



Province of British Columbia
Ministry of Energy, Mines and
Petroleum Resources

MINERAL RESOURCES DIVISION
Geological Survey Branch

**GEOLOGICAL
FIELDWORK
1990**

*A summary of Field Activities
and Current Research*

PAPER 1991-1

MINERAL RESOURCES DIVISION
Geological Survey Branch

British Columbia Cataloguing in Publication Data

Main entry under title:

Geological fieldwork. — 1974-

(Paper, ISSN 0226-9430)

Annual.

Issuing body varies: 1974-1980, Geological Division;
1981-1985, Geological Branch; 1986- , Geological
Survey Branch.

Subseries, 1979- , of: Paper (British Columbia,
Ministry of Energy, Mines and Petroleum Resources)

"A summary of field activities of the Geological
Division, Mineral Resources Branch."

ISBN 0381-243X=Geological fieldwork

1. Geology — British Columbia — Periodicals.
2. Geology, Economic — British Columbia — Periodicals.
3. Mines and mineral resources — British Columbia —
Periodicals. I. British Columbia. Geological Division.
II. British Columbia. Geological Branch. III. British
Columbia. Geological Survey Branch. IV. British
Columbia. Ministry of Energy, Mines and Petroleum
Resources. V. Series: Paper (British Columbia. Ministry
of Energy, Mines and Petroleum Resources)

QE187.G46

557.11'05

Rev. Dec. 1987

VICTORIA
BRITISH COLUMBIA
CANADA

January 1991

FOREWORD

Geological Fieldwork 1990: A Summary of Field Activities and Current Research is the sixteenth in this publication series. It contains reports on activities and project results during a year in which the Geological Survey Branch had budgets reduced due to the end of the Canada/British Columbia Mineral Development Agreement (MDA). Many of the Branch staff, particularly those engaged on MDA supported projects, are now producing final reports. This activity resulted in fewer field programs during 1990.

The base budget of the Branch for the 1990/91 fiscal year is \$7.05 million, with an additional \$300 700 provided by the MDA. The Geological Survey Branch is committed to a strong program of 1:50 000-scale regional mapping and mineral deposits, coal, surficial geology and industrial mineral studies. This includes 18 field programs in frontier areas or areas which are the focus of interest within the minerals industry.

Highlights of the 1990/91 program:

- Six 1:50 000-scale geological mapping programs were supported in areas across the province. Continuing programs were in the Iskut-North, Tagish Lake, Stikine River and Iskut-Sulphurets areas. New mapping projects were started in the Quatsino area of Vancouver Island and in the Mount Milligan area.
- Metallogenic field research continued in the Stewart-Sulphurets-Iskut "Golden Triangle", the Rossland Group of southeastern B.C., and precious metal enriched skarns. New research is supported in the area of the Mount Milligan porphyry Cu-Au deposit and on the potential for listwanite related lode-gold deposits in ultramafics.
- The newly created Surficial Geology unit carried out 3 field programs to improve the provincial database on surficial geology, geological hazards and placer geology. Data for the Peace River, Cariboo and northern Vancouver Island areas are reported herein.
- Reconnaissance geochemical surveys were completed in southeastern British Columbia (82G & J). Archived samples from 82E, F, K, L & M were analyzed for release later in 1991.
- The Coal unit continued studies on coal quality, resources and regional stratigraphy. Prominent projects are mapping on Vancouver Island and the Bowser Basin, as well as coalbed methane potential for the Vancouver Island, Rocky Mountain Foothills and Northeast B.C. deposits.
- The Industrial Minerals unit started a detailed geological evaluation of the Mount Brussilof magnesite deposit in southeastern B.C.
- The Branch continued to enhance computerized access to the provincial geoscience database. Research into Geographic Information Systems and the world-class MINFILE database are at the forefront of this activity.

The British Columbia Geoscience Research Program continued to encourage and support geoscience research. A total of 32 grants, funded by a budget of \$130 000, were made to researchers in 17 institutions across the country. Research topics covered such diverse topics as geologic mapping, isotopic dating, geochemistry, conodont research, Quaternary mapping, mineral deposit modelling and the application of Geographic Information Systems to geoscience data.

This volume of *Geological Fieldwork* contains forty-six technical manuscripts, down about 25 per cent from last year. However, producing this annual publication against very tight deadlines required a concerted effort from our editorial and publications staff and we acknowledge the efforts of Doreen Fehr and Janet Holland for formatting and page layout, John Newell for editing, and Brian Grant for managing the process. The quality of this publication is also due in part to Queen's Printer, who extended their cooperation and enthusiasm to ensure timely delivery.

*W.R. Smyth
Chief Geologist
Geological Survey Branch
Mineral Resources Division*

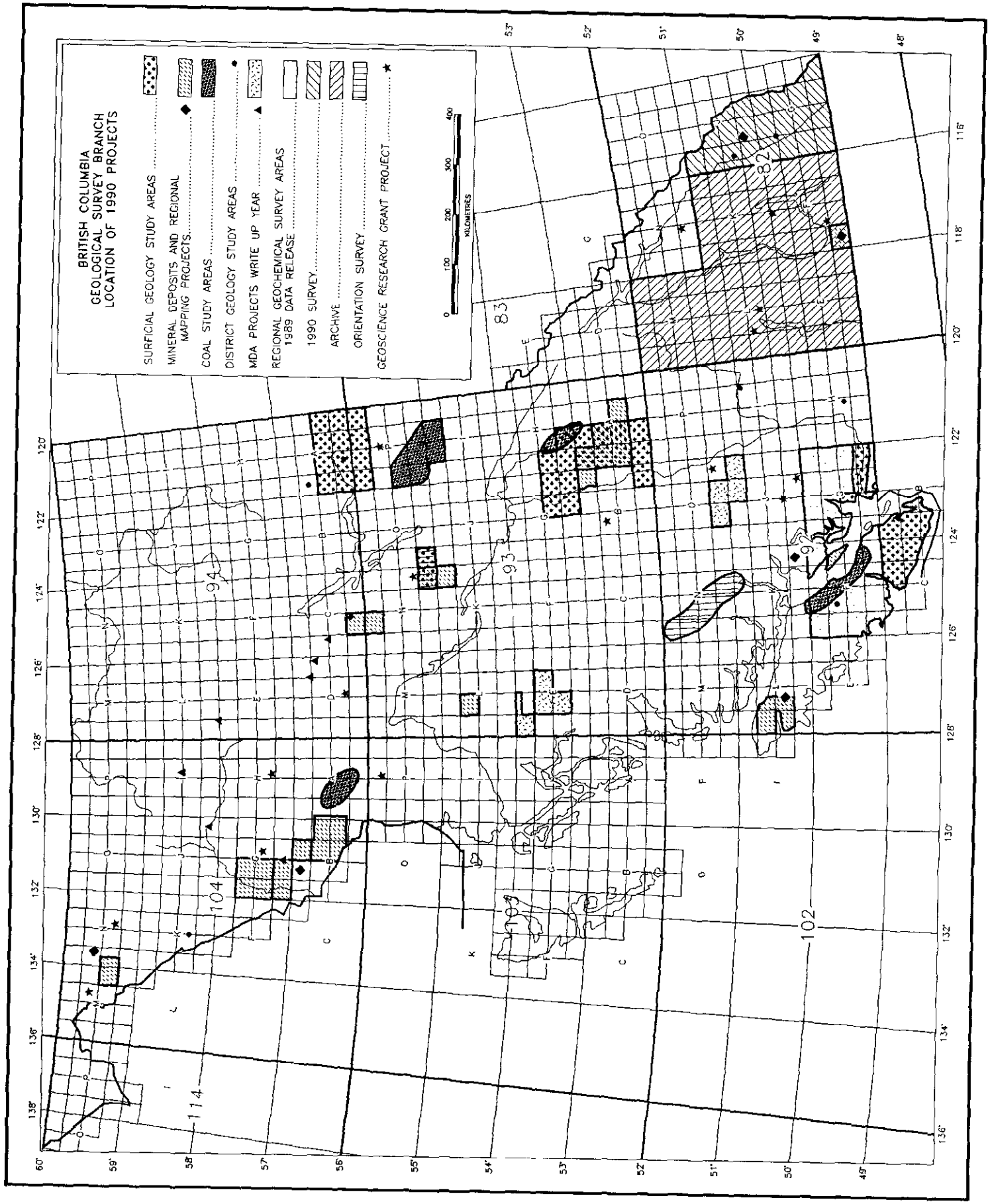


TABLE OF CONTENTS

	Page		Page
FOREWORD	3	1-12 G. Zhang and A. Hynes: Structure of the Takla Group East of the Finlay-Ingenika Fault, McConnell Creek Area, North-central B.C. (94D/8, 9)	121
REGIONAL AND DISTRICT MAPPING			
1-1 K.P.E. Andrew and T. Höy: Geology of the Rossland Group in the Erie Lake Area with Emphasis on Stratigraphy and Structure of the Hall Formation, Southeastern British Columbia (82F/3W)	9	1-13 J.M. Britton: Stratigraphic Notes from the Iskut-Sulphurets Project Area (104B)	131
1-2 T. Höy and K.P.E. Andrew: Geology of the Rossland Area, Southeastern British Columbia (82F/4E)	21	1-14 R.A. Donelick and J.R. Dickie: Low-temperature Thermal History of the Coast Plutonic Complex and Intermontane Belt, Northwest British Columbia (104M, N)	139
1-3 A. de Rosen-Spence and A.J. Sinclair: Metchosin Volcanics: A Low-titanium Emergent Seamount at the Base of the Crescent Terrane (92B)	33	1-15 M.G. Mihalynuk, K.J. Mountjoy, W.J. McMillan, C.H. Ash and J.L. Hammack: Highlights of 1990 Fieldwork in the Atlin Area (104N/12W)	145
1-4 G.E. Ray: The Geochemistry of Early Cretaceous Volcanic Rocks on the West Side of Harrison Lake, Southern British Columbia (92H/12)	41	1-16 J.L. Jackson, P.J. Patchett and G.E. Gehrels: Preliminary Nd and Sr Isotopic Analyses from the Nisling Assemblage, Northern Stikine and Northern Cache Creek Terranes, Northwestern British Columbia and Adjacent Yukon (104M, N)	153
1-5 H.R. Schmitt and G.G. Stewart: Preliminary Geology and Mineral Potential of the Cascade Recreation Area (92H/2, 3, 6, 7)	47	MINERAL DEPOSIT STUDIES	
1-6 J.M. Riddell: Stratigraphy of Mesozoic Rocks East of Pemberton, British Columbia, and the Setting of Mineral Showings (92J/2, 7, 10)....	57	2-1 B.N. Church, A.M. Jessop, R. Bell and A. Pettipas: Tertiary Outlier Studies: Recent Investigations in the Summerland Basin, South Okanagan Area, B.C. (82E/12)	163
1-7 J.I. Garver: Kinematic Analysis and Timing of Structures in the Bridge River Complex and Overlying Cretaceous Sedimentary Rocks, Cinnabar Creek Area, Southwestern British Columbia (92J/15)	65	2-2 G. Beaudoin and D.F. Sangster: The Use of Production Data as an Exploration Guideline for Ag-Pb-Zn-Au Vein and Replacement Deposits, Northern Kokanee Range, Southeastern British Columbia (82F, K)	171
1-8 D.A. Archibald, P. Schiarizza and J.I. Garver: ⁴⁰ Ar/ ³⁹ Ar Evidence for the Age of Igneous and Metamorphic Events in the Bridge River and Shulaps Complexes, Southwestern British Columbia (92O/2; 92J/15, 16)	75	2-3 X. Cheng, A.J. Sinclair, M.L. Thomson and Y. Zhang: Hydrothermal Alteration Associated with the Silver Queen Polymetallic Veins at Owen Lake, Central B.C. (93L/2)	179
1-9 N.W.D. Massey and D.M. Melville: Quatsino Sound Project (92L/5, 6, 11, 12)	85	2-4 C.T.S. Hood, C.H.B. Leitch and A.J. Sinclair: Mineralogic Variation Observed at the Silver Queen Mine, Owen Lake, Central British Columbia (93L/2)	185
1-10 J. Nelson, K. Bellefontaine, K. Green and M. MacLean: Regional Geological Mapping Near the Mount Milligan Copper-Gold Deposit (93K/16, 93N/1)	89	2-5 M.L. Thomson and A.J. Sinclair: Syn-Hydrothermal Development of Fractures in the Silver Queen Mine Area, Owen Lake, Central British Columbia (93L/2)	191
1-11 P.J. Desjardins, R.L. Arksey and D.G. McIntyre: Geology of the Lamprey Creek Map Sheet (93L/3)	111	2-6 R.C. DeLong, C.I. Godwin, M.W. Harris, N.M. Caira and C.M. Rebagliati: Geology and Alteration at the Mount Milligan Gold-Copper Porphyry Deposit, Central British Columbia (93N/1E)	199

TABLE OF CONTENTS (Continued)

		Page		Page	
2-7	J.R. Clark and A.E. Williams-Jones: ⁴⁰ Ar/ ³⁹ Ar Ages of Epithermal Alteration and Volcanic Rocks in the Toadoggone Au-Ag District, North-central British Columbia (94E)	207	4-4	P.M. Bartier and C.P. Keller: Integrating Bedrock Geology with Stream-sediment Geochemistry in a Geographic Information System (GIS): Case Study NTS 92H	315
2-8	J.L. Hammack, G.T. Nixon, W.P.E. Paterson and C. Nuttall: Geology and Noble Metal Geochemistry of the Lunar Creek Alaskan-type Complex, North-central British Columbia (94E/13, 14)	217	4-5	J.L. Gravel, S. Sibbick and D. Kerr: Geochemical Research, 1990: Coast Range – Chilcotin Orientation and Mount Milligan Drift Prospecting Studies (92O, N, 93N)	323
2-9	C.I. Godwin, A.D.R. Pickering, J.E. Gabites and D.J. Alldrick: Interpretation of Galena Lead Isotopes from the Stewart-Iskut Area (103O, P; 104A, B, G)	235	4-6	V.M. Levson and T.R. Giles: Stratigraphy and Geologic Settings of Gold Placers in the Cariboo Mining District (93A, B, G, H)	331
2-10	I.C.L. Webster and G.E. Ray: Skarns in the Iskut River - Scud River Region, Northwest British Columbia (104B, G)	245	4-7	P.T. Bobrowsky, N. Catto and V. Levson: Reconnaissance Quaternary Geological Investigations in Peace River District, British Columbia (93P, 94A)	345
2-11	G.E. Ray, V.A. Jaramillo and A.D. Ettlinger: The McLymont Northwest Zone, Northwest British Columbia: A Gold-rich Retrograde Skarn? (104B)	255	COAL STUDIES		
INDUSTRIAL MINERALS			5-1	D.A. Grieve and M.E. Holuszko: Trace Elements, Mineral Matter and Phosphorus in British Columbia Coals	361
3-1	L. Morin and J. Lamothe: Testing on Perlite and Vermiculite Samples from British Columbia	265	5-2	M.E. Holuszko and D.A. Grieve: Washability Characteristics of British Columbia Coals	371
3-2	G.J. Simandl and K.D. Hancock: Geology of the Mount Brussilof Magnesite Deposit, Southeastern British Columbia (82J/12, 13)	269	5-3	C.G. Cathyl-Bickford and G.L. Hoffman: Geology and Coal Resources of the Nanaimo Group in the Alberni, Ash River, Cowie Creek and Parksville Areas, Vancouver Island (92F/2, 6, 7, 8)	381
3-3	R.W. Renaut and D. Stead: Recent Magnesite-Hydromagnesite Sedimentation in Playa Basins of the Cariboo Plateau, British Columbia (92P)	279	5-4	C. Kenyon: The Suquash Coalfield, Vancouver Island (92L/11)	387
APPLIED GEOCHEMISTRY AND SURFICIAL GEOLOGY			5-5	A. Matheson and M. Sadre: Subsurface Coal Sampling Survey, Bowron River Coal Deposits, Central British Columbia (93H/13)	391
4-1	P.F. Matysek, W. Jackaman and S. Feulgen: 1991 Regional Geochemical Survey Release, Southeastern British Columbia. Delivering a New Generation of Geochemical Data (82E, F, G, J, K, L, M)	291	5-6	B. Ryan: Density of Coals from the Telkwa Coal Property, Northwestern British Columbia (93L/11)	399
4-2	J.M. Ryder and K. Fletcher: Exploration Geochemistry - Sediment Supply to Harris Creek (82L/2)	301	5-7	D.J. Hunter and J.M. Cunningham: Burnt River Mapping and Compilation Project (93P/5, 6)	407
4-3	P.T. Bobrowsky and J.J. Clague: Neotectonic Investigations on Western Vancouver Island, British Columbia (92F/4)	307	5-8	H.O. Cookenboo and R.M. Bustin: Coal-bearing Facies in the Northern Bowser Basin (104A, H)	415
			5-9	B. Ryan: Geology and Potential Coal and Coalbed Methane Resource of the Tuya River Coal Basin (104J/2,7)	419
			UNIVERSITY RESEARCH		
			6-1	University Research in British Columbia	433



GEOLOGY OF THE ROSSLAND GROUP IN THE ERIE LAKE AREA, WITH EMPHASIS ON STRATIGRAPHY AND STRUCTURE OF THE HALL FORMATION, SOUTHEASTERN BRITISH COLUMBIA (82F/3W)

By Kathryn P.E. Andrew and Trygve Höy

KEYWORDS: Regional geology, Rossland Group, Hall Formation, Elise Formation, Archibald Formation, Hall syncline, Erie Creek fault, Beaver Creek fault, Keystone deposit, Arlington mine, Clubine deposit.

INTRODUCTION

Regional mapping and mineral deposit studies have been carried out in the Rossland Group since 1987. The aim of the project is to develop a better understanding of the stratigraphic and structural setting of the Rossland Group and to assess controls on mineralization within it. The project includes systematic whole-rock and trace element analyses of volcanic rocks, uranium-lead dating of intrusive rocks and Elise volcanic rocks, and fluid inclusion, stable and radiogenic isotope studies of mineral occurrences.

During the 1990 field season, 1:20 000-scale regional mapping was completed in both the Salmo and Rossland map areas (Figure 1-1-1). The Salmo mapping ties together previous work in the Nelson map area to the north (Høy and Andrew, 1989b) and in the Mount Kelly – Hellroaring Creek and Beaver Creek areas to the south (Høy and Andrew, 1990b, Andrew *et al.*, 1990a, b). Previous to this study, the structural tie between the Nelson and Salmo map sheets was unresolved. Special emphasis is given to the distribution, facies changes and contact relationships of the Hall Formation in both the Salmo and Nelson map areas.

Previous regional mapping of the Rossland Group in the Erie Lake area has been by Little (1960, 1965), Fitzpatrick (1985), Mulligan (1951, 1952) and Walker (1934). Petrologic and geochemical studies of the Elise Formation have been undertaken by Beddoe-Stephens and Lambert (1981) and Beddoe-Stephens (1982).

STRATIGRAPHY

The Rossland Group is divided into a lower sequence of predominantly fine-grained clastic rocks of the Archibald Formation, a thick accumulation of mafic flows and pyroclastic and epiclastic rocks of the Elise Formation, and generally less intensely deformed clastic rocks of the overlying Hall Formation. The upper part of the Ymir Group, a fine-grained, strongly deformed clastic and carbonate package which underlies the Elise Formation in the Nelson area, is correlated with the Archibald Formation (Little 1960, 1965; Frebold, 1959; Höy and Andrew, 1989a). The age of the Elise Formation is bracketed by Sinemurian fossils in the Archibald Formation and Toarcian fossils in the overlying Hall Formation (Frebold and Tipper, 1970; Tipper, 1984); no fossils have been found in the Ymir Group.

Plagioclase porphyry and diorite plutons that intrude the Rossland Group are locally intensely sheared and conformable. These include the Silver King porphyry southwest of Nelson, the 'Shaft monzodiorite', and numerous other small alkaline intrusions. They have been interpreted to be coeval subvolcanic intrusions (Høy and Andrew, 1988, 1989a; Andrew and Höy, 1989); however, uranium-lead dating of the Silver King porphyry indicates a Middle Jurassic age of 178.1 ± 1.4 Ma. This age is between that of the Rossland Group (187 to 204 Ma), defined by macrofossil collections, and the Nelson batholith and related plutons, dated at 165 Ma. Other, more mafic intrusions, including the Shaft and Mammoth bodies are, however, still considered to be coeval with the Elise Formation.

Several granite to granodiorite stocks and plutons in the Erie Lake area are probably correlative with either the Middle to Late Jurassic Bonnington pluton or the Nelson batholith. Small biotite-rich monzonite stocks (Coryell intrusions) and quartz rhyolite dikes crosscut the Jurassic units and are of Eocene age (Little, 1960).

ARCHIBALD FORMATION

The Archibald Formation is the lowermost unit of the Rossland Group and is correlative with the upper part of the Ymir Group. The total exposed thickness of the formation varies from 825 to 2550 metres (Andrew *et al.*, 1990a); its base is not seen because it is either cut by faults or by Middle Jurassic intrusions. The contact between the Archibald and Elise formations is gradational, mapped where fine-grained interbedded siltstones and argillites with occasional thin flows give way to massive augite porphyry flows (Høy and Andrew, 1989a). In the Erie Lake area (Figure 1-1-2a), the Archibald Formation is exposed in the limbs of an anticline that parallels Erie Creek, in fault-bounded blocks west of the town of Salmo, in the Beaver Creek valley and on the northeast slopes of Mount Kelly.

The oldest rocks in the formation are massive to finely laminated, dark grey to black, rusty weathering argillite. These crop out on the northeastern slopes of Mount Kelly. This lower argillite unit is often either missing, not exposed or replaced by a coarser facies (Andrew *et al.*, 1990b). The lower argillite is overlain by an upper turbidite sequence of interbedded graded wacke, siltstone and silty argillite. This sequence generally coarsens upwards with over 400 metres of poorly lithified, matrix-supported conglomerate near the top. The conglomerate is best exposed in highway cuts in the Beaver Creek valley just west of the Crownsnest Highway cut-off. It contains approximately 10 per cent limestone and siltstone clasts; the limestone clasts contain Permian

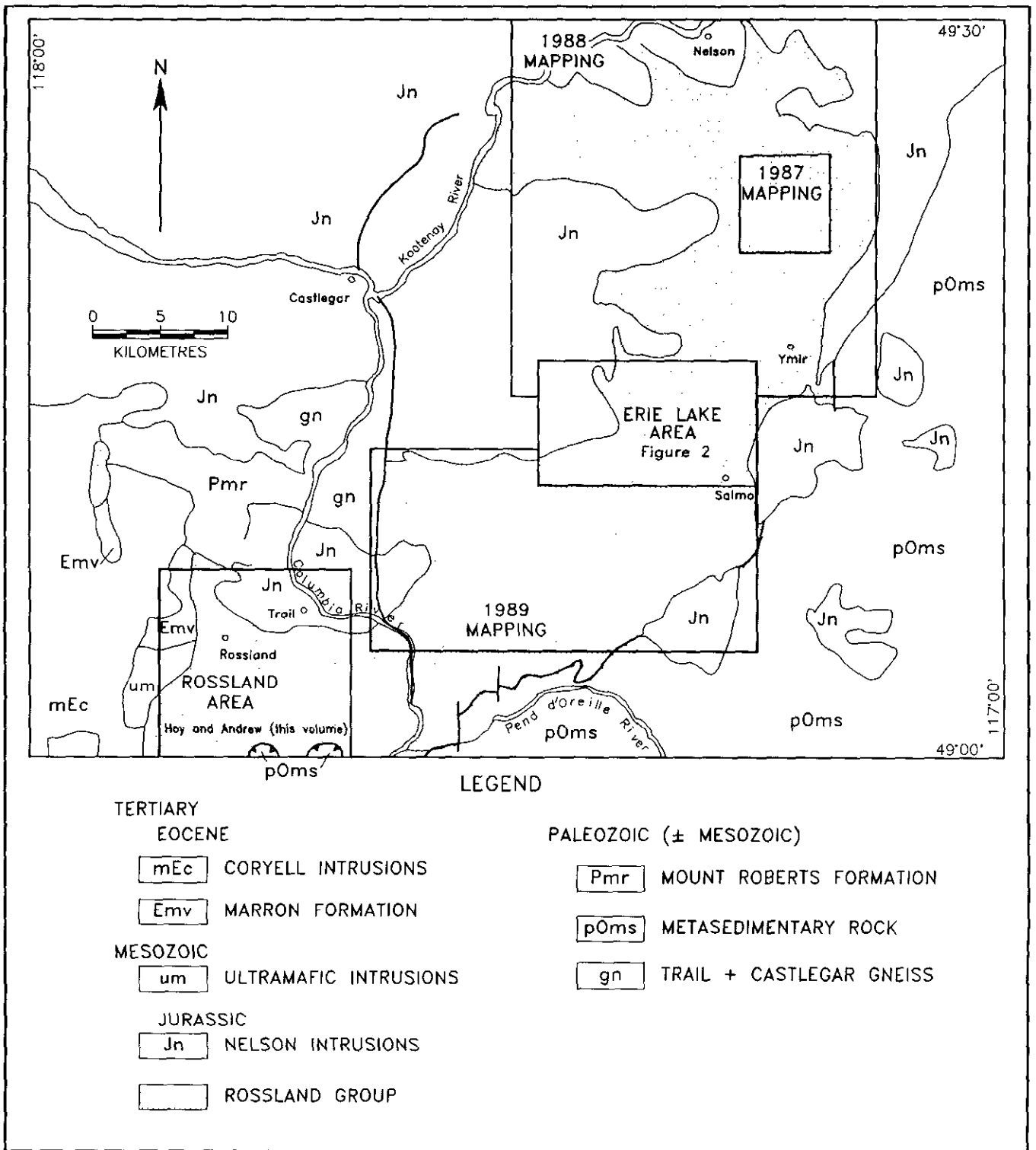


Figure 1-1-1. Location map and main physiographic and geologic features, Erie Lake area, southeastern British Columbia.

fossils probably derived from the Mount Roberts Formation (Little, 1982b). Augite porphyry sills, locally up to 50 metres thick, occur near the top of the succession in Erie Creek, on Bell Ridge and on the northeast ridge of Mount Kelly. In the Beaver Falls area (Andrew *et al.*, 1990b), the formation is capped by 100 metres of maroon siltstone and lithic wacke.

ELISE FORMATION

The Elise Formation occurs within fault-bounded blocks east of Hudu Creek, in the vicinity of Erie Mountain, on the northern slopes of Mount Kelly, northwest of Hellroaring Creek and as east and west-facing homoclinal panels on the limbs of the Hall Creek syncline. Interfingering lenses of massive to brecciated flows as well as pyroclastic, tuffite and epiclastic deposits characterise the formation. The total exposed thickness of the formation varies from 600 metres near Champion Lakes to 5100 metres in the Erie-Stewart Creek area (Andrew *et al.*, 1990a; Höy and Andrew, 1989a; Figure 1-1-3).

The basic subdivision of the Elise Formation in the Nelson area into a lower succession of mafic flows or pyroclastic breccias and an upper section of more intermediate pyroclastic and tuffite rocks, epiclastic deposits and minor fine sedimentary rocks, is not apparent in the Salmo area. This may be due to lack of outcrop in the Erie and Keystone Mountain areas or to structural complications.

The basal part of the Elise Formation shows rapid lateral facies changes. North of Beaver Creek, on the west limb of the Hall Creek syncline, the lower Elise comprises mafic pyroclastic breccia whereas south of Beaver Creek and near Ymir, mafic flows predominate. The top of the formation is poorly exposed in the limbs of the Hall syncline (Figure 1-1-2a). It includes intermediate lapilli and crystal tuff in the limbs of the Hellroaring Creek syncline south of Salmo. Elsewhere, the top of the formation is faulted out.

The thickest section of the Elise Formation is exposed in the Erie and Stewart Creeks areas. It comprises dominantly mafic lapilli tuff and pyroclastic breccia as well as more intermediate crystal tuff, tuffaceous conglomerate and 500 metres of finely laminated siltstone. It is possible that this siltstone succession, included as part of the Elise Formation (Figure 1-1-2a), may be the upper part of the Archibald Formation as mapped by Little (1960; 1982a).

HALL FORMATION

The 'Hall Series', from which the Hall Formation was named, was defined by Drysdale in 1917. It was renamed the Hall Group by Little in 1950 and subsequently referred to as the Hall Formation (Mulligan, 1952). The formation consists of conglomerate, lithic wacke, sandstone, siltstone and argillite with minor intercalated crystal tuffs. It is exposed in a belt extending from the headwaters of Noman Creek, just east of Toad Mountain in the Nelson area, southward to the town of Salmo, around Hellroaring Creek south of Salmo, near the head of Kelly Creek and in the Fruitvale area (Figure 1-1-4). The Hall Formation contains early Pleinsbachian and early Toarcian ammonites (Tipper,

1984). A plant fragment and pelecypods were also collected from the formation (Little, 1950).

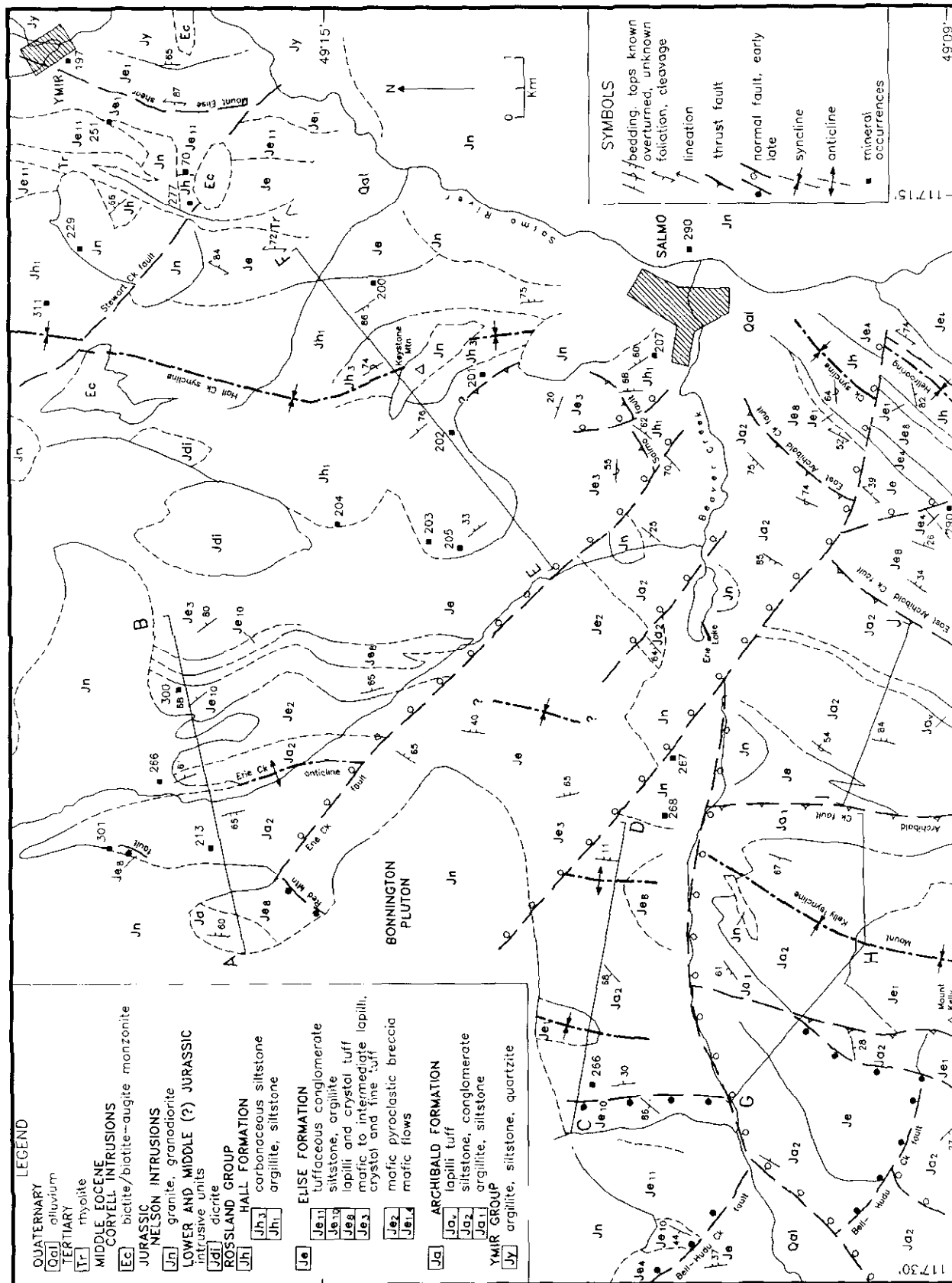
The exposed thickness of the Hall Formation (Figure 1-1-5) varies from at least 350 metres near Fruitvale, 550 metres near Kelly Creek, 1650 metres in Hellroaring Creek, 1700 metres on Keystone Mountain, 2100 metres in the Stewart Creek area and 1150 metres south of Hall Creek (Little, 1985; the type section of Drysdale, 1917). These are minimum estimates; the top of the Hall is not seen because the formation is either exposed in a syncline or faulted out (Figure 1-1-4).

Generally, the Hall Formation conformably overlies the Elise Formation; however, in the Salmo River valley, near Hall Creek, an erosional unconformity with development of basal conglomerates separates the two formations (Figure 1-1-6). The conglomerate varies in thickness from 10 to 20 metres and comprises subrounded clasts of augite porphyry and plagioclase lapilli and crystal tuff of the Elise Formation incorporated in a poorly consolidated muddy matrix. Elsewhere, as in highway cuts just south of Salmo and in Hellroaring Creek (Figure 1-1-4), moderate to intense shearing is exposed at the contact. Kinematic indicators, including c-s fabrics, kink bands and tension gashes, indicate a general right-lateral movement on the east side of the syncline and left-oblique dip-slip movement on the west side.

The Hall Formation can be subdivided into three broadly defined units: a lower, rusty black siltstone and argillite succession, a coarse sandstone and conglomerate succession and, locally, an upper carbonaceous siltstone unit (Figure 1-1-5). The base of the lower Hall is either conformable or marked by an erosional unconformity. Argillites within the lower Hall are rusted due to weathering of disseminated pyrite (Plate 1-1-1). Interbedded quartzitic siltstone and argillite, also typical of the lower part of the formation (Figure 1-1-6), are well exposed in Hall Creek (Plate 1-1-2). Although primary small-scale structures such as graded beds are absent or poorly developed in these rocks, rip-up clasts and flame structures are occasionally seen and can be used for top determinations (Plate 1-1-3). This unit hosts most of the vein deposits in the area (Figure 1-1-2a).

The middle unit of the Hall varies from a coarse polymict pebble conglomerate to lithic wacke and minor silty argillite. The conglomerate is characterised by elongate, subangular mudstone fragments 5 to 10 centimetres in diameter (Plate 1-1-4) and is probably the same unit described as 'intraformational' conglomerate by Mulligan (1952). The lithic wacke contains from 10 to 50 per cent quartz, feldspar, ferromagnesian minerals and angular rock fragments. The upper part of the Hall is characterised by massive fine-grained carbonaceous siltstone in the Keystone Mountain area (Figure 1-1-6).

Thickness and facies changes in the Hall Formation are summarized in the stratigraphic columns of Figure 1-1-5. The formation is absent in the Rossland area where Elise volcanic rocks are unconformably overlain by either late Cretaceous conglomerates of the Sophie Mountain Formation or Eocene volcanic rocks of the Marron Formation



Andrew and Höy (1991)

Figure 1-1-2a. Geology of the Eric Lake area after Höy and Andrew, 1989; 1990b; Little, 1960, 1965; Mulligan 1951, 1952; Fitzpatrick, 1985.

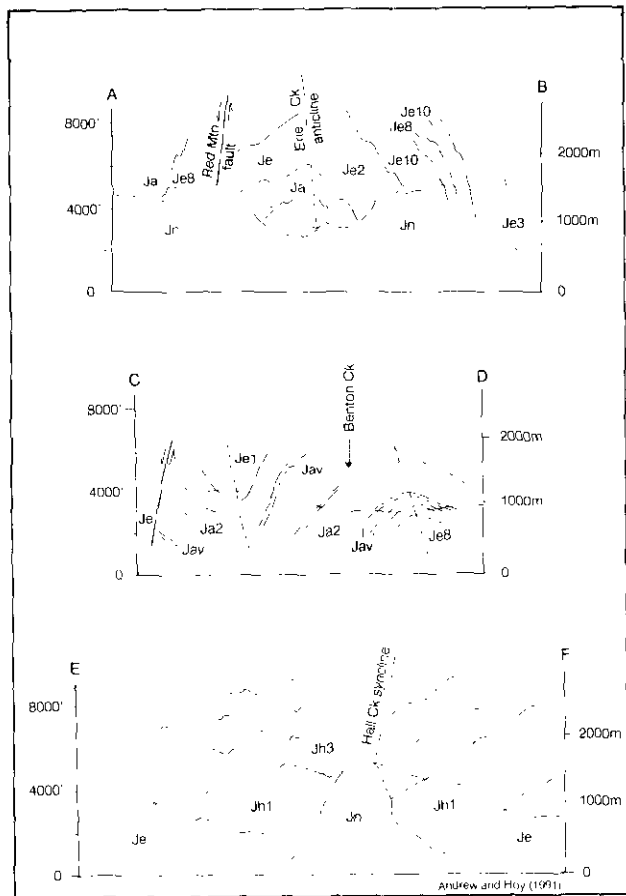
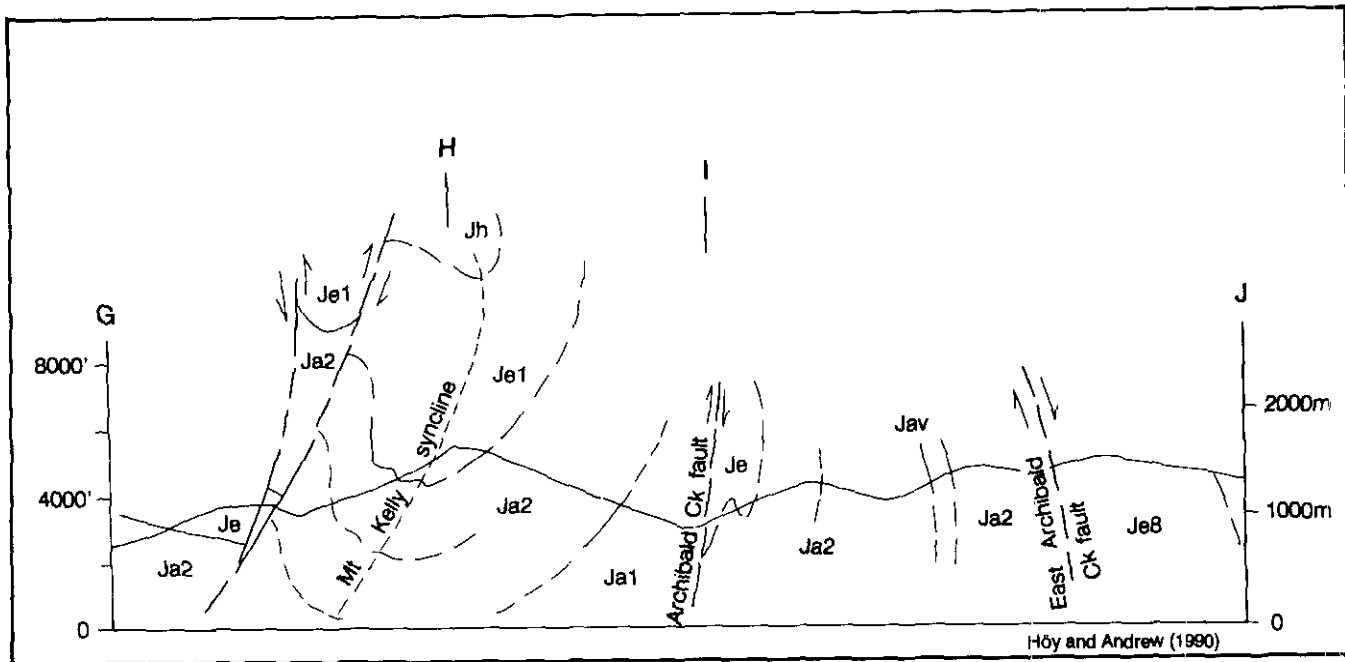


Figure 1-1-2b. Vertical structural sections, Erie Lake map area. Section locations are identified on Figure 1-1-2a.

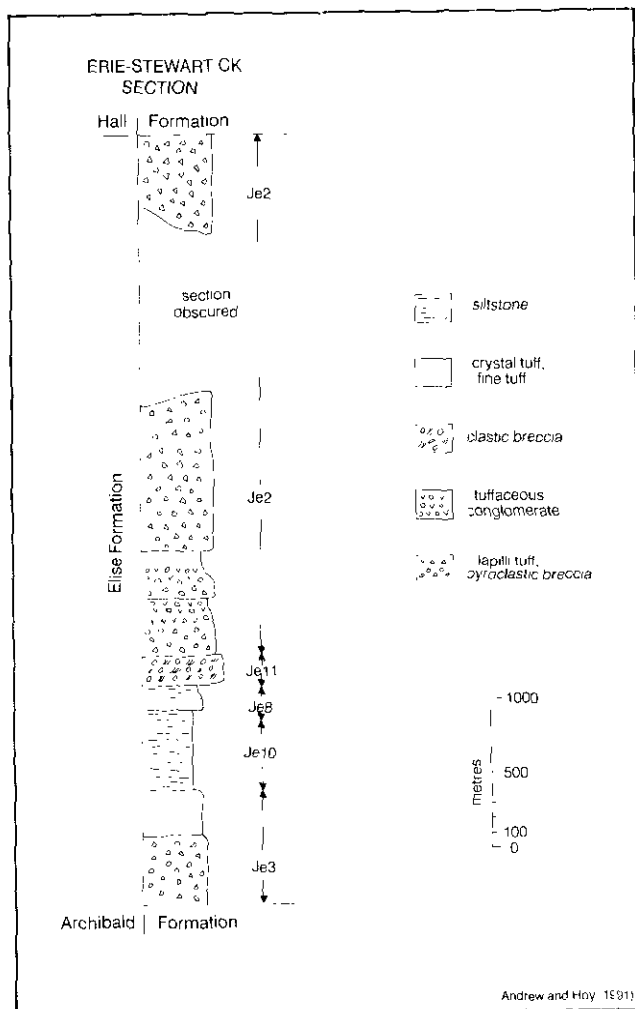


Figure 1-1-3. Composite stratigraphic section of the Elise Formation, Erie - Stewart Creek area.

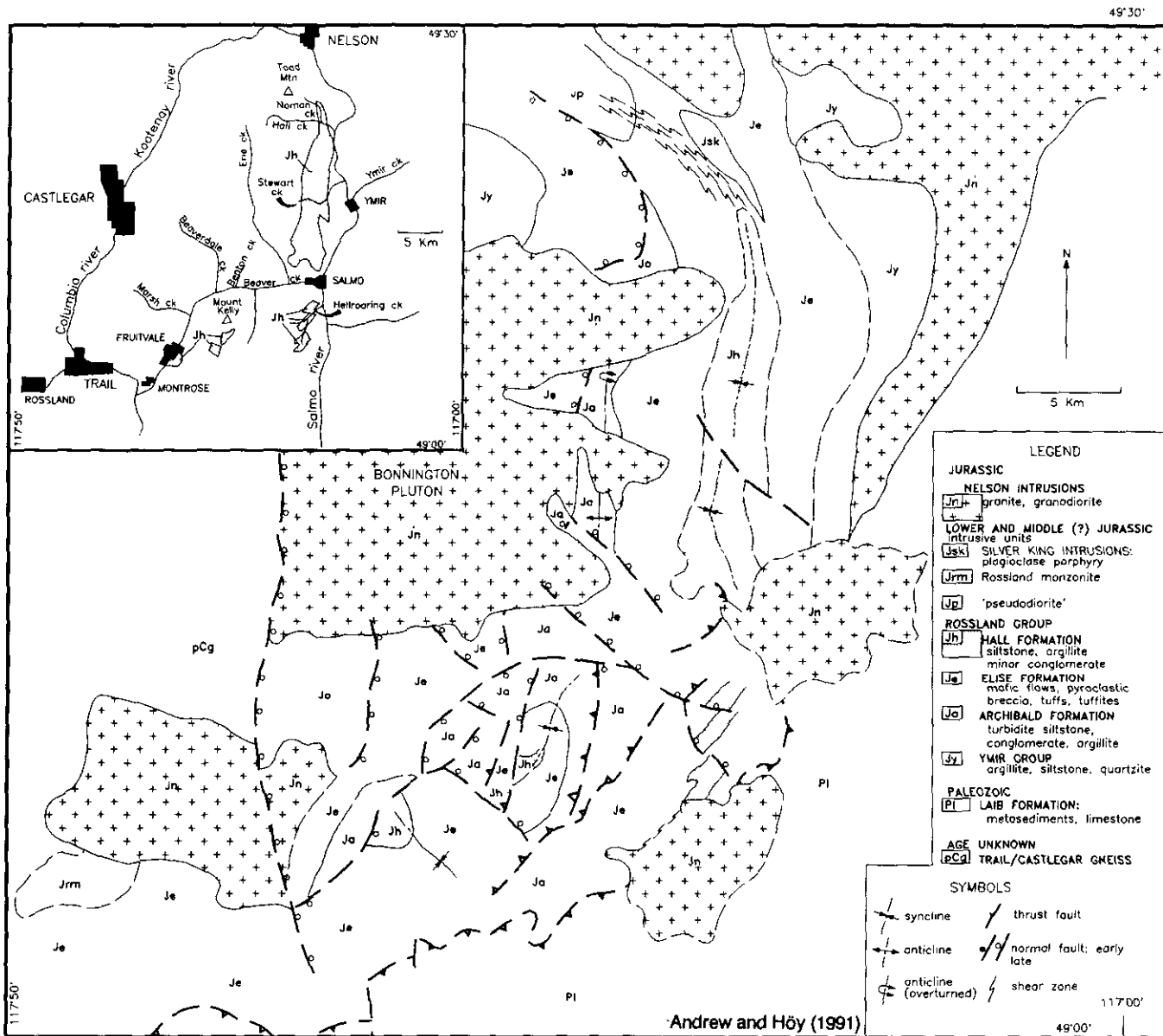


Figure 1-1-4. Distribution of the Hall Formation and main geologic and physiographic features in the Nelson (W1/2) southwest portion (82F/SW).

(Höy and Andrew, 1991a, this volume). To the east, in the Fruitvale area, the Hall Formation forms a wedge of fine-grained clastic beds that thicken and coarsen eastward (Figure 1-1-5). Farther east, in the Hall Creek and Stewart Creek areas, conglomerates are more predominant. The fine-grained, carbonaceous clastic units that occur at the top of the formation in the Keystone Mountain area appear to be laterally discontinuous; they are not recognized in the upper Hall to the west or north.

Based on sedimentary rock types and the abundance of marine fossils, the Hall Formation has been interpreted to have been deposited in a littoral to offshore environment (Little, 1950; Mulligan, 1951). Local development of a basal unconformity and, elsewhere, conformable deposition of laminated argillite above the Elise, suggests that the Hall

developed on an irregular paleosurface. Fanglomerates and clastic-wedge deposits within the Hall suggest deposition may have been modified by local fault scarps. In summary, the Hall Formation is interpreted to have been deposited in a shallow-marine structural basin at the end of a period of explosive pyroclastic volcanism.

STRUCTURE

The structure of the Salmo area is dominated by a complex pattern of rectilinear faults, superposed on an earlier thrust and fold terrain. Four phases of deformation are identified: intense shearing and development of a penetrative mineral foliation, north-trending folds associated with east-directed thrust faults, normal faulting prior to intrusion of Nelson batholithic rocks, and Eocene normal faulting.

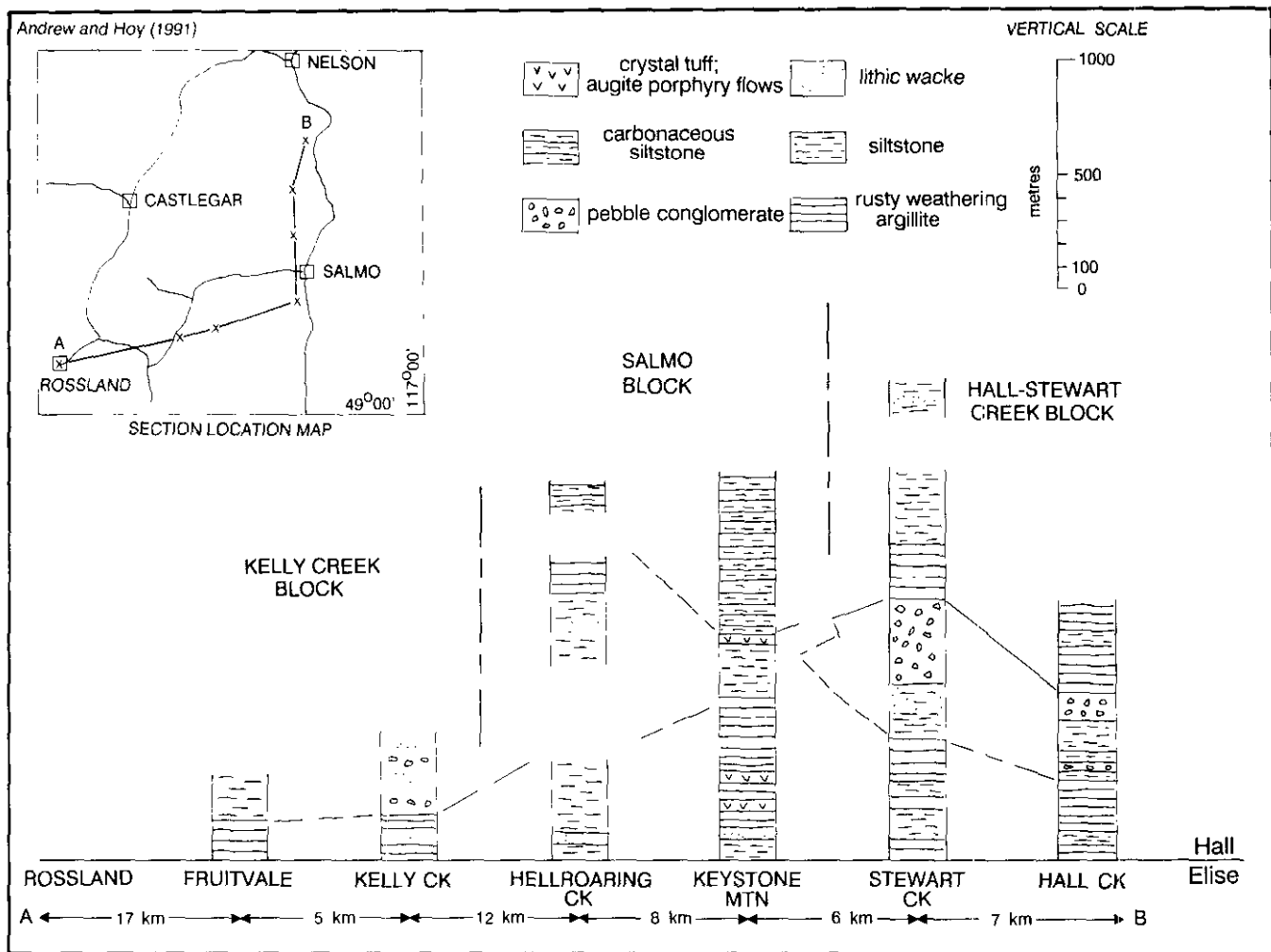


Figure 1-1-5. Correlation chart of the Hall Formation showing main lithologic and thickness changes.

Intense shearing along the eastern edge of exposed Rossland Group rocks, particularly in the Ymir Group northeast of Ymir and in the vicinity of the Hellroaring Creek syncline south of Salmo (Figure 1-1-2a; Höy and Andrew, 1989a), may result from collisional tectonics along the eastern margin of Quesnellia. With continued compressional tectonics, east-directed thrusts and east-verging to upright folds developed. The Hellroaring Creek syncline, the faulted continuation of the Hall Creek syncline north of Salmo (Höy and Andrew, 1990a), is an overturned, east-dipping syncline with Hall Formation in its core (see sections, Figure 1-1-2b). A number of layer-parallel faults or shear zones associated with intense penetrative deformation in Elise volcanic rocks parallel the margins of this syncline.

Farther west, folds are more upright, more open and appear to be associated with thrust faults. The Archibald Creek, East Archibald Creek and Salmo thrusts (Figure 1-1-2a) postdate early shearing and possibly related tight folds in the Hellroaring Creek area. The Salmo fault dips steeply to the northwest and places a west-facing lower Elise succession (Je3) on east-facing Hall Formation (Jh1, Figure 1-1-2a). Southwest of Salmo, the East Archibald Creek thrust juxtaposes west-facing Archibald Formation

(Ja2) in its hangingwall with east-facing upper Elise Formation (Je8). The Erie Creek anticline, mapped as slightly overturned to the east in the Nelson area (Höy and Andrew, 1989b), is upright and open south of the Bonnington pluton (section G-J, Figure 1-1-2b).

West and northeast-dipping normal faults that predate intrusion of Middle to Late Jurassic granitic plutons occur northwest of Mount Kelly; they may record similar extensional tectonics as the Red Mountain fault in the Nelson area (Höy and Andrew, 1989a, 1990a). The Hudu – Bell Creek fault has a rectilinear shape just northwest of Mount Kelly (Andrew and Höy, 1991b). It follows in part the locus of an earlier thrust fault (Figure 1-1-2a). The fault forms a down-dropped block which is then offset to the north by the Beaver Creek fault. The extension of the Red Mountain fault is seen farther north near Erie Creek (Figure 1-1-2a; Höy and Andrew, 1989a).

East and northeast-dipping normal faults cut all earlier structures. The Beaver Creek fault postdates the Archibald Creek thrust, downdrops earlier west-side-down normal faults and offsets Middle to Late Jurassic intrusive rocks. The Erie Creek fault and associated normal faults near Erie Mountain and Salmo downdrop strata to the northeast (Fig-

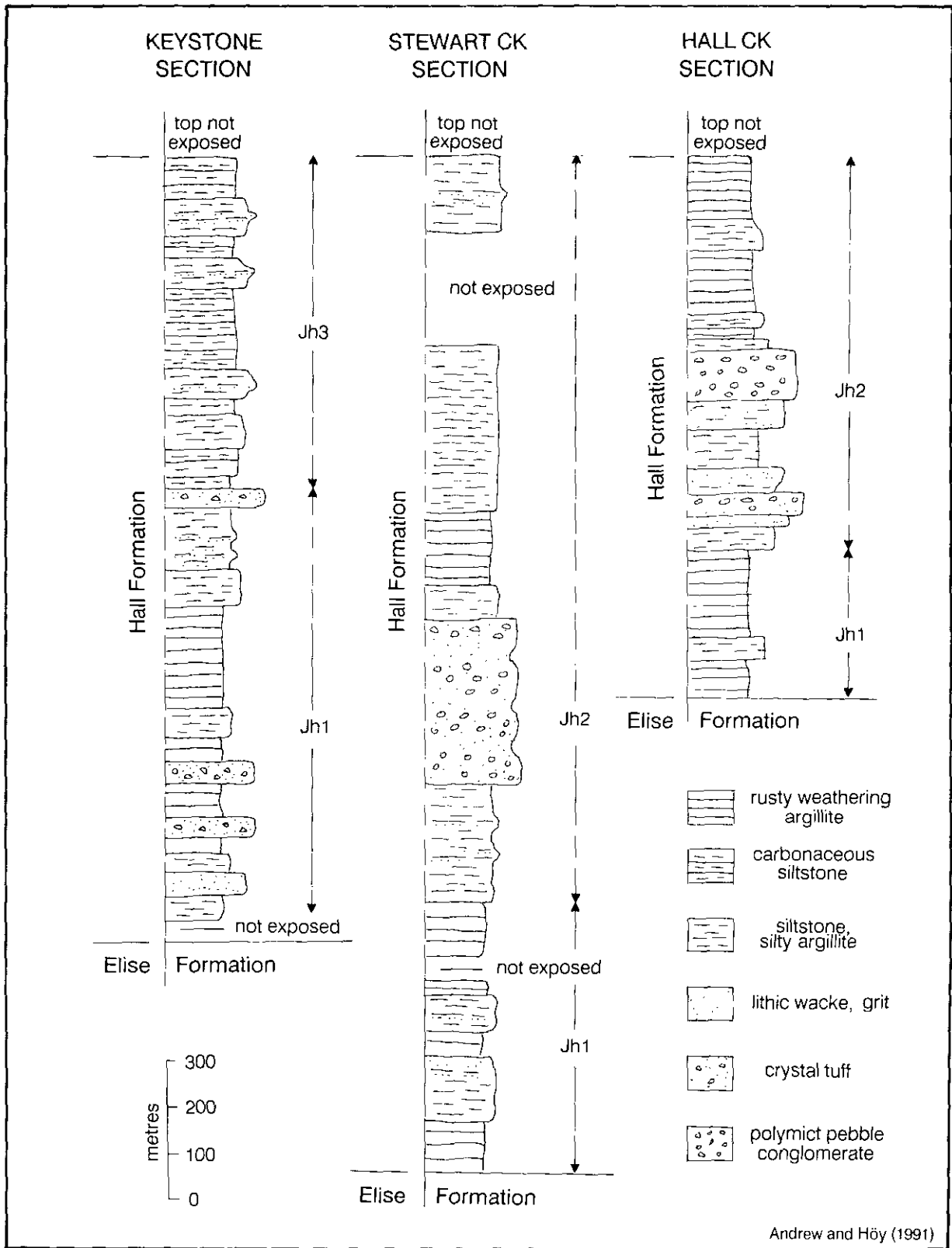


Figure 1-1-6. Stratigraphic sections of the Hall Formation, Keystone Mountain, Stewart Creek and Hall Creek areas.



Plate 1-1-1. Weathering of disseminated pyrite in siltstone of the Hall Formation, Hall Creek.



Plate 1-1-3. Rip-up clasts and flame structures in interbedded siltstone and sandstone beds, Stewart Creek area.



Plate 1-1-2. Interbedded quartzitic siltstone and argillite typical of the lower Hall Formation, Hall Creek type section.



Plate 1-1-4. Pebble conglomerate of the middle Hall Formation with 5 to 10-centimetre subangular mudstone fragments, south of Hall Creek.

ure 1-1-2a). The Stewart Creek fault (Höy and Andrew, 1989b) may also be a late east-dipping normal fault. These faults may be the same generation as the normal east-side-down Champion Lake and Slocan Lake faults which are part of an Eocene extensional event in southeastern British Columbia (Little, 1962; Simony, 1979; Parrish, 1984; Corbett and Simony, 1984; Parrish *et al.*, 1988).

In summary, the tectonic evolution of the Erie Lake area west of Salmo involved early compressive strain, with development of intense shearing, a penetrative mineral foliation and possible tight folds. This strain is concentrated along the eastern edge of Quesnellia and resulted from collision with cratonic North America in early Middle Jurassic time. Continued compressive strain spread westward, producing more open folds and associated east-verging thrust faults. Intrusion of the syntectonic Silver King suite of plutonic rocks (*ca* 178 Ma) records a magmatic event associated with this deformation.

Extensional tectonics produced large high-angle normal faults in the western part of the area. These faults are earlier than the late Middle Jurassic Nelson batholith (*ca* 165 Ma). Eocene extensional faults, associated with a suite of north-trending dikes, are the latest structures in the area.

MINERAL OCCURRENCES

Mineral occurrences in the Salmo area are shown on Figure 1-1-2a and listed in Table 1-1-1. These can be separated into:

TABLE 1-1-1
MINERAL PROPERTIES IN THE ERIE LAKE AREA

MINFILE No.	Name	Commodities	Type	Host	Status
82FSW070	May Blossom	Au,Pb,Zn,Mo,W	Vein	Je11	Showing
82FSW197	Myrtle	Au,Ag,Pb,Zn	Vein	Je1,4	Past producer
82FSW200	Clubine	Au,Ag,Pb,Zn	Vein	Jh1	Past producer
82FSW201	Second Chance	Au,Ag	Vein	Jh1	Past producer
82FSW202	Keystone	Au,Ag,Pb,Zn,Cu	Vein	Jh1	Past producer
82FSW203	Canadian King	Au,Ag,Pb	Vein	Jh1	Past producer
82FSW204	Gold Hill	Au,Ag	Vein	Jh1	Past producer
82FSW205	Arlington	Au,Ag,Pb,Zn	Vein	Jh1	Past producer
82FSW207	Silver Dollar	Au,Ag,Pb,Zn	Vein	Jh	Past producer
82FSW213	Drum Lummon	Au,Ag,Pb,Zn,Cu,W	Vein	Ja2	Showing
82FSW220	Curlett	Mo	Porphyry	Jn,e	Showing
82FSW226	Hattie	Mo,W,Cu,Ag	Porphyry	Jn	Showing
82FSW229	Stewart	Au,Mo,W	Porphyry	Jn	Developed prospect
82FSW251	Fresno	Mo	Porphyry	Jn	Showing
82FSW266	Rely	Au,Ag,Pb,Zn	Skarn	Ja2	Past producer
82FSW267	Armstrong	Au,Ag,Pb,Zn	Vein	Jn	Past producer
82FSW268	Meadows	Mo	Vein	Jn	Showing
82FSW277	Free Silver	Ag,Pb	Vein	Jh	Showing
82FSW283	Allouez	Au,Ag,Cu	Vein	Jn	Showing
82FSW290	Katie	Au,Cu	Shear-related	Je1,4	Showing
82FSW300	Ben Hassen	Au,Ag,Pb,Zn,Cu	Vein	Je10	Prospect
82FSW311	Arrow Tungsten	W,Mo	Skarn	Jh	Prospect

- pre and syntectonic types, which occur in the Elise Formation and are associated with tight folds and intense shearing (MINFILE 082FSW290); Andrew and Höy, 1989, 1990; Höy and Andrew, 1989c);
- intrusive-related types such as tungsten skarns and molybdenum porphyries, associated with Nelson or Coryell intrusions (MINFILE 082FSW311, 082FSW299, 082FSW268, 082FSW226); and,
- vein deposits associated with west-side-down, pre-Nelson normal faults (MINFILE 082FSW301, 082FSW266), east-side-down post-Nelson normal faults (MINFILE 082FSW70, 082FSW277), and the Hall-Elise contact (MINFILE 082FSW200-205).

A number of vein occurrences are hosted by the basal part of the Hall Formation, close to the Hall-Elise contact. They are characterised by generally north-trending shear-controlled quartz veins from about 0.5 to 1.5 metres wide with variable amounts of galena, pyrite, chalcopyrite and minor sphalerite, tetrahedrite and pyrrhotite. Arsenopyrite has been identified at the Gold Hill prospect (MINFILE 082FSW204).

The Clubine property (MINFILE 082FSW200) has recorded production from 1937 to 1939 of 2322 tonnes containing 28.8 grams per tonne gold and 42.6 grams per tonne silver. Trenching and drilling in new zones near the old Clubine-Comstock workings has been undertaken by Yellow Jack Resources Ltd. with return of high silver and lead assays (K. Murray, personal communication, 1990). On the Maggie zone, quartz veins 3 to 15 centimetres wide occur within shear zones 5 to 10 metres wide in the lower Hall Formation. Argillite and siltstone beds are contorted, displaying kink banding and crenulation cleavage. A distinctive yellow-green alteration envelope, 5 to 10 centimetres wide, that surrounds some of the veins, may be chrome mica and iron-rich carbonate.

The Arlington mine (MINFILE 082FSW205) produced over 765 kilograms of gold from approximately 64 000 tonnes of ore between 1899 and 1970. In 1988, a small tonnage was mined by Rimrock Gold Corporation and South Kootenay Goldfields Inc. (George Cross Newsletter, No. 6, 10 Jan. 1989) The Canadian King prospect occurs just north of the Arlington mine and is considered to be part of the Arlington vein system (MINFILE). This system is characterised by brecciated, milky white quartz with irregular patches of pyrite, galena, sphalerite and carbonaceous siltstone. The Keystone deposit may be the up-dip extension of the Arlington ore zone. Intermittent production of 1664 tonnes from 1901 to 1981 returned an average grade of about 50 grams per tonne gold and 100 grams per tonne silver (MINFILE). The results of detailed mapping and study of the Arlington and Clubine properties will be released in future editions of *Exploration in British Columbia*.

Drilling in 1990 on the Silver Dollar property northwest of Salmo was undertaken to explore for extensions of the Lucky Boy and Silver Dollar veins; these produced 52 kilograms of gold and 787 kilograms of silver between 1899 and 1970. Ore minerals include sphalerite, galena and minor chalcopyrite in a gangue of calcite, ankerite(?) and brecciated argillite (Walker, 1934).

ACKNOWLEDGMENTS

A number of people have contributed to the fieldwork in the Erie Lake map area. In particular, we would like to thank Darryl Lindsay for his careful mapping and help, Heather Blyth and Helena Karam for their cheerful and able field assistance and Mike Holmes and Cathy Lund for their reliable assistance in the 1988 season. We appreciate the property tours and information imparted by Ken Murray and Alex Fraser on the Clubine property and discussions with

Eric Denny. We thank Janet Gabites and Don Murphy for uranium-lead dating of the Silver King porphyry. We would also like to thank Aaron Pettipas for computer drafting of many of the diagrams. The manuscript was edited by J.M. Newell and B. Grant.

REFERENCES

- Andrew, K.P.E. and Höy, T. (1989): The Shaft Showing, Elise Formation, Rossland Group; *B.C. Ministry of Energy, Mines and Petroleum Resources*, Exploration in British Columbia 1988, pages B21-B28.
- Andrew, K.P.E. and Höy, T. (1990): Geology and Exploration of the Rossland Group in the Swift Creek Area; *B.C. Ministry of Energy, Mines and Petroleum Resources*, Exploration in British Columbia 1989, pages 73-80.
- Andrew, K.P.E., Höy, T. and Drobe, J. (1990a): Stratigraphy and Tectonic Setting of the Archibald and Elise Formations, Rossland Group, Beaver Creek Area, Southeastern British Columbia; *B.C. Ministry of Energy, Mines and Petroleum Resources*, Geological Fieldwork 1989, Paper 1990-1, pages 19-27.
- Andrew, K.P.E., Höy, T. and Drobe, J. (1990b): Geology of the Rossland Group in the Beaver Creek Area, Rossland-Trail (E1/2) Map Sheet, Southeastern British Columbia; *B.C. Ministry of Energy, Mines and Petroleum Resources*, Open File 1990-9.
- Beddoe-Stephens, B. (1982): The Petrology of the Rossland Volcanic Rocks, Southern British Columbia; *Geological Society of America*, Bulletin, Volume 93 pages 585-594.
- Beddoe-Stephens, B. and Lambert, R. St. J. (1981): Geochemical, Mineralogical, and Isotopic Data Relating to the Origin and Tectonic Setting of the Rossland Volcanic Rocks, Southern British Columbia; *Canadian Journal of Earth Sciences*, Volume 18, pages 858-868.
- Corbett, C.R. and Simony, P.S. (1984): The Champion Lake Fault in the Trail-Castlegar Area of Southeastern British Columbia; in Current Research, Part A, *Geological Survey of Canada*, Paper 84-1A, pages 103-104.
- Drysdale C.W. (1917): Ymir Mining Camp, British Columbia; *Geological Survey of Canada*, Memoir 94, 175 pages.
- Fitzpatrick, M. (1985): The Geology of the Rossland Group in the Beaver Valley Area, Southeastern British Columbia; unpublished M.Sc. thesis, *University of Calgary*, 150 pages.
- Frebold, H. (1959): Marine Jurassic Rocks in Nelson and Salmo Areas, Southern British Columbia; *Geological Survey of Canada*, Bulletin 49.
- Frebold, H. and Tipper, H.W. (1970): Status of the Jurassic in the Canadian Cordillera of British Columbia, Alberta, and Southern Yukon; *Canadian Journal of Earth Sciences*, Volume 7, pages 1-21.
- Höy, T. and Andrew, K.P.E. (1988): Preliminary Geology and Geochemistry of the Elise Formation, Rossland Group, between Nelson and Ymir, Southeastern British Columbia; *B.C. Ministry of Energy, Mines and Petroleum Resources*, Geological Fieldwork 1987, Paper 1988-1, pages 19-30.
- Höy, T. and Andrew, K.P.E. (1989a): The Rossland Group, Nelson Map Area, Southeastern British Columbia; *B.C. Ministry of Energy, Mines and Petroleum Resources*, Geological Fieldwork 1988, Paper 1989-1, pages 33-43.
- Höy, T. and Andrew, K.P.E. (1989b): Geology of the Rossland Group, Nelson Map Area, Southeastern British Columbia; *B.C. Ministry of Energy, Mines and Petroleum Resources*, Open File 1989-11.
- Höy, T. and Andrew, K.P.E. (1989c): The Great Western Group, Elise Formation, Rossland Group; *B.C. Ministry of Energy, Mines and Petroleum Resources*, Exploration in British Columbia 1988, pages B15-B19.
- Höy, T. and Andrew, K.P.E. (1990a): Structure and Tectonic Setting of the Rossland Group, Mount Kelly - Hellroaring Creek Area, Southeastern British Columbia; *B.C. Ministry of Energy, Mines and Petroleum Resources*, Geological Fieldwork 1989, Paper 1990-1, pages 11-17.
- Höy, T. and Andrew, K.P.E. (1990b): Geology of the Mount Kelly - Hellroaring Creek Area, Salmo Map Sheet (82F/3), Southeastern British Columbia; *B.C. Ministry of Energy, Mines and Petroleum Resources*, Open File 1990-8.
- Höy, T. and Andrew, K.P.E. (1991a): Geology of the Rossland Area, Southeastern British Columbia; *British Columbia Ministry of Energy, Mines and Petroleum Resources*, Geological Fieldwork 1990 Paper 1991-1, this volume.
- Höy, T. and Andrew, K.P.E. (1991b): Geology of the Rossland-Trail Area, Southeastern British Columbia (NTS 82F/4); *British Columbia Ministry of Energy, Mines and Petroleum Resources*, Open File 1991-2.
- Little, H.W. (1950): Salmo Map-area, British Columbia, *Geological Survey of Canada*, Paper 50-19, 43 pages.
- Little, H.W. (1960): Nelson Map-area, West-Half, British Columbia; *Geological Survey of Canada*, Memoir 308, 205 pages.
- Little, H.W. (1962): Trail Map-area; *Geological Survey of Canada*, Paper 62-5.
- Little, H.W. (1965): Geology, Salmo, British Columbia; *Geological Survey of Canada*, Map 1145A.
- Little, H.W. (1982a): Geology, Bonnington Map-area, British Columbia; *Geological Survey of Canada*, Map 1571A.
- Little, H.W. (1982b): Geology, Rossland-Trail Map-area, British Columbia; *Geological Survey of Canada*, Paper 79-26, 38 pages.
- Little, H.W. (1985): Geological Notes, Nelson West Half (82F, W1/2) Map Area; *Geological Survey of Canada*, Open File 1199.

- Mulligan, R. (1951): The Geology of the Nelson and adjoining part of Salmo Map Areas, British Columbia; unpublished Ph.D. thesis, *McGill University*, 202 pages.
- Mulligan, R. (1952): Bonnington Map-area, British Columbia; *Geological Survey of Canada*, Paper 52-13, 37 pages.
- Parrish, R. (1984): Slocan Lake Fault: A Low Angle Fault Zone Bounding the Valhalla Gneiss Complex, Nelson Map-area, Southern British Columbia; in Current Research, Part A, *Geological Survey of Canada*, Paper 84-1A, pages 323-330.
- Parrish, R.R., Carr, S.D. and Parkinson, D.L. (1988): Eocene Extensional Tectonics and Geochronology of the Southern Omineca Belt, British Columbia and Washington; *Tectonics*, Volume 7, pages 181-212.
- Simony, P.S. (1979): Pre-Carboniferous Basement near Trail, British Columbia; *Canadian Journal of Earth Sciences*, Volume 16, Number 1, pages 1-11.
- Tipper, H.W. (1984): The Age of the Jurassic Rosslund Group of Southeastern British Columbia; in Current Research, Part A, *Geological Survey of Canada*, Paper 84-1A, pages 631-632.
- Walker, J.F. (1934): Geology and Mineral Deposits of the Salmo Map-area, British Columbia; *Geological Survey of Canada*, Memoir 172, 102 pages.



**GEOLOGY OF THE ROSSLAND AREA, SOUTHEASTERN
BRITISH COLUMBIA
(82F/4E)**

By Trygve Höy and Kathryn P.E. Andrew

KEYWORDS: Regional geology, Rossland Group, Elise Formation, Archibald Formation, Mount Roberts Formation, Sophie Mountain Formation, Trail pluton, Rossland monzonite, Sheppard intrusions, Rossland tectonic high, growth faults, thrust faults, gold-copper veins.

INTRODUCTION

The Rossland map area extends north from the United States border to include the towns of Rossland and Trail in southeastern British Columbia (Figure 1-2-1). The area has been mapped at 1:50 000 scale by Little (1960, 1963, 1982), at 1:20 000 scale by Höy and Andrew (1991) and in more detail in the vicinity of the Rossland gold camp by Fyles (1984) and Drysdale (1915). The purpose of this paper is to describe and interpret the structural geology and tectonic evolution of the the Rossland area, to subdivide the Elise Formation of the Rossland Group in this area and to investigate tectonic and lithologic controls of gold mineralization in the camp. The geology of individual deposits and occurrences is described in considerable detail by Drysdale (*op. cit.*) and Fyles (*op. cit.*); those with more recent exploration activity will be described in forthcoming papers including *Exploration in British Columbia 1990*.

REGIONAL GEOLOGY

The southern part of the Rossland area is underlain primarily by volcanic rocks of the Lower Jurassic Elise Formation. These rest unconformably on metasedimentary rocks of the late Paleozoic Mount Roberts Formation and are in apparent fault contact with rocks of probable similar age but unknown correlation, referred to as Unit Cs (Fyles and Hewlett, 1959; Little, 1982). Locally, the Elise Formation is unconformably overlain by coarse conglomerates of the Late Cretaceous Sophie Mountain Formation.

Four prominent igneous suites intrude these rocks. The Rossland monzonite is an east-trending intrusive complex centred near the Rossland gold camp. It is cut by the Middle Jurassic Trail pluton and by alkaline Coryell intrusions of Middle Eocene age. The Eocene Sheppard intrusions occur as stocks in the southeastern part of the area and in north-trending felsic dikes; they are also cut(?) by the Coryell intrusions.

UNIT Cs

Rocks assigned to Unit Cs are exposed only in the southeastern part of the Rossland area. The western of the two exposures was mapped in detail (Figure 1-2-2). It includes tan to black-coloured argillite, silty argillite and minor siltstone, a massive light grey limestone, some massive dol-

omite and dolomitic siltstone. These rocks are locally silicified, sheared, brecciated and veined. Tight, minor folds occur locally, and crenulated phyllites indicate at least two periods of deformation.

The intense shearing and brecciation, particularly along the margins of Unit Cs, and the truncation of units in the Elise Formation, suggests a faulted contact between Unit Cs and the Elise. It is possible that this fault contact is the western extension of the Waneta fault, a thrust fault that is interpreted to mark the boundary of Quesnellia with North American rocks.

Unit Cs is of probable late Paleozoic age, possibly correlative with the Milford Group (Little, 1982). East of the Rossland area, it is in apparent conformable contact with the Laib and Nelway formations (Fyles and Hewlett, 1959). It is being extensively investigated as part of a Ph.D. thesis by Jon Einarsen at the University of Calgary.

MOUNT ROBERTS FORMATION

The Mount Roberts Formation comprises a succession of dominantly fine-grained siliceous rocks, argillite, carbonate and minor greenstone of Pennsylvanian and possibly Permian age (Little, 1982). It may correlate with the Milford Group farther north (Little, 1982; Klepacki, 1985). In the Rossland area, the formation is exposed near Patterson at the United States border, on the eastern slopes of Mount Roberts, Granite and OK mountains northwest of Rossland, and on the western slopes of Red Mountain within the Rossland mining camp (Figure 1-2-2). These localities are described in considerable detail by Little (1982) and the exposures on Mount Roberts, by Fyles (1984).

The Patterson exposures comprise dominantly fine-grained siliceous siltstone, dark grey to black argillite or pale grey-green silty chert. Numerous fine, irregular hairline fractures typically cut the more siliceous units; quartz veining is less common. These units are either massive or thinly laminated. Locally, graded and scoured sandstone lenses occur within the siltstone and provide rare stratigraphic-top indicators. Carbonate units, including grey brecciated limestone and rusty weathering, well-bedded fossiliferous dolomite, are conspicuous near the top of the Mount Roberts Formation.

Exposures on the eastern slopes of Mount Roberts and Granite Mountain are similar, comprising mainly black to grey siliceous argillite and siltstone. Rare silt scours, graded beds and a number of bedding-cleavage intersections indicate that the Mount Roberts Formation faces west. Thicker bedded, graded siltstone and sandstone beds, referred to as the sandstone member by Fyles (1984), are locally interbedded with thin, impure dolomite and limestone lenses. These

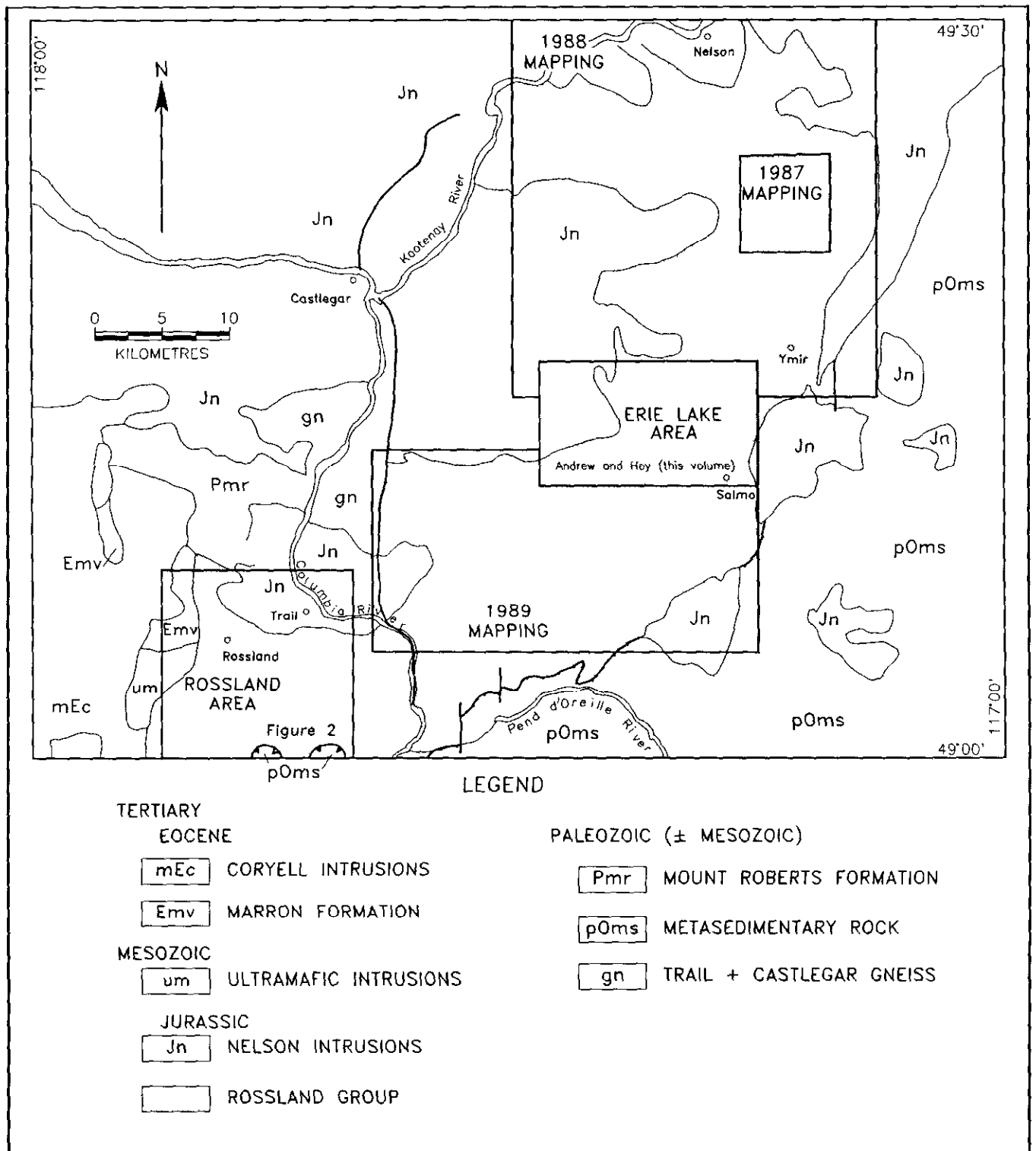


Figure 1-2-1. General location map showing distribution of the Rossland Group in southeastern British Columbia and the Rossland map area.

units also face west and occur directly beneath unconformably overlying volcanic breccias of the Elise Formation.

Siltstones on the western slopes of Red Mountain, which host the Red Mountain molybdenum deposits, are tentatively assigned to the Mount Roberts Formation. They were included in the Rossland Group by Fyles (1984), who noted their structural association with rocks of the Rossland Group and their similarity with Elise Formation siltstones. They include hornfelsed and skarned siltstones and argillites, calcisilicate gneisses suggestive of calcareous protoliths, and some white quartzite layers. Altered diorites within the Red Mountain succession may be sills or dikes; greenstones are recognized in the Mount Roberts Formation farther north (Little, 1982).

The assignment of the Red Mountain succession to the Mount Roberts Formation is based primarily on lithologic similarity. Calcareous rocks and quartzites are relatively common in the Mount Roberts, but are very rare in the Rossland Group. It is suggested that these rocks and a small section of overlying siltstone assigned to the Elise Formation by Fyles (1984), but possibly correlative with the Archibald Formation, are a structural panel thrust onto the Rossland sill. This interpretation infers that a small isolated exposure of Mount Roberts farther north is a klippe that overlies pyroclastic breccia of the Elise Formation (Figure 1-2-2).

ROSSLAND GROUP

The Rossland Group comprises a succession of dominantly coarse to fine clastic rocks of the Archibald Formation, volcanic rocks of the Elise Formation and overlying, dominantly fine-grained clastic rocks of the Hall Formation. These rocks are Early Jurassic in age, bracketed by Sinemurian fossils in the Archibald (Frebold and Tipper, 1970; Tipper, 1984) and Pleinsbachian and Toarcian macrofossils in the Hall (Frebold and Little, 1962; Tipper, 1984). Only the Elise Formation is well exposed in the Rossland area. The Hall Formation is missing, due to nondeposition or to erosion prior to deposition of the unconformably overlying Sophie Mountain Formation. A thin veneer of conglomerate that unconformably overlies the Mount Roberts Formation at Patterson, and was formerly included in the Elise (Little, 1982), is now assigned to the Archibald Formation.

ARCHIBALD FORMATION

The basal sedimentary succession of the Rossland Group, the Archibald Formation, is described in detail by Andrew *et al.* (1990). It comprises coarse conglomerates near Fruitvale, proximal turbidites farther east in Archibald Creek just west of Salmo, and more distal turbidites and argillite to the north, on the east slopes of Erie Creek in the Nelson map area. The only exposures assigned to the Archibald Formation in the Rossland area are a thin succession of conglomerates between the Mount Roberts Formation and overlying lapilli tuffs of the Elise Formation (Figure 1-2-2). These conglomerates were previously included in the basal part of the Elise (Little, 1982); however, their stratigraphic position at the base of the Rossland Group, their sedimentary nature and their inferred paleotectonic setting allow correlation with the Archibald Formation.

The Archibald Formation at Patterson comprises a veneer of conglomerates, up to several hundred metres thick, that lies unconformably on the Mount Roberts Formation. The Mount Roberts paleosurface is irregular, resulting in isolated patches of Archibald in depressions in the surface and small outcrops of Mount Roberts on paleohighs (Figure 1-2-3). Most commonly, a limestone unit in Mount Roberts lies near the paleosurface.

The Archibald Formation is typically a heterolithic pebble conglomerate with subrounded to subangular clasts of grey-green siliceous siltstone, argillaceous siltstone, limestone, and minor chert, quartzite and plagioclase porphyry in an argillaceous or granular sandy matrix. Locally, a coarse limestone breccia derived from the underlying Mount Roberts Formation is at the base of the Archibald (Plate 1-2-1). The argillaceous matrix is commonly tinged purple, suggestive of subaerial exposure. Bedding, clast-sorting or winnowing, grading or other features indicative of fluvial environments are lacking. These sedimentary conglomerates are distinct from tuffaceous conglomerates in the Elise as they contain virtually no volcanic clasts nor a tuffaceous matrix.

ELISE FORMATION

The Elise Formation is exposed in an arcuate belt that extends south from Nelson towards Salmo and west to Rossland. It hosts most of the gold deposits of the Rossland Group, including those in the Rossland camp. It comprises a succession of augite-phyric flows, tuffs, some epiclastic deposits and minor siltstone and argillite. In the Nelson area, the formation is readily subdivided into a basal unit of dominantly mafic flows and flow breccias overlain by intermediate pyroclastic rocks (Höy and Andrew, 1989a, b). In the Salmo map area and on the west limb of the Hall Creek syncline in the Nelson area, this distinction is less apparent and mafic flows or tuffs occur throughout the succession (Höy and Andrew, 1990; Andrew and Höy, 1991).

The Elise Formation in the Rossland map area comprises essentially a homoclinal succession that dips north to north-westerly and extends from Patterson in the south to Rossland in the north. Although this succession is offset by numerous north-trending faults, it does not appear to be repeated by thrust faulting. It is not a complete succession as it is developed on the Patterson paleohigh. To the east, in the Goodeve and Sheppard Creek areas, the Elise thickens, due in part to thickening of some units and introduction of others into the succession, but mainly to inclusion of a more complete lower section.

A composite section of the Elise Formation in the Rossland area is illustrated in Figure 1-2-4. Tuffaceous conglomerate (Unit Jellid) is in gradational contact with conglomerates of the underlying Archibald Formation. The Archibald-Elise contact is placed where either volcanic clasts are first noticed or the matrix becomes tuffaceous. The tuffaceous conglomerates are dominated by clasts of underlying Mount Roberts Formation, including prominent limestone clasts, in a green tuffaceous matrix. Rare augite porphyry and andesite clasts are also noted. The distribution of the basal tuffaceous conglomerate approximately follows

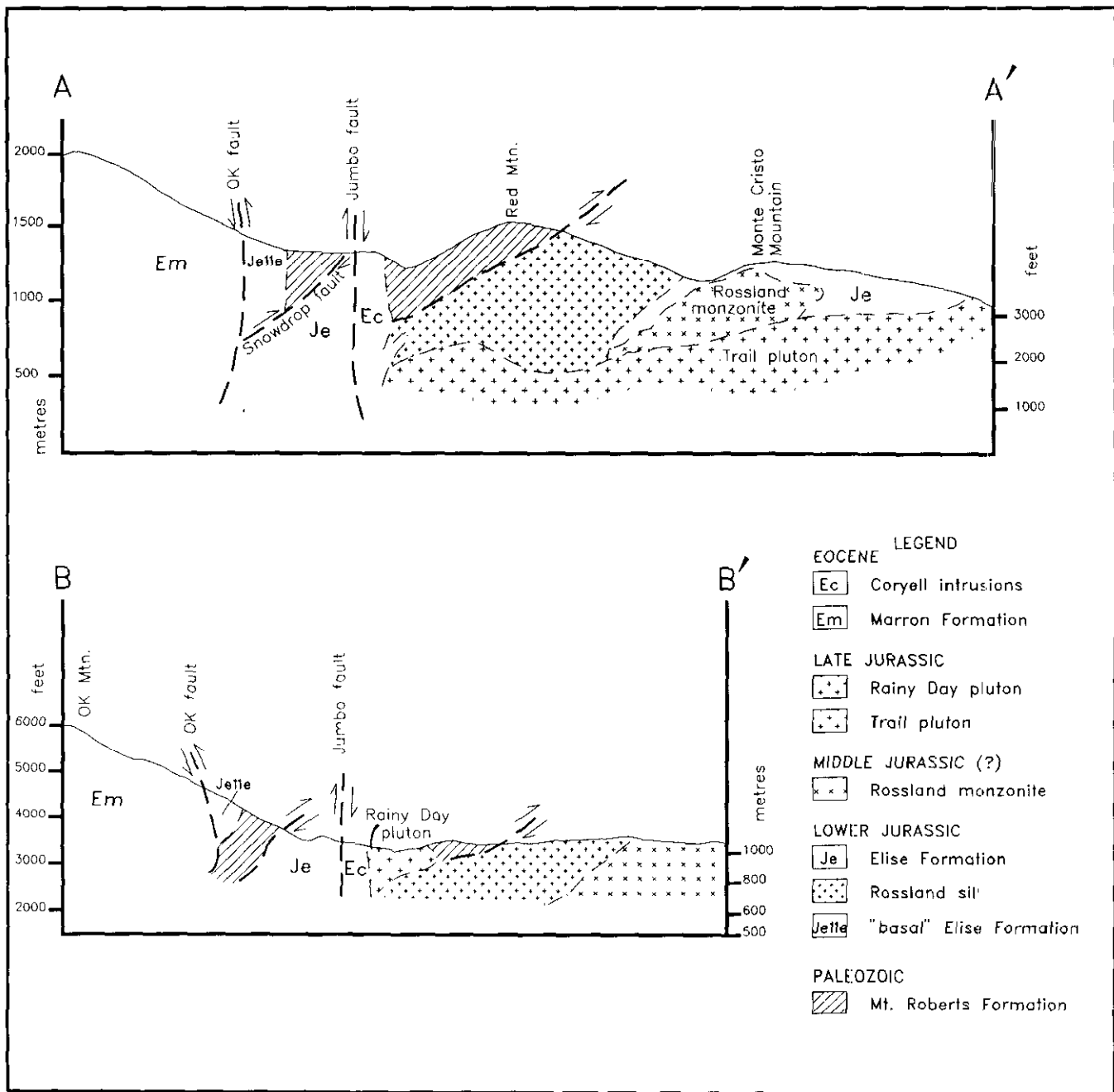


Figure 1-2-2b. Vertical structural sections, Rosland map area; (modified from Fyles, 1984).

that of the underlying Archibald and Mount Roberts formations whereas overlying Elise units thin dramatically as they approach the Patterson paleohigh.

Plagioclase-porphry lapilli tuff (Unit Je81) locally overlies the tuffaceous conglomerate. It thickens rapidly just east of Malde Creek. Farther east in the Sheppard Creek area, it is underlain by mafic lapilli tuff and the base of the Elise is not exposed. A sequence of argillaceous siltstone (Unit Je10a) and mafic flows and flow breccias (Unit Je4) overlies the tuffaceous conglomerate. The mafic flows comprise massive augite porphyry, flow breccias and possible minor lapilli tuff; it is the only significant mafic flow suc-

cession in the Rosland area. It appears to pinch out to the west, but can be traced or extrapolated eastward to the Tiger Creek fault. A similar succession of mafic flows east of Tiger Creek may be a faulted repetition of this unit (Figure 1-2-2). The interbedded siltstones are typically thin bedded, rusty weathering distal turbidites. Numerous sedimentary structures, including rip-ups, graded beds and load casts provide reliable top indicators. This sedimentary succession also thins westward, and increases in thickness to the east. Just west of the Tiger Creek fault a sequence of mafic lapilli tuffs is interbedded with the upper part of the siltstone succession (Figure 1-2-2).

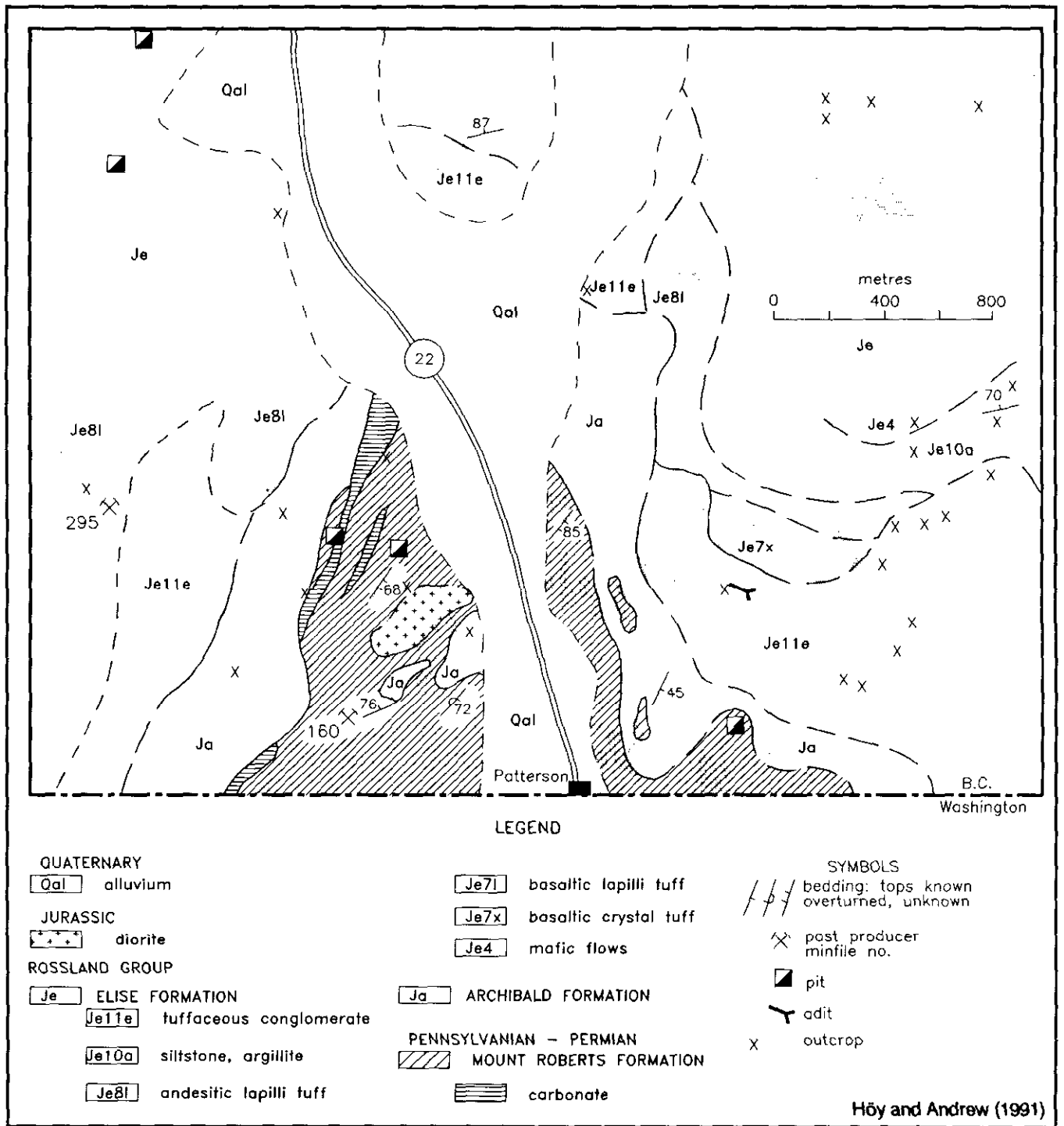


Figure 1-2-3. Geology of the Patterson area showing distribution of the Mount Roberts Formation and unconformably overlying Archibald (?) and Elise formations.

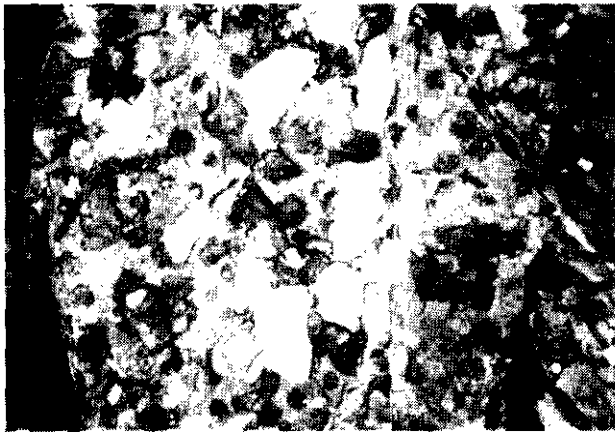


Plate 1-2-1. Limestone breccia of Archibald Formation, Patterson area.

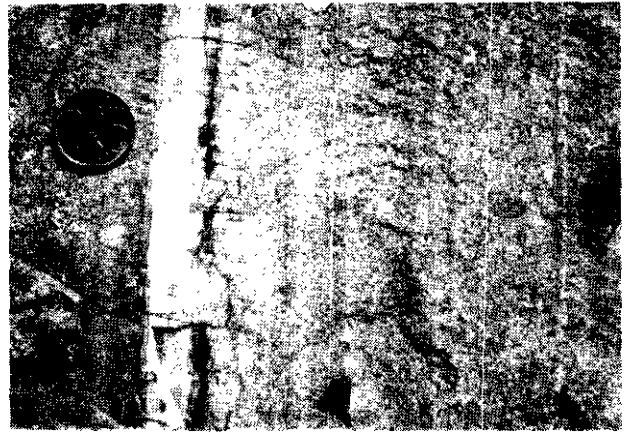


Plate 1-2-2a. Well-bedded, mafic waterlain tuffs of Unit Je7x south of Tamarac Mountain.

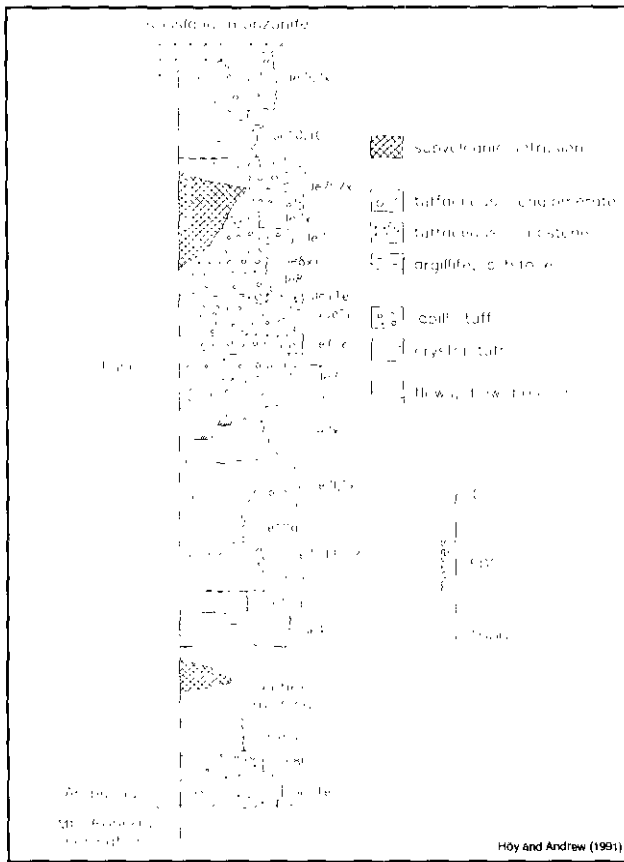


Figure 1-2-4. Composite stratigraphic section of the Rossland Group, Rossland map area.

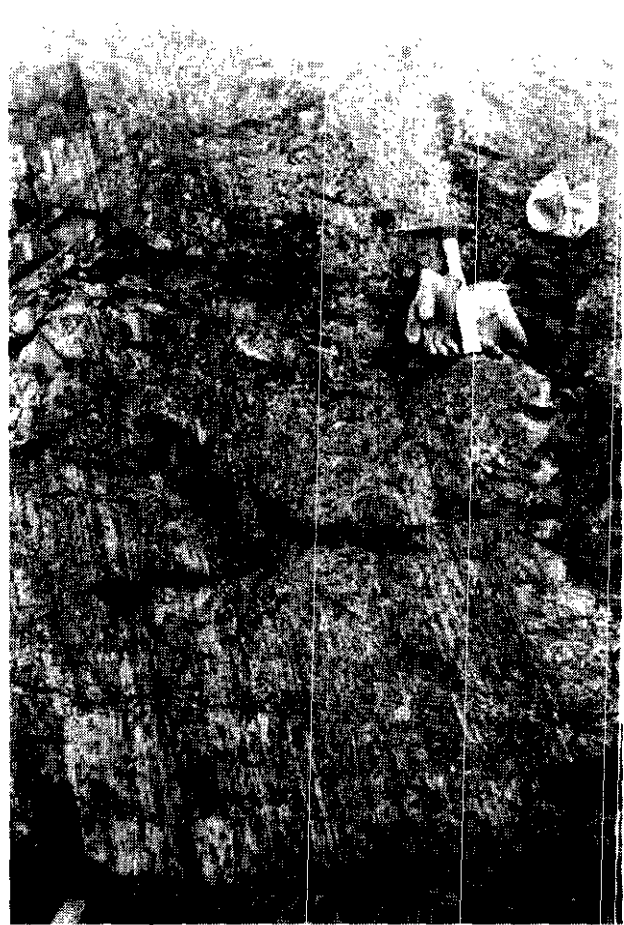


Plate 1-2-2b. Beds of mafic waterlain tuff (Unit Je7x) south of Violin Lake

A distinctive waterlain crystal tuff (Unit Je7x) extends from the western slopes of Tamarac Mountain to the north slopes of Baldy Mountain and in the Lake Mountain and Goodeve Creek areas. It coarsens upward and is supplanted to the east by mafic lapilli tuff (Unit Je7I). Unit Je7x is an interbedded succession of brown-weathering, massive to well-bedded mafic waterlain tuffs, minor tuffaceous sandstone and, at the base, minor argillite and silty argillite

(Plates 1-2-2a and 2b). The crystal tuffs commonly contain small, widely scattered augite porphyry lapilli and numerous plagioclase and augite crystals. Layers of lapilli tuff become more prominent near the top of the succession.

Unit Je7I (Figure 1-2-2) comprises dominantly mafic lapilli tuff, but includes pyroclastic breccia and waterlain

crystal tuffs. Clasts in the tuffs are dominantly augite porphyry; however, a variety of other clasts are noted, including limestone, plagioclase porphyry and green 'siltite' (Unit Je11d, Figure 1-2-3). A prominent, more felsic lapilli tuff, (Unit Je8) is recognized within Unit Je71 both east and west of the Tiger Creek fault. It contains fragments of both plagioclase porphyry and augite porphyry. Some plagioclase-rich crystal tuffs are also included in Unit Je8.

Interbedded argillaceous siltstone and tuffaceous sandstone (Units Je10) occur near the top of the exposed Elise succession, just south of the Rossland monzonite. These host a number of vein deposits (Höy and Andrew, 1991).

The Rossland sill, exposed south of the Rossland monzonite and on the east slopes of Red Mountain, intrudes the upper part of the Elise Formation. It has been described in detail by Fyles (1984). It is an augite porphyry intrusion that hosts a number of the principal orebodies of the Rossland camp. It is overlain (structurally?) to the west by the Mount Roberts Formation and is cut by the Rossland monzonite. A similar, but smaller augite porphyry intrusion is exposed just south of Mount Malde (Figure 1-2-2; Höy and Andrew, 1991).

In summary, the Elise Formation in the Rossland area comprises dominantly mafic to intermediate lapilli tuffs interlayered with prominent sections of tuffaceous siltstone and argillaceous siltstone. Mafic flows are subordinate and tuffaceous conglomerates are essentially restricted to the basal part of the succession. The Elise Formation was deposited on a structural high that is exposed in the Patterson area and on the eastern slopes of Mount Roberts. Virtually the entire basal succession of the Rossland Group, the Archibald Formation, and a considerable part of the lower Elise is missing. Despite this, the Elise in the Rossland area represents one of the thickest successions recognized, in excess of 5000 metres.

The Hall Formation, the upper sedimentary sequence of the Rossland Group, is also missing in the Rossland area. Rather, conglomerates of the Late Cretaceous Sophie Mountain or Eocene Marron volcanics unconformably overly Elise rocks, suggesting the Rossland area remained a tectonic high through considerable geologic time.

SOPHIE MOUNTAIN FORMATION

The Sophie Mountain Formation (Bruce, 1917; Little, 1960) is exposed on Mount Sophie and on the ridge a few kilometres southeast of Baldy Mountain. A small exposure is also recognized on the ridge north of Lake Mountain (Höy and Andrew, 1991) and in Hudu Creek 2 kilometres from its confluence with Beaver Creek (Andrew *et al.*, 1990). The formation comprises poorly sorted, heterolithic conglomerate with thin interbeds of argillite and argillaceous siltstone. The conglomerate consists dominantly of rounded clasts of quartzite and other sedimentary rocks. Clasts derived from the underlying Elise Formation are rare or absent.

MARRON FORMATION

The Middle Eocene Marron Formation (Bostock, 1940; Church, 1973; Little, 1982) is exposed on the eastern slopes

of OK Mountain and Mount Roberts just west of Rossland and just east of Goodeve Creek. The formation comprises dark grey, green and, locally, mauve andesitic flows and minor lapilli tuff, tuffaceous sandstone and tuffaceous conglomerate. It is in fault contact with the Elise Formation near Rossland (Fyles, 1984) but unconformably overlies the Elise in the southwest part of the map area; it is intruded by Middle Eocene Coryell intrusions.

INTRUSIVE ROCKS

Numerous intrusive rocks, ranging from batholithic bodies to stocks and dikes, occur throughout the Rossland area. They are described in considerable detail by Fyles (1984) and Little (1982) and hence will only be briefly described here.

The Rossland monzonite is an east-trending stock with a wide thermal aureole and, locally, a gradational contact with country rocks (Fyles, 1984). It is grey to green, fine to medium grained and comprises dominantly andesine (46%), hornblende (15%), orthoclase micropertthite (~13%), augite (~12%), biotite (11%) and quartz (2%) (Fyles, *op. cit.*). Its age is not known; however, it is cut by the Late Jurassic Trail pluton and hence may be part of a 178 to 180 Ma suite of calcalkaline intrusions in southeastern British Columbia, including the Silver King porphyries in the Nelson area, the Mount Cooper stock (Klepacki, 1985) and the Aylwin Creek stock (W.J. McMillan, personal communication, 1989).

The Trail pluton (Simony, 1979; Little, 1982) is part of the Late Jurassic Nelson plutonic suite. It is dominantly a medium to coarse-grained granodiorite, but locally includes quartz diorite and diorite phases.

The Sheppard intrusions include a number of large stocks and numerous smaller dikes that cut Nelson intrusive rocks and the Late Cretaceous Sophie Mountain Formation. These rocks are commonly fine to medium grained and leucocratic, ranging in composition from granite to syenite. North-trending Sheppard dike swarms are prominent northwest of Waneta on the west side of the Columbia River, in the Baldy Mountain area. They may record Middle Eocene east-west extension.

The Coryell intrusions are generally coarse grained and range in composition from syenite to monzonite and granite. Field relationships and numerous K-Ar dates (Little, 1982) indicate that these rocks are of similar age to the Middle Eocene Marron volcanics. Numerous small intrusions are present throughout the Rossland area; only the largest are shown on Figure 1-2-2.

STRUCTURE

The structure of the Rossland area has been well described by Fyles (1984) and Little (1982). Fyles divided the area into two domains separated by the "Rossland break", an east-trending zone marked by a number of faults and intrusions, including the Rossland monzonite, Rainy Day pluton and serpentinites. Fyles suggested that the Rossland break is a zone of "structural weakness that may have originated when the Rossland Group was laid down. . ." (Fyles, 1984, page 29). South of the break, structures trend northeasterly, whereas to the north, they trend northerly.

Detailed mapping, concentrated largely south of Rossland, has essentially confirmed the structures as outlined by Fyles. However, correlation of both units and structural patterns to those farther east has allowed a better understanding of the stratigraphic position of the Rossland mining camp and of the tectonic evolution of the area. Three phases of deformation are recognized:

1. extensional tectonics during deposition of lower Rossland Group rocks in Early Jurassic time;
2. east-directed thrust faults and associated minor folding before intrusion of Middle to Late Jurassic plutons;
3. normal faulting in Eocene time.

The Rossland area is underlain by a tectonic high, bounded by growth faults, that is first evident in early Rossland time. The basal sedimentary succession of the Rossland Group, the Archibald Formation, records deposition in a fault-bounded structural basin located just east of the Rossland map area, in the Beaver Creek valley (Andrew *et al.*, 1990). The source area, based on facies analyses, was inferred to lie immediately to the west. In the Rossland area, the Archibald Formation is missing or represented by a thin basal conglomerate and the entire lower part of the Elise Formation is generally missing (Figures 1-2-2, 4) confirming the suggestion of a tectonic high here. Neither the orientation nor the exact position of the bounding growth faults are known; however, the rapid facies changes in Elise rocks just east of Patterson suggest that the late north-trending faults located there may be the loci of some of the syndepositional Rossland growth faults. The location of other north-trending faults, including the Eocene Champion Lake fault, may also be controlled or modified by either fault-controlled facies changes in Rossland Group rocks or Rossland-age growth faults. Finally, the east-trending Rossland break also appears to record a zone of structural weakness in Rossland time (Fyles, 1984) suggesting that the uplifted tectonic high in the Rossland area may have been controlled by an orthogonal pattern of block faults. Block-faulted regions, with fault-bounded basins and tectonic highs, generally record extensional tectonics. These areas tend to localize later structures and intrusions and hence are favourable sites for structurally controlled mineral deposits.

A period of compressive tectonics, evident throughout the Rossland Group in Middle Jurassic time, is probably related to collision of the eastern edge of Quesnellia with cratonic North America. It produced tight folds, a penetrative cleavage and intense shearing in eastern exposures, and more open, upright folds and thrust faults farther west. In the Rossland area, it is marked by the Waneta fault and a number of east-directed thrust faults and possible associated minor folds. The Waneta fault, initially recognized by Fyles and Hewlett (1959) in the Salmo area, separates rocks of North America (Unit Cs) from those of Quesnellia. The fault has been traced westward to the Rossland area (Little, 1982) where it is covered by Eocene volcanic rocks of the Marron Formation. It is suggested that exposures of Unit Cs farther west are also thrust on younger Elise volcanic rocks (Figure 1-2-2). Both units are sheared and brecciated in the vicinity of the contact.

Thrust faults west and north of Rossland include the Snowdrop fault (Little, 1962; Fyles, 1984) and an inferred fault that separates Mount Roberts Formation from Elise Formation on Red Mountain (Figure 1-2-2). Folds are concentrated in only a few areas; the Rossland area is essentially a west to northwest-dipping homoclinal succession of Rossland Group rocks (Fyles, 1984).

The Snowdrop fault is a west-dipping structure, marked by intense shearing and brecciation, that places a west-facing panel of Mount Roberts Formation and basal Elise on younger Elise Formation (Sections A-A', B-B', Figure 1-2-2). The thrust fault on Red Mountain is inferred from stratigraphic relationships (see section on Mount Roberts Formation). It is placed at the contact of Mount Roberts with underlying Elise Formation, Rossland sill and Rossland monzonite. The faulted nature of this contact has not been previously recognized despite being exposed at surface and penetrated by numerous drill holes. It is suggested that intense alteration, both thermal and metasomatic, has obliterated evidence of fault movement along the contact.

The age of this compressive deformation is post-Toarcian (*ca.* 187 Ma), the youngest age of Rossland Group rocks, and pre-intrusion of late Jurassic plutons (*ca.* 165 Ma). In the Rossland area, the age of east-directed thrusts is bracketed by the age of the Rossland monzonite (Höy and Andrew, in preparation) and the Late Jurassic Rainy Day pluton.

Steeply dipping, generally north-trending normal(?) faults occur throughout the Rossland area. A number of these, including the OK and Jumbo faults (Fyles, 1984) and the Violin Lake fault (Little, 1982) have been recognized previously. The OK fault is a listric normal fault that is overturned to the east at higher structural levels (Sections A-A', B-B', Figure 1-2-2). Marron Formation rocks in the western block have been down-dropped in excess of 600 metres (Fyles, *op. cit.*). The Jumbo fault dips steeply east and has an inferred normal displacement of 600 to 700 metres. This movement is based on correlation of the Mount Roberts Formation on the eastern slopes of Mount Roberts with similar rocks on Red Mountain, and on the Snowdrop fault with the inferred thrust on Red Mountain.

The Violin Lake fault is a vertical structure with an unknown amount of displacement on it (Little, 1982). It appears to truncate the Waneta fault and possibly the Eocene Marron Formation in the south, but produces little, if any, offset of the Rossland monzonite; hence, it may die out to the north. The Tiger Creek fault is inferred from truncation and displacements of units in the Elise Formation (Figure 1-2-2). However, it also dies out northward as it displaces the Rossland monzonite only minimally. A number of north-trending faults with minor right-lateral displacement in the Malde Creek area, southwest of the Tiger Creek fault, may follow the loci of Rossland-age growth faults. They are associated with pronounced facies changes in the Rossland Group, and appear to die out up-section.

These late faults are younger than the Eocene intrusive and extrusive events. The Jumbo fault brecciates Middle Eocene Coryell intrusive rocks; the OK and Violin Lake faults truncate Middle Eocene lavas of the Marron Formation, and a western splay of the Tiger Creek fault truncates

Sheppard intrusions in the Mount Sophie Formation (Figure 1-2-2). These faults are undoubtedly related to an Eocene extensional event in southern British Columbia (Parrish *et al.*, 1988; Corbett and Simony, 1984).

In summary, structures in the Rosslund area record similar tectonic events as elsewhere in the Rosslund Group: extensional tectonics and growth faults during deposition of the lower part of the Rosslund Group in Early Jurassic time; compressional tectonics that initially occurred in eastern exposures, as Quesnellia impinged on rocks of North America, and continued with east-directed thrusts and folds in more western exposures in Middle Jurassic time; and Middle Eocene extensional tectonics.

ECONOMIC GEOLOGY

The Rosslund mining camp is the second largest gold-producing camp in British Columbia, with recovery of more than 84 000 kilograms of gold and 105 000 kilograms of silver between 1894 and 1941. These deposits are in three main groups referred to as the north belt, the main veins and the south belt. Mineralization in the Rosslund camp also includes molybdenum deposits on the western slopes of Red Mountain. These deposits have been described by a number of authors, including Drysdale (1915), Gilbert (1948), Little (1963), Stevenson (1935) and Fyles (1984); the paper by Fyles summarizes much of the previous work and describes the molybdenum mineralization in considerable detail. The following report only summarizes the geology of these deposits; it is taken largely from Fyles; more complete geology descriptions and interpretations will appear in forthcoming papers.

MOLYBDENUM DEPOSITS

Molybdenum deposits on Red Mountain (Plate 1-2-3) produced 1 748 871 kilograms of molybdenum from approximately 1 million tonnes of ore between 1966 and 1972 (MINFILE). Molybdenite occurs dominantly in quartz veins and veinlets cutting a coarse breccia complex in a west-dipping and facing, hornfelsed and skarned siltstone succession (Fyles, 1984). We correlate this succession with the Mount Roberts Formation and suggest that it has been



Plate 1-2-3. View of open-pit molybdenum mine on Red Mountain, town of Rosslund and Lake Mountain in distance.

thrust over the underlying Rosslund sill prior to intrusion of Middle to Late Jurassic plutons.

Molybdenum occurrences are spatially associated with the Jurassic Trail and Rainy Day plutons. In the Nelson map area, both skarn and porphyry molybdenum mineralization occur along the margins of Nelson plutonic rocks (Höy and Andrew, 1989a). Local crosscutting pyrrhotite-chalcopyrite veins on Red Mountain indicate that the mineralization is earlier than the copper-gold mineralization (Fyles, *op. cit.*).

GOLD-COPPER AND GOLD VEINS

The Rosslund gold-copper veins are dominantly pyrrhotite with chalcopyrite in a gangue of altered rock with minor lenses of quartz and calcite. In the north belt, a zone of discontinuous veins extends eastward from the northern ridge of Red Mountain to Monte Cristo Mountain. The veins trend east and dip north at 60° to 70°. The largest, on the Cliff and Consolidated St. Elmo claims, is in the Rosslund sill; it is 1 to 2 metres thick and is exposed for almost 100 metres strike length. Some veins in the north belt cross the molybdenum breccia zone on Red Mountain.

The main veins form a continuous well-defined fracture system that trends 070° from the southern slopes of Red Mountain northeastward to the eastern slopes of Columbia Kootenay Mountain. More than 98 per cent of the ore shipped from the Rosslund camp was produced from these veins and more than 80 per cent from deposits in a central core zone between two large north-trending lamprophyre dikes. These deposits include the Le Roi, Centre Star, Nickel Plate, Josie and War Eagle orebodies.

The main vein system consists of a series of veins, commonly en echelon, that dip steeply north. They are mostly within the Rosslund sill or the Rosslund monzonite, crosscut lithologies and early structures, but appear to be cut by the late north-trending faults and associated dikes.

The principal veins in the south belt trend 110° and dip steeply north or south. They are within siltstones, lapilli tuff and augite porphyry of the Rosslund Group several hundred metres south of the Rosslund monzonite. In addition to the typical copper-gold mineralization of the main veins and north belt, some veins in the south belt also contain sphalerite, galena, arsenopyrite and boulangerite.

High-grade gold veins also occur approximately 4 kilometres southwest of Rosslund in the Little Sheep Creek valley. They are in "greenstones" of the Rosslund Group adjacent to a small body of serpentinite. Gangue minerals include quartz and ankerite; sulphides are not common, but include pyrite, chalcopyrite and galena.

SUMMARY

Both skarn-porphyry molybdenum and copper-gold vein deposits have been extensively mined in the Rosslund area. They are in an area that has been tectonically active since Early Jurassic time and has been intruded repeatedly by plutonic rocks. Molybdenum mineralization, associated with intense brecciation and skarning, appears to be related to intrusion of Middle to Late Jurassic plutons, including the Trail and Rainy Day plutons. These intrusions postdate east-

directed thrust faults and related folds in the Rossland area. East-trending copper-gold veins cut these earlier structures, but are earlier than the north-south, Eocene extensional faults. The veins are parallel to and within the "Rossland break", a zone of fractures, faults and intrusions that marks a pronounced change in the structural grain. These structures, the anomalous thickness of the upper Elise Formation, prominent facies changes in Elise rocks and the higher concentration of intrusions suggest the influence of deep crustal structures, structures that may have controlled the distribution of metallic mineral deposits.

ACKNOWLEDGMENTS

We wish to acknowledge the cheerful and capable field assistance of Darryl Lindsay, Heather Blyth and Helena Karam during the 1990 field season. Discussions with a number of geologists, including Frank Fowler and Dan Werhle of Antelope Resources Inc.; Philip Simony, Jon Einarsen and Jim Vogel of the University of Calgary; Jim Fyles, consultant; and Bill McMillan of the British Columbia Geological Survey Branch were both informative and stimulating. Although these persons contributed substantially to many aspects of the paper, they do not necessarily agree with the interpretations. We wish to thank Aaron Pettipas for drafting the diagrams and John Newell for his editorial comments.

REFERENCES

- Andrew, K.P.E., Höy, T. and Drobe, J. (1990): Stratigraphy and Tectonic Setting of the Archibald and Elise Formations, Rossland Group, Beaver Creek Area, Southeastern British Columbia; *B.C. Ministry of Energy, Mines and Petroleum Resources*, Geological Fieldwork 1989, Paper 1990-1, pages 19-27.
- Andrew, K.P.E. and Höy, T. (1991): Geology of the Erie Lake Area with Emphasis on Stratigraphy and Structure of the Hall Formation, Southeastern British Columbia; *B.C. Ministry of Energy, Mines and Petroleum Resources*, Geological Fieldwork 1990, Paper 1991-1, this volume.
- Bostock, H.S. (1940): Keremeos, British Columbia; *Geological Survey of Canada*, Map 341A.
- Bruce, E.L. (1917): Geology and Ore Deposits of Rossland, British Columbia; *B.C. Ministry of Energy, Mines and Petroleum Resources*, Bulletin 4.
- Church, (1973): Geology of the White Lake Basin; *B.C. Ministry of Energy, Mines and Petroleum Resources*, Bulletin 61.
- Corbett, C.R. and Simony, P.S. (1984): The Champion Lake Fault in the Trail-Castlegar Area of Southeastern British Columbia; in *Current Research, Part A, Geological Survey of Canada*, Paper 84-1A, pages 103-104.
- Drysdale, (1915): Geology and Ore Deposits of Rossland, British Columbia; *Geological Survey of Canada*, Memoir 77.
- Frebold, H. and Little, H.W. (1962): Paleontology, Stratigraphy, and Structure of the Jurassic Rocks in Salmo Map-area, British Columbia; *Geological Survey of Canada*, Bulletin 81.
- Frebold, H. and Tipper, H.W. (1970): Status of the Jurassic in Canadian Cordillera of British Columbia, Alberta, and Southern Yukon; *Canadian Journal of Earth Sciences*, Volume 7, pages 1-21.
- Fyles, J.T. (1984): Geological Setting of the Rossland Mining Camp; *B.C. Ministry of Energy, Mines, and Petroleum Resources*, Bulletin 74, 61 pages.
- Fyles, J.T. and Hewlett, C.G. (1959): Stratigraphy and Structure of the Salmo Lead-Zinc Area; *B.C. Ministry of Energy, Mines and Petroleum Resources*, Bulletin 41, 162 pages.
- Gilbert, G. (1948): Rossland Camp; in *Structural Geology of Canadian Ore Deposits; Canadian Institute of Mining and Metallurgy*, Jubilee Volume, pages 189-196.
- Höy, T. and Andrew, K.P.E. (1989a): The Rossland Group, Nelson Map Area, Southeastern British Columbia; *B.C. Ministry of Energy, Mines and Petroleum Resources*, Geological Fieldwork 1988, Paper 1989-1, pages 33-43.
- Höy, T. and Andrew, K.P.E. (1989b): Geology of the Rossland Group, Nelson Map Area, Southeastern British Columbia; *B.C. Ministry of Energy, Mines and Petroleum Resources*, Open File 1989-1.
- Höy, T. and Andrew, K.P.E. (1990a): Structure and Tectonic Setting of the Rossland Group, Mount Kelly - Hellroaring Creek Area, Southeastern British Columbia; *B.C. Ministry of Energy, Mines and Petroleum Resources*, Geological Fieldwork 1989, Paper 1990-1, pages 11-17.
- Höy, T. and Andrew, K.P.E. (1991): Geology of the Rossland-Trail Area, Southeastern British Columbia (82F/4); *B.C. Ministry of Energy, Mines and Petroleum Resources*, Open File 1991-2.
- Klepacki, D.W. (1985): Stratigraphy and Structural Geology of the Goat Range Area, Southeastern British Columbia; unpublished Ph.D. thesis, *Massachusetts Institute of Technology*, 268 pages.
- Little, H.W. (1960): Nelson Map-area, West-half, British Columbia; *Geological Survey of Canada*, Memoir 308, 205 pages.
- Little, H.W. (1963): Rossland Map-area, British Columbia; *Geological Survey of Canada*; Paper 63-13.
- Little, H.W. (1982): Geology, Rossland-Trail Map-area, British Columbia; *Geological Survey of Canada*, Paper 79-26, 38 pages.
- Parrish, R.R., Carr, S.D. and Parkinson, D.L. (1983): Eocene Extensional Tectonics and Geochronology of the Southern Omineca Belt, British Columbia and Washington; *Tectonics*, Volume 7, pages 181-212.
- Simony, P.S. (1979): Pre-Carboniferous Basement near Trail, British Columbia; *Canadian Journal of Earth Sciences*, Volume 16, Number 1, pages 1-11.
- Stevenson, J.S. (1935): Rossland Camp; *Minister of Mines, British Columbia*, Annual Report 1935, pages E4-E11.
- Tipper, H.W. (1984): The Age of the Jurassic Rossland Group of Southeastern British Columbia; in *Current Research, Part A, Geological Survey of Canada*, Paper 84-1A, pages 631-632.

NOTES

**METCHOSIN VOLCANICS: A LOW-TITANIUM EMERGENT SEAMOUNT
AT THE BASE OF THE CRESCENT TERRANE***
(92B)

By Andrée de Rosen-Spence and A.J. Sinclair
The University of British Columbia

KEYWORDS: Litho-geochemistry, chemostratigraphy, Crescent Terrane, Metchosin volcanics, low-Ti seamount, Kula-Farallon Ridge, plume effects, collision.

INTRODUCTION

At the southern tip of Vancouver Island, the Metchosin volcanics are the northernmost occurrence of the Early Tertiary Crescent Terrane of Washington and Oregon. The allochthonous base of the Crescent Terrane consists of ocean-floor tholeiites, within-plate tholeiitic and alkalic seamounts and sediments (Snively *et al.*, 1968; Glassley, 1974; Cady, 1975; Muller, 1980) spanning the 62 to 49 Ma, or Paleocene to Early Eocene interval (Duncan, 1982). This base is a fragment of the Kula and Farallon plates sutured to the North American continent around 50 Ma (Magill *et al.*, 1981; Heller and Ryberg, 1983). The various tectonic models proposed generally emphasize the proximity and/or conjunction of an active ridge (Kula-Farallon) and hotspot (Yellowstone) close to the North American shore (Snively *et al.*, 1968; Glassley, 1974; Cady, 1975; Muller, 1980; Globerman, 1980; Duncan, 1982; Wells *et al.*, 1984). Duncan's model takes into account the apparent symmetrical aging of the volcanic sequences to the north and south, while some of Wells' models also attempt to integrate the different degrees of tectonic rotation measured in these sequences. Generation at a leaky transform fault, in a "pull-apart" basin of the Gulf of California type (Wells *et al.*, 1984) or in a basin at the back of an Eocene arc (Clowes *et al.*, 1987) have been suggested as alternative models which incorporate the northward motion of the Chugach and Prince William terranes towards Alaska at that time.

All models except that of Clowes *et al.* (1987) include subduction of the Kula and Farallon plates east of the Crescent Terrane boundary with concomitant generation of the Eocene continental arc which stretches from the Yukon to the Absaroka Mountains in Montana (Challis arc in the United States). In this context of lively debate, it is interesting to re-examine in more detail the composition of the Metchosin basalts and other basalts of the Crescent Terrane to determine their nature, their correlations, and the relationship between composition, time of docking and the evolution of the contemporaneous Eocene arc. The Metchosin volcanics are particularly unusual in that they are not only an emergent sequence with ocean-floor affinity (Muller, 1980), but as we will demonstrate, they are also an example of low-titanium normal mid-oceanic ridge basalts (low-Ti MORB-N).

In spite of some alteration and the sparsity of trace element data, it is possible to define the magmatic trends and tectonic settings of older volcanic sequences by using a particular screening method (de Rosen-Spence, 1976; Spence, 1985; de Rosen-Spence and Sinclair, 1987; and in preparation). This screening method is based on the plotting and subsetting of major element data on twelve discriminant diagrams, and the comparison of the treated data with well known suites. The twelve discriminant diagrams are MgO versus CaO, MgO versus SiO₂, CaO versus SiO₂, Na₂O versus SiO₂, K₂O versus SiO₂, Alkali versus SiO₂, MgO versus FeO_T, MgO versus 10xTiO₂/FeO_T, TiO₂ versus FeO_T, P₂O₅ versus TiO₂, MgO versus Al₂O₃ and K₂O/Na₂O versus SiO₂. This method, which can be used directly for small sets of data, has also been adapted for computers in the LITHCHEM system which is a database system for storage, retrieval and graphic representation of whole-rock geochemical data (Harrop and Sinclair, 1986; Radlowski and Sinclair, 1989).

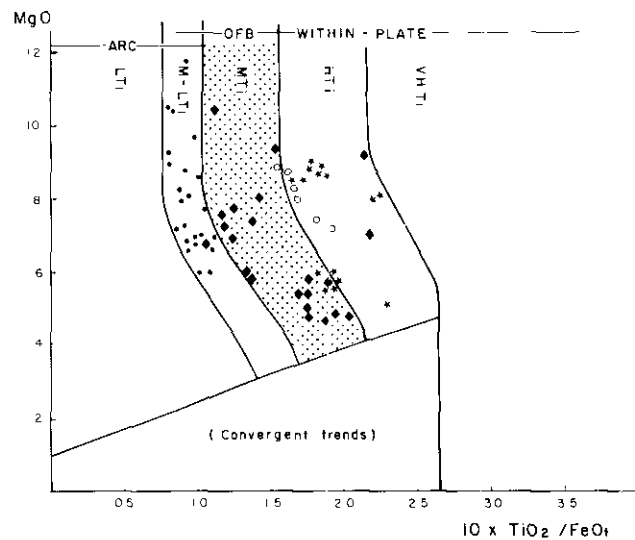


Figure 1-3-1. Different varieties of mid-oceanic ridge basalts (MORB) on MgO versus 10xTiO₂/FeO_T: Thulean MORB-N of Kolbeinsey Ridge (filled circles), Thulean MORB-P of the Icelandic Rift Zone (filled diamonds), common MORB-N (shaded pattern), common MORB-P of Azores on mid-Atlantic Ridge (stars) and fragmented MORB-N of Tamayo rift (open circles). Data from Schilling *et al.* (1983), Sigvaldason (1969) and Bender *et al.* (1984). Note the increase in titanium of MORB-P relative to MORB-N of the same variety.

* This project is a contribution to the Canada/British Columbia Mineral Development Agreement.

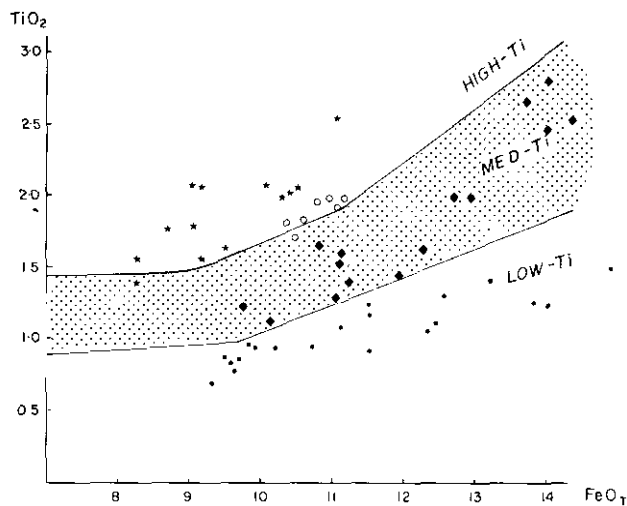


Figure 1-3-2. Different varieties of mid-oceanic ridge basalts (MORB) on TiO_2 versus FeO_1 . Symbols as in Figure 1-3-1. Oceanic island (plume) tholeiites would be in the high-titanium (high-Ti) domain like common MORB-P, but with higher iron content ($>10\%$ FeO_1).

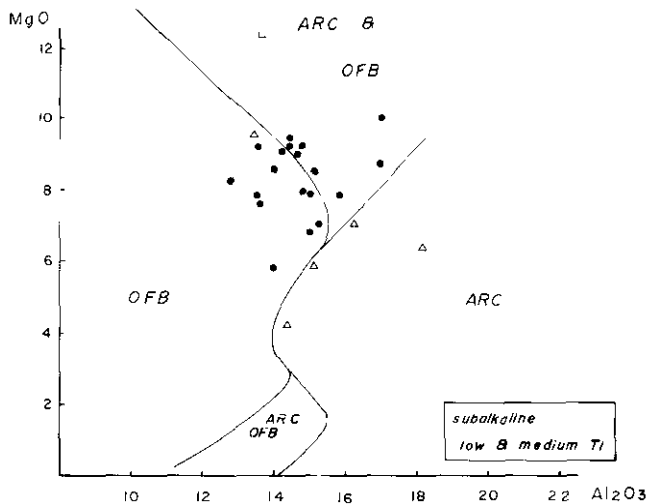


Figure 1-3-3. Metchosin volcanics on MgO versus Al_2O_3 showing the low aluminum content of Thulean MORB-N and slightly more aluminous composition of Thulean MORB-P. Symbols as in Figure 1-3-5.

DEFINITIONS

Much of our interpretation of the Metchosin and other Crescent Terrane basalts is based on the tectonic significance of their $\text{TiO}_2/\text{FeO}_1$ ratio and phosphorus content. On the MgO versus $\text{TiO}_2/\text{FeO}_1$ and TiO_2 versus FeO_1 diagrams (Figures 1-3-1 and 1-3-2), we distinguish three varieties of normal mid-oceanic ridge basalts (MORB-N) herein named "fragmented", "common" and "Thulean" MORB-N varieties (Note: fragmented because of numerous transform faults, Thulean from the Thulean Magmatic Province of Tyrrell, 1937). The decreasing $\text{TiO}_2/\text{FeO}_1$ ratios from fragmented to Thulean MORB correspond to increasing degrees of partial melting of the upper mantle, that is from 5 per cent

for fragmented (Bender *et al.*, 1984) to 20 per cent for Thulean MORB (Sun and Sharaskin, 1979). Any of these three varieties of MORB-N may be variably contaminated by a nearby enriched plume of lower mantle origin and enriched in light rare-earth elements (LREE), zirconium, titanium, and commonly alkali, phosphorus and water (Schilling *et al.*, 1983; Michael and Chase, 1987). Mid-oceanic ridge basalt markedly enriched in titanium and/or phosphorus is defined here as MORB-P. A substantial contamination in titanium results in the shift of Thulean and common MORB to higher titanium domains (Figures 1-3-1 and 1-3-2). On P_2O_5 versus TiO_2 (Figure 1-3-3), contamination involving phosphorus and water besides titanium results in a shift from the main oceanic domain [ocean-floor (OFB), oceanic-island tholeiites (OIT) and alkaline (OIA)] to the arc domain. This shift is an artifact created by the decrease in titanium (and iron) in the presence of water and is diagnostic of such MORB-P. The $\text{TiO}_2/\text{FeO}_1$ ratio remains unmodified and MORB-P therefore cannot be confused with arc basalts.

METCHOSIN VOLCANICS

PREVIOUS WORK

The Metchosin volcanics were mapped by Clapp and Cook (1917) and Muller (1977, 1980), and analyzed by Muller (1980). Recent drilling offshore of Vancouver Island revealed the northward extension of basalts with similar composition (Brandon, in Clowes *et al.*, 1987). The Metchosin volcanics, as described by Muller (1980): "consist of an estimated 3000 metres of pillow lavas, breccias and minor tuffs, succeeded by about 1000 metres of layered amygdaloidal flows . . . the transition of pillows to flows is marked by . . . a coquina of *Turitella* indicating Early Eocene age . . . the volcanics represent an emergent basaltic sequence". Recent dating gives an age of 55 Ma or earliest Eocene (Armstrong, in preparation).

Muller (1980) came to the conclusion that the Metchosin volcanics were of oceanic ridge (MORB) origin and not an oceanic island in spite of their emergent character. To explain their emergence, he proposed that they formed in a ridge-island setting similar to Iceland.

COMPOSITION RE-EXAMINED

The Metchosin basalts are only slightly altered and enough "unaltered" samples survived the altered-unaltered classification process (on a MgO versus CaO diagram, not shown) to characterize their original magmatic composition. Spilitization and small additions of magnesium and manganese in some samples were identified in flows and pillows. In tuffs, alteration is more varied and also includes leaching of sodium and calcium, and local addition of calcium.

The least altered or "unaltered" Metchosin samples, plotted on various discriminant diagrams (not reproduced), have been determined to be low-potassium, calcic tholeiites. Except for a few samples near the top of the pile, they are similar to common MORB-N in their aluminum, phos-

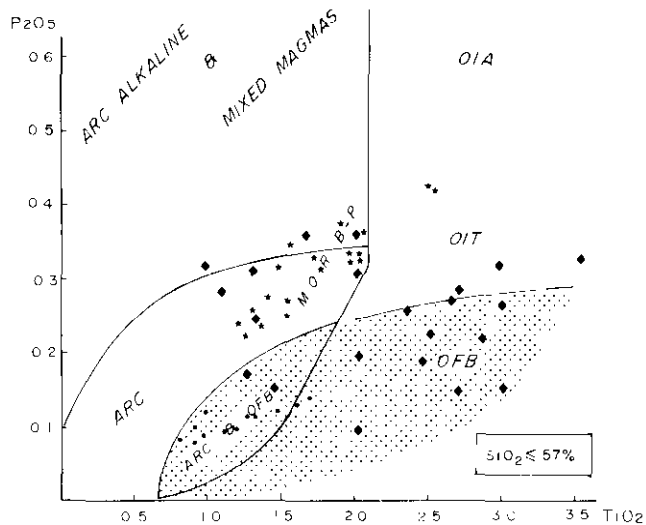


Figure 1-3-4. Different varieties of mid-oceanic ridge basalts (MORB) on P_2O_5 versus TiO_2 . Symbols as in Figure 1-3-1. The various domains overlap with each other, in particular MORB and oceanic-island tholeiite (OIT) domains. Thulean MORB-P of the Icelandic Rift Zone is widely scattered and only seven samples can be diagnosed as MORB-P without trace elements, these have the lowest iron content, the others could be confused with common MORB-N (see previous plots). This example is important to show the limitations faced in the absence of trace element data.

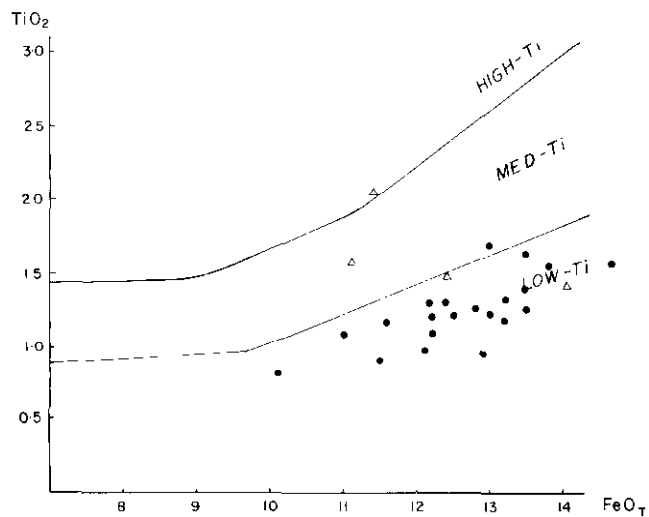


Figure 1-3-5. Metchosin volcanics on TiO_2 versus FeO_T illustrating their low titanium content. Thulean MORB-N, all samples (filled circles) and Thulean MORB-P (open triangles).

phorus and zirconium content but distinctly lower in titanium. As shown on MgO versus TiO_2/MgO (Figure 1-3-4) and TiO_2 versus FeO_T (Figure 1-3-5), they plot in the medium-low and lower titanium domain respectively, and so overlap with arc basalts. Their phosphorus content (Figure 1-3-6) is also compatible with both an arc or a MORB

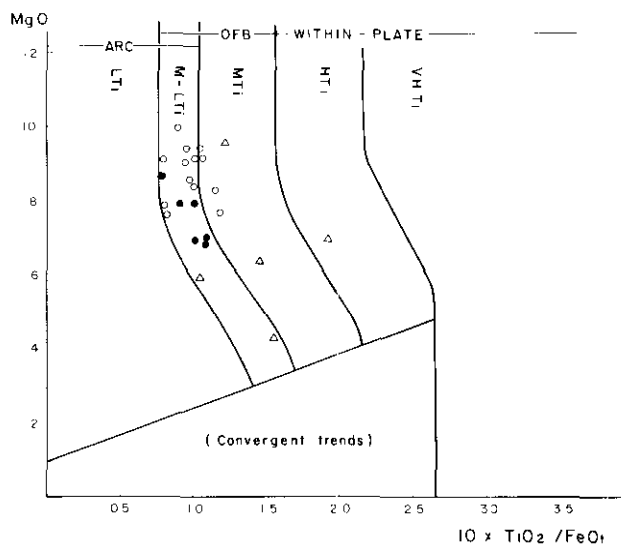


Figure 1-3-6. Metchosin volcanics on MgO versus $10 \times TiO_2 / FeO_T$ illustrating their low titanium content. Thulean MORB-N: unaltered samples (filled circles) and altered samples (open circles), Thulean-MORB-P (open triangles). Thulean MORB-N and -P determined by their phosphorus content on Figure 1-3-7. Data from Muller (1980).

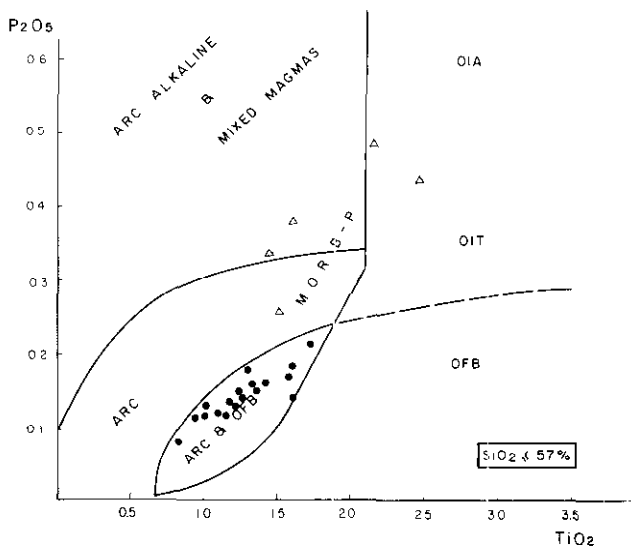


Figure 1-3-7. Metchosin volcanics on P_2O_5 versus TiO_2 showing the difference in phosphorus content leading to the separation of Thulean MORB-N and -P. Symbols as in Figure 1-3-5.

origin. Their MORB-like character, however, is evident on MgO versus Al_2O_3 (Figure 1-3-7) where their differentiation trend enters the low-alumina domain characteristic of ocean-floor basalts; it is also confirmed by their moderate zirconium content (Table 1-3-1, columns A to C). Thus, the Metchosin basalts show all the essential chemical characteristics of Thulean MORB-N-type basalts as defined earlier.

TABLE 1-3-1
SELECTED ANALYSES OF METCHOSIN VOLCANICS
(analyses from Muller (1980), recalculated 100% dry)

	Thulean MORB-N			Thulean MORB-P		
	A	B	C	D	E	F
SiO ₂	50.09	50.02	50.77	48.27	49.40	51.52
TiO ₂	0.83	1.21	1.73	1.61	2.15	2.45
Al ₂ O ₃	17.08	15.27	14.09	18.15	16.26	14.27
Fe ₂ O ₃	1.66	2.53	5.37	4.13	4.76	7.49
FeO	8.59	9.87	8.21	7.43	7.15	9.24
MnO	0.19	0.21	0.22	0.19	0.19	0.27
MgO	8.69	7.43	5.78	6.40	7.04	4.21
CaO	11.70	11.66	8.72	9.70	9.01	7.29
Na ₂ O	1.03	1.57	4.76	3.09	3.31	2.57
K ₂ O	0.06	0.08	0.14	0.66	0.24	0.27
P ₂ O ₅	0.08	0.14	0.21	0.38	0.49	0.44
Zr ppm	86	103	170	160	220	310
Cr ppm	260	161	54	140	130	40

Thulean MORB-N: A— most primitive unaltered sample (42 /76-21I); B= average of six intermediate unaltered samples (17 /76-6M, 27 /76-20B1, 9 /76-4A, 40 /76-21G, 41 /76-21H, 43 /76-21J); C— most differentiated sample, spilitized, note the higher TiO₂, P₂O₅ and Zr accompanying the high iron enrichment (20 /76-16E2). Thulean MORB-P: D= unaltered sample (12 /76-4I); E= slightly altered sample (10 /76-4G). F— Thulean MORB-P with exceptionally strong iron enrichment (11 /76-4B). Note the higher TiO₂, Al₂O₃, P₂O₅ and Zr content of Thulean MORB-P in Column E compared to average Thulean MORB-N in Column B, for about the same MgO and total iron content.

The few samples near the top of the pile are richer in titanium, phosphorus (Figures 1-3-4 to 6) and zirconium (Table 1-3-1, columns D to F), and are identified as Thulean MORB-P, reflecting contamination from a local enriched plume. In Table 1-3-1, a few selected analyses illustrate the variations in composition resulting from differentiation of the Thulean MORB-N Metchosin magma and the enrichment in titanium, phosphorus and zirconium of the Thulean MORB-P samples.

ORIGIN OF METCHOSIN BASALTS

The low-titanium (Thulean MORB) composition of the Metchosin basalts reflects a higher degree of partial melting of the upper mantle than found on most ridges and in marginal basins. It confirms their oceanic setting and precludes formation in a local pull-apart basin (3rd model of Wells *et al.*, 1984) or back-arc basin (Clowes *et al.*, 1987). Could this partial melting be sufficient to explain their emergence? Not necessarily so. The large degree of melting leads to voluminous outpourings of magma through fissures, but seemingly not to emergence in the largest occurrences of Thulean MORB-N: the North Atlantic ocean-floor including Kolbeinsey Ridge (Schilling, 1983), the Cretaceous mid-Pacific oceanic flood basalts (Tokuyama and Batiza, 1981; Saunders, 1986), and the tholeiites associated with Archean komatiites (de Rosen-Spence and Sinclair, in preparation). The build up of a seamount or an island seems to require a more localized source in the form of a plume. For the Metchosin volcanics, Muller (1980) proposed a situation similar to Iceland, but Iceland is a complex seamount built by an enriched lower mantle plume superimposed on a Thulean ridge, and the resulting tholeiites are

typical Thulean MORB-P with higher titanium as shown on Figures 1-3-1 to 1-3-3. The Metchosin volcanics, by contrast, are uncontaminated Thulean MORB-N-type products and thus their emergence cannot be explained by the superimposition of a similar enriched plume, this in spite of the vicinity of the Yellowstone hotspot. Since Muller's work, however, there have been a number of studies of seamounts with MORB-like composition attributed to upper mantle thermal plumes. These thermal plumes can be independent of the enriched lower mantle plumes (Batiza and Vanko, 1984; Desonic and Duncan, 1990; Rhodes *et al.*, 1990) or can be generated in the upper mantle by a thermal entrainment process (Griffiths, 1986) and dynamic upwelling of the enriched mantle plumes. The latter situation would be similar to that of Kolbeinsey Island and the Manihiki Plateau, both of Thulean MORB composition: Kolbeinsey Island, on Kolbeinsey Ridge, is uncontaminated by the nearby Iceland plume (Schilling *et al.*, 1983), and the Manihiki Plateau (northeast of New Zealand), emergent at the time of eruption, is on the site of a Cretaceous triple junction (Clague, 1976) and was close to a hotspot.

By analogy with these examples, we propose that the Metchosin basalts could reflect the presence of a local upper mantle thermal plume imposed either on the Kula-Farallon Ridge, or on the site of the Pacific-Farallon-Kula triple-junction which is thought to have been in the vicinity (Wells *et al.*, 1984). The few samples of Thulean MORB-P are a reminder of the proximity of the Yellowstone hotspot of enriched lower mantle composition (as shown below), and of its possible thermal and dynamic influence on the nearby independent ridge system.

CRESCENT TERRANE

We examined some of the data available for the Eocene Crescent Formation of the Olympic Peninsula (data from Glassley, 1974; Cady, 1975; Lyttle and Clarke, 1975) and Black Hills (data from Globerman, 1980) in Washington, and for the correlative Siletz River volcanics in Oregon (data from Snaveley *et al.*, 1968).

CRESCENT FORMATION

In the eastern Olympic Peninsula, the Crescent Formation is composed of two very distinct volcanic members separated by a tectonic contact (Glassley, 1974). These are an altered, ocean-floor lower member and a fresh plume-influenced upper member deposited in a shallow water to subaerial environment.

Our plots of the data for the lower member (Figures 1-3-8 to 10), are based mainly on Lyttle and Clarke's (*ibid.*) data because samples are separated into extrusive and possibly intrusive origin. They clearly indicate that this lower member is composed of Thulean MORB-N and Thulean MORB-P, and that all samples of possibly intrusive origin are of common MORB-N composition, suggesting that they are actually sills. One occurrence of flows is extremely poor in titanium (low-Ti plot on Figure 1-3-4) and phosphorus and may represent a case of extreme partial melting or of local depletion. Thulean MORB-N is also present in the basalts

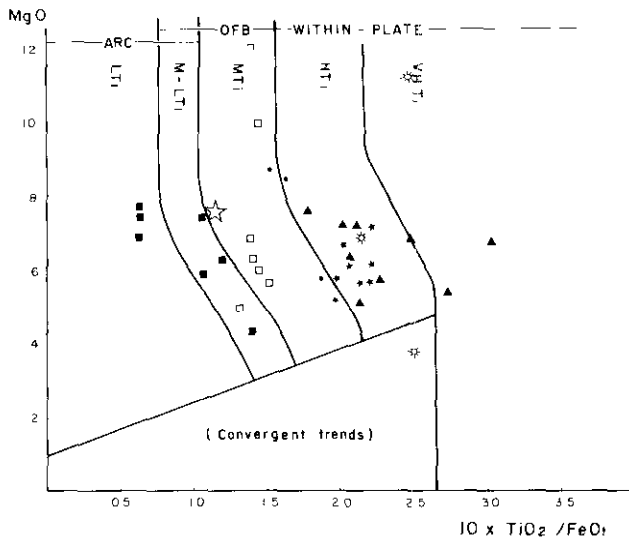


Figure 1-3-8. Crescent Terrane on MgO versus $10 \times \text{TiO}_2 / \text{FeO}_1$ illustrating its chemical complexity. Crescent Formation lower member is Thulean MORB-N (filled squares) and MORB-P (open squares); the upper member is common MORB-P (filled triangles). Siletz River volcanics are composed of common MORB (filled circles), oceanic-island tholeiites (filled stars), oceanic-island alkaline (open suns) and one isolated altered Thulean MORB-N (large open star). MORB-P character determined on Figures 1-3-9 and 1-3-10. Note the three samples in the low titanium domain (increased partial melting or initial depletion). Data from Glassley (1974), Lytle and Clarke (1975) and Snavely *et al.* (1968).

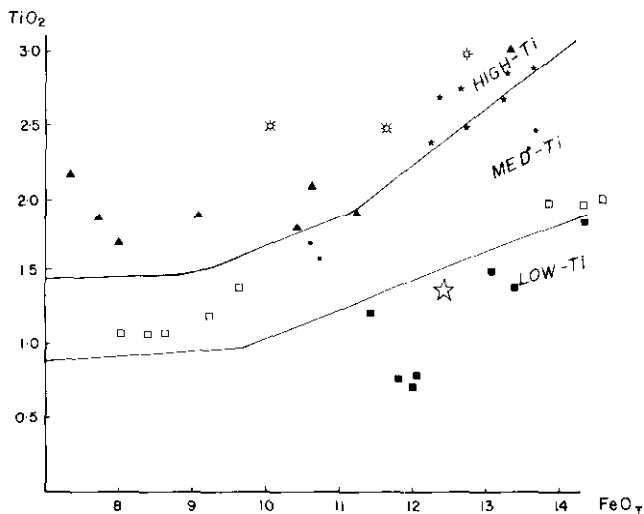


Figure 1-3-9. Crescent Terrane on TiO_2 versus FeO_1 . Note the low titanium content of Thulean MORB-N of the lower Crescent Formation (filled squares) and southeast Siletz River (open star), the generally low iron content of Thulean MORB-P (open squares) and common MORB-P (filled triangles) of the lower and upper Crescent Formation, the high titanium and high iron content of the Siletz River Seamount (stars and suns).

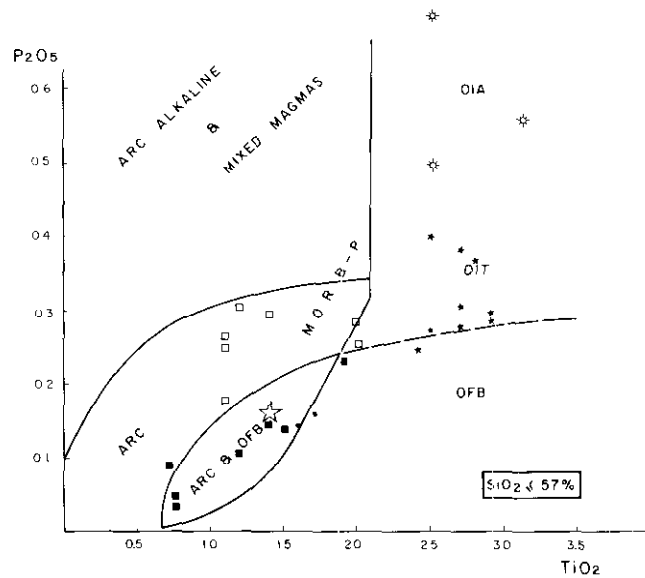


Figure 1-3-10. Crescent Terrane on P_2O_5 versus TiO_2 showing plume influence on the Thulean MORB of the lower Crescent Formation and the high titanium and phosphorus content of the Siletz River seamount. Symbols are as in Figure 1-3-8, but upper Crescent Formation was omitted owing to poor phosphorus analyses.

interbedded in the sediments of the "core rocks" of the central Olympic Peninsula, to the west (data from Cady, 1975).

The upper member, in the eastern Olympic Peninsula (data from Glassley, 1974) is interpreted to be composed of common MORB-P. It has the high $\text{TiO}_2 / \text{FeO}_1$ ratio of within-plate tholeiites but the lower iron content commonly associated with MORB-P (Figures 1-3-8 and 9). Analyses of phosphorus are too inaccurate to be useful in identifying MORB-P, but the moderate content of light rare-earth elements is also characteristic of MORB-P.

In the Black Hills to the southeast, Globerman (1980) has shown that the basalts, mainly subaerial, belong to the upper member of the Crescent Formation and are a mix of micro-oceanic-ridge basalts and enriched-plume tholeiites. They are richer in iron than the upper member in the Olympic Peninsula and probably were generated closer to the Yellowstone hotspot.

SILETZ RIVER VOLCANICS

The Siletz River volcanics were shown by Snavely *et al.* (1968) to be an emergent seamount composed essentially of oceanic tholeiites capped by alkaline rocks similar to Hawaiian lavas and resting on ocean-floor basalts. Our plots (Figures 1-3-8, 9 and 10) confirm this, although we can add that the isolated southeasternmost occurrence of Siletz volcanics contains Thulean MORB-N. The Siletz River volcanics are therefore products of the Yellowstone enriched plume and, with their ocean-floor base, represent the southern extension of the upper member of the Crescent Forma-

tion. The southeastern exposure, on the other hand, represents an extension of the Thulean lower member. It should be remembered that such chemostratigraphy may be time transgressive.

SUCCESSION AND CORRELATION OF EVENTS

Two eruptive episodes are clearly evident from the above determinations. During the first episode (Paleocene and earliest Eocene), Thulean MORB-N was generated close to the North American continent, and locally an island or a plateau emerged (Metchosin), while towards the top and to the south, the enriching influence of the Yellowstone plume was felt (presence of Thulean MORB-P in the upper Metchosin succession and in the lower member of the Crescent Formation). The remnants of this Thulean-type crust are identified as far south as the Siletz River but we suspect that it exists at the southernmost tip of the Crescent Terrane, in the Paleocene Roseburg Formation (Baldwin, 1974; Duncan, 1982) for which we have no data.

During the second episode (Early Eocene to early Middle Eocene) and corresponding to the upper member of the Crescent Formation, common MORB-N was generated (intrusives in the lower member of the Crescent Formation, base of the Siletz River volcanics), but was promptly modified by the Yellowstone hotspot into common MORB-P in the eastern Olympic Peninsula and Black Hills. To the south, the unmodified products of this hotspot formed a classic oceanic island (Siletz River).

Metamorphism and shearing, which are limited to rocks of the first episode, confirm the validity of this division.

Docking and suturing to the craton by 50 Ma (Magill *et al.*, 1981; Heller and Ryberg, 1983) and attendant steepening of the subduction zone profoundly modified the composition of the Eocene arc (de Rosen-Spence and Sinclair, in preparation): shoshonites of the Kamloops and Pentiction groups (Spence, 1985) started erupting at 51 Ma during a major period of extension (Ewing, 1981; Parrish *et al.*, 1988). Similar events occurred to the south, in the Challis arc down to the Absaroka Mountains (Armstrong, 1978; Iddings, 1895). Shoshonites are characteristic of collision episodes and it is symptomatic that they occur only in the southern segment of the arc opposite the Crescent Terrane, and not in its northern segment (central British Columbia to Yukon). If we take into account that there is a time lag of possibly 2 Ma between tectonic change and volcanism (Bardsell *et al.*, 1982), we can surmise that the actual docking must have occurred sometime about 53 Ma rather than 50 Ma ago.

Oblique collision at 53 Ma of an unobductible thickened crust could have generated numerous transform faults across the ridge, to absorb the first impact of the collision, and so would have locally slowed down the partial melting processes. Such a slow-down would account for the change from Thulean MORB in the lower member of the Crescent Formation to common MORB in the upper member. The colliding mass would have been composed of the Metchosin plateau or island to the north, the Roseburg Formation of

unknown composition (Thulean MORB ?) to the south, and some young, buoyant ridge fragment (lower Olympic Formation) thickened by addition of plume material (Thulean MORB-P) in between. The growth of seamounts (Black Hills, Siletz River) near the suture, and the buoyant activity of the Yellowstone hotspot prevented any further possibility of subduction. Finally, the plates attempted to reorganize around 48 Ma and, as a result, the subduction zone jumped west of the Crescent Terrane initiating the earliest Cascades volcanism (Wells *et al.* 1984), while activity waned in the Challis arc, starved by the demise of its own subduction zone.

This model of two distinct episodes, separated by collision and initiation of transform faults at 53 Ma, could reconcile some of the contradictory observations made by previous authors. It may explain some of the differences in rotation observed between the various sequences, while generation of transform faults in the second episode could be incorporated in the model of large-scale movements of detached terranes to Alaska, proposed by Wells *et al.* (*ibid.*).

METCHOSIN AS A SYMPTOM OF AN ACTIVE MANTLE

The generation of Thulean MORB can be a powerful and long-lived event (60 Ma in the North Atlantic and mid-Pacific) and so one should expect to find other similar occurrences in the Paleocene and Eocene oceanic crust of the Pacific Ocean. Unfortunately, only one sample of the Eocene of the northern Pacific plate has been analyzed, Hole 178 of Leg 18 near the Aleutian arc (MacLeod and Pratt, 1973). This single sample, approximately 50 Ma old, has the characteristics of a Thulean MORB-P. Another occurrence, though far from the Crescent Terrane, was found on Gorgona Island (Colombia) where an emergent fragment of the Eocene Farallon plate is composed of komatiites and basaltic komatiites interbedded with tholeiites (Aitken and Etcheverria, 1984); these tholeiites also plot as Thulean MORB. Seen in this larger context, the composition of the Metchosin volcanics should not be considered as a local quirk, but as one of the symptoms of an episode of more intense partial melting along the Pacific ridges, either widespread as in the North Atlantic or restricted to certain areas of the ridges, possibly close to large, new lower-mantle plumes. This surge of partial melting would be analogous to that which was responsible for the oceanic flood basalts across the mid-Pacific (Nauru basin and others) and the Ontong-Java and Manihiki plateaux during the Cretaceous.

It may be significant, on a global scale, that at about the same time (latest Cretaceous to earliest Tertiary) the Yellowstone hotspot became active and Metchosin Thulean basalts erupted, so did the Galapagos hotspot and the Gorgona Island Thulean tholeiites, the Iceland plume and the first Thulean basalts of the Faroes and Rockall Plateau (data from Noe-Nygaard and Rasmussen, 1968; Harrison *et al.*, 1984), the Reunion hotspot (Courtillot, 1990) and Thulean basalts of the nearby old (68 to 46 Ma) Indian Ocean floor (data from Melson *et al.*, 1976). Note that, at

present, only the North Atlantic ridge system has remained undisturbed and is still erupting Thulcan MORB on Kolbeinsey and Reykjanes ridges.

ACKNOWLEDGMENTS

This paper represents a small part of an ongoing study of whole-rock chemical data for volcanic sequences in the Canadian Cordillera, undertaken at The University of British Columbia. The project was funded initially by the Science Secretariat of British Columbia and the B.C. Ministry of Energy, Mines and Petroleum Resources through the Canada/British Columbia Mineral Development Agreement 1985-1990, and more recently by a Natural Science and Engineering Council operation grant. We also wish to thank Dr. R.L. Chase for pointing out the importance of non-enriched seamounts in the northeastern Pacific in the context of this study.

REFERENCES

- Aitken, B.G. and Etcheverria, L.M. (1984): Petrology and Geochemistry of Komatiites and Tholeiites from Gorgona Island, Colombia; *Contributions to Mineralogy and Petrology*, Volume 86, pages 94-105.
- Armstrong, R.L. (1978): Cenozoic Igneous History of the U.S. Cordillera from Lat 42° to 49°; *Geological Society of America, Memoir 152*, pages 265-282.
- Baldwin, E.M. (1974): Eocene Stratigraphy of Southwestern Oregon; *Oregon Department of Geology and Mineral Industry Bulletin*, Volume 83, 40 pages.
- Barsdell, M., Smith, I.E.M. and Spörli, K.B. (1982): The Origin of the Reverse Zoning in the Northern New Hebrides Volcanic Arc; *Contributions to Mineralogy and Petrology*, Volume 81, pages 148-155.
- Batiza, R. and Vanko, D. (1984): Petrology of Young Pacific Seamounts; *Journal of Geophysical Research*, Volume 89, pages 11,235-11,260.
- Bender, J.F., Langmuir, C.H. and Nanson, G.N. (1984): Petrogenesis of Basaltic Glasses in the Tamayo Region, East Pacific Rise; *Journal of Petrology*, Volume 25, pages 213-254.
- Cady, W.M. (1975): Tectonic Setting of the Tertiary Volcanic Rocks of the Olympic Peninsula, Washington; *U.S. Geological Survey Journal of Research*, Volume 3, pages 573-582.
- Clague, D.A. (1976): Petrology of Basaltic and Gabbroic Rocks Dredged from the Danger Island Troughs, Manihiki Plateau; *Initial Reports, Deep Sea Drilling Project 33*, pages 891-913.
- Clapp, C.H. and Cooke, H.C. (1917): Sooke and Duncan Map-areas, Vancouver Island; *Geological Survey of Canada, Memoir 96*, 445 pages.
- Clowes, R.M., Brandon, M.T., Green, A.G., Yorath, C.J., Sutherland-Brown, A., Kanasevich, E.R. and Spencer, C. (1987): LITHOPROBE - Southern Vancouver Island: Cenozoic Subduction Complex Imaged by Deep Seismic Reflections; *Canadian Journal of Earth Sciences*, Volume 24, pages 31-51.
- Courtillot, V.E. (1990): A Volcanic Eruption; *Scientific American*, Volume 263, Number 4, pages 85-92.
- de Rosen-Spence, A.F. (1976): Stratigraphy, Development and Petrogenesis of the Central Noranda Volcanic Pile; unpublished Ph.D. thesis, *University of Toronto*.
- de Rosen-Spence, A.F. and Sinclair, A.J. (1987): Classification of the Cretaceous Volcanic Sequences of British Columbia and Yukon; *B.C. Ministry of Energy, Mines and Petroleum Resources, Geological Fieldwork 1986, Paper 1987-1*, pages 419-426.
- Desonie, D.L. and Duncan, R.A. (1990): The Cobb-Eickelberg Seamount Chain: Hotspot Volcanism with Mid-oceanic Ridge Basalt Affinity; *Journal of Geophysical Research*, Volume 95, pages 12,697-12,711.
- Duncan, R.A. (1982): A Captured Island Chain in the Coast Range of Washington and Oregon; *Journal of Geophysical Research*, Volume 87, pages 827-837.
- Ewing, T.E. (1981): Regional Stratigraphy and Structural Setting of the Kamloops Group, South-Central British Columbia; *Canadian Journal of Earth Sciences*, Volume 18, pages 1464-1477.
- Glassley, W. (1974): Geochemistry and Tectonics of the Crescent Volcanic Rocks, Olympic Peninsula, Washington; *Geological Society of America Bulletin*, Volume 85, pages 785-794.
- Globerman, B.R. (1980): Geology, Petrology and Paleomagnetism of Eocene Basalts from the Black Hills, Washington Coast Range; unpublished M.Sc. thesis, *Western Washington University, Bellingham, Washington*.
- Griffiths, R.W. (1986): The Differing Effects of Compositional and Thermal Buycancies on the Evolution of Mantle Diapirs; *Physics of the Earth and Planetary Interior*, Volume 43, pages 261-273.
- Harrison, R.K., Merriman, R.J. et al. (1984): Petrology, Mineralogy and Chemistry of Basaltic Rocks: LEG 81; *Initial Reports, Deep Sea Drilling Project 81*, pages 743-770.
- Harrop, J.C. and Sinclair, A.J. (1986): Lithchem: an Integrated Geological Database for Microcomputers; *B.C. Ministry of Energy, Mines and Petroleum Resources, Geological Fieldwork 1985, Paper 1986-1*, pages 285-287.
- Heller, P.L. and Ryberg, P.T. (1983): Sedimentary Record of Subduction to Forearc Transition in the Rotated Eocene Basin of Western Oregon; *Geology*, Volume 11, pages 380-383.
- Iddings, J.P. (1895): Absarokite-Shoshonite-Banakite Series; *Journal of Geology*, Volume 3, pages 935-959.
- Lytle, N.A. and Clarke, D.B. (1975): New Analyses of Eocene Basalt from the Olympic Peninsula, Washington; *Geological Society of America Bulletin*, Volume 85, pages 421-427.
- MacLeod, N.S. and Pratt, R.M. (1973): Petrology of Volcanic Rocks Recovered on Leg 18; *Initial Reports, Deep Sea Drilling Project 18*, pages 935-945.

- Magill, J.R., Cox, A.V. and Duncan, R.A. (1981): Tillamook Volcanic Series: Further Evidence for Tectonic Rotation of the Oregon Coast Range; *Journal of Geophysical Research*, Volume 86, pages 2953-2970.
- Melson, W.G., Vallier, T.L., Wright, T.L., Byerly, G. and Nelen, J. (1976): Chemical Diversity of Abyssal Volcanic Glass Along Pacific, Atlantic and Indian Ocean Sea-floor Spreading Centers; in *Plate Tectonics, Selected papers from publications of the American Geophysical Union* (J.M. Bird, Editor), pages 622-636.
- Michael, P.J. and Chase, R.L. (1987): The Influence of Primary Magma Composition, H₂O Pressure on Mid-oceanic Ridge Basalt Differentiation; *Contributions to Mineralogy and Petrology*, Volume 96, pages 245-263.
- Muller, J.E. (1977): Evolution of the Pacific Margin, Vancouver Island and Adjacent Regions; *Canadian Journal of Earth Sciences*, Volume 9, pages 2062-2085.
- Muller, J.E. (1980): Chemistry and Origin of the Eocene Metchoshin Volcanics, Vancouver Island, British Columbia; *Canadian Journal of Earth Sciences*, Volume 17, pages 199-209.
- Noe-Nygaard, A. and Rasmussen, J. (1968): Petrology of a 3,000 metre Sequence of Basaltic Lavas in the Faroes Islands; *Lithos*, Volume 1, pages 286-304.
- Parrish, R.R., Carr, S.D. and Parkinson, D.L. (1988): Eocene Extensional Tectonics and Geochronology of the Southern Omineca Belt, British Columbia and Washington; *Tectonics*, Volume 7, pages 181-212.
- Radlowski, Z.A. and Sinclair, A.J. (1989): Lithchem — Geological Database System: Recent Developments; *B.C. Ministry of Energy, Mines and Petroleum Resources*, Geological Fieldwork 1988, Paper 1989-1, pages 619-620.
- Rhodes, J.M., Morgan, C. and Lias, R.A. (1990): Geochemistry of Axial Seamount Lavas: Magmatic Relationship between the Cobb Hotspot and the Juan de Fuca Ridge; *Journal of Geophysical Research*, Volume 95, pages 12,713-12,733.
- Saunders, A.D. (1986): Geochemistry of Basalts from the Nauru Basin, Deep Sea Drilling Project Legs 61 and 89: Implications for the Origin of Oceanic Flood Basalts; *Initial Reports, Deep Sea Drilling Project 89*, pages 499-517.
- Schilling, J.G., Zajac, M., Evans, R., Johnston, T., White, W., Devine, J.D. and Kingsley, R. (1983): Petrologic and Geochemical Variations along the Mid-Atlantic Ridge from 29°N to 73°N; *American Journal of Science*, Volume 283, pages 510-586.
- Sigvaldason, G.E. (1969): Chemistry of Basalts from the Icelandic Rift Zone; *Contributions to Mineralogy and Petrology*, Volume 20, pages 357-370.
- Snavely, P.D., MacLeod, N.S. and Wagner, H.C. (1968): Tholeiitic and Alkalic Basalts of the Eocene Siletz River Volcanics, Oregon Coast Range; *American Journal of Science*, Volume 266, pages 454-481.
- Spence, A.F. (1985): Shoshonites and Associated Rocks of Central British Columbia, Canada; *B.C. Ministry of Energy, Mines and Petroleum Resources*, Geological Fieldwork 1984, Paper 1985-1, pages 426-442.
- Sun, S.S. and Sharaskin, A.Y. (1979): Geochemical Characteristics of Mid-ocean Ridge Basalts; *Earth and Planetary Sciences Letters*, Volume 44, pages 119-138.
- Tokuyama, H. and Batiza, R. (1981): Chemical Composition of Igneous Rocks and Origin of the Sill and Pillow-lava Complex of Nauru Basin, Southwest Pacific; *Initial Reports, Deep Sea Drilling Project 61*, pages 673-695.
- Tyrrell, G.W. (1937): Flood Basalts and Fissure Eruption; *Bulletin de Volcanologie*, Volume 1, pages 89-111.
- Wells, R.E., Engerbretson, D.C., Snavely, P.D. and Coe, R.S. (1984): Cenozoic Plate Motions and the Volcanotectonic Evolution of Western Oregon and Washington; *Tectonics*, Volume 3, pages 275-294.



**THE GEOCHEMISTRY OF EARLY CRETACEOUS VOLCANIC
ROCKS ON THE WEST SIDE OF HARRISON LAKE,
SOUTHERN BRITISH COLUMBIA
(92H/12)**

By G.E. Ray

KEYWORDS: Litho-geochemistry, Brokenback Hill Formation, Gambier assemblage, Fire Lake Group, arc volcanism, volcanoclastics.

INTRODUCTION

This paper presents analytical data on 21 representative samples of volcanic and volcanoclastic rocks collected from the Early Cretaceous Brokenback Hill Formation on the west side of Harrison Lake. The area lies approximately 100 kilometres east-northeast of Vancouver and 45 kilometres north-northeast of Harrison Hot Springs (Figure 1-4-1), close to vein-hosted gold-silver mineralization at Doctors Point and the small, abandoned Providence mine (Ray *et al.*, 1984, 1985).

REGIONAL GEOLOGY

The Harrison Lake fault system is a major dislocation exceeding 100 kilometres in length that passes through Harrison Lake (Figure 1-4-1). It separates rocks of contrasting geological settings (Roddick, 1965; Monger, 1970). To the northeast are highly deformed, largely supracrustal rocks that were originally called the Stollicum series (Crickmay, 1925, 1930) but which are now termed the Stollicum package (Monger, 1986). These schistose rocks are penetratively deformed and regionally metamorphosed to greenschist and lower amphibolite facies (Journey and Csontos, 1989); they may be metamorphosed equivalents of the Late Triassic Cadwallader Group (Monger, 1986). With the exception of the Chilliwack-Cultus package, which outcrops south of the lake, rocks on the southwest side of the fault are younger, less deformed and of lower metamorphic grade. They include a variety of volcanic, volcanoclastic and sedimentary rocks of largely Jura-Cretaceous age, as well as some plutonic and migmatitic rocks.

The southwest part of the area, west of Harrison Lake, is underlain by the Lower to Middle Jurassic Harrison Lake Formation (Crickmay, 1925; Arthur, 1986). This formation is a sequence of intermediate to acid volcanic flows and pyroclastics that hosts the Seneca copper-zinc massive sulphide deposit (Watanabe, 1974; Urabe *et al.*, 1983). To the north are Middle to Upper Jurassic sediments and tuffs of the Mysterious Creek and Billhook Creek formations which are unconformably overlain by a sequence of Lower Cretaceous rocks. The thin, lowermost portion of this Cretaceous sequence is occupied by sediments of the Peninsula Formation; these pass conformably upward into the Brokenback Hill Formation. Journey and Csontos (1989) and Lynch (1990) correlate the latter formation as part of the

Fire Lake Group (Roddick, 1965), which lies at the north end of Harrison Lake; Wheeler and McFeely (1987) place both these packages within the Gambier assemblage. The Brokenback Hill Formation on the west side of Harrison Lake comprises the volcanic rocks which are the subject of this paper, as well as tuffs and a variety of sediments that range in age from upper Valanginian to middle Albian (Ray *et al.*, 1985; Arthur, 1986). The upper part of this formation to the north is intruded by several high-level, dioritic plutons (Figure 1-4-2) of mid-Tertiary age that are associated with auriferous vein mineralization at Doctors Point. Approximately 5 kilometres south of Doctors Point, on the shoreline of Harrison Lake, the old Providence mine contains both gold-bearing quartz veins and gold-poor, silver-rich quartz-carbonate veins. Minor gold production came from the quartz veins at the turn of the century (B.C. Minister of Mines Annual Reports; 1897, 1901). The steeply dipping silver-rich veins are up to 0.7 metre thick and are hosted by basaltic flows and tuffs of the Brokenback Hill Formation (Ray *et al.*, 1985).

The Harrison Lake fault is associated with a deformation zone 1 to 2 kilometres wide, marked by an intense slaty cleavage and gently plunging linear stretch fabrics (Arthur, 1986). The fault has had a long history of recurrent thrust, strike-slip and normal fault movements that ended prior to development of the Fraser fault system during Eocene time (Monger, 1986; Journey and Csontos, 1989).

GEOLOGY OF THE BROKENBACK HILL FORMATION, AND SAMPLE LOCATIONS

The locations of samples collected for geochemical analysis are shown on Figure 1-4-2. Between Doctors Point and the Providence mine, the Brokenback Hill Formation dips northeasterly. Bedding and fracture cleavage intersections indicate that this section occupies the northeastern limb of a major northerly trending anticline; there is no evidence of structural repetition and graded bedding shows the sequence is upright. Consequently, rocks between Providence mine and Doctors Point are considered to form part of a continuous, northerly younging sequence. Mafic volcanic flows and tuffs predominate in the lower, more southerly part of the section. Farther north, however, toward Doctors Bay, flows are uncommon, and the abundant tuffs are interbedded with black argillite, volcanic sandstone, siltstone, and rare, thin beds of polymictic conglomerate. Locally, the siltstones contain graded bedding, argillite rip-up clasts, soft-sediment deformation features, load casts and chaotic slump structures.

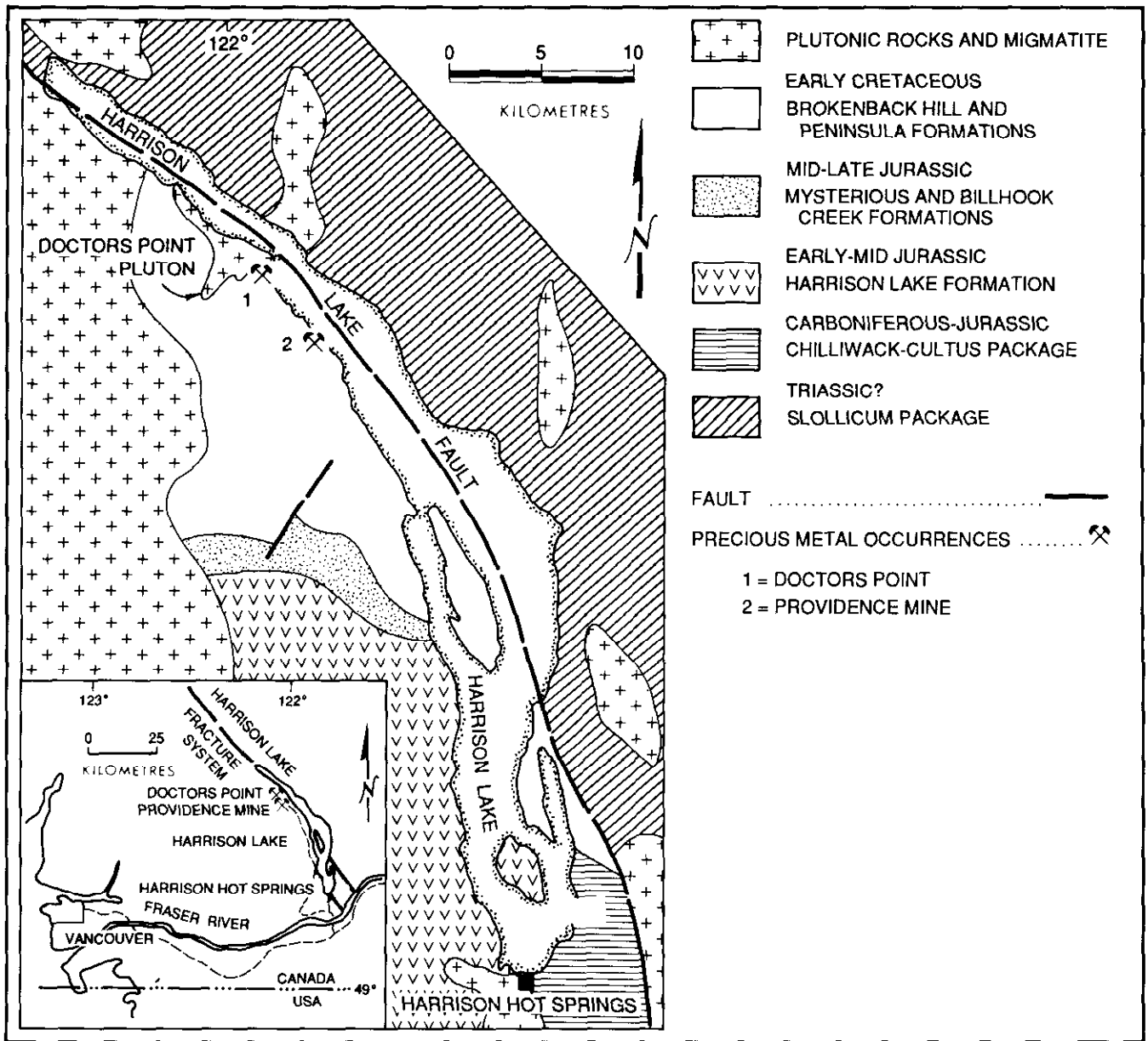


Figure 1-4-1. Regional geology of the Harrison Lake area and location of the Doctors Point and Providence mine mineralization in the sampled area (adapted after Roddick, 1965; Monger, 1970;1986, Arthur, 1986).

The volcanoclastic rocks throughout the section vary from massive to thinly bedded crystal-lithic tuffs and lapilli tuffs, through to chaotic, coarse volcanic breccias and aquagene breccias containing abundant angular to subangular clasts up to 15 centimetres in diameter. Most of the clasts are basalt and andesite, although some fragments in the upper part of the succession are dacitic. The mafic aquagene breccias are characterized by rounded clots of carbonate rimmed with epidote, and most of the tuffs and flows are strongly chloritized.

The varied character of the sedimentary and volcanoclastic rocks in the Brokenback Hill Formation suggests it was deposited during alternating episodes of low and high-

energy sedimentation with some periodic explosive volcanic activity.

The volcanic rocks are generally massive; pillowed flows have only been identified in the lower part of the succession, close to the Providence mine. Individual pillows are vesicular and reach 75 centimetres in diameter. The more mafic flows contain altered remnant crystals of augite up to 4 millimetres in length that enclose interlocking laths of andesine-labradorite plagioclase. Alteration products include chlorite, epidote and tremolite-actinolite. Some basaltic rocks with abundant coarse plagioclase phenocrysts up to 0.5 centimetre in diameter may represent subvolcanic intrusions.

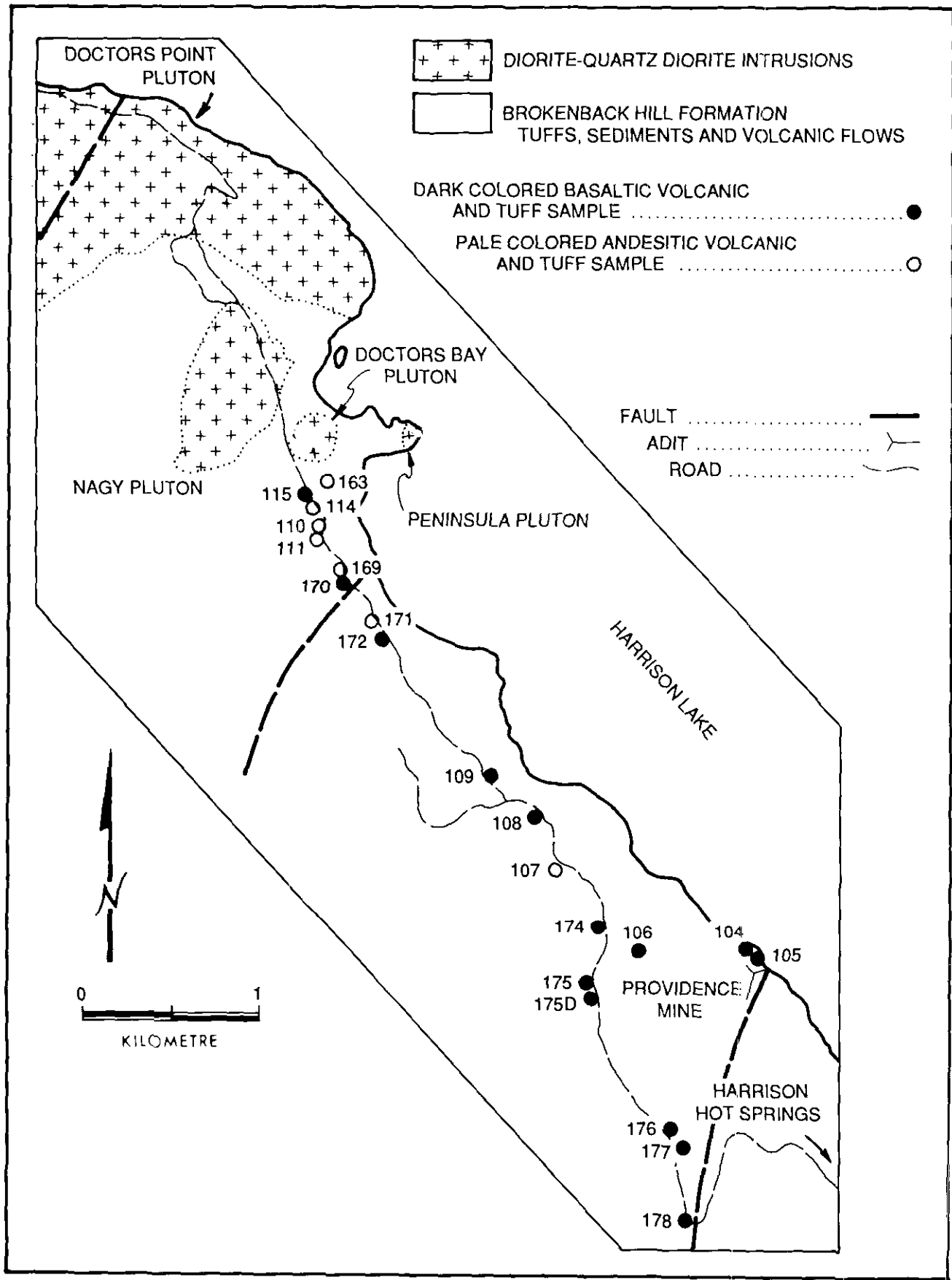


Figure 1-4-2. Location of the rock samples collected from the Brokenback Hill Formation between Doctors Point and Providence mine. (Numbers refer to sample numbers in Table 1-4-1).

TABLE 1-4-1
ANALYTICAL RESULTS OF VOLCANIC AND VOLCANICLASTIC SAMPLES,
DOCTORS POINT, BRITISH COLUMBIA

Sample No.	SiO ₂	TiO ₂	Al ₂ O ₃	Fe ₂ O ₃ *	MnO	MgO	CaO	Na ₂ O	K ₂ O	LOI	TOTAL	Y	Zr
RR 104	47.75	1.04	19.33	9.75	0.35	4.28	7.82	2.48	1.73	4.6	99.13	20	51
RR 105	45.69	0.93	14.95	9.99	1.01	2.39	7.41	0.80	6.65	8.7	98.52	20	45
RR 106	53.44	0.71	17.91	9.05	0.19	3.68	6.49	2.55	0.58	5.1	99.70	18	72
RR 108	46.96	1.07	18.29	10.72	0.26	5.47	11.12	2.02	0.14	3.8	99.85	20	66
RR 109	56.15	0.90	19.34	7.37	0.13	1.85	7.76	3.67	1.53	1.5	100.20	24	84
RR 115	53.40	1.42	16.06	13.19	0.34	4.13	7.35	3.19	0.54	0.9	100.52	24	66
RR 170	53.36	0.95	17.12	7.35	0.12	4.70	6.72	4.01	1.15	5.1	100.58	18	120
RR 172	56.07	0.75	17.13	7.65	0.14	3.84	7.98	2.77	0.68	2.6	99.61	16	63
RR 174	48.58	1.03	19.31	9.95	0.50	5.25	6.12	2.87	0.43	5.7	99.74	18	45
RR 175	50.69	0.81	18.47	10.12	0.17	4.73	6.84	3.38	0.58	4.1	99.89	16	39
RR 176	50.66	0.81	18.57	8.98	0.25	3.00	10.36	2.39	0.62	4.9	100.54	16	42
RR 177	52.38	1.19	19.08	9.12	0.18	3.29	7.11	4.36	0.28	3.6	100.59	20	60
RR 178	48.29	0.94	18.15	11.32	0.20	5.06	9.91	1.18	0.54	5.2	100.79	16	36
RR 175D	51.08	0.80	18.42	10.07	0.18	4.79	6.88	3.39	0.56	4.3	100.47	18	39
RR 107	59.07	0.78	16.82	6.47	0.17	3.47	5.24	2.89	0.94	4.6	100.45	26	90
RR 110	53.11	0.96	18.76	9.15	0.12	4.18	5.52	3.41	0.62	4.4	100.23	22	72
RR 111	61.82	0.79	18.06	7.32	0.13	2.09	4.07	2.79	1.14	2.5	100.71	26	100
RR 114	62.02	0.81	17.61	7.30	0.13	2.08	4.13	2.72	1.13	2.5	100.43	26	90
RR 163	62.12	1.21	17.69	8.70	0.16	1.70	2.01	2.62	1.83	2.3	100.34	42	160
RR 169	61.87	0.80	16.52	6.64	0.04	2.74	0.83	0.08	4.93	3.9	98.35	28	140
RR 171	61.01	0.86	17.16	7.27	0.06	3.67	1.49	1.00	3.25	4.1	99.87	28	130

* Total iron expressed as Fe₂O₃.

Y and Zr in ppm; all other values in per cent.

Analytical methods used for data in Table 1-4-1.

Major elements by flame AAS. Precision for major and trace elements averages 5-10% relative error, depending on element concentration.

LOI calculated by heating predried samples to 1050°C for 2 hours.

Y and Zr by XRF.

Y and Zr analyses completed by X-Ray Laboratories Ltd., Don Mills, Ontario.

All other analyses in Table 1-4-1, completed at the B.C. Ministry of Energy, Mines and Petroleum Resources Laboratory, Victoria.

SAMPLE DESCRIPTIONS (for locations see Figure 1-4-2)

Dark colored volcanic and tuff samples, generally of basaltic composition.

RR 104 - Mafic, vesicular, pillowed volcanic.

RR 105 - Mafic, chloritized aquagene breccia.

RR 106 - Chloritized volcanic. Ophitic-textured plagioclase crystals up to 3 millimetres long; original pyroxenes replaced by chlorite.

RR 108 - Mafic volcanic. Ophitic-textured plagioclase (An₆₂) with chloritized amphibole; minor epidote and carbonate.

RR 109 - Coarse feldspar porphyry flow or subvolcanic intrusion. Plagioclase phenocrysts up to 5 millimetres long with minor hornblende.

RR 115 - Mafic, massive volcanic. Ophitic textures; altered amphibole.

RR 170 - Mafic, chloritized volcanic. Minor epidote.

RR 172 - Mafic crystal-lapilli tuff.

RR 174 - Crystal tuff. Abundant plagioclase crystals with minor amphibole.

RR 175 - Fresh crystal tuff. Abundant plagioclase with some augite crystals up to 5 millimetres long.

RR 176 - Chloritized crystal tuff. Abundant altered plagioclase with some augite and remnant amphibole crystals.

RR 177 - Chloritized crystal tuff. Minor epidote and carbonate.

RR 178 - Chloritized crystal tuff. Minor epidote.

RR 175D - Altered crystal tuff containing some augite crystals.

Pale colored volcanic and tuff samples, generally of andesitic composition.

RR 107 - Altered crystal tuff with minor veinlets of tremolite-actinolite.

RR 110 - Unaltered crystal-lapilli tuff. Fresh volcanic fragments up to 8 millimetres in diameter.

RR 111 - Silicious lapilli tuff. Chloritized volcanic fragments up to 5 millimetres in diameter.

RR 114 - Weakly hornfelsed lapilli tuff with abundant andesitic volcanic clasts and rare dacitic fragments.

RR 163 - Silicious, hornfelsed crystal tuff.

RR 169 - Silicious bedded crystal tuff. Minor pyrite.

RR 171 - Silicious crystal-lapilli tuff. Abundant fresh andesite volcanic fragments.

The appearance of the volcanic and tuffaceous rocks changes from north to south up the Brokenback Hill Formation stratigraphic sequence. In the southern, more basal section the volcanics are mafic, but higher in the sequence, toward Doctors Bay, they are pale grey coloured and generally more silicious (Figure 1-4-2); these pale rocks were originally mapped as dacites by Ray *et al.* (1985), but this work indicates they are andesites.

CHEMISTRY OF THE VOLCANIC ROCKS

Analytical results for the major oxides, yttrium and zirconium are shown in Table 1-4-1. The samples analysed comprise seven from volcanic flows and fourteen from volcaniclastic rocks. Fourteen of the samples represent mafic volcanics and tuffs from the lower part of the succession, and the remaining seven samples are paler coloured

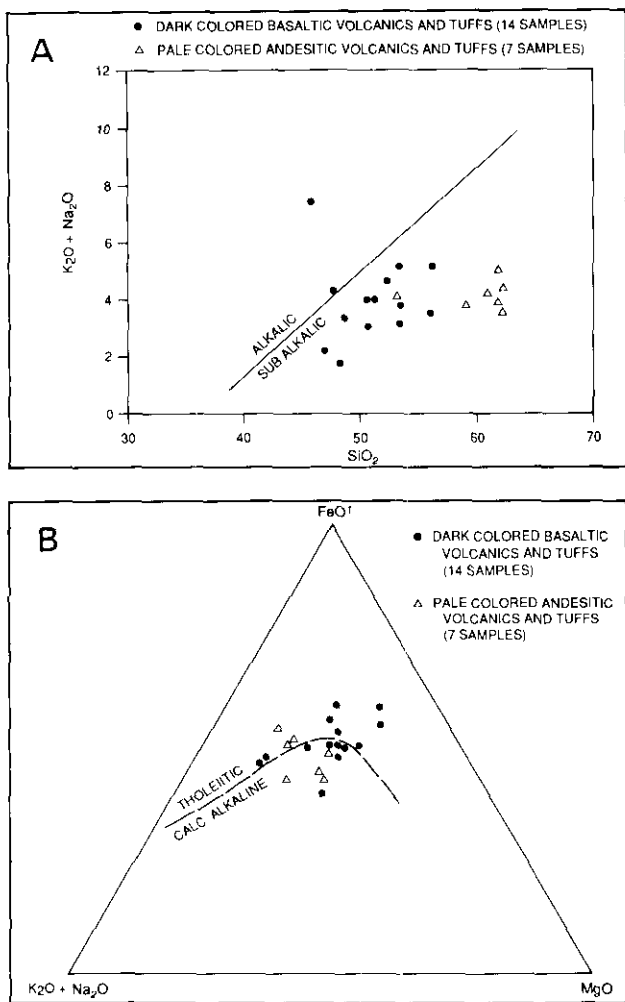


Figure 1-4-3. (A) Alkali versus silica plot (after Macdonald, 1968; Irvine and Barager, 1971) illustrating the subalkalic nature of volcanic and tuffaceous rocks, Brokenback Hill Formation. (B) AFM plot of the volcanic and tuffaceous rocks, Brokenback Hill Formation.

rocks in the upper part of the sequence (Figure 1-4-2; Table 1-4-1).

An alkali/silica plot of the data (Figure 1-4-3A) indicates the majority of the samples are subalkalic while an AFM plot (Figure 1-4-3B) suggests they are of tholeiitic to transitional calcalkaline affinity. Figure 1-4-4 shows that the mafic volcanics in the lower section of the Brokenback Hill Formation are subalkaline basalts while the pale grey rocks originally believed to be dacites (Ray *et al.*, 1985) are subalkalic andesites. The stratigraphic variation in the composition probably marks an original progressive temporal change from basaltic to andesitic volcanism due to differentiation. A discrimination plot (Figure 1-4-5) suggests the basaltic rocks are low-potassium island-arc tholeiites.

CONCLUSIONS

The Early Cretaceous Brokenback Hill Formation on the west side of Harrison Lake contains two compositional

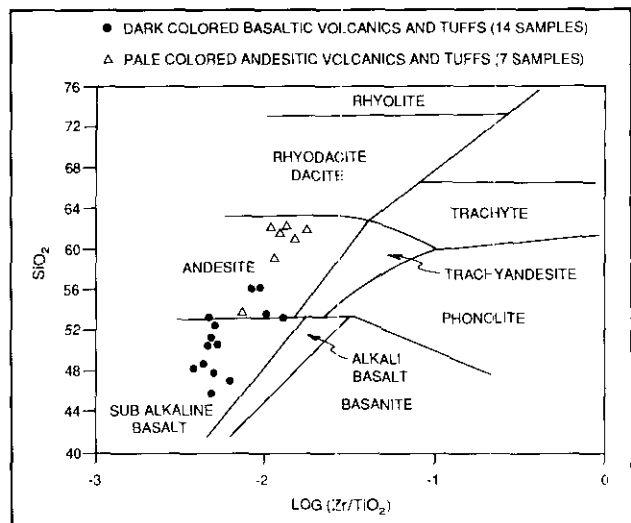


Figure 1-4-4. Plot of SiO₂ versus log(Zr/TiO₂) (after Floyd and Winchester, 1978) illustrating the subalkaline basaltic and andesitic compositions of the volcanic and tuffaceous rocks, Brokenback Hill Formation.

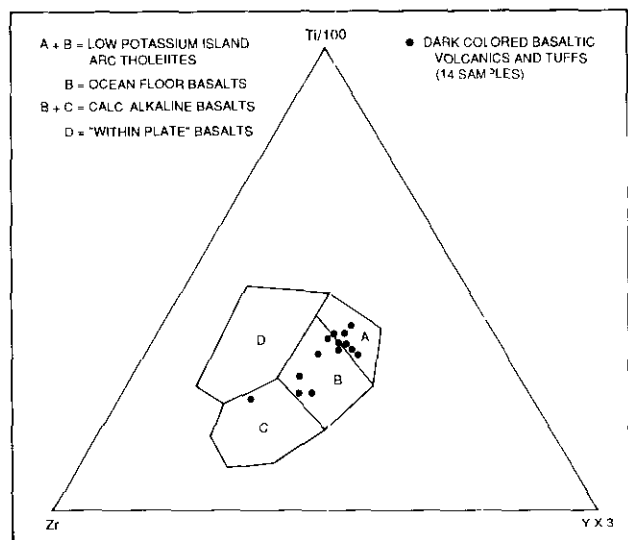


Figure 1-4-5. Zr-Ti-Y plot (after Pearce, 1975) of the volcanic and tuffaceous rocks, Brokenback Hill Formation.

suites of volcanic rocks. The lower part of the formation is dominated by mafic, subalkaline basalts; they largely represent low-potassium island-arc tholeiites that were probably erupted in an island-arc environment. Higher in the formation, volcanic flows are subordinate to tuffs and sediments. These volcanics, which were previously incorrectly described as dacites, are subalkaline andesites of transitional tholeiitic to calcalkaline affinity. The change up the succession from basalt to andesite probably reflects volcanic differentiation during arc volcanism.

ACKNOWLEDGMENTS

The following are thanked for their assistance: S. Coombes, G. Nagy, P. Desjardins, B.N. Church, M.A. Fournier, J.M. Journeay, the management, staff and associates of Rhyolite Resources Inc., including J. Stewart and P. Dasler, and the staff of the Ministry of Energy, Mines and Petroleum Resources Laboratory, Victoria.

REFERENCES

- Arthur, A.J. (1986): Stratigraphy along the West Side of Harrison Lake, Southwestern British Columbia; in Current Research, Part B, *Geological Survey of Canada*, Paper 86-1B, pages 715-720.
- Crickmay, C.H. (1925): The Geology and Paleontology of the Harrison Lake District, British Columbia, together with a General Review of the Jurassic Faunas and Stratigraphy of Western North America; unpublished. Ph.D. thesis, *Stanford University*, 140 pages.
- Crickmay, C.H. (1930): The Structural Connection between the Coast Range of British Columbia and the Cascade Range of Washington; *Geological Magazine*, Volume 67, pages 482-491.
- Floyd, P.A. and Winchester, J.A. (1978): Identification and Discrimination of Altered and Metamorphosed Volcanic Rocks Using Immobile Elements; *Chemical Geology*, Volume 21, pages 291-306.
- Irvine, T.N. and Baragar, W.R.A. (1971): A Guide to the Chemical Classification of the Common Volcanic Rocks; *Canadian Journal of Earth Sciences*, Volume 8, pages 523-547.
- Journeay, J.M. and Csontos, L. (1989): Preliminary Report on the Structural Setting along the Southeast Flank of the Coast Belt, British Columbia; in Current Research, Part E, *Geological Survey of Canada*, Paper 89-1E, pages 177-187, 1989.
- Lynch, J.V.G. (1990): Geology of the Fire Lake Group, South East British Columbia; in Current research, Part E, *Geological Survey of Canada*, Paper 90-1E, pages 197-205.
- MacDonald, G.A. (1968): Composition and Origin of Hawaiian Lavas; *Geological Society of America*, Memoir 116, pages 477-522.
- Monger, J.W.H. (1970): Hope Map-area, West Half (92H W1/2), British Columbia; *Geological Survey of Canada*, Paper 69-47, 75 pages.
- Monger, J.W.H. (1986): Geology between Harrison Lake and Fraser River, Hope Map Area, Southwestern British Columbia; in Current Research, Part B, *Geological Survey of Canada*, Paper 86-1B, pages 699-706.
- Pearce, J.A. (1975): Basalt Geochemistry Used to Investigate Past Tectonic Environments on Cyprus; *Tectonophysics*, Volume 25, pages 41-67.
- Ray, G.E., Coombes, S. and White G. (1984): Harrison Lake Project (92H/5, 12; 92G/9); *B.C. Ministry of Energy, Mines and Petroleum Resources*, Geological Fieldwork 1983, Paper 1984-1, pages 42-53.
- Ray, G.E., Coombes, S., MacQuarrie, D.R., Niels, R.J.E., Shearer, J.T. and Cardinal, D.G. (1985): Precious Metal Mineralization in Southwestern British Columbia; *Geological Society of America*, Field Trip 9, Guidebook, pages 9-1 to 9-31.
- Roddick, J.A. (1965): Vancouver North, Coquitlam and Pitt Lake Map-area, British Columbia; *Geological Survey of Canada*, Memoir 335, 276 pages.
- Urabe, T., Scott, S.D. and Hattori, K. (1983): A Comparison of Footwall-rock Alteration and Geothermal Systems beneath some Japanese and Canadian Volcanogenic Massive Sulphide Deposits; *Economic Geology*, Monograph 5, pages 345-364.
- Watanabe, R.Y. (1974): Seneca Deposit, an Example of Kuroko Mineralization; *Geological Association of Canada*, Cordilleran Section, Program and Abstracts, page 2.
- Wheeler, J.O. and McFeely, P. (1987): Tectonic Assemblage Map of the Canadian Cordillera; *Geological Survey of Canada*, Open File 1565.

PRELIMINARY GEOLOGY AND MINERAL POTENTIAL OF THE CASCADE RECREATION AREA (92H/2, 3, 6, 7)

By H.R. Schmitt and G.G. Stewart

KEYWORDS: Regional geology, Cascade Recreation Area, mineral potential, Methow basin, Hozameen fault, Dewdney Creek Formation, geochemistry, veins, skarns.

INTRODUCTION

The Cascade Recreation Area was created in 1987 to preserve wilderness and heritage recreation opportunities in 167 square kilometres of the northern Cascade Mountains. The area encompasses the headwaters of the Tulameen, Snass and Skaist rivers in the Hozameen Ranges, 30 kilometres southeast of Hope and is bordered by Manning Provincial Park on the southeast and Skagit Valley Recreation Area on the south (Figure 1-5-1). The Recreation Area contains parts of several provincially significant heritage trails, including the 1858 Whatcom Trail and the 1860 Dewdney Trail. Present resource use of the area includes backcountry hiking, grazing and trail riding.

In 1990, a mineral potential study of the Cascade Recreation Area was begun, to provide government and industry with mineral resource information prior to further time-limited exploration and decisions regarding suitability for park status. The study is modelled after the methodologies developed by McLaren (1990) in the Chilko Lake area and is the first government-sponsored mineral potential study of a Section 19 Recreation Area.

The 1990 field project consisted of examining the regional geology, a geochemical drainage survey over the entire Recreation Area, and limited geological mapping at 1:20 000 scale in the Punchbowl Lake–Turnbull Creek area. Mineralized and unmineralized rocks, additional drainage-sediment samples, and macrofossils were collected for mineral potential and geological interpretation.

The Giant Copper (AM and Invermay) copper-gold-silver-molybdenum, Treasure Mountain silver-lead-zinc, and Ladner Creek gold properties are hosted by rocks known to extend into the Recreation Area. Despite considerable regional mineral exploration, the area received little exploration attention until the discovery of gold-silver-copper mineralization in the Punch Bowl Creek watershed in 1984 by Mr. R. Rabbit, while prospecting for the source of placer gold in the upper Tulameen River.

In 1986, the provincial Wilderness Advisory Committee (1986) studied the initial 410 square kilometre Cascade Wilderness proposal, and recommended creation of the 167 square kilometre Cascade Recreation Area. Subsequently, a mineral and placer no-staking reserve was established over the Recreation Area to prohibit further mineral exploration and mine development, including exploration on existing mineral claims. It is anticipated that the Recreation Area will be re-opened to mineral exploration, following completion of this government-sponsored mineral potential study as required under Section 19 of the *Mineral Tenure Act*.

REGIONAL SETTING AND PREVIOUS WORK

The Cascade Recreation Area is situated in the northern Cascade belt between the Coast plutonic complex to the west and the Intermontane Belt to the east. It is underlain primarily by the Methow basin, a fault-bounded, northwest-trending sequence of Lower Jurassic to Upper Cretaceous sedimentary and volcanic rocks (Jeletzky and Tipper, 1968; Coates, 1974) that records the progressive evolution of a back-arc to nonmarine basin (Davis *et al.*, 1978; Anderson, 1976; Ray, 1990). Methow basin stratigraphy can be correlated with the Tyaughton trough in the Chilcotin Mountains (Jeletzky and Tipper, 1968; Kleinspehn, 1985) and with other Mesozoic sedimentary-volcanic successions along the Coast-Intermontane boundary.

The Methow basin is bounded on the west by the Hozameen fault, which separates the basin from the Paleozoic Hozameen complex of the Bridge River Terrane, and on the east by the Pasayten fault which separates it from the Cretaceous Eagle plutonic complex of Quesnellia Terrane (Monger *et al.*, 1982; Monger, 1989; Greig, 1983;

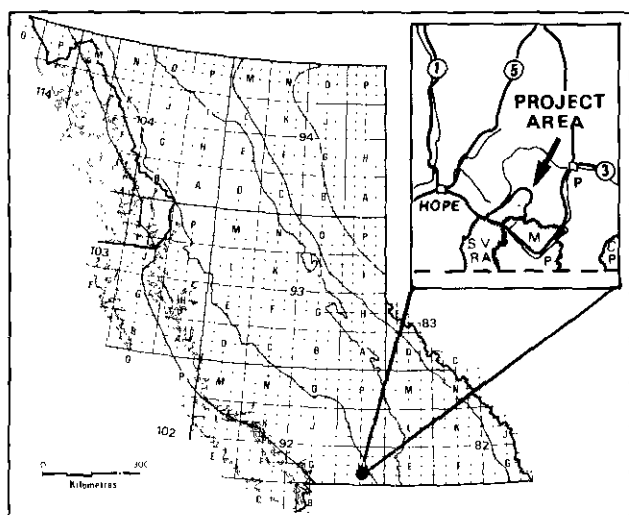


Figure 1-5-1. Location of Cascade Recreation Area, NTS 92H/2,3,6 and 7, in relation to Hope, Princeton (P), Skagit Valley Recreation Area (SVRA), Manning Provincial Park (MP), and Cathedral Provincial Park (CP).

LEGEND

TERTIARY



GRANODIORITE (NPP - NEEDLE PEAK PLUTON, MOP - MOUNT OUTRAM PLUTON, GB - CHILLIWACK BATHOLITH)

LATE OLIGOCENE TO EARLY MIOCENE



COQUIHALLA FORMATION INTERMEDIATE FELSIC PYROCLASTICS AND FLOWS

EOCENE



PRINCETON GROUP

INTERMEDIATE FLOWS, VOLCANICLASTICS, ES SANDSTONE, CONGLOMERATE, ARGILLITE

CRETACEOUS

LATE EARLY, EARLY LATE CRETACEOUS



PASAYTEN GROUP

NONMARINE SANDSTONE, CONGLOMERATE, ARGILLITE, MINOR RED BEDS, TUFF

EARLY AND MIDDLE CRETACEOUS



JACKASS MOUNTAIN GROUP

SANDSTONE, ARGILLITE, POLYMYCTIC CONGLOMERATE

JURASSIC

LATE JURASSIC AND EARLY CRETACEOUS



EAGLE PLUTONIC COMPLEX

GRANODIORITE, GNEISS, AMPHIBOLITE, MUSCOVITE BIOTITE GRANITE, MONZONITE, DIORITE, PEGMATITE

LATE JURASSIC



THUNDER LAKE SEQUENCE, SANDSTONE, CONGLOMERATE, ARGILLITE

EARLY AND MIDDLE JURASSIC



LADNER GROUP

ARGILLITE, SLATE, SILTSTONE, TUFF



DEWDEY CREEK FORMATION OF LADNER GROUP: VOLCANIC SANDSTONE AND ARGILLITE, TUFFACEOUS SILTSTONE, WACKE, MAFIC TO INTERMEDIATE VOLCANIC FLOW, BRECCIA, RARE LIMESTONE (ON FIGURE 1-XX-3, JGV - COARSE ANDESITE BRECCIA, AGGLOMERATE AND FLOWS; JDC - MASSIVE VOLCANIC-PEBBLE CONGLOMERATE AND TUFFACEOUS SANDSTONE)

TRIASSIC AND/OR JURASSIC



TULAMEEN COMPLEX

ULTRAMAFICS, GABBRO, SYENODIORITE

LATE TRIASSIC



NICOLA GROUP

MAFIC TO FELSIC VOLCANIC FLOWS, PYROCLASTICS, AND RELATED SEDIMENTS

TRIASSIC



ULTRAMAFIC ROCK, SERPENTINITE, GABBRO

PERMIAN TO JURASSIC



HOZAMEEN COMPLEX

UNDIFFERENTIATED CHERT, PELITE, BASALT, MINOR LIMESTONE, GABBRO AND ULTRAMAFIC ROCK

SYMBOLS

Geological boundary (defined, approximate)	
Fault (defined, approximate, minor)	
Thrust fault, teeth on overthrust plate	
Fold axis and form	
Bedding, foliation	
Glacial striae	
Mine or significant deposit (LC: Ladner Creek Au; E: Emancipation Au; TM: Treasure Mountain Ag-Pb-Zn; GC: Giant Copper Cu-Au-Mo)	
Mineral occurrence (Figure 1-5-3)	
Macrofossil site	
Park or Recreation Area boundary	

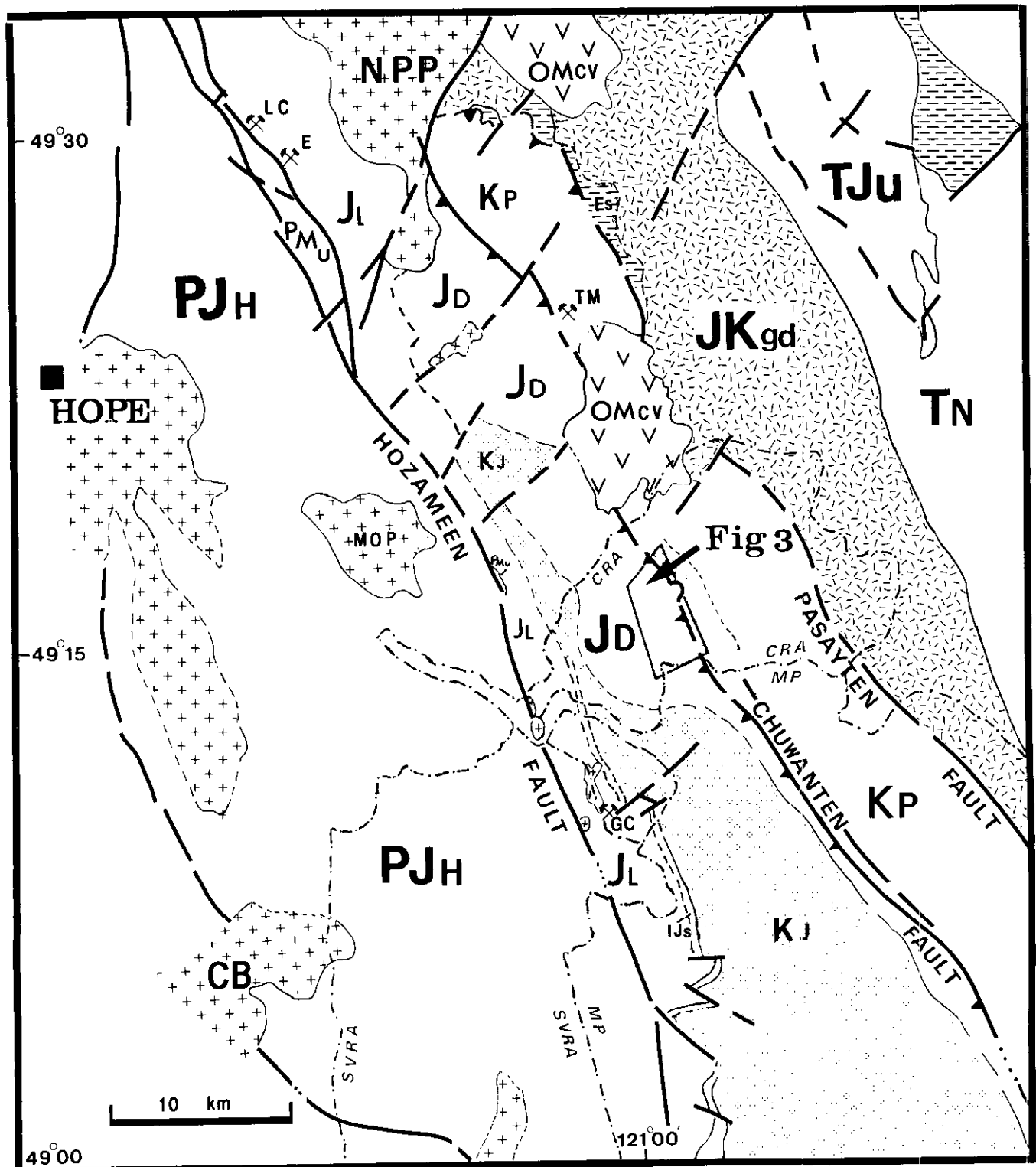


Figure 1-5-2. Regional geological setting of the Cascade Recreation Area, modified from Monger (1989) and O'Brien (1986). Methow basin lies between Hozameen and Pasayten faults and includes units JL, JD, KJ, and KP. Bridge River Terrane lies west of the Hozameen fault, Quesnellia Terrane lies east of the Pasayten fault. LC - Ladner Creek (Au); E - Emancipation (Au); TM - Treasure Mountain (Ag,Pb,Zn); GC - Giant Copper (Cu,Au,Mo). See text for description of units.

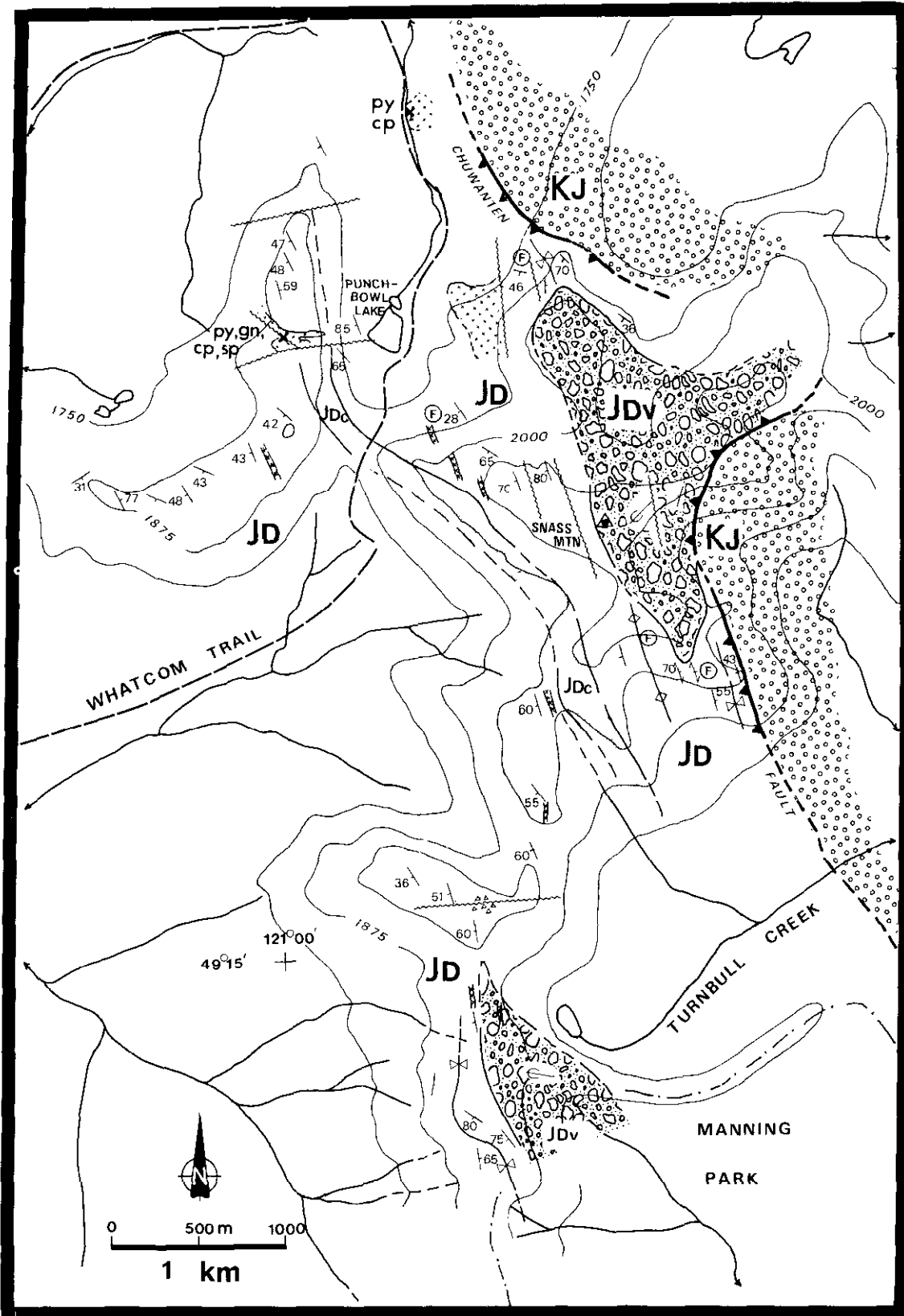


Figure 1-5-3. Detailed geology of the Snass Mountain area. See text for description of units.

McGroder and Miller, 1989: Figure 1-5-2). Oligocene to Miocene volcanic rocks of the Coquihalla Formation unconformably overlie the Methow basin and Eagle plutonic complex along the northern margin of the Recreation Area (Berman and Armstrong, 1980). A thin wedge of Eocene clastic rocks overlies the Eagle plutonic complex in places along the Pasayten fault. Tertiary plutons, dikes and sills intrude most rock types in the region.

The central part of the Methow basin is occupied by the northwest-trending Chuwanten fault, along which Middle to Lower Jurassic Dewdney Creek Formation is thrust eastwards onto Early to early Late Cretaceous Jackass Mountain and Pasayten groups (Coates, 1974; O'Brien, 1986). Late Cretaceous to Early Tertiary transcurrent movement along the Fraser River–Straight Creek fault system resulted in the development of a complex system of northeast-trending horsts, grabens and normal faults (Monger, 1985).

The earliest geological investigations were conducted by Lt. Palmer in 1861 and G. M. Dawson in 1877 along the Dewdney Trail (Cairnes, 1924). Geological mapping in the Recreation Area is limited to 1:50 000-scale studies of Cairnes (1924, 1944) along the north and west boundary, and Coates (1974) and O'Brien (1986) along the south and southeast boundary. Monger (1989) provides the most recent regional compilation at 1:250 000 scale. Recent metallogenic studies by Ray (1990) on geology and gold deposits of the Coquihalla gold belt and Hozameen fault system, by Meyers and Hubner (1990) at the Treasure Mountain silver-lead-zinc deposit, and by Wilton and Pfeutzenreuter (1990) at the Giant Copper deposit, provide important mineral-potential analogues.

Regional geochemical drainage-sediment data (Geological Survey of Canada Open File 865; B.C. Regional Geochemical Survey 07), and Geological Survey of Canada regional aeromagnetic survey data (Maps 8529G, 8530G, 8533G and 8534G) cover the study area at reconnaissance scales.

STRATIGRAPHY

Permian to Miocene rocks in the Cascade Recreation Area strike northwest, parallel to the axis of the Methow basin, and are divisible into five major units. Mapping in 1990 (Figure 1-5-3) concentrated on a 15 square kilometre area west of the Chuwanten fault, primarily in Jurassic strata.

HOZAMEEN COMPLEX – UNIT PJH

The Hozameen complex is exposed adjacent to the southwesternmost part of the area, north of the Sumallo River and west of the Hozameen fault. The Hozameen complex is a tectonically deformed, oceanic assemblage consisting of chert, argillite, greenstone and minor limestone (McTaggart and Thompson, 1967; Monger, 1970) of Permian to mid-Jurassic age (Haugerud, 1985). It represents a southern, faulted extension of the Bridge River complex (Scharizza *et al.*, 1989), which together comprise the Bridge River Terrane (Potter, 1986).

LADNER GROUP – UNITS JL, JD

The Ladner Group rocks (Cairnes, 1944) of Early to Middle Jurassic age are the oldest marine clastic sediments of the Methow basin. Ray (1986) suggests a total thickness of 1500 metres for the group. Ladner sediments are exposed in two parallel, northwest-striking belts between the Hozameen fault on the west and Chuwanten fault on the east. The belts are separated by the Early to late Early Cretaceous Jackass Mountain Group (Monger, 1989).

The Ladner Group consists of a lower, marine clastic sequence (Unit JL) recording a period of tectonic quiescence, and an upper, generally conformable sequence of coarser, volcanic-rich sediments, breccia and minor flows represented by the Dewdney Creek Formation (Unit JD) which record the onset of regional volcanic activity. The lower, undivided sequence comprises lower Pleinsbachian to Bajocian argillite, siltstone and subordinate tuffaceous siltstone, wacke and conglomerate (O'Brien, 1986; Ray, 1986). It is exposed along the east side of the Hozameen fault where it underlies the west boundary of the Cascade Recreation Area near Mount Dewdney (Monger, 1989) outside the area mapped in 1990.

DEWDNEY CREEK FORMATION – UNIT JD

The upper part of the Ladner Group is represented by the Toarcian to Bajocian Dewdney Creek Formation (O'Brien, 1986, Coates, 1974). In the Recreation Area, Dewdney Creek Formation dominates the east and west belts of the Ladner Group (O'Brien, 1986; Monger, 1989).

During 1990 fieldwork, over 2000 metres of Dewdney strata west of the Chuwanten fault, from Punchbowl Lake southeast to Turnbull Creek (Figure 1-5-3), were examined. These rocks are lithologically diverse and include tuffaceous siltstones, sandstones and pebble conglomerates, crystal and crystal-lithic tuff, argillite, coarse volcanic conglomerate, agglomerate and breccia, intermediate volcanic flows, rare limestone, and calcareous siltstone. Rocks are thinly laminated to thickly bedded and are commonly well indurated and massive. Dark green to dark brown coloration dominates although there are local pale buff to grey-black colour variants. Argillites and pyritic tuffaceous units display prominent rusty weathering. Graded bedding, cross-bedding, ball-and-pillow, flame, and rip-up clast features were widely observed in finer grained strata. These features mostly indicated stratigraphic tops to the southwest. Deformation is manifest at the outcrop scale as kink banding, chevron and open undulating folds, as well as larger southeast-plunging isoclinal folds.

Much of the section is dominated by alternating thinly laminated tuffaceous siltstone and argillite interbedded with volcanic sandstone and pebble conglomerate. Plate 1-5-1 shows a typical turbiditic D-E Bouma sequence (Walker, 1984) 1.5 kilometres southwest of Punchbowl Lake.

A massive volcanic-pebble conglomerate (Unit JDc), and a massive andesitic breccia and agglomerate with subordinate intermediate volcanic flows (Unit JDv) comprise two distinct mappable units. The pebble conglomerate is characterized by resistant cliff-forming beds, 50 to 100 metres



Plate 1-5-1. Dewdney Creek Formation (Unit JD): interbedded tuffaceous siltstone, sandstone and argillite showing D-E Bouma sequence and undulating folds. Minor fold below hammer plunges into hill. Located 1.5 kilometres southwest of Punchbowl Lake.

thick, extending over a strike length of more than 4 kilometres. The andesitic volcanics crop out west of the Chuwanten fault, generally north of Snass Mountain, and comprise primarily breccia and agglomerate with angular to subangular fragments up to 0.8 metre across, and lesser andesitic flows and volcanic conglomerate with subrounded clasts less than 10 centimetres in diameter, and rare limestone. Locally, the underlying tuffaceous sediments coarsen upwards into the coarse volcanic sequence; elsewhere the coarse breccia unconformably overlies the finer grained strata.

The Dewdney Creek Formation is intruded by a variety of aplite, diorite and gabbro dikes and sills, typically less than 2 metres thick and rarely exposed for more than 20 metres along strike.

Although the Dewdney Creek Formation contains thick sections of unfossiliferous strata, several intervals contain an abundant ammonite and bivalve fauna.



Plate 1-5-2. Jackass Mountain Group (Unit KJ): imbricated polymictic conglomerate adjacent to the Chuwanten fault north of Snass Mountain. Cobbles are mostly derived from Eagle plutonic complex (Unit JKgd).

JACKASS MOUNTAIN GROUP – UNIT KJ

The Jackass Mountain Group comprises Hauterivian to Albian marine sandstone, polymictic conglomerate, volcanic lithic wacke and pelite. It is exposed in a narrow belt separating the two Ladner Group belts (Monger, 1989). Jackass Mountain strata were mapped in this study east of the Chuwanten fault, east of Punchbowl Creek and east and south of Snass Mountain, where they are overthrust by the Dewdney Creek Formation. Along the Chuwanten fault, the Jackass Mountain strata consist of massive polymictic conglomerate with imbricated and well-rounded granitic cobbles (Plate 1-5-2), and minor interbedded light grey sandstone.

PASAYTEN GROUP – UNIT KP

The upper Albian to Cenomanian Pasayten Group (Rice, 1947; Coates, 1974) represents a nonmarine succession of

predominantly sandstone, siltstone, minor conglomerate and shale which underlies the eastern part of the Methow basin. These rocks were not mapped during the 1990 field area.

COQUIHALLA FORMATION – OMCv

Oligocene to Miocene calcalkaline intermediate to acid pyroclastics, flows and intrusions unconformably overlie and crosscut the Dewdney Creek Formation and the Pasayten Group along the northern boundary of the Recreation Area. These rocks belong to the Coquihalla Formation (Monger, 1989) and were recently studied near Coquihalla Mountain by Berman and Armstrong (1980), who concluded that the volcanics are coeval with the Pemberton volcanic belt.

INTRUSIVE ROCKS

UNIT PMu

Ultramafic rocks consisting of gabbro and serpentinite, related to the Coquihalla serpentinite belt (Ray, 1986; 1990) are exposed as a narrow fault-bounded sliver along the Hozameen fault north of the Sumallo River. Gabbro dikes and sills up to 3 metres wide and several metres long intrude the Dewdney Creek Formation in several locations.

EAGLE PLUTONIC COMPLEX – UNIT JKGD

The Cretaceous Eagle plutonic complex underlies the northeastern part of the Recreation Area east of the Pasayten fault. Greig (1988) mapped the complex to the north and recognized three major units: a western muscovite granite and an eastern foliated to gneissic granodiorite, separated by a heterogeneous gneiss. Although these rocks were not examined, numerous glacial erratics derived from the complex were encountered at elevations over 2000 metres, indicating a minimum of 10 kilometres southwest-directed ice transport.

TERTIARY INTRUSIONS – UNITS MGD, Mb

Tertiary stocks, plugs, dikes and sills are widespread through the region. A Miocene granodiorite plug dated at 87 Ma (Coates *in* Wanless *et al.*, 1967) intrudes the Hozameen fault, Hozameen complex, Ladner Group and ultramafic rocks where the fault crosses Highway 3 in the southwestern corner of the Recreation Area.

Near Punchbowl Lake, several aplite and diorite dikes invade Tertiary(?) brittle faults, and occur as sills and dikes in Dewdney Creek strata. A granodiorite intrusion of unknown dimensions is exposed in lower Punchbowl Creek where it is associated with disseminated pyrite and chalcopyrite mineralization.

South of Punchbowl Lake, and in the headwall above upper Turnbull Creek, several gabbro and diorite dikes and sills intrude the Dewdney Creek Formation. Narrow zones

of hornfelsing and pyritization occur locally at the contacts with argillaceous sediments.

GEOCHEMISTRY

A drainage-sediment (moss-mat) and water geochemical survey was conducted over the entire Recreation Area, under contract to MPH Consulting Ltd. A total of 74 sites were sampled, for a site density of 1 per 2.3 square kilometres. Standard RGS collection and quality-control methods were used. Sediment analyses for a wide range of elements, currently in progress, will be used to guide further mineral-potential mapping and interpretation.

MINERAL OCCURRENCES

Five mineral occurrences are known in the Recreation Area and are briefly described below. Information on two previously undocumented occurrences will be added to MINFILE.

ULTRAMAFIC-HOSTED GOLD AND NICKEL-BEARING VEINS:

Forks (092HSW040): Nickeliferous pyrrhotite occurs in serpentinite along the Hozameen fault north of Highway 3 in the southwest corner of the Recreation Area.

SKARNS

BB (Rainbow) (092HSW042): Skarn and related vein mineralization occur along the contact of a Miocene quartz diorite and Hozameen greenstone and limestone. Mineralization consists of pyrite, arsenopyrite, sphalerite and minor chalcopyrite and galena, with variable concentrations of gold, silver, copper, zinc, lead and antimony.

GRANITE AND PEGMATITE-HOSTED MOLYBDENUM AND TUNGSTEN:

Granite Scheelite (092HSE101): Quartz veins in Eagle granodiorite and pegmatite reportedly contain molybdenite and scheelite.

MESOTHERMAL VEINS:

Punchbowl Claims: Southwest of Punchbowl Lake, quartz veins exposed along the contact between several diorite dikes and fine-grained clastics of the Dewdney Creek Formation, contain variable amounts of pyrite, galena, chalcopyrite and sphalerite. Several trenches are located near the ridgetop southwest of Punchbowl Lake, in the area of most intense mineralization and ankeritic alteration. In this mineralized area, a 3-metre-wide diorite dike shows minor right-lateral displacement along a splay of an east-trending fault. Cardinal

(1986a, b) and Kallock (1987) report concentrations of 770 ppm zinc, 720 ppm lead, 1100 ppm arsenic and 215 ppb gold in quartz veins from the occurrence. The occurrence was mapped and sampled in detail during 1990, and geochemical analyses are in progress.

Punchbowl Creek: Approximately 1 kilometre north of Punchbowl Lake, a poorly exposed hornblende diorite plug intrudes Dewdney Creek Formation argillite and tuffaceous siltstone in a deeply incised part of Punchbowl Creek. Pyrite and chalcopyrite occur in quartz veins and as disseminations and streaks along cleavage and fracture planes. Mineralization is exposed intermittently over a length of 100 metres along the creek. Several mineralized samples were collected to determine the trace element content. The areal extent of the intrusive rocks and their possible relationship to the nearby Chuwanten fault will be further examined during the 1991 field season.

SUMMARY: MINERAL POTENTIAL

The Cascade Recreation Area encompasses a thick succession of marine and nonmarine sedimentary and volcanoclastic rocks. These rocks record Early Jurassic to Late Cretaceous progressive restriction and infill of the Methow basin. The margins of the basin are delineated by the Hozameen fault on the west, which separates the basin from the Bridge River Terrane, and by the Pasayten fault on the east, against which Eagle plutonic complex rocks are juxtaposed. Accretionary tectonics have produced a system of major northwest-trending faults and Tertiary transtensional faults and associated intrusions. The varied depositional settings and complex structural history have created a variety of metallogenic environments.

The Chuwanten fault trends northwest through the area to Treasure Mountain and the Summit Camp, where it has provided the locus for intrusive and hydrothermal activity giving rise to numerous silver-lead-zinc vein deposits. Preliminary investigation of the Punchbowl Creek occurrences provides evidence that similar metallogenic environments may exist in the Cascade Recreation Area. Additional fieldwork will be carried out in this area in 1991.

In the southwest corner of the Recreation Area, a variety of base and precious metal skarn and vein deposits occur in a complex geological setting. A Miocene granodiorite has intruded the Hozameen fault zone, Hozameen greenstone and limestone, Ladner sediments, and ultramafic rocks. Mineralization in this area contains copper, zinc, gold, silver, tungsten, nickel, arsenic and antimony. The occurrences will be examined in the 1991 field season and the potential for discovering similar additional mineralization will be assessed.

The Eagle plutonic complex is exposed in a belt 1 to 4 kilometres wide along the eastern side of the Recreation Area. Recent mapping of the complex to the north indicates that the dominant rock types along its western margin are muscovite granite, monzonite and pegmatite. Molybdenum and tungsten prospects are recognized to the north in these rocks, and therefore potential also exists for discovery of

these commodities in the Recreation Area. There is largely untested potential for tin, fluorine and rare-earth elements in these rocks. Heavy-mineral drainage-sediment samples will be collected during the 1991 field program to further test these possibilities.

ACKNOWLEDGMENTS

The following individuals are thanked for their varied contributions to this project: G. Ralph and staff of the Ministry of Parks, Manning Park Zone, for their cooperation and hospitality during our fieldwork; H.P. Wilton, V.A. Preto, and J.W.H. Monger for discussions on regional geology; W. Jackaman and T. O'Niell, for directing the geochemical survey; and Valley Helicopters Ltd. in Hope for exemplary helicopter service.

REFERENCES

- Anderson, P. (1976): Oceanic Crust and Arc-trench Gap Tectonics in Southwestern British Columbia; *Geology*, Volume 4, pages 443-446.
- Berman, R.G. and Armstrong, R.L.A. (1980): Geology of the Coquihalla Volcanic Complex, Southwestern British Columbia; *Canadian Journal of Earth Sciences*, Volume 17, pages 985-995.
- Cairnes, C.E. (1924): Coquihalla Area, British Columbia; *Geological Survey of Canada*, Memoir 139, 187 pages.
- Cairnes, C.E. (1944): Hope; *Geological Survey of Canada*, Map 737A, 1:253 440.
- Cardinal, D.G. (1986a): Reconnaissance Geochemical and Geological Assessment Report on the Punch Bowl Claim Group, Similkameen and New Westminster Mining Divisions, NTS 92H/6E, 7W; *B.C. Ministry of Energy, Mines and Petroleum Resources*; Assessment Report 15146, 13 pages.
- Cardinal, D.G. (1986b): Reconnaissance Geochemical and Geological Assessment Report on the K.C.M. Claim Group, Similkameen and New Westminster Mining Divisions, NTS 92H/6E, 7W; *B.C. Ministry of Energy, Mines and Petroleum Resources*, Assessment Report 15212, 14 pages with maps.
- Coates, J.A. (1974): Geology of the Manning Park Area, British Columbia; *Geological Survey of Canada*, Bulletin 238, 177 pages.
- Davis, G.A., Monger, J.W.H. and Burchfield, B.C. (1978): Mesozoic Construction of the Cordilleran "Collage", Central British Columbia to Central California; in *Mesozoic Paleogeography of the Western United States*, D.G. Howell and K.A. McDougall, Editors, *Society of Economic Paleontologists and Mineralogists, Pacific Section*, Pacific Coast Paleogeography Symposium 2, pages 1 - 32.
- Greig, C.J. (1988): Geology and Geochronometry of the Eagle Plutonic Complex, Hope Map-area, Southwestern British Columbia; *Geological Survey of Canada*, in *Current Research*, Part E, Paper 88-1E, pages 177-183.

- Haugerud, R.A. (1985): Geology of the Hozameen Group and the Ross Lake Shear Zone, Maselpalik Area, North Cascades, Southwest British Columbia; *University of Washington*, unpublished Ph.D. thesis, 263 pages.
- Jeletzky, J.A. and Tipper, H.W. (1968): Upper Jurassic and Cretaceous Rocks of Taseko Lakes Map-area and their bearing on the Geological History of Southwestern British Columbia; *Geological Survey of Canada*, Paper 67-54, 218 pages.
- Kallock, P. (1987): Geological and Geochemical Investigation, Punch West, Punch East, KCM West and KCM East Mineral Claims, Snass Creek-Tulameen River Area, Hope, B.C., Similkameen and New Westminster Mining Divisions, NTS 92H/6E, 7W; *B.C. Ministry of Energy, Mines and Petroleum Resources*, Assessment Report 16279, 14 pages.
- Kleinspehn, K.L. (1985): Cretaceous Sedimentation and Tectonics, Tyaughton-Methow Basin, Southwestern British Columbia; *Canadian Journal of Earth Sciences*, Volume 22, pages 154-174.
- McGroder, M.F. and Miller, R.B. (1989): Geology of the Eastern North Cascades; in *Geologic Guidebook for Washington and Adjacent Areas*, N.L. Joseph *et al.*, Editors, *Washington Division of Geology and Earth Resources*, Information Circular 86, pages 97-118.
- McLaren, G.P. (1990): A Mineral Resource Assessment of the Chilko Lake Planning Area; *B.C. Ministry of Energy, Mines and Petroleum Resources*, Bulletin 81, 117 pages.
- McTaggart, K.C. and Thompson, R.M. (1967): Geology of part of the Northern Cascades in Southern British Columbia; *Canadian Journal of Earth Sciences*, Volume 4, pages 1199-1228.
- Meyers, R.E. and Hubner, T.B. (1990): Preliminary Geology of the Treasure Mountain Silver-Lead-Zinc Vein Deposit; *B.C. Ministry of Energy, Mines and Petroleum Resources*, Exploration in British Columbia 1989, pages 95-103.
- Monger, J.W.H. (1970): Hope Map-area, West-half, British Columbia; *Geological Survey of Canada*, Paper 69-47, 75 pages.
- Monger, J.W.H. (1985): Structural Evolution of the Southwestern Intermontane Belt, Ashcroft and Hope Map-areas, British Columbia; *Geological Survey of Canada*, in *Current Research*, Part A, Paper 85-1A, pages 349-358.
- Monger, J.W.H. (1989): Geology, Hope, British Columbia; *Geological Survey of Canada*, Map 41-1989, 1:250 000.
- Monger, J.W.H., Price, R.A. and Tempelman-Kluit, D.J. (1982): Tectonic Accretion and the Origin of the Two Major Metamorphic and Plutonic Belts in the Canadian Cordillera; *Geology*, Volume 10, pages 70-75.
- O'Brien, J. (1986): Jurassic Stratigraphy of the Methow Trough, Southwestern British Columbia; *Geological Survey of Canada*, in *Current Research*, Part B, Paper 86-1B, pages 749-756.
- Potter, C.J. (1986): Origin, Accretion, and Post-accretionary Evolution of the Bridge River Terrane, Southwestern British Columbia; *Tectonics*, Volume 5, pages 1027-1041.
- Ray, G.E. (1986): The Hozameen Fault System and Related Coquihalla Serpentine Belt of Southwestern British Columbia; *Canadian Journal of Earth Sciences*, Volume 23, pages 1022-1041.
- Ray, G.E. (1990): The Geology and Mineralization of the Coquihalla Gold Belt and Hozameen Fault System, Southwestern British Columbia; *B.C. Ministry of Energy Mines and Petroleum Resources*, Bulletin 79, 97 pages.
- Rice, H.M.A. (1947): Geology and Mineral Deposits of the Princeton Map-area, British Columbia; *Geological Survey of Canada*, Memoir 243.
- Schiarizza, P., Gaba, R.G., Glover, J.K. and Garver, J.I. (1989): Geology and Mineral Occurrences of the Tyaughton Creek Area (92O/2, 92J/15, 16); *B.C. Ministry of Energy, Mines and Petroleum Resources*, Geological Fieldwork 1988, Paper 1989-1, pages 115-130.
- Walker, R.G. (1984): Turbidites and Associated Coarse Clastic Deposits; in *Facies Models - Second Edition*, R.G. Walker, Editor, *Geoscience Canada*, pages 171-188.
- Wanless, R.K., Stevens, R.D., Lachance, G.R. and Edmonds, C.M. (1967): Age Determinations and Geological Studies, K-Ar Isotopic Ages, Report 7; *Geological Survey of Canada*, Paper 66-17.
- Wilderness Advisory Committee (1986): The Wilderness Mosaic; *B.C. Wilderness Advisory Committee*, 132 pages and 6 Appendices.
- Wilton, H.P. and Pfuetschenreuter, S. (1990): Giant Copper; *B.C. Ministry of Energy, Mines and Petroleum Resources*, Exploration in British Columbia 1989, pages 91-93.

NOTES

STRATIGRAPHY OF MESOZOIC ROCKS EAST OF PEMBERTON, BRITISH COLUMBIA, AND THE SETTING OF MINERAL SHOWINGS (92J/2, 7, 10)

By J.M. Riddell
University of Montana

KEYWORDS: Stratigraphy, Mesozoic, Lillooet Lake, roof pendant, correlations, Cadwallader Group, shear zone, felsic volcanics, volcanogenic massive sulphides.

INTRODUCTION

East of Pemberton, British Columbia (Figure 1-6-1), Mesozoic volcanic and sedimentary rocks form a northwest-striking pendant about 70 kilometres long and 10 to 30 kilometres wide that is almost entirely surrounded by rocks of the Coast plutonic complex (Woodsworth, 1977). During the 1989 field season, mapping in the southernmost part of this Mesozoic band, adjacent to Lillooet Lake, confirmed that a major north-northwest-striking fault cuts the pendant.

Triassic rocks, probably of the Cadwallader Group, lie to the east, Cretaceous Fire Lake Group rocks to the west (Riddell, 1990). The goals of this project for the 1990 field season were to trace the fault to the north through the pendant, to improve the map coverage east of the fault and to expand the map area to the north to compare the stratigraphy in the Lillooet Lake area to that near Tenquille Lake.

The major thrust fault can be traced through the Owl Creek valley, and probably extends through the topographic notch east of Mount Pauline (Figures 1-6-2 and 3).

The Triassic rocks throughout the expanded map area generally comprise a lower unit of massive basaltic and andesitic flows (Tr1) and unsorted lithic tuffs (Tr2), overlain

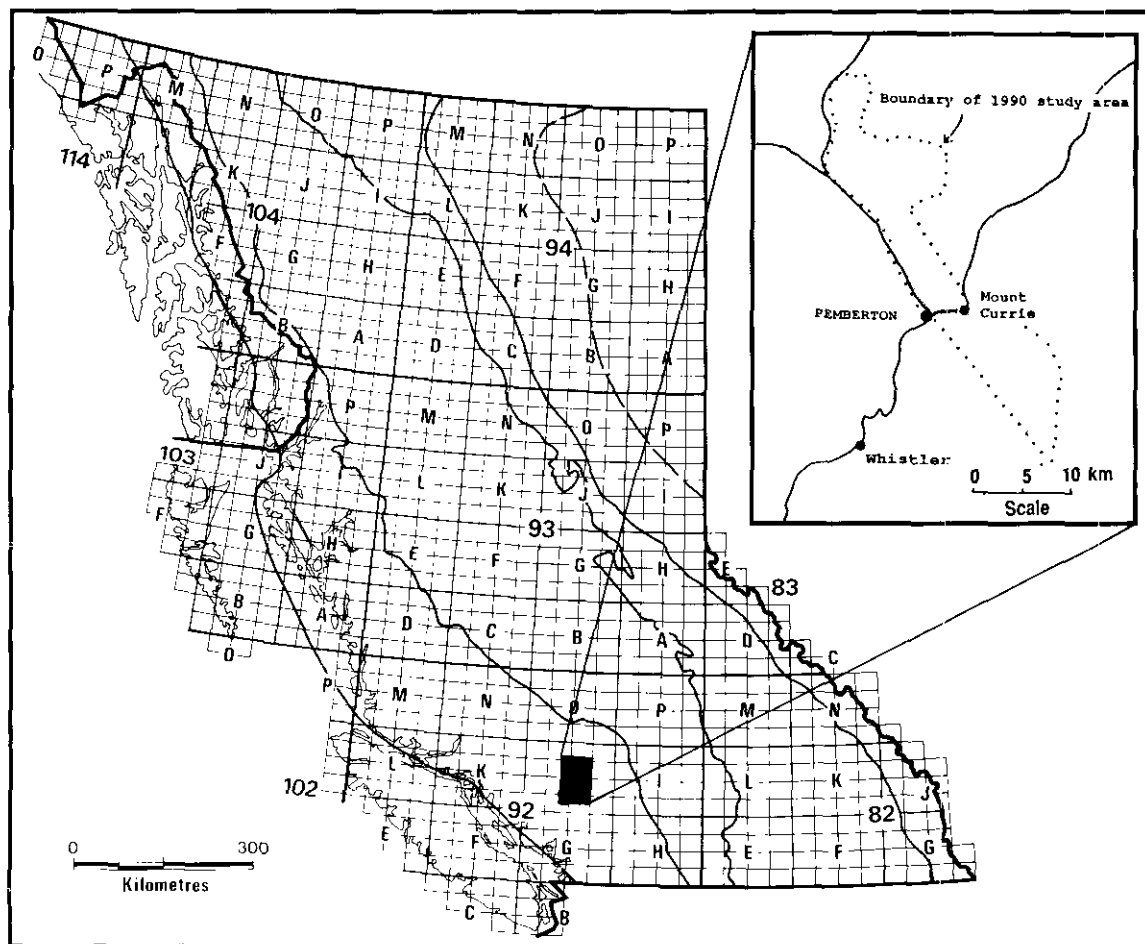


Figure 1-6-1. Location map.

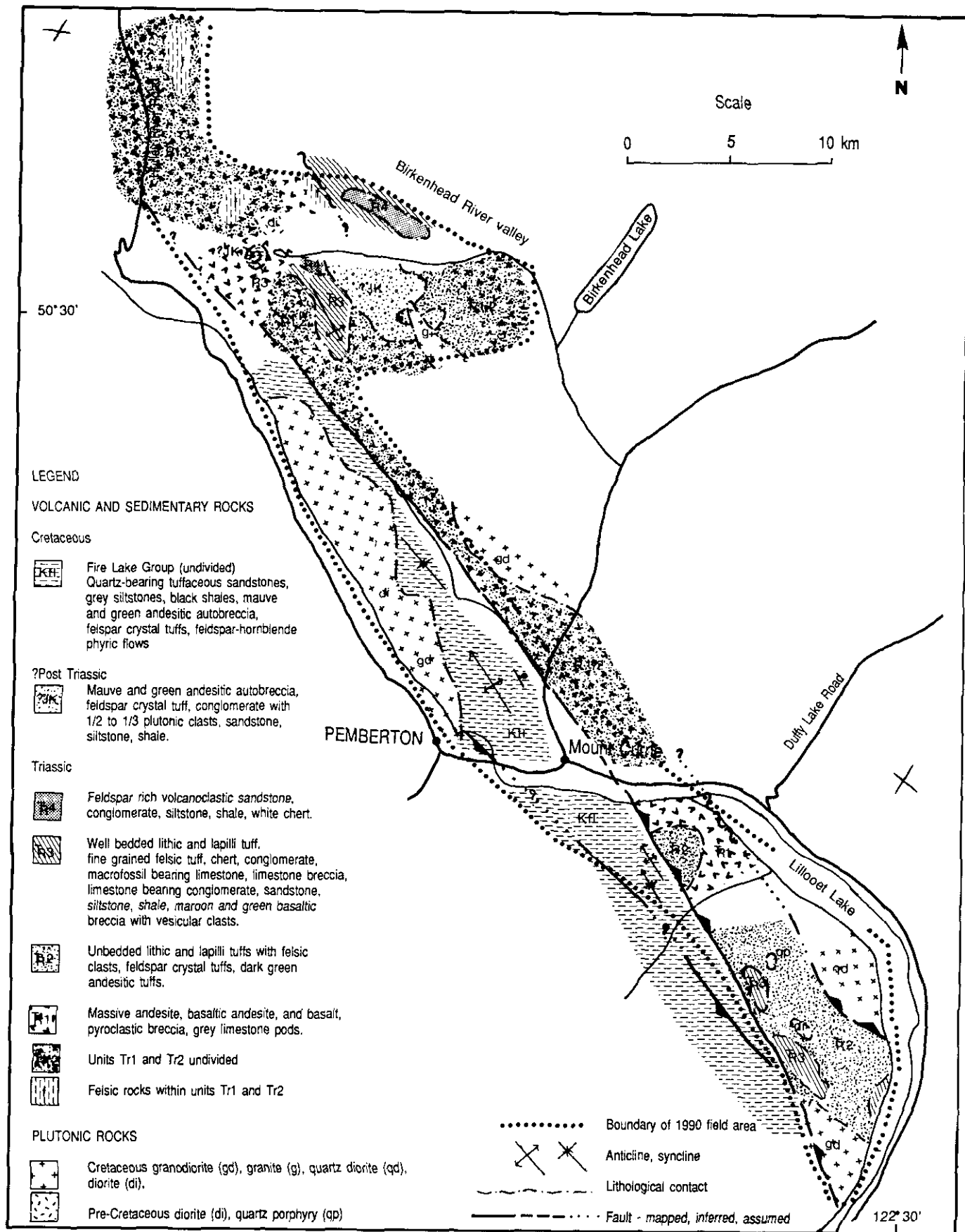


Figure 1-6-2. Geology map.

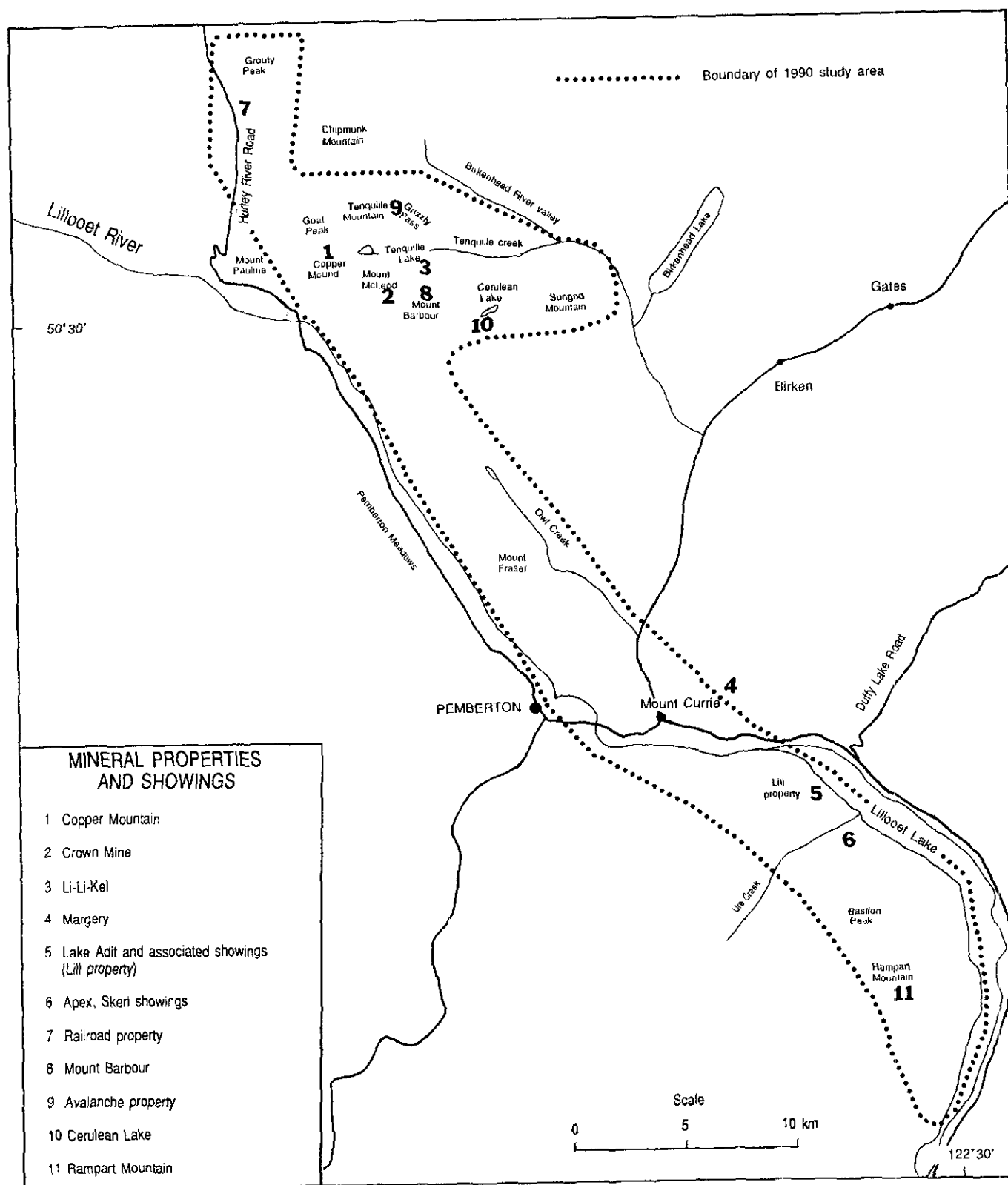


Figure 1-6-3. Place names and mineral showings in the Pemberton belt.

by a section of well-bedded tuffaceous and sedimentary rocks (Tr3). In some localities, a thin section of predominantly sedimentary rocks (Tr4) overlies Unit Tr3.

In the Tenquille Lake area, a relatively thin section of volcanic and sedimentary rocks sits unconformably on top of the rocks of the Triassic sequence. This section does not resemble rocks of the Cadwallader Group, and probably represents a younger overlap assemblage. If the age of this section can be determined, it will provide an upper constraint on the timing of accretion of the Triassic section.

TRIASSIC STRATIGRAPHY CORRELATION WITH THE CADWALLADER GROUP

Triassic rocks in the Pemberton belt have been mapped as Cadwallader Group (Cairnes, 1925; Roddick and Hutchison, 1973; Woodsworth, 1977). The validity of this correlation is still a matter of discussion. My observations in the Pemberton belt, especially in the Mount Barbour area south of Tenquille Creek, support the correlation of these

rocks with the Cadwallader section described by Rusmore (1985) in the Eldorado Creek area near Gold Bridge. There are, however, some significant differences between the two sections. Figure 1-6-4 compares the major stratigraphic components of the two sections. The important similarities between the sections are:

- A basal, massive, submarine mafic volcanic unit (the Pioneer Formation of the Cadwallader Group). Comparison of major and trace element analyses of mafic rocks from the Pemberton belt with those from Rusmore's study area shows that their chemical signatures are similar, and they could have formed within the same island arc (Schick, 1990).
- A transitional unit of mixed volcanic, volcanoclastic, and sedimentary rocks. Distinctive features common to the two sections include limestone beds containing Late Triassic microfossils and bivalve macrofossils (Woodsworth, 1977), felsic tuffs, a distinctive conglomerate with limestone clasts, and limestone breccias.

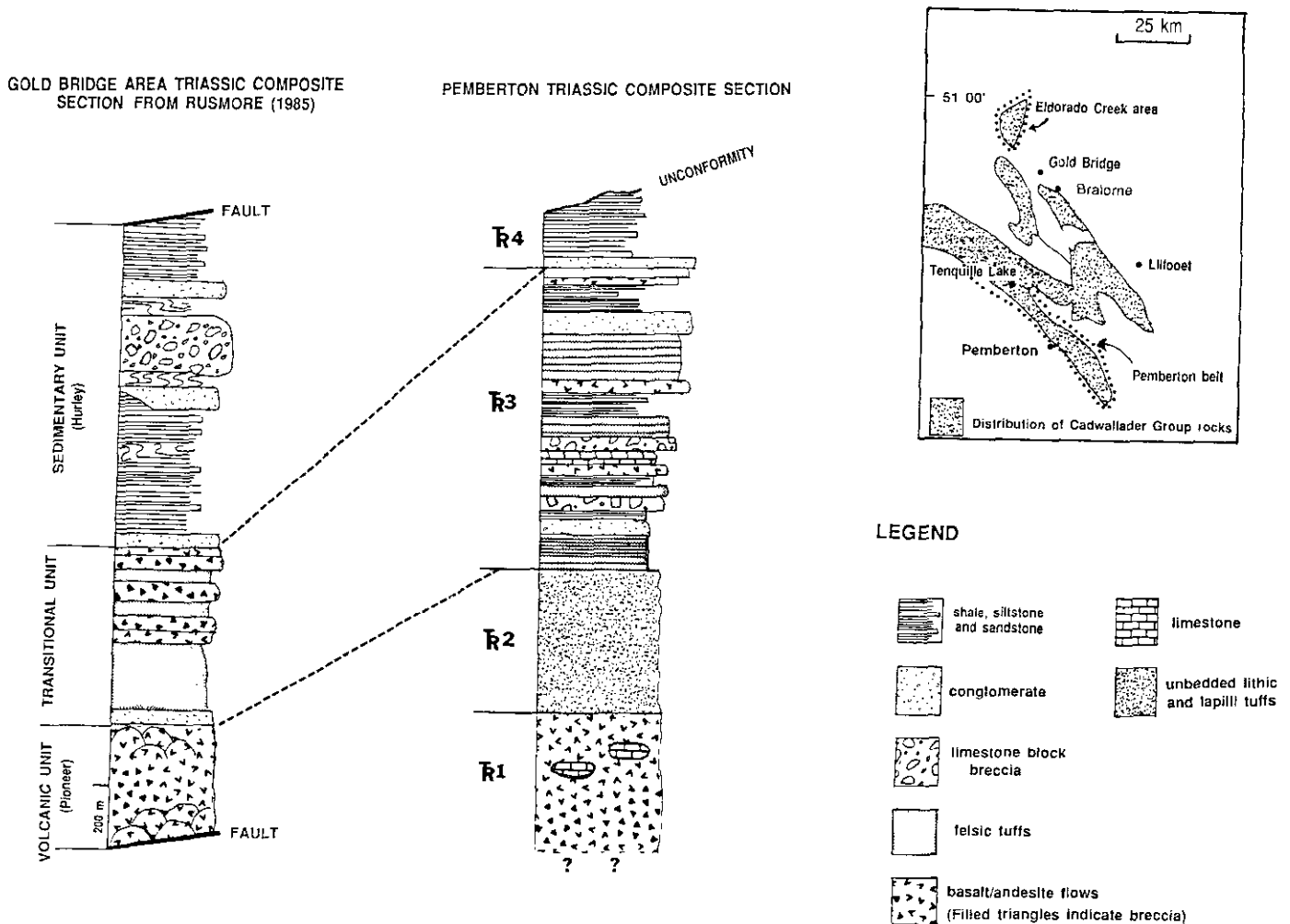


Figure 1-6-4. Composite Triassic sections from the Gold Bridge and Pemberton areas; Gold Bridge section from Rusmore (1985).

- A predominantly sedimentary unit at the top of the section (the Hurley Formation of the Cadwallader Group).

The most convincing evidence that the two sections are correlative lies in the striking similarities between Rusmore's "transitional unit" and the mixed bedded sequence (Tr3) of the Pemberton belt Triassic section. Most of Cairnes' (1937) observations of the Pioneer Formation in the Cadwallader valley near Bralorne accurately describe Units Tr1 and Tr2 of the Pemberton belt Triassic section. The two sections differ most significantly in that the Pemberton section contains a much greater volume of volcanoclastic rock, and a much smaller volume of purely sedimentary material than the Gold Bridge section. Also, the basal volcanic unit near Gold Bridge is dominantly basaltic and amygdaloidal, and often pillowed, whereas in the basal unit of the Pemberton Triassic section, andesite is dominant over basalt by volume, it is rarely amygdaloidal, and pillowed flows are absent. In the Pemberton section, isolated car-sized limestone pods are commonly found "floating" in the basal volcanic pile. Such pods are absent in the type Cadwallader section, and are more suggestive of stratigraphy in the Bridge River complex than of the Cadwallader Group.

THE PEMBERTON TRIASSIC COMPOSITE SECTION

The Pemberton Triassic section comprises four distinct mappable units (see Figure 1-6-4) but the idealized composite section is not preserved intact anywhere in the map area. There is wide variation with respect to both the internal stratigraphy of the units, and spatial relationships between them. For further discussion of this variation, the reader is referred to Riddell (1991).

MASSIVE BASALT AND ANDESITE (Tr1)

The lowermost, mafic volcanic unit is well exposed on the Lill property at the north end of Lillooet Lake, on the east side of the Owl Creek valley, below the 2000-metre elevation on Mount McLeod and Copper Mound, and in the bluffs of Finch Ridge west of the Grizzly Pass fault zone. This unit is characterized by massive, dark green basaltic andesite and lesser basalt flows, with common feldspar-porphyrific phases and abundant epidote clots and veinlets. Pyroclastic breccias with clasts 3 centimetres and smaller are common. Limestone pods 2 to 30 metres across are also present, and they are especially abundant in the Mount McLeod area. The massive nature of this unit makes it difficult to estimate its thickness. At Copper Mound, where the section is flat lying, it appears to be about 1000 metres thick. A belt of felsic rocks sits within this massive unit in the Goat Peak and Grouty Peak areas.

UNBEDDED TUFFACEOUS ROCKS (Tr2)

A thick sequence of unbedded lithic, lapilli and feldspar-crystal tuffs and fine andesitic tuffs lies above Unit Tr1. It is well exposed on the mountain above the Lill property, on the flank of the ridge west of Lillooet Lake, in the eastern

Owl Creek valley, and on the eastern flank of Sungod Mountain. Rocks in this unit are all rich in feldspar crystal fragments in the matrix. The fine andesitic tuffs are dark green on the fresh surface; the crystal, lapilli and lithic tuffs are pale green, and weather pale green or white. Clasts are subangular and are normally 3 to 4 centimetres across or smaller, but locally clasts twice this size are present. Andesitic and felsic volcanic fragments are the most common clast types in the lithic tuffs. Pale green chert, diorite and basalt clasts were found locally. Textures are best displayed on weathered surfaces. The lithic and lapilli tuffs tend to support a rusty coloured lichen that gives the rock a distinctive appearance in outcrop.

WELL-BEDDED MIXED VOLCANIC AND SEDIMENTARY ROCKS (Tr3)

The transition from massive lithic tuffs to well-bedded tuffs (without compositional change) marks the base of Unit Tr3. It is best exposed on the Mount Barbour ridge, or Bastion Peak and on Rampart Mountain. It comprises white and rusty weathering lithic and lapilli tuffs, macrofossil-bearing grey limestone beds, conglomerate, calcareous wackes rich in feldspar, grey siltstone and black shale, fine-grained felsic tuffs with cherty tops, limestone breccias, and mafic to intermediate flows. An outcrop of the distinctive limestone-clast 'Cadwallader' conglomerate described by Cairnes (1937) and Rusmore (1985) has been mapped northeast of Mount McLeod by M. Journeay (oral communication, 1990). A deep maroon and green basaltic breccia with vesicular clasts is associated with this section at Mount Barbour and Rampart Mountain.

SEDIMENTARY ROCKS (Tr4)

Predominantly sedimentary sequences are quite rare in the Pemberton Triassic section. Shales, siltstones, sandstones and conglomerates are present, but in almost all localities they are intermixed with tuffaceous sediments, tuffs, and flows, and are included in Unit Tr3. Exceptions are at the top of the Mount Barbour Triassic section, and on the eastern end of the ridge east of Grizzly Pass. These rocks are dominantly feldspar-rich, volcanoclastic sediments. Clasts of the underlying rock types are easily recognized. The sequence contains multiple, rapid fining-upward sequences from cobble conglomerate to black shale. White cherty beds are common.

POST-TRIASSIC(?) VOLCANIC AND SEDIMENTARY SECTION (?JK)

Southeast of Tenquille Lake, a relatively thin section of volcanic and sedimentary rocks sits unconformably on the Triassic sequence (Figure 1-6-2). This section does not resemble any known Cadwallader stratigraphy. It is well exposed in the area surrounding Cerulean Lake, and small outliers are preserved at the very top of Copper Mound and on the northern flank of Goat Peak. The lowest exposed rocks in this section are mauve and green andesitic auto-breccia, with beige feldspar and hornblende-phyric flows, and mauve and green lapilli and feldspar-crystal tuffs. These rocks are remarkably similar in appearance to the auto-

breccia unit of the Cretaceous Brokenback Hill Formation mapped in the Lillooet Lake pendant (Riddell, 1990), but the bounding stratigraphy is different. About 100 metres of sedimentary rock overlies the volcanic pile. Its base is a boulder conglomerate and it grades smoothly, apparently through only one major cycle, through cobble, pebble and granule conglomerate, into quartz and feldspar-rich calcareous sandstone, grey siltstone and black shale. One third to one half of the clasts in the conglomerate are fresh hornblende granodiorite, quartz diorite and granite. Their source is unknown. Remaining clasts tend to be representative of the local underlying rocks. Clasts of feldspar-phyric andesitic volcanics, argillite, green aphanitic volcanics and mafic volcanics are common, chert pebbles, gneissic granitoids and pyroxene granitoid clasts appear locally. Thin crossbedded magnetite-rich sandstone beds are present within the conglomerate in a few places. North of Cerulean Lake these beds are several centimetres thick (P. Newman, oral communication, 1990). A granodiorite boulder from the conglomerate has been sampled for radiometric dating.

CRETACEOUS STRATIGRAPHY (K)

Cretaceous stratigraphy west of the Owl Creek fault is not well exposed within the map area north of Pemberton; much of the area is underlain by quartz diorites and granodiorites of the Coast plutonic complex. The mauve and green volcanic breccia of the Brokenback Hill Formation can be traced northwest to the Mount Fraser ridge system. Volcanic wackes, siltstones and shale, probably of the Peninsula Formation, underlie the breccia.

TERTIARY VOLCANICS (T)

Chipmunk Mountain, just north of Tenquille Mountain, is a Tertiary volcanic centre. Dikes and small isolated outcrops of related basalt flows, volcanic breccias and rhyolite are found throughout the map area. These rocks have distinctive, drab brown and beige colours, and outcrops are often crumbly or flaggy. The basaltic rocks commonly contain euhedral biotite crystals up to 5 millimetres across. Basalt is the most dominant clast type in the breccias, and they also contain biotite crystals and clear, anhedral quartz eyes.

INTRUSIVE ROCKS

Diorites are associated with volcanic rocks of Units Tr1 and Tr2 on Tenquille Mountain and southeast of Bastion Peak. These rocks show mutually crosscutting relationships with the volcanic rocks and so appear to be coeval. The diorites are characteristically altered or contaminated near the contacts with the Triassic rocks. Some appear to grade into tuffaceous rocks of Unit Tr2, and in some places it is difficult to distinguish contaminated diorites from feldspar-crystal tuffs. Large bodies of granodiorite and quartz diorite of the Cretaceous Coast plutonic complex are exposed within the map area.

STRUCTURE

The major fault that cuts the Lillooet Lake pendant continues to the northwest through the Owl Creek valley (Fig-

ure 1-6-3). Near Lillooet Lake, Cretaceous rocks of the Fire Lake Group (equivalent to the Gambier Group), are gently deformed, probably by the east-side-up movement on the fault (Riddell, 1990), into broad, open folds with gently plunging, north-northwest-trending fold axes that parallel the fault trace. East of the fault, the Triassic outcrops show a moderate to intense north-northwest-trending penetrative shear foliation, parallel or subparallel to bedding, indicating that the rocks have suffered high shear stress. This deformation is not apparent in the rocks east of the fault in the Tenquille Lake area. There, the Triassic rocks and the overlying post-Triassic(?) rocks are gently folded into a broad anticline with a gentle southeast-plunging axis that lies just east of Mount McLeod (Figure 1-6-3). Only one axial planar cleavage is present, so it appears that the Triassic rocks and the post-Triassic(?) section were deformed together by one event some time during or after deposition of Unit ?JK.

Part of a large shear zone is exposed in a new road on the Lill property, along the shoreline at the mouth of the Lillooet River. The andesites and andesite breccias are intensely silicified and bleached to a pale silver-grey colour, and massive and disseminated pyrite is abundant. This is probably a continuation of an east-side-up thrust fault that lies along strike to the south, on the western shore at the bend in Lillooet Lake. This structure continues across the lake farther to the south (Journeay, 1990) and appears to be an important regional feature. It may be related to the Grizzly Pass shear zone. Alternatively, it may continue north through the valley of the Birkenhead River (Figure 1-6-3).

STRATIGRAPHIC SETTING OF MINERAL SHOWINGS

Most of the mineral exploration that was done in the Pemberton area in the late 1890s and the 1930s was focused on the magnetite-garnet-epidote skarns that are commonly

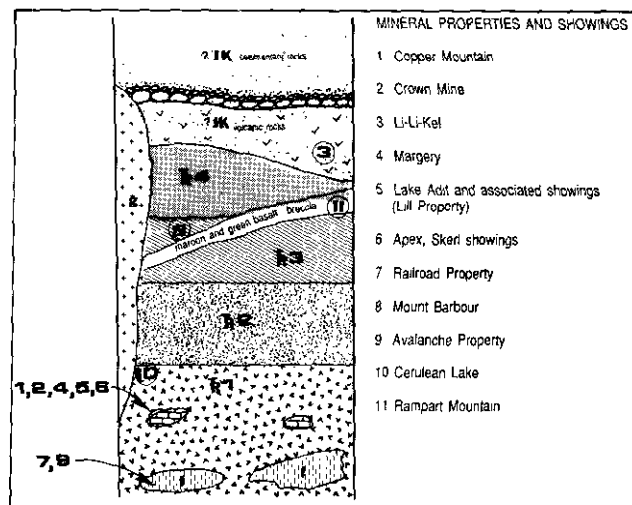


Figure 1-6-5. Locations of mineral showings within the Pemberton Triassic section. See text for details. Symbols as per Figure 1-6-2.

associated with limestone pods in Unit Tr1. A summary of the early exploration history of the area is provided by Cairnes (1925). In recent years attention has turned to volcanogenic massive sulphide deposit models. Favourable features such as a thick submarine volcanic pile with a history of explosive activity and the presence of felsic volcanic and exhalative rock types are found within the stratigraphy of both the Fire Lake Group (Lynch, 1990), and the Cadwallader Group. Historically, the Tenquille Lake area has received most of the attention from prospectors, while the southern part of the Lillooet Lake pendant has been ignored. This may be due to the more difficult terrain in the Lillooet Lake area; below tree-line outcrop is scarce, and much of the alpine outcrop is too precipitous to walk on. Another factor is that Unit Tr1 does not outcrop south of Ure Creek, and the area is therefore not prospective for skarns. The remainder of the Triassic section is present, however, so there is potential for a volcanogenic massive sulphide occurrence in the Lillooet Lake pendant.

During the 1990 field season, I visited the mineral showings and properties shown on Figure 1-6-3. Figure 1-6-5 illustrates how they fit into the Pemberton belt stratigraphy. The following comments pertain to the general geology and stratigraphic setting of the showings. Cairnes (1925) visited localities 1 to 6 and other Pemberton area showings during September of 1924. His reports are detailed and complete, and I will not add to them here.

RAILROAD PROPERTY

The Railroad property covers a large rusty zone that extends over most of the southwest flank of Grouty Peak, at the north end of a zone of felsic volcanic rocks that sits within andesites and tuffs of Units Tr1 and Tr2. This zone stretches from Grouty Peak through Goat Peak and Tenquille Mountain to Grizzly Pass. The property is underlain by massive andesite flows and tuffs with abundant coeval quartz feldspar porphyry dikes and rhyolite flows. Mutually crosscutting relationships between quartz feldspar porphyries, and dacitic and andesitic feldspar porphyry dikes are abundant, as are breccias with mixed felsic and intermediate volcanic clasts. The rocks on this property are intensely to moderately silicified, and disseminated pyrite is ubiquitous. Quartz-sericite schists are common; most shear foliations strike north-northwest and dip gently to very steeply to the northeast.

MOUNT BARBOUR

A new showing, mapped by McLaren (1989), is hosted by Unit Tr3, adjacent to an icefield in the cirque on the north side of the peak of Mount Barbour. The showing is a pod of massive, banded pyrrhotite within a conspicuous northwest-striking rusty scar that cuts through the ridges east and west of the snowfield. The host rocks are well-bedded felsic tuffs with cherty tops. The stratigraphy dips moderately to the northeast, and the associated rocks are well-bedded lithic tuffs and feldspar-rich wackes with pyritic quartz-sericite schists. Just south of the showing, a deep maroon and green basalt breccia outcrops on the peak of Mount Barbour. It is

unclear how this breccia fits in with the Unit Tr3 stratigraphy, or if it is related to the showing.

AVALANCHE PROPERTY

The Avalanche property covers a wide, rusty alteration zone east of Tenquille Mountain. The rocks on the property are deformed by a complex set of anastomosing north-northwest-striking shears associated with a fault that passes through Grizzly Pass. The shear zone is bounded to the southwest by competent, unsheared massive basaltic andesite of Unit Tr1, and to the north by overlapping Tertiary basalt breccias. Rocks within the shear zone are banded parallel to the strike of the fault, and individual bands can be traced along strike for hundreds of metres. The sequence includes rhyolite flows, lithic and lapilli tuffs, rusty quartz-muscovite schists, bluish green chloritic tuffs and aplite with rhodonite specks. Large quartz grains or quartz grain clusters are present in all outcrops. Dark green chloritic flows with blue quartz eyes outcrop along the northeast edge of the shear zone. A thick ferrocrete deposit about 150 metres wide has formed around a rusty seep that is fed by a creek that drains the saddle at the top of the pass.

CERULEAN LAKE

A pod of massive pyrrhotite about 3 metres thick and 30 metres long lies along the contact zone between massive andesite flows (Tr1) and the Late Cretaceous Spetch Creek pluton, on the creek that flows into the southwest end of Cerulean Lake. It is surrounded by a large rusty zone on the west bank above the creek. Mineralized boulders have conspicuous black and iridescent manganese oxide coatings.

TEXAS SHOWING

The Texas showing on the Birkenhead Lake road is an iron-copper-gold skarn within quartz-bearing calcareous andesitic lapilli tuff of the Unit Tr2. Banded and disseminated pyrite, chalcopyrite and malachite are associated with garnet-diopside calcisilicate rocks. No limestones were seen. The skarn mineralization may have formed by a reaction between the limy tuffs and a quartz feldspar porphyry dike that is exposed on the south end of the property.

RAMPART MOUNTAIN

A large, intensely rusty zone is associated with a deep maroon and green basalt breccia on Rampart Mountain, near where the breccia lies unconformably on top of mixed tuffs and sediments of Unit Tr3. Quartz-bearing breccias and felsic porphyries within the maroon and green rocks are strongly pyritized. The rocks all show strong to intense north-northwest shear foliation. Pyritic quartz-sericite schists are abundant.

ACKNOWLEDGMENTS

Funding for the 1990 field season was provided by British Columbia Geoscience Research Grant RG89-38. Teck Explorations Limited and the Geological Survey of Canada (Pemberton Project) provided logistical support. I would

like to thank Teck for allowing me to release information gathered while I was employed by the company. I am grateful to Murray Journeay and Paul Schiarizza for providing good advice and encouragement. Jean Pautler of Teck provided helpful insight, and was a most compatible field companion. Scott Helm's voluntary mapping contribution is most gratefully acknowledged. Pemberton Helicopters provided another season of safe and dependable transportation.

REFERENCES

- Cairnes, C.E. (1925): Pemberton Area, Lillooet District, British Columbia; in Summary Report 1924, Part A, *Geological Survey of Canada*, pages 76-99.
- Cairnes, C.E. (1937): Geology and Mineral Deposits of the Bridge River Mining Camp, British Columbia; *Geological Survey of Canada*, Memoir 213, 140 pages.
- Journeay, J.M. (1990): Structural and Tectonic Framework of the Southern Coast Belt: a Progress Report; in Current Research, Part E, *Geological Survey of Canada*, Paper 90-1E.
- Lynch, J.V.G. (1990): Geology of the Fire Lake Group, Southeast Coast Mountains, British Columbia; in Current Research, Part E, *Geological Survey of Canada*, Paper 90-1E, pages 197-204.
- McLaren, G.P. (1989): Geology of the Tenquille Creek to Owl Mountain Area, NTS 92J/07 and 10, 1:50 000 scale; *B.C. Ministry of Energy, Mines and Petroleum Resources*, Open File 1989-6.
- Riddell, J.M. (1990): Preliminary Report on the Lillooet Lake Mapping Project, Southwestern British Columbia. (92J/1, 2, 7); *B.C. Ministry of Energy, Mines and Petroleum Resources*, Geological Fieldwork 1989, Paper 1990-1, pages 39-44.
- Riddell, J.M. (1991): Geology of the Mesozoic Volcanic and Sedimentary Rocks East of Pemberton, British Columbia; in Current Research, Part I, *Geological Survey of Canada*, Paper 91-1A.
- Roddick, J.A. and Hutchison, W.W. (1973): Pemberton (East Half) Map Area, British Columbia; *Geological Survey of Canada*, Paper 73-17, 21 pages.
- Rusmore, M.E. (1985): Geology and Tectonic Significance of the Upper Triassic Cadwallader Group and its Bounding Faults, Southwest British Columbia; unpublished Ph.D. dissertation, *University of Washington*, 174 pages.
- Schick, J.D. (1990): Geochemistry and Tectonic Significance of Greenstones from the Fire Lake Pendant and Twin Islands Group, British Columbia; unpublished B.A. thesis, *Middlebury College*, Middlebury, Vermont, 58 pages.
- Woodsworth, G.J. (1977): Pemberton (92J) Map Area, British Columbia; *Geological Survey of Canada*, Open File 482.



KINEMATIC ANALYSIS AND TIMING OF STRUCTURES IN THE BRIDGE RIVER COMPLEX AND OVERLYING CRETACEOUS SEDIMENTARY ROCKS, CINNABAR CREEK AREA, SOUTHWESTERN BRITISH COLUMBIA* (92J/15)

By John I. Garver
Union College

KEYWORDS: Regional geology, structure, kinematic analysis, Bridge River complex, Taylor Creek Group, Silverquick conglomerate, Bralorne, Eldorado pluton, blueschist, deformation, strike-slip faulting, thrusting.

INTRODUCTION

The North Cinnabar Creek area is located approximately 200 kilometres north of Vancouver on the eastern flank of the Coast Range. The 12-square-kilometre study area is underlain by strongly deformed rocks of the Bridge River complex (informal) and an unconformably overlying synorogenic clastic sequence that is also deformed (Figure 1-7-1). The area is of particular interest because several fault-bounded panels of rocks belonging to the Bridge River complex contain newly discovered blueschist (Garver *et al.*, 1989a, b, and c; Garver, 1989). Detailed mapping

(1:10 000; Figure 1-7-2) and kinematic analysis of the structures in this area was undertaken to better understand the structural setting of the blueschists. This recent effort was largely concentrated in the imbricated rocks of the Bridge River complex, which are exposed east of the Castle Pass fault and south of the unconformably overlying sedimentary sequence, and it follows earlier 1:20 000 mapping (Figure 1-7-2). The Castle Pass fault, which separates the different lithologic units of the Bridge River complex, was originally interpreted as a dextral strike-slip fault in the Castle Pass area some 10 kilometres along strike to the northwest (Glover *et al.*, 1988a and b; Schiarizza *et al.*, 1989a and b). Recent mapping, however, suggests that although a late history of dextral strike-slip faulting may be recorded along parts of the Castle Pass fault, this fault (and the Tyaughton Creek fault to the east) has a history of sinistral transpressional deformation (Schiarizza *et al.*, 1990).

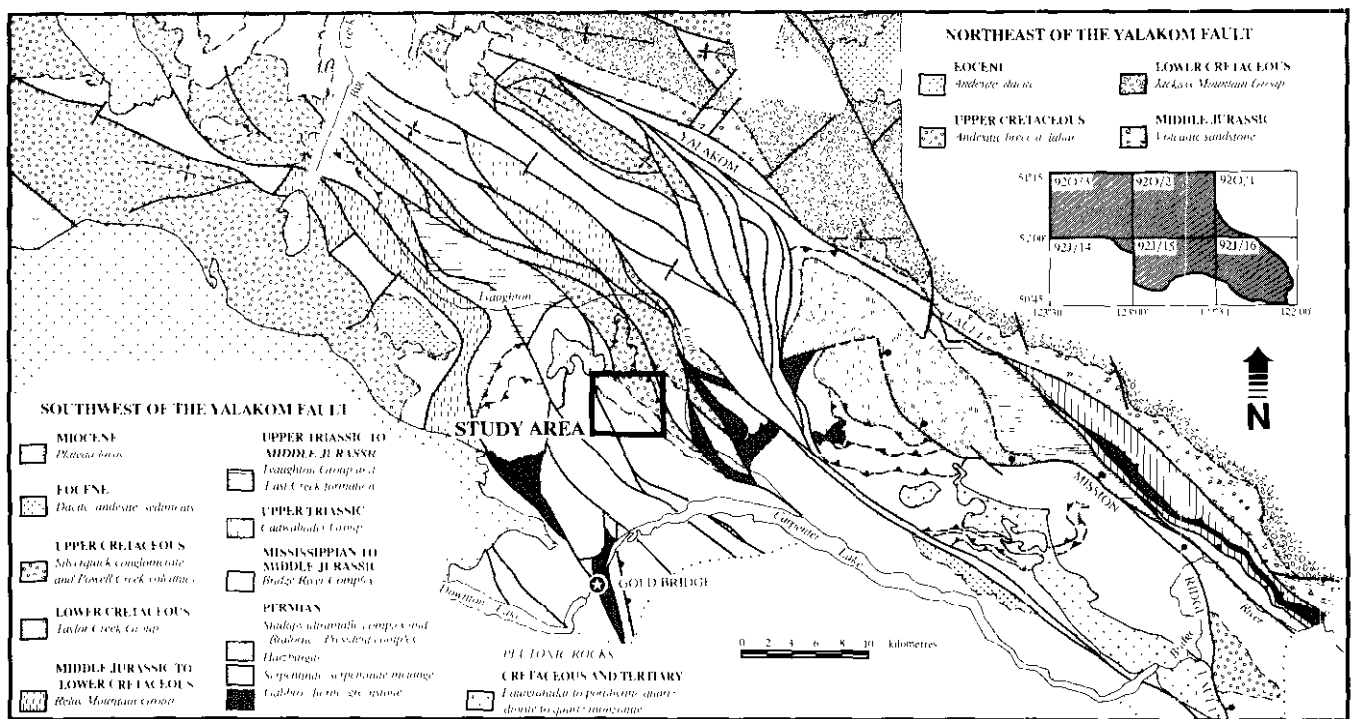


Figure 1-7-1. Generalized geology of the Taseko - Bridge River project area (from Schiarizza *et al.*, 1990). The study area is some 4 to 5 kilometres west of Tyaughton Lake, which is not shown on this map. Note the proximity of the 64 Ma Eldorado pluton directly to the north of the study area: it is not cut by northwest-trending strike-slip faults, but it does have faulted margins.

* This project is a contribution to the Canada/British Columbia Mineral Development Agreement.

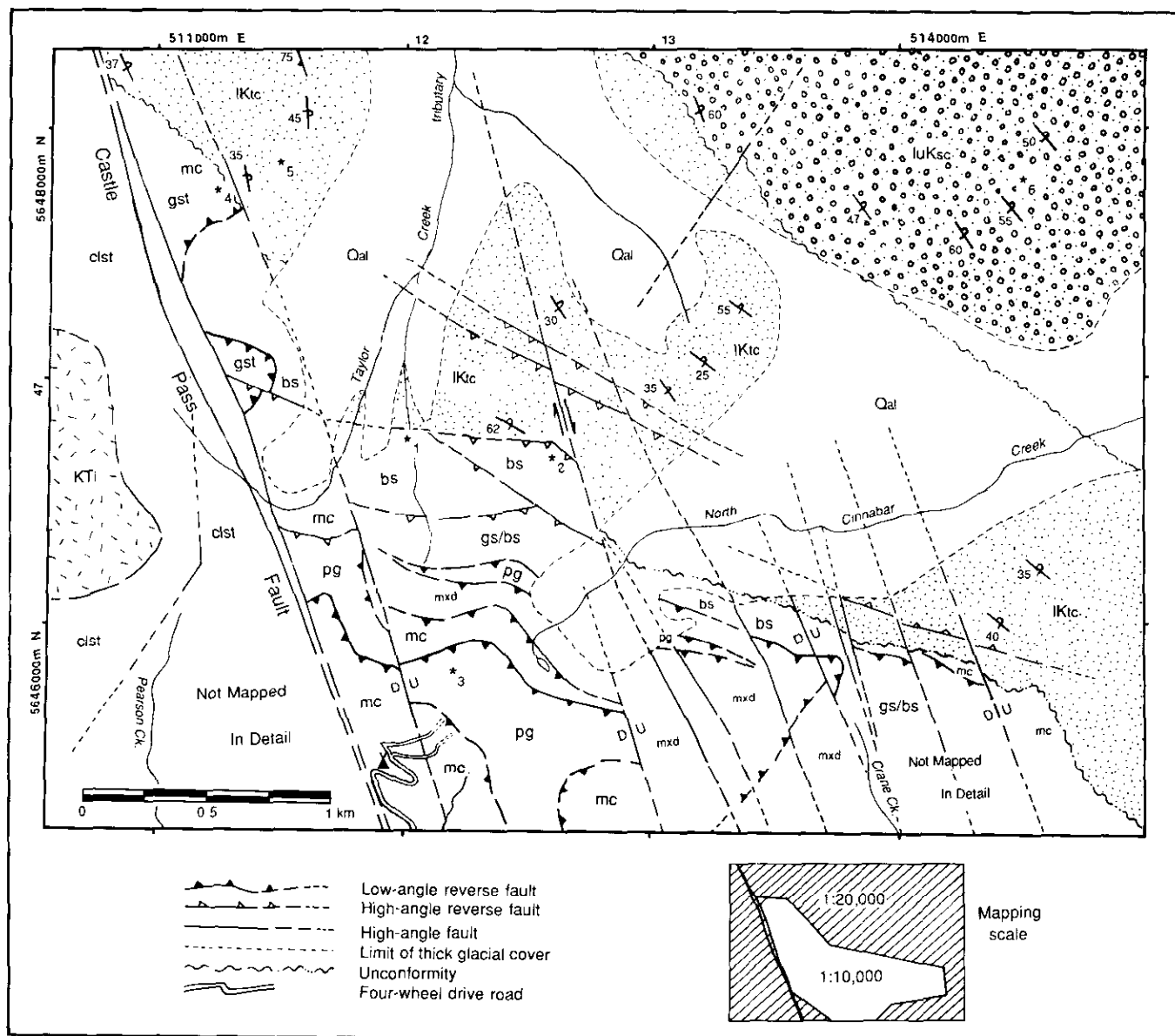


Figure 1-7-2. Simplified geologic map of the study area. Note that detailed mapping (1:10 000) was concentrated in the southern part of this area, east of the Castle Pass fault; the detail here is much better than elsewhere on the map sheet. The end of the Pearson Creek road, which begins near Tyaughton Lake, is shown on the southern part of the map. This four-wheel-drive road provides convenient access to the study area; camp sites are present at the end of the road. The Bridge River complex, which is unshaded, contains the following lithologies in this area: pg – prehnite-pumpellyite-grade pillowed greenstone; mc – highly deformed metachert; bs – blueschist; gs/bs – rocks that contain both green and blue schistose metamorphic rocks, both of which have blueschist-facies metamorphic minerals; mx – a mixed zone of lithologies that are similar to all lithologies in the Bridge River complex east of the Castle Pass fault; gst – massive greenstone without blueschist facies minerals; clst – clastic rocks, which occur east of the Castle Pass fault. These clastic rocks include black argillite, chert and volcanic-lithic sandstone and conglomerates, and minor interbedded chert. Other units include: KTi – a small stock that may be related to the Eldorado pluton to the north; IKtc – middle to upper Albian Taylor Creek Group; luKsc – Albian to Cenomanian Silverquick conglomerate; Qal – thick deposits of Quaternary alluvium. Numbers refer to dated rocks as follows: (1) white mica in blueschist gives 244 ± 7 Ma (K-Ar, Garver *et al.*, 1989b), 217 ± 5 Ma (Rb-Sr, Garver *et al.*, 1989b), 218.1 ± 1.2 Ma (Ar/Ar, Archibald *et al.*, 1989); (2) blueschist from several outcrops give 195 ± 6 , 222 ± 8 , and 250 ± 9 Ma (wholerock, Garver *et al.*, 1989b); an Ar/Ar sample from this locality is in progress, Archibald, personal communication, 1990); (3) conodonts from limestone interbedded with pillowed greenstone are early Norian (Upper Triassic – P. Schiarizza, unpublished data); (4) conodonts from bedded chert give a Triassic age (P. Schiarizza, unpublished data); (5) middle to upper Albian (Lower Cretaceous) ammonites from the Taylor Creek Group (Garver, 1989); (6) Albian to Cenomanian flora from the Silverquick conglomerate (see Garver, 1989).

In addition to the intrinsic scientific value of the blueschists, this area is also important in a regional sense because the rocks are well dated and therefore the timing of structural development is fairly well constrained. This project is an outgrowth of mapping done during the author's Ph.D. research (which focused on the mid-Cretaceous basin development in this area), which was conducted, in part, with the M.D.A.-sponsored Taseko—Bridge River mapping project (Figure 1-7-1; *see* also Glover and Schiarizza, 1987; Glover *et al.*, 1987, 1988a, b; Umhoefer *et al.*, 1988; Schiarizza *et al.*, 1989a, 1989b, 1990; Garver *et al.*, 1989a, b, c).

The structures and their timing bear on the tectonic evolution of the Bridge River and Cadwallader terranes in the immediate area as well as the Intermontane Superterrane to the east and the Insular Superterrane to the west. This structural information also has a bearing on mineral exploration in the area because the earlier structures (*circa* 100 to 80 Ma) outlined in this report are broadly coeval with the Bralorne fault system which hosts well-known mesothermal gold deposits about 20 kilometres to the south; thrusts in the North Cinnabar Creek area are probably a high-level expression of the same contractional event. These contractional structures are cut by a younger dextral fault system that may have experienced several episodes of movement and mineralization. In this area, these brittle high-angle faults host fairly common polymetallic vein mineralization (Minto mine, located on the Castle Pass fault to the southeast of the study area – Schiarizza *et al.*, 1990) and mercury mineralization.

LITHOLOGY

The rocks in the study area belong to two principal units that are cut by intrusive rocks: upper Paleozoic to lower Mesozoic rocks of the Bridge River complex, an oceanic assemblage that includes various imbricated panels of chert, greenstone, clastic rocks, serpentinite and, notably, blueschist; and a mid-Cretaceous sedimentary package that unconformably overlies the deformed Bridge River complex. This sequence includes the middle to upper Albian Taylor Creek Group and the Albian to Cenomanian Silverquick conglomerate (informal; Garver, 1989). Quartz diorite to granodiorite of the Eldorado pluton and related stocks, which are exposed immediately north and west of the map area, intrude both the Bridge River complex and the overlying Cretaceous strata (Figure 1-7-1). The Eldorado pluton has a satellite stock (the Robson stock) with a K-Ar age of 63.7 ± 2.2 Ma on biotite (Leitch *et al.*, 1989); this is taken as the age of the Eldorado pluton. Details concerning the different lithologic units in this area can be found in Garver *et al.* (1989a); Garver (1989); and Schiarizza *et al.* (1989a)

STRUCTURAL GEOLOGY

Our understanding of the structural development in the Bridge River – Taseko area has been greatly enhanced by MDA-sponsored mapping and thesis research. Recent detailed mapping in the Shulaps Range, slightly to the east of this study area, has revealed some of the intricacies of

this deformation. In essence, five deformational events are recognized: (1) lower Mesozoic blueschist deformation (Garver *et al.*, 1989 a, b); (2) southwest-vergent thrusting, which is best displayed in the Shulaps Range and slightly younger thrusts and reverse faults with the same vergence (Calon *et al.*, 1990; Schiarizza *et al.*, 1989a, 1990), both of which were probably contemporaneous with the deposition of a mid-Cretaceous synorogenic clastic wedge (Garver, 1989); (3) northeast-vergent thrusts and folds that probably immediately postdate the earlier thrusting (Schiarizza *et al.*, 1989; Garver *et al.*, 1989; Garver, 1989); (4) northwest-striking dextral strike-slip faulting and extension with significant movement on the Yalakom, Relay Creek and Mission Ridge faults during the Eocene (Glover *et al.*, 1988a and b; Schiarizza *et al.*, 1989a, 1990; Umhoefer, 1989; Coleman, 1989); and (5) north-striking dextral strike-slip faulting that is probably synthetic with the Fraser fault (Schiarizza *et al.*, 1990; Coleman 1989; Umhoefer, 1989; Coleman and Parrish, 1990). The North Cinnabar Creek area is important because it contains well-dated rocks and because structures related to the blueschist deformation, the northeast-vergent thrusting, and the strike-slip faulting are particularly well displayed. Indeed, this area is the one of the few areas in the region where northeast-vergent thrusting can be documented.

Specifically, the area contains internally imbricated panels of rocks within the Bridge River complex that are unconformably overlain by overturned rocks of the Albian Taylor Creek Group (Figure 1-7-2). The orientation and asymmetry of the overturned rocks and small-scale folds suggest that this phase of deformation was caused by northeast-vergent thrusting. These thrust-related structures are cut by a late, brittle, northwest-trending dextral fault system that is apparently plugged by the Eldorado pluton, but internally the pluton has not been mapped in detail. The pluton is cut by faults along its eastern margin. Deformation older than the strike-slip faulting and the northeast-vergent thrusting is present within the Bridge River complex but its nature cannot be resolved. Pre-unconformity deformation must have occurred, however, because the Taylor Creek Group rests above different rock types of the Bridge River complex. The sedimentology and pattern of basin infilling suggest that the Bridge River complex was thrust westward and internally imbricated during the sedimentation (Albian – *circa* 110 to 100 Ma; Garver, 1989). Older, poorly understood deformation is recorded in both units within the Bridge River complex. Notably, the blueschist experienced synkinematic deformation that was approximately contemporaneous with its Permo-Triassic metamorphism.

POST 64 MA STRIKE-SLIP FAULTING

Several of the main strands of the strike-slip faults in the study area can be mapped to the edge of the 64 Ma Eldorado pluton. These faults, which are discussed in detail in the next section, do not extend into the pluton and are therefore presumed to predate it. Although there is certainly a significant rheological contrast between the pluton and the surrounding sediments, deflection of these faults seems

unlikely because significant or cumulative offset within the Dash conglomerate of the Taylor Creek Group along the east edge of the pluton is not recognised (Figure 1-7-1; Garver *et al.*, 1989). Recent examination of the central and eastern parts of the pluton suggests that the Castle Pass fault does not cut the pluton where the fault is projected through it. As discussed above, the Castle Pass fault is presumed to have an earlier history of sinistral oblique movement and parts of it had a later history of dextral strike-slip (Scharizza *et al.*, 1990). It also suggests that the eastern edge of the pluton is faulted. These faults are north-striking, moderately dipping and have horizontal slickenside lineations and down-dip lineations. The nature of this young deformation is incompletely studied but it may have developed at the same time as the north-striking Fraser fault system to the east, or the northwest-striking Yalakom fault which has Eocene movement. The Fraser fault system, some 30 kilometres to the east, characterized by north-trending dextral strike-slip faulting, moved between 46.5 and 35 Ma, according to recent work by Coleman and Parrish (1990). The Yalakom fault is known to have had Eocene movement in this area that was largely transtensional in nature (Scharizza *et al.*, 1989a; Umhoefer, 1989; Scharizza *et al.*, 1990; Coleman, 1989). These young episodes of faulting appear to be poorly developed, but they may explain some of the multiple episodes of movement recognized on these brittle faults.

PRE 64 MA DEXTRAL STRIKE-SLIP FAULTING

The rocks in the map area are cut by numerous northwest-trending, high-angle faults that are interpreted to have dex-

tral strike-slip movement as suggested by map-scale relationships, small-scale structures and observed offsets. In the following discussion, only faults with known sense of movement are considered. The offset or movement history was determined by: net displacement of piercing points; calcite/quartz fibre mineral growth; or asymmetric fabrics in the faults themselves. Although none of these methods unequivocally gives net displacement, the results show a coherent pattern (Figure 1-7-3). Reverse faults, normal faults and sinistral faults with known net displacement and, generally, only minor movement, are compatible with the strain ellipse for dextral strike-slip faulting. Several small (metre scale) and medium-scale (tens of metres) faults have observable dextral displacement and, where exposed, near-horizontal slickenside striations (Plate 1-7-1), although both vertical and horizontal striations are present on some faults; vertical slickensides record the latest movement, which may be significantly younger, as discussed above. The average strike of faults with known dextral offset is 344° (Figure 1-7-3).

In addition to the dextral faults, many brittle faults indicate north-northeast to south-southwest contraction and nearly east to west extension, and are probably cogenetic with the strike-slip faults. Of all dip-slip faults observed, reverse displacements (indicating NNE-SSW contraction at 025° - 225°) are common; faults with normal displacement are rare. Small-scale (<1-2 m) antithetic sinistral faults with an average strike of about 055° are also common, but on a smaller scale, as shown in Plate 1-7-2. Collectively, these late brittle faults with minor displacement fit a strain ellipse for dextral strike-slip faulting with an orientation of about

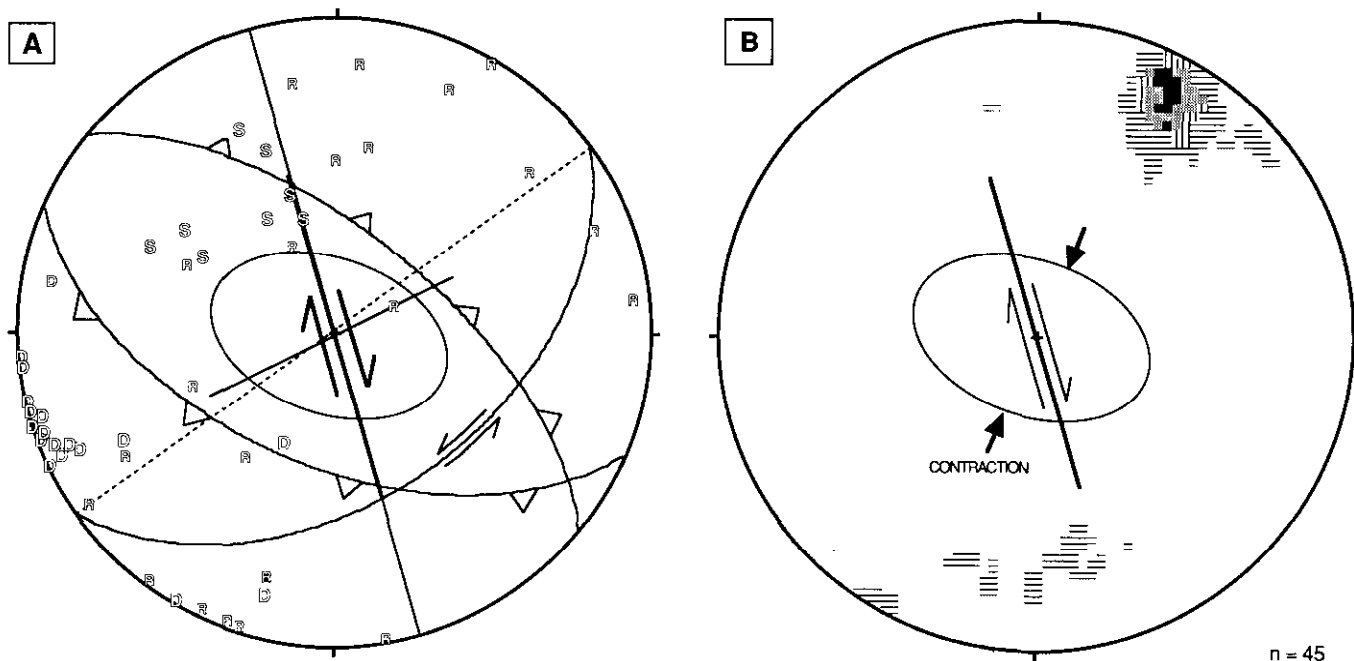


Figure 1-7-3. Small-scale structures related to dextral strike-slip faulting. (A) Poles to faults with known displacement. These faults have metres to tens of metres of displacement. Most have slickensides that corroborate the inferred sense of movement. Great circles indicate the estimated average of each data set. The strain ellipse for dextral strike-slip faulting overlies the data. (B) Poles to the crenulation cleavage in the blueschist. Asymmetry in the crenulations in both sets indicates reverse movement. Contour intervals are 2.2-5.8%, 5.8-9.3%, 9.3-12.9%, 12.9-16.4%, and 16.4-20.0% per 1% area.

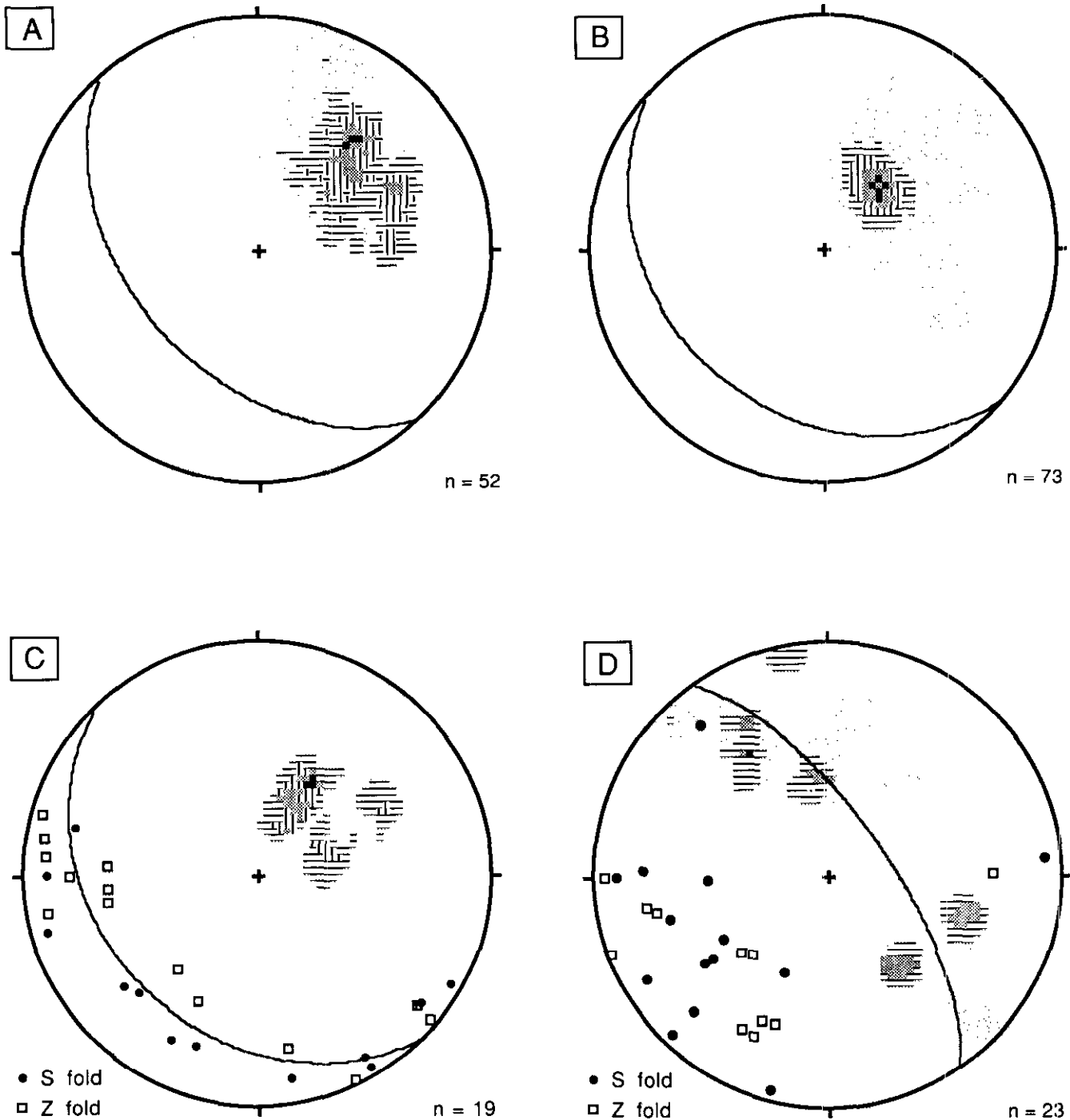


Figure 1-7-4. Stereographic projections of measurements of: (A) poles to foliations within rocks of the Bridge River complex. Contour intervals are 1.9-5.4%, 5.4-8.8%, 8.8-12.3%, 12.3-15.8%, 15.8-19.2% per 1% area. Mean pole to foliation is about $135^{\circ}/45^{\circ}$; (B) poles to bedding of the Cretaceous sedimentary rocks. Contour intervals are 1.4-10.7%, 10.7-20.0%, 20.0-29.3%, 29.3-38.6%, 38.6-47.9% per 1% area. These data include both upright and overturned attitudes; (C) poles to axial planes (contoured) of fold axes (squares and zeros) from small-scale folds within the Bridge River complex. These data include only those measurements where axial planes are coplaner with the dominant foliation in the Bridge River complex (*see A* above). The mean axial plane (great circle) has an orientation of $135^{\circ}/30^{\circ}$. The asymmetry of the folds is shown. Contour intervals are 5.3-9.5%, 9.5-13.5%, 13.7-17.9%, 17.9-22.1%, 22.1-26.3% per 1% area; (D) poles to axial planes (contoured) and the associated fold axes of small-scale folds that do not lie on the dominant foliation plane. These "residuals" almost certainly represent an earlier folding event that was overprinted by structures associated with northeast-vergent thrusting, but refolding of these "older" folds cannot be demonstrated in the field. Contour intervals are 4.3-6.1%, 6.1-9.6%, 9.6-12.2%, 12.2-14.8%, 14.8-17.4% per 1% area.

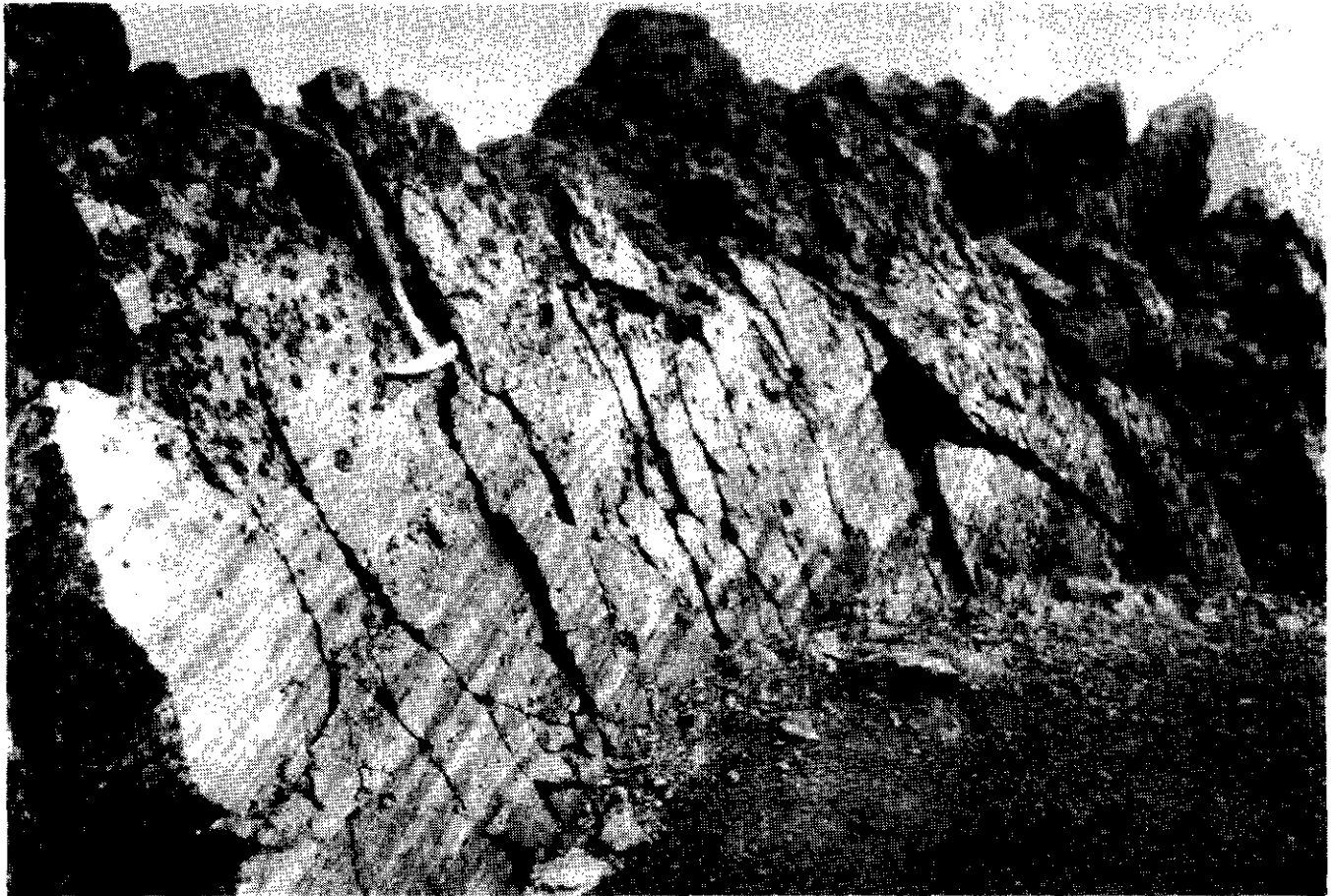


Plate 1-7-1. Northwest-trending high-angle faults with dextral offset. These particular brittle faults, with prominent nearly horizontal slickenside striations, are seen here cutting rocks of the Taylor Creek Group.



Plate 1-7-2. Northwest-striking, high-angle fault with gently plunging slickenside striations that is cut by very small scale northeast-striking sinistral faults. On this fault, the sinistral faults are clearly younger than the strike-slip fault but both are interpreted to have occurred in the same dextral strike-slip fault regime. A white Brunton compass is in the lower right of the photo for scale.

345° (Figure 1-7-3). These minor faults may have been produced during the later phases of movement on the Castle Pass fault in the western part of the map area (Figures 1-7-1 and 2)

Small-scale north-northeast to south-southwest contraction is also indicated by a pronounced crenulation cleavage in the blueschist. The average strike of the cleavage is parallel to the average strike of the relatively common high-angle reverse faults in the area (Figure 1-7-2); both are between 55° and 60° from the orientation of the strike-slip faults, almost exactly what is predicted in a strain ellipse for dextral strike-slip faulting with a strike of 345° (Figure 1-7-3b). Locally, the blueschist contains an earlier crenulation cleavage that is intersected by the late east-trending cleavage, which is dominant. The paucity of observations makes this earlier feature difficult to interpret. Although several faults with apparent normal separation and down-dip slickensides have been recognized, there is a dearth of extensional structures in the map area. The relative lack of extensional structures and abundance of contractional structures may suggest that this area was subject to transpressive dextral strike-slip faulting.

As indicated above, this pervasive system of brittle faults appears not to cut the 64 Ma Eldorado pluton. The north-

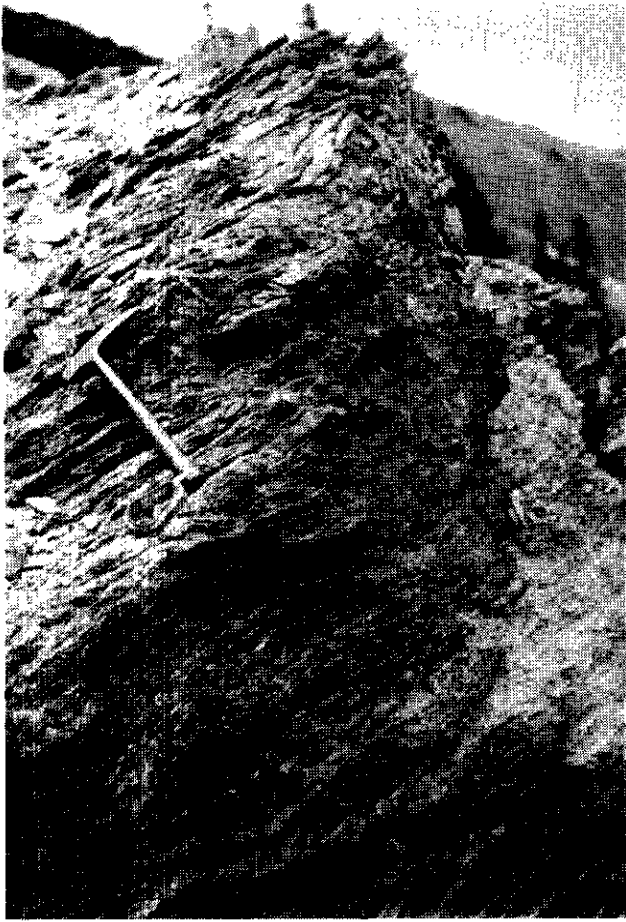


Plate 1-7-3. Thrust fault in metachert of the Bridge River complex. These highly strained rocks are characterised by a penetrative and anastomosing foliation that is defined by strongly attenuated compositional layering. Isolated fold hinges are present and occur as a pronounced streaking lineation on the foliation plane. The streaking lineation (orientated at about $240^{\circ}/40^{\circ}$), and the dominance of Z-folds in this outcrop, indicate that the tectonic transport was upper plate to the northeast (060°).

striking faults that bound the eastern edge may be related to this movement, or may possibly indicate the latest episode of movement in a protracted event. The system of faults does cut folded and faulted rocks of the Taylor Creek Group and the overlying Silverquick conglomerate. The Taylor Creek Group contains middle to upper Albian fossils (*circa* 105–97 Ma) and the Silverquick conglomerate is undated at this locality, but correlation suggests that it is upper Albian to Cenomanian (*circa* 100–91 Ma; Garver, 1989). Therefore the northwest-trending dextral faulting occurred between about 95 and 64 Ma, during the Late Cretaceous.

NORTHEAST-VERGENT FOLDING AND THRUSTING

The recent mapping indicates that the North Cinnabar area comprises a system of northeast-vergent, imbricate

thrust faults with a major (kilometre-scale) overturned fold of mid-Cretaceous rocks in the footwall. The asymmetry of the folds and kinematic indicators in the fault zones indicate that tectonic transport was to the northeast.

FOLDED MID-CRETACEOUS STRATA

A kilometre-scale, overturned, and nearly isoclinal fold occurs in Silverquick conglomerate, the Taylor Creek Group, and presumably in parts of the underlying Bridge River complex. The overturned limb contains the unconformable relationship with the Taylor Creek Group (Dash conglomerate) resting above blueschist and other rock types of the Bridge River complex (Figure 1-7-2). As discussed below, some fault zones in the Bridge River complex were probably produced during this northeast-vergent thrusting; however, any earlier structures must have been overturned or rotated some 150° from the horizontal during this folding event. A plot of poles to bedding (Figure 1-7-4b) shows both upright and overturned bedding attitudes in a relatively tight cluster, with a mean value of about $130^{\circ}/30^{\circ}$. This asymmetric folding, therefore, has a horizontal fold axis with an orientation of 130° to 310° with a vergence direction to the northeast (040°). Both the scale of this folding and crosscutting relationships suggest that it was a discreet and earlier event from the younger strike-slip faulting. The scale of the folding (a wavelength of 5 kilometres or greater, as some 3 kilometres of strata occur in the overturned limb) is at least an order of magnitude greater than the offset associated with the younger strike-slip faults (metres to tens of metres); folding associated with the strike-slip faulting has not been recognized here. Additionally, numerous synthetic strike-slip faults cut all parts of this nappe-like fold.

BRIDGE RIVER COMPLEX

Within the study area, all units mapped in the Bridge River complex locally contain metre-scale zones of high strain that are characterized by a penetrative foliation (Figures 1-7-2 and 4, Plate 1-7-3). Most of the principal contacts between units are interpreted to be southwest-dipping thrusts (Figure 1-7-2). Where these faults are well exposed, the fabric and the small-scale structures indicate top-to-the-northeast thrusting (Plate 1-7-3). In layered lithologies, such as chert, asymmetric folds are common in these zones and their asymmetry tends to suggest vergence to the northeast. A plot of axial planes to these small-scale folds (centimetre to decimetre scale) is shown in Figure 1-7-4c. Asymmetric folds (both Z and S-folds as viewed down plunge) with axial planes parallel to the dominant foliation suggest that these are developed in northeast-vergent thrusts; however, these data show significant scatter and a slip-line analysis is difficult and speculative. According to the slip-line theory, both S-folds and Z-folds typically form along a common slip plane. The slip line, or direction of tectonic transport, is defined by the area on the slip plane with the least overlap between fold shapes, or the separation arc (Hansen, 1971). These data show most Z-shaped folds plunge gently in the northwest quadrant and most S-shaped folds plot in the southeast quadrant, both reflect northeast vergence but it is not possible to determine a slip-line (Figure 1-7-4c).

The northeast-vergent folds involve the middle to upper Albian Taylor Creek Group and the Albian to Cenomanian(?) Silverquick conglomerate. Recent mapping to the south suggests that these thrusts postdate and cut the 91 to 84 Ma structures in the Bralorne area. (Schiarizza *et al.*, 1990; Schiarizza, personal communication, 1990). The overturned strata of the Taylor Creek Group are also intruded by the 64 Ma Eldorado pluton (Garver *et al.*, 1989a). The timing of this thrusting is probably between 91 to 84 Ma and 64 Ma, or Late Cretaceous.

SOUTHWEST-VERGENT THRUSTING

Regionally, workers have recognised an earlier contractional event that was characterized by southwest-vergent thrusting. The occurrence of southwest-vergent thrusts in the Shulaps Range, which are cut by northeast-vergent thrusts, and the depositional patterns of the Albian Taylor Creek Group and the overlying Albian-Cenomanian Silverquick conglomerate suggest that this initial phase of contraction occurred during Albian to Cenomanian time. Structural evidence for this event in the North Cinnabar area is scant and difficult to interpret due to the profound structural reworking during younger thrusting. It is possible that the folds interpreted to be unrelated to the northeast-vergent thrusting (Figure 1-7-4d) were produced during this earlier event. If these small-scale folds were overturned with the Cretaceous sediments then they must be rotated 150° around a horizontal northwest-trending axis to ascertain their pre-deformational orientation. This rotation takes the originally gently southwest-plunging fold axes, which are dominated by S-folds (Figure 1-7-4d), and restores them to gently northeast-plunging folds with the opposite sense of vergence. Although this restoration is speculative, the restored orientation would be consistent with westerly vergent thrusting. Elsewhere in the Chilcotin Ranges, the nature of this earlier contractional event is difficult to resolve because younger deformation has reoriented or reworked structures related to this older deformation.

The earlier southwest-vergent thrusting and the slightly younger northeast-vergent thrusting are both probably related to the same contractional event that is marked, in this area, by a vergence reversal and the cessation of sedimentation. The timing of southwest-vergent thrusting can be only indirectly determined in the North Cinnabar Creek area. Here, the synorogenic clastic wedge that is interpreted to have been shed westward from active thrusts is middle-late Albian to Cenomanian(?) in age (Garver, 1989). Elsewhere in the basin, however, the clastic wedge is upper lower Albian to Cenomanian (*circa* 110 to 95 Ma) and is presumed to be the best estimate of the timing of southwest-vergent thrusting (Garver, 1989).

SYNKINEMATIC BLUESCHIST-FACIES METAMORPHISM AND DEFORMATION

One of the thrust-bounded packages within the Bridge River complex consists of highly deformed blueschist (Figure

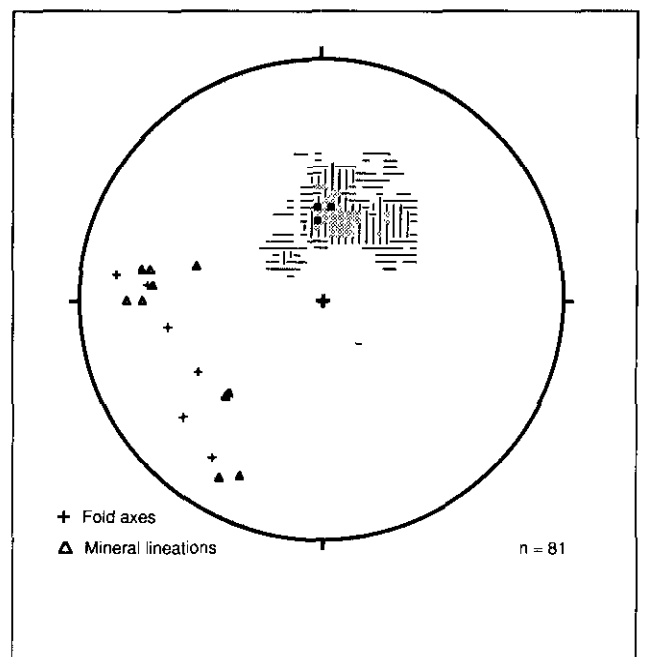


Figure 1-7-5. Stereographic projection of poles to schistosity in the blueschist. Contour intervals are 1.2-3.1%, 3.1-6.7%, 6.7-9.4%, 9.4-12.1%, 12.1-14.8% per 1% area. Also plotted are fold axes from tight to isoclinal folds of compositional layering, and mineral lineations that occur on the schistosity plane.

1-7-2). Brittle high-angle faults and a well-developed crenulation cleavage are present in these schists and are interpreted to represent a relatively young deformation as discussed. These schists have spectacular synkinematic isoclinal folds, a well-developed mineral lineation, and a very well developed schistosity. The schistosity dips moderately to the southwest and both the fold axes and the mineral lineations lie on the schistosity plane and plunge gently to the southwest (Figure 1-7-5). This fabric seems to mimic the foliation planes produced in faults during northeast-vergent thrusting (Figure 1-7-4a); this observation suggests that the blueschist schistosity has been rotated into parallelism with this younger foliation plane, which is common in other rocks of the Bridge River complex. The significance of these structures is unknown because the effects of younger deformation cannot be accurately determined.

The age of the blueschist-facies metamorphism is constrained by K-Ar, Ar-Ar, and Rb-Sr ages on whole-rock samples and white mica separates that range in age between 195 and 250 Ma (Archibald *et al.*, 1990, 1991, this volume; Garver *et al.*, 1989b). The spread of ages is certainly related to perturbations within the isotopic systems caused by younger deformation. Recently collected ⁴⁰Ar/³⁹Ar data from white mica separates suggest that the blueschist-facies metamorphism and associated deformation was complete by 230 Ma (Archibald *et al.*, 1990, 1991, this volume). Although the significance of these synmetamorphic structures is obscure at best, they are certainly the oldest dated structures in the Bridge River complex.

SUMMARY

- The eastern edge of the 64 Ma Eldorado pluton is cut by north-striking faults with near-horizontal slicken-side striations. These faults are parallel to dextral faults that are synthetic to the Fraser fault system and therefore may be related to this episode of strike-slip movement, which is bracketed between 46.5 and 35 Ma some 30 to 40 kilometres to the east (Coleman and Parrish, 1990). These faults could also be related to transtension on the Yalakom fault and related faults that are known to have occurred in this area in the Eocene (Umhoefer, 1989; Coleman, 1989; Schiarizza *et al.*, 1990)
- Northwest-striking dextral strike-slip faulting is pervasive but total distributed movement is minimal (hundreds of metres to perhaps a kilometre). Synthetic dextral, antithetic sinistral, and reverse faults fit the strain ellipse for dextral (transpressive) faulting with an orientation of about 345°. This faulting is post-Cenomanian (*circa* 95 Ma) and probably pre-64 Ma. This deformation may have occurred during a post 91 to 86, to pre-64 Ma interval, as suggested by regional relationships (Garver, 1989).
- Kilometre-scale northeast-vergent thrusting and folding involves rocks as young as Albian-Cenomanian. Folds and thrusts have good kinematic indicators suggesting northeast-vergence. Folds and thrusts are clearly cut by the small-scale dextral fault system and appear to cut structures related to the Bralorne fault system to the south. Regionally, therefore, this deformation is considered to have occurred between 91 to 86 Ma and 64 Ma (Garver, 1989).
- Southwest-vergent thrusting, recognized elsewhere in the region, is difficult to demonstrate in the North Cinnabar Creek area but evidence in the form of overturned small-scale folds may be present in rocks of the Bridge River complex. Other lines of evidence suggest this was an Albian to Cenomanian event (Garver, 1989).
- Isoclinally folded, blueschist experienced deformation and synkinematic metamorphism in the Triassic. This deformation occurred at or before 230 Ma (Archibald *et al.*, 1991, this volume).

ACKNOWLEDGMENTS

This project was partially funded by the Canada/British Columbia Mineral Development Agreement 1985-1990, the British Columbia Ministry of Energy, Mines and Petroleum Resources, and the Union College Faculty Research Fund. Doug Archibald, Alison Till, Murry Journaey, Todd Smick and Paul Schiarizza provided valuable insight into different aspects of the study. Todd Smick is gratefully acknowledged for his enthusiastic assistance in the field. This manuscript has benefited from reviews by Paul Schiarizza, Doug Archibald and Jacqueline Smith.

REFERENCES

- Archibald, D.A., Glover, J.K. and Schiarizza, P. (1989): Preliminary Report on $^{40}\text{Ar}/^{39}\text{Ar}$ Geochronology of the Warner Pass (92O/3) and Noaxe Creek (92O/2) Map Areas; *B.C. Ministry of Energy, Mines, and Petroleum Resources*, Geological Fieldwork 1988, Paper 1989-1, pages 145-151.
- Archibald, D.A., Schiarizza, P. and Garver, J.I. (1990): $^{40}\text{Ar}/^{39}\text{Ar}$ Dating and the Timing of Deformation and Metamorphism in the Bridge River Terrane, Southwestern British Columbia (92O/2; 92J/15, /16); *B.C. Ministry of Energy, Mines, and Petroleum Resources*, Geological Fieldwork 1989, Paper 1990-1, pages 45-51.
- Archibald, D.A., Schiarizza, P. and Garver, J.I. (1991): $^{40}\text{Ar}/^{39}\text{Ar}$ Evidence for the Age of Metamorphic Events in the Bridge River and Shulaps Complexes, Southwestern British Columbia, (92O/2; 92J/15, 16); *B.C. Ministry of Energy, Mines, and Petroleum Resources*, Geological Fieldwork 1990, Paper 1991-1, this volume.
- Calon, T.J., Malpas, J.G. and McDonald, R. (1990): Anatomy of the Shulaps Ophiolite, Canadian Cordillera; *Geological Association of Canada - Mineralogical Association of Canada*, Program with Abstracts, Volume 15, page A20.
- Coleman, M. (1989): Early Tertiary Deformation in the Bridge River Terrane near Lillooet, British Columbia; *Geological Society of America*, Abstracts with Programs, Volume 21, Number 5, page 68.
- Coleman, M. and Parrish, R.R. (1990): Eocene Deformation in the Bridge River Terrane, B.C.: Constraints on Dextral Movement of the Fraser Fault; *Geological Association of Canada - Mineralogical Association of Canada*, Program with Abstracts, Volume 15, page A26.
- Garver, J.I. (1989): Basin Evolution and Source Terranes of Albian-Cenomanian Rocks in the Tyaughton Basin, Southern British Columbia: Implications for Mid-Cretaceous Tectonics in the Canadian Cordillera; unpublished Ph.D. thesis, *University of Washington*, Seattle, 227 pages.
- Garver, J.I., Schiarizza, P. and Gaba, R.G. (1989a): Stratigraphy and Structure of the Eldorado Mountain Area Cariboo—Chilcotin Mountains, Southern B.C. (92O/02, 92J/15); *B.C. Ministry of Energy, Mines and Petroleum Resources*, Geological Fieldwork 1988, Paper 1989-1, pages 131-143.
- Garver, J.I., Till, A.B., Armstrong, R.L. and Schiarizza, P. (1989b): Blueschist in the Bridge River Complex, Southern British Columbia; *Geological Society of America*, Abstracts with Programs, Volume 21, Number 5, page 82.
- Garver, J.I., Umhoefer, P.J., Rusmore, M. and Schiarizza, P. (1989c): Geology of the Eldorado Mountain Area; *B.C. Ministry of Energy, Mines and Petroleum Resources*, Open File 1989-3.

- Glover J.K. and Schiarizza, P. (1987): Geology and Mineral Potential of the Warner Pass Map Area (92O/03); *B.C. Ministry of Energy, Mines and Petroleum Resources*, Geological Fieldwork 1986, Paper 1987-1, pages 157-169.
- Glover, J.K., Schiarizza, P. and Garver, J.I. (1988a): Geology of the Noaxe Creek Map Area (92O/2); *B.C. Ministry of Energy, Mines and Petroleum Resources*, Geological Fieldwork 1987, Paper 1988-1, pages 105-123.
- Glover, J.K., Schiarizza, P., Garver, J.I. and Umhoefer, P. (1988b): Geology of the Noaxe Creek Map Area (92O/02); *B.C. Ministry of Energy, Mines and Petroleum Resources*, Open File 1988-3.
- Glover, J.K., Schiarizza, P., Umhoefer, P. and Garver, J.I. (1987): Geology of the Warner Pass Map Area (92O/03); *B.C. Ministry of Energy, Mines and Petroleum Resources*, Open File 1987-3A.
- Hansen, E. (1971): *Strain Facies*; Springer-Verlag, New York, 207 pages.
- Leitch, C.H.B., Dawson, K.M. and Godwin, C.I. (1989): Late Cretaceous – Early Tertiary Gold Mineralization: A Galena Lead Isotope Study of the Bridge River Mining Camp, Southwestern British Columbia; *Economic Geology*, Volume 84, pages 2226-36.
- Schiarizza, P., Gaba, R.G., Glover, J.K. and Garver, J.I. (1989a): Geology of the Tyaughton Creek Area (92O/02, 03, 92J/15, 16); *B.C. Ministry of Energy, Mines and Petroleum Resources*, Geological Fieldwork 1988, Paper 1989-1, pages 115-130.
- Schiarizza, P., Gaba, R.J., Garver, J.I., Glover, J.K. and 11 others (1989b): Geology of the Tyaughton Creek Area (92J/15,16; 92O/02,); *B.C. Ministry of Energy, Mines and Petroleum Resources*, Open File 1989-4.
- Schiarizza, P., Gaba, R.J., Coleman, M., Garver, J.I. and Glover, J.K. (1990): Geology and Mineral Occurrences of the Yalakom River Area (92O/1, 2, 92J/15, 16); *B.C. Ministry of Energy, Mines and Petroleum Resources*, Geological Fieldwork 1989, Paper 1990-1, pages 53-72.
- Umhoefer, P.J. (1989): Stratigraphy and Tectonic Setting of the Upper Cadwallader Terrane and Overlying Relay Mountain Group, and Cretaceous to Eocene Structural Evolution of the Eastern Tyaughton Basin, British Columbia; unpublished Ph.D.thesis, *University of Washington*, 186 pages.
- Umhoefer, P.J., Garver, J.I. and Tipper, H.W. (1988): Geology of the Relay Mountain Area (92O/2, 92O/3); *B.C. Ministry of Energy, Mines and Petroleum Resources*, Open File 1988-16.



**⁴⁰Ar/³⁹Ar EVIDENCE FOR THE AGE OF IGNEOUS AND METAMORPHIC
EVENTS IN THE BRIDGE RIVER AND SHULAPS COMPLEXES,
SOUTHWESTERN BRITISH COLUMBIA*
(92O/2; 92J/15, 16)**

By **D.A. Archibald, Queen's University**
P. Schiarizza, Geological Survey Branch
and
J.I. Garver, Union College

KEYWORDS: Geochronology, argon-argon dating, Bridge River complex, Tyaughton Creek, Bralorne, Noaxe Creek, Shulaps ultramafic complex, Yalakom fault, blueschist, deformation, metamorphism.

INTRODUCTION

The Taseko Lakes–Bridge River area is situated approximately 200 kilometres north of Vancouver on the eastern margin of the Coast plutonic complex and west of the Yalakom fault (Figure 1-8-1). This area is the focus of a regional program of ⁴⁰Ar/³⁹Ar dating which was initiated in 1987 in the Warner Pass (92O/3) and Noaxe Creek (92O/2) map areas (Archibald *et al.*, 1989). In 1988 and 1989, the program continued with sampling in the Bralorne (92J/15) and Bridge River (92J/16) map areas. These latter areas are underlain by rocks of the Bridge River complex, and include a fault-bounded panel of blueschist-facies metamorphic rocks (Garver *et al.*, 1989a), the Shulaps ultramafic complex and the Cadwallader Group (Schiarizza *et al.*, 1989, 1990a). Additional, detailed sampling and mapping in the blueschist locality (Bralorne, 92J/15) were completed in 1990. In this note we report ⁴⁰Ar/³⁹Ar step-heating data for a white mica sample from the blueschist rocks, a hornblende sample from a package of sheeted mafic dikes emplaced into Bridge River volcanic rocks, and biotite and hornblende samples from rocks in the Shulaps ultramafic complex.

GEOLOGIC SETTING OF THE SAMPLES

The regional and detailed geology has been outlined in a series of British Columbia Ministry of Energy, Mines and Petroleum Resources publications and preliminary maps (see Figure 1-8-2). Of particular relevance to this study are the reports of the blueschist locality in the Eldorado Mountain area (Garver *et al.*, 1989a; Garver, 1991, this volume) and the summary of the geology within and adjacent to the Shulaps ultramafic complex (Schiarizza *et al.*, 1989, 1990a; Calon *et al.*, 1990).

BLUESCHIST FACIES ROCKS

In the Tyaughton Creek area, there are three areas of blueschist and greenschist-facies metamorphic rocks struc-

turally interleaved with typical Bridge River rocks of lower metamorphic grade. The larger area is in the watershed of North Cinnabar Creek and is a narrow tectonic lens with a strike length of some 4 kilometres. This package is unconformably overlain by middle to upper Albian rocks of the Taylor Creek Group which contain boulders of blueschist, chert and greenstone.

The blueschist is strongly flattened, locally records isoclinal folding, and commonly has a pronounced crenulation cleavage of variable intensity (Garver *et al.*, 1989a). Two principal mineral assemblages have been recognized in this area: crossite/glaucophane+lawsonite, and crossite/glaucophane+garnet+epidote+white mica. These two assemblages, which represent slightly different pressure/temperature conditions during metamorphism, occur in the same area but are probably separated by faults. Prehnite is present as crosscutting veins in both rock types (Garver *et al.*, 1989b). The sample dated in this study contains the second mineral assemblage and the medium to coarse-grained white mica lies nearly in the plane of the schistosity. Previous K-Ar and Rb-Sr dating of rocks and white mica separates from the same structural panel yielded dates between 195 and 250 Ma (Garver *et al.*, 1989b). Step-heating experiments were undertaken to refine the primary cooling age and to determine the magnitude and timing of later thermal events that are thought to have affected the area.

**AMPHIBOLITE KNOCKER FROM THE SHULAPS
ULTRAMAFIC COMPLEX**

The Shulaps ultramafic complex underlies about 180 square kilometres of the Shulaps Range. The southwestern part of the complex sits structurally above the Cadwallader Group and Bridge River complex in a block of relatively high grade (lower to upper greenschist facies) metamorphic rocks bounded by the Mission Ridge and Marshall Creek faults (Coleman, 1989; Potter, 1986). This part of the Shulaps complex comprises harzburgite tectonite structurally underlain by a thick unit of serpentinite mélange that includes knockers of an ultramafic-mafic plutonic-volcanic suite characteristic of the upper part of an ophiolite complex (Calon *et al.*, 1990; Schiarizza *et al.*, 1990a), as well as knockers of bedded chert, limestone, sandstone and pebble

* This project is a contribution to the Canada/British Columbia Mineral Development Agreement.

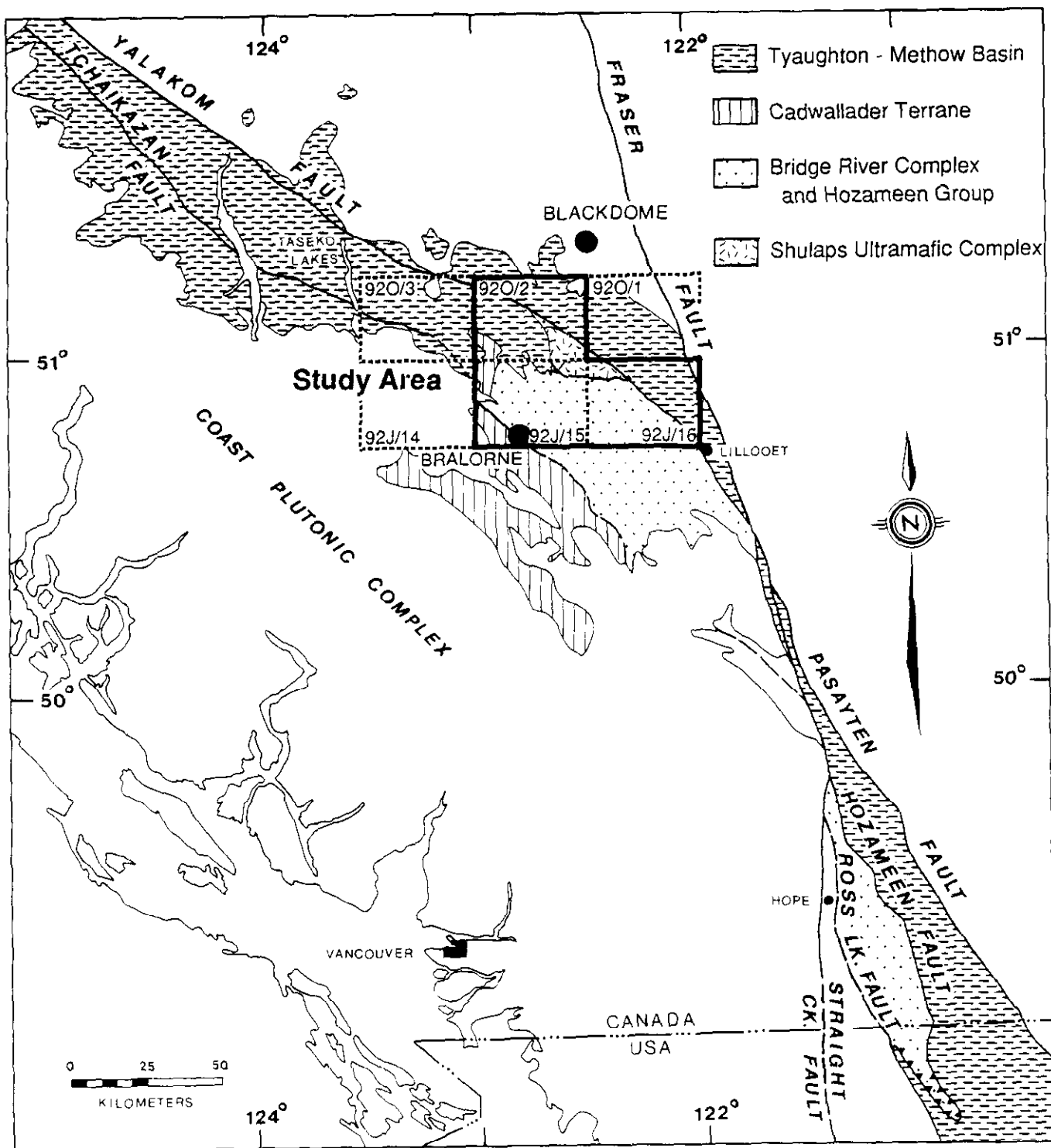


Figure 1-8-1. Location and geological setting, Taseko Lakes-Bridge River map area.

conglomerate. The serpentinite mélangé unit sits structurally above the Cadwallader Group, which in turn sits structurally above the Bridge River complex. The southwestern serpentinite mélangé unit has been sampled extensively for dating and amphibole has yielded a 73 Ma date that is thought to reflect uplift and cooling following synkinematic metamorphism during the latest stages of emplacement-related deformation within the complex (Archibald *et al.*, 1989).

The northwestern, northern and eastern portions of the Shulaps complex comprise harzburgite and underlying serpentinite and serpentinite mélangé which sit structurally above sub-greenschist facies rocks of the Bridge River complex (Schiarizza *et al.*, 1990a, b). These rocks are separated from the higher metamorphic-grade rocks to the southwest by a system of faults that may be a northwestward extension of the northeast-dipping Mission Ridge normal fault (Coleman, 1989; Schiarizza *et al.*, 1990a, b); they may comprise a relatively higher slice within the southwest-vergent Shulaps thrust system than the southwestern Shulaps complex. Dating of samples from the serpentinite mélangé belt along the western margin of the Shulaps complex was therefore undertaken to compare its thermal history with that of the southwestern belt. For this study we selected amphibole from a lens of coarse-grained, massive to weakly lineated, coarsely brecciated amphibolite 6 metres thick. The sample contains well-preserved brown amphibole, saussuritized plagioclase and epidote; it is cut by closely spaced quartz veins.

BIOTITE REACTION ZONE IN THE SHULAPS ULTRAMAFIC COMPLEX

The sample is from a metasomatic reaction zone that formed around a 1 to 2-metre, siliceous phacoid within serpentinite of the Shulaps ultramafic complex. The locality is approximately 10 metres north of a near-vertical, east-striking fault that juxtaposes serpentinitized ultramafic rock on the north against greenschist-facies metachert, marble and metabasalt of the Bridge River complex. This fault is considered to be a component of the Mission Ridge fault system (Coleman, 1989) because it traces eastward into the Mission Ridge fault, and westward into a kinematically congruent east-side-down normal fault system that cuts through the Shulaps complex (Schiarizza *et al.*, 1990a, b).

The sample was collected from the biotite-rich part of the reaction zone that surrounds the phacoid of strongly altered quartz-biotite-feldspar rock. The biotite reaction rim is several centimetres thick and is mantled by a thicker zone rich in quartz-chromite-talc which separates it from unaltered, dark green serpentinite. The phacoid may be a tectonic inclusion of the underlying Bridge River schists incorporated during an earlier episode of thrust faulting, or a tectonothermally reworked, intermediate to felsic dike. As the Mission Ridge pluton and Rexmount porphyry outcrop a short distance to the southeast and metasedimentary knockers have not been mapped in the vicinity, the latter seems more probable.

The sample consists of quartz, plagioclase and biotite. In thin section, the biotite is brown, randomly oriented, dis-

plays even extinction, and has very ragged grain boundaries. The lack of a penetrative fabric in the phacoid or its margin indicates postemplacement recrystallization that was primarily static in nature. This sample was selected for dating because potassic rocks are rare in this part of the Shulaps ultramafic complex, and a biotite date would provide information about the late-stage thermal history of this part of the complex.

SHEETED DIKES IN THE BRIDGE RIVER COMPLEX

Schiarizza *et al.* (1989) describe sheeted mafic dikes from the Bridge River complex. The dikes selected for this study outcrop along the Carpenter Lake road and comprise a set of nearly east-striking, steeply dipping dikes approximately 15 metres thick. Individually, they are less than 2 metres thick, massive, and display a range of grain sizes; medium to coarse-grained dikes are most common. Locally, some of the thicker dikes contain patches of more pegmatitic and leucocratic rock, as well as 1-centimetre phenocrysts of plagioclase. They are in intrusive contact with pillowed volcanic rocks of the Bridge River complex. However, at the southern contact, the dike appears to be chilled against, and to follow a linear, altered breccia zone. Some internal contacts and most fracture surfaces in the dikes and the enclosing volcanic rocks have slickensides with highly variable orientation.

Although these dikes have well-defined internal intrusive contacts, they are locally severely altered rocks composed of brown and green amphibole, chlorite, quartz, calcite and saussuritized plagioclase. Clinopyroxene occurs as remnant grains, as phenocrysts in chilled margins and as rounded inclusions in the hornblende. The amphibole occurs as subhedral to euhedral laths and needles and, although well preserved, commonly displays fracturing and undulatory extinction in thin section. The green amphibole overgrows the brown amphibole, forming a thin rind suggesting a minor greenschist-facies metamorphic overprint, although regionally, rocks from this part of the Bridge River complex contain prehnite-pumpellyite facies mineral assemblages. For this study an attempt was made to separate, and date, the paragenetically older, brown amphibole.

$^{40}\text{Ar}/^{39}\text{Ar}$ ANALYTICAL METHODS

Mineral separates were prepared using a Frantz magnetic separator, heavy organic liquids and, where appropriate, by hand-picking.

Samples and six flux monitors (standards) were irradiated with fast neutrons in position 5C of the McMaster nuclear reactor (Hamilton, Ontario) for 29 hours. The monitors were distributed throughout the irradiation container, and *J*-values for individual samples were determined by interpolation.

Both step-heating experiments and analysis of the monitors were done in a quartz tube heated using a Lindberg furnace. The bakeable, ultrahigh-vacuum, stainless steel argon-extraction system is operated online to a substantially modified, A.E.I. MS-10 mass-spectrometer run in the static

TABLE 1-8-1
⁴⁰Ar/³⁹Ar STEP-HEATING DATA

TL-88-1a White Mica (7-40 mesh)									TL-88-24 Biotite 80/140 mesh																										
Weight (mg) = 100 J = 0.006888									Weight (mg) = 185 J = 0.007																										
Temp. °C	Vol. ³⁹ Ar × 10 ⁻⁸								DATE (4, 5)	± 2σ Ma	Temp. °C	Vol. ³⁹ Ar × 10 ⁻⁸								DATE (4, 5)	± 2σ Ma														
	40/39 (1)	36/39 (1)	37/39 (1, 2)	cc NTP (3)	f39	% ⁴⁰ Ar Rad.	40/39 (1)	36/39 (1)				37/39 (1, 2)	cc NTP (3)	f39	% ⁴⁰ Ar Rad.																				
500	38.423	0.0845	0.592	0.156	0.0044	34.81	158.3	± 33.4										500	22.217	0.0697	0.155	0.523	0.0084	7.26	20.27	± 3.82	540	6.845	0.0116	0.118	1.263	0.0203	50.05	42.76	± 0.77
575	27.209	0.0254	4.707	0.326	0.0093	73.71	234.1	± 7.3										580	4.789	0.0037	0.083	3.598	0.0579	76.98	45.96	± 0.64	625	4.196	0.0015	0.023	7.742	0.1247	89.39	46.75	± 0.35
675	22.104	0.0050	0.919	1.051	0.0299	93.55	240.4	± 4.3										670	4.079	0.0012	0.001	6.764	0.1089	90.99	46.28	± 0.26	710	4.299	0.0019	0.000	3.350	0.0539	86.68	46.46	± 0.72
725	20.909	0.0043	0.130	2.056	0.0585	93.96	229.0	± 2.5										760	4.662	0.0034	0.000	2.001	0.0322	77.89	45.29	± 1.30	810	4.594	0.0027	0.000	2.127	0.0342	82.18	47.06	± 1.53
775	20.631	0.0034	0.017	3.294	0.0937	95.00	228.5	± 0.4										860	4.221	0.0014	0.000	3.819	0.0615	89.65	47.17	± 0.51	910	4.011	0.0008	0.000	9.026	0.1453	93.82	46.91	± 0.35
800	20.440	0.0018	0.009	4.310	0.1226	97.36	231.8	± 0.7										960	3.959	0.0007	0.000	11.216	0.1806	94.38	46.58	± 0.31	1010	4.073	0.0011	0.010	9.331	0.1502	91.95	46.69	± 0.42
825	20.364	0.0022	0.015	8.643	0.2458	96.78	229.6	± 0.8										1060	5.298	0.0050	0.341	0.809	0.0130	72.40	47.82	± 4.55	1200	7.299	0.0105	0.755	0.536	0.0086	57.94	52.66	± 3.55
850	20.497	0.0027	0.014	4.832	0.1374	96.07	229.5	± 0.8																											
875	20.509	0.0025	0.006	5.920	0.1684	96.37	230.3	± 0.8																											
900	20.236	0.0021	0.015	2.220	0.0631	96.88	228.5	± 1.3																											
1000	20.507	0.0027	0.028	1.795	0.0510	96.11	229.7	± 2.4																											
1200	21.908	0.0066	0.250	0.560	0.0159	91.18	232.6	± 5.0																											
				35.163			229.9	± 1.3																											

Total ³⁹Ar = 35.163 × 10⁻⁸ cm³ NTP
 I.A. = 229.9 ± 1.3 Ma
 P.A. = 229.8 ± 1.0 Ma
 Plateau steps: 725 to 1000°C

TL-88-23 Hornblende 80/140 mesh									TL-88-10 Brown Hornblende 80/120 mesh																										
Weight (mg) = 200 J = 0.007									Weight (mg) = 200 J = 0.007																										
Temp. °C	Vol. ³⁹ Ar × 10 ⁻⁸								DATE (4, 5)	± 2σ Ma	Temp. °C	Vol. ³⁹ Ar × 10 ⁻⁸								DATE (4, 5)	± 2σ Ma														
	40/39 (1)	36/39 (1)	37/39 (1, 2)	cc NTP (3)	f39	% ⁴⁰ Ar Rad.	40/39 (1)	36/39 (1)				37/39 (1, 2)	cc NTP (3)	f39	% ⁴⁰ Ar Rad.																				
700	100.838	0.2808	12.947	0.0897	0.0601	18.65	224.8	± 40.4										825	25.987	0.0582	11.421	0.2009	0.0563	37.00	118.4	± 1.1									
800	34.480	0.0682	11.829	0.0524	0.0351	44.03	183.6	± 19.8										900	20.062	0.0337	28.618	0.0803	0.0225	60.87	150.6	± 18.4									
870	41.555	0.0981	13.367	0.0349	0.0234	32.59	164.7	± 91.0										925	19.529	0.0417	16.726	0.0563	0.0158	43.20	104.6	± 43.9									
940	35.333	0.0556	26.631	0.0780	0.0523	59.03	249.8	± 32.0										950	14.552	0.0210	13.807	0.0798	0.0224	64.25	115.4	± 13.8									
1000	27.030	0.0246	28.050	0.4842	0.3247	80.68	260.6	± 8.1										980	10.346	0.0080	12.278	0.3226	0.0905	85.97	109.8	± 7.7									
1040	31.048	0.0391	24.846	0.1333	0.0894	68.64	254.7	± 6.8										1010	9.735	0.0067	11.043	0.4535	0.1272	87.83	105.6	± 4.7									
1070	35.353	0.0512	25.984	0.0955	0.0640	62.59	263.9	± 30.1										1040	9.672	0.0067	9.207	0.8371	0.2348	86.52	103.3	± 6.2									
1100	28.684	0.0285	28.741	0.3090	0.2072	77.95	266.9	± 6.3										1070	10.260	0.0080	9.527	0.6117	0.1716	83.62	105.9	± 1.7									
1200	29.893	0.0348	28.069	0.2144	0.1438	72.44	259.0	± 8.8										1100	11.189	0.0107	9.533	0.5013	0.1406	77.99	107.6	± 4.4									
				1.4912			253.7	± 14.7										1130	13.090	0.0179	9.299	0.2760	0.0774	64.68	104.5	± 12.6									
																		1160	21.174	0.0497	9.066	0.0760	0.0213	33.82	88.8	± 8.1									
																		1200	22.816	0.0461	9.699	0.0702	0.0197	43.36	121.5	± 22.1									

Total ³⁹Ar = 1.4912 × 10⁻⁸ cm³ NTP
 I.A. = 253.7 ± 14.7 Ma
 P.A. = 260.8 ± 10.7 Ma
 Plateau steps: 940 to 1200°C

Total ³⁹Ar = 62.105 × 10⁻⁸ cm³ NTP
 I.A. = 46.37 ± 0.58 Ma
 P.A. = 46.62 ± 0.52 Ma
 Plateau steps: 580 to 1060°C

Total ³⁹Ar = 3.5655 × 10⁻⁸ cm³ NTP
 I.A. = 107.6 ± 6.7 Ma
 P.A. = 105.2 ± 5.7 Ma
 Plateau steps: 1010 to 1200°C

- (1) True ratios corrected for fractionation and discrimination.
- (2) ³⁷Ar/³⁹Ar is corrected for the decay of ³⁷Ar during and after irradiation using a ³⁷Ar half-life of 35.1 days.
- (3) Volume of ³⁹Ar is determined using equilibration peak height and mass spectrometer sensitivity.
- (4) Isotope production ratios for the McMaster reactor are from Masliwec (1981).
- (5) Ages calculated using the constants recommended by Steiger and Jäger (1977). Errors represent the analytical precision only (*i.e.* error in J value = 0). Flux monitor used: LP-6 Biotite at 128.5 Ma.
- (6) I.A. = integrated age for all steps. P.A. = plateau age.

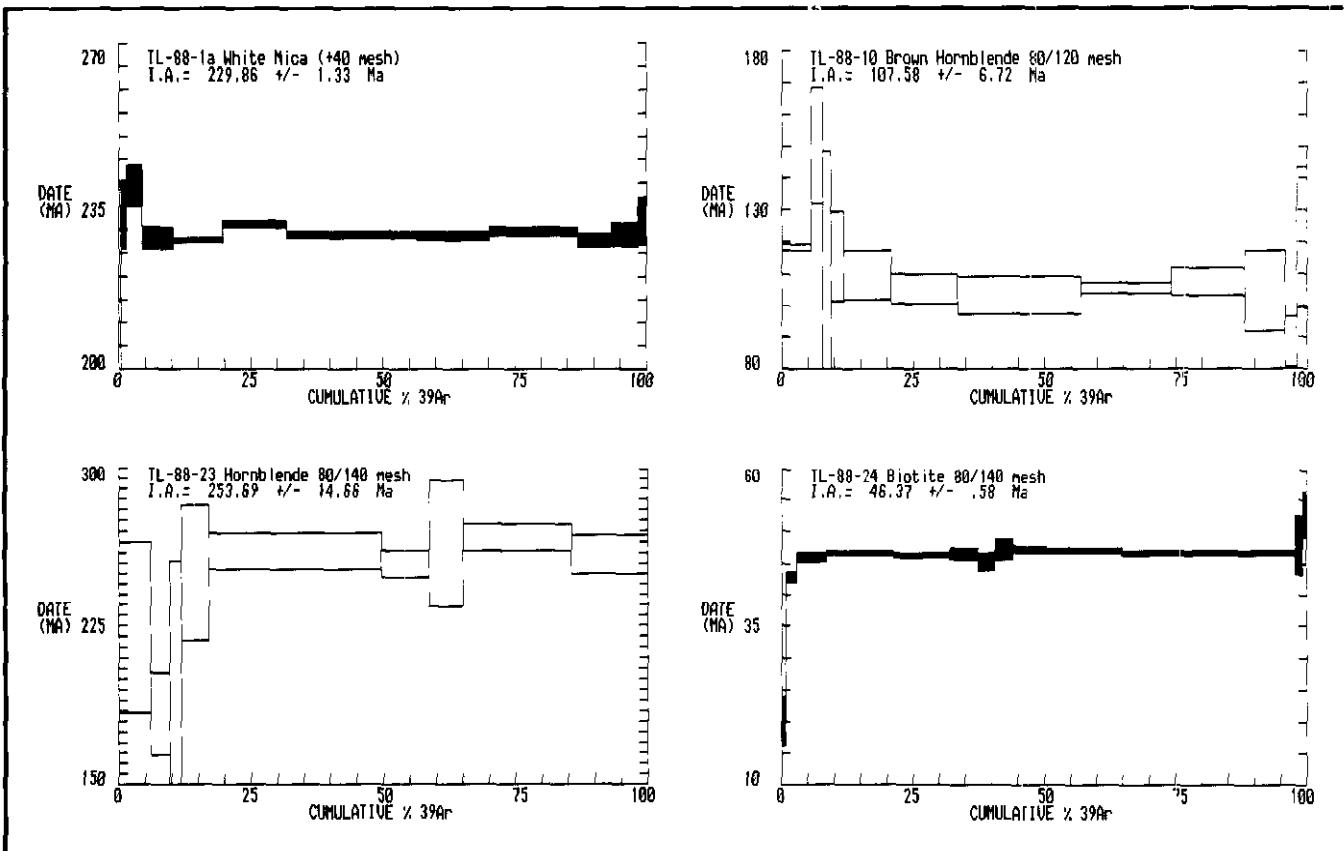
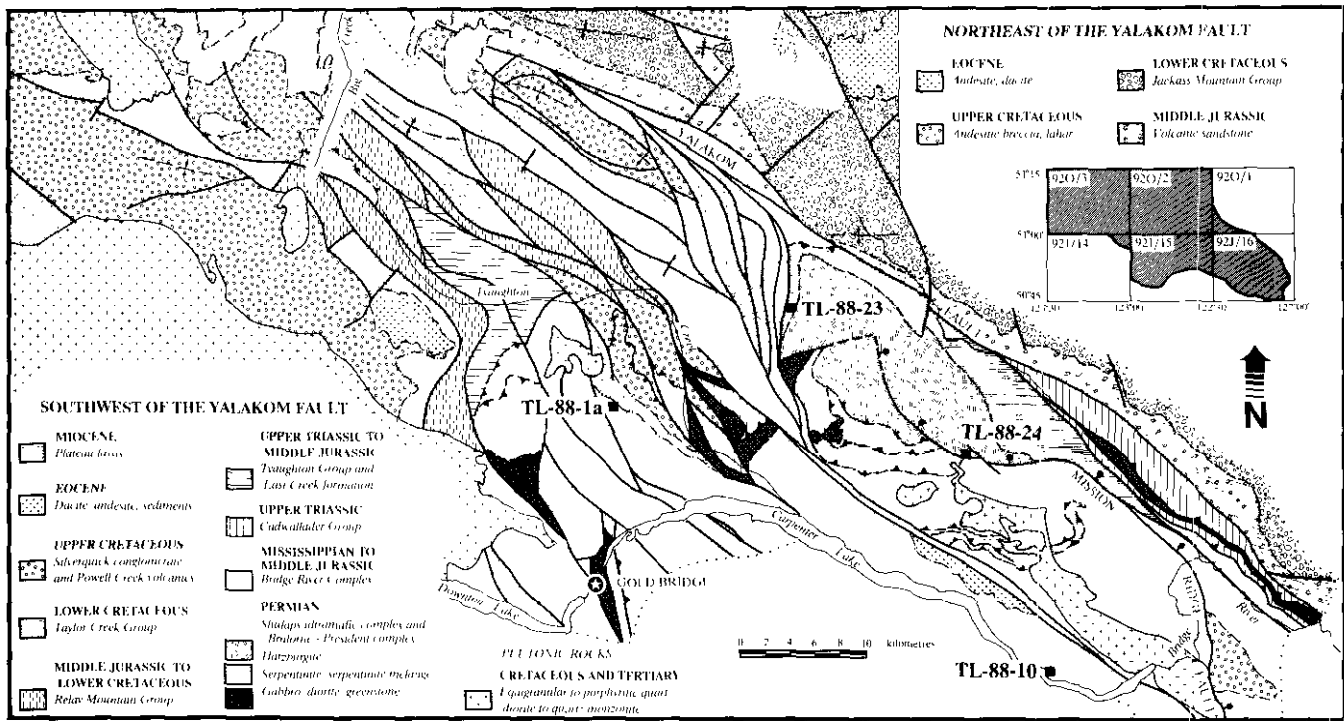


Figure 1-8-2. Sample locations and $^{40}\text{Ar}/^{39}\text{Ar}$ age spectra for rocks from the Bridge River and Shufaps complexes, southwestern British Columbia.

mode. Measured mass-spectrometric ratios were extrapolated to zero-time, corrected to an $^{40}\text{Ar}/^{36}\text{Ar}$ atmospheric ratio of 295.5, and corrected for neutron induced ^{40}Ar from potassium, and ^{39}Ar and ^{36}Ar from calcium. Dates and errors were calculated using formulae given by Dalrymple *et al.* (1981), and the constants recommended by Steiger and Jäger (1977). The errors shown in Table 1-8-1 were used to plot the age spectra in Figure 1-8-2: these represent the analytical precision at 2σ assuming that the error in the J-value is zero.

RESULTS AND DISCUSSION

BLUESCHIST-FACIES ROCKS

RESULTS

The age spectrum for the white mica from the blueschist locality (TL-88-1a) is shown in Figure 1-8-2; analytical data are listed in Table 1-8-1. The integrated age of this sample is 229.9 ± 1.3 (2σ) Ma which is in the range of previous dates for this site (Permo-Triassic; Garver *et al.*, 1989b). The 500°C step yields a date of 158 Ma, and dates for subsequent steps are all in excess of 228 Ma. The steps from 725° to 1200°C yield a well-defined plateau date of 229.8 ± 1.0 (2σ) Ma for 95 per cent of the ^{39}Ar released from the sample. In this temperature range, the $^{37}\text{Ar}/^{39}\text{Ar}$ ratio ranges from 0.006 to 0.25 which corresponds to the low Ca/K ratio of phengite (*e.g.* Sisson and Onstott, 1986). The age spectrum does not record any evidence of a post-Triassic, thermal perturbation. Thus, it appears that blueschist facies metamorphism in the Bridge River complex is a Middle Triassic or older event that ended by 230 Ma.

DISCUSSION

The white mica from the blueschist contains a record of only one tectonothermal event. Blueschist-facies metamorphism is a low-temperature event ($300\text{-}400^\circ\text{C}$; Sisson and Onstott, 1986) and the mica may have grown in this temperature range. As the mica grew syntectonically, the 230 Ma plateau date for the mica implies that both deformation (development of schistosity) and metamorphism are at least this old. The two K-Ar dates older than this (reported by Garver *et al.*, 1989b) remain problematic, and additional analyses of white mica are planned; these will include white mica from blueschist cobbles in the Dash conglomerate at the base of the Taylor Creek Group.

Archibald *et al.* (1990) reported an age spectrum for nearly identical white mica (but from a different sample) that yielded a 221 Ma plateau segment as well as a 500°C step, indicating that the area was affected by a thermal event in post-Late Triassic time. Based on modelling of this previously reported age spectrum, the thermal event must have been of short duration and/or of low temperature (the closure temperature of argon diffusion in white mica is 350°C); an original cooling age only slightly greater than the 221 Ma plateau date ($225\text{-}230$ Ma) was favoured for this sample. The new data support this conclusion and suggest that blueschist-facies metamorphism ended in Middle Triassic time.

The post-Triassic thermal overprint was inferred by Archibald *et al.* (1990) to reflect structural thickening associated with a protracted episode of contractional deformation that affected the region in mid-Cretaceous time. The latest manifestation of this deformation is reflected in the sample area by a system of northeast-vergent thrusts within the Bridge River complex and a large overturned footwall fold outlined by unconformably overlying mid-Cretaceous rocks of the Taylor Creek Group and Silverquick conglomerate (*see* Garver, 1991, this volume). These mid-Cretaceous clastics were deposited during the earlier stages of contractional deformation, which generated a complex system of southwest-vergent thrust and reverse faults (Garver, 1989; Schiarizza *et al.*, 1990a, c; Calon *et al.*, 1990). Partial argon loss during this protracted contractional event may explain the wide range of K-Ar dates for blueschist rocks reported by Garver *et al.* (1989a); crenulation of the blueschist rocks is variable and most white mica porphyroblasts show degrees of kinking. It is possible that the variable development of a crenulation cleavage, interpreted by Garver (1991, this volume) to be related to Cretaceous contraction, may have facilitated partial argon loss.

AMPHIBOLITE KNOCKER FROM THE SHULAPS ULTRAMAFIC COMPLEX

RESULTS

The age spectrum for the amphibole from the knocker (TL-88-23) is shown in Figure 1-8-2; analytical data are listed in Table 1-8-1. The integrated date for this age spectrum is 253.7 ± 14.7 Ma (2σ). The four lowest temperature steps are characterized by low radiogenic content, erratic $^{37}\text{Ar}/^{39}\text{Ar}$ ratios and large errors. In contrast, the remaining, higher temperature steps representing 83 per cent of the total ^{39}Ar , have a consistent $^{37}\text{Ar}/^{39}\text{Ar}$ ratio averaging 27 ± 3 (2σ), are much more radiogenic and represent the main pulse of argon release from the amphibole. These steps define a plateau date of 260.8 ± 10.7 (2σ) Ma. Although the analytical errors are large (due to the small volume of argon released in each step), there is no evidence in the age spectrum of a later thermal overprint. To test for the presence of initial argon, an Ar-Ar correlation analysis was done for the plateau segment. This revealed an initial $^{40}\text{Ar}/^{36}\text{Ar}$ ratio of 257 ± 68 (2σ) (slightly less than the expected atmospheric argon ratio of 295.5) and an older age for the plateau segment of 271 ± 16 Ma (2σ ; MSWD=0.9 for steps: 940° to 1200°C). We consider the correlation plot date to be a reliable cooling age for this sample. This age spectrum indicates that this part of the Shulaps complex records a different thermal history than the southwestern part of the complex, and that the amphibolite cooled following metamorphism in Early Permian time.

DISCUSSION

The amphibolite knocker sampled from the serpentinite mélange along the northwestern margin of the Shulaps complex is lithologically similar to the samples from the southwestern part of the complex reported on previously (Archibald *et al.*, 1989). Both samples are thought to have been

derived from mafic plutonic rocks of the Shulaps ophiolite complex. Synkinematic metamorphism indicated by their textures and mineralogy is attributed to ocean-floor processes during the protracted constructional phase of the ophiolite complex; this interpretation follows the recognition of similar ductile deformation fabrics in the large ultramafic-mafic plutonic blocks of the southwestern serpentinite mélangé belt which developed during and between plutonic episodes (Calon *et al.*, 1990). Amphibole from the knocker in the southwestern mélangé belt yielded a plateau date of 72.6 ± 0.5 Ma, suggesting that it was reheated to at least greenschist-facies conditions and cooled through approximately 500°C in Late Cretaceous time (Archibald *et al.*, 1989). Cretaceous heating of the southwestern serpentinite mélangé belt is consistent with its structural setting within the metamorphic belt bounded by the Mission Ridge and Marshall Creek faults (Potter, 1986; Coleman, 1989; Schiarizza *et al.*, 1990a, b); at least some of the heating is attributed to intrusion of a suite of late kinematic dioritic dikes which caused local prograde metamorphism within the mélangé (Archibald *et al.*, 1989, 1990; Calon *et al.*, 1990).

The 271 Ma date for the amphibolite knocker along the northwestern margin of the Shulaps complex is interpreted to be the age of cooling following metamorphism, deformation and plutonism related to ocean-floor construction of the Shulaps ophiolite. There is no indication of the Late Cretaceous heating that affected the southwestern serpentinite mélangé belt, despite the fact that Late Cretaceous dikes and plugs are found throughout the northern part of the complex (Leech, 1953; Archibald *et al.*, 1989, 1990; Schiarizza *et al.*, 1990a, b). The lack of a Cretaceous overprint may reflect a structurally high origin for the northern and eastern Shulaps complex; these rocks may have been subsequently down-dropped on faults related to the Eocene Mission Ridge fault (Figure 1-8-2).

The Early Permian date provides the first direct evidence of the age of the oceanic crust and upper mantle represented by the Shulaps ultramafic complex. The new date is almost identical to recent U-Pb zircon dates obtained by Leitch (1989) from diorite and soda granite of the Bralorne intrusive complex, 20 kilometres to the southwest, which, together with associated ultramafic rocks, has also been inferred to be of ophiolitic affinity (Wright, 1974; Leitch, 1989). The Permian dates corroborate the correlation implied by Wright *et al.* (1982) who included the Shulaps complex, together with ultramafic and associated rocks near Bralorne, in the Bridge River ophiolite assemblage. The Permian dates also corroborate the structural interpretation advanced by Schiarizza *et al.* (1990c) which suggests that the rocks near Bralorne are actually part of the same imbricate thrust sheet as the Shulaps complex, which is repeated across a relatively late southwest-vergent reverse fault defining the eastern margin of the Bralorne fault system.

BIOTITE REACTION ZONE IN THE SHULAPS ULTRAMAFIC COMPLEX

RESULTS

The age spectrum for biotite from the biotite reaction zone (TL-88-24) is shown in Figure 1-8-2 and the analytical

data are presented in Table 1-8-1. The sample yielded an integrated age of 46.4 ± 0.6 Ma. With the exception of the first two and the last two steps (representing $< 5\%$ of the gas released) the sample yields a well-defined plateau corresponding to an age of 46.6 ± 0.5 Ma. This is interpreted as indicating the time the rock cooled through the argon closure temperature of biotite (*ca.* 280°C).

DISCUSSION

In light of the probable igneous origin, boudinage and postkinematic recrystallization of this rock, the $^{40}\text{Ar}/^{39}\text{Ar}$ plateau from the biotite is interpreted as the time of postemplacement cooling. In rocks 20 kilometres to the southeast, Coleman and Parrish (1990) have documented an Eocene plutonic event broadly synchronous with ductile deformation associated with dextral strike-slip faulting. Their U-Pb data indicate a period (48.5 and 46.5 Ma) of ductile deformation and dextral movement within the Bridge River schists related to strike-slip faulting on the northwest-trending Yalakom fault system. Intrusion of hornblende porphyry and felsite continued through later brittle phases of deformation, which included rapid uplift and tectonic denudation along the Mission Ridge fault (Coleman, 1989). Our data suggest that the southern part of the Shulaps ultramafic complex was the locus of Eocene granitoid emplacement and was involved in this Eocene tectonic event.

SHEETED DIKES IN THE BRIDGE RIVER COMPLEX

RESULTS

The age spectrum for a separate of brown amphibole from the centre of a 1.5-metre dike (TL-88-10) is shown in Figure 1-8-2; analytical data appear in Table 1-8-1. The sample yielded an integrated date of 108 ± 7 Ma. The low-temperature steps ($< 980^\circ\text{C}$) are characterized by high $^{37}\text{Ar}/^{39}\text{Ar}$ ratios and high atmospheric argon contamination and account for 12 per cent of the ^{39}Ar released from the sample. The higher temperature steps are more radiogenic and most of the gas released in these steps has a $^{37}\text{Ar}/^{39}\text{Ar}$ ratio of approximately 9.5 suggestive of release from a single phase. The release of ^{39}Ar centred on a temperature of 1040°C is typical of hornblende rather than actinolite. These higher temperature steps (1010 to 1200°C) define a plateau date of 105 ± 6 Ma. A correlation plot for the eight steps from 980 to 1200°C yields a well-defined isochron age of 107 ± 3 Ma (2σ) and an initial $^{40}\text{Ar}/^{39}\text{Ar}$ ratio of 277 ± 36 (2σ) with an MSWD of 2. The initial ratio is slightly lower than atmospheric argon and does not indicate the presence of excess argon. This date is the best estimate of the age of this sample and suggests that the area cooled through the argon closure temperature of hornblende in mid-Cretaceous time.

DISCUSSION

The sheeted dikes within the Bridge River complex were presumed by Schiarizza *et al.* (1989) to be an intrusive phase of the Bridge River greenstones, emplaced in a

spreading-centre environment within the Bridge River ocean basin. It is unlikely, however, that the mid-Cretaceous date reflects the age of relict Bridge River oceanic crust because cherts from the immediate area are Late Triassic in age (Cordey, 1986) and are only known to be as young as Middle Jurassic for the complex as a whole (F. Cordey, personal communication, July, 1990). The presence of the green amphibole rims suggests that the date may reflect cooling following reheating of the dikes under conditions sufficient to reset the K-Ar system of amphibole, but any such reheating is not reflected in surrounding Bridge River rocks which are at prehnite-pumpellyite metamorphic grade (Potter, 1986; Schiarizza *et al.*, 1989, 1990a). It is considered more likely that the dikes are the products of a relatively young magmatic event, unrelated to the ocean-floor construction of the plutonic-volcanic elements of the Bridge River complex. The multiple emplacement of the dikes may have been the source of heat for the alteration event (auto-metamorphism); thus the 107 Ma date is thought to indicate that dike emplacement and related alteration processes ended in late Early Cretaceous time. If dike emplacement was not a protracted event, then the 107 Ma date for the amphibole would provide a good estimate of the age of the dikes.

Regionally the latter part of the Early Cretaceous marked the beginning of a protracted episode of contractional deformation that extended into Late Cretaceous time (Garver, 1989; Schiarizza *et al.*, 1990c). The early stages of deformation involved southwest-verging thrust imbrication of the Shulaps complex, Bridge River complex and Cadwallader Group, and deposition of a thick accumulation of syn-orogenic clastic sediments represented by the Taylor Creek Group. Therefore the sheeted gabbroic dikes were apparently emplaced during the final collapse and destruction of the Bridge River ocean basin, rather than during construction of Bridge River oceanic crust as previously inferred (Schiarizza *et al.*, 1989). The Early Cretaceous gabbroic dikes described herein, together with Late Cretaceous dioritic dikes emplaced during the late stages of contractional deformation within the Shulaps complex (Archibald *et al.*, 1989, 1990), suggest that a prolonged episode of mafic to intermediate magmatism was coincident with the contractional deformation.

SUMMARY AND CONCLUSIONS

There are several conclusions which may be drawn concerning the timing of deformation, metamorphism and magmatism in the Taseko Lakes – Bridge River area:

- Blueschist-facies metamorphism and attendant deformation within the fault-bounded panels of blueschist are Middle Triassic or older events (230 Ma).
- The Shulaps complex is at least Permian (270 Ma) as the northwestern part of the complex records probable sea-floor metamorphism of at least this age. This age is nearly identical to the age of the Bralorne diorite and supports the correlation of the two mafic-ultramafic suites.
- The southern Shulaps ultramafic complex cooled through the argon closure temperature of biotite at 46.6 Ma during the waning stages of Middle Eocene magmatism and tectonism.
- Undeformed but hydrothermally altered, sheeted, gabbroic dikes were emplaced into the Bridge River complex at or before 107 Ma. They may be part of a suite of synorogenic mafic to intermediate intrusions emplaced during Early to Late Cretaceous contractional deformation.
- The step-heating results for amphibole from the Shulaps complex are consistent with a structural interpretation which suggests that the northern and eastern parts of the complex have been down-dropped and juxtaposed against higher grade rocks in the south-western part of the complex by Eocene extension faults.

ACKNOWLEDGMENTS

This project was funded in part by the Canada/British Columbia Mineral Development Agreement through research agreements to D.A.A. and J.I.G. Partial support for field and laboratory expenses was provided by Energy, Mines and Resources Canada Research Agreement to D.A.A. The Geochronology Laboratory at Queen's University is supported by Natural Sciences and Engineering Research Council operating and Queen's University Advisory Research Committee grants to E. Farrar.

REFERENCES

- Archibald, D.A., Glover, J.K. and Schiarizza, P. (1989): Preliminary Report on $^{40}\text{Ar}/^{39}\text{Ar}$ Geochronology of the Warner Pass, Noaxe Creek and Bridge River Map Areas (92O/3, 2; 92J/16); *B.C. Ministry of Energy, Mines and Petroleum Resources, Geological Fieldwork 1988, Paper 1989-1, pages 145-151.*
- Archibald, D.A., Schiarizza, P. and Garver, J.I. (1990): $^{40}\text{Ar}/^{39}\text{Ar}$ Dating and the Timing of Deformation and Metamorphism in the Bridge River Terrane, South-western British Columbia (92O/2; 92J/15); *B.C. Ministry of Energy, Mines and Petroleum Resources, Geological Fieldwork 1989, Paper 1990-1, pages 45-51.*
- Calon, T.J., Malpas, J.G. and Macdonald, R. (1990): The Anatomy of the Shulaps Ophiolite; *B.C. Ministry of Energy, Mines and Petroleum Resources, Geological Fieldwork 1989, Paper 1990-1, pages 375-386.*
- Coleman, M.E. (1989): Geology of Mission Ridge, near Lillooet, British Columbia (92I, J); *B.C. Ministry of Energy, Mines and Petroleum Resources, Geological Fieldwork 1988, Paper 1989-1, pages 99-104.*
- Coleman, M.E. and Parrish, R.R. (1990): Eocene Deformation in the Bridge River Terrane, British Columbia: Constraints on Dextral Movement on the Fraser Fault; *Geological Association of Canada, Program with Abstracts, Volume 15, page A26.*

- Cordey, F. (1986): Radiolarian Ages from the Cache Creek and Bridge River Complexes and from Chert Pebbles in Cretaceous Conglomerates, Southwestern British Columbia; in *Current Research, Part A, Geological Survey of Canada*, Paper 86-1A, pages 596-602.
- Dalrymple, G.B., Alexander, Jr., E.C., Lanphere, M.A. and Kraker, G.P. (1981): Irradiation of Samples for $^{40}\text{Ar}/^{39}\text{Ar}$ Dating Using the Geological Survey TRIGA Reactor; *U.S. Geological Survey*, Professional Paper 1176, 55 pages.
- Garver, J.I. (1989): Basin Evolution and Source Terranes of Albian-Cenomanian Rocks in the Tyaughton Basin, Southern British Columbia: Implications for Mid-Cretaceous Tectonics in the Canadian Cordillera; unpublished Ph.D. thesis, *University of Washington*, Seattle, Washington.
- Garver J.I. (1991): Kinematic Analysis and Timing of Structures in the Bridge River Complex and Overlying Cretaceous Sedimentary Rocks, Cinnabar Creek Area, Southwestern British Columbia (92J/5); *B.C. Ministry of Energy, Mines and Petroleum Resources*, Geological Fieldwork 1990, Paper 1991-1, this volume.
- Garver, J.I., Schiarizza, P. and Gaba, R.G. (1989a): Stratigraphy and Structure of the Eldorado Mountain Area, Chilcotin Ranges, Southwestern British Columbia (92O/2; 92J/15); *B.C. Ministry of Energy, Mines and Petroleum Resources*, Geological Fieldwork 1988, Paper 1989-1, pages 131-143.
- Garver, J.I., Till, A.B., Armstrong, R.L. and Schiarizza, P. (1989b): Permo-Triassic Blueschist in the Bridge River Complex, Southern British Columbia; *Geological Society of America*, Abstracts with Program, Volume 21, Number 5, page 82.
- Leech, G.B. (1953): Geology and Mineral Deposits of the Shulaps Range; *B.C. Ministry of Energy, Mines and Petroleum Resources*, Bulletin 32, 54 pages.
- Leitch, C.H.B. (1989): Geology, Wallrock Alteration, and Characteristics of the Ore Fluid at the Bralorne Mesothermal Gold Vein Deposit, Southwestern British Columbia; unpublished Ph.D. thesis, *The University of British Columbia*, 483 pages.
- Masliwec, A. (1981): The Direct Dating of Ore Minerals; unpublished M.Sc. thesis, *University of Toronto*.
- Potter, C.J. (1986): Origin, Accretion and Post-accretionary Evolution of the Bridge River Terrane, Southwest British Columbia; *Tectonics*, Volume 5, pages 1027-1041.
- Schiarizza, P., Gaba, R.G., Glover, J.K. and Garver, J.I. (1989): Geology and Mineral Occurrences of the Tyaughton Creek Area (92O/2, 92J/15,16); *B.C. Ministry of Energy, Mines and Petroleum Resources*, Geological Fieldwork 1988, Paper 1989-1, pages 115-130.
- Schiarizza, P., Gaba, R.G., Coleman, M., Garver, J.I. and Glover, J.K. (1990a): Geology and Mineral Occurrences of the Yalakom River Area (92O/1, 2, 92J/15, 16); *B.C. Ministry of Energy, Mines and Petroleum Resources*, Geological Fieldwork 1989, Paper 1990-1, pages 53-72.
- Schiarizza, P., Gaba, R.G., Coleman, M., Glover, J.K., Macdonald, R., Calon, T., Malpas, J., Garver, J.I. and Archibald, D.A. (1990b): Geology and Mineral Potential of the Yalakom River Area; *B.C. Ministry of Energy, Mines and Petroleum Resources*, Open File 1990-10.
- Schiarizza, P., Garver, J.I., Glover, J.K., Gaba, R.G. and Umhoefer, P.J. (1990c): Mid-Cretaceous Structural History of the Taseko Lakes – Bridge River Area, Southwestern British Columbia: Part of the Boundary between the Intermontane and Insular Superterrane; *Geological Association of Canada*, Program with Abstracts, Volume 15, page A118.
- Sisson, V.B. and Onstott, T.C. (1986): Dating Blueschist Metamorphism: A Combined $^{40}\text{Ar}/^{39}\text{Ar}$ and Electron Microprobe Approach; *Geochimica et Cosmochimica Acta*, Volume 50, pages 2111-2117.
- Steiger, R.H. and Jäger, E. (1977): Subcommission on Geochronology: Convention on the Use of Decay Constants in Geo- and Cosmo-chronology; *Earth and Planetary Science Letters*, Volume 36, pages 359-362.
- Wright, R.L. (1974): Geology of the Pioneer Ultramafite, Bralorne, British Columbia; unpublished M.Sc. thesis, *The University of British Columbia*, 178 pages.
- Wright, R.L., Nagel, J. and McTaggart, K.C. (1982): Alpine Ultramafic Rocks of Southwestern British Columbia; *Canadian Journal of Earth Sciences*, Volume 19, pages 1156-1173.

NOTES



QUATSINO SOUND PROJECT (92L/5, 6, 11, 12)

By N.W.D. Massey and D.M. Melville

KEYWORDS: Regional mapping, Quatsino Sound, Wrangellia, stratigraphy, mineral occurrences.

INTRODUCTION

The Quatsino Sound project is a five-year 1:50 000-scale regional mapping program in northern Vancouver Island, begun in 1990. The project area is centred upon Quatsino Sound and extends from Port Hardy in the north to Merry Widow Mountain in the south, and from the Benson River in the east to Holberg in the west. It comprises the Quatsino (92L/12) and Mahatta Creek (92L/5) map sheets and the western halves of the Port McNeil (92L/11) and Alice Lake (92L/6) sheets. Access throughout the area is generally good with an extensive network of public and logging roads. Logging activity continues to open up the area, particularly in the west. Shorelines of the inlets and many lakes are accessible in most areas by small boats, and water taxis serve some of the areas inaccessible by road.

Previous mapping in the Quatsino Sound area has been carried out by both provincial and federal government agencies beginning with the pioneering work of Dawson (1887). Studies of the geology and mineral deposits have included those of Gunning (1930), Jeffrey (1962), McCammon (1969) and Northcote (1969, 1971, 1973). The most recent published mapping is that of Muller *et al.* (1974).

In addition to geological studies, the project area has recently been covered by the 1:50 000 Vancouver Island aeromagnetic survey, and is within the 1988 Regional Geochemical Survey area (Matysek *et al.*, 1989).

REGIONAL GEOLOGY

The project area is part of the Wrangellia Terrane and has similar stratigraphy to both Vancouver Island and the Queen Charlotte Islands. It is underlain by a thick sequence of Upper Triassic and Lower Jurassic volcanic and sedimentary rocks, overlain by Cretaceous sediments (Figure 1-9-1). The following stratigraphic units have been recognized:

Vancouver Group – an Upper Triassic oceanic assemblage, related to submarine rifting or eruption of widespread flood-basalts, includes pillowed and massive flows (Karmutsen Formation), and is overlain by shallow-water platformal limestones and shales (Quatsino and Parson Bay formations).

Bonanza Group – a Lower Jurassic calcalkaline volcanic assemblage developed in a continental arc on the Wrangellian basement of the western margin of Vancouver Island. It comprises a lower, marine sedimentary suite and an upper, marine to subaerial volcanic package.

Island Plutonic Suite – several stocks intrude the lower Mesozoic sequences. They vary in composition from

gabbro to granodiorite and are coeval with the Bonanza Group volcanics.

Longarm Formation (Kyuquot Group) – marine clastic sediment wedges of Early Cretaceous age onlap onto the older basement.

Queen Charlotte Group – a Lower Cretaceous fluvial sequence that includes coaly intervals.

Nanaimo Group – Upper Cretaceous clastic sediments underlie the Squash basin on the northeast margin of the project area. They are regarded as the northernmost extension of the Nanaimo Group.

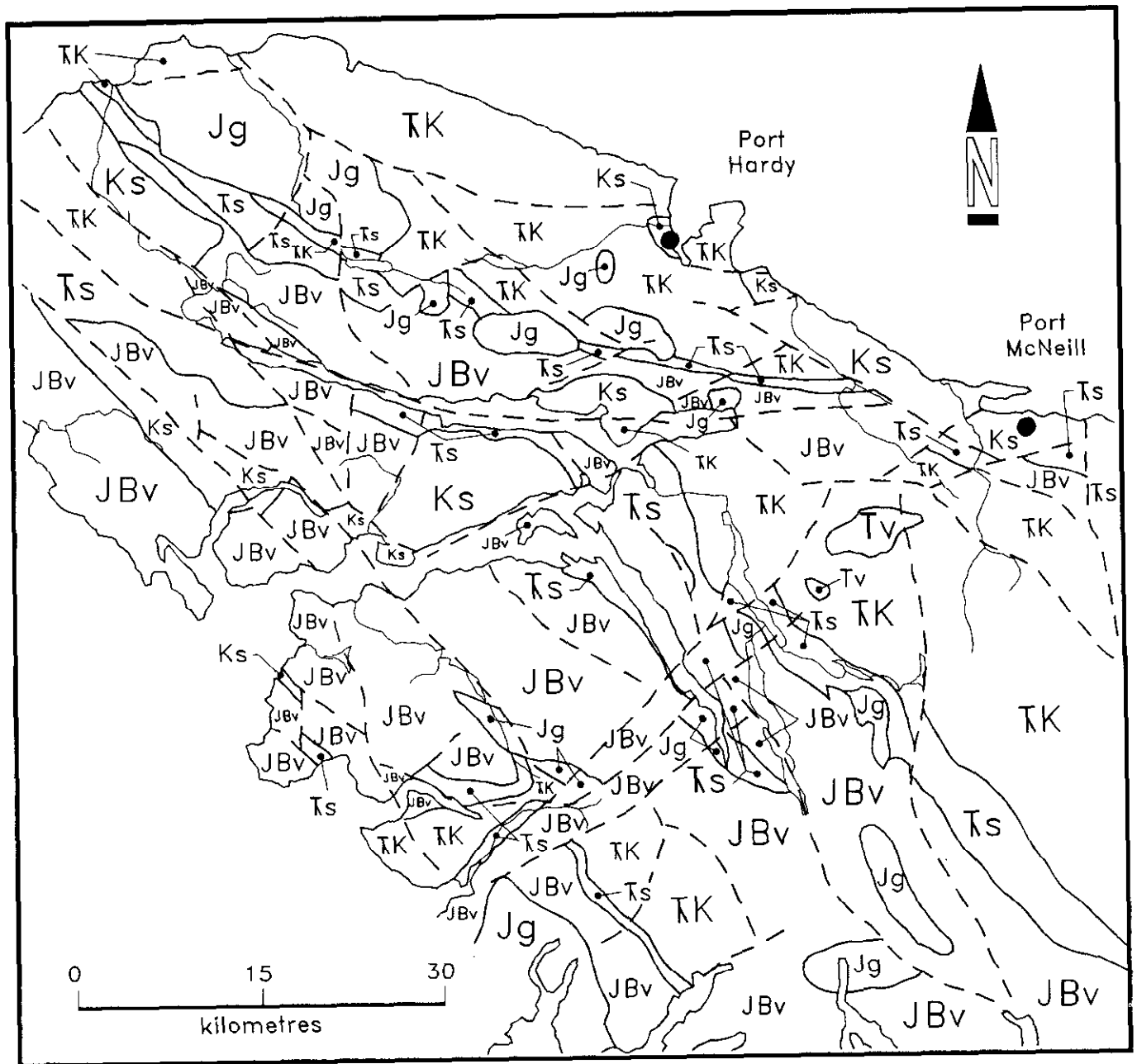
Alert Bay Volcanics – Miocene mafic to felsic fore-arc volcanic and volcanoclastic rocks form a northeasterly trending chain across the southern part of the project area.

Muller *et al.* (1974) described the major structural architecture of northern Vancouver Island as being dominated by fault-bound blocks each with essentially homoclinal south-westerly dipping strata. The northeast-trending Brooks Peninsula fault zone is spatially associated with late Tertiary volcanics and has been interpreted as being related to the Miocene position of the Juan de Fuca Ridge, near the Brooks Peninsula (Riddihough, 1977; Armstrong *et al.*, 1985). The tectonics, age and sense of motion on most other faults in the area are not well constrained. Northwest-trending faults may result from a late Cretaceous or Tertiary dextral transpressive regime. The more westerly trending Holberg fault was interpreted by Muller *et al.* as being a sinistral strike-slip fault, possibly of mid-Cretaceous age, but could also be a thrust fault within the dextral transpressive regime (T.D.J. England, personal communication, 1990).

ECONOMIC GEOLOGY

Known metal mineralization in the project area includes:

- Iron-copper-molybdenum-(?)gold skarns are hosted principally within limestone and limy tuffs in the upper Karmutsen and the Quatsino formations. Examples include the past-producing Merry Widow and Coast Copper mines.
- Copper-molybdenum porphyry stockworks are hosted by Bonanza Group volcanics intruded by several suites of Jurassic porphyry dikes. The Island Copper mine is presently producing, and exploration is in progress on the Expo and Red Dog properties north of Holberg Inlet.
- Lead-zinc mantos and replacement bodies are hosted by Quatsino and Parson Bay limestones. Examples include the H.P.H. showing near Nahwiti Lake.



LEGEND

- Tv - Tertiary volcanics
- Ks - Cretaceous sediments
- JBv - Bonanza volcanics
- Jg - Jurassic Island plutonic suite
- Ts - Upper Triassic sediments
- TK - Triassic Karmutsen Formation

Figure 1-9-1: Simplified geological map of northern Vancouver Island (after Muller, 1974).

- Epithermal to mesothermal, shear-hosted quartz-carbonate veins containing gold, silver, arsenic, antimony and mercury are found in basalts and diabase of the Karmutsen Formation.

The porphyry, skarn and manto deposits appear to be interrelated in a major metallogenic system associated with an early Jurassic arc. Models of similar arc-related deposits suggest a potential for epithermal gold in Bonanza volcanics and possibly for Carlin-style gold in Parson Bay and Bonanza sediments (Panteleyev, 1986; Sillitoe and Bonham, 1990).

Alaskan equivalents of the Quatsino limestones are the host to stratiform copper deposits (Armstrong *et al.*, 1969;

Armstrong and MacKevett, 1982); similar deposits have not yet been explored for on Vancouver Island. There is also an unknown potential for base metal massive sulphide deposits in the lower marine sections of the Bonanza Group.

Cretaceous sediments in the Coal Harbour area, and particularly the Suquash basin, are the host to historically important coal deposits. These coal deposits are no longer economically viable but they offer some potential for the recovery of coalbed methane. On the Queen Charlotte Islands, parts of the Lower Cretaceous sedimentary sequence have some potential as reservoir rock for petroleum, but source rocks are probably absent on Vancouver Island. White recrystallized limestone is currently quar-

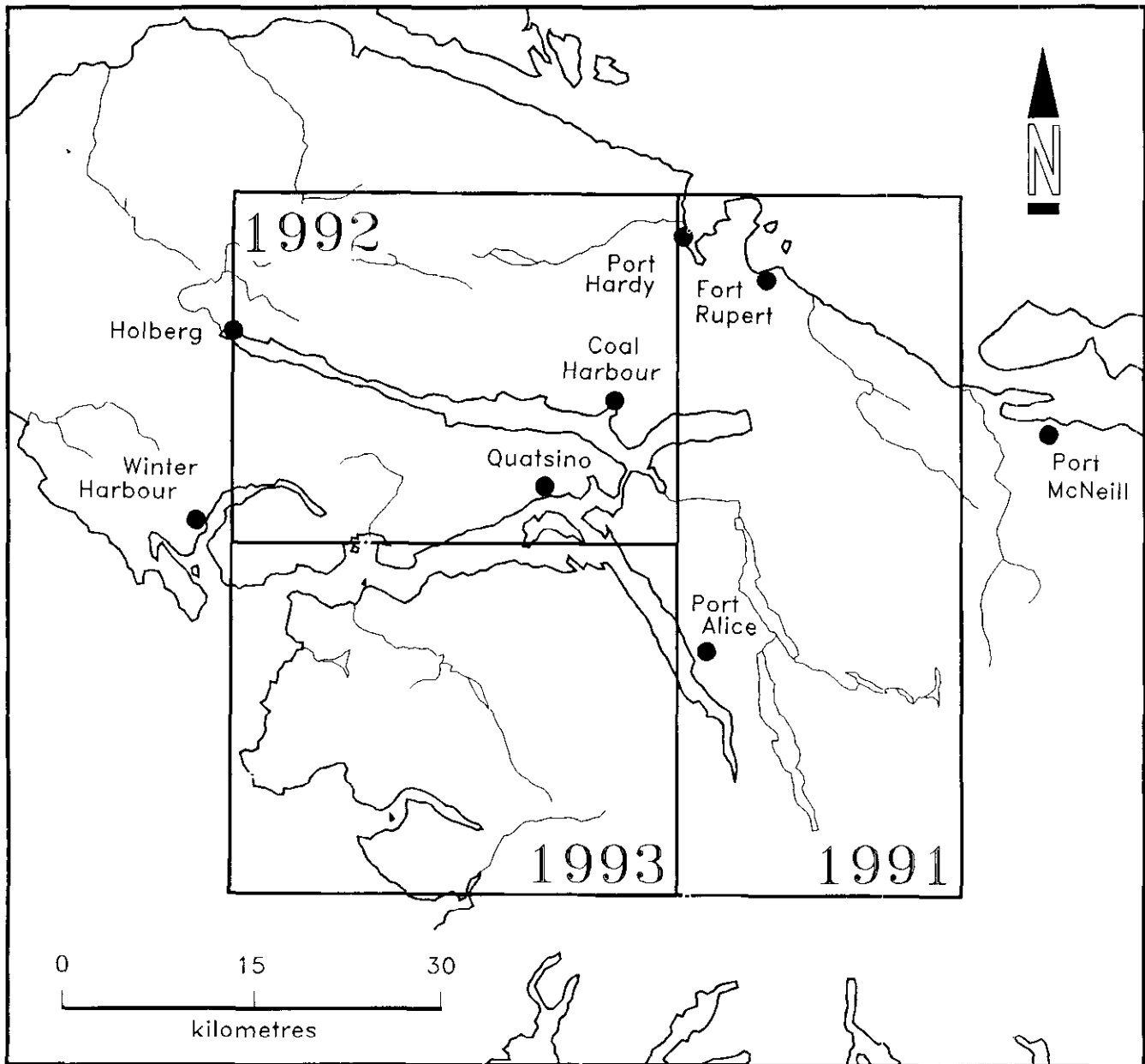


Figure 1-9-2: The location of the Quatsino Project. Proposed map areas are 1991 Benson River Area (92L/6W and 92L/11W), 1992 Quatsino (92L/12) and 1993 Mahatta Creek (92L/5).

ried from the Quatsino Formation near Benson Lake for use as fillers, road metal and other applications.

OBJECTIVES OF THE PROJECT

The 1990 field season was restricted to a four-week reconnaissance of the project area by the authors to obtain some familiarization with the region, its logistical problems, principal geologic units and mineral deposits. Full-scale fieldwork will begin in 1991 in the eastern part of the project area (Figure 1-9-2) and continue over the next three years. Apart from 1:50 000 regional geologic maps of the project area, it is also proposed to conduct further moss-mat stream-sediment sampling throughout the area to complement the 1988 Regional Geochemical Survey. D.M. Melville will also undertake thesis studies to characterize the alteration assemblages associated with the porphyry copper deposits of the Coal Harbour – Holberg area.

Several ancillary studies focused on specific topics will be undertaken during the course of the project, in cooperation with colleagues from provincial and federal governments and universities. These include a study of the sedimentology and biostratigraphy of the Triassic sediments, in collaboration with M.J. Orchard and E.T. Tozer of the Geological Survey of Canada and A. Desrochers of the University of Ottawa; and studies of the development and regional setting of the iron-copper-gold skarns in cooperation with G.E. Ray of this Ministry.

ACKNOWLEDGMENTS

The authors would like to acknowledge the help, support and encouragement for this project given by John Fleming (BHP-Utah Mines Ltd.), Peter Dasler (Daiwan Engineering Ltd.), Jim Laird, Paul Wilton, Gerry Ray, Tim England and staff of Western Forest Products Ltd., MacMillan-Bloedel Limited, Interfor and the British Columbia Ministry of Forests.

REFERENCES

- Armstrong, A.K. and MacKevett, E.M. (1982): Stratigraphy and Diagenetic History of the Lower Part of the Triassic Chitistone Limestone, Alaska; *United States Geological Survey*, Professional Paper 1212-A.
- Armstrong, A.K. and MacKevett, E.M. and Silberling, N.J. (1969): The Chitistone and Nizina Limestones of the Southern Wrangell Mountains, Alaska – a Preliminary Report Stressing Carbonate Petrography and Depositional Environments; *United States Geological Survey*, Professional Paper 650-D, pages 49-62.
- Armstrong, R.L., Muller, J.E., Harakal, J.E. and Muehlenbachs, K. (1985): The Neogene Alert Bay Volcanic Belt of Northern Vancouver Island, Canada: Descending-plate-edge Volcanism in the Arc-trench Gap; *Journal of Volcanology and Geothermal Research*, Volume 26, pages 75-97.
- Dawson, G.M. (1887): Report on a Geological Examination of the Northern Part of Vancouver Island and Adjacent Coasts; *Geological Survey of Canada*, Annual Report 1886, Volume 2, Part B, pages 1-107.
- Gunning, H.C. (1930): Geology and Mineral Deposits of the Quatsino-Nimpkish Area, Vancouver Island, British Columbia; *Geological Survey of Canada*, Summary Report 1929, Part A, pages 94-143.
- Jeffrey, W.G. (1962): Alice Lake – Benson Lake Map-area; *B.C. Ministry of Energy, Mines and Petroleum Resources*, unnumbered Preliminary Geological Map.
- Matysek, P.F., Gravel, J.L. and Jackaman, W. (1989): 1988 British Columbia Regional Geochemical Survey, Stream Sediment and Water Geochemical Data, NTS 92L/102I – Alert Bay/Cape Scott; *B.C. Ministry of Energy, Mines and Petroleum Resources*, RGS 23.
- McCammon, J.W. (1969): Limestone Deposits at the North End of Vancouver Island; *B.C. Ministry of Energy, Mines and Petroleum Resources*, Annual Report 1968, pages 312-318.
- Muller, J.E., Northcote, K.E. and Carlisle, D. (1974): Geology and Mineral Deposits of Alert – Cape Scott Map-area (92L – 102I), Vancouver Island, British Columbia; *Geological Survey of Canada*, Paper 74-8, includes Map 4-1974, scale 1:250 000.
- Northcote, K.E. (1969): Geology of the Port Hardy – Coal Harbour Area; *B.C. Ministry of Energy, Mines and Petroleum Resources*, Annual Report 1968, pages 84-87.
- Northcote, K.E. (1971): Rupert Inlet – Cape Scott Map-area; *B.C. Ministry of Energy, Mines and Petroleum Resources*, Geology, Exploration and Mining in British Columbia 1970, pages 254-258.
- Northcote, K.E. and Robinson, W.C. (1973): Island Copper Mine; *B.C. Ministry of Energy, Mines and Petroleum Resources*, Geology, Exploration and Mining in British Columbia 1972, pages 293-301.
- Panteleyev, A. (1986): A Canadian Cordilleran Model for Epithermal Gold-silver Deposits; *Geoscience Canada*, Volume 13, pages 101-111.
- Riddihough, R.P. (1977): A Model for Recent Plate Interactions off Canada's West Coast; *Canadian Journal of Earth Sciences*, Volume 14, pages 384-396.

**REGIONAL GEOLOGICAL MAPPING NEAR THE
MOUNT MILLIGAN COPPER-GOLD DEPOSIT
(93K/16, 93N/1)**

By JoAnne Nelson, Kim Bellefontaine, Kim Green and Mary MacLean

KEYWORDS: Regional geology, Mount Milligan, porphyry Cu-Au, alkaline intrusions, Takla Group, Rainbow Creek formation, Inzana Lake formation, Witch Lake formation, Chuchi Lake formation, Tertiary basins, Takla intrusions, structural geology, Mount Milligan horst, metamorphism, alteration, mineralization.

INTRODUCTION

The Nation Lakes area of central British Columbia is located approximately 75 kilometres north of Fort St. James and is accessed by well-maintained logging roads from Fort St. James and MacKenzie (Figure 1-10-1). Its current exploration importance is due to the 1987 discovery of the Mount Milligan porphyry copper-gold deposit by Lincoln Resources Inc. At present, the Mount Milligan deposit is nearing feasibility stage with geological reserves, currently under revision, of approximately 400 million tonnes grading 0.48 grams per tonne gold and 0.2 per cent copper (Rebagliatti, 1990, DeLong *et al.*, 1991, this volume). Exploration for other copper-gold porphyry deposits is very active in the area; by August 1990 approximately 90 per cent of the Wittsichica Creek (93N/1) and Tezzeron Creek (93K/16) map areas was staked.

The Nation Lakes regional mapping project was started in 1990 to assist exploration efforts by providing a geological database in this virtually unmapped area. Two 1:50 000 map sheets were covered in the summer of 1990. They are

available as Open File 1991-3 (Nelson *et al.*, 1991). This high productivity was made possible due to the sparseness of outcrop, less than 5 per cent, and the excellent access to much of the area by logging roads. Goals of the project are as follows:

- To outline stratigraphic subdivisions of the Takla Group, which is undivided on previous reconnaissance-scale geological maps (Armstrong, 1949; Garnett, 1978).
- To locate intrusions and alteration zones as an aid to mineral exploration.
- To accurately locate previously documented mineral occurrences and add new showings.
- To provide lithogeochemical and stream-sediment data.
- To evaluate the potential of the area for new discoveries of porphyry-style mineralization and other types of mineral deposits.

REGIONAL GEOLOGIC SETTING

THE TAKLA ARC

The Nation Lakes area is predominantly underlain by Early Mesozoic Takla Group rocks of island-arc affinity. The Takla Group and its southern equivalent, the Nicola Group, define the Quesnel Terrane or Quesnellia (Monger *et al.*, 1990). The northwest-elongate Hogem batholith is intruded into this terrane. The southern tip of this intrusion lies within the map area on the north shore of Chuchi Lake (Figure 1-10-2). The main phase of the Hogem batholith is dated by K-Ar methods as 176 to 212 Ma, and is considered to be an intrusive equivalent of at least part of the Takla Group (Garnett, 1978).

At the latitude of the map area the western border of Quesnellia is the Pinchi fault. Here the Takla Group lies in tectonic contact with oceanic rocks of the Cache Creek Terrane (Figure 1-10-2). The presence of Triassic blueschists along the Pinchi fault (Paterson, 1977) suggests that a subduction zone lay west of the Takla arc. The eastern border of Quesnellia is a complex zone of faults that place lower Takla rocks against the Late Paleozoic Slide Mountain Terrane (Ferri and Melville, in preparation) and metamorphic rocks of autochthonous North America, notably the southern Wolverine complex near Carp Lake (Struik, 1990).

Regionally, the Takla Group comprises a lower Late Triassic sedimentary unit which interfingers with and is overlain by voluminous volcanic, pyroclastic and epiclastic rocks. These rocks are intruded by coeval plutons which range up to Early Jurassic in age. Augite-phyric rocks predominate, although plagioclase and hornblende are present

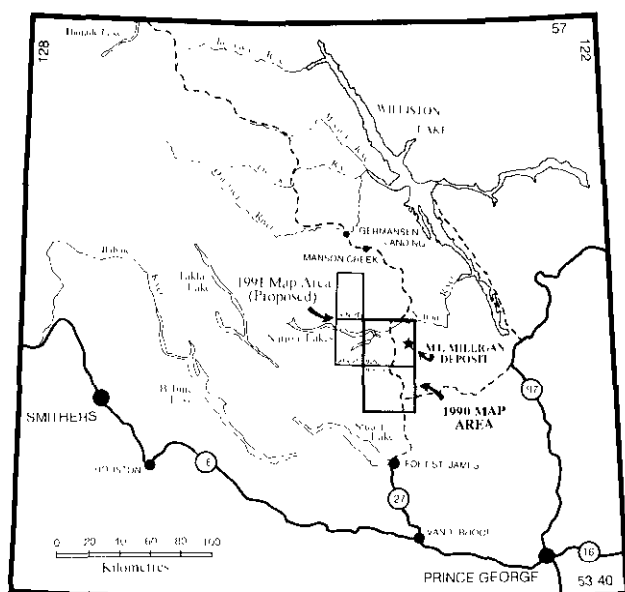


Figure 1-10-1. Location of Wittsichica Creek and Tezzeron Creek map areas (93N/1, 93K/16).

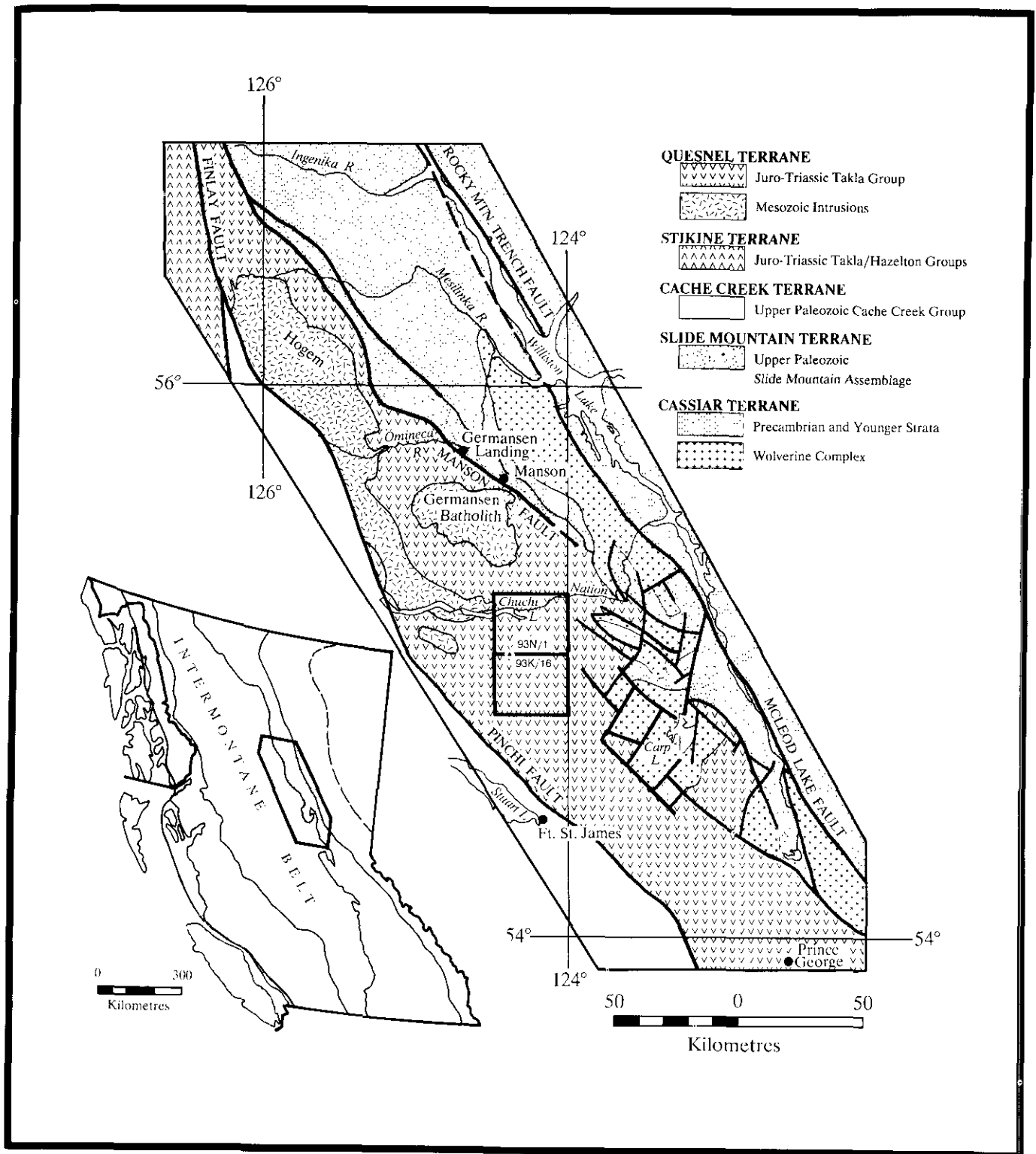


Figure 1-10-1. Location of Wittsichica Creek and Tezzeron Creek map areas (93N/1, 93K/16).

and can be abundant. Takla volcanics tend to be unusually potassium rich and are transitional to alkalic in their major-element chemistry (Rebagliati, 1990; Ferri and Melville, in preparation). They share this characteristic with contempo-

aneous arc-volcanic rocks of the Nicola Group in the Quesnel Terrane (Mortimer, 1987) and the Stuhini Group in the Stikine Terrane near Galore Creek (Logan and Koyanagi, 1989). The Stikine Terrane is separated from

Quesnellia either by major faults or by the strongly allochthonous Cache Creek Terrane (Monger *et al.*, 1990). These petrologic and petrochemical parallels between Quesnellia and Stikinia, two apparently disparate tectonic entities, pose an interesting question in Cordilleran geology. Stratigraphies of the two Early Mesozoic arcs show further similarities as discussed later.

THE ALKALINE PORPHYRY COPPER-GOLD ASSOCIATION

The potassium-rich volcanics of the Takla and Nicola groups have been classified as shoshonites by Mortimer (1987) and de Rosen-Spence (1985). Shoshonites are thought to arise from unusual conditions within magmatic arcs. A variety of tectonic mechanisms have been called upon to explain the strongly alkalic nature of these rocks, including the breaking off and foundering of the downgoing slab (de Rosen-Spence, 1985), mantle metasomatism (Foden and Varne, 1980) and the melting of subcontinental lithosphere during subduction (Varne, 1985). Whatever the ultimate origin of shoshonites, their coeval and cogenetic alkaline intrusions tend to host or nucleate porphyry-style deposits that are enriched in both copper and gold. There are many excellent examples of alkalic porphyry copper-gold deposits in British Columbia, most of them associated with Late Triassic to Early Jurassic intrusive bodies in Quesnellia and Stikinia (Barr *et al.*, 1976). Operating mines include Similco (Copper Mountain) and Afton; mine prospects include Mount Milligan, Mount Polley and Stikine Copper (Figure 1-10-3).

Barr *et al.* (1976) outlined exploration parameters for alkalic porphyry copper-gold deposits. These are summarized here to provide a context for the following discussion of local geology. One of the most important characteristics of alkaline porphyry deposits is that they tend to be spatially related to long-lived faults. Faults that control early intrusive activity are later reactivated and also control much younger features such as Eocene extensional basins. Both Copper Mountain and Afton/Ajax lie near important Eocene basin-bounding faults, which are interpreted as reactivated Triassic-Jurassic structures (V.A. Preto, personal communication, 1990).

The alkalic intrusive bodies associated with porphyry copper-gold deposits are typically small and high level to subvolcanic. Their textures strongly resemble those of volcanic flows. These intrusions consist of densely crowded, blocky plagioclase phenocrysts about 2 millimetres in diameter, and perhaps less abundant biotite, augite, hornblende, or orthoclase, in a dense very fine grained feldspar matrix. They are distinguished from surrounding flows by their limited areal extent, lack of volcanic features such as amygdules and pyroclastic facies, extremely crowded phenocrysts and a relatively more felsic composition. Intrusive breccias and diatremes are also an important aspect of alkaline porphyry systems (Barr *et al.*, 1976; Sillitoe, 1990).

Alkalic porphyries often have associated propylitic and potassic alteration. Abundant magnetite, part of the potassic suite, makes airborne and ground magnetic surveys an important exploration tool. Extensive pyrite haloes outline the porphyry systems and can aid the prospector who does



Figure 1-10-3. Distribution of porphyry copper-gold deposits associated with alkaline intrusions within the Intermontane Belt of British Columbia. Modified after Legun *et al.* (1990).

not have access to a petrographic microscope or feldspar-staining apparatus. Small, high-grade veins such as the Esker veins at Mount Milligan (Rebagliati, 1990) and the gold-magnetite veins and magnetite-matrix breccias at the Cat property, may signal the presence of nearby large-tonnage, lower grade zones.

REGIONAL STRUCTURAL SETTING

The Nation Lakes area lies between two regional-scale northwest-trending fault systems that probably had significant dextral offsets in Late Mesozoic to Eocene time; the Pinchi fault to the west and the Manson, McLeod and Northern Rocky Mountain Trench faults to the east. Struik (1990) has shown how transcurrent motion in this area was transferred from one fault system to the other through sets of subsidiary faults in the block between. The southern Wolverine complex, centred on Carp Lake 20 kilometres southeast of the present map area (Figure 1-10-2), is an uplifted horst of basement gneisses, it is bounded by a series of steep, northwest-trending dextral faults and northeast-trending low-angle normal faults (Struik, 1989, 1990). Several of the northwest-trending bounding faults project into the Nation Lakes map area (Figure 1-10-2).

CAPSULE EXPLORATION HISTORY

Figure 1-10-3 shows the distribution of significant copper-gold deposits associated with alkaline porphyry systems in Quesnellia and Stikinia. The Nation Lakes region has seen two phases of intense exploration activity in the last two decades. The first pulse, dating roughly from 1970 to 1975, concentrated on deposits in and near the Hogem

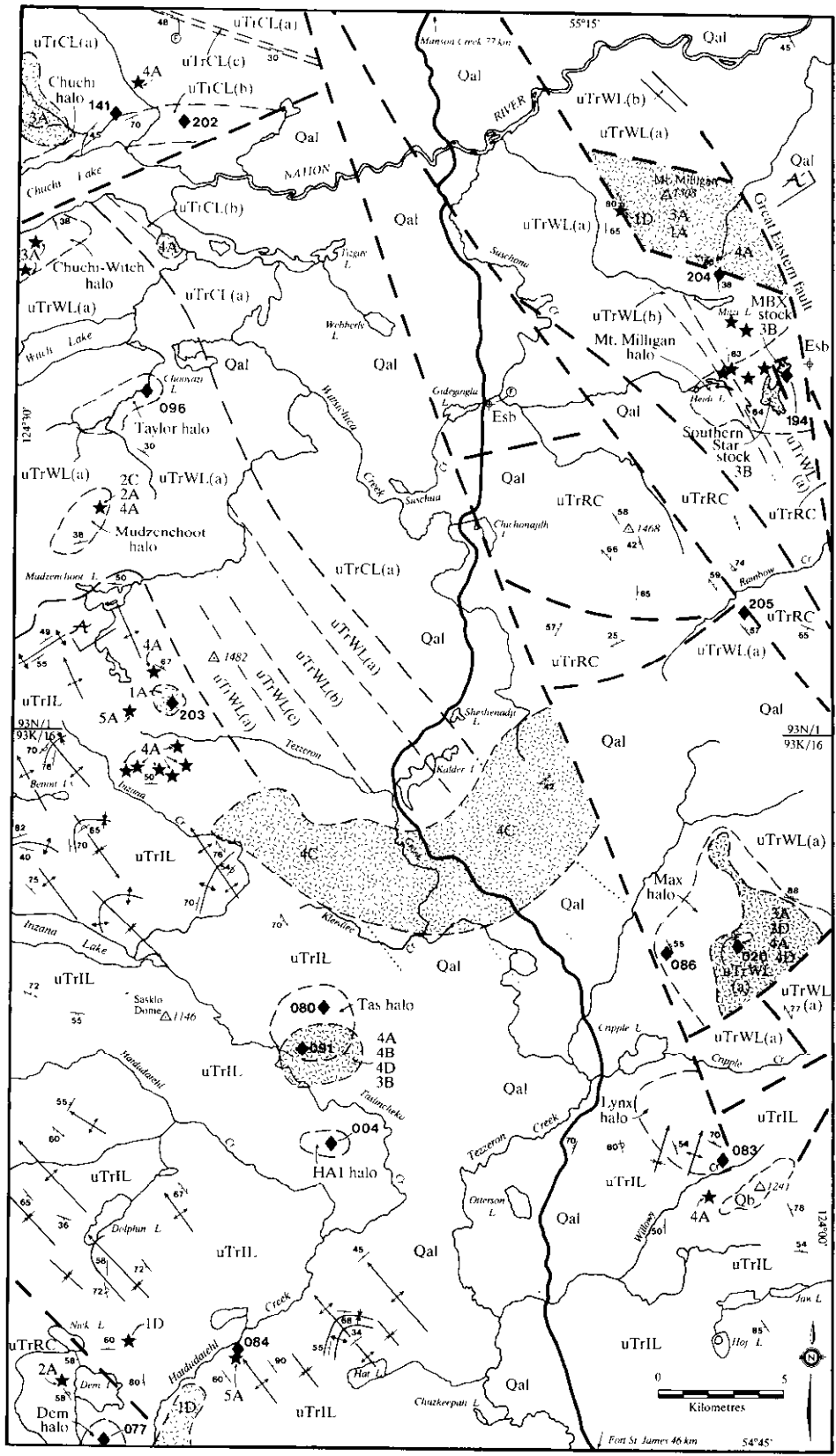


Figure 1-10-4a. Generalized geology and mineral occurrences in the Nation Lakes map area (Wittsichica Creek 93N/1 and Tezzeron Creek 93K/16 map areas). Refer to MINFILE descriptions in text.

LEGEND

LAYERED ROCKS

QUATERNARY

Qal UNCONSOLIDATED GLACIAL TILL AND ALLUVIUM

QUATERNARY?

Qb OLIVINE-BEARING BASALT

EOCENE - OLIGOCENE

Esb BASALT, VOLCANIC WACKE AND FOSSILIFEROUS VOLCANIC ASH-RICH MUDSTONE

UPPER TRIASSIC-(JURASSIC?)

TAKLA GROUP

uTrCL CHUCHI LAKE FORMATION: (A) GREEN AND MAROON HETEROLITHIC AGGLOMERATE; (B) PLAGIOCLASE-PORPHYRY TRACHYTE FLOWS AND BRECCIAS; (C) INTERVOLCANIC SEDIMENTS

uTrWL WITCH LAKE FORMATION: (A) AUGITE (\pm PLAGIOCLASE \pm HORNBLENDE) PORPHYRY AGGLOMERATE, VOLCANIC BRECCIA, LAPILLI TUFF AND EPICLASTIC SEDIMENTS; (B) TRACHYTE FLOWS AND TUFF-BRECCIAS; (C) PLAGIOCLASE (\pm AUGITE) PORPHYRY LATITE FLOWS AND AGGLOMERATES

uTrIL INZANA LAKE FORMATION: VOLCANIC SANDSTONE, SILTSTONE, MUDSTONE, ARGILLITE, LAPILLI TUFF AND SEDIMENTARY BRECCIA

uTrRC RAINBOW CREEK FORMATION: GREY SLATE, THIN-BEDDED SILTSTONE, MINOR VOLCANICLASTIC SEDIMENTS

INTRUSIVE ROCKS

LATE CRETACEOUS-EARLY TERTIARY?

1 GRANITE SUITE: (1A) EQUIGRANULAR, COARSE GRAINED GRANITE; (1D) RHYODACITE/DACITE

LATE TRIASSIC-EARLY JURASSIC

2 SYENITE SUITE: (2A) COARSE GRAINED, EQUIGRANULAR SYENITE; (2C) MEGACRYSTIC SYENITE

3 MONZONITE SUITE: (3A) EQUIGRANULAR, COARSE GRAINED MONZONITE; (3B) CROWDED PLAGIOCLASE PORPHYRITIC MONZONITE; (3D) SPARSELY PORPHYRITIC LATITE

4 DIORITE/MONZODIORITE SUITE: (4A) COARSE GRAINED, EQUIGRANULAR DIORITE/MONZODIORITE; (4B) CROWDED PLAGIOCLASE PORPHYRITIC DIORITE; (4C) MEGACRYSTIC PLAGIOCLASE (\pm AUGITE) PORPHYRITIC DIORITE; (4D) SPARSELY PORPHYRITIC ANDESITE

5 GABBRO/MONZOGABBRO SUITE: (5A) COARSE GRAINED, EQUIGRANULAR GABBRO/MONZOGABBRO

SYMBOLS

geologic contact (approximate, inferred).....	
lithologic contact (approximate, inferred)	
fault (defined, inferred)	
F ₁ axial trace (anticlinal, synclinal).....	
F ₂ axial trace (antiformal, synformal).....	
bedding (tops known, tops unknown, overt	
foliation.....	
large intrusion	
small intrusion	
area of alteration	
mineral occurrence and MINFILE number...	
fossil locality	
diamond drill hole.....	
elevation in metres	

batholith. This led to the discovery of the Lorraine deposit by Granby Mining Corporation (Wilkinson *et al.*, 1976) and the Takla Rainbow prospect. Porphyry systems were also identified south of Chuchi Lake (reported in Campbell, 1990). Interest in porphyry systems declined until the mid-1980s when strong market prices for both copper and gold made alkaline porphyry deposits desirable exploration targets. Recent exploration efforts have extended outside the Hogen batholith to the entire Intermontane Belt. The most important result so far of this resumed interest in the Nation Lakes area was the 1987 discovery of the Mount Milligan deposit and its subsequent development to feasibility stage. Major drilling programs were conducted in the summer of 1990 on the Cat property owned by BP Resources Canada Limited and Lysander Gold Corporation, on Cathedral Gold Corporation's Takla Rainbow property, on Rio Algom Exploration Inc.'s Klawli property, and on the BP-Digger Resources Limited Chuchi property north of Chuchi Lake. The Lorraine is being investigated by Kennco Explorations (Canada) Limited. In addition, large alteration systems with anomalous copper and gold values are under investigation south of Chuchi Lake by Rio Algom, Westmin Resources Limited, and Noranda Exploration Company, Limited, on the Max claims by Rio Algom, on Grand America Minerals Ltd. Webb claims, and on Placer Dome Inc.'s Windy property. Noranda's promising Tas property has been inactive since 1989, its potential still unclear. Most other properties and projects are in the early stages of exploration.

LOCAL GEOLOGY

STRATIGRAPHY OF THE TAKLA GROUP

Mapping in the Nation Lakes area in 1990 resulted in a provisional subdivision of the Takla Group into four informal formations, the Rainbow Creek, Inzana Lake, Witch Lake and Chuchi Lake formations. A nearly complete stratigraphic succession can be seen in the broad anticline that outcrops from south of Chuchi Lake to the southern limit of mapping near Dem Lake (Figure 1-10-4A). Epiclastic sediments of the Inzana Lake formation are overlain by augite and other porphyritic volcanics and pyroclastics of the Witch Lake formation. These in turn pass upward into polymictic lahars and subaerial flows of the Chuchi Lake formation. Elsewhere, Takla units occur in incomplete, fault-bounded panels (Figures 1-10-4A, 4B and 5.)

RAINBOW CREEK FORMATION (uTrRC)

The Rainbow Creek formation is a basinal package of dark grey slate with lesser siltstone and, in some exposures, epiclastic interbeds. It occurs in three fault-bounded structural blocks in the Nation Lakes map area – one north of Rainbow Creek, one near Dem Lake in the far southwest corner of the map area, and one intersected in a drillhole southeast of the Mount Milligan deposit.

The exposures north of Rainbow Creek are divided into two sub-blocks based on different trending schistosities and distinctive lithologic suites (Figures 1-10-4 and 5). The northern block consists mostly of monotonous grey slate with sparse, thin siltstone interbeds and minor quartz sand-

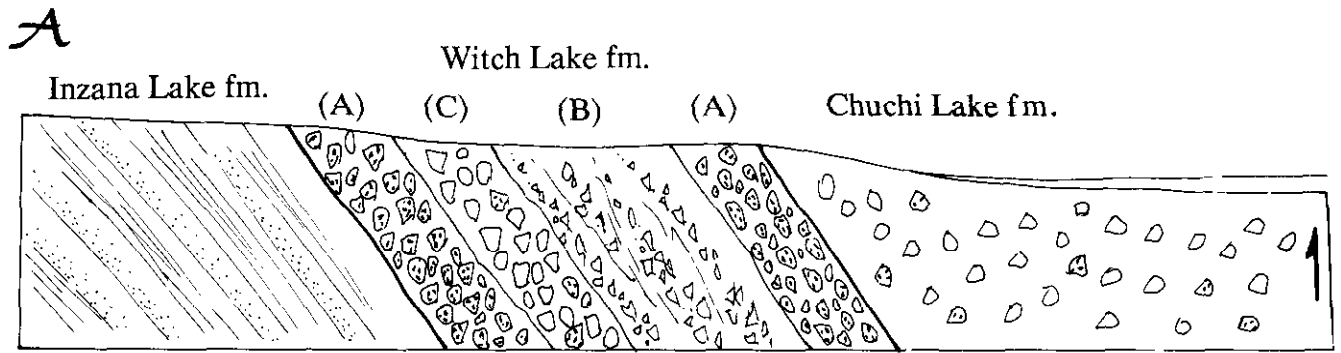


Figure 1-10-4b. Cross-section of Wittsichica Creek map area.

stones. The southern block, next to Rainbow Creek, is also dominated by slate, but contains some volcanic and volcanoclastic components. Near Dem Lake, the grey slate contains very common siltstone interbeds and also sedimentary breccias composed of slate interclasts. The black slate intersected in drill hole DDH-274, southeast of the Mount Milligan deposit, is limy, graphitic and soot-black.

All of these exposures are completely fault-bounded. Their original relationships to the rest of the Takla Group are not known. Regionally, the lowest unit of the Takla Group is a package of dark grey to black slates or phyllites with interbedded quartz-rich siltstones and sandstones and minor limy beds and limestones. Near Quesnel this unit is termed the "Triassic black phyllite" (Struik, 1988, Bloodgood, 1987, 1988). More locally, Ferri and Melville (in preparation) recognize dark grey slates, limy slates, siliciclastics and limestones of Late Triassic age in the Manson Creek area, which they propose to include in the lower part of the Slate Creek formation. The Rainbow Creek formation is correlated to these on lithologic grounds.

INZANA LAKE FORMATION (uTrIL)

Extensive sedimentary, epiclastic and lesser pyroclastic rocks outcrop in the map area from north of Inzana Lake to the southern map border. Due to the lithologic monotony shown by this package over large areas, and to the tight folding within it, no subdivisions were made. It consists of abundant grey, green and black siliceous argillite with lesser green to grey volcanic sandstones and siltstones, green, augite bearing crystal and lapilli tuffs, sedimentary breccia, siliceous waterlain dust tuffs, heterolithic volcanic agglomerates and rare, small limestone pods. The argillite is siliceous and poorly cleaved; it contrasts strongly with the alumina-rich grey slates of the Rainbow Creek formation. Although the sandstones tend to be thick bedded and relatively featureless, graded bedding and load casts are common within the thin-bedded siltstones. They provide extensive control on sedimentary tops. Two separate sets of flame structures, and imbricated volcanic agglomerates, indicate arc-parallel northwesterly transport into the basin, suggesting a volcanic centre to the south.

Crystal and lapilli tuffs occur mostly along the western margin of the map area. Fragments in the lapilli tuffs are

characteristically sparse, less than 10 per cent in a sandy matrix. These units may represent an upward transition to the overlying augite porphyry flows and coarse pyroclastic deposits. They contain fragments of augite and lesser hornblende (plagioclase) porphyry. Fresh olivine crystals are rare but notable.

The sedimentary breccias contain mostly intrabasinal clasts of argillite, sandstone and fine-grained, green siliceous tuff. Volcanic and high-level plutonic clasts are also present, including plagioclase and pyroxene porphyry. At one exposure 300 metres east of the Fort St. James-Germansen road and 200 metres north of the Germansen-Cripple subsidiary road, a broad channel in the sedimentary breccia is filled with a slump of rounded augite porphyry clasts. These breccias attest to high-energy conditions within the basin, possibly induced by syndimentary faulting.

The Inzana Lake formation is transitionally overlain by augite porphyry agglomerates of the Witch Lake formation on the low ridge north of Mudzenchoot Lake. Its low stratigraphic position in the Takla Group and its character as facies equivalent of distant volcanic centres suggests that the Inzana Lake formation correlates with Unit 7 of the Takla Group near Quesnel (Bloodgood, 1988) and with the upper part of the Slate Creek formation of the Takla Group near Germansen Lake (Ferri and Melville, in preparation).

WITCH LAKE FORMATION (uTrWL)

The best-known lithologies of the Takla Group are augite porphyry flows and pyroclastics. In the Nation Lakes area they are included in the Witch Lake formation, named for the thick, well-exposed sequences around Witch Lake. The Witch Lake formation has two main areas of exposure, one between Mudzenchoot and Chuchi lakes, where it is in stratigraphic continuity with the underlying Inzana Lake and overlying Chuchi Lake formations; and a fault-bounded structural panel on the eastern side of the Wittsichica Creek map sheet, which hosts the Mount Milligan deposit.

In addition to augite porphyry, a thick section dominated by plagioclase-porphyrific latites occurs in the Witch Lake formation south of Witch Lake. Acicular hornblende-plagioclase porphyries are locally abundant, particularly

A'

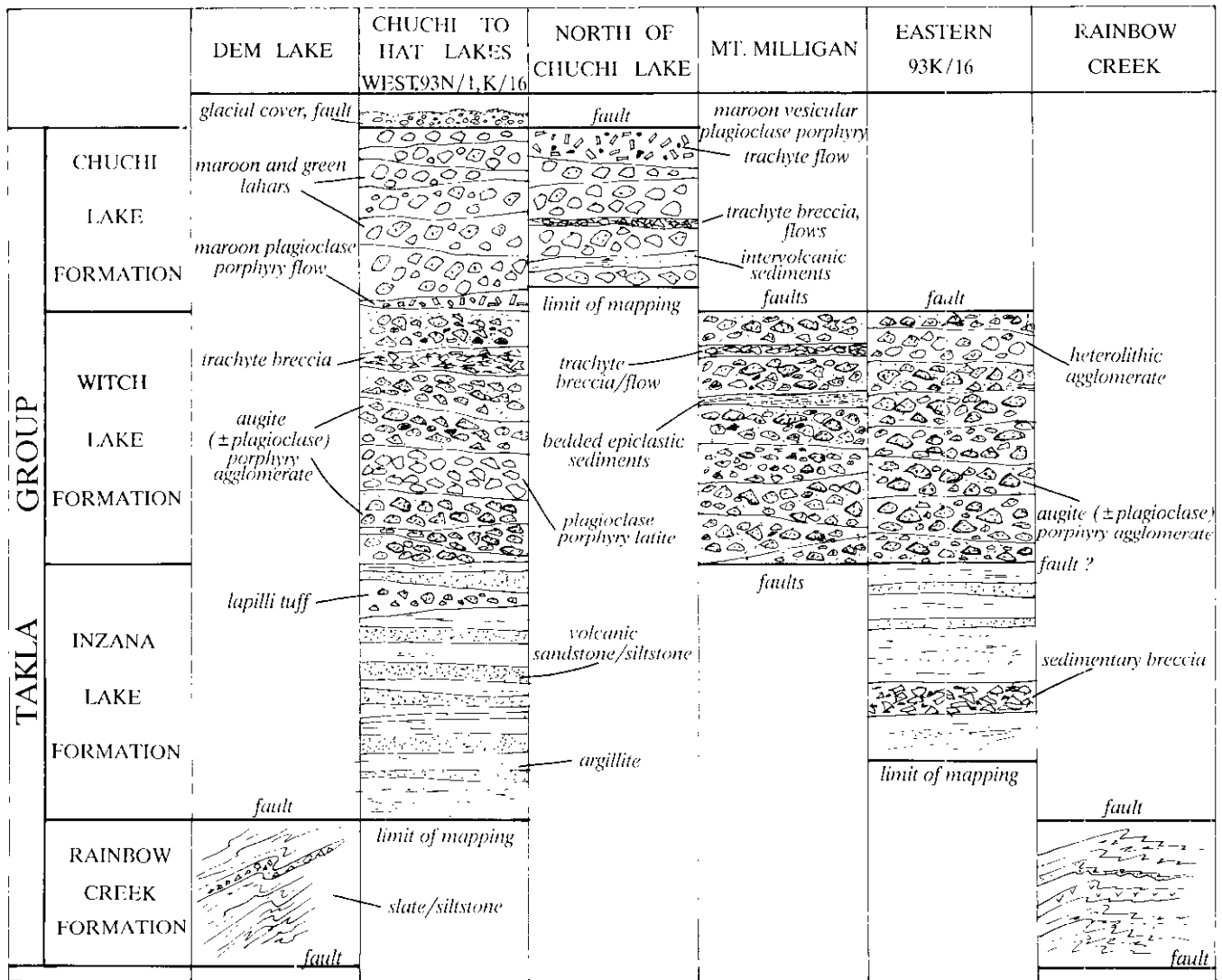
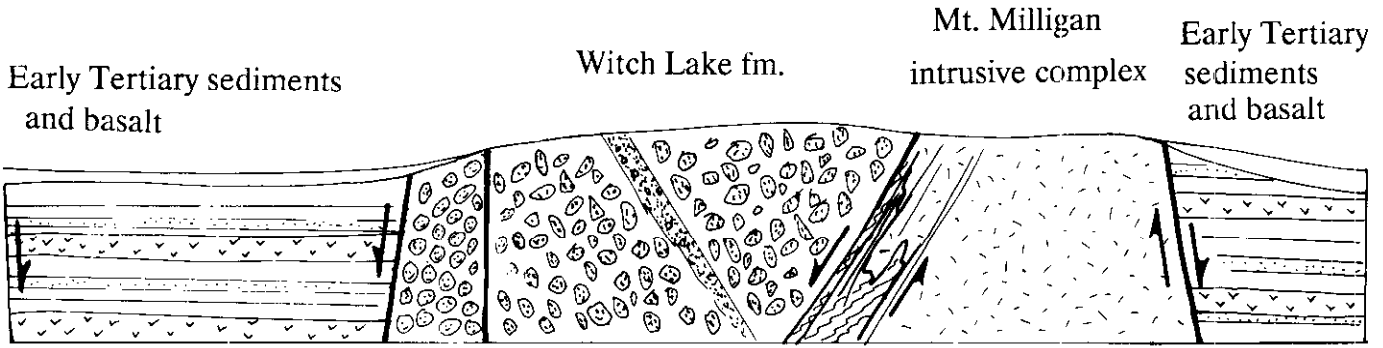


Figure 1-10-5. Composite stratigraphy of the Takla Group in the Nation Lakes area.

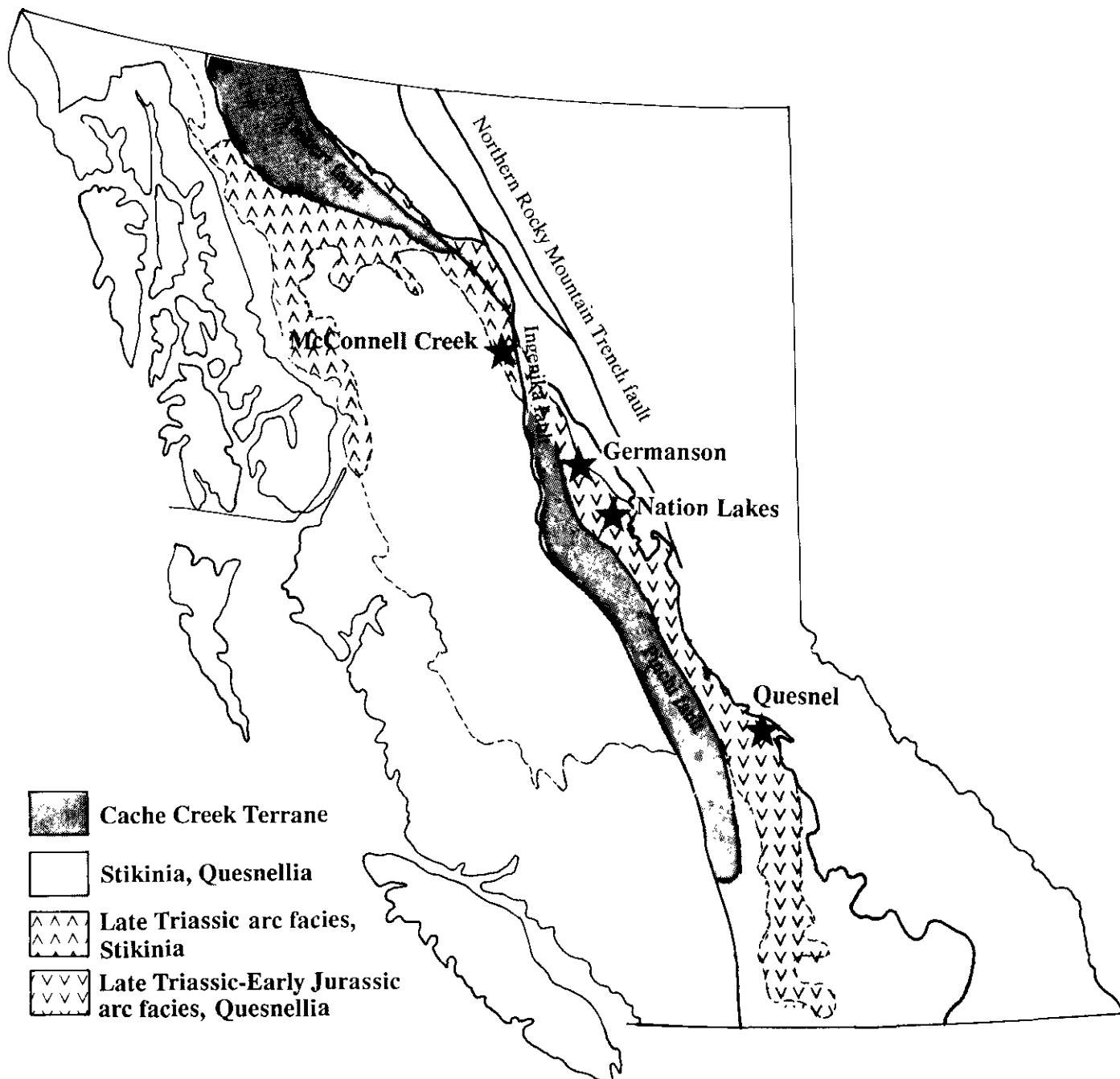


Figure 1-10-6a. Regional comparisons of Takla Group stratigraphy. Locations of stratigraphic sections and their terrane context.

south of Rainbow Creek and extending southward into the northeastern corner of the Tezzeron Creek map sheet. Here hornblende porphyries are the dominant lithology in agglomerates and in heterolithic aggregates that also contain the more common augite porphyries. At one locality south of Rainbow Creek, hornblendite and amphibolite clasts occur within the hornblende porphyries. One clast consists of clinopyroxenite in contact with amphibolite, reminiscent of Polaris-type ultramafic bodies (Nixon *et al.*, 1990).

Trachyte breccia occurs near the top of the western Witch Lake formation in the headwaters of the south fork of

Wittsichica Creek. In the Mount Milligan panel, two thin trachyte units can be traced over several kilometres. They are composite units that include pale-coloured flows with large, ovoid amygdules, flow breccias, and lapilli tuffs that contain deformed glass shards.

The augite porphyry suite that dominates the Witch Lake formation is typical of explosive intermediate volcanism. It includes all gradations from flows and probable hypabyssal intrusions to coarse volcanic breccias and agglomerates, lapilli and crystal-rich tuffs and thinly bedded, subaqueous epiclastic sandstones and siltstones. Both small-augite por-

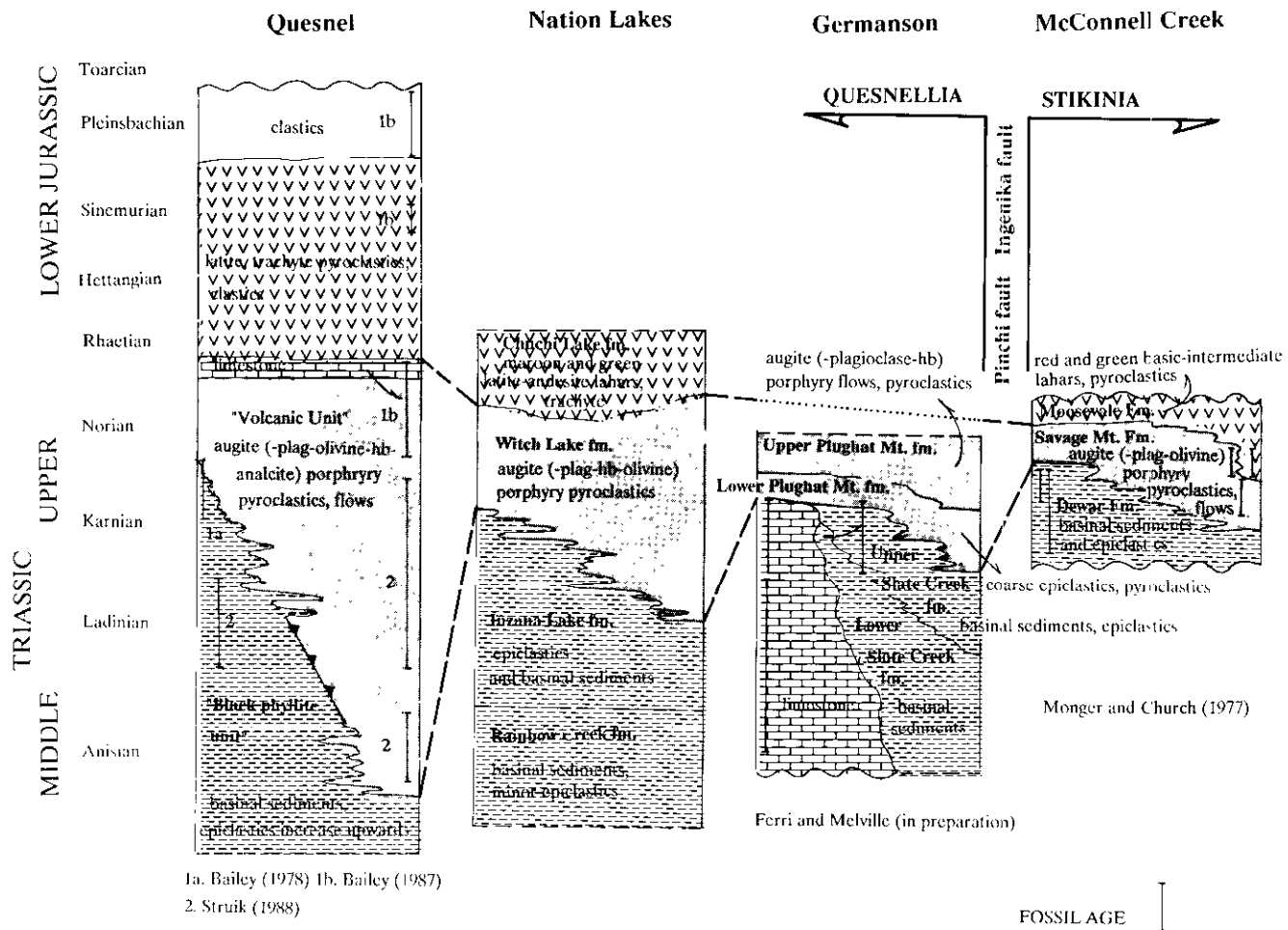


Figure 1-10-6b. Stratigraphic sections.

phyry and large-augite porphyry variations are present. Plagioclase and hornblende phenocrysts are subordinate and olivines rare. In terms of composition, the augite porphyries contain between 20 and 80 per cent matrix and phenocrystic plagioclase and in rare examples, primary potassium feldspar as a matrix phase. They are classified as andesites and basaltic andesites. The abundance of potassium feldspar in the volcanic rocks at and near the Mount Milligan deposit, has led past authors (Rebagliati, 1990) to classify them as augite-porphyrific latites and banded trachytes. However, microscopic examination of andesites and derived sediments up to 4 kilometres from the MBX and Southern Star stocks shows the invasion of secondary potassium feldspar occurring as veinlets, as clumps with pyrite and epidote, as seams in plagioclase phenocrysts, and as fine-grained aggregates along bedding planes in the sediments. Such replacement distal to the deposit suggests that the highly potassic nature of the rocks within the deposit is due to wholesale replacement, converting andesites to "latites" and bedded andesitic sediments to "trachytes".

CHUCHI LAKE FORMATION (uTrCL)

The intermediate to felsic Chuchi Lake formation transitionally overlies the Witch Lake formation along a

northwest-trending contact that can be traced for 25 kilometres south of Chuchi Lake. The best exposures are seen north of Chuchi Lake; however, in this area the basal contact with the Witch Lake formation lies north of the Witsichica Creek map sheet. In contrast with the marine Witch Lake formation, the Chuchi Lake formation shows evidence of deposition in a partly subaerial environment. It is dominated by polymictic plagioclase porphyry agglomerates and breccias. They are typically matrix supported and grey-green to pale maroon in colour. One of these lahars is in contact with a thin volcanic sandstone bed containing abundant wood fragments on bedding planes. Wood fragments caught up in the hot lahar are evidenced by black cores of remnant carbonaceous material with reaction rims.

The plagioclase (\pm augite \pm hornblende) porphyries contain from 70 to 80 per cent plagioclase and from zero to 15 per cent matrix potassium feldspar. They are andesites and latitic-andesites.

Another characteristic lithology of the Chuchi Lake formation is dark maroon, felsic latite to trachyte flows with large, irregular, partly filled amygdules. Microscopically, the flows consist of potassium feldspar and plagioclase in varying proportions. Some are plagioclase phyrific. The amygdules are filled with calcite and albite. A single large-

plagioclase intrusion and flow unit, with individual phenocrysts averaging several centimetres long, is exposed north of Chuchi Lake. Although megacrystic intrusions are fairly common, this is the only documented volcanic occurrence of megacrystic feldspar porphyry in the map area. Farther north and down-section, a partly welded trachyte tuff-breccia is cut by the Hogem batholith.

Hornblende porphyry with acicular phenocrysts occurs as clasts in polymictic breccias at the base of the Chuchi Lake formation between Witch and Chuchi lakes, and also up-section north of Chuchi Lake. This textural variant is also seen in dikes. In some exposures the acicular hornblende porphyries contain small inclusions of hornblendite and amphibolite.

The basal contact of the Chuchi Lake formation is gradational; it lies within a zone where mainly augite porphyry agglomerates of the Witch Lake formation pass upwards into polymictic agglomerates with small, abundant plagioclase phenocrysts in the clasts. As well, the dark green

TABLE 1-10-1
FOSSIL IDENTIFICATIONS

Macrofossils identified by Elisabeth McIver of the Institute of Sedimentary and Petroleum Geology.

C-168233

Sample Number: JN-90-34-1

From thinly bedded, dark grey-black, volcanic-ash-rich mudstones and siltstones in drill hole DDH-89-2 located on the Assunta claims near Gidegingla Lake. Sample taken from drill-hole interval 270-288.5 metres.

NTS 93N/1

UTM ZONE 10; N6107925 E422600

Identifications:

SUBDIVISION: Gymnospermophytina

CLASS: Gymnospermopsida

FAMILY: Taxodiaceae

Metasequoia occidentalis – leafy twigs

FAMILY: Pinaceae

Pinus – seeds, and probably leaves, but without fascicles, identification of the leaves as *Pinus* is impossible.

Picea – seeds

SUBDIVISION: Angiospermophytina

CLASS: Magnoliopsida

FAMILY: Betulaceae

cf. *Betula* – leaves betulaceous and could be *Betula* but, as the leaves are poorly preserved or only fragments, they should not be assigned to the genus.

FAMILY: Proteaceae

Lomatia lineata (Lesquereux) MacGinitie – leaves and probably seeds (seeds are incomplete but resemble those of the taxon).

FAMILY: Myricaceae

Comptonia hesperia Berry – leaves

AGE: Eocene or Oligocene

colours of the Witch Lake formation change to maroon, reddish and green shades. The top contact of the Chuchi Lake formation is not observed in the map area.

COMPARISON WITH OTHER TAKLA GROUP LOCALITIES

In the Nation Lakes area dark grey to black siliciclastic and limy strata of the Rainbow Creek formation are inferred to pass upward into the mixed epiclastic/basinal Inzana Lake formation, which in turn is succeeded by the predominantly augite-phyric porphyritic volcanics of the Witch Lake formation, and finally by somewhat more felsic and polymictic subaerial pyroclastics and flows of the Chuchi Lake formation (Figure 1-10-5). As shown on Figure 1-10-6, this stratigraphy is closely analogous to the Takla Group near Quesnel (Struik, 1988; Bailey, 1988; Bloodgood, 1987; 1988) and in the Manson Creek area (Ferri and Melville, 1989 and in preparation). It also strongly resembles the Takla stratigraphy outlined by Monger (1977) and Monger and Church (1977) in the McConnell Creek map area (Figure 1-10-6). The Rainbow Creek and Inzana formations are equivalent to the Dewar Formation; the Witch Lake to the Savage Mountain Formation; and the Chuchi Lake to the Moosevale Formation. In both the McConnell Creek and Nation Lakes map areas Late Triassic marine sedimentation is succeeded by voluminous volcanism that becomes increasingly intermediate in composition and sub-aerial through time. The McConnell Creek map area lies within Stikinia (Figure 1-10-6A), therefore these stratigraphic parallels are present across a major terrane boundary.

POST-TAKLA STRATIGRAPHIC UNITS EARLY TERTIARY SEDIMENTARY ROCKS AND BASALTS (Esb)

Recessive Early Tertiary strata may underlie fairly extensive regions of the map area. Evidence for this comes from a few drill holes east of the Mount Milligan deposit (DDH-426, DDH-433, DDH-440, DDH-445, DDH-446, DDH-449) and one near Gidegingla Lake (DDH NR-89-2; Ronning, 1989). East of the Mount Milligan deposit lithologies include sandstone, mudstone, coal, pebble conglomerate and basalt. Clasts in the pebble conglomerate are of Takla lithologies, some of which are altered, suggesting local derivation from the deposit area. This may be a slump breccia associated with the Great Eastern fault (*see* discussion on faults).

Near Gidegingla Lake, sandstone, siltstone and shale and thin-bedded volcanic ash form an interval 19 metres thick between basalt flows. Abundant broad-leaf and *Metasequoia* prints are well-preserved on bedding surfaces. A collection submitted to Elisabeth McIver of the Institute of Sedimentary and Petroleum Geology, Geological Survey of Canada, includes *Metasequoia occidentalis*, *Pinus* and *Picea* seeds, Betulaceae (birch) family, *Lomatia lineata*, and *Comptonia hesperia* Berry (Table 1-10-1). This flora is of Early Tertiary age (E. McIver, personal communication, 1990). Samples of this material have been submitted for

pollen analysis. The basalts are brown to black and aphanitic to finely plagioclase phyrlic. They contain partly filled vesicles that vary from pin-prick size to cavities several centimetres in diameter. Filling materials include chalcidony, crystalline calcite, celadonite and zeolites such as mordenite. These basalts strongly resemble Early Tertiary basalts in the Gang Ranch area as well as basalts of the Endako Group.

These subsurface data point to the existence of previously unrecognized Early Tertiary basins within the map area, probably controlled by penecontemporaneous block faults. This point is further developed in the discussion of structures following.

QUATERNARY(?) BASALT (Qb)

Fresh olivine-bearing basalt is exposed on an east-trending ridge near Willow Creek in the southeastern corner of the Tezzeron Creek map area (Figure 1-10-4A). It unconformably overlies the Inzana Lake formation on a bevelled surface. It may be a separate outlier of the young basalt mapped by Armstrong (1949, Unit 15A) on Hunitlin Mountain 15 kilometres to the south, although he assigned it to the older Endako Group. The basalts are brown weathering and columnar or platy jointed. They contain xenoliths of dunite and also of gneissic leucogranite derived from North American basement that structurally underlies the Takla Group.

QUATERNARY GLACIAL OVERBURDEN (Qal)

A large north-trending belt of glacial and glaciofluvial deposits, approximately 100 kilometres long and 10 to 20 kilometres wide, extends from Fort St. James to north of the Nation River (Armstrong, 1949). Glacial drift in the Nation Lakes area can reach thicknesses exceeding 200 metres (Ronning, 1989) and can make geological, geophysical and geochemical interpretation extremely difficult. Recent surficial studies by Gravel *et al.* (1991, this volume) and Kerr and Bobrowsky (in preparation) at and near the Mount Milligan deposit have helped to explain its surficial geochemical signature.

Geological interpretation in the heavily glaciated regions of the map area is based on small isolated outcrops that poke through the Quaternary cover and, on several key drill holes on the Mount Milligan (DDH-426, DDH-433, DDH-440, DDH-445, DDH-446, DDH-449) and Assunta (DDH NR-89-2) properties. These drill holes show that significant thicknesses of glacial material overlie down-dropped Tertiary basins. Thick glacial deposits may have an application as a regional-scale exploration tool for Tertiary basins in this part of the Intermontane Belt.

INTRUSIVE ROCKS

CLASSIFICATION: COMPOSITIONS AND TEXTURES

Prior to this project, two intrusive bodies appeared on published regional maps of the Nation Lakes area; the Hogem batholith and the Mount Milligan intrusion. Several other small intrusions had been located by exploration work. Presently, six bodies mappable at 1:50 000 scale have

been located in the area, in addition to many small ones. The large intrusions are: the southern end of the Hogem batholith north of Chuchi Lake, the Mount Milligan complex situated 10 kilometres north of the deposit, the MBX and Southern Star intrusions at the Mount Milligan deposit, a complex monzonite-diorite intrusion on the Max claims northeast of Cripple Lake, the extensive plagioclase-megacrystic diorite south of Kalder Lake, and the Tas intrusive complex. Most are multiphase, complex intrusive bodies. The highly variable nature of the intrusions is shown by the following classification scheme, in which we attempt to logically subdivide the range of textures and compositions that are present. This classification emphasizes hand-sample character, because we believe this to be most useful to the field geologist. The rock names and modal compositions were confirmed microscopically. All but those noted below are considered to be part of the Triassic-Jurassic Takla intrusive suite.

Using the classification scheme of Streckeisen (1967) the following compositions are represented in the area: (1) granite, (2) syenite, (3) monzonite/monzodiorite, (4) diorite, and (5) gabbro/monzogabbro. This numbering scheme is used on the map (Figure 1-10-4A), however it does not imply relative ages for the intrusions. The variations in potassium feldspar content between and within individual intrusions makes sodium cobaltinitrate staining necessary for correct identification. Texturally, the intrusions may be (A) coarse-grained equigranular to somewhat porphyritic; (B) crowded-porphyritic; (C) porphyritic with megacrysts; or (D) porphyritic with sparse phenocrysts in a very fine grained matrix. Because of the abundance of fine-grained matrix material in the sparsely porphyritic intrusions, they are named using volcanic terminology: (1) rhyodacite/dacite, (2) trachyte, (3) latite/latitic andesite and (4) andesite.

THE GRANITE SUITE (1)

COARSE-GRAINED EQUIGRANULAR GRANITE (1A)

Two phases of this lithology are seen on Mount Milligan peak. The first is a sphene-bearing hornblende granite, which is probably a quartz-rich differentiate of the main Mount Milligan monzonites (3A). The second phase forms discrete bodies near the southern end of the Mount Milligan ridge. Large plagioclase phenocrysts and smaller quartz and biotite crystals are spaced in a foliated, medium-grained (2 mm) equigranular matrix of quartz, orthoclase and plagioclase. This texture is indicative of subsolidus recrystallization.

SPARSELY PORPHYRITIC RHYODACITE/DACITE (1D)

These bodies may be partly or wholly of Late Cretaceous to Early Tertiary age. They are concentrated in two areas; at the Mount Milligan deposit north to the western flank of Mount Milligan peak, and around Dem Lake in the southwestern corner of the map area. They generally occur as dikes, except for one large body east of Dem Lake. They are white, tan and grey in colour. Most contain clear, round to embayed quartz phenocrysts. Plagioclase phenocrysts range from millimetre size to megacrystic. Biotite and hornblende form small phenocrysts. The rhyodacites and dacites may be

fine-grained textural variants of the porphyritic granite on Mount Milligan (1A).

THE SYENITE SUITE (2)

COARSE GRAINED, EQUIGRANULAR SYENITE (2A)

These coarse-grained intrusive rocks contain sparse to fairly abundant 5 to 8-millimetre plagioclase phenocrysts in ioclase. They form small intrusions west of Dem Lake and 6 kilometres south of Witch Lake. They are also found as cognate inclusions in a welded trachyte tuff/breccia of the Chuchi Lake formation.

MEGACRYSTIC SYENITE (2C)

In one dike south of Witch Lake, large, centimetre-sized, tabular white plagioclase and pink orthoclase(microcline?) phenocrysts occur in a felsic matrix. North of Heidi Lake, orthoclase megacrysts are present in a dike which occurs in a swarm with sparsely porphyritic monzonites and latites.

THE MONZONITE SUITE (3)

This is the most important intrusive suite in the map area. It dominates the Mount Milligan intrusion and the southern

end of the Hogem batholith. The MBX and Southern Star stocks are monzonite porphyries.

COARSE-GRAINED EQUIGRANULAR MONZONITE (3A)

Coarse-grained monzonite is seen most prominently on Mount Milligan. It also occurs in the southern end of the Hogem batholith, as small intrusions immediately south of Chuchi Lake, and on the central ridge on the Max Claims. The large Mount Milligan body varies gradationally in mineralogy and fabric. Constituents include plagioclase, clinopyroxene, hornblende and biotite with interstitial orthoclase and minor quartz (less than 10%). Hornblende and biotite are in some cases poikilitic to skeletal. Hornblende commonly forms mantles on early-crystallizing clinopyroxene. Also noteworthy in thin section are the relatively large (0.2-0.4 millimetre), abundant accessory sphene, magnetite and apatite. The Mount Milligan body also contains less abundant phases ranging from diorite to granite. Fabrics in the body vary from massive to foliated. The planar fabric is due to igneous plagioclase alignment and/or subsolidus recrystallization.

The Chuchi monzonite is unfoliated and varies in texture from coarse-grained to medium-grained "salt-and-pepper"



Plate 1-10-1. Creek zone crowded monzonite porphyry, near 66 zone. Plagioclase and minor chlorite-sericite-altered biotite phenocrysts in dark-stained K-spar-rich matrix. Station 90-JN2-4.



Plate 1-10-2. Somewhat crowded plagioclase-hornblende porphyry monzonite, West zone north of Heidi Lake. Station 90JN1-1.

textured to porphyritic. Diorite is also present in this body. The main mafic minerals are clinopyroxene and biotite.

CROWDED PLAGIOCLASE-PORPHYRITIC MONZONITE (3B)

This lithology is key to porphyry copper-gold deposits in the Nation Lakes area, as it is throughout the Quesnel trough. It makes up the MBX and Southern Star stocks at the Mount Milligan deposit and is also seen north of Heidi Lake, on the hill immediately south of Cripple Lake, and on the ridge at the centre of the Max claims. In general these rocks are quite felsic and mafic poor. Plagioclase phenocrysts 2 millimetres in size predominate, and hornblende, clinopyroxene and biotite may also be present (Plates 1-10-1 and 1-10-2). The MBX and Southern Star stocks are plagioclase biotite porphyries, the only occurrence of phenocrystic biotite in crowded porphyritic monzonites. The matrix is mostly plagioclase and potassium feldspar. Because of their low potassium contents, textural equivalents of the crowded monzonite porphyries on the Tas claims are classified here as diorites.

SPARSELY PORPHYRITIC LATITE (3D)

Plagioclase ± Hornblende, Clinopyroxene Porphyritic Latite

This lithology occurs mainly as dikes. Small, elongate plagioclase phenocrysts with subordinate hornblende and/or clinopyroxene are sparse in a very fine grained, pale greenish matrix that consists of plagioclase, potassium feldspar and mafic minerals. Many dikes of these lithologic types occur south of Heidi Lake on the western fringes of the Mount Milligan deposit. They have also been mapped near Mitzi Lake, north and south of Chuchi Lake, on the Max claims, and near Cripple Lake. They occur either as isolated bodies or as parts of larger intrusive complexes. The composition, mineralogy and texture of these intrusive rocks are comparable to some of the extrusive plagioclase-phyrlic latites within the Witch Lake and Chuchi Lake formations; they may be feeders to the more evolved volcanic flows.

Acicular Hornblende ± Plagioclase Porphyritic Latite

This highly distinctive intrusive type contains abundant needle-like hornblende crystals between 5 millimetres and 1 centimetre long. More irregular or blocky hornblendes may also be present, as well as xenoliths of hornblendite and amphibolite. The matrix consists of plagioclase, orthoclase, and smaller hornblende and augite crystals. Dikes of this lithology occur immediately west of the Mount Milligan deposit, near Mitzi Lake, south of Chuchi Lake, near Rainbow Creek, and in the southwestern corner of the Witsichica Creek map area. Their composition, mineralogy and texture are comparable to extrusive hornblende porphyries near Rainbow Creek and along the outlet of Witch Lake. A few andesite (potassium feldspar free) dikes exhibit an identical field character to these hornblende latites; they can only be distinguished by staining.

THE DIORITE/MONZODIORITE SUITE (4)

COARSE-GRAINED EQUIGRANULAR DIORITE/MONZODIORITE (4A)

A few examples of coarse-grained diorite were distinguished by potassium feldspar staining and thin-section examination. They are texturally similar to the orthoclase-rich monzonites and form in association with them. They occur on Mount Milligan, in the southern "tail" of the Hagem batholith, north of Benoit Lakes, and on the Max and Tas claims. Tas seems to be exceptional in that many of the intrusive phases are orthoclase poor. A large, multiphase pluton is shown in poor subcrop exposures east from the Free Gold zone. It is mostly diorite, although syenite with large orthoclase phenocrysts is also present.

CROWDED PLAGIOCLASE-PORPHYRITIC DIORITE (4B)

This lithology is seen on the top of the hill on the Tas property, south of Chuchi Lake, and in a dike north of Chuchi Lake that cuts the Chuchi Lake formation. On the Tas, plagioclase hornblende porphyry intrudes earlier, blocky hornblende porphyry andesite dikes. South of Chuchi Lake, the crowded porphyritic diorite shows intrusive-breccia and shattered textures in thin section.

MEGACRYSTIC PLAGIOCLASE (± AUGITE) PORPHYRITIC DIORITE (4C)

This lithology is restricted to one large body south of Kalder Lake. Large, pale greenish plagioclase phenocrysts over a centimetre in size, and much smaller blocky augites, occur in a fairly dark green, very fine grained matrix. The matrix contains plagioclase and secondary actinolite needles. An accompanying phase contains smaller plagioclases.

SPARSELY PORPHYRITIC ANDESITE (4D)

Hornblende-porphyritic Andesite

A swarm of hornblende-porphyritic andesite dikes is exposed on the hill at the centre of the Tas property. Well-formed blocky hornblende phenocrysts, roughly 5 millimetres in length, and smaller plagioclase crystals are sparse to abundant in a dark green, nearly aphanitic matrix of plagioclase and hornblende. Scattered examples of these "Tas" dikes are seen as far west as Inzana Lake. One acicular hornblende porphyritic andesite dike was mapped south of the Mount Milligan deposit.

Clinopyroxene-porphyritic Andesite

Intrusive equivalents of the Witch Lake augite porphyries are rare and small, but notable. They occur north of Heidi Lake, north of the monzonite intrusive complex on the Max claims, and at the Lynx showing.

THE GABBRO AND MONZOGABBRO SUITE (5)

COARSE-GRAINED, EQUIGRANULAR GABBRO/MONZOGABBRO (5A)

Hornblende-rich gabbros form a small part of the intrusive suite on Mount Milligan.

Another small, but very interesting, variable-textured gabbroic dike crops out south of Hat Lake. Its composition ranges from monzodiorite to hornblendite over a few metres; it varies in texture from an intrusive breccia to hornblende pegmatite. The gabbro and hornblendite clasts that occur as xenoliths in the Tas crowded porphyries and in intrusive and extrusive acicular-hornblende biotite porphyries may well have been derived from such a source.

A small coarse-grained augite-biotite-magnetite gabbro body is exposed near the northwestern corner of the map area.

IGNEOUS CLASTS IN VOLCANIC HOSTS

Keying intrusive episodes to the volcanic cycle is an important aspect of porphyry deposit modelling. The existence of plutonic and subvolcanic clasts in surface deposits gives stratigraphic constraint to the development of magma chambers. In the present map area, plutonic clasts other than hornblendites and gabbros occur only within the Chuchi Lake Formation. Many of the plagioclase-phyric clasts in the lahars could be equally of hypabyssal or volcanic origin. Coarse-grained monzonites and syenites are noted at three localities. The stratigraphically lowest locality south of Chuchi Lake contains acicular-hornblende monzonites in a host of plagioclase-hornblende polymictic breccias. The two localities north of Chuchi Lake contain coarse, equigranular, felsic clasts that are hosted in plagioclase-phyric agglomerate and a partly welded trachytic tuff-breccia. Although clasts precisely equivalent in texture to the MBX stock were not seen, it is likely that the intermediate to felsic magma chambers that produced it were probably not active until after the transition to Chuchi Lake subaerial volcanism had occurred. The coincidence of elevation above wave base – and its implication of crustal thickening – with the development of evolved magma chambers carries a pleasing symmetry, which may be substantiated by zircon dates!

METAMORPHISM

Three distinct metamorphic facies are seen in volcanic and plutonic rocks of the Takla Group. The lowest grade is subgreenschist, developed in the western and southern part of the map area. Metamorphic minerals include chlorite, carbonate, albite and rare pumpellyite. In general clinopyroxenes are fresh, and plagioclases are fresh to albitized and sericitized.

In the eastern part of the map area, including the vicinity of the Mount Milligan deposit and south to Cripple Lake, abundant clear to pale green actinolite indicates lower greenschist facies conditions. Actinolite occurs as mats of tiny acicular crystals and also as overgrowths on, and replacements of, clinopyroxene phenocrysts. This facies is developed in the megacrystic diorite south of Kalder Lake, and thus is not a contact metamorphic effect of Takla intrusions.

Near the peak of Mount Milligan, the lower greenschist passes into texturally destructive upper greenschist facies. Actinolites are more intense green. In many samples biotite and actinolite form well-oriented trains that wrap around

phenocrysts and lithic fragments, and appear to develop at the expense of randomly oriented clusters. Hornfelses without visible fabric are also present. Within the Mount Milligan complex itself, there are screens of well-foliated hornblende-clinopyroxene-biotite-plagioclase-orthoclase granulites. The transition outwards from the Mount Milligan plutonic complex seems to be in part a thermal, and in part, a strain gradient.

STRUCTURAL GEOLOGY

A strong northwesterly structural grain manifests itself in the Nation Lakes map area. It is defined by formation contacts, faults and several generations of folds. Each structural element is discussed separately below.

FOLDS

The Takla Group in the western part of the map area occupies a regional-scale, gently northwest-plunging, upright anticline that extends from the south shore of Chuchi Lake to the southern limit of mapping. The trace of the fold is outlined by formational contacts between the Inzana Lake, Witch Lake and Chuchi Lake formations. They define a kilometre-scale fold closure near Mudzenchoot Lake and a northeastern limb that trends southeasterly to around Kalder Lake (Figure 1-10-2). Relatively incompetent sediments of the Inzana Lake formation are exposed in the core of the anticline and are strongly deformed. Although the Inzana Lake formation is well bed-

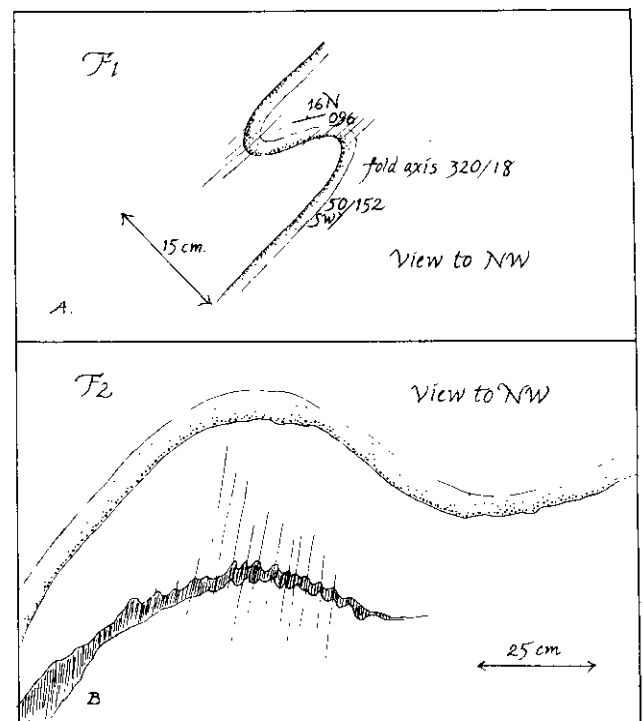


Figure 1-10-7. Sketches of F_1 and F_2 mesoscopic folds from the Inzana Lake formation. A) Overturned F_1 minor fold located on western limb of the major F_2 antiform. B) F_2 upright fold on the western limb of the major antiform.

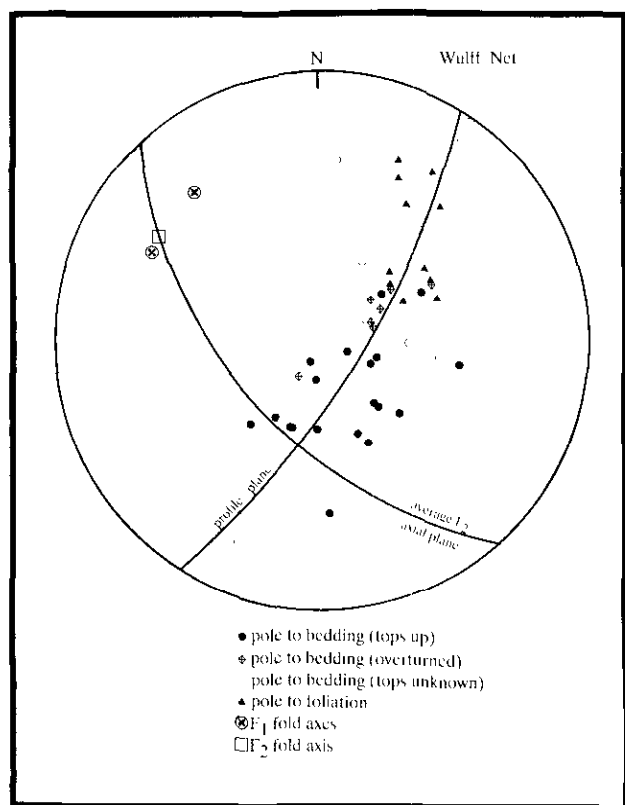


Figure 1-10-8. Stereonet plot of F_1 and F_2 structural data from north of Hat Lake.

ded, it lacks marker units. Thus structural interpretation of the region relies on rare minor folds and folds inferred on the basis of dip direction changes and facing reversals. Facing directions and bed orientations can change many times in a single outcrop due to the small scale of the folds. This, together with soft-sediment deformation, inverse grading, block faulting and rotation can make structures difficult to interpret. None the less, two coaxial phases of folding are clearly evident in the Inzana Lake formation.

The major evidence for two discrete phases of folding is the presence of overturned beds in the hinges of large scale F_2 upright folds, which indicate tight, recumbent refolded F_1 hinges. An excellent example of this occurs in the regional anticlinal hinge zone near Mudzenchoot Lake. An earlier phase of tight folding is clearly apparent where a facing/dip reversal occurs in northeast-striking strata. Other examples of F_1 folds defined by changes in facing directions in F_2 fold closures occur near Inzana Creek, north of Benoit Lake and north of Chuchi Lake. Although F_1 and F_2 folds are readily distinguishable in the closures of F_2 folds, the two are not easily discernible on the limbs of F_2 folds due to their apparently coaxial orientations.

Mesoscopic F_1 folds were only observed in a single outcrop north of Hat Lake (Figure 1-10-7a). Tight F_1 folds with gently northwest-plunging axes are overturned and show a northeast-directed asymmetry. These folds are superimposed on the southwest-dipping limb of a large-scale F_2 fold that has a well-developed axial planar cleav-

age. At the Hat Lake locality the axial planes of the two phases are parallel due to their location on the limb of an F_2 fold. A stereonet plot for the outcrop shows a great circle distribution of bedding around both F_1 and F_2 fold axes (Figure 1-10-8). A small circle distribution of poles to bedding may be expected due to refolding, however, the lack of structural data from the hinge zone and northeast limb of the F_2 fold limits stereonet interpretation. An overturned bed that occurs close to the hinge of the F_2 fold also supports the existence of two phases of folding north of Hat Lake. The pole to this bed plots in the axial region of the F_2 fold on Figure 1-10-7.

Several examples of outcrop-scale F_2 folds were seen in the field (Figure 1-10-7b). They have gently northwest-plunging fold axes similar to F_1 and are characteristically open and upright. These folds appear to be parasitic to the regional anticlinal structure.

The large-scale fold closures shown on the map probably represent an oversimplified structural interpretation, as they are based on minor structures with dimensions that are too small to be accurately represented at 1:50 000 scale. The map pattern is still useful in that it shows the types of structures that are probably present in the map area.

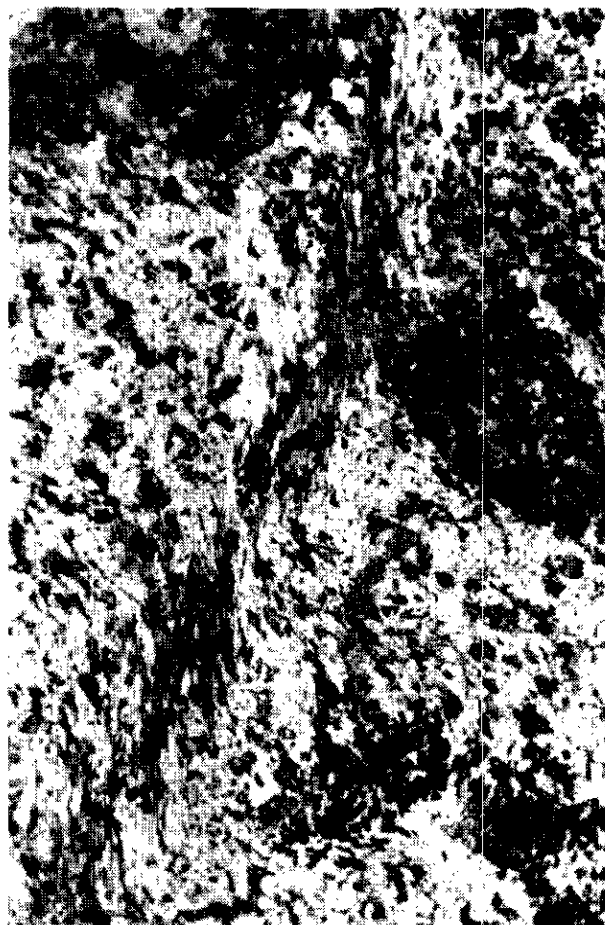


Plate 1-10-3. Shear band defined by actinolite needles in megacrystic diorite, southeast of Kalder Lake. Station 90JN19-2.

The two phases of folding apparent in the Inzana Lake formation are probably part of a progressive deformation. F_1 and F_2 folds are coaxial but not coplanar; their axial planes are approximately perpendicular to each other. F_1 folds are tight and recumbent. A regional northeast transport direction is suggested by their symmetry. The vergences of F_2 minor folds are geometrically related to the map-scale upright anticlinal structure, rather than to regional tectonic transport. Folding is probably late Triassic to early Jurassic in age and is most likely related to docking of the Quesnel Terrane (Rees, 1987).

FAULTS

Faults play an important role in the interpreted map pattern of the area. Most of them are conjectural. Their basis is in small exposures of strongly deformed rocks, and in offsets of stratigraphy and abrupt changes of structural grain. Fault zones outcrop on the northeast shore of Dem Lake, west of Mount Milligan, in the valley of Rainbow Creek, on the ridge due east of Kalder Lake (Plate 1-10-3), on the southeast spur of the ridge on the Max claims, and a kilometre east of the map area on the Germansen-Cripple road. Except at Dem Lake, where deformation is purely brittle, all of these zones show strong penetrative fabrics. At



Plate 1-10-4. Biotite trains in deformed, schistose augite porphyry lapilli tuff northeast of Mount Milligan peak. Station 90JN8-11.

the Germansen-Cripple locality, large-augite porphyry agglomerate has been smeared into a northeasterly trending tectonite with moderately plunging stretching lineations. West of Mount Milligan peak, the intrusive complex is in faulted contact with slightly metamorphosed Takla rocks. Quartz-plagioclase-biotite porphyry dikes within this fault zone are strongly deformed to mylonitized and have steep, northwesterly-striking foliations parallel to the inferred fault trace. Subhorizontal lineations and asymmetric pressure shadows in the outcrop indicate a dextral strike-slip motion for the fault. These plastically deformed rocks lie in contact with foliated, green clay gouge, which shows later, post-uplift, brittle deformation.

At the eastern edge of the Mount Milligan deposit, Takla stratigraphy is truncated by the "Great Eastern fault", a broad zone of milling and brittle shear zones seen only in drill-core. The Great Eastern fault juxtaposes Takla rocks against Early Tertiary continental clastics, basalt and coal. It is crosscut by quartz and plagioclase-porphyrific dikes, which show only minor shearing (C. DeLong, personal communication, 1990). These dikes are texturally unique but still part of the rhyodacite/dacite suite. One dike is an amygdaloidal plagioclase porphyry; the other contains white plagioclase and pink orthoclase megacrysts and smaller, rounded quartz phenocrysts.

Other faults are inferred in order to explain map patterns. A northeasterly trending fault under Chuchi Lake is needed to separate the south-facing Chuchi Lake formation to the north from the east-facing Witch Lake formation to the south. The Early Tertiary sediments and basalts near Gidegingla Lake occupy a fault-bounded basin. The northwesterly trending bounding faults are necessary, in any event, to separate eastward-younging Chuchi Lake formation to the west from Witch Lake formation near Mount Milligan to the east, while the inferred northeasterly-trending faults are strong VLF linears (Ronning, 1989).

The overall map pattern shows a series of long, but ultimately discontinuous northwest-trending faults, linked by shorter, second-order northeast-trending faults (Figure 1-10-4A). This pattern is exactly that predicted for an area in which motion is transferred between two different northwest-trending dextral faults. The map pattern implies the same stress regime as Struik (1990) envisages for the contiguous McLeod Lake area.

THE MOUNT MILLIGAN HORST

The Mount Milligan intrusive complex is far from an ordinary plutonic body. It consists of at least two separate intrusive phases: sphene-bearing monzonite with gabbro and hornblende granite end-members; and porphyritic granite. Its wallrocks and numerous pendants include regionally metamorphosed amphibolites and granulites as well as contact hornfelses. The transition from the plutonic/high-grade metamorphic core of the complex into low-grade metamorphic, ordinary Witch Lake rocks occurs variously across both contact metamorphic zones and strain gradients (Plate 1-10-4). The western contact of the complex is a major transcurrent fault.

The earlier of the two plutonic bodies on Mount Milligan is an equigranular, massive to foliated quartz-deficient monzonite. Near its southern margin this body is cut by a wide-spaced biotite or chlorite schistosity. This same strong but widely spaced schistosity is seen sporadically in the country rocks. The later plutonic body is a porphyritic, medium-grained granite with peripheral pegmatite and aplite stringers. This much smaller body crosscuts the amphibolite foliation but is itself foliated in places. Some of its most felsic apophyses are postkinematic. Therefore, this intrusion was emplaced during the waning stages of deformation.

The equigranular monzonite phase on Mount Milligan is probably a Takla intrusion. Perhaps it is a deep-level equivalent of the MBX and Southern Star monzonites. The presence of amphibolites among its wallrocks suggests that it was emplaced at a considerably deeper crustal level than anything else now exposed in the map area. The juxtaposition of these amphibolites against texturally unaffected augite porphyries – outcropping in one case less than 300 metres apart – requires significant uplift of the central Mount Milligan block. On the other hand, some Takla Group rocks south of the complex are strongly hornfelsed. The late-kinematic granite is a likely culprit. Although its exposed extent is small, it may be an offshoot of a larger body. Rhyodacite/dacite porphyry dikes of inferred Cretaceous to Early Tertiary age concentrate in the Mount Milligan area. All of them are recrystallized and many of them are strongly deformed. Plagioclase and quartz phenocrysts are subgrained and partly recrystallized to aggregates of tiny neoblasts; the matrix shows an incipient to well-developed biotite schistosity.

Uplift of the Mount Milligan complex as a horst, accompanied by Late Cretaceous to Early Tertiary felsic intrusions, fits well with the overall fault pattern of the Nation Lakes area. It also suggests an explanation for the anomalously young K-Ar dates (1094 Ma and 66.32.3 Ma) that have been obtained from the Mount Milligan deposit (Faulkner *et al.*, 1990). They were probably thermally updated by the quartz-bearing intrusions and by rapid uplift as well.

Like other large alkalic porphyry copper-gold deposits, the Mount Milligan deposit has had a complex later structural history. Its present structural setting near Early Tertiary down-dropped sedimentary basins and an uplifted basement complex, is very like that of Copper Mountain and Afton. Speculatively, these later faults such as the Great Eastern fault may have had antecedents in early Mesozoic intrabasin faults.

ALTERATION AND MINERALIZATION

ALTERATION HALOES

Broad alteration haloes occur throughout the mapped area. Most of them contain intrusive bodies and all coincide with magnetic anomalies. The alteration haloes are interesting as exploration targets on their own. Many of them contain known or newly discovered mineral occurrences, so they provide a context for discussing mineralization. They are given names for ease of reference.

The Mount Milligan halo extends at least 3 kilometres from the deposit to the skarn occurrence west of Heidi Lake, and north along the ridge towards Mitzi Lake. It includes a complex suite of small monzonitic intrusive bodies. Very strong potassic alteration occurs in the core of the halo. Secondary biotite clumps and pervasive fine-grained interlocking secondary potassium feldspar are abundant. Near the periphery, secondary potassium feldspar forms veinlets and clumps, as well as fine seams in plagioclase and augite phenocrysts. It also penetrates along the bedding planes of epiclastic sediments.

The Chuchi halo, north of Chuchi Lake, extends westward onto Noranda's Chuchi property. It occurs mostly within monzonites of the Hogem batholith. Disseminated pyrrhotite and pyrite and secondary potassium feldspar veins and veinlets are locally abundant.

The Chuchi-Witch halo lies between the two lakes it is named for and continues west onto Rio Algom's Witch claim group. The halo contains several small, crowded porphyry diorite and coarse-grained monzonite bodies. Intense alteration is extensive. Actinolite-diopside hornfels is overprinted by secondary biotite, potassium feldspar and epidote. Copper and gold showings occur within the halo off the western edge of the map area (Campbell, 1990).

The Taylor halo south of Witch Lake, includes the Taylor showing. Disseminated pyrite, pyrrhotite and silicification are abundant. The eastern side of the halo disappears under cover; most of the associated magnetic anomaly is in an area covered by glacial overburden.

The Mudzenchoot halo north of Mudzenchoot Lake contains several small outcrops of fine-grained diorite and orthoclase-megacrystic syenite. The surrounding fine-grained volcanic rocks are silicified and strongly hornfelsed. Stringers and disseminations of pyrite are abundant.

The Max halo, which lies on and near the Max claims northeast of Cripple Lake, includes the Max, Lynx and K-2 mineral showings. A complex intrusive system with local intrusion breccia has areas of epidote flooding and associated pervasive potassic and propylitic alteration. Abundant disseminated pyrite and pyrrhotite also occur.

The Lynx halo south of Cripple Creek covers an area of bleached, silicified and hornfelsed sediments that host the Lynx showing. Pyrite, chalcopyrite, pyrrhotite, malachite and skarn mineralization are present in the halo.

The Tas halo, on and near the Tas claims, shows a strong, pervasive alteration in the vicinity of the East and West zones, where hornblende porphyry dikes and crowded porphyry diorites are most abundant. To the south, a large body of coarse-grained diorite to syenite is mostly propylitically altered but also has scattered potassium feldspar veins.

The HAI halo south of the Tas property consists of silicified sediments with minor pyrite and chalcopyrite.

The Dem halo affects Rainbow Creek sediments south of Dem Lake. It hosts the Dem showing. It is characterized by hornfelsing, abundant disseminated pyrite, hairline magnetite veinlets and local strong alteration with associated syenite dikes.

The most common feature of these alteration haloes is the abundance of disseminated pyrite and/or pyrrhotite. Second most common is propylitic alteration, expressed generally as epidote flooding. Secondary potassium feldspar is widespread but generally detectable only by chemical staining or in thin section as hairline veinlets and scattered patches. Pervasive, texture-destructive alteration occurs only in the centres of the haloes, where it succeeds early purple-brown biotite hornfels.

The potential for undiscovered alteration haloes is still present in the map area due to extensive glacial overburden.

MINERAL OCCURRENCES

MOUNT MILLIGAN (MINFILE 093N 194)

The Mount Milligan deposit, with published reserves of 400 million tonnes of 0.48 gram per tonne gold and 0.2 per cent copper (DeLong *et al.*, 1991), is one of the most exciting finds of the 1980s. More complete descriptions of the deposit can be found in Faulkner *et al.* (1990) and DeLong *et al.* (1991, this volume). At present, two potential orebodies have been identified on the property: the MBX zone associated with the MBX stock, which grades into the peripheral, gold-rich 66 zone; and the Southern Star zone, associated with the Southern Star stock. Gold and copper mineralization correlate with intense potassic alteration. The copper-to-gold ratio is highest in the Southern Star stock. The gold-rich 66 zone developed by bedding-parallel infiltration and replacement of volcanic sediments and andesites of the Witch Lake formation above, and spreading away from, the MBX stock. Rotation of northeasterly dipping and facing stratigraphy to horizontal shows the MBX stock as a vertical feeder to the laccolithic, sill-like Rainbow dike. Dilation along bedding planes may have controlled the emplacement of the Rainbow dike and also provided increased permeability, which channelled ore fluids to create the 66 zone.

TAS (MINFILE 093K 080)

The Tas (East zone) is located on a small hill just north of the Germansen–Inzana forest road, approximately 10 kilometres from its junction with the Fort St. James–Germansen logging road. Hornfelsed and bleached siliceous argillites of the Inzana Lake formation are intruded by texturally variable hornblende±biotite±plagioclase porphyry. The hornblende porphyry often forms intrusive breccia with xenoliths of sediments and hornblendite. It is weakly propylitized. Later, more felsic diorite intrudes this package.

Mineralization in the sedimentary and intrusive rocks is confined to minor amounts (<2%) of disseminated pyrite and pyrrhotite. Semimassive sulphide pods are found in steeply dipping, north-trending shear zones, 10 to 20 centimetres wide. On surface these zones contain up to 70 per cent sulphides: mainly pyrite and pyrrhotite with minor chalcopyrite and marcasite(?).

An unmineralized diatreme containing milled fragments of tuffs, hornblende porphyry and monzodiorite appears to grade into a hydrothermal breccia containing quartz and fine-grained massive actinolite. No sulphides were noted.

FREE GOLD ZONE (MINFILE 093K 091)

The Free Gold zone is located on the Tas claims on the Germansen–Inzana forest road. A small zone of intense quartz-carbonate alteration is exposed in a quarry. Up to 10 per cent pyrite with traces of magnetite and malachite and rare native gold occur in the rock. Propylitized hornblende diorite with sporadic potassium feldspar veins and traces of malachite on fractures outcrop near the showing. The diorite and the Free Gold zone are hosted by the Inzana Lake formation.

MAX (MINFILE 093K 020)

The Max claims are located east of the Fort St. James–Germansen logging road near Cripple Lake; approximately 14 kilometres east of the Tas property and 22 kilometres south of the Mount Milligan deposit. The property covers an extensive area of propylitic alteration and sporadic mineralization that is associated with a complex polyphase intrusive body. The occurrence location recorded in MINFILE is at the highest elevation on the Max claims (1370 metres), the approximate centre of the alteration zone. The Max prospect includes several small showings in and around the main intrusive body.

The complex intrusive suite includes texturally variable monzonite, diorites and monzodiorites. Hornblendite and aplite dikes have also been mapped on the property. In one locality hornblendite apparently grades into amygdaloidal extrusive equivalents. Similar hornblendite dikes have been documented on the Tas property.

Propylitic alteration is extensive in the intrusive rocks; epidote and secondary chlorite are abundant. Minor potassic alteration also occurs. The intrusions contain up to 20 per cent pyrite in places, but average sulphide contents are closer to 3 per cent.

The intrusions cut heterolithic augite±plagioclase porphyry flows and agglomerates, black siliceous argillite and volcanic siltstones and sandstones of the Witch Lake formation. The sediments are intensely hornfelsed with abundant secondary biotite; the volcanic rocks are strongly epidotized. Up to 30 per cent pyrite occurs in these rocks. Minor disseminated pyrrhotite is found with chlorite in veinlets. Chalcopyrite and magnetite have also been identified.

LYNX (MINFILE 093K 083)

The Lynx showing is located on the southern portion of the Max claims south of Cripple Creek. It occurs within a large area (approximately 2 km by 1 km) of bleached, silicified and mineralized rocks. This alteration zone may be part of a larger propylitic alteration halo associated with the intrusive body on the Max claims to the north.

The main part of the Lynx showing occurs in a trench adjacent to the Germansen–Cripple logging road. A three-metre square sulphide-rich oxidized zone occurs within light green, silicified and brecciated ash and dust tuffs of the Inzana Lake formation. The zone contains up to 30 per cent massive and crystalline pyrite, up to 5 per cent chalcopyrite and minor malachite. The rocks have a well-developed network of hairline fractures with alteration envelopes along

them. Both propylitic and potassic alteration are present. The rocks are strongly hornfelsed and contain abundant secondary biotite, however, no intrusive rocks have been identified on the property. Adjacent to the gossan a north-west trending, steeply dipping fault contains a 30-centimetre gouge zone that hosts quartz but no sulphides.

Stratigraphically above the main showing and approximately 1.25 kilometres to the west-northwest, tuffaceous siltstones and minor lapilli tuffs are sporadically converted to skarn. Biotite and diopside hornfelsing are widespread for several hundred metres. One zoned garnet-epidote-diopside-biotite skarn contains concentrations of massive pyrrhotite (50 to 70%) with minor flecks of chalcopyrite and possibly covellite. The meta-tuffs are interbedded with intermediate plagioclase+augite±hornblende porphyry flows or sills. They contain disseminated pyrite and abundant epidote in streaky veins.

K-2 (MINFILE 093K 086)

The K-2 showing is located near the western boundary of the Max claims, approximately 3 kilometres north-northeast of Cripple Lake. The showing is a hydrothermally brecciated quartz-carbonate vein which is exposed in a subcrop zone approximately 2 metres wide that trends south-southeast over 50 metres. The vein contains bleached and milled wallrock and is strongly hematite stained. Up to 30 per cent chalcopyrite with minor malachite and an unidentified grey-silver-coloured sulphide occur in the rock. The vein is hosted by clinopyroxene-rich flows and agglomerates of the Witch Lake formation. Secondary biotite and epidote are locally abundant in the rocks around the showing. These alteration minerals are probably part of the large propylitic alteration halo around the multiphase intrusion on the Max claims to the east.

DEM (MINFILE 093K 077)

The Dem showings are hosted by metasomatically altered sediments of the Inzana Lake formation, within the Dem halo described above. Well-laminated sandstones and siltstones are intruded, hornfelsed and altered by syenomonzonite dikes. Areal extensive alteration in the sediments ranges from local massive epidote-tremolite skarning to biotite-diopside hornfelsing. Samples contain up to 137 ppm copper.

The main showing is a pod-shaped subcrop exposure (20 centimetres by 1 metre) of brecciated quartz vein. The vein contains between 5 and 10 per cent arsenopyrite that forms in clumps with epidote and tremolite. A grab sample of this vein contains 361 ppb gold, 2.11 per cent arsenic and 66 ppm antimony.

Approximately 500 metres south of the arsenopyrite quartz-breccia vein, another massive skarn pod (0.5 metre wide) occurs within the sediments close to syenomonzonite dikes. Skarn mineralization consists of pyrite and pyrrhotite with secondary biotite and actinolite veinlets. A grab sample contains 204 ppb gold and 41 ppm copper.

MITZI (MINFILE 093N 204)

The Mitzi showing is located on the Phil claim group, 1 kilometre north-northeast of the east end of Mitzi Lake and 4.5 kilometres northwest of the Mount Milligan deposit. The showing is a tetrahedrite-chalcopyrite-bearing quartz-ankerite breccia vein hosted in hornfelsed augite porphyry agglomerate of the Witch Lake formation. The 20-centimetre vein trending 045°/65°NW contains up to 5 per cent tetrahedrite with minor chalcopyrite. Alteration in the metavolcanics includes massive garnet and biotite. Prominent red-weathering zones occur within 500 metres of the vein, but contain no visible sulphides.

Outcrops around the showing include strongly foliated biotite-rich mafic schists that are intruded by and occur as pods in coarse-grained equigranular diorite/syenodiorite. These regionally metamorphosed amphibolitic schists are part of the Mount Milligan horst.

CHIC (MINFILE 093N 202)

The Chic showing is located on the Goldfinger claim group approximately 3 kilometres north of the outlet of the Nation River on Chuchi Lake, 2.5 kilometres east of the Wit prospect. The showing is a poddy epithermal vein that cuts a megacrystic-feldspar porphyry intrusion. The vein contains light green kaolinite and quartz with abundant blebs of disseminated pyrite and traces of chalcopyrite.

The feldspar porphyry is probably the intrusive equivalent of nearby potassium feldspar porphyritic andesites and purple amygdaloidal dacitic flows of the Chuchi Lake formation.

KBE (MINFILE 093N 203)

This small, isolated showing is located approximately 10 kilometres north-northeast of the east end of Inzana Lake and 5 kilometres southeast of Mudzenchoot Lake. The showing consists of less than 1 per cent disseminated malachite in a bleached and slightly gossanous hornblende granite or granodiorite intrusion. No visible pyrite or other sulphides are associated with the malachite. A grab sample from this showing contains 196 ppb gold and 0.2 per cent copper. Minor amounts of epidote and magnetite occur in the granite within 100 metres of the showing. The granite intrudes epiclastic sediments of the Inzana Lake formation.

HAT LAKE (MINFILE 093K 084)

The Hat Lake showing is located on the Hat Lake claim group 1.5 kilometres south of Hat Lake on the Germansen-Hat logging road. Bedrock is best exposed along road cuts and in trenches on the property. Silicified, hornfelsed and fractured black argillite, cherty tuffs and green sandstone of the Inzana Lake formation contain disseminated pyrite. The sediments are cut by texturally highly variable gabbro and diorite intrusions, gabbro pegmatite and intrusion breccias. These mafic intrusive phases appear very similar to those that form xenoliths in crowded porphyry diorite on the Tas property. A trench exposes a plagioclase-augite-hornblende diorite dike that contains 10 per cent pyrrhotite. Pale quartz

carbonate alteration and a shear zone were also noted at the showing.

Several gold and silver geochemical anomalies are present in soils on the property; one coincides with a quartz-carbonate stockwork 1 metre wide containing minor sulphides. Sulphides at the showing include up to 5 per cent pyrite and pyrrhotite with traces of chalcopyrite (Schmidt, 1987).

HAI (MINFILE 093K 004)

The HAI showing is located on the HAI claim near Taslinchecko Creek, approximately 5.5 kilometres south of the Tas property. The showing consists of 5 per cent pyrite and less than 1 per cent chalcopyrite disseminated in siliceous black argillite of the Inzana Lake formation. Quartz-carbonate stringers are abundant in the rocks; some of them contain minor pyrite. Abundant hematite-coated fractures occur in silicified sediments in a trench exposure.

Previous drilling on the property has shown the presence of subsurface diorite and gabbro intrusions on the HAI claim. Fine to coarse-grained gabbro with 20 to 25 per cent hornblende phenocrysts contains 2 to 3 per cent pyrite and pyrrhotite. Fine to medium-grained, equigranular to weakly porphyritic diorite contain less than 1 per cent pyrite. Hornfelsed sediments contain 2 to 5 per cent disseminated pyrite and quartz-carbonate altered zones contain 5 to 10 per cent (Maxwell, 1987).

RAINBOW CREEK (MINFILE 093N 205)

The Rainbow Creek showing is located on the Rain claims along a north-flowing tributary of Rainbow Creek, about 15 kilometres south of the Mount Milligan deposit. There is a strong base metal geochemical anomaly in silts at the creek junction. The following values have been identified in a *Regional Geochemical Survey (RGS)* stream-sediment sample collected near the mouth of the tributary: 21.5 ppm arsenic, 9.4 ppm antimony and 128 ppm zinc.

A grey to black fault-zone breccia with quartz and carbonate veining and up to 20 per cent pyrite outcrops on the banks of the tributary. The fault zone cuts through augite porphyry agglomerates and white-weathering tuffaceous black siltstone and mudstone of the Witch Lake formation. Gossanous zones contain 3 per cent disseminated pyrite with magnesite and traces of fuchsite. A few discontinuous chalcedony veins cut the pyritic breccia. The fault breccia itself is geochemically flat except for one sample that contains 140 ppm copper, but a grab sample of one of the veins returned an anomalous analysis of 1400 ppb gold and 180 ppm arsenic.

TAYLOR (MINFILE 093N 096)

The Taylor showing lies on the Mitzi claim group, within the Taylor halo. It outcrops in a northeast-flowing tributary of Wittsichica Creek, 3 kilometres south of the outlet of Witch Lake. Diverse alteration assemblages including secondary biotite, chlorite, secondary amphibole, black tourmaline, garnet skarning and white bleaching are intermixed

in an outcrop less than 20 metres long. Up to 10 per cent pyrrhotite occurs with fine-grained pyrite and chalcopyrite. Assays of 1.59 per cent copper and 4.93 grams per tonne gold have been obtained from grab samples (Roney and Maxwell, 1989).

The showing is hosted in trachytic plagioclase-augite-porphyrific latites of the Witch Lake formation. Intrusive rocks on the Mitzi claims include diorite and gabbro dikes (Roney and Maxwell, 1989).

WIT (MINFILE 093N 141)

The Wit showing was initially covered by the Wit and Wag claim groups, but due to restaking in the 1980s is now on the Skook claim group. The showing is located on the north shore of Chuchi Lake and is reached by a forest road that joins the Fort St. James-Germansen logging road 5 kilometres north of the Nation River crossing.

The main showing is an irregular epithermal vein (5 metres wide by 20 metres vertical extent) of banded white and grey quartz and chalcedony that is exposed in and around a trench. The vein hosts small pods and disseminations of galena and sphalerite with possible argentite and tetrahedrite. Banded chalcedony and quartz with calcite, pyrite and trace galena occur 150 metres east of the main vein outcrop.

Exploration work on the property (Holcapek, 1981; Campbell, 1988) has delineated an estimated geological reserve of 20 000 tonnes grading 7 per cent combined lead-zinc. The surface showing seems to be the top of a larger epithermal system. Barite lenses and stockworks as well as strongly oxidized and limonitic zones have also been documented by previous workers on the property.

The hostrocks are maroon and green matrix-supported polymictic breccias and lahars of the Chuchi Lake formation. The volcanics are in places scoriaceous and amygdaloidal and have calcite, albite and celadonite vesicle infillings. Sulphides are also disseminated in the hostrocks and in fracture fillings.

CONCLUSIONS AND SUMMARY OF MINERAL POTENTIAL

Regional mapping in the Nation Lakes area has documented the potential for alkaline porphyry copper-gold deposits throughout the entire area where the Takla Group is exposed. No firm stratigraphic or structural constraints on the Mount Milligan deposit are shown in the regional geology. Instead, small intrusions associated with strong potassic-propylitic-pyritic alteration haloes and coincident magnetic anomalies occur scattered throughout the Takla Group. Recognition of these alteration zones, both through field tracing of sulphide-rich areas and through petrographic determination of potassic assemblages, is an important aspect of porphyry exploration efforts.

ACKNOWLEDGMENTS

The development of the ideas presented in this paper benefited greatly from discussions with exploration person-

nel and from the willingness of exploration companies to share information. We are particularly indebted to Doug Forster and Mike Harris of Continental Gold Corp., Peter Leriche of Reliance Geological Limited and Chris Bates, Russ Wong and Tucker Barrie of BP Resources Canada Limited. Vic Preto and Fil Ferri visited the project and added valuable insights. Vic Preto and Bill McMillan reviewed the manuscript and offered valuable suggestions.

REFERENCES

- Armstrong, J.E. (1949): Fort St. James Map-area, Cassiar and Coast Districts, British Columbia; *Geological Survey of Canada*, Memoir 252, 210 pages.
- Bailey, D.G. (1978): Geology of the Morehead Lake Area, South Central British Columbia; unpublished Ph.D. thesis, *Queen's University*, 198 pages.
- Bailey, D.G. (1988): Geology of the Central Quesnel Belt, Hydraulic, South-central British Columbia (93A/12); *B.C. Ministry of Energy, Mines and Petroleum Resources*, Geological Fieldwork 1987, Paper 1988-1, pages 147-153.
- Barr, D.A., Fox, P.E., Northcote, K.E. and Preto, V.A. (1976): The Alkaline Suite Porphyry Deposits – A Summary; in Porphyry Deposits of the Canadian Cordillera, A. Sutherland Brown, Editor, *Canadian Institute of Mining and Metallurgy*, Special Volume 15, pages 359-367.
- Bloodgood, M.A. (1987): Geology of the Triassic Black Phyllite in the Eureka Peak Area, Central British Columbia (93A/7); *B.C. Ministry of Energy, Mines and Petroleum Resources*, Geological Fieldwork 1986, Paper 1987-1, pages 135-142.
- Bloodgood, M.A. (1988): Geology of the Quesnel Terrane in the Spanish Lake Area, Central British Columbia (93A/11); *B.C. Ministry of Energy, Mines and Petroleum Resources*, Geological Fieldwork 1987, Paper 1988-1, pages 139-153.
- Campbell, C. (1988): Preliminary Geochemical and Geological Report on the Skook 3-6 Mineral Claims (93N/1E and 2W); *B.C. Ministry of Energy, Mines and Petroleum Resources*, Assessment Report 18073.
- Campbell, E.A. (1990): Witch Option, NTS: 93N1&2, Geology, Geophysics and Geochemistry 1989, Rio Algom Exploration Inc.; *B.C. Ministry of Energy, Mines and Petroleum Resources*, Assessment Report 19720.
- DeLong, R.C., Godwin, C.I., Harris, M.K., Cairn, N. and Rebagliatti, C.M. (1991): Geology and Alteration at the Mount Milligan Property; *B.C. Ministry of Energy, Mines and Petroleum Resources*, Geological Fieldwork 1990, Paper 1991-1, this volume.
- de Rosen-Spence, A.F. (1985): Shoshonites and Associated Rocks of Central British Columbia; *B.C. Ministry of Energy, Mines and Petroleum Resources*, Geological Fieldwork 1984, Paper 1985-1, pages 426-442.
- Faulkner, E.L., Preto, V.A., Rebagliatti, C.M. and Schroeter, T.G. (1990): Mount Milligan (93N 194); *B.C. Ministry of Energy, Mines and Petroleum Resources*, Exploration in British Columbia 1989, Part B, pages 181-192.
- Ferri, F. and Melville, D. (1989): Geology of the Germansen Landing Area, British Columbia (93N/10, 15); *B.C. Ministry of Energy, Mines and Petroleum Resources*, Geological Fieldwork 1988, Paper 1989-1, pages 209-220.
- Ferri, F. and Melville, D. (in preparation): Geology of the Germansen Landing – Manson Creek Area, B.C.; *B.C. Ministry of Energy, Mines and Petroleum Resources*.
- Foden, J.D. and Varne, R. (1980): The Petrology and Tectonic Setting of Quaternary-Recent Volcanic Centres of Lombok and Sumbawa, Sunda Arc; *Chemical Geology*, Volume 30, pages 201-226.
- Garnett, J.A. (1978): Geology and Mineral Occurrences of the Southern Hogem Batholith; *B.C. Ministry of Energy, Mines and Petroleum Resources*, Bulletin 70, 75 pages.
- Gravel, J.L., Sibbick, S. and Kerr, D. (1991): Geochemical Research, 1990: Chilcotin Orientation and Mount Milligan Drift Prospecting Studies (92O, 92N, 93N); *B.C. Ministry of Energy, Mines and Petroleum Resources*, Geological Fieldwork 1990, Paper 1991-1, this volume.
- Holcapek, F. (1981): Geological and Geochemical Report on the Wit Mineral Claim (93N/1W); *B.C. Ministry of Energy, Mines and Petroleum Resources*, Assessment Report 9705.
- Kerr, D.E. and Bobrowsky, P.T. (in preparation): Quaternary Geology and Drift Exploration at Mount Milligan (93N/1E, 93O/4W) and Johnny Mountain (104B/6E, 7W, 10W, 11E), British Columbia.
- Legun, A., Faulkner, E.L., Lefebvre, D.V., Meyers, R.E. and Wilton, H.P. (1990): 1989 Producers and Potential Producers, Mineral and Coal; *B.C. Ministry of Energy, Mines and Petroleum Resources*, Preliminary Map 65.
- Logan, J.M. and Koyanagi, V.M. (1989): Geology and Mineral Deposits of the Galore Creek Area, Northwestern British Columbia (104G/3, 4); *B.C. Ministry of Energy, Mines and Petroleum Resources*, Geological Fieldwork 1988, Paper 1989-1, pages 269-284.
- Maxwell, G. (1987): Geological and Geochemical Report on the HA1 Claim (93K/16); *B.C. Ministry of Energy, Mines and Petroleum Resources*, Assessment Report 16272.
- Monger, J.W.H. (1977): The Triassic Takla Group in McConnell Creek Map-area, North-central British Columbia; *Geological Survey of Canada*, Paper 76-29, 45 pages.
- Monger, J.W.H. and Church, B.N. (1977): Revised Stratigraphy of the Takla Group, North-central British Columbia; *Canadian Journal of Earth Sciences*, Volume 14, pages 318-326.

- Monger, J.W.H., Wheeler, J.O., Tipper, H.W., Gabrielse, H., Harms, T., Struik, L.C., Campbell, R.B., Dodds, C.J., Gehrels, G.E. and O'Brien, J. (1990): Cordilleran Terranes; in *The Cordilleran Orogen: Canada*, Chapter 8, Upper Devonian to Middle Jurassic Assemblages, H. Gabrielse and C.J. Yorath, Editors, *Geological Survey of Canada*, Geology of Canada, Number 4.
- Mortimer, N. (1987): The Nicola Group: Late Triassic and Early Jurassic Subduction-related Volcanism in British Columbia; *Canadian Journal of Earth Sciences*, Volume 24, pages 2521-2536.
- Nelson, J., Bellefontaine, K.A., Green, K.C. and MacLean, M. (1991): Geology and Mineral Potential of the Witsichica Creek and Tezzeron Creek Map-areas (NTS 93N/1, 93K/16); *B.C. Ministry of Energy, Mines and Petroleum Resources*, Open File 1990-3.
- Nixon, G.T., Hammack, J.L., Connelly, J.N., Case, G. and Paterson, W.P.E. (1990): Geology and Noble Metal Geochemistry of the Polaris Ultramafic Complex, North-central British Columbia (94C/5, 12); *B.C. Ministry of Energy, Mines and Petroleum Resources*, Geological Fieldwork 1989, Paper 1990-1, pages 387-404.
- Paterson, I.A. (1977): The Geology and Evolution of the Pinchi Fault Zone at Pinchi Lake, Central British Columbia; *Canadian Journal of Earth Sciences*, Volume 14, pages 1324-1342.
- Rebagliati, C.M. (1990): Mount Milligan – Alkalic Porphyry Cu-Au Deposits; *Geological Association of Canada, Mineralogical Association of Canada*, Program with Abstracts, Volume 15, page A109, Vancouver.
- Rees, C.J. (1987): The Intermontane-Omineca Belt Boundary in the Quesnel Lake Area, East-central B.C.: Tectonic Implications Based on Geology, Structure and Paleomagnetism; unpublished Ph.D. thesis, *Carleton University*, 409 pages.
- Roney, C. and Maxwell, G. (1989): Geochemistry Report on the Mitzi Option (93N/1); *B.C. Ministry of Energy, Mines and Petroleum Resources*, Assessment Report 19184.
- Ronning, P.A. (1989): Pacific Sentinel Gold Corporation, Nation River Property, Report on Diamond Drilling (93N/1); *B.C. Ministry of Energy, Mines and Petroleum Resources*, Assessment Report 19296.
- Schmidt, U. (1987): Geochemistry and Geological Mapping of the Hat Grid, Hat Claim Group (93K/16W); *B.C. Ministry of Energy, Mines and Petroleum Resources*, Assessment Report 15943.
- Sillitoe, R.H. (1990): Gold Rich Porphyry Copper Deposits; *Geological Association of Canada, Mineralogical Association of Canada*, Program with Abstracts, Volume 15, page A122, Vancouver.
- Streckeisen, A.L. (1967): Classification and Nomenclature of Igneous Rocks; *Neues Jahrbuch Fur Mineralogie Abhandlungen*, Volume 107, pages 144-240.
- Struik, L.C. (1989): Regional Geology of the MacLeod Lake Map Area; *Geological Survey of Canada*, Report of Activities, Paper 1989-1E, pages 109-114.
- Struik, L.C. (1990): Wolverine Core Complex, Transforms and Metals, McLeod Lake Map Area, Central British Columbia; *Geological Association of Canada, Mineralogical Association of Canada*, Program with Abstracts, Volume 15, page A126, Vancouver.
- Varne, R. (1985): Ancient Subcontinental Mantle: A Source for K-Rich Orogenic Volcanics; *Geology*, Volume 13, pages 405-408.
- Wheeler, J.O., Brookfield, A.J., Gabrielse, H., Monger, J.W.H., Tipper, H.W. and Woodsworth, G.J. (1988): Terrane Map of the Canadian Cordillera; *Geological Survey of Canada*, Open File 1894, 9 pages and 1:2 000 000 map.
- Wheeler, J.O. and McFeely, P. (1987): Tectonic Assemblage Map of the Canadian Cordillera; *Geological Survey of Canada*, Open File 1565.
- Wilkinson, W.J., Stevenson, R.W. and Garnett, J.A. (1976): Lorraine, The Alkaline Suite Porphyry Deposits – A Summary; in *Porphyry Deposits of the Canadian Cordillera*, A. Sutherland Brown, Editor, *Canadian Institute of Mining and Metallurgy*, Special Volume 15, pages 397-401.



GEOLOGY OF THE LAMPREY CREEK MAP SHEET (93L/3)

By P.J. Desjardins, R.L. Arksey and D.G. MacIntyre

KEYWORDS: Regional geology, Jurassic stratigraphy, Hazelton Group, Telkwa Formation, structure, Skeena Group, Mount Ney volcanics, Kasalka Group, Ootsa Lake Group, Thautil River sediments, Buck Creek volcanics, Bulkley intrusions, Topley intrusions.

INTRODUCTION

This report discusses the geology and mineral occurrences of the Lamprey Creek map area (93L/3). These observations are based on 1:50 000 mapping conducted as part of the Telkwa project (Figure 1-11-1) in 1990. The project area includes the Babine and Telkwa ranges; approximately six 1:50 000 scale-map sheets have now been completed.

REGIONAL GEOLOGIC SETTING

The project area is located within the Stikine Terrane, a collage of Jurassic, Cretaceous and Tertiary magmatic arcs and related successor basins (MacIntyre *et al.*, 1989). Mineral deposits are associated with Late Triassic to Early Jurassic, Middle to Late Cretaceous and Eocene granitic intrusions (Carter, 1981). The most economically important exploration targets are porphyry copper and molybdenum deposits and related mesothermal and epithermal precious metal veins. A few small massive sulphide occurrences have also been discovered.

TECTONIC HISTORY

The geologic history of the project area can be traced from Early to Middle Jurassic time when the area was part

of the regionally extensive Hazelton calcalkaline island arc. From late Middle Jurassic to Early Cretaceous time thick deposits of molasse derived from an uplifted Skeena arch and Omineca crystalline belt were deposited in fault-controlled basins. A major plate collision in Middle Cretaceous time resulted in uplift of the Coast Range and extensive folding of rocks to the east. Debris was shed eastward across the area from the rising metamorphic-plutonic complex and this was followed by the growth of a north-trending Andean-type volcanic arc in Middle to Late Cretaceous time. A transtensional tectonic regime in Late Cretaceous to Early Tertiary time produced the basin-and-range geomorphology that controls the current pattern of the map area. The latest tectonic event appears to be northeast shearing and tilting of fault blocks to the southeast. This shearing has offset earlier northwest-trending grabens and horsts (MacIntyre *et al.*, 1989).

LITHOSTRATIGRAPHY OF THE STUDY AREA

The generalized geology of the Lamprey Creek area is shown in Figure 1-11-2. In this area Early Jurassic to Tertiary volcanic and sedimentary rocks are preserved in a series of north-trending grabens and horsts. The youngest rocks are Miocene and crop out as a northwest-trending ridge east of Nanika Mountain. Tertiary sediments are preserved within the north-trending Thautil River graben which follows the southern reaches of the Thautil River and continues south to the Morice River. Inliers of Eocene Ootsa Lake

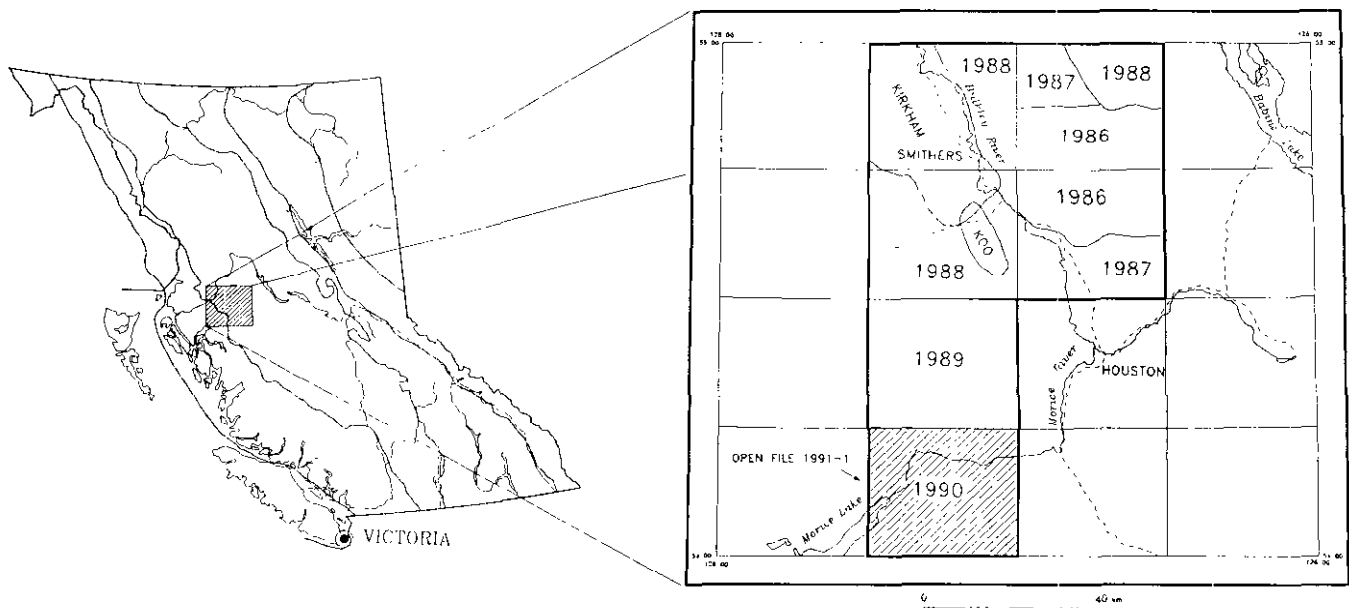


Figure 1-11-1. Location of the Lamprey Creek map sheet, (NTS 93L/3) relative to the area covered by the Babine and Telkwa projects to date.

LAYERED ROCKS

EOCENE TO OLIGOCENE

ENDAKO GROUP

EO_B

Buck Creek volcanics: basalt flows (olivine-phyric), columnar-jointed, amygdaloidal basalt, breccia

PALEOCENE TO EOCENE

PE_s

Thaultil River sediments: heterolithic, poorly sorted conglomerate, sandstone, siltstone, minor coal, wood fragments; biotite-phyric Ootsa Lake clasts

OOTSALA LAKE GROUP

EO

rhyolite to dacite flows and tuffs, layered, light grey, pink to chalky white, typically biotite-phyric, flow banded; local basalt flows; felsic biotite bearing lapilli, crystal and lithic tuff; minor breccia

UPPER CRETACEOUS

KASALKA GROUP

uKK

hornblende-feldspar and hornblende-biotite-feldspar porphyry flows; lapilli and crystal tuff; lahar of andesitic composition

LOWER CRETACEOUS (ALBIAN)

SKEENA GROUP

IK_s

sandstone, siltstone, shale, micaceous greywacke, coal bearing

IK_v

Mount Ney volcanics: andesitic flows, grey, porphyritic, thin platy plagioclase, amygdaloidal

LOWER JURASSIC (SINEMURIAN TO TOARCIAN)

HAZELTON GROUP

IJT

Telikwa Formation: undivided andesite, dacite, rhyolite, basalt, flows and pyroclastics

IJT_d

Shallow marine sedimentary unit: well-bedded limestone, calcareous sandstone, siltstone; interbedded with epiclastics and air-fall tuff; fossiliferous; may be early facies of Nikitkwa Formation

IJT_c

Siliceous pyroclastic facies: well-bedded quartz-feldspar-phyric ash flows, ignimbrite, breccia, siliceous air-fall tuff, red tuff, basalt, rhyolite flows.

IJT_b

Basaltic flow facies: massive maroon to green augite-feldspar-phyric to aphyric basalt flows; minor maroon tuff between flows; flow-top breccia common; locally amygdaloidal

IJT_a

Andesitic pyroclastic facies: andesitic air-fall tuff, breccia, feldspathic epiclastics, minor welded lapilli tuff

INTRUSIVE ROCKS

EOCENE

Erh

Rhyolite intrusions: biotite-phyric felsic intrusives

En

Nanika intrusions: porphyritic quartz monzonite, hornblende-quartz-biotite-feldspar porphyry

LATE CRETACEOUS

Kg

Bulkley intrusions: gr - undivided granitic intrusions; gd - granodiorite; dr - diorite; th - rhyolite; fp - feldspar porphyry; hbqfp - hornblende-biotite-quartz-feldspar porphyry; qm - quartz monzonite

EARLY JURASSIC

eJt

Topley intrusions: undivided granitic intrusions

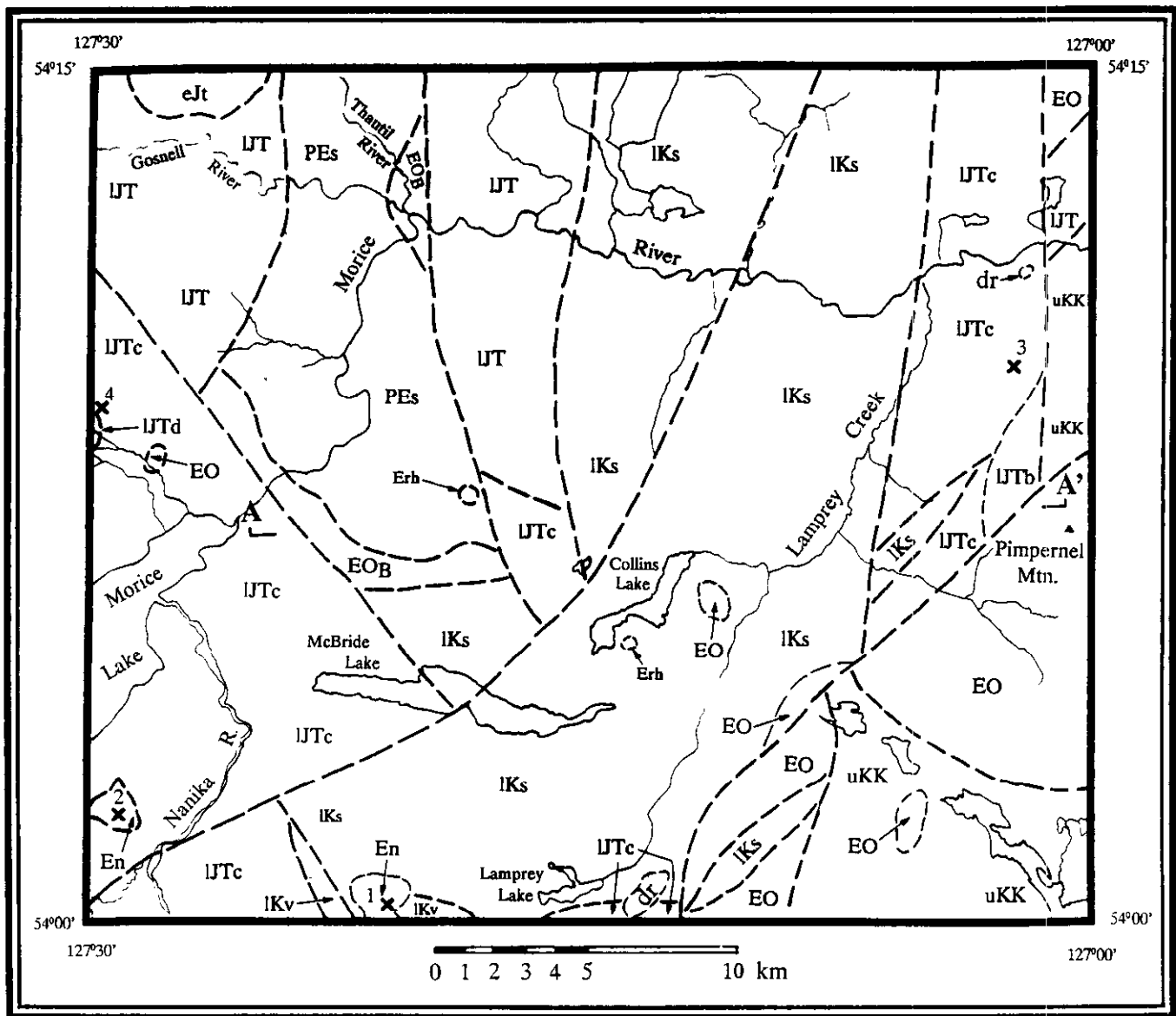


Figure 1-11-2. General geology of the Lamprey Creek area, (NTS 93L/3).

OCCURRENCE	NAME	MINFILE NO.
1	King	052
2	Lucky Ship	053
3	Hagas	221
4	Fire Lookout	309

volcanics occur in the southeast part of the map area where they overlie Upper Cretaceous Kasalka Group volcanic rocks. Similar relationships occur northeast of Morice Lake. Lower Cretaceous sediments are exposed in the Chisholm Lake area and extend to the area south of McBride Lake. Lower Jurassic volcanics crop out on the eastern border and southwest corner of the map area, and just east and south of Morice River. A generalized stratigraphic column is shown in Figure 1-11-3.

HAZELTON GROUP

The Hazelton Group (Leach, 1910) is a calcalkaline island-arc assemblage that evolved in Early to Middle Jurassic time. Tipper and Richards (1976) divide the group into three major formations in the Smithers map area (93L). These are the Sinemurian to early Pliensbachian Telkwa Formation, the early Pliensbachian to middle Toarcian Nilkitkwa Formation and the middle Toarcian to early Callovian Smithers Formation. Only the Telkwa Formation is found in the Lamprey Creek map area.

TELKWA FORMATION

In the Telkwa Range north of the study area, a thick section of Early Jurassic volcanic rocks constitutes the type area for the Telkwa Formation of the Hazelton Group (Tipper and Richards, 1976; Desjardins *et al.*, 1990). Here the

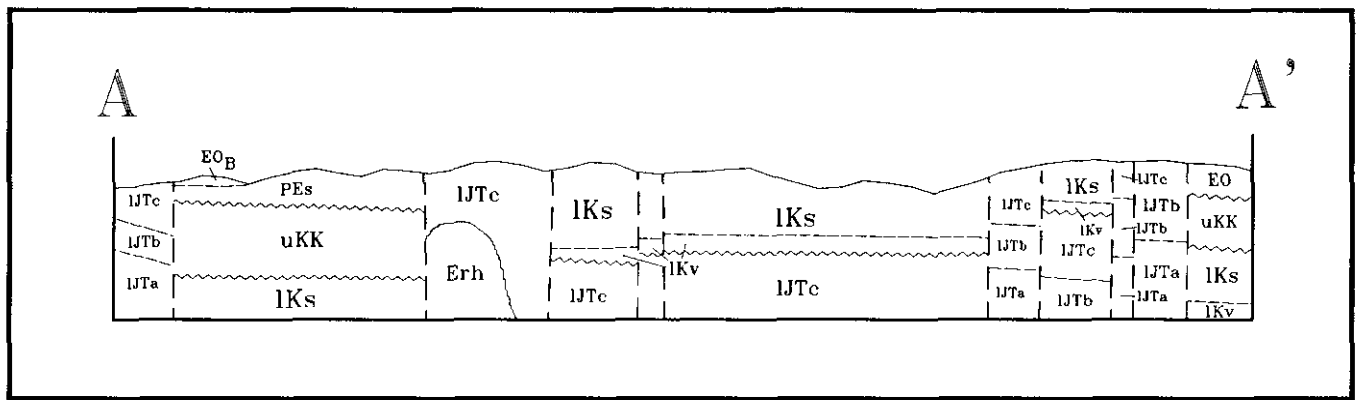


Figure 1-11-3. Cross-section showing typical structural style of the map area. See Figure 1-11-2 for location of section.

formation is predominantly subaerial and is mainly Sinemurian or older.

Mapping in the Telkwa range (Desjardins *et al.*, 1990) suggests the Telkwa Formation (IJT) is divisible into five major lithostratigraphic units, each representing distinct cycles of arc volcanism. These units are characterized by their predominant lithologies although internal facies variations are common. In ascending stratigraphic order they are: an andesitic pyroclastic unit comprised of thick-bedded, massive, maroon andesitic lapilli, crystal and ash tuffs with minor interbeds of siliceous, banded ash flows and grey, welded lapilli tuffs; a flow unit which is predominantly massive, cliff-forming, augite-feldspar-phyric to aphyric, dark green to maroon basalt; a siliceous pyroclastic unit that is well bedded and includes felsic epiclastics, welded lapilli tuffs, flow-banded ash flows, feldspathic breccias, pebble conglomerates, lahars, sandstones, air-fall lapilli and crystal-lithic tuffs; a marine sedimentary unit characterized by well-bedded, near-shore, fossiliferous limy sandstone, siltstone, conglomerate, grey bioclastic and massive limestone; and a recessive unit of well-bedded maroon to red crystal, lapilli and ash tuff and associated epiclastics with lesser flows of amygdaloidal augite-feldspar-phyric basalt. A similar stratigraphic sequence underlies the Middle Jurassic Smithers and Ashman formations on Ashman Ridge, 85 kilometres northwest of the map area. Only the siliceous pyroclastic (IJTc) and marine sedimentary (IJTd) units are recognized in the study area; other units of the Telkwa Formation are missing or not exposed.

SILICEOUS PYROCLASTIC UNIT (IJTc)

Well-bedded lapilli tuffs, with lesser breccias and flows occur throughout the map area. This unit is typically well bedded and consists of a mixture of maroon and green lapilli tuffs, grey welded crystal and lapilli tuffs, minor feldspar-phyric flows, and minor green and maroon feldspathic volcanic-clast breccias. The siliceous pyroclastic unit is widespread within the Lamprey Creek map area but its thickness is unknown. Tuff breccias consisting mainly of angular felsic, minor irregular-shaped feldspar-phyric andesite and basalt clasts crop out north of McBride Lake. White-weathering, fine-grained angular rhyolite clasts up to 30 centimetres long, occur locally. Heterolithic lapilli tuffs

with mainly felsic, minor maroon or green basalt and flow-banded clasts are also exposed. Minor augite-feldspar-phyric basalt flows occur here as well. Maroon lapilli tuffs with quartz crystal fragments are exposed just northwest of Tableland Mountain.

MARINE SEDIMENTARY UNIT (IJTd)

Marine sedimentary strata with graded bedding and ripple marks are exposed near the top of Nanika Mountain, on the western margin of the map area. These rocks stratigraphically overlie and are in part interfingering with well-bedded siliceous pyroclastic rocks.

These sedimentary rocks are probably equivalent to the Sinemurian marine sedimentary unit (IJTd) recognized in the Telkwa Mountains north of the map area (Desjardins *et al.*, 1990).

AGE OF THE TELKWA FORMATION

The Telkwa Formation is Sinemurian or older based on sporadic fossil fauna within the stratigraphic succession (Tipper and Richards, 1976). In the map area, which covers part of the Skeena arch, the granitic Topley intrusions cut the Telkwa Formation. These intrusions give K-Ar ages between 195 and 205 Ma (Carter, 1981). This is further evidence that the formation is predominantly Sinemurian or older. Fossils collected from the marine sedimentary unit (IJTd) in the Thautil River map area are early Sinemurian to early Pliensbachian in age (Desjardins *et al.*, 1990). No fossils were found in the study area, however.

MOUNT NEY VOLCANICS

In the Tahtsa Lake area amygdaloidal basalts conformably underlie Early Cretaceous marine turbidites of the Skeena Group (MacIntyre, 1985). These volcanics are well exposed on the east flank of Mount Ney and the name Mount Ney volcanics has been proposed. Rocks correlative with this unit were mapped by Diakow and Drobe (1989) in the northern half of the Newcombe Lake map area where they crop out on the north flank of Tableland Mountain. Here the characteristic lithology is an augite-feldspar-phyric basalt. This rock is dark green in colour and contains 10 to 15 per cent feldspar laths between 1 to 3 millimetres long.

Chlorite-altered augite crystals are 3 millimetres long and comprise 2 per cent of the rock. The rock is amygdaloidal and slightly magnetic.

SKEENA GROUP

The Skeena Group (Leach, 1910) comprises interbedded marine and nonmarine sedimentary strata of an Early Cretaceous successor basin. West of Telkwa these rocks unconformably overlie the Telkwa Formation and contain important coal seams (Koo, 1984). The coal seams occur in upward-fining fluvial clastic sequences of conglomerate, sandstone, siltstone and mudstone.

Strata of the Skeena Group crop out in the middle of the map area from north of Chisholm Lake to south of McBride Lake. Here lithologies include massive sandstone, conglomerate, minor mudstone and siltstone. The predominant lithology is a fine-grained, equigranular, massive, blocky weathering sandstone. It is micaceous, commonly has concretions ranging from 4 to 30 centimetres in diameter, and weathers reddish brown. Crossbedding and wisps of organic matter occur locally, particularly north of McBride Lake. Elsewhere in the region, this unit contains Albian macrofossils, although fossils were not found in the study area.

Probable Early Cretaceous conglomerates crop out in a west-flowing tributary of Lamprey Creek approximately 3 kilometres north of Pimpnel Creek. The clasts in the

pebble conglomerate are mainly feldspar-phyric andesite and siltstone averaging 8 centimetres across. The rock is clast-supported with a sandy matrix. Medium-grained, green micaceous sandstone crops out in the central area. This rock, which has an exfoliation weathering style, also contains concretions 4 to 30 centimetres in diameter. Minor mudstone, siltstone, and well-jointed micaceous sandstone with organic wisps paralleling bedding are exposed in the same area.

UPPER CRETACEOUS KASALKA GROUP

The Kasalka Group is an informal name proposed by MacIntyre (1976) for an Upper Cretaceous volcanic succession that unconformably overlies the Skeena Group in the Tahtsa Lake area. The succession varies from early silicic to late mafic eruptive rocks that collectively represent a cauldron-forming eruptive cycle. Rocks lithologically similar to the Kasalka Group occur in the Tagetochlain Lake area of the Newcombe Lake map sheet where a comagmatic intrusion has been dated at 85 Ma (Diakow and Drobe, 1989). These same volcanics extend northward into the southeast corner of the Lamprey Creek map area. There are also small inliers north of McBride Lake and on Nanika Mountain.

The main Kasalka Group lithologies in the map area are porphyritic andesite, lapilli tuff, breccia, and crystal tuff. In



Plate 1-11-1. View looking east near Tagetochlain Lake. The white-weathering unit is bedded rhyolite flows of the Ootsa Lake Group.

the Tagetochlain Lake area, the flows are hornblende-biotite-feldspar-porphyrific andesites containing 15 to 40 per cent feldspar phenocrysts (4 to 15 millimetres) and 5 per cent hornblende plus or minus biotite phenocrysts (1 to 2 millimetres). Quartz-biotite-feldspar-phyric andesite flows, maroon crystal-lapilli tuffs containing irregular shaped angular volcanic clasts and feldspar crystal fragments, and tuff breccias with irregular shaped volcanic clasts are also present.

OOTSALAKE GROUP

The Ootsa Lake Group (Duffell, 1959) is a succession of continental calcalkaline volcanic rocks and less abundant sedimentary rocks. Recent mapping has recognized six lithologic divisions in the Whitesail Lake area. The volcanic members are differentiated andesites, dacites and rhyolites. The dacites and rhyolites are sporadic, extrusive flow and flow-breccia dome complexes while the andesite flows and tuffs are more extensive. Several dates determined in the Whitesail Lake area constrain the timing of volcanic eruptions. The Ootsa Lake volcanics erupted 50 million years ago for a period of 1 million years (Diakow and Mihalynuk, 1987). The volcanic succession is capped by a polymitic conglomerate similar to the one that crops out in the Thautil River graben on the Lamprey Creek map sheet.

Small inliers of predominantly flat-lying rhyolitic flows crop out in the Lamprey Creek area (Plate 1-11-1). These rocks are correlated with the Eocene Ootsa Lake Group based on lithology. Biotite-phyric rhyolite, biotite-feldspar-quartz-phyric dacite, feldspar-hornblende-phyric rhyolite, flow-banded rhyolite, rhyolitic tuff and dacitic tuff are exposed in the southeast corner of the map area. Purple welded rhyolite with biotite phenocrysts crops out just north of Tagetochlain Lake. Feldspar-phyric andesite with variable biotite phenocrysts occurs locally. This rock usually has a fine foliated texture. Feldspar-quartz-phyric dacite with minor biotite phenocrysts is common just south of Pimpernel Mountain.

Flow-banded feldspar-phyric rhyolite, biotite-phyric rhyolite and rhyolite tuffs crop out in the area near the head of Pimpernel Creek. The rhyolite has less than 1 per cent feldspar phenocrysts that are aligned parallel to the flow direction. This rock locally contains minor quartz crystals. Rhyolite flows may also contain up to 2 per cent biotite phenocrysts. Locally the flows are columnar jointed and bedded. The rhyolite tuff has 30 to 40 per cent subangular fragments ranging from 1 to 4 millimetres in length.

A dull greyish white dacitic tuff, with minor aligned hornblende crystal fragments, is exposed in the Tagetochlain Lake area. Dull grey to chalky white, well-banded feldspar-hornblende-phyric rhyolite crops out near Lamprey Lake.

Tuffs with felsic clasts and biotite crystal fragments are exposed east of Lamprey Creek and are also mapped as part of the Ootsa Lake Group. These rocks are locally strongly fractured and brecciated with minor jasper occurring between clasts. Biotite-feldspar-porphyrific andesite with chalcedonic veins and veinlets crops out north of McBride Lake.

PALEOCENE TO EOCENE THAUTIL RIVER SEDIMENTS

Interbedded pebble conglomerate, sandstone and siltstone, with minor coal seams, crop out in the northwest quadrant of the map area, within the Thautil River graben. These rocks are correlated with the Paleocene to Eocene Thautil River sediments described in a previous report (Desjardins *et al.*, 1990). Exposures include a clast-supported heterolithic pebble conglomerate north of McBride Lake. Here clasts are feldspar-phyric andesite, amygdaloidal andesite, biotite-hornblende-feldspar-phyric andesite, maroon and red volcanics, and sandstone. Clasts range from 2 to 20 centimetres across, averaging 6 centimetres; the matrix is green sandstone. Semiconsolidated, clast-supported, heterolithic conglomerates with a fine to medium-grained, dirty sandstone to mudstone matrix crop out west of Morice River. Clasts are well rounded, range from 2 to 20 centimetres across and make up 60 to 75 per cent of the rock. Lithologies include trachyte with feldspar laths 2 to 6 millimetres long; biotite-phyric felsic intrusive; diorite; quartz-feldspar crystal tuff and green medium-grained sandstone. Well-bedded fine-grained black to dark green shale underlies the conglomerate. Bedding is laminar and defined by wispy partings. Wood fragments occur locally.

Lithologies similar to the Thautil River sediments also crop out in Gosnell River. Here beds of bright green to turquoise, medium-grained sandstone and medium-grained well-fractured siltstone, 30 to 50 centimetres thick, contain wood fragments, particularly near the top of the unit. Sandstone is interbedded with siltstone and laminar-bedded mudstone. The sandstone and siltstone beds are 50 centimetres thick. This unit is overlain by a thick bed of pebble conglomerate. The conglomerate contains lapilli tuff, augite porphyry, basalt, maroon tuff and sandstone clasts. A layer of coal 25 centimetres thick overlies an organic-rich mudstone.

Conglomerates in the Thautil River area contain 40 to 50 per cent clasts of mafic, biotite or hornblende-feldspar-phyric flows, ranging from 1 to 3 centimetres in diameter; feldspar-phyric, very magnetic basalt clasts, 2 to 8 centimetres in length; 10 to 15 per cent micaceous sandstone; and 2 to 5 per cent wood fragments. There are minor clasts of chlorite and calcite-filled amygdaloidal basalt. The matrix is coarse grained, grey, green and white. Locally 1 to 2-metre beds of medium to coarse-grained arkosic sandstone are interbedded in the conglomerate. The sandstone is mottled olive-green to white on fresh surfaces. Interbedded conglomerate, sandstone, siltstone, and very thin coal partings contain abundant wood fragments.

Some of the clasts in Thautil River conglomerates are tentatively recognized as specific older lithologies. Micaceous sandstone clasts are most likely from the Skeena Group; feldspar-phyric andesite clasts are probably from the Upper Cretaceous Kasalka Group.

BUCK CREEK VOLCANICS

Inliers of fine-grained dark green to black basalt crop out east of Nanika Mountain and in the Thautil River graben.

Type 2 showings in the Smithers area are preferentially associated with the upper facies of the Telkwa Formation and the overlying Nilkitkwa Formation. In the Lamprey Creek map area showings are generally small and isolated. This results from the sparse outcrop and the scarcity of exposed upper Telkwa facies or Nilkitkwa Formation. Porphyry deposits are confined to intrusions of Late Cretaceous and Early Tertiary age and adjacent hornfelsed country rocks.

KING (MINFILE 93L 052)

A plagioclase biotite porphyry intrudes and has hornfelsed sediments of the Skeena Group. Disseminated and fracture-filling molybdenite, chalcopyrite and pyrite (as pyritohedrons) are hosted by the pervasively silicified porphyry. A narrow shear zone trending northwest and dipping moderately to the northeast carries little mineralization. A breccia zone is reported to host arsenopyrite, pyrite and pyrrhotite (Helgesen, 1969).

LUCKY SHIP (MINFILE 93L 053)

The Lucky Ship prospect is located on a ridge between Morice Lake and the mouth of the Nanika River. It has been described by Sutherland Brown (1966) and Carter (1981).

The Lucky Ship stock cuts and has hornfelsed lapilli tuffs of the siliceous pyroclastic facies (IJTc) of the Telkwa Formation. The stock, like most other Nanika intrusions, is a multiphase body and has two porphyry and two breccia phases. Most of the plug is a white aphanitic rock with sparse quartz and feldspar phenocrysts. The other porphyry is unaltered, light grey and has abundant feldspar, quartz and biotite phenocrysts. One breccia is comprised largely of fragments of the first porphyry, with some exotic fragments. The other breccia is homogeneous and composed of variably sized fragments of the first porphyry. The four phases do not necessarily represent unique intrusions or episodes and age relationships are uncertain (Sutherland Brown, 1966). Molybdenite mineralization is associated with the initial phase, but appears to have been overprinted by a later, unmineralized rhyolite porphyry phase. Sulphides are concentrated in an annular zone of intense silicification and quartz veining around the later stage quartz monzonite porphyry plug.

The prospect is marked by an extensive gossanous zone resulting from the oxidation of pyrite and chalcopyrite. Sulphides comprise 2 to 10 per cent of some samples, but appear to be preferentially concentrated in the more intermediate phases of the rhyolite breccia. This zone has undergone phyllic and minor propylitic alteration and silicification.

Mafic phases occur as dikes and have also been subjected to intense silicification. The dikes follow the dominant northeasterly structural trend. Sulphide mineralization, associated with the mafic phases occurs in a stockwork of quartz veins which cut earlier, unmineralized quartz veins.

A K-Ar whole-rock date on a biotite hornfels sample from the Lucky Ship deposit yielded an age of 49.9 ± 2.3 Ma

(Carter, 1981). This date corresponds well with whole-rock ages obtained from other Nanika intrusions in the Smithers area and the age of the Lucky Ship intrusion may be inferred from this. The age of mineralization is believed to be contemporaneous or slightly younger than the age of intrusion.

HAGAS (MINFILE 93L 221)

Quartz stringers and fractures within propylitically and argillically altered maroon tuffs of the siliceous pyroclastic facies (IJTc) contain chalcopyrite, sphalerite and minor native copper. These shear zones trend east and dip steeply to the south. Malachite staining is associated with a silicified and propylitically altered gabbroic body. Follow-up trenching exposed an extensive gossanous zone, but little sulphide mineralization.

FIRE LOOKOUT (MINFILE 93L 309)

Malachite staining, discovered during the 1990 field season, is extensive in a small gossanous zone and appears to follow bedding in the siliceous pyroclastic facies of the Telkwa Formation (IJTc). Bedding in the maroon lapilli tuffs strikes easterly and dips moderately to the south. A prominent east-trending, north-dipping joint set may have acted as the conduit for mineralizing fluids. Augite-bearing basalt is also present and has been extensively altered to carbonate. No significant veining was noted.

SUMMARY

Conclusions based on this field season's work are:

- North-trending horst-and-graben structures, such as the Thautil River graben, characterize the study area.
- Clasts of Skeena Group and Kasalka Group in the Thautil River conglomerate suggest these sediments are Tertiary in age.
- Ootsa Lake Group volcanics are present and overlie the Kasalka Group.
- The siliceous pyroclastic unit (IJTc) of the Telkwa Formation is more felsic in the Lamprey Creek area than it is to the north.
- Kasalka Group volcanics mapped by Diakow and Drobe (1989) in the northeast corner of the Newcombe Lake map area extend northward into the Lamprey Creek area. This unit has been informally named the Pimpernel Mountain volcanics.

ACKNOWLEDGMENTS

The authors would like to acknowledge Dr. T.A. Richards and Dr. L.J. Diakow for informative discussions; Victor Koyanagi for his contribution in the field; Clayton Brown ably assisted the authors during the course of fieldwork.

REFERENCES

- Carter, N.C. (1981): Porphyry Copper and Molybdenum Deposits West-central British Columbia; *B.C. Ministry of Energy, Mines and Petroleum Resources*, Bulletin 64, 150 pages.

- Desjardins, P.J., MacIntyre, D.G., Hunt, J., Lyons, L. and Pattenden S. (1990): Geology of the Thautil River Map Area; *B.C. Ministry of Energy, Mines and Petroleum Resources*, Geological Fieldwork 1989, Paper 1990-1, pages 91-99.
- Diakow, L.J. and Drobe, J. (1989): Geology and Mineral Occurrences in North Newcombe Lake Map Sheet; *B.C. Ministry of Energy, Mines and Petroleum Resources*, Geological Fieldwork 1988, Paper 1989-1, pages 183-188.
- Diakow, L.J. and Mihalynuk, M. (1987): Geology of the Whitesail Reach and Troitsa Lake Areas; *B.C. Ministry of Energy, Mines and Petroleum Resources*, Geological Fieldwork 1986, Paper 1987-1, pages 171-179.
- Duffell, S. (1959): Whitesail Lake Map-area, British Columbia; *Geological Survey of Canada*, Memoir 299, 119 pages.
- Helgesen, D.H. (1969): Geochemical Report on the King, Queen, Jack, Pine, PI and Squeek Mineral Claims, Lamprey Lake, B.C.; *B.C. Ministry of Energy, Mines and Petroleum Resources*, Assessment Report 1809, 6 pages.
- Koo, J. (1984): The Telkwa, Red Rose, and Klappan Coal Measures in Northwestern British Columbia; *B.C. Ministry of Energy, Mines and Petroleum Resources*, Geological Fieldwork 1983, Paper 1984-1, pages 81-90.
- Leach, W.W. (1910): The Skeena River District; *Geological Survey of Canada*, Summary Report, 1909.
- MacIntyre, D.G. (1976): Evolution of Upper Cretaceous Volcanic and Plutonic Centres and Associated Porphyry Copper Occurrences, Tahtsa Lake Area, British Columbia; unpublished Ph.D. thesis, *University of Western Ontario*, 149 pages.
- MacIntyre, D.G. (1985): Geology and Mineral Deposits of the Tahtsa Lake District, West-central British Columbia; *B.C. Ministry of Energy, Mines and Petroleum Resources*, Bulletin 75, 82 pages.
- MacIntyre, D.G., Brown, D., Desjardins, P. and Mallett, P. (1987): Babine Project (93L/10,15); *B.C. Ministry of Energy, Mines and Petroleum Resources*, Geological Fieldwork 1986, Paper 1987-1, pages 201-222.
- MacIntyre, D.G., Desjardins, P. and Tercier, P. (1989): Jurassic Stratigraphic Relationships in the Babine and Telkwa Ranges (93L/10, 11, 14, 15); *B.C. Ministry of Energy, Mines, and Petroleum Resources*, Geological Fieldwork 1989, Paper 1989-1, pages 195-208.
- Sutherland Brown A. (1966): Lucky Ship (Amax Exploration, Inc.); *B.C. Ministry of Energy, Mines and Petroleum Resources*, Annual Report 1965, pages 84-87.
- Tipper, H.W. and Richards, T.A. (1976): Jurassic Stratigraphy and History of North-central British Columbia; *Geological Survey of Canada*, Bulletin 270, 73 pages

NOTES



**STRUCTURE OF THE TAKLA GROUP EAST OF THE
FINLAY-INGENIKA FAULT, McCONNELL CREEK AREA,
NORTH-CENTRAL B.C.
(94D/8, 9)**

**By G. Zhang and A. Hynes
McGill University**

KEYWORDS: Regional geology, Takla Group, Johanson Lake, stratigraphy, Darb Creek, Goldway Peak, Osilinka Ranges, Kliyul Creek, Dortatelle Creek, Wrede Range, transcurrent faulting, rotational structure.

INTRODUCTION

The study area is located northwest and south of Johanson Lake, bounded to the northeast by the northwest-trending Lay fault and to the west by the north-northwest-trending Finlay-Ingenika fault. The Finlay-Ingenika fault is a dextral transcurrent fault, and is part of the very prominent strike-slip fault system in north-central British Columbia (Gabrielse, 1985). This project was undertaken to examine the structures on the east side of the Finlay-Ingenika fault, to provide geological evidence for the dextral transcurrent displacement and to study local deformation associated with it.

This report summarizes the results of 1:50 000-scale geological mapping in July and August 1990 in parts of map sheets 94D/8 and 94D/9. Fieldwork concentrated on stratigraphic and structural relationships.

GEOLOGICAL SETTING

The study area is in the Intermontane Belt of Monger (1984), and forms part of the Quesnellia tectonostratigraphic terrane. North and south of the study area, rocks of Quesnellia are separated from Stikinia rocks to the west by the Cache Creek Terrane, which is generally regarded as a subduction-related assemblage. These terranes were amalgamated by latest Triassic to earliest Jurassic time, to form a large, composite terrane, Terrane I, that accreted to the ancient margin of North America in Jurassic time (Monger, 1984). There is widespread evidence of dextral transcurrent motion of Terrane I, and possibly part of the Omineca metamorphic belt, during the late Cretaceous (Gabrielse, 1985) and some workers have advocated as much as 2400 kilometres of transport (*e.g.* Umhoefer, 1987). The Finlay-Ingenika fault, the boundary between Quesnellia and Stikinia in the project area, is one of the system of dextral strike-slip faults on which the motion occurred.

The area is underlain predominantly by Upper Triassic Takla Group volcanic, volcanoclastic and sedimentary rocks. West of the Finlay-Ingenika fault the Takla Group was subdivided during 1:250 000 mapping of the McConnell Creek map area (Lord, 1948; Church, 1974, 1975; Richards, 1976a, b; Monger, 1977) into a lower Dewar Formation

consisting of volcanic sandstone, siltstone and black argillite, a middle Savage Mountain Formation of dark grey-green basalt, volcanic breccia and siltstone and an upper Moosevale Formation, consisting of red and green or reddish grey marine and nonmarine volcanoclastics together with intermediate alkaline feldspar porphyry (Monger, 1977). Takla Group east of the Finlay-Ingenika fault remains undivided. It is dominated by grey green, dark and pale grey volcanic breccia, sandstone and siltstone, interbedded with minor augite and feldspar-porphyrific lava flows, with minor black argillite and dark grey and purplish grey limestone. No conclusive stratigraphic correlations have been made between the Takla Group rocks on either side of the fault, and Minehan (1989b) has suggested that the rocks east of the fault should be assigned to a different group (Johanson Group) because they are geochemically very different (calcalkaline rather than alkaline) from the western Takla Group, despite their similar appearance.

LOCAL STRATIGRAPHY

The Takla Group east of the Finlay-Ingenika fault is predominantly volcanoclastic, with minor volcanic and sedimentary rocks. Stratigraphic successions and rock assemblages vary greatly from one locality to another. The stratigraphy and petrology are therefore described separately for three different regions of the map area: the northwest, southwest and southeast (Figure 1-12-1).

The stratigraphic succession in the Wrede Range in the northwest has been described by Bellefontaine and Minehan (1988) and Minehan (1989a, b). The typical stratigraphic section occurs within Minehan's (1989a) Block C. It attains thicknesses of up to 1800 metres and can be divided into four units (Figure 1-12-2a).

A lowest Unit 1 has a minimum thickness of about 800 metres but the base is not exposed. The lowest part of this unit is exposed along a small northeast-trending ridge in the south of the region and is dominated by dark green and greenish grey, massive volcanic breccia, sandstone and siltstone, together with minor clinopyroxene or plagioclase-porphyrific lava flows. The dark grey to greenish grey breccia is compositionally heterogeneous. There are crystals of plagioclase and clinopyroxene together with fragments of porphyry, volcanic sandstone and siltstone. The fragments are angular to subrounded, and average less than 10 centimetres in diameter. The breccias are poorly bedded and poorly sorted. The grey-green volcanic sandstone is com-

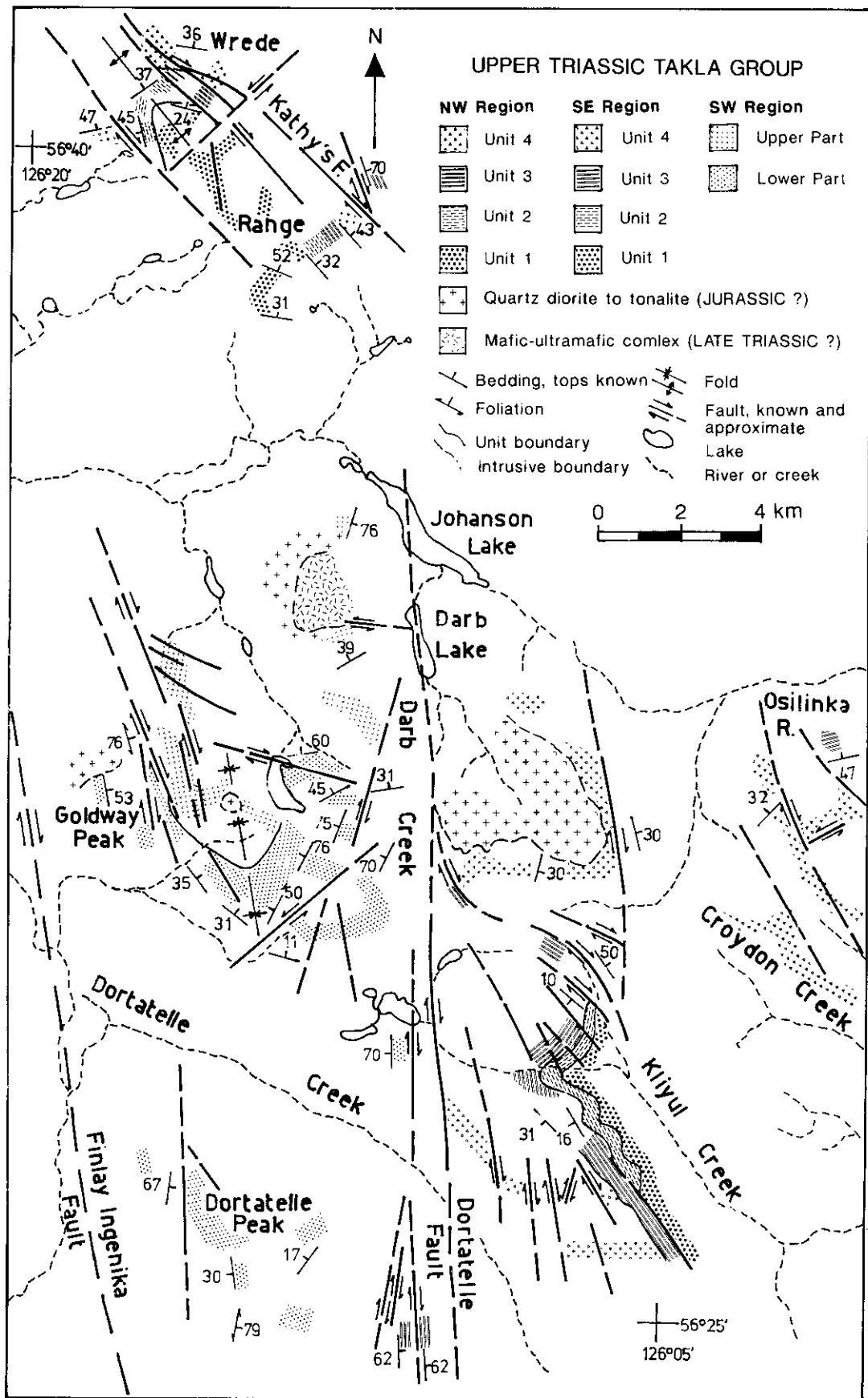


Figure 1-12-1. Generalized geology of the Johanson Lake area.

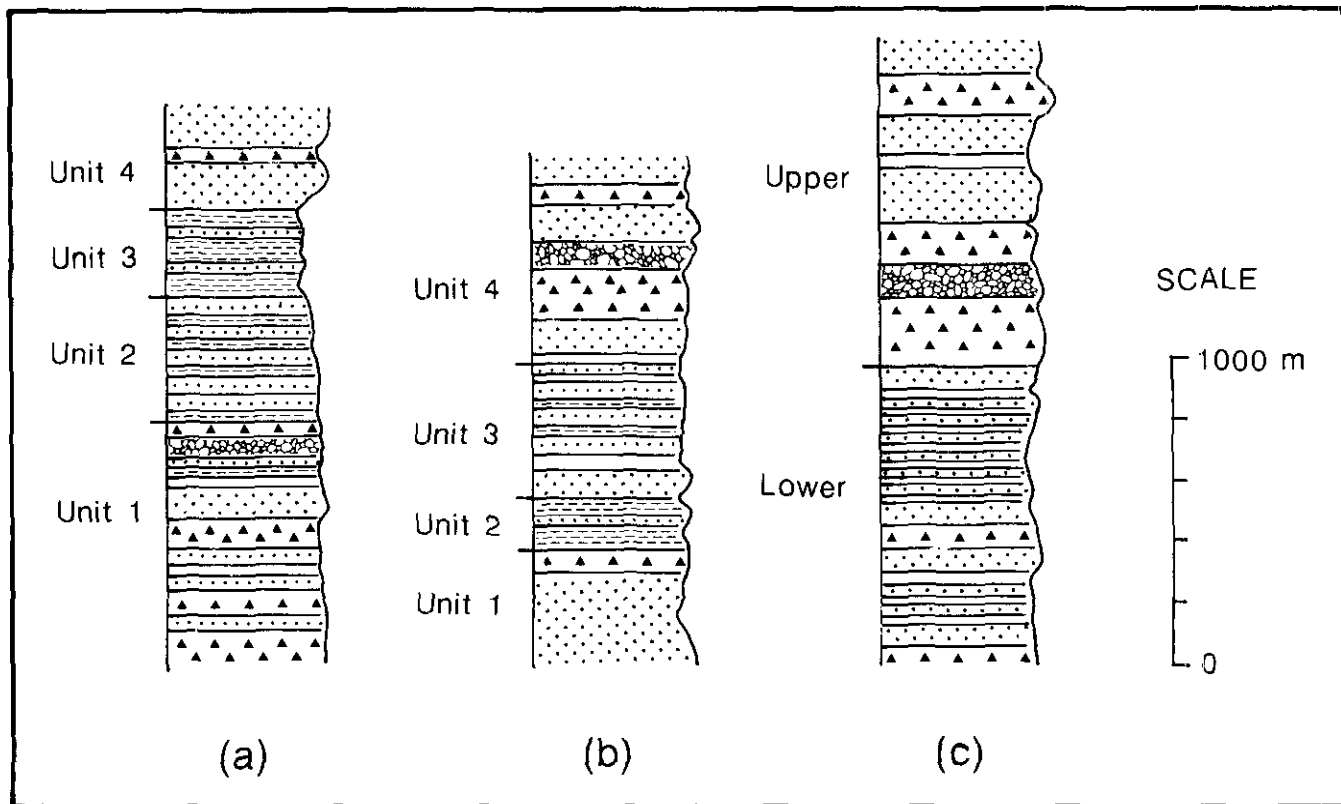


Figure 1-12-2. Generalized stratigraphic columns of Takla Group in the northwest (a) southeast (b) and southwest (c) regions. Triangles: volcanic breccia; dots: volcanic sandstone; horizontal lines: volcanic siltstones; dashed horizontal lines: black argillite and limestone; irregular circles: lava flows.

posed predominantly of plagioclase, amphibole and clinopyroxene crystals, with minor small lithic fragments similar to those in the breccia. It may occur as graded, upward-facing beds, typically 20 centimetres thick, or as massive units up to 300 metres thick. Volcanic siltstone is minor, greenish or pale grey, and commonly shows very fine, alternating dark and pale grey laminations, presumably reflecting alternation of clinopyroxene/amphibole and plagioclase-rich layers. Clinopyroxene and clinopyroxene-plagioclase-porphyrific flows are greenish grey, dark grey or dark purple and are characterized by equant euhedral clinopyroxene and anhedral plagioclase phenocrysts typically up to 5 millimetres long but locally as long as 1 centimetre. Commonly, clinopyroxene is fresh, dark green to pale greenish yellow and displays sector twinning and pseudodimetric shape in cross-section. These lava flows closely resemble the breccia in the field but are distinguished by the complete absence of fragmentation, even on the weathered surfaces.

The middle part of Unit 1, exposed on the col to the northeast, consists of greenish grey and pale grey volcanic sandstone and siltstone interbedded with black, reddish weathering, thin-layered argillite and purplish grey limestone with individual beds up to 30 centimetres thick. The upper part of Unit 1 consists of characteristically greenish grey, massive lava flows of clinopyroxene and clinopyrox-

ene plagioclase porphyry and volcanic sandstone. The flows contain fragments of purple limestone typically 10 to 20 centimetres and locally up to 2 metres in diameter. It is therefore likely that the lava flow disrupted the limestone of the middle part of the unit.

Unit 2, up to 400 metres thick, is well exposed along the northeast-trending ridge northeast of Unit 1. This unit is made up of greenish grey and pale grey, well-bedded volcanic sandstone and siltstone interbedded, with black, thin-layered argillite and marly limestone. The sedimentary rocks account for about 40 per cent of the unit and individual argillite beds are typically 2 centimetres thick. Toward the top of the unit sedimentary rocks become progressively more abundant.

Unit 3, a predominantly sedimentary package about 270 metres thick, consists mainly of black, reddish weathering, thin-layered argillite and dark grey or black, thin-layered, marly limestone. Thirty per cent of the unit is thick-bedded (40 to 50 cm), greenish grey and dark grey volcanic sandstone and siltstone.

Unit 4, the uppermost unit of the succession, is exposed on the highest peak in the southern part of the region. It is dominated by massive, greenish grey volcanic sandstones and has a minimum thickness of 300 metres. To the northeast this unit is cut by the northwest-trending Kathy's fault (Figure 1-12-1).

In the southeastern region, west of Kliyul Creek, four units are recognized and a minimum thickness of 1600 metres is estimated for the whole succession, although the estimate is imprecise because of widespread shearing and fault truncation at its top. Thicknesses of Units 2 and 3 have been well defined and measured (Figure 1-12-2b).

Unit 1, exposed along the west side of Kliyul Creek, is dominated by grey volcanic sandstone. Most of this unit is covered by vegetation and moraine but a minimum thickness of 400 metres can be estimated. The top of the unit contains abundant recessive clasts of carbonate.

Unit 2 is up to 170 metres thick, and consists mainly of black, reddish weathering argillite and dark grey or black, 2 to 10-centimetre layered limestone. The unit also contains minor interbedded, grey or greenish grey volcanic sandstone and siltstone. This unit extends to the south and is truncated by a northwest-trending fault which juxtaposes Unit 3 and Unit 1.

Unit 3, well exposed on the ridge west of the Kliyul Creek, consists of grey or greenish grey volcanic sandstone and siltstone interbedded with dark grey or black limestone and minor black argillite, and is up to 440 metres thick. The lower part is dominated by greenish grey volcanic siltstone which contains abundant fragments of dark grey or purplish, well-bedded limestone, ranging from several centimetres to several metres in diameter. The upper part is greenish grey or pale grey, medium-layered (10 to 20 cm) volcanic sandstone interbedded with dark grey or black, thin-layered limestone or argillite. These limestone beds are very widespread and are useful marker horizons in the region. At the top of the unit there is a thin-layered, fine-grained volcanic sandstone, which is the boundary between Units 3 and 4.

Unit 4 consists mainly of massive, greenish grey volcanic sandstone and breccia with minor siltstone and clinopyroxene porphyry and is well exposed in the western part of the region. Rocks of this unit are very resistant and commonly form high peaks and steep cliffs. In the west, near the Dortatelle fault (Monger, 1977), these rocks are sheared into protomylonite. Lineations defined by stretched mineral crystals and elongated breccia fragments are very common. Because of the intense shearing, the total thickness of the unit cannot be measured, but a minimum thickness of 600 metres is estimated.

The stratigraphic succession in the Osilinka Ranges, east of Johanson Lake (Figure 1-12-1), appears similar to that in the northwest, but exact correlations between them have not proved possible.

The Goldway Peak and Dortatelle Peak area (Figure 1-12-1), in the southwest, has a stratigraphic succession very different from that east of the Dortatelle fault. It is dominated by volcanics and volcanoclastics and can be divided into two parts. The lower part consists of greenish grey, thin-layered volcanic sandstone interbedded with pale grey, thin-layered volcanic sandstone and siltstone, commonly with individual bed thickness less than 2 centimetres. Nonvolcanic sedimentary rocks are rare, but are observed near the glacier southeast of Goldway Peak and on the eastern flank of Dortatelle Peak where there are small

amounts of thin-bedded (2 cm) dark grey or black limestone and argillite. The upper part consists of massive or poorly bedded, greenish grey volcanic sandstone and breccia with minor clinopyroxene porphyry. The breccias are polymictic and made up of predominantly subrounded fragments of volcanic sandstone and clinopyroxene porphyry. Thickness of this succession has not been measured but a minimum thickness of 2000 metres can be estimated (Figure 1-12-2c).

INTRUSIVE ROCKS

The upper Triassic Takla Group rocks are intruded by the Johanson Lake mafic-ultramafic complex, an Alaskan-type *intrusive complex* (Nixon and Hammack, 1990), the Darb Lake dioritic body which is located in the centre of the map area, and many intermediate to felsic dikes and sills, typically less than 3 metres wide. These intermediate to felsic rocks are probably related to the Hogen batholith and Jurassic to Cretaceous in age (Monger, 1977).

DEFORMATION

Rocks in the map area experienced deformation predominantly, and perhaps exclusively, associated with the dextral, transpressive displacement along the Finlay-Ingenika fault. This deformation is characterized by dextral strike-slip faults trending northwest, north-northwest and north-northeast, and sinistral strike-slip faults trending east-northeast. The faults cut the rocks into a number of fault-bounded, weakly deformed blocks, in which cleavages and small-scale shear zones are the only visible structures. These characteristics are typical of continental crustal deformation associated with large-scale transcurrent faulting (*e.g.* Nelson and Jones, 1986; Geissman *et al.*, 1989). There are also some large-scale, open to medium folds with axes trending northwest.

FOLDS

Two large-scale folds, an anticline and a syncline, have been recognized. The Wrede Range anticline, in the north-western region of the map area, has Unit 1 volcanics and volcanoclastics in its core and Unit 2 volcanoclastic and interbedded sedimentary rocks on the two limbs. Bedding attitudes measured in Unit 2 define a fold axis trending 325° and plunging 30°. Axial-surface cleavage is common on both limbs, especially in the Unit 2 argillitic beds. The anticline is truncated on both northeast and southwest sides by northwest-trending, dextral strike-slip faults.

The Goldway Peak syncline is exposed around Goldway Peak, in the southwestern region. The core of the syncline consists of the upper, massive volcanic breccia and sandstone and the limbs are dominated by the lower, well-bedded, thin-layered volcanic sandstone and siltstone. The fold-axis trends 340° and plunges 40°. On both limbs near the nose, secondary, outcrop-scale folds are well developed. They are either box-type or chevron folds. The east limb of the Goldway Peak syncline is truncated by a northwest-trending, dextral strike-slip fault and the strata have been rotated clockwise through about 30° due to drag on the fault.

In contrast, the west limb was sheared by north-northwest-trending dextral strike-slip faults, which are parallel to the bedding surface, leading to steep dips for the strata.

Small-scale folds are also common in the well-bedded, thin-layered units throughout the map area, especially in the Unit 3 thin-layered limestone interbedded with volcanic siltstone west of Kliyul Creek. Most folds have axial surfaces at small ($<45^\circ$) angles to the bedding surfaces and are probably due to bedding-parallel slip.

Timing of formation of the folds is uncertain. They pre-date the faults but may well have formed in the early stages of the dextral transpression (*cf.* Wilcox *et al.*, 1973; Sylvester, 1988).

FAULTS

Steeply dipping or vertical strike-slip faults are the most significant structural features in the map area. The faults may be divided into northwest, north-northwest, north-northeast and east-northeast-trending structures, which show different slip senses.

Northwest-trending faults are predominantly dextral and occur mainly in the Wrede Range and west of Kliyul Creek. In the Wrede Range, two northwest-trending faults cut the northeastern limb of the Wrede Range anticline and bring reddish sedimentary rocks of Unit 3 into contact with volcanic rocks of Units 1 and 4. These faults are well exposed to the northwest, where the volcanic rocks are sheared into protomylonite over a zone 20 metres wide. Drag folds and Riedel shears (Tchalenko, 1970; Sylvester, 1988) in the fault zone indicate dextral slip. By matching the offsets, a dextral displacement of 1 kilometre has been estimated along the faults. Some faults provide evidence of an early stage of dip-slip motion. For example, two sets of slickenlines are observed on the cleaved rock surfaces in a fault zone on Darb Creek near the Dortatelle fault. The earlier is dip-slip with a thrust sense, and the later is horizontal, dextral. These faults may originally have been thrust faults that were associated with the initiation of dextral displacement on the Finlay-Ingenika fault in the Ingenika valley west of the map area (*cf.* Sylvester, 1988).

North-northwest-trending faults are predominant in the southern part of the map area, and all show dextral displacement. The biggest and most obvious one is the Dortatelle fault. It extends 30 kilometres from north of Johanson Lake through Darb Creek to the south and is well exposed near the biggest lake north of Dortatelle Creek. Rocks in a fault zone 40 metres wide were sheared into protomylonite. In the mylonitic rocks kinematic indicators such as mylonitic foliation fish and S-C fabrics (Berthe *et al.*, 1979) are common (Plate 1-12-1c). Centimetre-scale drag folds, plunging steeply north-northwest, with axial planes striking northwest and dipping steeply northeast, are widespread. All the kinematic indicators are consistent with dextral strike-slip on the fault. To the south the fault passes through a col in which the volcanic rocks are mylonitic over a zone 50 metres wide. A fault-parallel, horizontal mineral-stretching lineation is very well developed, especially in the sheared clinopyroxene porphyry. A similar lineation is

defined elsewhere by elongated fragments of volcanic breccia (Plate 1-12-1b). In a fault east of the Darb Creek dioritic body, a quartz diorite dike is incorporated in the mylonitic zone, indicating that fault motion occurred after emplacement of the extensive dioritic plutons in the map area, *i.e.* during the Jurassic or later (Monger, 1977). Faults in this group are parallel to, and have the same slip senses as, the Finlay-Ingenika fault west of the map area. They are also better developed and more closely spaced approaching the major fault to the west. It is therefore inferred that they were formed as a result of the dextral transcurrent movement on the Finlay-Ingenika fault.

North-northeast-trending faults are not as common in the map area as those of the other two sets. This may be due to vegetation and moraine cover in north-northeast-trending valleys. Two large-scale, north-northeast trending faults were mapped on the ridges west of Darb Creek. They cut the lower part of the volcanic sandstone and are characterized by protomylonites, with a mineral-stretching lineation parallel to the fault strike. S-C structures in the mylonitic zone, which is up to 20 metres wide, indicate dextral movement. Another shear zone with the same trend was mapped on the ridge behind the glacier west of Kliyul Creek. The Unit 4 greenish clinopyroxene porphyry is sheared into a narrow (10 cm) mylonitic band, in which S-C structures show dextral slip. On the east wall there is a small rotational structure, characterized by a number of curved cleavage planes that project to the south and diverge towards and converge away from the shear zone (Plate 1-12-1d). They are approximately parallel to the mylonitic foliation and die out outside the shear zone. The rotational structure is therefore a local feature and was probably associated with dextral transpression. The attitudes and slip senses on this north-northeast trending fault set are consistent with their formation as Riedel shears (R) related to the main motion on the Finlay-Ingenika fault (*cf.* Tchalenko, 1970; Sylvester, 1988).

East-northeast-trending faults generally display sinistral displacement. Although faults of this group are not well developed, they were found at several places within the map area. One such fault lies in the valley west of Darb Creek and is inferred from stratigraphic relationships. A 750-metre sinistral displacement of the lower part of the thin-layered, greenish grey volcanic sandstone and pale grey volcanic siltstone unit is required to match stratigraphic offsets. Another fault, striking approximately east, was mapped within the Johanson Lake mafic-ultramafic block, west of Darb Creek. It is characterized by a mylonitic zone, about 1 metre wide, and the drag folds of mylonitic foliation show a sinistral strike-slip sense. Approaching the Dortatelle fault, this small fault, together with the fault-bounded block, has been rotated clockwise through 35° . Small east-northeast-trending shear zones are also present in the area. A mylonitic zone 40 centimetres wide, striking 055° , observed on the peak of the Osilinka Ranges in massive, greenish grey volcanoclastics, has S-C fabrics indicative of sinistral displacement. The east-northeast-trending faults may be conjugate to the north-northeast-trending set, reflecting the R' Riedel set (Tchalenko, 1970; Keller *et al.*, 1982; Sylvester,

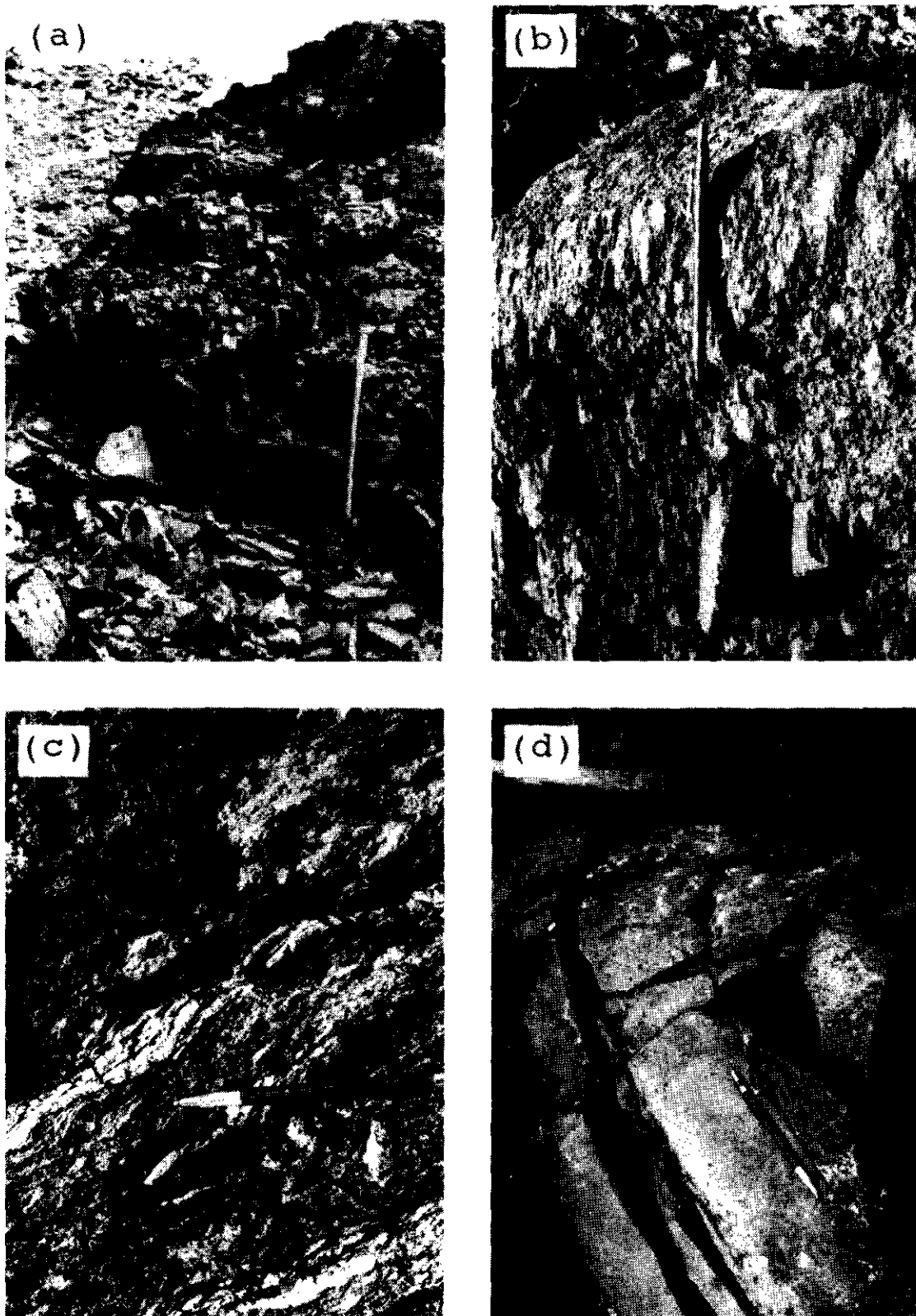


Plate 1-12 (a) Cleavage defined by closely spaced shear planes; (b) Lineation of stretched volcanic breccia in a north-northwest-trending, strike-slip fault; pencil parallel to the lineation, looking at north-northwest down; (c) S-C fabrics of the mylonitic rocks in Dortatelle fault, pencil parallel to the C planes, looking at south down; (d) Transpressive rotational structure consisting of curved cleavage planes; pencil parallel to the cleavage planes, hammer handle parallel to the small shear zone, looking at west down.

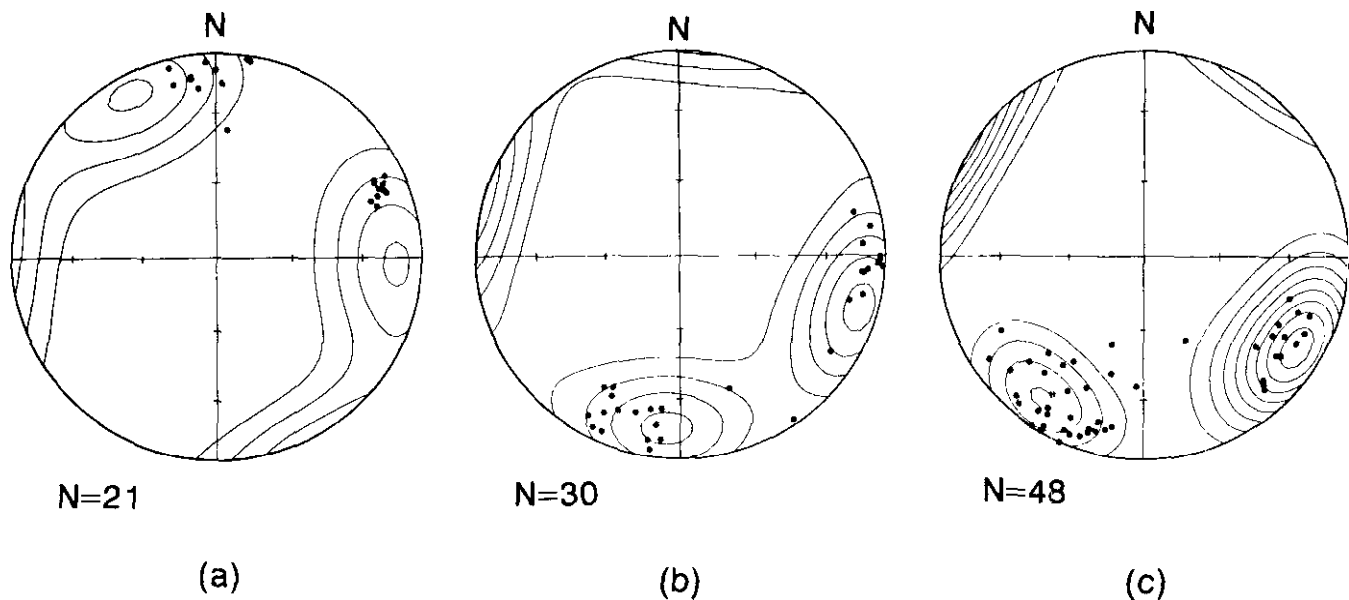


Figure 1-12-3. Stereonet plots of conjugate cleavages from the ridge north of Croydon Creek (a) the southern margin of Darb Creek dioritic body (b) and Goldway Peak (c). Solid circles: slickenlines; lines: contours of poles to the cleavages; N: number of cleavage planes measured.

1988) associated with faulting on the Finlay-Ingenika system.

All the faults, although they trend differently and have different slip senses, may be explained by association with the Finlay-Ingenika faulting. They cut the rocks into fault-bounded, weakly deformed blocks, ranging in size from several square kilometres to tens of square kilometres. With progressive displacement on the Finlay-Ingenika fault, deformation was apparently concentrated in the previously formed faults, while the fault-bounded blocks remained only very weakly deformed. Typically the only visible deformation outside the fault zones themselves is a cleavage and weak shear zones.

CLEAVAGE

Cleavage is extensively developed in the map area. It is characterized by spaced shear planes and in the cleaved rocks no apparent fabrics have been found. The shear planes are usually steeply dipping and closely spaced, at intervals of 2 to 10 centimetres (Plate 1-12-1a). They are commonly slickensides with slickenlines, and many are characterized by crystals of tremolite or patches of chlorite and epidote. Shear senses are evident from the slickenline steps and offset of such features as quartz veins or the conjugate cleavage. Most cleavage is regional but some is local in its distribution. The local cleavage is commonly associated with nearby faults and can be easily distinguished from the regional by tracing away from the fault. Regionally distributed cleavage generally occurs in conjugate sets trending north to north-northeast and east-northeast to east, although there is considerable variation. Assuming the regional cleavage was homogeneously distributed before the widespread faulting in this region, its

attitudes may be used to indicate the bulk rotation of fault-bounded blocks.

Several hundred shear planes were measured in the field, and a preliminary analysis (Figure 1-12-3) indicates significant variations between the three major fault blocks. On the ridge north of Croydon Creek two sets of conjugate cleavages trend north and east-northeast, respectively (Figure 1-12-3a), which are consistent with those caused by Finlay-Ingenika faulting. To the west, in the block near the southern margin of the Darb Creek dioritic body, they trend north-northeast and east, respectively (Figure 1-12-3b). Near the Finlay-Ingenika fault at Goldway Peak, they are oriented northeast and east-southeast, respectively (Figure 1-12-3c). Based on the above assumption, this variation of the orientations of the regional, conjugate cleavages indicates that the fault-bounded blocks have been rotated clockwise, and the amount of block rotation varies, reaching a maximum close to the Finlay-Ingenika fault.

CONCLUSIONS

The deformation observed in the Takla Group rocks east of the Finlay-Ingenika fault can therefore all be explained by dextral transcurrent motions on the Finlay-Ingenika fault. There is no compelling evidence for deformation associated with the collision of Quesnellia with Stikinia or of Terrane 1 with North America. During the early stages of deformation, folds with axes trending northwest, northwest-trending thrust faults and two sets of conjugate strike-slip faults, striking north-northeast and east-northeast, were formed, together with north-northwest-trending, secondary dextral strike-slip faults. These structures cut the Takla Group rocks into a number of fault-bounded, weakly deformed blocks. With progressive displacement on the

Finlay-Ingenika fault, deformation became concentrated in early-formed fault zones. The northwest-trending thrust faults may have been rotated and dextral strike-slip motion appears to have been superimposed on them. The fault-bounded, brittle, upper crustal blocks appear to have been rotated clockwise in response to the large amount of dextral transcurrent displacement, the amount of rotation increasing toward the major faults. This rotation of discrete blocks is a mode of deformation common at shallow crustal levels in many strike-slip zones (Nelson and Jones, 1986; Ron *et al.*, 1986; Hudson and Geissman, 1987; Geissman *et al.*, 1989) and may provide one means of rationalizing the disparities between estimates of the amount of tectonic displacement derived from geological and paleomagnetic studies (Monger and Irving, 1980; Irving *et al.*, 1985; Rees *et al.*, 1985; Gabrielse, 1985).

ACKNOWLEDGMENTS

This research was made possible by grants from the British Columbia Ministry of Energy, Mines and Petroleum Resources, the Geological Survey of Canada and the Natural Sciences and Engineering Research Council. Their support is gratefully acknowledged.

REFERENCES

- Bellefontaine, K.A. and Minehan, K. (1988): Summary of Fieldwork in the Ingenika Range, North-central British Columbia (94D/09; 94C/12); *B.C. Ministry of Energy, Mines and Petroleum Resources*, Geological Fieldwork 1987, Paper 1988-1, pages 195-198.
- Berthé, D., Choukroune, P. and Jegouzo, P. (1979): Orthogneiss, Mylonite and Non-coaxial Deformation of Granites: the Example of the South Armorican Shear Zone; *Journal of Structural Geology*, Volume 1, pages 31-42.
- Church, B.N. (1974): Geology of the Sustut Area; *B.C. Ministry of Energy, Mines and Petroleum Resources*, Geology, Exploration and Mining in British Columbia 1973, pages 411-455.
- Church, B.N. (1975): Geology of the Sustut Area; *B.C. Ministry of Energy, Mines and Petroleum Resources*, Geology, Exploration and Mining in British Columbia 1974, pages 305-309.
- Gabrielse, H. (1985): Major Dextral Transcurrent Displacements along the Northern Rocky Mountain Trench and Related Lineaments in North-central British Columbia; *Geological Society of America*, Bulletin, Volume 96, pages 1-14.
- Geissman, J.W., Harlan, S.S. and Wawrzyniec, T.F. (1989). Strike-slip Faulting and Block Rotation in the Lake Mead Fault System; *Geology*, Volume 17, pages 1057-1058.
- Hudson, M.R. and Geissman, J.W. (1987): Paleomagnetic and Structural Evidence for Middle Tertiary Counterclockwise Block Rotation in the Dixie Valley Region, West-central Nevada; *Geology*, Volume 15, pages 638-642.
- Irving, E., Woodsworth, G.J., Wynne, P.J. and Morrison, A. (1985): Paleomagnetic Evidence for Displacement from the South of the Coast Plutonic Complex, British Columbia; *Canadian Journal of Earth Sciences*, Volume 22, pages 584-598.
- Keller, E.A., Bonkowski, M.S., Korsch, R.J. and Shlemon, R.J. (1982): Tectonic Geomorphology of the San Andreas Fault Zone in the Southern Indio Hills, Coachella Valley, California; *Geological Society of America*, Bulletin, Volume 93, pages 46-56.
- Lord, C.S. (1948): McConnell Creek Map-area, Cassiar District, British Columbia; *Geological Survey of Canada*, Memoir 251, 72 pages.
- Minehan, K. (1989a): Takla Group Volcano-sedimentary Rocks, North-central British Columbia; *B.C. Ministry of Energy, Mines and Petroleum Resources*, Geological Fieldwork 1988, Paper 1989-1, pages 227-232.
- Minehan, K. (1989b): Paleotectonic Setting of Takla Group Volcano-sedimentary Rocks, Quesnellia, North-central Columbia; unpublished M.Sc. thesis, *McGill University*, 102 pages.
- Monger, J.W.H. (1977): The Triassic Takla Group in McConnell Creek Map-area, North-central British Columbia; *Geological Survey of Canada*, Paper 76-29, 45 pages.
- Monger, J.W.H. (1984): Cordilleran Tectonics: a Canadian Perspective; *Bulletin Société Géologique de France*, Volume 7, pages 255- 278.
- Monger, J.W.H. and Irving, E. (1980): Northward Displacement of North-central British Columbia; *Nature*, Volume 285, pages 289-293.
- Nelson, M.R. and Jones, C.H. (1986): Paleomagnetism and Crustal Rotations along a Shear Zone, Las Vegas Range, Southern Nevada; *Tectonics*, Volume 6, pages 13-33.
- Nixon, G.T. and Hammack, J.L. (1990): Geology and Noble Metal Geochemistry of the Johanson Lake Mafic-Ultramafic Complex, North-central British Columbia; *Geological Fieldwork 1989*, *B.C. Ministry of Energy, Mines and Petroleum Resources*, Paper 1990-1, pages 417-424.
- Rees, C.J., Irving, E. and Brown, R.L. (1985): Secondary Magnetization of Triassic-Jurassic Volcaniclastic Rocks of Quesnel Terrane, Quesnel Lake, B.C.; *Geophysical Research Letters*, Volume 12, pages 498-501.
- Richards, T.A. (1976a): McConnell Creek Map Area (94D/E), Geology; *Geological Survey of Canada*, Open File 342.
- Richards, T.A. (1976b): Takla Group (Reports 10-16): McConnell Creek Map Area (94D, East Half). British Columbia; *Geological Survey of Canada*, Paper 76-1a, pages 43-50.
- Ron, H., Aydin, A. and Nur, A. (1986): Strike-slip Faulting and Block Rotation in the Lake Mead Fault System; *Geology*, Volume 14, pages 1020-1023.

Sylvester, A.G. (1988): Strike-slip Faults; *Geological Society of America, Bulletin*, Volume 100, pages 1666-1703.

Tchalenko, J.S. (1970): Similarities between Shear Zones of Different Magnitudes; *Geological Society of America, Bulletin*, Volume 81, pages 1625-1640.

Umhoefer, P.J. (1987): Northward Translation of "Baja British Columbia" along the Late Cretaceous to Paleocene Margin of Western North America; *Tectonics*, Volume 6, pages 377-394.

Wilcox, R.E., Harding, T.P. and Seely, D.R. (1973): Basic Wrench Tectonics; *American Association of Petroleum Geologists, Bulletin*, Volume 57, pages 74-96.

NOTES



STRATIGRAPHIC NOTES FROM THE ISKUT-SULPHURETS PROJECT AREA (104B)

By J. M. Britton

KEYWORDS: Regional geology, stratigraphy, Stikine assemblage, Stuhini Group, Hazelton Group, Texas Creek intrusive suite.

INTRODUCTION

The Iskut-Sulphurets project (Figure 1-13-1) completed its final field season with an abbreviated program of fill-in mapping and examination of major mineral properties. This report emphasizes stratigraphic revisions based on the mapping and on new fossil identifications.

PREVIOUS AND CURRENT WORK

The list of published geological reports on the Iskut-Sulphurets gold camp continues to grow. The regional geologic framework has been presented by Anderson (1989), Anderson and Thorkelson (1990) and Anderson and Bevier (1990). The geology and mineralization of the Sulphurets, Unuk and Snippaker areas have been described in maps and reports by Alldrick and Britton (1988), Alldrick *et al.* (1989, 1990), Britton and Alldrick (1988), Britton *et al.* (1989, 1990b). Maps and reports of contiguous areas include Alldrick (1985, 1987), Read *et al.* (1989) and Logan *et al.* (1990a, b). There are detailed geologic maps of the Bronson Creek - Johnny Mountain area by Lefebure and Gunning (1989) and Fletcher and Hiebert (1990). Published mineral deposit descriptions include the E&L nickel prospect (Hancock, 1990), the Colagh prospect (MacLean, 1990), the recent discoveries at Eskay Creek (Britton *et al.*, 1990a), and skarns (Ray and Webster, 1991, this volume). New galena-lead isotope data from many deposits of this region are presented in Godwin *et al.* (1991, this volume).

In addition to these reports are rock and stream-sediment geochemical data (Lefebure and Gunning, 1988, 1989; National Geochemical Reconnaissance, 1988), MINFILE descriptions of 360 mineral occurrences, and more than 225 assessment reports now in the public domain.

The Geological Survey of Canada will continue regional mapping of the Iskut River sheet (104B) under the direction of R.G. Anderson. In July, 1990 the recently established Mineral Deposit Research Unit began studies of the major mineral deposits in the Iskut-Sulphurets camp, including Sulphurets, Kerr, Eskay Creek, Snip and Johnny Mountain.

Our 1990 field area extended from Mount Verrett in the northwest to McQuillan Ridge in the southeast, mainly between Snippaker and Harymel creeks (Figure 1-13-2). This area had been only briefly reconnoitred in 1988 and 1989 and there remained the task of correlating our units with those of adjacent map areas (Read *et al.*, 1989; Logan *et al.*, 1990b).

STRATIGRAPHIC NOMENCLATURE

Stratigraphic nomenclature in this part of the Intermontane Belt is evolving (Figure 1-13-3). Anderson (1989) defined the regional stratigraphic framework in terms of four tectonostratigraphic assemblages:

- Paleozoic Stikine assemblage;
- Triassic to Jurassic volcanic-plutonic arc complexes;
- Middle and Upper Jurassic Bowser overlap assemblage; and,
- Tertiary Coast plutonic complex.

The Paleozoic Stikine assemblage comprises three separate lithologic sequences deposited, respectively, in the Early Devonian, Mississippian and Early Permian. Lithologies include coralline limestone, chert, mafic to felsic volcanic and volcanoclastic rocks, and derived sediments. Of the four tectonostratigraphic assemblages this is the least well known. None of its sequences has been named, nor have contact relationships between them been defined.

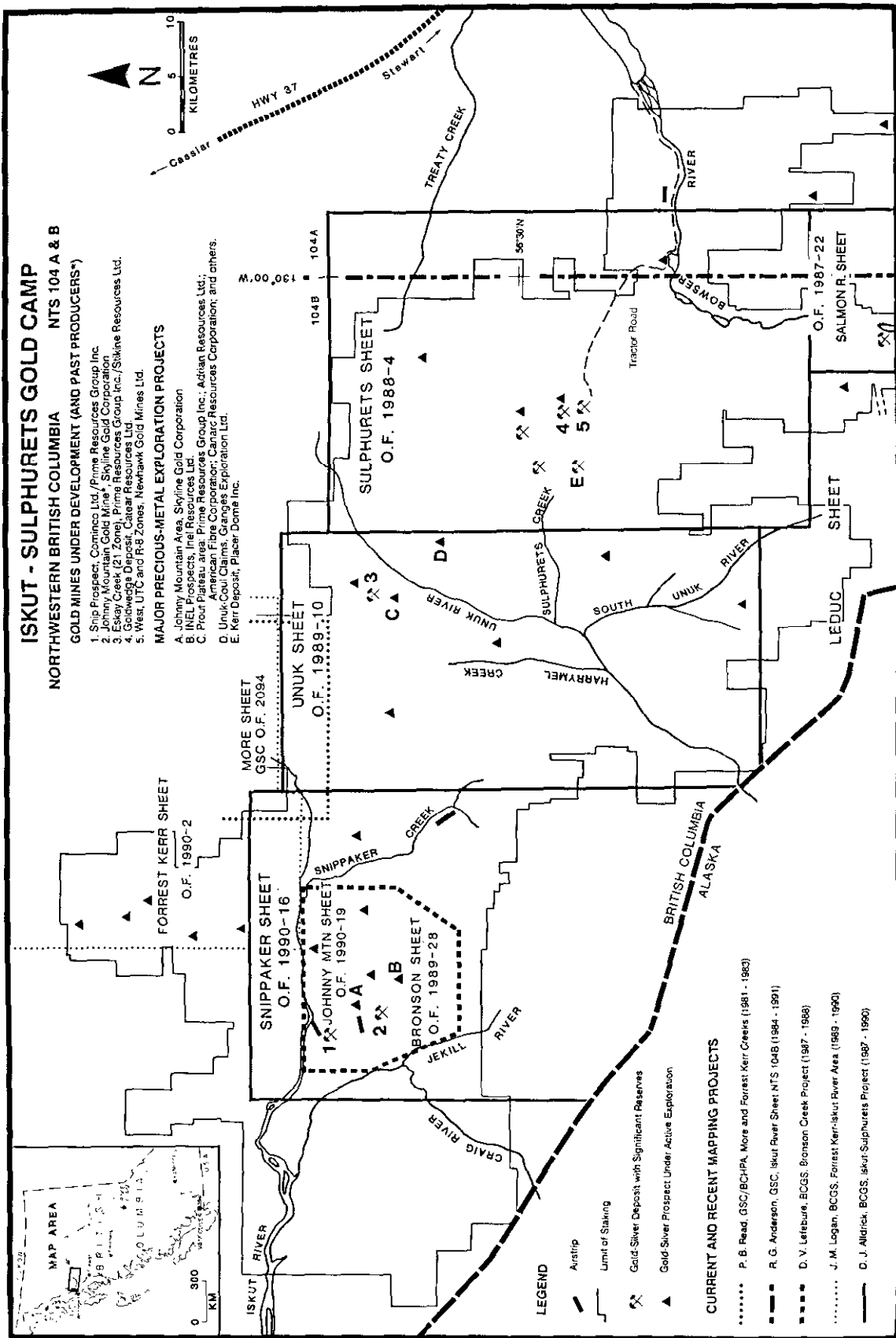
Triassic and Jurassic arc rocks are divided into two main groups: the Upper Triassic Stuhini (Takla) Group and the Lower (to Middle) Jurassic Hazelton Group. Read *et al.* (1989) identified Middle Triassic rocks that may represent a third, as yet unnamed group. Lower to Middle Jurassic rocks (basinal sediments and distal tuffs) mark the end of arc volcanism.

[Note: Before the early 1980s Takla was the usual name for Triassic strata in the project area (Grove, 1986). Since then the term Stuhini has become more common. The Stuhini Group was first defined by Kerr in 1948; the Takla, by Armstrong in 1949. The groups comprise Upper Triassic strata that fringe the Bowser basin. As terrane concepts emerged and became entrenched in the literature, a new convention has developed. Stuhini is now the preferred term for Triassic strata west of the Cache Creek Terrane (*i.e.* in Stikinia). Takla is used for similar strata east of the Cache Creek Terrane (*i.e.* in Quesnellia). There is little difference in age, lithology, rock associations or chemistry between the two groups.]

The overlap assemblage of basinal marine and nonmarine sedimentary rocks is the Middle to Upper Jurassic Bowser Lake Group.

The Tertiary Coast plutonic complex is mostly granitic intrusive rocks but includes some (probably older) metamorphic rocks and tectonites that have been exhumed by rapid uplift and erosion.

Regional mapping has added refinements to this simple scheme. The Upper Triassic Stuhini Group has not yet been divided into formations but Anderson and Thorkelson



Map courtesy of Teulon Resources Corporation, used & modified with permission.

Figure 1-13-1. Iskut-Sulphurets gold camp: precious metal deposits and current mapping projects.

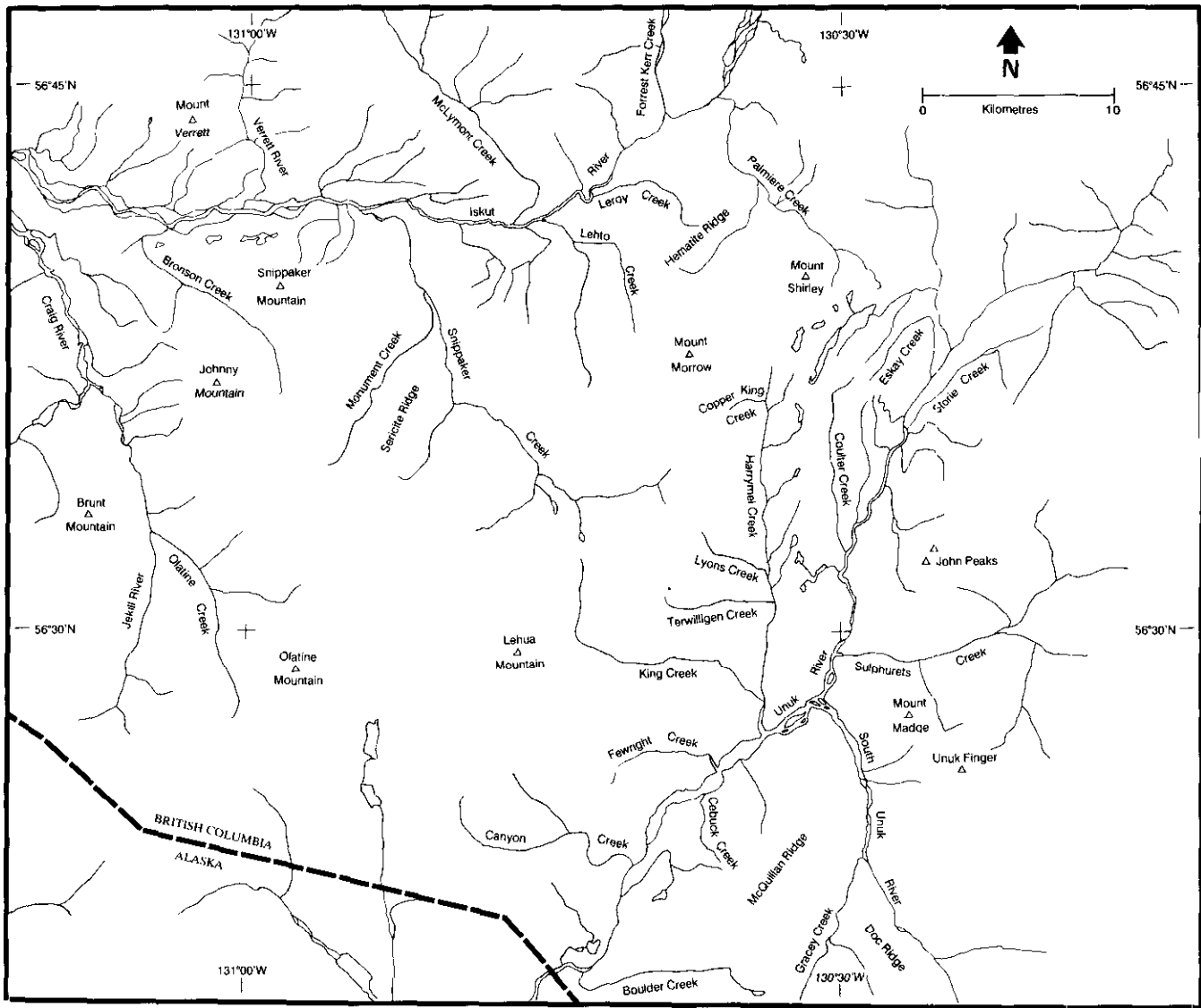


Figure 1-13-2. Location map for areas discussed in the text.

(1990) discuss this group in terms of unnamed eastern and western facies.

Only Jurassic strata (Hazelton and Bowser Lake groups) have been divided into named formations, most of which are not yet formally defined. The lowermost strata of the Hazelton Group are mainly volcanic or volcanogenic units. In order of decreasing age these have been divided into the Unuk River, Betty Creek and Mount Dilworth formations. Upper Lower Jurassic basal sediments and distal tuffs (the Salmon River formation) follow the end of arc volcanism. Because rocks of the Salmon River formation are transitional between mostly volcanic Hazelton Group and the wholly sedimentary Bowser Lake Group they have been treated differently by different authors. Some consider them part of the Hazelton Group, others part of the Bowser Lake Group, still others part of the Spatsizi Group [defined by Thomson *et al.* (1986) in an area 160 kilometres to the northeast]. Because of lithological similarities and the difficulty of defining the upper boundary of the Salmon River

formation it may be best to include it as a basal formation of the Bowser Lake Group. So far, the only basal formation of this group that has been recognized is the Ashman.

MOUNT VERRETT/HEMATITE RIDGE

North and south of the Iskut River, extending from the southern flank of Mount Verrett to Snippaker, Lehto and Leroy creeks, are thick, monotonous sequences of massive andesitic tuffs and flows, locally with clasts and lenses of limestone, and interbeds of siltstone and wacke. Correct stratigraphic assignment of these rocks remains an unresolved problem, it creates the most noticeable difference between various geological maps published to date.

Based on lithostratigraphic correlations the rocks have been variously assigned to Jurassic Hazelton Group (Grove, 1986; Alldrick *et al.*, 1989), Triassic Stuhini Group (Lefebvre and Gunning, 1989; Alldrick *et al.*, 1990) and Paleozoic Stikine assemblage (Read *et al.*, 1989; Logan *et al.*, 1990b). As stratigraphic correlations have been

PERIOD	FORMATION	GROUP
MIDDLE JURASSIC	ASHMAN	BOWSER LAKE
190 Ma	SALMON RIVER	HAZELTON
	MOUNT DILWORTH	
LOWER JURASSIC	BETTY CREEK	
210 Ma	UNUK RIVER	
UPPER TRIASSIC		STUHINI
230 Ma		
MIDDLE TRIASSIC		
245 Ma		
PERMIAN		STIKINE
285 Ma		
320 Ma		
MISSISSIPPIAN		ASSEMBLAGE
360 Ma		
DEVONIAN		

Figure 1-13-3. Simplified table of formations for the Iskut-Sulphurets project area.

developed north of the Iskut and extended south (e.g. by P.B. Read, J.M. Logan and others) the tendency has been to place them in the Paleozoic. Based on correlations developed to the south and extended north they can be fitted without difficulty into Mesozoic sequences. If nothing else, these rocks serve as an object lesson in the limitations of lithostratigraphic correlation. To date the limestones have proven to be barren of conodonts and carry only rare, nondiagnostic crinoid fragments.

Hard evidence for a Paleozoic age for some of these rocks comes from three Early Permian fossils found by Read *et al.* (1989) 5 kilometres south of the confluence of Forrest Kerr Creek and Iskut River, on the northeast end of "Hematite Ridge" (Unit "Ptf" of Read *et al.*, 1989). Previously they were mapped as Lower Jurassic Hazelton Group (Unit "3a" of Alldrick *et al.*, 1989). Hematite Ridge was re-examined this year and found to be very complexly faulted. The fossil-bearing strata occur both structurally above and below a volcanic conglomerate unit assigned to the Stuhini Group (Unit "Trs" of Read *et al.*, 1989). The fossil locations were resampled for conodonts and it is hoped these samples will help resolve the apparent discrepancies.

Read *et al.* (1989) also assigned andesitic volcanics to the Paleozoic on the basis of greater structural deformation, such as zones of foliation or widespread phyllite, that appear to be lacking in younger sequences. On these grounds rocks near Lehto Creek were assigned to the Upper Permian. Phyllonitic to mylonitic zones are fairly common along the major faults and splay off them. Given the

abundance of faults in the area, rock fabric is at best an equivocal criterion for dating the rocks.

Lithostratigraphic association can also provide some help in assigning a relative age.

A body of coarsely recrystallized limestone, 200 metres thick, on the east side of Mount Verrett, may correlate with a Permian limestone marker (Kerr, 1948) that occurs near the top of the Paleozoic succession. If so the Mount Verrett limestone may mark the Permo-Triassic boundary at Verrett Creek. The unit strikes northerly and dips moderately to steeply to the west. Beneath it are mixed sediments and andesitic tuffs of probable Early Permian age, above it similar lithologies of probable Triassic age. The principal difference between andesites above the limestone and those below it is that the former have more prominent feldspar phenocrysts (A. Travis, personal communication, 1990). Minor limestone lenses also seem less abundant above the marker.

Farther east, near Snippaker and Lehto creeks, andesitic rocks locally have pyroxene phenocrysts and are generally unfoliated, except near faults or shears. In some exposures they appear to be immediately overlain by dated Lower Jurassic strata. For these reasons they are more likely part of the Stuhini Group than the Paleozoic Stikine assemblage.

SERICITE RIDGE

The tentative identification of *Weyla* (H.W. Tipper, personal communication, 1990) suggests an Early Jurassic age for a sequence of wackes and siltstones that crop out near the northern end of Sericite Ridge. These sediments can be assigned to the Hazelton Group. Structurally beneath them are thin pyroxene-porphyrific andesitic tuffs that, on the basis of phenocryst association, may be part of the Late Triassic Stuhini Group.

Monument Creek valley, especially its lower slopes along Monument and Pyramid glaciers, is underlain by quartz-poor monzonitic to dioritic intrusive rocks, locally with coarse potassium feldspar phenocrysts. These resemble an Early Jurassic (189 to 195 Ma) suite of plutons that includes the Texas Creek, Mitchell Glacier and McLymont Creek plutons (Anderson and Bevier, 1990) and may include the Lehto pluton (Britton *et al.*, 1989). Important base and precious metal deposits are spatially associated with these intrusives and a genetic link seems probable. The extensive gossans found on Sericite Ridge, Pyramid Hill and Khyber Pass (and perhaps the Inel property) are developed in volcanic and sedimentary rocks that form a roof over relatively fresh monzodiorite stocks and are probably caused by these intrusions. The Lehto pluton has also generated several small skarns (Ray and Webster, 1991, this volume).

NICKEL MOUNTAIN

Black, thinly bedded siltstone and shale cap the western slopes of Nickel Mountain in upper Snippaker Creek. Fossils collected in 1989 include an ammonoid of late Early Jurassic age (probably middle Toarcian; H.W. Tipper, personal communication, 1990). These sediments have been intruded by small olivine and pyroxene-bearing gabbro

plugs that host the E&L nickel-copper deposit (Hancock, 1990). Fossil data thus confirm a post-Early Jurassic age of *intrusion and sulphide mineralization*. These gabbroic plugs are the youngest mafic plutons in the map area (apart from basaltic dikes related to Pleistocene and Recent volcanism: Stasiuk and Russell, 1990). Well dated Middle Jurassic plutons are not common in the Iskut area (Anderson and Bevier, 1990). Magmatism of that age (175-180 Ma) may have a mainly volcanic expression in the pillow lavas of the Eskay Creek facies of the Salmon River formation, of Anderson and Thorkelson (1990).

The northeast quarter of NTS 104B (National Geochemical Reconnaissance, 1988) is an area mostly underlain by Toarcian and younger siltstones and shales of the Salmon River formation and Bowser Lake Group. Regional stream-sediment samples collected in this area have consistently higher nickel values than the rest of the sheet. The source of the nickel is not known but could be nickeliferous plugs intruded into this stratigraphic level.

WEST OF HARRYMEL CREEK

Immediately west of Harrymel Creek, from the outflow of Copper King Glacier south to Fewright Creek, is a thick sequence of mainly fine-grained siliciclastic sedimentary rocks locally with thin to thick limestones and minor dacitic and andesitic tuffs. Both Late Triassic and Early Jurassic fossils have been reported from this sequence.

Smith and Carter (1990) reported Early Jurassic (upper Pliensbachian, Kunaie zone) fauna from a sequence of black siltstones and shales overlying a rusty buff limestone-mudstone unit, 180 metres thick, that in turn overlies red and green mottled polymictic conglomerate. Along strike to the north, a Late Triassic (probably Carnian) fauna was documented in 1961 (E.T. Tozer in Grove, 1986). To the south, in tan-weathering fine-grained wackes and coarse polymictic conglomerate (with pyroxene porphyry and rare limestone clasts) another probable Triassic fauna was found this year (H.W. Tipper, personal communication, 1990). Higher in the section the sediments give way to unfossiliferous dacitic pyroclastic rocks, including airfall tuffs.

The importance of these fossil discoveries is that they demonstrate a *conformable, possibly even gradational* transition between the Stuhini and Hazelton groups. East of the Unuk River, between Storie and Treaty creeks, a similar contact relationship has also been described (Britton *et al.*, 1989; Anderson and Thorkelson, 1990). More commonly this contact is a marked *unconformity* (Anderson, 1989).

MCQUILLAN RIDGE

On ridges south of the confluence of Unuk and South Unuk rivers (McQuillan and Doc) a thick sequence of andesitic tuffs, tuffaceous siltstones and limestone lenses were included as part of the Hazelton Group (Unuk River formation; Alldrick *et al.*, 1989). Dating of crosscutting dioritic stocks indicates that they are all at least Late Triassic or older (about 221 and 226 Ma; Anderson and Bevier, 1990). In keeping with the current convention of including



Plate 1-13-1. Coarse hornblende-phyric andesite tuff of the Stuhini Group, near Cebuck Creek on McQuillan Ridge. X-ray diffractometer analysis indicates the phenocrysts are ferroan magnesio-hornblende.

Upper Triassic rocks in the Stuhini Group and Lower Jurassic rocks in the Hazelton Group, all these rocks should be assigned to the Stuhini Group.

Dips of strata on McQuillan Ridge appear to define a broad syncline with a northerly trending axis. From oldest to youngest the lithologic sequence is: *metasiltstone and fine-grained meta-andesite tuff; foliated to gneissic andesite with minor siltstone; foliated to layered andesitic ash and lapilli tuff intercalated with siltstone and thin limestone lenses up to 10 metres thick; overlain by andesitic to dacitic ash and lapilli tuff, commonly with hornblende and pyroxene phenocrysts. Hornblende phenocrysts increase in abundance up-section and are locally very coarse (Plate 1-13-1).*

Metamorphic fabrics increase down-section and have been attributed to thermal effects of the Coast plutonic complex which occupies the southern end of McQuillan Ridge, or to numerous faults. There appears to be a marked change in deformational intensity between the hornblende-

pyroxene-phyric pyroclastics above and mixed andesite-siltstone-limestone sequence below. In view of the observation of widespread phyllite in Permian and older rocks (Read *et al.*, 1989) the possibility remains that these rocks are part of the Paleozoic Stikine assemblage.

ACKNOWLEDGMENTS

Thanks go to Jan Hammack for her capable fieldwork despite the rain, vertigo and *Oplopanax horridum* of a typical Iskut summer, and to Victor Koyanagi who, in a ten-day visit, made a substantial contribution to the success of this short season.

I am grateful for discussions with Rex Pegg, Rick Honsinger, Piotr Lutynski, Adam Travis and Andy Muirhead of Keewatin Engineering Ltd.; Dave Kuran and Paul Jones of Corona Corporation; Scott Casselman of Western Canadian Mining Corporation; Steve Todoruk of Pamicon Developments Ltd.; and Bernie Gaboury, Karen Pelletier and Lawrence Solkoski of Granges Exploration Inc. Keewatin Engineering and Granges Exploration provided exceptional hospitality.

Jaycox Industries Ltd. supplied reliable expediting services; Northern Mountain Helicopters Inc. and Central Mountain Air Ltd. safe air travel.

REFERENCES

- Alldrick, D.J. (1985): Stratigraphy and Petrology of the Stewart Mining Camp (104B/1); *B.C. Ministry of Energy, Mines and Petroleum Resources*, Geological Fieldwork 1984, Paper 1985-1, pages 316-341.
- Alldrick, D.J. (1987): Geology and Mineral Deposits of the Salmon River Valley, Stewart Area (104A, 104B); *B.C. Ministry of Energy, Mines and Petroleum Resources*, Open File 1987-22.
- Alldrick, D.J. and Britton, J.M. (1988): Geology and Mineral Deposits of the Sulphurets Area (104A/5, 104A/12, 104B/8, 104B/9); *B.C. Ministry of Energy, Mines and Petroleum Resources*, Open File 1988-4.
- Alldrick, D.J., Britton, J.M., Webster, I.C.L. and Russell, C.W.P. (1989): Geology and Mineral Deposits of the Unuk Area (104B/7E, 8W, 9W, 10E); *B.C. Ministry of Energy, Mines and Petroleum Resources*, Open File 1989-10.
- Alldrick, D.J., Britton, J.M., MacLean, M.E., Hancock, K.D., Fletcher, B.A. and Hiebert, S.N. (1990): Geology and Mineral Deposits of the Snippaker Area (104B/6E, 7W, 10W, 11E); *B.C. Ministry of Energy, Mines and Petroleum Resources*, Open File 1990-16.
- Anderson, R.G. (1989): A Stratigraphic, Plutonic, and Structural Framework for the Iskut River Map Area, Northwestern British Columbia; in Current Research, Part E, *Geological Survey of Canada*, Paper 89-1E, pages 145-154.
- Anderson, R.G. and Bevier, M.L. (1990): A Note on Mesozoic and Tertiary K-Ar Geochronometry of Plutonic Suites, Iskut River Map Area, Northwestern British Columbia; in Current Research, Part E, *Geological Survey of Canada*, Paper 90-1E, pages 141-147.
- Anderson, R.G. and Thorkelson, D.J. (1990): Mesozoic Stratigraphy and Setting for some Mineral Deposits in the Iskut River Map Area, Northwestern British Columbia; in Current Research, Part E, *Geological Survey of Canada*, Paper 90-1E, pages 131-139.
- Armstrong, J.E. (1949): Fort St. James Map-area, Cassiar and Coast Districts, British Columbia; *Geological Survey of Canada*, Memoir 252.
- Britton, J.M. and Alldrick, D.J. (1988): Sulphurets Map Area (104A/5W, 12W; 104B/8E, 9E); *B.C. Ministry of Energy, Mines and Petroleum Resources*, Geological Fieldwork 1987, Paper 1988-1, pages 199-209.
- Britton, J.M., Webster, I.C.L. and Alldrick, D.J. (1989): Unuk Map Area (104B/7E, 8W, 9W, 10E); *B.C. Ministry of Energy, Mines and Petroleum Resources*, Geological Fieldwork 1988, Paper 1989-1, pages 241-250.
- Britton, J.M., Blackwell, J.D. and Schroeter, T.G. (1990a): #21 Zone Deposits, Eskay Creek, Northwestern British Columbia; *B.C. Ministry of Energy, Mines and Petroleum Resources*, Exploration in British Columbia 1989, pages 197-223.
- Britton, J.M., Fletcher, B.A. and Alldrick, D.J. (1990b): Snippaker Map Area (104B/6E, 7W, 10W, 11E); *B.C. Ministry of Energy, Mines and Petroleum Resources*, Geological Fieldwork 1989, Paper 1990-1, pages 199-209.
- Fletcher, B.A. and Hiebert, S.N. (1990): Geology of the Johnny Mountain Area (104B/11E); *B.C. Ministry of Energy, Mines and Petroleum Resources*, Open File 1990-19.
- Godwin, C.L., Pickering, A.D.R., Gabites, J.E. and Alldrick, D.J. (1991): Interpretation of Galena Lead Isotopes from the Stewart-Iskut Area (103O & P and 104A, B & G); *B.C. Ministry of Energy, Mines and Petroleum Resources*, Geological Fieldwork 1990, Paper 1991-1, this volume.
- Grove, E.W. (1986): Geology and Mineral Deposits of the Unuk River – Salmon River – Anyox Area; *B.C. Ministry of Energy, Mines and Petroleum Resources*, Bulletin 63, 152 pages.
- Hancock, K.D. (1990): Geology of Nickel Mountain and the E&L Nickel-Copper Prospect (NTS 104B/10E); *B.C. Ministry of Energy, Mines and Petroleum Resources*, Geological Fieldwork 1989, Paper 1990-1, pages 337-341.
- Kerr, F.A. (1948): Lower Stikine and Western Iskut River Areas, British Columbia; *Geological Survey of Canada*, Memoir 246, 94 pages.
- Lefebvre, D.V. and Gunning, M.H. (1988): Gold Lithogeochemistry of Bronson Creek Area, British Columbia (104B/10W, 11E); *B.C. Ministry of Energy, Mines and Petroleum Resources*, Exploration in British Columbia 1987, pages B71-B77.

- Lefebure, D.V. and Gunning, M.H. (1989): Geology of the Bronson Creek Area (104B/10W, 11E); *B.C. Ministry of Energy, Mines and Petroleum Resources*, Open File 1989-28.
- Logan, J.M., Koyanagi, V.M. and Drobe, J.R. (1990a): Geology and Mineral Deposits of the Forrest Kerr Map Area (104B/15); *B.C. Ministry of Energy, Mines and Petroleum Resources*, Geological Fieldwork 1989, Paper 1990-1, pages 127-139.
- Logan, J.M., Koyanagi, V.M. and Drobe, J.R. (1990b): Geology and Mineral Occurrences of the Forrest Kerr – Iskut River Area (104B/15 and part of 104B/10); *B.C. Ministry of Energy, Mines and Petroleum Resources*, Open File 1990-2.
- MacLean, M.E. (1990): Geology of the Colagh Prospect, Unuk Map Area (104B/10E); *B.C. Ministry of Energy, Mines and Petroleum Resources*, Geological Fieldwork 1989, Paper 1990-1, pages 343-346.
- National Geochemical Reconnaissance, 1:250,000 Map Series (1988): Iskut River, British Columbia (NTS 104B); *Geological Survey of Canada*, Open File 1645; *B.C. Ministry of Energy, Mines and Petroleum Resources*, RGS-18.
- Ray, G.E. and Webster, I.C.L. (1991): Skarns in the Iskut and Scud River Region, Northwestern British Columbia; *B.C. Ministry of Energy, Mines and Petroleum Resources*, Geological Fieldwork 1990, Paper 1991-1, this volume.
- Read, P.B., Brown, R.L., Psutka, J.F., Moore, J.M., Journey, M., Lane, L.S. and Orchard, M.J. (1989): Geology, More and Forrest Kerr Creeks (Parts of 104B/10, 15, 16 and 104G/1,2), Northwestern British Columbia; *Geological Survey of Canada*, Open File 2094.
- Smith, P.L. and Carter, E.S. (1990): Jurassic Correlations in the Iskut River Map Area, British Columbia: Constraints on the Age of the Eskay Creek Deposit; in Current Research, Part E, *Geological Survey of Canada*, Paper 90-1E, pages 149-151.
- Stasiuk, M.V. and Russell, J.K. (1990): Quaternary Volcanic Rocks of the Iskut River Region, Northwestern British Columbia; in Current Research, Part E, *Geological Survey of Canada*, Paper 90-1E, pages 153-157.
- Thomson, R.C., Smith, P.L. and Tipper, H.W. (1986): Lower to Middle Jurassic (Pliensbachian to Bajocian) Stratigraphy of the Northern Spatsizi Area, North-central British Columbia; *Canadian Journal of Earth Sciences*, Volume 23, Number 12, pages 1963-1973.

NOTES



LOW-TEMPERATURE THERMAL HISTORY OF THE COAST PLUTONIC COMPLEX AND INTERMONTANE BELT, NORTHWEST BRITISH COLUMBIA (104M, N)

By Raymond A. Donelick and John R. Dickie
Dalhousie University

KEYWORDS: Geothermometry, Tagish Lake, fission-track age, apatite, zircon, Cache Creek Terrane, Whitehorse trough, Coast plutonic complex, Llewellyn fault.

INTRODUCTION

Fieldwork completed in 1990 focused on Laberge Group sediments along the shores of southern Tagish Lake, northwestern British Columbia (Figure 1-14-1). The objective of this study is to determine the low-temperature thermal evolution of this part of the Intermontane Belt, using apatite fission-track techniques and, if possible, place constraints on the timing of mineralization at the Engineer gold deposit. Sample analyses are currently underway, with new results forthcoming. The remainder of this paper focuses on previously unpublished fission-track data for northwestern

British Columbia, reported and discussed in two graduate theses by the first author (Donelick, 1986; 1988; *see also* Donelick and Miller, 1986). These data constrain the regional low-temperature cooling pattern of the Coast plutonic complex and Intermontane Belt in the vicinity of Tagish Lake.

GENERAL GEOLOGY

The studied area is situated in the Cordillera of northwestern British Columbia between Atlin and the Alaska Panhandle (Figure 1-14-1; NTS 1:250 000 maps 104M and 104N). Geological mapping of this area was conducted by Christie (1957), Aitken (1959), Bultman (1979), Mihalynuk and Rouse (1988a, b), Mihalynuk *et al.* (1989a, b), Mihalynuk and Mountjoy (1990), and Mihalynuk *et al.* (1990). From east to west, the area crosses parts of (a) the Cache Creek Terrane, (b) the Whitehorse trough, (c) the Nisling Terrane, and (d) the Coast plutonic complex. The Cache Creek Terrane is composed of upper Paleozoic rocks of oceanic affinity and is inferred to have been metamorphosed no later than pre-Late Triassic time (Aitken, 1959; Eisbacher, 1974; Monger, 1977; Bultman, 1979). The Whitehorse trough is composed primarily of the Lower Jurassic Laberge Group fore-arc sequence which was folded and thrust by Early Cretaceous time (*e.g.* Bultman, 1979; Dickie, 1989). The Nisling Terrane is composed of metamorphosed Proterozoic to Paleozoic volcanic arc and continental margin rocks (Mihalynuk and Mountjoy, 1990; Currie, 1990). Numerous Mesozoic to Cenozoic granitoid intrusions of the Coast plutonic complex form the western part of the study area and are present in all of the eastern assemblages.

LOW-TEMPERATURE HISTORY OF NORTHWESTERN BRITISH COLUMBIA

No previous work is published concerning the low-temperature thermal history of northwestern British Columbia, however, relevant studies are reported for the southern part of the Coast plutonic complex (Harrison *et al.*, 1979; Parrish, 1982; 1983) and the Omineca crystalline belt (Parrish *et al.*, 1988; Sevigny *et al.*, 1990). These studies primarily document large-scale cooling of much of the Cordillera following latest Cretaceous to Eocene compressive orogeny. Of greatest significance to the present study is the 30-kilometre-wide belt of Late Cretaceous to Middle Eocene epizonal calcalkaline plutons situated along the International Boundary between Atlin, British Columbia

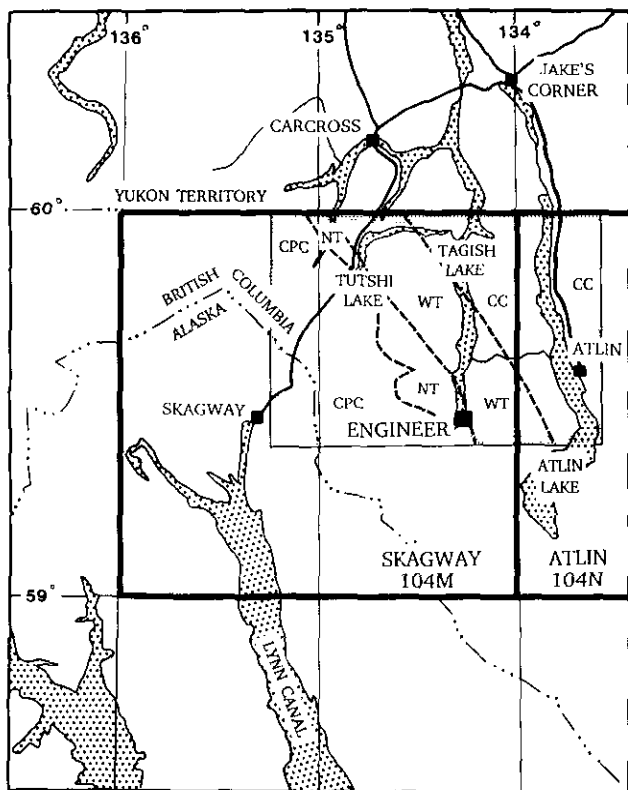


Figure 1-14-1. Location map of the study area (small box with dotted outline). CC = Cache Creek Terrane; WT = Whitehorse trough; NT = Nisling Terrane; CPC = Coast plutonic complex.

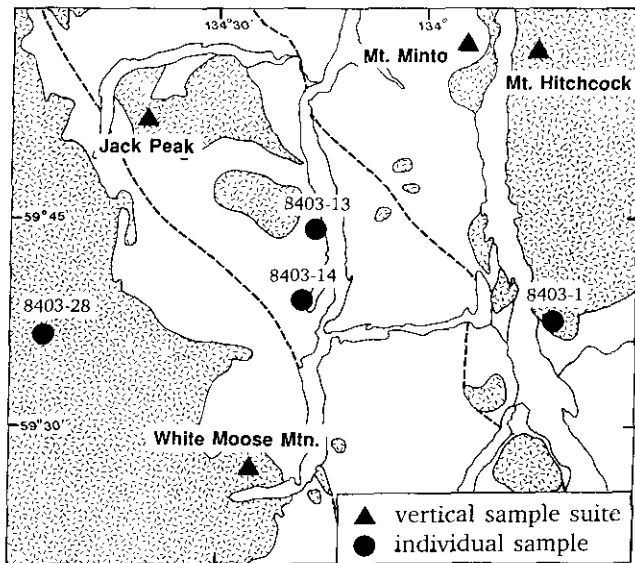


Figure 1-14-2. Sample location map. The patterned areas correspond to major granitoid intrusive bodies that were preferentially sampled; dashed lines indicate approximate terrane boundaries from Figure 1-14-1.

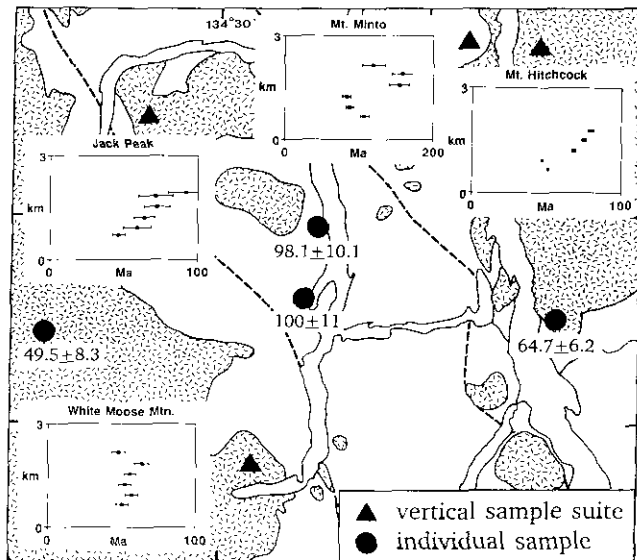


Figure 1-14-3. Summary of apatite fission-track ages (after Donelick, 1986). Errors given as one standard deviation.

and Juneau, Alaska (e.g. Bultman, 1979; Gehrels *et al.*, 1984; Brew, 1988), and several isolated plutons of the same age that intrude the Cache Creek Terrane to the east (Atlin Mountain, Birch Mountain; Aitken, 1959; Bultman, 1979). It is expected that the thermal histories recorded by these intrusions and adjacent country rock will reflect postintrusive cooling, no older than the age of the respective intrusive events.

Twenty-seven samples were collected from throughout the study area for fission-track analysis; sample locations

TABLE 1-14-1
SAMPLE LOCATIONS

Sample	Rock type	Elevation above m.s.l. (km)	Longitude	Latitude
Cache Creek Terrane				
Como Lake				
8403-1	intrusive	0.92	133°40' 0"	59°36'40"
Mount Hitchcock				
8403-2	intrusive	0.67	133°48'10"	59°55'20"
8403-3	intrusive	0.92	133°47'20"	59°55'10"
8403-4	intrusive	1.22	133°46'20"	59°55'40"
8403-5	intrusive	1.53	133°46' 0"	59°56' 0"
8403-6	intrusive	1.80	133°45' 0"	59°56'20"
Mount Minto				
8403-7	intrusive	0.67	133°50'50"	59°56'20"
8403-8	intrusive	0.92	133°51' 0"	59°56'50"
8403-9	intrusive	1.22	133°51'50"	59°56'50"
8403-10	volcanic	1.53	133°52'50"	59°56'20"
8403-11	volcanic	1.84	133°53'50"	59°56'40"
8403-12	volcanic	2.11	133°53'50"	59°57' 0"
Whitehorse Trough				
Tagish Lake				
8403-13	sedimentary	0.92	134°16'20"	59°45'20"
8403-14	sedimentary	0.66	134°17'40"	59°37'30"
Jack Peak				
8403-21	intrusive	0.71	134°44'10"	59°55'30"
8403-22	intrusive	0.92	134°44'30"	59°55'10"
8403-23	intrusive	1.22	134°44' 0"	59°54'50"
8403-24	intrusive	1.53	134°43'10"	59°54'40"
8403-25	intrusive	1.84	134°42'20"	59°54'40"
8403-26	intrusive	1.94	134°42'10"	59°52'50"
Coast Plutonic Complex				
White Moose Mountain				
8403-15	intrusive	0.66	134°27'40"	59°25' 0"
8503-16	intrusive	0.92	134°27'50"	59°25'20"
8403-17	intrusive	1.22	134°27'10"	59°25'30"
8403-18	intrusive	1.53	134°27'10"	59°25'50"
8403-19	intrusive	1.84	134°26'50"	59°26' 0"
8403-20	intrusive	2.17	134°26'50"	59°26'30"
White Pass				
8403-28	intrusive	0.92	135° 7'10"	59°39'50"

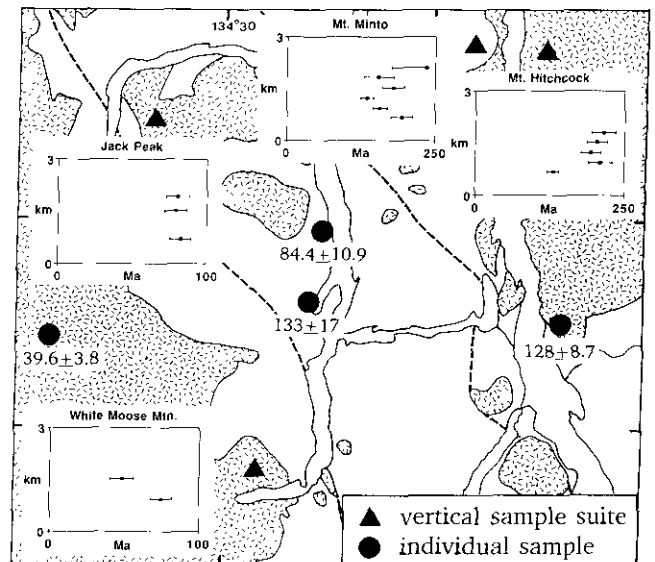


Figure 1-14-4. Summary of zircon fission-track ages (after Donelick, 1988). Errors given as one standard deviation.

TABLE 1-14-2
SUMMARY OF APATITE FISSION-TRACK ANALYSES

Sample	ρ_z^a	N	ρ_i^a	N	ρ_d^a	N	Grains	Chi ²	Test ^b	Fission Track Age ^c (Ma)	Track Lengths ^d	Mean Track Length (μm)	Std. Dev. (μm)
Cache Creek Terrane													
Como Lake													
8403-1	0.660	145	2.45	539	1.36	6520	15	7.48	PASS	64.7 \pm 6.2	301	13.24 \pm 0.10	1.70
Mount Hitchcock													
8403-2	0.674	220	4.03	1316	1.70	10719	15	32.9	FAIL	51.2 \pm 6.6	301	13.02 \pm 0.10	1.65
8403-3	0.674	169	4.17	1044	1.63	11025	15	16.5	PASS	47.0 \pm 4.0	306	13.48 \pm 0.11	1.90
8403-4	2.75	339	12.3	1516	1.71	10719	15	12.8	PASS	68.0 \pm 4.3	306	13.24 \pm 0.09	1.49
8403-5	2.33	287	9.39	1157	1.72	10719	15	4.30	PASS	75.7 \pm 5.2	313	13.24 \pm 0.09	1.56
8403-6	2.69	332	9.83	1211	1.65	11025	15	9.46	PASS	79.9 \pm 5.2	310	12.93 \pm 0.11	1.88
Mount Minto													
8403-7	4.17	548	11.3	1486	1.66	11025	15	15.1	PASS	108 \pm 5.8	311	12.73 \pm 0.11	2.01
8403-8	2.50	441	6.92	1222	1.38	6520	15	11.3	PASS	88.0 \pm 5.2	n.m.		
8403-9	1.57	328	5.51	1154	1.67	11025	15	17.1	PASS	83.8 \pm 5.5	n.m.		
8403-10	4.87	220	9.87	446	1.77	10719	15	17.4	PASS	154 \pm 13	n.m.		
8403-11	0.900	194	1.69	365	1.69	11025	16	18.9	PASS	158 \pm 14	n.m.		
8403-12	0.634	86	1.59	216	1.70	11025	15	22.6	PASS	119 \pm 15	n.m.		
Whitehorse Trough													
Tagish Lake													
8403-13	0.480	131	1.48	403	1.72	11025	15	19.6	PASS	98.1 \pm 10.1	n.m.		
8403-14	0.346	106	0.850	260	1.39	6520	15	13.3	PASS	100 \pm 11	n.m.		
Jack Peak													
8403-21	0.752	142	4.75	897	1.66	11025	15	7.90	PASS	46.7 \pm 4.3	n.m.		
8403-22	0.564	51	2.31	209	1.36	6520	10	7.97	PASS	59.1 \pm 9.3	110	13.88 \pm 0.19	1.99
8403-23	0.730	117	3.38	541	1.68	11025	15	11.6	PASS	64.4 \pm 6.7	n.m.		
8403-24	0.571	88	2.49	382	1.78	10719	15	7.20	PASS	72.6 \pm 8.7	n.m.		
8403-25	0.905	119	4.15	546	1.70	10719	13	27.5	FAIL	71.6 \pm 11.5	n.m.		
8403-26	0.771	76	2.50	246	1.69	11025	15	13.0	PASS	92.4 \pm 12.3	n.m.		
Coast Plutonic Complex													
White Moose Mountain													
8403-15	0.884	198	5.06	1132	1.63	11025	15	16.4	PASS	50.8 \pm 4.0	n.m.		
8403-16	1.31	244	5.66	1058	1.40	6520	15	14.4	PASS	57.2 \pm 4.2	306	13.79 \pm 0.09	1.55
8403-17	0.798	195	4.44	1085	1.64	11025	15	15.8	PASS	52.4 \pm 4.2	n.m.		
8403-18	1.16	233	6.11	1230	1.65	11025	15	4.99	PASS	55.5 \pm 4.1	n.m.		
8403-19	0.703	215	3.39	1037	1.73	10719	15	17.9	PASS	63.7 \pm 4.9	n.m.		
8403-20	0.632	131	4.09	848	1.76	10719	15	11.1	PASS	48.3 \pm 4.6	n.m.		
White Pass													
8403-28	0.273	41	1.64	246	1.63	11025	22	16.0	PASS	49.5 \pm 8.3	n.m.		

^a in units of 10^6 tracks/cm²

^b pass or fail at the 95% confidence level for Chi² calculated using the method of Galbraith (1981)

^c zeta calibration factor 357.0 \pm 6.3 relative to neutron dosimeter glass standard SRM-612; ages determined using the criteria of Green (1981); error given as 1 standard deviation

^d confined horizontal fission tracks as recommended by Laslett *et al.* (1982); n.m. = not measured

are shown in Figure 1-14-2 and listed in Table 1-14-1. The samples represent: (a) vertical suites from four mountains collected over their accessible elevation ranges and (b) four additional samples collected from selected sites interspersed among the vertical suites. Apatite fission-track ages were measured for all 27 samples (Table 1-14-2 and Figure 1-14-3); etchable fission-track length distributions in apatite for nine samples (Table 1-14-2); and zircon fission-track ages for twenty samples (Table 1-14-3 and Figure 1-14-4). Full details regarding the mineral separation techniques, sample preparation procedures and analytical methods employed for the fission-track analyses are presented in Donelick (1986; 1988). In this paper, each apatite fission-track age is interpreted as the time when its sample cooled through the 100°C crustal isotherm. This interpretation is appropriate due to the limited degree of fission-track annealing present in the apatites as evidenced by the rela-

tively long, mean etchable track lengths (*e.g.* Naeser and Forbes, 1976; Green *et al.*, 1986). Furthermore, we interpret each zircon fission-track age as a minimum age of formation of the igneous rock samples (either intrusive or volcanic), as each age probably reflects the time when its rock cooled through the 200°C crustal isotherm (*e.g.* Harrison *et al.*, 1979). It is convenient to consider separately, the data obtained for the Cache Creek Terrane, the Whitehorse trough, and the Coast plutonic complex.

CACHE CREEK TERRANE

Figure 1-14-3 shows all apatite fission-track ages measured in this study, including plots of apatite fission-track age versus sample elevation for Mount Hitchcock, on the eastern shore of Atlin Lake, and Mount Minto, 5 kilometres from Mount Hitchcock on the western shore. It is apparent

TABLE 1-14-3
SUMMARY OF ZIRCON FISSION-TRACK ANALYSES

Sample	ρ_s^a	N	ρ_i^a	N	ρ_d^a	N	Grains	Chi ²	Test ^b	Fission Track Age ^c (Ma)
Cache Creek Terrane										
Como Lake										
8403-1	35.2	650	25.6	474	1.46	15879	7	9.78	PASS	128±8.7
Mount Hitchcock										
8403-2	24.4	501	17.4	358	1.48	15879	8	7.60	PASS	132±10
8403-3	22.7	467	10.2	210	1.49	15879	10	6.72	PASS	210±19
8403-4	26.6	546	13.2	271	1.52	15879	10	9.78	PASS	194±16
8403-5	22.3	549	10.6	261	1.53	15879	10	12.2	PASS	204±17
8403-6	25.8	424	11.7	192	1.53	15879	8	10.5	PASS	215±20
Mount Minto										
8403-7	24.6	405	11.9	195	1.46	15879	8	10.3	PASS	193±18
8403-8	29.7	549	17.6	325	1.47	15879	8	11.1	PASS	158±12
8403-9	28.5	410	19.8	284	1.48	15879	7	10.1	PASS	136±11
8403-10	34.3	282	18.3	150	1.51	15879	2	0.29	PASS	180±19
8403-11	30.5	438	17.1	246	1.52	15879	5	14.4	FAIL	155±25
8403-12	28.2	58	11.2	23	1.47	15879	2	3.11	PASS	235±58
Whitehorse Trough										
Tagish Lake										
8403-13	11.6	119	13.0	134	1.48	15879	4	0.35	PASS	84.4±10.9
8403-14	15.0	154	10.7	110	1.49	15879	4	0.49	PASS	133±17
Jack Peak										
8403-21	22.6	278	26.9	331	1.53	15879	6	1.60	PASS	82.5±7.2
8403-22										n.m.
8403-23										n.m.
8403-24	23.4	240	28.1	289	1.48	15879	4	1.29	PASS	79.0±7.3
8403-25										n.m.
8403-26	20.7	213	25.2	259	1.52	15879	4	0.90	PASS	80.1±7.8
Coast Plutonic Complex										
White Moose Mountain										
8403-15										n.m.
8403-16	8.15	201	10.6	261	1.52	15879	6	2.72	PASS	75.0±7.4
8403-17										n.m.
8403-18	15.3	63	29.9	123	1.48	15879	2	1.98	PASS	48.6±7.7
8403-19										n.m.
8403-20										n.m.
White Pass										
8403-28	13.8	170	33.0	407	1.48	15879	6	4.77	PASS	39.6±3.8

^a in units of 10⁶ tracks/cm²

^b pass or fail at the 95% confidence level for Chi² calculated using the method of Galbraith (1981)

^c zeta calibration factor 129.0±3.8 relative to neutron dosimeter glass standard CN-1; ages determined using the criteria of Green (1981); error given as 1 standard deviation; n.m. = not measured

from these data that opposite sides of northern Atlin Lake experienced markedly different Mesozoic to Cenozoic cooling histories. Apatite fission-track ages for Mount Hitchcock range from 47.0±4.0 Ma to 79.9±5.2 Ma (one standard deviation). Mount Minto, however, exhibits significantly older apatite fission-track ages, ranging from 83.8±5.5 Ma to 158±14 Ma. The Mount Hitchcock samples and the three lowest elevation samples from Mount Minto (samples 8403-7, 8, 9) are from the Black Mountain body, as mapped by Aitken (1959). The zircon fission-track ages for these samples range from 132±10 Ma to 215±20 Ma (Figure 1-14-4), indicating this intrusion is no younger than Triassic. The volcanic rocks that cap Mount Minto (samples 8403-10, 11, 12) exhibit zircon fission-track ages that range from 155±25 Ma to 235±58 Ma (Figure 1-14-4) indicating that these rocks are at least Mesozoic in age.

WHITEHORSE TROUGH

Figure 1-14-3 also contains a plot of apatite fission-track age versus sample elevation for Jack Peak, an intrusion into Whitehorse trough stada for which Bultman (1979) reports a K-Ar biotite age of 90±3.0 Ma. The fission-track ages range from 46.7±4.3 Ma to 92.4±12.3 Ma, similar to those observed for Mount Hitchcock in the Cache Creek Terrane. In contrast, two Lower Jurassic Laberge Group samples from the western shore of Tagish Lake (samples 8403-13 and 14; Figure 1-14-2) yield apatite fission-track ages of 98.1±10.1 Ma and 100±11 Ma respectively (Figure 1-14-3), significantly older than those for Jack Peak. The zircon fission-track ages for the Jack Peak samples range from 79.0±7.3 Ma to 82.5±7.2 Ma (Figure 1-14-4). The Laberge Group samples yield zircon fission-track ages of 84.4±10.9 Ma and 133±17 Ma respectively (Figure

1-14-4), significantly younger than their depositional ages indicating that these rocks experienced postdepositional temperatures in excess of approximately 200°C.

COAST PLUTONIC COMPLEX

The apatite fission-track age versus sample elevation plot for White Moose Mountain is included in Figure 1-14-3. The ages range from 48.3 ± 4.6 Ma to 63.7 ± 4.9 Ma, representing the youngest age range of the vertical suites analyzed. The zircon fission-track ages for these samples range from 39.6 ± 3.8 Ma to 75.0 ± 7.4 Ma (Figure 1-14-4).

DISCUSSION

The results summarized above, in particular the apatite fission-track ages, indicate that the Whitehorse trough in the vicinity of Tagish Lake, and part of the Cache Creek Terrane near Mount Minto, experienced a different cooling history relative to surrounding areas. The differential cooling, evidenced by the zone of 100 Ma fission-track ages at low elevations along Tagish Lake and at Mount Minto (at or below 920 metres above m.s.l.; Table 1-14-1), most likely resulted from differential vertical motion in the region between approximately 100 Ma and 50 Ma. It appears that an as yet unrecognized structure beneath the northern part of Atlin Lake forms the eastern boundary of this zone of 100 Ma apatite-cooling ages. The western boundary may be the Llewellyn fault, but this has yet to be proven. Mihalynuk and Hart (in press) document at least 100 kilometres of dextral motion on the Llewellyn fault zone – Tally Ho shear zone coincident with the boundary between Stikine Terrane to the east and Nisling Terrane to the west. Furthermore, these authors state that “thick accumulations of coarse clastic sedimentary rocks of the Lower Jurassic Whitehorse trough overlie the Stikine Terrane, but are thin and discontinuously exposed west of the fault zone on the Nisling Terrane.” Greater erosion on the west side of the Llewellyn fault zone between 100 Ma and 50 Ma would account for both the fission track data summarized here and the greater preservation of Whitehorse Trough strata on the east side.

Our current research in this region is aimed at delimiting the zone of 100 Ma apatite fission-track ages along southern Tagish Lake. If this zone includes the Engineer mine, it may be possible to determine the timing of mineralization at this historically important deposit. Preliminary fluid-inclusion data from the Engineer deposit indicate homogenization temperatures of approximately 185°C, sufficient to completely anneal fission tracks in apatite (M. Mihalynuk, personal communication, 1990). If the hydrothermal activity was localized near the Engineer deposit and occurred post-100 Ma, apatites from country rocks heated by these fluids will yield fission-track ages less than 100 Ma, indicating the timing of mineralization.

ACKNOWLEDGMENTS

Fieldwork in 1990 was supported by British Columbia Ministry of Energy, Mines and Petroleum Resources Grant RG90-23. The authors wish to thank Mitch Mihalynuk,

Keith Mountjoy, Jim Brook and Miriam Brook for their support and assistance in the field and Mai Nguyen for her excellent drafting assistance.

REFERENCES

- Aitken, J.D. (1959): Atlin Map-area, British Columbia; *Geological Survey of Canada*, Memoir 307, 83 pages.
- Brew, D.A. (1988): Latest Mesozoic and Cenozoic Igneous Rocks of Southeastern Alaska — a Synopsis; *U.S. Geological Survey*, Open-File Report 88-405, 29 pages.
- Bultman, T.R. (1979): Geology and Tectonic History of the Whitehorse Trough West of Atlin, British Columbia; unpublished Ph.D. thesis, *Yale University*, New Haven, Connecticut, 284 pages.
- Christie, R.L. (1957): Bennett, British Columbia; *Geological Survey of Canada*, Map 19-1957 with descriptive notes.
- Currie, L.D. (1990): Metamorphic Rocks in the Florence Range, Coast Mountains, Northwestern British Columbia; *B.C. Ministry of Energy, Mines and Petroleum Resources*, Geological Fieldwork 1989, Paper 1990-1, pages 197-203.
- Dickie, J.R. (1989): Sedimentary Response to Arc-Continent Transpressive Tectonics, Laberge Conglomerates (Jurassic), Whitehorse Trough, Yukon Territory; unpublished M.Sc. thesis, *Dalhousie University*, Halifax, Nova Scotia, 361 pages.
- Donelick, R.A. (1986): Mesozoic-Cenozoic Thermal Evolution of the Atlin Terrane, Whitehorse Trough, and Coast Plutonic Complex from Atlin, British Columbia to Haines, Alaska as Revealed by Fission Track Geothermometry Techniques; unpublished M.Sc. thesis, *Rensselaer Polytechnic Institute*, Troy, New York, 167 pages.
- Donelick, R.A. (1988): Etchable Fission Track Length Reduction in Apatite: Experimental Observations. Theory and Geological Applications; unpublished Ph.D. thesis, *Rensselaer Polytechnic Institute*, Troy, New York, 414 pages.
- Donelick, R.A. and Miller, D.S. (1986): Low-temperature Geothermometry of the Coast Plutonic Complex, Whitehorse Trough and Atlin Terrane from Atlin, B.C. to Haines, AK; *Geological Society of America*, Abstracts with Programs, Volume 18, page 102.
- Eisbacher, G.H. (1974): Evolution of Successor Basins in the Canadian Cordillera; *Society of Economic Paleontologists and Mineralogists*, Special Publication 19, pages 274-291.
- Galbraith, R.F. (1981): On Statistical Models for Fission Track Counts; *International Association of Mathematical Geology*, Journal, Volume 13, pages 471-478.

- Gehrels, G.E., Brew, D.A. and Saleeby, J.B. (1984): Progress Report on U/Pb (Zircon) Geochronologic Studies in the Coast Plutonic-Metamorphic Complex East of Juneau, Southeastern Alaska; in *The United States Geological Survey in Alaska: Accomplishments during 1982*; K.M. Reed and S. Bartsch-Winkler, Editors, *U.S. Geological Survey, Circular 939*, pages 100-102.
- Green, P.F. (1981): A New Look at Statistics in Fission-track Dating; *Nuclear Tracks*, Volume 5, pages 77-86.
- Green, P.F., Duddy, I.R., Gleadow, A.J.W., Laslett, G.M. and Tingate, P.R. (1986): Thermal Annealing of Fission Tracks in Apatite - A Qualitative Description; *Chemical Geology (Isotope Geoscience Section)*, Volume 59, pages 237-253.
- Harrison, T.M., Armstrong, R.L., Naeser, C.W. and Harakal, J.E. (1979): Geochronology and Thermal History of the Coast Plutonic Complex, near Prince Rupert, British Columbia; *Canadian Journal of Earth Sciences*, Volume 16, pages 400-410.
- Laslett, G.M., Kendall, W.S., Gleadow, A.J.W. and Duddy, I.R. (1982): Bias in Measurement of Fission-track Length Distributions; *Nuclear Tracks*, Volume 6, pages 79-85.
- Mihalynuk, M.B., Currie, L.D. and Arksey, R.L. (1989a): Geology of the Tagish Lake Area (Fantail Lake and Warm Creek, 104M/9W and 10E); *B.C. Ministry of Energy, Mines and Petroleum Resources*, Geological Fieldwork 1988, Paper 1989-1, pages 293-310.
- Mihalynuk, M.B., Currie, L.D., Mountjoy, K. and Wallace, C. (1989b): Geology of the Fantail Lake (West) and Warm Creek (East) Map Area (NTS 104M/9W and 10E); *B.C. Ministry of Energy, Mines and Petroleum Resources*, Open File 1989-13.
- Mihalynuk, M.B. and Hart, C.J.R. (in press): Constraints on Timing, Styles and Amount of Offset on the Llewellyn Fault - Tally Ho Shear System; *Geology*.
- Mihalynuk, M.B. and Mountjoy, K.J. (1990): Geology of the Tagish Lake Area (104M/8, 9E); *B.C. Ministry of Energy, Mines and Petroleum Resources*, Geological Fieldwork 1989, Paper 1990-1, pages 181-196.
- Mihalynuk, M.B., Mountjoy, K.J., Currie, L.D., Lofthouse, D.L., and Winder, N. (1990): Geology and Geochemistry of the Edgar Lake and Fantail Lake Map Area NTS (104M/8, 9E); *B.C. Ministry of Energy, Mines and Petroleum Resources*, Open File 1990-4.
- Mihalynuk, M.G. and Rouse, J.N. (1988a): Preliminary Geology of the Tutshi Lake Area, Northwestern British Columbia (104M/15); *B.C. Ministry of Energy, Mines and Petroleum Resources*, Geological Fieldwork 1987, Paper 1988-1, pages 217-231.
- Mihalynuk, M.B. and Rouse, J.N. (1988b): Geology of the Tutshi Lake Area (104M/15); *B.C. Ministry of Energy, Mines and Petroleum Resources*, Open File 1988-5.
- Monger, J.H.W. (1977): Upper Paleozoic Rocks of the Western Canadian Cordillera and their bearing on Cordilleran Evolution; *Canadian Journal of Earth Sciences*, Volume 14, pages 1832-1859.
- Naeser, C.W. and Forbes, R.B. (1976): Variation of Fission Track Ages with Depth in Two Deep Drill Holes (abstract); *EOS*, Volume 57, page 363.
- Parrish, R.R. (1982): Cenozoic Thermal and Tectonic History of the Coast Mountains of British Columbia as Revealed by Fission Track and Geological Data and Quantitative Thermal Models; unpublished Ph.D. thesis, *The University of British Columbia*, 166 pages.
- Parrish, R.R. (1983): Cenozoic Thermal Evolution and Tectonics of the Coast Mountains of British Columbia - Fission Track Dating, Apparent Uplift Rates, and Patterns of Uplift; *Tectonics*, Volume 2, pages 601-631.
- Parrish, R.R., Carr, S.D. and Parkinson, D.L. (1988): Eocene Extensional Tectonics and Geochronology of the Southern Omineca Belt, British Columbia and Washington; *Tectonics*, Volume 7, pages 181-212.
- Sevigny, J.H., Parrish, R.R., Donelick, R.A. and Ghent, E.D. (1990): Northern Monashee Mountains, Omineca Crystalline Belt, British Columbia: Timing of Metamorphism, Anatexis, and Tectonic Denudation; *Geology*, Volume 18, pages 103-106.

**HIGHLIGHTS OF 1990 FIELDWORK IN THE ATLIN AREA
(104N/12W)**

By M.G. Mihalynuk, K.J. Mountjoy, W.J. McMillan,
C.H. Ash and J.L. Hammack

KEYWORDS: Regional geology, Cache Creek complex, Peninsula Mountain suite, Graham Creek suite, Laberge Group, Sloko Group, Fourth of July batholith, Nahlin fault, isotopic age, rare-earth elements, geochemistry, gold, metallogeny.

INTRODUCTION

Fieldwork in the Atlin area was confined to a four-week period in 1990. About two weeks were spent on reconnaissance mapping of the western half of the Atlin 1:50 000 map-sheet (104N/12W) incorporating mapping done in 1989 as part of a study by Bloodgood and Bellefontaine (1990). The contact zone between the Cache Creek Terrane and terranes to the west is exposed in this half map-sheet (Figure 1-15-1). This paper focuses on geological highlights of mapping along the contact zone and presents new rare-earth element data, anomalous geochemical gold analyses and previously unpublished isotopic age data.

GENERAL GEOLOGIC SETTING

The geology of the area is dominated by three lithotectonic packages. From east to west these are: oceanic crustal rocks and overlying sediments of the Triassic to Mississippian Cache Creek complex; probable Middle to Upper Triassic intermediate to felsic volcanic-arc strata of the Peninsula Mountain suite, and Lower to Middle Jurassic sedimentary rocks of the Laberge Group. In the southern part of the map area the Cache Creek rocks are juxtaposed against the Laberge Group across the Nahlin fault. To the north, the Peninsula Mountain volcanic package separates these packages and displays structural and stratigraphic relationships with both the Laberge Group and Cache Creek complex. The Fourth of July batholith intrudes deformed Cache Creek Complex and probable Peninsula Mountain lithologies. All of these rocks are overlain by at least two younger volcanic suites.

PREVIOUS WORK

A more regional geological perspective can be found in Cairns (1913), Aitken (1959) and Bultman (1979). Geology west of NTS mapsheet 104N/12W is covered by Mihalynuk *et al.* (1988a,b; 1989a,b; 1990), Mihalynuk and Mountjoy (1990) and Mihalynuk and Rouse (1988a,b), and to the immediate east by Ash and Arksey (1990b). Geological data compiled in Figure 1-15-2 were augmented in specific areas by property-scale mapping (Aspinall, 1969; Anuik, 1970).

CACHE CREEK COMPLEX

“Cache Creek complex” is used here in preference to the more commonly used “Cache Creek Group” as component units include rocks of sedimentary, volcanic, metamorphic (ultramafic) and structural (fault mélangé) origin.

Within the complex, units are generally fault bounded and vary in dimension from just a few metres to several kilometres. In 104N/12W, Cache Creek lithologies include

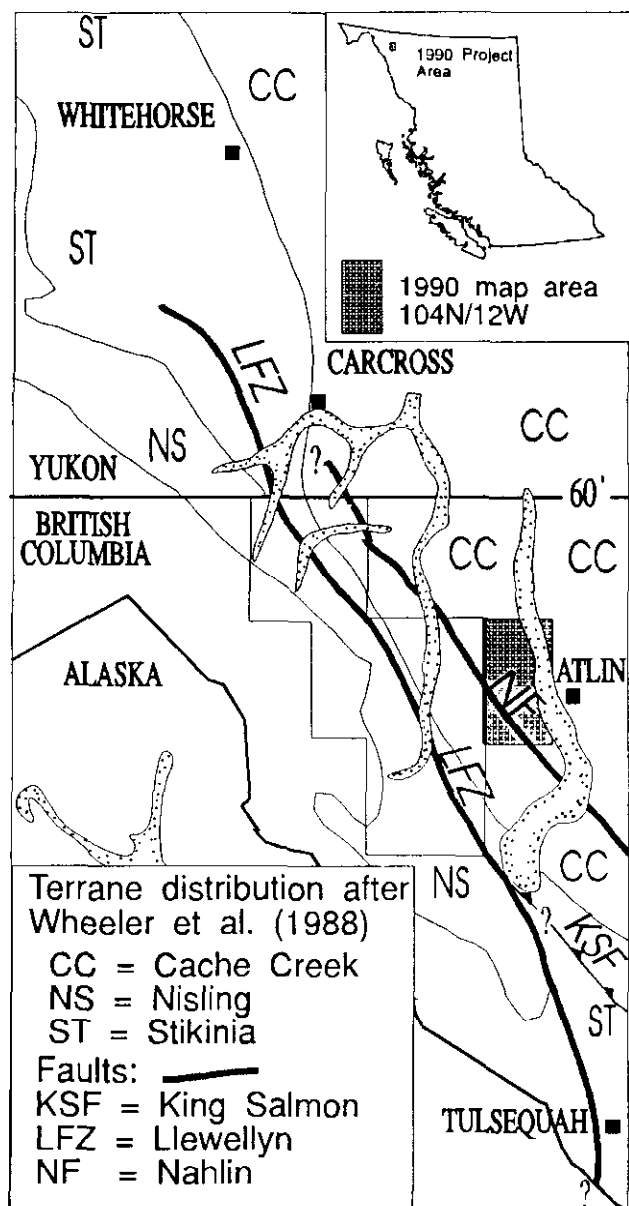
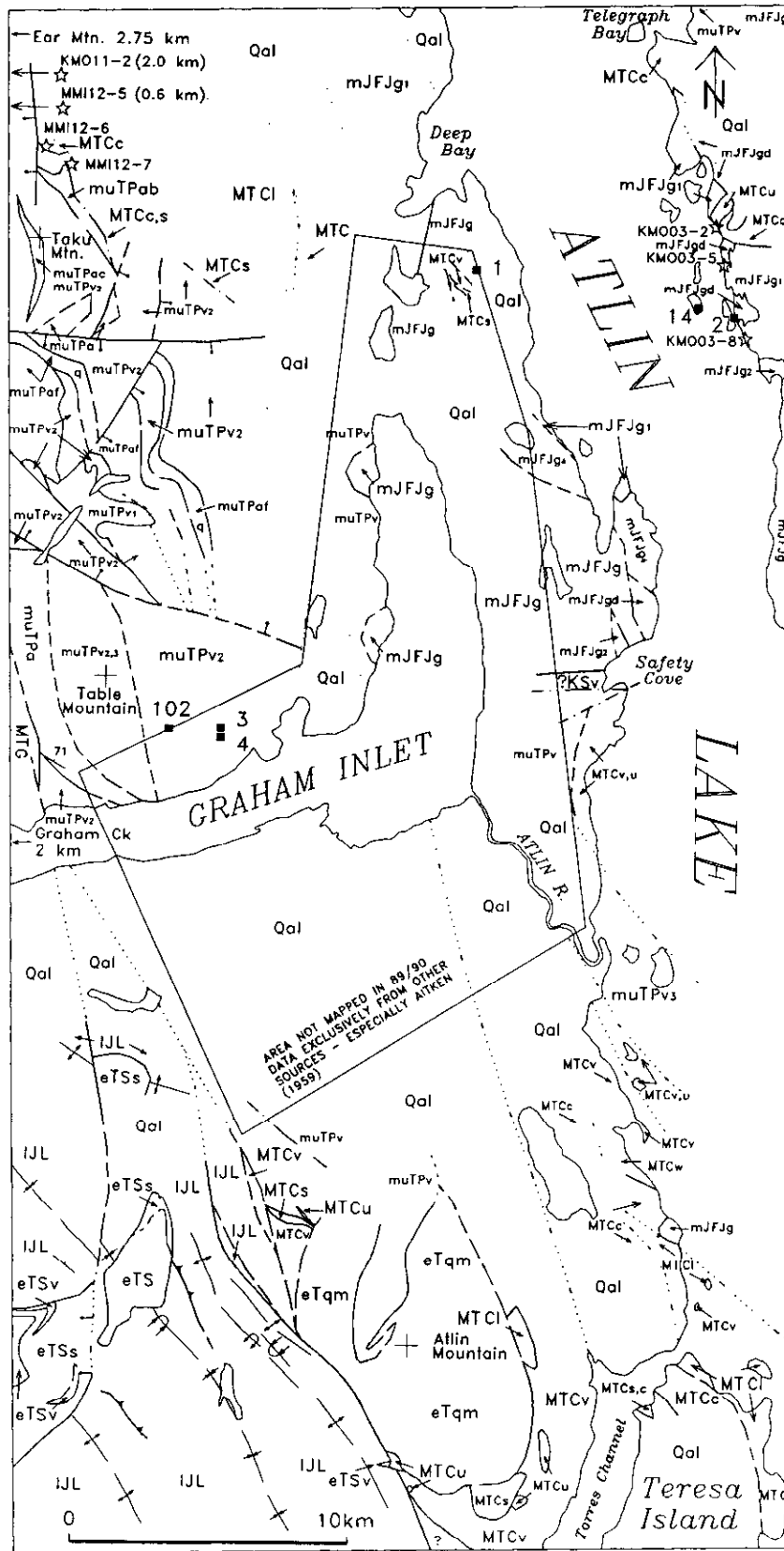


Figure 1-15-1. Tectonic elements of northwestern British Columbia in the vicinity of 104N/12W.



LEGEND

Layered Rocks

- Qal** unconsolidated glacial fill and poorly sorted alluvium
- eTS** Sloko Group - undivided
 - eTSs** wacke and conglomerate
 - eTSv** felsic tuff, flows, ignimbrite
- ?KSv** Safety Cove volcanic suite
- IJL** Laberge Group - undivided; mainly interbedded wackes and argillites
- muTPv** Peninsula Mountain Volcanic-Sedimentary suite
 - muTPa** feldspar rhyolite flows and breccias
 - muTPaf** feldspar-quartz-biotite ash flows; q=quartz
 - muTPac** volcanic sandstone and conglomerate
 - muTPab** basal rhyolite breccia & small domes? +/- chert fragments
 - muTPv3** coarse, mainly monolithologic lahar? & interbedded sediments
 - muTPv2** varicolored, feldspar-phyric lapilli tuff & breccia
 - muTPv1** fragmentals; +/- pyroxene
- MTG** Graham Creek suite - undivided
- MTC** Cache Creek Group - undivided
 - MTCc** chert; well bedded with argillite or massive
 - MTCi** massive recrystallized limestone
 - MTCs** sediments - undivided or mixed
 - MTCv** generally fine grained mafic volcanic flows and breccia
 - MTCw** quartz and chert-rich wackes (probably mid to Upper Triassic)
 - MTCu** Cache Creek - hornburgites & dunites

Intrusive Rocks

- eTqm** Atlin Mountain intrusive
- mJFJg** Fourth of July intrusive suite - quartz diorite to granite
 - mJFJg1** hornblende > biotite
 - mJFJg2** hornblende-rich
 - mJFJg3** biotite-rich
 - mJFJg4** K-feldspar megacrystic
 - mJFJgd** dark grey to light pink granite to diorite border phase; hbf & bt-rich

Symbols

- contacts defined, approximated, assumed
- Faults
- Intrusive
- Unconformable
- Conformable
- Quaternary limits
- Geochemical sample sites
- MINFILE localities

Figure 1-15-2. Generalized geological map of the Tagish area.

massive, white carbonate, chert, mint-green basalt breccia, harzburgite, dunite (and serpentinized equivalents), and a variety of clastic sediments including silty argillite and coarse quartz-bearing wackes.

Descriptions of lithologic units have been furnished previously by Monger (1975, regional geology and paleontology), Ash and Arksey (1990b, ultramafic rocks), and Bloodgood and Bellefontaine (1990, sedimentary rocks) among others, and are not reproduced here. However, quartz-rich strata within the Cache Creek complex are less well known in this region. Such strata are potentially very useful for establishing linkages between the oceanic Cache Creek Terrane and adjacent, more evolved crustal masses. An investigation of possible linkages is currently in progress.

GRAHAM CREEK IGNEOUS SUITE AND PENINSULA MOUNTAIN VOLCANIC SUITE: RELATIONS AND CORRELATIONS

Rocks of the Graham Creek and Peninsula Mountain suites form a northwest-trending belt beginning at Atlin Mountain, with best exposures on Table and Taku mountains. Along the northwest flank of the belt, tectonized harzburgite has a recurrent spatial association with chert and pillow basalt; together these rocks comprise the Graham Creek suite (Mihalynuk and Mountjoy, 1990). In most cases contacts between the two suites are verifiably faulted. There is some evidence for local stratigraphic continuity between the pillow basalts and lower Peninsula Mountain volcanics, but it is circumspect (*cf.* Mihalynuk and Mountjoy, 1990). Rare-earth element (REE) data emphasize the differences between the two suites. However, they represent two compositionally distinct volcanic packages, with the Peninsula Mountain volcanic rocks tending to be porphyritic and more felsic overall, such that preliminary REE data from the two suites (Figure 1-15-3) cannot be directly compared. The data do show that the Graham Creek pillow basalt and

gabbro fall in the centre of the mid-ocean ridge basalt (MORB) field of Saunders and Tarney (1979), confirming their genetic association with spatially affiliated tectonized harzburgites.

Within the Peninsula Mountain suite, widespread eruptive units, particularly quartz-phyric ash flows and other distinct lithologies, are marker horizons that allow for the development of a tentative stratigraphy consisting of six eruptive packages. Stratigraphic relationships are not simple as interfingering and onlapping of units is probably common.

At the base of the succession are green and light grey to tan, epidote and chlorite-altered, coarse, vesicular andesitic breccias containing medium-grained feldspar and sparse medium to coarse-grained pyroxene. These rocks are well exposed in a steep valley that dissects Table Mountain, where they stratigraphically underlie feldspar-phyric lapilli tuffs and abundant feldspar-quartz-biotite-phyric ash flows.

North of Table Mountain, fine to medium-grained tabular feldspar-phyric lapilli tuffs of intermediate composition are interfingering with, and underlie, ash flows. Maroon, green, and orange varieties may be locally foliated, particularly near their contacts with pyritic white rhyolite which occurs as small domes(?) or as chert-bearing breccias and interbedded epiclastics.

Ash flows are mauve, tan, grey and light green and generally display crude flow layering and lapilli elongation. Individual cooling units are generally homogeneous and monolithologic. Thin, well-bedded epiclastic interbeds are common.

The rhyolite unit separates the bulk of the volcanic strata from sediments of the Cache Creek Terrane. Lithologically it resembles younger rhyolites. It is, however, thought to be part of the Peninsula Mountain suite as the provenance of associated epiclastics (particularly chert cobbles) appears to be the same as for epiclastic beds within some of the oldest Peninsula Mountain lapilli tuffs. Relationships between the rhyolite breccia and other volcanics of the Middle to Upper Triassic package are illustrated in Figure 1-15-4.

Volcanic strata near the mouth of the Atlin River are included as part of the Peninsula Mountain suite on the basis of limited lithologic similarities. These rocks are relatively undeformed and may actually be younger than the Peninsula Mountain suite. They comprise massive, coarse, predominantly clast-supported laharic breccias and lesser pyroclastic units with minor interbeds of well-layered epiclastics which dip gently to moderately eastward. They are bordered on all sides by Cache Creek lithologies, although nowhere can the contact be observed directly.

Blocks within laharic units are typically rounded and of decimetre size, but range up to several metres diameter. They are generally of one or two compositions. Rounded, red, purple, orange or green andesitic blocks containing about 35 per cent fine to medium-grained, trachytically aligned feldspar are most common. Less common are white, grey or light green blocks which may be slightly more angular, are flow layered and have a planar fracture and a waxy fresh surface.

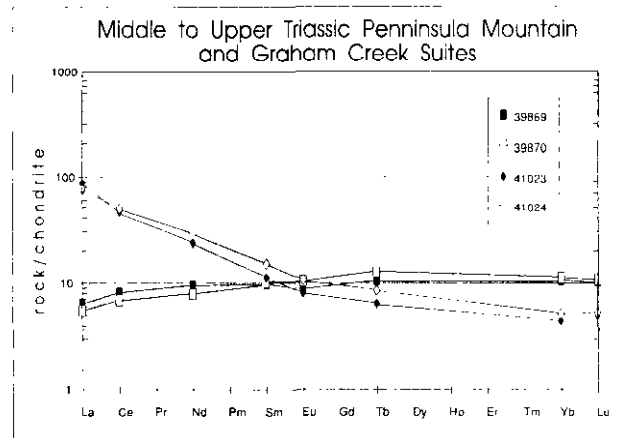


Figure 1-15-3. Chondrite normalized REE plot of selected samples from the Graham Creek igneous suite (squares) and the Peninsula Mountain volcanic suite (diamonds). Normalizing factors used are those of Nakamura (1974); the shaded MORB field is adapted from Saunders and Tarney (1979).

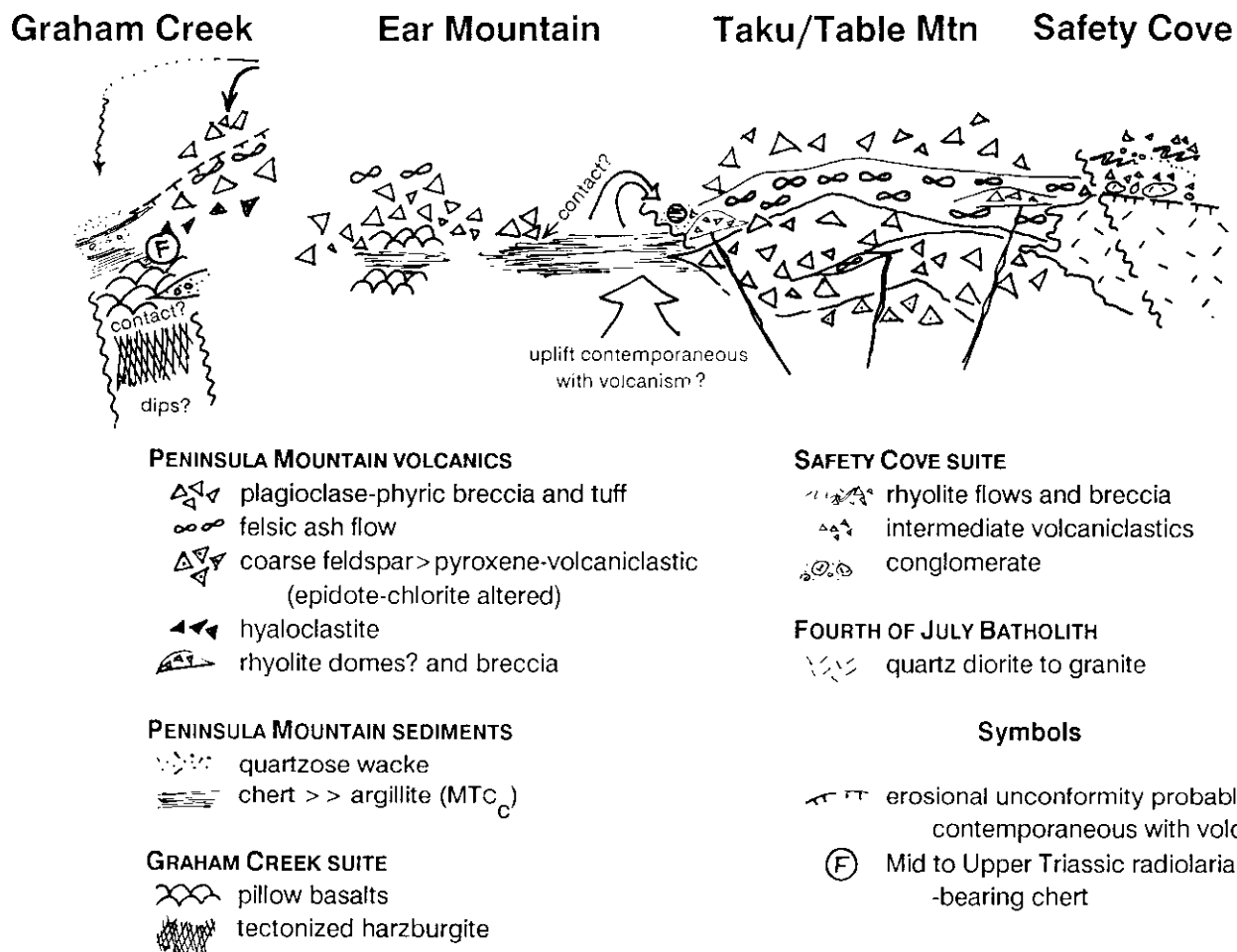


Figure 1-15-4. Schematic representation of stratigraphic relationships between the Peninsula Mountain suite and the Graham Creek suite which may both be partly correlative with rocks of the Cache Creek complex. (Especially tectonized harzburgite and cherts).

At the mouth of the Atlin River, pyroclastic breccia units from 1 metre to greater than 5 metres thick are interbedded with dense, ochre-coloured flows that have vesicular tops. Pyroclastic units are distinctive in that they incorporate abundant charred plant fragments. In places they appear to grade into flow-top breccia, but are otherwise quite similar in appearance to laharic units.

AGE AND CORRELATION

Just off the northwest corner of 104N/12W hornblende-quartz-phyric volcanoclastic rocks are interbedded with massive white to tan chert (Ear Mountain, Figure 1-15-4). A few kilometres to the southwest, well-bedded, tan chert is interbedded with coarse quartz, feldspar and hornblende-bearing wackes probably derived from the volcanics. These well-bedded cherts yield radiolarians identified by Cordey (1990) as Middle to Upper Triassic age. Pyroclastic rocks associated with the massive cherts are believed to be part of the intermediate and felsic Peninsula Mountain suite volcanics. At Telegraph Bay, Peninsula Mountain volcanic

strata are thermally metamorphosed by the 171 Ma Fourth of July batholith. The same intrusive relationship is shown by Aitken (1959) on northern Graham Inlet; such relationships support the Middle to Upper Triassic age of these rocks. Furthermore, the Peninsula Mountain suite shares many characteristics with the Upper Triassic massive sulphide bearing Kutcho Formation in the Dease Lake area (Thorstad and Gabrielse, 1986; Mihalynuk and Mountjoy, 1990).

Despite a growing body of geological evidence that indicates a Middle to Upper Triassic age for the Peninsula Mountain suite, a Rb-Sr isochron, defined largely on the basis of a sample collected from Table Mountain, returned an age of 72.4 ± 2.1 Ma (Grond *et al.*, 1984). At present we are unable to accommodate this date. We do not recognize a separate, younger volcanic package above the Peninsula Mountain suite, nor are we able to reasonably apply this date to the Peninsula Mountain suite as a whole. We suspect that either the sample was atypical, either a dike or a fault sliver, or it is chemically aberrant (perhaps altered).

FOURTH OF JULY BATHOLITH AND RELATED DIKES

Just north of the town of Atlin, the Fourth of July batholith underlies an area of approximately 650 square kilometres. In the map area, this polyphase intrusive body is composed primarily of pink granite, granodiorite and monzonite. Zoning is apparent with varying abundances of porphyritic potassium feldspar, biotite and hornblende. Zoning is particularly evident near the margins, where biotite and, to a lesser degree, hornblende are much more abundant within a monzodiorite or monzonite phase (*cf.* Aitken (1959) for a more detailed description).

Everywhere the batholith is crosscut by dikes that are thought to be residuals of late-stage magmatic intrusion. These dikes generally have the same composition as the more mafic portions of the batholith. Very biotite-rich varieties have a distinctive knobby weathering habit in which sparse, pink feldspar clots (xenocrysts? or immiscible droplets) may form resistant spikes. Dikes are typically 0.3 to 3 metres thick and trend 315° with moderately steep dips to the east. They comprise 10 to 20 per cent of the outcrop volume and extend into the Cache Creek section where abundance decreases and their orientation is less consistent.

AGE OF FOURTH OF JULY BATHOLITH

Until recently an inferred Jurassic age for the Fourth of July batholith was based on relative geologic age constraints (Aitken, 1959). Bloodgood *et al.* (1989) referenced K-Ar (hornblende and biotite) dates of 110 ± 4 and 73.3 ± 2.6 Ma from rocks collected within 150 metres of the younger Surprise Lake batholith by Christopher and Pinsent (1982). In the latter paper Christopher and Pinsent list these dates in "Table 2. K/Ar Ages from the Surprise Lake Batholith" and they are indicated as having been obtained from a sample with "Reference Number A-KAR-5". The same sample is listed in their "Table 1" of whole-rock geochemical data where it is labelled "Fourth of July" and displays a geo-

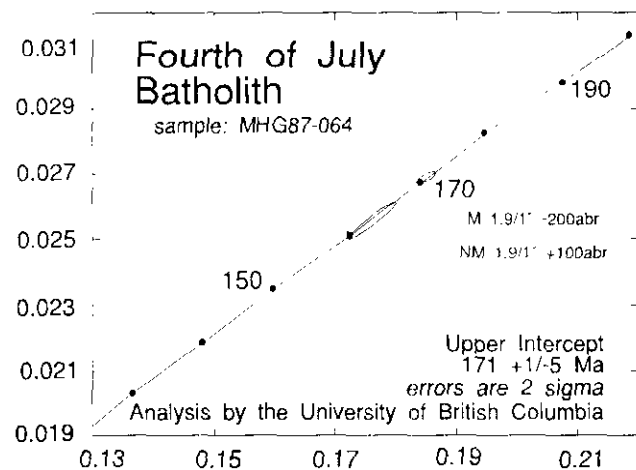


Figure 1-15-5. Concordia plot for clear, colourless, euhedral, doubly terminated zircons of the Fourth of July batholith (analyzed by The University of British Columbia). Analyses of both fractions are essentially concordant giving a $^{206}\text{U}/^{238}\text{Pb}$ date of 171 ± 5 Ma.

chemical signature that is radically different from other samples from the Surprise Lake batholith. Their written location description of Sample A-KAR-5 places it as part of the Fourth of July batholith on both their map and the map of Sutherland Brown (1970). Thus, these data do appear to have been derived from Fourth of July rocks as inferred by Bloodgood *et al.*; however, as implied by Christopher and Pinsent, the ages probably reflect resetting during the intrusion of the nearby Surprise Lake batholith.

Donelick (1988) determined a zircon fission-track age of 215 ± 20 Ma from the Fourth of July batholith at Mount Hitchcock and 193 ± 18 Ma and 128 ± 8.7 Ma were acquired from other Fourth of July localities. This Upper Triassic age indicates the time at which these rocks cooled through 200°C and, if not misrepresentative, should be the minimum age of the intrusive body. However, a sample collected by the Geological Survey Branch recently returned a concordant U-Pb zircon date of 171 ± 5 Ma. These new data, shown in Figure 1-15-5, are thought to most accurately reflect the age of the Fourth of July batholith and most closely replicate the early age assignment of Aitken (1959) based upon geological relationships. However, since the Fourth of July batholith is a composite intrusive body, some variability in the isotopic age data is to be expected.

TECTONIC IMPLICATIONS

In the northeast corner of 104M/12W, intermediate and felsic pyroclastic rocks, like those on Atlin Mountain, sit adjacent to well-bedded, deformed ribbon cherts of the Cache Creek complex (contact not exposed). Both are thermally metamorphosed and crosscut by the Fourth of July batholith as well as later dikes which also extensively cut the batholith. This association indicates that: the volcanic rocks are older than 171 Ma; unless the Fourth of July batholith is decapitated, it represents a pin point that pierced the Cache Creek succession (which is apparently a stack of thrust slices) during the Middle Jurassic and limits the age of ophiolite emplacement to before this time; North of Atlin volcanic and batholithic rocks cross Atlin Lake, indicating no major structural offset across this portion of the lake since the Middle Jurassic. Thus, any major post-Middle Jurassic motion must have been accommodated along the northward continuation of the Nahlin fault (Mihalynuk *et al.*, 1990).

Within a few hundred metres south of Safety Cove, biotite-rich dikes of the Fourth of July suite are not only offset by extensive high-angle brittle faults, but also cut these fault planes. Clearly this style of deformation accompanied late stages of Fourth of July batholith emplacement. Furthermore, a very consistent dike swarm orientation of about $315^\circ/75^\circ\text{E}$ suggests crustal extension of 10 to 20 per cent southwestward during their emplacement.

JURASSIC TO TERTIARY VOLCANIC SUITES

Two separate packages of volcanic strata appear to post-date the Fourth of July batholith. At Safety Cove, a deformed package of volcanic rocks has obscure contacts

TABLE 1-15-1
REGIONAL GEOCHEMICAL SURVEY RESULTS*

Sample Number	Easting	Northing	NTS 104 . . .	Au ppb	Ag ppm	Cu ppm	Pb ppm	Zn ppm	Co ppm	As ppm	Sb ppm	Ba ppm
KMO90-3-2B	569000	6620100	N12/W	7	<5	22	4	37	36	36	7.5	1900
KMO90-3-5	569150	6619400	N12/W	6	<5	80	41	110	41	41	0.5	3700
KMO90-3-8	569550	6618050	N12/W	6	<5	43	11	72	42	42	0.3	1500
KMO90-11-2	554100	6622750	M/9E	37	<5	4	15	71	17	17	6.2	8600
MMI90-12-5	555450	6622150	M/9E	<5	<5	6	41	217	27	9	1.6	250
MMI90-12-6	556775	6621450	N12/W	1510	<5	11	13	27	100	9	8.9	270
MMI90-12-7	557250	6621125	N12/W	<5	<5	9	19	26	28	13	0.9	1800

* Au and Ba determinations by NAA, all others by AAS.

Note the anomalous gold values obtained in an argillite-quartz breccia in the contact zone between Cache Creek Complex and Peninsula Mountain suites (MMI90-12-6).

and can not be reliably correlated, whereas, in west-central 104N/12W, undeformed volcanic rocks of the Sloko Group can be correlated with certainty.

SAFETY COVE VOLCANIC SUITE

Probably the oldest of the two volcanic packages crops out on the western shore of Atlin Lake, at Safety Cove. These rocks vary compositionally from dark, andesitic(?), nonporphyritic ash and sparse-lapilli tuffs, to rhyolite flows and breccia. Where well exposed they are extensively crosscut by dikes of equally variable composition.

The age of these rocks is not established, but is partly constrained by their relationship to the Fourth of July batholith. At Safety Cove, a significantly altered biotite-rich border phase of the batholith shares an enigmatic contact with structurally overlying and generally fine-grained, brown and green tuffs with sparse fragmental texture. Locally these rocks are highly strained and appear, in places, to contain blocks of the Fourth of July border phase. Several metres "above" the contact zone, a white rhyolite breccia displays thin (<10 cm) epiclastic interbeds containing altered biotite-rich pebbles, presumably derived from the mafic border phase. It appears then, that though the contact is now deformed, originally it was probably an unconformity. Thus, alteration of the Fourth of July batholith at Safety Cove is probably due to weathering at or beneath an erosional surface, and rounded blocks of border phase intrusive are probably conglomerate boulders, not milled fault blocks. If this is correct, Safety Cove volcanics are post-Middle Jurassic in age and their unconformable contact with the Fourth of July batholith, like many other unconformities within the Tagish area, is rather strongly deformed.

SLOKO GROUP

The Sloko Group are the youngest rocks recognized in 104N/12W where they occur as erosional remnants on several of the highest mountains. They are composed mainly of rhyolite and derived epiclastic strata and rest on a well-exposed, deeply incised paleosurface on deformed Laberge Group strata. Numerous rhyolite dikes cutting the Laberge Group probably represent feeders to the Sloko rhyolite. Except where involved in high-angle faulting, they are flat-lying and undeformed.

Contact relationships, composition and the flat-lying nature of these strata are diagnostic. There is little doubt that they correlate with the main mass of Sloko Group rocks at the south end of Atlin Lake.

METALLOTECTS IN 104N/12W

Metallotects of particular interest within 104N/12W include altered ultramafic rocks, deep-seated faults, and acid volcanic rocks that may in part be submarine.

Fault-bounded, carbonatized serpentinites along the west shore of Atlin Lake are potential candidates for the ultramafic lode gold association that is thought to be the source of placer gold in the Atlin camp (Ash and Arksey, 1990a, b). Of note, but not shown in Table 1-15-1, are analyses from a northwest-trending belt of pillow basalts mapped as the Peninsula Mountain Group by Mihalynuk *et al.* (1990). Unaltered samples of these rocks yield high background gold values and, in combination with carbonatized ultramafics, may be the ultimate sources for the placer gold in Graham Creek. Along-strike continuation of these rocks may also explain a delapidated sluice operation on the unnamed drainage northwest of Graham Creek (UTM 551450, 6615900).

Deep-seated faults such as the Nahlin (*cf.* Mihalynuk and Mountjoy, 1990; Mihalynuk *et al.*, 1990), and perhaps related structures at the eastern margin of Peninsula Mountain suite exposures, are metallotects with largely undetermined potential. A silicified breccia zone of untested extent marks the contact between volcanic rocks on Taku Mountain and cherts and argillites of the Cache Creek complex (Figure 1-15-2). A single sample collected from the breccia yielded a gold assay of 1510 ppb (Table 1-15-1). Motion in this zone is difficult to assess. It could be regional in scale or merely localized at the contact of contrasting lithologies.

Also near the eastern boundary of the Peninsula Mountain suite are small pyritic rhyolite domes(?) and breccia bodies closely associated with argillite and chert of the Cache Creek complex. Although the exact relationship between the two lithotectonic packages is not clear, the setting contains many of the lithologic elements typical of a Kuroko deposit setting (*e.g.* Urabe and Sato, 1978). Tentative correlation of the Peninsula suite with the Kutcho Formation, host to the Kutcho Creek massive sulphide

deposit (Thorstad and Gabrielse, 1986), underscores the importance of these strata as a potential metallotect.

ACKNOWLEDGMENTS

This paper has benefited from discussions with Craig Hart and Jay Jackson. Norm Graham of Capital Helicopters Inc., in his typical good style, helped us make the best use of a short field season and a limited budget. Dave Lefebure and Mike Gunning collected a sample of the Fourth of July batholith for isotopic age dating, and Dave kindly agreed to have the date published in this paper.

REFERENCES

- Aitken, J.D. (1959): Atlin Map-area, British Columbia; *Geological Survey of Canada*, Memoir 307, 89 pages.
- Anuik, E.L. (1970): Geological Report on the Deep Bay Uranium Property, Atlin Area; *B.C. Ministry of Energy, Mines and Petroleum Resources*, Assessment Report 2786, 16 pages, appendices and maps.
- Ash, C.H. and Arksey, R.L. (1990a): The Listwanite-Lode Gold Association in British Columbia; *B.C. Ministry of Energy, Mines and Petroleum Resources*, Geological Fieldwork 1989, Paper 1990-1, pages 359-364.
- Ash, C.H. and Arksey, R.L. (1990b): The Atlin Ultramafic Allochthon: Ophiolitic Basement Within the Cache Creek Terrane; Tectonic and Metallogenic Significance (104N/12); *B.C. Ministry of Energy, Mines and Petroleum Resources*, Geological Fieldwork 1989, Paper 1990-1, pages 365-374.
- Aspinall, N.C. (1969): Report on Mapping and Scintillometer Survey, the Norsk-Sally-Balm Claims, Burnt Creek Area; *B.C. Ministry of Energy, Mines and Petroleum Resources*, Assessment Report 2118, 11 pages, appendices and maps.
- Bloodgood, M.A., Rees, C.J. and Lefebure, D.V. (1989): Geology and Mineralization of the Atlin Area, Northwestern British Columbia (104N/11W and 12E); *B.C. Ministry of Energy, Mines and Petroleum Resources*, Geological Fieldwork 1988, Paper 1989-1, pages 311-322.
- Bloodgood, M.A. and Bellefontaine, K.A. (1990): The Geology of the Atlin Area (Dixie Lake and Teresa Island 104N/6 and Parts of 104N/5 and 12); *B.C. Ministry of Energy, Mines and Petroleum Resources*, Geological Fieldwork 1989, Paper 1990-1, pages 205-215.
- Bultman, T.R. (1979): Geology and Tectonic History of the Whitehorse Trough West of Atlin, British Columbia; unpublished Ph.D. thesis, *Yale University*, 284 pages.
- Cairns, D.D. (1913): Portions of Atlin District British Columbia: with Special Reference to Lode Mining; *Geological Survey of Canada*, Memoir 37, 129 pages.
- Christopher, P.A. and Pinsent, R.II. (1982): Geology of the Ruby Creek and Boulder Creek Area Near Atlin (104N/11W); *B.C. Ministry of Energy, Mines and Petroleum Resources*, Preliminary Map 52 with notes.
- Cordey, F. (1990): Comparative Study of Radiolarian Faunas from the Sedimentary Basins of the Insular, Coast and Intermontane Belts; unpublished manuscript, 57 pages.
- Donelick, R.A. (1988): Etchable Fission Track Length Reduction in Apatite: Experimental Observations, Theory and Geological Applications; unpublished Ph.D. thesis, *Rensselaer Polytechnic Institute*, 371 pages.
- Grond, H.C., Churchill, S.J., Armstrong, R.L., Harakal, J.E. and Nixon, G.T. (1984): Late Cretaceous Age of the Hutshi, Mount Nansen, and Carmacks groups, Southwestern Yukon Territory and Northwestern British Columbia; *Canadian Journal of Earth Sciences*, Volume 21, pages 554-558.
- Mihalynuk, M.G. and Rouse, J.N. (1988a): Preliminary Geology of the Tutshi Lake Area, Northwestern British Columbia (104M/15); *B.C. Ministry of Energy, Mines and Petroleum Resources*, Geological Fieldwork 1987, Paper 1988-1, pages 217-231.
- Mihalynuk, M.G. and Rouse, J.N. (1988b): Geology of the Tutshi Lake Area (104M/15); *B.C. Ministry of Energy, Mines and Petroleum Resources*, Open File 1988-5.
- Mihalynuk, M.G., Currie, L.D. and Arksey, R.L. (1989a): Geology of the Tagish Lake Area (Fantail Lake and Warm Creek, 104M/9W and 10E); *B.C. Ministry of Energy, Mines and Petroleum Resources*, Geological Fieldwork 1988, Paper 1989-1, pages 293-310.
- Mihalynuk, M.G., Currie, L.D., Mountjoy, K. and Wallace, C. (1989b): Geology of the Fantail Lake (West) and Warm Creek (East) Map Area (NTS 104M/9W and 10E); *B.C. Ministry of Energy, Mines and Petroleum Resources*, Open File 1989-13.
- Mihalynuk, M.G. and Mountjoy, K.J. (1990): Geology of the Tagish Lake Area (104M/8, 9E); *B.C. Ministry of Energy, Mines and Petroleum Resources*, Geological Fieldwork 1989, Paper 1990-1, pages 181-196.
- Mihalynuk, M.G., Mountjoy, K.J., Currie, L.D., Lofthouse, D.L. and Winder, N. (1990): Geology and Geochemistry of the Edgar Lake and Fantail Lake Map Area, NTS (104M/8, 9E); *B.C. Ministry of Energy, Mines and Petroleum Resources*, Open File 1990-4.
- Monger, J.W.H. (1975): Upper Paleozoic Rocks of the Atlin Terrane; *Geological Survey of Canada*, Paper 74-47, 63 pages.
- Nakamura, N. (1974): Determination of REE, Ba, Fe, Mg, Na and K in Carbonaceous and Ordinary Chondrites; *Geochimica et Cosmochimica Acta*, Volume 38, pages 757-775.
- Saunders, A.D. and Tarney, J. (1979): The Geochemistry of Basalts from a Back-arc Spreading Center in the Scotia Sea; *Geochimica et Cosmochimica Acta*, Volume 43, pages 555-572.
- Sutherland Brown, A. (1970): Adera; *B.C. Ministry of Energy, Mines and Petroleum Resources*, Geology, Exploration and Mining in British Columbia 1969, pages 29-35.

Thorstad, L.E. and Gabrielse, H. (1986): The Upper Triassic Kutcho Formation, Cassiar Mountains, North-central British Columbia; *Geological Survey of Canada*, Paper 86-16, 53 pages.

Urabe, T. and Sato, T. (1978): Kuroko Deposits of the Kosaka Mine, Northeast Honshu, Japan – Products of

Submarine Hot Springs on Miocene Sea Floor; *Economic Geology*, Volume 73, pages 161-179.

Wheeler, J.O., Brookfield, A.J., Gabrielse, H., Monger, J.W.H., Tipper, H.W. and Woodsworth, G.J. (1988): Terrane Map of the Canadian Cordillera; *Geological Survey of Canada*, Open File 1894, 9 pages and 1:2 000 000 map.



PRELIMINARY Nd AND Sr ISOTOPIC ANALYSES FROM THE NISLING ASSEMBLAGE, NORTHERN STIKINE AND NORTHERN CACHE CREEK TERRANES, NORTHWESTERN BRITISH COLUMBIA AND ADJACENT YUKON (104M, N)

By Jay L. Jackson, P. Jonathan Patchett and George E. Gehrels
The University of Arizona

KEYWORDS: Regional geology, geochronology, neodymium isotopes, strontium isotopes, Nisling Terrane, Stikine Terrane, Cache Creek Terrane, Stuhini Group, Laberge Group, Tantalus Group.

INTRODUCTION

One of the fundamental tectonic problems in the western Canadian Cordillera is constraining the age of initial juxtaposition of the disparate terranes that underlie this region. Understanding of the temporal and spatial relationships between terranes is hindered by the unique stratigraphy of each terrane and by the fault-bounded nature of these fragments. To unravel relationships between terranes, one must examine the evolution of a terrane through time and look for changes that signal its proximity to another crustal fragment.

The use of radiogenic isotopes is one method by which we can examine changes in terrane stratigraphy through time. The Sm-Nd isotopic system is of particular value because most crustal rocks contain trace quantities of these elements, and samarium and neodymium are not significantly fractionated within the sedimentary system or during metamorphism (*e.g.* DePaolo, 1988). This latter quality allows analysis and direct comparison of values from all rock types that comprise a particular terrane, from sedimentary and volcanic rocks to plutons that intrude these fragments, as well as their metamorphosed equivalents. Although sometimes subject to disturbance, Rb-Sr isotopic analyses are valuable for comparison with existing data sets (*e.g.* Armstrong, 1988).

In this paper we report preliminary interpretations for data from 45 samples taken from the Nisling assemblage, northern Stikine Terrane and northern Cache Creek Terrane in northern British Columbia and adjacent Yukon. Full results of these analyses and precise sample locations will be published elsewhere (Jackson *et al.*, 1990b; in review; in preparation).

REGIONAL GEOLOGIC FRAMEWORK

Researchers have long recognized the oceanic Cache Creek Terrane as one of the most enigmatic terranes in the Cordillera, largely due to Permian Tethyan fauna that are distinct from coeval North American forms (*e.g.* Monger and Ross, 1971). The Quesnel and Stikine terranes border Cache Creek Terrane on the east and west respectively (Figure 1-16-1). The Quesnel and Stikine terranes are characterized by Upper Triassic strata characteristic of an

intra-oceanic volcanic arc, including pyroxene-porphyritic basalt and related sedimentary rocks (Monger, 1977; Mortimer, 1986). The area west of the Stikine Terrane near Atlin, British Columbia, is underlain by the pericratonic basinal assemblage of metasedimentary and metavolcanic rocks termed the Nisling assemblage by Wheeler and McFeely (1987).

The initial juxtaposition of these terranes, with each other and with the North American margin, is generally accepted to have occurred in early Mesozoic time (Monger *et al.*, 1982), but the exact timing and method of this juxtaposition remains poorly constrained. Recent research has illustrated two additional reasons for examining the relations between these terranes:

- (1) Workers have shown that metamorphic rocks in and west of the Coast Range batholith (Figure 1-16-1) have an ancient isotopic signature, both in neodymium isotopic studies (Samson, 1990) and detrital and inherited U-Pb zircon geochronology (Gehrels *et al.*, 1990a, b). These studies suggest that a significant component of Precambrian material has been recycled into these metamorphic rocks. Nisling rocks north and east of the Coast Range batholith also have this ancient crustal signature (Armstrong, 1988; Werner in Monger and Berg, 1987; Jackson *et al.*, 1990b). The Nisling assemblage has been correlated with the lower section of the Yukon-Tanana Terrane (Mortensen, in press) and the latter has in turn been correlated with portions of the North American miogeocline by isotopic and geochronologic studies (*e.g.* Bennett and Hansen, 1988). If the Nisling assemblage represents a part of the North American margin, a complex accretionary history is required to place the Stikine, Cache Creek and Quesnel terranes inboard of it.
- (2) In central and northwestern British Columbia, the Upper Triassic Stuhini Group of the Stikine Terrane unconformably overlies the Paleozoic Stikine assemblage which comprises multiply deformed mafic and felsic volcanic rocks, related sedimentary rocks, chert and marble (Anderson, 1989). Both the Stuhini Group and Paleozoic Stikine assemblage in this region have juvenile neodymium and strontium isotopic signatures, indicating a lack of any significant quantity of recycled Precambrian material in this part of the Stikine Terrane (Samson *et al.*, 1989). In contrast, Stuhini Group and equivalent Lewes River Group rocks in extreme northwestern British Columbia and southern

NORTHERN CANADIAN CORDILLERA GENERALIZED ASSEMBLAGE MAP

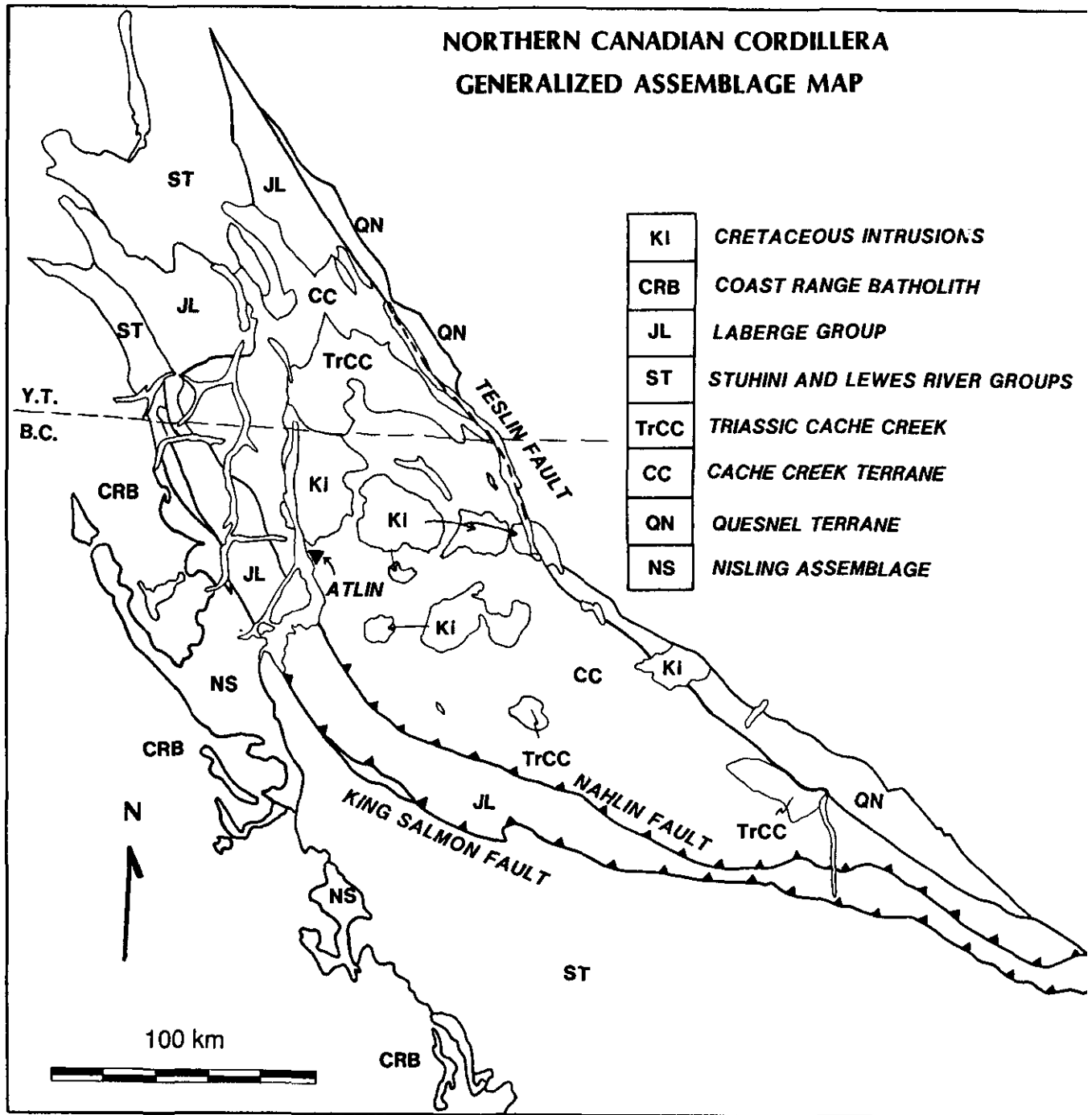


Figure 1-16-1. Generalized geology of the northern Canadian Cordillera (modified after Wheeler and McFeely, 1987).

Yukon have been interpreted to unconformably overlie the Nisling assemblage (Werner, 1978; Bultman, 1979; Mihalyuk and Rouse, 1988). Recent isotopic work shows that local clastic strata in the Stuhini Group of the northern Stikine Terrane contain a significant amount of ancient crustal material, seeming to confirm this interpretation (Jackson *et al.*, 1990b). This Nisling – northern Stikine Terrane link calls into question relations between the northern and southern parts of the Stikine Terrane and their along-strike continuity.

ISOTOPIC STUDIES

We have analyzed 43 samples for Sm-Nd isotopic composition and 19 samples for Rb-Sr isotopic composition. Neodymium data are summarized for this report by their depleted mantle model ages (DePaolo, 1981). For igneous rocks, the model age is a measure of the time at which the pluton or volcanic rock was removed from the mantle, plus any contamination from existing crustal material in the surrounding country rock which could have a very different

model age. For sedimentary and metasedimentary rocks, the model age is a measure of the average age at which detritus that comprises these rocks was separated from the mantle. We use the depleted mantle form rather than the more traditional epsilon value because depositional ages or crystallization ages of many of the samples are poorly known.

Strontium data were obtained for igneous and metamorphic rocks in the study. Data for volcanic and plutonic rocks are reported by their initial $^{87}\text{Sr}/^{86}\text{Sr}$ values because the crystallization ages of samples collected are fairly well known. Metamorphic rocks, however, are reported by their measured $^{87}\text{Sr}/^{86}\text{Sr}$ value because neither depositional ages of their protoliths nor the age of metamorphism are known.

NISLING ASSEMBLAGE

The Nisling assemblage comprises metamorphic rocks interpreted as a pericratonic basinal assemblage (Wheeler and McFeely, 1987). Currie (1990) described these rocks in detail and broke out two subdivisions of metasedimentary

rocks: the Florence Range suite, dominated by quartz-rich metaclastic strata and marble; and the Boundary Ranges suite, primarily composed of metavolcanic and related metasedimentary rocks. Relative ages of the two suites are unknown.

Neodymium isotopic data confirm that the rocks of the Florence Range suite contain a substantial amount of older Precambrian material, with neodymium depleted mantle model ages ranging from 2700 Ma to 1600 Ma (Figure 1-16-2). Strontium data also show strongly evolved values, but these numbers are less meaningful due to severe disturbance during metamorphism (Jackson, unpublished data). Rocks of the Boundary Ranges suite, on the other hand, show younger average depleted mantle model ages between 1550 and 800 Ma and lower measured strontium ratios. This is consistent with, but does not require, the interpretation that Boundary Ranges rocks are younger than those of the Florence Range suite. Alternatively, these rocks may simply be derived from a more primitive source area.

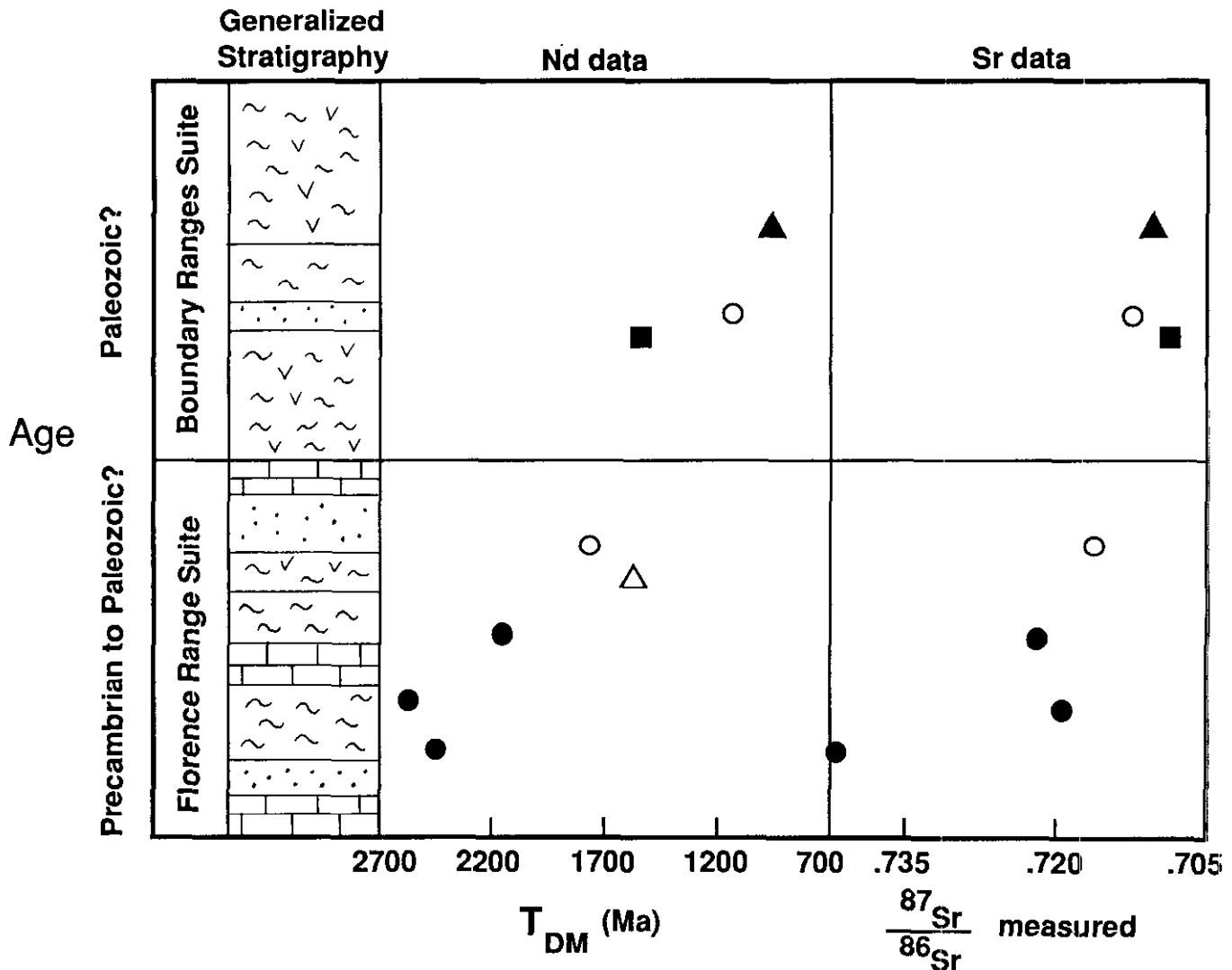


Figure 1-16-2. Nd and Sr isotopic data from the Nisling assemblage. Black circles are carbonaceous schist, open circles are quartzite, black squares are chlorite-actinolite schist, black triangles are quartz-chlorite schist and open triangles are a chlorite schist clast within Stuhini conglomerate.

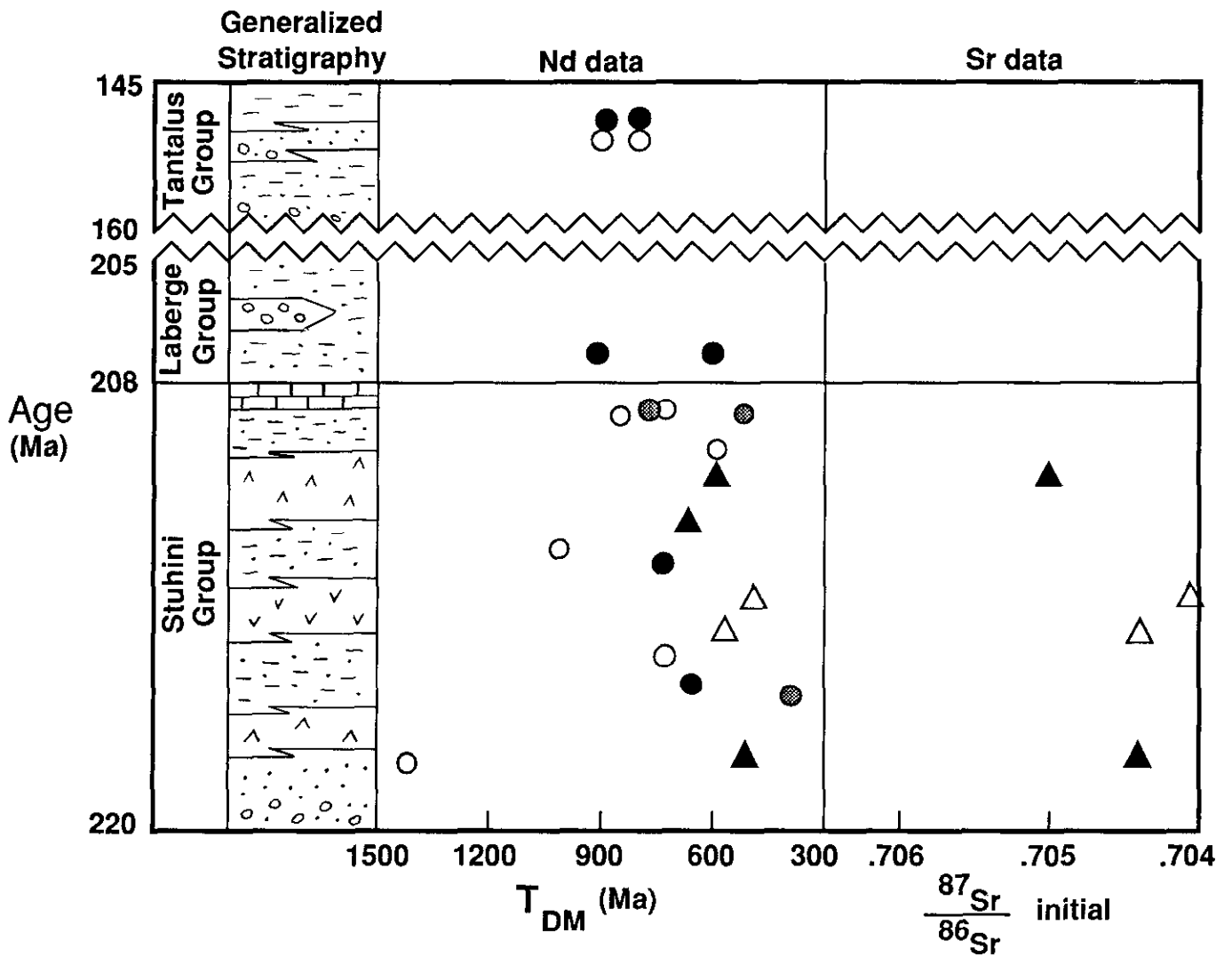


Figure 1-16-3. Nd and Sr isotopic data from the northern Stikine Terrane. Black circles are argillite and shale, shaded circles are siltstone, open circles are sandstone, black triangles are mafic volcanic rock and open triangles are felsic volcanic rock.

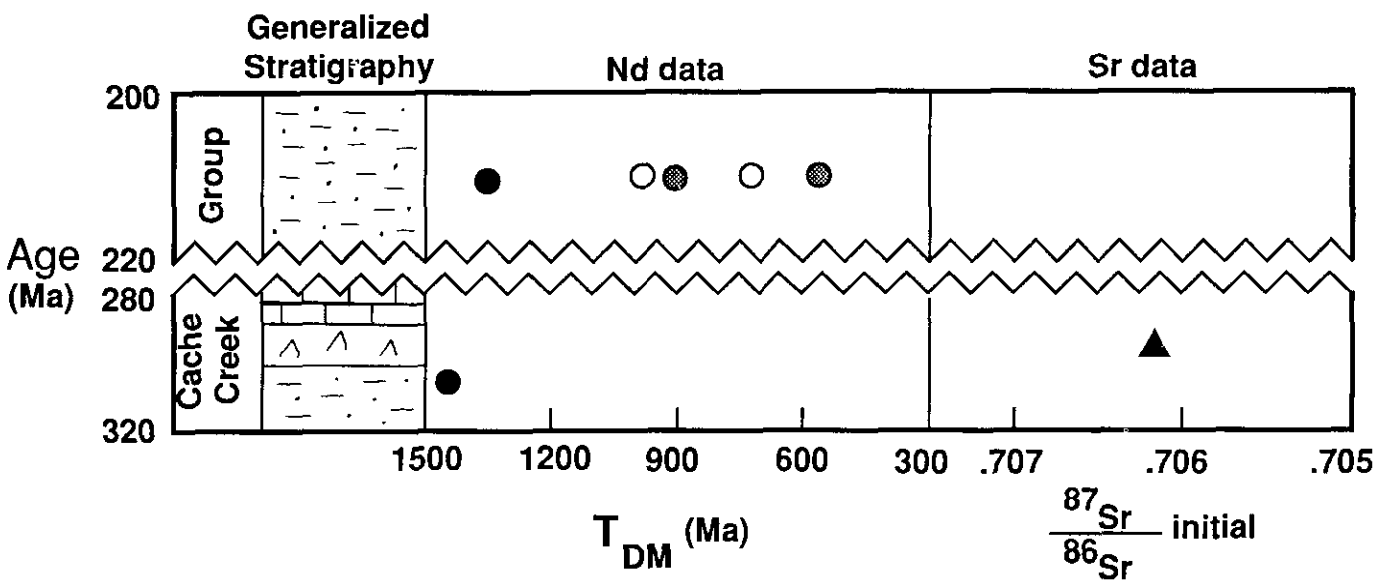


Figure 1-16-4. Nd and Sr isotopic data from the northern Cache Creek Terrane. Symbols are the same as in Figure 1-16-3.

NORTHERN STIKINE TERRANE

Samples analyzed from the northern Stikine Terrane include sedimentary and volcanic rocks from the Upper Triassic Stuhini and age-equivalent Lewes River groups, and clastic rocks from the Lower to Middle Jurassic Laberge Group and the Upper Jurassic to Lower Cretaceous Tantalus Group (Figure 1-16-3; for stratigraphic descriptions see Mihalynuk and Mountjoy, 1990; Hart and Radloff, 1990). In general, the Stuhini rocks have a primitive isotopic signature quite similar to rocks in the southern sections of Stikinia (cf. Samson *et al.*, 1990). With younger depositional ages, however, the neodymium data show a slight trend toward older depleted mantle model ages. Two Stuhini Group sandstone samples in the northern Stikine Terrane, however, are a marked exception to this pattern with model ages of 1410 and 1010 Ma (Figure 1-16-3). The most likely source for the old detritus in this arkose is the adjacent Nisling assemblage which is interpreted to have been linked with northern Stikine Terrane by Late Triassic time (Werner, 1978; Bultman, 1979; Jackson *et al.*, 1990b).

NORTHERN CACHE CREEK TERRANE

A sample of late Paleozoic (Pennsylvanian to Permian?) argillite has a model age of 1450 Ma which indicates a

significant component of Precambrian detritus (Figure 1-16-4). This reflects either: pelagic deposition in an open ocean basin where clastic strata have been derived from the continents surrounding it (Ben Othman *et al.*, 1989; Jackson *et al.*, 1990a); or deposition near a continent or continental fragment composed of rocks with Precambrian model ages. The Upper Triassic argillite carries this same ancient crustal signature, reflecting a similar depositional setting. Interbedded Late Triassic, coarse clastic strata, however, have younger model ages. This suggests input of detritus from a source of juvenile crustal material in the Late Triassic, periodically interrupting the pelagic deposition of chert and argillite. This juvenile source is most likely one of the flanking volcanic-arc terranes (Samson *et al.*, 1989; Jackson *et al.*, 1990b).

An upper Paleozoic metabasalt has an initial $^{87}\text{Sr}/^{86}\text{Sr}$ ratio of 0.7064. This slightly evolved signature is most likely due to alteration during greenschist-facies metamorphism. Analyses of 14 additional Cache Creek samples, currently in progress, will add details to these preliminary interpretations.

PLUTONIC ROCKS

Felsic plutonic rocks that intrude the Nisling assemblage, northern Stikine and northern Cache Creek terranes show

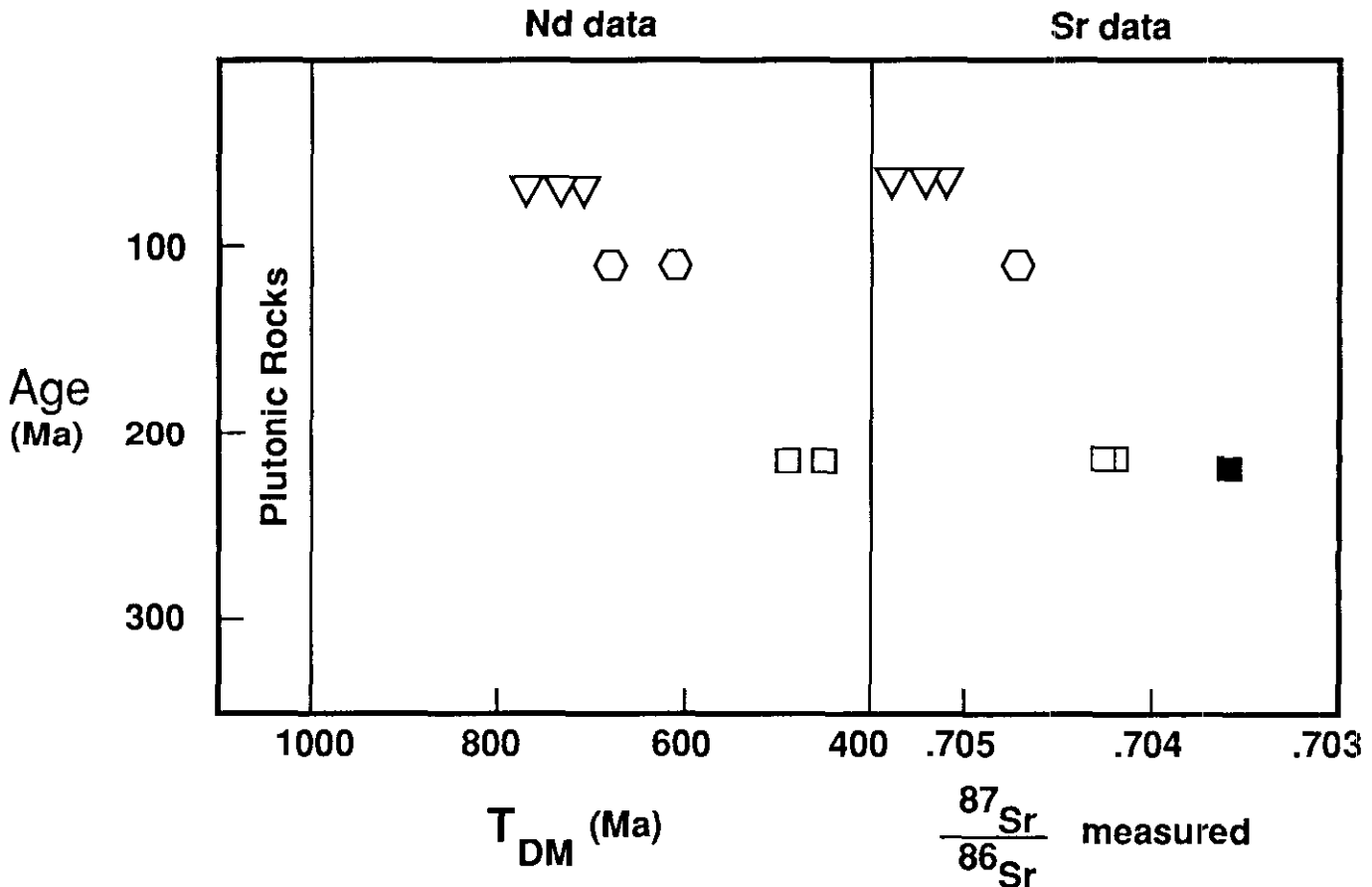


Figure 1-16-5. Nd and Sr isotopic data from plutons. Open triangles are felsic plutons that intrude the Nisling assemblage, open hexagons are felsic plutons that intrude the Cache Creek Group, open squares are felsic plutons that intrude the Stikine Terrane and the black square is a gabbro that intrudes Stikinia.

distinct differences in their neodymium and strontium isotopic signatures. The oldest model ages, ranging from 710 to 770 Ma, are found in Cretaceous granodiorite and tonalite plutons that intrude Nisling assemblage rocks southwest of Atlin. (Figures 1-16-1; 1-16-5). Northern Cache Creek granodiorite shows intermediate model ages of 610 to 680 Ma. Northern Stikine granodiorite samples have young model ages of 450 to 490 Ma. Initial strontium data mimic the neodymium model age trends. Two possible controls on these isotopic ratios are as follows. First, wallrock contamination may affect the model ages of these plutons. Nisling assemblage rocks have the oldest neodymium model ages, whereas those of Stikinia are the youngest. Strata in the Cache Creek Terrane are intermediate with old model ages for argillite and young model ages for interbedded siltstone and sandstone. Second, the data show an increase in model age with decreasing crystallization age (Figure 1-16-5). This may be a function of plutons intruding a crustal section that has become progressively thickened through Jurassic and Cretaceous structural shortening (Monger, 1977; Monger *et al.*, 1982; Bloodgood and Bellefontaine, 1990).

TECTONIC SIGNIFICANCE

Examination of the neodymium and strontium isotopic signatures of three terranes in the northern Canadian Cordillera can help place constraints on the timing of juxtaposition of these fragments. Local layers of Late Triassic sandstone in the northern Stikine Terrane contain a significant component of older crustal material (Figure 1-16-3) which provides a link between northern Stikine Terrane and the Nisling assemblage at this time (Jackson *et al.*, 1990b).

In the northern Cache Creek Terrane, sandstone beds with isotopic ratios indicative of juvenile crust are interstratified with argillite carrying an ancient crustal signature. Two possible models can account for this pattern. In one model, the argillite could reflect pelagic deposition in an ocean basin as described above, whereas sandstone beds would demonstrate increasing proximity to a source of juvenile detritus, most likely from the Stikine Terrane or the Quesnel Terrane. Alternatively, the ancient component of detritus in Cache Creek argillite could signal proximity to either the Nisling assemblage or the North American continental margin, with sandstone beds representing periodic input from a nearby source of juvenile material (Quesnel Terrane or Stikine Terrane). Further isotopic and petrographic analyses will aid in discriminating between these models.

ACKNOWLEDGMENTS

Thanks to Lisel Currie, Craig Hart, Bill McClelland, Mitch Mihalyuk and Scott Samson for discussions and logistical assistance throughout the course of this project. This work was funded by U.S. National Science Foundation grant EAR-8903764 to Gehrels and Patchett, research grants to Jackson from the Geological Society of America, Sigma Xi Grants-In-Aid of Research, British Columbia Geoscience Research Grant Program (grants RG89-13 and

RG90-11), Homestake Mineral Development Company of Canada, Shell Oil Company (U.S.), and British Petroleum, and a fellowship to Jackson from Chevron U.S.A. The Exploration and Geological Services Division of Indian and Northern Affairs Canada in Whitehorse and the Geological Survey of Canada in Vancouver provided additional logistical support. Julie Roska and Barb Waugh served as field assistants.

REFERENCES

- Anderson, R.G. (1989): A Stratigraphic, Plutonic, and Structural Framework for the Iskut River Map Area, Northwestern British Columbia; *in* Current Research, Part E, *Geological Survey of Canada*, Paper 89-1E, pages 145-154.
- Armstrong, R.L. (1988): Mesozoic and Early Cenozoic Magmatic Evolution of the Canadian Cordillera; *Geological Society of America*, Special Paper 218, pages 55-90.
- Ben Othman, D., White, W.M. and Patchett, P.J. (1989): The Geochemistry of Marine Sediments, Island Arc Magma Genesis, and Crust-Mantle Recycling; *Earth and Planetary Science Letters*, Volume 94, pages 1-21.
- Bennett, V.C. and Hansen, V.L. (1988): Neodymium Isotopic Similarities between the Yukon-Tanana Terrane, Yukon Territory and Continental North America; *Geological Society of America*, Abstracts with Programs, Volume 20, Number 7, page A111.
- Bloodgood, M.A. and Bellefontaine, K.A. (1990): The Geology of the Atlin Area (Dixie Lake and Teresa Island) (104N/6 and parts of 104N/5 and 12); *B.C. Ministry of Energy, Mines and Petroleum Resources*, Geological Fieldwork 1990, Paper 1990-1, pages 205-215.
- Bultman, T.R. (1979): Geology and Tectonic History of the Whitehorse Trough West of Atlin, British Columbia; unpublished Ph.D. thesis, *Yale University*, 284 pages.
- Currie, L.D. (1990): Metamorphic Rocks of the Florence Range, Coast Mountains, Northwestern British Columbia; *B. C. Ministry of Energy, Mines and Petroleum Resources*, Geological Fieldwork 1989, Paper 1990-1, pages 197-203.
- DePaolo, D.J. (1981): Neodymium Isotopes in the Colorado Front Range and Crust-Mantle Evolution in the Proterozoic; *Nature*, Volume 291, pages 193-196.
- DePaolo, D.J. (1988): Neodymium Isotope Geochemistry; *Springer Verlag*, 187 pages.
- Gehrels, G.E., McClelland, W.C., Samson, S.D., Patchett, P.J. and Jackson, J.L. (1990): Ancient Continental Margin Assemblage in the Northern Coast Mountains, Southeast Alaska and Northwest Canada; *Geology*, Volume 18, pages 208-211.
- Gehrels, G.E., McClelland, W.C., Samson, S.D. and Patchett, P.J. (1990): U-Pb Geochronology of Detrital Zircons from the Yukon Crystalline Terrane along the Western Flank of the Coast Mountains Batholith

- (abstract); *Geological Association of Canada/ Mineralogical Association of Canada, Programs with Abstracts, Volume 15, page A44.*
- Hart, C.J.R. and Radloff, J.K. (1990): Geology of the Whitehorse, Alligator Lake, Fenwick Creek, Carcross and Part of Robinson Map Areas (105D/11, 6, 3, 2 & 7); *Indian and Northern Affairs Canada, Open File 1990-4, 113 pages.*
- Jackson, J.L., Gehrels, G.E. and Patchett P.J. (1990a): Geology and Nd Isotope Geochemistry of Part of the Northern Cache Creek Terrane, Yukon: Implications for Tectonic Relations Between Cache Creek and Stikine (abstract); *Geological Association of Canada/ Mineralogical Association of Canada, Programs with Abstracts, Volume 15, page A64.*
- Jackson, J.L., Gehrels, G.E., Patchett, P.J. and Mihalynuk, M.G. (1990b): Late Triassic Depositional Link Between the Northern Stikine Terrane and Nisling Assemblage, Northwestern Canada (abstract); *Geological Society of America, Abstracts with Programs, Volume 22, Number 7, page A325.*
- Mihalynuk, M.G. and Mountjoy, K.J. (1990): Geology of the Tagish Lake Area (104M/8, 9E); *B.C. Ministry of Energy, Mines and Petroleum Resources, Geological Fieldwork 1989, pages 181-196.*
- Mihalynuk, M.G. and Rouse, J.N. (1988): Preliminary Geology of the Tutshi Lake Area, Northwestern British Columbia (105M/15); *B.C. Ministry of Energy, Mines and Petroleum Resources, Geological Fieldwork 1987, Paper 1988-1, pages 217-231.*
- Monger, J.W.H. (1977): Upper Paleozoic Rocks of the Western Canadian Cordillera and their Bearing on Cordilleran Evolution; *Canadian Journal of Earth Sciences, Volume 14, pages 1832-1859.*
- Monger, J.W.H. and Berg, H.C. (1987): Lithotectonic Terrane Map of Western Canada and Southeastern Alaska; *U.S. Geological Survey, Miscellaneous Field Studies Map MF-1874-B, scale 1:2 500 000.*
- Monger, J.W.H., Price, R.A. and Tempelman-Kluit, D.J. (1982): Tectonic Accretion and the Origin of the Two Major Metamorphic and Plutonic Belts in the Canadian Cordillera; *Geology, Volume 10, pages 70-75.*
- Monger, J.W.H. and Ross, C.A. (1971): Distribution of Fusulinaceans in the Western Canadian Cordillera; *Canadian Journal of Earth Sciences, Volume 8, pages 259-278.*
- Mortensen, J.K. (in press): Pre-Mid-Mesozoic Tectonic Evolution of the Yukon-Tanana Terrane, Yukon and Alaska; *Tectonics.*
- Mortimer, N. (1986): Late Triassic, Arc-related, Potassic Igneous Rocks in the North American Cordillera; *Geology, Volume 14, pages 1035-1038.*
- Samson, S.D., McClelland, W.C., Patchett, P.J., Gehrels, G.E. and Anderson, R.G. (1989): Evidence from Neodymium Isotopes for Mantle Contributions to Phanerozoic Crustal Genesis in the Canadian Cordillera; *Nature, Volume 337, pages 705-709.*
- Samson, S.D. (1990): Nd and Sr Isotopic Characterization of the Wrangellia, Alexander, Stikine, Taku and Yukon Crystalline Terranes of the Canadian Cordillera; unpublished Ph.D. thesis: *University of Arizona, 155 pages.*
- Werner, L.J. (1978): Metamorphic Terrane, Northern Coast Mountains West of Atlin Lake, British Columbia; in *Current Research, Part A, Geological Survey of Canada, Paper 78-1A, pages 69-70.*
- Wheeler, J.O. and McFeely, P. (1987): Tectonic Assemblage Map of the Canadian Cordillera and Adjacent Parts of the United States of America; *Geological Survey of Canada, Open File 1565, scale 1:2 000 000.*

NOTES



TERTIARY OUTLIER STUDIES: RECENT INVESTIGATIONS IN THE SUMMERLAND BASIN, SOUTH OKANAGAN AREA, B.C. (82E/12)

By B.N. Church, G.S.B., A.M. Jessop, Geological Survey of Canada,
R. Bell, Geological Survey of Canada and A. Pettipas, G.S.B.

KEYWORDS: Tertiary basins, geothermal resources, environment, uranium, molybdenum.

INTRODUCTION

The Tertiary basins in the interior of British Columbia present opportunities for the development of geothermal resources but not without appropriate regard for environmental considerations such as the dispersion of heavy metals, the radioactivity of country rocks and the quality of groundwater.

The main object of this project was to test the geothermal potential of the Summerland basin with a view to locating a low-grade thermal source for space heating (mainly the local greenhouses). To this end the first phase of a drilling, Hole No. EPB/GSC 495, began in March 1990 at Summerland, sponsored by the South Okanagan – Similkameen Community Futures Group (based in Penticton), the Geological Survey of Canada and the British Columbia Ministry of Energy, Mines and Petroleum Resources.

The weakly lithified beds, characteristic of the Tertiary basins, are poor thermal conductors that commonly blanket older more conductive crystalline basement rocks. The natural dissipation of heat from the earth's interior is impeded by this blanket, causing thermal accumulation. Combined with this, the inherent structural weakness of these young cover rocks facilitates faulting and fracturing allowing the entry of groundwater into the strata and the possible development of warm-water reservoirs at depth (Nevin, Sadlier-Brown, Goodbrand Ltd., 1987).

The mixing of mineral-laden ground waters from deep sources with surface waters may present environmental concerns in ranching and urban areas. For example specific concerns were expressed by Bates *et al.* (1979, page 4):

“A problem exists at Eneas Creek west of Summerland, where uranium in creek water at the present time appears to be naturally in excess of the proposed public drinking water standard (20 ppb uranium)”.

Elevated uranium in surface water in the area, up to 2.5 ppm, was also noted by Church, 1980. The ultimate source of the uranium is believed to be groundwater from surrounding hills.

GEOLOGICAL SETTING

The Summerland basin is an Eocene volcanic caldera that was once part of a larger contiguous mass of volcanic and sedimentary rocks known as the “Penticton Tertiary outlier” (Church, 1982). The rocks in the Summerland basin

consist of several major units of the Penticton Group such as the basal conglomerates (Kettle River Formation), massive volcanic beds (Marron Formation), feldspar porphyry trachyandesite lavas (Kitley Lake member), fine-grained trachytic lavas and ash flows (Nimpit Lake member), dome-forming dacitic lava and breccia (Marama Formation) and fluvial and lacustrine sedimentary rocks (White Lake Formation). The total stratigraphic thickness of this assemblage is in excess of 1000 metres (Figures 2-1-1 and 2-1-2). A drill hole through to the keel of the basin in a central location would be expected to encounter most of the stratigraphic units.

Rifting and graben development caused by crustal extension along the Okanagan valley occurred about 50 million years ago (Church, 1973). At this time, and subsequently, the rocks of the Summerland area were tilted and folded into an elliptical 5 by 10 kilometre synclinal trough, forming a natural catchment area for resupply of groundwater. Down dip on the beds the lateral movement of groundwater is impeded (and ponded?) along the Summerland fault at the southeast margin of the basin where down-faulted strata are juxtaposed against impervious massive granite.

Eneas Creek enters from the north, through the breached rim of the basin. It becomes intermittent and marshy toward the centre of the basin and eventually disappears into the glacial overburden. Elsewhere there are few streams; a number of ponds and marshes in closed depressions receive drainage directly from adjacent slopes.

At depth, groundwater is channelled along joints, bedding planes and faults, becoming trapped in permeable units such as conglomerate and sandstone beds and lenses of breccia in fault zones. In the elastic beds permeability is greatly reduced because of carbonate cement and abundant interstitial volcanic ash. Consequently much of the available groundwater is believed to be contained in the fractures. Slippage, as the result of folding, between the individual beds and along formational contacts, is believed to be the most promising mechanism for the formation of aquifers at depth.

DRILLING

The search for renewable energy sources began prior to the energy crisis of the mid-70s. To this end, Energy Mines and Resources Canada and the British Columbia Ministry of Energy, Mines and Petroleum Resources have supported a number of geothermal energy projects. The Geothermal Potential Map of British Columbia (Church *et al.*, 1983)

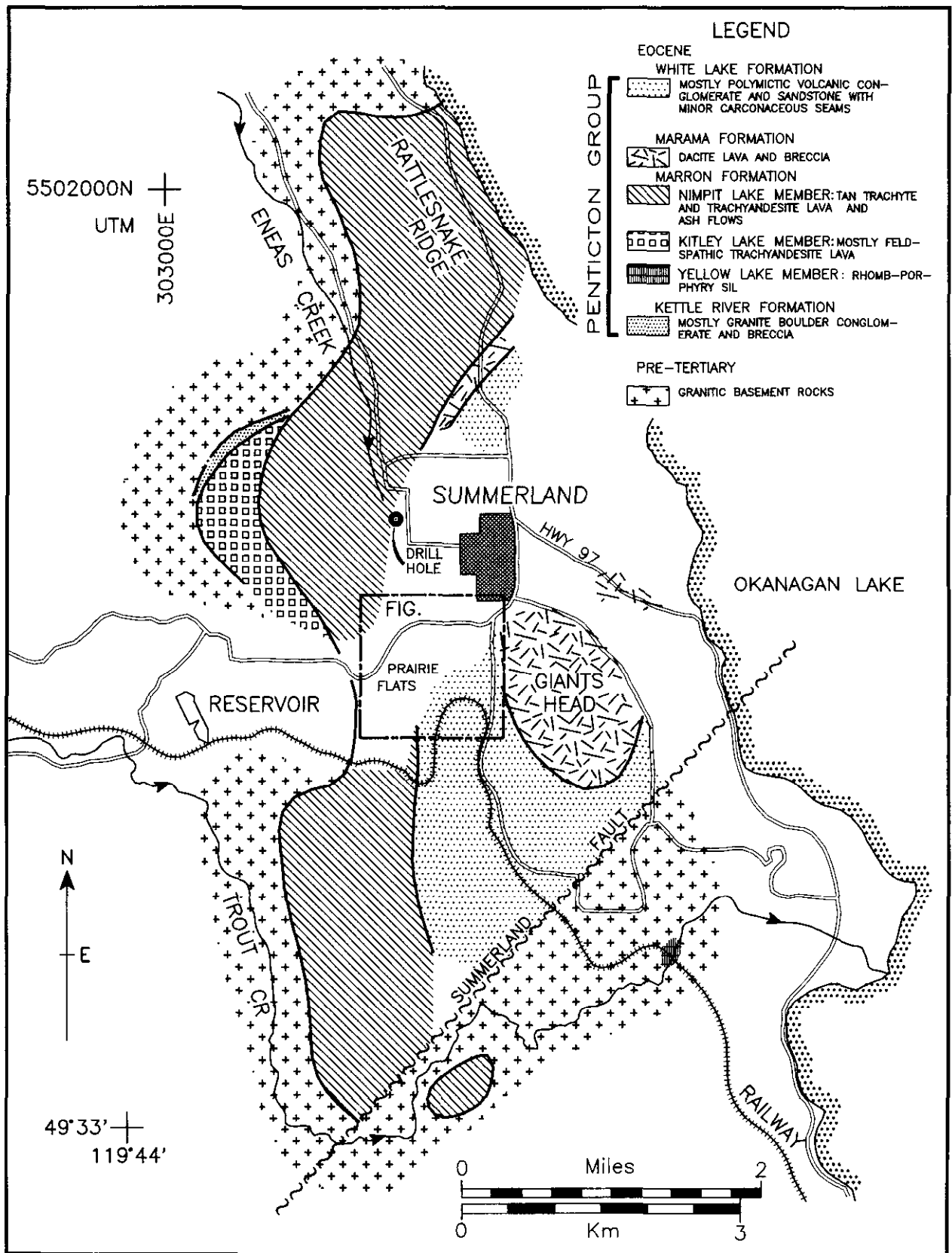


Figure 2-I-1. Location of geothermal drill hole in the Summerland basin.

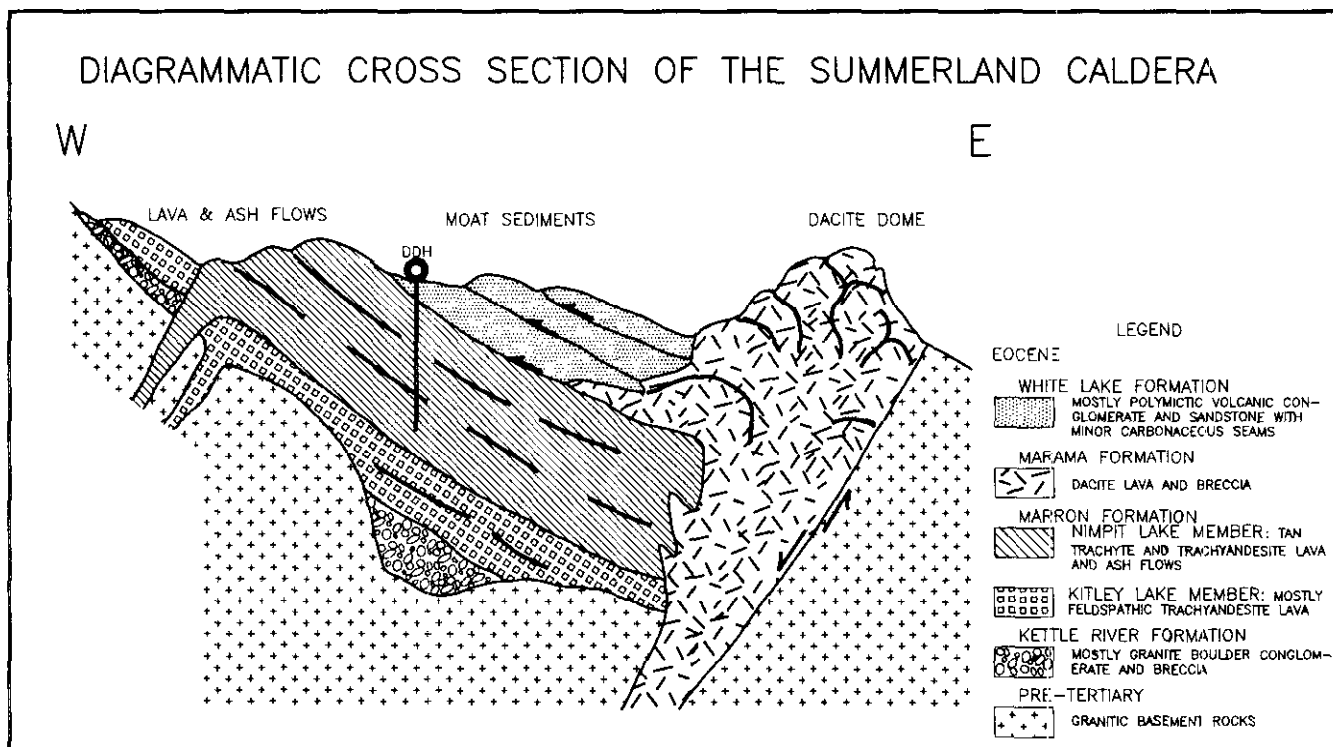


Figure 2-1-2. Diagrammatic cross-section of the Summerland basin.

was preceded by more detailed investigations suggesting geothermal potential in the White Lake basin and other Tertiary outliers in south-central British Columbia (Church, 1973; Jessop and Judge, 1971).

The first borehole in the area was sponsored by the federal government as part of the Geothermal Energy Program (Lewis and Werner, 1982). This was a diamond-drill hole intended to test the geophysical and geological properties of granitic rocks just south of the Summerland basin. Later, a second hole, the "Mraz well", was drilled to a depth of 200 metres to test the bedded Tertiary rocks in the southern part of the basin.

Lewis (1984) confirmed a regional high heat-flow and suggested targets for further research. He concluded that a more quantitative evaluation of the geothermal reserve required additional test wells.

The most recent hole (EPB/GSC 495) is located on the Boreboon farm (Mountain View Farms), just south of Encas Creek, approximately 1 kilometre northwest from the centre of Summerland (Plate 2-1-1): (latitude 49°36'30", longitude 119°41'18"; elevation 505 metres). The location of this hole was chosen based on geology and proximity to a potential customer. The Boreboon farm proved to be well positioned on the west limb of the basin where a drill hole of reasonable depth could penetrate to the base of the Tertiary pile. This optimized the blanket effect and increased the possibility of intercepting a warm-water aquifer at the contact of the Tertiary beds with the underlying granite. The farm is a large user of natural gas for heating greenhouses and the owner was clearly interested in a cheaper source of energy.



Plate 2-1-1. Logging geothermal well at Summerland (Giant's Head in background)

The new well began as a 6-inch (15.2 cm) diameter rotary hole. It was drilled (March 10 to May 15th) to a depth of 544 metres, penetrating 56 metres of gravel and glacial till before entering bedrock. The hole was completed by BQ diamond drilling (July 2nd to July 31st) to a depth of 712 metres.

The geological profile of the bed-rock in this hole shows mostly alternating ash flows and lava flows typical of the Nimpit member of the Marron Formation, that is tan to dark grey trachyte/trachyandesite with small phenocrysts of diopsidic pyroxene and microlites of plagioclase and alkali feldspar in a fine-grained matrix. Quartz is rarely seen. Some admixture of shale and coal with the volcanic fragments recovered from the rotary drilling suggests penetration of part of the White Lake Formation or intercalation of similar sedimentary rocks in the volcanic pile.

The petrography of the lower, cored section of the drill hole is consistent with the chip samples obtained above. Most of this section appears to be Nimpit tuff-breccia with a few interlayered lava flows and crosscutting dikes. Flattening and welding of pumice fragments is seen at several levels. The angle between bedding and core axis averaged 45°.

A temporary water-flow of about 100 litres per minute was reported at approximately 150 metres depth; a geophysical log of the hole indicated possible water movement at 523 metres and other disturbances at 50 and 350 metres. Water movement is also believed to have been responsible for hematization in shear zones such as between 569 and 573 metres and by the local abundance of calcite and laumontite-filled fractures between 554 and 557 metres.

Preliminary results (Jessop, unpublished) gives a bottom hole temperature of slightly more than 33°C (at 706 metres) and a uniform thermal gradient close to 34 microkelvins per metre in the lower part of the hole.

ENVIRONMENTAL CONSIDERATIONS

The first caution regarding the environmental hazard of uranium in the Summerland area was from Bates *et al.* (1979, page 4): "A recent intensification of exploration and drilling in this area might have the effect of further increasing the uranium content in this (Eneas Creek) and other creeks".

In this regard it is noteworthy that testing rock samples and water from hole EPB/GSC 495 has shown no anomalous uranium concentrations nor high radioactive levels (Leaming, personal communication, 1990). However, accumulation of young uranium in the peat of nearby Prairie Flats was noted by Culbert (1980) and Culbert and Leighton (1988).

The Prairie Flats area is marshland on the edge of Summerland (Figures 2-1-1 and 3). According to Culbert *et al.* (1984) concentration of uranium in peat samples from Prairie Flats locally exceeds 1000 ppm in the surface layer; a maximum of value of 623 ppm uranium was obtained by the writer from a suite of 28 samples collected from the same general area (Table 2-1-1). The total accumulation of U₃O₈, to a depth of 1 to 3 metres, is estimated to be 230

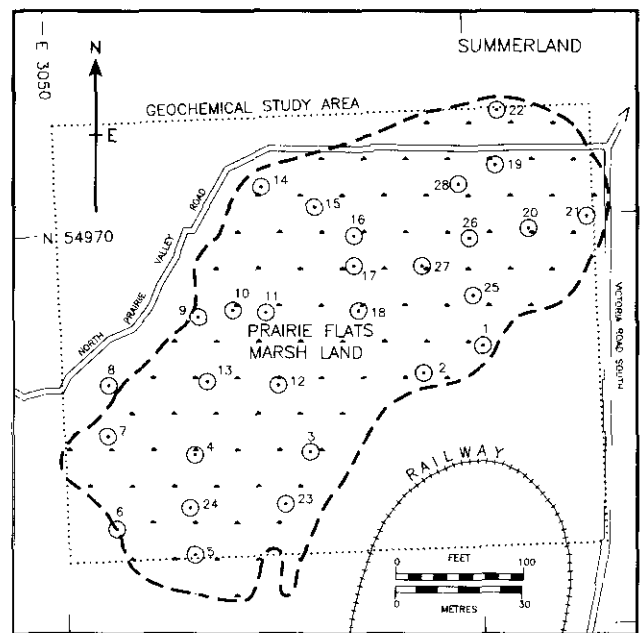


Figure 2-1-3. Sample locations, Prairie Flats marshland.

tonnes (Culbert *et al.*, 1984). It is believed that this uranium was deposited since the last ice age and mostly within the last 2000 years (Levinson *et al.*, 1984).

Young uranium with few gamma-active daughter products occurs in semi-arid regions of the southern interior of British Columbia and northeastern Washington State. The uranium was leached from felsic igneous rocks and fixed in organic-rich sediments. In the Flodelle Creek area of Washington uranium has been recovered from organic-rich sediments in a series of old beaver ponds — the source is a nearby uranium-rich granodiorite (Johnson *et al.*, 1987). Similarly, in the Eneas Creek area near Summerland the source of uranium appears to be groundwater feeding from fractured granitic rocks underlying the upper course of the stream.

The semi-arid climate of the Okanagan region has facilitated transport of uranium in streams. Evaporation has resulted in an increase in the alkalinity and bicarbonate content of these waters, both of which are important local factors for the solution of uranium at surface (Culbert and Leighton, 1978; Church and Johnson, 1978). Uranium was concentrated initially by evaporation and held by adsorption and ion exchange such as occurred in the Flodelle Creek deposit (Johnson *et al.*, 1987). Zielinski and Meier (1988) indicate that uranium at Flodelle Creek may be held loosely on organic matter as uranyl carbonate and phosphate complexes, then fixed, together with other metals, by the reducing action of bacteria. However, no specific uranium-bearing minerals have been identified and the exact mechanism of metal fixation on organic matter is not completely understood.

These young deposits are not readily detectable by conventional scintillometer surveys because of the lack of significant radioactive daughter products. They are of environ-

TABLE 2-1-1
ANALYSES OF PRAIRIE FLAT PEAT SAMPLES

No.	EASTING	NORTHING	LOI %	SiO ₂ %	Ba PPM	Ce PPM	Cs PPM	La PPM	Mo PPM	Sc PPM	Th PPM	U PPM	V PPM
1	30603	549670	27.47	46.04	1106	58	6	34	39	8.8	8	106	267
2	30588	549663	23.12	50.99	979	58	4	26	82	9.3	18	222	214
3	30560	549644	17.64	51.75	997	47	2	28	7	10.6	5	10	153
4	30531	549643	20.97	52.53	1054	48	4	24	24	8.9	12	172	127
5	30530	549620	12.85	56.78	1050	48	4	43	7	8.0	5	2	77
6	30502	549621	13.80	55.33	874	50	1	30	7	7.4	5	8	61
7	30510	549650	35.33	31.78	402	1	13	1	3	18.7	17	25	32
8	30511	549662	6.82	63.53	1193	72	0	39	1	5.1	5	7	81
9	30533	549679	21.20	45.83	724	39	4	27	7	12.1	5	6	69
10	30543	549680	30.47	35.80	764	23	12	24	5	18.2	5	21	10
11	30550	549679	22.00	47.45	903	41	6	24	1	11.8	5	17	84
12	30552	549661	25.82	48.61	937	56	3	37	5	7.7	2	34	111
13	30536	549661	14.81	51.91	868	57	5	38	3	13.1	5	16	96
14	30551	549709	40.16	37.69	509	30	6	19	13	9.6	5	34	168
15	30562	549704	18.70	55.86	708	31	6	20	7	7.2	5	58	134
16	30573	549698	49.23	30.93	609	28	7	15	72	7.5	11	577	184
17	30572	549690	61.02	22.31	558	13	8	4	54	6.7	1	623	179
18	30572	549678	50.77	25.69	657	16	10	9	36	10.3	2	133	161
19	30609	549712	19.95	54.00	949	51	1	26	4	6.7	12	30	106
20	30617	549698	17.01	52.96	908	46	3	30	27	8.5	5	80	134
21	30630	549700	28.12	44.61	773	46	3	12	4	7.4	5	46	125
22	30610	549726	12.22	60.92	1019	50	0	21	7	5.9	5	10	72
23	30552	549632	14.18	55.55	916	37	1	15	7	7.8	5	2	67
24	30530	549632	18.26	54.89	1145	56	2	32	7	7.7	5	46	99
25	30600	549682	34.17	42.22	712	24	5	8	68	6.9	0	187	135
26	30601	549697	33.20	41.43	684	28	5	15	49	8.4	0	193	109
27	30588	549690	47.17	28.81	532	11	6	15	66	8.7	10	393	139
28	30599	549708	19.72	56.49	969	46	2	8	3	6.9	3	33	78

mental concern because they contain significant concentrations of poorly fixed uranium and some other elements such as molybdenum, and inadvertant cultural disruption may generate transient, perhaps harmful, levels of dissolved uranium in local ground and surface waters (Zeilinski *et al.*, 1987).

ANALYTICAL RESULTS

Table 2-1-1 gives the results of analyses of 28 samples of peat from Prairie Flats (Figure 2-1-3). Eleven chemical variables were chosen to characterize the deposit, the main variables being loss on ignition (LOI) representing organics (mostly carbon), silica (SiO₂) representing the clastic sedimentary fraction; and uranium (U) representing chemical precipitate. Other elements analysed are barium (Ba), cerium (Ce), lanthanum (La), molybdenum (Mo), scandium (Sc), thorium (Th) and vanadium (V).

Loss on ignition is the weight loss of the sample after heating to 550°C. This is an indication of its organic content.

Silica ranges from 22.3 to 63.5 per cent and is generally the most abundant component in the peat. It is concentrated in the silty layers as detrital quartz and in silicates such as feldspar, the clay minerals and mica.

Other major oxides and LOI constituents comprise much of the remainder. These include alumina (Al₂O₃), carbon (C), carbon dioxide (CO₂), water (H₂O), and probably minor amounts of lime (CaO), magnesia (MgO), potash (K₂O), soda (Na₂O) and phosphate (P₂O₅), although these variables have not been individually determined for this report. The LOI ranges from 6.8 to 61.0 per cent.

The minor element values are mostly elevated compared to other sediments. It is well known that peatbogs and marshlands can be sites for anomalous concentrations of metals, especially heavy metals (Zeilinski *et al.*, 1987). This is especially true for uranium, molybdenum (Mo), and vanadium which are concentrated up to two or three magnitudes above the levels in source rocks. The exception is thorium which averages 5 ppm, a value lower than some of the source rocks in the region (Church and Johnson, 1978).

TABLE 2-1-2
CORRELATION MATRIX OF CHEMICAL DATA*

VARIABLE	LOI	SiO ₂	Ba	Ce	Cs	La	Mo	Sc	Th	U	V
LIO	1	-.909	-.754	-.57	.742	-.567	.611	.284	-.196	.742	.237
SiO ₂ 1		.798	.684	-.736	.617	-.501	-.33	.201	-.61	-.087
Ba 1			.829	-.652	.728	-.302	-.389	.077	-.395	.059
Ce 1				-.592	.868	-.138	-.495	-.07	-.248	.274
Cs 1					-.428	.361	.629	-.064	.508	-.014
La 1						-.15	-.23	.118	-.325	.124
Mo 1							-.125	-.134	.75	.542
Sc 1								.264	-.098	-.483
Th 1									-.109	-.073
U 1										.519
V 1										

* Based on log transformation of data in Table 2-1-1.

Molybdenum is commonly associated with uranium and enrichment of vanadium is noted in some deposits (Levinson *et al.*, 1984). In the sedimentary cycle, under oxidizing conditions, molybdate ions are mobile and travel together with vanadium. Under strongly reducing conditions, such as found in peat bogs and carbonaceous sedimentary rocks, molybdenum may precipitate as molybdenite (MoS₂) if hydrogen sulphide (H₂S) is available.

Thorium can also be adsorbed by organic material, however, this element is relatively insoluble in most surface and groundwaters and its presence can usually be explained by silicate variations in the silt fraction.

Table 2-1-2 presents the correlation matrix (r-coefficients) for the elements listed in Table 2-1-1 (log transformed). It can be seen that the abundances of uranium and molybdenum are positively correlated with LOI as is cesium (Cs), which is a heavy alkali metal absorbed in clays. Scandium adsorbs on clay explaining the positive correlation of this element with cesium — it may also substitute to some extent for ferrous iron, especially in micas. The association of clay and organic material in the peat deposit suggested by these data, is not surprising and the strong negative correlation of silica (representing clastic material) and LOI (that includes organics), r=-0.909, fits a

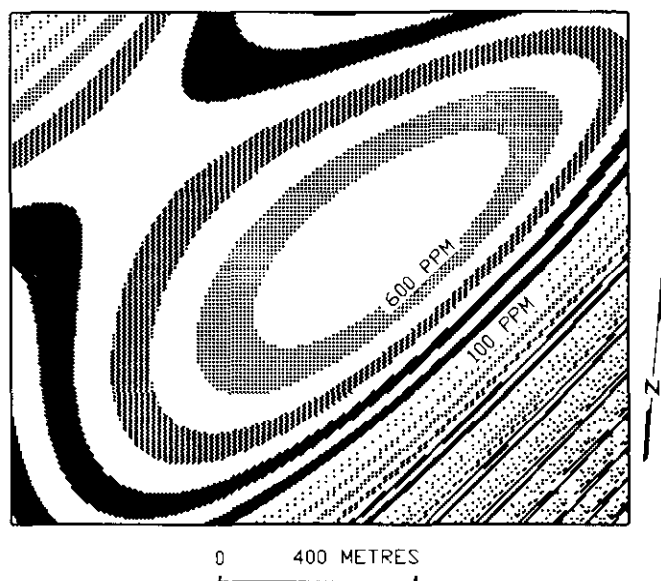


Figure 2-1-4. Trend surface map of uranium (U), Prairie Flats area (6th order polynomial surface)

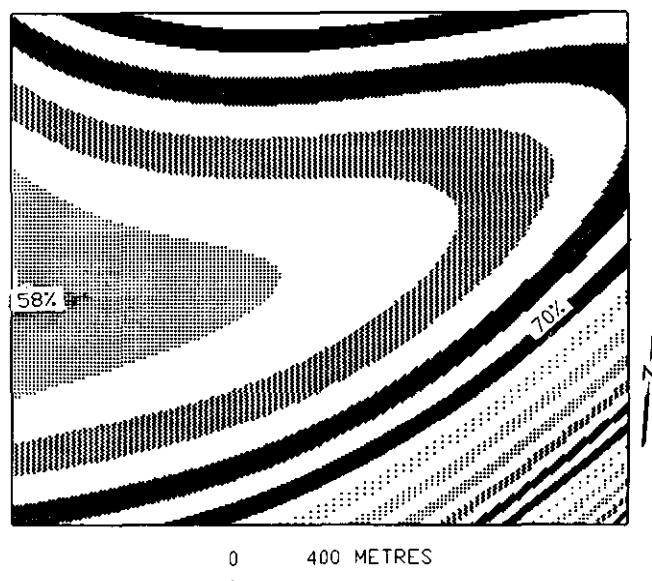


Figure 2-1-5. Trend surface map of SiO₂, Prairie Flats area (6th order polynomial surface).

model indicating that some of the peat is relatively free of clastic input, perhaps distal from the source area. The alkaline-earth and lanthanide elements, barium, lanthanum and cerium, are positively correlated with silica suggesting transportation in clastic minerals, perhaps in alkali feldspar. Lanthanum and cerium are also known to concentrate in apatite which may survive transport as a clastic component, together with quartz.

Figure 2-1-4 is a trend-surface map of uranium content based on the random array of sampling stations in the Prairie Flats area (Figure 2-1-3). The contours form an asymmetric elliptical bull's eye rising abruptly on the southeast side of the deposit from 100 to more than 600 ppm over a distance of 200 metres. This is a 6th order polynomial surface (coefficient $r=0.57$); the procedure for preparation of trend-surface maps is described in detail by Krumbein, 1959. The general shape of the contours coincides with the northeast elongation of the marshland, with the highest concentration of uranium in the east-central part. Possible erosion or leaching of the deposit along the southeast side may account for the rapid change in uranium values here. Alternatively, the uranium may already have migrated from the centre of peat accumulation farther to the west.

Figure 2-1-5 is the result of trend-surface analysis of normalized silica data for the Prairie Flats area. The silica is normalized to a LOI-free basis to better reflect the distribution of the clastic sedimentary fraction in the area. This assumes that the coarse clastic fraction is mainly quartz. Normalized silica ranges from 51.49 to 70.37 per cent, with the highest values peripheral to much of the marshland area. The map contours have a parabolic outline with values diminishing from the maximum of about 70 per cent on the north and southeast margins of the Prairie Flats area to about 50 per cent on the west. This is also a 6th order polynomial surface (coefficient $r=0.61$). It appears that these contours are roughly parallel to the original margin or strand line of the peat basin which evidently had a northeast-southwest elongation.

In conclusion, variations in the abundance of selected elements show the influence of a combined clastic and chemical depositional environment on the formation of the Prairie Flats marshland — an environment where alkalinity and oxidizing/reducing conditions were important.

The original geometry of the basin is suggested by the shape of the trend-surface contours for normalized silica. These contours are parabolic in outline and open to the west possibly defining the strand line of the original marsh. This suggests that the centre of the marshland may have been farther west (prior to erosion) than the present Prairie Flats location.

The highest concentration of uranium, over 600 ppm, is in the east-central part of the Prairie Flats area. Steep uranium contours on the southeast side suggest some chemical remobilization of uranium in the marshland to the southeast.

This may have been caused by inadvertent cultural disturbance such as farming or urban activities at the outer Summerland town limits. However, further studies in the area are necessary to confirm these conclusions.

ACKNOWLEDGMENTS

The support and encouragement of the Community Futures group in Penticton, especially G. Stayberg, M. Cook, B. Dehart, S. Leaming and A. Daniels, was essential for the implementation and completion of the project.

The writers are obliged to T. Lewis of the Geological Survey of Canada for cooperation and scientific advice and support for this study. Technical data supplied by S.A.S. Croft of Nevin, Sadlier-Brown, Goodbrand Ltd., D.G. Leighton of D.G. Leighton and Associates Ltd., S.Y. Johnson and R.A. Zielinski of the United States Geological Survey are gratefully acknowledged.

REFERENCES

- Bates, D.V., Murray, J.W. and Raudsepp, V. (1979): The Commissioners First Interim Report on Uranium Exploration; *Royal Commission of Inquiry, Health and Environmental Protection, Uranium Mining, Province of British Columbia*; 18 pages.
- Church, B.N. (1973): Geology of the White Lake Basin; *B.C. Ministry of Energy, Mines and Petroleum Resources, Bulletin 61*.
- Church, B.N. (1980): Anomalous Uranium in the Summerland Caldera; *B.C. Ministry of Energy, Mines and Petroleum Resources, Geological Fieldwork 1979, Paper 1980-1, pages 11-15*.
- Church, B.N. (1982): Geology of the Penticton Tertiary Outlier; *B.C. Ministry of Energy, Mines and Petroleum Resources, Revised Preliminary Map 35*.
- Church, B.N. and Johnson, W.M. (1978): Uranium and Thorium in Tertiary Alkaline Volcanic Rocks of South-central British Columbia; *Western Miner.* Volume 51, Number 5, pages 33-34.
- Church, B.N., McAdam, K. and Hudson, J. (1983): Geothermal Potential Map of British Columbia; *B.C. Ministry of Energy, Mines and Petroleum Resources*.
- Culbert, R.R. (1980): Report on Post-glacial Uranium Concentrations in the Southern Okanagan Valley; report for the *B.C. Ministry of Health*, released by the B.C. Royal Commission of Inquiry, Health and Environmental Protection — Uranium Mining.
- Culbert, R.R., Boyle, D.R. and Levinson, A.A. (1984): Surficial Uranium Deposits in Canada; in Surficial Uranium Deposits, P.D. Toens, Editor, *International Atomic Energy Agency, Vienna, Tecdoc-322, pages 179-191*.
- Culbert, R.R. and Leighton, D.G. (1978): Uranium in Alkaline Waters, Okanagan Area, British Columbia; *Canadian Institute of Mining and Metallurgy, Bulletin, Volume 71, Number 793, pages 103-110*.
- Culbert, R.R. and Leighton, D.G. (1988): Young Uranium; *Ore Geology Reviews, Volume 3, pages 313-330*
- Jessop, A.M. and Judge, A.S. (1971): Five Measurements of Heat Flow in Southern Canada; *Canadian Journal of Earth Sciences, Volume 8, Number 6, pages 711-716*.

- Johnson, S.Y., Otton, J.K. and Macke, D.L. (1987): Geology of the Holocene Surficial Uranium Deposit of the North Fork of Flodelle Creek, Northeastern Washington; *Geological Society of America*, Bulletin, Volume 98, pages 77-85
- Krumbein, W.C. (1959): Trend Surface Analysis of Contour-type Maps with Irregular Control-point Spacing; *Journal of Geophysical Research*, Volume 64, Number 7, pages 823-834.
- Levinson, A.A., Bland, C.J. and Dean, J.R. (1984): Uranium Series Disequilibrium in Young Surficial Uranium Deposits in Southern British Columbia; *Canadian Journal of Earth Sciences*, Volume 21, pages 559-566.
- Lewis, T. (1984): Geothermal Energy from the Penticton Tertiary Outlier, British Columbia: an Initial Assessment; *Canadian Journal of Earth Sciences*, Volume 21, pages 181-188.
- Lewis, T.J. and Werner, L. (1982): Geothermal Gradients on the West Side of Okanagan Lake, B.C.; *Energy, Mines and Resources Canada, Earth Physics Branch*, Ottawa, Ontario, Open File 82-6.
- Nevin, Sadlier-Brown, Goodbrand Ltd. (1987): Feasibility Study for Direct Utilization of Geothermal Energy Resources at Summerland, B.C.; unpublished report, 85 pages.
- Zielinski, R.A. and Meier, A.L. (1988): The Association of Uranium with Organic Matter in Holocene Peat: an Experimental Leaching Study; *Applied Geochemistry*, Volume 3, pages 631-643.
- Zielinski, R.A., Otton, J.K., Wanty, R.B. and Pierson, C.T. (1987): The Geochemistry of Water near a Surficial Organic-rich Uranium Deposit, Northeastern Washington State, U.S.A.; *Chemical Geology*, Volume 62, pages 263-289.



**THE USE OF PRODUCTION DATA AS AN EXPLORATION GUIDELINE
FOR Ag-Pb-Zn-Au VEIN AND REPLACEMENT DEPOSITS,
NORTHERN KOKANEE RANGE, SOUTHEASTERN BRITISH COLUMBIA
(82F, K)**

**By Georges Beaudoin
University of Ottawa
D.F. Sangster
Geological Survey of Canada**

KEYWORDS: Economic geology, vein, silver, lead, zinc, Sandon, Ainsworth, Slocan, production data, exploration, Kokanee Range

INTRODUCTION

In a series of papers Orr (1971), Orr and Sinclair (1971), Sinclair (1974, 1979, 1982), Goldsmith and Sinclair (1985), and Goldsmith *et al.* (1986) used production statistics to investigate metal grades, metal ratios, and deposit density zonation on a mining-camp scale and attempted to define statistical relationships between metal grades and the size of an orebody using multiple regression and discriminant analysis. Goldsmith and Sinclair (1985) found that statistical models differed significantly from camp to camp and standard errors could be reduced using multiple independent variables (*i.e.* metal grades). The most important variable controlling the variance of their models, although different from camp to camp, in each case was negatively correlated to tonnage and of minor economic importance.

In the present study, we investigate the use of production data as guidelines to the exploration for new mineral resources in a formerly very active mining area. The study area is located north of the city of Nelson, southeastern British Columbia, between Slocan and Kootenay lakes and comprises the old mining camps of Slocan, Slocan City and Ainsworth. The deposits consist of silver-lead-zinc-gold veins and replacements which occur in all sedimentary and intrusive rocks outcropping in the area, with the exception of a few of the Eocene lamprophyre dikes which are post mineralization. The deposits consist mainly of: veins and lenses in fault zones of various widths and fabrics, where mineralization typically displays open space filling textures and is commonly brecciated and deformed by later fault movements; and massive replacements of limestone surrounding fractures. Although replacement deposits are less numerous than vein deposits, they account for about 55 per cent of ore production in the study area, with the Bluebell replacement deposit representing 46 per cent of total production. Mineralogy is predominantly galena and sphalerite with accessory pyrite, pyrrhotite, chalcopyrite and a variegated suite of silver minerals and sulphosalts in a gangue of siderite, dolomite, calcite or quartz. The reader is referred to Cairnes (1934, 1935), Hedley (1945, 1952), Little (1960),

Brown and Logan (1989), Beaudoin (1990) and Beaudoin and Sangster (1990) for more details of individual deposits and regional geology.

Cumulative production data for the study area are presented in Table 2-2-1. Metals such as zinc were not mined in the early years because their occurrence in the ore concentrate resulted in a penalty from the smelter. Zinc production data must therefore be used with caution and we have limited its use to a minimum in this study. Similarly, cadmium data are suspect because of the close association of the metal with sphalerite. Copper was recovered from only a few deposits and was not deemed to be sufficiently ubiquitous to warrant investigation in this study. Additionally, in small operations rich ore shoots were mined selectively, thus tending to increase overall ore grades. Accordingly we tried to avoid the use of grades in our study and, instead, used cumulative tonnages of ore mined, metal recovered, and metal ratios. Data for silver, lead, zinc and gold were selected for this study.

The British Columbia Ministry of Energy, Mines and Petroleum Resources MINFILE database was used as our source of production data. Each of the 272 deposits selected produced more than one tonne of ore. No attempts were made to verify the accuracy of individual records except for the Silvana mine of Treminco Resources Limited, the only current producer in the area, for which cumulative production to 1988 was used.

**TABLE 2-2-1
CUMULATIVE PRODUCTION FROM THE
NORTHERN KOKANEE RANGE**

Tonnage	10 432 412 tonnes
Pb	530 240 663 kg
Zn	505 399 616 kg
Cu	2 867 915 kg
Cd	1 771 485 kg
Ag	2 623 406 019 g
Au	961 483 g
Cumulative metal ratios ¹	
Pb/(Pb+Zn)	0.51
(Ag · 1000)/[(Ag · 1000)+Pb]	0.83
Ag/[Ag + (Au · 1000)]	0.73

¹ ratios computed using mass units of cumulative production

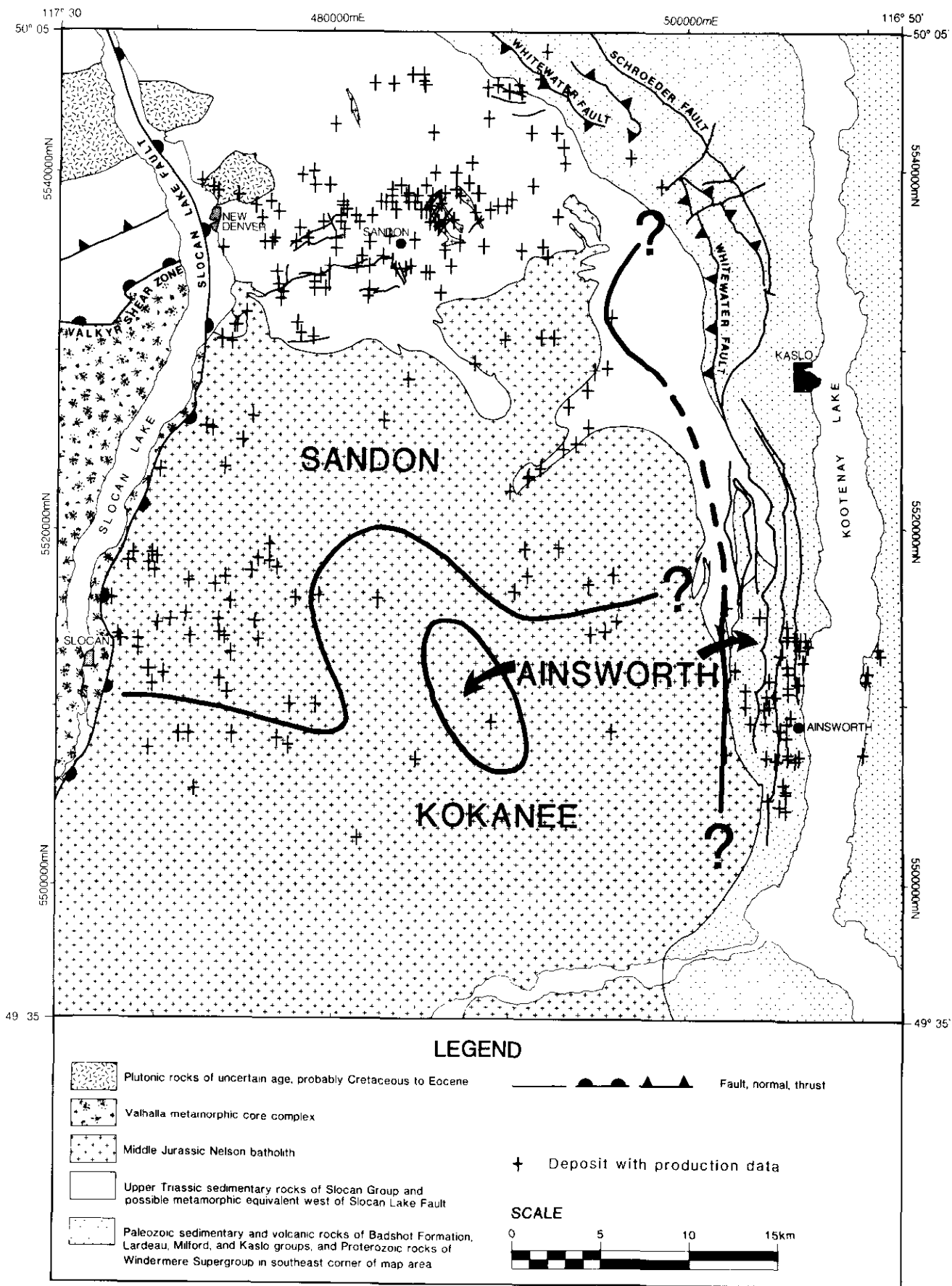


Figure 2-2-1. Location of deposits from the study area with production data recorded in MINFILE database. The areas containing deposits with lead isotope ratios typical of Sandon, Ainsworth, and Kokanee groups are broadly outlined.

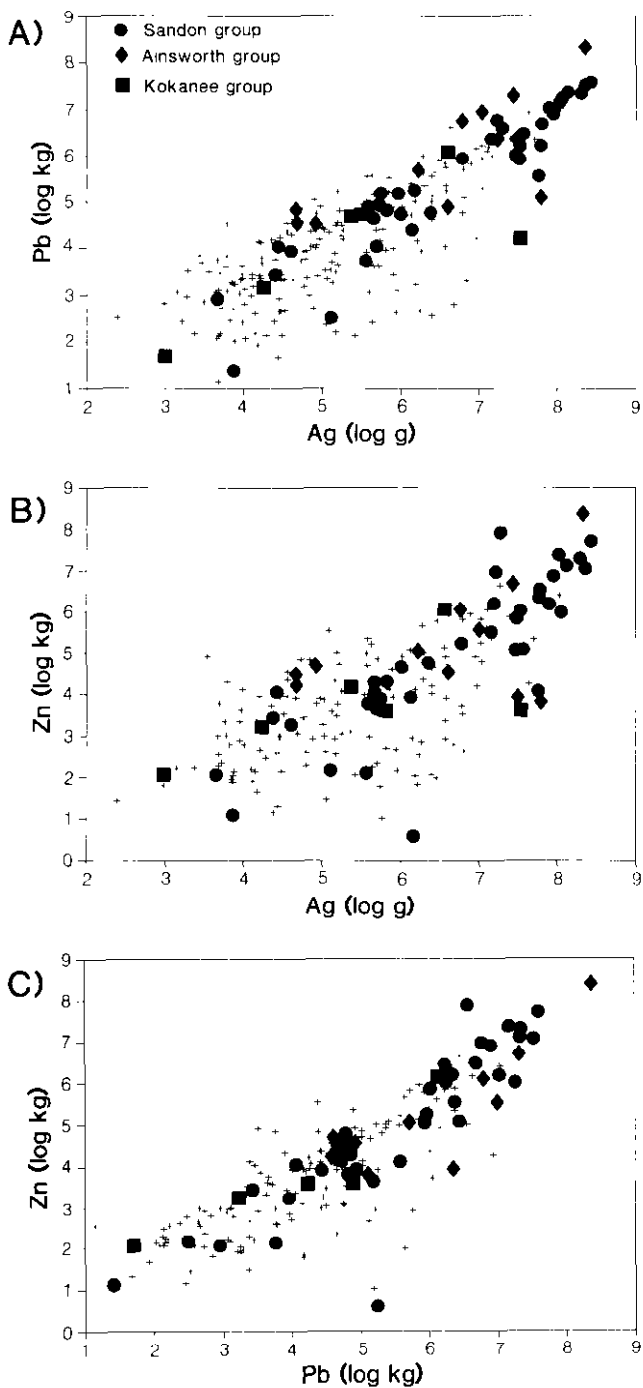


Figure 2-2. Log-log scatter plots of total metal production per deposit. See text for discussion. (A) Pb versus Ag. (B) Zn versus Ag. (C) Pb versus Zn.

DESCRIPTION OF CUMULATIVE PRODUCTION DATA

Deposits in the Slocan, Slocan City and Ainsworth mining camps are either hosted by the Middle Jurassic Nelson batholith or occur peripheral to it in sedimentary rocks of

the Badshot Formation, Lardeau, Kaslo, Milford and Slocan groups of Early Cambrian to Late Triassic age. Logan *et al.* (1987) found that lead isotope ratios of galena from some of the deposits fell into three groups. This grouping was confirmed using all published galena lead isotope ratios. The three groups of deposits have a distinct geographical distribution and we have used this grouping to study the production statistics. Due to lack of lead isotope data, however, only 24 per cent of the deposits could be assigned to a group. The locations of the mineral deposits for which production data exist are shown in Figure 2-2-1, with a broad outline of the geographical distribution of the three groups of lead isotopes. The three groups of lead isotopes are named Sandon, Kokanee and Ainsworth, and production data will be discussed in relation to the location of the deposits within the areas defined by the three groups.

The three most abundant metals, silver, lead and zinc display log-log linear relationships (Figure 2-2-2). Scatter plots of the log of the amount of metal extracted from each deposit exhibit a sharp upper limit and a convex lower limit. The peculiar half-moon shape of the log-log arrays does not seem to be related to population statistics but to anthropogenic artifacts as discussed below. On each of these plots the three lead isotope groups cannot be distinguished from one another and will therefore be treated as a single statistical population.

In Figures 2-2-2b and 2c the lower limit of the scatter plots comprises deposits with high contents of silver or lead relative to zinc. As zinc was an unwelcome commodity in the early days of mining (backfilling with zinc-bearing waste is reported for the Payne deposit) selective mining probably resulted in lower cumulative production of zinc. The reasons for the irregular lower limit of the array in the log Pb versus log Ag (Figure 2-2-2a) is less obvious as galena was one of the ore minerals specifically sought during mining. For small deposits, it can be argued that selective mining of a specific texture of foliated galena ("steel galena"), considered by miners to be rich in silver, is responsible for the scatter. Visible pyrrargyrite is almost always found in foliated, fine-grained galena at the Silvana mine, whereas it is rarely found in large lenses of massive galena. Another explanation for deposits with high cumulative production of silver relative to lead and also zinc, is that these deposits represent the so-called "dry ores" of Cairnes (1934), which are characterized by quartz veins with disseminated silver minerals and sulphosalts and little galena or sphalerite. Their lead isotopes, however, are similar to the other deposits richer in lead and zinc.

Interestingly, gold does not show a linear relationship with either lead, zinc or silver. There is a weak negative correlation between copper and gold. The reasons for the apparently different behavior of gold are unresolved, but may be related to its associated minerals.

EXPLORATION GUIDELINES

Production tonnage is a minimum estimate of the size of a deposit because unrecovered reserves are excluded, and losses during beneficiation must have occurred. To some

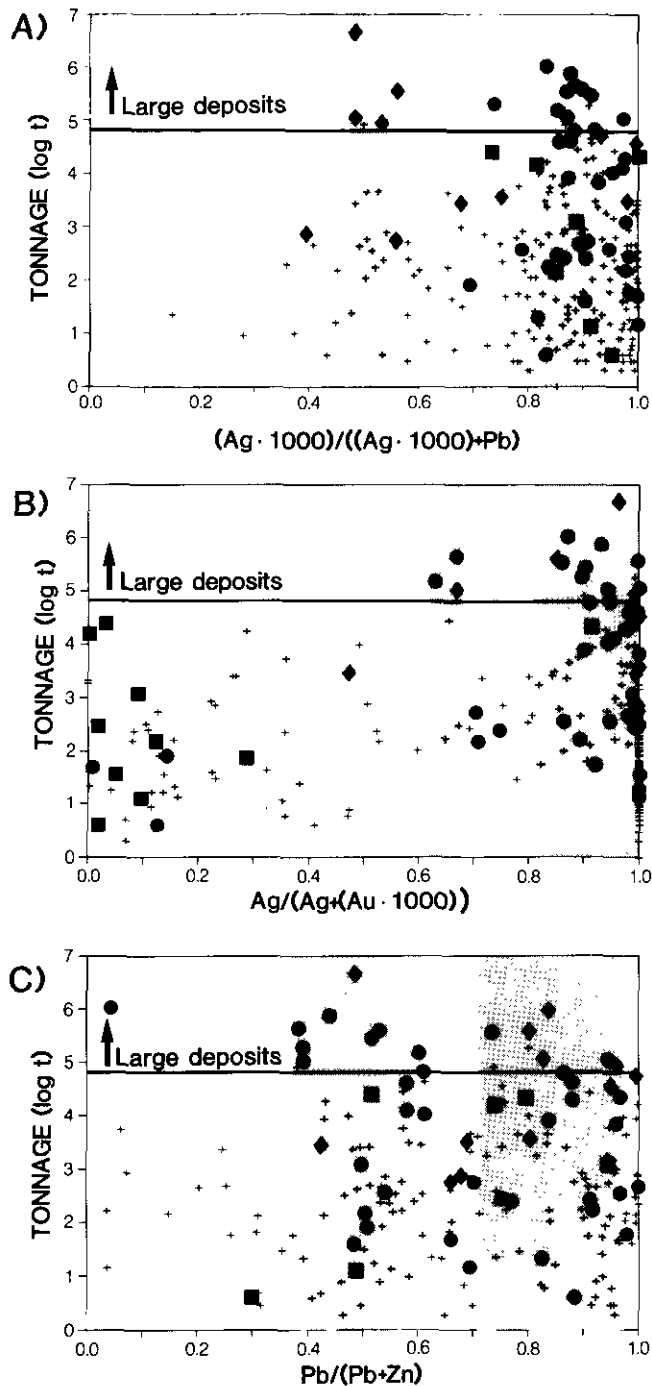


Figure 2-2-3. Log total production tonnage per deposit relative to metal ratios. Shaded areas comprise the ranges of ratios of the large deposits. The horizontal line at 63 000 tonnes separates large deposits from the rest of the data. Symbols as in Figure 2-2-2, all metals in kg. See text for discussion. (A) Tonnage versus $(Ag \cdot 1000)/[(Ag \cdot 1000)+Pb]$ (B) Tonnage versus $Ag/[Ag+(Au \cdot 1000)]$. (C) Tonnage versus $Pb/(Pb+Zn)$.

extent, production tonnage is also a function of mining methods, especially in districts with a long mining history. For the purpose of this study, large orebodies are defined as those greater than 63 000 tonnes, the 50th percentile value for Canadian lead-zinc vein and replacement deposits (Sangster, 1986). Metal ratios for these large orebodies were used to provide empirical exploration guidelines to identify former small producers that may have potential for being larger. The technique should, of course, be regarded as only one of many tools to evaluate mineral occurrences or past producers. Nevertheless, there is a striking consistency in the metal ratios of large producers and the use of their ratios in assessing mineral exploration targets in the study area is proposed.

SILVER:LEAD RATIOS

The graph of $(Ag \cdot 1000)/[(Ag \cdot 1000)+Pb]$ versus log tonnage (Figure 2-2-3a) demonstrates that most of the large orebodies correspond with two ranges of ratios. The first range, between 0.47 and 0.57, comprises all the large orebodies of the Ainsworth group. The second range, from 0.82 to 0.93, comprises most of the large orebodies from the Sandon group. The Cork-Province deposit (082FNW094) ratio (0.74) is intermediate between Ainsworth and Sandon ranges. This deposit has lead isotope ratios typical of the Sandon group and the reason for its anomalous $(Ag \cdot 1000)/[(Ag \cdot 1000)+Pb]$ ratio remains unknown. The Hewitt deposit (082FNW065), with a ratio of 0.97 is outside the Sandon range but is contained within the same fault zone as the Sandon group Van Roi deposit (082FNW064). Both have similar lead, sulphur, carbon and oxygen isotope ratios (Beaudoin, unpublished data) whereas the Van Roi has a $(Ag \cdot 1000)/[(Ag \cdot 1000)+Pb]$ ratio within the Sandon range. There is thus justification for regarding the Van Roi and Hewitt as parts of the same orebody and calculating a new, weighted, ratio of 0.94. This, in turn, would redefine the Sandon range to extend from 0.82 to 0.95. This results in a Sandon range which excludes only one large orebody (Cork-Province). No deposit of the Kokanee group has a sufficiently large tonnage to qualify as a large orebody as defined in this study. The average $(Ag \cdot 1000)/[(Ag \cdot$

TABLE 2-2-2
STUDENT'S t TEST COMPARING THE DATABASE
WITH THE AU SUBSET

		Pb/(Pb+Zn)	Ag · 1000/[(Ag · 1000)+Pb]
1) Database	\bar{x} ¹	0.69	0.84
	n ²	195	251
2) Au subset	\bar{x}	0.67	0.87
	n	114	125
Student's t test	DF ³	307	374
	t ⁴	0.083	0.036
	t_c ⁵	2.576	2.576

¹ average

² number of observations

³ degrees of freedom

⁴ Student's t test of the ratio after logistic transformation

⁵ critical value of Student's t test at a level of significance of $2\alpha=0.01$

1000)+Pb] ratio of the Kokanee group, however, falls within the Sandon group range (Table 2-2-2).

SILVER:GOLD RATIOS

The graph of $Ag/[Ag+(Au \cdot 1000)]$ versus log tonnage (Figure 2-2-3b) also exhibits two ranges of ratios which contain all the large orebodies. One of the ranges, 0.84 to 1.00, contains a majority of the large deposits of both the Ainsworth and Sandon groups. A large number of deposits possess a ratio of 1.00; this is caused either by very low gold content in the orebody or, more commonly, by the absence of gold production data.

A second range of ratios, between 0.62 and 0.68, includes only three large orebodies. Two of them, the Victor (082FNW204) and Whitewater (082KSW033), are from the Sandon group whereas the other, the Kootenay Florence (082FNE016), is from the Ainsworth group. There is no obvious geographic or geologic reason for their higher gold content.

LEAD:ZINC RATIOS

A graph of $Pb/(Pb+Zn)$ ratios versus log tonnage (Figure 2-2-3c) indicates that this ratio has a wide range, even for large orebodies. All but one large deposit (Lucky Jim, 082KSW023) are contained within two broad ranges extending from 0.37 to 0.61 and 0.71 to 0.97. Both contain deposits from the Ainsworth and Sandon groups.

ANALYSIS OF EXPLORATION GUIDELINES

Based on this analysis of metal ratios and deposit size, it is suggested that those small deposits in the study area which possess all three metal ratios falling within the favourable ranges defined here be considered exploration targets with good potential to contain further, undiscovered, ore reserves.

Gold data are available for 137 of the 272 deposits studied. We tested to see if the deposits with gold data are from a representative subset of the database. We have applied the logistic transformation to $(Ag \cdot 1000)/[(Ag \cdot 1000)+Pb]$ and $Pb/(Pb+Zn)$ ratios since they are constrained between 0 and 1 and have a skewed distribution. Student's t tests indicate that there is no statistical evidence suggesting that the means of the transformed ratios from the gold data subset come from a different population than does the entire database (Table 2-2-2). Also, there are similar proportions in the gold data subset and the database of deposits within both favourable ranges of $(Ag \cdot 1000)/[(Ag \cdot 1000)+Pb]$ ratios. Accordingly we conclude that the gold data subset is representative of the database.

Within the Ainsworth group, only one deposit falls within the favourable ranges of $(Ag \cdot 1000)/[(Ag \cdot 1000)+Pb]$, $Ag/[Ag+(Au \cdot 1000)]$, and $Pb/(Pb+Zn)$ ratios and hence, by this criterion, would be regarded as potentially larger than its past production would indicate (Table 2-2-3). Within the Sandon and Kokanee groups, 24 deposits are considered to have potential for being larger than their past production

(Table 2-2-3). These 24 exploration targets represent 40 per cent of the deposits with favourable $(Ag \cdot 1000)/[(Ag \cdot 1000)+Pb]$ ratios from the gold data subset. They represent 18 per cent of the gold data subset and about 9 per cent of the whole database. If, in fact, the gold data subset is representative of the database, as suggested above, the empirical exploration guidelines proposed in this paper should enable one to select about 18 per cent of the known deposits as potential new development targets in the study area. We suggest that this percentage is also a better estimate than the percentage (0.7%) obtained for the Ainsworth group because of the small number of deposits within the favourable ranges of ratios available in that group.

The efficiency of these exploration guidelines can be checked by verifying the past production of the targets identified in the study area. Of the 25 targets identified, nine (36%) produced more than 10 000 tonnes of ore including one with production over 50 000 tonnes, twelve (48%) have produced between 10 000 tonnes and 1000 tonnes and the remaining four (16%) have produced less than 1 000 tonnes. There are 38 deposits with more than 10 000 tonnes of production in the study area. Excluding the large orebodies as defined in this study, the nine deposits that have each produced more than 10 000 tonnes of ore represent 24 per cent of the deposits within this class of tonnage in the area. The proposed exploration guidelines are not biased by the larger scale mining operations and therefore permit selection of targets which have produced varied quantities of ore.

Figure 2-2-4 shows the locations of the 25 targets relative to the known large orebodies in the area. An obvious feature is the clustering of large orebodies in two relatively small areas; one near Sandon and the other near Ainsworth.

TABLE 2-2-3
LIST OF EXPLORATION TARGETS

MINFILE	NAME	PRODUCTION (Tonnes)
082FNE005	VIGILANT	4684
082FNW008	ALAMO	357
082FNW015	ALTOONA	8041
082FNW020	LAST CHANCE	9445
082FNW021	SURPRISE	44476
082FNW028	BELL	4146
082FNW035	RECO	6697
082FNW036	SLOCAN SOVEREIGN	4539
082FNW037	NOBLE FIVE	39812
082FNW042	ELKHORN	3071
082FNW043	WONDERFUL	28382
082FNW052	RUTH-HOPE	59753
082FNW054	RICHMOND-EUREKA	36651
082FNW057	IVANHOE	40294
082FNW060	MAMMOTH	19283
082FNW063	LUCKY THOUGHT	8951
082FNW068	NOONDAY	572
082FNW083	FLINT	171
082FNW148	ENTERPRISE	10687
082FNW177	MOUNTAIN CHIEF	2989
082FNW181	AMERICAN BOY	5948
082FNW197	CANADIAN	855
082KSW011	ANTOINE	10127
082KSW030	WELLINGTON	1779
082KSW031	CHARLESTON	2324

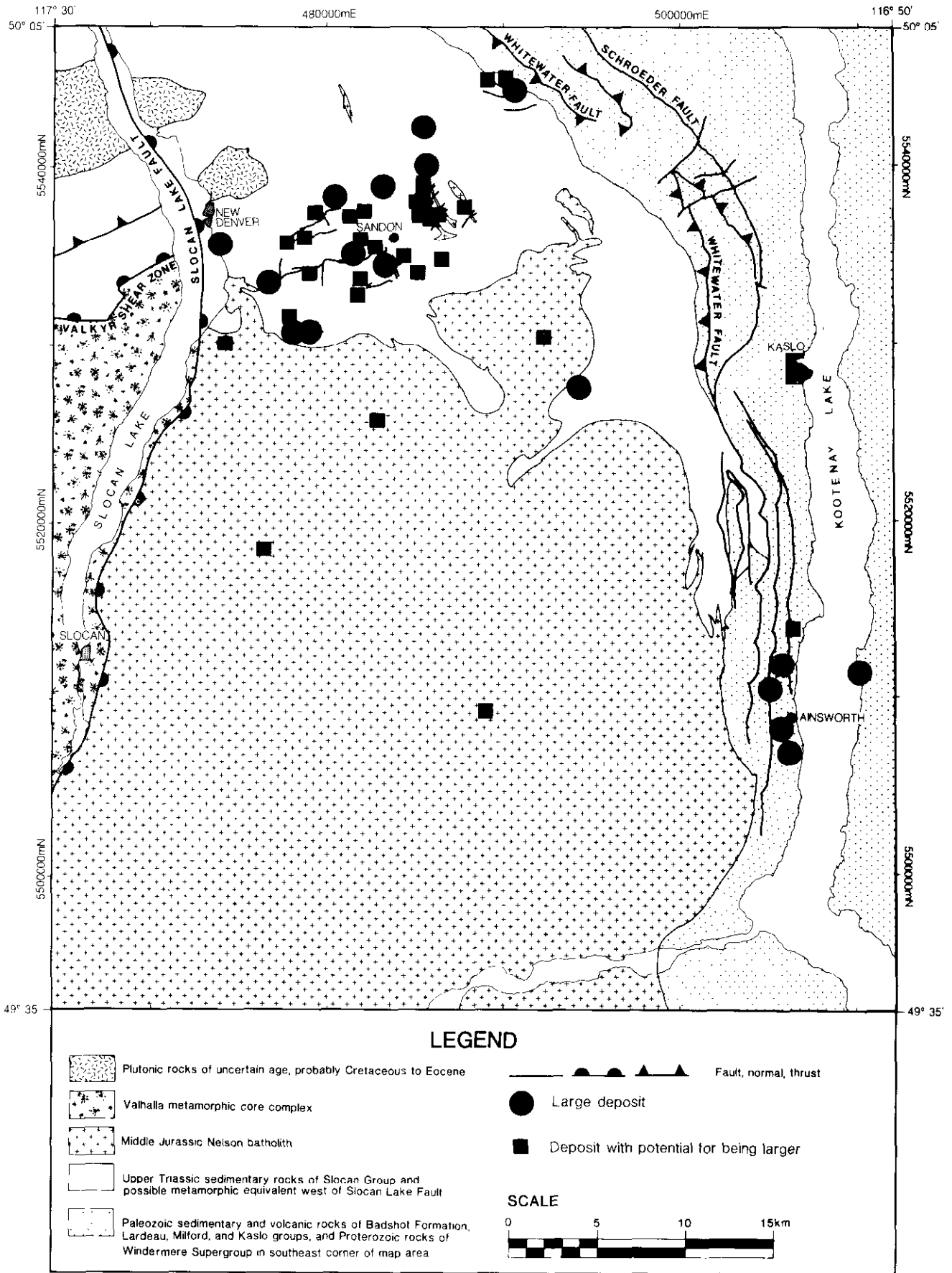


Figure 2-2-4. Location of large deposits and others with potential for being larger, based on their metal ratios.

Almost all the exploration targets are, however, confined to the area near Sandon.

Some of the targets are hosted by the same structure as some large orebodies. The most striking example is the "Main Lode" near Sandon. The "Main Lode" has been interpreted by numerous mine geologists and Hedley (1952) as a continuous fault zone containing several large orebodies: the Standard (082FNE180), Silvana (082FNE050) and Silversmith (082FNE053). Two of the proposed targets, the Ruth-Hope (082FNE052) and Richmond-Eureka (082FNE054) are also contained within the "Main Lode" and occur respectively between the Silvana and Silversmith deposits and to the east of the Silversmith deposit.

Metal zoning in the orebodies could reduce the accuracy of these exploration guidelines because a zoned deposit, if partially mined, would yield production metal ratios not representative of the deposit as a whole. Vertical mineralogical zoning is reported in the literature from nine deposits, although there is no quantitative information on this zoning. Metal zoning has also not been documented but would be expected if, indeed, there is mineralogical zoning. Reported vertical mineralogical zoning generally consists of increased abundances of sphalerite or siderite with depth relative to galena or quartz. At Silvana, metal ratios in millhead assays for individual stopes do not show evidence of either lateral or vertical zoning across the orebody. A poorly defined increase of $(Ag \cdot 1000)/[(Ag \cdot 1000)+Pb]$ with depth may be present although detailed study of individual sections through the orebody shows similar, reverse, or nonsystematic variation of the same ratio. Careful investigation of paragenesis has shown neither vertical nor lateral mineralogical zoning at Silvana. Therefore it is concluded that vertical mineralogical and metal zoning, although

reported, have not been conclusively demonstrated and, where investigated, have been shown to be nonexistent. Consequently, metal-ratio zoning is unlikely to have influenced the exploration guidelines proposed here.

Systematic channel sampling is a common method employed in the determination of metal grades and has been carried out in some stopes in the Silvana orebody. A typical histogram of $(Ag \cdot 1000)/[(Ag \cdot 1000)+Pb]$ ratios from one of the stopes at Silvana (Figure 2-2-5a) shows that the ratios cluster between 0.97 and 1.00. No sample had a ratio either in the previously determined favourable range for the Sandon group (0.82-0.95) or close to the ratio for cumulative production data at Silvana (0.90). This contrasts with a strong mode for the $(Ag \cdot 1000)/[(Ag \cdot 1000)+Pb]$ ratios of all millhead stope data between 0.88 and 0.90, similar to cumulative production data (Figure 2-2-5). It thus appears that channel sampling within individual stopes or lodes does not produce metal ratios directly comparable with production data. The reasons for the contrast remain obscure. It appears therefore that only production data should be used in conjunction with the exploration guidelines proposed here.

CONCLUSIONS

It is concluded that cumulative production data can be useful to assess the potential of past producers when a large database exists for a group of deposits which may be considered as a single population. In the study area, large deposits have a limited range of silver, lead, zinc, and gold metal ratios. We suggest that these common parameters can be used to identify those past producers which have the potential for being larger than indicated by their production record. The empirical exploration guidelines developed here could be modified by the discovery of new large orebodies with different metal ratios. From the currently available database, we propose that deposits in the study area with metal ratios within the following ranges have potential for being larger:

- i) Deposits from the Ainsworth group having $(Ag \cdot 1000)/[(Ag \cdot 1000)+Pb]$ ratios between 0.47 and 0.57 and deposits in the Sandon group having $(Ag \cdot 1000)/[(Ag \cdot 1000)+Pb]$ ratios ranging from 0.82 to 0.95.
- ii) Deposits in the Ainsworth and Sandon groups having $Ag/[Ag+(Au \cdot 1000)]$ ratios ranging from 0.84 to 1.00. It is also apparent that some deposits with ratios around 0.62 to 0.68 are also more likely to be large, with the added interest of being richer in gold.
- iii) Deposits in the Ainsworth and Sandon groups having $Pb/(Pb+Zn)$ ratios ranging from 0.36 to 0.61 and from 0.71 to 0.97.

ACKNOWLEDGMENTS

This study is being funded jointly by Natural Sciences and Engineering Research Council (NSERC) Operating Grant OGP 0038460 to D.F.S., by the Geological Survey of Canada, and by the British Columbia Ministry of Energy.

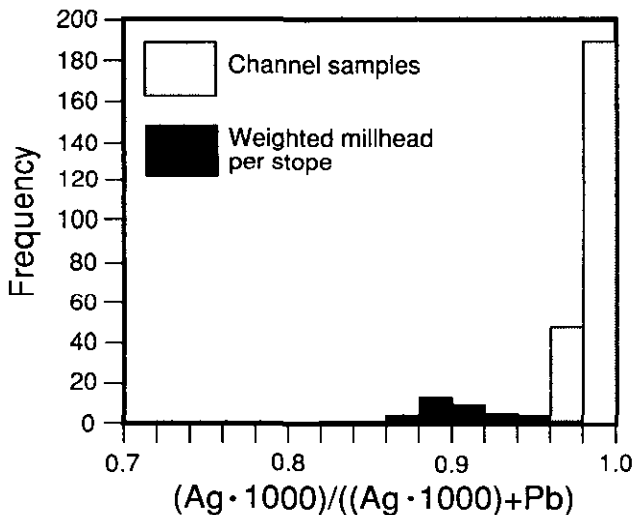


Figure 2-2-5. The histogram of $(Ag \cdot 1000)/[(Ag \cdot 1000)+Pb]$ ratio, using weighted millhead data for each stope, is superposed over a typical histogram of $(Ag \cdot 1000)/[(Ag \cdot 1000)+Pb]$ ratios from channel samples across the lode in stope 45-13-7, 8, Silvana Mine, Tremincio Resources Limited.

Mines and Petroleum Resources (Geoscience Research Grant RG89-04 and RG89-37). G. Beaudoin is supported by NSERC, Fonds pour la formation de chercheurs et l'aide à la recherche and University of Ottawa scholarships. We wish to express our gratitude to Silvana Division of Tremco Resources Limited for allowing use of their production data. The MINFILE database was provided by the Geological Survey Branch, British Columbia Ministry of Energy, Mines and Petroleum Resources. We wish to thank W.D. Sinclair and R.G. Garrett for reviewing the report.

REFERENCES

- Beaudoin, G. (1990): Geological Compilation Map, Northern Kokanee and Southern Goat Ranges, British Columbia; *B.C. Ministry of Energy, Mines and Petroleum Resources*, Open File 1990-18.
- Beaudoin, G. and Sangster, D.F. (1990): Preliminary Report on the Silvana Mine and other Ag-Pb-Zn Vein Deposits, Northern Kokanee Range, British Columbia; *B.C. Ministry of Energy, Mines and Petroleum Resources*, Geological Fieldwork 1989, Paper 1990-1: pages 251-255.
- Brown D.A. and Logan, J.M. (1989): Geology and Mineral Evaluation of Kokanee Glacier Provincial Park, (82S/11, 14) Southeastern British Columbia; *B.C. Ministry of Energy, Mines and Petroleum Resources*, Paper 1989-5, 47 pages.
- Cairnes, C.E. (1934): Slocan Mining Camp, British Columbia; *Geological Survey of Canada*, Memoir 173, 137 pages.
- Cairnes, C.E. (1935): Description of Properties, Slocan Mining Camp, British Columbia; *Geological Survey of Canada*, Memoir 184, 274 pages.
- Goldsmith, L.B. and Sinclair, A.J. (1985): Multiple Regression, a Useful Quantitative Approach in Evaluating Production Data from Vein-type Mining Camps, Southern British Columbia; *B.C. Ministry of Energy, Mines and Petroleum Resources*, Geological Fieldwork 1984, Paper 1985-1: pages 411-418.
- Goldsmith, L.B., Sinclair, A.J. and Read, P.B. (1986): Exploration Implications of Production and Location Data for Ag-rich Vein Deposits, Trout Lake Mining Camp, Southeastern B.C.; *Canadian Journal of Earth Sciences*, Volume 23: pages 1627-1640.
- Hedley, M.S. (1945): Geology of the Whitewater and Lucky Jim Mine Areas, Slocan District, British Columbia; *B.C. Ministry of Energy, Mines and Petroleum Resources*, Bulletin 22, 54 pages.
- Hedley, M.S. (1952): Geology and Ore Deposits of the Sandon Area, Slocan Mining Camp, British Columbia; *B.C. Ministry of Energy, Mines and Petroleum Resources*, Bulletin 29, 130 pages.
- Little, H.W. (1960): Nelson Map-area, West Half, British Columbia (82FW1/2); *Geological Survey of Canada*, Memoir 308, 205 pages.
- Logan, J.M., Gabites, J.E. and Brown, D.A. (1987): Galena Lead Isotope Characteristics of Mineralization in Kokanee Glacier Provincial Park, Southeastern British Columbia; *B.C. Ministry of Energy, Mines and Petroleum Resources*, Geological Fieldwork, Paper 1988-1: pages 535-541.
- Orr, J.F.W. (1971): Mineralogy and Computer-oriented Study of Mineral Deposits in Slocan City Camp, Nelson Mining Division, British Columbia; unpublished M.Sc. thesis, *The University of British Columbia*, 143 pages.
- Orr, J.F.W. and Sinclair, A.J. (1971): Mineral Deposits in the Slocan and Slocan City Areas of British Columbia; *Western Miner.* Volume 44: pages 22-34.
- Sangster, D.F. (1986): Classification, Distribution and Grade-tonnage Summaries of Canadian Lead-Zinc Deposits; *Geological Survey of Canada*, Economic Geology Report 37: 68 pages.
- Sinclair, A.J. (1974): Probability Graphs of Ore Tonnages in Mining Camps – A Guide to Exploration; *Canadian Institute of Mining and Metallurgy*, Bulletin, Volume 67: pages 71-75.
- Sinclair, A.J. (1979): Preliminary Evaluation of Summary Production Statistics and Location Data for Vein Deposits, Slocan, Ainsworth, and Slocan City Camps, Southern British Columbia; *Geological Survey of Canada*, Current Research, Part B, Paper 79-1B: pages 173-178.
- Sinclair, A.J. (1982): Multivariate Models for Relative Mineral Potential, Slocan Silver-Lead-Zinc Camp; *B.C. Ministry of Energy, Mines and Petroleum Resources*, Geological Fieldwork 1981, Paper 1982-1: pages 167-175.

**HYDROTHERMAL ALTERATION ASSOCIATED WITH THE SILVER QUEEN
POLYMETALLIC VEINS AT OWEN LAKE, CENTRAL B.C.***
(93L/2)

By **Xiaolin Cheng, A. J. Sinclair**
Margaret L. Thomson and Yuening Zhang
The University of British Columbia

KEYWORDS: Economic geology, Silver Queen, hydrothermal alteration, polymetallic vein, volcanic sequence, mineral assemblage, zoning.

INTRODUCTION

The Silver Queen polymetallic vein deposit is in the Intermontane Belt in central British Columbia (54°05'N; 126°44'W) about 100 kilometres southeast of Smithers and 35 kilometres south of Houston (*see Hood et al., 1991, this volume; Figure 2-3-1*). The study area lies in the central portion of the Nechako trough, just south of the Skeena arch. The deposit occurs near the rim of the Buck Creek basin, interpreted as a resurgent caldera delineated by intrusions and a semicircular alignment of Upper Cretaceous to Eocene volcanic centres (Church and Barakso, 1990).

Hydrothermal alteration in the mine area has not previously been studied in detail. Church (1970) noted that wallrock alteration included kaolinization of feldspar and replacement of ferromagnesian minerals by fine-grained carbonates, epidote and pyrite; altered rock characteristically is nonmagnetic. Church and Pettipas (1990) noted that the veins commonly have an argillic envelope and a broad aureole of propylitic alteration. Fyles (1984) indicated that kaolinite with or without sericite is common, and that the principal carbonate is siderite.

This study concentrates on alteration mineral assemblages and their spatial relationships to the No. 3 vein, the most explored mineralized zone in the study area. Results are based on petrographic examination and X-ray diffraction analysis of rock samples collected during under-

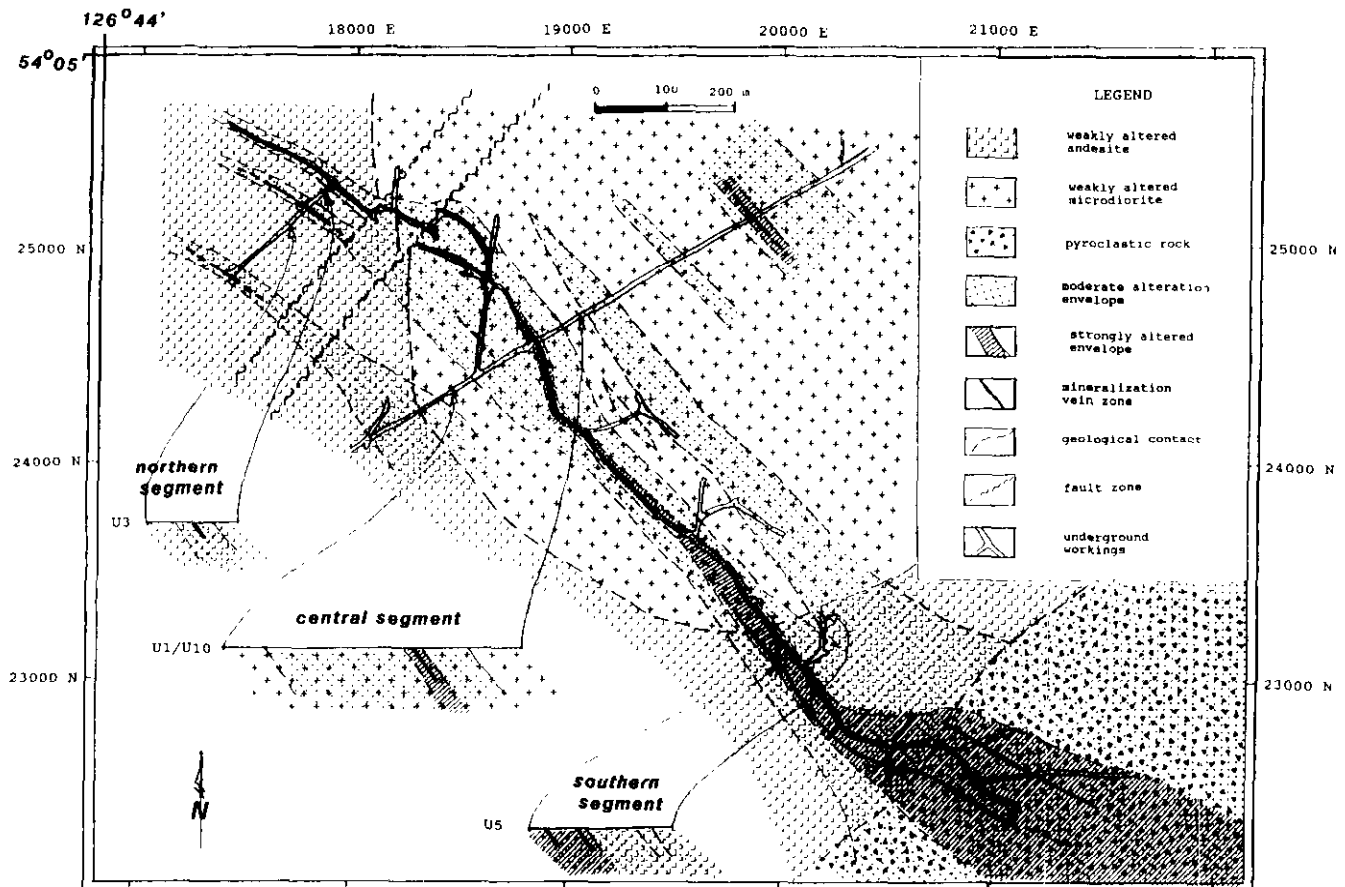


Figure 2-3-1. Schematic plan of alteration on the 2600-foot level, Silver Queen mine.

* This project is a contribution to the Canada/British Columbia Mineral Development Agreement.

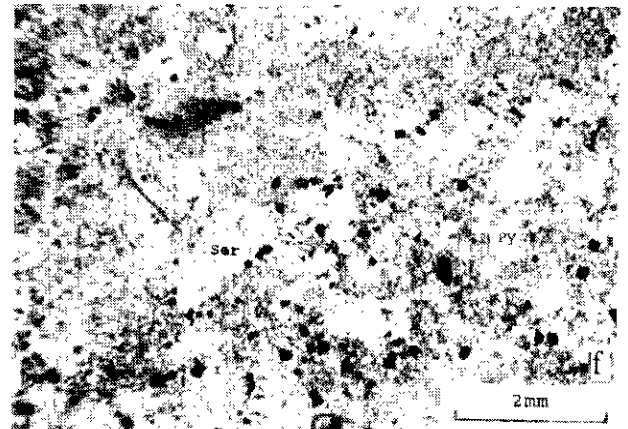
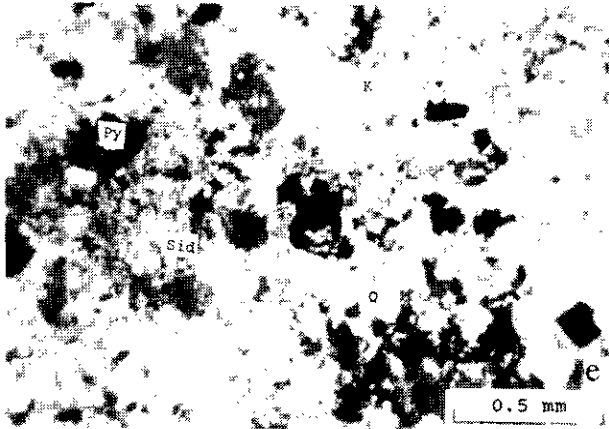
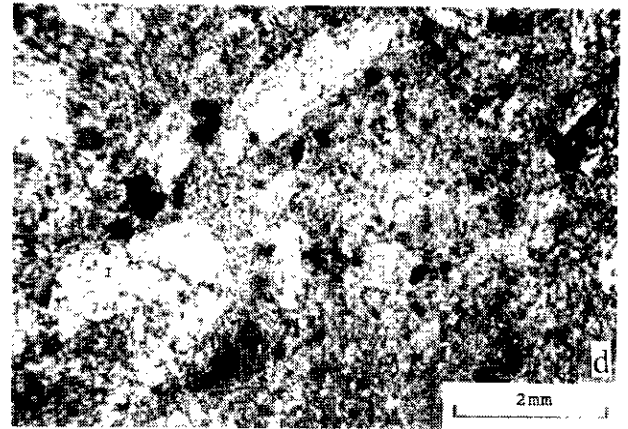
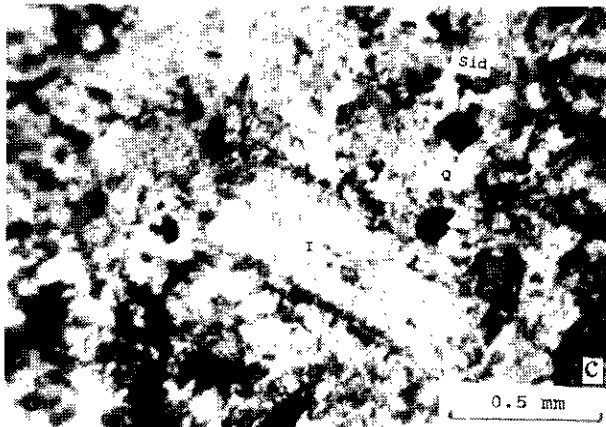
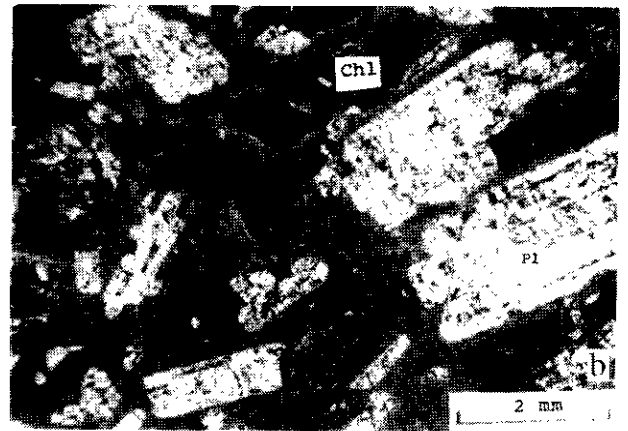
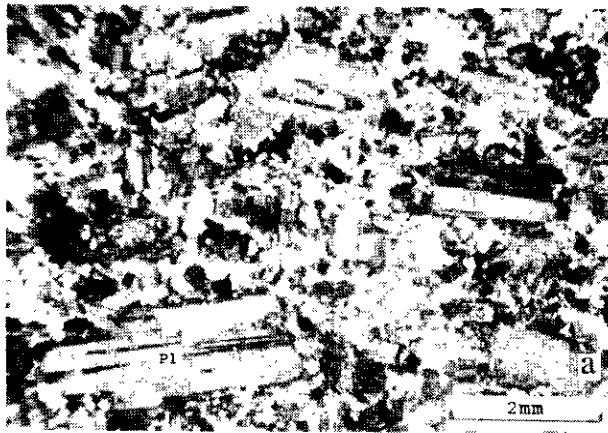


Plate 2-3-1. (a) Weakly altered microdiorite from the central segment of the No. 3 vein; (b) weakly altered andesite from the northern segment of the No. 3 vein. Photomicrographs a and b show that chlorite replaces augite, kaolinite partially replaces plagioclase along its margins and cleavages and aphanitic matrix remains unaltered; (c) moderately altered microdiorite from the central segment of the No. 3 vein; (d) moderately altered andesite from southern segment of the No. 3 vein. Photomicrographs c and d show that illite and kaolinite almost completely replace primary plagioclase, and the recrystallization and silicification of aphanitic matrix. (e) strongly altered microdiorite from the central segment of the No. 3 vein with kaolinite replacing plagioclase, carbonate replacing mafic mineral and matrix intensely recrystallized and silicified. Disseminated pyrite is common. (f) strongly altered andesite from the southern segment of the No. 3 vein with simple alteration mineral assemblage of sericite-quartz-pyrite. (Q = quartz; Pl = plagioclase; K = kaolinite; Sid = siderite; I = illite; Ser = sericite; Py = pyrite.)

ground mapping and drill-core logging. The sample base consists of 60 thin sections and their corresponding hand specimens, and 38 whole-rock analyses by X-ray diffraction. These samples represent northern, central, and southern cross-sections of the No. 3 vein on the 2600-foot underground level (Figure 2-3-1). Due to the fine grain size, the X-ray diffraction method has been used to distinguish different species among the phyllosilicates and carbonates including sericite, illite, kaolinite, chlorite, calcite and siderite, after methods suggested by Moore and Reynolds (1989).

DEPOSIT GEOLOGY

Rocks hosting the Silver Queen deposit are thought to be correlative with Upper Cretaceous Kasalka Group (Leitch *et al.*, 1990). At Silver Queen they consist mainly of porphyritic andesite flows, hypabyssal microdiorite and various pyroclastic units. The hypidiomorphic microdiorite texturally grades into the porphyritic andesite flows and they are interpreted to be two facies of the same volcanic event. Epithermal, polymetallic quartz-carbonate-barite veins with associated hydrothermal alteration cut these rocks on north-westerly and southeasterly trends.

No. 3 vein has a southeasterly strike (135°) and a steep to moderate northeast dip (55°). Width varies from a few centimetres to 1 metre in the sections studied in detail, but is locally greater. Pinching and swelling, branching and converging of the veins are common. The vein mineral assemblages are different in the northern, central and southern segments of the deposit. Sphalerite and rhodochrosite are the dominant vein minerals in the northern segment. Pyrite, sphalerite and hematite are the major components in the central segment. Quartz, calcite, barite and massive sphalerite-galena-pyrite are characteristic of the southern segment (Hood *et al.*, 1991, this volume). Correspondingly, the wallrock alteration varies from north to south, as discussed below.

WALLROCK ALTERATION

Hydrothermal alteration of the host microdiorite and andesite has been characterized as weak, moderate and strong.

Weakly altered rock is ubiquitous throughout the study area (Figure 2-3-1). The rock is black, hard, and magnetic. Primary plagioclase phenocrysts have limited alteration to clay along crystal margins and cleavages. Most primary mafic phenocrysts are extensively altered to chlorite and/or iron carbonate. Aphanitic matrix is largely unaltered (Plate 2-3-1, a and b). Based on petrographic similarities to rarely noted unaltered microdiorite and andesite, these weakly altered rocks are assumed, for the purpose of this study, to be the "fresh" rock parent to the moderately and strongly altered rocks described below.

Moderately altered rock occurs as broad envelopes around veins. It is buff coloured, softer than weakly altered rock, and nonmagnetic. Primary minerals have been altered almost completely. Generally, plagioclase is delicately pseudomorphed to sericite, illite or kaolinite. Mafic minerals are altered to chlorite or iron carbonate. Recrystalliza-

tion and silicification are obvious in the matrix (Plate 2-3-1, c and d). The contact between weakly altered and moderately altered rock is relatively sharp, commonly grading over less than 2 centimetres.

Strongly altered rock occurs as an envelope adjacent to the vein. It is commonly pale apple-green when freshly broken and orange-yellow on weathered surfaces; it is moderately hard and nonmagnetic. All primary minerals have been completely altered to quartz, sericite or kaolinite, carbonates and pyrite. Pseudomorphs of plagioclase are not as well defined as in moderately altered rocks. Recrystallization and silicification of the matrix are more intense than in moderately altered rock. Disseminated fine-grained pyrite is ubiquitous (Plate 2-3-1, e and f). The contact between moderately and strongly altered rocks is typically gradational.

As there is variation in the alteration assemblage perpendicular to the vein, so too there is variation in the assemblage parallel to the vein. These variations are described for each of the major segments.

In the northern segment of the No. 3 vein (north of section 24700N on the mine grid; Figure 2-3-1), the alteration envelope is narrow (about 7 metres wide). There is no significant difference between the alteration envelope at the hangingwall and the footwall. Consequently, only the alteration data from the hangingwall are presented in detail. The strongly altered envelope is 1 metre wide, followed outward by a moderately altered envelope 3 metres wide. Figure 2-3-2a presents the typical X-ray diffraction pattern charts for strongly, moderately and weakly altered samples.

The alteration envelope in the central segment of the No. 3 vein (between sections 24700N and 23600N on the mine grid) is wider than to the north. It extends about 30 metres into the hangingwall, but up to 100 metres into the footwall where dikes and fractures are more abundant. The hangingwall data are presented. The strongly altered rock envelope, 1.2 metres wide, is followed by the moderately altered envelope that is 30 metres wide. The weakly, moderately and strongly altered assemblages are not unlike those of the northern segment, as illustrated in Figure 2-3-2b.

Samples from the southern segment of the No. 3 vein (south of section 23600N on the mine grid) are limited to the hangingwall due to problems of access. The alteration intensity is stronger than in the northern and central segments of the vein, and the alteration mineral assemblage differs (Figure 2-3-2c). Kaolinite and siderite are absent from the strongly altered envelope (0 to 1.6 metres from the vein), which consists of quartz, mixed-layer sericite(2M₁)/illite(2M₂) and pyrite. Kaolinite and siderite appear in the moderately altered envelope (1.6 to 35 metres from the vein). The weakly altered andesite samples are similar to those from the north and central segments of the vein, however, the proportions of alteration minerals are relatively higher in the southern segment.

DISCUSSION

The mineralogical data presented above is preliminary and does not allow for rigorous treatment. However, the

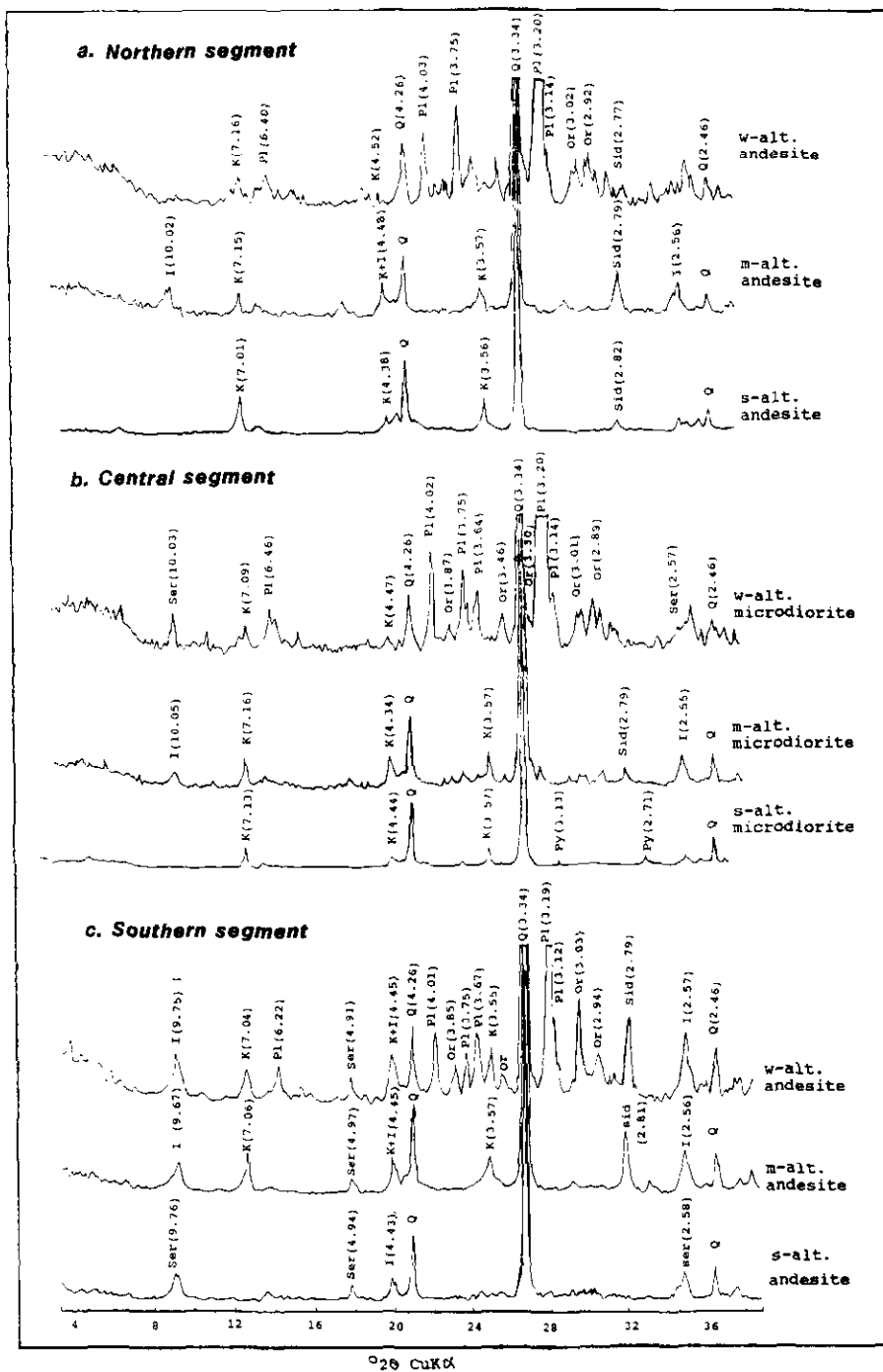


Figure 2-3-2. X-ray diffraction patterns for whole-rocks. Stack of three diffraction patterns represents sequence from weakly altered (w-alt.) to moderately altered (m-alt.) to strongly altered (s-alt.). Location of these sections (a) northern segment, (b) central segment and (c) southern segment are illustrated in Figure 2-3-1 (Symbols are the same as in Plate 2-3-1).

lateral or cross-section mineral zonation of weakly to strongly altered rocks, and the north to south mineralogical variation in the strongly and moderately altered envelope is significant.

The process related to the distribution of weakly altered rocks is unclear. This assemblage may represent either a low-temperature regional metamorphic effect resulting from loading, or the waning stages of the 78 Ma volcanic event (Leitch *et al.*, 1990). Thus it might predate the ore-forming hydrothermal activity, or represent incipient alteration related to it. More detailed petrography of regionally distal rocks will resolve this issue. Important, however, is the recognition that weakly altered rock represents the background or parent assemblage to the moderately and strongly altered rock.

The distribution of strongly to weakly altered rocks around the No. 3 vein is interpreted to be a function of decreasing intensity of alteration. Two processes may account for this decrease. Simple diffusion resulting in a chemical gradient, and therefore, reaction-front boundaries, may explain the variation on a small scale (less than 1 metre), but does not account for the large-scale alteration envelope up to 100 metres wide noted in this study. The second possible process involves varying water to rock ratios due to decreased permeability with distance from the vein. Thomson and Sinclair (1991, this volume) show that with decreased proximity to the vein, the intensity of fracturing also decreases. High water to rock ratios result in complete alteration of the hosting microdiorite and andesite as represented by the strongly altered rock assemblage, and low water to rock ratios result in the weakly altered rock. Moderately altered rock formed in intermediate conditions.

The processes accounting for the difference in the assemblage of quartz-sericite/illite-pyrite of the strongly altered rock in the southern segment compared to quartz-clay(kaolinite)-carbonate-pyrite in the northern and central segments may be twofold: presence of quartz-sericite-pyrite suggests the southern segment assemblage represent a higher temperature relative to the northern and central segment; and the activity of K^+ in the fluid increases to the south and Ca^{2+} decreases to the south. Further speculation on the specifics is beyond the scope of these data.

More questions are proposed from these data than are answered. Isotope and fluid inclusion analyses will facilitate the interpretation of the apparent variations.

ACKNOWLEDGMENTS

This work is supported by Pacific Houston Resources Inc. and by a cooperative research grant from the Natural

Science and Engineering Research Council to A.J. Sinclair. Special thanks are given to Craig H. B. Leitch and Chris Hood for helpful discussions. We particularly thank Webb Cummings and Jim Hutter for their assistance in the field. L. Groat and K. N. Nicholson provided advice and assistance with the X-ray diffraction studies. Colin I. Godwin and John M. Newell reviewed early versions of the manuscript.

REFERENCES

- Church, B.N. (1970): Nadina (Silver Queen); *B. C. Ministry of Mines, Energy and Petroleum Resources*, Geology, Exploration and Mining 1969, pages 122-141.
- Church, B.N. and Barakso, I.J. (1990): Geology, Lithochemistry and Mineralization in the Buck Creek Area, British Columbia; *B. C. Ministry of Mines, Energy and Petroleum Resources*, Paper 1990-2, 95 pages.
- Church, B.N. and Pettipas, A.R. (1990): Interpretation of Second Derivative Aeromagnetic Maps at the Silver Queen and Equity Silver Mines, Houston, B.C.; *Canadian Institute of Mining and Metallurgy*, Bulletin, Volume 83, No.934, pages 69-76.
- Fyles, J.T. (1984): Report on Notes on Thin Sections of New Nadina DDH 84-15; Department of Geological Sciences, *The University of British Columbia*, unpublished report.
- Hood, C.T.H., Leitch, C.H.B. and Sinclair, A.J. (1991): Mineralogy of Vein Systems at the Silver Queen Mine, Owen Lake, West-central British Columbia (93L/2); *B.C. Ministry of Energy, Mines and Petroleum Resources*, Geological Fieldwork 1990, Paper 1991-1, this volume.
- Leitch, C.H.B., Hood, C.T., Cheng, X-L. and Sinclair, A.J. (1990): Geology of the Silver Queen Mine Area, Owen Lake, Central British Columbia; *B.C. Ministry of Energy, Mines and Petroleum Resources*, Geological Fieldwork 1989, Paper 1990-1, pages 287-295.
- Moore, D.M. and Reynolds, Jr., R.C. (1989): X-ray Diffraction and the Identification and Analysis of Clay Minerals; *Oxford University Press Inc.* 332 pages.
- Thompson, M.L. and Sinclair, A.J. (1991): Syn-hydrothermal Development of Fractures in the Silver Queen Mine Area, Owen Lake Central British Columbia (93L/2); *B.C. Ministry of Energy, Mines and Petroleum Resources*, Geological Fieldwork 1990, Paper 1991, this volume.

NOTES



MINERALOGIC VARIATION OBSERVED AT THE SILVER QUEEN MINE, OWEN LAKE, CENTRAL BRITISH COLUMBIA (93L/2)*

By C.T.S. Hood, C.H.B. Leitch and A.J. Sinclair
The University of British Columbia

KEYWORDS: Economic geology, Silver Queen, epithermal, Kasalka Group, paragenesis, mineralogy, sulphosalts, vein zonation.

INTRODUCTION

The Silver Queen (Owen Lake, Nadina) vein system, lies within the Buck Creek basin near Houston, 100 kilometres southeast of Smithers, in the Bulkley Valley region of central British Columbia (Figure 2-4-1). The mine, which produced 98 285 grams of gold, 5225 kilograms of silver, 405 000 kilograms of copper, 703 000 kilograms of lead, 5 million kilograms of zinc and 15 800 kilograms of cadmium from 190 700 tonnes of ore over a brief period from 1972 to 1973, has current reserves of approximately 500 000 tonnes grading 3 grams gold and 200 grams silver per tonne, 0.23 per cent copper, 0.92 per cent lead and 6.20 per cent zinc. Problems arising from the complex mineralogy and variability of the ore zones were, to some extent, responsible for the closure of the mine. The mineralogic study of the Owen Lake property reported on here is part of a more extensive project dealing with the geology and origin of polymetallic vein deposits in the Owen Lake area.

REGIONAL SETTING

West-central British Columbia lies within the Stikine Terrane, which includes submarine calcalkaline to alkaline immature volcanic island-arc rocks of the Late Triassic Takla Group, subaerial to submarine calcalkaline volcanic, volcanoclastic and sedimentary rocks of the Early to Middle Jurassic Hazelton Group, successor basin sedimentary rocks of the Late Jurassic and Early Cretaceous Bowser Lake, Skeena and Sustut groups, and Late Cretaceous to Tertiary calcalkaline continental volcanic-arc rocks of the Kasalka, Ootsa Lake and Endako groups (MacIntyre and Desjardins, 1988). The younger volcanic rocks occur sporadically throughout the terrane, mainly in downthrown fault blocks and grabens. Plutonic rocks of Jurassic, Cretaceous and Tertiary ages form distinct intrusive belts (Carter, 1981), with which porphyry copper, stockwork molybdenum, mesothermal and epithermal base and precious metal veins are associated.

The area surrounding the Silver Queen mine forms part of the Buck Creek basin, characterized as a resurgent caldera with the Equity Silver mine (Figure 2-4-1) located within the central uplift area (Church and Barakso, 1990). The study area lies on the western margin of the basin, which is roughly defined by a series of rhyolite outliers and a semi-circular alignment of Upper Cretaceous and Eocene vol-

canic centres. Block faulting is common within the basin, locally juxtaposing the various sequences of volcanic rocks. The Silver Queen veins are hosted by some of the oldest rocks in the basin and the succession has been correlated with rocks of the Kasalka Group (Leitch *et al.*, 1990). However, Armstrong (1988) argues that this correlation is incorrect and that the rocks hosting the Silver Queen deposit are, in fact, part of the Tip Top Hill Formation, as suggested originally by Church (1970). The type section of the Kasalka rocks, which are Late Cretaceous (MacIntyre, 1985) or Early Cretaceous (Armstrong, 1988) in age, is in the Kasalka Range near Tahtsa Lake, approximately 75 kilometres southeast of Houston.

PROPERTY GEOLOGY

The stratigraphy hosting the Silver Queen deposit is subdivided into five major units which form a gently northwest-dipping succession (Leitch *et al.*, 1990). The oldest rocks are exposed near Riddeck Creek in the south and the youngest in Emil Creek to the north (Figure 2-4-1). The lowest unit in the succession is a reddish purple, polymictic conglomerate (Unit 1). It is overlain by fragmental rocks ranging from thick crystal tuff (Unit 2) to coarse lapilli tuff and breccia (Unit 3), which are succeeded upwards by a thick feldspar-porphyrific andesite flow unit (Unit 4). The flows are intruded by microdiorite sills (Unit 5) and other feldspar porphyry (Unit 5a) and quartz porphyry (Unit 5b) dikes and stocks. All the units are cut by dikes that can be divided into three groups: amygdaloidal dikes (Unit 6), bladed-feldspar trachyandesite dikes (Unit 7), and diabase dikes. The succession is unconformably overlain by basaltic to possibly trachyandesitic volcanic rocks that outcrop in Riddeck Creek and farther south. These volcanics may be correlative with the Goosly Lake Formation of the Equity Silver mine area (Church and Barakso, 1990).

The bladed-feldspar trachyandesite (Unit 7) and amygdaloidal dike (Unit 6) units are of particular importance in relation to age of mineralization. Rocks of Unit 7 are generally unaltered in the vicinity of major veins and give a whole-rock K-Ar date of 51.9 ± 1.2 Ma, whereas Unit 6, which is commonly strongly altered near veins, produces a whole-rock K-Ar date of 51.3 ± 1.2 Ma. These dates allow for close bracketing of the age of mineralization, with all three dike types commonly paralleling the strike of the major vein systems. The major veins, including the No. 3 vein (Figure 2-4-1) which is the most important economically, tend to strike northwest and are controlled by both strike-slip and reverse faults.

* This project is a contribution to the Canada/British Columbia Mineral Development Agreement.

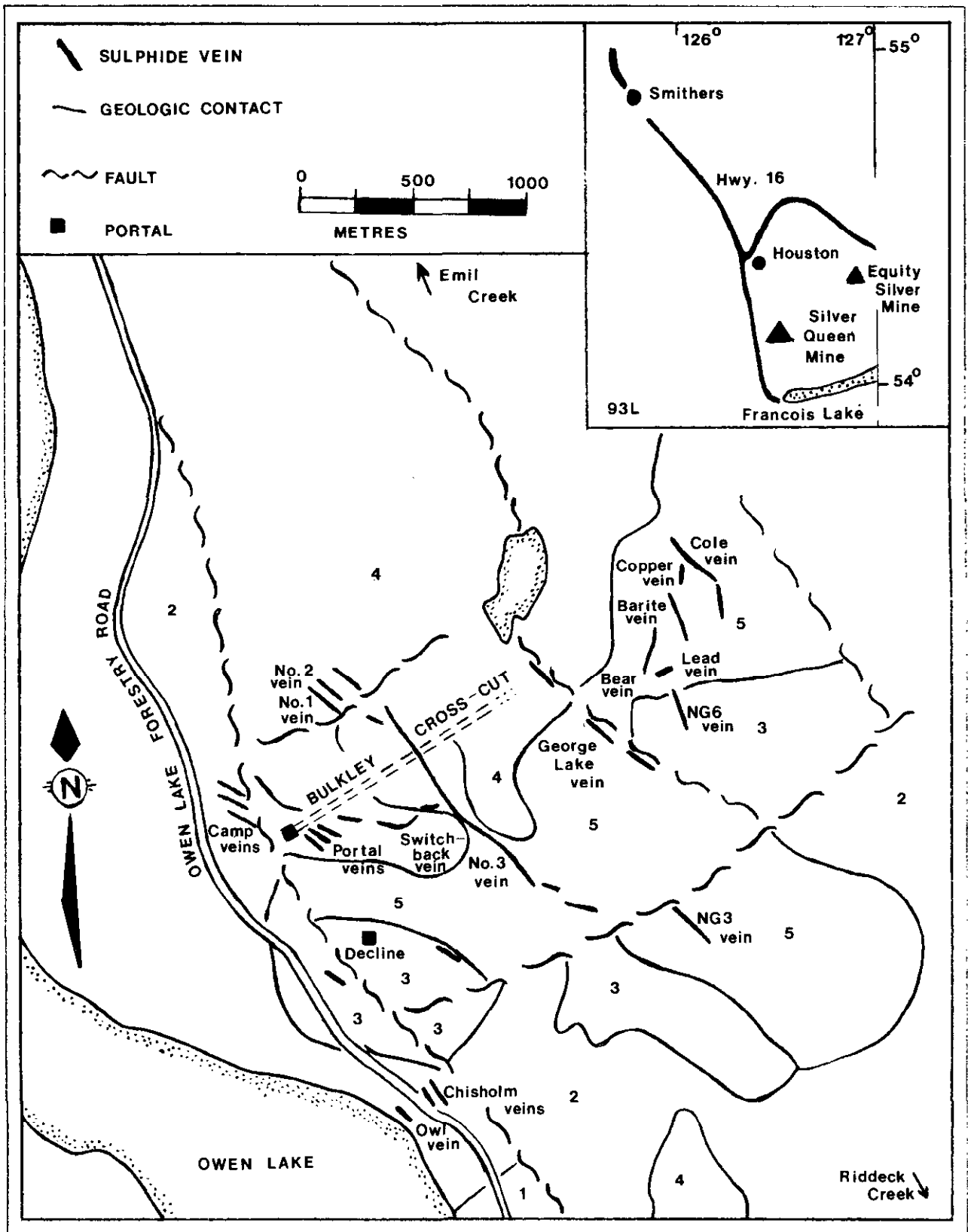


Figure 2-4-1. Map of Silver Queen mine showing locations of geologic contacts (Leitch *et al.*, 1990) and major mineralized structures. Legend: 1=polymictic basal conglomerate; 2=crystal tuff; 3=medium to coarse tuff-breccia; 4=feldspar-porphyrific andesite; 5=microdiorite.

Inset: Location of Silver Queen mine.

VEIN MINERALOGY

The Silver Queen vein system displays a great degree of complexity on the centimetre to metre scale, but, when examined over the strike lengths of individual structures, such as the No. 3 and George Lake systems, several large-scale patterns become evident. The No. 3 vein, with its extensive surface exposure, large number of drill-hole intersections, and structural continuity, provides the best opportunity for analysis of a complete system. Despite differences in mineralogy within the No. 3 structure and other veins on the Owen Lake property, a surprising paragenetic continuity (summarized in Tables 2-4-1 and 2) exists throughout the mineralized area.

No. 3 VEIN SYSTEM

The No. 3 vein system is the largest and, to date, most intensively explored structure at the Silver Queen mine. It is well defined on surface, underground and in drill-hole intersections, and displays a wide range of mineralogies over the length of the structure. Several smaller veins with similar mineralogy lie adjacent to the main vein.

The No. 3 vein can be divided into five zones based on bulk mineralogical content (Table 2-4-1). The northernmost segment of the vein system (Zone I) consists of narrow, commonly multiple, smaller veins dominated by inter-banded rhodochrosite and quartz. Prominent, if irregular, bands of coarse-grained euhedral sphalerite and galena are an important distinguishing feature. Toward the south, hematite, chalcopyrite and the sulphosalts (matildite, aikinite and berryite) increase in abundance until a distinct new zone (Zone II) is entered. Chalcopyrite, comprising as much as 60 volume per cent of the opaque assemblage, is the definitive mineral for Zone II, with bismuth-bearing sulphosalts and tennantite present in significant amounts. Vein walls are generally brecciated in this segment, with hematite, pyrite and carbonate among the first minerals to be deposited. To the south of the relatively short chalcopyrite-rich zone, the mineralogy in Zone III becomes less complex. The vein attains widths of up to 2.5 metres in this central segment and is generally very lean (<10 per cent) in opaque minerals. The sulphide assemblage is dominated by pyrite and sphalerite, commonly occurring as colloform masses overgrowing carbonate (manganosiderite) and quartz. Hematite is also present and in some places has been overgrown and replaced by later sphalerite, pyrite and galena. Seligmannite-bournonite and tetrahedrite-tennantite are present in minor amounts, generally as myrmekitic intergrowths with galena.

The most unusual zone (Zone IV) within the No. 3 system forms the southern one-third of the structure exposed underground. The vein displays well-defined boundaries, but locally splits into several closely associated narrower veins. The mineralogy is generally dominated by pyrite and sphalerite, with an earlier pyrite-quartz-barite phase frequently brecciated and surrounded by later, finer grained pyrite and quartz. Complexly intergrown galena and multiple-composition tetrahedrite-tennantite locally form up to 40 per cent of the opaque assemblage and are the princi-

TABLE 2-4-1
MINERALOGY OF MAJOR VEIN SYSTEMS

Vein	Mineralogy		Important Textures
	Sulfide	Gangue	
#3 North (Zone I)	sphl, gln, py, tet cpy, sel, elec	rho, qtz Mn-sid, pybit	banded (rho) sparry (qtz) coarse-grained euhedral (sphl, gln)
#3 Cpy-rich (Zone II)	cpy, ten, py, sphl mtd, ber, aik, gln, elec, hem-mag, pc-plb	rho, qtz, Mn-sid, pybit	breccia (qtz, py) myrmekitic (cpy gln, ten, mtd)
#3 Central (Zone III)	cpy, sphl, gln, py tet-ten, hem-mag, sel, elec, mc	qtz, Mn-sid, ba, rho	sparry (qtz Mn-sid) breccia (py, mc) colloform (sphl, py) myrmekitic (sel, tet-ten)
#3 South (Zone IV)	gln, aik, tet-ten, sphl, aspb, fr, py, pyg, sel, elec, bn, cv, cc, UNssx #2	ba, qtz, clc, pybit, hins, svan, Ti-ox	colloform (py, sphl), breccia (py-qtz), bladed (ba), myrmekitic (sel, cpy, tet-ten), web (aik, tet-ten, gln)
NG3 (Zone V)	gln, sphl, tet-ten, cpy, pu-pyg, UNssx #1, bs, cpb, py	ba, clc, qz, hins, svan	web (bis, cpb), lamellae(UNssx #1, cpb, bs), myrmekitic (pu-pyg, UNssx #1, tet-ten, gln)
Twinkle Zone	sphl, tet-ten, gln cpy, py	clc, qtz	
Porial	cpy, sphl, gln, mtd, tet-ten, py, elec, aik, aspy, mc, pc	qtz, rho Mn-sid, ba, pybit	sparry (qtz, Mn-sid), breccia (py, ba, sphl) myrmekitic (mtd, gln, aik, cpy, tet-ten)
Camp	py, aspy, sphl, gln, tet-ten, po, pu-pyg, elec, pc-plb, dig, ac, bn, fr, cpy	qtz, ba, rho, Mn-sid, pybit	dendritic (aspy, py) colloform (sphl), myrmekitic (py, tet-ten, gln, cpy) breccia (py, aspy)
George Lake	sphl, py, gln, cpy hem-mag, tet-ten, mc, pc-plb, elec	qz, clc, ba	breccia (py-qtz) myrmekitic (gln, tet-ten) crustiform (py on hem-mag)
Cole Lake	sphl, cpy, py, mc, hem-mag, aspy, fr, tet-ten, aik, gln, mtd, elec, sel, pc-plb, UNssx #3	qz, ba, rho Mn-sid, clc, pybit	sparry (qtz, rho) myrmekitic (gln, aik, mtd, sel) breccia (py-qtz)
#1	aspy, py, elec, po, pc-plb, cpy, tet-ten, sphl, gln	rho, qtz, phbit	breccia (py, aspy)
#2	aspy, py, tet-ten, pu-pyg, elec, mc, sphl, gln, cpy, pc-plb, hem-mag	rho, qz, pybit	sparry (qtz) breccia (py) banded (rho)
Chisholm/Owl	sphl, py, gln, cpy, tet-ten, sel, pu-pyg, pc-plb	qtz, ba, clc	breccia (py, aspy) myrmekitic (gln, sel)

**Symbols for minerals are as follows:

qtz= quartz	ba= barite
clc= calcite	pybit= pyrobitumen
gln= galena	cpy= chalcopyrite
aik= aikinite	sphl= sphalerite
pc= pearcite	plb= polybasite
ber= berryite	tet= tetrahedrite
pu= proussite	elec= electrum
cb= unidentified carbonate	py= pyrite
UNssx= unidentified sulfosalt	bn= bornite
hem= hematite	mag= magnetite
cv= covellite	mc= marcasite
ac= acanthite	cc= chalcocite
hins= hindsite	fr= freibergite

Mn-sid= Mn-rich siderite
rho= rhodochrosite
sel= seligmannite
aspb= arsenopolybasite
pyg= pyrargyrite
ten= tennantite
cpb= cuprobismutite
bs= bismuthinite
mtd= matildite
po= pyrrotite
dig= digenite
svan= svanbergite
Ti-ox= titanium oxide phase

TABLE 2-4-2
PARAGENESIS IN THE SILVER QUEEN VEIN SYSTEM

STAGE	I	II	III	IV
TYPE OF MINERALIZATION	Fe-Ba	Mn-Zn-Cd-Ge-Ga	Cu	Pb-Ag-Bi-Au-As-Sb-Cu
quartz	---	---		---
pyrite	---	---		---
sphalerite		---		---
arsenopyrite	---			
galena		---		---
pyrobitumen				---
barite	---	---		
svanbergite	---			
hinsdalite	---			
marcasite	---			
pyrrhotite	---			
rhodochrosite	---	---		---
manganosiderite		---	---	
hematite	---			
magnetite	---			
calcite		---		---
aikinite				---
matildite				---
electrum				---
tetrahedrite			---	---
tennantite				---
pearcite-polybasite				---
proustite-pyrargyrite				---
chalcopyrite			---	
acanthite				---
berryite				---
bismuthinite			---	
cuprobismutite			---	
covellite-chalcocite			---	
bornite			---	
seligmannite				---
Unknown sulphosalts (all)				---

pal host for gold (in the form of electrum grains within the galena) and silver (some tetrahedrite contains as much as 8 per cent silver). Of particular interest is a northwesterly plunging section of the vein system, centred on the decline area, displaying anomalously high (up to 3 per cent of opaque minerals) amounts of aikinite intergrown with galena and tetrahedrite-tennantite. Myrmekitic intergrowths of seligmannite and galena are also widespread in the southern part of the vein.

The least defined of the No. 3 vein segments is that known as the NG3 vein (Zone V). This part of the structure has only been intersected in a few widely spaced drill holes and few samples are available. The mineralogy appears to be dominated by coarse-grained galena, sphalerite and pyrite, with earlier barite and quartz gangue. The whole

assemblage is cut and brecciated by calcite. Unusual exsolution features, consisting of proustite and an unidentified silver-bearing sulphosalt, are present in galena from drill-hole NG3. Bismuthinite and cuprobismutite were recorded occurring in tetrahedrite from a pyrite-rich portion of the vein and appear to be penecontemporaneous with a period of silver-bearing tetrahedrite mineralization.

PORTAL AND CAMP VEINS

The Portal veins are a series of highly irregular structures near the entrance to the Silver Queen underground workings (Figure 2-4-1). Orientation, thickness and mineralogy vary from vein to vein; individual structures attain widths of up to a metre, only to disappear tens of metres away. The veins

can, however, be roughly classified into three groups on the basis of mineralogy. The most important economically are those containing substantial amounts of chalcopyrite (up to 60 per cent of the total sulphide) and associated later galena-matildite intergrowths. Widespread tennantite veining cuts this assemblage, with manganosiderite and quartz making up the gangue mineralogy. In places, spectacular concentrations of electrum are also associated with the galena-matildite assemblage characteristic of chalcopyrite-rich veins.

Several of the westernmost veins within the Portal system have mineralogies closely resembling the nearby Camp veins (*see description below*). Early, bladed barite, with quartz, pyrite and rare arsenopyrite, followed by coarse-grained sphalerite and lesser galena and chalcopyrite, are the dominant components of this group of veins. Later sulphosalts, electrum, rhodochrosite and pyrobitumen are conspicuously absent. Many of the easternmost veins, and the Switchback vein (Figure 2-4-1), are dominated by early phases (barite, quartz, pyrite and sphalerite), with relatively minor amounts of chalcopyrite, carbonate and tetrahedrite-tennantite usually confined to narrow bands near the foot-wall of each vein.

The Camp veins lie to the west of the Portal vein system (Figure 2-4-1) and are known only from an extensive pattern of drill-holes. They are distinctive because of their anomalously high silver grades associated with pearcite, acanthite and the ruby silvers. Many of the veins are actually mineralized breccias, with the first episode of mineralization characterized by narrow drusy-quartz bands surrounding fragments. Bladed barite, pyrite, sphalerite and arsenopyrite follow, forming up to 50 per cent of the mineral assemblage, and galena, tetrahedrite-tennantite and the silver-bearing minerals are the final phases of economic interest. A volumetrically important period of rhodochrosite deposition was the last major episode of mineralization in the Camp veins.

GEORGE LAKE VEINS

The George Lake veins (Figure 2-4-1) are part of the second most important vein system (next to the No. 3 vein) on the property, in terms of structural continuity and potential reserves. Overall mineralogy roughly compares to that of the No. 3 system, with slightly greater abundances of fine-grained quartz and hematite being the chief difference. Sulphosalts are generally absent in the available samples and pyrite is the most important sulphide constituent throughout the vein. Galena, tetrahedrite-tennantite and rare pearcite-polybasite are most commonly found filling fractures within the pyrite and sphalerite. As with the No. 3 vein system, chalcopyrite and manganooan carbonates generally appear to increase in abundance towards the north.

COLE LAKE VEINS

The Cole Lake veins (Figure 2-4-1) are a widely spaced group of structures with a northerly trend and highly varied mineralogy. Mineralogy is somewhat similar to the Portal vein system; in the Cole Lake veins, the characteristic

assemblage changes from hematite-carbonate-pyrite in the westernmost veins (Bear vein), through chalcopyrite and sulphosalt-bearing assemblages in the central veins (Copper and Lead veins) to sphalerite and barite-rich veins in the easternmost area (Cole vein). The Cole vein has the longest strike length in the Cole Lake system, but presents a relatively simple mineralogy in contrast to smaller but more complex veins such as the Copper vein. The sulphide mineralogy in the Cole vein is dominated by coarse-grained, euhedral sphalerite and galena in a matrix of manganooan carbonate, barite and quartz. Toward the north, arsenopyrite becomes abundant, overgrowing pre-existing hematite grains that have been replaced by carbonate, pyrite and galena. Freibergite (argentian tetrahedrite) also appears within this portion of the vein.

In contrast to the relatively simple Cole vein, the adjacent Copper vein is mineralogically complex. Although the walls of the vein are similar to the Cole vein, the Copper vein is distinctive because of an important later chalcopyrite-sulphosalt episode (possibly correlative with Stage IV of the No. 3 vein). Symplectic intergrowths of galena, aikinite and matildite are widespread, with rare tennantite veinlets cutting the entire assemblage. To the west of the Copper vein, the Barite, NG6 and Lead veins, though chalcopyrite poor, contain unusual concentrations (to 3 per cent of total sulphide) of pearcite polybasite and seligmannite. The Bear vein is the westernmost vein within the system and is characterized by early stage mineralization dominated by hematite, carbonate, pyrite and quartz.

OTHER VEINS

The most important of the remaining veins are the Chisholm veins (Figure 2-4-1), located near the south boundary of the property. Mineralogy of these veins is similar to the Camp veins, dominated by early quartz, barite, pyrite, arsenopyrite and sphalerite, followed by less abundant galena, carbonate, quartz and tetrahedrite-tennantite. Up to 5 per cent of the galena in sections from the Chisholm veins and the nearby Owl vein (Figure 2-4-1) has undergone replacement by ruby silvers, pearcite-polybasite and tennantite. Very fine grained symplectic intergrowths of seligmannite in galena have also been noted.

The No. 1 and No. 2 veins split off the northern segment of the No. 3 vein and retain many of its characteristics. The No. 2 vein, actually a set of closely associated parallel veins, is quite similar to Zone I of the No. 3 vein in that the mineralogy is dominated by banded rhodochrosite and quartz, with prominent coarse-grained sphalerite bands throughout. Farther north on the No. 2 system, arsenopyrite, pearcite-polybasite and the ruby silvers appear within the opaque assemblage.

The No. 1 vein is singular in that arsenopyrite forms an important part of the assemblage (up to 10 per cent of the total sulphide), surrounding and brecciating pre-existing pyrite while predating other sulphides. Pearcite-polybasite and possibly acanthite are also present within the vein, representing the final stage of sulphide mineralization.

The remaining mineralized structures on the property are quite simple mineralogically, generally consisting of pyrite, sphalerite and galena with quartz-carbonate-dominated gangue. A vein intersected in Hole NG4 (near the south boundary of the property) containing an anomalous amount of late chalcopyrite (to 5 per cent of sulphide component) is perhaps the most unusual.

DISCUSSION

The mineral assemblages in the Silver Queen vein system present a paragenetic sequence that is remarkably consistent throughout the property (summarized in Table 2-4-2). This suggests that all veins at Owen Lake originated from a single source during a single mineralizing event, a concept that is generally supported by relationships with the series of dikes that closely bracket the time of mineralization (Leitch *et al.*, in preparation). Evolution of the deposit can be divided roughly into four stages, each displaying typical characteristics of low-temperature, open-space deposition (*i.e.* colloform sphalerite, sparry quartz, vuggy nature throughout). The first stage (refer to Table 2-4-2) is distinguished by an initial minor quartz-pyrite episode, followed by hematite, pyrobitumen, barite, svanbergite and hinsdalite (the latter two minerals are unusual strontium-bearing sulphates). More voluminous influxes of pyrite, quartz and minor carbonate followed, with later arsenopyrite, pyrite and marcasite marking the end of this stage. The second stage is defined by the deposition of sphalerite (containing up to 0.1 weight per cent germanium), galena, minor pyrite, and manganosiderite, followed by a stage of copper-bearing mineralization and associated manganous carbonates. The latter stage is particularly prominent toward the north of the property, although isolated occurrences of relatively chalcopyrite-tetrahedrite-rich material occur in the southernmost areas as well. The final stage is characterized by rhodochrosite (or calcite in the south), galena and sulphosalts, and is associated with the deposition of electrum, the principal source of gold at Silver Queen mine. The galena-sulphosalt assemblage is cut by tennantite veining (consisting of bismuth and arsenic-bearing phases) in the north and a weak quartz-pyrobitumen event marks the end of mineralization in Stage IV and in the system as a whole.

Textures within the individual veins indicate that the veins were deposited along fractures and joints that were repeatedly opened and sealed as mineralization proceeded. The initial quartz-pyrite vein material has, in many sites, undergone brecciation and has subsequently been surrounded by later pyrite. These breccias often show signs of renewed vein dilation and subsequent sealing by later phases such as galena. Remobilization of the "soft sulphides", such as galena, has been discounted to a large extent due to the preservation of the more fragile open-space filling textures. A single exception to the above observation was noted in the George Lake vein, where postmineralization fault movement has resulted in the formation of "sulphide slickensides". Of particular note are offsets perpendicular to the veins that cut Stages I and II material, but are often filled by later minerals such as galena. Dilation and lateral motion were, therefore, active processes during mineralization.

Constraints on pressure, temperature and composition of the ore fluids are conjectural at this stage. A more in-depth examination of the more complex mineral assemblages (particularly where multiple compositions of the fahlore group are concerned) as well as stable isotope and fluid inclusion work, will be conducted.

CONCLUSION

The Owen Lake property covers a series of base and precious metal veins that display great consistency with respect to mineral paragenesis. Four distinct stages of mineralization are recognized within most of the major structures and are interpreted to be derived from a single fluid source with deposition accompanied by repeated opening and sealing of the individual veins.

ACKNOWLEDGMENTS

Funding for mineralogical studies was provided by a cooperative research agreement between the Natural Sciences and Engineering Research Council and Pacific Houston Resources Inc.. The authors thank M.L. Thomson, J. Hutter, W.W. Cummings and X. Cheng for their helpful discussions in and out of the field. Technical assistance of J. Knight and Y. Douma is appreciated. The authors also thank J.M. Newell for helpful reviews of an earlier draft of the paper.

REFERENCES

- Armstrong, R.L. (1988): Mesozoic and Early Cenozoic Magmatic Evolution of the Canadian Cordillera; *Geological Society of America*, Special Paper 218, pages 55-91.
- Carter, N.C. (1981): Porphyry Copper and Molybdenum Deposits, West-central British Columbia; *B.C. Ministry of Energy, Mines and Petroleum Resources*, Bulletin 64, 150 pages.
- Church, B.N. (1970): Nadina (Silver Queen); *B.C. Ministry of Energy, Mines and Petroleum Resources*, Geology, Exploration, and Mining in British Columbia, 1969, pages 126-139.
- Church, B.N. and Barakso, J.J. (1990): Geology, Lithochemistry and Mineralization of the Buck Creek Area, British Columbia; *B.C. Ministry of Energy, Mines and Petroleum Resources*, Paper 1990-2, 95 pages.
- Leitch, C.H.B., Hood, C.T., Cheng, X-L. and Sinclair, A.J. (1990): Geology of the Silver Queen Mine Area, Owen Lake, Central British Columbia; *B.C. Ministry of Energy, Mines and Petroleum Resources*, Geological Fieldwork 1989, Paper 1990-1, pages 287-295.
- MacIntyre, D.G. (1985): Geology and Mineral Deposits of the Tahtsa Lake District, West-central British Columbia; *B.C. Ministry of Energy, Mines and Petroleum Resources*, Bulletin 75, 82 pages.
- MacIntyre, D.G. and Desjardins, P. (1988): Babine Project (93L/15); *B.C. Ministry of Energy, Mines and Petroleum Resources*, Geological Fieldwork 1987, Paper 1988-1, pages 181-193.



**SYN-HYDROTHERMAL DEVELOPMENT OF FRACTURES IN THE
SILVER QUEEN MINE AREA, OWEN LAKE,
CENTRAL BRITISH COLUMBIA***
(93L/2)

By Margaret L. Thomson and Alastair J. Sinclair
The University of British Columbia

KEYWORDS: Economic geology, Silver Queen, epithermal, polymetallic vein, hydrothermal fracturing.

INTRODUCTION

The site and character of precious and basemetal epithermal deposits is determined by several principal factors which include: structure, stratigraphy, lithology, pressure and temperature, hydrology, chemistry of the mineralizing fluid, and syn-hydrothermal development of permeability or changes in hydraulic gradient (White and Hedenquist, 1990). This study investigates the syn-hydrothermal development of permeability by documenting the attitude and style of fracturing in the immediate area of the Silver Queen mine (Figure 2-5-1). This work represents a portion of a more extensive study investigating the mineralizing processes at the Silver Queen mine (*see Cheng et al. and Hood et al., this volume*).

DEPOSIT GEOLOGY

The Silver Queen (Nadina, Bradina) deposit is located 100 kilometres southeast of Smithers, 30 kilometres south of Houston and 30 kilometres southwest of the Equity Silver mine (Figure 2-5-1, inset). It is hosted by Upper Cretaceous (77 to 75 Ma; Church and Barakso, 1990) andesitic volcanic rocks, tentatively correlated with the Kasalka Group (Leitch *et al.*, 1990). Mineralization is bracketed in age by altered, and therefore older, amygdaloidal dikes (51.3 ± 1.8 Ma, K-Ar, whole-rock) which parallel the veins described below, and unaltered bladed-feldspar porphyry dikes (51.9 ± 1.8 Ma, K-Ar, whole-rock).

Mineralization occurs in veins varying in width from 1 centimetre to 2 metres and consisting of silver, copper, lead and zinc sulphides in a gangue of quartz, carbonate and barite (*see Hood et al., this volume*). The No. 3 vein (Figure 2-5-1), the focus of previous mining activity and the largest discovered in the immediate area, has a known length of 1.5 kilometres, a depth of at least 200 metres and a width varying from 0.1 to 2.0 metres. Country rocks are Tip Top Hill feldspar porphyry at the north end, Mine Hill microdiorite in the central segment, and medium to coarse tuff-breccia to the south (Figure 2-5-1). A distinct alteration envelope, consisting of strongly to weakly altered rocks, extends tens of metres into both the footwall and hanging-wall of the vein (Cheng *et al.*, this volume).

FIELD OBSERVATIONS

The Wrinch Creek canyon west of the No. 3 vein, and a section 30 metres east of the vein along the underground Bulkley cross-cut (Figure 2-5-1) were chosen as study areas to obtain structural orientation data. Complimenting these observations are regional determinations and measurements on several sequences of diamond-drill core through the No. 3 vein.

DEFINITIONS

Based on experimental deformation studies (reviews in Price, 1966; Hobbs *et al.*, 1976) two general classes of fractures can be related to three axes of compressive stress: principal (σ^1), intermediate (σ^2) and minor (σ^3). The resulting fractures are referred to as extension (E), and shear (S) fractures (Figure 2-5-2). The 2θ angle for extension fractures is 0° , and for shear fractures it ranges from greater than 0° to 90° . The acute bisector of conjugate shear fractures is developed parallel to the principal compressive stress direction (σ^1).

As an aid to field interpretation of fracture patterns Hancock (1985) suggests classifying fractures by shapes of letters in the alphabet. Summarizing this work: I-shapes suggest unidirectional extension (E) fractures; K-shapes suggest extension fractures formed under conditions of near hydrostatic stress; T-shapes suggest two episodes of orthogonal extension fracturing; H-shapes suggest non-systematic overprinting of orthogonal extension; V, Y and X-shapes suggest conjugate shear (S) fractures and non-systematic crossfractures resulting in an A-shape.

In this study, joints are defined as fractures with no megascopic indications of relative motion or accumulation of secondary minerals (Plate 2-5-1a).

Veins are fractures filled with secondary minerals, with or without an envelope of alteration. Three groups of veins are distinguished by width: less than 1 millimetre, 1 millimetre to 1 centimetre and greater than 1 centimetre (Plate 2-5-1a, b, c).

Faults are defined as fractures with evidence of relative motion. The most common type recognized in this study is identified by slickensides on planar surfaces with the sense of last motion determined by hackle-marks, if present (Plate 2-5-1a). Strongly silicified breccia zones are restricted to the footwall and hangingwall of veins greater than 1 centimetre wide and the margins of amygdaloidal dikes (Plate

* This project is a contribution to the Canada/British Columbia Mineral Development Agreement.

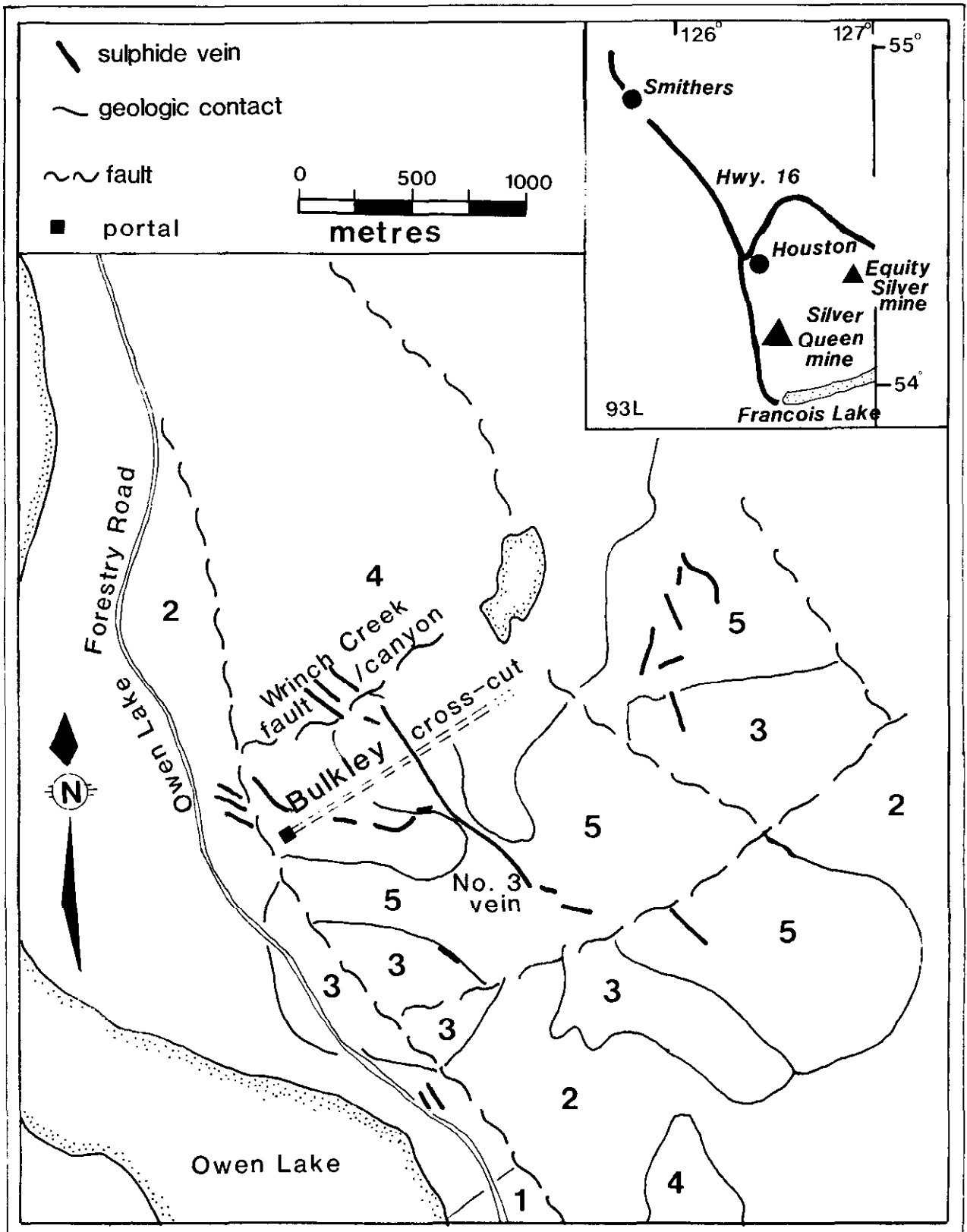


Figure 2-5-1. Simplified surface geologic map of the Silver Queen mine, highlighting the surface trace of the No. 3 vein and the other significant sulphide-bearing veins. Legend: 1=polymictic basal conglomerate; 2=crystal tuff; 3=medium to coarse tuff-breccia; 4=Tip Top Hill feldspar porphyry; 5=Mine Hill microdiorite (after Leitch *et al.*, 1990). Inset: location map of Silver Queen Mine.

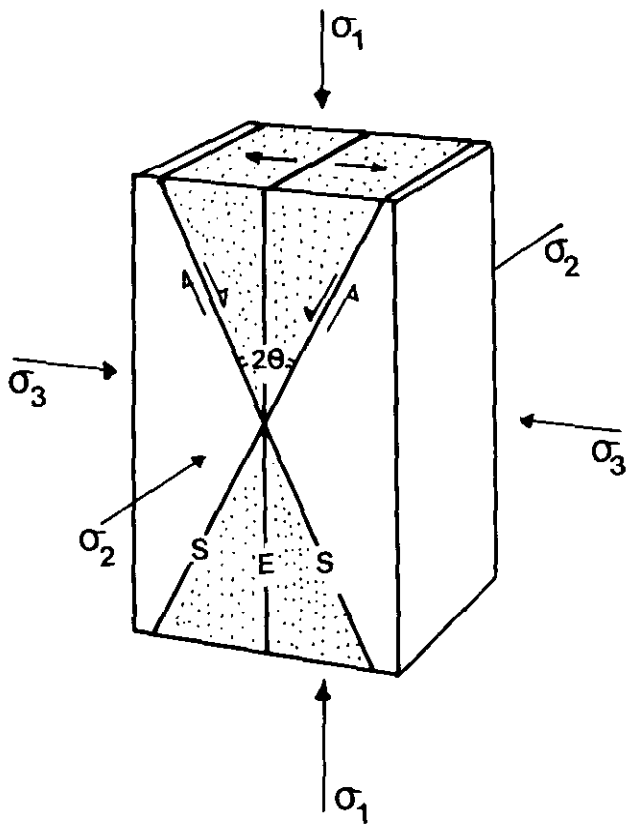


Figure 2-5-2. Block diagram showing the relationship of principal stress directions and extension fractures (E) and conjugate shear fractures (S) developed in a mechanically isotropic brittle rock.

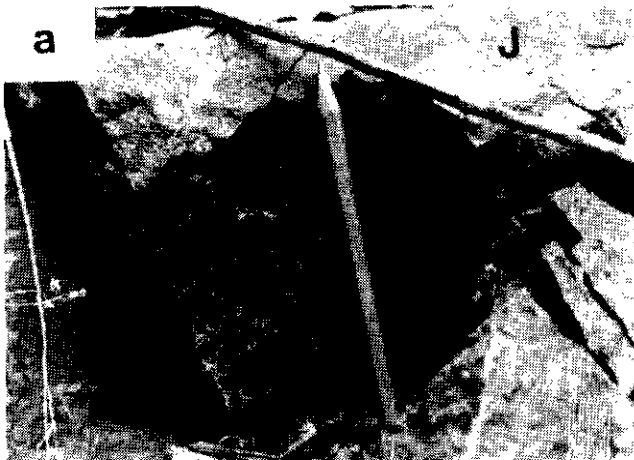
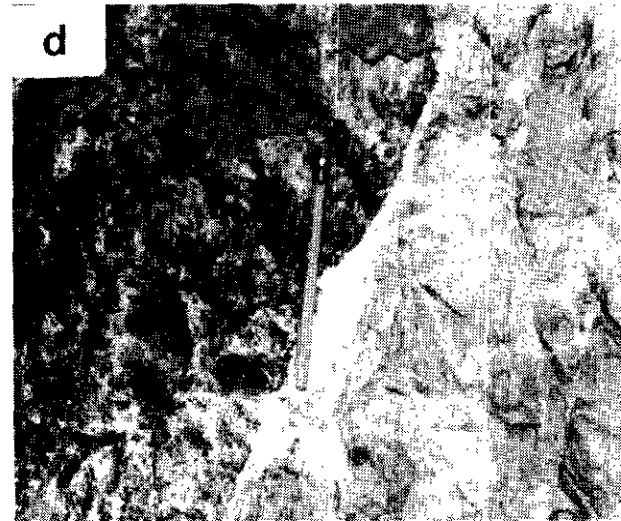
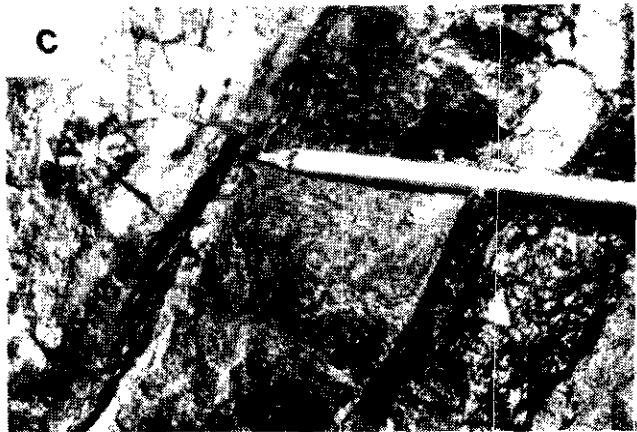
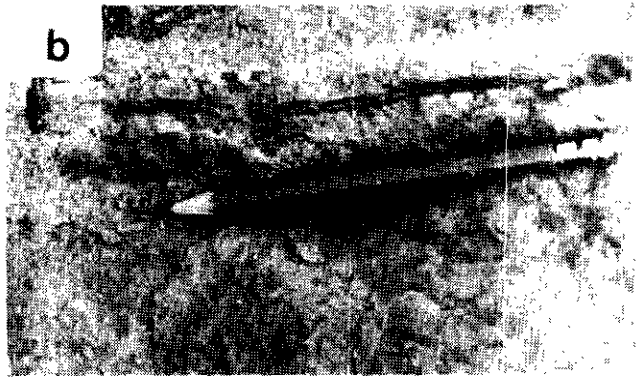


Plate 2-5-1. (a) Joint fractures (J) in fresh feldspar porphyry. Gently plunging slickensides (SS) on a plane parallel to Wrinch Creek canyon. (b) I-shaped, 1 millimetre to 1 centimetre wide veins cutting weakly altered microdiorite. (c) Sulphide-rich vein greater than 1 centimetre wide with footwall (left) and hangingwall (right) brecciation. (d) Pencil-tip sticking into clay-rich fault gouge in the footwall of a vein greater than 1 centimetre wide. Note the internal chaotic nature of the vein.

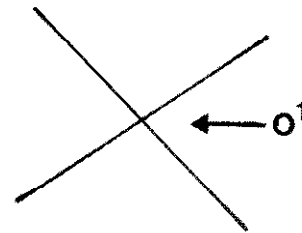
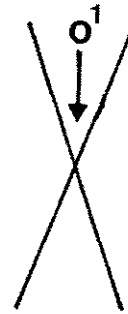


Plate 2-5-2. (a) Steeply dipping, conjugate shear fractures developed 20 metres away from the No. 3 vein. Acute bisector (σ^1) is vertical. (b) Gently dipping conjugate shear fractures 10 metres from the No. 3 vein. Acute bisector (σ^1) is horizontal. Arrow points to sulphide-bearing vein.

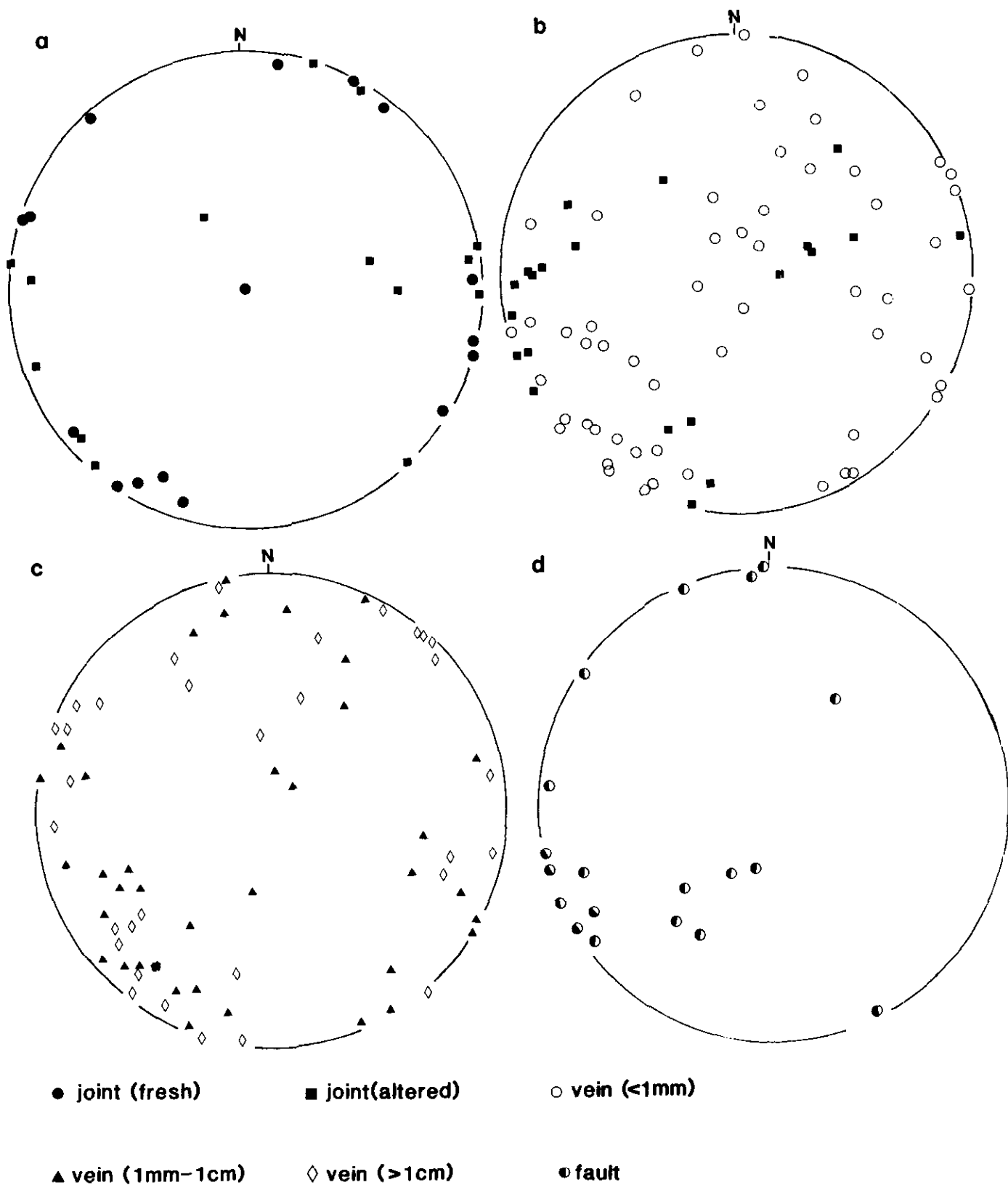


Figure 2-5-3. Lower hemisphere equal-area projection of fracture orientation data. (a) Joints and veins in unaltered to weakly altered rock 30 metres away from No. 3 vein, (b) Joints and veins in altered rock 20 metres away from No. 3 vein, (c) Veins 0 to 10 metres away from No. 3 vein, star is average orientation of No. 3 vein, (d) faults 0 to 10 metres away from No. 3 vein.

2-5-1c). Clay-rich gouge on faults is noted underground and in diamond-drill core (Plate 2-5-1d).

STRUCTURAL ORIENTATION DATA

Fractures in fresh feldspar porphyry and microdiorite, at a distance approximately 30 metres from the No. 3 vein, are orthogonally oriented, I-shaped joints (Plate 2-5-1a). They are regularly spaced at 20 to 50-centimetre intervals, and are both steeply dipping and flat lying (Figure 2-5-3a).

Close to the No. 3 vein (~20 m), narrow (less than 1 millimetre wide) vertical to steeply dipping quartz veins are characterized by buff-coloured envelopes of alteration 1 to 5 millimetres wide (Plate 2-5-1b). The veins are I-shaped, suggesting extension. They show a similar density and orientation to joints within the fresh rock (Figure 2-5-3a).

Within 10 to 20 metres of the No. 3 vein the fracture density increases to a 5 to 10-centimetre spacing, and veins less than 1 millimetre wide become more abundant. The veins are X and A-shaped conjugate shear fractures, with a vertical acute bisector (Figure 2-5-3a, Plate 2-5-2a).

At approximately 10 metres from the No. 3 vein, steeply and gently dipping X and A-shaped joints and 1-millimetre, and 1-millimetre to 1-centimetre-wide X and A-shaped veins are more abundant than I-shaped joints and veins (Figure 2-5-3b, Plate 2-5-2b). The acute bisectors of the steeply and gently dipping conjugate joints and veins are vertical and horizontal, respectively.

The No. 3 vein and most adjacent veins greater than 1 centimetre wide are commonly I-shaped and steeply dipping (Plate 2-5-1c, d, Figure 2-5-3c). However, a second population of gently dipping conjugate shear veins (1 millimetre to greater than 1 centimetre wide) are cut by the I-shaped veins, more than 1 centimetre wide.

Clay-rich fault planes are commonly developed marginal to veins greater than 1 centimetre wide (Plate 2-5-1d). The plunge of slickenside lineations is at a high angle and where hackle-marks are preserved, normal faulting is interpreted. A second set of fault planes has a shallow dip (Figure 2-5-3d), similar in attitude to the low-angle shear planes illustrated in Figures 2-5-3b and c.

The silicified breccias in the footwall of the No. 3 vein predate the vein, as the vein boundary is sharp against the breccia (Plate 2-5-1c, d) and postdate the amygdaloidal dike, as it is brecciated. Brecciation, however, was not a single event, but rather episodic, with evidence of internal brecciation within the No. 3 vein.

INTERPRETATION

Hubbert and Rubey (1959) and Secor (1965) have shown that the total effective stress (σ') across any plane can be resolved into a normal stress (σ^n) less the fluid pressure (p). This relationship has dramatic consequences with regard to the brittle failure of a rock. Figure 2-5-4 illustrates that an increase in fluid pressure will result in a shift to the left (A-A', B-B') of the Mohr stress circle, without changing the differential stress value ($\sigma^1 - \sigma^3$). If the diameter of the stress circle (differential stress) is large (A), increases in fluid pressure will shift the stress circle tangent to the failure

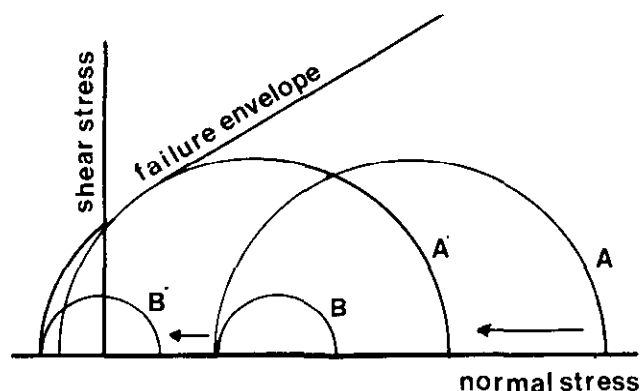


Figure 2-5-4. Mohr diagram with modified Griffith failure envelope and stress circles representing the influence of fluid pressure on the effective stress states. In the case A-A', increasing fluid pressure results in shear failure. In the case B-B', the increasing fluid pressure results in extension failure.

envelope, right of the ordinate (A'), the rock will fail through shear fracturing and conjugate shear planes will develop. If, however, the diameter of the stress circle is small (B), increases in fluid pressure will result in the circle becoming tangent to the failure envelope on the abscissa, in the tensile quadrant (B'), and the rock will fail through the development of extension planes. Simply stated, if σ^3 equals the tensile strength of the rock, extension will result.

The joint and fracture system within the unaltered feldspar porphyry and microdiorite (greater than 30 metres from the No. 3 vein) is assumed to reflect the regional stress field. The vertical and horizontal orientation of joint sets suggests that the orientation of σ^1 and σ^3 have shifted from horizontal to vertical. This type of variation may be a product of unloading of the crust under near hydrostatic conditions (Price, 1966).

Approaching the No. 3 vein, the first indication of overprinting of the regional stress field comes with the development of conjugate shear veins with a vertical acute bisector (σ^1 -vertical). The presence of an alteration assemblage marginal to the conjugate shear veins suggests that an increase in fluid pressure in the rock may have resulted in shear failure as illustrated in Figure 2-5-4.

With increased proximity to the No. 3 vein, steeply and gently dipping conjugate shear planes are both developed, indicating that σ^1 was both vertical and horizontal (Plate 2-5-2a, b). One possible explanation for this is the intrusion of a magma at depth, causing the inflation and extension of overlying rocks (Shaw, 1980). Evidence for a contemporaneous magma at depth comes from the occurrence of the amygdaloidal dikes parallel to the joint and vein attitudes.

Brecciation within the footwall and hangingwall of the No. 3 vein may be explained by a model of seismic pumping (Sibson *et al.*, 1975). This model suggests that prior to seismic shear failure, the region around the focus of the subsequent earthquake dilates in response to rising tectonic shear stress. Extension cracks and fractures open normal to the least compressive stress. The development of fracture

porosity causes the fluid pressure in the dilatant zone to decrease, inducing a slow inward migration of fluids from the surrounding rock mass. At the onset of dilatancy, the drop in the fluid pressure causes a rise in the frictional resistance to shear along the fault. The migrating fluids fill the cracks, the fluid pressure rises again and frictional resistance decreases. Seismic failure eventually occurs when the rising shear stress equals the frictional resistance. The fluids in the dilatant zone are expelled upward through the fault and adjacent fractures. Cooling of silica and metal-saturated fluids, near the surface, will result in the deposition of quartz and sulphide-rich veins in the fault plane and adjacent fractures above the seismic epicentre. The No. 3 vein is therefore interpreted as a fault plane, which acted as a conduit for metal-bearing fluids, with the smaller veins of variable attitude hydraulically connected to the "seismic pump".

A model of an intruding magma at depth, with associated increased fluid pressure and seismicity, unifies most structural elements described above into a single process. There are, however, several observations which have not been discussed. For instance, as Church and Barakso (1990) point out, strike-slip and normal faulting are noted in the area, however, the relationship between normal and strike-slip faulting is unclear. Future work will have to accommodate these observations into the broader Eocene geologic history of the area.

ACKNOWLEDGMENTS

The opportunity to work on this project comes through a joint industry (Pacific Houston Resources Inc.) and National Science and Engineering Research Council research grant to AJS. Jim Hunter provided able assistance during the underground examination. Discussions with Craig Leitch and Ken Wilks are greatly appreciated. Editing by Colin Godwin and John Newell greatly improved earlier drafts.

REFERENCES

Cheng, X. and Sinclair, A.J. (1991): Hydrothermal Alteration Associated with the Silver Queen Polymetallic Veins at Owen Lake, Central B.C. (93L/2); *B.C. Ministry of Energy, Mines and Petroleum Resources*, Geological Fieldwork 1990, Paper 1991-1, this volume.

- Church B.N. and Barakso, J.J. (1990): Geology, Lithochemistry and Mineralization in the Buck Creek Area, British Columbia; *B.C. Ministry of Energy, Mines and Petroleum Resources*, Paper 1990-2, 95 pages.
- Hancock, P.L. (1985): Bittle Microtectonics: Principles and Practice; *Journal of Structural Geology*, Volume 7, pages 437-457.
- Hobbs, B.E., Means, W.D. and Williams P.F. (1976): An Outline of Structural Geology; *John Wiley & Sons, Inc.*, 571 pages.
- Hood, T.S., Leitch, C.H.B. and Sinclair, A.J. (1991): Mineralogic Variation Observed at the Silver Queen Mine, Owen Lake, Central British Columbia; *B.C. Ministry of Energy, Mines and Petroleum Resources*, Geological Fieldwork 1990, Paper 1991-1, this volume.
- Hubbert, M.K. and Rubey, W.W. (1959): Role of Fluid Pressure in Mechanics of Over-thrust Faulting; *Geological Society of America, Bulletin*, Volume 70, pages 115-205.
- Leitch, C.H.B., Hood, C.T., Cheng, X.C. and Sinclair, A.J. (1990): Geology of the Silver Queen Mine Area, Owen Lake, Central British Columbia (93L); *B.C. Ministry of Energy, Mines and Petroleum Resources*, Geological Fieldwork 1989, Paper 1990-1, pages 287-295.
- Price, N.J. (1966): Fault and Joint Development in Brittle and Semi-brittle Rock; *Pergamon*, 186 pages.
- Secor, D.T. (1965): Role of Fluid Pressure in Jointing; *American Journal of Science*, Volume 263, pages 633-646.
- Shaw, H.R. (1980): The Fracture Mechanisms of Magma Transport from the Mantle to the Surface; in *Physics of Magmatic Process*, R.B. Hargraves, Editor; *Princeton University Press*, pages 201-264.
- Sibson, R.H., McMoore, J. and Rankin, R.H. (1975): Seismic Pumping – A Hydrothermal Fluid Transport Mechanism; *Journal of the Geological Society of London*, Volume 131, pages 653-659.
- White, N.C. and Hedenquist, J.W. (1990): Epithermal Environments and Styles of Mineralization: Variations and Their Causes, and Guidelines for Exploration, II; in *Epithermal Gold Mineralization of the Circum-Pacific: Geology, Geochemistry, Origin and Exploration*, J.W. Hedenquist, N.C. White and G. Siddeley Editors, *Journal of Geochemical Exploration*, Volume 36, pages 445-474.

NOTES



**GEOLOGY AND ALTERATION AT THE MOUNT MILLIGAN
GOLD-COPPER PORPHYRY DEPOSIT,
CENTRAL BRITISH COLUMBIA
(93N/1E)**

**By R.C. DeLong and C.I. Godwin
The University of British Columbia
M.W. Harris and N.M. Caira
Continental Gold Corp.
C.M. Rebagliati
Rebagliati Geological Consulting Ltd.**

KEYWORDS: Economic geology, Mount Milligan, alkaline porphyry, Quesnellia, Takla Group, gold, copper, potassic alteration, propylitic alteration.

INTRODUCTION

The Mount Milligan deposit, centred at latitude 55°08' north and longitude 124°04' west, is 100 kilometres west-southwest of Mackenzie and 160 kilometres northwest of Prince George in central British Columbia. The deposit occurs in gently rolling topography (Plate 2-6-1) 5 kilometres due south of Mount Milligan. Access to the property

is by a 93-kilometre logging road that connects with the Hart Highway 30 kilometres south of Mackenzie.

Estimated geological reserves for the deposit, including the Southern Star deposit to the south, are 400 million tonnes grading about 0.20 per cent copper and 0.48 gram per tonne gold (Preto, 1990).

The property was originally held by a joint venture between Continental Gold Corp. and B.P. Resources Canada Ltd. (69.8 and 30.2 per cent, respectively). Placer Dome Inc. bought all of B.P. Canada Ltd.'s interest in the property in October 1990. On October 22 Placer Dome acted on a



Plate 2-6-1. Oblique view looking westerly across the main part of the Mount Milligan gold-copper porphyry deposit. The MBX stock (Figure 2-6-1) occurs in the north-central part of the photo. Coordinates (metres) for the borders of the grid used in Figures 2-6-3 to 2-6-8 are: north = 10 000, south = 8500, east = 18 750 and west = 11 750.

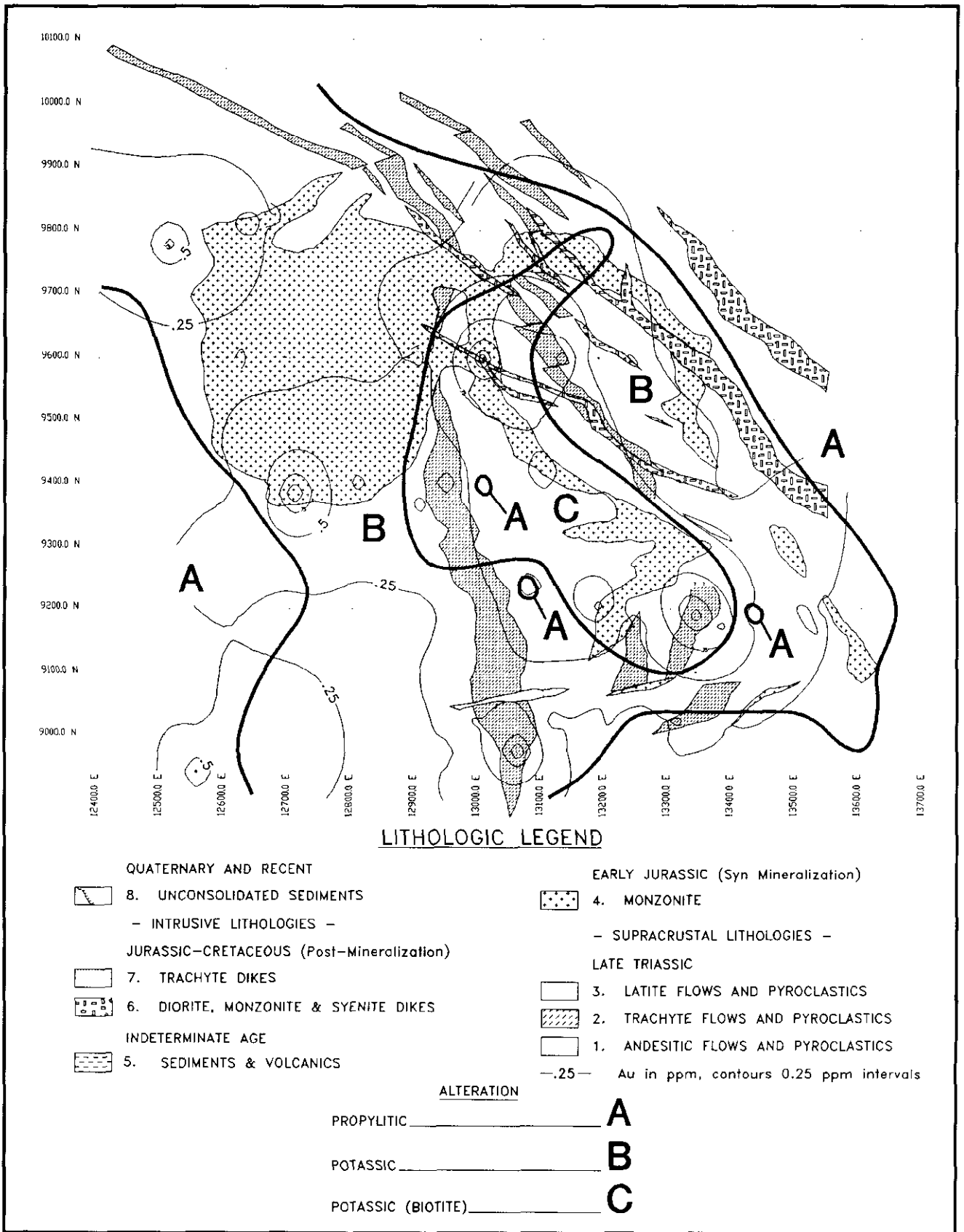


Figure 2-6-1. Geology and alteration of the Mount Milligan gold-copper porphyry deposit. Mineralization is concentrated around the stock, especially its east flank. Geological plan 995-metre level.

previous agreement with Continental Gold to purchase all its outstanding shares and now holds 97 per cent of all shares.

This report incorporates data from company reports with a compilation of drill-core data collected by DeLong and Godwin. The latter data are the basis of research by DeLong at The University of British Columbia.

METHODS

Figures 2-6-1, and 2-6-3 to 2-6-8 were prepared by collecting and examining samples from drill-hole intersections at the 1000-metre elevation in the Mount Milligan deposit. The area surveyed lies between coordinates 8500 and 10 000 metres north, and 11 750 and 13 750 metres east on the property grid (*see* Plate 2-6-1 and Figures 2-6-1 and 2-6-3 to 8).

Holes sampled are on east-west lines 200 metres apart. The vertical 10-metre interval, from 995 to 1005 metres around the piercing point for each hole, was described by examination of the core in the field, the samples in the laboratory and the existing geological logs. The values assigned to each 10-metre interval are averages of assay data. Assays of postmineral dikes have been excluded. About 100 piercing points on the 945-metre level plan were examined. All data were collated into a computer file for statistical examination and computer plotting. Figures 2-6-5 to 2-6-8 define the qualitative geometry of the distribution of alteration minerals. The 1000-metre level geological map (Figure 2-6-1) is constrained by geological interpretation of sections and adjacent levels.

REGIONAL GEOLOGY

The Mount Milligan property lies within the Quesnel Terrane in the Intermontane Belt of the Canadian Cordillera (Monger *et al.*, in press). The region is underlain mainly by Early Mesozoic Takla Group rocks (Armstrong, 1949; Garnett, 1978) of island-arc affinity (Mortimer, 1986; Nelson *et al.*, 1991, this volume). The Takla Group is equivalent to the Nicola Group in southern British Columbia.

The Takla Group in the area studied is Late Triassic to Early Jurassic in age. It is represented by volcanic, pyroclastic and epiclastic rocks overlying and, in part, interfingering with, an early Late Triassic sedimentary unit (Nelson *et al.*, 1991, this volume). The volcanic rocks are mainly augite phyric, although plagioclase and hornblende phenocrysts are present and occasionally abundant.

The Takla Group and Nicola Group are intruded by coeval plutons up to Early Jurassic in age (Mortimer, 1986). Most of these plutons are alkalic and closely related to alkaline copper porphyry deposits enriched in gold, such as the Copper Mountain, Ingerbelle, Afton and Ajax mines (Barr *et al.*, 1976). The Mount Milligan porphyry gold-copper deposit belongs to this clan.

LOCAL GEOLOGY

Outcrops and subcrops on the Mount Milligan property are Takla Group volcanic rocks intruded by small alkaline

stocks and dikes. Three volcanic units, the MBX stock and associated dikes, and three types of postmineral dikes are described below.

VOLCANIC ROCKS

Volcanic rocks are divided into three units in Figure 2-6-1 (*cf.* Rebagliati *et al.*, 1990): Unit 1, andesitic flows and fragmentals; Unit 2, trachyte flows and tuffs; and Unit 3, latitic flows and fragmentals. The andesitic and latitic units are similar texturally. Rocks where more than one-third of the total feldspar is potassic (based on staining) are classified as latite.

Andesitic volcanic rocks (Unit 1), stratigraphically the lowest unit mapped, consist of flows, and commonly, monolithic fragmental rocks. Clasts are lapilli-sized and augite (altered to actinolite) phyric. Flow and fragmental units are often interbedded with ash to fine lapilli augite-crystal tuffs.

Trachyte flows and tuffs (Unit 2) are potassic. Rocks interpreted as flows commonly contain over 70 per cent potassium feldspar as fine-grained felted microlites in the groundmass (Harris, 1989). Flows are massive but locally exhibit curvilinear banded textures defined by partings of pyrite with chlorite. This texture may mimic primary flow banding. Potassium feldspar rich ash to fine lapilli tuffs are well bedded. Sometimes they show sedimentary structures such as crossbedding, grading and load casts. These units are lensoidal. Although thickness of the trachyte flows and spatially related tuffaceous units varies abruptly, they are the best stratigraphic markers on the property.

Latite flows and fragmental rocks (Unit 3) are augite (altered to actinolite) phyric. They host most of the copper and gold mineralization in the Mount Milligan deposit. These rocks may be potassically altered andesite. If so, the stratigraphic interpretation of a lower andesite and a higher latite is a result of the geometry of the intruding stock and corresponding alteration patterns. Fragmental rocks vary from augite and augite plagioclase crystal ash tuff to lapilli tuff. Lapilli tuffs are commonly monolithic. Clasts are mainly augite-phyric fragments. Subordinate, discontinuous, heterolithic, coarse fragmental units are occasionally associated with a turbiditic cap. These are interpreted as submarine debris flows and contain clasts of latite, andesite, trachyte, and rarely, monzonite.

Most of the stratigraphy trends south-southeast and dips steeply (70°) east. Near the southeastern end of the Mount Milligan deposit (Figure 2-6-1) the strike swings east and dips shallow to 20° north. Based on textures within the tuffaceous and turbidite units, the stratigraphy is upright and faces east or north.

INTRUSIVE ROCKS

Intrusive rocks at the Mount Milligan deposit include the MBX stock and Rainbow dike (Figure 2-6-1). Postmineral dikes are common throughout the property.

The MBX stock and Rainbow dike (Unit 4) occur in the centre of the area covered by Figure 2-6-1. Unit 4 also

includes a swarm of smaller cogenetic stocks and dikes. These rocks are monzonitic and are contemporaneous with the associated porphyry-style alteration and gold-copper mineralization (Rebagliati *et al.*, 1990). The MBX stock, about 400 metres in diameter at the 1000-metre level, is typically a crowded plagioclase porphyry with an aphanitic groundmass rich in potassium feldspar. Plagioclase phenocrysts, 1.0 to 4.0 millimetres long and locally trachytoid, make up 25 to 50 per cent of the rock. Hornblende and biotite are variable and, together, average 10 per cent. They occur as single grains and aggregates. Quartz usually forms less than 3 per cent of the matrix (Harris, 1989). Accessory magnetite is often present in the matrix.

The Rainbow dike is an extension of the east side of the MBX stock (Figure 2-6-1). It is up to 50 metres wide and forms an elongate bowl or trough with gently dipping sides. The southwest part is subparallel to stratigraphy. The northeast part cross cuts stratigraphy to the bedrock surface. The southwest part also follows a segment of the Rainbow fault, one of several large structures on the property.

Postmineral dikes (Unit 6 and 7), volumetrically minor, occur throughout the deposit. Three distinct types are recognized: grey fine-grained trachyte, augite-plagioclase-porphyrific monzodiorite, and plagioclase porphyritic diorite.

ALTERATION AND MINERALIZATION

Alteration and mineralization assemblages at Mount Miligan are either potassic or propylitic – emphasized by correlation coefficients and the tree diagram shown in Figure 2-6-2. This is compatible with detailed geological observations, although detailed patterns are complex where alteration assemblages overlap. Locally, propylitic alteration overprints the potassic assemblage. The reverse is noted occasionally. The two-fold division of alteration is an important exploration guide because gold and copper are concentrated in the potassic assemblage.

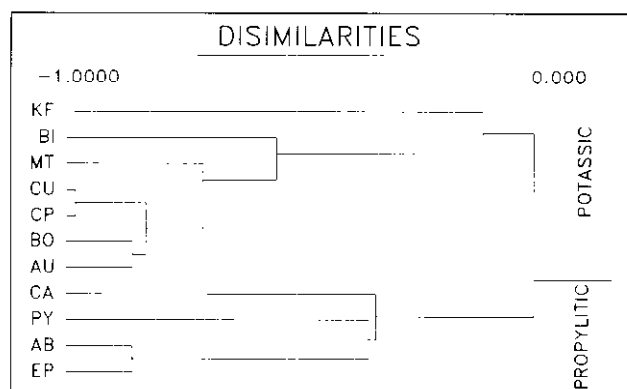


Figure 2-6-2. Tree diagram (Wilkinson, 1989) generated from Gutman mu^2 monotonicity coefficients (Shye, 1978). The potassic assemblage, in order of closest correlation, is copper [CU], chalcopyrite [CP], bornite [BO], gold [AU], magnetite [MT], biotite [BI] and potassium feldspar [KF]. The propylitic assemblage, in the same order, is albite [AB], epidote [EP], pyrite [PY] and calcite [CA]. Note that potassic alteration is independent of propylitic alteration.

POTASSIC ALTERATION

Potassic alteration is concentrated around the contacts of the monzonite intrusions. Alteration may extend several hundred metres outward from the contact, into fractured volcanic rocks, for example, along structures such as the Rainbow fault. Potassic alteration also occurs within the monzonite.

The potassic alteration assemblage (Figure 2-6-2) is characterized by widespread development of secondary potassium feldspar. However, hydrothermal biotite, bornite, chalcopyrite and magnetite are better indicators of areas of intense potassic alteration.

The potassic alteration is crudely zoned. Biotite is most abundant close to the stock and around parts of the Rainbow dike (Figures 2-6-1 and 2-6-5). Figure 2-6-2 shows the close statistical correlation between gold and copper, bornite and chalcopyrite, and magnetite and biotite. The broader relationship to potassium feldspar is also shown. Figure 2-6-2 shows that potassic alteration is independent of the propylitic assemblage of epidote, albite and pyrite.

Figures 2-6-3 to 2-6-6 show the distribution of gold and copper with respect to minerals characteristic of the potassic assemblage. Gold abundance in Figure 2-6-3 is represented by a smoothed surface such that the influence of neighboring points decreases exponentially with distance. The other three-dimensional plots that represent abundances use surfaces that are more smoothed by a distance-weighted least-squares fit. The plots and methods are from the computer program SYGRAPH (Wilkinson, 1988).

Fine-grained secondary biotite commonly forms 30 per cent (up to 60 per cent in places) of the volcanic rocks near the intrusive contact. It is most abundant in intermediate to basic protoliths. Biotite is usually pervasive, but it also occurs as envelopes to potassium feldspar veinlets. Pervasive biotite alteration usually leaves relict porphyritic textures. Augite phenocrysts are not biotitized, but are always actinolitized. Locally, intense biotitization has destroyed primary textures.

Secondary potassium feldspar, present throughout and beyond the biotite zone, is the most abundant alteration mineral in the potassic assemblage. It occurs as veinlets and microveinlets, sometimes with accessory quartz. However, it is also present as patchy to pervasive, grey to occasionally pink, aphanitic alteration of the groundmass that obliterates primary textures. This type of alteration floods parts of the Rainbow dike. Some of the rocks mapped as trachyte could be pervasively altered units.

Chalcopyrite (Figure 2-6-6) occurs as fine-grained disseminations, often in biotitic envelopes around veinlets especially near the MBX stock. Less commonly, it forms veinlets and selvages of veins and veinlets. In veins and veinlets it is associated with either calcite, or quartz and potassium feldspar.

Bornite is not abundant but occurs exclusively with potassic alteration. It is correlated with higher gold assays. Chalcopyrite has a broader association with potassic alteration and gold (Figures 2-6-2 and 2-6-6).

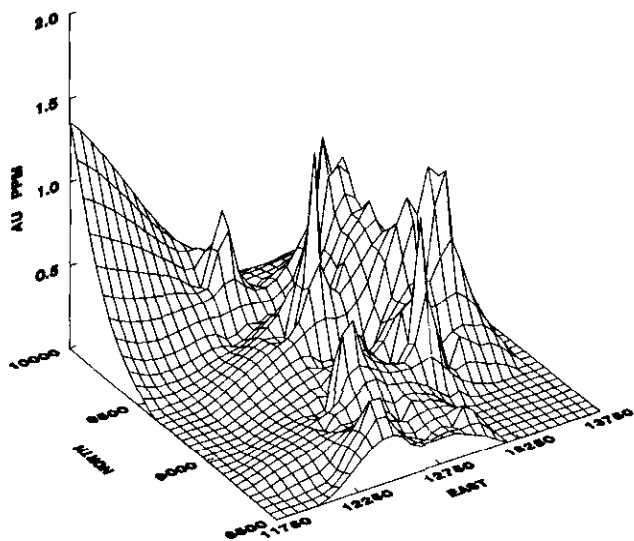


Figure 2-6-3. Gold [AU] surface in parts per million. Edge effects in the northwestern corner should be ignored.

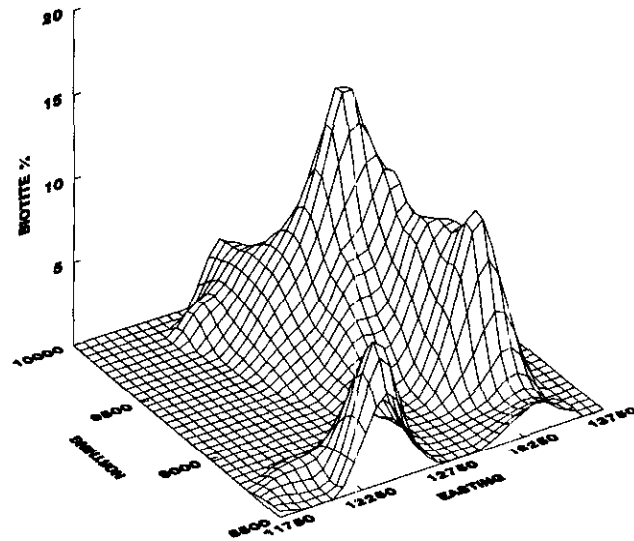


Figure 2-6-5. Biotite surface in visually estimated per cent. The potassic core to the deposit is well outlined.

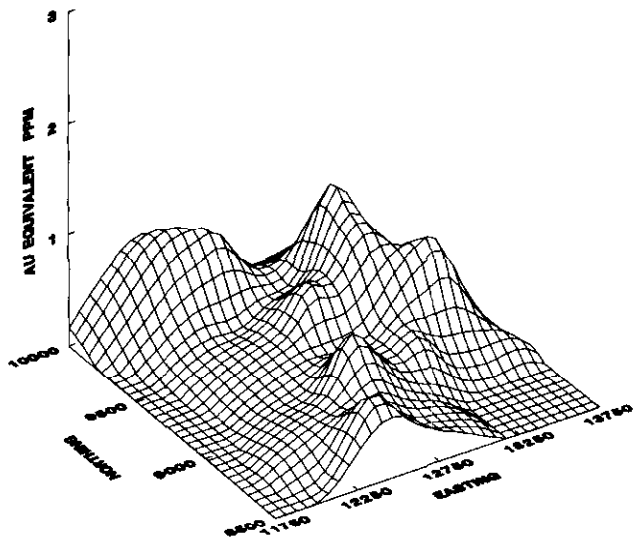


Figure 2-6-4. Gold [AU] equivalent (gold in parts per million plus copper in per cent) surface in parts per million. This surface is more smoothed, but is clearly similar to Figure 2-6-3.

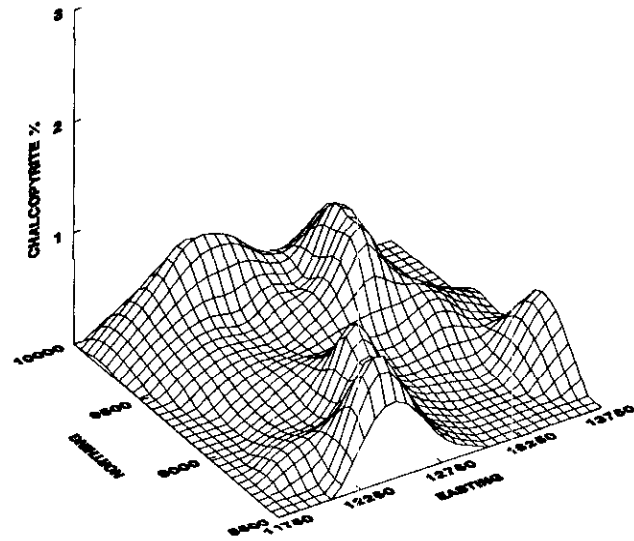


Figure 2-6-6. Chalcopyrite surface in visually estimated per cent. Note that abundant chalcopyrite coincides with concentrations of gold and biotite.

Secondary magnetite occurs throughout the potassic assemblage, and only locally in the propylitic assemblage. Most commonly it occurs as disseminations in biotite-rich areas. Within the MBX stock some of the magnetite may be primary. Magnetite also occurs locally as flooding, as veins and microveins, and as matrix to small breccia bodies around the eastern contact of the MBX stock. It also forms partings in trachyte flows and is concentrated along bedding planes in some tuffs. Abundant magnetite is associated with high copper and gold contents, and low pyrite estimates (Figure 2-6-2).

PROPYLITIC ALTERATION

Propylitic alteration (Figures 2-6-7 and 2-6-8) is widespread and characterized by epidote with varying amounts of calcite, chlorite, albite and pyrite. The greatest volume of propylitic alteration is peripheral to the potassic alteration zone. Except for postmineral dikes, the rocks are never fresh; where they are not potassically altered, they are propylitized.

Potassic and propylitic zones locally overlap. Propylitic alteration, in part, is contemporaneous with potassic altera-

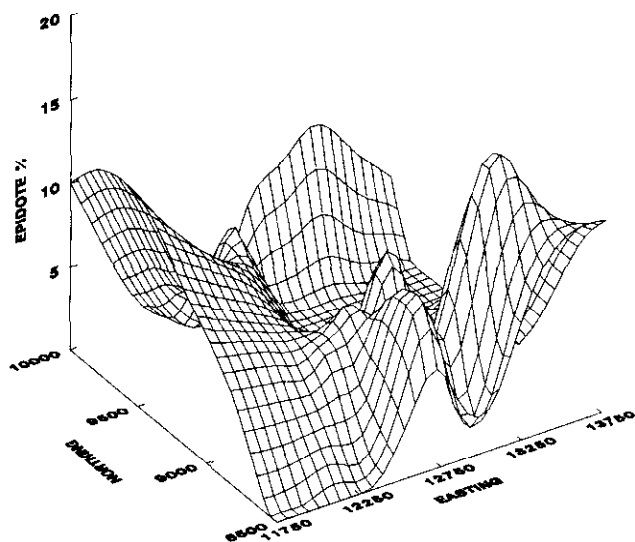


Figure 2-6-7. Epidote surface in visually estimated per cent. Epidote concentration is marginal to mineral concentrations in the potassic core (Figures 2-6-5 and 2-6-6). It is the inverse of the gold and gold-equivalent surfaces (Figures 2-6-3 and 2-6-4) except for the anomaly mentioned in the text around 9100 north and 12 800 east.

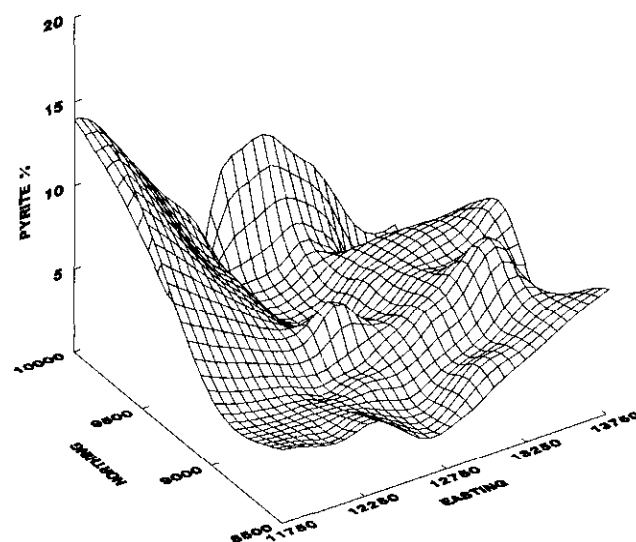


Figure 2-6-8. Pyrite surface in visually estimated per cent. Pyrite distribution is similar to epidote (Figure 2-6-7).

tion. It represents the peripheral part of the same hydrothermal system that generated the potassic alteration. However, some of the propylitic alteration is later. Retrograde alteration formed during the collapse of the hydrothermal system may account for some overprinting relationships.

Epidote (Figure 2-6-7) is the most common propylitic mineral. It is almost always associated with pyrite blebs and disseminations. Epidote forms in alteration envelopes up to 1.5 centimetres thick around pyrite-calcite veinlets, as *medium-grained clots nucleated on mafic grains*, as *irregular aggregates* in the groundmass of volcanics, and as cores to circular porphyroblastic aggregates with albite and calcite that are up to 5 centimetres across. Epidote envelopes may crosscut potassium feldspar and biotite alteration. Thin-section observations show that epidote replaces actinolite. Late, minor epidote occurs along fractures in postmineral dikes.

Albite forms irregular, creamy fine-grained patches of groundmass alteration. Mafic grains and phenocrysts are not albitized. Albite sometimes forms very fine grained pale yellow-green aggregates when intergrown with epidote. It has a negative correlation with gold and copper (Figure 2-6-2). However, this relationship is locally inconsistent, because high-grade mineralization occurs around rare, intensely albitized pipe-like zones in the order of 50 metres in diameter (Rebagliati *et al.*, 1990).

Calcite is present as groundmass alteration, replacement of actinolite, and in at least two generations of veins and veinlets. Both sparry and pink calcite veins crosscut most textures.

Pyrite (Figure 2-6-8) is widespread. Although present in the potassic zone, it is more abundantly developed in the

propylitic zone. It forms veins, microveins, disseminations in wallrock, and pseudomorphs mafic grains. Several generations of pyrite veining are indicated by crosscutting relationships. Figure 2-6-8 shows an irregular pyrite halo around the potassic core of the deposit.

Carbonate, chlorite and clays occur in fault and fracture zones that locally show elevated gold and copper values. Most of the carbonate is calcite. Dolomite and iron carbonate form late crosscutting veins and the matrix of tectonic breccias.

SUMMARY

The Mount Milligan gold-copper alkaline porphyry deposit is large compared to Afton, Copper Mountain and other similar deposits. It formed by hydrothermal activity related to emplacement of the MBX stock into the Takla Group. On a property scale the alteration and mineral zoning are consistent with previously described models for alkaline porphyry deposits (*cf.*: diorite model of Lowell and Guilbert, 1970; Barr *et al.*, 1976; Fox, 1989). As in most porphyry deposits detailed patterns of alteration and metal zoning are complex where alteration assemblages overprint each other. The overprinting probably represents either separate pulses of alteration, or changes of the physical and chemical properties of the hydrothermal solutions with time and distance.

The highest gold assays and chalcopryrite estimates correlate directly with potassic alteration. This is particularly clear from the close correlation (Figure 2-6-2) between the distribution of gold and copper (Figures 2-6-3, 4 and 6) and the biotite-rich zones (Figure 2-6-5). Gold distribution in the southeastern part of the deposit (Figure 2-6-1) is unusual. A gold zone, centred at 9250 north and 13 300 east (Figures 2-6-1 and 2-6-3) is anomalous. Copper concentrations are low and gold values are high. Both potassic and propylitic alteration are associated with this mineralization.

This might be explained by overprinting of earlier potassic alteration by later propylitic alteration. This anomaly, gold associated with epidote, is being investigated.

ACKNOWLEDGMENTS

Continental Gold Corp. has provided research funding, employment to DeLong and open access to company information. Fellow employees at Continental Gold Corp. have been helpful in many ways. Research funding has been given to Godwin by grants from the National Science and Engineering Research Council and the British Columbia Ministry of Energy, Mines and Petroleum Resources. DeLong is partly supported by a Science Council of British Columbia GREAT Award.

REFERENCES

- Armstrong, J.E. (1949): Fort St. James Map-area; *Geological Survey of Canada*, Memoir 252.
- Barr, D.A., Fox, P.E., Northcote, K.E. and Preto, V.A. (1976): The Alkaline Suite Porphyry Copper Deposits – A Summary; in *Porphyry Deposits of the Canadian Cordillera*, A. Sutherland Brown, Editor, *Canadian Institute of Mining and Metallurgy*, Special Volume 15, pages 359-367.
- Fox, P.E. (1989): Alkaline Cu-Au Porphyries – Schizophrenic Cousins of Real Porphyry Coppers; in *Cu-Au Porphyry Workshop*, April 5, 1989, Vancouver, *Geological Association of Canada, Mineral Deposits Division*, reprinted in *The Gangue*, No. 28.
- Garnett, J. (1978): Geology and Mineral Occurrences of the Southern Hogen Batholith; *B.C. Ministry of Energy, Mines and Petroleum Resources*, Bulletin 70.
- Harris, J.F. (1989): A Petrographic Study of Rocks from the Mount Milligan Gold Deposit; unpublished report for Continental Gold Corp.; *Harris Exploration Services Ltd.*
- Lowell, J.D. and Guilbert, J.M. (1970): Lateral and Vertical Alteration-Mineralization Zoning in Porphyry Ore Deposits; *Economic Geology*, Volume 65, pages 373-408.
- Monger, J.W.H., Wheeler, J.O., Tipper, H.W., Gabrielse, H., Struik, L.T., Campbell, R.B., Dodds, C., Garrels, R., and O'Brien, J. (in press): Cordilleran Terranes; in *The Cordilleran Orogen: Canada*, H. Gabrielse and C.J. Yorath, Editors, Chapter 8, Upper Devonian to Middle Jurassic Assemblages; *Geological Survey of Canada*, Geology of Canada, No. 4. (also *Geological Society of America*, The Geology of North America, No. G-2).
- Mortimer, N. (1986): Late Triassic, Arc Related, Potassic Igneous Rocks in the North American Cordillera; *Geology*, Volume 14, pages 1035-1038.
- Nelson, J., Bellefontaine, K., Green, K. and MacLean, M. (1991): Regional Geological Mapping Near the Mount Milligan Deposit (93N/1, 93K/16); *B.C. Ministry of Energy, Mines and Petroleum Resources*, Geological Fieldwork 1990, Paper 1991-1, this volume.
- Preto, V.A. (1990): British Columbia Exploration and Development Highlights for 1990: Gold and Porphyry Deposits Continue to Excite Investors; *B.C. Ministry of Energy, Mines and Petroleum Resources*, Information Circular 1990-25, page 7.
- Rebagliati, C.M., Harris, M.W. and Caira, N.M. (1990): Interim Geological Report, Mount Milligan Project; *Continental Gold Corp.*, unpublished report.
- Shye, S. (1978): Theory, Construction and Data Analysis in the Behavioral Sciences; *Jossey-Bass*, San Francisco.
- Wilkinson, L. (1989): Systat: The System for Statistics; *Systat Inc.*, Evanston, IL.

NOTES



⁴⁰Ar/³⁹Ar AGES OF EPITHERMAL ALTERATION AND VOLCANIC ROCKS IN THE TOODOGGONE Au-Ag DISTRICT, NORTH-CENTRAL BRITISH COLUMBIA (94E)

By James R. Clark and A.E. Williams-Jones
Mineral Exploration Research Institute
McGill University

KEYWORDS: Regional geology, Toodoggone, geochronology, ⁴⁰Ar/³⁹Ar, epithermal, gold, silver, alteration, potassium feldspar, adularia, sericite, volcanic, hornblende.

INTRODUCTION

For the past decade, the Toodoggone district has been an active area of mineral exploration, and has recently become an important area of gold and silver production. The district contains one of British Columbia's largest gold-silver mines (Lawyers), as well as smaller scale current and past-producers (Shasta and Baker mines, respectively). Several gold deposits have drill-indicated reserves and await production decisions (e.g. Bonanza), and numerous other gold-silver-copper prospects are in various stages of exploration.

The deposits range from gold-rich porphyry-style deposits, to deep-seated precious and base metal bearing stockworks and veins, to near-surface replacement-type gold mineralization. The most economically significant deposits exhibit characteristics typical of epithermal alteration and mineralization of both adularia-sericite and acid-sulphate affinities. The former class of deposits is represented by the Lawyers AGB and Cliff Creek zones and the Shasta deposit, and the latter by the Bonanza deposit. These four deposits also contain most of the known reserves in the district.

The most important lithologic assemblage in the area is the "Toodoggone volcanics" (Carter, 1972). These consist of dominantly andesitic to dacitic pyroclastics and flows of apparent Early to Middle Jurassic age, and have been described by Schroeter (1981; 1982), Panteleyev (1982; 1983), Diakow (1984), Forster (1984), Diakow *et al.* (1985), and Marsden and Moore (1989, 1990). The Toodoggone volcanics are underlain by Upper Triassic mafic to intermediate volcanics of the Stuhini Group, and are overlain by Cretaceous-Tertiary clastic sediments of the Sustut Group. Gold-silver mineralization is primarily hosted by the Toodoggone volcanics, and to a lesser extent, by the Stuhini and Asitka groups, and Lower Jurassic felsic to intermediate intrusive rocks. The major ore deposits in the district have been described by Vulimiri *et al.* (1987; Lawyers), Thiersch and Williams-Jones (1990; Shasta), Clark and Williams-Jones (1986; Bonanza), and Barr (1978; Baker).

The objective of the current study is to clarify the age of the Toodoggone volcanics and the related epithermal gold-silver deposits. This report presents seven new ⁴⁰Ar/³⁹Ar age determinations, and discusses the results in terms of the implications for mineral exploration and metallogeny in the Toodoggone district.

PREVIOUS DETERMINATIONS OF AGE RELATIONSHIPS

Several K-Ar studies have been conducted on the Toodoggone volcanics, and have yielded ages that range from 204 to 182 Ma. When correlated with geological observations, these ages appear divisible into groups that correspond to two stages of volcanism: an older, lower stage with ages of 204 ± 7 Ma (Panteleyev, 1983), 202 ± 7, 200 ± 7, 200 ± 7, 199 ± 7 and 197 ± 7 Ma (Diakow, 1985), and 189 ± 6 Ma (Carter, 1972; age recalculated using the constants of Steiger and Jäger, 1977); and a younger, upper stage with ages of 183 ± 8 and 182 ± 8 Ma (Gabrielse *et al.*, 1980; first value recalculated using constants of Steiger and Jäger, 1977). The lower volcanics are dominantly andesitic pyroclastic and flow rocks, and are characterized by widespread propylitic and zeolitic alteration. The upper volcanics correspond to the "grey dacite" and equivalent units of Diakow *et al.* (1985), and overlying rocks recently mapped by Marsden and Moore (1990). These volcanics consist of dominantly andesitic to dacitic ash-flow tuffs that generally lack significant epithermal alteration. All epithermal gold-silver deposits and prospects discovered thus far in the district are restricted to the lower Toodoggone volcanics and underlying units. On the basis of these geological relationships, Clark and Williams-Jones (1987, 1988) proposed division of the Toodoggone volcanics into two stages, with mineralization having occurred during Stage I and/or between Stages I and II.

The timing of Toodoggone Stage I volcanism is constrained by K-Ar age determinations spanning 204 to 189 Ma. However, the sample of the oldest Stage I rock (204 Ma, Panteleyev, 1983; "Adoogacho Formation" of Diakow *et al.*, 1985) was re-analysed by the ⁴⁰Ar/³⁹Ar method by Shepard (1986) and yielded a plateau age of 197.6 ± 0.5 Ma. This suggested that the Stage I volcanics range between 198 and 189 Ma in age. Toodoggone Stage II volcanics are more poorly constrained by two K-Ar determinations of 183 and 182 Ma. The relatively wide range of K-Ar ages for volcanic rocks in the district is greater than that expected for Hazelton-equivalent volcanism elsewhere in north-central and northwestern British Columbia. There is a clear need for additional high-precision age determinations to elucidate the ages and relationships of the Toodoggone volcanics.

Whereas the ages of the volcanics are at least somewhat constrained, there is poor agreement on the timing of mineralization. Potassium-argon ages of epithermal alteration range from Early to Late Jurassic, and most dates appear to

be too young to be geologically reasonable. Schroeter *et al.* (1986) reported K-Ar ages for adularia from the Lawyers AGB deposit (180 ± 6 Ma), the Golden Lion prospect (176 ± 6 Ma) and the Metsantan prospect (168 ± 6 Ma). The K-Ar ages of acid-sulphate alteration and related deposits have been determined for the Alberts Hump alunite zone (190 ± 7 Ma, alunite; Schroeter, 1982), the Jan alunite zone (193 ± 7 Ma, alunite; Clark and Williams-Jones, 1989), and the Bonanza and BV deposits (171 ± 6 and 152 ± 5 Ma, sericite; Clark and Williams-Jones, 1989). Clark and Williams-Jones (1989) suggested that the adularia and sericite dates were minimum ages due to loss of small amounts of radiogenic argon. Whether Toodoggone gold-silver mineralization is restricted to mid-Toarcian (~ 190 Ma) and older rocks (Clark and Williams-Jones, 1987) or postdates the youngest volcanism in the area by several million years (Schroeter *et al.*, 1986), remains to be clarified by our $^{40}\text{Ar}/^{39}\text{Ar}$ study.

$^{40}\text{Ar}/^{39}\text{Ar}$ ANALYSES

Step-heating $^{40}\text{Ar}/^{39}\text{Ar}$ analyses were conducted on three samples of hornblende separated from Toodoggone volcanic rocks, and four samples of potassium feldspar and sericite separated from hydrothermal alteration zones directly associated with gold-silver mineralization. The samples from volcanic rocks were selected to evaluate the age relationship between the two main stages of Toodoggone volcanism. Samples from ore zones were chosen to accurately date the most important deposits in the area, to provide information on the relationship between deposits associated with both adularia-sericite and acid-sulphate alteration styles, and to constrain metallogenic events in the district.

SAMPLE DESCRIPTIONS

Sample SH-11 is from an andesitic crystal-lapilli tuff unit ("Unit 9" of Marsden and Moore, 1990) located 1.5 kilometres north of the Shasta mine (Figure 2-7-1). The tuff is the youngest unit of the Toodoggone Stage I volcanics in the Jock Creek area. Hornblende comprises 3 per cent of the rock, and consists of euhedral to broken crystals ($200\text{-}1000 \mu\text{m}$) that exhibit no evidence of alteration. Lithic fragments in the tuff sample are similar in composition to the matrix and crystals, and contain optically identical hornblende grains.

Sample BK87-03 was collected from the "Tiger Notch area", 1.8 kilometres north of the Baker mine (Figure 2-7-1). The sample is from the basal part of an andesitic/dacitic ash-flow tuff that forms the major unit of the second stage of the Toodoggone volcanics ("grey dacite" unit of Diakow *et al.*, 1985). Hornblende comprises 5 per cent of the rock and consists of euhedral to broken crystals ($200\text{-}1500 \mu\text{m}$) with slightly oxidized rims ($5\text{-}10 \mu\text{m}$ thick).

The material used from sample GSC 76-77 consists of a hornblende separate, part of which has been previously analysed by the K-Ar method. The original sample was obtained from an outcrop mapped by Diakow *et al.* (1985) as part of the "grey dacite" unit, located approximately 9 kilometres north-northeast of the Kemess prospect (Figure

2-7-1). The hornblende gave a K-Ar age of 183 ± 8 Ma (Gabrielse *et al.*, 1980; age recalculated using the constants of Steiger and Jäger, 1977).

Sample LW-037 is from an andesitic/dacitic tuff ("welded trachyte tuff" unit of Vulimiri *et al.*, 1987) exposed in the 1750-level adit of the AGB zone at the Lawyers mine (Figure 2-7-1). The sample exhibits strong potassic alteration, brecciation and gold-silver mineralization. Alteration is complete, and no primary potassium-bearing phases remain from the original tuff. The sample consists of 40 to 50 per cent potassium feldspar as replacements of plagioclase crystals ($200\text{-}3000 \mu\text{m}$), and as alteration of the tuff matrix ($20\text{-}100 \mu\text{m}$). Minor sericite (<3 per cent) occurs as irregular alteration patches in the potassium feldspar, but is considered to be synmineralization in age. Fracture-controlled ankerite alteration locally overprints the potassium feldspar.

A similar sample of material rich in potassium feldspar (LW-011) was obtained from a trench on the Cliff Creek zone at the Lawyers mine (Figure 2-7-1). The sample is from an andesitic/dacitic tuff unit ("upper andesite" of Vulimiri *et al.*, 1987) that has been potassically altered and locally brecciated, and contains gold-silver mineralization. Alteration is complete, and no primary potassic phases remain in the rock. Potassium feldspar comprises 30 to 40 per cent of the sample, and consists of replacements of plagioclase crystals ($200\text{-}2000 \mu\text{m}$) and alteration of the tuff matrix ($20\text{-}100 \mu\text{m}$). Sericitic alteration of the potassium feldspar is minor (<1 per cent), and is considered to be associated with the mineralizing event.

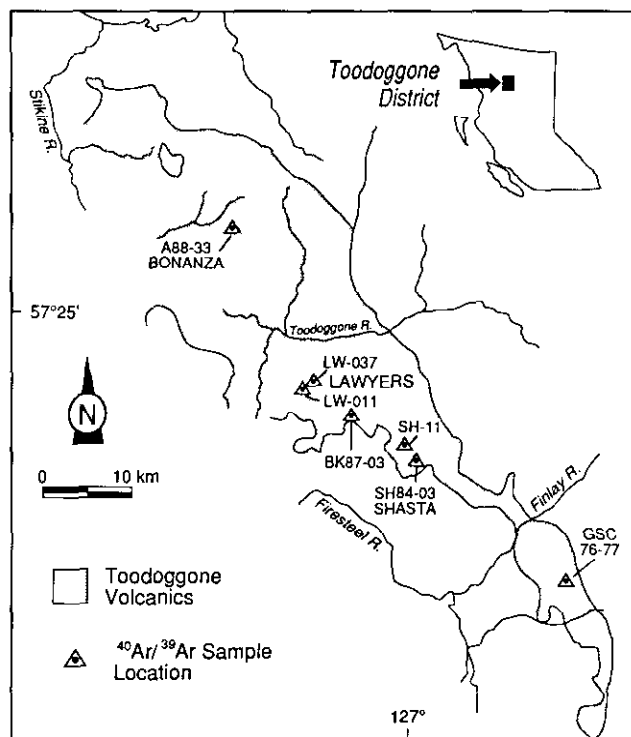


Figure 2-7-1. Distribution of the Toodoggone volcanics and locations of samples used for $^{40}\text{Ar}/^{39}\text{Ar}$ analyses.

Sample SH84-03 is from 94.5 metres depth in drill hole 84-03 on the Creek zone at the Shasta mine (Figure 2-7-1). The rock is a dacitic ash-flow tuff ("Unit 5" of Marsden and Moore, 1990) that has undergone intense potassic alteration, and contains quartz stockworks and weak gold-silver mineralization. Potassium feldspar in the sample is well crystallized, and generally appears to have been precipitated in open spaces created by an earlier alteration and dissolution event. The potassium feldspar exhibits an adularia-type habit (Felsobanya), and comprises 80 to 90 per cent of the sample. Adularia occurs as euhedral to subhedral grains (50-800 μm) and as fine-grained (<25 μm) flooding of the matrix. Larger grains contain slightly turbid centres due to finely disseminated hematite. Minor sericitic alteration (<5 per cent) occurs as irregular patches throughout the sample, but is considered to have formed closely after mineralization.

Sample A88-33 is from 73.8 metres depth in drill hole 88-33 on the South Bonanza zone of the Bonanza deposit (Figure 2-7-1). The Bonanza deposit is characterized by acid-sulphate alteration, but locally contains sericite at depth. The host rock is an andesitic to dacitic ash-flow tuff that has undergone complete alteration to a sericite-quartz-pyrite assemblage that contains gold. The sample consists of 60 to 70 per cent sericite that X-ray diffraction indicates to be dominantly 1M illite. The sericite grains are subhedral (20-200 μm) and generally replace the originally feldspathic components of the tuff. Traces of dickite occur locally in quartz and sericite.

ANALYTICAL METHODS

Most of the mineral separations, and all the argon determinations were conducted in the Department of Geology, University of Maine at Orono, under the direction of Daniel R. Lux. Samples were crushed and sieved to uniform grain sizes, and standard magnetic and density methods were used to extract hornblende, potassium feldspar and sericite. The mineral separates were encapsulated in foil and sealed in silica-glass tubes, and then irradiated in the HS facility of the Ford nuclear reactor at the University of Michigan. MMhb-1 (Alexander *et al.*, 1978) and several internal standards were used as irradiation monitors. The irradiated samples were heated in molybdenum crucibles in an ultra-high vacuum system using a radio frequency induction furnace. Standard gettering techniques were employed to purify the rare gases from the sample. The argon isotopic compositions were measured with a Nuclide 6-60-SGA mass spectrometer. Peak height-time values were extrapolated to time-zero by both linear and quadratic routines. Aliquots of atmospheric argon were analysed daily in order to determine mass discrimination values. Potassium and calcium salts were analysed with each batch of samples to determine correction factors for unwanted argon irradiation products.

Ages and errors were calculated using the equations of Dalrymple *et al.* (1981), and the decay constants and isotopic compositions of Steiger and Jäger (1977). Errors are given for two standard deviations, plus a 0.5 per cent uncertainty in the irradiation parameter (J). Plateaus were deter-

mined using the criteria of Fleck *et al.* (1977), and the critical value test (Dalrymple and Lanphere, 1969) was used to evaluate concordance between successive increments.

RESULTS

The results of the $^{40}\text{Ar}/^{39}\text{Ar}$ analyses and apparent ages of the gas fractions are given in Table 2-7-1.

Sample SH-11, from the upper strata of the first stage of the Toodoggone volcanics, has a total gas age of 197.9 ± 2.2 Ma. The high ages of the lower temperature gas fractions show that the hornblende contains some excess ^{40}Ar . Standard data treatment yields a plateau age of 195.1 ± 1.6 Ma (Figure 2-7-2a). Use of the isotope correlation data treatment (Fig. 2-7-2b) indicates that the sample has a non-atmospheric $^{40}\text{Ar}/^{36}\text{Ar}$ ratio of 337 ± 9 , which allows calculation of an adjusted plateau age of 193.8 ± 2.6 Ma (Figure 2-7-2c). This result can be considered to approximate the minimum age for the Toodoggone Stage I volcanic rocks.

Hornblende (BK87-03) from near the base of Toodoggone Stage II volcanics also contains minor excess argon, and has a total gas age of 197.8 ± 2.5 Ma. Standard treatment of the data suggests a plateau age of 194.4 ± 1.9 Ma (Figure 2-7-3a). The isotope correlation method indicates a relatively high $^{40}\text{Ar}/^{36}\text{Ar}$ composition of 349 ± 27 (Figure 2-7-3b), and yields a recalculated plateau age of 192.9 ± 2.7 Ma (Figure 2-7-3c).

In order to check the apparent closeness in age of the upper Stage I and lower Stage II volcanics, we analysed an additional hornblende separate (GSC 76-77) from the "grey dacite" unit. The sample shows evidence of a disturbed argon history in the lower temperature gas fractions which may be due to a superimposed excess ^{40}Ar component and a slight argon loss. The total gas age is 193.0 ± 2.4 Ma, and the plateau age is 193.8 ± 2.5 Ma (Figure 2-7-4a). The isotope correlation treatment indicates a near-atmospheric $^{40}\text{Ar}/^{36}\text{Ar}$ ratio of 278 ± 12 , and a concordant intercept age of 194.2 ± 3.6 Ma (Figure 2-7-4b). The age of the basal Toodoggone Stage II volcanics thus falls in the range of 194 to 193 Ma, and must be only slightly younger than the underlying Stage I rocks.

Sample LW-037, a potassium feldspar separate from the AGB deposit at the Lawyers mine, yields quite straightforward results. The lower temperature steps of the age spectrum show that the feldspar has undergone minor loss of radiogenic argon (^{40}Ar); the sample has a total gas age of 186.0 ± 1.9 Ma. The plateau age is 188.2 ± 2.3 Ma (Figure 2-7-5), and the isotope correlation method indicates an atmospheric $^{40}\text{Ar}/^{36}\text{Ar}$ composition of 291 ± 77 and an intercept age of 188.0 ± 1.8 Ma.

A potassium feldspar separate (LW-011) from the Cliff Creek zone of the Lawyers mine yields results similar to those for the AGB deposit. There is a very slight ^{40}Ar loss, suggested by the lowest temperature gas fractions, and the total gas age is 188.1 ± 3.9 Ma. The plateau age is 189.7 ± 2.6 Ma (Figure 2-7-6). The main orebodies at the Lawyers mine are therefore well constrained, with an age of 190 to 188 Ma.

The results from the Shasta mine adularia sample (SH84-03) are quite similar to those from the Lawyers

TABLE 2-7-1
⁴⁰Ar/³⁹Ar ANALYTICAL RESULTS AND APPARENT AGES OF MINERALS FROM TOODOGGONE VOLCANIC ROCKS
AND EPITHERMAL GOLD-SILVER DEPOSITS.

Temp. °C	⁴⁰ Ar/ ³⁹ Ar	³⁷ Ar/ ³⁹ Ar	³⁶ Ar/ ³⁹ Ar	³⁹ Ar 10 ⁻¹³ mol	³⁹ Ar % tot.	⁴⁰ Ar* %	K/Ca	Age±2σ Ma
SH-11 Hornblende (J=0.006075)								
865.....	33.39	1.152	0.0372	36.4	2.3	67.3	0.425	231.0±4.1
1015.....	33.13	1.224	0.0387	76.7	4.8	65.7	0.400	224.3±2.5
1120.....	27.05	3.007	0.0254	76.7	4.8	73.0	0.163	204.8±2.0
1175.....	22.38	4.495	0.0128	117.0	7.3	84.7	0.109	197.2±2.2
1220.....	19.79	5.298	0.0051	321.1	20.1	94.5	0.092	194.7±1.9
1265.....	19.46	5.386	0.0039	378.3	23.7	96.2	0.091	195.0±2.2
1305.....	19.47	5.447	0.0038	256.1	16.0	96.4	0.090	195.5±1.9
1345.....	19.47	5.627	0.0041	161.2	10.1	96.1	0.087	194.8±2.3
FUSE.....	19.59	5.965	0.0044	175.5	11.0	95.7	0.082	195.2±2.1
Total.....				1599.0	100.0			197.9±2.2
BK87-03 Hornblende (J=0.05984)								
865.....	74.49	16.560	0.1602	23.4	2.1	38.2	0.029	287.0±14.5
975.....	53.60	11.170	0.1070	26.0	2.3	42.7	0.044	233.0±7.3
1070.....	22.53	5.302	0.0124	117.0	10.3	85.6	0.092	197.7±2.0
1160.....	21.73	5.127	0.0094	74.1	6.5	89.0	0.095	198.3±2.3
1235.....	19.94	4.926	0.0048	140.4	12.3	94.8	0.099	193.9±2.3
1305.....	19.66	4.889	0.0037	374.4	32.8	96.4	0.100	194.4±2.1
FUSE.....	20.00	5.224	0.0048	384.8	33.8	94.9	0.093	194.8±2.2
Total.....				1140.1	100.0			197.8±2.5
GSC 76-77 Hornblende (J=0.00622)								
650.....	69.12	0.666	0.1736	22.4	1.0	25.8	0.735	190.1±4.4
740.....	45.80	0.544	0.0974	31.2	1.3	37.2	0.900	181.8±8.7
830.....	38.95	0.653	0.0782	27.2	1.2	40.7	0.749	169.9±4.8
900.....	36.11	1.360	0.0710	20.8	0.9	42.1	0.360	163.4±4.2
970.....	22.91	4.536	0.0182	149.6	6.5	78.2	0.108	191.3±2.8
1040.....	20.79	4.846	0.0098	314.4	13.6	88.1	0.101	195.3±2.6
1100.....	19.92	4.993	0.0076	668.0	28.9	90.8	0.098	193.1±2.0
1170.....	19.90	5.058	0.0073	612.8	26.5	91.2	0.096	193.7±1.9
FUSE.....	20.09	5.120	0.0077	467.2	20.2	90.8	0.095	194.6±2.5
Total.....				2313.6	100.0			193.0±2.4

mine. The lowest temperature gas fractions indicate that there has been minor loss of radiogenic argon; the total gas age is 187.1±1.9 Ma. The standard data treatment yields a plateau age of 188.1±1.8 Ma (Figure 2-7-7a), but the isotope correlation technique suggests a slightly higher than atmospheric ⁴⁰Ar/³⁶Ar ratio of 326±49 and an intercept age of 186.7±2.0 Ma (Figure 2-7-7b). Applying the non-atmospheric ⁴⁰Ar/³⁶Ar composition to the data results in an adjusted plateau age of 186.7±1.7 Ma (Figure 2-7-7c).

Sample A88-33, consisting of sericite from the Bonanza deposit, gives a fairly complicated gas-release pattern. In addition, the sample was heated to relatively high temperatures prior to the first gas analyses, which further complicates interpretation of the results. Most of the argon was released from the sericite in the first three steps, and yielded unexpectedly old apparent ages for these gas fractions. Higher temperature increments give younger ages but involve only small amounts of argon. The total gas age for the sample is 206.8±2.3 Ma, and the plateau age by standard calculation is 207.7±2.7 Ma (Figure 2-7-8a). These ages are geologically unreasonable (*i.e.* older than the host-rocks), as is the intercept age from the isochron diagram. However, the age spectrum only provides a model age, and following the approach of Heizler and Harrison (1988), may

be resolved into thermally and compositionally distinct argon components. For example, the last three gas fractions define an isochron which has an atmospheric ⁴⁰Ar/³⁶Ar ratio of 291±23, and an intercept age of 195.9±5.9 Ma (Figure 2-7-8b). Steps 1, 2 and 5 indicate a high ⁴⁰Ar/³⁶Ar ratio of 544±192 and an intercept age of 196.4±4.7 Ma (Figure 2-7-8b). The inclusion of steps 3 and 4 in the treatment of isotope correlation data results in unreasonably old ages. The preferred interpretation for the age of the sericite is thus approximately 196 Ma. As ages older than approximately 197 Ma are not geologically reasonable, the 2σ error limit allows for ages in the range of 197 to 190 Ma.

Sample A88-33 may have been affected by processes that could have disturbed the argon systematics: excess argon, recoil phenomena and mixed phases. Excess argon could have been introduced into the sericite during emplacement of dacitic porphyry dikes thought to postdate, but be closely related to formation of the Bonanza deposit. Two narrow (1-2 m) dikes occur within 10 metres of the sample location, and a larger dike (20-30 m thick) is projected to occur approximately 100 metres away. Argon, with a non-atmospheric ⁴⁰Ar/³⁶Ar signature, may have affected the sericite during the thermal disturbance associated with dike emplacement, and be responsible for the difficulties in inter-

TABLE 2-7-1 — Continued
⁴⁰Ar/³⁹Ar ANALYTICAL RESULTS AND APPARENT AGES OF MINERALS FROM TOODOGGONE VOLCANIC ROCKS
AND EPITHERMAL GOLD-SILVER DEPOSITS.

Temp. °C	⁴⁰ Ar/ ³⁹ Ar	³⁷ Ar/ ³⁹ Ar	³⁶ Ar/ ³⁹ Ar	³⁹ Ar 10 ⁻¹³ mol	³⁹ Ar % tot.	⁴⁰ Ar* %	K/Ca	Age ± 2σ Ma
LW-037 K-Feldspar (J=0.006145)								
840.....	18.88	0.0104	0.0072	829.4	9.1	88.6	47.06	176.5 ± 1.7
935.....	18.55	0.0069	0.0044	1183.0	13.0	92.8	70.64	181.4 ± 1.7
1015.....	18.51	0.0047	0.0028	750.1	8.2	95.3	104.57	185.7 ± 1.8
1090.....	18.36	0.0051	0.0017	655.2	7.2	97.1	95.64	187.5 ± 2.6
1160.....	18.27	0.0032	0.0009	646.1	7.1	98.5	155.29	189.2 ± 1.8
1220.....	18.23	0.0039	0.0009	770.9	8.4	98.4	125.03	188.6 ± 1.8
1280.....	18.38	0.0043	0.0016	739.7	8.1	97.3	113.22	188.0 ± 2.1
1335.....	18.61	0.0037	0.0027	1366.3	15.0	95.6	133.78	187.1 ± 1.8
1385.....	18.96	0.0035	0.0035	1021.8	11.2	94.4	141.87	188.2 ± 1.8
FUSE.....	19.09	0.0038	0.0039	1166.1	12.8	93.9	128.43	188.4 ± 1.8
Total.....				9128.6	100.0			186.0 ± 1.9
LW-011 K-Feldspar (J=0.006207)								
840.....	19.69	0.0011	0.0081	843.7	16.3	87.7	427.98	183.8 ± 2.1
935.....	19.53	0.0007	0.0070	751.4	14.5	89.3	705.65	185.4 ± 2.1
1015.....	19.26	0.0008	0.0047	464.1	9.0	92.7	627.59	189.5 ± 1.9
1090.....	19.23	0.0003	0.0042	356.2	6.9	93.4	1549.21	190.7 ± 1.9
1160.....	19.21	0.0008	0.0041	296.4	5.7	93.5	600.43	190.8 ± 1.9
1220.....	19.28	0.0010	0.0045	466.7	9.0	92.9	497.52	190.2 ± 1.8
1280.....	19.64	0.0007	0.0058	608.4	11.7	91.1	750.44	189.9 ± 1.9
1350.....	19.77	0.0008	0.0068	508.3	9.8	89.7	606.59	188.3 ± 1.8
1450.....	19.90	0.0008	0.0069	377.0	7.3	89.6	613.73	189.3 ± 1.8
FUSE.....	20.04	0.0011	0.0074	508.3	9.8	88.9	440.41	189.2 ± 1.8
Total.....				5180.5	100.0			88.1 ± 3.9
SH84-03 Adularia (J=0.00619)								
840.....	22.70	0.004	0.0196	582.4	5.9	74.4	128.32	179.3 ± 2.2
935.....	21.13	0.003	0.0130	759.2	7.7	81.6	170.57	183.0 ± 2.1
1015.....	19.62	0.003	0.0069	609.7	6.2	89.4	165.41	186.1 ± 1.9
1090.....	18.83	0.003	0.0036	595.4	6.1	94.1	166.97	187.8 ± 2.0
1160.....	18.86	0.003	0.0035	1034.8	10.6	94.3	174.93	188.4 ± 1.8
1220.....	18.99	0.003	0.0042	1249.3	12.7	93.3	177.77	187.8 ± 1.8
1280.....	19.09	0.003	0.0045	1353.3	13.8	92.9	162.00	187.9 ± 1.8
1335.....	19.17	0.003	0.0048	1290.9	13.2	92.5	152.81	187.9 ± 1.8
1385.....	19.26	0.003	0.0050	1223.3	12.5	92.1	166.72	188.0 ± 1.8
FUSE.....	19.47	0.003	0.0055	1102.4	11.2	91.6	151.26	188.9 ± 1.8
Total.....				9800.7	100.0			187.1 ± 1.9
A88-33 Sericite (J=0.006215)								
840.....	21.28	0.0071	0.0052	629.2	27.7	92.7	69.23	208.7 ± 2.0
935.....	20.71	0.0071	0.0038	765.7	33.8	94.5	68.62	207.0 ± 2.0
1015.....	20.30	0.0070	0.0023	439.4	19.4	96.5	69.96	207.3 ± 2.4
1090.....	20.14	0.0110	0.0023	249.6	11.0	96.5	44.66	205.7 ± 2.0
1160.....	20.09	0.0217	0.0030	102.7	4.5	95.5	22.55	203.3 ± 2.7
1220.....	20.77	0.0592	0.0069	46.8	2.1	90.1	8.27	198.6 ± 3.6
1280.....	24.99	0.1576	0.0242	19.5	0.9	71.4	3.11	189.7 ± 15.5
FUSE.....	51.87	0.7206	0.1140	15.6	0.7	35.1	0.68	193.6 ± 10.8
Total.....				2268.5	100.0			206.8 ± 2.3

preting steps 3 and 4. It is not possible to resolve these steps without an additional heating experiment using a larger number of steps. A less likely problem, but one worth considering, is the possibility of recoil effects during irradiation. For illite, Halliday (1978) has shown that ³⁹Ar can be readily lost from fine-grained (<5 μm) material during irradiation, which leads to anomalously high apparent ages. The illite in sample A88-33 is significantly coarser grained, averaging 20-200 micrometres, but some of the grains at the lower end of this range could have been affected by recoil to some degree. However, the illite in sample A88-33 is domi-

nantly of the 1m polytype, and may be less affected by recoil than more disordered illite. For example, Hunziker *et al.* (1986) found that 2m₁ illites were more resistant to recoil than 1Md illite, even in similar size fractions. Therefore, recoil effects were probably not sufficient to control the distribution of argon in this sample. A final possible problem with sample A88-33 is the purity of the mineral separate. Although every effort was made to attain a high degree of purity, the drop in calculated potassium/calcium ratios in the last few heating steps suggests degassing of a small amount of a low-potassium mineral phase. The only

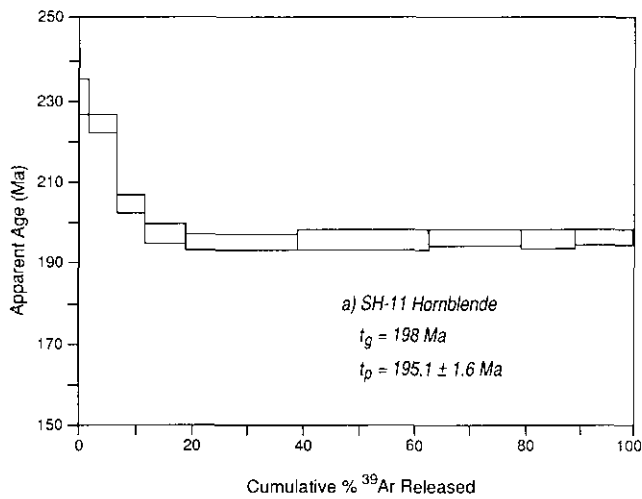


Figure 2-7-2a. Age spectrum for hornblende SH-11, from the upper strata of the Toodoggone Stage I volcanics, calculated assuming an atmospheric composition ($^{40}\text{Ar}/^{36}\text{Ar}=295.5$) for trapped argon. T_g is the total gas age, and T_p is the plateau age.

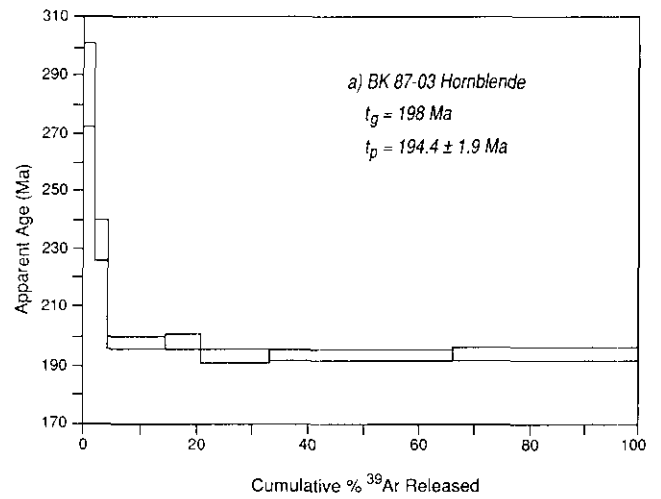


Figure 2-7-3a. Age spectrum for hornblende BK87-03, from the lower strata of the Toodoggone Stage II volcanics, calculated assuming an atmospheric argon composition.

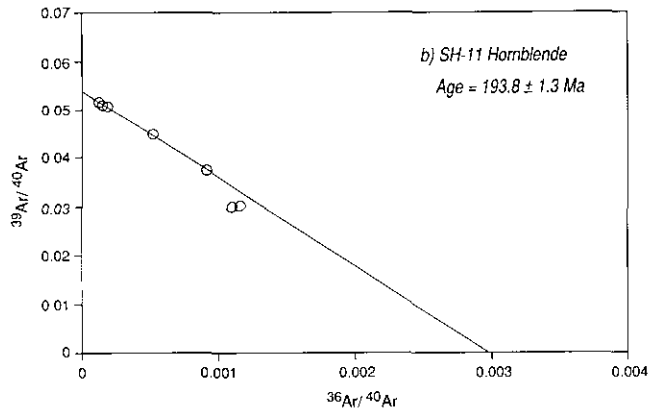


Figure 2-7-2b. Isochron diagram for step-heating data from hornblende SH-11. The $^{40}\text{Ar}/^{36}\text{Ar}_i=3379$, and the intercept age is 193.8 ± 1.3 Ma (MSWD=2.8).

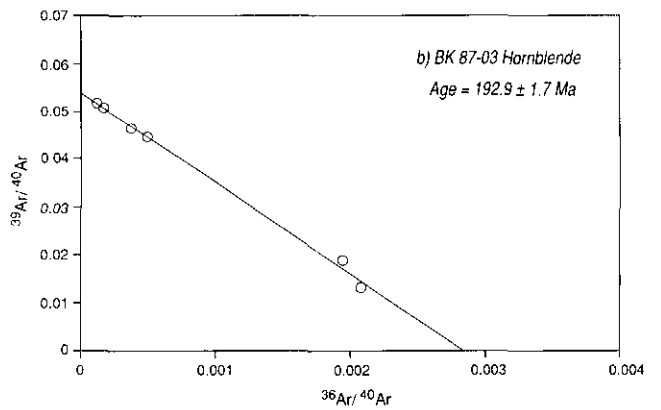


Figure 2-7-3b. Isochron diagram for step-heating data from hornblende BK87-03. The $^{40}\text{Ar}/^{36}\text{Ar}_i=349 \pm 27$, and the intercept age is 192.9 ± 1.7 Ma (MSWD=3.3).

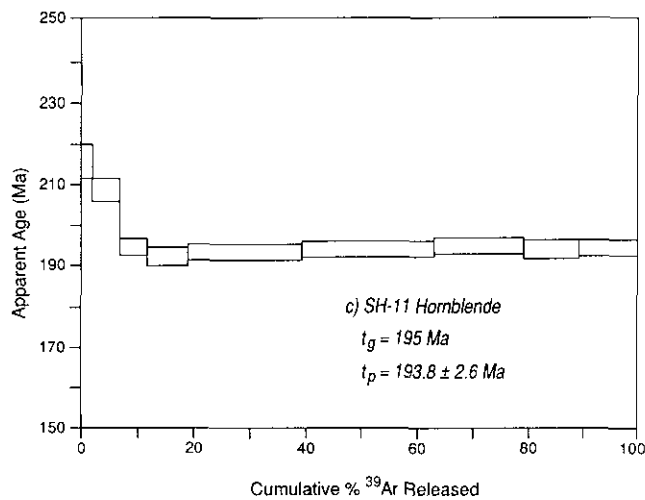


Figure 2-7-2c. Age spectrum for hornblende SH-11 calculated using the trapped $^{40}\text{Ar}/^{36}\text{Ar}$ ratio indicated by the isotope correlation data treatment.

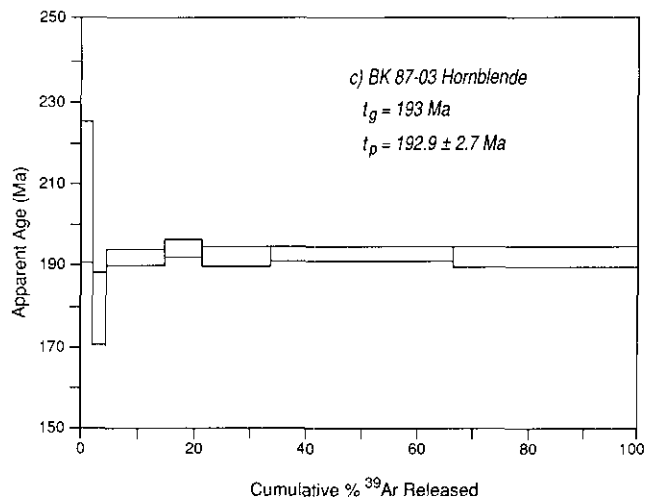


Figure 2-7-3c. Age spectrum for hornblende BK87-03 calculated using the trapped $^{40}\text{Ar}/^{36}\text{Ar}$ ratio indicated by the isotope correlation data treatment.

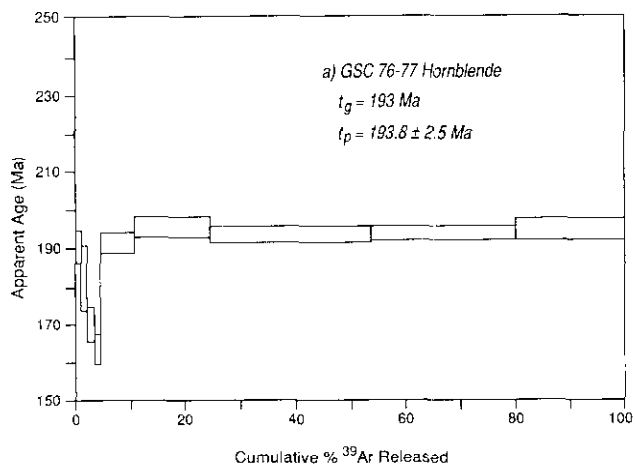


Figure 2-7-4a. Age spectrum for hornblende GSC 76-77, from the Toodogone Stage II volcanics, calculated assuming an atmospheric composition for trapped argon.

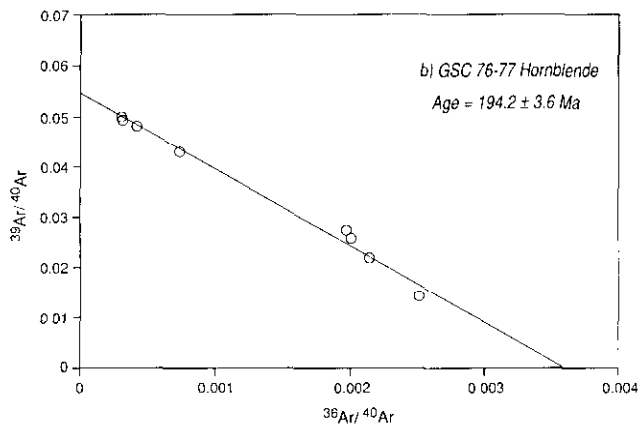


Figure 2-7-4b. Isochron diagram for step-heating data from hornblende GSC 76-77. The $^{40}\text{Ar}/^{36}\text{Ar}_i = 278 \pm 12$, and the intercept age is 194.2 ± 3.6 Ma (MSWD=2.6).

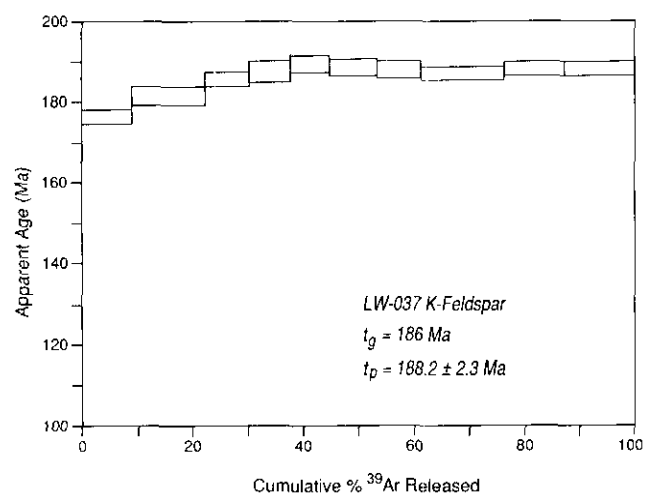


Figure 2-7-5. Age spectrum for potassium feldspar LW-037 from the AGB deposit at the Lawyers mine, calculated using an atmospheric composition for trapped argon.

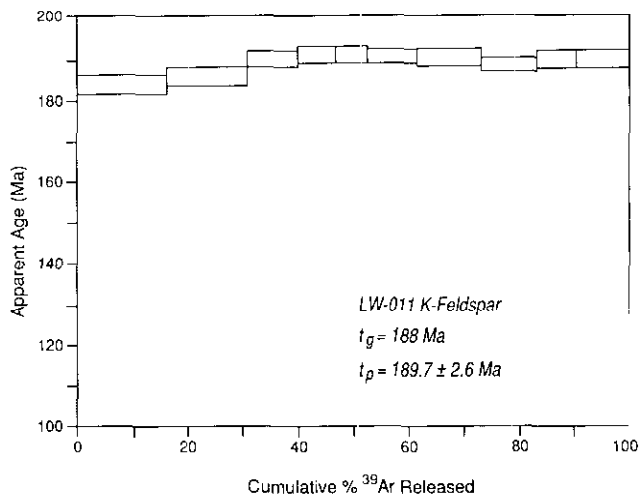


Figure 2-7-6. Age spectrum for potassium feldspar LW-011 from the Cliff Creek deposit at the Lawyers mine, calculated using an atmospheric composition for trapped argon.

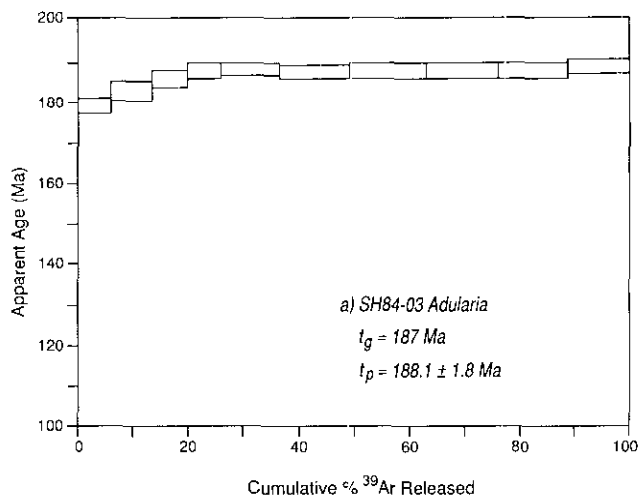


Figure 2-7-7a. Age spectrum for adularia SH84-03, from the Shasta mine, calculated assuming an atmospheric composition for trapped argon.

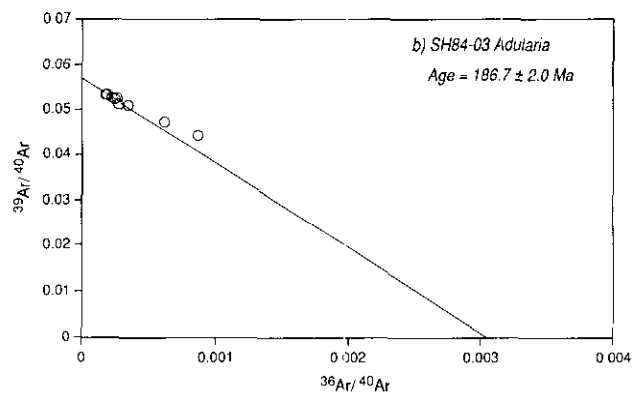


Figure 2-7-7b. Isochron diagram for step-heating data from adularia SH84-03. The $^{40}\text{Ar}/^{36}\text{Ar}_i = 326 \pm 49$, and the intercept age is 186.7 ± 2.0 Ma (MSWD=2.8).

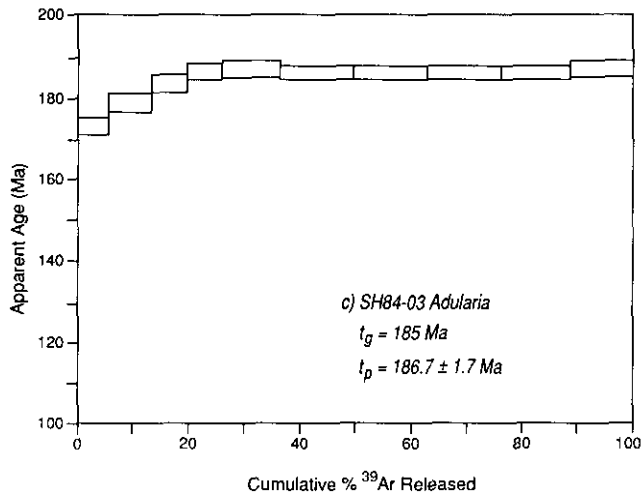


Figure 2-7-7c. Age spectrum for adularia SH84-03 calculated using the trapped $^{40}\text{Ar}/^{36}\text{Ar}$ ratio indicated by the isotope correlation data treatment.

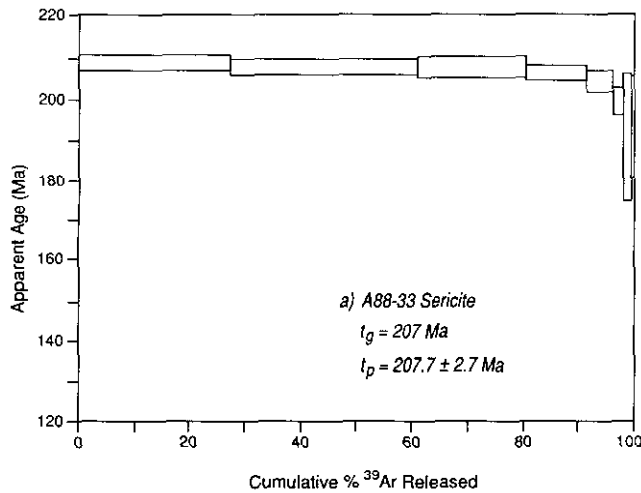


Figure 2-7-8a. Age spectrum for sericite A88-33, from the Bonanza deposit, calculated assuming an atmospheric composition for trapped argon. The total gas and plateau ages are too old to be geologically reasonable.

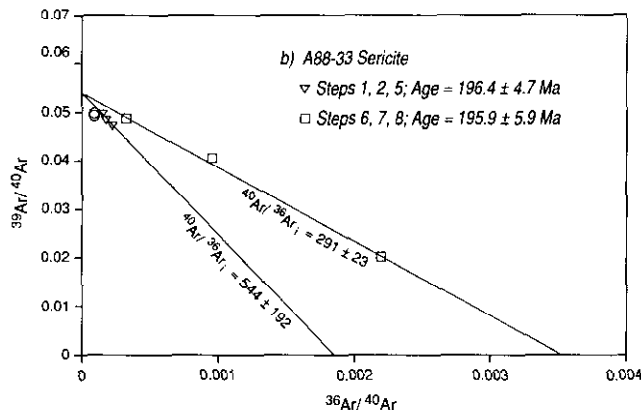


Figure 2-7-8b. Isochron diagram for step-heating data from sericite A88-33. Two linear arrays are defined by the data which yield an age of 196 Ma, but appear to have different trapped $^{40}\text{Ar}/^{36}\text{Ar}$ ratios of 543 ± 192 (MSWD=6) and 291 ± 23 (MSWD=6). Steps 3 and 4 (circles) cannot be resolved without additional information.

possible contaminants are quartz and dickite. Both these minerals formed contemporaneously with the sericite; trace amounts of potassium from inclusions, and recoil-induced ^{39}Ar may have been released from these minerals during the higher temperature heating steps.

The concordance of isochrons using both low and high-temperature gas fractions (Figure 2-7-8b) suggests that, despite the complications discussed above, the $^{40}\text{Ar}/^{39}\text{Ar}$ data provide a reasonable estimate of the age of alteration in the Bonanza deposit.

DISCUSSION

The results of this $^{40}\text{Ar}/^{39}\text{Ar}$ study have important implications for the age of both the Toodoggone volcanics and related epithermal gold-silver deposits.

In general, the Toodoggone volcanics are older than was suggested by previous K-Ar data, and are much more restricted in their range of ages. The basal Toodoggone units have been fixed at ~ 197.6 Ma by the $^{40}\text{Ar}/^{39}\text{Ar}$ analysis of Shepard (1986), and the youngest age determined in our study for rocks near the top of the volcanics ("grey dacite" unit) is ~ 192.9 Ma. Although a small volume of younger volcanics overlying the "grey dacite" unit has been mapped by Marsden and Moore (1990), and erosion has not been taken into account, most of the Toodoggone volcanics appear to have formed during the earliest Pleinsbachian through the earliest Toarcian (*i.e.* entirely Early Jurassic; boundary estimates from Kent and Gradstein, 1985). Within this range it is possible to divide the volcanics into two stages on the basis of geological observations, but the stages cannot be distinguished from the geochronological data alone. Stage I rocks exhibit widespread, low-grade alteration, contain numerous gold-silver showings and range in age between 198 and 194 Ma. Stage II volcanics are less altered than Stage I, are not known to host significant mineralization, and have an age range in of 194 to 193 Ma. The 2σ errors in the $^{40}\text{Ar}/^{39}\text{Ar}$ ages are large enough to allow a hiatus of up to several million years between stages, but the stages are of essentially the same statistical age. For these reasons, we prefer to retain the division of the Toodoggone volcanics into two stages until such time as data clearly to the contrary become available.

The timing of the gold-silver mineralizing event in the district is significantly older than was suggested by previous K-Ar data. Deposits related to adularia-sericite alteration (*e.g.* Lawyers AGB and Cliff Creek, Shasta) formed between 187 and 190 million years ago, that is up to several million years following cessation of the main part of Toodoggone volcanism. In contrast, deposits associated with acid-sulphate alteration may have formed earlier in the Toodoggone volcanic history. The Bonanza deposit has an age of ~ 196 Ma and thus formed synchronously with Toodoggone Stage I volcanism. Although alunite $^{40}\text{Ar}/^{39}\text{Ar}$ ages were not determined in this study, the previous K-Ar ages for alunite of 190 ± 7 Ma (Alberts Hump; Schroeter, 1982) and 193 ± 7 Ma (Jan; Clark and Williams-Jones, 1989) are much older than K-Ar adularia and sericite dates. These alunitic alteration zones may also have formed during Stage I volcanism. A similar relationship, with adularia-

sericite-related deposits forming up to several million years after the hostrocks, and acid-sulphate-type deposits forming almost contemporaneously with volcanism, has been documented for a number of other epithermal districts (*cf.* Heald *et al.*, 1987).

In spite of the paucity of alteration and mineralization in the Toodoggone Stage II volcanics, it appears that these rocks do constitute prospective units for exploration for Lawyers-type gold-silver deposits. Our revised metallogenic model suggests that all Toodoggone volcanics, underlying units, and coeval intrusions could contain epithermal mineralization. Regional-scale, low-grade alteration and acid-sulphate style gold mineralization appear to be restricted to the older, Stage I volcanics and possibly underlying units. However, all epithermal gold-silver mineralization in the district appears to have been related to Pleinsbachian to earliest Toarcian volcanic events, and mid-Pleinsbachian to mid-late Toarcian hydrothermal activity.

ACKNOWLEDGMENTS

Most of the $^{40}\text{Ar}/^{39}\text{Ar}$ analyses were conducted with funding through grant number RG89-17 from the British Columbia Geoscience Research Grant Program. Additional support was provided by the Natural Sciences and Engineering Research Council and Energy, Mines and Resources Canada (AEWJ), and the Ixion Research Group (JRC). Daniel R. Lux directed the $^{40}\text{Ar}/^{39}\text{Ar}$ analytical work at the University of Maine at Orono, and provided invaluable assistance with data interpretation. We are also grateful to Hugh Gabrielse for donating mineral separate GSC 76-77, and to Peter Thiersch and Henry Marsden for providing samples SH84-03 and SH-11, respectively. The study would not have been possible without the cooperation of Cheni Gold Mines Inc., Homestake Mining Canada Ltd., and Energex Minerals Ltd.

REFERENCES

- Alexander, E.C., Mickelson, G.M. and Lanphere, M.A. (1978): MMhb-1: A New $^{40}\text{Ar}/^{39}\text{Ar}$ Dating Standard; in Short Papers of the Fourth International Conference on Geochronology, Cosmochronology and Isotope Geology, *United States Geological Survey*, Open File Report 78-701, pages 6-8.
- Barr, D.A. (1978): Chappelle Gold-Silver Deposit, British Columbia; *Canadian Institute of Mining and Metallurgy*, Bulletin, Volume 72, Number 790, pages 66-79.
- Carter, N.C. (1972): Toodoggone River Area; *B.C. Ministry of Energy, Mines and Petroleum Resources*, Geology, Exploration and Mining in British Columbia 1971, pages 63-71.
- Clark, J.R. and Williams-Jones, A.E. (1986): Geology and Genesis of Epithermal Gold-Barite Mineralization, Verrenass Deposit, Toodoggone District, British Columbia; *Geological Association of Canada*, Program with Abstracts, Volume 11, page 57.
- Clark, J.R. and Williams-Jones, A.E. (1987): Metallogenic Implications of Lithotectonic Assemblages in the Toodoggone Au-Ag District, North-central B.C.; *Geological Association of Canada*, Program with Abstracts, Volume 12, page 32.
- Clark, J.R. and Williams-Jones, A.E. (1988): A Preliminary Appraisal of the Au-Ag Metallogeny of the Toodoggone District, North-central British Columbia; in Geology and Metallogeny of Northwestern British Columbia Workshop, *Smithers Exploration Group – Geological Association of Canada*, Program with Abstracts, pages A33-A37.
- Clark, J.R. and Williams-Jones, A.E. (1989): New K-Ar Isotopic Ages of Epithermal Alteration in the Toodoggone River Area, British Columbia (94E); *B.C. Ministry of Energy, Mines and Petroleum Resources*, Geological Fieldwork 1988, Paper 1989-1, pages 409-412.
- Dalrymple, G.B., Alexander, E.C., Lanphere, M.A. and Kraker, G.P. (1981): Irradiation of Samples for $^{40}\text{Ar}/^{39}\text{Ar}$ Dating Using the Geological Survey TRIGA Reactor; *United States Geological Survey*, Professional Paper 1176, 55 pages.
- Dalrymple, G.B. and Lanphere, M.A. (1969): Potassium-Argon Dating; *W.H. Freeman*, San Francisco, 258 pages.
- Diakow, L.J. (1984): Geology between Toodoggone and Chukachida Rivers (94E); *B.C. Ministry of Energy, Mines and Petroleum Resources*, Geological Fieldwork 1983, Paper 1984-1, pages 139-145.
- Diakow, L.J. (1985): Potassium-Argon Age Determinations from Biotite and Hornblende in Toodoggone Volcanic Rocks (94E); *B.C. Ministry of Energy, Mines and Petroleum Resources*, Geological Fieldwork 1984, Paper 1985-1, pages 298-301.
- Diakow, L.J., Panteleyev, A. and Schroeter, T.G. (1985): Geology of the Toodoggone River Area (94E); *B.C. Ministry of Energy, Mines and Petroleum Resources*, Preliminary Map 61.
- Fleck, R.J., Sutter, J.F. and Elliot, D.H. (1977): Interpretation of Discordant $^{40}\text{Ar}/^{39}\text{Ar}$ Age Spectra of Mesozoic Tholeiites from Antarctica; *Geochimica et Cosmochimica Acta*, Volume 41, pages 15-32.
- Forster, D.B. (1984): Geology, Petrology and Precious Metal Mineralization, Toodoggone River Area, North-central British Columbia; unpublished Ph.D. thesis, *The University of British Columbia*, 223 pages.
- Gabrielse, H., Wanless, R.K., Armstrong, R.L. and Erdman, L.R. (1980): Isotopic Dating of Early Jurassic Volcanism and Plutonism in North-central British Columbia; in Current Research, Part A, *Geological Survey of Canada*, Paper 80-1A, pages 27-32.
- Halliday, A.N. (1978): $^{40}\text{Ar}/^{39}\text{Ar}$ Stepheating Studies of Clay Concentrates from Irish Orebodies; *Geochimica et Cosmochimica Acta*, Volume 42, pages 1851-1858.
- Heald, P., Foley, N.K. and Hayba, D.O. (1987): Comparative Anatomy of Volcanic-hosted Epithermal Deposits: Acid-Sulfate and Adularia-Sericite Types; *Economic Geology*, Volume 82, pages 1-26.

- Heizler, M.T. and Harrison, T.M. (1988): Multiple Trapped Argon Isotope Components Revealed by $^{40}\text{Ar}/^{39}\text{Ar}$ Isochron Analysis; *Geochimica et Cosmochimica Acta*, Volume 52, pages 1295-1303.
- Hunziker, J.C., Frey, M., Clauer, N., Dallmeyer, R.D., Friedrichsen, H., Flehmig, W., Hochstrasser, K., Roggwiler, P. and Schwander, H. (1986): The Evolution of Illite to Muscovite: Mineralogical and Isotopic Data from the Glarus Alps, Switzerland; *Contributions to Mineralogy and Petrology*, Volume 92, pages 157-180.
- Kent, D.V. and Gradstein, F.M., (1985): A Cretaceous and Jurassic Geochronology; *Geological Society of America Bulletin*, Volume 96, pages 1419-1427.
- Marsden, H. and Moore, J.M. (1989): Stratigraphic and Structural Setting of the Shasta Ag-Au Deposit, North-central British Columbia (94E); *B.C. Ministry of Energy, Mines and Petroleum Resources*, Geological Fieldwork 1988, Paper 1989-1, pages 395-407.
- Marsden, H. and Moore, J.M. (1990): Stratigraphic and Structural Setting of the Shasta Ag-Au Deposit (94E); *B.C. Ministry of Energy, Mines and Petroleum Resources*, Geological Fieldwork 1989, Paper 1990-1, pages 305-314.
- Panteleyev, A. (1982): Toodoggone Volcanics South of Finlay River (94E/2); *B.C. Ministry of Energy, Mines and Petroleum Resources*, Geological Fieldwork 1981, Paper 1982-1, pages 135-141.
- Panteleyev, A. (1983): Geology Between Toodoggone and Sturdee Rivers; *B.C. Ministry of Energy, Mines and Petroleum Resources*, Geological Fieldwork 1982, Paper 1983-1, pages 143-148.
- Schroeter, T.G. (1981): Toodoggone River Area (94E); *B.C. Ministry of Energy, Mines and Petroleum Resources*, Geological Fieldwork 1980, Paper 1981-1, pages 124-131.
- Schroeter, T.G. (1982): Toodoggone River Area (94E); *B.C. Ministry of Energy, Mines and Petroleum Resources*, Geological Fieldwork 1981, Paper 1982-1, pages 122-133.
- Schroeter, T.G., Diakow, L.J. and Panteleyev, A. (1986): Toodoggone River Area (94E); *B.C. Ministry of Energy, Mines and Petroleum Resources*, Geological Fieldwork 1985, Paper 1986-1, pages 167-174.
- Shepard, J.B. (1986): The Triassic-Jurassic Boundary and the Manicouagan Impact: Implications of $^{40}\text{Ar}/^{39}\text{Ar}$ Dates on Periodic Extinction Models; unpublished B.Sc. thesis, *Princeton University*, 38 pages.
- Steiger, R.H. and Jäger, E. (1977): Subcommittee on Geochronology; Convention on the Use of Decay Constants in Geo- and Cosmochronology, *Earth and Planetary Science Letters*, Volume 36, pages 359-362.
- Thiersch, P. and Williams-Jones, A.E. (1990): Paragenesis and Ore Controls of the Shasta Ag-Au Deposit, Toodoggone River Area, British Columbia (94E); *B.C. Ministry of Energy, Mines and Petroleum Resources*, Geological Fieldwork 1989, Paper 1990-1, pages 315-321.
- Vulimiri, M.R., Tegart, P. and Stammers, M.A. (1987): Lawyers Gold-Silver Deposits, British Columbia: in Mineral Deposits of the Northern Cordillera, A. Morin, Editor, *Canadian Institute of Mining and Metallurgy*, Special Volume 37, pages 191-201.



GEOLOGY AND NOBLE-METAL GEOCHEMISTRY OF THE LUNAR CREEK ALASKAN-TYPE COMPLEX, NORTH-CENTRAL BRITISH COLUMBIA* (94E/13, 14)

By J.L. Hammack and G.T. Nixon;
W.P.E. Paterson and C. Nuttall, Consultants

KEYWORDS: Economic geology, Alaskan-type complex, Lunar Creek, mafic-ultramafic complex, structure, geochemistry, platinum group elements.

INTRODUCTION

Alaskan-type complexes in British Columbia are potentially important hosts for economic concentrations of platinum-group elements (PGEs; Rublee, 1986; Evenchick *et al.*, 1986) as well as other commodities such as chrome, nickel, cobalt, gold, jade and asbestos. To date, only the platinum-rich placers of the Tulameen complex have been exploited economically, yielding some 680 000 grams of impure platinum nuggets between the years 1885 and 1932 (O'Neil and Gunning, 1934). The source of the placer nuggets has been traced to chromitite horizons within the dunite core of the Tulameen complex (Nixon *et al.*, 1990a), and the chromitite-PGE association appears to be one of the most favourable exploration targets for lode occurrences of PGEs in British Columbia (Nixon and Hammack, 1990).

The Lunar Creek complex is part of the "Polaris suite" of Alaskan-type intrusions, a series of mafic-ultramafic complexes concentrated in northern British Columbia along an arcuate zone around the northern and eastern margin of the Bowser basin (Figure 2-8-1). All lie within the allochthonous Quesnel and Stikine terranes which were amalgamated prior to accretion with the North American craton in the Mesozoic (Wheeler and McFeeley, 1987) and form part of the Intermontane Superterrane. These intrusions are typically spatially associated, and believed to be coeval, with augite-phyric volcanic rocks of the Upper Triassic Takla and Stuhini groups (Irvine, 1976). The size of individual intrusive bodies ranges from less than 1 square kilometre to 60 square kilometres, and outcrop patterns vary from round or elliptical to markedly elongate. Elongate intrusions have a northwesterly orientation, parallel to the tectonic grain of the region. These intrusions generally exhibit a crude concentric zonation such that ultramafic lithologies in the centre grade outward into gabbroic lithologies at the margins. In all, nine Alaskan-type intrusions have been examined over the course of this project: the Polaris (Nixon *et al.*, 1990d, e), Wrede (Hammack *et al.*, 1990a, b), Johanson (Nixon *et al.*, 1990b), Turnagain (Nixon *et al.*, 1989a), Menard, Gnat Lakes, Hickman (Nixon *et al.*, 1989b) in northern British Columbia, and the Tulameen complex (Nixon and Rublee, 1988; Nixon, 1988; Nixon *et al.*, 1989c, 1990a) in south-central British Colum-

bia. Although similar in many respects, each has its own unique characteristics.

Ultramafic lithologies characteristic of Alaskan-type intrusions lie along the join between olivine and clinopyroxene in Figure 2-8-2. This diagram essentially illustrates the IUGS classification scheme (LeMaitre, 1989) with modifications to include the olivine wehrlite field (65 to 90 per cent olivine and 10 to 35 per cent clinopyroxene) that was found to be useful for mapping purposes.

Fieldwork at Lunar Creek was conducted during the summer of 1989, and this report summarizes the geology of the previously published Open File map (Nixon *et al.*, 1990c). The project area is covered at a scale of 1:250 000 by the Finlay River map sheet (94E) and 1:50 000 topography maps (94E/13 and 14). Aeromagnetic maps are not currently available.

LOCATION AND ACCESS

The Lunar Creek ultramafic complex (57°55'N, 127°28'W) lies within the Stikine Ranges of the Omineca Mountains, approximately 1 kilometre northwest of the headwaters of Lunar Creek (Figure 2-8-3). Lunar Creek drains southward into the Chuckachida River, a tributary of the Stikine River. Access to the complex was by helicopter from Sturdee airstrip in the Toodoggone River area, which is serviced by scheduled flights from Smithers, or by vehicle along a well-maintained dirt road stretching from Fort St. James to the Cheni mine. Access to the northern part of the road is restricted and requires permission from mine management. The complex lies completely above treeline and is best exposed along ridge crests and high on valley walls. Glacial till and talus aprons cover lower valley walls and floors.

GEOLOGIC SETTING AND GEOCHRONOMETRY

The Lunar Creek ultramafic complex was first recognized in 1973 during regional geologic mapping by the Geological Survey of Canada (Gabrielse and Dodds, 1974). Later, more detailed mapping was completed by Irvine (1976) as part of a study of Alaskan-type ultramafic bodies in the Finlay River map area (Irvine, 1974a, 1976).

The complex lies within Quesnellia, at the boundary between the Stikine and the Quesnel tectonostratigraphic terranes. In the study area, this boundary is defined by the Kutcho fault which marks the western margin of the ultramafite (Figure 2-8-4). Zircon from diorite within the Lunar

* This project is a contribution to the Canada/British Columbia Mineral Development Agreement.

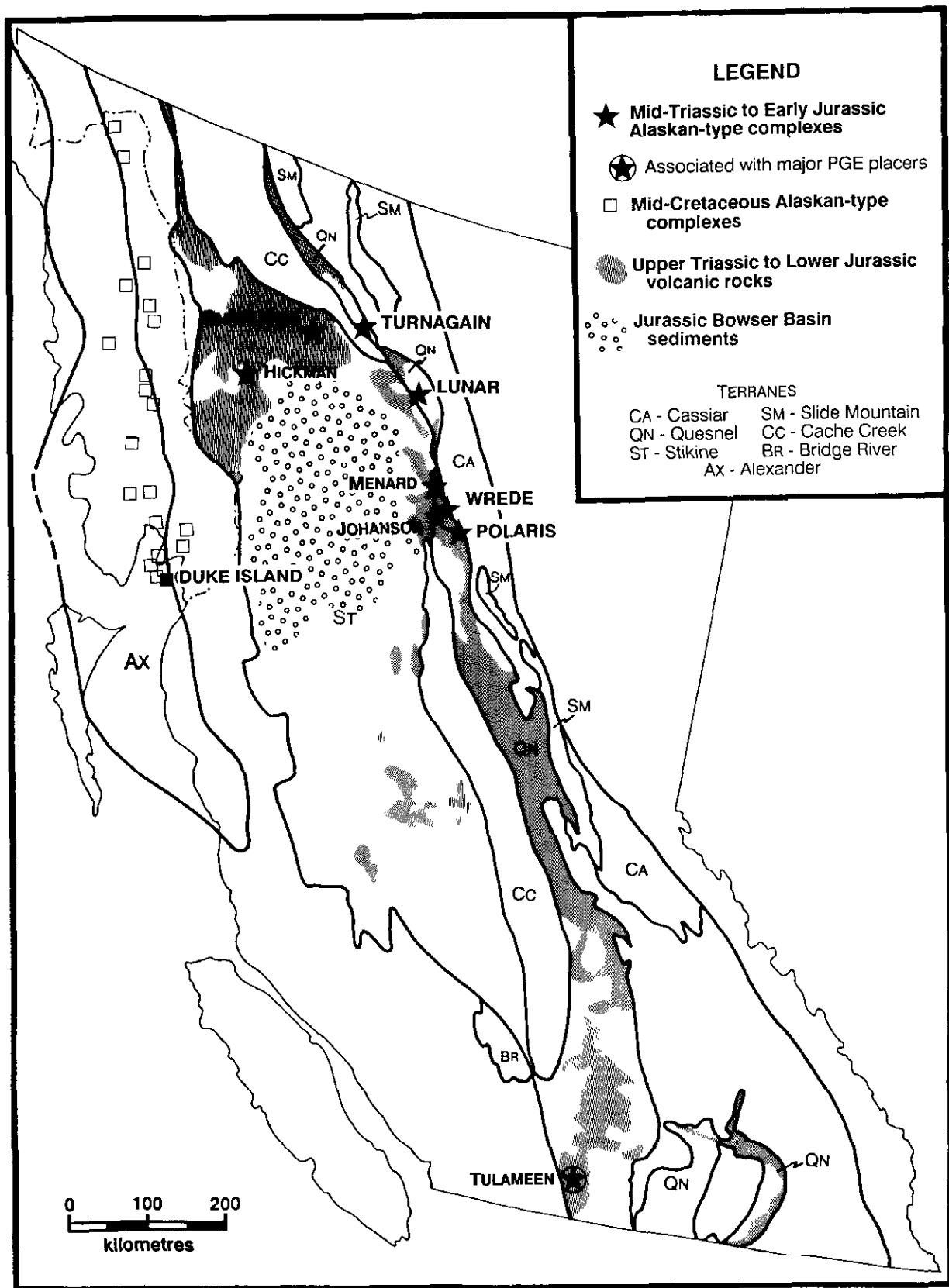


Figure 2-8-1. Distribution of major Alaskan-type ultramafic-mafic complexes in British Columbia and southeastern Alaska and coeval volcanic rocks in relation to tectonostratigraphic terranes of the Cordillera.

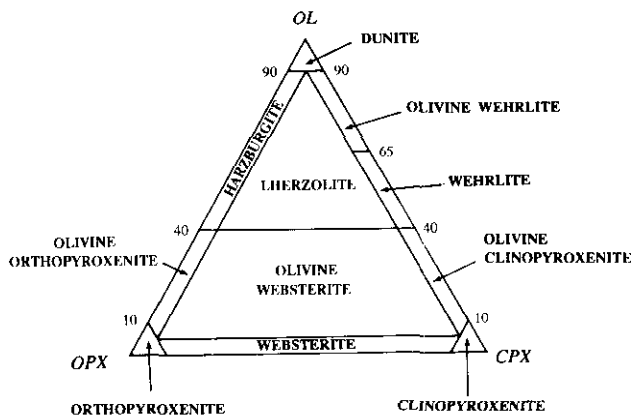


Figure 2-8-2. Classification of ultramafic rocks (modified after Le Maitre, 1989). Lithologies encountered in Alaskan-type complexes in British Columbia lie along the olivine-clinopyroxene join; other common rock types include hornblende clinopyroxenite (<50 per cent hornblende), clinopyroxene hornblende (>50 per cent hornblende) and hornblende.

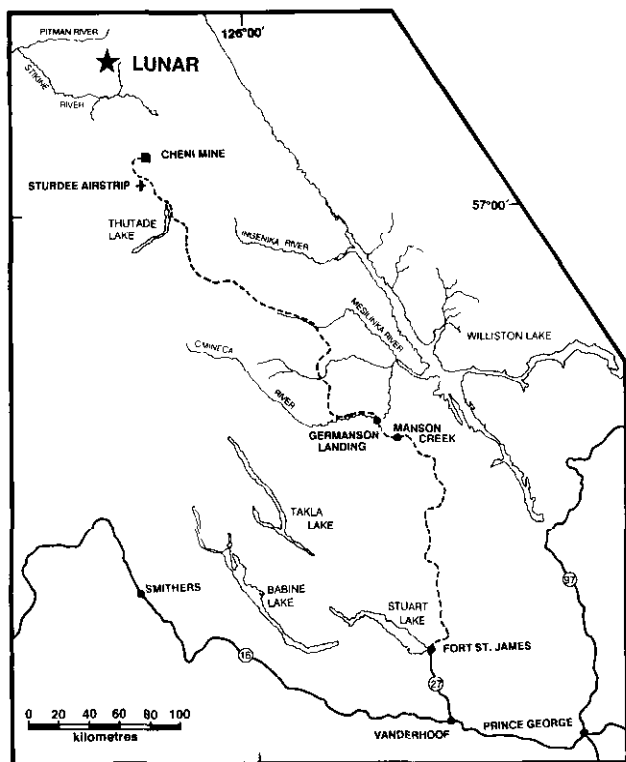


Figure 2-8-3. Location of the Lunar Creek mafic-ultramafic complex.

Creek complex has yielded a U-Pb age of Middle Triassic (237 ± 2 Ma; L. Heaman, personal communication, 1990). Along its eastern margin, the ultramafite lies in contact with, and may intrude, foliated augite-phyric volcanic rocks which, on the basis of lithology, are assigned to the Upper Triassic Takla Group. Granitoids of the Early Jurassic Pit-

man batholith, part of the Guichon suite of intrusions (Woodsworth *et al.*, in press), intrude these volcanic rocks as well as ultramafic rocks of the complex. Potassium-argon ages, determined on hornblende from this batholith, are 182 ± 13 (2σ) Ma (Gabrielse *et al.*, 1980) and 190 ± 8 Ma (Wanless *et al.*, 1979; Gabrielse *et al.*, 1980).

The Kutcho fault separates the southwest margin of the ultramafic complex, which lies in Quesnellia, from Paleozoic and younger rocks within Stikinia. Paleozoic rocks in the area are believed to range in age from Devonian to Permian (Thorstad, 1980; H. Gabrielse, personal communication, 1990). Rocks of the Upper Triassic Stuhini Group are also represented west and south of the study area. These arc-derived volcanic and clastic rocks have been intruded by granitoids of the Late Triassic to Early Jurassic Stikine batholith [222 ± 10 (2σ) Ma, K-Ar date on hornblende: Dodds in Wanless *et al.*, 1979; Anderson, 1984] as well as granitoids of the previously mentioned Early Jurassic Guichon suite. Biotite from granite of the Mount Albert Dease pluton, which is part of the Three Sisters suite of intrusions found south of the ultramafic complex, has yielded a K-Ar age of 167 ± 6 (2σ) Ma (Dodds in Wanless *et al.*, 1979; Woodsworth *et al.*, in press). The Three Sisters suite is spatially and temporally associated with volcanic and clastic rocks of the Lower to Middle Jurassic Hazelton Group.

STRATIFIED ROCKS

Stratified rocks within the study area include both meta-volcanic and metasedimentary rocks of the Takla Group, which crop out north and east of the complex and lie within Quesnellia, and an unnamed package of metavolcanic and metasedimentary rocks of Paleozoic age, which lies southwest of the Kutcho fault, within Stikinia.

TAKLA GROUP

Rocks tentatively assigned to the Upper Triassic Takla Group crop out north and east of the complex (Figures 2-8-4 and 2-8-5). To the north, augite-plagioclase porphyry, volcanic wackes and siltstones have been metamorphosed to lower amphibolite grade. To the east, the country rock is strongly sheared and metamorphosed, and varies from a medium-grained biotite schist to well-foliated amphibolite.

The contact between rocks of the Takla Group and the Lunar Creek complex is a ductile fault zone. Along it, both lithologies have been mylonitized. Mylonitized meta-volcanic rocks of the Takla Group (near Localities 3 and 4; Figure 2-8-6) are medium to dark grey to green-grey augite, augite-plagioclase and plagioclase-porphyrific actinolite schists. Augite augen, up to 0.7 centimetre in diameter, have been partially to completely altered to pale green actinolite. Actinolite, seen in thin section, is the most common constituent of the matrix, forming laths parallel to the foliation. The remainder of the matrix consists of albite, epidote and clay minerals. Northeast of Locality 2, away from the mylonitic zone, the most common lithology is dark grey augite porphyry that is metamorphosed to lower amphibolite grade.

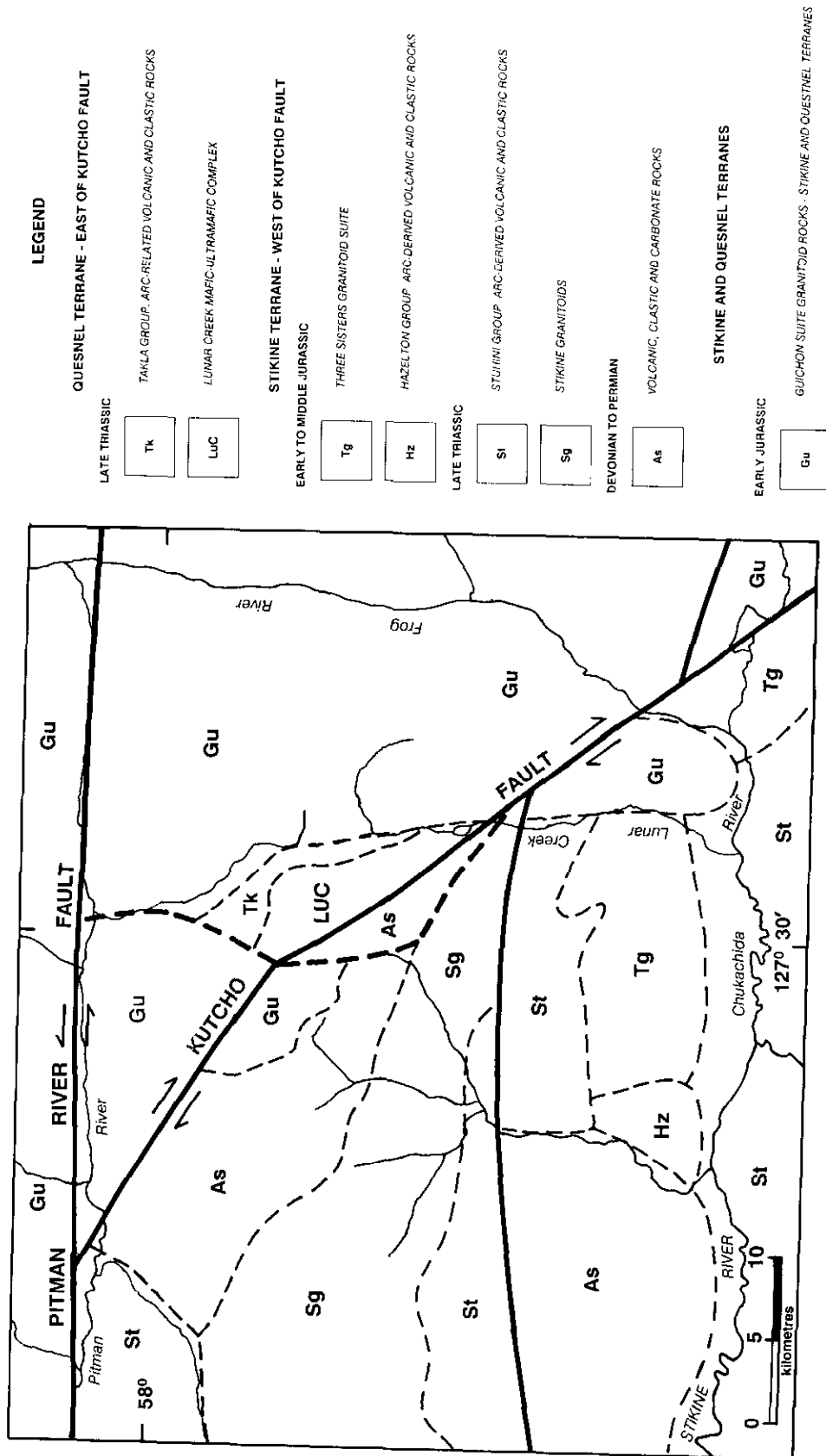


Figure 2-8-4. Regional geological setting of the Lunar Creek mafic-ultramafic complex (LuC).

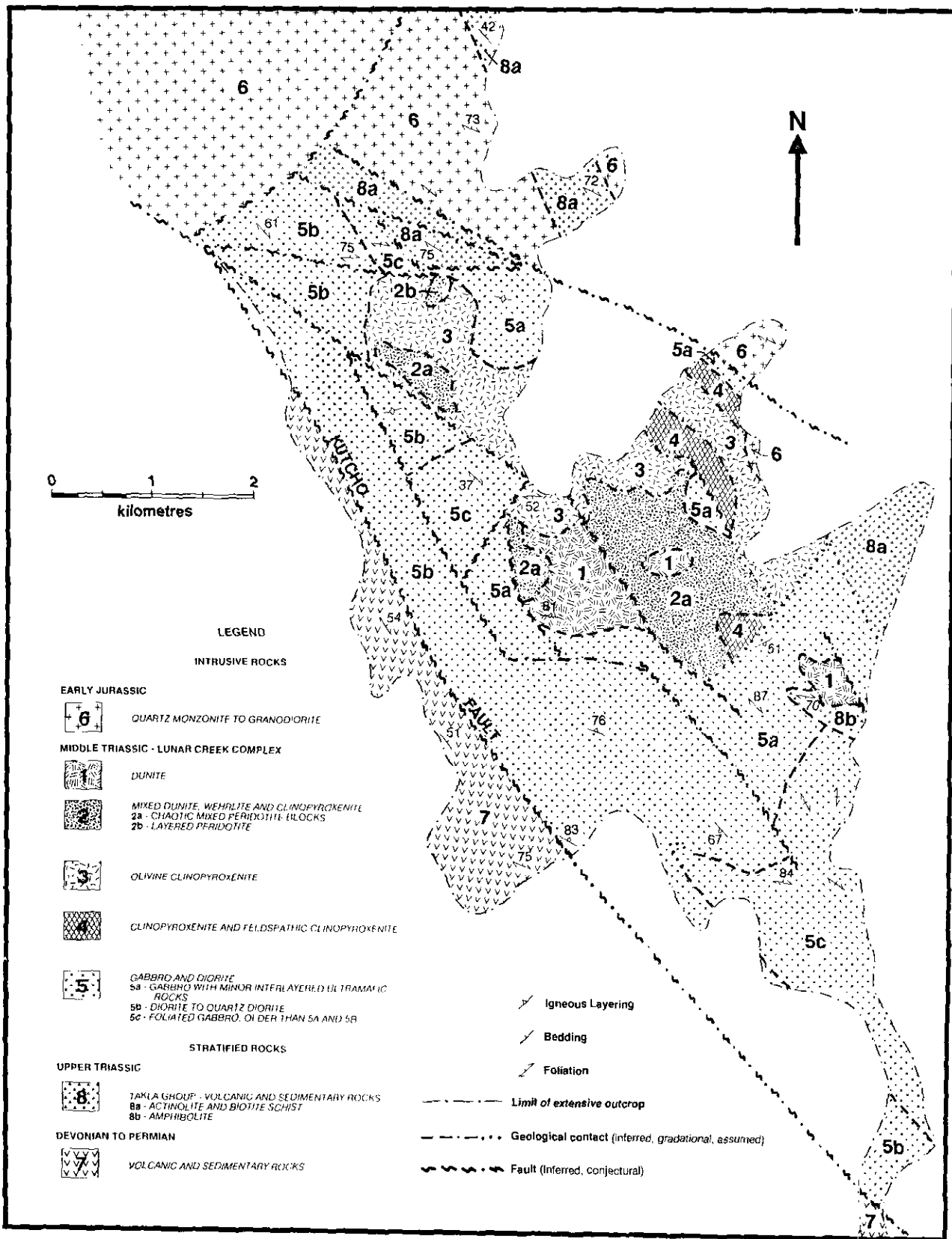


Figure 2-8-5. Generalized geology of the Lunar Creek mafic-ultramafic complex (modified after Nixon *et al.*, 1990).

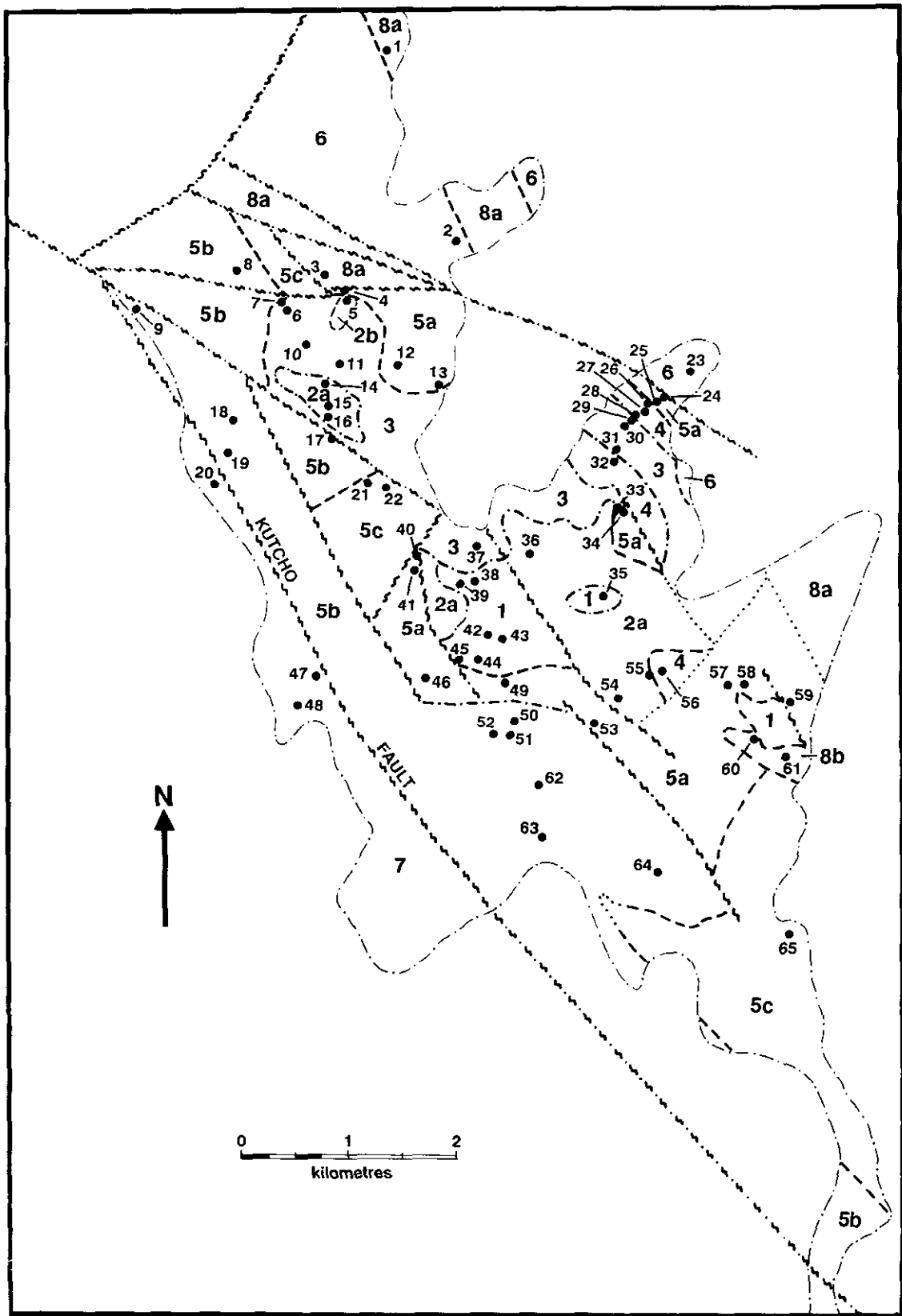


Figure 2-8-6. Location of lithogeochemical sample sites, numbered sequentially from north to south (*cf.* Table 2-8-1). Units and symbols as in Figure 2-8-5.

Medium grey weathering, medium to dark grey siltstones and fine-grained volcanic wackes at Locality 1 have been metamorphosed to lower amphibolite grade. These rocks are well bedded, dip moderately toward the northeast and have a weak bedding-parallel foliation. Common constituent minerals are plagioclase, potassium feldspar, green pleochroic hornblende and abundant idioblastic biotite that is oriented within the foliation.

UNNAMED PALEOZOIC ROCKS OF STIKINIA

Paleozoic rocks west of the Kutcho fault have not been assigned to a defined stratigraphic unit. Conodont analysis has shown that some of them are Mississippian in age (Thorstad, 1980), and may range from Devonian through Permian (H. Gabrielse, personal communication, 1990). Regionally, lithologies include chlorite schist, sericite schist, phyllite, rhyolite flows and tuffs, chert, sandstone and carbonate (Thorstad, 1980). In the study area, these Paleozoic rocks crop out adjacent to the southwestern margin of the ultramafic complex, west of the Kutcho fault. They have been metamorphosed to upper greenschist grade and include medium grey-green to dark grey quartz-potassium feldspar-actinolite schist, medium green-grey siliceous siltstone and medium grey, gritty micritic limestone with thin chert beds.

LUNAR CREEK MAFIC-ULTRAMAFIC COMPLEX

The Lunar Creek ultramafic complex is an elongate body which measures more than 11 kilometres in length and 4 kilometres in width at its widest point. The northwesterly trending long axis of the body parallels the structural grain of the region. The southwestern margin lies adjacent to the Kutcho fault, a major structure that juxtaposes the Quesnel and Stikine terranes.

Several attributes set the Lunar Creek complex apart from other Alaskan-type complexes:

- Two gabbroic phases are present, one of which is ductily deformed and older than the main part of the complex.
- Cumulate layering is locally very well developed in the ultramafic rocks, a rare feature in the Alaskan-type intrusions of British Columbia.
- Quartz-rich pegmatitic segregations are common in the gabbroic to dioritic phases, which also appears to be relatively uncommon in Alaskan-type intrusions.

ULTRAMAFIC ROCKS

All ultramafic lithologies which typify Alaskan-type ultramafic intrusions are represented in the Lunar Creek complex. Dunite, chromitiferous dunite, wehrlite, olivine wehrlite, olivine clinopyroxenite, clinopyroxenite and gabbroic rocks are found. Of interest is the relatively low abundance of massive wehrlitic lithologies relative to, for example, the Polaris complex (Nixon *et al.*, 1990d, e), and the presence instead of chaotically mixed wehrlite and clinopyroxenite units. These chaotic domains often occur in

gradational contact with adjacent ultramafic rocks and are most common at the transition between massive dunite and olivine clinopyroxenite (Figure 2-8-5).

DUNITE AND CHROMITITE

Massive dunite crops out in three areas (near Localities 35, 42 and 59; Figure 2-8-6), underlying a total area of approximately 1.5 square kilometres. Dunite also occurs as irregular blocks within chaotic mixed zones, interlayered with wehrlite, and as dikes within massive dunite, wehrlite and olivine clinopyroxenite (Localities 5 and 14; Figure 2-8-6).

Commonly dunite is medium grained and weathers pale orange-brown. Outcrops are characteristically smooth and rounded. Contacts with clinopyroxene-rich lithologies (wehrlite and clinopyroxenite) are gradational and marked by a gradual increase in clinopyroxene crystals. Serpentinization is pervasive near faults and near contacts with gabbroic units and country rock. Away from these areas the rock is comparatively fresh and composed mainly of glassy, dark olive-green olivine.

Although the contact between dunite and country rock was not observed, relationships suggest that it may be intrusive in at least one location (Locality 60; Figure 2-8-6). In this area, dunite adjacent to the contact is weakly serpentinized but shows no evidence of shearing, implying that the contact here is not faulted. Further, amphibolite-grade metamorphism of adjacent country rock may represent a contact metamorphic aureole.

Disseminated chromite is ubiquitous in dunite, typically forming 1 to 2 per cent of the rock. Chromitite schlieren occur locally, generally in clusters of two or more (Plate 2-8-1). Individual schlieren range in thickness from 1 to

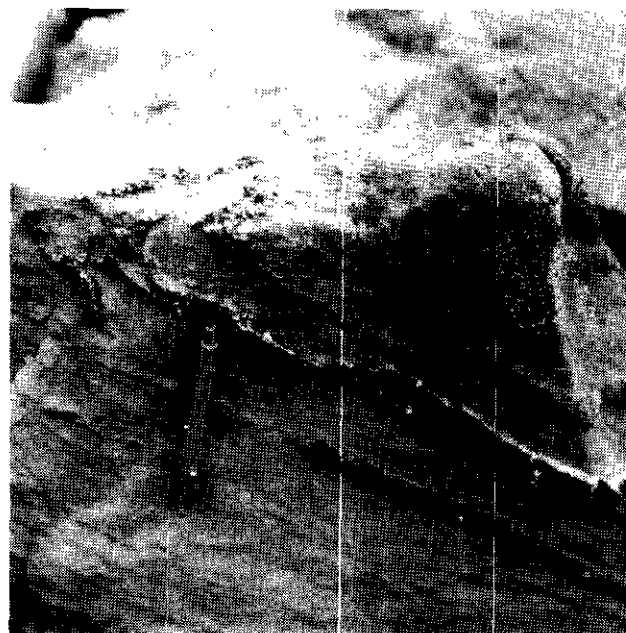


Plate 2-8-1. Deformed chromitite schlieren in dunite at Locality 44, Figure 2-8-6.



Plate 2-8-2. Olivine clinopyroxenite to clinopyroxenite dikes in dunite.

4 centimetres and in length from 20 to 30 centimetres. Locally, these schlieren are very strongly magnetic, suggesting that some of the chromite has been altered to magnetite.

Chromitite schlieren are known to host platinum group element mineralization within the Tulameen complex (Nixon *et al.*, 1990a) and the Wrede complex (Hammack *et al.*, 1990a, b). The Lunar Creek complex is no exception to this trend. However, the amount of chromitite observed is small, which minimizes the economic potential for platinum group elements.

Dunite bodies are commonly cut by swarms of anastomosing wehrlite, olivine clinopyroxenite, clinopyroxenite and rare dunite dikes (Plate 2-8-2). These dikes range in width from 1 to 20 centimetres and are most common near gradational contacts with clinopyroxene-rich lithologies.

OLIVINE CLINOPYROXENITE AND CLINOPYROXENITE

Olivine clinopyroxenite is the most extensive of the ultramafic lithologies exposed at the Lunar Creek complex (greater than 5 square kilometres). It is characterized by dark green to rusty brown, knobby-weathering outcrops. Fresh surfaces are dark green-grey and the rock is weakly magnetic. Clinopyroxene crystals vary from 2 millimetres to 3 centimetres in diameter, with a modal grain size of approximately 0.5 centimetre. Olivine grain size is fairly constant at 1 to 2 millimetres. Locally, both minerals show cumulate textures. In some cases, clinopyroxene is intercumulus and poikilitically encloses olivine. Phlogopite exists locally as an accessory phase.

Contacts between olivine clinopyroxenite and other ultramafic lithologies are gradational, marked by an increasing



Plate 2-8-3. Layering of coarse-grained clinopyroxenite-olivine wehrlite offset by small syndepositional fault, mixed layered unit 2b, south of Locality 5, Figure 2-8-6.

or decreasing olivine component. A gradational relationship is also seen between clinopyroxenite and feldspathic clinopyroxenite, marked by the appearance of plagioclase as an intercumulus phase. Rare layering, showing compositional and/or size grading, was observed in all of these lithologies (Plate 2-8-3).

Pods of dunite and wehrlite, up to 8 metres in diameter, are fairly common within the olivine clinopyroxenite unit, and are most common near gradational contacts with the chaotic mixed units described below. These pods may represent fragments of crystalline material that broke away from the walls or roof of the magma chamber, or they might be disrupted ultramafic dikes. Locally, pods have been flattened and stretched into schlieren which reach 1 metre in width and several metres in length. Locally these schlieren have a well-developed foliation parallel to their margins.

Hornblende clinopyroxenite is a rare rock type within this complex. Microscopic examination has shown that much of the hornblende observed in hand samples of clinopyroxenite is secondary, after clinopyroxene. Primary hornblende in clinopyroxenite was observed only at the narrow, gradational contacts between clinopyroxenite and hornblende-clinopyroxene gabbro.

MIXED ULTRAMAFIC ROCK UNITS

Mixed units comprise a variety of distinct ultramafic lithologies that are not mappable at 1:16 000 scale. Three varieties of mixed ultramafic rocks are observed: layered units which are sequences of interlayered clinopyroxenite,



Plate 2-8-4. Fine modal layering of olivine and clinopyroxene in mixed layered unit 2b near Locality 5, Figure 2-8-6.

olivine clinopyroxenite, wehrlite and dunite; chaotic units which consist of blocks of one ultramafic lithology mixed into another; and replacement zones which are sites where dunite has partially replaced clinopyroxenite.

LAYERED MIXED UNITS

Layering is locally well developed in peridotites of the Lunar Creek complex. Near Locality 5 (Figure 2-8-6), dunite, wehrlite, olivine clinopyroxenite and clinopyroxenite exhibit layering produced by modal and/or grain size variations. Most layering in this area is discontinuous: layers vary from less than 1 metre to several metres in thickness. Centimetre-scale layering and rhythmic layering are observed locally (Plate 2-8-4). Interlayered wehrlite, clinopyroxenite and rare dunite are seen farther south at Locality 14 (Figure 2-8-6). Here, dunite layers up to 2 metres thick, with rare chromite accumulations, grade into wehrlite. The dunite layers have sharp, nongradational contacts with adjacent olivine clinopyroxenite.

Soft-sediment deformation-like features are well exposed at Locality 5 (Figure 2-8-6). Locally, large blocks, possibly derived from the walls and roof of the magma chamber, fell onto layered material resulting in compressed and distorted layering. Further crystallization within the chamber led to deposition of more layers, which drape over both the block and the distorted material. Angular unconformities caused by the truncation of layers were observed in several outcrops. These features bear many similarities to sedimentary crossbedding and undoubtedly reflect similar processes (*i.e.* the deposition of cumulate crystals by magmatic currents).

Overall, there is no consistency in layer orientation between outcrops. Facing direction, determined by the truncation of layering and deformed layering below slumped boulders, is also variable. This suggests that significant

rotation has occurred since deposition, possibly as a result of slumping within the magma chamber prior to complete solidification.

CHAOTIC MIXED ZONES

Chaotic mixed zones are more widespread than layered zones. They consist of blocks of massive olivine clinopyroxenite to clinopyroxenite, up to 5 metres in diameter, set in a matrix of wehrlite to dunite; or blocks of olivine wehrlite/dunite/wehrlite in a clinopyroxenite matrix. Blocks are typically angular to subrounded (infrequently rounded) and commonly exhibit sharp contacts with their hosts. Contacts between mixed zones and massive peridotite are gradational and expressed by the appearance of scattered, irregular blocks in the massive host rock. The mixed zones can be subdivided into wehrlite-dominated and clinopyroxenite-dominated domains.

The chaotic mixed zones may represent density flows resulting from the spalling of crystalline material from the walls and roof of the magma chamber; in some cases, they may have formed by dike intrusion into consolidated cumulate rocks that subsequently were deformed plastically. Clinopyroxenite to wehrlite dikes are very common in chaotic zones and add to the chaotic nature of the rock by further subdividing large blocks. It is likely that some diking resulted from overpressuring of the underlying crystal mush, causing expulsion and upward migration of residual pore fluid through the cumulate pile. In fact, diking may have been promoted in chaotic zones, where slumping of large blocks from the chamber walls and roof would result in rapid loading.

REPLACEMENT DUNITE

Locally, in clinopyroxene-rich lithologies, clinopyroxene crystals have been partially to completely replaced by olivine. This process resulted in the development of irregular bodies of dunite and wehrlite within clinopyroxenites and olivine clinopyroxenites. A similar replacement phenomenon has been observed at the Duke Island complex in southeastern Alaska (Irvine, 1974b, 1986). Replacement dunite appears to have resulted from the migration of an olivine-rich magma through a porous, clinopyroxene-rich, crystal mush. The resulting disequilibrium between olivine-rich magma within the pore spaces and the adjacent clinopyroxene crystals likely led to replacement of clinopyroxene by olivine.

At Lunar Creek, replacement dunite is most common in olivine clinopyroxenite, particularly in the layered and chaotic mixed units. The effect is most spectacular in layered olivine clinopyroxenite that grades from fine to coarse grained (Locality 5, Figure 2-8-6). Here, irregular bodies of replacement dunite are up to a metre wide and cut layering at a high angle. Coarse-grained layers show pervasive replacement, whereas finer grained layers are virtually unaffected. This strongly supports the hypothesis that porosity plays an important role in the development of replacement dunite. The lower porosity of fine-grained layers restricted the amount of olivine-rich fluid in the pore

spaces and thus limited the degree of replacement in these layers.

Passive infiltration through pore spaces is one mechanism for magma migration through the cumulate pile. Where cumulates were consolidated, and pore spaces were closed, magma movement was accomplished by diking. Ultramafic dikes are fairly common in all of the ultramafic lithologies observed at Lunar Creek, as well as in most other Alaskan-type complexes within the Polaris suite of intrusions.

Dynamic processes within the magma chamber (slumping, infiltration, diking, convection, *etc.*) might explain the lack of layering in most of the ultramafic rocks of this complex, and the scarcity of layering in the ultramafic rocks of the Polaris suite as a whole.

GABBROIC ROCKS

Two suites of gabbroic rocks are found at the Lunar Creek complex. The oldest is a strongly foliated hornblende-clinopyroxene gabbro/diorite. Foliation in this unit predates the intrusion of the main body of the ultramafite and the emplacement of the younger suite of gabbroic rocks. The latter consists of massive equigranular gabbro and diorite which are virtually undeformed and appear to be the youngest rocks associated with the complex.

FOLIATED GABBRO/DIORITE

Weakly to strongly foliated hornblende-clinopyroxene gabbro/diorite is similar in mineralogy to the younger unfoliated gabbros at Lunar Creek. However, crosscutting relationships demonstrate that this foliation predates crystallization of the massive gabbro. The age of deformation of the foliated gabbroic rocks is unknown, but it is possible that they belong to an early phase of the ultramafic complex



Plate 2-8-5. Mylonitic fabrics in older, foliated gabbro/diorite unit 5c.

which was ductily deformed prior to emplacement of the remainder of the complex.

Foliated rock consists of alternating mafic and feldspathic foliae, typically less than 1 centimetre in width (Plate 2-8-5). Mafic layers are composed of black hornblende or dark green clinopyroxene or both. Feldspathic layers are composed of white plagioclase with rare quartz. Clinopyroxenes are subhedral to euhedral and commonly rimmed by hornblende. In many cases, euhedral clinopyroxene crystals have grown across foliation.

Where original igneous layering is preserved it is parallel to foliation; it is commonly boudinaged. Fabric orientation is variable throughout the complex. However, layering and foliation are crudely parallel to contacts with ultramafic components. This feature is well exposed southeast of Locality 58 (Figures 2-8-5 and 2-8-6) where the fabric appears to arch over a large body of dunite.

GABBRO/DIORITE

Gabbro, diorite and quartz diorite underlie a total area of approximately 16 square kilometres (Figure 2-8-5). Of this, diorite to quartz diorite, exposed along the western margin of the complex, make up the majority of outcrop. Gabbro/diorite forms a large body on the southeast end of the complex, and a narrow band along its eastern margin. It is also found as thick units within layered, clinopyroxenite and gabbro sequences (*e.g.* 500 metres north of Locality 12; Figure 2-8-6).

Gabbro/diorite forms massive, resistant, medium grey outcrops. Fresh rock varies in colour from medium grey to black, mafic minerals vary from 50 to 90 per cent. It is typically equigranular and medium to coarse grained, but fine-grained and pegmatitic varieties are also found. Subhedral to euhedral, cumulate hornblende and clinopyroxene

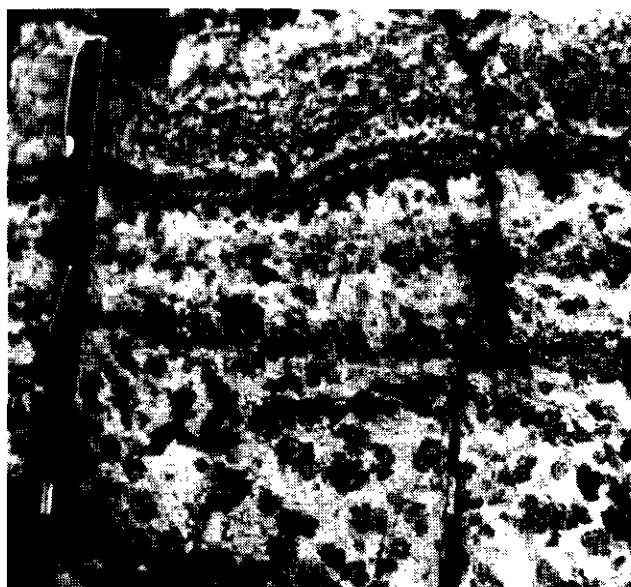


Plate 2-8-6. Fine modal layering of poikilitic hornblende and plagioclase in leucocratic layer within the gabbro/diorite unit 5a.

are the common mafic components, anhedral plagioclase occurs as an intercumulus phase. Minor net-textured sulphides were observed locally. Hornblende is typically more abundant than clinopyroxene, except near gradational contacts with ultramafic rocks. Igneous layering, in the form of alternating mafic and feldspathic layers, is fairly common (Plate 2-8-6). Locally layers are leucocratic, with as little as 20 per cent mafic minerals. This leucogabbro/leucodiorite also occurs as thick dikes which crosscut both gabbroic and ultramafic rocks.

Gabbro/diorite has a narrow gradational contact with ultramafic lithologies along the northeastern edge of the complex. In this area, gabbroic rocks form a thin wedge along the margin and lie in fault contact with Takla Group rocks to the northeast. Massive gabbro is also found in gradational contact with zones of interlayered olivine clinopyroxenite, clinopyroxenite, feldspathic clinopyroxenite, hornblende clinopyroxenite and gabbro. In addition, gabbro occurs as dikes which crosscut the foliated gabbro unit described above (Locality 22; Figure 2-8-5).

Rocks of diorite to quartz diorite composition form medium to light grey weathering, blocky outcrops. Fresh surfaces are medium grey in colour. Grain size varies from medium to coarse; the rock is locally pegmatitic. Hornblende ± biotite, composes 30 to 50 per cent of the rock. Variably altered plagioclase, together with quartz, constitute the felsic component. Quartz varies in abundance from 1 to 25 per cent and forms an interstitial phase.

Diorite/quartz diorite intrudes ultramafic rocks as well as rocks of the foliated gabbro unit. Contacts with massive gabbro/diorite appear to be gradational. It is therefore believed to be the youngest and most highly differentiated



Plate 2-8-7. Zoned quartz-feldspar pegmatite vein cutting coarse-grained hornblende gabbro/diorite (upper left) and tapering into feldspathic groundmass (lower right) where it is continuous with its host (unit 5b). Note concentration of quartz (pale grey) in centre of vein.

component of the Lunar Creek complex. Zircon from this diorite has yielded a U-Pb age of Middle Triassic (237 ± 2 Ma; L. Heaman, personal communication, 1990) which therefore represents a minimum age for the complex.

QUARTZ-PLAGIOCLASE VEINS

Quartz-plagioclase veins occur exclusively in ultramafic and mafic rocks of the complex. At one location they were observed to pinch out into, and become continuous with, pegmatitic hornblende-bearing quartz diorite (Plate 2-8-7). They are therefore believed to represent late-stage, silica-rich differentiates.

Veins range from 2 to 20 centimetres in width; most are approximately 4 centimetres. Typically, vein margins are lined with white plagioclase crystals up to 2 centimetres in diameter. Light grey quartz forms vein cores. Graphic feldspar-quartz intergrowths are common in the marginal zones.

PITMAN BATHOLITH GRANITOIDS

Granitoids north and east of the complex are associated with the Early Jurassic Pitman batholith, part of the Guichon suite of intrusions (Gabrielse *et al.*, 1980). Granodiorite dikes emanating from this batholith intrude ultramafic and mafic rocks of the complex as well as Takla Group rocks to the north. Outcrops are commonly lichen covered and form resistant, dark grey cliffs; where not covered by lichen, they are light grey. Fresh surfaces are light to medium grey and the rock is medium grained and equigranular. Composition of the granitoid varies from quartz monzonite to granodiorite. Mafic minerals, chloritized biotite and hornblende, comprise approximately 20 per cent of the rock and quartz varies from 10 to 25 per cent.

PLAGIOCLASE PORPHYRY DIKES

Plagioclase porphyry dikes intrude ultramafic and mafic rocks in the study area, and are intruded by hornblende microdiorite dikes described following. Euhedral to subhedral plagioclase phenocrysts up to 2 centimetres in diameter lie in a dark grey, fine-grained to aphanitic groundmass, which locally has hornblende microphenocrysts. In some dikes, plagioclase crystals are aligned and flattened parallel to the dike walls. These plagioclase porphyry dikes are believed to be derived from granitoids of the Early Jurassic Pitman batholith.

QUARTZ VEINS

Quartz veins cut mafic and ultramafic rocks of the complex, as well as rocks of the Takla Group to the northeast. They average 20 to 40 centimetres in width and consist of massive white quartz with less than 1 per cent pyrite. These veins commonly follow pre-existing foliation planes and often are sheared and folded, illustrating the complex history of deformation.

The veins may represent fluids emanating from Pitman batholith granitoids or they might be metamorphic dewatering features. Geochemical analysis of grab samples shows no evidence of precious metals (Table 2-8-1).

TABLE 2-8-1
ABUNDANCES OF NOBLE METALS IN THE LUNAR CREEK COMPLEX AND ASSOCIATED ROCKS

Locality	Sample Number	UTM Grid Zone 9V		Pt	Pd	Rh (ppb)	Au
		Northing	Easting				
Dunite (Units 1 and 2)							
14	GN-89-9077A	6421870N	589260E	41	6	<2	10
14	GN-89-9077B	6421870N	589260E	62	7	<2	11
14	GN-89-9077F	6421870N	589260E	343	10	<2	<1
35	GN-89-8096	6419960N	591800E	173	3	12	3
39	GN-89-9060	6420010N	590450E	41	4	<2	4
42	GN 89 7116B*	6419520N	590430E	1017	26	<2	<1
43	GN-89-9100B	6429480N	590850E	14	4	<2	<1
44	GN-89-9101	6419280N	590660E	18	3	<2	<1
Olivine Wehrlite and Wehrlite (Units 2, 3 and dike in Unit 1)							
5	GN-89-9075B	6422695N	584275E	9	3	<2	9
14	GN-89-9077E	6421870N	589260E	15	<2	<2	4
14	GN-89-9077D	6421870N	589260E	60	12	<2	11
15	GN-89-9070B	6421620N	589300E	135	4	4	2
31	GN-89-9065	6421330N	591860E	85	3	<2	<1
36	GN-89-9080A	6420340N	591090E	29	3	<2	4
45	GN-89-7073A	6419250N	590440E	9	24	<2	47
Olivine Clinopyroxenite and Clinopyroxenite (mainly Units 3 and 4)							
10	GN-89-6077	6422240N	589900E	13	<2	<2	5
11	GN-89-9076	6422060N	598225E	136	8	4	<1
15	GN-89-8070B	6421620N	589300E	57	9	<2	12
15	GN-89-9070A	6421620N	589300E	21	<2	<2	111
25	GN-89-9087	6421800N	592170E	41	4	<2	3
28	GN-89-9085	6421670N	592040E	40	6	<2	3
29	GN-89-9084	6421620N	592000E	28	5	<2	<1
30	GN-89-9066D	6421570N	591950E	26	4	<2	<1
33	GN-89-8082	6420760N	591890E	31	11	<2	3
37	GN-89-9064	6420385N	590590E	111	12	7	6
46	GN-89-7076A	6419085N	590150E	3	<2	<2	4
55	GN-89-8117B	6421310N	592290E	12	8	<2	3
59	GN-89-9113A	6418990N	593600E	55	3	<2	175
Hornblende Clinopyroxenite and Feldspathic Hornblende Clinopyroxenite (Units 4, 5a and 5b)							
13	GN-89-7092	6421890N	590180E	27	3	<2	94
27	GN-89-9068	6421710N	592120E	10	6	<2	12
52	GN-89-7099B	6418600N	590810E	7	12	<2	123
56	GN-89-8118	6419240N	592400E	15	16	<2	5
62	GN-89-7111	6418110N	591270E	34	63	<2	8
Clinopyroxene Hornblende and Hornblende (Unit 5a)							
40	GN-89-9056	6420290N	590010E	13	18	<2	4
41	GN-89-9058	6420150N	590010E	11	13	<2	3
Gabbro/Diorite (Unit 5a)							
24	GN-89-9090	6421850N	592300E	17	89	<2	8
49	GN-89-7097	6419070N	590880E	3	<2	<2	216
54	GN-89-8103	6418990N	591990E	8	16	<2	9
57	GN-89-9107	6419130N	593020E	<1	2	2	8
58	GN-89-9119	6419250N	593020E	15	8	<2	2
58	GN-89-9119	6419250N	593020E	10	8	<2	81
Diorite/Quartz Diorite (Unit 5b)							
8	GN-89-6110	6422890N	588240E	8	17	<2	64
9	GN-89-8080	6422510N	587290E	6	9	<2	4
17	GN-89-8043	6421340N	589330E	3	<2	<2	64
19	GN-89-8075	6421180N	588210E	2	<2	<2	18
51	GN-89-7107	6418590N	590990E	3	<2	<2	12
52	GN-89-7099A	6418600N	590810E	<1	<2	<2	2
64	GN-89-7120	6417320N	592400E	5	<2	<2	4
Leucogabbro/Leucodiorite (Units 5a and 5b)							
7	GN-89-6107	6422600N	588670E	13	5	<2	373
34	GN-89-8084	6427600N	591940E	13	53	<2	10
51	GN-89-9106	6418590N	590990E	2	<2	<2	<1

* Chromite-rich dunite. Detection limits: Pt and Au 1 ppb; Pd and Rh 2 ppb.

TABLE 2-8-1
ABUNDANCES OF NOBLE METALS IN THE LUNAR CREEK COMPLEX AND ASSOCIATED ROCKS — *Continued*

Locality	Sample Number	UTM Grid Zone 9V		Pt	Pd	Rh	Au
		Northing	Easting				
Foliated Gabbro/Diorite (Unit 5c)							
4	GN-89-9073C	6422780N	584240E	12	3	<2	10
12	GN-89-9074B	6422060N	589950E	8	6	<2	2
21	GN-89-9049A	6420930N	589680E	8	7	<2	2
65	GN-89-6149	6416780N	593670E	9	9	<2	9
Leucogabbro/Leucodiorite Dikes							
6	GN-89-6078	6422530N	588725E	2	<2	<2	3
21	GN-89-9049	6420930N	589680E	<1	<2	<2	442
22	GN-89-8046	6420890N	589840E	31	4	<2	17
Quartz Monzonite to Granodiorite (Unit 6)							
2	GN-89-6094B	6423280N	590290E	<1	<2	<2	3
26	GN-89-9069	6421780N	592160E	3	<2	<2	11
Granodiorite Dikes							
26	GN-89-9069B	6421780N	592160E	<1	3	<2	14
30	GN-89-9066C	6421570N	591950E	<1	<2	<2	8
Plagioclase Porphyry Dikes							
30	GN-89-9066A	6421570N	591950E	<1	<2	<2	31
36	GN-89-9080B	6420340N	591090E	<1	<2	<2	<1
53	GN-89-6112B	6418700N	591730E	4	17	<2	21
55	GN-89-8117A	6421310N	592290E	4	6	<2	4
Hornblende Microgabbro/Microdiorite Dikes							
18	GN-89-8077	6421490N	588250E	<1	<2	<2	55
38	GN-89-9063	6420030N	590550E	6	<2	<2	142
50	GN-89-9105	6418720N	591010E	<1	<2	<2	43
53	GN-89-6112A	6418700N	591730E	<1	<2	<2	5
Devonian-Permian Metavolcanic and Metasedimentary Rocks (Unit 7)							
20	GN-89-8073	6420000N	588100E	<1	3	<2	20
47	GN-89-7085	6419060N	589115E	<1	<2	<2	133
48	GN-89-6124	6418790N	589080E	<1	<2	<2	15
Takla Group Metavolcanic and Metasedimentary Rocks (Units 8a and 8b)							
1	GN-89-6090	6425050N	590550E	<1	<2	<2	4
23	GN-89-9094C	6422090N	592550E	<1	4	<2	5
23	GN-89-9094B	6422090N	592550E	9	8	<2	89
60	GN-89-9121	6418460N	593300E	10	5	<2	35
61	GN-89-9115	6418610N	593590E	4	<2	<2	37
Quartz Veins							
3	GN-89-6099	6422900N	589075E	2	<2	<2	17
16	GN-89-8069A	6421550N	589290E	3	<2	<2	3
16	GN-89-8069B	6421550N	589290E	2	<2	<2	<1
21	GN-89-8045B	6420930N	589680E	3	<2	<2	5
32	GN-89-8055A	6421250N	591860E	2	<2	<2	11
51	GN-89-9106C	6418590N	590990E	2	<2	<2	3
63	GN-89-7112	6417630N	591310E	2	3	<2	8

* Chromite-rich dunitic. Detection limits: Pt and Au 1 ppb; Pd and Rh 2 ppb.

HORNBLENDE MICRODIORITE DIKES OF DUBIOUS AFFINITY

Medium to dark grey hornblende microdiorite dikes intrude Pitman batholith granitoids, plagioclase porphyry dikes (described above), Takla Group volcanic rocks and ultramafic and mafic rocks of the Lunar Creek complex, (Plate 2-8-8). These dikes were not observed southwest of the Kutcho fault, but this area was not mapped in detail.

Dikes weather dark grey to pale brown and have an average width of approximately 50 centimetres. They are fine grained to aphanitic with microphenocrysts of euhedral

hornblende and rare euhedral to subhedral white plagioclase. Dike margins are commonly foliated, implying at least some postemplacement deformation.

STRUCTURE

The Lunar Creek ultramafite is bounded on the west by the Kutcho fault, a major structure that forms the boundary between the Quesnel and Stikine terranes. Transcurrent movement on this fault may have been initiated as early as the Middle Jurassic and may have continued through to Eocene time, resulting in an estimated 100 kilometres of

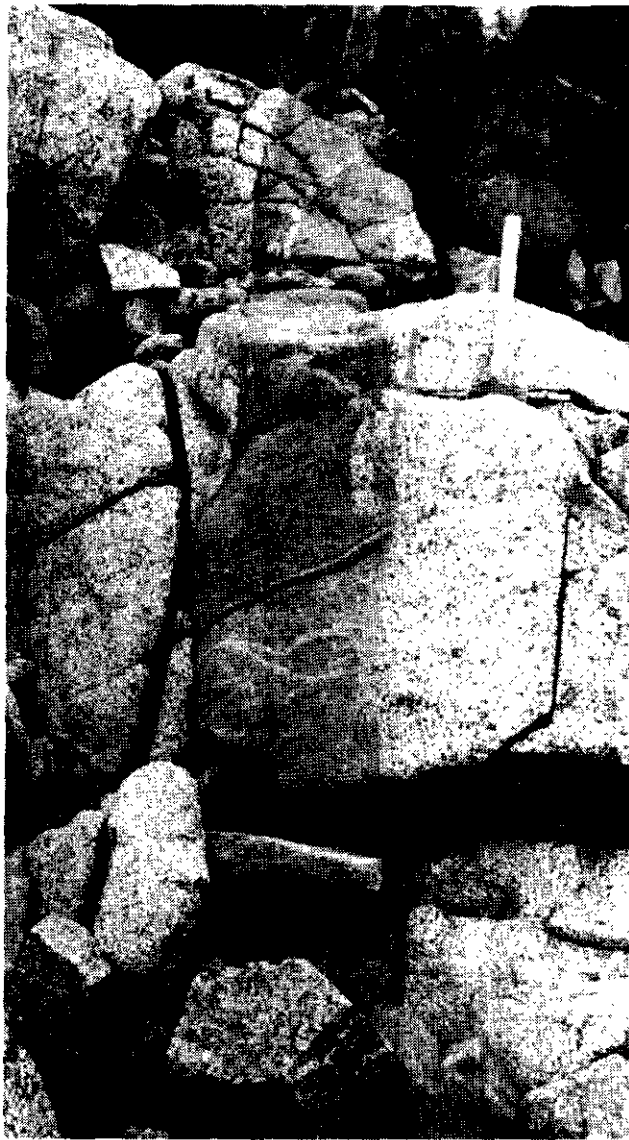


Plate 2-8-8. Hornblende microdiorite dike cutting leucocratic gabbro/diorite unit 5a and enclosing xenoliths of its host.

dextral displacement (Gabielse, 1985). It is therefore believed to be one of the more important structures in the northern Canadian Cordillera.

Northwest-trending, steeply dipping faults, subparallel to the Kutcho fault, are the dominant structures in the study area. Less abundant, steeply dipping northeast and east-trending faults are also found. Intense faulting has resulted in an outcrop pattern which is a mosaic of disrupted, disconnected blocks. This, coupled with the lack of any marker horizon within the complex, has made the detailed structure irresolvable at the scale of mapping.

At the north and east margin of the complex, Takla Group volcanic rocks and Pitman batholith granitoids, lie in fault contact with gabbroic rocks. All three lithologies are mylonitized along this fault. North of this contact, both the

granitoid and volcanic rocks have a steeply dipping, northwest-trending penetrative foliation. Bedding in Takla Group rocks dips moderately to the northeast.

Rocks immediately adjacent to the Kutcho fault are not exposed. Approximately 250 metres southwest of the fault (near Locality 47, Figure 2-8-6), stratified rocks have a steeply dipping, northwest-trending, penetrative foliation, (subparallel to the fault). Bedding within these rocks dips moderately to the northeast. Diorite and quartz diorite, approximately 100 metres north of the Kutcho fault are extensively altered but are not foliated.

An older episode of deformation is preserved in the foliated gabbro unit (Unit 5c, Figure 2-8-5). Crosscutting relationships show that ductile deformation in this unit predates intrusion of the main body of the complex, that is, prior to the collision of the Stikine Terrane with Quesnellia. In other words, this fabric predates regional deformation events proposed for this area.

The outcrop distribution of the foliated gabbro unit is commonly controlled by faults. The orientation of the foliation appears to be fairly consistent within individual fault blocks, but varies between blocks. Outcrops near the north and south margins of the complex tend to have a steeply dipping, east-trending foliation, whereas most other outcrops have a steeply dipping, northwest-trending orientation. The origin and timing of ductile deformation of this unit remains a mystery.

MINERALIZATION AND LITHOGEOCHEMISTRY

Analytical results for platinum, palladium, rhodium and gold in 84 representative rock samples from the Lunar Creek complex, its country rocks, and various dikes and quartz veins in the map area are presented in Table 2-8-1. Sample localities are shown on Figure 2-8-6. The noble metals were preconcentrated by fire assay using 30-gram splits of approximately 200 grams of rock powder (-200 mesh) and analyzed by inductively coupled plasma emission spectroscopy by Acme Analytical Laboratories, Vancouver. Accuracy was checked by international and in-house standards, and analytical precision (and any nugget effect) monitored by hidden duplicates.

Platinum abundances are generally low except in dunites (up to 343 ppb) and a chromite-rich dunite (1017 ppb). Palladium abundances are low overall, and reach their highest values in gabbroic rocks (<90 ppb). With the exception of one weakly anomalous dunite (12 ppb), rhodium is at or near the limit of detection. Gold abundances attain their highest levels in gabbroic rocks (216 to 442 ppb) but show no correlation with platinum-group elements. Quartz veins are uniformly low in gold.

Anomalous abundances of platinum in chromitite and chromiteiferous dunite have been documented in many other Alaskan-type intrusions including some in British Columbia such as Tulameen (St. Louis *et al.*, 1986; Nixon and Hammack, 1990) and Wrede Creek (Hammack *et al.*, 1990a). In the Tulameen complex, platinum in the chromitites occurs

as discrete platinum-iron alloys enclosed within chromite (Nixon *et al.*, 1990a). The high Pt:Pd ratio (39) in chromite-rich dunite (Sample 7116B, Table 2-8-1) suggests a similar mineralogical association. Unfortunately, chromite is scarce and dunite is not abundant, which suggests that the Lunar Creek complex is not a prime target for further prospecting for platinum-group elements.

Potential for industrial minerals, such as asbestos and chromite, also appears to be low. Asbestiform serpentine occurs as narrow veins within dunite, and near contacts and fault zones. Overall, however serpentine is not abundant.

Other mineralization has been described near the eastern margin of the complex. A copper showing, hosted in skarn and porphyry-style alteration at the West property, was explored in the early 1970s and has been described in assessment reports (Jones, 1970; Ryback-Hardy, 1972). These claims covered minor garnet-epidote skarn that is locally enriched in copper (chalcopyrite, malachite and covellite; Jones, 1970). Malachite staining was also observed along fractures and foliation planes in biotite schists (Ryback-Hardy, 1972). Silt, soil and rock sample geochemistry outlined several zones with modestly anomalous copper values. Skarn samples were also analysed for gold but were found to be barren (Jones, 1970). This mineralization is probably unrelated to the ultramafic complex and is more likely associated with granitoids of the Pitman batholith to the east.

SUMMARY AND CONCLUSIONS

Economic potential for platinum-group elements and economic concentrations of chromite appear to be low at the Lunar Creek complex. Lithochemical analyses were completed on 84 samples from the study area (Table 2-8-1). Samples included ultramafic and mafic rocks, dikes and quartz veins which crosscut the complex, and stratified and granitoid rocks at the periphery of the complex. Anomalous platinum was found in some samples of all of the ultramafic rocks, dunite was particularly enriched. One sample of chromite-bearing dunite contained 1017 ppb platinum, suggesting that platinum is hosted within the chromite. This association of platinum-group elements with chromite has been documented at other Alaskan-type intrusions in British Columbia (Nixon and Hammack, 1990). Unfortunately, chromite horizons are rare at this complex, and economic platinum concentrations are unlikely.

The Lunar Creek complex is set in a unique structural environment, at the juncture between the Quesnel and the Stikine tectonostratigraphic terranes. Movement on the Kutcho fault, which lies at the southwestern margin, is believed to have been responsible for as much as 100 kilometres of right-lateral displacement. Due to its close proximity to this major structure, the complex is intensely faulted, and interpretation of the internal stratigraphy is impossible at the scale of mapping done.

A wide range of ultramafic and mafic lithologies are represented in the Lunar Creek complex. Dunite outcrop is limited, and with only minor chromite concentrations. Massive olivine clinopyroxenite is the most extensive ultra-

mafic lithology exposed. Hornblende clinopyroxenite is present along narrow gradational contacts between clinopyroxenite and gabbro, but appears to be absent elsewhere. Zones where blocks of one ultramafic lithology have been mixed into another, are common. Much of the mixing of these rocks appears to have resulted from density flows within the magma chamber. Magmatic layering is locally very well preserved in the ultramafic rocks. Comparable layering has been reported at the Duke Island complex in southeastern Alaska, but is rare in the Alaskan-type complexes in British Columbia.

Gabbroic rocks formed during two phases. The oldest phase has a well-developed foliation which predates intrusion of the ultramafic rocks. The younger phase is massive and includes rocks which range in lithology from gabbro to quartz diorite. This latter phase includes the youngest rocks of the complex. Silica oversaturation, rare in Alaskan-type complexes, is common in the massive dioritic rocks at Lunar Creek. Characteristics indicative of oversaturation are quartz-rich segregations and veins, as well as the presence of interstitial quartz within gabbro/diorite phases.

Alaskan-type complexes are believed to be coeval with widespread Upper Triassic to Lower Jurassic arc volcanics of Stikinia and Quesnellia. The somewhat older Middle Triassic age (L. Heaman, personal communication, 1990) determined for the Lunar Creek complex, confirms that arc volcanism was ongoing within Quesnellia in Middle Triassic time.

ACKNOWLEDGMENTS

Fieldwork at the Polaris complex was funded by the Canada/British Columbia Mineral Development Agreement 1985-1990. We would like to thank our expeditor, Sandy Jaycox of Jaycox Industries, and Keith Buchanan of Northern Mountain Helicopters, for their caring and personal service. Thanks are also due to Tom Brooks of Canadian Helicopters, for allowing us the use of their facilities at Sturdee airstrip. We also owe many thanks to the crew of the Shasta camp for their friendly hospitality. This manuscript benefitted from reviews by Bill McMillan and John Newell, thanks are due them for their insightful comments and suggestions.

REFERENCES

- Anderson, R.G. (1984): Late Triassic and Jurassic Magmatism Along the Stikine Arch and the Geology of the Stikine Batholith, North-central British Columbia; in Report of Activities; *Geological Survey of Canada*, Paper 84-1A, pages 67-73.
- Evenchick, C.A., Friday, S.J. and Monger, J.W.H. (1986): Potential Hosts to Platinum Group Element Concentrations in the Canadian Cordillera; *Geological Survey of Canada*, Open File 1433.
- Gabrielse, H. (1985): Major Dextral Transcurrent Displacements along the Northern Rocky Mountain Trench and Related Lineaments in North-central British Columbia; *Geological Society of America*, Bulletin, Volume 96, pages 1-14.

- Gabrielse, H. and Dodds, C.J. (1974): Operation Finlay; *Geological Survey of Canada*, Paper 74-1A, pages 13-16.
- Gabrielse, H., Wanless, R.K., Armstrong, R.L. and Erdman, L.R. (1980): Isotopic Dating of Early Jurassic Volcanism and Plutonism in North-central British Columbia; *Geological Survey of Canada*, Paper 80-1A, pages 27-32.
- Hammack, J.L., Nixon, G.T., Wong, R.H. and Paterson, W.P.E. (1990a): Geology and Noble Metal Geochemistry of the Wrede Creek Ultramafic Complex, North-central British Columbia; *B.C. Ministry of Energy, Mines and Petroleum Resources*, Geological Fieldwork 1989, Paper 1990-1, pages 405-415.
- Hammack, J.L., Nixon, G.T., Wong, R.H., Paterson, W.P.E. and Nuttall, C. (1990b): Geology and Noble Metal Geochemistry of the Wrede Creek Ultramafic Complex; *B.C. Ministry of Energy, Mines and Petroleum Resources*, Open File 1990-14.
- Irvine, T.N. (1974a): Ultramafic and Gabbroic rocks in the Aiken Lake and McConnell Creek Map-areas, British Columbia; *Geological Survey of Canada*, Paper 74-1A, pages 149-152.
- Irvine, T.N. (1974b): Petrology of the Duke Island Ultramafic Complex, Southeastern Alaska; *Geological Society of America*, Memoir 138, 240 pages.
- Irvine, T.N. (1976): Alaskan-type Ultramafic-Gabbroic Bodies in the Aiken Lake, McConnell Creek and Toodoggone Map-areas; *Geological Survey of Canada*, Paper 76-1A, pages 76-81.
- Irvine, T.N. (1986): Layering and Related Structures in the Duke Island and Skaergaard Intrusions: Similarities, Differences, and Origins; in *Origins of Igneous Layering*, I. Parsons, Editor, NATO ASI Series, 196, pages 185-245.
- Jones, H.M. (1970): Geological and Geochemical Report on the West Nos. 1-14 Mineral Claims; *B.C. Ministry of Energy, Mines and Petroleum Resources*, Assessment Report 2548, 10 pages.
- Le Maitre, R.W. (1989): A Classification of Igneous Rocks and Glossary of Terms; *Blackwell Scientific Publications*, Oxford, 193 pages.
- Nixon, G.T. (1988): Geology of the Tulameen Complex; *B.C. Ministry of Energy, Mines and Petroleum Resources*, Open File 1988-25.
- Nixon, G.T., Ash, C.H., Connelly, J.N. and Case, G. (1989a): Geology and Noble Metal Geochemistry of the Tumagain Ultramafic Complex, Northern British Columbia; *B.C. Ministry of Energy, Mines and Petroleum Resources*, Open File 1989-18.
- Nixon, G.T., Ash, C.H., Connelly, J.N. and Case, G. (1989b): Alaskan-type Mafic-Ultramafic Rocks in British Columbia: The Gnat Lakes, Hickman, and Menard Creek Complexes; *B.C. Ministry of Energy, Mines and Petroleum Resources*, Geological Fieldwork 1988, Paper 1989-1, pages 429-442.
- Nixon, G.T., Cabri L.J. and LaFlamme J.H.G. (1989c) Tulameen Placers, 92H/7, 10: Origin of Platinum Nuggets in Tulameen Placers: A Mineral Chemistry Approach with Potential for Exploration; *B.C. Ministry of Energy, Mines and Petroleum Resources*, Exploration in British Columbia 1988, pages B83-B89.
- Nixon, G.T. and Hammack, J.L. (1990): Metallogeny of Ultramafic Rocks; in *Ore Deposits, Tectonics and Metallogeny in the Canadian Cordillera*, *Geological Association of Canada*, Short Course Notes, Vancouver, 1990.
- Nixon, G.T., Cabri L.J. and LaFlamme J.H.G. (1990a): Platinum-group Element Mineralization in Lode and Placer Deposits associated with the Tulameen Alaskan-type Complex, British Columbia; *Canadian Mineralogist*, 28, pages 503-535.
- Nixon, G.T., Hammack, J.L. and Paterson, W.P.E. (1990b): Geology and Noble Metal Geochemistry of the Johanson Lake Mafic-Ultramafic Complex, North-central British Columbia; *B.C. Ministry of Energy, Mines and Petroleum Resources*, Geological Fieldwork 1989, Paper 1990-1, pages 417-424.
- Nixon, G.T., Hammack, J.L., Paterson, W.P.E. and Nuttall, C. (1990c): Geology and Noble Metal Geochemistry of the Lunar Creek Mafic-Ultramafic Complex; *B.C. Ministry of Energy, Mines and Petroleum Resources*, Open File 1990-12.
- Nixon, G.T., Hammack, J.L., Ash, C.H., Connelly, J.N., Case, G., Paterson, W.P.E. and Nuttall, C. (1990d): Geology of the Polaris Mafic-Ultramafic Complex; *B.C. Ministry of Energy, Mines and Petroleum Resources*, Open File 1990-13.
- Nixon, G.T., Hammack, J.L., Connelly, J.N., Case, G. and Paterson, W.P.E. (1990e): Geology and Noble Metal Geochemistry of the Polaris Ultramafic Complex, North-central British Columbia; *B.C. Ministry of Energy, Mines and Petroleum Resources*, Geological Fieldwork 1989, Paper 1990-1, pages 387-404.
- Nixon, G.T. and Rublee, V.J. (1988): Alaskan-type Ultramafic Rocks in British Columbia: New Concepts of the Structure of the Tulameen Complex; *B.C. Ministry of Energy, Mines and Petroleum Resources*, Geological Fieldwork 1987, Paper 1988-1, pages 281-294.
- O'Neil, J.J. and Gunning, H.C. (1934): Platinum and Allied Metal Deposits of Canada; *Geological Survey of Canada*, Economic Geology Series 13, 165 pages.
- Rublee, V.J. (1986): Occurrence and Distribution of Platinum-group Elements in British Columbia; *B.C. Ministry of Energy, Mines and Petroleum Resources*, Open File 1986-7, 94 pages.
- Ryback-Hardy, V. (1972): Geological-Geochemical Report on the South Group of the West Property; *B.C. Ministry of Energy, Mines and Petroleum Resources*, Assessment Report 3835, 10 pages.
- St. Louis, R.M., Nesbitt, B.E. and Morton, R.D. (1986): Geochemistry of Platinum Group Elements in the Tulameen Ultramafic Complex, Southern British Columbia; *Economic Geology*, Volume 81, pages 961-973.

- Thorstad, L. (1980): Upper Palaeozoic Volcanic and Volcaniclastic Rocks in Northwest Toadogone Map Area, British Columbia; *Geological Survey of Canada*, Paper 80-1B, pages 207-211.
- Wanless, R.K., Stevens, R.D., Lachance, G.R. and Delabio, R.N. (1979): Age Determinations and Geological Studies: K-Ar Isotopic Ages, Report 14; *Geological Survey of Canada*, Paper 79-2, 67 pages.
- Wheeler, J.O. and McFeely, P. (1987): Tectonic Assemblage Map of the Canadian Cordillera and Adjacent Parts of the United States of America; *Geological Survey of Canada*, Open File 1565.
- Woodsworth, G.J., Anderson, R.G., Armstrong, R.L., Struik, L.C. and Van der Heyden, P. (In press): Plutonic Regimes; Chapter 15, in *The Cordilleran Orogen: Canada*, H. Gabrielse and C.J. Yorath, Editors; *Geological Survey of Canada*, Geology of Canada, Number 4.

NOTES



**INTERPRETATION OF GALENA LEAD ISOTOPES
FROM THE STEWART-ISKUT AREA***
(1030, P; 104A, B, G)

By **Colin I. Godwin, Anne D.R. Pickering and Janet E. Gabites**
The University of British Columbia
and
Dani J. Alldrick

KEYWORDS: Galena lead isotope, lead fingerprint, deposit age, deposit origin, Jurassic, Hazelton Group, Tertiary, plutons, Stewart, Iskut, Stikine Terrane.

INTRODUCTION

The Stewart-Iskut area has had the most exploration activity in the Canadian Cordillera for the last decade. Consequently, this paper examines all available galena lead isotope data related to this area. These data are from LEAD-TABLE, a dBaseIV file of about 2000 deposits in British Columbia, Yukon Territory and adjacent Northwest Territories (Godwin *et al.*, 1988).

Table 2-9-1 has 197 galena lead isotope analyses from 60 mineral occurrences. This represents less than 10 per cent of the almost 800 showings in the study area, as listed in MINFILE, the mineral inventory database of the British Columbia Ministry of Energy, Mines and Petroleum Resources. The importance of the Stewart-Iskut area is emphasized by the observation that it contains about eight per cent of the total mineral occurrence inventory of the province.

This paper shows how galena lead isotope fingerprints can be used to date deposits in the Stewart-Iskut area (Figure 2-9-1). The isotope data in Table 2-9-1 define two clusters of points (Figures 2-9-2 and 2-9-3). One represents Jurassic gold-silver-copper-zinc-lead mineralization that is cogenetic with the Hazelton Group and associated plutons. The second cluster identifies Tertiary silver-zinc-lead \pm molybdenum showings that are related to plutons. Historically, the Jurassic deposits have been of more economic significance than the Tertiary showings. So, galena lead isotopes provide a simple, effective method for evaluating the economic potential of newly discovered or poorly exposed showings.

GENERAL GEOLOGY

Most of the Stewart-Iskut area is within the Stikine Terrane of the Intermontane Belt. The western edge of the area probably includes portions of the Wrangell Terrane of the Insular Belt. All rocks of the region have been intruded by Eocene plutons and dikes of the Coast plutonic complex. The following description of the general geology is confined to Stikinia because it contains most of the occurrences examined here.

Stikine Terrane in the study area consists mainly of Mesozoic Hazelton Group that rests on rarely exposed Paleozoic "basement". Triassic to Early Jurassic strata of the Hazelton Group represent an evolving volcanic arc. This arc consists of a lower mafic volcanic complex that evolved to a thick andesite package which grades upward into dacites of the Mount Dilworth Formation. The Early Jurassic Texas Creek plutonic suite, characterized by potassium-feldspar megacrystic granodiorite, is cogenetic with Hazelton Group volcanics. In the Middle Jurassic the volcanic arc foundered and was covered by a thick succession of turbidites. In the mid-Cretaceous the entire area was regionally metamorphosed to lower greenschist facies.

LEAD FINGERPRINTS

The lead fingerprints (Figures 2-9-2, and 3) divide all but 10 per cent of the showings examined into two groups. Table 2-9-2 shows that 37 of the showings are Jurassic, 24 are Tertiary, and 5 are not clearly defined. Table 2-9-4 summarizes the galena lead isotope ratios for the two clusters.

DISCUSSION

The regional mid-Cretaceous metamorphism makes dating of Triassic to Jurassic mineralization by simple radiogenic isotopes (potassium-argon or rubidium-strontium) impossible. Galena lead isotopes, however, are not reset by thermal events alone. This emphasizes one of the advantages of the analyses presented here. In addition, at \$300 an analysis, the method is relatively inexpensive.

Jurassic and Tertiary clusters of galena lead isotope ratios in the Stewart area were first recognized by Godwin *et al.* (1980). In 1986 Alldrick submitted a suite of samples from ten deposits on eight properties from the same area. The results of this work, reported in Alldrick *et al.* (1987), were so definitive that additional samples were collected from as many showings in the Stewart-Iskut area as possible. A preliminary interpretation of resulting data was presented by Alldrick *et al.* (1990).

The clusters clearly define two separate, relatively short-lived metallogenic events. An Early Jurassic and a Tertiary interpretation for these events is consistent with stratigraphic information and other radiogenic dates. Brief

* This project is a contribution to the Canada/British Columbia Mineral Development Agreement.

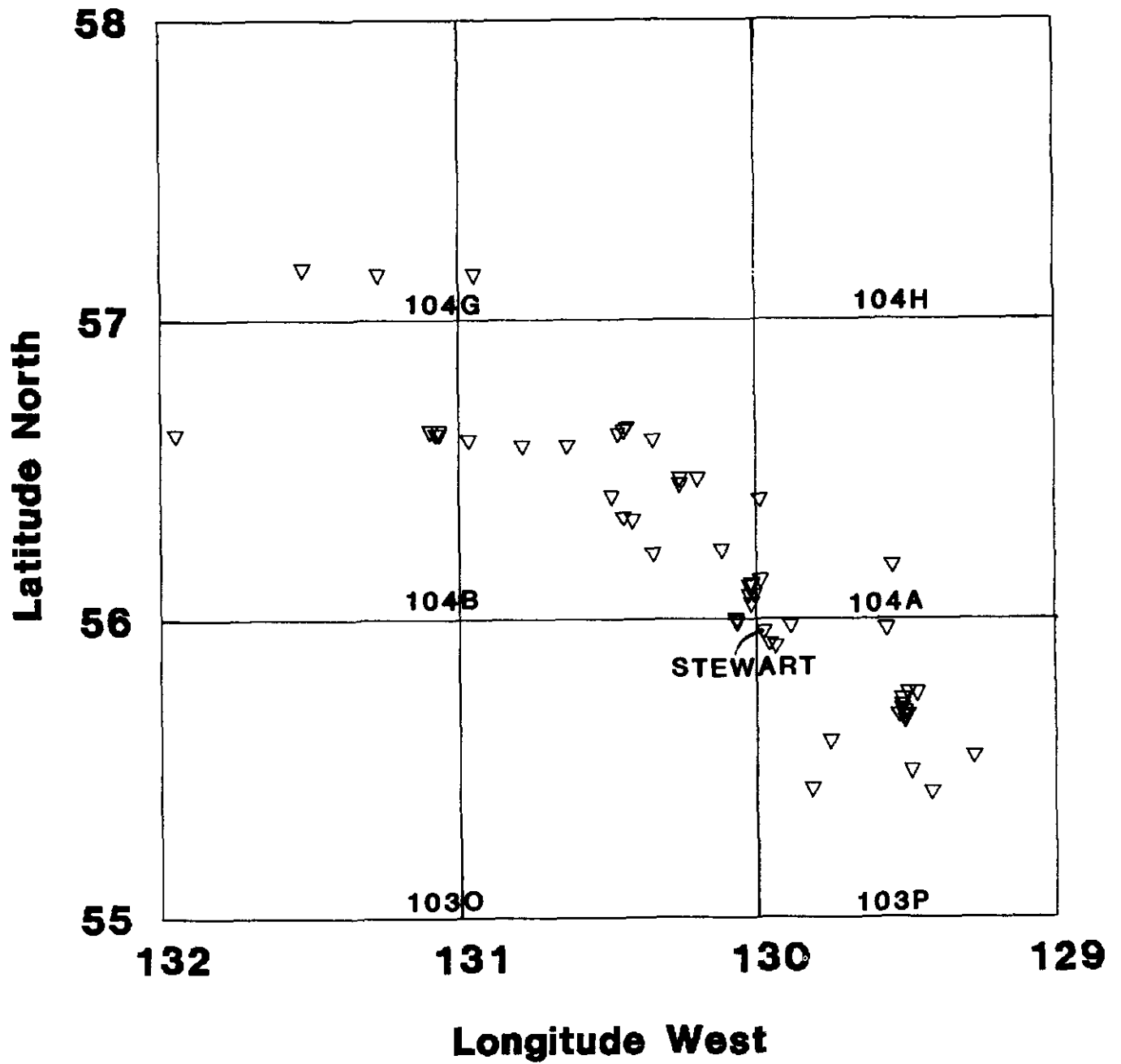


Figure 2-9-1. Location of analyses and deposits in Tables 2-9-1 and 2-9-2, Stewart-Iskut area, northwestern British Columbia.

**TABLE 2-9-1
GALENA LEAD ISOTOPE ANALYSES FOR THE STEWART – ISKUT AREA, NORTHWESTERN B.C.
(103O&P AND 104A, B&G)**

Lab Number	Deposit Name	Analyst	²⁰⁶ Pb/ ²⁰⁴ Pb	²⁰⁷ Pb/ ²⁰⁴ Pb	²⁰⁸ Pb/ ²⁰⁴ Pb	²⁰⁷ Pb/ ²⁰⁶ Pb	²⁰⁸ Pb/ ²⁰⁶ Pb	Date
NTS: 103O								
50055-001A1	JARVIS	86GA	19.164	15.607	38.579	0.81439	2.0131	R
50055-001A2	JARVIS	87GA	19.114	15.642	38.555	0.81835	2.0171	R
50055-002A1	JARVIS	86GA	19.158	15.625	38.616	0.81556	2.0156	R
50055-002A2	JARVIS	86GA	19.180	15.643	38.695	0.81561	2.0175	R
50055-003A	JARVIS	86GA	19.174	15.635	38.656	0.81545	2.0161	R
NTS: 103P								
30062-001A	WILBY	88GA	19.031	15.644	38.788	0.82202	2.0381	-
30062-001B1	WILBY	89PI	18.949	15.597	38.361	0.82310	2.0245	-
30062-001B2	WILBY	89PI	18.951	15.596	38.356	0.82296	2.0240	-
30062-002A1	WILBY	89PI	18.976	15.614	38.412	0.82285	2.0243	-
30062-002A2	WILBY	89PI	18.959	15.600	38.371	0.82284	2.0239	-
30492-001A	PROSPER-IDAHO	84GA	19.130	15.627	38.644	0.81687	2.0201	R
30492-002A	PROSPER-IDAHO	84GA	19.116	15.624	38.616	0.81732	2.0201	R
30492-003A1	PROSPER-IDAHO	84GA	19.114	15.610	38.589	0.81667	2.0189	R
30492-003A2	PROSPER-IDAHO	84GA	19.122	15.619	38.614	0.81677	2.0193	R
30555-001A1	RED POINT	84GA	18.814	15.608	38.394	0.82956	2.0407	J
30555-001A2	RED POINT	85GA	18.824	15.612	38.327	0.82940	2.0414	J
30556-001A	NORTH STAR	84GA	18.874	15.623	38.482	0.82775	2.0389	J
30556-002A	NORTH STAR	79GA	18.856	15.610	38.287	0.82785	2.0305	J
30556-002B	NORTH STAR	87GA	18.885	15.636	38.532	0.82796	2.0404	J
30556-003A	NORTH STAR	90PI	18.889	15.630	38.519	0.82744	2.0392	J
30556-003B	NORTH STAR	90PI	18.886	15.626	38.503	0.82742	2.0388	J
30557-001A	TORBRIT	79RY	18.844	15.580	38.295	0.82679	2.0322	-
30557-001B	TORBRIT	87GA	18.869	15.609	38.438	0.82725	2.0371	J
30557-003A	TORBRIT	85GA	18.875	15.625	38.485	0.82778	2.0389	J
30557-095A	TORBRIT	79RY	18.918	15.642	38.546	0.82683	2.0375	J
30557-095B	TORBRIT	87GA	18.902	15.629	38.524	0.82681	2.0381	J
30557-502	TORBRIT	60RU	19.566	16.082	39.573	0.82194	2.0225	-
30717-001A	RUTH & FRANC	79RY	19.231	15.629	38.712	0.81270	2.0130	R
30718-001A	KITSAULT	86GA	19.098	15.627	38.671	0.81826	2.0249	R
30718-002A	KITSAULT	79RY	19.203	15.637	38.893	0.81430	2.0254	R
30718-002B	KITSAULT	86GA	19.088	15.617	38.640	0.81817	2.0243	R
30765-001A	BAYVIEW	79RY	18.501	15.592	38.213	0.84276	2.0655	-
30765-002A	BAYVIEW	86GA	19.153	15.616	38.608	0.81532	2.0158	R
30765-003A	BAYVIEW	86GA	19.151	15.623	38.633	0.81582	2.0173	R
30765-004A	BAYVIEW	86GA	19.152	15.622	38.633	0.81570	2.0171	R
30766-001A1	SILVERADO	86GA	19.162	15.650	38.731	0.81669	2.0212	R
30766-001A2	SILVERADO	86GA	19.148	15.631	38.656	0.81634	2.0188	R
30766-002A1	SILVERADO	86GA	19.167	15.645	38.713	0.81623	2.0197	R
30766-002A2	SILVERADO	86GA	19.156	15.630	38.672	0.81595	2.0188	R
30771-001A	DOLLY VARDEN	79RY	18.948	15.673	38.779	0.82716	2.0466	-
30771-002A	DOLLY VARDEN	79RY	18.866	15.629	38.432	0.82842	2.0371	J
30771-003A	DOLLY VARDEN	85GA	18.852	15.612	38.452	0.82814	2.0397	J
30771-004A	DOLLY VARDEN	85GA	18.898	15.624	38.519	0.82675	2.0383	J
30773-001A	ESPERANZA	79RY	18.791	15.617	38.620	0.83109	2.0552	?
30773-001B	ESPERANZA	87GA	19.072	15.635	38.643	0.81979	2.0262	R
30776-136A	ROBIN	79RY	18.912	15.688	38.784	0.82953	2.0508	-
30776-136B	ROBIN	86GA	18.908	15.622	38.533	0.82622	2.0379	J
30776-136C	ROBIN	87GA	18.523	15.641	37.766	0.84442	2.0389	-
30777-001A	HIDDEN CK	79RY	18.489	15.590	38.380	0.84320	2.0758	-
30777-001B	HIDDEN CK	87GA	19.310	15.866	39.245	0.82164	2.0324	-
30777-001C	HIDDEN CK	87GA	19.211	15.765	39.193	0.82061	2.0401	-
30785-001A	MASTODON	79RY	18.758	15.654	38.546	0.83452	2.0549	J
30785-001B	MASTODON	86GA	18.793	15.682	38.578	0.83446	2.0528	J
30785-001C	MASTODON	87GA	18.806	15.692	38.622	0.83443	2.0537	J
30798-198A	BELLEVUE	79RY	18.858	15.671	38.503	0.83100	2.0417	-
30798-198B	BELLEVUE	87GA	18.818	15.603	38.415	0.82915	2.0414	J
30904-001A	WOLF	85GA	18.859	15.613	38.464	0.82789	2.0396	J
30993-001A	KIT	90PI	18.902	15.624	38.520	0.82656	2.0379	J

TABLE 2-9-1 — Continued
GALENA LEAD ISOTOPE ANALYSES FOR THE STEWART – ISKUT AREA, NORTHWESTERN B.C.
(1030&P AND 104A, B&G)

Lab Number	Deposit Name	Analyst	²⁰⁶ Pb/ ²⁰⁴ Pb	²⁰⁷ Pb/ ²⁰⁴ Pb	²⁰⁸ Pb/ ²⁰⁴ Pb	²⁰⁷ Pb/ ²⁰⁶ Pb	²⁰⁸ Pb/ ²⁰⁶ Pb	Date
30994-001A1	SUMMIT	90PI	18.882	15.610	38.460	0.82673	2.0369	J
30994-001A2	SUMMIT	90PI	18.909	15.644	38.574	0.82733	2.0400	J
30994-001B1	SUMMIT	90PI	18.868	15.606	38.475	0.82712	2.0392	J
30994-001B2	SUMMIT	90PI	18.878	15.611	38.467	0.82693	2.0377	J
31026-001A	E AND D	90PI	18.920	15.628	38.545	0.82600	2.0373	J
31027-001A	COPPERFIELD	90PI	18.864	15.618	38.465	0.82793	2.0391	J
NTS: 104A								
30455-001A1	KNIP	90PI	19.159	15.628	38.643	0.81570	2.0170	R
30455-001A2	KNIP	90PI	19.137	15.605	38.576	0.81543	2.0158	R
30455-001A3	KNIP	90PI	19.181	15.646	38.701	0.81572	2.0177	R
30455-002A	KNIP	90PI	19.159	15.625	38.635	0.81557	2.0166	R
30616-001A	SPIDER	86GA	19.085	15.609	38.590	0.81788	2.0220	R
30929-001A	SURPRISE CK	87GA	19.125	15.611	38.589	0.81628	2.0177	R
30929-002A	SURPRISE CK	87GA	19.144	15.630	38.637	0.81644	2.0182	R
NTS: 104B								
30361-001A	GRACY	90PI	19.157	15.635	38.673	0.81616	2.0188	R
30361-001B	GRACY	90PI	19.149	15.629	38.651	0.81618	2.0184	R
30361-002A1	GRACY	90PI	19.132	15.637	38.659	0.81729	2.0206	R
30361-002A2	GRACY	90PI	19.188	15.642	38.724	0.81521	2.0181	R
30361-002B1	GRACY	90PI	19.169	15.624	38.676	0.81508	2.0177	R
30361-002B2	GRACY	90GO	19.218	15.674	38.824	0.81561	2.0202	-
30361-002C	GRACY	90PI	19.186	15.638	38.717	0.81506	2.0180	R
30415-001A	BIG MISSOURI	81RY	18.857	15.603	38.489	0.82744	2.0411	J
30415-002A	BIG MISSOURI	81RY	18.857	15.645	38.474	0.82966	2.0403	J
30415-003A	BIG MISSOURI	81RY	18.816	15.624	38.535	0.83036	2.0480	J
30415-004A	BIG MISSOURI	81RY	18.803	15.655	38.512	0.83258	2.0482	J
30415-005A	BIG MISSOURI	81RY	18.780	15.642	38.530	0.83291	2.0517	J
30415-006A	BIG MISSOURI	84GA	18.820	15.615	38.456	0.82970	2.0433	J
30415-007A	BIG MISSOURI	84GA	18.823	15.609	38.435	0.82927	2.0420	J
30415-008A1	BIG MISSOURI	84GA	18.824	15.610	38.458	0.82928	2.0430	J
30415-008A2	BIG MISSOURI	84GA	18.822	15.611	38.453	0.82939	2.0430	J
30415-009A	BIG MISSOURI	86GA	18.812	15.592	38.373	0.82882	2.0399	J
30415-009B	BIG MISSOURI	87GA	18.835	15.615	38.450	0.82904	2.0414	J
30415-010A	BIG MISSOURI	79RY	18.175	15.521	37.634	0.85398	2.0707	-
30415-011A	BIG MISSOURI	87GA	18.827	15.616	38.464	0.82945	2.0430	J
30415-012A	BIG MISSOURI	87GA	18.828	15.617	38.474	0.82949	2.0435	J
30415-013A	BIG MISSOURI	79RY	18.753	15.634	39.057	0.83368	2.0827	J
30415-013B	BIG MISSOURI	87GA	18.734	15.612	38.990	0.83333	2.0813	J
30441-001A1	GLOBE	90PI	19.133	15.624	38.614	0.81656	2.0181	R
30441-001A2	GLOBE	90PI	19.135	15.632	38.656	0.81690	2.0201	R
30441-001A3	GLOBE	90PI	19.133	15.627	38.624	0.81677	2.0187	R
30446-001A	BRUCE GLACIER	90PI	18.828	15.589	38.338	0.82797	2.0362	J
30453-001A	COLAGH	90PI	18.847	15.609	38.433	0.82820	2.0392	J
30459-001A	KERR 15	90GO	18.801	15.613	38.427	0.83042	2.0439	J
30493-001A	SCOTTIE GOLD	84GA	18.804	15.608	38.426	0.83007	2.0435	J
30494-001A	SILBAK PREMIER	79RY	18.825	15.577	38.357	0.82746	2.0376	-
30494-002A	SILBAK PREMIER	79RY	18.849	15.639	38.551	0.82970	2.0453	J
30494-003A	SILBAK PREMIER	79RY	18.839	15.632	38.475	0.82977	2.0423	J
30494-004A	SILBAK PREMIER	79RY	18.767	15.594	38.494	0.83093	2.0512	J
30494-004B	SILBAK PREMIER	87GA	18.833	15.611	38.450	0.82891	2.0417	J
30494-005A	SILBAK PREMIER	86GA	19.229	15.758	38.251	0.81947	2.0412	-
30494-005B	SILBAK PREMIER	87GA	19.210	15.738	39.201	0.81923	2.0406	-
30494-006A	SILBAK PREMIER	87GA	18.836	15.617	38.464	0.82907	2.0420	J
30494-007A	SILBAK PREMIER	84GA	18.825	15.611	38.421	0.82926	2.0410	J
30494-010A	SILBAK PREMIER	87GA	18.817	15.602	38.382	0.82915	2.0397	J
30494-011A	SILBAK PREMIER	87GA	18.838	15.612	38.421	0.82871	2.0395	J
30494-012A	SILBAK PREMIER	87GA	18.841	15.619	38.465	0.82901	2.0416	J
30494-013A	SILBAK PREMIER	87GA	18.833	15.618	38.450	0.82930	2.0416	J
30495-001A	SILVER CONSOL	84GA	18.828	15.619	38.474	0.82954	2.0435	J
30495-001A	SILVER CONSOL	85GA	18.812	15.605	38.432	0.82957	2.0430	J
30629-001A	TAMI	85GA	18.857	15.610	38.456	0.82781	2.0394	J

TABLE 2-9-1 — *Continued*
 GALENA LEAD ISOTOPE ANALYSES FOR THE STEWART – ISKUT AREA, NORTHWESTERN B.C.
 (103O&P AND 104A, B&G)

Lab Number	Deposit Name	Analyst	²⁰⁶ Pb/ ²⁰⁴ Pb	²⁰⁷ Pb/ ²⁰⁴ Pb	²⁰⁸ Pb/ ²⁰⁴ Pb	²⁰⁷ Pb/ ²⁰⁶ Pb	²⁰⁸ Pb/ ²⁰⁶ Pb	Date
30631-002A1	SNIPPAKER	85GA	19.146	15.616	38.584	0.81565	2.0152	R
30631-002A2	SNIPPAKER	85GA	19.155	15.624	38.614	0.81565	2.0159	R
30631-003A	SNIPPAKER	85GA	18.812	15.614	38.441	0.83001	2.0434	J
30631-004A1	SNIPPAKER	85GA	18.806	15.599	38.419	0.82944	2.0429	J
30631-004A2	INEL	87GA	18.823	15.610	38.424	0.82927	2.0413	J
30720-001A	PACKER FRACT	79RY	19.155	15.585	39.602	0.81363	2.0675	R
30720-001B	PACKER FRACT	87GA	19.177	15.629	38.661	0.81500	2.0160	R
30772-001A1	ESKAY CK	90PI	18.812	15.602	38.348	0.82938	2.0385	J
30772-001A2	ESKAY CK	90PI	18.801	15.597	38.344	0.82957	2.0395	J
30772-002A	ESKAY CK	90PI	18.810	15.598	38.335	0.82924	2.0380	J
30772-003A1	ESKAY CK	90PI	18.844	15.635	38.461	0.82968	2.0410	J
30772-003A2	ESKAY CK	90PI	18.835	15.624	38.445	0.82952	2.0411	J
30772-004A	ESKAY CK	90PI	18.817	15.603	38.351	0.82920	2.0381	J
30772-005A	ESKAY CK	90PI	18.806	15.594	38.309	0.82922	2.0371	J
30772-006A1	ESKAY CK	90GO	18.832	15.632	38.466	0.83008	2.0426	J
30772-006A2	ESKAY CK	90GO	18.838	15.626	38.432	0.82947	2.0401	J
30772-007A	ESKAY CK	90PI	18.826	15.613	38.385	0.82932	2.0389	J
30772-008A	ESKAY CK	90PI	18.821	15.605	38.349	0.82916	2.0376	J
30772-009A	ESKAY CK	90PI	18.823	15.609	38.371	0.82923	2.0385	J
30772-013A	ESKAY CK	90PI	18.856	15.660	38.541	0.83053	2.0440	J
30772-013B	ESKAY CK	90PI	18.820	15.608	38.366	0.82930	2.0385	J
30772-014A	ESKAY CK	90PI	18.801	15.595	38.336	0.82951	2.0391	J
30775-001A	GRANDUC	86GA	19.099	15.614	38.561	0.81754	2.0190	R
30775-002A	GRANDUC	87GA	19.144	15.609	38.592	0.81532	2.0159	R
30775-003A	GRANDUC	79RY	18.722	15.600	38.428	0.83324	2.0526	-
30775-003B	GRANDUC	87GA	18.671	15.578	38.256	0.83438	2.0490	-
30775-005A	GRANDUC	88GA	19.085	15.602	38.532	0.81758	2.0190	R
30794-001A	TOM MACKAY LK	79RY	18.773	15.600	38.330	0.83098	2.0418	J
30794-002A	TOM MACKAY LK	79RY	18.792	15.589	38.438	0.82956	2.0454	J
30794-003A	EMMA	90PI	18.819	15.608	38.383	0.82939	2.0396	J
30794-004A1	EMMA	90PI	18.815	15.605	38.370	0.82939	2.0393	J
30794-004A2	EMMA	90PI	18.802	15.593	38.341	0.82936	2.0392	J
30797-001A	UNUK	79RY	18.861	15.629	38.373	0.82864	2.0345	J
30799-001A	MACKAY	90GO	18.816	15.601	38.339	0.82911	2.0376	J
30799-002A	MACKAY	90PI	18.820	15.606	38.348	0.82922	2.0376	J
30799-003A	MACKAY	90PI	18.811	15.596	38.319	0.82910	2.037	J
30813-001A	TWO BARREL	85GA	18.837	15.595	38.399	0.82788	2.0384	J
30814-001A	JOHNNY MT	85GA	18.848	15.605	38.427	0.82797	2.0388	J
30814-001B	JOHNNY MT	87GA	18.855	15.611	38.450	0.82796	2.0393	J
30814-002A1	JOHNNY MT	85GA	19.065	15.625	38.586	0.81956	2.0239	R
30814-002A2	JOHNNY MT	85GA	19.054	15.615	38.562	0.81952	2.0238	R
30814-003A	JOHNNY MT	90PI	18.842	15.591	38.403	0.82746	2.0381	J
30814-005A	JOHNNY MT	90PI	18.853	15.603	38.430	0.82762	2.0385	J
30889-001A	KERR (NANCY)	85GA	18.779	15.599	38.327	0.83066	2.0410	J
30890-001A	SULPHURETS	85GA	18.809	15.626	38.477	0.83077	2.0457	J
30890-002A	SULPHURETS	86GA	18.809	15.608	38.430	0.82979	2.0431	J
30890-002B	SULPHURETS	87GA	18.822	15.617	38.452	0.82969	2.0429	J
30890-003A1	SULPHURETS	85GA	18.803	15.600	38.399	0.82965	2.0422	J
30890-003A2	SULPHURETS	86GA	18.804	15.598	38.388	0.82952	2.0415	J
30890-004A	SULPHURETS	87GA	18.818	15.616	38.444	0.82986	2.0430	J
30890-005A	SULPHURETS	87GA	18.815	15.595	38.407	0.82885	2.0413	J
30890-006A	SULPHURETS	88GA	19.196	15.668	38.842	0.81631	2.0234	R
30891-001A	KHYBER PASS	85GA	19.134	15.615	38.585	0.81610	2.0166	R
30891-002A1	KHYBER PASS	85GA	18.862	15.630	38.526	0.82862	2.0425	J
30891-002B	KHYBER PASS	87GA	18.846	15.611	38.470	0.82835	2.0413	J
30891-002A2	KHYBER PASS	85GA	18.842	15.611	38.448	0.82854	2.0406	J
30923-001A1	START	86GA	19.150	15.654	38.749	0.81747	2.0235	R
30923-001A2	START	86GA	19.132	15.629	38.642	0.81689	2.0198	R
30923-002A1	START	86GA	19.159	15.663	38.719	0.81755	2.0210	R
30923-002A2	START	86GA	19.134	15.641	38.683	0.81746	2.0218	R
30923-003A	START	86GA	19.114	15.621	38.629	0.81729	2.0210	R
30923-003B	START	86GA	19.121	15.628	38.643	0.81733	2.0210	R

TABLE 2-9-1 — *Continued*
 GALENA LEAD ISOTOPE ANALYSES FOR THE STEWART – ISKUT AREA, NORTHWESTERN B.C.
 (1030&P AND 104A, B&G)

Lab Number	Deposit Name	Analyst	²⁰⁶ Pb/ ²⁰⁴ Pb	²⁰⁷ Pb/ ²⁰⁴ Pb	²⁰⁸ Pb/ ²⁰⁴ Pb	²⁰⁷ Pb/ ²⁰⁶ Pb	²⁰⁸ Pb/ ²⁰⁶ Pb	Date
30939-001A	INDIAN	84GA	19.150	15.625	38.665	0.81595	2.0191	R
30939-002A	INDIAN	84GA	19.159	15.621	38.650	0.81537	2.0174	R
30989-001A	TRISH	90PI	18.838	15.588	38.370	0.82747	2.0368	J
30990-001A	TWIN CK	90PI	18.829	15.586	38.366	0.82779	2.0377	J
30991-001A	C-1	90PI	19.176	15.622	38.634	0.81466	2.0147	R
31002-001A	SNIP	90PI	18.847	15.606	38.429	0.82802	2.0390	J
31002-002A	SNIP	90PI	18.809	15.598	38.393	0.82931	2.0412	J
31002-003A	SNIP	90PI	18.865	15.611	38.450	0.82752	2.0382	J
31025-001A	CE ZONE	90PI	18.819	15.624	38.465	0.83021	2.0439	J
50058-001A1	RIVERSIDE	86GA	19.191	15.656	38.726	0.81578	2.0179	R
50058-001A2	RIVERSIDE	87GA	19.160	15.621	38.594	0.81529	2.0143	R
NTS: 104G								
30074-001A	PTARMIGAN	88GA	19.119	15.643	38.639	0.81829	2.0210	R
30074-002A	PTARMIGAN	88GA	19.098	15.622	38.576	0.81806	2.0199	R
30420-001A	BJ	82AN	18.718	15.545	38.183	0.83048	2.0399	-
30420-002A	BJ	82AN	18.741	15.448	37.985	0.82429	2.0268	-
30420-005A	BJ	82AN	19.291	15.702	38.987	0.81395	2.0210	R
30421-002A	SHAFT CK	90PI	18.686	15.584	38.271	0.83399	2.0481	-
30558-001A1	HORN SILVER	85GA	18.846	15.590	38.364	0.82721	2.0357	J
30558-001A2	HORN SILVER	85GA	18.858	15.598	38.393	0.82712	2.0359	J

geological descriptions of hostrock and style of mineralization are in Table 2-9-2. An explanation of abbreviations in Tables 2-9-1 and 2-9-2 is in Table 2-9-3).

Jurassic deposits (Table 2-9-2) include: Eskay Creek, Premier, Scotty Gold, Kerr, Johnny Mountain, Snip and Dolly Varden. Eskay Creek is Early Jurassic on preliminary fossil evidence (P.L. Smith, personal communication, 1990). The Premier, Scotty Gold, Kerr and Johnny Mountain deposits are closely associated with granodiorites of the Texas Creek plutonic suite. This has been dated throughout the study area as Early Jurassic (U-Pb from zircon: Brown, 1987). The Dolly Varden and Snip deposits have the same lead and therefore are also Early Jurassic.

The Early Jurassic produced a wide variety of deposit types. First, they are precious metal rich, but most have associated copper, lead and zinc. Classification of deposits is varied and includes: mesothermal gold veins at Snip and Johnny Mountain, porphyry copper-gold systems at Kerr, epithermal gold-silver and base metal deposits at Sulphurets and Premier, and volcanogenic (Donnelly, 1976; Devlin, 1987) precious metal rich deposits at Eskay Creek (gold rich) and Dolly Varden (silver rich). Overall metal association is gold and silver with copper, lead and zinc (Table 2-9-4).

Tertiary deposits (Table 2-9-2) include Indian, Prosperity-Idaho and Kitsault. These represent the two main deposit types associated with this Eocene metallogenic event. Indian and Prosperity-Idaho are representative of silver-lead-zinc-rich mesothermal veins. These are abundant throughout the study area, but are generally smaller than these examples. Kitsault, dated as Eocene (K-Ar: Carter, 1982), is a porphyry molybdenum deposit with potentially recoverable silver. Thus, the overall metal association

is silver and lead with zinc and, sometimes, molybdenum (Table 2-9-4).

Deposits with both Jurassic and Tertiary lead in Table 2-9-2 are Snippaker, Sulphurets, BJ and Granduc. In all cases the area of these deposits contains Tertiary veins as well as mineralization that is apparently older. This emphasizes the strong overprint by Tertiary intrusions associated with the Coast plutonic complex throughout the study area.

Undefined deposits in Table 2-9-2 are BJ, Granduc, Hidden Creek, Shaft Creek and Wilby. In all cases, additional analyses are desirable. However, tentative ages are assigned in the table. The BJ deposit is hosted by Permian schist, and Granduc by Triassic basalt. As neither of these units are part of the Hazelton Group, their associated lead might reflect a different model of lead evolution. Shaft Creek lead plots at the lower, left-hand edge of the Jurassic cluster in Figures 2-9-2 and 3. Consequently, it is slightly anomalous given its Middle Jurassic age (Panteleyev, 1974). Wilby lead is more radiogenic than most deposits examined here. This deposit is stratabound. Markedly radiogenic lead can be characteristic of such deposits (Godwin *et al.*, 1982; 1988).

CONCLUSIONS

Distinctions between the Jurassic and Tertiary galena lead isotope clusters in the Stewart-Iskut area are summarized in Table 2-9-4. Distinctive galena lead ratios conveniently discriminate Jurassic from Tertiary deposits. Historically, the Jurassic deposits are more significant because they tend to be larger and richer in precious metals – especially gold. Deposits with lead isotope ratios that are outside the well-defined Jurassic and Tertiary clusters need more analyses. Some of them formed from lead with a different source.

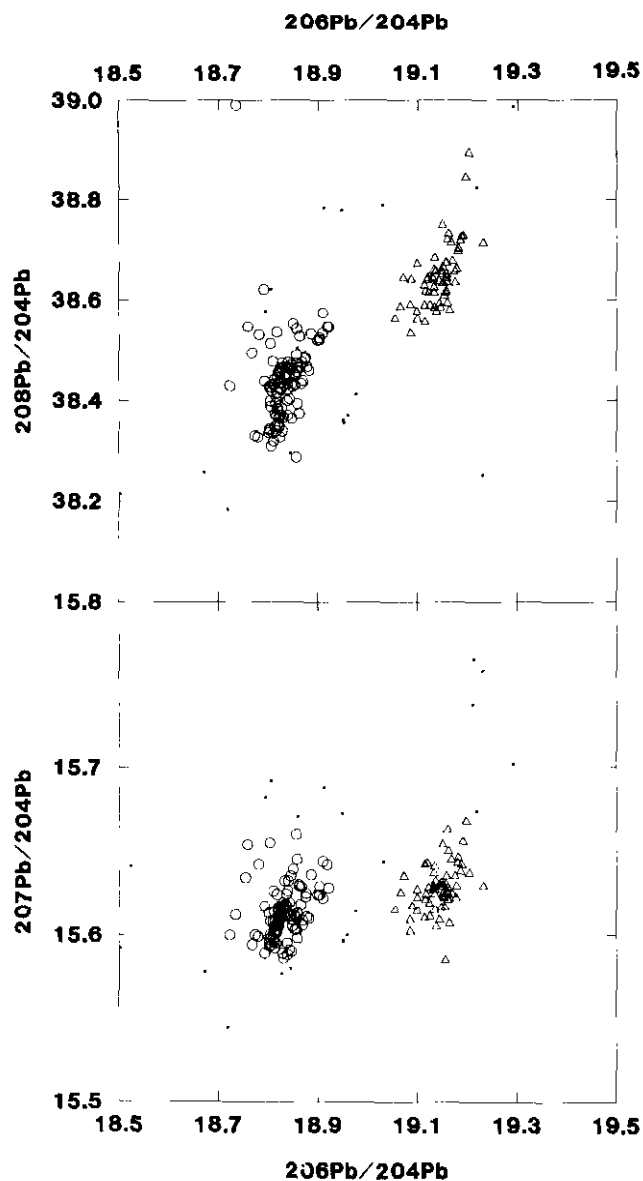


Figure 2-9-2. Lead-lead plots of galena lead isotopes from mineral deposits in the Stewart-Iskut area. The data plot in two clusters. Circles represent Early Jurassic, gold-silver and base metal mineralization that is coeval with the Hazelton Group. Triangles represent Tertiary, silver-lead-zinc±molybdenum deposits generated by granitic intrusions. Dots represent analyses that cannot be assigned or are of poor quality. See also Figure 2-9-3.

Galena lead isotope analysis is a powerful tool for evaluation of mineral showings in the Stewart-Iskut area. The method enables definition of the age and precious metal potential for poorly exposed or newly discovered mineral showings. It therefore allows exploration priorities to be set up for occurrences on a regional, district or local property scale. Application of this scheme should lead to improved success in mine discovery. It allows efforts to be focused on the potentially most productive showings under investigation. Time is a particularly precious commodity during the short field seasons in northwestern British Columbia.

TABLE 2-9-2
ALPHABETICAL LISTING OF DEPOSITS CLASSIFIED
BY DATE AND DESCRIBED BY LOCATION,
HOST AGE AND DEPOSIT TYPE
(103O&P AND 104A, B&G)

Dep No.	Deposit Name	NTS-MINFILE	Lat N	Long W	Host	Type	Date
<i>Jurassic Deposits</i>							
30798	Bellevue	103P-NW139	55.54	129.28	JM	?	J
30415	Big Missouri	104B-SE092	56.12	130.02	JE	?	J
30446	Bruce GLC	104B-NE072	56.60	130.35	JE	V	J
31025	CF Zone	104B-NW	56.63	131.07	?	V	J
31027	Copperfield	103P-NW185	55.67	129.51	JE	L	J
30453	Colagh	104B-NE252	56.58	130.64	JE	L	J
30771	Dolly Varden	103P-NW188	55.68	129.53	JE	L	J
31026	E and D	103P-NW183	55.66	129.51	J	?	J
30794	Emma	104B-NE008	56.63	130.45	JE	L	J
30772	Eskay Ck	104B-NE008	56.64	130.44	JM	L	J
30558	Horn Silver	104G-SW059	57.17	131.52	J	V	J
30631	Inel	104B-NE113	56.62	131.95	T-J	V	J
30814	Johnny Mt	104B-NW107	56.62	131.07	T-J	V	J
30459	Kerr 15	104B-SE278	56.45	130.26	JE	V	J
30889	Kerr (Nancy)	104B-SE100	56.47	130.26	JE	L	J
30993	Kit	103P-NW239	55.75	129.47	J	L	J
30891	Khyber Pass	104B-NW138	56.60	130.97	JE	V	J
30799	Mackay	104B-NE008	56.62	130.47	JE	L	J
30785	Mastodon	103P-NW020	55.59	129.76	?	?	J
30556	North Star	103P-NW189	55.68	129.50	JE	L	J
30555	Red Point	103P-NW196	55.70	129.52	JE	V	J
30776	Robin	103P-NW208	55.73	129.52	J	V	J
30493	Scottie Gold	104B-SE074	56.23	130.12	JE	V	J
30494	Silbak Premier	104B-SE054	56.05	130.02	JE	V	J
30495	Silver Consol	104B-SE095	56.11	130.03	JE	V	J
30631	Snippaker	104B-NE113	56.62	131.95	T-J	V	J
31002	Snip	104B-NW250	56.67	131.10	JE	V	J
30994	Summit	103P-NW172	55.75	129.50	JLM	V	J
30890	Sulphurets	104B-SE022	56.47	130.20	JE	V	J
30629	Tami	104B-NE116	56.58	130.79	JE	V	J
30794	Tom Mackay Lk	104B-NE008	56.63	130.45	JE	L	J
30557	Torbrit	103P-NW191	55.69	129.51	JE	L	J
30989	Trish	104B-NW107	56.63	131.07	T-J	V	J
30990	Twin Ck	104B-NW107	56.63	131.10	T-J	V	J
30813	Two Barrel	104B-NW261	56.62	131.07	T-J	V	J
30797	Unuk	104B-SE018	56.41	130.49	?	?	J
30904	Wolf	103P-NW198	55.71	129.52	JE	V	J
<i>Tertiary Deposits</i>							
30765	Bayview	103P-NW051	55.96	129.98	JE	V	R
30420	BJ	104G-SE070	57.15	130.95	P	V	R
30991	C-1	104B-NW262	56.62	131.08	T-J	V	R
30773	Esperanza	103P-SW126	55.49	129.49	JM	V	R
30441	Globe	104B-SE015	56.33	130.42	F-JE	V	R
30361	Gracy	104B-SE014	56.34	130.45	T-JE	V	R
30775	Granduc	104B-SE021	56.22	130.35	TL	V	R
30939	Indian	104B-SE031	56.08	130.03	JE	V	R
50055	Jarvis	103O-NE	55.99	130.07	JE	V	R
30814	Johnny Mt	104B-NW107	56.62	131.07	T-J	V	R
30891	Khyber Pass	104B-NW138	56.60	130.97	JE	V	R
30718	Kitsault	103P-SW120	55.42	129.42	R	#	R
30455	Knip	104A-SW095	56.40	129.99	JE	V	R
30720	Packer Fract	104B-SE	56.11	130.02	JE	V	R
30492	Prosper-Idaho	103P-NW089	55.91	129.94	J	V	R
30074	Ptamigan	104G-SW053	57.15	131.27	T	V	R
50058	Riverside	104B-SE073	56.00	130.07	JE	V	R
30717	Ruth & Franc	103P-NW062	55.98	129.89	J	V	R
30766	Silverado	103P-NW088	55.92	129.96	J	V	R
30631	Snippaker	104B-NE113	56.62	131.95	T-J	V	R
30616	Spider	104A-SW010	56.13	129.99	JE	V	R
30923	Start	104B-SW051	56.08	130.01	JE	V	R
30890	Sulphurets	104B-SE022	56.47	130.20	JE	V	R
30929	Surprise Ck	104A-SW002	56.18	129.55	J	V	R
<i>Undefined Deposits</i>							
30420	BJ	104G-SE070	57.15	130.95	P	V	J?
30775	Granduc	104B-SE021	56.22	130.35	TL	V	T?
30777	Hidden Ck	103P-SW021	55.43	129.82	T	?	R?
30421	Shafi Ck	104G-SE015	57.33	131.01	J	#	J?
30062	Wilby	103P-NW006	55.97	129.57	J	B	R?

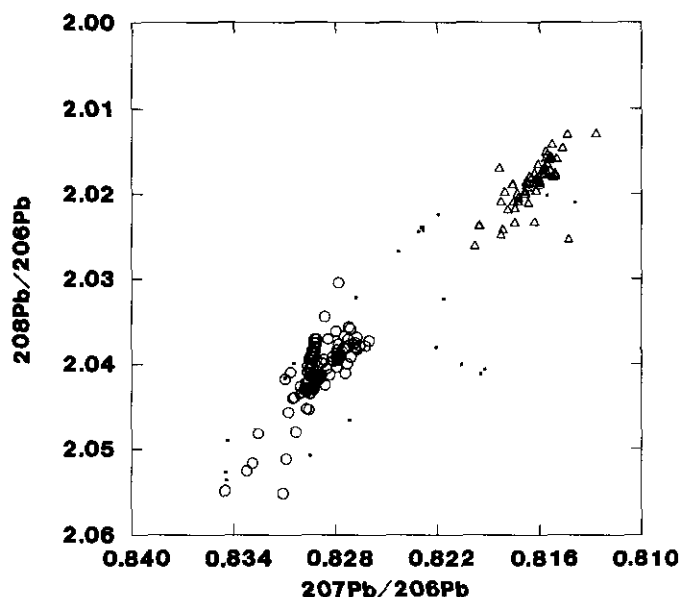


Figure 2-9-3. Lead-lead plot of galena lead isotopes as defined in Figure 2-9-2. However, different ratios are plotted. This plot minimizes effects of ^{204}Pb error.

TABLE 2-9-3
CODES USED IN TABLES 2-0-1 AND 2-0-2

Date and Host (Deposit Date and Host Age)	Type (Deposit Type)
R = Tertiary	V = Vein
J = Jurassic	L = Volcanogenic
T = Triassic	E = Early
P = Permian	B = Stratabound
? = Unknown	# = Porphyry
	? = Unknown

Analyst
(Analyst or Reference)

60-90 = Year of Analysis or reference

GA = Gabites¹

GO = Godwin²

PI = Pickering²

RU = Russell and Farquhar, 1960³

RY = Ryan³

¹ GA analyses have been normalized to the Broken Hill Standard sample UBCBHS1 with accepted values (absolute error) from Richards (1981) of: $^{206}\text{Pb}/^{204}\text{Pb} = 16.004$ (0.006), $^{207}\text{Pb}/^{204}\text{Pb} = 15.390$ (0.007), $^{208}\text{Pb}/^{204}\text{Pb} = 35.651$ (0.017), $^{207}\text{Pb}/^{206}\text{Pb} = 0.96163$ (0.00057), and $^{208}\text{Pb}/^{206}\text{Pb} = 2.2276$ (0.0014). Sample preparation and analytical techniques are described in Godwin *et al.* (1988).

² GO & PI analyses have been normalized to the National Bureau of Standard sample NBS981 with accepted values (absolute error) of: $^{206}\text{Pb}/^{204}\text{Pb} = 16.937$ (0.001), $^{207}\text{Pb}/^{204}\text{Pb} = 15.493$ (0.001), $^{208}\text{Pb}/^{204}\text{Pb} = 36.705$ (0.004), $^{207}\text{Pb}/^{206}\text{Pb} = 0.91470$ (0.00003), and $^{208}\text{Pb}/^{206}\text{Pb} = 2.1671$ (0.0001). Sample preparation and analytical techniques are described in Godwin *et al.* (1988).

³ These analyses are older and sometimes less accurate. See Godwin *et al.* (1988) for normalization factors.

TABLE 2-9-4
SUMMARY FOR THE TWO CLUSTERS OF
GALENA LEAD ISOTOPE RATIOS,
STEWART-ISKUT AREA
(1030&P AND 104A, B&G)

Cogenesis	Age	Metals	$^{206}\text{Pb}/^{204}\text{Pb}$	$^{207}\text{Pb}/^{204}\text{Pb}$	$^{208}\text{Pb}/^{204}\text{Pb}$	$^{207}\text{Pb}/^{206}\text{Pb}$	$^{208}\text{Pb}/^{206}\text{Pb}$
Hazelton Group	Jurassic	Au-Ag-Cu-Zn-Pb	18.82	15.61	38.41	0.8290	2.040
Plutons	Tertiary	Ag-Pb-Zn±Mo	19.15	15.64	38.68	0.8150	2.018

ACKNOWLEDGMENTS

Support to Colin Godwin for analytical costs was received from the British Columbia Ministry of Energy, Mines and Petroleum Resources, the Canada/British Columbia Mineral Development Agreement, the British Columbia Science Council and National Science and Engineering Research Council. Placer Dome Inc., Rio Algom Limited and Minnova Inc. gave grants to this research. Galena samples for this study were obtained from the Economic Geology Collection at The University of British Columbia, and from many geologists, in both government and industry.

REFERENCES

- Alldrick, D.J., Gabites, J.E. and Godwin, C.I. (1987): Lead Isotope Data from the Stewart Mining Camp (104B/1); *B.C. Ministry of Energy, Mines and Petroleum Resources*, Geological Fieldwork 1986, Paper 1987-1, pages 93-102.
- Alldrick, D.J., Godwin, C.I., Gabites, J.E. and Pickering, A.D.R. (1990): Turning Lead into Gold – Galena Lead Isotope Data from the Anyox, Kitsault, Stewart, Sulphurets and Iskut Mining Camps, Northwest B.C.; *Geological Association of Canada and Mineralogical Association of Canada*, Vancouver '90, Programs and Abstracts, Volume 15, page A2.
- Brown, D.A. (1987): Geological Setting of the Silbak Premier Mine, Northwestern British Columbia (104A/4, B/1); unpublished M.Sc. thesis, *The University of British Columbia*, 216 pages.
- Carter, N.C. (1982): Porphyry Copper and Molybdenum Deposits, West-central British Columbia; *B.C. Ministry of Energy, Mines and Petroleum Resources*, Bulletin 64, 150 pages.
- Devlin, B.D. (1987): Geology and Genesis of the Dolly Varden Silver Camp, Alice Arm Area, Northwestern British Columbia; unpublished M.Sc. thesis, *The University of British Columbia*, 131 pages.
- Donnelly, D.A. (1976): A Study of the Volcanic Stratigraphy and Volcanogenic Mineralization on the Kay Claim Group, Northwestern British Columbia; *The University of British Columbia*, unpublished B.Sc. thesis, 61 pages.
- Godwin, C.I., Gabites, J.E. and Andrew, A. (1988): LEAD-TABLE: A Galena Lead Isotope Data Base for the Canadian Cordillera, With a Guide to its Use by Explorationists; *B.C. Ministry of Energy, Mines and Petroleum Resources*, Paper 1988-4, 188 pages.
- Godwin, C.I., Sinclair, A.J. and Ryan, B.D. (1980): Preliminary Interpretation of Lead Isotopes in Galena-Lead from British Columbia Mineral Deposits; *B.C. Ministry of Energy, Mines and Petroleum Resources*, Geological Fieldwork 1979, Paper 1980-1, pages 171-182.
- Godwin, C.I., Sinclair, A.J. and Ryan, B.D. (1982): Lead Isotope Models for the Genesis of Carbonate-hosted

- Zn-Pb, Shale-hosted Ba-Zn-Pb, and Silver-rich Deposits in the Northern Canadian Cordillera; *Economic Geology*, Volume 77, pages 82-92.
- Panteleyev, A. (1974): Stikine Copper; *B.C. Ministry of Energy, Mines and Petroleum Resources*, Geology, Exploration and Mining in British Columbia 1973, pages 520-528.
- Richards, J.R. (1981): Some Thoughts on the Time-dependence of Lead Isotope Ratios; *Geokhimiya*, Number 1, pages 17-36.

NOTES



**SKARNS IN THE ISKUT RIVER – SCUD RIVER REGION,
NORTHWEST BRITISH COLUMBIA
(104B, G)**

By I.C.L. Webster and G.E. Ray

KEYWORDS: Economic geology, skarn, gold, copper, magnetite, Iskut River, Scud River.

INTRODUCTION

This report describes a number of mineralized skarns in the Iskut River–Scud River region of northwest British Columbia. The study forms part of an on-going project to determine the distribution, controls and metallogeny of skarns in the province. It is hoped to establish genetic models for skarn formation and examine the distribution of skarns with regard to tectonic belts and lithostructural terranes.

Nearly all the skarn occurrences described in this paper are located along the upper reaches of McLymont and Forrest Kerr creeks and on the east and west sides of lower Snippaker Creek (Figure 2-10-1). Two skarns, the Devils Elbow (MINFILE 104G 012), situated 30 kilometres south of Telegraph Creek and another in the Scud River area, were investigated but are not shown on Figure 2-10-1. The details in this paper are based largely on field observations and on some preliminary trace element analyses (Table 2-10-1). Whole-rock analyses of the intrusions, and microprobe studies of skarn minerals will be completed at a later date.

GEOLOGICAL SETTING

The study area is situated in the Boundary Ranges of the Coast Mountains physiographic belt. It lies on the western edge of the Intermontane tectonic belt within the Stikine lithostructural terrane. The Quesnel Terrane in southern British Columbia has produced over 90 per cent of the province's gold derived from skarn (Fittlinger and Ray, 1989), as well as major amounts of copper. Since the Quesnel and Stikine terranes are believed to be correlative (Monger *et al.*, 1982) it suggests that the Iskut River – Scud River area has potential for gold and copper skarn mineralization.

The geology of the area has been outlined by Anderson (1989), Logan *et al.* (1990a and b), Britton *et al.* (1989; 1990), Brown and Greig (1990), and Webster and McMillan (1990). Anderson proposes a regional stratigraphy for the area comprising four tectono stratigraphic assemblages, each bounded by unconformities:

- Tertiary Coast plutonic complex
- Middle and Upper Jurassic Bowser overlap assemblage
- Triassic – Jurassic volcanic-plutonic arc complexes
- Paleozoic Stikine assemblage

The Paleozoic Stikine assemblage underlies most of the study area in the upper McLymont and Forrest Kerr creek

area and is characterized by coralline reef limestone members intercalated with mafic to felsic volcanic rocks. In the upper Forrest Kerr Creek area, Mississippian rocks are distinguished from the Lower to Middle Devonian rocks by the presence of thick beds, local coarse bioclastic textures (large crinoidal columnals) and an association with pillowed basalt flows (Anderson, 1989).

Mesozoic strata underlie most of the area of study on the south side of the Iskut River. They comprises a 3-kilometre-thick sequence of volcanics and sediments that shows a decrease in its limestone content toward the top of the succession; it is distinguished from the Paleozoic rocks by an absence of macrofossils (Britton *et al.*, 1990).

At least four intrusive episodes, spanning Late Triassic to Quaternary time, cut this stratigraphy. These include syn-volcanic plugs, stocks, dike and sill swarms, as well as the batholithic Coast plutonic complex (Britton *et al.*, 1990).

SKARN PROSPECTS

DIRK: MINFILE 104B 114 (KEN, CHANDI, W.D., DIRK 1-324, AU 1-2, BIZ AND NEZ)

Skarn mineralogy: pyrite, chalcopyrite, bornite, chalcocite, magnetite, hematite, garnet, epidote.

The Dirk skarn is located on the southeast side of a nunatak about 6.5 kilometres northwest of Newmont Lake (Figure 2-10-1), at an elevation of approximately 1700 to 1800 metres (5580 to 5900 feet). The area is underlain by Paleozoic limestone, ash and lapilli tuff, and tuff breccias that strike north-northeasterly and dip moderately to the northwest. The white to cream-coloured limestone is locally metamorphosed to a fine to medium-grained marble. Tectonically dismembered blocks of bedded limestone, up to 3 metres by 8 metres in size, occur in the tuff breccia. Some blocks are surrounded by zones of pyrrhotite mineralization 10 centimetres thick. Higher in the sequence, lapilli and ash tuffs predominate over the tuff breccia and limestone. These rocks are intruded by early syenites containing potassium feldspar megacrysts and later sill-like bodies of orange-coloured syenite. The early porphyries form sills, dikes and irregular plugs. The euhedral, platy feldspar megacrysts are up to 3 centimetres in length, and are often aligned parallel to intrusive contacts; hostrocks immediately adjacent to the porphyries are often brecciated. The later syenites are characterized by an aphanitic matrix with large, green biotite phenocrysts and rare crystals of hornblende and potassium feldspar.

Skarn mineralization is locally developed within the early porphyries as subcircular to irregular shaped zones of brown

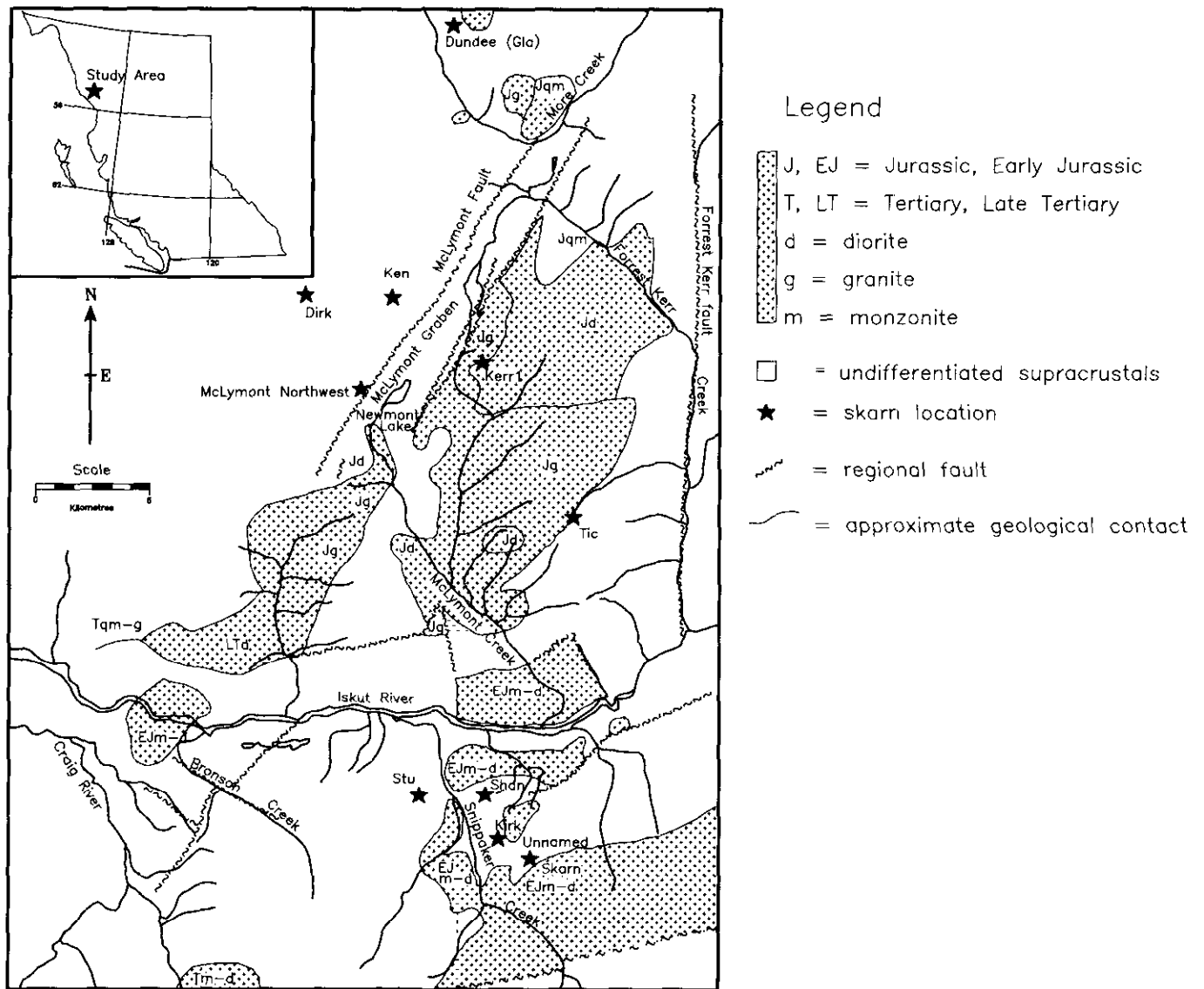


Figure 2-10-1. Generalized geological map of the study area with skarn locations. (Geology after Logan *et al.*, 1990b and Britton *et al.*, 1990)

garnet and epidote that carry pyrite, chalcocite, bornite, magnetite and hematite. These zones are generally less than 3 metres square in area and are heavily stained by malachite and azurite. Two diamond-drill holes put down by Newmont Corporation of Canada Limited gave assays of 0.3 per cent copper over 1.8 metres and 2.27 per cent over 6.0 metres. Channel samples from trenches returned assays of 0.8 per cent copper and 7.9 grams per tonne silver over 22 metres (Klesman and Ikona, 1988).

KEN: MINFILE 104B 027 (DIRK, GLACIER, ROPE, WARRIOR, GAB, CREVASSE, CONSOLIDATED AND SEA GOLD.)

Skarn mineralogy: magnetite, pyrite, chalcocopyrite, gold, garnet, carbonate, epidote, wollastonite, (?)barite.

The Ken showing is exposed on several nunataks about 3.2 kilometres northwest of Newmont Lake (Figure 2-10-1) between elevations 1500 and 1585 metres (4920 to 5200 feet). Most of the property is underlain by bedded to massive, mafic andesitic ash and lapilli tuffs of probable Permian age. These rocks strike easterly and dip moderately to steeply south. Epidote alteration is locally pervasive and also occurs in veins with pink potassium feldspar and calcite. Magnetite, chalcocopyrite and specular hematite also occur in some of these veins. The higher western flank of the largest nunatak is underlain by an intrusive quartz diorite and partly covered by a moraine consisting of 95 per cent pink granite to granodiorite boulders; some of these boulders are epidotized and cut by potassium feldspar veins, and may represent endoskarn.

A garnetite skarn zone, 5 metres wide, that trends northerly and dips steeply to the west, crosscuts the bedding in

TABLE 2-10-1
ASSAY RESULTS OF SKARN SAMPLES: ISKUT RIVER – SCUD RIVER AREA

Lab No.	Au	Ag	Cu	Pb	Zn	Co	Ni	Mo	As	Sb	Bi	Te	Se
041354	226	14	0.60%	3	233	9	<2	<8	6	<0.5	28	0.3	0.1
041356	412	57	3.83%	5	15.8%	69	9	13	2	3	<5	1.0	34.0
041357	18	1	515	3	270	20	<2	40	2	<0.5	<5	0.1	0.8
041358	5113	44	2.44%	3	660	91	6	405	7	2	<5	0.1	0.1
041359	16	4	0.17%	11	126	14	3	700	10	1	<5	0.1	0.4
041364	141	2	0.22%	6	38	238	5	<8	25	1	<5	0.8	0.2
041365	26	4	0.53%	29	445	360	19	<8	124	4	<5	1.0	3.0
041366	445	24	3.74%	33	175	402	38	<8	330	2	78	1.0	1.4
041367	23	0.7	27	3	21	55	11	14	4	2	<5	0.1	1.2
841368	23	<0.5	87	5	55	13	6	<8	10	3	<5	0.2	0.3
041369	64	3	62	<3	54	377	446	<8	22	2	<5	0.8	12.4
041370	14	3	478	11	307	47	6	<8	36	2	<5	0.2	2.2
041379	1335	106	17.5%	38	0.49%	243	10	<8	*<80	*<20	<5	0.5	0.5
041381	7	21	343	290	5.32%	32	4	8	20	1	0.16%	12.0	13.7
041383	7	28	18.2%	11	115	2	4	12	3	2	<5	0.5	0.5
041384	24	5	52	134	21.0%	101	3	8	16	2	144	15.1	25.4
041385	6	7	0.46%	9	84	118	17	19	30	1	44	2.1	0.3

Units and Methods:

Au, in ppb; all other elements in ppm except where noted in per cent (%).
Au, FA/ICP; Te and Se, AH/ICP; all other elements are by AAS.

* = interference due to high copper

Sample Descriptions and Property

041354: magnetite-pyrrhotite-chalcopyrite-garnet skarn boulder, Scud River
041356: pyrrhotite-pyrite-sphalerite-chalcopyrite-garnet skarn boulder, Scud River
041357: garnet-pyrrhotite-pyrite skarn boulder, Scud River
041358: chloritized, pyrite and chalcopyrite-rich boulder, Scud River
041359: pyrite-chalcopyrite-garnet skarn boulder, Scud River

041364: pyrite-chalcopyrite-garnet skarn boulder, Scud River
041365: pyrite-chalcopyrite-carbonat skarn, Stu skarn
041366: pyrite-chalcopyrite-actinolite skarn, Stu skarn
041367: pyrite-carbonate mineralization, Unnamed skarn
841368: magnetite-pyrite-epidote-pyroxene skarn, Unnamed skarn
041369: pyrite-magnetite-carbonate mineralization, Kirk magnetite skarn
041370: pyrite-carbonate-quartz mineralization, Kirk magnetite skarn
041379: chalcopyrite-pyrite mineralization, Dundee (Gla) skarn
041381: quartz-sphalerite vein, Shan skarn
041383: quartz-chalcopyrite breccia, Shan skarn
041384: quartz-actinolite-sphalerite mineralization, Shan skarn
041385: quartz-pyrite mineralization, Shan skarn

the lower part of the sequence. Alternating garnet-rich and epidote-rich layers trend approximately east and dip moderately south. The coarse, brown garnet-epidote-calcite skarn carries massive magnetite, chalcopyrite and coarse pyrite and cubes of pyrite. The pyrite occurs as veins and as coarse crystals and blebs, up to 2 centimetres in diameter, which are intergrown with calcite and magnetite. Chalcopyrite forms veins subparallel to bedding and disseminations intergrown with coarse calcite.

DEVILS ELBOW: MINFILE 104G 012 (STIKINE, PEACH AND APRICOT)

Skarn mineralogy: magnetite, chalcopyrite, sphalerite, galena, pyrite, scheelite, pyrrhotite, garnet, quartz, epidote, wollastonite.

This scheelite-bearing skarn is located approximately 30 kilometres south of Telegraph Creek on the northwest side of Devils Elbow Mountain at an elevation of between 600 and 690 metres (1970 to 2260 feet). Three adits (two of which are now caved) and a number of open-cuts were opened during the early part of this century.

The area is underlain by Stikine assemblage limestone, argillites and minor tuffs, of possible Carboniferous age, that are intruded by Mid-Jurassic granodiorites and the Eocene Sawback granite (Brown and Greig, 1990; Brown *et*

al., 1990). Near the lowest adit (elevation 630 metres), biotite-hornfelsed tuffaceous argillites trend northeasterly and dip approximately 60° northwest. These are intruded by a hornblende-bearing granodiorite body as well as numerous sills up to 2 metres wide; these are probably related to the Mid-Jurassic granodiorite bodies that outcrop elsewhere on Devils Elbow Mountain. The 91-metre adit follows lenses rich in magnetite, pyrrhotite, sphalerite and copper minerals. The lenses reach 15 metres in length and 1.5 metres in width and generally occupy the contact between the intrusion and sediments, although some endo-skarn mineralization is also reported in the granodiorite (Kerr, 1948). Skarn minerals include quartz, garnet, epidote and wollastonite. Mineralization in the two upper adits appears to be both lithologically and structurally controlled, and has an east-southeast strike and a steep northerly dip. It comprises galena and sphalerite with garnet, wollastonite and quartz.

Two other skarn occurrences are reported in the vicinity of the Devils Elbow prospect (Kerr, 1948). One of these, the Apex (MINFILE 104G 013), situated about 4 kilometres southeast of the Devils Elbow skarn, is hosted in limestone. The other, the Drapich (MINFILE 104G 011), situated on the west side of the Stikine River, lies along the contact between hornblende-bearing diorite and limestone. It contains lenses of chalcopyrite mineralization up to 1.5 metres thick.

SHAN: MINFILE 104B 023 (SHAN 1-6, SNIP, SNIP 5-6, JOSH AND MAY)

Skarn mineralogy: sphalerite, chalcopyrite, magnetite, pyrite, galena, tetrahedrite, epidote, actinolite, quartz, garnet, (?) bismuth tellurides.

The Shan skarn is situated 1 kilometre east of Snippaker Creek and 4 kilometres south of the Iskut River at an elevation of 1125 metres (3690 feet). The area is underlain by dark green to black andesitic tuffs which are intercalated with beds of tectonically dismembered limestone and siltstone. These strike easterly and dip moderately north. To the south these rocks are intruded by the Early Jurassic Lehto pluton, a potassium feldspar megacrystic porphyry of quartz monzonitic to dioritic composition (Britton *et al.*, 1990). The country rocks adjacent to the pluton are cut by numerous dikes and sills of quartz diorite. The Shan skarn is located close to the northern contact of the pluton; it includes abundant, coarse radiating actinolite crystals intergrown with lesser amounts of epidote, quartz and minor garnet. Metallic minerals include pods of sphalerite, pyrite, magnetite, galena and tetrahedrite. At one locality, angular fragments of strongly brecciated volcanic rocks are cemented by cockscomb quartz and chalcopyrite. Assays of chalcopyrite and sphalerite-bearing samples show no gold enrichment, although one sample contains anomalous bismuth and tellurium (Table 2-10-1).

SCUD RIVER

Skarn mineralogy: pyrrhotite, pyrite, chalcopyrite, sphalerite, gold, garnet, potassium feldspar, epidote, lizardite.

A train of mineralized skarn boulders occurs in a southeast-trending tributary to the Scud River (between UTM coordinates 354400E, 6348750N and 353550E, 6349450N; Zone 9). These boulders, which are up to 1.5 metres in diameter, can be followed up the valley in a northwest direction for at least 1.5 kilometres to the toe of a receding glacier at an elevation of 1210 metres (3970 feet). The source of the mineralized boulders was not discovered, although a helicopter traverse revealed gossanous nunataks farther up the glacier to the north. The boulders may come from these nunataks or from beneath the glacier. Mineralization comprises massive pyrrhotite with lesser pyrite, chalcopyrite and sphalerite in a reddish brown garnetite matrix. Some boulders contain irregular, pale green masses of lizardite.

The bedrock geology and float at the toe of the glacier were examined in some detail. Besides large boulders of sulphide-bearing skarn, there are also numerous boulders of epidotized granodiorite which contain disseminated pyrite and pyrrhotite and some potassium feldspar and chloritic alteration. It is possible that this is endoskarn alteration. Bedrock is exposed in a large, semicircular cliff at the toe of the glacier. Thick-bedded, impure, brownish grey tuffaceous and crinoidal limestone strikes southeast and dips steeply northeast. These sediments are cut by several intrusives, including an early irregular body of granodiorite,

and later dikes and sills of altered diorite to quartz diorite. A set of pre-dike tension gash fractures in the early granodiorite are filled with irregular, vuggy quartz-carbonate-chlorite veins up to 10 centimetres in thickness. The granodiorite adjacent to the veins is highly chloritized and weakly pyritic.

Assay results of samples collected from assorted mineralized skarn boulders are shown in Table 2-10-1. The pyrrhotite-rich skarn can contain high copper and zinc values but is low in gold. One boulder of intensely chloritized granodiorite with pyrite and chalcopyrite contained over 5 grams gold per tonne. This boulder was collected close to the toe of the glacier (UTM 353550E, 6349450N); it is uncertain whether it is skarn, or represents chloritic wallrock alteration similar to that adjacent to the quartz veins in the nearby granodiorite outcrops.

TIC

Skarn mineralogy: magnetite, pyrite, epidote, garnet, quartz, potassium feldspar, carbonate, quartz.

The Tic skarn is located approximately 11.5 kilometres southeast of Newmont Lake at an elevation of 1430 metres (4700 feet). The area is underlain by a steeply dipping, deformed package of andesitic ash and lapilli tuffs, bedded tuffaceous sediments and thin marble beds. These are locally epidotized and silicified, and are intruded by numerous sills and dikes of hornblende plagioclase-porphyrific quartz diorite and granodiorite. In places these intrusions contain elongate screens of the host tuffs.

The skarn is developed along the southeast margin of a steeply dipping and northeast-striking marble unit, 70 to 100 metres thick. The coarse-grained, recrystallized marble is strongly foliated and contains thin, deformed silty layers and pods of pink, crystalline calcite. A zone of massive magnetite, 5 to 7 metres wide, lies along the contact between the marble to the northwest and tuffs and mafic quartz diorite to the southeast. The contact between the magnetite zone and the marble is generally sharp but locally it is marked by either a 1-metre zone of orange-coloured ankeritic alteration or irregular pods of coarse crystalline pyrite up to 15 centimetres in diameter. Deformed pods of pyrite up to 30 centimetres wide, and thin pyrite veins, occur within the magnetite unit and the adjacent marble. Locally, the magnetite also contains some carbonate clots and small, euhedral quartz crystals.

A nearby sill of mafic hornblende quartz diorite is moderately to extensively altered to endoskarn; it contains widespread epidote, local pocket-rich in brown-coloured garnet, and veins of pyrite and potassium feldspar. Farther from the skarn, the intrusions tend to be fresher. Local silicification and epidote-carbonate-pyrite alteration occurs in both the intrusions and country rocks up to 400 metres south and southwest of the Tic skarn, though no additional magnetite-rich skarn was seen. In places the rocks are overprinted by narrow, southeast-trending, fracture-controlled zones of orange to brown-coloured ankeritic alteration. At one locality southwest of the skarn, the altered tuffs are also cut

by thin veins (<2 centimetres) that contain calcite, epidote and coarse, black tourmaline; X-ray diffraction analysis indicates the latter is dravite (M. Chowdry, personal communication, 1990).

KERR I

Skarn mineralogy: magnetite, pyrite, chalcopyrite, hematite, epidote, garnet, quartz, calcite, potassium feldspar, pyroxene, (?)barite.

The Kerr I skarn is situated approximately 5.5 kilometres east-northeast of Newmont Lake (Figure 2-10-1) at an elevation of 1730 metres (5680 feet); it is on claims currently held by Pamicon Developments Limited. Only one magnetite-pyrite-chalcopyrite skarn occurrence was examined, but abundant and extensive skarn-altered float suggests that there are other occurrences in the area. The vicinity of the Kerr I skarn is underlain by highly altered mafic ash and crystal tuffs that are massive to weakly bedded. These rocks are cut by swarms of sills and dikes representing several generations of intrusion; early mafic, feldspar-porphyratic diorite is cut by a phase of leucocratic, pink, granodiorite to quartz monzonite which is cut in turn by andesitic dikes with chilled margins. The granodiorite to quartz monzonite contains abundant rounded to subangular xenoliths of tuff and diorite as well as crosscutting veins of potassium feldspar and epidote.

The skarn occurrence examined is hosted by epidotized mafic tuffs; no intrusive rocks were identified in the immediate vicinity. A zone of magnetite and epidote skarn, 1 to 2 metres thick, strikes northeast and dips 45° northwest. This zone, which is irregular and discontinuous, includes large pods of massive pyrite and trace chalcopyrite. It is structurally overlain by a zone of massive brown garnetite 2 to 3 metres thick, which in turn passes upward into epidote-rich skarn. The latter contains small, irregular pods of garnetite as well as massive blebs of hematite surrounded by dark green pyroxene. Contacts between the magnetite, garnet and epidote-pyroxene-rich zones are sharp. The occurrence is crosscut by several weakly mineralized veins up to 7 centimetres wide. One set strikes southeast to east-southeast and is steeply dipping; these veins contain calcite, dolomite, quartz, barite and trace pyrite and chalcopyrite. The vein barite seen in outcrop did not exceed 1.5 centimetres in width, but float containing pods of barite up to 9 centimetres wide occurs in the area. Irregular, discontinuous veins with quartz, carbonate, magnetite and specular hematite also cut the garnetite skarn. The quartz forms euhedral, elongate crystals intergrown with carbonate, while the magnetite is coarse and bladed. Another set of ankeritic veins is associated with a minor, northeast-trending, southwest-dipping fault zone.

KIRK MAGNETITE: MINFILE 104B 362

Skarn mineralogy: magnetite, pyrite, chalcopyrite, azurite, epidote, garnet, pyroxene, chlorite, potassium feldspar, lizardite, carbonate, (?)barite.

The Kirk skarn is situated east of Snippaker Creek (Figure 2-10-1), about 5.5 kilometres north-northwest of Snip-

paker airstrip, at an elevation of 1465 metres (4800 feet). It lies close to the toe of a receding glacier and appears to have been uncovered relatively recently. The area is underlain by a package of altered siltstone, bedded to massive mafic tuff and marble, and lies close to the northern margin of the Early Jurassic Lehto pluton. Farther south, the pluton mainly comprises a fresh, pink, coarse-grained quartz monzonite that is rich in potassium feldspar and contains hornblende phenocrysts. Approximately 200 metres south of the Kirk magnetite skarn, however, the pluton becomes green coloured and pervasively altered; it contains chlorite, epidote and veins of carbonate. Nearby, the tuffs and sediments strike southeast to north-northeast and dip between 30° and 55° easterly. They are cut by potassium feldspar rich granitic dikes that are presumed to be derived from the adjacent Lehto pluton.

The mineralized stratiform skarn is developed along the lower contact of a major unit of grey to white, foliated and banded marble that is estimated to be at least 150 metres thick. A zone of massive magnetite, 2 to 8 metres thick, outcrops over a 150-metre strike length; like the structurally overlying marble it dips northeastwards into the hillside at about 45°. The marble close to the magnetite contains thin stringers of magnetite orientated parallel to the banding. In the main magnetite zone, magnetite is intergrown with white calcite, minor epidote and chlorite, as well as with irregular masses and veins of a massive yellow-green mineral which X-ray diffraction studies indicate to be lizardite (M. Chowdry, personal communication, 1990). Locally, the magnetite zone contains thin, discontinuous interlayers of marble up to 0.6 metre thick which contain coarse masses of crystalline, amber-coloured garnet that reach 9 centimetres in diameter. The lower part of the zone contains some sulphides and the magnetite is intergrown with pods and stringers of pyrite up to 7 centimetres wide. Traces of chalcopyrite and azurite also occur together with malachite staining. Assay results of two mineralized samples from the Kirk skarn are shown in Table 2-10-1. Gold and silver values are very low.

Immediately beneath the magnetite-rich zone is a thin, discontinuous unit of bleached, massive and siliceous rock that contains disseminations and veinlets of pyrite and carbonate with traces of chalcopyrite. Locally, these veinlets penetrate the overlying magnetite.

Structurally underlying the mineralized skarn is a zone of pyroxene-garnet-epidote skarn that is at least 100 metres thick. The protolith of this unit comprises interbanded layers of feldspar crystal tuff and bedded tuffaceous sediment. The sediments are overprinted by abundant pyroxene-garnet-epidote alteration that has preferentially replaced certain beds to produce banded skarn; the brown garnet forms discontinuous bands up to 0.3 metre thick. This skarn contains patches of black to dark green chlorite, as well as some white carbonate clots that are rimmed by bands of pyrite and epidote. The massive, mafic crystal tuffs in this unit, particularly those close to the magnetite skarn, are less strongly altered to garnet-pyroxene skarn. Instead, they are partially to completely replaced by a dense vein network of bleached, siliceous alteration.

The magnetite skarn is cut by a closely spaced set of steeply dipping, east-northeast-trending faults that are downthrown to the north. Where these faults displace the marble they are often marked by orange-weathering ankeritic zones up to 1 metre wide. Locally, the skarn is also cut by thin veins of dolomitic and white barite; float of Lehto pluton cut by carbonate-barite veins was also observed at the occurrence.

STU

Skarn mineralogy: magnetite, pyrite, chalcopyrite, pyrrhotite, galena, sphalerite, tremolite-actinolite, epidote, quartz, garnet, chlorite, ferrocarbonate.

The Stu skarn occurrence is situated approximately 5 kilometres south of the confluence of Snippaker Creek and the Iskut River (Figure 2-10-1), at an elevation of 1390 metres (4560 feet). In 1988 the property was trenched and sampled by Kestrel Resources Ltd., (Blanchflower, 1988). The area is underlain by a steeply dipping, east-northeast to northeast-trending package of massive to bedded tuffs, thin andesitic flows, flow breccias, and occasional bands of white to grey marble up to 20 metres thick. The volcanoclastic rocks include ash and lapilli tuffs as well as some tuff breccias with clasts up to 0.3 metre across. Some rare, fresh-looking dioritic sills, less than 1.5 metres thick, intrude the sequence.

An elongate zone of tremolite-actinolite-quartz-carbonate skarn follows the contact between tuffs and a 20-metre-thick marble unit. The skarn lies along the southeastern margin of the marble; it reaches 20 metres in thickness and is traceable along strike to the southeast for at least 600 metres. It largely comprises veins, rounded pods and irregular masses of tremolite-actinolite-epidote-quartz skarn that cut the marble. Locally, the skarn encloses subrounded to angular masses of marble several metres in diameter. The contacts between the skarn and marble are sharp, except where they are separated by narrow zones of ferrocarbonate alteration. The tremolite-actinolite generally occurs as elongate, radiating crystals up to 10 centimetres long. The quartz forms coarse crystals intergrown with the tremolite-actinolite; where quartz grows adjacent to calcite it develops good, euhedral faces. The skarn is also cut by massive to vuggy quartz veins up to 0.3 metre wide that can contain abundant pyrrhotite and lesser pyrite and carbonate. Locally the tremolite-actinolite-quartz skarn includes minor amounts of massive brown garnet and disseminated epidote.

Mineralization is characterized by magnetite with lesser pyrite and pyrrhotite and trace chalcopyrite. Blanchflower (1988) reports trace galena, sphalerite and possible scheelite. Metallic minerals occur as disseminations or lenticular masses in the skarn, as magnetite-sulphide veins up to 10 centimetres wide, or in quartz veins that cut the tremolite-actinolite skarn. Some quartz veins contain large blebs of pyrrhotite with minor pyrite, tremolite, chlorite and traces of chalcopyrite. Pyrite is often concentrated along the margins of the quartz veins. Assay results on two mineralized grab samples are listed in Table 2-10-1. The samples

contain high copper and silver values, are weakly anomalous in arsenic, but contain only low quantities of gold.

Late, orange-coloured ferrocarbonate alteration is extensive. It occurs in a vein network cutting the marble adjacent to the skarn and as veins that postdate the tremolite-actinolite, the magnetite and the sulphides. The sequence of crystallization at the Stu skarn was as follows: 1) tremolite-actinolite, 2) magnetite, 3) pyrite and chalcopyrite, followed by 4) ferrocarbonate.

DUNDEE (GLA)

Skarn mineralogy: magnetite, pyrrhotite, pyrite, chalcopyrite, sphalerite, gold, garnet, epidote, pyroxene, wollastonite, quartz, carbonate, potassium feldspar, (?) barite.

The Dundee (Gla) property, currently held by Kestrel Resources Ltd., straddles the south fork of More Creek between elevations 730 metres (2400 feet) and 1500 metres (5000 feet) (Figure 2-10-1). The area is largely underlain by a deformed, highly altered package of tuffs, tuffaceous sediments, siltstones and argillites with lesser volcanics and rare limestone beds (Figure 2-10-2). Many of the tuffs and volcanics are massive; poorly preserved bedding is seen locally. The strike and dip of the bedding is highly variable throughout the area. The sedimentary and volcanic package is intruded by a body that varies compositionally from quartz monzonite to quartz diorite. The margins of this intrusion are irregular, but it reaches at least 500 metres in width in its southern section, and could be much wider to the north (Figure 2-10-2). The sediments and volcanics close to the intrusion are commonly hornfelsed and silicified, making it difficult to recognize their origin. Mineralized skarns are differentially developed where the intrusion crosscuts limestone sequences.

Numerous andesitic dikes cut both the volcanic-sedimentary package and the major intrusion. Dikes are particularly common close to the margin of the intrusion; they form densely packed, highly irregular, crosscutting swarms that disrupt bedding in the sediments. They include massive equigranular forms, and coarsely feldspar-porphyrific phases that display flow fabrics. These dikes postdate the main intrusive body, but may represent a late phase of the same magmatic event. However, their relationship to skarn alteration is uncertain. Two narrow dikes of fresh potassium feldspar megacrystic syenite are seen in the area. These resemble the intrusion associated with the Dirk skarn elsewhere in the district.

Three fault sets are seen on the Dundee property. An early north-striking set trends parallel to the More Creek valley. A later east-trending set displaces the major intrusive body and cuts some skarn zones. Slickensides on this set indicate subhorizontal dextral movement. The latest, northeast-trending set apparently displaces the east-striking faults (Figure 2-10-2).

Three types of mineralization are recognized. Thin, irregular veins of quartz, carbonate and pyrite, with sporadic chalcopyrite, cut both the intrusions and the volcanic-

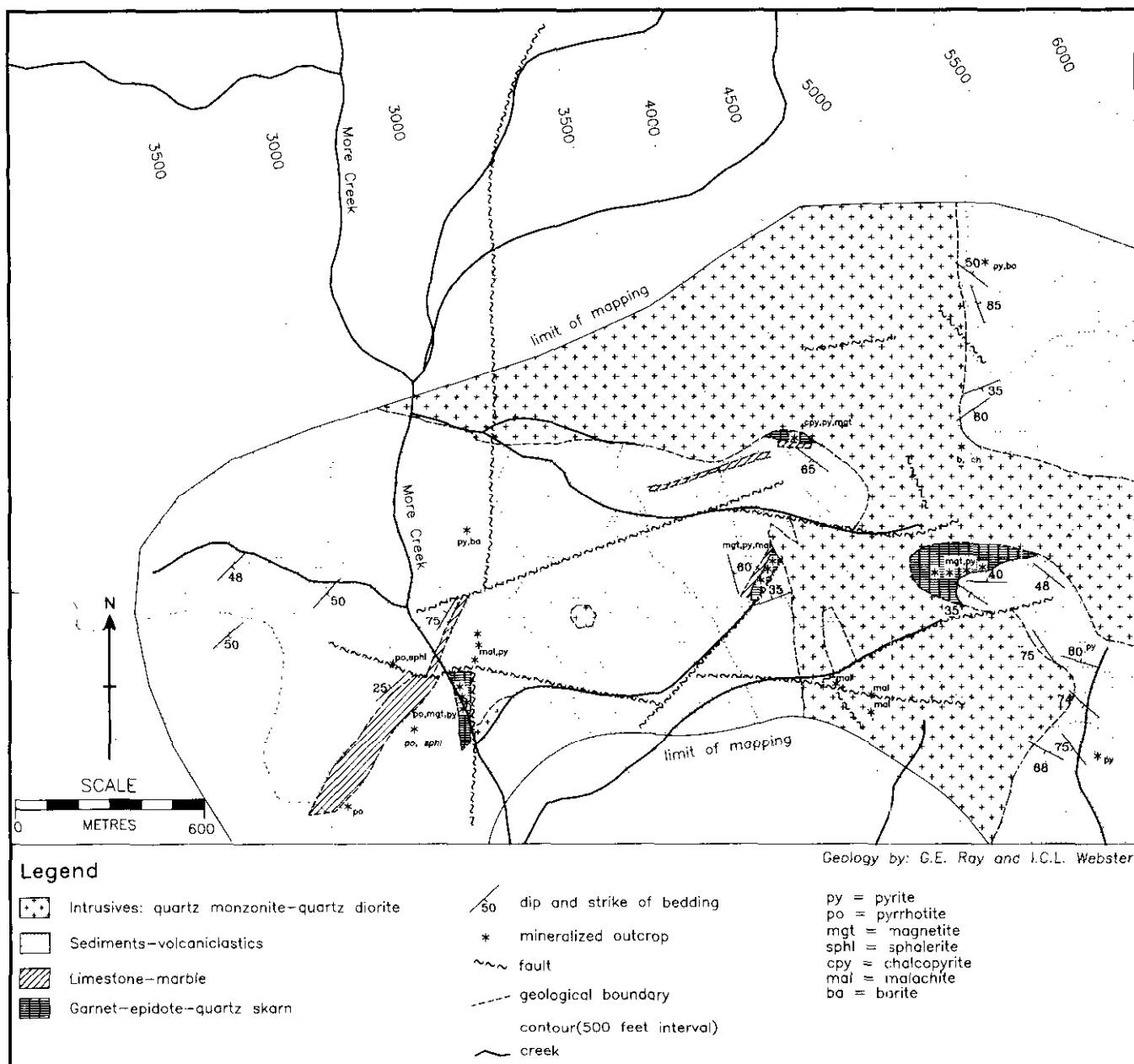


Figure 2-10-2. Geological map of the Dundee (Gla) skarn, showing areas of mineralization.

sedimentary package; these are locally weakly stained with malachite. In at least two localities, narrow veins also carry dolomite, chalcopyrite and barite.

In addition to the veins, pervasive silicification with disseminated pyrite mineralization overprints the quartz monzonite and the country rocks. It appears to be related to the nearby intrusion and it is locally associated with structurally controlled zones of intense pyritic alteration, up to 4 metres thick, that crosscut bedding.

The third type of mineralization is related to skarns, and appears to be the only type with economic potential. Four major areas of skarn alteration are seen (Figure 2-10-2), although numerous minor skarn zones are present on the

property. The northernmost skarn, exposed at an elevation of 1375 metres (4520 feet) lies close to the contact between quartz monzonite, to the north, and an east-southeast-trending marble unit 30 to 35 metres thick. The skarn is largely covered by talus, but above the scree slope, chalcopyrite-pyrite mineralization occurs along the sheared contact between the monzonite and a feldspar-porphyrific andesite dike. Immediately to the east of the scree, outcrops of steeply dipping marble pass gradationally into massive garnetite skarn that is cut by veins and lenses of magnetite and pyrite. At this locality, the sulphide and magnetite-rich zone tends to separate garnetite skarn from sheared and hornfelsed metasediments and plagioclase porphyry sills

and dikes. Assay results on a chalcopyrite-bearing sample collected from this skarn locality are shown in Table 2-10-1. The sample is enriched in gold, silver, copper and zinc, and contains anomalous antimony.

The second area of extensive skarn alteration crops out about 600 metres farther east-southeast. Massive garnetite-epidote skarn is exposed over a 200-metre width. This skarn is cut by numerous epidotized monzonite-diorite dikes. Veins and masses of magnetite contain white clots of quartz and carbonate that are often rimmed with brown garnet. Both brown and yellowish green garnets are seen in this skarn, and several generations of garnet are recognized; late veins of garnetite cut earlier, banded garnet-epidote skarn.

The third extensive garnet-epidote skarn on the property lies about 600 metres farther west at an elevation of 1250 metres (4100 feet). It is developed at the contact between marble and the quartz monzonite intrusion. Skarn assemblages include coarse brownish green euhedral garnet, up to 3 centimetres across, with variable amounts of epidote, and carbonate. Metallic minerals include magnetite, pyrite, minor pyrrhotite and chalcopyrite.

The fourth major skarn is located close to More Creek at the 760-metre elevation (2500 feet). It lies along a northerly trending fault and differs from the other three major skarns in that it does not lie close to the major quartz monzonite to quartz diorite intrusion. It includes two types of mineralization. One of these forms semimassive pods and lenses of pyrrhotite. The host rock is a silicified and epidotized, green andesitic ash and lapilli tuff that is locally cut by quartz and carbonate veins. At least eight of the pyrrhotite lenses have been mapped. They are up to 5 metres long and 2 metres wide, outcrop on both sides of More Creek and trend approximately north-northeast and dip 30 to 35° west. The other type of mineralization, associated with pale, reddish brown garnetite skarn, includes coarse, radiating magnetite crystals intergrown with minor pyrite, as well as irregular pods of pyrite, up to 20 centimetres wide.

To summarize, the Dundee (Gla) skarns include garnet, epidote, quartz, potassium feldspar, carbonate with rare pyroxene and wollastonite. Mineralization comprises massive and veined magnetite with variable amounts of pyrite, pyrrhotite, chalcopyrite, sphalerite and gold. The westernmost skarn is characterized by semimassive lenses of pyrrhotite. Most of the Dundee skarns are garnet-rich exoskarns that replace limestone; they differ from many other skarns in the district in being locally pyrrhotite-rich.

McLYMONT NORTHWEST ZONE: MINFILE 104B 281 (McLYMONT 3, WARRIOR 4, DIRK AND KEN)

Skarn mineralogy: Magnetite, pyrite, chalcopyrite, gold, galena, sphalerite, tetrahedrite, chlorite, quartz, calcite, dolomite, siderite, jasper, potassium feldspar. (?) barite.

This property lies about 2 kilometres southwest of Newmont Lake (Figure 2-10-1) and is currently being explored by Gulf International Minerals Ltd. The mineralogy and morphology of this gold deposit, which is described by Ray *et al.*, (this volume), is distinct from most of the other skarns

in the district. It is tentatively classified as a retrograde-altered gold-rich skarn that contains chimney and manto-type ore zones.

UNNAMED SKARN

Skarn mineralogy: magnetite, pyrite, chalcopyrite, garnet, epidote, tremolite-actinolite, potassium feldspar, lizardite, (?) barite.

This skarn is situated east of Snippaker Creek (Figure 1-10-1), about 4.5 kilometres north of the Snippaker airstrip, at an elevation of between 1575 and 1725 metres (5180 to 5660 feet). The area is underlain by a package of altered, massive to bedded ash tuffs, tuffaceous sediments and massive limestones that strike east-southeast and dip steeply north. These are intruded by early sills and dikes of altered, porphyritic quartz monzonite, as well as thin, late sills of epidotized mafic andesite. The quartz monzonite contains variable amounts of megacrystic potassium feldspar, up to 2.5 centimetres long, together with some coarse hornblende phenocrysts. These intrusions, which locally contain xenoliths, are sporadically epidotized and cut by veinlets of potassium feldspar and pyrite. Both the tuff-sediment package and the intrusions are cut by numerous northeast to north-northeast-striking faults.

The extensive gossanous skarn visited in this survey occurs on a steep, west-facing slope at an elevation of 1725 metres. Farther upslope to the east, the mountaintop appears to be largely underlain by carbonate and there are numerous gossans that could mark other skarns. The visited skarn is hosted by bedded tuff close to its faulted contact with a quartz monzonite intrusion. The banded skarn is characterized by an assemblage of epidote, potassium feldspar, tremolite-actinolite, quartz, carbonate and minor pyroxene cut by veinlets of epidote and potassium feldspar. Metallic minerals include magnetite, with moderate amounts of pyrite and traces of chalcopyrite. Pyrite veins ranging up to 4 centimetres in width also occur. No garnet was seen in outcrop, but mafic hornblende diorite and marble float at the toe of the glacier below the skarn outcrop contain veins of brown garnet rimmed with epidote. Boulders of magnetite-pyrite-bearing marble with yellow-green lizardite were also seen at this locality.

Assay results on two mineralized samples collected from this skarn are shown in Table 2-10-1; they show only low values of gold, silver and base metals.

CONCLUSIONS

The Iskut River-Scud River area contains numerous mineralized skarns that have only recently received serious exploration attention. Many of the occurrences, based on their predominant economic commodity, appear to represent copper or iron-copper skarns, some of which are sporadically enriched in gold. The McLymont Northwest zone, however, may represent a retrograde-altered gold-rich skarn. The occurrence of lizardite at the Scud River and Kirk skarns, together with the presence of dolomites in the region, suggests that some occurrences may have magne-sian skarn affinities.

This preliminary field investigation suggests the following conclusions with respect to skarns in the Iskut River–Scud River area:

- They are commonly associated with monzonite, quartz monzonite or quartz monzodiorite intrusions rich in potassium feldspar. Skarn-related diorites and gabbros are rare.
- They are commonly hosted in carbonate-rich sediments and tuffs where these rocks are intruded by either large plutons or small dikes and sills. In some cases, however, (e.g. McLymont) no intrusions have been identified immediately adjacent to the skarn.
- The skarn morphology varies from stratiform (Kirk magnetite) to irregular (Dirk) to chimney and mantle-like (McLymont).
- Most skarns have high garnet/pyroxene ratios and low pyrrhotite/pyrite ratios. Pyroxene-rich assemblages are seen only in the footwall of the Kirk magnetite skarn. Some skarns, such as the Stu and Shan, contain coarse tremolite-actinolite.
- Many skarns are characterized by abundant magnetite, and minor amounts of hematite. Pyrite and chalcopyrite are the most abundant sulphides; no arsenopyrite was positively identified, although trace amounts may exist in the McLymont Northwest zone (Ray *et al.*, this volume), and at the Stu.
- Preliminary trace element analyses indicate some skarns such as the Dundee, and possibly the Scud River, are sporadically enriched in gold. The anomalous bismuth and tellurium at the Shan skarn suggests the presence of bismuth tellurides.
- Late barite-carbonate veining is seen at many skarns, but it is uncertain whether this is associated with the skarn or to some later, unrelated mineralizing event.
- The most common skarn silicates are garnet and epidote. Potassium feldspar is also a common minor constituent. The McLymont mineralization is associated with intense silicification and carbonate alteration of the wallrocks.
- The low pyrrhotite/pyrite ratios, abundance of garnet and the presence of hematite suggest most skarns in the Iskut River area formed in a relatively oxidized environment. The Scud River skarn and some of the Dundee (Gla) skarns are unusual in being pyrrhotite-rich.

ACKNOWLEDGMENTS

We wish to thank the following for their help: I. Hagemoen, J. Buccholz and S.J. Tennant of Kestrel Resources Ltd., R. Davis, G.G. Carlson, V.A. Jaramillo and P. Carter of Gulf International Minerals Ltd. and S. Todoruk of Pamicon Developments Ltd. The generous provision of helicopter support by these three companies was largely instrumental in our completing this field project. Bob Paul and Kenton McNutt provided good field assistance.

Geological Fieldwork 1990, Paper 1991-1

REFERENCES

- Anderson, R.G. (1989): A Stratigraphic, Plutonic, and Structural Framework for the Iskut River Map Area, Northwestern British Columbia; *in* Current Research, Part E: *Geological Survey of Canada*, Paper 89-1E, pages 145-154.
- Blanchflower, J.D. (1988): Geology of the Stu Claims, Iskut River Area; unpublished report for *Kestrel Resources Ltd.*
- Britton, J.M., Fletcher, B.A., Alldrick, D.J. (1990): Snip-paker Map Area (104B/6E, 7W, 10W, 11E); *B.C. Ministry of Energy, Mines and Petroleum Resources, Geological Fieldwork 1989*, Paper 1990-1, pages 115-125.
- Britton, J.M., Webster, I.C.L. and Alldrick, D.J. (1989): Unuk Map Area (104B/7E, 8W, 9W, 10E); *B.C. Ministry of Energy, Mines and Petroleum Resources, Geological Fieldwork 1988*, Paper 1989-1, pages 241-250.
- Brown, D.A., and Greig, C.J. (1990): Geology of the Stikine River – Yehiniko Lake Area, Northwestern British Columbia (104G/11W and 12E); *B.C. Ministry of Energy, Mines and Petroleum Resources, Geological Fieldwork 1989*, Paper 1990-1, pages 141-151.
- Brown, D.A., Greig, C.J. and Gunning, M.H. (1990): Geology of the Stikine River–Yehiniko Area, Northwestern B.C.; *B.C. Ministry of Energy, Mines and Petroleum Resources*, Open File 1990-1.
- Ettlinger, A.D. and Ray, G.E. (1989): Precious Metal Enriched Skarns in British Columbia: an Overview and Geological Study; *B.C. Ministry of Energy, Mines and Petroleum Resources*, Paper 1989-3, 128 pages.
- Logan, J.M., Koyanagi, V.M., and Drobe, J.R. (1990a): Geology of the Forrest Kerr Creek Area, Northwestern British Columbia (104B/15); *B.C. Ministry of Energy Mines and Petroleum Resources, Geological Fieldwork 1989*, Paper 1990-1, pages 127-139.
- Logan, J.M., V.M. Koyanagi and J.R. Drobe (1990b): Geology, Geochemistry and Mineral Occurrences of the Forrest Kerr–Iskut River Area, Northwestern British Columbia; *B.C. Ministry of Energy Mines and Petroleum Resources*, Open File 1990-2, 2 sheets.
- Kerr, F.A., (1948): Lower Stikine and Western Iskut River Areas, British Columbia; *Geological Survey of Canada*, Memoir 246, 94 pages.
- Klesman, W.D. and Ikona, C.K. (1988): *Geological Report on the Au1, Au2, Biz, Nez Mineral Claims*; unpublished report for *Chandi Resources Corporation*, June 1988.
- Monger, J.W.H., Price, R.A., Tempelman-Kluit, D.J. (1982): Tectonic Accretion and the Origin of Two Major Metamorphic Belts in the Canadian Cordillera; *Geology*, Volume 10, pages 70-75.
- Ray, G.E., Jaramillo, A.V. and Ettlinger, A.D. (1991): The McLymont Northwest Zone, Northwest British Columbia: A Gold-rich Retrograde Skarn?; *B.C. Ministry of Energy, Mines and Petroleum Resources, Geological Fieldwork 1990*, Paper 1991-1, this volume.
- Webster, I.C.L. and McMillan, W.J. (1990): Structural Interpretation of Airborne Synthetic Aperture Radar Imagery in the Sulphurets–Unuk–Iskut River Area, Northwest British Columbia (104B); *B.C. Ministry of Energy, Mines and Petroleum Resources*, Open File 1990-7.

NOTES



**THE McLYMONT NORTHWEST ZONE, NORTHWEST BRITISH COLUMBIA:
A GOLD-RICH RETROGRADE SKARN? (104B)**

**By G.E. Ray, Geological Survey Branch
V.A. Jaramillo, Gulf International Minerals Limited
and A.D. Ettlinger, Mineral Deposit Research Unit, U.B.C.**

KEYWORDS: Economic geology, skarn, gold, Iskut River, manto, retrograde skarn, garnet microprobe analyses, silicification, galena-lead isotopes.

INTRODUCTION

The McLymont property is located close to the headwaters of McLymont Creek, a tributary of the Iskut River; it lies at an elevation of approximately 1170 metres (3800 feet), about 2 kilometres southwest of Newmont Lake (Figure 2-11-1). The property is currently being explored by Gulf International Minerals Ltd. It contains two styles of mineralization whose relationship to each other is uncertain. One of these, the "Camp zone", consists of auriferous quartz-ankerite-pyrite-chalcopyrite veins hosted by a quartz-rich granite close to its contact with Triassic and Jurassic rocks. The second style, the "Northwest zone", comprises steeply dipping and subhorizontal zones of magnetite-sulphide-gold mineralization hosted in Mississippian rocks. This paper describes the geology and mineralization of the Northwest zone, and is based on preliminary work that includes core logging, polished thin-section studies, microprobe analyses of garnets, galena-lead isotope analyses, and some trace element analyses (Table 2-11-1).

REGIONAL GEOLOGY

The first major geological study of the region was presented by Kerr (1948). Recent work includes 1:50 000-scale geological mapping by Logan *et al.* (1990a) as well as other work by Read *et al.* (1989), Anderson (1989), Britton *et al.*

(1989, 1990), Webster and McMillan (1990), Anderson and Bevier (1990) and Logan *et al.* (1990b). A descriptive report of the skarn occurrences in the district is given by Webster and Ray (1991, this volume).

The area lies within the Stikine lithostructural terrane which represents a mid-Paleozoic to Mesozoic island-arc sequence of volcanic and sedimentary rocks. The Paleozoic rocks range from Devonian to Permian in age and form part of the Stikine assemblage, while the Mesozoic includes both the Upper Triassic Stuhini Group and the Jurassic Hazelton Group. These supracrustal rocks are intruded by Early Jurassic to Cretaceous and Tertiary plutons (Logan *et al.*, 1990b).

The region is cut by two sets of major faults. The most abundant are narrow, north-striking linear faults; one of these, the Forrest Kerr fault (Logan *et al.*, 1990a), has influenced the lower course of the Forrest Kerr Creek (Figure 2-11-1). The other set forms complex, north-northeast to northeast-trending fault zones. The faults bounding the Newmont graben belong to this set; the graben is 1 to 2 kilometres wide and contains downdropped Jurassic and Triassic sediments, tuffs and some intrusions that are juxtaposed against Paleozoic rocks to the east and west (Figure 2-11-1).

PROPERTY GEOLOGY

Previous studies on the property have been by Grove (1986, 1989), who first identified the McLymont Northwest zone as a skarn, and by Koyanagi (1990). The Camp zone

**TABLE 2-11-1
ASSAY RESULTS OF SELECTED UNMINERALIZED AND MINERALIZED SAMPLES: McLYMONT NORTHWEST ZONE**

Lab No.	Au	Ag	Cu	Pb	Zn	Co	Ni	Mo	As	Sb	Bi	Te	Se
041347	239	5	0.36%	38	81	21	4	8	110	8	<5	1.4	0.1
041348	176	5	0.49%	7	48	51	112	8	80	3	<5	4.0	18.0
041349	444	20	0.16%	125	28	38	10	8	424	10	<5	1.6	0.1
041350	1670	23	2.10%	255	52	129	42	8	835	16	11	4.0	0.1
041374	11938	30	1.18%	313	51	75	4	8	690	21	8	1.4	0.1
041375	2848	8	0.34%	13	73	6	6	52	115	4	<5	0.3	0.1

Units and Methods:

Au, in ppb; all other values in ppm except where noted in per cent (%).
Au, FA/ICP; Te and Se AH/ICP; all other elements are by AAS.

Sample description:

- 041347: magnetite-pyrite-ankerite alteration adjacent to ore zone, Drillhole 89-19.
- 041348: pyrite-quartz veining adjacent to ore zone, Drillhole 89-19.
- 041349: chlorite-pyrite-carbonate alteration adjacent to ore zone, Drillhole 89-19.
- 041350: coarse pyrite-magnetite-chlorite alteration, Drillhole 89-19.
- 041374: pyrite-chalcopyrite-carbonate mineralization from ore in mushroom zone, Drillhole 89-20.
- 041375: magnetite-pyrite-carbonate mineralization from ore in mushroom zone, Drillhole 89-18.

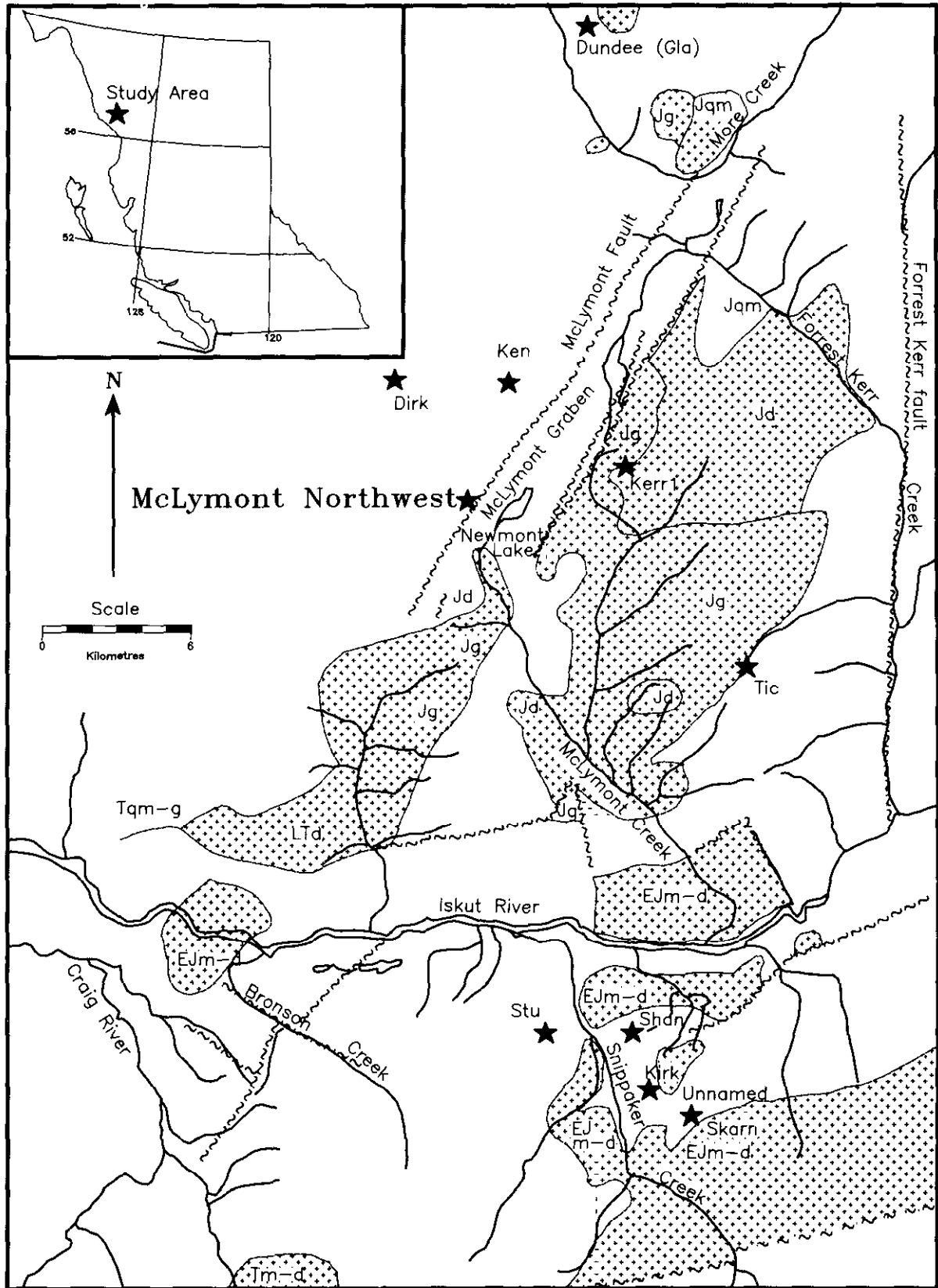


Figure 2-11-1. Location of the McLymont Northwest zone in relation to the McLymont graben and other skarn occurrences in the district. (see Webster and Ray, 1991, this volume). Geology after Logan *et al.* (1990b) and Britton *et al.* (1990).

Legend

- J, EJ = Jurassic, Early Jurassic
- T, LT = Tertiary, Late Tertiary
- d = diorite
- g = granite
- m = monzonite

- = undifferentiated supracrustals
- ★ = skarn location
- = regional fault
- = approximate geological contact

vein mineralization is exposed in the McLymont graben, east of the bounding McLymont fault (Logan *et al.*, 1990a). By contrast, the McLymont Northwest zone lies immediately west of the McLymont fault (Figure 2-11-1). The dip direction of the fault is unknown; consequently it is uncertain whether it represents a normal or high-angle reverse fault. Airphoto interpretation indicates that the rocks on both sides of the McLymont fault are cut by northerly trending fractures that probably represent second-order splay structures off the main fault. Several sets of faults are recognized on surface above the Northwest zone. An early, north-striking, steeply east-dipping set is probably related to these second-order structures; slickenslides on this set plunge steeply east. This set is cut by younger, east-trending faults with slickenslides indicating subhorizontal dextral movement.

The deposit is hosted by a Mississippian clastic marine succession that is several hundred metres thick. The upper part comprises fresh, green, massive andesitic ash and lapilli tuffs with thin units of marble. Lower down, where the mineralization occurs, is a sequence of bedded tuffs, thin-bedded tuffaceous siltstones, occasional units of massive ash and crystal tuff, and some horizons of white to grey marble, some of which contain remnant crinoids. The lowest part of the sequence, which is seen in drill-core, includes lapilli and ash tuff, with minor tuff breccia and tuffaceous siltstone. Excellent grading in the tuffaceous siltstones indicates the Mississippian package hosting the mineralization is upright. Poorly defined bedding attitudes measured on surface suggest that the area of drilling lies close to a northerly striking and plunging fold; the western limb of this fold dips 35 to 75° northwest while the eastern limb apparently dips steeply southeast. This structure is not well understood but it has possibly controlled some of the ore zones.

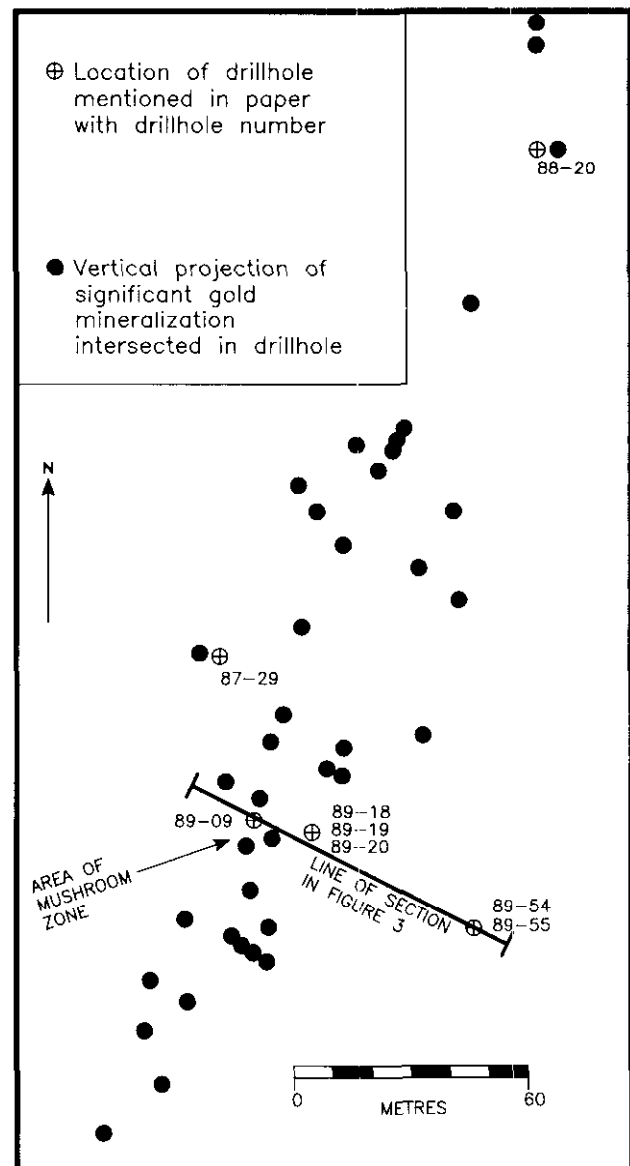


Figure 2-11-2. Location of mineralized drillholes – McLymont Northwest zone. Note line of section for Figure 2-11-3. Data courtesy of Gulf International Minerals Ltd.

MINERALIZATION IN THE NORTHWEST ZONE

The deposit plunges north and has been traced by drilling for over 300 metres in a north-northeast direction (Figure 2-11-2), although it remains unexplored to the north and south. It occurs both in steep, generally narrow, possibly fracture-controlled zones, and in gently dipping, thicker zones that appear to have replaced units of coarse, crinoidal marble and lesser amounts of calcareous siltstone and tuff. In one southern section, several steeply dipping mineralized zones pass upwards into an extensive, sulphide-rich “mushroom zone” (Figure 2-11-3); it is uncertain whether this represents a mineralized fold structure or is the result of

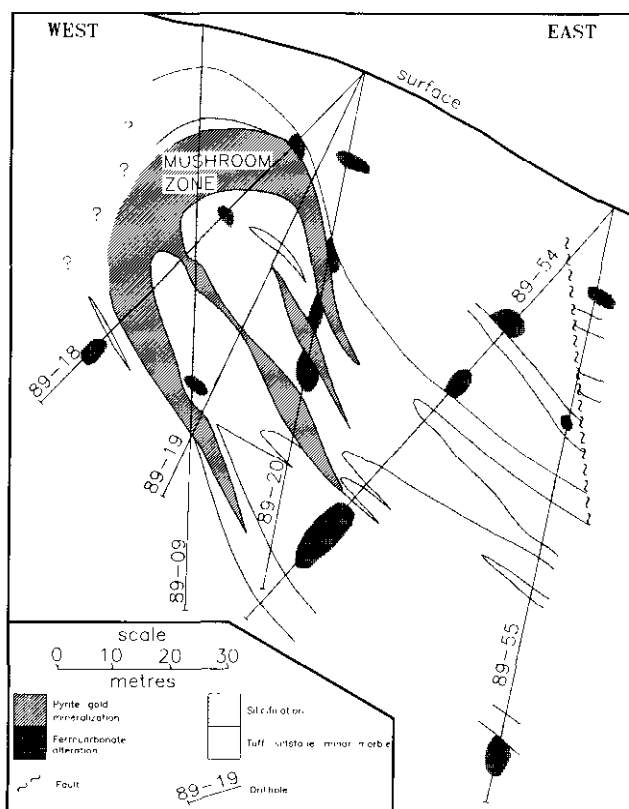


Figure 2-11-3. Generalized geological cross-section across the southern part of the McLymont Northwest zone, (for location see Figure 2-11-3). Interpretation based on core logging by G.E. Ray.

mineralization controlled by the intersection of steep fractures and a subhorizontal carbonate unit. At the northern end of the deposit, the ore zones are shallow dipping. Gold grades are sometimes very high. For example, the MINFILE database records that Drillhole 87-29, located north of the mushroom zone (Figure 2-11-2), cut an 11.2-metre intercept that assayed 55.02 grams gold and 1362 grams silver per tonne, and 0.97 per cent copper. Trace element analytical results on unmineralized and mineralized drill-core samples are shown in Table 2-11-1. Besides gold and copper enrichment, weakly anomalous antimony, arsenic, bismuth and tellurium values are recorded in some samples.

Mineralization consists principally of pyrite and magnetite, with subordinate chalcopyrite and trace galena, sphalerite and gold, in a carbonate-quartz-chlorite gangue. Other minerals present include hematite, sericite, jasper, garnet, rutile, sphene, covellite, tetrahedrite, barite and gypsum; graphite is sporadically present, particularly along fault zones. Trace amounts of a minute bladed mineral, tentatively identified as arsenopyrite, were noted in one thin section.

The magnetite is irregularly distributed; it displays two habits: a rounded to nodular form which apparently replaces carbonate, and an acicular to bladed form that results in crystals up to 2 centimetres long (Plate 2-11-1). Similar elongate magnetite crystals are observed in other skarns such as those at the Merry Widow mine and Nanaimo Lakes

on Vancouver Island, and the Texada Island iron mines (Ettlinger and Ray, 1989). At McLymont, this magnetite appears to replace an early, pale green mineral, which is tentatively identified as tremolite-actinolite.

Small isolated remnants of garnet, as well as pseudomorphs after garnet (Plate 2-11-2), are observed throughout the deposit. Garnet is commonly fractured (Plate 2-11-3) and retrograde-altered to jasper, carbonate or chlorite; generally, only millimetre-sized glassy fragments of unaltered garnet remain. Most garnet replaces marble, where it originally formed either isolated, euhedral crystals or small masses. Garnet pseudomorphs occur as concentric zones of deep red jasper alternating with brown jasper and carbonate. Thin-section studies show the unaltered garnets commonly have isotropic, yellowish brown cores and clear, birefringent, zoned overgrowths. Microprobe analyses indicate they are iron-rich and contain less than 5 per cent manganese. The isotropic cores are generally Ad₉₅ to Ad₁₀₀ mole per cent while the overgrowths range from Ad₅₉ to Ad₆₄ mole per cent (Figure 2-11-4).

Pyrite also occurs in two habits, both of which carry gold. The commonest forms coarse, rounded subhedral crystals up to 1 centimetre in diameter; these may occur as single, isolated crystals within carbonate, or as large clusters and irregular masses that, in thin section, are seen to contain cataclastic textures (Plate 2-11-4) and abundant inclusions. Some of this pyrite replaces either large carbonate crystals, remnant crinoid ossicles or garnet. The other pyrite is fine grained and massive, and locally carries very high gold values. It occurs as veins and masses that postdate the coarse crystalline pyrite. In polished section it is seen to comprise densely packed clusters of small, euhedral, subhedral and anhedral crystals in a carbonate, quartz or chloritic matrix (Plate 2-11-5).

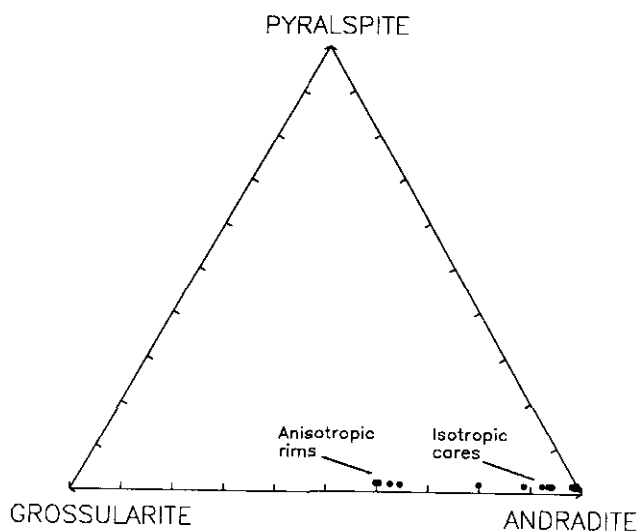


Figure 2-11-4. Composition of garnets from the McLymont Northwest zone (25 analyses). Note andraditic cores and more grossularitic rims. Microprobe analyses by A.D.Ettlinger at The University of British Columbia.

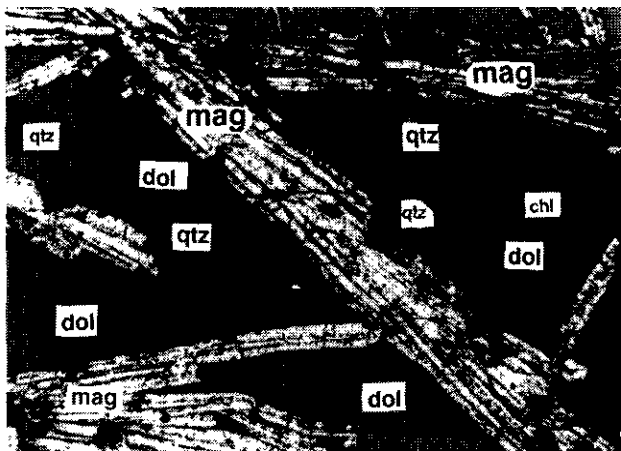


Plate 2-11-1. Photomicrograph of elongate magnetite (mag) in a matrix of dolomite (dol), chlorite (chl) and euhedral quartz crystals (qtz), Drillhole 89-18. Reflected PPL, x 100 magnification.



Plate 2-11-4. Brecciated, coarse, first generation pyrite in a carbonate matrix, Drillhole 89-18. Reflected PPL, x 150 magnification.



Plate 2-11-2. Jasper-chlorite pseudomorphs after euhedral garnet in marble, Drillhole 88-36.

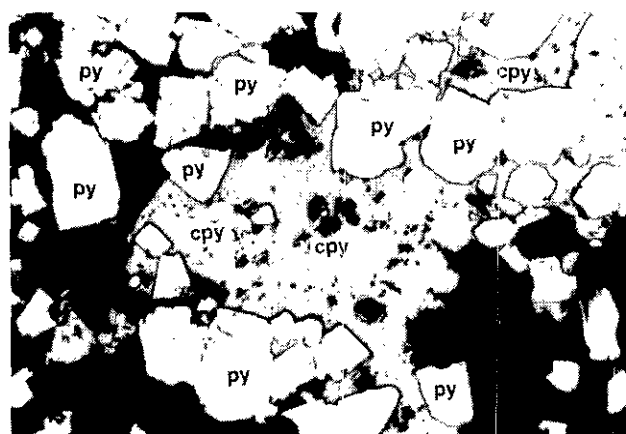


Plate 2-11-5. Anhedral to subhedral, second generation pyrite (py) overgrown by chalcopyrite (cpy), Drillhole 89-29. Reflected PPL, x 150 magnification.

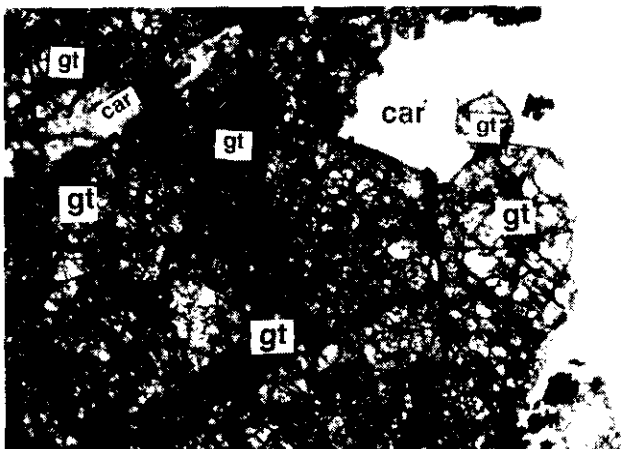


Plate 2-11-3. Photomicrograph of fractured euhedral garnet crystals (gt) intergrown with carbonate (car), Drillhole 89-09. Transmitted PPL, x 100 magnification.

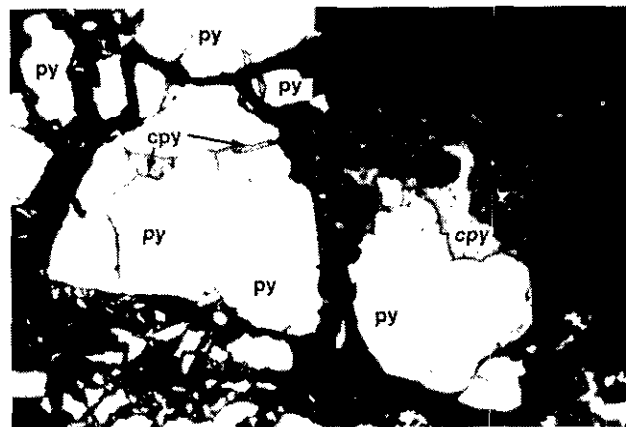


Plate 2-11-6. Brecciated, first generation pyrite (py), with overgrowths and veins of chalcopyrite (cpy), Drillhole 89-18. Reflected PPL, x 100 magnification.

Chalcopyrite is widespread throughout the mineralized zones. It occurs as overgrowths or veinlets that cut both the coarse and fine pyrite (Plates 2-11-5 and 6), as small inclusions within sphalerite, or as late veinlets with barite, carbonate and quartz. Galena, sphalerite, tetrahedrite and covellite are rare and tend to occur in small veins. Galena forms anhedral skeletal masses that are spatially associated with pyrite and chalcopyrite. Sphalerite forms coarse to fine clots, while covellite is fine grained and occurs with chalcopyrite and tetrahedrite. Hematite forms isolated crystals and veinlets that cut both the magnetite and the coarse and fine pyrite.

Chlorite is sporadically distributed, but tends to show a spatial correlation with the magnetite-sulphide zones and can carry visible gold. It forms large, black to dark green, irregular and deformed masses as well as fine-grained clots. It appears to replace and pseudomorph quartz, carbonate, garnet and possibly pyroxene.

Quartz occurs in veins and as isolated, euhedral crystals. The irregular, thin white veins cut the coarse and fine pyrite; they contain vugs lined with elongate, euhedral quartz crystals. These crystals reach 2 centimetres in length and commonly grow within carbonate (Plate 2-11-1).

Disseminations and small masses of sericite can make up to 20 per cent of the rock in some thin sections; it appears to be a relatively late alteration mineral and largely replaces original feldspar. Trace amounts of sphene and rutile are present; the latter as disseminated, small (<20 micrometres) subhedral crystals.

The mineralized zones are also characterized by abundant white to cream to pale brown carbonate that includes calcite, dolomite, ankerite and siderite. Carbonate occurs both as a groundmass to the magnetite and sulphides (Plate 2-11-1) and as late crosscutting veins. Some of the late dolomitic and ankeritic veins contain stringers of chalcopyrite and small masses of white barite.

Although some coarse visible gold is seen in chlorite, polished-section studies suggest that most of the gold is very fine grained (<15 micrometres). These minute grains of gold are seen in chlorite and as inclusions in both the coarse pyrite crystals and the younger, fine-grained pyrite.

The mineralized zones and the adjacent white marble can contain small amounts of red, podiform jasper that have replaced garnet. Isolated jasper pseudomorphs of large euhedral garnet crystals are occasionally seen in the marble (Plate 2-11-2). Locally, jasper is partially replaced by pyrite, and some jasper pseudomorphs are rimmed with magnetite and chlorite.

The mineralized zones are surrounded by irregular envelopes of early silicification and later ankeritic-dolomitic alteration up to 25 metres wide (Figure 2-11-3). The silicified rocks vary from grey to pale green to pale brown in colour. Silica can crosscut bedding or may selectively replace certain beds in the tuffaceous siltstones, resulting in alternating layers of unaltered and silicified rock. Where complete silicification has occurred, extensive zones of

massive chert-like rock are formed. Silicification was followed by the introduction of brown-coloured carbonate that includes siderite, ankerite and dolomite; this occurs either as a massive overprinting or as fracture-related ferrocarbonate veins and breccias. Some of the carbonate veins contain small euhedral quartz crystals, stringers of chalcopyrite, and clots of white barite.

Mineral textures suggest the following broad paragenesis: 1. garnet, 2. jasper and chlorite, (the chlorite possibly replaced early pyroxene), 3. magnetite, 4. coarse pyrite, 5. fine-grained pyrite, 6. quartz veining and silicification, 7. pervasive and vein-carbonate alteration.

There are at least two generations of chalcopyrite: the first is associated with, but postdates pyrite, while the second is found in late quartz-carbonate-barite veins. Sphalerite may postdate the early chalcopyrite. Specular hematite postdates both the magnetite and pyrite. The relative age of the gold is uncertain although it appears to be associated with pyrite and chlorite, but not with chalcopyrite.

GALENA-LEAD ISOTOPES

Sphalerite-galena veins tend to be more common on the outer margins of the Northwest zone and are interpreted to represent a distal part of the hydrothermal system. A galena sample from a sphalerite-galena vein in Drillhole 88-20, at the north end of the deposit (Figure 2-11-2), was analysed at The University of British Columbia for its lead isotope ratios; $^{208}\text{Pb}/^{206}\text{Pb}$ and $^{207}\text{Pb}/^{206}\text{Pb}$ ratios of 2.0429 and 0.83223 respectively (± 0.01 per cent error for each) were measured (A.D.R. Pickering, personal communication, 1990).

When these galena-lead isotope ratios are compared to similar data from other deposits in the Iskut-Stewart area (*see Godwin et al.*, 1991, this volume), an Early Jurassic, or older age for the mineralization is indicated. The measured ratios are consistent with a tight cluster of precious metal deposits that are cogenetic with the Jurassic Hazelton Group. These include Eskay Creek, Premier, Scotty Gold, Kerr, Johnny Mountain and Snip. All but Eskay Creek and Snip are closely associated with the Texas Creek plutonic suite which has been dated as Early Jurassic (Brown, 1987).

DISCUSSION

The silicate-sulphide mineral assemblages in the Northwest zone deposit indicate it may represent a retrograde skarn, while the abundant dolomitic alteration suggests it could have magnesian skarn affinities. The importance of retrograde activity in developing an ore-grade skarn deposit has previously been described by Meinert (1986). Remnant early andradite garnet is preserved in the deposit, particularly within the mushroom zone, although most of the garnet is now a retrograde assemblage of jasper, hematite, carbonate, chlorite and quartz. The mushroom zone is underlain and enveloped by a halo of intense silicification (Figure 2-11-3) in which the marble and clastic rocks are replaced largely by silica and chlorite with lesser magnetite

and pyrite. At the outer margins of this envelope, and distal to the deposit, are thin veins containing sphalerite and galena; one of these veins was sampled for galena-lead isotope analysis.

Development of garnet skarn close to a source of hydrothermal fluids, with more distal hydrous silicate alteration and silicification, and peripheral base metal mineralization is well documented (Zharikov, 1970; Einaudi *et al.*, 1981; Meinert, 1983). The alteration paragenesis observed in the Northwest zone suggests the mushroom zone was a garnet-bearing skarn that formed close to the source of the hydrothermal fluids. Outwards from this feeder zone, pyroxene may originally have crystallized and later been destroyed during the subsequent retrogression that accompanied sulphide deposition, as no pyroxene has been positively identified in the deposit.

The gold-rich Northwest zone is unusual in that it does not contain the reduced mineral assemblages that characterized other gold skarns in British Columbia (Ettlinger and Ray, 1989; Ray *et al.*, 1990). Iron-bearing phases in the deposit are hematite, jasper, magnetite and andradite which all contain abundant Fe³⁺. Pyrite is the most abundant sulphide, while pyrrhotite and arsenopyrite, which characterize other gold skarns, are generally absent. Although pyroxene has not been seen, the abundant chlorite suggests that if prograde pyroxene was originally present, it was probably diopsidic in composition. This contrasts with true gold skarns, such as those in the Hedley district, which are marked by iron-rich, hedenbergitic pyroxenes (Ray *et al.*, 1988; Ettlinger *et al.*, in press).

To summarize, the oxidized assemblage at the McLymont Northwest zone is atypical for Hedley-type gold skarns, but instead resembles those found in skarns associated with porphyry copper systems. Similar, oxidized skarn assemblages occur in the gold-rich McCoy and Surprise deposits in Nevada (Brooks *et al.*, 1990; J.W. Brooks, personal communication, 1990).

CONCLUSIONS

The McLymont Northwest zone is believed to represent a highly retrograde-altered, gold-rich skarn deposit, which, on the basis of galena-lead isotope analyses, is probably Early Jurassic or older in age. Although some coarse visible gold is present, much of the gold is fine grained (<15 micrometres) and commonly occurs as inclusions in pyrite. The pyrite-magnetite-hematite-andradite assemblages indicate the deposit formed under oxidized conditions which are atypical of other gold skarns in British Columbia. Alteration envelopes of silicification and distal base metal veining are present around the deposit; extensive dolomitic alteration may indicate the deposit has magnesian skarn affinities.

Precise controls of the ore zones are not yet fully understood. Mineralization is believed to be both lithologically and structurally controlled, and it is possible that the flat-lying and steeply dipping ore zones represent mantos and chimneys. It is uncertain, however, whether the richest part of the deposit, the mushroom zone, represents a mineralized fold hinge, a stockwork feeder or a pipe.

ACKNOWLEDGMENTS

We are grateful for the assistance and cooperation of the management and staff of Gulf International Minerals Ltd., particularly Reg Davis, Bob Gifford and Paul Carter. Thanks are also expressed to Gerry Carlson for his help, to Colin Godwin and Anne Pickering of The University of British Columbia, for the galena-lead isotope data, and to John Knight for help with the microprobe analyses. Geological discussions with Ian Webster, and the assistance of Bob Paul are also acknowledged.

REFERENCES

- Anderson, R.G. (1989): A Stratigraphic, Plutonic, and Structural Framework for the Iskut River Map Area, Northwestern British Columbia; in Current Research, Part E; *Geological Survey of Canada*, Paper 89-1E, pages 145-154.
- Anderson, R.G. and Bevier, M.L. (1990): A Note on Mesozoic and Tertiary K-Ar Geochronometry of Plutonic Suites, Iskut River Map Area, Northwestern British Columbia; in Current Research, Part E, *Geological Survey of Canada*, Paper 90-1E, (in press).
- Britton, J.M., Webster, I.C.L. and Alldrick, D.J. (1989): Unuk Map Area (104B/7E, 8W, 9W, 10E); *B.C. Ministry of Energy, Mines and Petroleum Resources*, Geological Fieldwork 1988, Paper 1989-1, pages 241-250.
- Britton, J.M., Fletcher, B.A. and Alldrick, D.J. (1990): Snip-paker Map Area (104B/6E, 7W, 10W, 11E); *B.C. Ministry of Energy, Mines and Petroleum Resources*, Geological Fieldwork 1989, Paper 1990-1, pages 115-125.
- Brooks, J.W., Meinert, L.D., Kuyper, B.A. and Lane, M.L. (1990): Petrology and Geochemistry of the McCoy Gold Skarn, Lander County, Nevada; in *Geology and Ore Deposits of the Great Basin*, Symposium Proceedings, *Geological Society of Nevada*, April 1-5, 1990, Sparks, Nevada.
- Brown, D.A. (1987): Geological Setting of the Silbak-Premier Mine, Northwestern British Columbia (104A/4, B/1); unpublished M.Sc. thesis, *The University of British Columbia*, 216 pages.
- Ettlinger, A.D. and Ray, G.E. (1989): Precious Metal Enriched Skarns in British Columbia: an Overview and Geological Study; *B.C. Ministry of Energy, Mines and Petroleum Resources*, Paper 1989-3, 128 pages.
- Ettlinger, A.D., Meinert, L.D. and Ray, G.E. (in press): Skarn Evolution and Hydrothermal Fluid Characteristics in the Nickel Plate Deposit, Hedley District, British Columbia; *Economic Geology*.
- Einaudi, M.T., Meinert, L.D. and Newberry, R.J. (1981): Skarn Deposits; in 75th Anniversary Volume, 1906-1980; *Economic Geology*, B.J. Skinner, Editor, *The Economic Geology Publishing Company*, pages 317-391.

- Godwin, C.I., Pickering, A.D.R. and Gabites, J.E. (1991): Interpretation of Galena-lead Isotopes from the Stewart – Iskut Area (1030, P, 104A, B, G); *B.C. Ministry of Energy, Mines and Petroleum Resources*, Geological Fieldwork 1990, Paper 1991-1, this volume.
- Grove, E.W. (1986): Geology and Mineral Deposits of the Unuk River – Salmon River – Anyox Area; *B.C. Ministry of Energy, Mines and Petroleum Resources*, Bulletin 63, 152 pages.
- Grove, E.W. (1989): Geological Report and Development Proposal on the McLymont Creek Property in the Iskut River Area, N.W. British Columbia; *Gulf International Minerals Ltd.*, unpublished report.
- Logan, J.M., Koyanagi, V.M. and Drobe, J.R. (1990a): Geology, Geochemistry and Mineral Occurrences of the Forrest Kerr – Iskut River Area, Northwestern British Columbia, (104B/15 and part of 104B/10); *B.C. Ministry of Energy, Mines and Petroleum Resources*, Open File 1990-2.
- Logan, J.M., Koyanagi, V.M. and Drobe, J.R. (1990b): Geology of the Forrest Kerr Creek Area, Northwestern British Columbia (104B/15); *B.C. Ministry of Energy, Mines and Petroleum Resources*, Geological Fieldwork 1989, Paper 1990-1, pages 127-139.
- Kerr, F.A. (1948): Lower Stikine and Western Iskut River Areas, British Columbia; *Geological Survey of Canada*, Memoir 246, 94 pages.
- Koyanagi, V.M. (1990): Northwest Zone, McLymont Property, Northwestern British Columbia; *B.C. Ministry of Energy, Mines and Petroleum Resources*, Exploration in British Columbia 1989, pages 225-227.
- Meinert, L.D. (1983): Variability of Skarn Deposits; in *Guides to Exploration; in Revolution in the Earth Sciences – Advances in the Past Half-Century*, S.J. Boardman, Editor, *Kendall/Hunt Publishing Company*, pages 301-316.
- Meinert, L.D. (1986): Gold in Skarns of the Whitehorse Copper Belt, Southern Yukon; in *Yukon Geology*; J.A. Moran and D.S. Emond, Editors; *Indian and Northern Affairs Canada*, Exploration and Geological Services Division, Volume 1, pages 19-43.
- Ray, G.E., Dawson, G.L. and Simpson, R. (1988): Geology, Geochemistry and Metallogenic Zoning in the Hedley Gold-skarn Camp; *B.C. Ministry of Energy, Mines and Petroleum Resources*, Geological Fieldwork 1987, Paper 1988-1, pages 59-80.
- Ray, G.E., Ettliger, A.D. and Meinert, L.D. (1990): Gold Skarns: Their Distribution, Characteristics and Problems in Classification; *B.C. Ministry of Energy, Mines and Petroleum Resources*, Geological Fieldwork 1989, Paper 1990-1, pages 237-246.
- Read, P.B., Brown, R.L., Psutka, J.F., Moore, J.M., Journey, M., Lane, L.S. and Orchard, M.J. (1989): Geology of Parts of Snippaker Creek (104B/10), Forrest Kerr Creek (104B/15), Bob Quinn Lake (104B/16), Iskut River (104G/1), and More Creek (104G/2); *Geological Survey of Canada*, Open File 2094.
- Webster, I.C.L. and McMillan, W.J. (1990): Structural Interpretation of Airborne Synthetic Aperture Radar Imagery in the Sulphurets–Unuk–Iskut River Area, Northwest British Columbia (104B); *B.C. Ministry of Energy Mines and Petroleum Resources*, Open File 1990-7.
- Webster, I.C.L. and Ray, G.E. (1991): Skarns in the Iskut River – Scud River Region, Northwest British Columbia; *B.C. Ministry of Energy, Mines and Petroleum Resources*, Geological Fieldwork 1990, Paper 1991-1, this volume.
- Zharikov, V.A. (1970): Skarns; *International Geological Review*, Volume 12, pages 541-559, 619-647, 760-775.



TESTING ON PERLITE AND VERMICULITE SAMPLES FROM BRITISH COLUMBIA

By Lucie Morin and Jean-Marc Lamothe
CANMET Mineral Processing Laboratory, Ottawa

KEYWORDS: Industrial minerals, perlite, vermiculite, thermogravimetric balance, softening-point temperature, bulk density, exfoliation tests.

INTRODUCTION

In November 1989, CANMET was approached by the British Columbia Ministry of Energy, Mines and Petroleum Resources to perform an assessment of potential perlite and vermiculite resources, as represented by samples provided to us. The samples, totalling 520 kilograms, were from seven perlite occurrences (the Frenier deposit on the eastern slope of Blackdome Mountain, northwest of Clinton; the Francois Lake, Ootsa Lake and Uncha Lake prospects south of Burns Lake; and the Blackwater Creek, Florence Creek and Gold Creek occurrences in the Port Clements area of the Queen Charlotte Islands) and two vermiculite prospects (the Joseph Lake occurrence southeast of Fraser Lake and the Sowchea Creek showing near Fort St. James). The material for testing, as received, was a mixture of grab samples and chunk specimens shipped in jute bags. Brief descriptions of the geology of the sample sites are given by White (1990).

TESTING ON SAMPLES OF PERLITE

PREPARATION OF HEAD SAMPLE

Because of the nature of the material, a preliminary examination was made by removing a scoopful of material from each bag and combining the scoops as one lot weighing approximately 2 kilograms. This composite was reduced to less than 6 millimetres (1/4 inch) in a jaw crusher. A 100-gram sample was riffled and pulverized for thermal testing in a thermogravimetric balance. The rest of the material was used for subsequent beneficiation studies.

DESCRIPTION OF TESTING

The samples were subjected to three tests. The first used the thermogravimetric balance to determine the percentage water loss when heated to about 800°C. In the second test the samples were heated under a heating microscope for determination of the softening point and the results were used in the subsequent thermal treatment. Thermal treatment involved heating the sample to 700°C in a horizontal stationary furnace for 5 minutes, then transferring it to a vibrating tube furnace set at the softening-point temperature. The small tube furnace, measuring 15 by 30 inches (≈40 by 80 cm) was set at an angle of 50° to the horizontal, with a stainless steel tube 48 inches (≈120 cm) long and 2 inches (≈5 cm) in diameter, centred within it. The total time for the material to pass through the tube was about 15 seconds, the retention time in the hot zone being about

5 seconds. A portion of the sample from each of the deposits was passed through the tube. The approximate bulk density of the material recovered from each test was obtained by measuring the weight in a 250 cubic centimetre graduate cylinder.

RESULTS AND DISCUSSION

THERMOGRAVIMETRIC BALANCE

Figure 3-1-1 shows that samples from Uncha Lake, Ootsa Lake, Francois Lake and Blackwater Creek are quite comparable to the sample from the Frenier deposit. The Gold Creek sample showed much higher weight loss (7.9%) than the Frenier sample (3.6%). The lowest water loss, the Florence Creek sample, was only 1.2 per cent.

SOFTENING-POINT TEMPERATURE

Figure 3-1-2 shows softening-point temperatures; the Florence Creek sample was found to soften at the lowest temperature, between 1210 and 1235°C. Softening of the Gold Creek perlite occurred between 1235 and 1270°C, comparable to the Frenier perlite and other samples. Plate 3-1-1 is a series of photomicrographs illustrating the stages in the softening process.

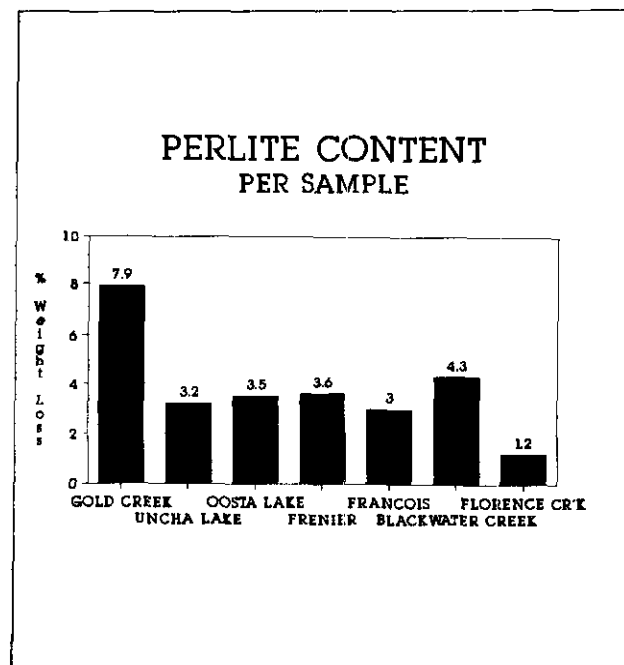
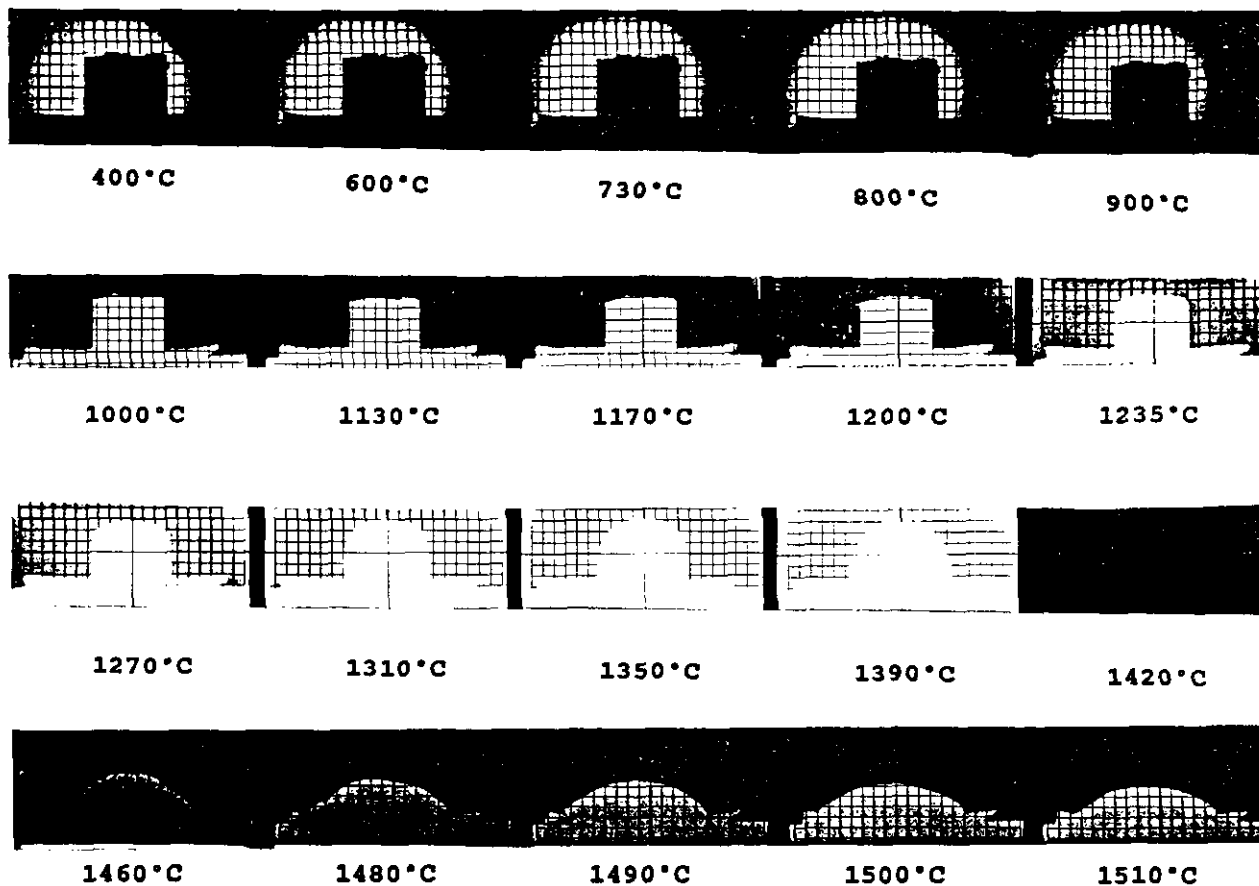


Figure 3-1-1. Histogram showing perlite content of samples from Gold Creek, Uncha Lake, Ootsa Lake, Frenier, Francois Lake, Blackwater Creek and Florence Creek.



REPORT OF A SERIES OF PHOTOMICROGRAPHS

Material: Perlite, Gold Creek
 Film: PX-125
 Developed with: D-76, 5 min.
 Printed with: Dektol 112

Date: May 3/1990

Velox paper F-3 for contact printing

Shot No	Time	Temperature	Light	Filter	Remarks
1	9:30	400	4	0	
2	9:48	600	4	0	
3	9:57	730	4	0	
4	10:02	800	4	0	
5	10:10	900	4	0	
6	10:18	1000	4	0	
7	10:25	1130	2	0	
8	10:33	1170	2	0	
9	10:35	1200	2	0	
10	10:38	1235	2	0	
11	10:41	1270	2	0	corner start rounded
12	10:44	1310	2	0	
13	10:49	1350	0	0	
14	10:53	1390	0	0	
15	10:56	1420	0	GREEN	hemisphere point
16	11:00	1460	0	GREEN	
17	11:04	1480	0	GREEN	
18	11:05	1490	0	GREEN	
19	11:06	1500	0	GREEN	
20	11:07	1510	0	GREEN	

Plate 3-1-1. Photomicrographs showing silhouettes of a perlite sample under heating treatment. At 1270°C the outline of the silhouette has rounded, indicating that at this stage the ashes have passed into the softening phase. The softening temperature is found to be between 1235 and 1270°C. After swelling slightly at 1350°C, the specimen eventually melts. The photomicrograph obtained at 1420°C shows the "hemisphere point", which is accepted as the melting point.

HEATING TREATMENT

The results of the third test are illustrated by Figures 3-1-3 and 4. The Gold Creek sample expanded the most, decreasing to a bulk density of 166 kilograms per cubic metre. Bulk densities of expanded Frenier and Blackwater Creek perlite were 258 and 450 kilograms per cubic metre respectively and the Florence Creek sample gave the highest value (928 kg/m³).

CONCLUSIONS

All results indicate that samples from Gold Creek and Florence Creek are significantly different from all other samples. The Gold Creek sample showed much higher water loss and was noticeably more expansible than all other samples. The Florence Creek sample shows very much lower water loss than the other samples and had the highest bulk density after the heating treatment. The other four perlite samples show similar and comparable results.

The temperature of the furnace could not be controlled as closely as desired to permit uniform heat treatment and the firing conditions were therefore not necessarily those which would give the best results. Considering this, the Gold Creek sample has the best potential application as filler, and possibly in concrete and plaster aggregates. Further testing, using equipment permitting an optimum heat treatment, might give better results and would be necessary to measure the actual potential of all the sampled deposits.

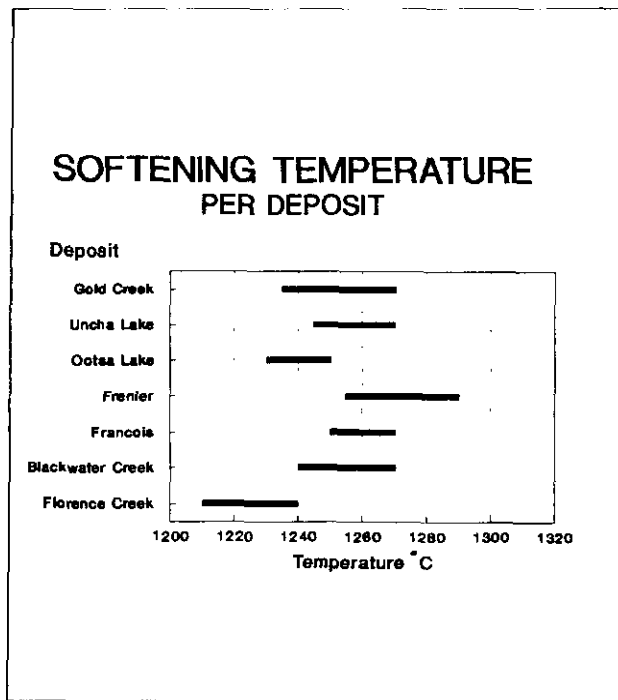


Figure 3-1-2. Softening temperatures of perlite samples from Gold Creek, Uncha Lake, Ootsa Lake, Frenier, Francois Lake, Blackwater Creek and Florence Creek.

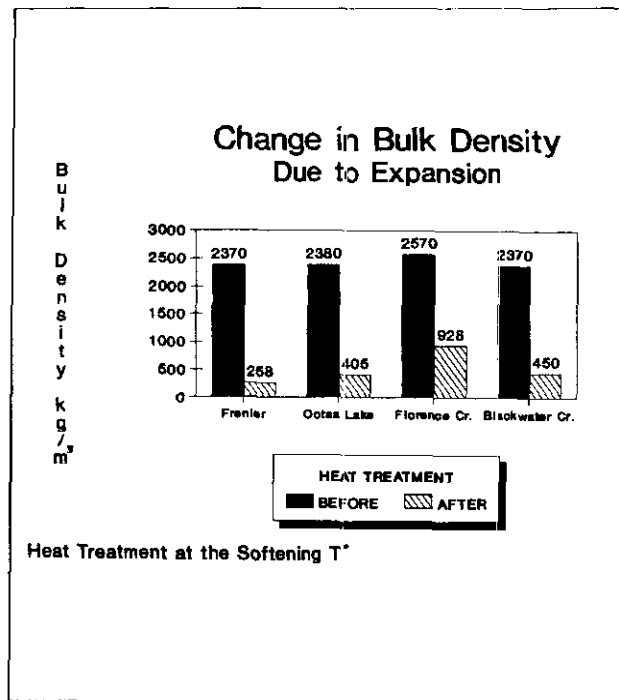


Figure 3-1-3. Change in bulk density due to expansion of perlite samples from Gold Creek, Uncha Lake, Frenier and Francois Lake.

TESTING ON SAMPLES OF VERMICULITE

PREPARATION OF HEAD SAMPLE

Five kilograms of material from each sample was riffled down to a 1-kilogram portion which was scrubbed in a Wemco attrition scrubber for 10 minutes at 20 per cent solids. After scrubbing, the samples were wet screened over an 8 mesh screen and crushed in a roll crusher to less than 3.36 millimetres ($\approx 1/8$ inch).

DESCRIPTION OF TESTING

The vermiculite samples were subjected to exfoliation tests using the same small tube furnace as for the tests on the perlite samples. The total time for the material to pass through the furnace, and the retention time in the hot zone, were the same as in the perlite tests. A portion of each size fraction was passed through the tube with the maximum temperature of the furnace maintained between 930 and 960°C.

RESULTS AND DISCUSSION

Each product contained material that did not exfoliate and which was removed from the sample by air separation using an air table. The percentage by weight of vermiculite was calculated and an approximate density of the exfoliated vermiculite obtained (Tables 3-1-1 and 3-1-2). Figures in brackets under the heading "Vermiculite %" in the tables

TABLE 3-1-1
EXFOLIATION TESTS ON SOWCHEA CREEK SAMPLE

Size Fraction mm	Product Wt %	Vermiculite %		Bulk Density (kg/m ³) (lb/ft ³)	
-3.36+2.38	5	(7.2)*	0.4	308	19
-2.38+1.65	4	(20.6)	0.9	267	17
-1.65+1.40	11	(22.9)	2.5	382	24
-1.40+800 μ m	27	(12.4)	3.3	413	26
-800+630 μ m	39	(8.6)	3.3	357	22
-630+500 μ m	14	(10.2)	1.4	434	27
Total	100		11.8		

The vermiculite obtained from Sowchea Creek sample was dark golden-brown in colour, and was fairly well exfoliated. The plus 500 μ m (35 mesh) portion of the sample contained 11.8% vermiculite.

TABLE 3-1-2
EXFOLIATION TESTS ON JOSEPH LAKE SAMPLE

Size Fraction mm	Product Wt %	Vermiculite %		Bulk Density (kg/m ³) (lb/ft ³)	
-3.36+2.38	2	(0.1)	0.0	—	—
-2.38+1.65	3	(0.3)	0.1	—	—
-1.65+1.40	8	(0.5)	0.4	—	—
-1.40+800 μ m	28	(2.4)	0.7	398	25
-800+630 μ m	43	(7.9)	3.4	427	27
-630+500 μ m	16	(5.9)	1.0	326	20
Total	100		5.6		

* Figures in brackets under the heading "% Vermiculite" are the percentage of vermiculite in each fraction.

are the percentage of vermiculite in the whole minus 3.36 millimetres fraction. The +500-micron fraction (35 mesh) had been discarded because of its lack of commercial value and the percentages were recalculated on the basis of grading the material to obtain the total percentage of vermiculite in the whole - 3.36-millimetre fraction.

As in the case of the perlite tests, the conditions of crushing and exfoliation were not necessarily those that would give optimum exfoliation and recovery of vermiculite.

CONCLUSIONS

Neither of the samples tested shows significant promise of being suitable for use as loose insulation as both are too fine grained. More than 60 per cent of Canadian production was used for this purpose in 1980. Bulk densities greatly exceed ASTM specifications for this application which are in the range 88 to 128 kilograms per cubic metre.

The material tested might be used in other ways, such as filler or aggregates in insulating concrete or plaster, although the maximum bulk density permitted by ASTM specifications for lightweight aggregates in insulating concrete is 160 kilograms per cubic metre. The Sowchea Creek sample contained the most vermiculite, but the density obtained in these preliminary tests was not close enough to the specified limit to indicate that the material might be suitable for commercial purposes. The vermiculite content of the Joseph Lake sample appears to be too low to be of commercial value.

REFERENCES

- White, G.V. (1990): Perlite and Vermiculite Occurrences in British Columbia; *B.C. Ministry of Energy, Mines and Petroleum Resources*, Geological Fieldwork 1989, Paper 1990-1, pages 481-487.

GEOLOGY OF THE MOUNT BRUSSILOF MAGNESITE DEPOSIT, SOUTHEASTERN BRITISH COLUMBIA (82J/12, 13)

By George J. Simandl and Kirk D. Hancock

KEYWORDS: Industrial minerals, economic geology, magnesite, Cathedral Formation, Middle Cambrian, dolomitization, porosity, base metal association, deposit model.

INTRODUCTION

Magnesite ($MgCO_3$) is an industrial mineral that can be converted into either caustic, fused or dead-burned magnesia. Dead-burned magnesia is used mainly in the manufacture of refractory products; caustic magnesia is used in treatment of water, in animal feedstuffs, fertilizers, magnesia cements, insulating boards and wood-pulp processing, in chemicals and pharmaceuticals and as a curing agent in rubber (Coope, 1987). Magnesium metal is produced either from magnesite or from caustic magnesia.

In the short term future, production of dead-burned magnesia is expected to remain constant, however, demand for caustic magnesia is increasing (Duncan, 1990). With the increasing trend toward the use of high-performance "mag-carbon" refractories, future demand for fused magnesia looks promising.

A number of magnesite deposits are known in British Columbia (Grant, 1987), the most important of these is the Mount Brussilof orebody. It is hosted by dolomites of the Middle Cambrian Cathedral Formation.

HISTORY

The Mount Brussilof deposit was discovered during regional mapping by the Geological Survey of Canada (Lecch, 1965). Baykal Minerals Ltd. and Brussilof Resources Ltd. staked and explored the deposit. In 1971, the two companies merged to form Baymag Mines Co. Ltd. In 1979, Refratechnik GmbH. acquired Baymag Mines (MacLean, 1988). In 1980, proven and probable geological reserves were 9.5 million tonnes grading over 95 per cent magnesia in the calcined product and 13.6 million tonnes of 93 to 95 percent magnesia in calcined product. Possible reserves were estimated at 17.6 million tonnes averaging 92.44 per cent magnesia in calcinated product (Schultes, 1986). Previous investigations, including mapping, are described in detail by MacLean (1988).

LOCATION

The Mount Brussilof deposit is located in southeastern British Columbia, approximately 35 kilometres northeast of Radium Hot Springs. It is accessible from Highway 93 by an all-weather unpaved road (Figure 3-2-1). Elevations in the area range from 1250 to 3045 metres above sea level.

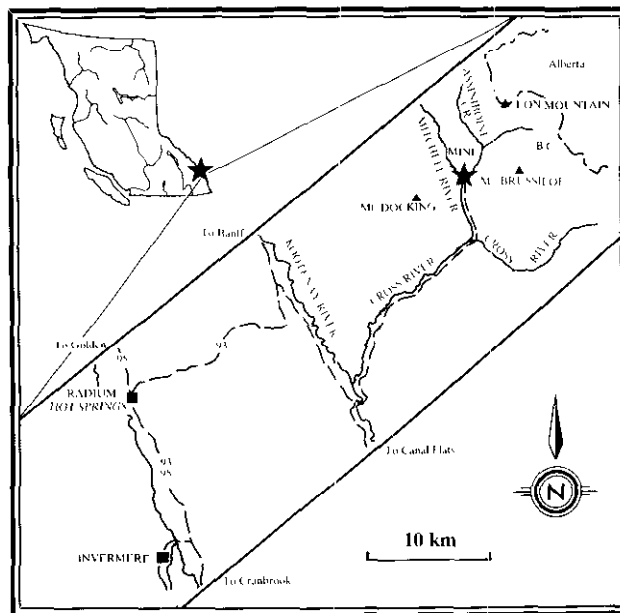


Figure 3-2-1. Location of the Mount Brussilof magnesite mine.

TECTONIC SETTING

The Mount Brussilof deposit is located in the Foreland tectonostratigraphic belt and within the "Kicking Horse Rim", as defined by Aitken (1971, 1989). It is situated east of a Cambrian bathymetric feature commonly referred to as the Cathedral escarpment (Fritz, 1990; Aitken and McIlreath, 1984, 1990). Existence of the escarpment is challenged by Ludwigsen (1989, 1990) who suggests that this feature is a shale-carbonate facies change on a ramp. Lecch (1966) described the same feature in the Mount Brussilof mine area (Figure 3-2-2) as a "faulted facies change". In any event, the carbonate rocks east of this feature, which host the magnesite mineralization, were deposited in a shallower marine environment than their stratigraphic equivalents to the west.

STRATIGRAPHY AND LITHOLOGY

The stratigraphic relationship between rocks east of the Cathedral escarpment, and their deeper water equivalents to the west, commonly referred to as the Chancellor Formation, is described by Aitken and McIlreath (1984) and Stewart (1989).

All known occurrences of sparry carbonate, other than veins of calcite or dolomite a few centimetres thick, are located east of the Cathedral escarpment. A composite stratigraphic section of this area is shown on Figure 3-2-3

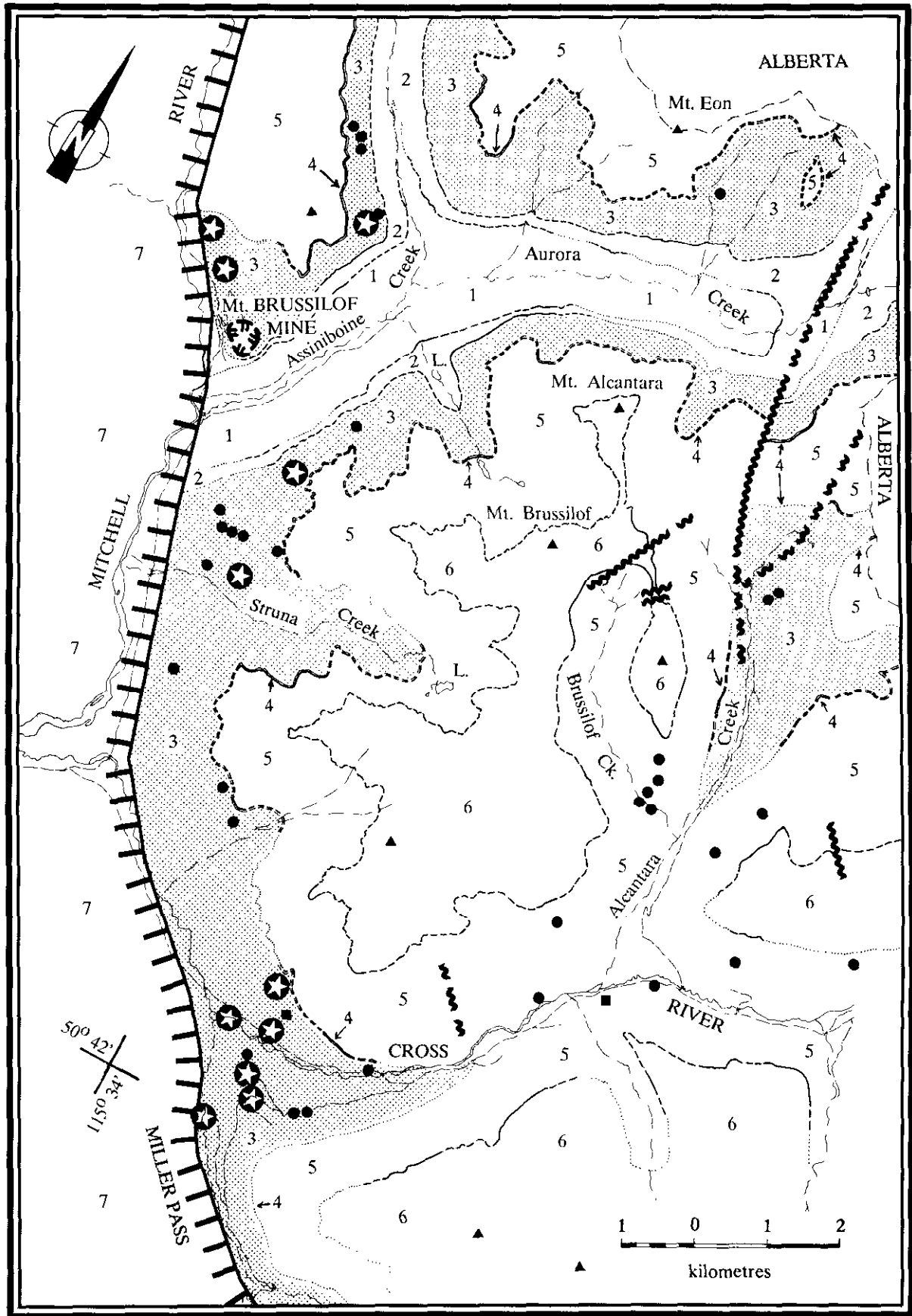


Figure 3-2-2. Geology of the Mount Brussilof area.

LEGEND

Middle Cambrian

- 7 **Chancellor Formation:** Argillaceous limestone and shales. Basinal equivalent of the Pika, Eldon, Stephen and Cathedral formations
- 6 **Arctomys Formation:** Purple and red shales with beige dolomite. Overlain by the Waterfowl and Sullivan formations.
- 5 **Eldon and Pika formations (undivided):** Buff, grey and black massive dolomite, argillaceous dolomite and limestone.
- 4 **Stephen Formation:** Brown and tan shales. Fossiliferous.
-  3 **Cathedral Formation:** Buff and grey dolomite and limestone
- 2 **Naiset Formation:** Thin-bedded, brown and green shale.

Lower Cambrian

- 1 **Gog Formation:** Massive, tan, quartz sandstone.

SYMBOLS

	Open pit
	Magnesite
	Sparry carbonate
	Magnesite (Leech, 1966)
	Cathedral Escarpment
	Geological contact: defined, approximate, assumed
	Fault: defined, approximate

Stratigraphic thicknesses of the formations are approximate. The formations are described below, in order from oldest to youngest.

The Gog Formation is a rusty, grey or buff, medium to coarse-grained, massive to thick-bedded Lower Cambrian sandstone more than 250 metres thick.

The Naiset Formation comprises thinly bedded, brown and green Middle Cambrian shale overlying the Gog Formation. It is 65 to 170 metres thick, characterized by blue-green chlorite spots and by a well-developed cleavage

oblique to bedding. Near the Cathedral escarpment this shale may become grey or partially converted to talc and serpentine.

The Cathedral Formation, which hosts the magnesite deposits, is also Middle Cambrian in age. It is about 340 metres thick and consists of buff, white and grey limestones and dolomites. Laminations, ripple marks, intraformational breccias, *yoholaminites* (McIlreath and Aitken, 1976), algal mats, oolites, pisolites, fenestrae and burrows are well preserved. Pyrite is common either as disseminations or pods and veins.

The Stephen Formation consists of tan to grey, thinly bedded to laminated shale about 16 metres thick, with a cleavage subparallel to bedding. It is of Middle Cambrian age and contains abundant fossil fragments and locally well-preserved trilobites and inarticulate brachiopods.

The Eldon and Pika formations cannot be subdivided in the map area. The lowermost beds of the Eldon Formation, overlying the Stephen Formation, are black limestones approximately 50 metres thick. This basal unit is very distinctive, containing millimetre to centimetre-scale argillaceous layers that weather to a red, rusty colour; elsewhere these formations cannot be readily distinguished from the Cathedral Formation, except by fossil evidence.

The Arctomys Formation, also Middle Cambrian in age, is characterized by green and purple shales and siltstones interbedded with beige, fine-grained dolomites. Mud cracks and halite crystal prints are commonly preserved. The thickness of this formation was not determined, as the base marked the limit of mapping.

All the formations are well exposed over the area, except the recessive Stephen Formation, which was not observed in the southern part of the map area. It is not clear if this lack of exposure is due to lack of outcrops or to nondeposition.

STRUCTURE

Rocks west of the Cathedral escarpment are strongly deformed. The deformation is characterized by numerous small-scale folds with subhorizontal fold axes oriented 160° Minor thrust faults, and a well-developed steeply dipping cleavage striking 160° are other typical features. Along the Cathedral escarpment, cleavage is subvertical, closely spaced and injected by dolomite, calcite and siderite(?) veins.

East of the Cathedral escarpment, cleavage is generally absent in carbonates (Cathedral, Eldon and Pika formations), well developed in the Stephen Formation and strongly developed in the Naiset Formation. The rocks outcropping immediately east of the escarpment strike 170° and dip 20° west.

Farther east the bedding is subhorizontal and characterized, by minor, upright, open folds. Several subvertical faults transect this area (Figure 3-2-2). These faults have vertical displacements of tens to hundreds of metres. In the northeastern corner of the study area, deformation in the Naiset Formation is similar to that of the Chancellor Formation, due to a thrust fault outcropping farther east.

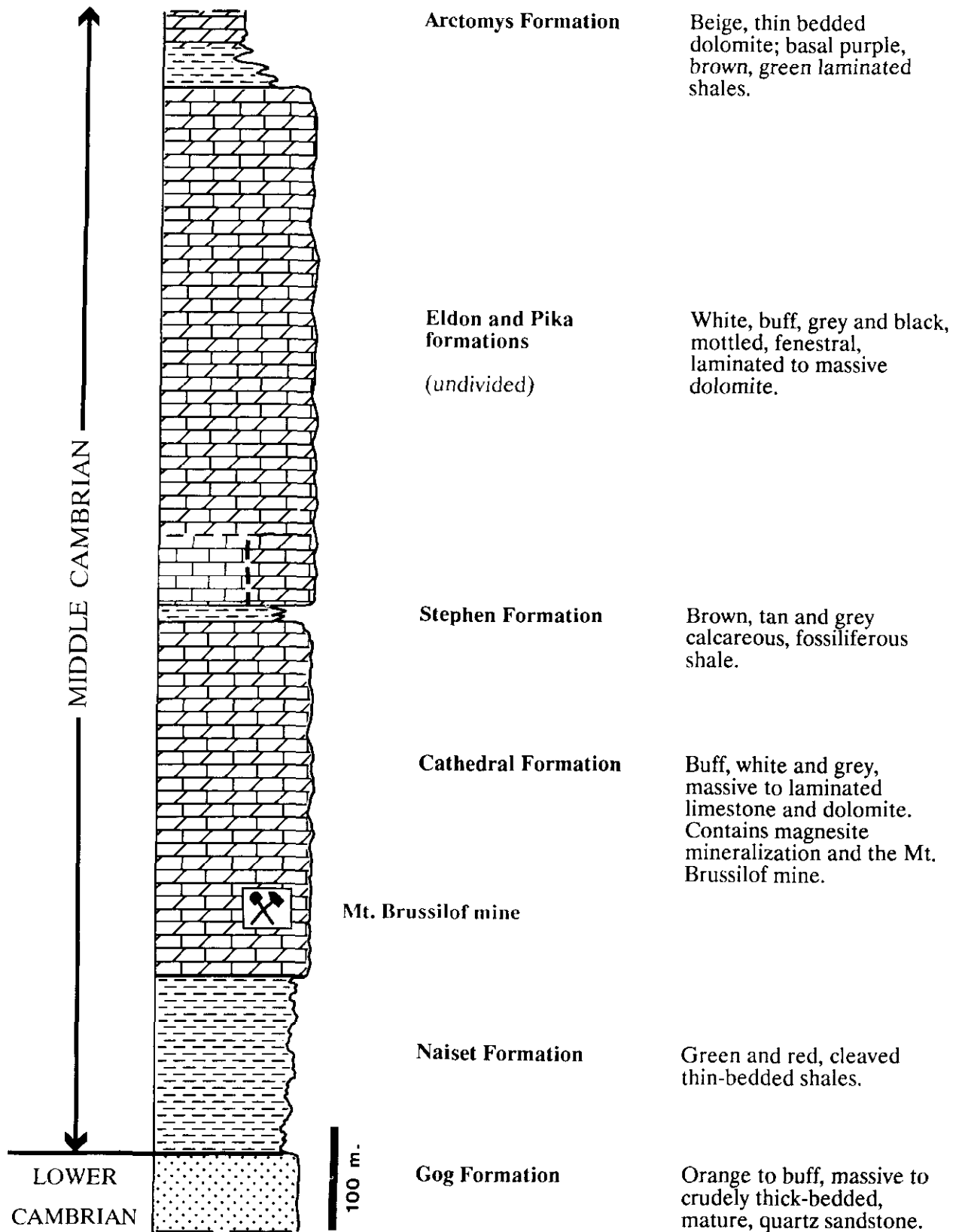


Figure 3-2-3. Composite stratigraphic column of the sedimentary sequence east of the Cathedral escarpment, Mount Brussilof mine area.

MAGNESITE DEPOSITS

Sparry carbonate rocks occur within the Cathedral, Eldon and Pika formations (Figure 3-2-2). They consist mainly of coarse dolomite and magnesite crystals in varying proportions. Magnesite-rich sparry carbonates are restricted to the Cathedral Formation, where they form lenses, pods and irregular masses.

Barren Cathedral Formation consists mainly of fine-grained, massive or laminated dolomites interbedded with limestones. It contains well-preserved sedimentary and diagenetic features. These fine-grained carbonates are locally brecciated and cemented by coarse white dolomite, indicating a strong secondary porosity (Plate 3-2-1).

Parts of the Cathedral Formation are entirely altered to sparry magnesite, forming deposits of economic interest.

Sparry carbonates are separated from limestone by light grey, massive dolomite, which may contain needle-shaped quartz crystals (Plate 3-2-2). The contacts between sparry carbonate masses and the fine-grained dolomite are sharp and may be concordant or discordant (Plates 3-2-3 and 4).

Magnesitic sparry carbonate is usually white or light grey in colour and buff when weathered. It consists of regularly spaced, alternating white and grey magnesite layers (Plate 3-2-5), randomly oriented centimetre-scale white magnesite

crystals (Plate 3-2-6) or a mixture of light grey and white magnesite crystals. Common impurities in magnesite ore are isolated rhombohedral dolomite crystals, calcite veins, pyrite veins (Plate 3-2-7), subvertical fractures filled by a mixture of beige ankerite, calcite and chlorite, coarse radiat-



Plate 3-2-2. Fine-grained dolomite containing acicular quartz crystals (QZ). These crystals are commonly present near the contact of sparry carbonates with dolomite.



Plate 3-2-1. Dark grey dolomite fragments cemented by coarser white dolomite: Cathedral Formation, outcrop adjacent to Cathedral escarpment.



Plate 3-2-3. Concordant contacts between sparry carbonate (SC) and fine-grained dolomite (DO).



Plate 3-2-4. Discordant, sharp and irregular contact between sparry carbonate (SC) and fine-grained dolomite (DO).

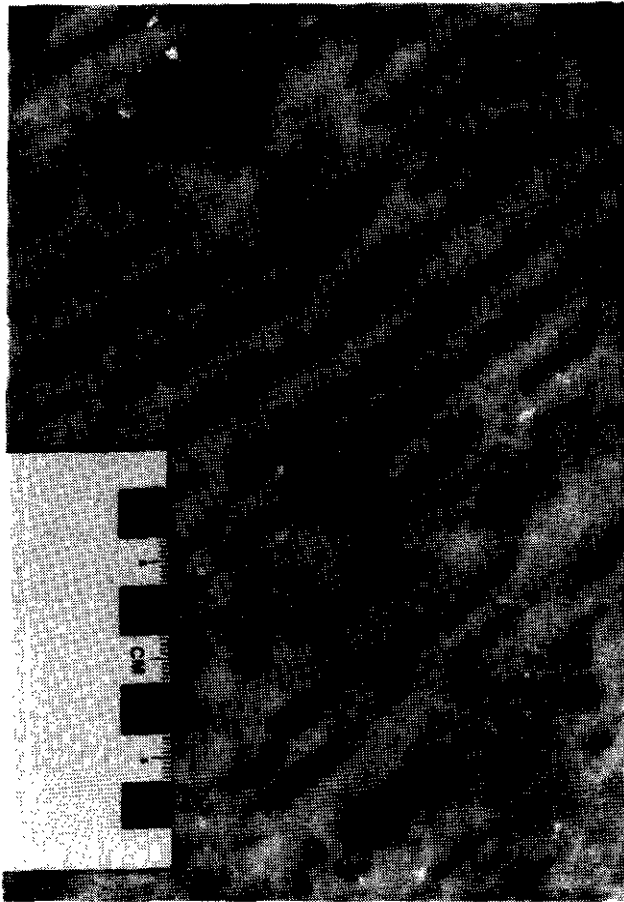


Plate 3-2-5. White and grey, layered sparry magnesite ore from the Mount Brussilof mine.

ing or single quartz crystals and coarse pyrite pyritohedrons and octahedrons disseminated within sparry magnesite. Chalcocite, fersmite, phlogopite, talc and coarse, white, acicular palygorskite were also observed in the mine. Boulangerite, huntite and brucite were reported from laboratory analysis by White (1972).

Where fine-grained dolomite is not entirely converted to magnesite, replacement features such as coarse, white carbonate crystals growing perpendicular to fracture planes (Plate 3-2-8) or partings (Plate 3-2-9) and lenses of fine-grained dolomite enclosed by sparry carbonates are common. Bipolar growths of zoned magnesite crystals (Plate 3-2-10), magnesite pinolite (Plate 3-2-11), rosettes and coarse carbonate crystals having lozenge-shaped cross-sections (Plate 3-2-12). All these features are interpreted as replacement textures. Some long magnesite crystals are deformed, suggesting that at least some magnesite predates or is penecontemporaneous with the last period of deformation.

Sparry dolomite rock consists mainly of dolomite rhombs. It forms lenses, veins or irregular masses in fine-grained dolomite and is believed to occur at the same stratigraphic horizons and to contain the same impurities as coarse sparry magnesite.



Plate 3-2-6. Randomly oriented sparry magnesite crystals, Cathedral Formation, 100 metres east of the Mount Brussilof mine.

Dolomite veins cutting magnesite ore occur at the mine, however, magnesite veins were never observed to cut sparry dolomite.

CHEMISTRY OF CARBONATE ROCKS

Analyses of 19 samples of magnesite and dolomite-bearing rocks were available in time for this publication. These samples were analyzed for MgO, CaO, FeO, SiO₂ and Al₂O₃. The major constituents are MgO and CaO, which are negatively correlated (Figure 3-2-4).

The magnesium content of the carbonate rocks varies continuously from dolomite to magnesite. Stoichiometric dolomite and magnesite are given for reference. Fine-grained massive or laminated carbonates are dolomitic in composition. Coarse and sparry carbonates have higher magnesia contents than fine-grained carbonates.

ELEMENTS OF THE GENETIC MODEL

Several elements of a genetic model explaining the origin of the Mount Brussilof deposit are indicated by the tectonic, stratigraphic and structural setting, secondary porosity features, replacement textures, paragenesis and absence of fine-grained magnesite, protodolomite or hydromagnesite. The presence of huntite (White, 1972) remains to be explained.

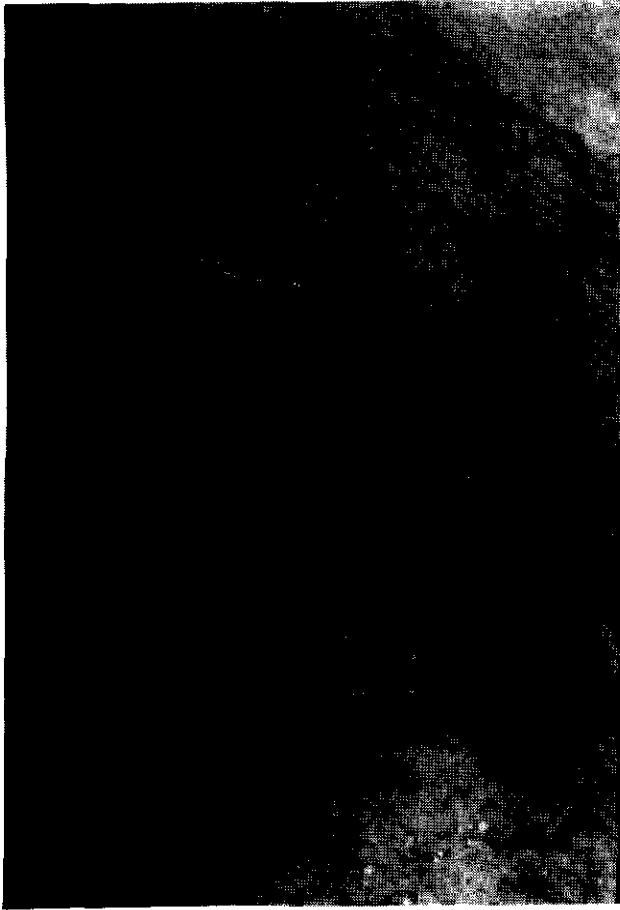


Plate 3-2-7. Pyrite veinlets cutting magnesite rock: Mount Brussilof mine.

It is suggested that the magnesite postdates early diagenesis of the Cathedral Formation and probably of the Stephen, Eldon and Pika formations as well. Widespread dolomitization and subsequent fracturing and brecciation contributed significantly to an increase in porosity. Some of the fracturing may be due to reactivation of a pre-Cathedral escarpment fault or to a difference in competence of deep and shallow-water sediments during the post-Middle Cambrian tectonic activity. However, most of the breccias were probably produced by a partial dissolution and collapse of the carbonate hostrock, caused by incursion of meteoric water or hydrothermal solutions in the manner described by Sangster (1988).

Fluids responsible for crystallization of coarse sparry carbonates reacted with dolomitized, permeable and fractured reef facies along the Cathedral escarpment and moved up-dip along the permeable zones. The fluid cooled and evolved chemically along its path due to interaction with dolomitic hostrock. The most important parameters determining the ability of the fluid to increase the magnesium content of carbonate rock are temperature, the mole $\text{Ca}^{2+}/\text{mole Mg}^{2+}$ ratio of the solution, the fluid/rock ratio and the salinity of the fluid as well as the permeability, porosity and physical and chemical characteristics of the protolith. The relationship between temperature and mole $\text{Ca}^{2+}/\text{mole}$



Plate 3-2-8. Bipolar growth of sparry carbonates from a fracture plane in fine-grained dolomite that hosts the Mount Brussilof deposit.

Mg^{2+} ratio is illustrated in Figure 3-2-5, high temperature and low mole $\text{Ca}^{2+}/\text{mole Mg}^{2+}$ ratio increases the potential of the fluid to convert carbonates to magnesite.

Predictions based on this model suggest that the highest grade magnesite deposits should be located along the edge of the Cathedral escarpment, within the reef facies. Lower grade magnesite deposits and sparry dolomites would be located at a greater distance up-dip from the Cathedral escarpment along the same permeable zones, or adjacent to the escarpment but in the zones of lesser permeability.

This model conforms well to the field observations. It requires confirmation and integration with the results of future petrographic work, geochemical (isotopic, REE, minor and major element) analysis, fluid inclusion and crystallinity studies, mass balance determinations and further thermodynamic considerations. Future studies will focus on constraints on the origin, temperature and composition of the mineralizing fluid, geochemical gradients, paragenetic relationships and fluid/rock ratios.

ECONOMIC CONSIDERATIONS

Several new magnesite showings that are part of a continuous sparry carbonate belt parallel to the Cathedral escarp-

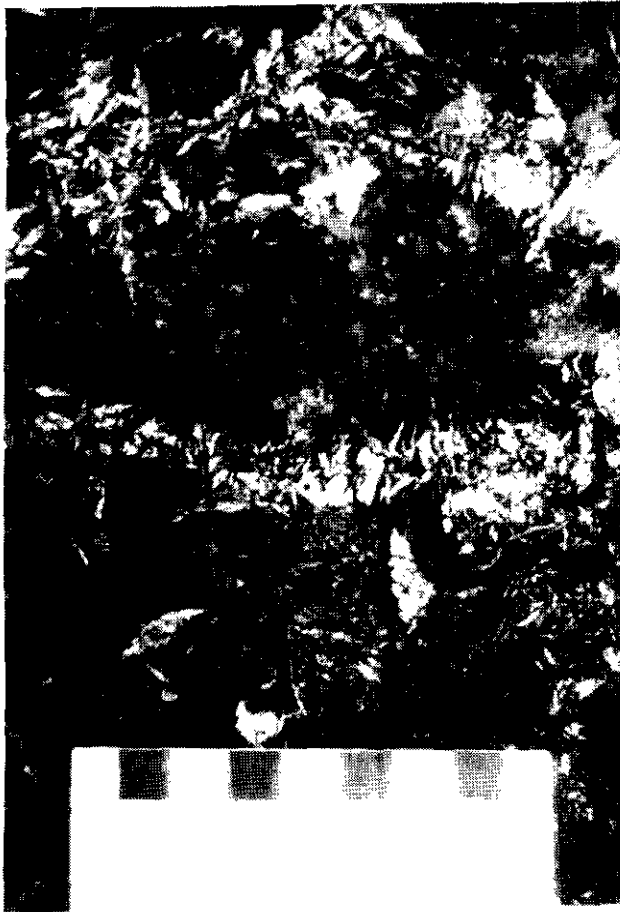


Plate 3-2-9. Subparallel layers of sparry carbonates (white) growing along original parting within fine-grained dolomite: 150 metres east of the Mount Brussilof mine.

ment were identified in the course of fieldwork. Magnesia content varies considerably within this belt. About 1 kilometre north of the mine the favorable horizon of the Cathedral Formation is covered by barren Eldon Formation. However the continuity of the mineralization beneath this cover is proved by sparry carbonate showings along the Assiniboine Creek valley. The belt may extend south of the known Miller Pass showings (Figure 3-2-2). Very little is known about the grade of these occurrences and further exploration is justified.

Mapping confirmed that magnesite is not confined to a single stratigraphic horizon within the Cathedral Formation. Sparry dolomite is widespread throughout the formation, and also occurs within the Eldon Formation. The possibility that the Cathedral escarpment is not the only permeable zone that was open to magnesite-forming fluids should be considered by prospectors.

The known association of base metal deposits with the Cathedral escarpment (Aitken and McIlreath, 1984), similarities between the dolomitization styles in the Kicking Horse mine (Rasetti, 1951) and in the Mount Brussilof area indicate that exploration should not be restricted to magnesite.

Discovery of a fluorapatite float on Mount Brussilof, the identification of fersmite (a niobium-bearing mineral) and

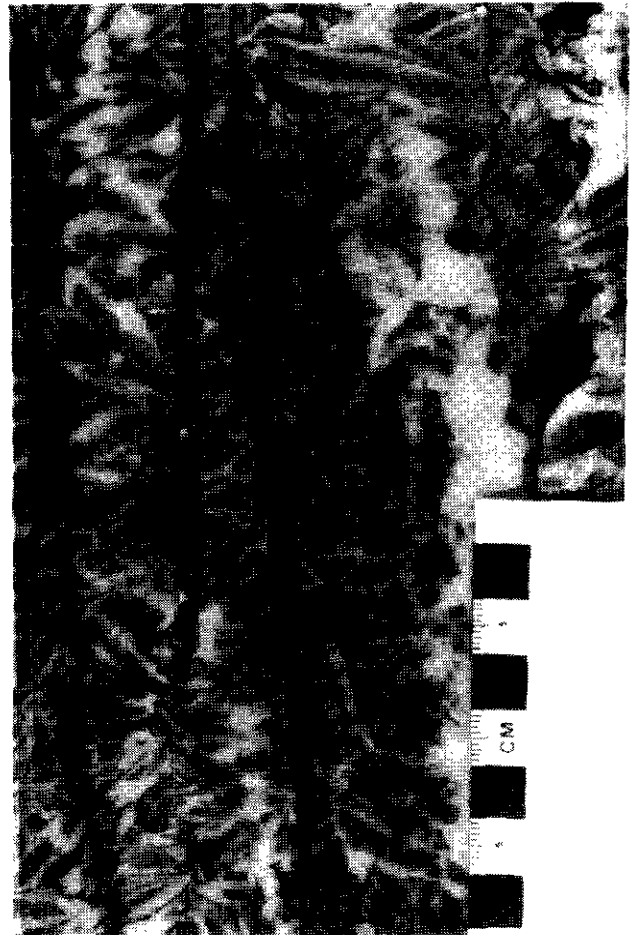


Plate 3-2-10. Bipolar magnesite pinolite: vestigial silty dolomitic protolith (black), zoned magnesite crystals (white and light grey); Mount Brussilof mine.

chalcocite, the previously reported occurrence of boulangerite (White, 1972) and abundant pyrite in the Mount Brussilof mine further encourage exploration programs in the Mount Brussilof area.

ACKNOWLEDGMENTS

Baymag Mines Co. Ltd. kindly provided access to company documents and a field office during the lengthy rainy periods of the 1990 field season. Twenty major element analyses were performed by Baymag free of charge. Special thanks are extended to H. Fergen, Mine Manager, and I. Knuckey, Mine Geologist, for their cooperation and assistance. R. Matthew, Consulting Engineer, directed our attention to the mineralogical particularities of the Mount Brussilof mine. Dr. S. Paradis of the Geological Survey of Canada in Quebec, performed most of the density studies used to determine the proportions of magnesite and dolomite. Z.D. Hora of the British Columbia Ministry of Energy, Mines and Petroleum Resources proposed the project and kindly proof-read an earlier version of this manuscript. Enriching discussions with Dr. J.M. Aitken, Dr. I. Jonasson and Dr. D. Sangster from the Geological Survey of Canada are acknowledged.



Plate 3-2-11. Magnesite pinolites (light grey) growing within a fine-grained dolomite matrix; Mount Brussilof mine.

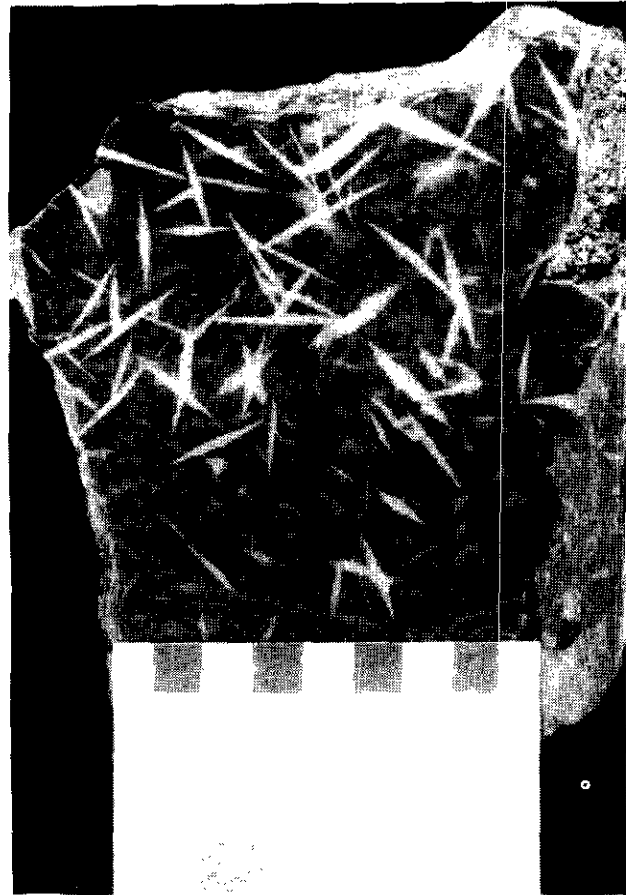


Plate 3-2-12. Lozenge-shaped cross-sections of dolomite crystals (white) growing within fine-grained dolomite: less than 15 metres from the contact between sparry dolomite and sparry magnesite; Miller Pass Road showing.

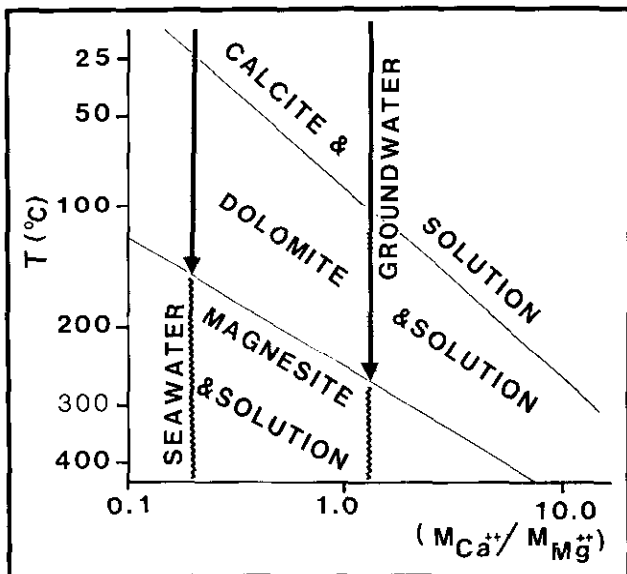


Figure 3-2-5. Potential of a solution to convert carbonate to magnesite as a function of temperature and $M_{Ca^{2+}}/M_{Mg^{2+}}$ ratios. Compositions of ideal seawater and groundwater are shown for reference. 1 mole chloride solution assumed. After Wilson *et al.* (1990), data extrapolated from Rosenberg, Burt and Holland (1967).

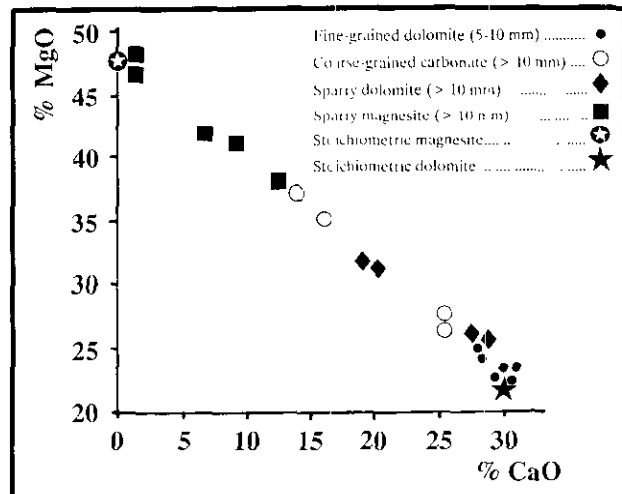


Figure 3-2-4. Negative correlation between CaO and MgO in carbonate rocks, Mount Brussilof area. The distribution of the data suggests a continuum in composition. Coarse-grained and sparry dolomites have higher MgO content than fine-grained carbonate rocks.

REFERENCES

- Aitken, J.D. (1971): Control of Lower Paleozoic Sedimentary Facies by the Kicking Horse Rim, Southern Rocky Mountains, Canada; *Bulletin of Canadian Petroleum Geology*, Volume 19, pages 557-569.
- Aitken, J.D. (1989): Birth, Growth and Death of the Middle Cambrian Cathedral Lithosome, Southern Rocky Mountains; *Bulletin of Canadian Petroleum Geology*, Volume 37, pages 316-333.
- Aitken, J.D. and McIlreath, I.A. (1984): The Cathedral Reef Escarpment, a Cambrian Great Wall with Humble Origins; *Geos*, Volume 13, pages 17-19.
- Aitken, J.D. and McIlreath (1990): Comment on "The Burgess Shale: Not in the Shadow of the Cathedral Escarpment"; *Geoscience Canada*, Volume 17, pages 111-115.
- Coope, B.(1987): The World Magnesite Industry; *Industrial Minerals*, Number 223, pages 21-31.
- Duncan, L.R. (1990): Magnesite; *Mining Engineering*, Volume 191, Number 6, page 569.
- Fritz, W.H. (1990): Comment: In Defence of the Escarpment near the Burgess Shale Fossil Locality; *Geoscience Canada*, Volume 17, pages 106-110.
- Grant, B. (1987): Magnesite, Brucite and Hydromagnesite Occurrences in British Columbia; *B.C. Ministry of Energy, Mines and Petroleum Resources*, Open File 1987-13, 68 pages.
- Leech, G.B. (1965): Kananaskis Lakes, W 1/2 Area; in Report of Activities, May to October, 1965; *Geological Survey of Canada*, Paper 66-1, pages 65-66.
- Leech, G.B. (1966): Kananaskis Lakes; *Geological Survey of Canada*, Open File 634.
- Ludwigsen, R. (1989): The Burgess Shale : Not in the Shadow of the Cathedral Escarpment; *Geoscience Canada*, Volume 16, pages 139-154.
- Ludwigsen, R. (1990): Reply to Comments by Fritz, and Aitken and McIlreath; *Geoscience Canada*, Volume 17, pages 116-118.
- MacLean, M.E. (1988): Mount Brussilof Magnesite Project, Southeast British Columbia (82/13E); *B.C. Ministry of Energy, Mines and Petroleum Resources*, Geological Fieldwork 1988, Paper 1989-1, pages 507-510.
- McIlreath, I.A and Aitken, J.D. (1976): *Yoholaminites* (Middle Cambrian) Problematic Calcareous Sediment-stabilizing Organism; *Geological Association of Canada*, Program with Abstracts, 1976 Annual Meeting, page 84.
- Rasetti, F. (1951): Middle Cambrian Stratigraphy and Fauna of the Canadian Rocky Mountains; *Smithsonian Miscellaneous Collections*, Volume 116, Number 5, 277 pages.
- Rosenberg, P.E., Burt, D.M. and Holland, H.D., (1967): Calcite – Dolomite – Magnesite Stability Relations in Solutions: the Effect of Ionic Strength; *Geochimica et Cosmochimica Acta*, Volume 31, pages 391-396.
- Sangster, D.F. (1988): Breccia-hosted Lead-Zinc Deposits in Carbonate Rocks; in Paleocarst, N.P. James, and P.W. Choquette, Editors, *Springer-Verlag New York Inc.*, pages 102-116.
- Schultes, H.B. (1986): Baymag – High Purity MgO from Natural Magnesite; *Canadian Institute of Mining and Metallurgy*, Bulletin, May 1986, pages 43-47.
- Stewart, W.D. (1989): A Preliminary Report on Stratigraphy and Sedimentology (Middle to Upper Cambrian) in the Zone of Facies Transition, Rocky Mountain Main Ranges, Southeastern British Columbia; in Current Research, Part D, *Geological Survey of Canada*, Paper 89-1D, pages 61-68.
- Wilson, E.M., Hardie, A.L. and Phillips, O.M. (1990): Dolomitization Front Geometry, Fluid Flow Patterns, and the Origin of Massive Dolomite: The Triassic Latemar Buildup, Northern Italy; *American Journal of Science*, Volume 290, pages 741-796.
- White, G.P.E. (1972): Mineralogy of the Baymag Mines Ltd. Magnesite Prospect, South Kootenay Area, B.C.; *Acrers Western Limited*, unpublished report, 17 pages.



**RECENT MAGNESITE-HYDROMAGNESITE SEDIMENTATION
IN PLAYA BASINS OF THE CARIBOO PLATEAU,
BRITISH COLUMBIA
(92P)**

**By Robin W. Renaut and Douglas Stead
University of Saskatchewan**

KEYWORDS: Industrial minerals, magnesite, Cariboo Plateau, playa, Holocene, salinity, chemical composition, depositional environments.

INTRODUCTION

Deposits of sedimentary magnesite and hydromagnesite of Holocene age are common on the semi-arid Cariboo Plateau of interior British Columbia. They occur as surficial deposits in playas and many other small closed depressions, mainly between Williams Lake and Clinton.

Reinecke (1920) and Cummings (1940) have provided the only descriptions of the deposits to date. Grant (1987) has reviewed these and other occurrences. Recent studies of Cariboo playa sedimentation have shown that magnesium carbonates are far more widespread than previously reported (Renaut and Long, 1987, 1989). Although Reinecke and Cummings speculated upon their genesis, no attempts have been made to determine their mode of formation and the age of the deposits.

Therefore, during June and July 1990, we began a study of the origins of the magnesite and hydromagnesite. This included a reconnaissance to determine the types of occurrence, and a detailed survey of Milk Lake, a small playa basin where they are well developed. We summarize results of the fieldwork at Milk Lake and provide some preliminary mineralogical data. These show that magnesium carbonates are probably forming in many Cariboo basins today, both subaqueously and in zones of shallow groundwater discharge.

GEOLOGY AND ENVIRONMENTAL SETTING

The intermontane Cariboo Plateau (Figure 3-3-1) lies at an elevation of 1050 to 1250 metres above sea level. The plateau is underlain mostly by Neogene basalts (Campbell and Tipper, 1971; Mathews, 1989), with a thin (0 to 5 m) mantle of till and glaciofluvial sediments (Tipper, 1971; Valentine and Schori, 1980). Ice retreated from the region about 10 000 years ago (Fulton, 1984). The adjacent Marble Range (Figure 3-3-1) is composed of marine sediments, basic lavas and ultramafic rocks of the Permian-Jurassic Cache Creek Terrane (Monger, 1989). Inliers of Cache Creek rocks occur locally within the plateau basalts (e.g. hills northwest of Meadow Lake).

The plateau surface is gently undulating with extensive coniferous forest cover, locally broken by grassy meadows.

Drainage is disordered with few streams, abundant marshy ground, and several thousand lakes, both fresh and saline.

The climate is semi-arid to sub-humid with a mean annual precipitation of 300 to 400 millimetres, which is a similar value to the mean annual moisture deficit (Valentine and Schori, 1980). Mean July temperatures range from 13 to 17°C, compared with -9 to -11°C in January. Less than 90 days each year are frost free. Snow and ice usually cover the plateau from November until late March. Further details of the environmental setting are given in Renaut and Long (1989).

THE PLAYAS AND SALINE LAKES OF THE CARIBOO PLATEAU

There are more than one thousand saline lakes on the Cariboo Plateau, ranging from small ephemeral ponds and playas to large perennial meromictic lakes. Commonly they lie in small, closed basins between elongate mounds of till or eskers, or in small, kettle-like depressions. Many are clustered along paleomeltwater channels produced during the last deglaciation. Most lakes have small catchments, lack channelled inflow, and are fed directly by groundwater, snowmelt and unchannelled wash. Subaerial and sub-lacustrine springs are present at several lakes.

Although extensive magnesite-hydromagnesite deposits are also found around the margins of only a few perennial saline lakes (e.g. Meadow Lake, Figure 3-3-1), they are most common in the ephemeral lake (playa) basins. The playas are defined as those lakes that desiccate annually or every few years.

Three main groups of playas have been recognized (Renaut and Long, 1989; Renaut, 1990a):

- *Siliciclastic playas* are small and fed predominantly with clastic debris derived from slope wash and small slope failures.
- *Carbonate playas* are very shallow, alkaline lakes that desiccate producing hard, dry mudflats composed predominantly of carbonates, but with a peripheral zone of mixed carbonate and siliciclastic debris.
- *Saline mudflat - ephemeral lake complexes* have mixed carbonate-siliciclastic mudflats surrounding a shallow brine or pan in which salts (natron, mirabilite or epsomite, according to brine composition) are precipitated.

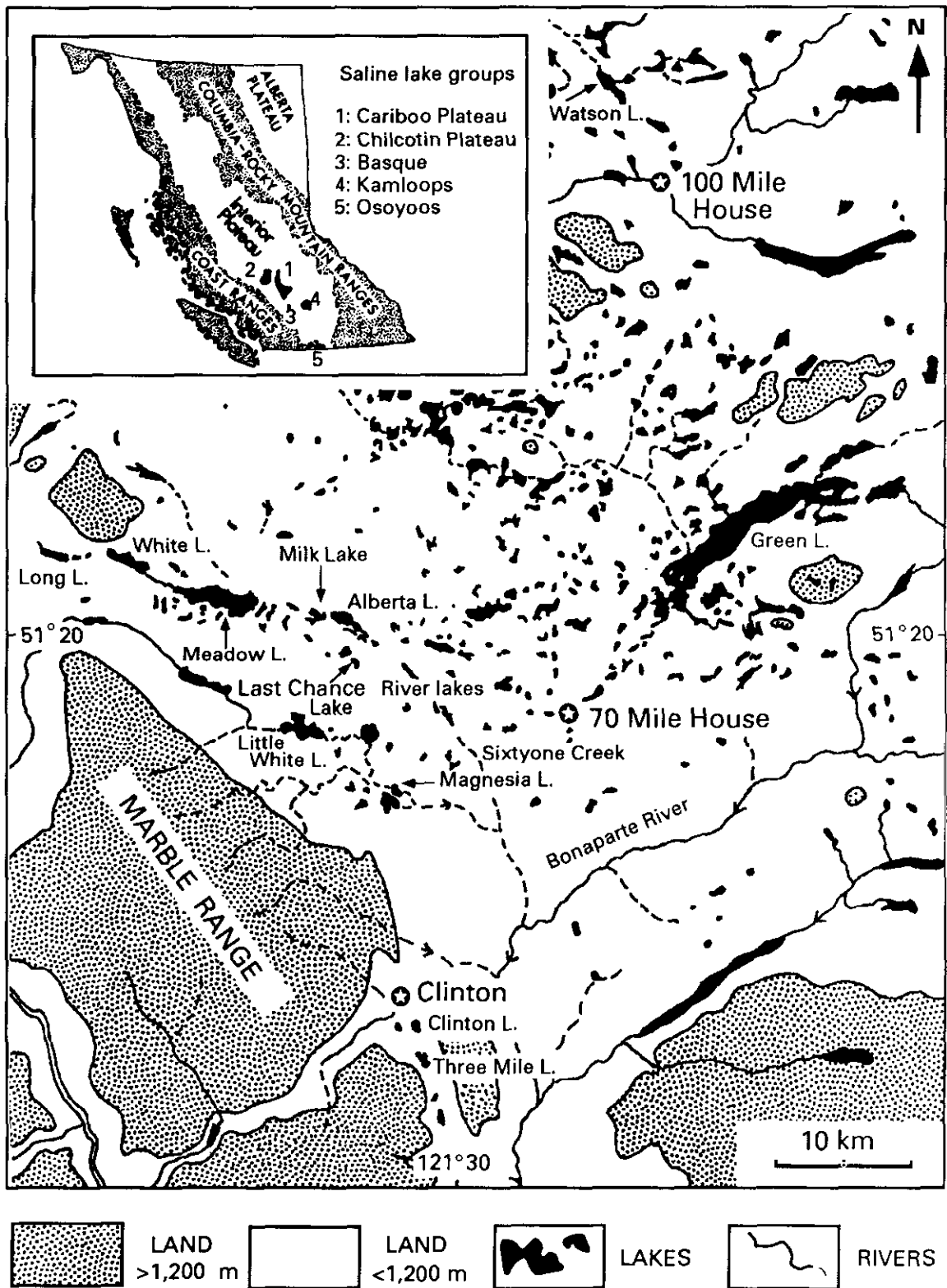


Figure 3-3-1. The southern Cariboo Plateau showing the location of Milk Lake.

More than 150 analyses have been made of Cariboo Plateau waters (Topping and Scudder, 1977; Renaut and Long, 1987; Renaut, 1990b). These have demonstrated a very wide range, both in salinity (<1 to >350 g L⁻¹ TDS) and in chemical composition. Notable are the exceptionally high magnesium/calcium ratios, which range from 0.7 to greater than 300. Evaporative concentration appears to be the dominant method of increasing salinity.

The main ions in runoff, spring waters, and fresh lakes (<3 g L⁻¹) are usually Mg²⁺, Na⁺, HCO₃⁻ and SO₄²⁻, and in many, Mg²⁺ and HCO₃⁻ are dominant. Lake waters with moderate salinities (3 to 50 g L⁻¹), including several carbonate playa-lakes, also have similar compositions.

There are three main types of hypersaline brine (>50 g L⁻¹) on the plateau: highly alkaline brines (pH: 8.5 to 10.5), poor in calcium and magnesium, with Na-CO₃-(SO₄)-Cl composition; more neutral brines (pH: 7.5 to 8.8), poor in HCO₃⁻ and CO₃²⁻, with Mg-Na-SO₄ composition; and Na-Mg-SO₄-CO₃ brines with somewhat lower salinities (pH: 8.0 to 9.5). The origins of the brines are discussed in Renaut (1990b).

THE MAGNESITE-HYDROMAGNESITE DEPOSITS OF MILK LAKE

A reconnaissance of magnesite and hydromagnesite deposits across the plateau suggests that they are found in four main depositional settings: (1) as the dominant minerals in carbonate-playa basins, where they precipitate subaqueously and in zones of shallow groundwater discharge; (2) in peripheral mudflats surrounding closed perennial lakes (e.g. Meadow Lake, Watson Lake of Cummings, 1940); (3) in marshy valley-bottom sites (e.g. Clinton, Basque, Riske Creek); and (4) either alone or associated with other mineral precipitates in saline mudflat – ephemeral lake complexes, where they may occur in peripheral mudflats or near sites of spring water discharge (e.g. Last Chance Lake).

Only the first type will be discussed here, using the example of Milk Lake. However, the processes in the mudflats of Types 2 and 3 are believed to be similar to those operative in Type 1.

SETTING OF MILK LAKE

Milk Lake is a small carbonate playa with well-developed magnesium carbonate muds (Figure 3-3-2). It lies on part of a southeast-trending paleodrainage channel network that extends from Long Lake, through Meadow Lake and Alberta Lake, and continues through to Sixtyone Creek (Figure 3-3-1). Large hydromagnesite-magnesite deposits are found west of Meadow Lake (Reinecke, 1920) and are reported in Sixtyone Creek (Cummings, 1940). It appears, therefore, that Milk Lake is but one of several magnesite-hydromagnesite lake basins located along the paleochannel.

Milk Lake has an irregular shape, consisting of three elongate lobes and a broad, central playa flat. It has a surface area of 0.3 square kilometre and the playa floor lies at an elevation of approximately 1095 metres. The playa is

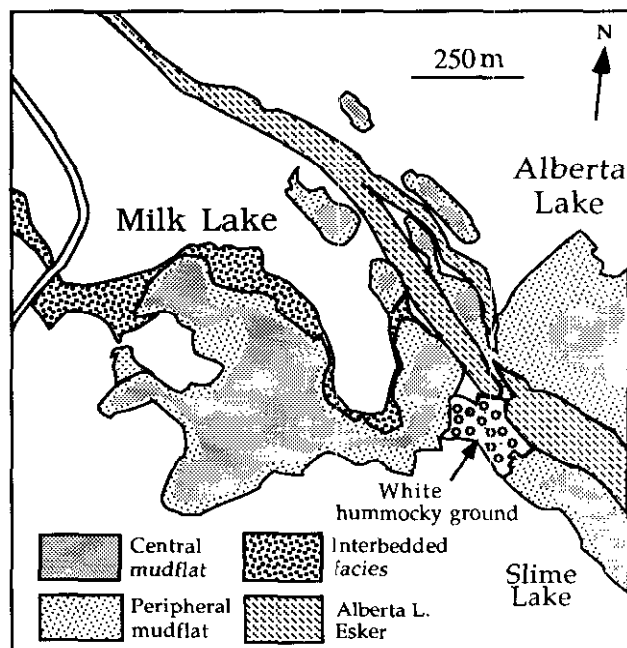


Figure 3-3-2. Depositional subenvironments of the Milk Lake playa basin.

confined by low vegetated hills, composed of glacial deposits, that rise abruptly from the shoreline on all sides. At the northwestern margin, the valley continues across a low col, now crossed by a road (Figure 3-3-2). The eastern margin of the basin is defined by the Alberta Lake esker, which rises 10 to 15 metres above the valley floor. Several smaller ephemeral lakes are separated from Milk Lake by vegetated carbonate mudflats.

The lake is fed mainly by groundwater, direct precipitation and unchannelled wash. Small lake-floor spring seeps are periodically visible. Milk Lake normally only holds water for 2 to 4 months a year, following spring snowmelt and for brief periods after heavy rains. During June 1990, which was exceptionally wet, the entire lake bed was submerged to an estimated maximum depth of 20 to 30 centimetres. The pH was 7.4 to 7.6. In contrast, in June 1988, the lake bed was already dry mud with small residual pools with waters having a pH of 8.7. The lake bed is usually ice covered from November until late March.

DEPOSITIONAL SUBENVIRONMENTS

Milk Lake is a typical Cariboo playa with three main depositional subenvironments (Figure 3-3-3). The centre of the basin is a broad mudflat that is seasonally occupied by an ephemeral lake. This passes transitionally into peripheral mudflats that, in turn, give way to vegetated hillslopes.

HILLSLOPE

The grass and tree-covered hillslopes are predominantly sites of erosion. Siliciclastic sediment is moved to the adjacent mudflats by slopewash. Periodically, small slumps and arcuate slope failures occur, projecting as lobes onto the

mudflats and exposing the glacial sediments to rapid erosion. As the slopes retreat, coarse gravels remain as surficial lag aprons along the base of slope.

PERIPHERAL MUDFLAT

The contact between the hillslope and the peripheral mudflat is commonly abrupt. The peripheral mudflats are a site of extensive magnesium carbonate precipitation. They are a zone where groundwater fluctuates at or close to the surface and is seeping basinward.

The peripheral mudflats are usually zoned with several types of surface (Figure 3-3-3). Below relatively steep hillslopes, the junction may be marked by dense, reedy vegetation; locally, there is standing water. This passes lakeward into a zone of vegetated hummocky ground on which sub-circular earthy hummocks rise up to 40 centimetres above the damp intervening hollows. The mounds range from 20 to 100 centimetres in diameter. Most hummocks are partially covered by pink and orange, leathery microbial (cyanobacterial) mats, 1 to 2 centimetres thick.

Sediments in this zone are typically a mixture of slope-derived siliciclastic detritus, mixed with precipitated magnesium carbonates, and are commonly rich in organic matter. They are massive to crudely bedded, may be granular, and are commonly disrupted by roots. Along the southern

shore, three main units can be recognized in the upper metre: an upper, dark grey stromatolitic carbonate layer; a brown, middle clastic unit with grey carbonate mottling and macrovegetal remains; and a lower, pale grey to cream carbonate layer (Figure 3-3-3). The intervening hollows are commonly rich in stromatolite intraclasts. This zone ranges in width from a few metres to approximately 20 metres, and is typically 5 to 10 metres wide.

Beyond the vegetated hummocks, there is usually a zone of white hummocky ground composed predominantly of magnesium carbonates. This differs from the former by being purer carbonate (often greater than 95%), having far less surficial vegetation, and displaying a more regular polygonal pattern (Plates 3-3-1 and 2). The subcircular hummocks ("cauliflowers" of Cummings, 1940) rise from a few decimetres to a metre above normal maximum lake level. They are typically 50 to 120 centimetres across, and separated by narrow, often damp depressions, normally with tufted grasses. The hummock surfaces have stromatolitic crusts 1 to 2 centimetres thick that break up as the surface dries out, producing intraclasts and finely powdered mud. Below these friable crusts, there is a layer of grey to white, mottled massive carbonate mud, that progressively becomes more cream in colour and granular at depths of 60 to 80 centimetres.

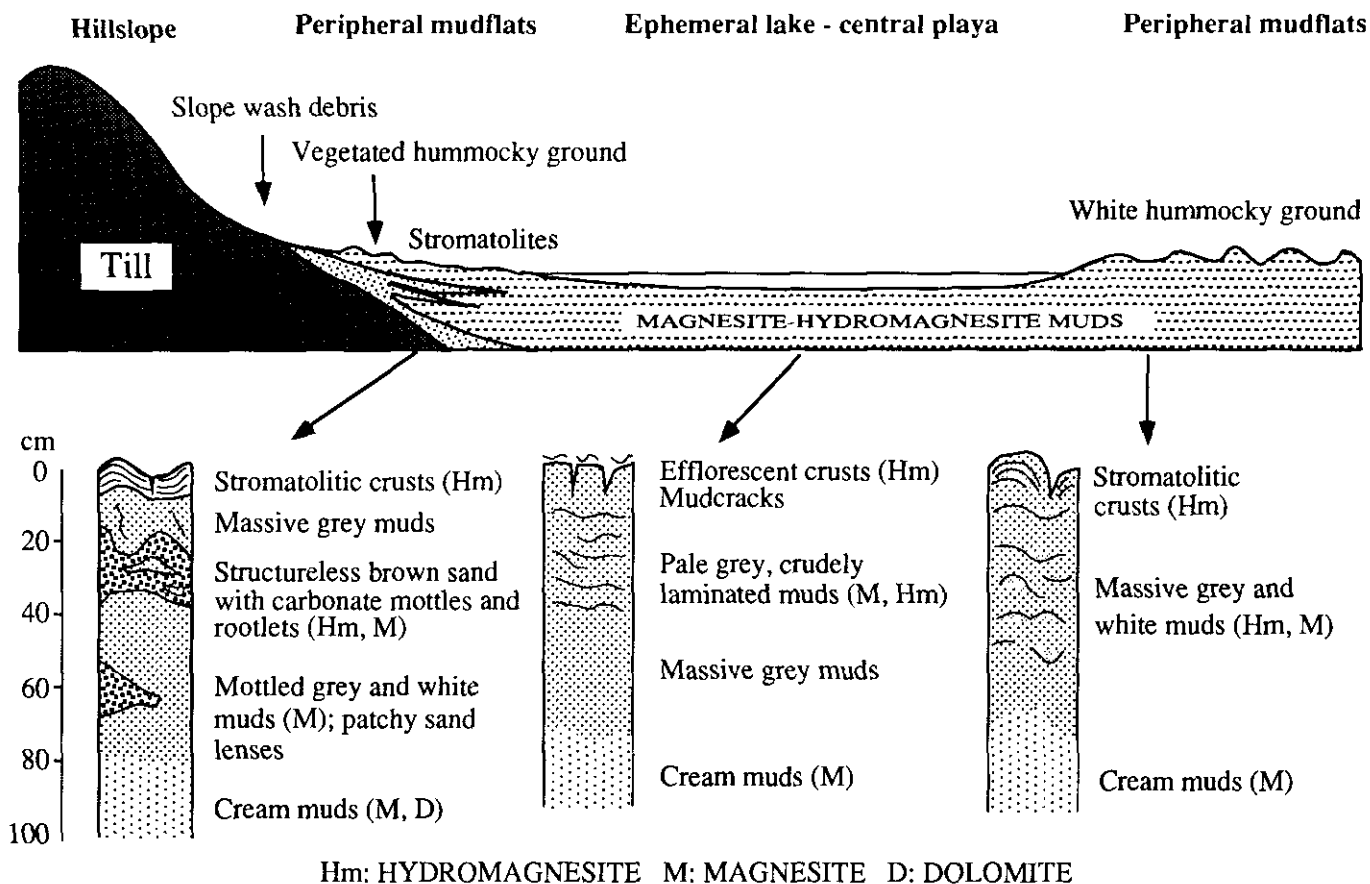


Figure 3-3-3. Schematic section through the southern margins of Milk Lake, showing selected profiles through the near-surface sediments.



Plate 3-3-1. White hummocky ground (hydromagnesite) at the southeastern margin of Milk Lake. The upper surface of the hummocks is composed of desiccated, fragmented microbial mats. The Alberta Lake esker is visible in the background.

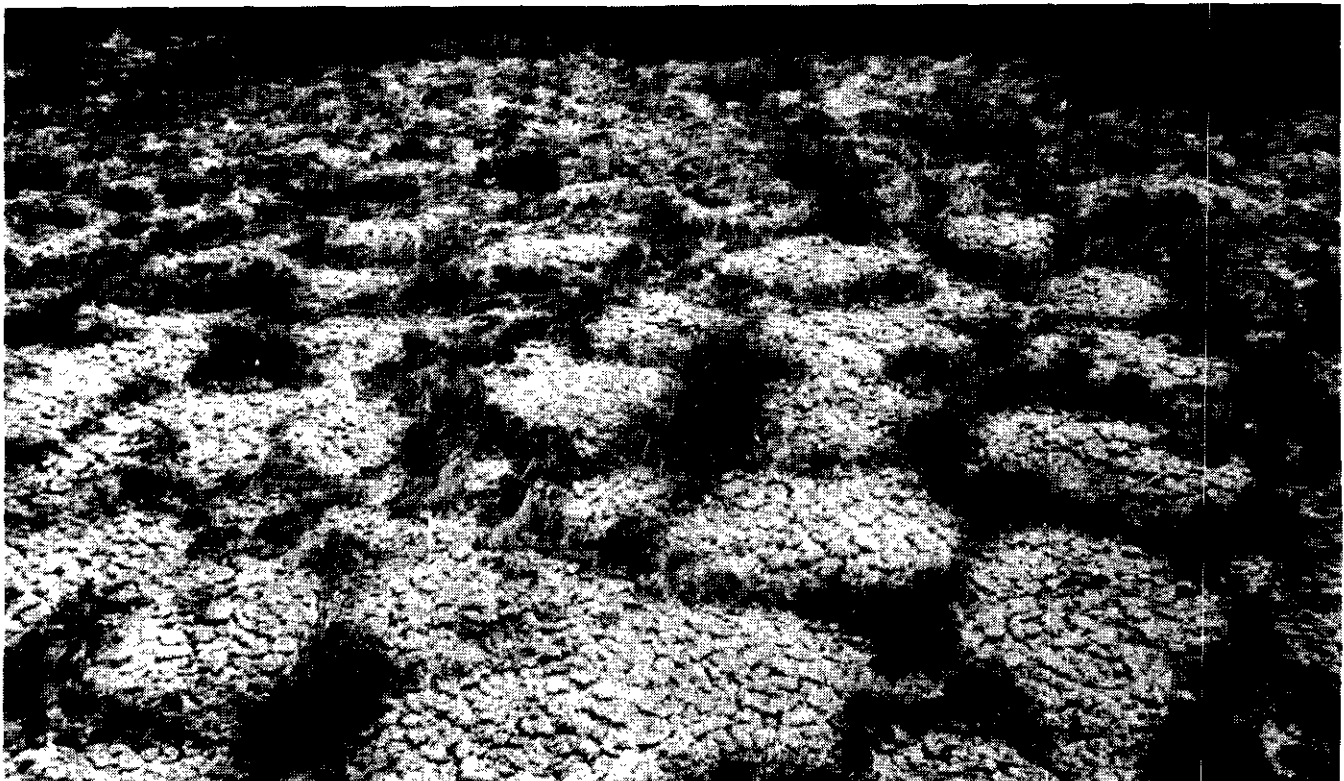


Plate 3-3-2. White hummocky ground (hydromagnesite) between Milk Lake and Slime Lake, showing polygonal pattern. Polygon at bottom centre is about 80 centimetres in diameter.



Plate 3-3-3. Hydromagnesite stromatolites on the southern margin of Milk Lake, which is visible at top right. Tufts of grasses are about 30 centimetres high.

This type of surface is common to most hydromagnesite-magnesite deposits across the plateau, including those at Meadow Lake, Watson Lake, Sixtyone Creek and Clinton Lake (Reinecke, 1920; Cummings, 1940; Renaut and Stead, 1990). This zone is not continuous around most lakes. It typically develops on mudflats at the extreme ends of elongate lakes, and may separate adjoining playa basins, as for example, between Milk Lake and Slime Lake (Figure 3-3-2).

Toward the shoreline, hummocky ground gives way to a broad zone of microbial mats (stromatolites) with extensive mudcracks (Plate 3-3-3). During June 1990 this zone was 5 to 20 metres wide and extended for at least 2 metres offshore. The stromatolites themselves show morphological zonation from broadly domal and pustular mats to nearly horizontal mats as the shoreline is approached. Sediments in the upper metre of this zone are typically white and grey, massive muds, locally with stromatolite intraclasts, becoming cream coloured at depth. Significantly, all the microbial mats of the peripheral mudflat were developed above the maximum lake level for spring of 1990.

CENTRAL MUDFLAT

The central mudflat, when dry, is a hard, flat surface of pale grey carbonate muds showing extensive, dense, small (2 to 20 cm) polygonal mudcracks. A few larger crack

networks also develop 2 to 4 metres apart. Although generally flat, small saucer-like depressions a few metres across and less than 10 centimetres deep, are scattered across the surface. They are commonly damp and are visible on aerial photographs. It is unclear whether these are loci of upward groundwater seepage or withdrawal, or both. Recessional strandlines, marked by concentrations of vegetative and/or microbial debris, and, more rarely, small (1 to 2 cm) wave-cut notches, are also present. Shallow rills less than 5 centimetres deep and from 10 to 50 centimetres wide, are found normal to the recessional shorelines. White efflorescent carbonate crusts from 1 to 10 millimetres thick develop locally, particularly toward the shoreline.

A shallow pit dug near the centre of the playa muds during June 1988 revealed massive grey muds which continue to a depth of at least 80 centimetres, becoming mottled with whiter patches and lenses 40 to 60 centimetres below the surface, and cream at about 1 metre. Samples allowed to dry at room temperature, and split subvertically with respect to the lake bed, revealed a crude, but disrupted, coarse (0.5 to 1 cm) lamination.

INTERBEDDED CARBONATES AND SILICICLASTICS OF THE NORTHERN LAKE MARGINS

The gentle grassy slopes along the northwestern playa margins are underlain by massive to weakly bedded, grey

and white, magnesium carbonate muds that interfinger with slope-derived siliciclastic sands. The carbonates lie up to a metre above the adjacent playa mudflats and, unlike the other playa margins, they are incised by broad shallow gulleys. They are also truncated by an erosional bluff along the modern littoral zone. Hummocky ground is only well developed close to the modern maximum level shoreline.

The significance of these sediments is uncertain. Although carbonates may be forming near the shore zone, the eroding sediments upslope may be somewhat older than those elsewhere in the basin.

MINERALOGY

Preliminary analyses of the mineralogy of 30 bulk samples of the carbonate muds were made by X-ray diffraction. Samples were prepared as cavity mounts and analysed using a Rigaku X-ray diffractometer with Cu K- α radiation. These have confirmed that the muds are predominantly magnesite ($MgCO_3$) and hydromagnesite ($Mg(OH)_2 \cdot 4MgCO_3 \cdot 4H_2O$) (Figure 3-3-4). Dolomite is present in two of the muds. Although the sample size is still small, several trends in the mineral distribution are apparent.

Hydromagnesite is the dominant, and commonly the only, mineral in the stromatolites and surficial efflorescent crusts that surround the lake. Hydromagnesite, normally mixed with some magnesite, is also the principal carbonate in the upper 10 to 30 centimetres of the zones of white hummocky ground. The carbonates interbedded with siliciclastics along the northern shore are a mixture of hydromagnesite and magnesite, the latter increasing downward in the profile.

Magnesite is the principal carbonate in the modern ephemeral lake muds. It is found at the surface of the dry lake bed (or below a thin, ephemeral hydromagnesite efflorescence) and continues to depths of at least 80 centimetres. Hydromagnesite was found in two cores at depths of 10 to 20 centimetres below the central playa surface, accounting for about 25 to 30 per cent of the total carbonate.

Magnesite also occurs in the peripheral mudflats. Although an accessory in some surficial crusts and stromatolites, it usually increases in abundance about 20 to 30 centimetres below the surface, down to about a metre, occurring as the only carbonate or accompanied by minor hydromagnesite or dolomite.

Partially ordered dolomite occurs at a depth of 40 to 80 centimetres below the stromatolites in the southern peripheral mudflat sediments, associated with magnesite (Figure 3-3-4). At Milk Lake, no other carbonate minerals were found in the initial batch of samples analysed. However, in the Clinton Lake basin (Figure 3-3-1), where similar hydromagnesite-magnesite muds are forming, aragonite, calcian dolomite and magnesian calcite are found mixed with hydromagnesite in peripheral mudflats (Renaut and Stead, 1990; Renaut *et al.*, in press). Nesquehonite ($MgCO_3 \cdot 3H_2O$) and huntite [$CaMg_3(CO_3)_4$] have been recorded from unnamed carbonate playas a few kilometres west of 70 Mile House.

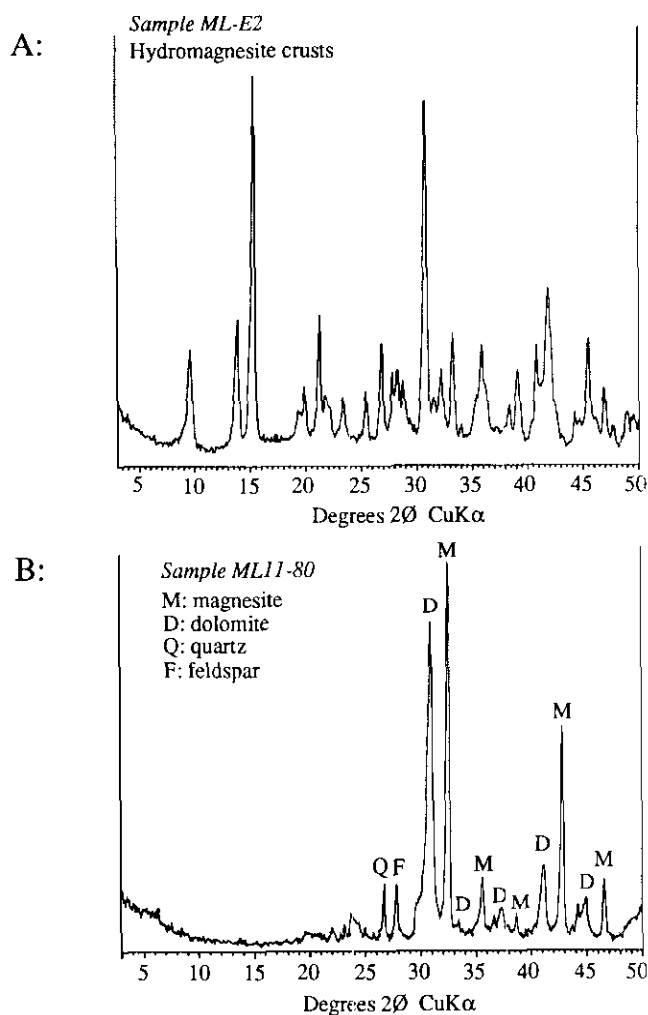


Figure 3-3-4: X-ray diffractograms of Milk Lake carbonates. A: Hydromagnesite crusts from white hummocky ground southeast of the lake; B: Magnesite-dolomite muds from 80 centimetres depth in a pit located in the peripheral mudflats of the southern shoreline.

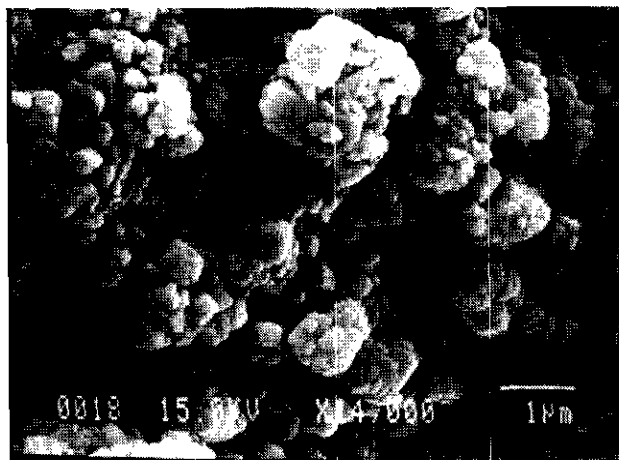


Plate 3-3-4. Scanning electron microscope photomicrograph showing aggregates of magnesite-hydromagnesite crystals, from a depth of 20 centimetres, central playa.

Four lacustrine muds were examined using a scanning electron microscope (Plate 3-3-4). They show that the muds are extremely fine grained. For both magnesite and hydromagnesite, individual crystals range from subhedral to anhedral and are less than 1 micron. Most occur as aggregates from 0.5 to 2 microns across.

The carbonates of the central mudflat are relatively pure. The acid-insoluble fraction of four samples ranged from 1.2 to 5.4 weight per cent. The principal impurities are clay minerals (mostly smectite), plagioclase silt, corroded diatom debris and organic detritus.

The peripheral mudflats generally contain a higher percentage of non-carbonates, reflecting detrital wash from adjacent slopes. The principal non-carbonate minerals detected by X-ray diffraction are plagioclase, quartz and clay minerals. Preliminary results suggest that smectites predominate (14Å). Palygorskite, sepiolite and opal-A have been found in samples from mudflats west of Meadow Lake, and may account for the silica reported in hydromagnesite analyses by Reinecke (1920) and Cummings (1940).

ORIGIN OF THE MAGNESITE-HYDROMAGNESITE DEPOSITS

Magnesite and hydromagnesite deposits have been described from playa lakes on several continents. Both primary and diagenetic origins for the minerals have been proposed (*e.g.* von der Borch, 1965; Irion and Müller, 1968; Müller *et al.*, 1972; Popov and Sadykov, 1987; Pueyo-Mur and Ingles-Urpinell, 1987; Molnar, 1990).

Although analyses are at a very preliminary stage, and chemical analyses of the basin waters are incomplete, the field evidence indicates that the magnesium carbonates are probably forming today. Magnesium-rich groundwaters are discharging into the basin, and through evaporation and/or biomediation, magnesite and hydromagnesite (and/or possibly a calcium-bearing precursor) are forming both in peripheral mudflats and within the central playa-lake.

The groundwaters acquire a high magnesium/calcium ratio on contact with the underlying basaltic rocks, and by widespread precipitation of calcite and magnesian calcite in soils and near-surface sediments (Renaut, 1990b). Previous analyses of Cariboo groundwaters have revealed magnesium/calcium ratios of 1.5 to 41, and salinities from <1 to 40 g L⁻¹ TDS (unpublished data). Although the hydrogeology is poorly understood, they move basinward through permeable layers within the tills and glaciofluvial deposits, or at their contact with the underlying lavas. Elsewhere on the plateau, especially along paleomeltwater channels, permeable sands and gravels underlie playa sediments and may also do so at Milk Lake.

In the peripheral mudflats, shallow groundwaters seeping lakeward undergo capillary evaporation and perhaps degassing of carbon dioxide. Hummocky and self-rising ground are commonly associated with groundwater discharge in the capillary fringe (*e.g.* Motts, 1970). The upward growth of hummocks may be related to interstitial carbonate precipitation within granular permeable sediments.

Hydromagnesite appears to be forming today at or close to the surface as a product of complete evaporation. Whether associated cyanobacteria mediate in precipitation is uncertain, but scanning electron microscope examination has shown that their filaments and mucilage are heavily encrusted by hydromagnesite.

The origin of the underlying magnesite and dolomite requires investigation. Cummings (1940) noted a common downward increase in calcium content of the muds which he attributed to differences in solubility, the calcium-bearing carbonates being first to precipitate from waters progressively concentrated as they are drawn upwards. There are, however, other possibilities that require testing. For example, groundwater composition may have varied through time as a result of a climatic change. A relative increase in evaporation, for example, might increase early calcium carbonate precipitation in soils, thereby increasing the magnesium/calcium ratio of the groundwaters. Dolomitization of a calcium carbonate precursor might result, and magnesium carbonates could precipitate. The common downward transition from hydromagnesite to magnesite may be diagenetic, due to dewatering of original hydromagnesite, which is the metastable phase (Christ and Hostetler, 1970). The effects of seasonal changes in groundwater composition, already noted in other lake basins (Renaut, 1990b), and flushing of the sediment by runoff are also unknown.

Most carbonate precipitation within the lake occurs as it gradually desiccates from its maximum level during May and June. During June 1990, the lake waters were milky with a fine suspension of white carbonate crystals and had a pH of 7.6.

A preliminary examination by scanning electron microscope of a small filtered sample collected at the shoreline revealed very fine aggregates of subhedral magnesium carbonate crystals, the individual crystals being less than 0.5 micron in diameter. Qualitative energy-dispersive analyses (EDS) on a JEOL JXA 8600 microprobe, confirmed that these are calcium-free. X-ray diffraction analysis of a smear of the very small sample produced a dominant, but weak, reflection at 2.735 Å, suggesting that they are magnesite, but further confirmation is required. Whether this is evidence of primary precipitation of magnesite, or resuspension of bottom muds, awaits investigation.

Although evaporative concentration and warming are probably important factors in precipitation, biomediation may also occur. During June and July, the waters were locally green with dense blooms of algae and cyanobacteria. Photosynthetic assimilation of carbon dioxide may, therefore, contribute to carbonate precipitation (*e.g.* Kelts and Hsü, 1978). Recently, Thompson and Ferris (1990) demonstrated cyanobacterial mineralization of magnesite in the laboratory and speculated that it may occur in high pH (8.5 to 10), saline aquatic environments, such as Milk Lake.

It is unclear whether magnesite is the initial and only precipitate, or whether hydromagnesite also precipitates from the lake waters or central playa groundwaters after the lake desiccates. Elsewhere on the plateau, hydromagnesite is apparently precipitating from lake water. In a small

gravel-pit pond 1 kilometre west of Clinton Lake, brief whittings of hydromagnesite have twice been observed during early summer. The sediments are nearly pure aggregates of hydromagnesite.

CONCLUSIONS

Magnesite and hydromagnesite are forming today at Milk Lake and in many other playa basins on the Cariboo Plateau. At Milk Lake, hydromagnesite is precipitating as surficial crusts from shallow magnesium-rich groundwaters in the capillary fringe of peripheral mudflats, and is commonly associated with cyanobacterial mats. It overlies magnesite and dolomite at a few decimetres depth.

Subaqueous precipitation of magnesium carbonates occurs in the desiccating playa lake, by evaporative concentration and possibly by biomediation. The original precipitate remains to be determined. The central playa muds are relatively pure and dominated by magnesite with subsidiary hydromagnesite.

ACKNOWLEDGMENTS

This work is supported by grants from the British Columbia Ministry of Energy, Mines and Petroleum Geoscience Research Grant program and the Natural Science and Engineering Research Council for which we gratefully acknowledge. We thank Cherdsak Utha-aroon for his assistance during fieldwork.

REFERENCES

- Campbell, R.B. and Tipper, H.W. (1971): *Geology of the Bonaparte Lake Map-area, British Columbia; Geological Survey of Canada, Memoir 363*, 100 pages.
- Christ, C.L. and Hostetler, P.B. (1970): Studies in the System $MgO-SiO_2-CO_2-H_2O$ (II): The Activity Product Constant of Magnesite; *American Journal of Science*, Volume 268, pages 439-453.
- Cummings, J.M. (1940): Saline and Hydromagnesite Deposits of British Columbia; *B.C. Ministry of Energy, Mines and Petroleum Resources, Bulletin 4*, 160 pages.
- Fulton, R.J. (1984): Quaternary Glaciation, Canadian Cordillera; in *Quaternary Stratigraphy of Canada - A Canadian Contribution To I.G.C.P. Project 24*, R.J. Fulton, Editor, *Geological Survey of Canada, Paper 84-10*, pages 39-47.
- Grant, B. (1987): Magnesite, Brucite and Hydromagnesite Occurrences in British Columbia; *B.C. Ministry of Energy, Mines and Petroleum Resources, Open File 1987-13*, 80 pages.
- Irion, G. and Müller, G. (1968): Huntite, Dolomite, Magnesite and Polyhalite of Recent Age from Toz Gölü, Turkey; *Nature*, Volume 220, pages 130-131.
- Kelts, K. and Hsü, K. (1978): Freshwater Carbonate Sedimentation; in *Lakes: Chemistry, Geology, Physics*; A. Lerman, Editor, *Springer*, New York, pages 295-324.

- Mathews, W.H. (1989): Neogene Chilcotin Basalts in South-central British Columbia: Geology, Ages, and Geomorphic History; *Canadian Journal of Earth Sciences*, Volume 26, pages 969-982.
- Molnar, B. (1990): Modern Lacustrine Carbonate (Calcite, Dolomite, Magnesite) Formation and Environments in the Hungary; *Thirteenth International Sedimentological Congress*, Nottingham, U.K., Abstracts (Papers), pages 363-364.
- Monger, J.W.H. (1989): Overview of Cordilleran Geology; in *Western Canada Sedimentary Basin - A Case History*, B.D. Ricketts, Editor, *Canadian Society of Petroleum Geologists*, pages 9-32.
- Motts, W. (Editor): 1970: *Geology and Hydrology of Selected Playas in Western United States; U.S. Air Force Cambridge Research Laboratories, Bedford, Massachusetts, Final Scientific Report (Part II), AFCRL-69-0214*, 288 pages.
- Müller, G., Irion G. and Förstner, U. (1972): Formation and Diagenesis of Inorganic Ca-Mg Carbonates in the Lacustrine Environment; *Naturwissenschaften*, Volume 59, pages 158-164.
- Popov, V.S. and Sadykov, T.S. (1987): Magnesium Carbonate Deposits of the Lake Beshkhod Region (Western Uzbekistan); *Lithology and Mineral Resources*, Volume 21, pages 394-400 (translation from *Litologiyai Poleznye Iskopaemye*, Volume 4, pages 112-118, 1986).
- Pueyo-Mur, J.J. and Ingles-Urpinell, M. (1987): Magnesite Formation in Recent Playa Lakes, Los Menegros, Spain; in *Diagenesis of Sedimentary Sequences*, J.D. Marshall, Editor, *Geological Society of London, Special Publication 36*, pages 119-122.
- Reinecke, L. (1920): Mineral Deposits between Lillooet and Prince George, British Columbia; *Geological Survey of Canada, Memoir 118*.
- Renaut, R.W. (1990a): Recent Sedimentation in the Saline, Alkaline Playa-lake Basins of Interior British Columbia, Canada; *Thirteenth International Sedimentological Congress*, Nottingham, U.K., Abstracts (Papers), pages 455-456.
- Renaut, R.W. (1990b): Recent Carbonate Sedimentation and Brine Evolution in the Saline Lake Basins of the Cariboo Plateau, British Columbia, Canada; *Hydrobiologia*, Volume 197, pages 67-81.
- Renaut, R.W. and Long, P.R. (1987): Freeze-out Precipitation of Salts in Saline Lakes - Examples from Western Canada; in *Crystallization and Precipitation*, G. Stratford, M.O. Klein and L.A. Melis, Editors, *Pergamon Press, Oxford*, pages 33-42.
- Renaut, R.W. and Long, P.R. (1989): Sedimentology of the Saline Lakes of the Cariboo Plateau, Interior British Columbia, Canada; *Sedimentary Geology*, Volume 64, pages 239-264.

- Renaut, R.W. and Stead, D. (1990): Sedimentology, Mineralogy and Hydrochemistry of the Magnesium Sulphate Playa-lakes of Alkali Valley, British Columbia, Canada; *Thirteenth International Sedimentological Congress*, Nottingham, U.K., Abstracts (Posters), pages 187-188.
- Renaut, R.W., Stead, D. and Owen, R.B. (in press): The Saline Lakes of the Fraser Plateau, British Columbia, Canada; in *Global Geological Record of Lake Basins*, E. Gierlowski-Kordesch and K. Kelts, Editors, *Cambridge University Press*.
- Thompson, J.B. and Ferris, F.G. (1990): Cyanobacterial Precipitation of Gypsum, Calcite and Magnesite from Natural Lake Water; *Geology*, Volume 18, pages 995-998.
- Tipper, H.W. (1971): Glacial Geomorphology and Pleistocene History of Central British Columbia; *Geological Survey of Canada, Bulletin* 196, 89 pages.
- Topping, M.S. and Scudder, C.G.E. (1977): Some Physical and Chemical Features of Saline Lakes in Central British Columbia; *Syesis*, Volume 10, pages 145-166.
- Valentine, K.W.G. and Schori, A. (1980): Soils of the Lac La Hache–Clinton Area, British Columbia; *B.C. Soil Survey Report*, Volume 25, 118 pages.
- von der Borch, C. (1965): The Distribution and Preliminary Geochemistry of Modern Carbonate Sediments of the Coorong Area, South Australia; *Geochimica Cosmochimica Acta*, Volume 29, pages 781-799.



**1991 REGIONAL GEOCHEMICAL SURVEY RELEASE,
SOUTHEASTERN BRITISH COLUMBIA:
DELIVERING A NEW GENERATION OF GEOCHEMICAL DATA*
(82E, F, G, J, K, L, M)**

By P.F. Matysek, W. Jackaman and S. Feulgen

KEYWORDS: Regional Geochemical Survey, reconnaissance, multi-element, stream sediment, water, Fernie, Kananaskis Lakes, Penticton, Nelson, Lardeau, Vernon, Seymour Arm.

INTRODUCTION

Since the inception of the joint federal-provincial Regional Geochemical Survey (RGS) program in 1976, high-quality geochemical data have been effectively disseminated to the exploration and mining industry (Figure 4-1-1). A great many new mineral prospects have been discovered, old ones have been re-evaluated and a number of areas previously thought to have little mineral potential have been investigated as a result of these surveys. Over time, the program has evolved in its scope and mandate in response to the changing demands of the exploration industry, the development of fast, inexpensive high-quality analytical techniques, increased knowledge of trace element dispersion and the growing concern with environmental and land-use issues.

The 1990 programs covering southeastern British Columbia reflect the continued efforts of the Applied Geochemistry Unit to meet the needs of the exploration industry as well as to enhance the inherent qualities of the data as a tool for other research. Highlights of these programs include:

- The completion of two regional geochemical surveys in southeastern British Columbia, covering NTS map sheets, Fernie (82G) and Kananaskis Lakes (82J).
- The expansion of the RGS stream-sediment analytical suite to include neutron activation analyses of 26 additional metals and pathfinder elements.
- The expansion of the stream-water chemistry database to include analytical results for copper, lead, zinc, mercury, cadmium and arsenic.
- The analysis of 25 000 archived regional geochemical stream-sediment samples (seventeen 1:250 000 map sheets, Figure 4-1-1) for 26 previously undetermined elements. The 1991 release will include results from NTS map sheets Penticton (82E), Nelson (82F), Lardeau (82K), Vernon (82L) and Seymour Arm (82M).

The forthcoming 1991 RGS release will present explorationists with the formidable task of assessing over 500 000 analytical results from approximately 8400 sites covering 110 000 square kilometres of one of British Columbia's most diverse geological regions (Table 4-1-1). Preliminary interpretation of the data indicates that sites occurring

TABLE 4-1-1
SAMPLE DISTRIBUTION IN SOUTHEASTERN
BRITISH COLUMBIA

Map Sheet	Sample Year	Number of Sites	Area km sq.	Density km sq./site
82G - Fernie	1990	922	11400	12
82J - Kananaskis	1990	583	6500	11
82E - Penticton	1976	1631	16600	10
82F - Nelson	1977	1394	16600	12
82K - Lardeau	1977	1297	16400	13
82L - Vernon	1976	1385	16400	12
82M - Seymour Arm	1977	1219	16200	13
TOTALS		8431	100100	12

within the Lower Paleozoic Lardeau group, Triassic-Jurassic Nicola and Rossland groups and Jurassic granodiorites contain a high proportion of samples anomalous in base and precious metals. Additionally, the expanded stream-water database will aid in the evaluation of the background metal concentrations in this area of high mineral potential.

This report will outline the regional geologic setting and the associated mineralization found in the survey areas. Survey parameters (sample collection, preparation and analytical procedures) and a preliminary evaluation of the base and precious metal results are also presented.

REGIONAL SETTING

LOCATION

The areas surveyed in 1976, 1977 and 1990 cover southeastern British Columbia from 49° to 52° north latitude and 114° to 120° west longitude. The region is characterized by a varied physiography (Table 4-1-2) and complex geology (Figure 4-1-2).

PHYSIOGRAPHY

Southeastern British Columbia consists of two major physiographic regions, the Columbia Mountains and Southern Rockies, and the Interior Plateau (Holland, 1976). Extending westward from the Alberta border to the Monashee Range, the Columbia Mountains and Southern Rockies physiographic region accommodates the majority of the survey area. These parallel mountain belts trend northwest and are separated by the Rocky Mountain Trench.

* This project was funded in part by the Sustainable Environment Fund and is a contribution to the Canada/British Columbia Mineral Development Agreement 1985-1990.

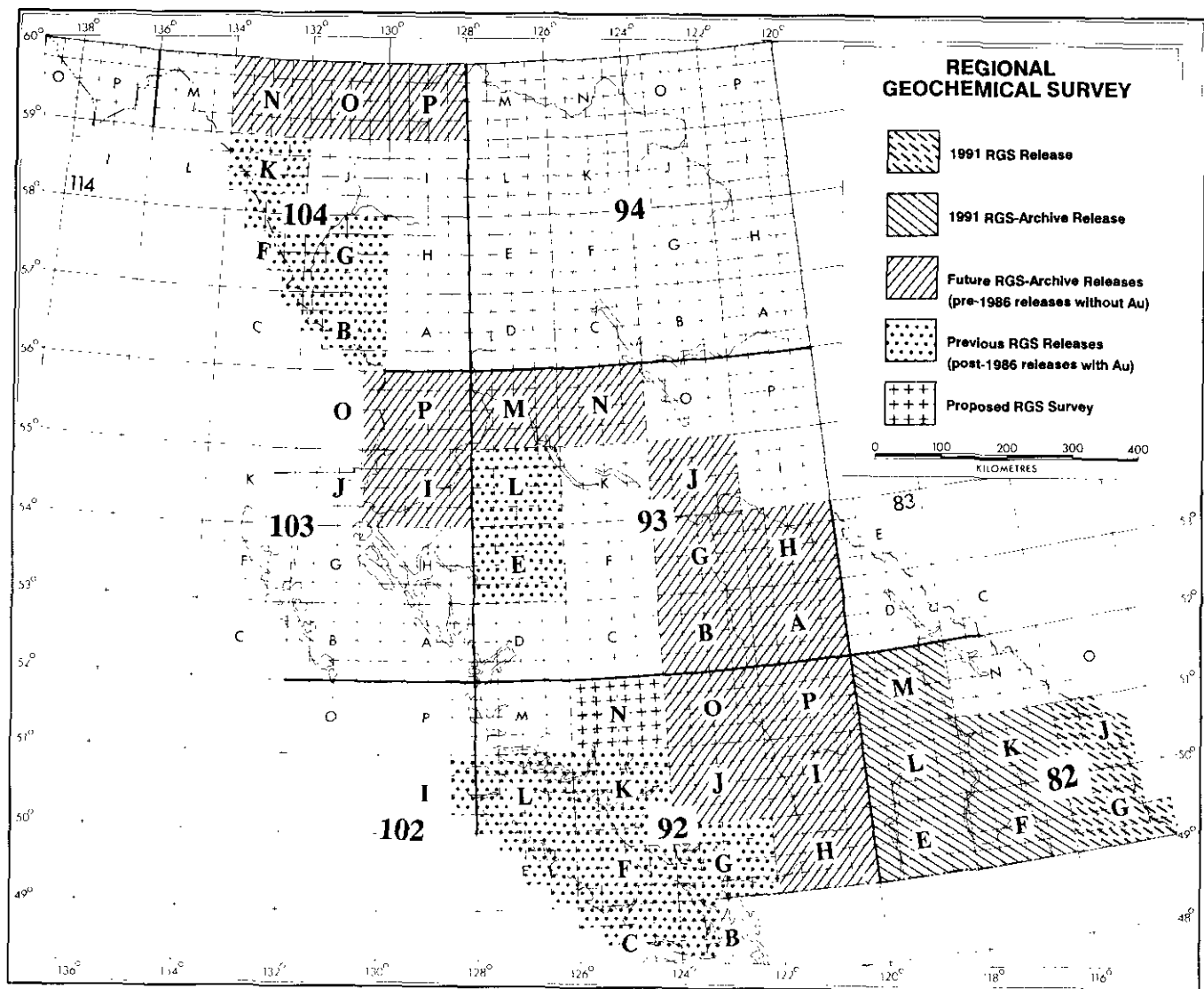


Figure 4-1-1. Current status of British Columbia Regional Geochemical Survey program.

The Rocky Mountains are strongly faulted, folded and glaciated. Summit elevations range above 2500 metres and extremely rugged mountains are separated by deep, narrow valleys. The peaks and ridges are predominantly exposed bedrock. The steeply sloping valley sides are covered with talus or colluvium and the valley bottoms contain alluvium and till. The primary and secondary stream drainages found in these high mountain areas are generally characterized by a herringbone pattern.

The Columbia Range averages 2000 metres in elevation. The peaks are well rounded and the corresponding stream patterns are primarily dendritic. Till and colluvium cover the middle to upper slopes and alluvium is found in the stream basins.

As many of the mountain ranges within this major physiographic region exceed 3000 metres elevation, they are very effective barriers to the eastward movement of moist Pacific air masses. This rainshadow effect produces drier climates in the major valleys such as the Rocky Moun-

tain Trench, especially on their east-facing slopes. As a result, dry, overgrown creek beds, which no longer contain stream-sediment material, are commonly found in these areas.

The survey area also extends into the eastern margin of the Interior Plateau. The Shuswap and Okanagan Highlands consist of well-rounded ridges and summits ranging from 1500 to 2000 metres elevation. Glacial erosion has produced deep valleys with steeply sloping sides. The higher elevations are characterized by relatively resistant bedrock and the valley floors are covered with drift material. The drainage patterns are primarily dendritic.

GEOLOGY

The survey area includes parts of three of the five structurally and physiographically distinct belts which constitute the Canadian segment of the North American Cordillera. From east to west, these are: the Foreland Belt, the Omineca Belt and the Intermontane Belt.

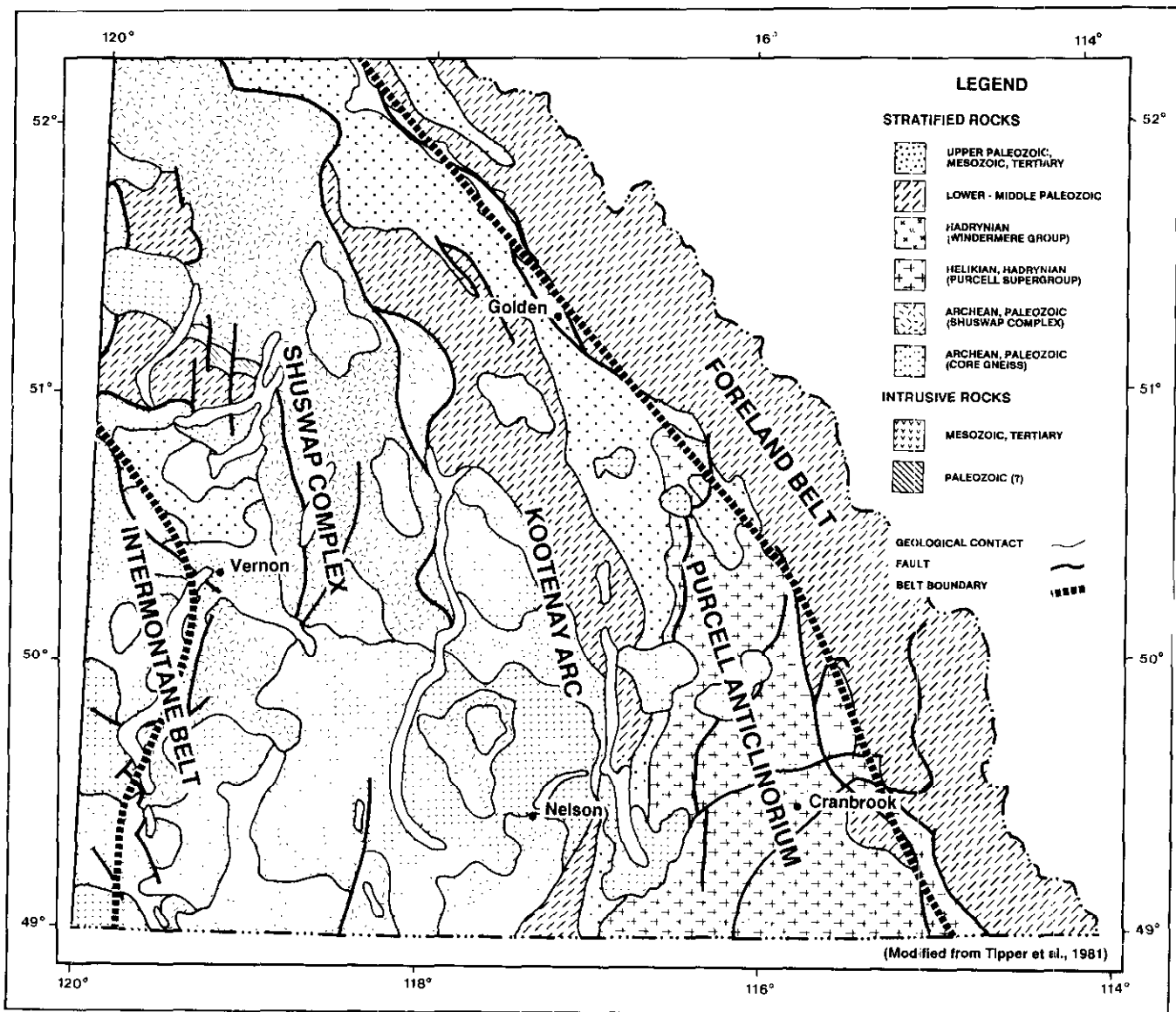


Figure 4-1-2. Geology of southeastern British Columbia.

The Foreland and Intermontane belts are primarily composed of unmetamorphosed and low-grade metamorphic stratified rocks. Separating these two belts, and characteristically distinct, is the Omineca Belt, a high-grade metamorphic and granitic belt that reflects a history of tectonic uplift and the intrusion of granitic rocks between mid-Jurassic and early Tertiary time.

On the eastern margin of southern British Columbia lie miogeoclinal clastic and carbonate sediments of mid-Proterozoic to Mesozoic age which comprise the Foreland Belt. These were deposited on the western edge of cratonic North America and subsequently thrust eastward during Mesozoic and Tertiary times. Small Cretaceous intrusions are found within this belt. The region is bounded by the Omineca Belt to the west.

Most of the study area lies within the Omineca Belt. It is characterized by a succession of strongly deformed and

locally strongly metamorphosed Proterozoic and Paleozoic miogeoclinal rocks, younger volcanics, pelitic rocks and a large number of Mesozoic intrusions (Höy, 1983). The Purcell anticlinorium, Kootenay arc, and Shuswap metamorphic complex are structural provinces defined within this belt and host several important mineral deposits.

The Purcell anticlinorium comprises a succession of northward-plunging rocks of Proterozoic age. One of the largest known stratiform base metal deposits in the world, the Sullivan mine, is hosted by Helikian turbidites (Aldridge Formation) along the eastern edge of the Purcell anticlinorium and other deposits are found to the south, in the United States, in rocks equivalent to the Purcell Supergroup strata.

The Kootenay arc is described as a north-trending arcuate belt containing sediments of Hadrynian to early Mesozoic age which have been folded and thrust faulted. A major

TABLE 4-1-2
ABRIDGED DESCRIPTION OF PHYSIOGRAPHY AND GEOLOGY

PHYSIOGRAPHIC REGIONS	PHYSIOGRAPHIC SUBUNITS	GEOLOGY AND STRUCTURE
INTERIOR PLATEAU	Shuswap Highland	gneiss and schistose metamorphic rocks
	Okanagan Highland	metamorphic rocks (chiefly gneiss) with granitic intrusions
COLUMBIA MOUNTAINS AND SOUTHERN ROCKIES	Rocky Mountains	folded and faulted sedimentary and metasedimentary (chiefly limestone, quartzite, schist and slate) rocks
	Rocky Mountain Trench	chiefly Quaternary sediments
	Purcell Mountains	folded sedimentary and metamorphic rocks (chiefly quartzite, argillite and limestone) with granitic intrusions
	Selkirk Mountains	folded sedimentary and metamorphic rocks with granitic stocks and batholiths
	Monashee Mountains	folded sedimentary and metamorphic (chiefly gneiss) rocks with intrusions
	Cariboo Mountains	folded sedimentary and metamorphic rocks

regional structure, it is primarily a lead-zinc belt as is evidenced by the Salmo mining camp, Bluebell and Wigwam deposits, which are typified by shallow-water Lower Cambrian carbonate hosts. The Rossland volcanics of Jurassic age continue to be actively explored for large gold-bearing shear zones and the Cretaceous Nelson batholith is host to the old silver mining camp known as the "Silver Slocan".

The Shuswap metamorphic complex is separated from the Kootenay arc by the eastward-dipping Columbia River fault. The metamorphic complex consists primarily of Archean paragneisses which form domal structures containing core gneisses of Aphebian age. A number of large stratabound lead-zinc deposits, such as Big Ledge and Ruddock Creek, are found along its eastern margin.

The Intermontane Belt, west of the Omineca Belt, crosses the extreme southwest corner of the study area. Moderately folded upper Paleozoic strata, overlain unconformably by folded and faulted Late Triassic volcanics, are intruded by Late Triassic to Early Jurassic plutons which have caused low-grade metamorphism of the strata (Schau, 1970).

MINERAL DEPOSITS

The styles of mineralization found in the 1991 RGS-release area can be categorized according to tectonic terrane and deposit type. Table 4-1-3 is a compilation of some past and presently active exploration properties within the survey area (British Columbia Mineral Exploration Review 1990, Information Circular 1990-1).

The Omineca Belt remains the centre of exploration activity in southeastern British Columbia. Current exploration within the belt is concentrated on Sullivan-type deposits within the Purcell Supergroup. Other activities include the evaluation of lode gold deposits within the

Rossland volcanics; sedex deposits in the Upper Proterozoic Dutch Creek Formation; massive sulphide deposits in the Eagle Bay assemblage; stratabound copper deposits found in the Grinnell Formation of the Purcell Supergroup; and gold in Cambrian limestones adjacent to the Sheep Creek camp.

In the Foreland Belt, recent exploration has centred on the Jubilee Formation carbonates which host lead-zinc-copper-(silver) mineralization at intrusive contacts; and on gold associated with Cretaceous alkalic intrusions in the Flathead area.

Most exploration within the Intermontane Belt is focused on porphyry deposits and gold-bearing skarns similar to the Nickel Plate deposit. Interesting possibilities also continue to be explored in the Eocene and Tertiary volcanic rocks of the area and several epithermal vein systems hosting gold have been discovered.

1990 PROGRAMS

RGS PROGRAM — SOUTHERN ROCKY MOUNTAINS (82G, J) STREAM-SEDIMENT AND STREAM-WATER SAMPLE COLLECTION

MPH Consulting Limited (Vancouver) was selected by competitive bid to carry out the 1990 RGS sampling program. The sample-collection team consisted of five samplers and a crew chief. Field operations were conducted from several strategically located base camps. Ministry representation was maintained throughout the 40-day program to ensure all aspects of sample collection, data recording, drying, packing and shipping were in accordance with standards set by the National Geochemical Reconnaissance Program.

TABLE 4-1-3
COMMON DEPOSIT TYPES AND ASSOCIATED GEOLOGICAL ENVIRONMENTS

CLASS	SUBCLASS	EXAMPLE	COMMODITIES	HOST ROCK
INTERMONTANE BELT				
PORPHYRY	Calc alkaline	Brenda	Cu, Mo	hosted within a zoned and composite quartz diorite body known as the Brenda stock
VEIN	Epithermal	Vault	Au	a deep, structurally complex epithermal vein system hosted by Eocene volcanic rocks
SKARN		Dividend-Lakeview	Au	hosted by Triassic Kobau or Paleozoic Anarchist groups, associated with Osoyoos batholith
		Crystal Peak	Industrial Garnet	hosted in an inlier of upper Triassic Nicola group granite, associated with Bromley pluton
OMINECA BELT				
SHUSWAP METAMORPHIC COMPLEX				
MASSIVE SULPHIDE	Stratabound	Ruddock Creek	Zn, Pb, Ag, (F, Ba)	stratabound layers in quartzite, calc silicate gneiss, marble Helikian-Hadrynian(?) age
	Stratiform	Victory	Ag, Au, Cu, Zn, Pb	hosted by Eagle Bay assemblage and Fennell Formation, Samatosum mine extension?
	Volcanogenic Kuroko Type	Homestake	Pb, Zn, Cu, Ag, Ba	hosted by Eagle Bay assemblage in sequence of schists and felsic volcanic lenses
VEIN	Epithermal	Venner	Au	gold-bearing epithermal quartz carbonate vein in a trachytic volcanoclastic sequence
SKARN		Greenwood Camp	Au, Ag, Cu	associated with late Paleozoic Knob Hill group and rocks of the Triassic Brooklyn Formation
KOOTENAY ARC				
MASSIVE SULPHIDE	Sedex	Reeves-McDonald	Zn, Pb, Ag, (Cd, Ga, Ge)	well-banded, parallel lenses hosted by Reeves Formation dolomite (associated breccia)
	Volcanogenic Besshi Type	Goldstream	Cu, Zn, (Pb)	stratabound layers hosted in the Lardeau group
VEIN	Mesothermal	Rossland Camp	Au	lodes and replacements along fractures and faults cutting Jurassic Rossland volcanics
		Slocan Camp	Ag, Pb, Zn	lodes and replacements in Slocan group sediments and the Nelson batholith
SKARN		Tillicum Mountain	Au, Ag	hosted by Rossland volcanics associated with quartz monzonite sills
PORPHYRY-BRECCIA	Calc alkaline	Willa	Cu, Au	hosted by Rossland volcanics
PLACER	Gold	Wild Horse River	Au	
PURCELL ANTICLINORIUM				
MASSIVE SULPHIDE	Sedex	Sullivan	Pb, Zn, Ag	hosted by lower Middle Aldridge siltstone
	"Kupferschiefer"		Cu, U (Ag, Pb, Mo)	stratabound layers in Grinnell Formation sandstone red beds
VEIN		Vine	Zn, Pb, Cu	hosted by the Aldridge Formation; associated with fault zone
FORELAND BELT				
SKARN		Cash	Pb, Zn, Cu (Ag)	hosted by brecciated Jubilee Formation limestones at intrusive contacts with Cretaceous syenite
PORPHYRY	Alkaline	Flathead	Au	hosted by Cretaceous alkalic intrusions
INDUSTRIAL MINERALS		Mt. Brussilof	Magnesite	replacement in Cambrian Cathedral Formation

TABLE 4-1-4
METHODS AND SPECIFICATIONS FOR SAMPLE ANALYSES (AFTER MATYSEK *ET AL.*, 1989)

Element	Detection Limits	Sample Weight	Digestion Technique	Determination Method	
Gold Silver	1 ppb 100 ppb	10 g	fire assay fusion - Palladium inquarting agent	FA-AA	atomic absorption spectrophotometry after digestion of doré bead by aqua regia
Cadmium Cobalt Copper Iron Lead Manganese Nickel Zinc	0.2 ppm 2 ppm 2 ppm 0.02 pct 2 ppm 5 ppm 2 ppm 2 ppm	1 g	3 ml HNO ₃ let sit overnight, add 1 ml HCl in 90°C water bath, for 2 hrs. cool, add 2 ml H ₂ O, wait 2 hrs.	AAS	atomic absorption spectrophotometry using air-acetylene burner and standard solutions for calibration, background corrections made for Pb, Ni, Co, Ag, Cd
Molybdenum	1 ppm	0.5 g	Al added to above solution		
Barium Vanadium Chromium	10 ppm 5 ppm 5 ppm	1 g	HNO ₃ - HCl - HF taken to dryness, hot HCl added to leach residue		
Bismuth Antimony	0.2 ppm 0.2 ppm	2 g	HCl - KClO ₂ digestion, KI added to reduce Fe, MIBK and TOPO for extraction	AAS-H	organic layer analyzed by atomic absorption spectrophotometry with background correction
Tin	1 ppm	1 g	sintered with NH ₄ I, HCl and ascorbic acid leach	AAS	atomic absorption spectrophotometry
Arsenic	1 ppm	0.5 g	add 2 ml KI and dilute HCl to 0.8M HNO ₃ • 0.2M HCl	AAS-H	2 ml borohydride solution added to produce AsH ₃ gas which is passed through heated quartz tube in the light path of atomic absorption spectrophotometer
Mercury	10 ppb	0.5 g	20 ml HNO ₃ • 1 ml HCl	AAS-F	10% stannous sulphate added to evolve mercury vapour, determined by atomic absorption spectrometry
Tungsten	1 ppm	0.5 g	K ₂ SO ₄ fusion, HCl leach	COLOR	colorimetric: reduced tungsten complexed with toluene 3, 4 dithiol
Fluorine	40 ppm	0.25 g	NaCO ₃ - KNO ₃ fusion, H ₂ O leach	ION	citric acid added and diluted with water, fluorine determined with specific ion electrode
Uranium	0.5 ppm	1 g	nil	NADNC	neutron activation with delayed neutron counting
LOI	0.1 pct	0.5 g	ash sample at 500°C	GRAV	weight difference
pH - water	0.1 pH unit	25 ml	nil	GCE	glass - calomel electrode system
U - water	0.05 ppb	5 ml	add 0.5 ml fluran solution	LIF	place in Scintrex UA-3
F - water	20 ppb	25 ml	nil	ION	fluorine ion specific electrode

Stream-sediment and stream-water samples were collected from 922 sites within the Fernie map area (82G), and 583 sample sites were sampled within the Kananaskis Lakes map area (82J). The surveys covered approximately 18 000 square kilometres at an average density of one sample site every 11.9 square kilometres. Sixty-five per cent of the sites were accessed by truck or trail bike, the remainder were reached by helicopter. The program included sample collection in Kootenay National Park, Elk Lakes Recreation Area, Akamina Kishinena Recreation Area and Height of the Rockies Forest Wilderness Area. However, samples were not collected from Mount Assiniboine, Elk Lakes and Top of the World provincial parks.

In general, sample sites were restricted to primary and secondary drainages having catchment basins of less than 10 square kilometres. Contaminated or poor-quality sample sites were avoided by choosing an alternative stream or sampling a minimum of 100 metres upstream from the identified problem. At each site fine-grained stream sediments weighing 1 to 2 kilograms were collected from the active (subject to annual flooding) stream channel and placed in kraft-paper bags. Unfiltered water samples were collected in sterilized 250-millilitre bottles. Precautions were taken to ensure suspended solids were excluded from the water sample. Field observations regarding sample media, sample site and local terrain were recorded and, to assist follow-up, aluminum tags inscribed with a unique RGS sample identification number were fixed to permanent objects at each site. Numerous field-site checks were conducted to monitor, control and assess sample-collection procedures.

SAMPLE PREPARATION — FIELD

Collected samples were field processed by the sample collection contractor at a central facility in Cranbrook. Sediment samples were dried and all sediment material finer than 1 millimetre was recovered by sieving each sample through a -18 mesh ASTM screen. Samples were assessed for quality and content of fine-grained sediment and samples which appeared deficient in fine-grained material were routinely sieved through a -80 mesh screen (less than 177 microns). Sites yielding organic-rich samples and samples containing less than 40 grams of -80 mesh stream sediment were resampled.

SAMPLE PREPARATION — LAB

Field-processed sediment samples and the water samples were shipped to Rossbacher Analytical Laboratory in Burnaby for final preparation. Sediment samples were sieved to -80 mesh ASTM fraction and blind duplicate samples and control reference materials were inserted into each analytical batch of 20 sediment samples. Control reference water standards were also inserted into each analytical batch of 20 water samples. At this stage, a quantity of -80 mesh sediment and a representative sample of the +80 to -18 mesh fraction was archived for future studies.

TABLE 4-1-5
REPORTED DETECTION LIMITS FOR INSTRUMENTAL
NEUTRON ACTIVATION ANALYSES

Element	Detection Limits	Element	Detection Limits
Gold	2 ppb	Molybdenum	1 ppm
Antimony	0.1 ppm	Nickel	10 ppm
Arsenic	0.5 ppm	Rubidium	5 ppm
Barium	100 ppm	Samarium	0.5 ppm
Bromine	0.5 ppm	Scandium	0.5 ppm
Cerium	10 ppm	Sodium	0.1 pct
Cesium	0.5 ppm	Tantalum	0.5 ppm
Chromium	5 ppm	Terbium	0.5 ppm
Cobalt	5 ppm	Thorium	0.5 ppm
Hafnium	1 ppm	Tungsten	2 ppm
Iron	0.2 pct	Uranium	0.2 ppm
Lanthanum	5 ppm	Ytterbium	2 ppm
Lutetium	0.2 ppm	Zirconium	200 ppm

ANALYTICAL PROCEDURES

Table 4-1-4 outlines the standard RGS procedures used to analyze the sediment and water samples. These methods and specifications have been successfully employed in previous surveys. In addition to the standard RGS analytical package, the sediment samples will also be shipped to Becquerel Laboratories (Ontario) for analysis of 26 elements (Table 4-1-5) by instrumental neutron activation analyses.

Instrumental neutron activation analyses involves irradiating the sediment samples, which on average weigh 20 grams, for 20 minutes in a neutron flux. Most of the elements in the sample become radioactive and emit radiation in the form of gamma rays which have energies (wavelengths) characteristic of particular elements. Samples are then removed from the neutron flux and placed close to a gamma-ray detector, commonly a germanium crystal held at the temperature of liquid nitrogen. Counting data are accumulated on a computer and converted to concentrations.

Field site duplicates, blind analytical duplicates and control reference materials are used to ensure that analytical data satisfy National Geochemical Reconnaissance quality control standards.

EXPANDED STREAM-WATER CHEMISTRY DATABASE

BACKGROUND

Until quite recently, explorationists have made relatively little use of stream water as a sample medium for geochemical drainage surveys (Learned *et al.*, 1985). The recent availability of instrumentation allowing inexpensive, rapid and direct determination of metals in water to concentrations below the parts per billion level has made the collection and analysis of stream water more economically feasible. In order to test the relative effectiveness of stream water

as a geochemical exploration medium, and to further the understanding of background metal concentrations (Cu, Pb, Zn, As, Cd, Hg) in stream waters, an additional water sample was collected from each RGS sample site. The results will also be used for developing water-quality objectives for existing and future mining operations, trans-boundary water-quality issues and the setting of water-quality criteria for fish habitat and human consumption.

SAMPLE COLLECTION AND PREPARATION

A total of 1259 water samples were collected and prepared according to Ministry of Environment (MOE) water-sampling protocols.

A 250-millilitre unfiltered water sample was taken in midstream from the same stream drainages sampled during the RGS program. Samples were stored in coolers immediately after collection. On average, sample preparation was completed within 6 to 8 hours and involved the filtering of a 125-millilitre portion of the unfiltered sample through a 0.45 micron cellulose acetate filter. Both the unfiltered and filtered samples were acidified with 1 millilitre of nitric acid to produce a pH below 2.

ANALYTICAL PROCEDURES

Can Test Laboratory (Vancouver) was selected by competitive bid to analyze water samples according to MOE guidelines and quality control and assurance standards.

Copper and lead concentrations in both field-filtered and unfiltered water will be determined by graphite-furnace atomic absorption spectrometry with a detection limit of 0.5 ppb. Zinc concentrations in both field-filtered and unfiltered waters will be estimated by flame atomic absorption with a 1.0 ppb detection limit. Cadmium and arsenic concentrations in unfiltered waters will be determined by graphite-furnace atomic absorption spectrometry with detection limits of 0.2 ppb and 1 ppb, respectively. Mercury concentrations in unfiltered waters will be determined by cold-vapour atomic absorption with a 0.05 ppb detection level.

ARCHIVE PROGRAM — KOOTENAYS (82E, F, K, L, M)

BACKGROUND

During the initial development of the National Reconnaissance Program the Geological Survey of Canada (GSC) recognized the importance of preserving RGS stream-sediment samples for future studies. At the completion of each survey, remaining sediment was routinely saved and stored at GSC facilities in Ottawa. To encourage mineral exploration in previously surveyed areas (Figure 4-1-1), over 24 500 of these archived sediment samples have been retrieved and analyzed for a number of previously undetermined elements, including gold. The analyses of archived pulps have been performed through nondestructive instrumental neutron activation analysis by Becquerel Laboratories in Ontario. The initiative has added over one million analytical determinations to the existing RGS database. Due to the size of the expanded data set, the results will be released over an extended period of time. The five Kootenay

map sheets, originally surveyed in 1976 and 1977, will represent the first RGS Archive Program release.

1990 RGS ARCHIVE PROGRAM

Approximately 6900 stream-sediment and water samples were collected in southeastern British Columbia during the 1976 and 1977 Federal-Provincial Regional Geochemical Surveys (Figure 4-1-1). The samples were collected at an average density of 1 sample every 12 square kilometres and covered an area in excess of 82 000 square kilometres (Table 4-1-1). The field and analytical data were initially released as GSC Open Files 409 (82E), 410 (82L), 514 (82F), 515 (82K) and 516 (82M) and are available in hard copy and floppy diskette.

Original stream-sediment analytical data included results for Zn, Cu, Pb, Ni, Co, Ag, Mn, Fe, Mo, W, Hg and Sn. The methods and specifications of analyses are similar to those listed in Table 4-1-4. The additional elements determined by instrumental neutron activation analyses are listed in Table 4-1-5.

PRELIMINARY RESULTS

In order to assist explorationists in planning for their follow-up of the 1991 release of archive data, some preliminary comments and statistics for gold, copper, lead and zinc results are provided below. In addition, Figure 4-1-3 identifies key geologic formations (Okulitch and Woodsworth, 1977) within the survey area that contain a high proportion of anomalous base metal and gold samples.

GOLD (1990 DATA)

Over half of the gold analyses (n = 3060 samples) returned concentrations greater than the detection limit. The mean value is 10 ppb and the 90th, 95th and 98th percentile concentrations are 14, 28 and 62 ppb, respectively. The maximum value obtained was 3530 ppb. Anomalous gold results are particularly associated with samples collected from the Lower Paleozoic Lardeau Group, Carboniferous-Permian Thompson assemblage, Triassic-Jurassic Nicola and Rossland groups, and Early Cretaceous granodiorites.

COPPER (1976 AND 1977 DATA)

Over 99 per cent of the copper analyses (n = 6451 samples) returned concentrations greater than the detection limit. The mean value is 24 ppm and the 90th, 95th and 98th percentile concentrations are 46, 59 and 81 ppm, respectively. The maximum value obtained was 1800 ppm. Anomalous copper results are particularly associated with samples obtained from the Lower Paleozoic Lardeau Group, Triassic-Jurassic Nicola and Rossland groups, and Proterozoic Miette and Horsethief Creek groups.

LEAD (1976 AND 1977 DATA)

Over 82 per cent of the lead analyses (n = 5396 samples) returned concentrations greater than the detection limit. The mean value is 20 ppm and the 90th, 95th and 98th percentile concentrations are 25, 37 and 70 ppm, respectively. The maximum value obtained is 20 000 ppm. Anomalous lead results are particularly associated with samples

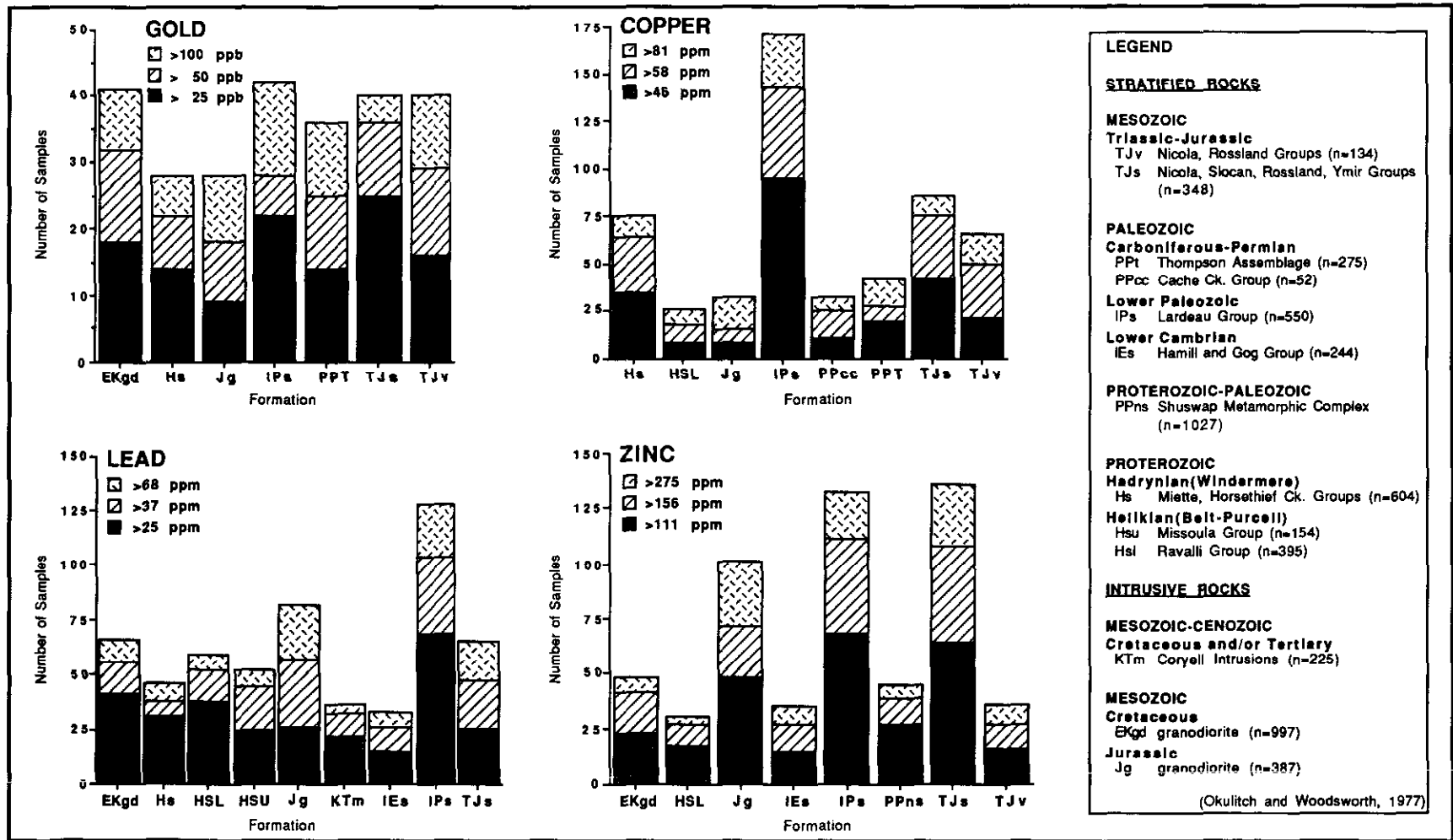


Figure 4-1-3. Number of samples exhibiting anomalous concentrations for selected elements (by formation).

collected from the Proterozoic Windermere and Purcell belts, Lower Paleozoic Lardeau Group, Triassic-Jurassic Nicola and Rossland groups, and Cretaceous and Jurassic granodiorite intrusions.

ZINC (1976 AND 1977 DATA)

All samples (n = 6540 samples) returned concentrations greater than the detection limit. The mean value is 94 ppm and the 90th, 95th and 98th percentile concentrations are 111, 156 and 275 ppm respectively. The maximum value obtained is 20 000 ppm. Anomalous zinc results are particularly associated with samples obtained from the Lower Paleozoic Lardeau Group, Triassic-Jurassic Nicola and Rossland groups, and Cretaceous and Jurassic granodiorite intrusions.

1991 RGS RELEASE INFORMATION

The 1991 RGS release will include field and analytical data from the 1990 surveys. The Open File data packages will be identified as follows:

- RGS-27 Fernie (NTS 82G)
- RGS-28 Kananaskis Lakes (NTS 82J).

The 1991 RGS-archive release will include field and analytical data from the original 1976 and 1977 surveys, plus results of the INAA program. The Open File data packages will be identified as follows:

- RGS-29 Penticton (NTS 82E)
- RGS-30 Nelson (NTS 82F)
- RGS-31 Lardeau (NTS 82K)
- RGS-32 Vernon (NTS 82L)
- RGS-33 Seymour Arm (NTS 82M)

The Open File data packages will be released in the following hard-copy and digital data formats:

- The hard-copy data packages will contain 1:100 000 and 1:500 000-scale sample-location maps, 1:500 000-scale geochemical maps for each element, listings of field and analytical data, and summary statistics and data analyses.
- Digital data packages will consist of MS-DOS formatted, 5¼" floppy diskettes containing listings of field and analytical data together with files outlining methods and specifications. A 1:250 000-scale sample-location map will also be included.

All seven Open Files are tentatively scheduled for release in the spring of 1991. Release centres will be established in Nelson and Vancouver.

ACKNOWLEDGMENTS

The delivery of the 1990 RGS program required the cooperation and assistance of numerous private companies and government agencies. We acknowledge the high quality of work performed by contractors involved with sample collection, preparation and analyses. The valuable assistance provided by the Kootenay Park Warden Office (Environment Canada), the Invermere Forest District Office (Ministry of Forests), the East Kootenay District Office (Ministry of Parks), the Water Quality Unit (Ministry of Environment) and the Mineral Policy Branch (Ministry of Energy, Mines and Petroleum Resources) is also appreciated.

REFERENCES

- Holland, S.S. (1976): Landforms of British Columbia, a Physiographic Outline; *B.C. Ministry of Energy, Mines and Petroleum Resources*, Bulletin 48.
- Höy, T. (1983): Stratabound Base Metal Deposits in South-eastern British Columbia and Northwestern Montana, Geological Framework; *Geological Association of Canada*, Field Trip Guidebook, pages 1-15.
- Learned, R.E., Chao, T.T. and Sanzolone, R.F. (1985): A Comparative Study of Stream Water and Stream Sediment as Geochemical Exploration Media in the Rio Tanama Porphyry Copper District, Puerto Rico; *Journal of Geochemical Exploration*, Volume 24, pages 175-195.
- Matysek, P.F., Gravel, J.L. and Jackman, W. (1989): 1988 British Columbia Regional Geochemical Survey; *B.C. Ministry of Energy, Mines and Petroleum Resources*, B.C. RGS 21, 22, 23; *Geological Survey of Canada*, Open File 2038, 2039, 2040.
- Okulitch, A.V. and Woodsworth, G.J. (1977): Geology of the Kootenay River Map Sheet; *Geological Survey of Canada*, Open File 481.
- Schau, M. (1970): Stratigraphy and Structure of the Type Area of the Upper Triassic Nicola Group of South-central British Columbia; in Wheeler, J.O. (Editor), Structure of the Southern Canadian Cordillera, *Geological Association of Canada*, Special Paper No. 6, pages 123-135.
- Tipper, H.W., Woodsworth, G.J. and Gabrielse, H. (1981): Tectonic Assemblage Map of the Canadian Cordillera; *Geological Survey of Canada*, Map 1505A.

EXPLORATION GEOCHEMISTRY – SEDIMENT SUPPLY TO HARRIS CREEK (82L/2)

By J. M. Ryder and W. K. Fletcher
The University of British Columbia

KEYWORDS: Applied geochemistry, anomaly decay, catchment area, sediment supply, mass wasting, debris flow, stream bank erosion, sediment storage.

INTRODUCTION

Stream sediment geochemical anomalies are often interpreted with reference to an idealized dilution model, based on catchment area, that supposes a smooth exponential decay of the anomaly away from its source (*e.g.* Rose *et al.*, 1979, pages 399-400). The model involves several assumptions, one of which is that supply of sediment to the stream by erosion is constant throughout the catchment. However, in streams in hilly or mountainous terrain, significant amounts of sediment are derived from individual mass-wasting events (*e.g.* debris flows) or are locally stored in the stream channel and only intermittently released. The frequency and distribution of such events is not constant throughout a catchment, and this will clearly influence decay rates for geochemical anomalies both locally and throughout the length of the stream. This has not been studied. Our objectives, therefore, are to investigate the magnitude of these effects and to establish practical limits to the idealized dilution model. We have initiated the study with an investigation of sediment supply in Harris Creek,

east of Vernon (Figure 4-2-1), the site of ongoing studies of fluvial processes and transport of gold in streams (Day and Fletcher, 1989, *in press*; Fletcher, 1990; Fletcher and Day, 1988; Fletcher and Wolcott, submitted).

A preliminary inventory of sediment sources has been conducted by terrain mapping of the 225 square kilometre basin of Harris Creek. The 1:20 000-scale terrain map shows the distribution of active mass-wasting and bank erosion, as well as the distribution of surficial materials and landforms. Many mass-wasting sites were examined in the field in order to assess their relation to Harris Creek. Estimation was attempted of the volume of sediment supplied, and the timing of events was investigated by dendrochronology.

PHYSIOGRAPHY OF THE STUDY AREA

Harris Creek basin occupies part of the dissected plateau of the Okanagan Highland. The gently undulating plateau surface, between 1300 and 2000 metres above sea level, constitutes about two-thirds of the catchment (Figure 4-2-2). The downstream sections of Harris Creek and its major tributaries, however, occupy steep-sided valleys that are incised as much as 750 metres below the plateau surface. Mean valley side gradients range from 20° to 38°.

Three types of stream course are clearly differentiated within this physiographic setting (Figure 4-2-2).

- On the plateau surface, stream gradients are gentle, generally between 1° and 5°. Numerous lakes and bogs along the stream courses trap any sediment that is mobile. Consequently, sediment supply from the uplands to points downstream is negligible.
- Streams descend steeply (6° to 17°) from the uplands through V-shaped valleys where colluvial slopes adjoin the stream channel and no valley flat is present.
- On the main valley floor, stream gradients are between 1° and 2°, and a valley flat is present. This type of stream course is restricted to lower Harris Creek.

Bedrock in the study area was mapped by Jones (1959). The eastern part of the basin is underlain by Tertiary volcanic rocks of the Kamloops Group. Tuffs and breccias are widespread, as well as basalt and other lavas. Tertiary gravels (conglomerates) were noted in a few places. These various lithologies contribute a range of detritus, including a silty till matrix and abundant pebbles, to overlying Quaternary sediments. The volcanic rocks, particularly breccias, form prominent scarps along the plateau margins. In several places, topographic features downslope from the scarps suggest that massive slope movements within the volcanic rocks have affected many square kilometres of the study

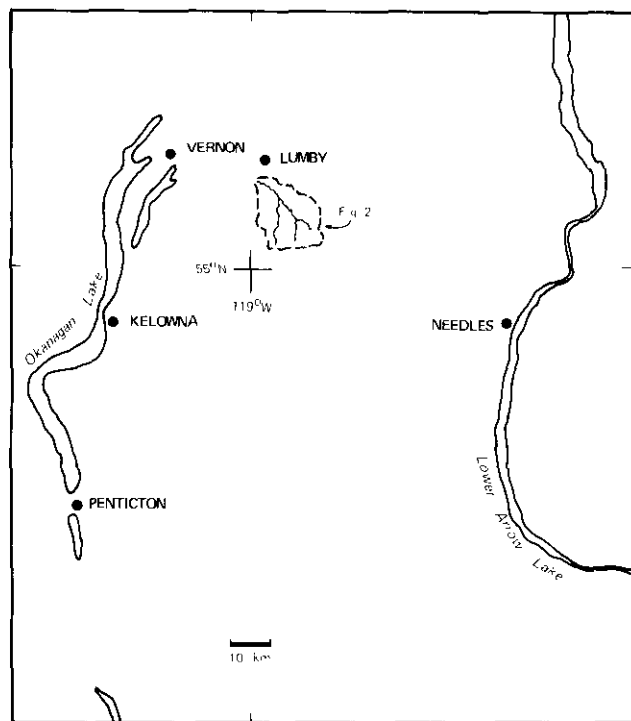


Figure 4-2-1. Location map for Harris Creek study area.

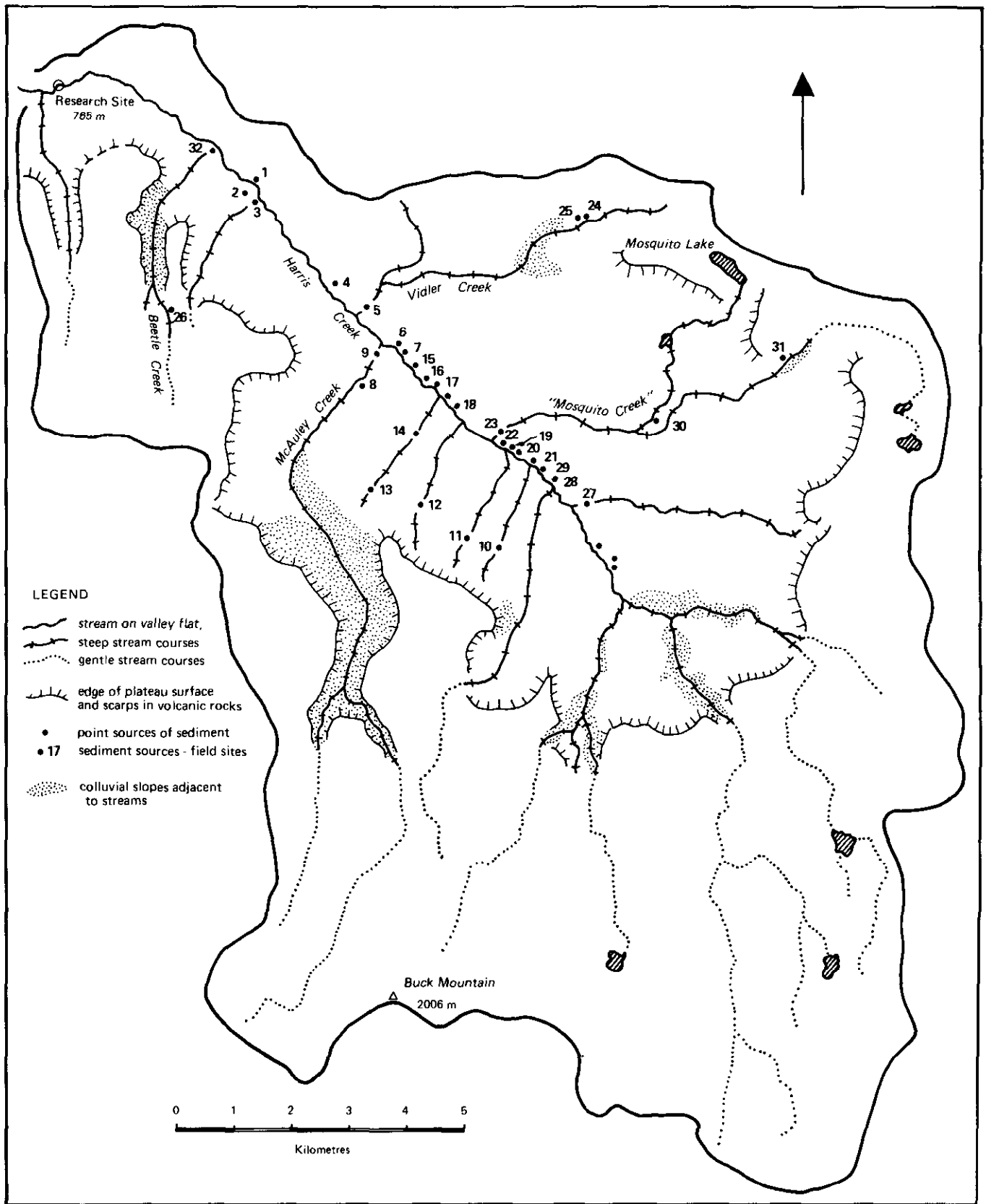


Figure 4-2-2. Harris Creek basin: physiographic features and field sites.

area. The features are till covered, however, suggesting that they predate the last glaciation.

The northwestern and southwestern parts of the study area are underlain, respectively, by acidic plutonic rocks and gneiss of the Shuswap complex. These provide relatively large clasts and coarse sand to the sediment system.

During Fraser Glaciation, the entire study area was buried beneath southward-flowing ice, and all but the steepest slopes still retain a drift cover. In many places, the characteristics of this material determine the mode of sediment supply to Harris Creek. Till is widespread on valley sides. Its texture and lithology are variable, being strongly influenced by the proximity and type of the underlying bedrock. Pockets of stratified drift are scattered throughout the till.

Within about 150 metres elevation of the valley floor along lower Harris Creek, terraces and undulating benches at several levels are underlain by thicker drift consisting of glaciofluvial gravels, glaciolacustrine silt and fine sand, and till. The till is sandwiched between two units of glaciolacustrine sediments, suggesting that Harris Creek drainage was impounded by ice during both early and late phases of Fraser Glaciation. Well-defined terraces are underlain by glaciofluvial sand and gravel.

Relatively little modification of the landscape has occurred during the past 10 000 years. A broad floodplain (now forested) has developed along lower Harris Creek, and small alluvial fans have formed at the mouths of the larger tributaries. Mass movements such as rockfall and debris flows on the steepest slopes have resulted in the accumulation of talus and colluvial fans. Widespread rock slumps (much smaller than the preglacial features mentioned above) have been active along the volcanic rock scarps during Holocene time. A few of these may influence sediment input to the steep middle courses of some streams.

THE SEDIMENT CASCADE

A framework for the analysis of sediment supply to lower Harris Creek is represented schematically in Figure 4-2-3. This demonstrates that sediment mobilization on valley sides does not necessarily coincide with sediment supply to a stream channel. For example, material moved in debris flows and landslides may reach a creek or it may be temporarily stored on lower valley sides and fans. Sediment that is transported by tributary creeks may accumulate on alluvial fans, rather than being entrained by the trunk stream. Remobilization of stored sediment may occur after a few years (*e.g.* trunk stream erosion of the toe of a fan), or it may not occur until the next regional glaciation (*e.g.* sediment buried beneath the apical part of a fan). The diagram also indicates that sediment supply from the upstream to the downstream reaches of lower Harris Creek is not a continuous process, but that channel material may be temporarily stored in the old floodplain or in channel bars for time periods ranging from one year to several millenia.

In view of these processes, and since research on sediment transport has, so far, been concentrated at the downstream end of Harris Creek, particular attention was paid to sediment supply to lower Harris Creek.

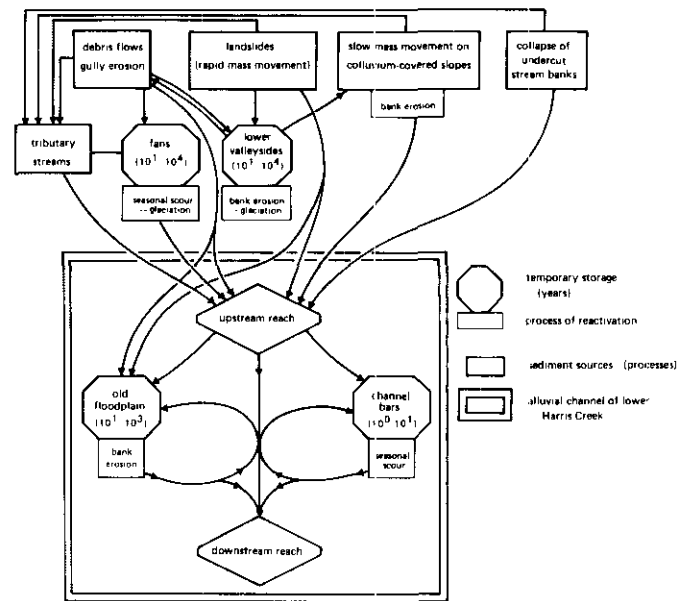


Figure 4-2-3. Sediment cascade for Harris Creek.

MASS MOVEMENTS

SLUMPS AND SLIDES IN DRIFT

Landslides in till and glaciolacustrine sediments (Figure 4-2-4) are common on the scarp of a more or less continuous bench that extends along the north side of lower Harris Creek. Conditions contributing to slope failure include steep slopes, thick and weak materials (silt with minor fine sand and clay, and silty diamict), and saturation by groundwater. Slope movements appear to have been triggered by undercutting by Harris Creek, because a stream channel (either the present channel or a recently abandoned channel) abuts the toe of almost every landslide.

Of the fourteen landslides of this type that were examined in the field (Figure 4-2-4, Table 4-2-1), only four appear to be active (moving slowly) at present: one of these (SS18) debouches into an abandoned channel, but the other three (SS1b, SS7a, SS28) feed directly into Harris Creek. Of ten inactive features, nine are adjacent to abandoned channels and one (SS17) is being undercut by the active channel of Harris Creek. Minor gully erosion and very small debris flows ($<10\text{ m}^3$) have occurred on the toes of some of the inactive features within the past one or two years.

Preliminary results from the analysis of increment cores from trees on stationary slump blocks suggest that they have not moved significantly for intervals that vary from 25 to 80 years. Trees on inactive (but sparsely vegetated) slide scars and on the slump toes indicate that sites have been stable for 6 to 80 years. Thus it appears that slumping occurs intermittently (Table 4-2-1). Consequently, the significance of these landslides as sediment sources (in the short term) depends upon whether or not a period of active slope movement coincided with the presence of an active channel at the toe of the slump. More dendrochronological dating of both slumps and fluvial features would possibly allow a more

precise assessment of the frequency of sediment input to Harris Creek. Success of such a dating program would depend upon the presence of pioneer trees on the critical sites.

Measurements were made of the approximate dimensions of most slump blocks and slide scars (Table 4-2-1) in order to attempt estimates of the volume of material displaced by slope movement. Determination of potential volumes contributed to the bedload (*i.e.* sand and gravel) of Harris Creek is complicated by the fact that the landslide materials include a high proportion of finer material that would be rapidly removed from the creek as wash load after a landslide event. Proportional clast content in till was estimated visually and the relative volumes of till and glaciolacustrine sediments involved in a slope failures were estimated

TABLE 4-2-1
LANDSLIDES IN DRIFT ADJACENT TO
LOWER HARRIS CREEK
CHARACTERISTICS AND RATING AS SEDIMENT SOURCES

Number ¹	Description ²	Material involved	Relation to stream ³	Width ⁴ (m)	Height (m)	Age ⁵ (yr)	Rating ⁶
SS1a	slump	till, silt	ic	107	58	>10	H
SS1b	slide/fall*	till, silt	ac	56	24	A	P
SS4	slide scar	silt	of	20	30	>3	h
SS6	slide scar	till, silt	ic	17	36	>30	h
SS7a	slide scar*	till, silt	ac	34	36	A	P
SS7b	slide scar	till, silt	of	20	36	>60	h
SS8	slump	till, silt	of ^m	25	20	>25	h
SS15	slump	till, silt	of	60-100	68	>80?	H
SS17	slump	till, sil	ac	50?	70	A	P
SS18	slump*	silt	ic	60	61	A	H
SS19	slide scar	till, silt	ic	30-40	40?	(-)	h
SS20	slide scar	till, silt	ic	30-40	40?	(-)	h
SS21	slide scar	till, silt	ic	40?	40?	(-)	h
SS28	slump*	gravel	ac	30?	24	A	P

¹ SS = sediment source.

² * = active or partly active landslide.

³ landslide descends to: ic = inactive (abandoned) channel; ac = active channel; of = old floodplain; m = lower McAuley Creek.

⁴ ? indicates approximate.

⁵ estimate only; based on age of one or two trees; (-) = no data; A = active.

⁶ H = former (historic) major source; h = former minor source; P = major source at present; p = minor source at present.

according to the area of their outcrops in the slide scar. These data were used to calculate approximate gravel volume equivalents for a few sites. Individual slump blocks appear to contain in the order of hundreds of cubic metres of gravel; total volumes of gravel that have been displaced from landslide scars, that is the volume of the empty concavities, range from hundreds to thousands of cubic metres.

DEBRIS FLOWS

Evidence of recent debris-flow activity was found at only one site (25 on Figure 4-2-2), although the presence of gullies cut into drift on steep slopes (both mountainsides and terrace scarps) suggests either that this process operates very sporadically or that it was more effective at some past period of time. Debris flows may also be contributing sediment to Harris Creek indirectly if debris-flow fans are being undercut by bank erosion (Figures 4-2-3), but no such sites were specifically noted.

OTHER FORMS OF RAPID MASS MOVEMENT

Collapse of undercut valley sides and rockfalls appear to contribute minor amounts of bed material to Harris Creek. Where the creek occupies a broad valley flat, it rarely impinges on the valley sides (except at sites where landslides have occurred as described above). Only two undercut banks in unconsolidated materials were identified; the one of these that was examined in the field had supplied about 1000 cubic metres of sediment directly to Harris Creek, but the time span over which this had occurred is not known. Along much of lower Harris Creek, the southern side of the valley flat is flanked by a bedrock scarp. Where the creek flows against the toe of this scarp, which is commonly a near-vertical cliff in such locations, angular blocks in the stream channel indicate where minor rockfalls (no more than a few cubic metres) have occurred. Very little mobile sediment seems to be contributed by this process.

In a few places, mostly along tributary streams, minor (100s of cubic metres) amounts of logging road materials have moved downslope to a stream channel (Figure 4-2-2, sites 21, 22, 39).

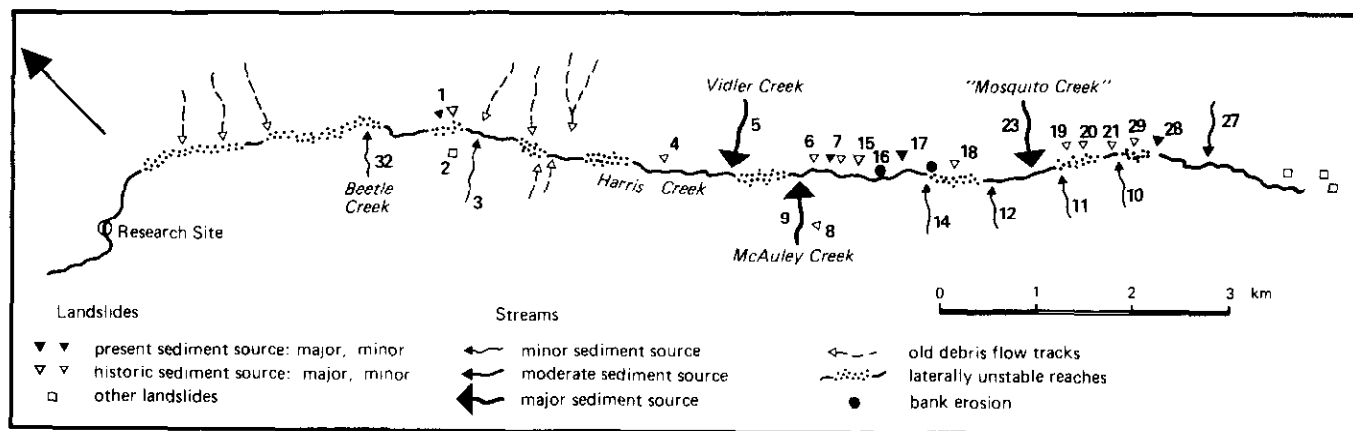


Figure 4-2-4. Sediment sources along lower Harris Creek.

**SLOW MASS MOVEMENT
ON COLLUVIAL SLOPES**

Slow mass movement of colluvium toward stream channels is occurring along the steep, mid-courses of Harris Creek and its tributaries (Figures 4-2-2 and 3).

SEDIMENT INPUT FROM TRIBUTARY STREAMS

Bedload transport in tributary streams that enter lower Harris Creek was assessed visually at sites adjacent to Harris Creek and, for some creeks, at more distant locations. Volumes of sediment contributed were rated qualitatively according to the width of the stream channel and active floodplain, the apparent freshness of gravel in the channel, and the presence of features such as pools and riffles, bars, and logjams (Table 4-2-2, Figure 4-2-4). Fortuitous deposition upstream of a culvert at Vidler Creek allowed an estimate of at least 120 cubic metres bedload transport during a recent flood.

**TABLE 4-2-2
TRIBUTARIES OF LOWER HARRIS CREEK
SEDIMENT SOURCE RATINGS**

Tributary (number)	Width of channel/ active zone (m)	Qualitative estimate of bedload transport	Rating as sediment source
1 km east of Beetle Cr. (SS3)	1.0	inactive	minor
Vidler Cr. (SS5)	2.0	very active*	major*
McAuley Cr. (SS9)	3.0/7.0	very active	major
(SS10)	1.0	inactive	minor
(SS11a)	1.5	mod. active	} minor
(SS11b)	2.0	inactive	
(SS12)	1.3	inactive	
(SS13/14)	1.5	inactive	minor
"Mosquito Cr." (SS23)	3.6	very active	major
(SS27)	3.3	mod. active	moderate
Beetle Cr. (SS32)	1	mod. active	minor

* Sediment transport to Harris Creek currently restricted by culvert.

FLUVIAL PROCESSES ALONG LOWER HARRIS CREEK

Lower Harris Creek occupies an active channel zone that is flanked by an extensive old floodplain. In places gravel is being supplied to the active channel from the old feature, and this appears to be a significant source of sediment for lower Harris Creek.

The old floodplain, which, together with the active channel zone, constitutes a valley flat that varies in width from about 100 to 350 metres, typically stands 0.5 to 1.5 metres above the gravel bars of the active channel zone. It is occupied by mature forest, suggesting an age of at least several hundred years. The floodplain surface is underlain by overbank sediments, 0.5 to 1.5 metres of thinly interbed-

ded silt and sand, which commonly contain paleosols, layers of forest litter, charcoal or wood fragments (Plate 4-2-5). Channel gravels underlie the overbank sediments along a contact which ranges in elevation from below present stream level to approximate high-water levels.

Preliminary assessment of the characteristics of the active channel zone suggest that it consists of alternating reaches of relatively active and less active sediment (largely bedload) transport (Figure 4-2-4). In active reaches, the stream channel is laterally unstable: the active channel zone is several times as wide as the stream channel and includes recently deposited (or reworked) gravel bars. The presence of numerous fallen trees attests to recent severe bank erosion and broadening of the active zone at the expense of the old floodplain. Such instability progresses downstream, leaving behind partly eroded bars that are above normal flood levels and undergoing recolonization by vegetation. Detailed surveys of fluvial features and dendrochronological dating could be used to estimate the magnitude and timing of sediment movement in these reaches. It is possible that instability in initially stable reaches could be triggered by the development of logjams or by a sudden influx of

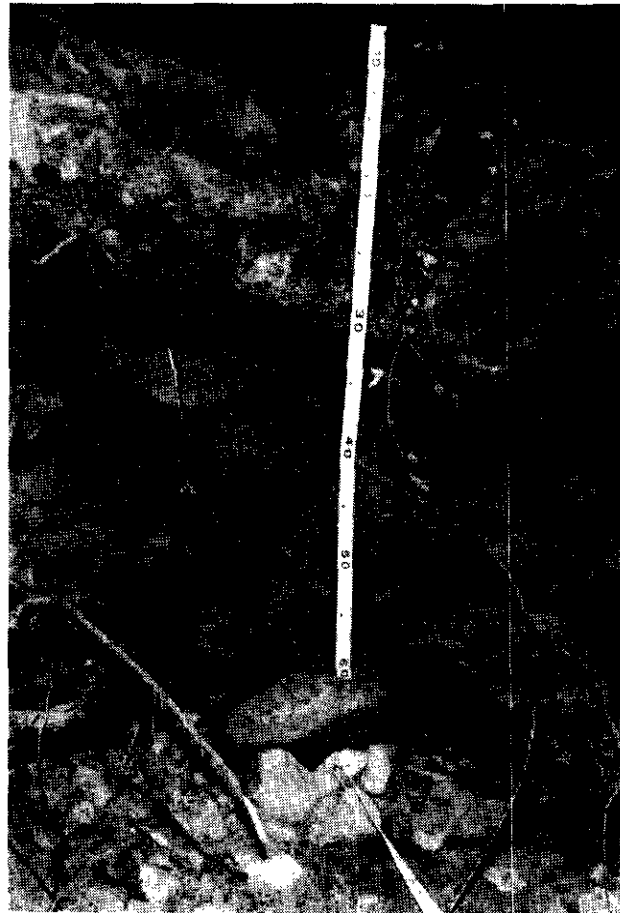


Plate 4-2-1. Overbank sediments exposed by recent erosion of Harris Creek about 1 km upstream from Research Site (Figure 4-2-2). Note well-defined paleosol at 31-35 cm, lower discontinuous paleosol (faintly defined at 50 cm), and underlying channel gravels (>60 cm).

sediment from a landslide, as well as by downstream progression. Estimates based on a few measurements at one site suggest that from several hundred to a few thousand cubic metres of sediment could be mobile in a single unstable reach. This quantity is of similar order of magnitude as estimates of the total volume of gravel represented by a single landslide scar, and an order of magnitude greater than the volume of gravel likely to be contained in a single slump block or a single landslide event.

In less active, laterally stable reaches, the active channel zone is relatively narrow, commonly no wider than the stream channel during floods. Bank erosion occurs on bends, resulting in the transfer of relatively minor amounts of sediment — no more than a few cubic metres per site per flood event — from the old floodplain to the active channel.

SUMMARY OF SEDIMENT SOURCES

A preliminary classification of sediment sources adjacent to lower Harris Creek is indicated in Tables 4-2-1 and 2 and Figure 4-2-4. Sources are rated according to their relative magnitudes, and in the case of landslides, according to their proximity to the present channel of Harris Creek. Landslide and tributary sources cannot be compared directly, however, since the dates and magnitude of specific landslide events and the volumes of stream sediment transport are not known.

CONCLUSIONS

Sediment supply to Harris Creek is discontinuous both spatially and temporally. Sediment that is mobilized on slopes or along tributary streams may be supplied to the trunk stream or it may be stored temporarily on lower valley sides, in fans, or on the old floodplain and abandoned channels of lower Harris Creek; storage times range from one to tens of thousands of years. Only four of fourteen landslides along lower Harris Creek are currently supplying sediment to the trunk stream; other landslides are stable at present or debouch into inactive channels. Only the three largest tributaries appear to regularly contribute significant bedload to the trunk stream. Along lower Harris Creek,

relatively large volumes of bedload material are being derived from the old floodplain by bank erosion in several laterally unstable reaches. The volume of mobile gravel within each unstable reach may be similar to the total volume of gravel supplied by a single landslide.

ACKNOWLEDGMENTS

This study was supported by the Geoscience Research Grant Program of the British Columbia Ministry of Energy, Mines and Petroleum Resources. Alan Paige was a thoughtful and careful field assistant.

REFERENCES

- Day, S. J. and Fletcher, W. K. (1989): Effects of Valley and Local Channel Morphology on the Distribution of Gold in Stream Sediments from Harris Creek, British Columbia, Canada; *Journal of Geochemical Exploration*, Volume 32, pages 1-16.
- Day, S. J. and Fletcher, W. K. (In press): Concentrations of Magnetite and Gold at Bar and Reach Scales in a Gravel-bed Stream, British Columbia, Canada; *Journal of Sedimentary Petrology*.
- Fletcher, W. K. (1990). Dispersion and Behaviour of Gold in Stream Sediments; *B.C. Ministry of Energy, Mines and Petroleum Resources*, Open File 1990-28.
- Fletcher, W. K. and Day, S. J. (1988): Seasonal Variation of Gold Content of Stream Sediments, Harris Creek, near Vernon: a Progress Report (82L/02); *B.C. Ministry of Energy, Mines and Petroleum Resources*, Geological Fieldwork 1987, Paper 1988-1, pages 511-514.
- Fletcher, W. K. and Wolcott, J. (Submitted): Transport of Magnetite and Gold in Harris Creek, British Columbia, and Implications for Exploration; *Journal of Geochemical Exploration*.
- Jones, A. G. (1959): Vernon Map-area, British Columbia; *Geological Survey of Canada*, Memoir 296.
- Rose, A. W., Hawkes, H. E. and Webb, J. S. (1979): Geochemistry; in *Mineral Exploration*, *Academic Press*, 657 pages.



**NEOTECTONIC INVESTIGATIONS ON WESTERN
VANCOUVER ISLAND, BRITISH COLUMBIA
(92F/4)**

By **P.T. Bobrowsky**
and
J.J. Clague, Geological Survey of Canada

KEYWORDS: Geological hazards, neotectonics, Quaternary, Tofino, Grice Bay, Maltby Bay, tsunami deposit, 1964 Alaska earthquake, sedimentology.

INTRODUCTION

Interest in the contemporary geodynamic setting of southwestern British Columbia stems from a concern that a large earthquake may impact the major urban centres of the province. Indeed, monitoring of seismic activity in western Canada indicates that numerous smaller magnitude (<M4) intraplate earthquakes affect the southern coastal region annually, and that very small tremors occur daily. Large (M6 to 7+) intraplate earthquakes are frequent, the most recent being the M7.2 event of 1946 near Comox on Vancouver Island. Recently, concern has been expressed that an unprecedented, great (>M8) earthquake could also occur in the eastern North Pacific Ocean near populated areas of British Columbia (Rogers, 1988).

The dire consequences of a great earthquake, as perceived by the public through popular articles (*cf.* Koppel, 1989), are warranted insofar as previous M8+ events elsewhere (*e.g.* M9.5 in Chile, 1960, and M8.6 in Alaska, 1964) have caused considerable property damage and loss of human life. Our understanding of these rare but devastating events has improved considerably during the last few decades. For example, they are now known to occur along zones of interaction between converging lithospheric plates. Commonly referred to as "megathrust" earthquakes, they result from the sudden release of large amounts of strain stored between two locked lithospheric plates (Rogers, 1988). In the case of western Canada, the Cascadia subduction zone west of Vancouver Island marks the interface between the eastward subducting Juan de Fuca plate and the over-riding North American plate. The Cascadia subduction zone shares many of the same attributes as other subduction zones bordering the Pacific Ocean that have experienced megathrust earthquakes in recorded history (Rogers, 1988).

Responding to concern that a megathrust event could effect southwestern British Columbia, the Geological Survey of Canada and the provincial Geological Survey Branch have undertaken integrated geological investigations as part of a neotectonics program. The primary purpose of this research is to locate and interpret the geologic evidence for past earthquakes, and if possible determine the frequency and magnitude of these events. Such information could prove invaluable in formulating and implementing proactive policy and actions for safer building codes, emergency response procedures, as well as general land-use planning.

SETTING

During the summer of 1990, geological investigations were undertaken in coastal areas of southern and western Vancouver Island. The primary objective of this work was to add to, and improve upon, the existing intertidal record of paleoseismicity and sea-level changes documented previously (Clague, 1989; Clague and Bobrowsky, 1990). This report provides details of field activities conducted in the area of Tofino, British Columbia.

Surficial geologic reconnaissance was restricted to the peninsula extending east from the town of Tofino to Grice Bay (Figure 4-3-1, Plate 4-3-1, Table 4-3-1). Marine and glaciomarine sand, silt and clay underlie low-lying areas of the peninsula, and veneers of colluviated till and marine sediments drape bedrock-cored hills. The West Coast fault, which extends in a northwest direction along the peninsula, separates the Pacific Rim Complex to the west from rocks of Wrangellia to the east. The Pacific Rim Complex consists mainly of Jura-Cretaceous mudstone, sandstone and chert, which overlie Triassic volcanics. The Wrangell Terrane comprises a diverse assemblage of Paleozoic and Mesozoic rocks which were metamorphosed during the Late Jurassic (Brandon, 1985).

**TABLE 4-3-1
LOCATION OF SAMPLE SITES**

Locality	Latitude	Longitude	UTM
90-90	49°04.5'	125°45.0'	BK992393
90-91	49°05.1'	125°50.4'	BK927405
90-92	49°05.7'	125°50.8'	BK922412
90-93	49°05.8'	125°50.9'	BK921420
90-94	49°06.0'	125°51.0'	BK920423
90-95	49°06.5'	125°52.3'	BK905436

RESULTS

Six sites were examined in detail (Figure 4-3-1). Three of these provide good evidence for glaciation of the area. Site PTB90-91 (Plate 4-3-1), located on a prominent topographic high called Radar Hill, consists of well-developed striae etched into glacially polished bedrock. Micro crag-and-tail features associated with the striae suggest ice flow toward 220°.

Section PTB90-92 (Tofino dump), northwest of Radar Hill (Plate 4-3-1), provides a good stratigraphic and sedimentologic record of the last glacial maximum (Figure 4-3-2; Plates 4-3-1 and 2). Basal, crossbedded coarse sand

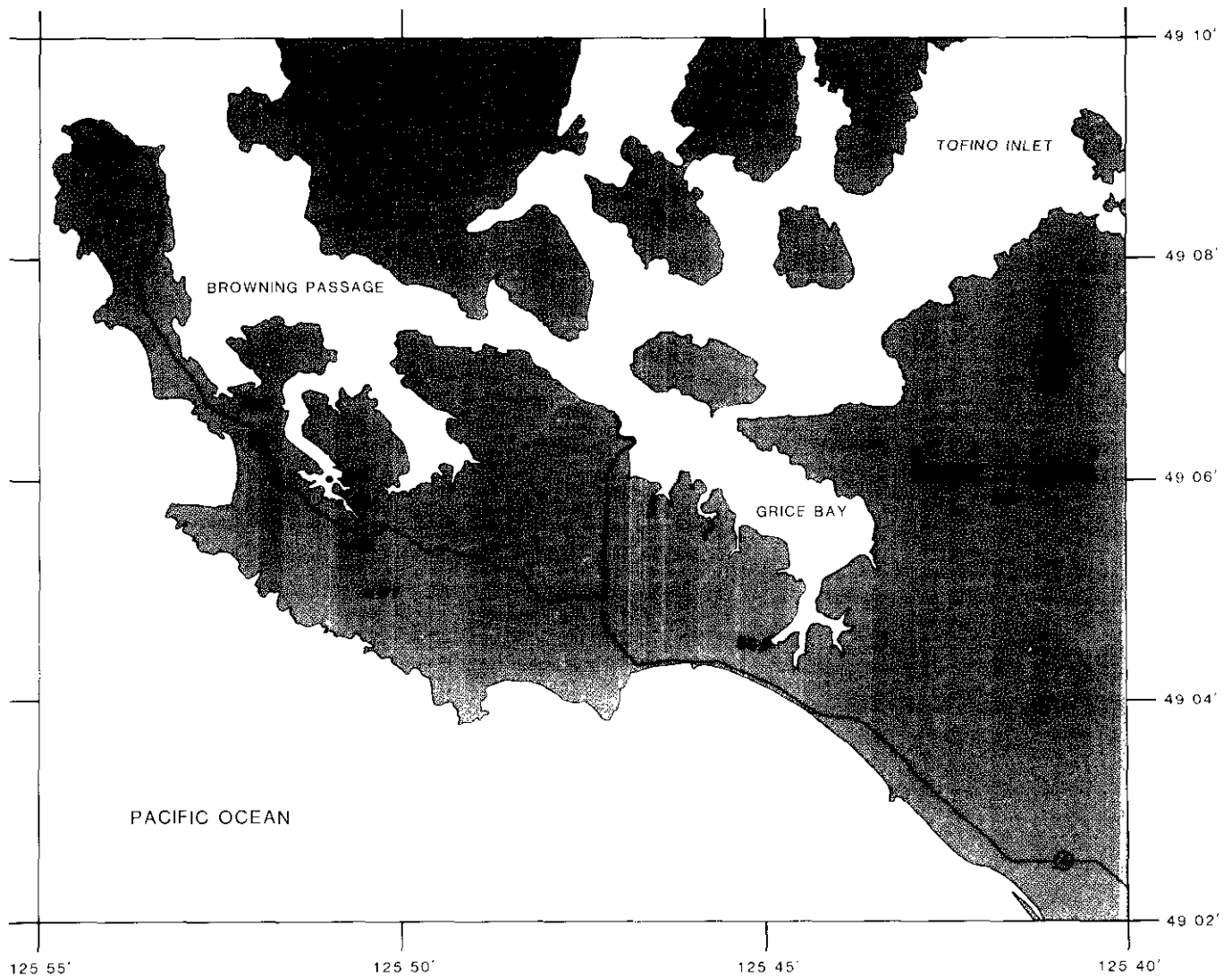


Figure 4-3-1. Location map showing sites in the Tofino area investigated in 1990 as part of the GSB/GSC neotectonics program. Numbers refer to sites discussed in the text. Coordinates for all sites are given in Table 4-3-1.

over 3 metres thick contains minor pebble lenses and ripple-laminated silty clay lenses indicating flow to the west (Unit 1). The sand grades upwards into 3 metres of chaotic, clast-supported, pebble-cobble gravel, supporting boulders up to 40 centimetres in diameter (Unit 2; Plate 4-3-2). Approximately 2 metres of poorly sorted, matrix-supported, crossbedded, sandy granules overlies the gravel (Unit 3). This unit, in turn, is overlain sharply by approximately 2 metres of clast-supported, bouldery cobble gravel (Unit 4). Finally, the gravel is overlain gradationally by approximately 10 metres of stratified, matrix-supported diamicton (Unit 5; Plate 4-3-3). Boulders up to 1.5 metres in diameter are present in the diamicton, and well-rounded pebbles (up to approximately 10 per cent of the sediment) accentuate a well-developed planar fabric. A radiocarbon age of $16\,700 \pm 150$ years B.P. (GSC-2768) on wood (*Pinus contorta*) from the top of Unit 4 at 37 metres elevation indicates the overlying diamicton was deposited during the Fraser

Glaciation (Clague *et al.*, 1980). Units 1 to 4 are interpreted to be different facies of advance outwash and ice-contact deposits.

Section PTB90-95 is a 2-metre-high road exposure of banded and locally deformed rhythmites consisting of silty sand and sandy silt. These sediments are interpreted to be glaciolacustrine or glaciomarine in origin, and were deposited during the Fraser Glaciation.

Several upright stumps with laterally extensive root systems up to several metres across are present in Maltby Bay (PTB90-93, 94; Plates 4-3-1 and 4). The stumps appear to be rooted in dense marine or glaciomarine clay and are overlain by up to 2 metres of mud. Level surveying indicated the root boles of the stumps are approximately 0.5 to 1.5 metres below Highest High Water.

Intertidal accumulations were examined in detail in a small inlet of Grice Bay (PTB90-90; Figure 4-3-3). Shovel

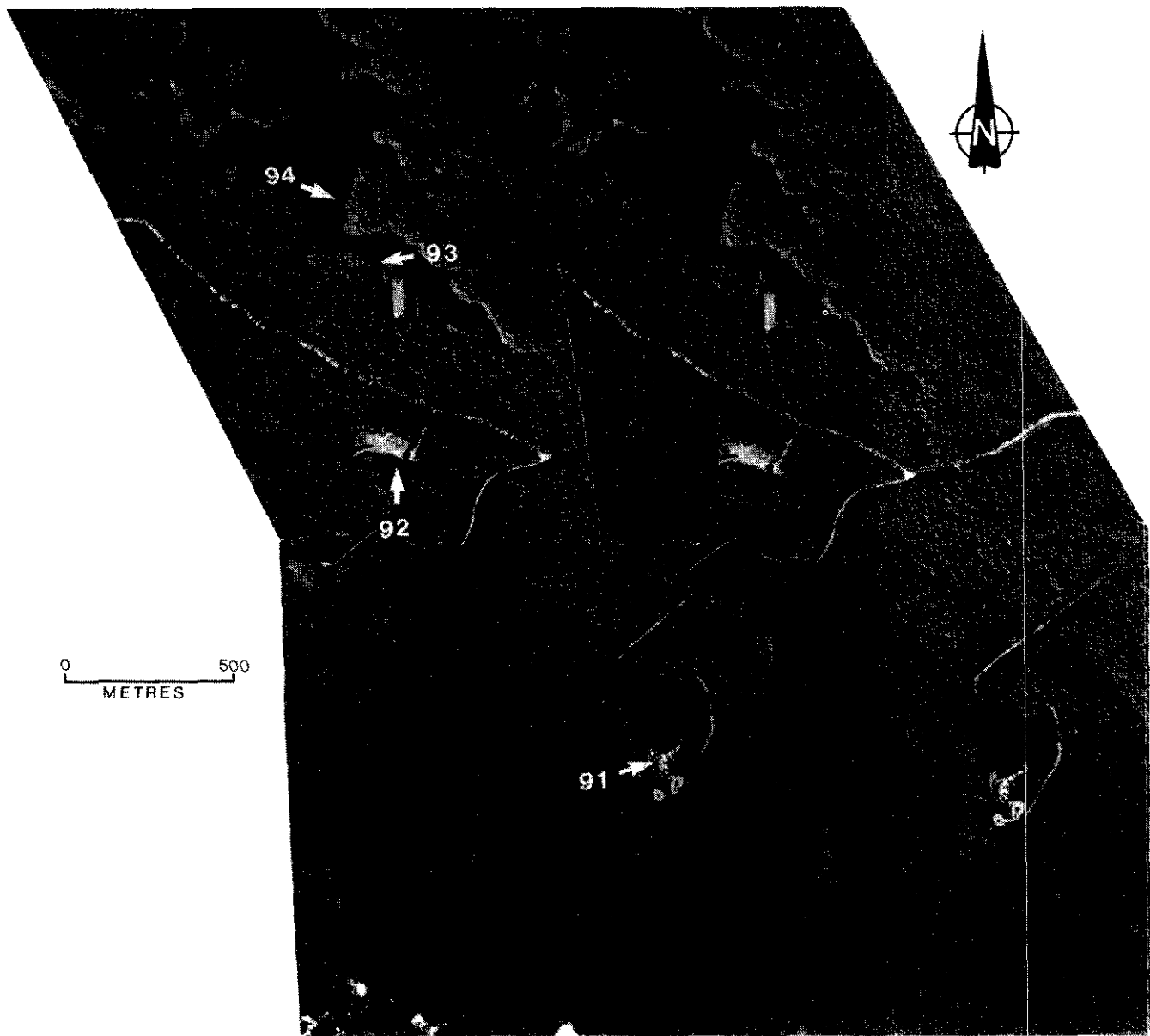


Plate 4-3-1. Photostereogram of Maltby Bay and surrounding area, southeast of Tofino, B.C. Numbered localities correspond to those discussed in text and shown on Figure 4-3-1. (Photographs BC84084-174 and 175).

holes and trenches, tidal-channel sections and cores along two transects provided stratigraphic and sedimentologic information. Cores were obtained using an Oakfield soil corer with a 2.54-centimetre (1") diameter sampling tube and extension rods capable of reaching over 2 metres in depth. Transect A-A' consisted of six holes spaced 10 metres apart along a line trending 161° (Figure 4-3-4). Holes were dug to depths of about 25 centimetres and cores were then taken from the base of each hole. Except for some differences in facies thickness, the observed stratigraphy is essentially similar at all six sites. Briefly, the lowest unit in each hole is compact grey mud and silty mud, which in some cases contains marine gastropods and bivalves. Some sand and silt stringers are present in the mud. This unit is overlain by a prominent deposit of massive sand and silty

sand, with minor shells, pebbles and cobbles. Organic detritus and silt increase in abundance in the upper part of the unit. The sand unit is gradationally overlain by interbedded muddy peat, silt and organic mud. The upper few centimetres of each hole are exclusively muddy peat. Of particular note is a massive, fine sand bed, 6 to 12 centimetres thick, with sharp contacts, in the upper peaty sediments of Holes 2 and 6 (Plate 4-3-5).

A second, nonlinear transect (B-B') of holes, cores and tidal-channel sections was established almost perpendicular to the first transect (Figure 4-3-5). Adjoining sites along this transect were 20 to 125 metres apart. The stratigraphy along Transect B-B', although more complex and variable than that of Transect A-A', shows several similarities. The basal mud unit was not encountered at all sites, but its local

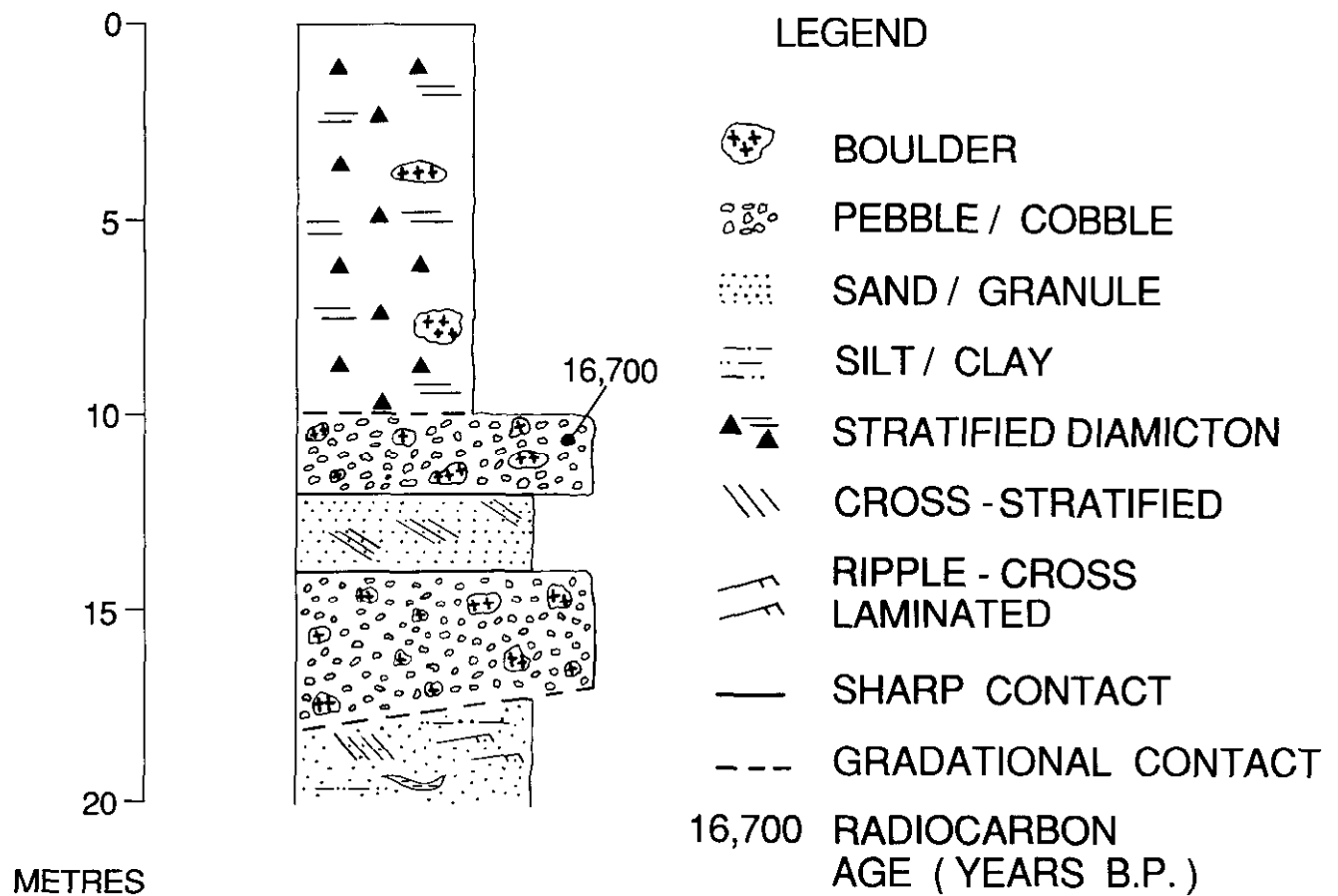


Figure 4-3-2. Composite stratigraphic section of site PTB90-92 (Tofino dump).

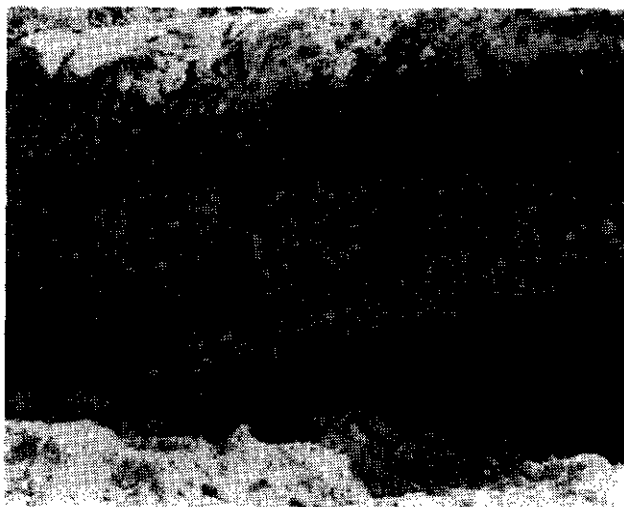


Plate 4-3-2. Section PTB90-92 (Tofino dump) showing Units 1, 2, 3 and 4 (see text for details). (GSB photograph PTB 90-16-14).



Plate 4-3-3. Stratified diamicton at section PTB90-92 (Tofino dump). Diamicton is >10 metres thick and overlies a sequence of poorly sorted sand and gravel deposits. Boulders up to 1.5 metres in diameter occur in the diamicton. Arrow points to knife. (GSB photograph PTB 90-16-99).



Plate 4-3-4. Stump at site PTB90-94 (Maltby Bay). (GSB photograph PTB 90-15-35).



Plate 4-3-5. View of upper part of Hole 2 of Transect A-A', locality PTB90-90 (Grice Bay), showing clean sand bed (arrow) within muddy organic sediments. White card is 9 centimetres long. (GSB photograph PTB 90-16-17).

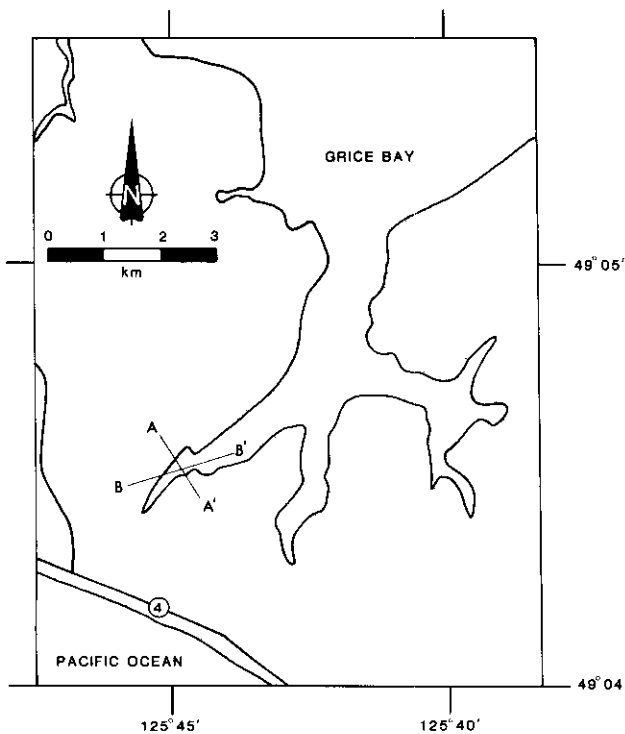


Figure 4-3-3. Locality PTB90-90 (Grice Bay). Locality is centred at the intersection of two transect lines. Lengths of transect lines exaggerated for clarity. Transect A-A' corresponds to Holes 1 to 6 (Figure 4-3-4), and Transect B-B' corresponds to various core and bank sections (Figure 4-3-5).

absence is most likely a function of shallow probing and increasing thickness of the overlying sand unit seaward. The mud commonly contains molluscs and wood fragments. Where observed in its entirety, the overlying sand unit was generally thick, attaining a maximum thickness of 1.6

metres in core 90-117. At some sites, significant amounts of shell occur in the lower part of the sand unit. The sand unit is overlain by alternating beds and lenses of mud, organic silt and muddy peat. Samples for radiocarbon dating and foraminiferal analysis were collected from the bank section at station 90-115. A series of samples for both foraminiferal and diatom study were also recovered from core 90-120.

DISCUSSION

The Pleistocene exposure at the Tofino dump indicates that there was at least one Late Wisconsinan ice advance over the study area sometime after 16 700 years B.P. Ice probably flowed from highlands northeast of the study area, across the peninsula southeast of Tofino, and out into the Pacific Ocean for an indeterminate distance, as interpreted from striations (PTB90-91) and deposits of stratified diamicton (Section PTB90-92). As ice retreated from the area, glaciomarine and marine muds probably accumulated over much of the isostatically depressed area. Subsequent uplift, resulting from isostatic and/or tectonic processes, may have caused the deposition of sandy, nearshore facies in Grice Bay (PTB90-90). Continued uplift during the late Holocene may have isolated Grice Bay from the open Pacific Ocean, causing silt, mud and peat to be deposited on the sand. Accretion of these fine sediments and organics has continued to the present day, essentially uninterrupted, except for deposition of the prominent, thin sand bed observed in several holes along the two transects at PTB90-90.

A genetic interpretation for the thin sand bed at PTB90-90 points to three possible influences: flood, storm, or tectonic. This bed is patchily distributed, massive, lacks grading, displays sharp contacts and appears to thicken seaward. Internal crossbedding, which might reflect oscillatory flow or traction-current transport, is absent. There is no

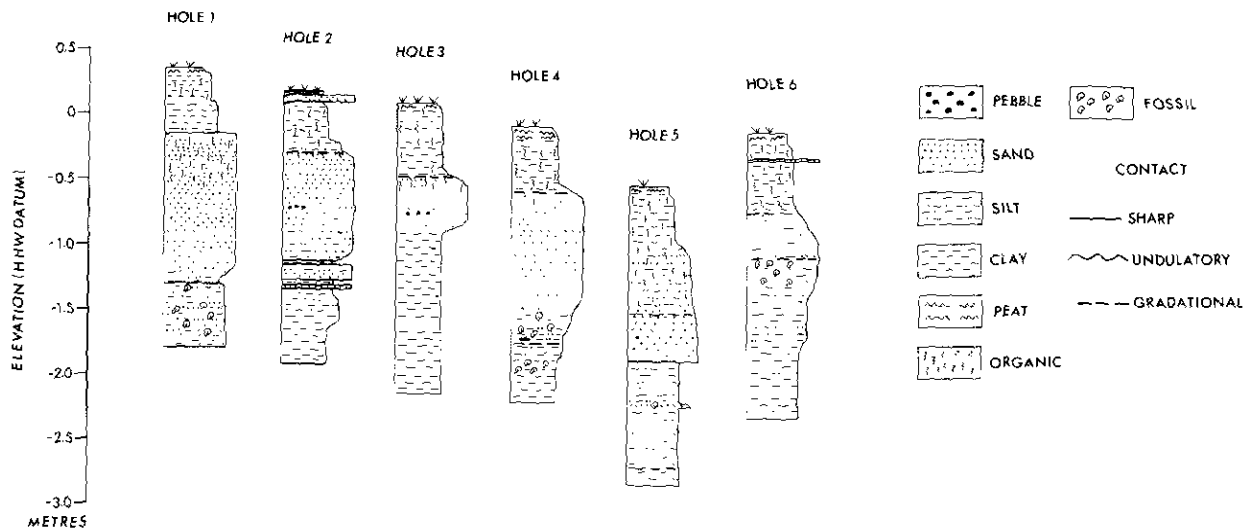


Figure 4-3-4. Stratigraphic sections along Transect A-A', PTB90-90.

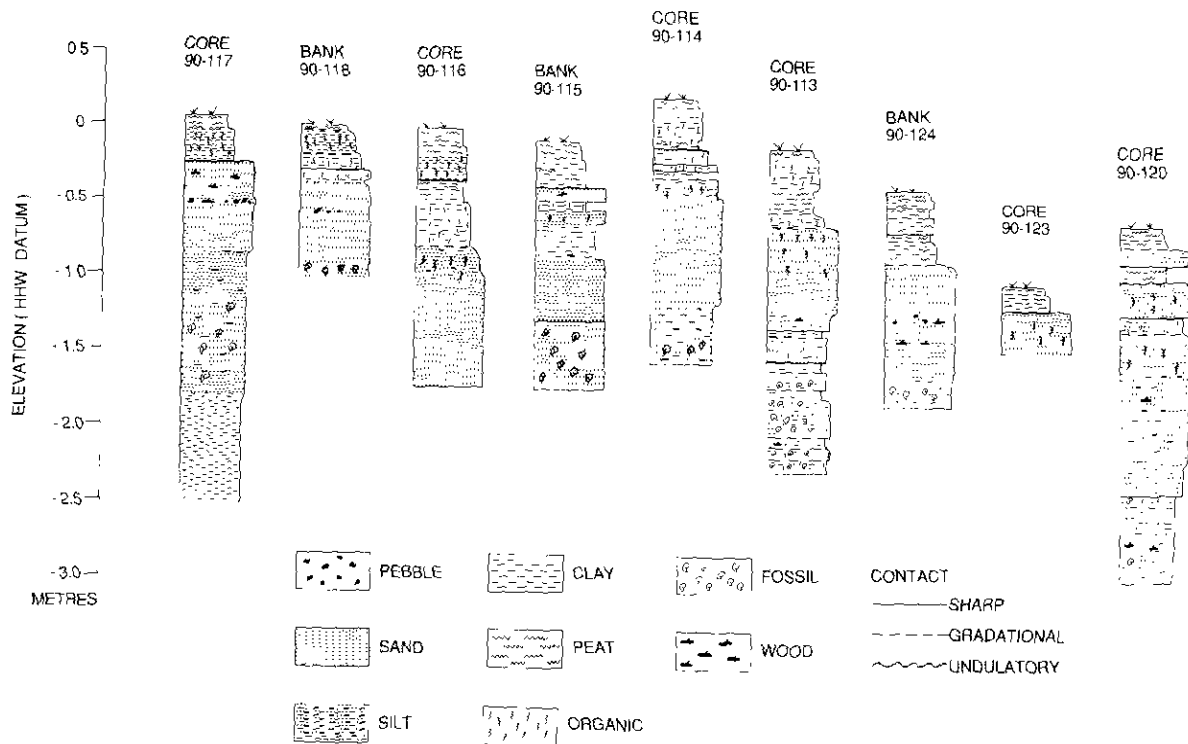


Figure 4-3-5. Stratigraphic sections along Transect B-B', PTB90-90.

significant source of riverine water entering the tidal inlet, ruling out a flood origin. On a geologic scale, severe storm surges are considered frequent events, suggesting that resulting depositional products should be common, where preservation permits; this seems to argue against a storm origin for the sand bed. In a similar setting in northern Oregon, the absence of stratification in sand beds has been cited as evidence against them being flood or storm-generated features (Peterson and Darienzo, 1988). A similar, laterally continuous, ungraded sand bed described from Scotland has been interpreted to be a tsunami deposit (Long

et al., 1989). We suggest that the thin sand bed near the top of the Grice Bay sequence may also have been deposited by a tsunami.

Attention focused on large-magnitude earthquakes during the last several years has led to a better understanding of the geologic effects of seismogenic phenomena such as coseismic subsidence, coseismic uplift and tsunamis (*e.g.* Atwater, 1987). For example, sandy units sharply overlying down-dropped peats in tidal sequences in Washington State have been interpreted as products of tsunami-genic earthquakes (Reinhart and Bourgeois, 1988).

To date there is no geologic evidence to support the contention that one or more megathrust earthquakes have occurred during the Holocene near Vancouver Island. However, tsunamis from earthquakes occurring elsewhere in the Pacific Ocean have impacted the British Columbia coast in historic times (Murty, 1977). The March 27, 1964, earthquake centred under Prince William Sound, Alaska (M8.6), generated a tsunami that caused millions of dollars damage to communities on Vancouver Island. (Wigen and White, 1964; White, 1966). Although no tidal records are available for Grice Bay, the tidal station at Tofino, recorded a maximum rise of 2.5 metres during this event (Murty, 1977). It is thus reasonable to conclude that a tsunami may have deposited the thin sand bed near the top of the Holocene sequence at Grice Bay.

The stumps in Maltby Bay are presently undecipherable. Although unquestionably Holocene in age, they could represent relict, submerged soil surfaces (gradual sea level rise or rapid subsidence), organic lag deposits, or could be a product of some recent cultural activity. These stumps and the thin sand bed are the focus of continuing research in this area. In particular, attempts are being made to date these features.

ACKNOWLEDGMENTS

The authors would like to thank A. Blais and H. Blyth for assistance in the field. Dr. I. Hutchinson directed the authors to features of interest in Maltby Bay. The figures were drafted by C. Smith.

REFERENCES

- Atwater, B.F. (1987): Evidence for Great Holocene Earthquakes Along the Outer Coast of Washington State; *Science*, Volume 236, pages 942-944.
- Brandon, M.T. (1985): Mesozoic Mélange of the Pacific Rim Complex, Western Vancouver Island; *Geological Society of America*, Cordilleran Section, Guidebook Trip 7, 28 pages.
- Clague, J.J. (1989): Late Quaternary Sea Levels and Crustal Movements, Coastal British Columbia; *Geological Survey of Canada*, Current Research, Part E, Paper 89-1E, pages 233-236.
- Clague, J.J., Armstrong, J.E. and Mathews, W.H. (1980): Advance of the Late Wisconsin Cordilleran Ice Sheet in Southern British Columbia Since 22,000 Yr B.P.; *Quaternary Research*, Volume 13, pages 322-326.
- Clague, J.J. and Bobrowsky, P.T. (1990): Holocene Sea Level Change and Crustal Deformation, Southwestern British Columbia; *Geological Survey of Canada*, Current Research, Part E, Paper 90-1E, pages 245-250.
- Koppel, T. (1989): Earthquake, Major Quake Overdue on the West Coast; *Canadian Geographic*, Aug/Sept., 12 pages.
- Long, D., Smith, D.E. and Dawson, A.G. (1989): A Holocene Tsunami Deposit in Eastern Scotland; *Journal of Quaternary Science*, Volume 4, pages 61-66.
- Murty, T.S. (1977): Seismic Sea Waves, Tsunamis; *Department of Fisheries and the Environment, Canada*, Bulletin 198, 337 pages.
- Peterson, C.D. and Darienzo, M.E. (1988): Discrimination of Flood, Storm and Tectonic Events in Coastal Marsh Records of the Southern Cascadia Margin; *Quaternary Research Center*, Spring Symposium, Seattle, Washington, page 11.
- Reinhart, M.A. and J. Bourgeois (1988): Testing the Tsunami Hypothesis at Willapa Bay, Washington: Evidence for Large Scale, Landward Directed Processes; *Quaternary Research Center*, Spring Symposium, Seattle, Washington, page 9.
- Rogers, G.C. (1988): An Assessment of the Megathrust Potential of the Cascadia Subduction Zone; *Canadian Journal of Earth Sciences*, Volume 25, pages 844-852.
- White, W.R.H. (1966): The Alaska Earthquake and its Effect in Canada; *Canadian Geographical Journal*, Volume LXXII, pages 210-219.
- Wigen, S.O. and White, W.R.H. (1964): Tsunami of March 27-29, 1964 West Coast of Canada; *Department of Mines and Technical Surveys, Canada*, unpublished manuscript, 12 pages.

NOTES



INTEGRATING BEDROCK GEOLOGY WITH STREAM-SEDIMENT GEOCHEMISTRY IN A GEOGRAPHIC INFORMATION SYSTEM (GIS): CASE STUDY NTS 92H

By P.M. Bartier and C. P. Keller, University of Victoria

KEYWORDS: Geographical information systems, GIS, geology, stream-sediment geochemistry, point transformation, data transformation, catchment basins, Thiessen polygons, integration, overlay, spatial analyses.

INTRODUCTION

Two data sets commonly used for geological resource assessment include bedrock geology and stream-sediment geochemistry. Traditional methods for determining relationships between these data include both qualitative and quantitative techniques. Qualitative interpretation and integration is generally based upon visual observations of spatial coincidence between the data. Quantitative results can be derived by summarising point values according to the dominant lithology of a sample's drainage area, or according to the geological unit it coincides with. Qualitative methods lack numerical explicitness, reproducibility and rigour. Quantitative methods struggle with the fact that stream-sediment geochemistry sample points are manipulated to represent areal distributions, where the area represented by each sample must somehow be inferred before quantitative analysis can take place. This study concerns quantitative techniques.

Geographical information systems (GIS) offer several methods for transforming geochemical points into areal coverage, allowing the resulting choropleth map to be integrated with maps depicting bedrock geology and used in the preparation of quantitative summaries or for further analysis. For example, points can be transformed into discrete homogeneous polygons (Thiessen polygons, drainage basins), or into continuous surfaces via interpolation (contouring, moving averages). This capability obviously has tremendous potential for geological interpretation and mineral exploration.

An ongoing research project at the University of Victoria, conducted in conjunction with the British Columbia Geological Survey Branch, is examining alternative methodologies for computationally integrating bedrock geology with stream-sediment geochemistry in GIS, including comparing and contrasting different results obtained. This research note presents a cursory discussion of general methodologies for interpolating stream-sediment geochemical sample points for integration with bedrock geology within GIS. Preliminary results are discussed.

Use of commercial names in this paper is for descriptive purposes only. It does not constitute endorsement by the University of Victoria or the British Columbia Geological Survey.

JUSTIFICATION FOR STREAM- SEDIMENT POINT TRANSFORMATION

For the purposes of the following discussion, the basis for transforming stream-sediment point samples into areal coverages can be discussed in terms of physical factors and spatial analytical concepts. Physical factors are those which are responsible for the sediment make-up of a sample site before collection takes place. They include surficial geomorphology, bedrock geology, structure, atmospheric pollutants, fauna, flora and other physiographical variables. Spatial concepts entail upstream analysis, spatial autocorrelation, proximity, and distance decay. There are also other non-physical factors, including sampling and recording techniques, and analytical procedures, which may contribute to error and uncertainty in geochemical determinations, but these do not constitute a basis for spatial transformation. The latter non-physical factors are beyond the control of this study and will not be considered further.

PHYSICAL FACTORS

The catchment basin associated with a given stream-sediment sample is the dominant physical factor controlling input of material. It can be determined by including successively adjacent locations with elevations higher than the point of sampling. Within a basin, various other physical factors may influence the composition of the stream sediment sample, or contribute to within-basin variation. These include slope, aspect, curvature, vegetation, differential weathering of bedrock, rainfall and wildlife. There are also factors which transcend drainage basin boundaries. Geological material from beyond the catchment boundary may be present due to glacial transport or atmospheric pollution; it is also possible for groundwater flow and biological activity to transport material across watershed boundaries.

SPATIAL ANALYSIS

'The first law of geography' states "... everything is related to everything else, but near things are more related than distant things." (Tobler, 1970). In map variables exhibiting spatial pattern due to proximity, spatial autocorrelation is said to exist (Johnston, 1986). Assuming spatial autocorrelation exists, how does it affect the nature of spatial patterns? Spatial autocorrelation is associated with the topological relationships and metric relationships between spatial phenomena. Spatial patterns can therefore be discerned based upon topological and metric analysis, including directional relationships (upstream versus downstream), adjacency, proximity and through metric-distance decay.

The role of stochastic processes, of course, should not be ignored. Given these constraints, a number of techniques have been developed to translate point data into areal coverage based upon the concept of spatial autocorrelation.

TECHNIQUES FOR TRANSFORMING POINT DATA

Techniques for transforming point data into thematic maps can be divided into discrete and continuous methods. Discrete methods assume that a distinct area can be associated with each point, and that there is no variation within this area; variation occurs abruptly along polygon boundaries only. In contrast, continuous methods assume that variation is gradual between observation points or over the entire area of interest. A number of transformations are briefly introduced below. Most commercial GIS support one or a number these techniques. The reader is referred to Burrough (1987), George and Bonham-Carter (1990), McCullagh (1988), Davis (1986) or Lam (1983) for in-depth discussions.

CATCHMENT BASINS

Catchment basins have been used to define area-of-influence polygons for stream-sediment samples (*see*, for example, Bonham-Carter *et al.*, 1988; Dwyer and Nash, 1987; Rogers *et al.*, 1990). Catchment basins assume elevation to be the defining criterion for area-of-influence of a sample point. This is a discrete polygon method and therefore assumes within-polygon uniformity of geochemistry. Catchment basins can be determined manually from elevation contours, a time-consuming and tedious task, or digitally from a digital terrain model. Not all GIS support automatic digital watershed-identification routines.

THIESSEN POLYGONS

Thiessen polygons, also known as Voronoi or proximal polygons, assume that the extent of a point's influence can be strictly defined by its proximity to neighbouring points. Thus, for a given distribution of points, Thiessen polygons are defined by joining right-angle bisectors of lines connecting all neighbouring points. All locations in resulting polygons are closer to the defining point than any other (assuming unweighted transformation). Thiessen polygons are a discrete method and the primary drawback is again their inability to reflect within-polygon variation and gradual changes between sample points (Saxton Branson, 1989). For a detailed discussion of Thiessen tessellations refer to Gold (1989) or Burrough (1987).

CONTOURING

This method is analogous to manual contouring approaches traditionally employed by geologists. A continuous surface can be created by determining the values of unknown locations through linear interpolation between known values. This method assumes sample points represent exact locational values, and the method may not be appropriate if critical values (local maxima, minima) are not

defined by the point distribution. Interpolation between sample points can be both linear or nonlinear.

WEIGHTED AVERAGES

This represents a local interpolation method which considers the values of several points within a defined window (or kernel) to determine an average value for any point within it. Averaging can be linear or nonlinear by defining appropriate distance-decay parameters. The method is discussed in detail by Burrough (1987) and George and Bonham-Carter (1990). A number of limitations have been identified. Problems may occur if the data points tend to be clustered (Burrough, 1987), and the original data values may be lost due to generalization. The user is also required to have some knowledge of the data which allows for the determination of appropriate kernel size and distance-decay parameters.

OPTIMAL INTERPOLATION

Optimal interpolation, or Kriging, assumes that variation is too complex to be modelled using mathematics, and that it therefore must be treated as a stochastic process. The technique depends upon the variogram for summarizing the form of the variation, its magnitude and spatial scale (Oliver and Webster, 1990). Original data values are maintained and estimates of error can be obtained (Burrough, 1987). This type of optimal interpolation procedure is largely absent in commercial GIS software, however, Oliver and Webster (1990) believe it can be incorporated.

TREND-SURFACE ANALYSIS

Trend-surface analysis is a global interpolation technique, that is values for a given location are determined by considering the entire data set (the methods listed above are local interpolators). This method employs multiple regression to determine a polynomial equation which can be used to estimate the value for any given location. It is susceptible to highly anomalous values (Burrough, 1987) and original data values are not represented in resulting surfaces.

CLASSIFYING CONTINUOUS SURFACES

Point data transformed into continuous surfaces can be made discrete through classification methods. This may be useful for display purposes but results in generalization and loss of resolution if used for analysis. Classifying continuous data also requires an appropriate scheme for grouping data values based upon some underlying nature (*e.g.* statistical). Refer to Burrough (1987) for a discussion on techniques and problems associated with classifying continuous data.

INTEGRATING STREAM-SEDIMENT GEOCHEMISTRY WITH GEOLOGY IN A GIS

The practical aspects of data input, transformation and integration of the two geoscience data sets are described in

**TABLE 4-4-1
DESCRIPTION OF GEOLOGICAL UNITS**

1	QUATERNARY Drift; alluvium; colluvium, recent deposits.	33	Intermediate volcanics.
2	Basaltic flows.	34	Argillite, tuff.
	TERTIARY	35	Intermediate, locally felsic flows and pyroclastics; local argillite, conglomerate.
3	Basalt, olivine basalt, minor flows.	36	Argillite, slate, siltstone, tuff.
4	Intermediate, felsic pyroclastics and flows.	37	Sandstone, argillite; local mafic, intermediate volcanics.
5	Granodiorite.		TRIASSIC AND/OR JURASSIC
6	Intermediate, felsic pyroclastics and flows.	38	Granodiorite.
7	Granodiorite.	39	Diorite, amphibolite.
8	Granodiorite.	40	Syenite, diorite, gabbro, ultramafic rock.
9	Intermediate with local mafic and felsic flows, volcanics.	41	Argillite, sandstone, minor carbonate.
10	Sandstone, conglomerate, argillite.	42	Mafic to felsic volcanics, minor argillite.
11	Granodioritic and intermediate intrusions.	43	Felsic to intermediate pyroclastics, argillite.
	CRETACEOUS AND/OR TERTIARY	44	Intermediate pyroclastics and flows.
12	Pegmatitic granite gneiss; pelitic schist, amphibolite, minor marble, ultramafic rocks.	45	Mafic pyroclastics and flows.
13	Blueschist, local amphibolite, minor marble and ultramafic rock.	46	Argillite, sandstone, tuff, breccia, conglomerate.
14	Greenschist: mafic to intermediate volcanics, phyllite, minor volcanic, conglomerate.	47	Amphibolite, diorite, mylonite, schist, marble.
	CRETACEOUS	48	Siliceous argillite, mafic volcanics.
15	Granodiorite, quartz monzonite.	49	Mafic volcanics.
16	Mainly granite.	50	Granite gneiss.
17	Felsic intrusions.	51	Carbonate.
18	Intermediate, locally felsic, mafic volcanics sandstone, shale, conglomerate.	52	Schist, metachert, pelite, amphibolite, marble, ultramafic rock.
19	Mafic volcanics.	53	Ultramafic rock, local gabbro.
20	Chert-grain sandstone and conglomerate.		PERMIAN TO JURASSIC
21	Undifferentiated sediments.	54	Chert, pelite, mafic volcanics, minor limestone, gabbro and ultramafic rock.
22	Sandstone, argillite, conglomerate.	55	Mafic volcanics.
23	Intermediate intrusions, minor ultramafic rock.	56	Siliceous and chlorite schist, phyllite.
24	Felsic and mafic gneiss.	57	Ultramafic rock and local gabbro.
	JURASSIC(?) AND CRETACEOUS		ORDOVICIAN TO TRIASSIC
25	Intermediate pyroclastics and flows.	58	Argillite, chert, mafic volcanics, minor carbonate and ultramafic rock.
26	Sandstone, conglomerate.	59	Amphibolite, gneiss, minor ultramafic rock.
27	Granodiorite and gneiss.		DEVONIAN TO PERMIAN
28	Diorite and amphibolite.	60	Pelite, sandstone, minor conglomerate, mafic and felsic volcanics; carbonate.
29	Granite and pegmatite.	61	Metadiorite and gabbro.
30	Sandstone, conglomerate, argillite.	70	Water bodies.
31	Conglomerate, sandstone, argillite.		
32	Granite and granodiorite.		

Generalized after Monger, 1989.

**TABLE 4-4-2
SUMMARY OF DATA VARIABLES USED FOR THE STUDY**

Data Variable	Data Type	Attributes	Input/Source
Stream-sediment Geochemistry Drainage Basins	Points Polygonal	Geochemical Elements Geochemical Elements	Digital files; GSC OF 865/MEMPR BC RGS 7 Digitized; derived from NTS 92H using geochemical points as criteria
Bedrock Geology Geology Cut To Drainage Cover Thiessen Polygons	Polygonal Polygonal Polygonal	Geological Classes Geological Classes Geochemical Elements	Digitized from 1:250 000 GSC geology map 92H Derived from intersection of geology/drainage maps Computed from geochemical point locations

this section. The study area used is as defined by the boundary of map-sheet NTS 92H, located in southwestern British Columbia.

DATA INPUT

A 1:250 000-scale bedrock geology map (NTS 92H, Monger, 1989) containing 791 polygons was manually digitized. Attribute tags identifying map units were added to

each polygon. Including water bodies, there are 62 classes; a generalized description of each class is provided in Table 4-4-1. Catchment basins were manually determined from elevation contours (NTS 92H) according to the location of stream-sediment sample points (BC-RGS-7). Of the 995 sample locations for 92H, 55 are duplicate samples and another 27 lack elemental analyses; these sample locations were discarded. Of the remaining 913, two fell on the southern map-sheet boundary and appreciable catchment

TABLE 4-4-3
OVERLAY SUMMARIES

Unit	Area (Square km)		Pts	Zinc (ppm)			Copper (ppm)			Lead (ppm)			Nickel (ppm)		
	B	T	PiP	B	T	PiP	B	T	PiP	B	T	PiP	B	T	PiP
1	964.6	2091.6	206	60.6	72.4	75.4	30.5	31.4	34.9	4.53	5.96	5.7	16.4	16.2	18.0
2	5.2	6.9	0	50.6	53.2		21.6	23.7		1.86	2.44		8.6	8.9	
3	8.4	11.8	0	57.7	64.4		16.2	20.8		3.82	6.30		7.3	13.6	
4	9.1	9.1	1	123.4	61.4	56.0	53.5	36.4	33.0	16.81	12.07	12.0	36.7	11.4	10.0
5	151.1	206.0	12	39.7	40.9	30.9	22.1	21.8	21.2	4.87	6.20	5.2	15.0	11.6	9.1
6	53.7	70.1	2	72.2	68.3	79.5	18.6	19.7	16.0	11.59	10.10	19.5	16.6	8.8	9.5
7	170.2	312.7	24	62.9	50.8	57.0	32.2	30.2	32.8	10.25	6.80	7.5	19.0	12.9	12.5
8	209.2	240.7	10	60.9	52.1	44.7	15.5	14.4	9.0	4.04	4.45	3.9	11.3	12.8	4.0
9	271.3	429.7	15	54.6	52.1	51.0	30.0	27.4	32.3	5.92	5.35	6.3	13.4	13.8	12.1
10	63.9	167.6	12	52.7	60.7	55.0	24.7	28.9	20.5	6.04	6.80	5.1	17.8	14.3	11.4
11	96.2	182.0	9	68.9	68.7	88.2	30.4	29.4	28.2	4.81	5.26	9.4	31.8	29.1	17.4
12	111.7	218.4	22	66.7	62.5	63.4	33.4	30.5	33.0	6.29	3.89	3.3	35.4	52.3	63.9
13	210.9	344.4	22	50.6	49.8	49.9	35.6	32.0	35.3	2.66	2.90	2.5	43.9	37.2	39.7
14	13.2	17.1	0	126.6	104.8		53.3	47.8		6.96	6.22		61.0	52.8	
15	495.4	705.3	32	43.6	36.9	34.7	6.7	4.7	3.2	3.09	3.27	3.0	8.9	7.0	5.9
16	315.6	377.5	13	93.5	83.9	49.3	41.8	33.0	15.8	10.77	9.07	5.8	5.8	5.1	5.7
17	45.0	93.9	6	125.5	172.1	84.7	93.6	95.5	48.2	14.14	19.58	11.7	7.8	10.3	9.0
18	401.2	696.6	41	61.6	63.5	62.9	18.9	20.5	20.2	4.15	4.48	3.8	9.3	9.4	9.4
19	115.5	264.0	17	58.5	64.2	62.5	32.1	37.4	39.1	2.81	3.22	3.6	51.2	36.4	25.2
20	12.0	13.0	1	70.2	70.1	73.0	29.7	38.7	29.0	4.50	3.97	1.0	8.3	10.2	9.0
21	346.0	478.3	21	60.7	62.3	63.0	20.3	21.3	20.0	4.48	5.58	8.0	14.3	14.4	12.0
22	165.1	294.5	22	102.2	102.2	102.7	31.0	38.4	54.5	6.20	7.52	9.0	21.4	18.6	17.6
23	455.0	816.2	52	39.8	42.6	43.6	22.0	21.7	20.0	2.97	3.59	3.7	26.1	24.5	24.0
24	29.7	71.0	2	32.6	37.4	34.5	32.6	30.4	18.0	4.43	4.60	3.0	3.7	4.7	8.0
25	50.6	87.5	7	63.2	70.1	68.4	31.7	31.4	34.1	3.84	4.61	5.9	9.0	9.8	9.6
26	5.8	61.3	2	73.7	89.3	105.0	26.3	37.5	46.0	3.11	3.05	2.5	10.8	26.6	35.0
27	370.5	611.4	38	46.8	50.5	50.9	16.5	17.2	16.3	3.14	3.81	4.1	7.0	7.0	8.5
28	15.6	46.7	2	58.6	66.0	57.0	29.4	23.6	20.0	6.18	9.30	9.0	14.8	14.9	30.0
29	125.4	161.9	8	54.7	53.0	51.2	22.3	17.6	15.2	4.32	5.01	5.6	10.3	7.9	6.8
30	6.0	10.3	0	130.2	201.8		58.9	91.9		9.64	16.64		20.8	26.7	
31		15.6	0		154.7			31.9			15.04			10.2	
32	660.6	993.4	33	58.6	64.1	86.3	12.3	13.6	13.7	5.50	5.41	7.8	4.1	4.1	4.2
33	6.0	9.4	1	79.8	84.5	70.0	23.9	22.9	20.0	4.68	6.45	4.0	7.4	7.0	6.0
34	12.4	13.7	2	85.0	92.8	95.0	23.4	23.9	24.0	8.21	9.62	9.0	6.4	6.2	6.5
35	127.1	258.7	13	192.3	131.6	111.5	30.0	30.9	31.2	12.06	9.58	7.9	5.3	5.5	4.8
36	219.8	281.2	15	128.5	142.1	97.7	35.5	59.5	26.9	17.87	22.49	5.5	43.4	35.9	36.8
37	227.2	331.1	19	109.1	97.3	90.1	24.1	24.1	21.8	8.60	6.35	5.0	16.7	14.8	11.6
38	533.3	1117.7	51	54.6	54.0	54.5	17.3	20.4	20.3	3.79	3.66	3.6	7.8	7.1	7.0
39	136.6	181.6	5	42.4	41.1	42.4	27.1	29.3	29.6	1.74	1.91	2.4	12.7	8.7	9.6
40	63.5	104.0	4	64.1	58.7	54.2	59.6	77.2	115.8	3.30	4.06	3.0	27.1	38.4	44.8
41	44.3	166.7	9	127.7	117.6	122.8	46.2	45.0	48.1	4.78	5.02	5.1	25.6	27.6	31.2
42	210.5	338.0	17	71.2	71.1	65.4	33.9	35.7	34.8	4.25	3.87	3.4	14.7	16.0	18.1
43	63.8	88.7	7	70.0	70.5	70.7	33.8	38.4	37.7	1.36	1.83	1.6	9.6	10.2	10.3
44	165.9	190.4	6	72.4	65.5	61.7	30.6	37.3	37.0	3.89	4.93	3.0	6.0	9.2	8.5
45	440.1	715.0	32	65.0	65.2	71.9	48.1	58.5	66.5	4.10	3.94	4.3	10.3	10.4	10.7
46	220.0	324.3	10	52.2	52.2	50.8	17.0	19.2	22.4	2.40	2.77	2.9	6.9	8.5	10.5
47	91.6	237.8	10	61.4	59.9	56.6	39.5	32.1	37.5	3.55	4.21	3.2	15.6	13.1	10.3
48		1.6	0		73.0			31.3			4.00			4.3	
49	4.2	6.3	0	68.5	71.8		27.2	25.7		3.05	5.02		98.4	103.0	
50	25.9	25.9	2	38.7	34.8	34.0	23.5	19.1	13.5	2.74	3.00	4.5	15.0	13.3	8.0
51	0.8	0.9	0	38.0	34.7		22.0	25.0		2.00	1.67		18.0	6.7	
52	49.3	71.3	5	43.1	46.8	47.8	28.4	32.6	43.2	2.93	3.23	2.0	47.2	48.0	39.0
53	28.7	40.2	2	69.5	70.3	65.5	31.9	31.3	23.0	3.48	4.75	3.5	165.6	174.0	
54	368.8	592.9	32	104.5	109.8	121.0	55.8	56.6	58.1	10.18	11.62	25.9	62.3	71.2	59.5
55	133.0	225.7	19	144.7	161.0	135.9	96.0	101.7	97.2	9.87	22.32	10.3	57.6	57.9	58.7
56	1.3	18.4	4	57.9	68.5	64.8	24.8	36.6	31.0	1.31	1.14	1.2	21.5	31.5	24.2
57	2.3	5.1	1	83.4	88.7	94.0	44.5	43.6	40.0	4.05	4.34	7.0	124.6	89.0	96.0
58	37.3	97.0	7	52.0	51.3	55.4	22.5	22.6	28.3	3.53	2.92	3.1	13.2	13.2	19.1
59		8.1	0		105.0			29.0			5.00			11.0	
60	74.9	219.9	8	98.0	101.5	111.5	38.7	39.9	44.0	5.16	5.51	5.6	27.6	24.0	21.8
61	8.8	21.1	0	58.1	60.9		37.4	33.9		4.47	4.54		55.0	60.2	
70	10.0	260.6	0	38.5	99.8		26.0	38.9		5.49	5.08		4.9	17.4	
Total	9261.3	16060.3	913	67.7	69.5	69.7	28.4	30.5	31.9	5.42	5.81	5.9	18.2	18.0	19.5

Note: B — Drainage basin; T — Thiessen polygon; PiP — Point-in-Polygon.

TABLE 4-4-3
OVERLAY SUMMARIES — Continued

Unit	Cobalt (ppm)			Silver (ppm)			Manganese (ppm)			Iron (%)			Molybdenum (ppm)			Tungsten (ppm)		
	B	T	PiP	B	T	PiP	B	T	PiP	B	T	PiP	B	T	PiP	B	T	PiP
1	8.4	8.4	8.3	0.12	0.14	0.13	467.1	527.5	461.4	1.93	2.14	2.04	1.3	1.5	1.7	1.2	1.2	1.3
2	7.0	7.1		0.10	0.10		476.7	536.8		1.87	1.87		2.1	1.8		1.0	1.0	
3	7.0	8.3		0.10	0.19		438.1	670.9		2.28	2.45		1.1	1.3		1.0	1.2	
4	16.6	9.8	9.0	0.18	0.10	0.10	811.8	308.4	275.0	3.78	2.58	2.50	2.8	1.9	2.0	1.3	1.0	1.0
5	6.2	5.6	5.4	0.10	0.11	0.10	195.0	214.2	173.0	1.75	1.61	1.49	1.5	1.5	1.4	2.3	2.2	2.2
6	7.0	7.1	7.0	0.22	0.11	0.10	483.8	559.2	810.0	1.68	1.88	1.83	1.2	1.4	2.0	1.0	1.0	1.0
7	7.4	6.4	6.6	0.18	0.13	0.11	325.5	306.7	464.0	1.91	1.76	1.74	1.7	1.3	1.5	2.1	3.6	4.6
8	6.3	6.1	5.1	0.10	0.16	0.10	282.1	270.1	251.2	2.05	2.11	1.38	1.6	1.7	2.4	2.5	1.9	1.0
9	6.4	6.6	6.1	0.13	0.11	0.11	438.8	457.9	298.1	1.69	1.66	1.59	1.3	1.1	1.1	1.0	1.1	1.0
10	7.0	7.6	7.3	0.11	0.12	0.10	361.6	446.1	481.3	1.70	1.82	1.74	1.1	1.2	1.1	1.2	1.2	1.2
11	10.1	9.4	8.3	0.12	0.13	0.16	353.4	373.6	455.1	2.28	2.15	2.21	1.4	1.5	1.7	1.0	1.0	1.1
12	8.2	9.6	10.6	0.12	0.11	0.11	300.4	303.9	310.9	2.11	2.14	2.27	1.7	1.3	1.3	2.3	1.0	1.0
13	8.5	8.6	8.9	0.11	0.11	0.10	197.3	194.6	175.6	1.73	1.70	1.75	1.6	1.5	1.4	3.8	2.7	1.3
14	17.2	14.9		0.10	0.10		619.4	504.0		4.32	3.72		3.0	2.5		1.0	1.0	
15	3.3	2.4	2.1	0.10	0.10	0.10	187.6	135.1	131.7	0.92	0.71	0.67	1.1	1.1	1.1	1.1	1.1	0.9
16	3.7	4.0	3.7	0.16	0.14	0.15	505.7	618.7	667.1	1.44	1.48	1.43	1.8	2.1	2.0	1.3	1.6	1.5
17	5.3	5.9	5.2	0.37	0.37	0.23	650.9	666.7	514.7	2.28	2.19	2.13	2.7	2.4	1.8	1.1	1.1	1.0
18	7.3	7.6	7.8	0.12	0.13	0.11	568.2	646.3	670.1	2.11	2.15	2.16	1.3	1.5	1.4	1.0	1.0	1.1
19	9.1	10.2	9.5	0.10	0.11	0.11	260.7	258.3	245.0	1.91	2.09	2.07	1.2	1.3	1.4	3.1	2.7	1.9
20	7.5	8.1	8.0	0.10	0.10	0.10	744.2	687.7	680.0	2.00	2.10	2.10	1.0	1.0	1.0	1.0	1.0	1.0
21	7.8	7.5	6.6	0.21	0.27	0.15	427.8	434.5	368.4	2.01	1.91	1.72	1.2	1.2	1.4	1.0	1.0	1.0
22	12.0	12.0	13.3	0.15	0.18	0.23	590.7	623.8	592.0	2.95	2.87	3.02	1.7	1.5	1.7	1.0	1.4	2.1
23	6.3	6.8	6.5	0.11	0.10	0.11	170.6	193.7	129.9	1.32	1.38	1.34	1.2	1.4	1.3	1.7	1.6	1.0
24	4.9	5.6	5.5	0.12	0.12	0.15	153.8	161.8	130.0	1.26	1.30	1.02	1.9	1.8	1.5	8.3	7.4	13.0
25	13.1	13.7	13.6	0.11	0.11	0.13	513.9	582.3	543.1	3.07	3.25	3.09	1.1	1.0	1.1	1.0	1.0	1.0
26	11.2	12.0	13.5	0.16	0.11	0.10	540.0	412.9	338.0	3.14	3.14	3.23	1.7	1.1	1.0	1.0	1.0	1.0
27	5.1	6.0	6.1	0.11	0.11	0.11	375.4	451.8	450.9	1.52	1.68	1.71	1.4	1.3	1.1	0.9	1.0	1.0
28	8.1	7.7	8.5	0.10	0.17	0.10	422.8	461.6	370.0	1.72	1.78	1.70	1.1	1.8	1.0	1.0	1.0	1.0
29	6.8	5.7	4.5	0.10	0.11	0.12	370.2	418.8	405.4	1.60	1.43	1.22	1.4	1.2	1.1	1.5	1.0	1.0
30	13.0	16.7		0.25	0.46		693.5	826.4		3.30	3.93		2.0	3.4		2.2	3.6	
31		8.9			0.21			1136.9			2.97			1.6			1.0	
32	4.1	4.1	4.6	0.11	0.12	0.14	639.6	589.9	744.0	1.73	1.61	1.74	1.5	1.7	1.5	1.1	1.5	1.5
33	12.7	12.6	9.0	0.14	0.11	0.10	728.0	792.1	467.0	3.63	3.76	3.00	1.4	1.1	1.0	1.0	1.0	1.0
34	11.4	12.7	14.0	0.16	0.16	0.15	745.6	898.0	990.0	3.36	3.77	4.15	1.6	1.6	1.5	1.0	1.0	1.0
35	10.4	9.1	8.7	0.19	0.14	0.12	1120.8	768.5	545.4	3.18	3.10	3.10	2.3	2.3	2.6	1.0	0.9	1.0
36	12.8	12.9	10.5	0.37	0.53	0.11	542.4	565.8	450.5	3.14	3.04	2.65	2.1	2.4	1.7	1.1	2.4	1.9
37	9.6	9.6	8.8	0.31	0.15	0.25	532.2	518.6	474.4	2.59	2.47	2.20	1.4	1.4	1.3	1.2	1.0	1.0
38	5.9	5.6	5.8	0.14	0.13	0.13	565.6	563.8	562.0	1.93	1.95	1.94	1.4	1.6	1.4	1.3	1.3	1.7
39	9.8	8.0	9.6	0.10	0.10	0.10	359.6	314.8	401.2	1.75	1.65	2.00	1.1	1.2	1.2	1.1	1.0	1.0
40	14.8	13.8	13.8	0.15	0.11	0.12	612.2	674.3	1113.8	2.79	2.53	2.45	1.2	1.0	1.0	1.0	1.0	1.0
41	13.3	13.0	13.8	0.18	0.16	0.17	643.2	758.4	852.7	3.80	3.61	3.70	2.4	2.0	1.8	1.0	1.0	1.0
42	11.1	11.7	11.7	0.20	0.13	0.15	502.0	567.5	600.6	2.53	2.49	2.47	1.3	1.3	1.4	1.0	1.1	1.1
43	9.3	9.7	9.4	0.10	0.10	0.10	2581.6	1127.4	1602.9	2.45	2.51	2.46	1.6	1.4	1.4	1.1	1.1	1.0
44	6.4	7.5	7.7	0.10	0.10	0.10	664.9	530.4	489.5	1.93	1.93	1.88	1.1	1.2	1.2	1.0	1.0	1.0
45	7.6	7.8	8.4	0.12	0.12	0.12	690.0	792.4	791.5	1.99	2.18	2.57	1.6	1.5	1.6	1.0	1.1	1.1
46	4.8	4.9	5.2	0.13	0.13	0.12	464.1	516.2	681.7	1.39	1.53	1.83	1.6	2.0	1.6	1.2	1.0	1.0
47	11.2	8.8	7.7	0.24	0.12	0.11	501.8	443.8	383.4	2.44	2.11	1.99	1.5	1.5	1.9	1.1	1.1	1.1
48		7.8			0.10			370.0			3.05			3.5			1.0	
49	13.8	14.3		0.10	0.11		413.9	432.3		2.70	2.75		1.3	1.5		1.0	1.0	
50	6.8	5.8	5.0	0.10	0.10	0.10	136.5	152.2	136.0	1.19	1.09	1.00	2.1	2.2	3.0	16.4	10.4	20.5
51	10.0	7.3		0.10	0.10		265.0	200.0		1.55	1.32		1.0	1.0		1.0	1.0	
52	8.9	9.3	10.4	0.10	0.10	0.10	159.1	174.7	175.6	1.35	1.46	1.52	1.3	1.2	1.0	5.5	1.7	1.0
53	17.7	18.2	26.0	0.11	0.13	0.10	395.6	399.7	470.0	2.63	2.58	2.95	1.2	1.2	1.0	1.1	1.1	1.0
54	17.5	18.5	18.7	0.17	0.20	0.51	613.1	637.5	675.8	3.51	3.46	3.66	2.3	2.4	2.4	1.6	1.4	1.2
55	26.9	27.3	26.1	0.16	0.38	0.18	748.3	754.3	733.4	4.28	4.11	3.91	3.2	3.7	3.6	1.5	1.9	2.2
56	9.9	12.1	11.0	0.10	0.10	0.10	234.7	237.4	218.0	1.88	2.26	2.11	1.0	1.3	1.0	1.0	1.0	1.0
57	20.0	17.1	20.0	0.10	0.10	0.10	519.8	461.2	435.0	3.34	3.01	3.80	2.1	2.1	2.0	1.0	1.0	1.0
58	7.0	6.7	8.4	0.12	0.14	0.14	383.6	368.2	360.6	1.96	1.83	1.94	1.3	1.3	1.3	2.5	2.5	1.6
59		9.0			0.20			2400.0			2.75			3.0			1.0	
60	11.5	11.5	12.0	0.15	0.16	0.21	483.9	515.3	507.9	3.30	3.34	3.62	2.2	2.0	2.0	1.0	1.1	1.0
61	11.6	11.2		0.11	0.11		275.4	271.6		2.13	2.00		1.7	1.4		1.0	1.0	
70	4.7	11.4		0.10	0.12		205.4	589.0		1.41	2.80		1.2	1.4		5.2	2.2	
Total	8.0	8.2	8.5	0.14	0.14	0.14	482.8	495.7	483.3	2.02	2.07	2.09	1.5	1.6	1.6	1.4	1.4	1.4

Note: B — Drainage basin; T — Thiessen polygon; PiP — Point-in-Polygon.

basins could not be determined. A total of 911 stream-sediment catchment polygons were thus determined and digitized. Each polygon on the catchment map is treated as a unique class unto itself, and geochemical records in flat ASCII format were attached to corresponding catchment polygon tags. Both maps were digitised in an arc-node vector format using PC-ARC/INFO software. Upon completion of input, both polygonal data sets were formatted into an ASCII file and re-input to TYDAC SPANS GIS for further processing. The original geochemistry point file (913 points including the two points along the southern boundary) was input to SPANS as a third primary data set.

DATA TRANSFORMATION

In the SPANS GIS environment, both polygonal maps were rasterized to a resolution such that the accuracy of the digitized boundaries was not compromised (final resolution exceeds 100 metres on the ground). Using the coverage of the catchment basins as a binary template (coverage present, coverage absent), a second geology map was "cut out" such that the resulting area matched exactly with the catchment coverage. A Thiessen polygon map, totalling 913 separate polygons, was generated from geochemical point locations, and geochemical determinations were assigned as attributes to each polygon. A summary of each map variable is provided in Table 4-4-2.

DATA INTEGRATION

Treating the geology and "cut-out" geology maps as dependent variables and the Thiessen and catchment maps as corresponding independent variables, each map-pair was overlaid to determine average elemental concentration for each geology class, weighted to area. Overlay of map-pairs was performed ten times, using the following elements as attributes for the independent maps: zinc, copper, lead, nickel, cobalt, silver, manganese, iron, molybdenum and tungsten. A point-in-polygon overlay was performed using the geochemical point data set as the dependent variable and the geology map as independent, such that the geology classes were appended to spatially coincident points. Subsequent processing on the updated point file using dBASE III+ allowed each geology class to be summarized according to average concentration for each of the ten elements listed above.

The raw results from each overlay set are summarized in Table 4-4-3. The results for the polygon overlay sets are average values weighted to area; the point-in-polygon overlay is averaged by the number of contained points in each geology class. Totals for the entire map are included. The Thiessen map covered the entire map area; therefore all geology classes contain summaries for this overlay set. The catchment map covered only those areas defined by catchment basins; therefore three geology units were missed and could not be summarized. The potential for "miss" is even greater for the point-in-polygon overlay as it is dependent upon point-area intersections: ten units lack summaries from this overlay.

Included in Table 4-4-3 are summaries of the total area and point intersections for each geology map unit as well as total map areas. From this information it can be determined that stream-sediment catchment basins cover 57.7 per cent of the map area. However stream-sediment sample coverage of bedrock is very good as most of the missing coverage is accounted for by Harrison Lake, the city of Hope, samples lacking analyses and valley bottoms.

EDGE PROBLEMS

Geoscience data sets tend to be collected and distributed according to NTS map boundaries. Such boundaries place limitations, or edge effects, when used as a basis for data integration. Catchment basins of stream-sediment samples are either cut off or not included, depending upon which side of the boundary they fall on. Points immediately adjacent to the map area will also change Thiessen polygon configurations and affect the transformation of geochemical points into continuously varying surfaces through contouring, Kriging and weighted averages. The point-in-polygon method appears to be the only one that is unaffected by edge effects.

SUMMARY AND PROSPECTS

Geological interpretation and explanation of the data is not attempted here since this research note focuses upon the application of various techniques for transforming geochemical point data for subsequent integration with geology. However, a visual examination reveals obvious correlations between the three techniques. Further interpretation is left up to the reader for the purpose of this study, but will be reported in a future paper.

Although there is a conceptual basis for both Thiessen and catchment-basin transformations, the latter is intuitively more appealing. Catchment basins account for a primary physical factor controlling the spatial influence of stream-sediment sample points. Strict proximity of Thiessen polygons is a more abstract concept based upon the assumption that spatial autocorrelation exists. In regions of high relief, where catchment basins are easily defined, it is difficult to understand how Thiessen polygons can offer any advantage. However, as relief becomes flat and drainage boundaries are not as easily defined, then proximity may offer some advantages. Neither method allows for within-polygon variation. If variation is perceived as being important, then techniques for interpolating points into continuous surfaces will be more appropriate.

In applying these techniques, basic questions are raised regarding the nature of geochemical point samples are put forth. Do the samples represent point or areal coverage? Are the distributions discrete or continuous, stochastic or deterministic? What physical and spatial factors determine a sample's area of influence? It is therefore important that the assumptions and limitations of the various methods are understood. Ongoing work includes expanding the study to include additional interpolation techniques and a study of the impact of edge problems on overlay results. Future

research will include a quantitative comparison and explanation of the results each interpolation method produces through overlay with geology.

The techniques presented here offer considerable potential to assist with geological research and mineral exploration. However, digital spatial integration of geological data sets currently is not widely practised. The barriers for doing so can be identified as expensive technologies and a lack of digital map databases (geology, topography). Price-performance ratios for computer hardware and software are doubling every one to two years, and provincial coverage of geochemistry and terrain data in digital formats will soon be complete. Development of digital geological map databases by the appropriate authorities must also take place. Such databases should include seamless concepts (geographical elements are logically connected across NTS boundaries) such that users are not restricted to analysis by NTS mapsheets, but can choose regions more appropriate to the task, such as major watershed or geological terrane. The development and adoption of map database standards by various government agencies would also be helpful.

ACKNOWLEDGMENTS

Financial support was provided by the Geoscience Research Grant Program (RG90-2), British Columbia Ministry of Energy, Mines and Petroleum Resources. Research was conducted at the GIS research laboratory, the Department of Geography, the University of Victoria. Cloverpoint Cartographics of Victoria provided some computer hardware and software for the project. Their assistance is gratefully acknowledged.

REFERENCES

- Bonham-Carter, G.F., Agterberg, F.P. and Wright, D.F. (1988): Integration of Geological Datasets for Gold Exploration in Nova Scotia; *Photogrammetric Engineering and Remote Sensing*, Volume 54, No. 11, pages 1585-1592.
- British Columbia Ministry of Energy, Mines and Petroleum Resources (1982): National Geochemical Reconnaissance, Hope, British Columbia (92H); BC RGS 7.
- Burrough, P.A. (1987): Principles of Geographical Information Systems for Land Resources Assessment; *Oxford University Press*, New York, 193 pages.
- Davis, J.C. (1986): *Statistics and Data Analysis in Geology*; Wiley, New York, Second Edition.
- Dwyer, J.L. and Nash, J.T. (1987): Spatial Analysis of Geochemical Information From the Tonopah, Nevada, CUSMAP Project; *U.S. Geological Survey*, Open-File Report 87-314, pages 9-10.
- George, H. and Bonham-Carter G.F. (1990): An Example of Spatial Modelling of Geological Data for Gold Exploration, Star Lake Area, Saskatchewan; *Geological Survey of Canada*, Paper 89-9, pages 157-169.
- Gold, C.M. (1989): Surface Interpolation, Spatial Adjacency and GIS; in *Three Dimensional Applications in Geographic Information Systems*, J. Raper, Editor, *Taylor and Francis*, U.K., pages 21-35.
- Lam, N. (1983): Spatial Interpolation Methods: A Review; *The American Cartographer*, Volume 10, No. 2, pages 129-149.
- Johnston, R.J., Editor (1986): *The Dictionary of Human Geography*; *Basil Blackwell Ltd.*, Oxford, U.K.
- McCullagh, M.J. (1988): Terrain and Surface Modelling Systems: Theory and Practises; *Photogrammetric Record*, Volume 12, No. 27.
- Monger, J.W.H. (1989): Geology, Hope, British Columbia; *Geological Survey of Canada*, Map 41-1989, Sheet 1, Scale 1:250 000.
- Oliver, M.A. and Webster, R. (1990): Kriging: A Method of Interpolation for Geographical Information Systems; *International Journal of Geographic Information Systems*, Volume 4, No. 3, pages 313-332.
- Ostrowski, J.A., Benmouffok, D., He, D.C. and Horler, D.H. (1990): Geoscience Applications of Digital Elevation Models; *Geological Survey of Canada*, Paper 89-9, pages 33-37.
- Rogers, P.J., Bonham-Carter, G.F. and Ellwood, D.J. (1990): Mineral Exploration Using Catchment Basin Analysis to Integrate Stream Sediment Geochemical and Geological Information in the Cobequid Highlands, Nova Scotia; *Geological Survey of Canada*, Paper 89-9, pages 212.
- Saxton Branson, W. (1989): The Role of Point Data in GIS; *The Operational Geographer*, Volume 7, No. 4, pages 9-12.
- Tobler, W. (1970): A Computer Movie Simulates Urban Growth in the Detroit Region; *Economic Geography*, Volume 46, No. 2, pages 234-240.

NOTES



**GEOCHEMICAL RESEARCH, 1990: COAST RANGE -
CHILCOTIN ORIENTATION AND MOUNT MILLIGAN DRIFT
PROSPECTING STUDIES*
(92O, 92N, 93N)**

By J. L. Gravel, S. Sibbick and D. Kerr

KEYWORDS: Applied geochemistry, Coast Range, Chilcotin, orientation, stream sediment, multi-element, drift prospecting, alkaline porphyry, copper-gold, Mount Milligan.

INTRODUCTION

The Applied Geochemistry Unit undertook two new research programs in 1990 (Figure 4-5-1). The Coast Range - Chilcotin orientation study examined geochemical characteristics of mineralized drainage basins in the southwest interior of British Columbia. Resultant data interpretation will aid planning for a proposed Regional Geochemical Survey in the Mount Waddington (92N) map area and also serve as a guide for industry on geochemical exploration strategies in this region. The Mount Milligan project is the inaugural program in what is to become a series of drift-prospecting case studies integrating expertise from the applied geochemistry, surficial geology, regional mapping and mineral deposits fields. These studies will evaluate various exploration techniques for more effective mineral exploration in areas of thick glacial drift in British Columbia.

Final output for both the Coast Range-Chilcotin orientation and Mount Milligan drift-prospecting studies will appear in the publication *Exploration in British Columbia 1990*.

**COAST RANGE — CHILCOTIN
ORIENTATION STUDY**

In anticipation of a Regional Geochemical Survey of the Mount Waddington map sheet (92N), a series of orientation surveys were conducted within map areas 92O (Taseko Lakes) and 92N during the 1990 field season. The Mount Waddington map area contains numerous mineral showings within a variety of physiographic settings, yet remains largely unexplored; between 1985 and 1988, only 0.4 per cent of the assessment reports filed in the province originated in the 92N map sheet. Land-use concerns in the Mount Waddington area may be addressed with the aid of a high-quality, multi-element geochemical database.

Increased knowledge of the effects of geology, mineralogy, climate, surficial materials and physiography upon stream sediment dispersion will increase the effectiveness of a Regional Geochemical Survey. To this end, six deposits were selected to assess the effectiveness of multi-element

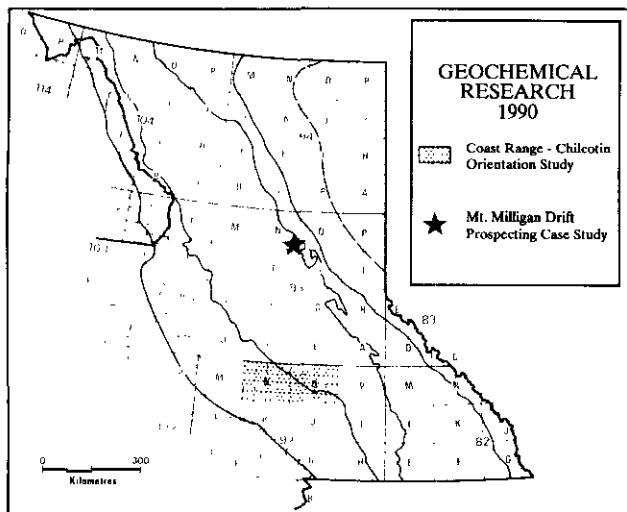


Figure 4-5-1. Location of Applied Geochemistry Unit research programs for 1990.

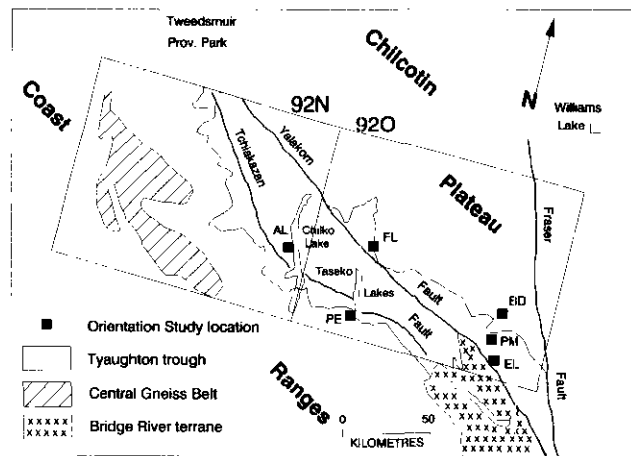


Figure 4-5-2. Geologic setting and orientation study locations Mount Waddington (92N) and Taseko Lakes (92O) map sheets. AL = Alexis; PE = Pellaire; FL = Fish Lake; EL = Elizabeth; PM = Poison Mountain; BD = Black Dome.

* This project is a contribution to the Canada/British Columbia Mineral Development Agreement.

stream-sediment geochemistry within this area (Figure 4-5-2). Five of the six deposits studied are located in the adjacent Taseko Lakes (92O) map area. These five deposits occur in geologic and physiographic settings comparable to the Mount Waddington area and are more accessible.

Objectives of the study are to:

- Typify the downstream dispersion of anomalous elements from the selected deposits.
- Observe the behavior of gold with downstream transport.
- Determine the impact of hydromorphic dispersion (in solution) and scavenging by organic and inorganic compounds in low-energy streams.
- Define the best sample media and analytical procedures for a Regional Geochemical Survey of the Mount Waddington (92N) map sheet.

DESCRIPTION OF STUDY AREA

PHYSIOGRAPHY

The Mount Waddington and Taseko Lakes map areas are characterized by a transition from the rugged, heavily glaciated Coast Range mountains to the semi-arid, subdued topography of the Chilcotin Plateau. Within the Mount Waddington map area, Coast Range mountains comprise approximately 75 per cent of the total area. Summit elevations commonly exceed 2500 metres, with intervening valleys averaging 1200 metres above sea level. Upper to mid-slopes are steep; bedrock is either exposed or covered with a thin veneer of till, colluvium and talus. Streams define a trellised pattern and are generally confined to narrow channels cut into bedrock. Valley floors are covered by thick glaciofluvial sediments; broad, gravel floodplains are actively reworked by shifting braided streams. The Chilcotin Plateau consists of flat to rolling terrain, generally at an elevation of 1200 to 1500 metres, dissected by glacially deranged, low-energy drainages with a moderate to high organic component. Precipitation decreases from over 3500 millimetres per year along the western edge of the Coast Range to 400 to 500 millimetres per year on the Chilcotin Plateau.

GEOLOGY

The Coast plutonic complex, composed of Cretaceous granites and granodiorites, dominates the Mount Waddington area and is a significant feature in the Taseko Lakes map area (Figure 4-5-2). Within the Coast Complex, roof pendants of gneiss, amphibolite, metasediments and meta-volcanics represent metamorphosed remnants of volcanic-arc rocks (Roddick and Tipper, 1985). Bordering the complex to the northeast are rocks of the Tyaughton trough, a back-arc sequence marking the boundary suture between the Stikinia and Wrangellia terranes (McLaren, 1990). The Tyaughton trough, comprising successions of Late Jurassic to Early Cretaceous volcanic and sedimentary rocks, stretches from north of Kleena Kleene southwards to the Fraser River, where it is truncated by the Fraser River fault (Tipper, 1969). Northeast of the Tyaughton trough, Tertiary

(and younger?) basalts and andesites are widespread, forming the subdued terrain of the Interior Plateau.

Several significant faults transect the study area. The Eocene Yalakom fault, a northwest-trending strike-slip fault approximately 300 kilometres long, displaces rocks within the Tyaughton trough by distances exceeding 100 kilometres (Tipper, 1969). A secondary structure, the Tchaikazan fault, parallels the Yalakom for 150 kilometres and has an estimated displacement of 30 kilometres (Tipper, 1969).

MINERAL OCCURENCES

At present, 48 mineral prospects, showings or occurrences within the Mount Waddington map area are recorded in MINFILE. Most notable are the Morris mine (Au, Ag, Sb), Alexis (Cu, Hg, Sb) and Daisie (Cu, W, Mo, Zn) prospects. Mesothermal and epithermal veins are the most common deposit type in the region (McLaren, 1990). Pel-laire (MINFILE 92O 045), located 30 kilometres east of Chilko Lake, is a mesothermal(?) gold-silver deposit containing 31 000 tonnes of ore grading 21 grams per tonne gold and 73 grams per tonne silver (Skerl, 1947). Two calcalkaline, copper-gold porphyry deposits [Fish Lake (MINFILE 92O 052) and Poison Mountain (MINFILE 92O 046)] are found within Tyaughton trough rocks to the east of Mount Waddington. Fish Lake has estimated reserves of 200 million tonnes grading 0.5 gram per tonne gold, 1.0 gram per tonne silver and 0.24 per cent copper; whereas Poison Mountain contains 193 million tonnes of ore grading 0.3 gram per tonne gold, 0.33 per cent copper and 0.015 per cent molybdenum (Schroeter and Panteleyev, 1986).

The Mount Waddington map sheet straddles a region of generally high mineral potential in British Columbia; the boundary between the Coast and Intermontane belts. However, few mineral deposits are known within the Mount Waddington area. The high mineral potential suggested by a clustering of mineral deposits north of Whitesail Lake and south of Taseko Lake has been extrapolated by McLaren (1990) into the Mount Waddington sheet. The scarcity of mineral occurrences may be attributed to the inaccessibility of the area. The rugged beauty and inaccessibility have also prompted consideration of parts of the map sheet as recreational or wilderness areas.

SAMPLING TECHNIQUES AND ANALYTICAL PROCEDURES

Six deposits were selected for detailed stream-sediment orientation studies (Table 4-5-1). These deposits were chosen to represent the most likely styles of mineralization and the characteristic physiographic regimes found in the Mount Waddington map area. Location of the deposit at or near the head of a drainage and the presence of only one known mineral occurrence within that drainage were prerequisites for selection. Sampling involved the collection of 1 to 2-kilogram stream-sediment samples at 500-metre intervals downstream from the deposit. Moss-mat samples were also taken when available. A duplicate sample was

**TABLE 4-5-1
SUMMARY OF ORIENTATION STUDY
HIGHLIGHTING DEPOSIT TYPES, GEOLOGY
AND SAMPLING PROGRAM**

Deposit (MINF #)	Deposit type (Commodities)	Deposit Geology	No. of Samples				Length of Traverse (km)
			Stream	Moss	Bulk	Rock	
Kizobeth (920/012)	Mesothermal vein (Au, Ag, Pb, Zn)	Qtz veins in Blue Creek porphyritic quartz diorite	19	19	1	0	5
Poison Min. (920/046)	Porphyry (Cu, Mo, Au)	Porphyritic stocks intrude Jackass Min. Group	15	1	1	1	55
Blackdome (920/052)	Epithermal vein (Au, Ag)	Qtz veins cut Kingsvale volcanics	21	0	2	0	55
Fish Lake (920/041)	Porphyry (Cu, Au, Sb)	Porphyritic stocks intrude Iyaughton volcanics	16	1	2	1	55
Pellare (920/044)	Mesothermal vein (Au, Ag, Cu)	Qtz veins in Coast Range granodiorite and L. Gref. rocks	7	0	0	0	71
Alexis (920/044)	Epithermal vein (Hg, Cu, Sb)	Faults cut altered U. Cretaceous volcanics	13	9	2	2	4

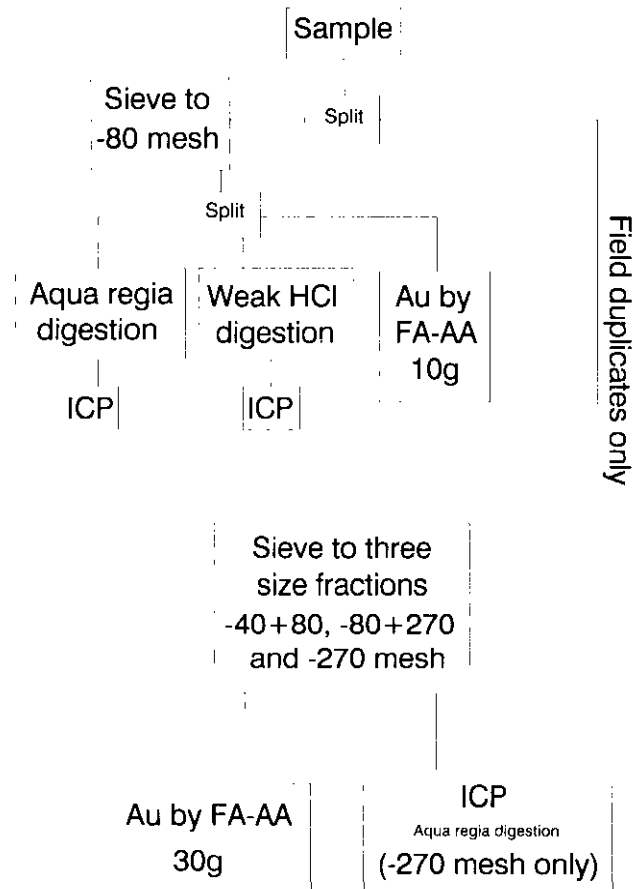


Figure 4-5-3. Flow chart detailing methods and specifications for analysis of orientation study samples.

collected at every second site. Bulk sediment samples for heavy mineral analysis were collected at the lowermost sample site of each drainage (Table 4-5-1). Major tributaries or adjacent streams draining similar geology but lacking known mineralization were sampled for background determinations.

Procedures for sample preparation and analysis are shown in Figure 4-5-3. Strong acid digestions are to be used on all samples. However, in cases where a hydromorphic component is suspected, a weak (10% HCl) digestion will also be employed.

PRELIMINARY CONCLUSIONS

Several preliminary conclusions can be drawn from the 1990 RGS orientation survey:

- The area is relatively inaccessible and will require extensive helicopter support to complete a Regional Geochemical Survey or other field programs.
- Moss-mat sampling is feasible, however, the sporadic distribution of mats may prevent its use on an RGS-style pay-per-sample survey.
- The presence of similar geologic environments found to the northwest and southeast of the map sheet suggest that areas of high mineral potential exist within the Mount Waddington map area.
- An RGS program covering the Mount Waddington map area would provide an excellent database for the resolution of potential land-use issues.

MOUNT MILLIGAN: A DRIFT-PROSPECTING CASE STUDY

Considerable research in drift prospecting in areas of continental glaciation has led to its regular use by industry in exploration programs in eastern and central Canada. Conversely, a lack of research on drift prospecting in areas of alpine glaciation, with particular reference to British Columbia, has impeded its use in this province. Notable exceptions include studies by Hoffman and Fletcher (1972), Mehrtens *et al.* (1973), Bradshaw (1975), Levinson and Carter (1979) and Hicock (1986). Most geochemical investigations, although recognizing the general nature of overburden, have rarely conducted in-depth analysis. The following case study, and those to follow, will attempt to provide guidelines that can be applied by the exploration community in British Columbia. The Mount Milligan copper-gold deposits were chosen for a detailed drift-prospecting study on the basis of several attributes:

- The deposit model (alkaline copper-gold porphyry), although known for some time (Barr *et al.*, 1976), is presently of great interest to the exploration community. Activity in the northern Quesnel trough which hosts these deposits has more than quintupled in the last five years (E.L. Faulkner, personal communication, 1990).
- Given the scale (up to 300 million tonnes) of these deposits, mineralized dispersion trains in glacial drift should be detectable by exploration geochemistry.
- The main orebodies are entirely covered by stratified and unstratified glacial drift of variable thickness which presents a challenge to routine exploration geochemical methods. There is potential for discovery of other alkaline porphyry deposits in the area, buried under similar drift.

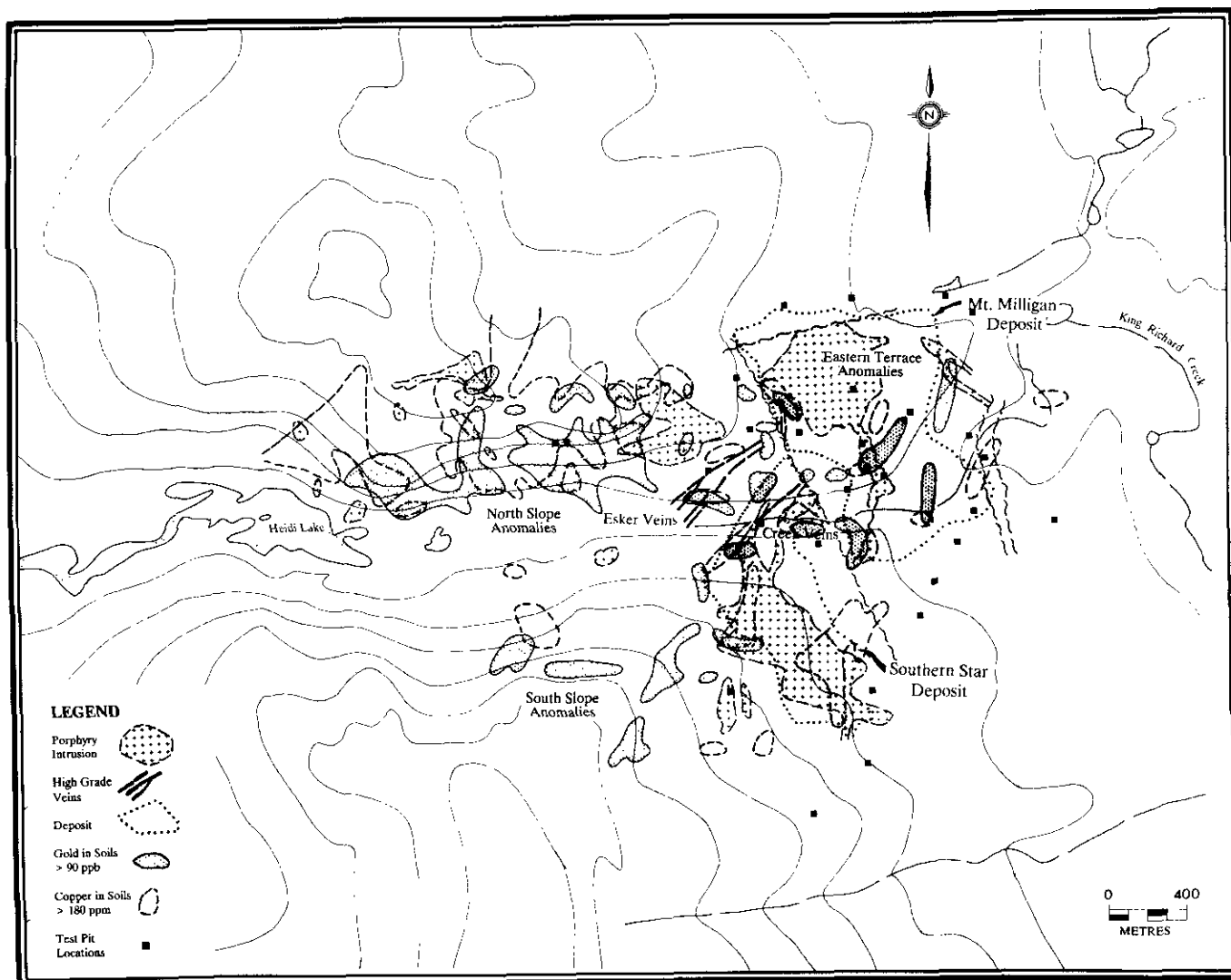


Figure 4-5-4. Summary of Mount Milligan soil geochemistry for copper and gold, and location of test pits.

EXPLORATION HISTORY

The Mount Milligan property lies along a northwest-trending mountainous ridge 60 kilometres north of Fort St. James. Initially explored in the 1970s as a porphyry copper prospect and subsequently dropped, the property was acquired in 1983 as an alkaline copper-gold porphyry target using the QR deposit as a model. Exploration from 1984 to 1986 defined several exploration targets (Figure 4-5-4):

- Broad copper-gold soil anomalies in thin colluvium and till mantling the northern and southern slopes (North and South Slope anomalies) of a minor east-trending valley.
- Discontinuous copper-gold anomalies following the meltwater paleocurrent direction in ice-contact moraine and stratified drift covering a terrace immediately east of the valley (Eastern Terrace anomalies).

- High-grade copper-gold (\pm arsenic, silver, lead, zinc and molybdenum) mineralization in quartz veins exposed along the banks of King Richard Creek (Esker and Creek zones) flowing from the minor valley and dissecting the eastern terrace.

By 1990 two well-mineralized alkaline porphyry stocks, the Mount Milligan and Southern Star deposits, and several smaller plugs, had been defined by extensive diamond-drilling (over 200 000 metres). Collectively, ore reserves are estimated at over 300 million tonnes grading 0.5 gram per tonne gold and between 0.25 per cent copper (DeLong *et al.*, 1991, this volume). Disseminated and stockwork sulphides are hosted by monzonite stocks and the surrounding cogenetic latite and andesite volcanics. For a complete overview of regional geology, local geology and mineralization, the reader is referred to contributions by Nelson *et al.* (1991) and DeLong *et al.* (1991) in this volume.



Plate 4-5-1. View of Test Pit 75; 5-metre section comprising glacial outwash overlying till. Samples were collected from the B and C soil horizons and from immediately above and below the outwash/till contact (dashed line).

PROGRAM DESIGN

Interpretation of soil anomalies prior to discovery of the main orebodies held that the North and South Slope anomalies were essentially formed *in situ* and the Eastern Terrace anomalies were dispersion trains of mineralized glaciofluvial sediments derived from either the Esker and Creek zones or a source on the North Slope. Subsequently the Eastern Terrace anomalies were found to directly overlie the Mount Milligan deposit; whether the anomalies are due to the underlying mineralization or simply coincidental was unclear. In addition, a bedrock source for the North Slope anomalies had not yet been located; could these anomalies be derived from a distant source? A drift-prospecting program was designed to study geochemical and surficial geology indicators which would determine direction, relative distance travelled and thus potential source areas for the various anomalies.

To resolve these questions, the following program was conducted during July, 1990:

- Surficial mapping of glacial stratigraphy in road-cut, drill-pad and test-pit exposures.

- Surficial mapping and airphoto interpretation of a 1:50 000-scale map area centred on the Mount Milligan deposits.
- Pebble counting to determine contributing lithologies in available till sections.
- Sampling and counting of mineralized boulders in test pits.
- Sampling of soil and various glacial stratigraphic horizons in drill-pad and test-pit exposures.
- Bulk soil sampling in the North Slope anomaly.
- Profile sampling of a trench traversing the Esker Creek zone.

SAMPLING PROGRAM

Test pits (22) and drill-pad cut faces (4) were profile sampled. Two-kilogram samples were collected from the B, upper C and lower C soil horizons and any distinctly different glacial horizons (Plate 4-5-1). Comparison of the B and C horizons will demonstrate if soil forming processes obscure geochemical trends. Comparison of samples from stratified versus unstratified material may aid in distinguishing between these parent materials. Computer-assisted regeneration (*i.e.* outwash versus unstratified till) of geochemical patterns using original data (1984-1985), but subdivided on overburden type, may help to interpret dispersion trends and potential source areas.

Gold grains from bulk soil samples (12) collected from strongly anomalous sites on the North Slope and the Esker zone will be recovered and examined by scanning electron microscopy (SEM). Shape and concentration of grains collected from basal till have been employed with success in eastern Canada to determine distance of travel from source (Averill, 1978, Averill and Zimmerman, 1984; Gray, 1983; Sauerbrei *et al.*, 1987).

Soil and rock-chip samples were collected down profile at intervals of 0.5 metre at sites spaced 20 metres apart along a trench which exposes the Esker Vein zone. This study will demonstrate the rapidity of anomaly dilution with vertical and horizontal distance from source in outwash material, much in the manner of Levinson and Carter (1979).

SAMPLE PREPARATION AND ANALYSIS

Samples were submitted to Acme Analytical Labs, Ltd., Vancouver. A flow-chart highlighting methods and specifications for analysis of the various samples is given in Figure 4-5-5.

TRACE METALS

Determination of 30 trace, minor and major elements by inductively coupled plasma-emission spectroscopy (ICP-ES) will be conducted on the -40+80 mesh (-425 to +180 microns) and -80 mesh (-180 microns) size fractions of soil and unweathered overburden samples and on rock chips crushed and pulverized to -100 mesh (-150 microns). Results will determine the contribution of boulders

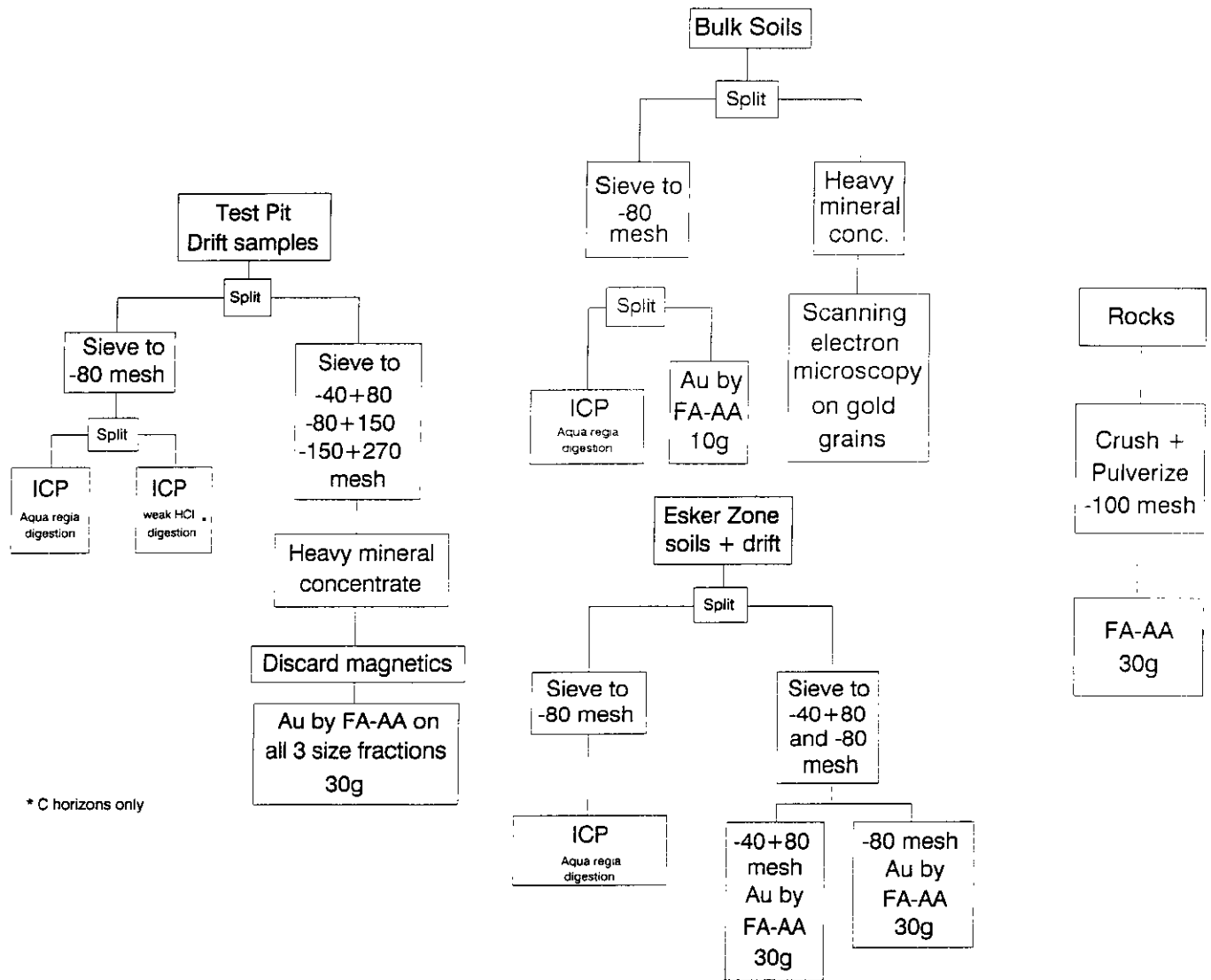


Figure 4-5-5. Flow chart detailing methods and specifications for analysis of drift-prospecting samples.

ders, coarse sand and matrix to the development of soil anomalies. Samples will be digested using hot aqua regia. To determine the hydromorphic component of anomalies, till samples (-80 mesh) will also be digested by warm dilute (10%) hydrochloric acid followed by ICP analysis.

GOLD

All soil, till and rock-chip samples will be analyzed for gold by fire assay using an atomic absorption determination. Till samples will be sieved to three size fractions (-40+80 mesh, -80+150 mesh and -150+270 mesh), concentrated by heavy liquid separation (2.96 SG) and separated into magnetic and nonmagnetic fractions, 30 grams of each size fraction will be analyzed. This will determine relative proportions of course to fine gold and reduce the influence of the nugget effect. Soil and till samples from the North Slope and Esker zones will be sieved into coarse (-40+80 mesh)

and fine (-80 mesh) size fractions, 30-gram unconcentrated subsamples will be analyzed. Rock-chip samples will be crushed and pulverized to -100 mesh and 30-gram subsamples of the oversize and undersize will be analyzed. As mentioned above, bulk soils will be concentrated by heavy liquid separation followed by extraction of gold grains for SEM examination.

SUMMARY OF PRELIMINARY RESULTS

Sample analyses are incomplete at the time of writing, however, some preliminary statements on surficial geology can be made, based on field observations.

The Mount Milligan area was glaciated during the last glacial episode and all glacial features observed in the study area are associated with this event. Ice-flow indicators such as drumlinoids and striae suggest a southwest to northeast direction of ice advance across the area. The surficial



Plate 4-5-2. Site of 19 000 ppb (0.54 oz/ton) gold soil anomaly on North Slope. Note the veneer (15-30 cm) of colluvium overlying bedrock. Bulk samples were collected from B-horizon soils for recovery of gold grains. Cursory field panning of duplicate samples produced numerous visible grains.

deposits, which may attain tens of metres in thickness, consist mainly of matrix-supported diamictons in the form of a till blanket, as well as glaciofluvial deposits of sand and gravel. The latter generally exhibit a southwest trend as defined by sinuous esker ridges and broad outwash plains; the dominant meltwater paleocurrent direction obtained from outwash sediments is to the northeast. Till veneer and colluvium deposits frequently mantle the steeper slopes of hills and valleys, whereas isolated deposits of fine glaciolacustrine sand, silt and clay are found in several topographic depressions. Thickness of surficial cover varies considerably over the copper-gold deposits, from less than 1 metre to in excess of 90 metres. Test pits, which were dug to a general depth of 2 to 3 metres, exposed a complex stratigraphic sequence. For a more complete discussion of the Quaternary geology and its relationship to drift prospecting, the reader is referred to Kerr and Bobrowsky (1991).

Several gold anomaly sites visited on the North Slope suggest local derivation. Surficial deposits, comprising till and colluvium, varied from 0.1 to 1 metre in thickness (Plate 4-5-2) and contained predominantly angular clasts of the underlying lithology.

Abundance, shape, size and composition of mineralized clasts encountered in test pits over the Mount Milligan deposit indicate incorporation of local material into till and outwash. Distance of travel in some instances may be relatively short, clasts of easily comminuted, oxidized supergene material were encountered in the upper layer of a till sheet in one test pit. The first drill-hole intercept of the supergene cap lies 150 metres to the southwest.

ACKNOWLEDGMENTS

The authors wish to thank Doug Forster, Mike Harris and the field crew of Continental Gold Corp. for their cooperation and hospitality. Chris Bates of BP Canada, Stan

Hoffman of Prime Geochemical Methods and Mark Rebagliatti of Rebagliatti Geological Consulting for their information and insights.

REFERENCES

- Averill, S.A. (1978): Overburden Exploration and the New Glacial History of Northern Canada; *Canadian Mining Journal*, Volume 99, pages 58-64.
- Averill, S.A. and Zimmerman, J.R. (1984): The Riddle Resolved: The Discovery of the Partridge Gold Zone Using Sonic Drilling in Glacial Overburden at Waddy Lake, Saskatchewan; paper presented at the 1984 Annual General Meeting, *Canadian Institute of Mining and Metallurgy*.
- Barr, D.A., Fox, P.E., Northcote, K.E. and Preto, V.A. (1976): The Alkaline Suite Porphyry Deposits – A Summary; in *Porphyry Deposits of the Canadian Cordillera*, A. Sutherland Brown, Editor, *Canadian Institute of Mining and Metallurgy*, Special Volume No. 15, pages 359-367.
- Bradshaw, P.M.D. (1975): Conceptual Models in Exploration Geochemistry; Association of Exploration Geochemists, Special Publication No. 3, *Elsevier Publishing Co.*, 223 pages.
- Delong, R.C., Godwin, C.I., Harris, M.K., Cairn, N.M. and Rebagliatti, C.M. (1991): Geology and Alteration at the Mount Milligan Gold-Copper Porphyry Deposit; *B.C. Ministry of Energy, Mines and Petroleum Resources*, Geological Fieldwork 1990, Paper 1991-1, this volume.
- Gray, R.S. (1983): Overburden Drilling as a Tool for Gold Exploration; paper presented at the 1983 Annual General Meeting, *Canadian Institute of Mining and Metallurgy*.
- Hicock, S.R. (1986): Pleistocene Glacial Dispersion and History in Buttle Valley, Vancouver Island, British Columbia: A Feasibility Study for Alpine Drift Prospecting; *Canadian Journal of Earth Sciences*, Volume 23, pages 1867-1879.
- Hoffman S.J. and Fletcher K. (1972): Distribution of Copper at the Dansey-Rayfield River Property, South-central British Columbia, Canada; *Journal of Geochemical Exploration*, Volume 1, No. 2, pages 163-180.
- Kerr, D.E. and Bobrowsky, P.T. (1991): Quaternary Geology and Drift Exploration at Mount Milligan (93N/1E, 93O/4W) and Johnny Mountain (104B/6E, 7W, 10W, 11E), British Columbia; *B.C. Ministry of Energy, Mines and Petroleum Resources*, Exploration in British Columbia 1990, in preparation.
- Levinson, A.A. and Carter, N.C. (1979): Glacial Overburden Profile Sampling for Porphyry Copper Exploration: Babine Lake Area, British Columbia; *Western Miner.* Volume 52, No. 5, pages 19-32.
- McLaren, G.P. (1990): A Mineral Resource Assessment of the Chilko Lake Planning Area; *B.C. Ministry of Energy, Mines and Petroleum Resources*, Bulletin 81.

- Mehrtens, M.B., Tooms, J.S. and Troup, A.G. (1973): Some Aspects of Geochemical Dispersion from Base-metal Mineralization within Glaciated Terrain in Norway, North Wales and British Columbia, Canada; in *Geochemical Exploration 1972*, M.J. Jones, Editor, *Institute of Mining and Metallurgy*, London, pages 105-115.
- Nelson, J., Bellefontane, K., Green, K. and MacLean, M. (1991): Regional Geological Mapping Near the Mount Milligan Deposit (93K/16, 93N/1); *B.C. Ministry of Energy, Mines and Petroleum Resources*, Geological Fieldwork 1990, Paper 1991-1, this volume.
- Roddick, J.A. and Tipper, H.W. (1985): Geology, Mount Waddington (92N) Map Area; *Geological Survey of Canada*, Open File 1163.
- Sauerbrei, J.A., Patterson, E.F. and Averill, S.A. (1987): Till Sampling in the Casa Berardi Gold Area, Quebec: A Case History in Orientation and Discovery; *Journal of Geochemical Exploration*, Volume 28, No. 1/3, pages 297-314.
- Schroeter, T.G. and Panteleyev, A. (1986): Gold in British Columbia; *B.C. Ministry of Energy, Mines and Petroleum Resources*, Preliminary Map 64.
- Skerl, A.C. (1947): Detailed Reserve Calculations; unpublished private report on the Pellaire gold mine.
- Tipper, H.W. (1969): Mesozoic and Cenozoic Geology of the Northeast Part of Mount Waddington Map Area (92N), Coast District, British Columbia; *Geological Survey of Canada*, Paper 68-33.



STRATIGRAPHY AND GEOLOGIC SETTINGS OF GOLD PLACERS IN THE CARIBOO MINING DISTRICT (93A, B, G, H)

By V.M. Levson and T.R. Giles

KEYWORDS: Economic geology, placer, Cariboo Mining District, gold, stratigraphy, auriferous gravels, exploration.

INTRODUCTION

This report provides details on field activities in placer geology conducted by the Surficial Geology Unit of the British Columbia Geological Survey Branch. In 1989, studies of gold-bearing placer deposits at active mines were undertaken with the objective of identifying geological criteria useful for recognizing placer potential. This research was continued in 1990 and a total of over 60 different placer properties have been studied (Figures 4-6-1 to 3). Stratigraphic, sedimentologic and geomorphic factors have been used to classify each of these placers by geologic environment. A suite of geologic settings representative of each of these placer-producing environments is presented in this paper, whereas a complete report discussing the geology of each described site is forthcoming. The complexity of the observed geology indicates that detailed sedimentologic and stratigraphic studies are required to understand both the distribution of placer deposits in a regional sense and the location and extent of gold-bearing units at the local level.

The Cariboo Mining District was selected for initial study because of its long history of placer gold production. Since 1860, the district has produced 75 000 to 100 000 kilograms (about 2.5 to 3 million ounces) of gold, more than any other placer area in British Columbia (Anon., 1963; Boyle, 1979). Several large (200 cubic metres per day processed) placer mines are now active in the region, as well as over 200 small operations, including hand mining and exploration projects. Sites selected for this study are producing mines offering good section exposure. Sections in the active mines were mapped and lithologic, pebble-fabric and sedimentological studies were conducted. Samples were collected for textural, mineralogical and geochemical analysis. Gold production in each stratigraphic unit was determined, where possible, by discussions with miners.

PREVIOUS WORK

General descriptions of placer deposits in the Cariboo area first appeared in 1874 in British Columbia Ministry of Mines Annual Reports. Johnson and Uglow (1926) completed descriptions of placer and lode gold deposits in the Wells-Barkerville area. Regional bedrock mapping was conducted by Tipper (1971) and more recently by Struick (1982). The Quaternary geology of the region was mapped by Tipper (1971) and recent investigations on the Quaternary and placer geology have been made by Clague (1987a, b, 1989) and Clague *et al.* (1990). Detailed sedimentologic evaluations of placer deposits have been completed in

unglaciated terrains, such as on the White Channel gravels in the Klondike area of the Yukon Territory (Morison and Hein, 1987). However, the geology of placer deposits in glaciated terrains remains poorly understood. Regional studies in British Columbia have been done, but detailed sedimentological analyses are lacking. Depositional environments of Cariboo placer deposits have recently been discussed by Eyles and Kocsis (1988, 1989a, b) and Levson *et al.* (1990).

STRATIGRAPHY AND GEOLOGIC SETTINGS OF GOLD PLACERS

TERTIARY PLACERS

Gold-bearing gravels of Tertiary or presumed Tertiary age have been mined in recent years in the Cariboo (Figure 4-6-1). Rouse *et al.* (1990) associated a number of placer deposits in the Cariboo with the late Tertiary Fraser Bend Formation. Dating was based on the palynology of the sediments, principally the occurrence of *Cedrus perilata* which became extinct in North America in the late Miocene, and the association of placers with volcanic clasts and ash that are generally limited to Tertiary successions. Gravels of the Fraser Bend Formation occur at elevations below 600 metres along the Fraser River in a north-south belt that is at least 150 kilometres long and less than 27 kilometres wide (Rouse and Mathews, 1979).

Recent and historical mining of Tertiary placer gravels has been concentrated along the Fraser River valley north of Quesnel. Underground mining was conducted at the Allstar mine on the west bank of the Quesnel River (Figure 4-6-1, Location 2) during the 1980s with reported approximate grades as high as 8.5 grams per tonne in the lowermost pay zone. Tertiary gravels in this area are confined by bedrock highs and 8.5 metres of the gravels are well exposed above river level (about 510 metres) at this location (Figure 4-6-4). At the base of the section up to 50 centimetres of sand, containing abundant fossil plant fragments, are overlain by cemented pebble gravels with some cobbly beds. The gravels are massive to crudely stratified and coarser beds exhibit scoured lower contacts. Trough-crossbedded sand and gravel lenses and horizontally laminated silt lenses also occur. Wood, at various stages of petrification, and coal fragments are common throughout the gravel succession.

Texturally mature gravels, believed to be Tertiary in age, and at least two other distinct younger gravel units, have been identified along the Big Bend (Quesnel Canyon) portion of the Quesnel River (Figure 4-6-1, Location 1). In the Horsefly area (Figure 4-6-1, Location 4), Miocene gravels have been mined since the start of the Cariboo gold rush in the 1850s; their age determined by bracketing K-Ar dates on volcanics. The gravels are underlain by a thick succession

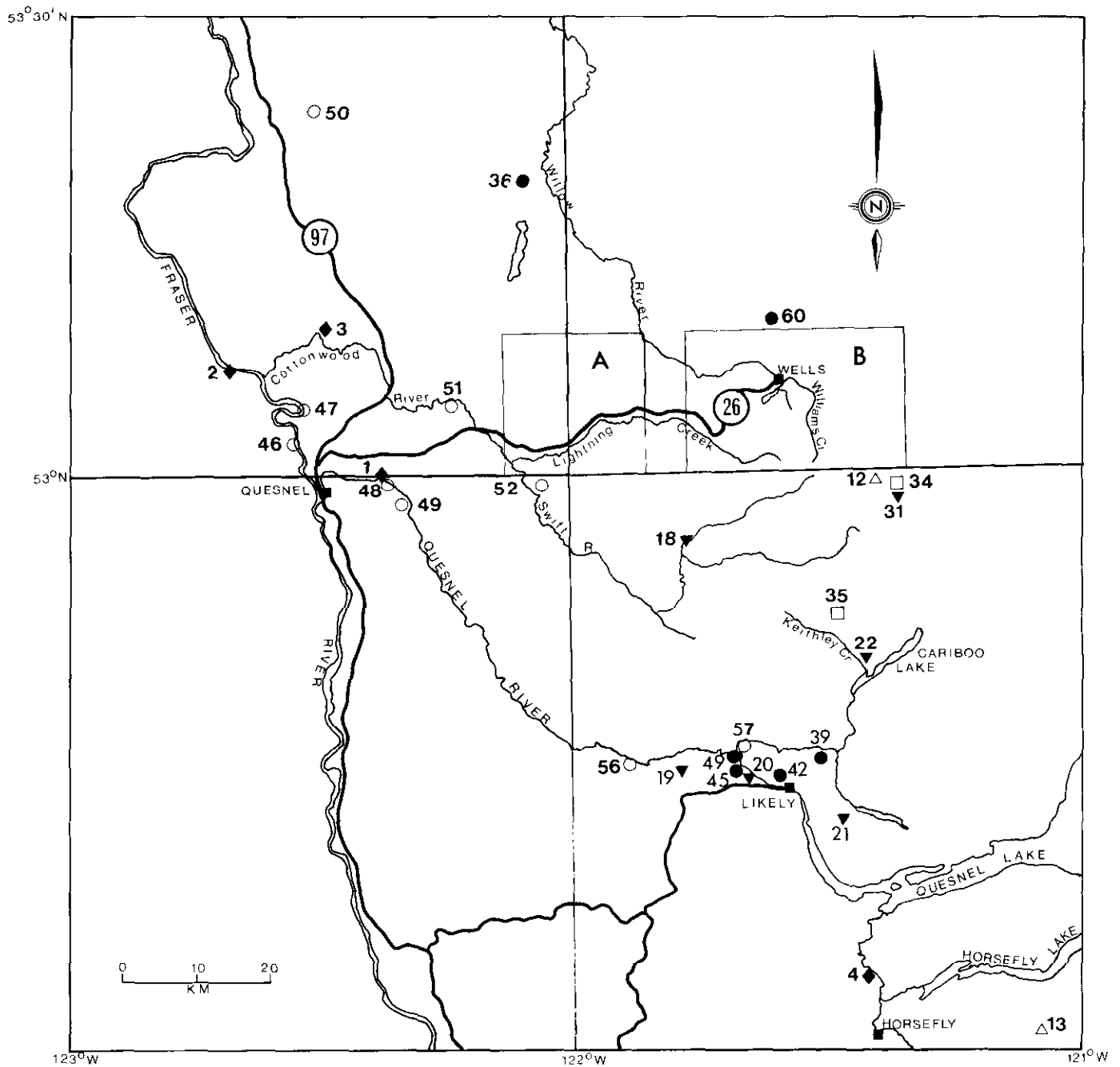


Figure 4-6-1. Location of the Cariboo placer mining area and study sites: solid diamonds – Tertiary placers; open triangles – paleogulch placers; solid triangles – buried channels; open squares – glacial placers; solid circles – outwash, colluvial and alluvial placers; open circles – low-terrace placers. Insets A and B show locations of Figures 4-6-2 and 3, respectively.

of horizontally laminated Eocene lacustrine sediments containing abundant plant fragments and fossil fish. Gold occurs mainly in the lower part of the gravels.

PREGLACIAL AND INTERGLACIAL PLACERS

PALEOCHANNEL SETTINGS

Preglacial and interglacial placers stratigraphically underlie till of the last (Late Wisconsinan) glaciation. Precise dating of these sediments is usually not possible as they are

beyond the limits of radiocarbon dating. A few finite radiocarbon dates have recently been recovered from Middle Wisconsinan interstadial sediments (Clague *et al.*, 1990) but such dates are rare due to the typical absence of organics in placer-gravel sequences. In addition, the coarse nature of most placer deposits precludes good preservation of pollen and volcanic ash, limiting the usefulness of palynological and radiometric dating techniques.

Preglacial and interglacial fluvial paleochannel placers occur in broad, low-gradient valleys and are potentially of

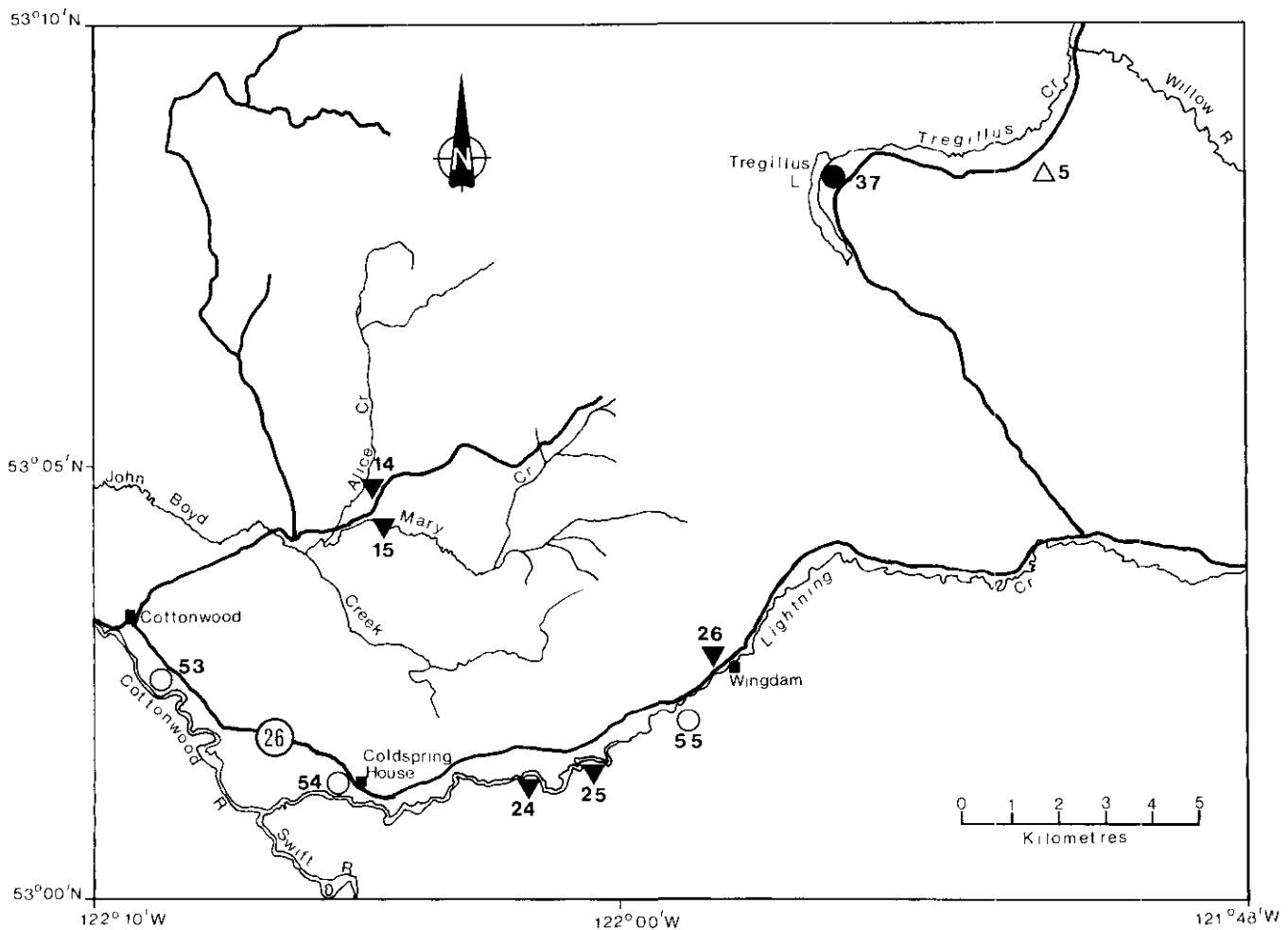


Figure 4-6-2. Location of study sites in the lower Lightning Creek area. Symbols as on Figure 4-6-1.

large volume. Three different types of buried-channel placer settings have been recognized in the Cariboo; abandoned trunk valleys, abandoned high-level valleys and buried channels in modern valleys. Abandoned trunk valleys are usually bedrock walled and infilled with stratigraphically complex sequences of sand, gravel and diamicton. Abandoned high-level valleys occur at elevations substantially higher than modern streams and may represent channel remnants from periods of relatively high base-level prior to more recent valley incision. Buried channels in modern valleys occur both below recent alluvium and in buried channels adjacent to modern creeks.

ABANDONED TRUNK VALLEYS

The valley excavated by hydraulic operations at the Bullion mine is a well-known example of a large abandoned Pleistocene valley in the Cariboo (Figure 4-6-1, Location 20). The Bullion mine occupies a bedrock-walled valley about 1 kilometre long and over 100 metres deep that is truncated at the north end by the modern Quesnel River. Sediments from two glacial periods (tills and glaciofluvial sands and gravels) and intervening nonglacial deposits are locally preserved in the mine area (Clague, 1987). The mine

has produced over 3860 kilograms (120 000 ounces) of gold. Gold was recovered mainly from the lowermost gravels on bedrock (Sharpe, 1939) but some gold also occurs in stratigraphically higher gravel units, probably overlying clay-rich till or lacustrine deposits that acted as false bedrock (Figure 4-6-5). North of Spanish Mountain, along the Cariboo River, Clague (1987b) identified a buried channel similar to the Bullion channel as a possible placer-exploration target.

Actively mined deposits at Spanish Mountain (Figure 4-6-1, Location 21) appear to infill the upper part of an elevated erosional channel cut in bedrock. Drilling results indicate that the bedrock channel is up to 74 metres deep. The lower 50 metres is infilled with clean pebble and boulder gravels. These gravels have not been mined extensively but there is a high potential that they are gold bearing, particularly at their base. The orientation of the channel is not well defined but appears to be oblique to the regional northwesterly strike of bedrock, topography and glacial ice flow. This orientation could provide an ideal situation for the development of a subglacial cavity and may account for the preservation of the placer deposits in the paleochannel (Levson *et al.*, 1990).

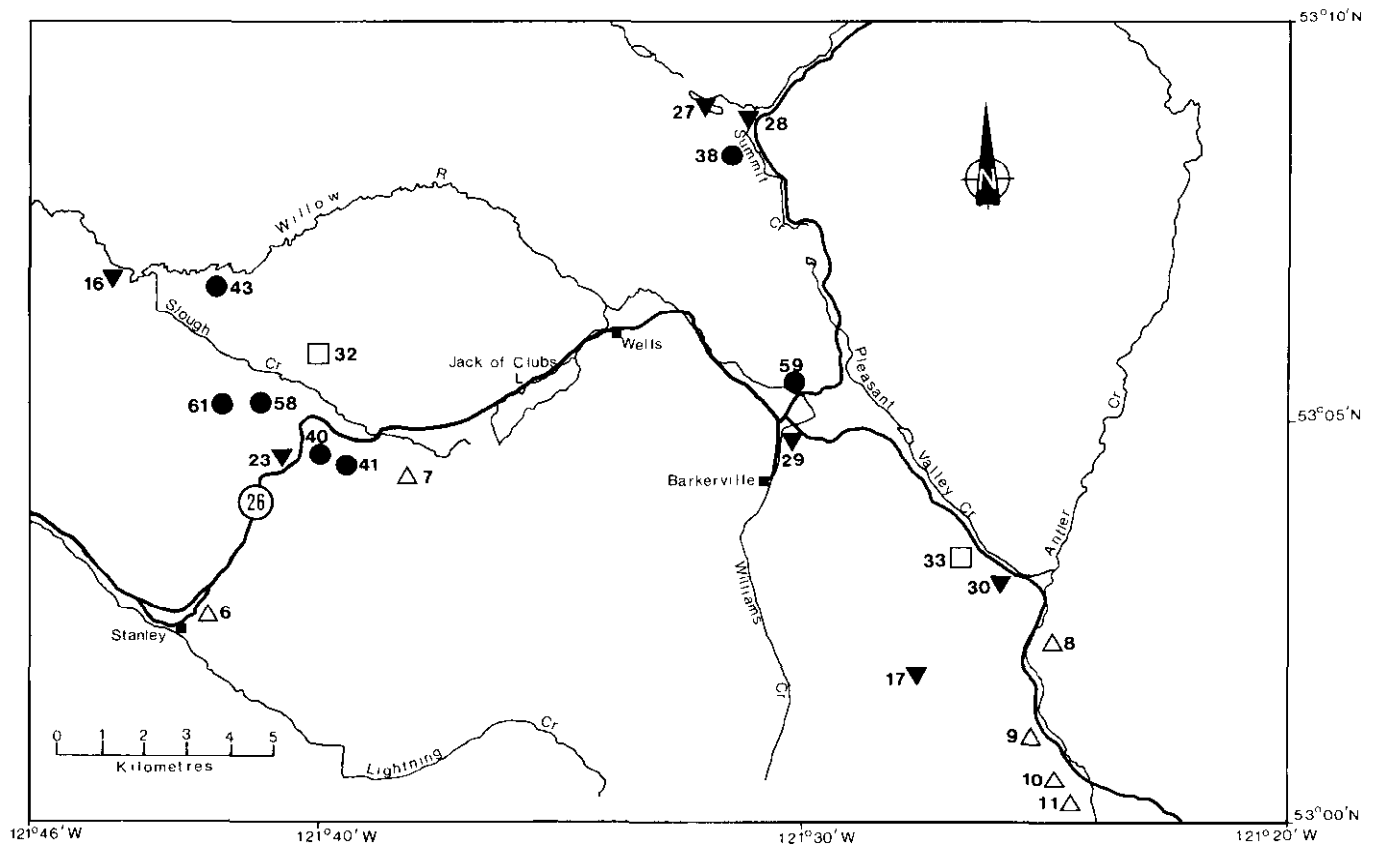


Figure 4-6-3. Location of study sites in the Wells-Barkerville area. Symbols as on Figure 4-6-1.

Preglacial and interglacial stream-channel placers in the Cottonwood River area have been mined in recent years at Mary and Alice creeks. The size, number and orientation of the channel(s) are unknown but outcrops of the channel gravels are spread over a distance of several hundred metres. A preglacial age of gold-bearing gravels in the region has recently been corroborated by palynological data (Rouse *et al.*, 1989). At Mary Creek (Figure 4-6-2, Location 15), the gold-bearing gravels are cemented, moderately to well sorted, imbricated, horizontally stratified and interbedded with trough-crossbedded sands (*cf.* Plate 6-3-1 in Levson *et al.*, 1990). They contain rich pay-zones with nuggets up to about 100 grams in size. Pay gravels at Alice Creek (Figure 4-6-2, Location 14) are similar, consisting of horizontally stratified sands interbedded with poorly to moderately sorted, clast-supported and discontinuously cemented gravels. They have been interpreted as low-sinuosity braided-river sediments (Eyles and Kocsis, 1989a). Gold values increase toward the base of the gravels with the main pay zone in the lower 3 to 5 metres over bedrock. Pay-streaks are sporadic, producing an average of 4 grams per cubic metre with a maximum return of about 9 grams.

Gold-bearing paleochannel gravels at both Mary and Alice creeks are stratigraphically overlain by a thick succession of Pleistocene sediments (*cf.* Figure 6-3-3 in Levson *et al.*, 1990). At Mary Creek the gold-bearing gravels are

overlain by two till units. Intertill sands and gravels and early postglacial gravels also contain some gold, probably reconcentrated from underlying units. At Mary Creek, glacial meltwater incised a channel and removed much (at least 20 metres) of the overburden. In contrast, gold-bearing gravels at the near-by Alice Creek mine are overlain by about 30 metres of overburden.

ABANDONED HIGH-LEVEL VALLEYS

An excellent example of a high-level buried valley placer is provided by the Streicek mine (Figure 4-6-3, Location 23). The southeast channel wall has been exposed down to a depth of 24 metres. The lowest exposed gold-bearing deposits are well-rounded to subrounded boulder gravels grading up into cobble to pebble gravels (Figure 4-6-6). Sorting and stratification increase with depth as does the abundance of openwork beds reflecting the increased influence of fluvial action. Overlying gravel units, exposed along the channel wall, are poorly sorted and have been reworked by gravity. They are dominated by angular clasts of local shale that dip steeply (45°) into the channel centre due to down-slope colluvial processes during channel infilling. The uppermost part of the gravel sequence was deposited as the channel was infilled prior to the last glaciation. These gravels are imbricated, poorly sorted, medium to large pebbles with an abundant silt and fine sand matrix. They are crudely stratified and some thin, openwork, small-

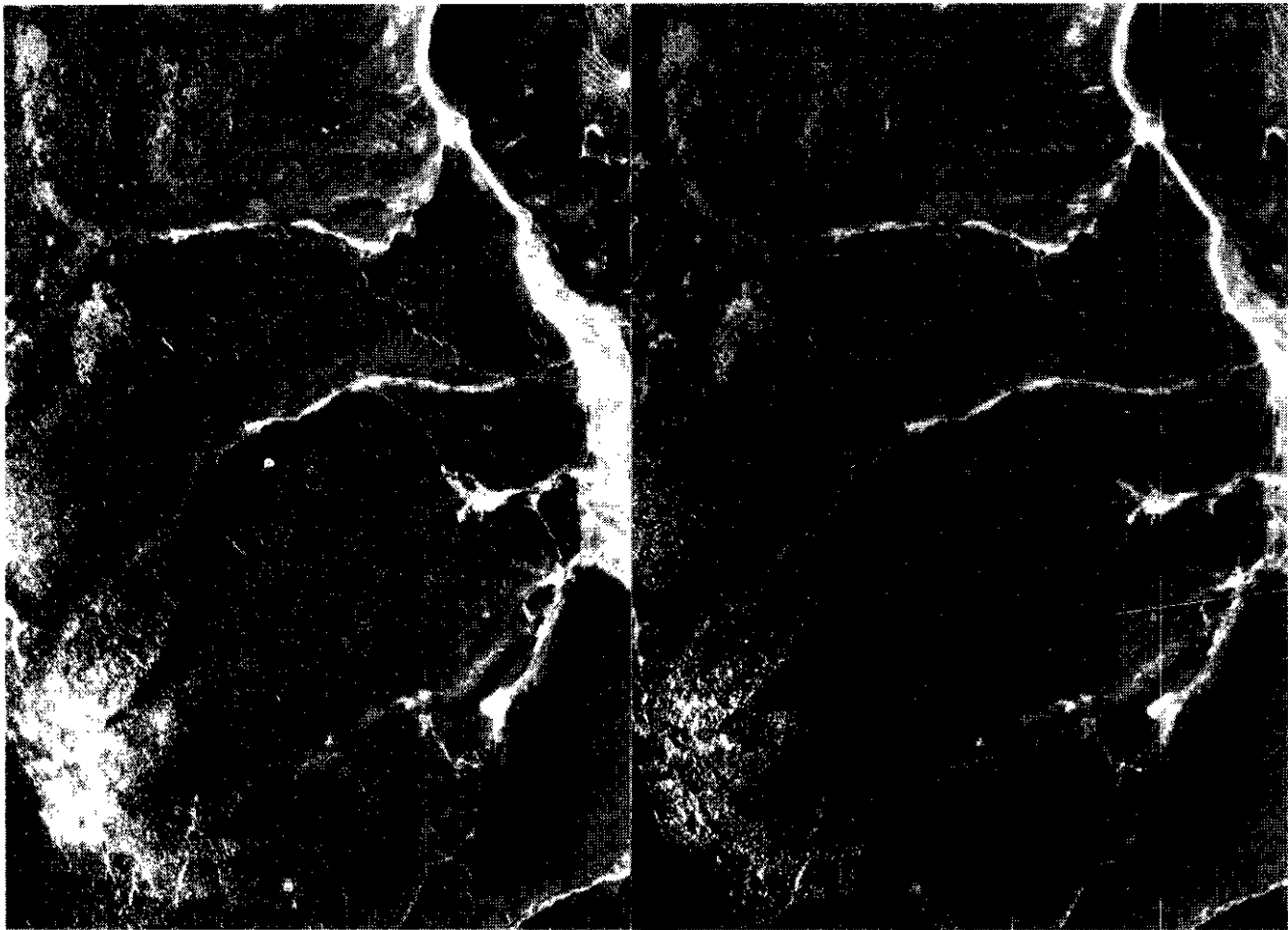


Plate 4-6-1. Airphoto stereo pair of gulch streams in the Antler Creek area.

pebble lenses occur. The gold-bearing gravel sequence is unconformably overlain by massive matrix-supported diamicton interpreted as a till deposited during the last glaciation.

BURIED CHANNELS IN MODERN VALLEYS

Buried-channel gravels in modern valleys are commonly exploited placers. The paleochannels may be buried directly under, or adjacent to, modern alluvial channels. Buried channels adjacent to modern streams are often segmented by recent erosion and their lateral extent is therefore often difficult to define. Paleochannels below modern streams commonly parallel the modern stream course but they can be deeply buried by alluvium and glacial deposits. In addition, these paleoplacers may be difficult to mine because of groundwater or surface-water problems.

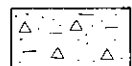
Gold-bearing deposits at the Ballarat mine (Figure 4-6-2, Location 29) infill an ancient bedrock channel adjacent to Williams Creek, which is one of the richest gold-producing streams in British Columbia. The lowest exposed gravels (Figure 4-6-7) in the Ballarat pit are moderately sorted, clast-supported, stratified pebbly gravels. Multiple scour

and channel-fill structures indicate deposition in a braided-river system. Lithologic analysis of these gravels suggests that they were not derived solely from a local tributary, but rather were deposited in the main valley system (Levson *et al.*, 1990). The gravels contain up to approximately 2 grams of gold per cubic metre and, in general, gold content increases with depth. Seismic, drilling and excavation results indicate that a variable gravel unit on the order of 10 metres thick is present below the lowest exposed gravel beds. Discontinuous, thin (< 2 to 3 metres thick), diamicton beds overlie bedrock highs along the south and north sides of the paleochannel. They exhibit sedimentary characteristics typical of modern debris-flow deposits such as poor sorting, disorganized fabric, gradational bed contacts and folded and boudinaged beds (Bull, 1972; Kochel and Johnson, 1984). Deposition of these locally derived debris-flow sediments along the margins of the channel was probably coeval with fluvial sedimentation in the channel centre.

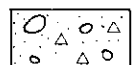
The gold-bearing gravels and associated debris-flow deposits that infill the paleochannel at the Ballarat mine were probably deposited in the last interglacial period. They are overlain by a complex succession of alluvial fan deposits (*see below*), ice-proximal gravels and an unconfor-

KEY TO FIGURES 4-6-4 through 4-6-14

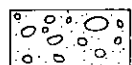
SEDIMENT TYPE:



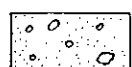
DIAMICTON - Matrix supported



GRAVELLY DIAMICTON - Matrix to Clast supported



GRAVEL - Clast supported, Matrix filled



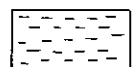
GRAVEL - Matrix supported



GRAVEL - Open framework



SANDS



SILTS



CLAYS



COVERED

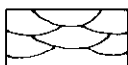
STRATIFICATION:



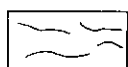
HORIZONTAL



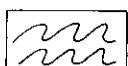
PLANAR - CROSS



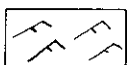
TROUGH - CROSS



CRUDE



DEFORMED



RIPPLED

CONTACTS:



GRADATIONAL



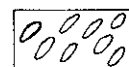
SHARP



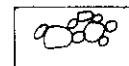
UNDULATORY



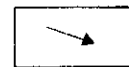
INTERBEDDED



IMBRICATED



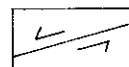
CLAST CLUSTERS



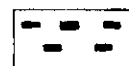
PALEOFLOW



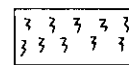
JOINTING



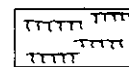
FAULTS



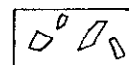
WOOD



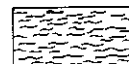
ORGANICS



SOIL or PALEOSOLS



INTRACLASTS



BEDROCK

mable capping sequence of till (Figure 4-6-7). Currently, economic gold placers occur only in reworked sediments that were deposited prior to the last glaciation.

Placer gravels in a buried channel adjacent to Lightning Creek (Figure 4-6-2, Location 24) are currently being mined. Paleoflow in the gold-bearing gravels was to the west, similar to the modern Lightning Creek channel which lies on the opposite side of the valley. Gravels yielding the highest gold concentrations are about 5 metres thick and sit unconformably on bedrock. More than 25 metres of glaciofluvial sand and gravel, with relatively low gold concentrations, conformably overlies the lower gravel sequence.

PALEOGULCH SETTINGS

Gulches are small narrow valleys with steep sides that commonly occur as tributaries to larger trunk valleys in

areas of high relief (Plate 4-6-1). They typically have steep gradients and carry large volumes of water and sediment during episodic flood events generated by unusual snow-melt or heavy rainfall events. These floods may recur at intervals of tens to hundreds of years and are capable of transporting large volumes of sediment. Large increases in the amount and size of material that can be moved by the stream occur as a result of the increased discharge and velocity. High stream capacity and competence are ideal for concentrating coarse placer gold and consequently gulch placers in the Cariboo have proven to be most productive. In many areas Holocene streams reoccupied preglacial and interglacial channels, eroding the overburden and, in some cases, reconcentrating the ancient placers. Holocene gulch placers were largely depleted in the 1800s due to ease of exploration and mining. Some paleogulch placers, however, were totally buried during the last glaciation. Locating,

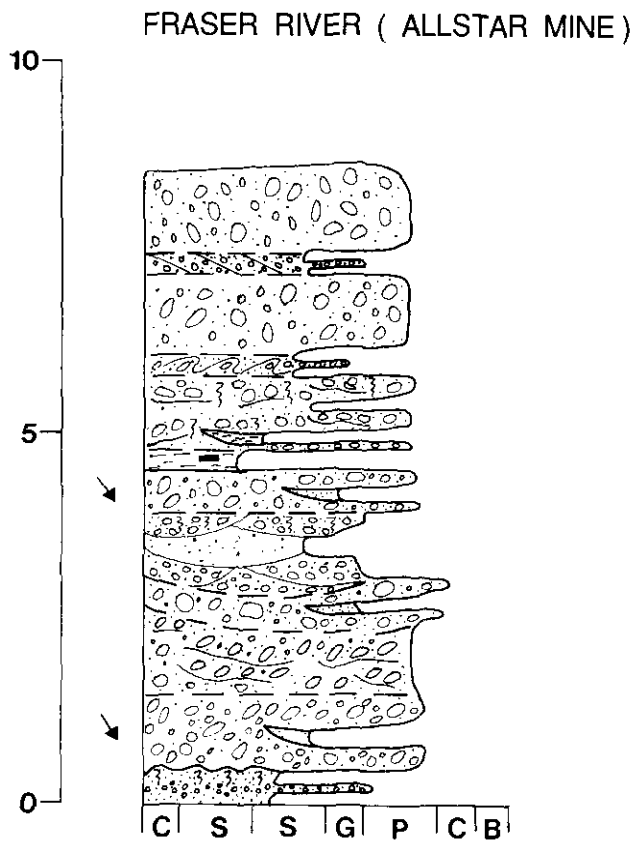


Figure 4-6-4. Stratigraphic column of Tertiary gravels and sands at the Allstar mine. Vertical scale in metres. Horizontal scale: C-clay S-sand S-silt G-granule P-pebble C-cobble B-boulder. Legend applies to all subsequent figures.

BULLION MINE

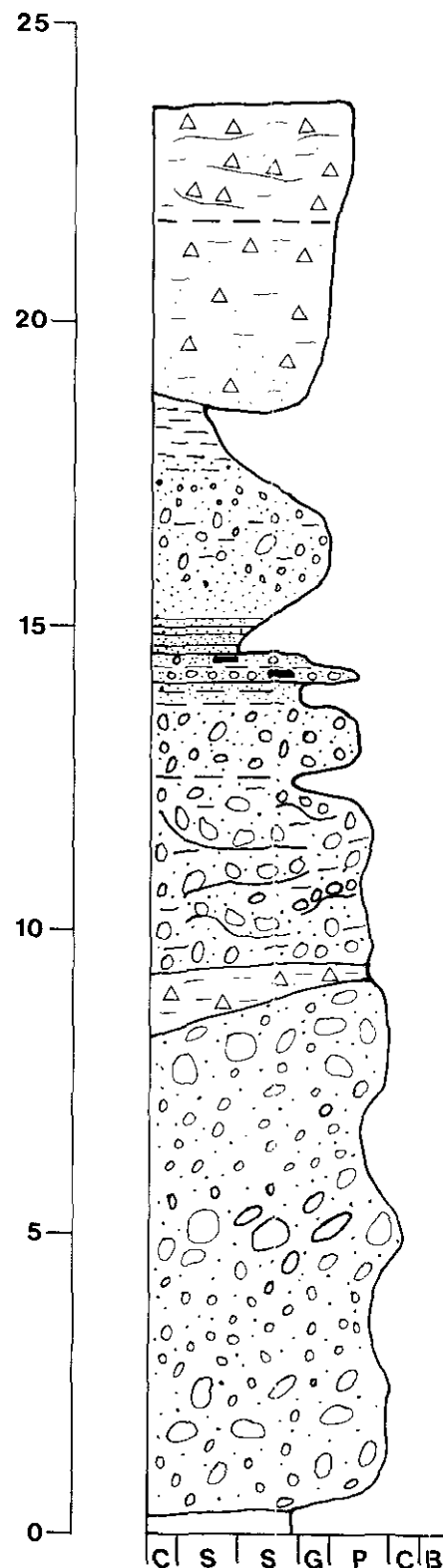


Figure 4-6-5. Stratigraphy of the Bullion mine (modified from Clague *et al.*, 1990) (Site 20).

evaluating and mining these buried, but potentially rich, placers can be both difficult and costly and usually requires detailed geologic information. At most active gulch-placer mines the glacial overburden is thick or has been partially excavated by *Holocene stream erosion*. Some of these paleoplacers were mined hydraulically in the past and modern workings commonly are either above the upper elevation reached by the hydraulic operations or along the valley sides where remnants of buried pay gravels are preserved.

Several mines along Antler Creek are typical of operations working buried gulch gravels (Plate 4-6-1). Mining at Stevens Gulch (Figure 4-6-3, Location 10) has exposed approximately 1 metre of poorly sorted, medium to large-pebble gold-bearing gravels sitting on bedrock, overlain by several metres of colluvial diamicton, sands and minor gravel (Figure 4-6-8). The lower gravel contains coarse nuggets (commonly 8 to 16 grams) and is probably a remnant gulch placer left along the valley side by previous mining activities. A debris-flow origin is suspected because of the massive structure, chaotic fabric, dominance of angular local clasts and poor sorting of the gravels.

At California Gulch (Figure 4-6-3, Location 11) pebble to cobble gravels with some boulders are buried by over 10 metres of glaciofluvial sand and gravel and 2 metres of

HIGH BENCH (STREICEK MINE)

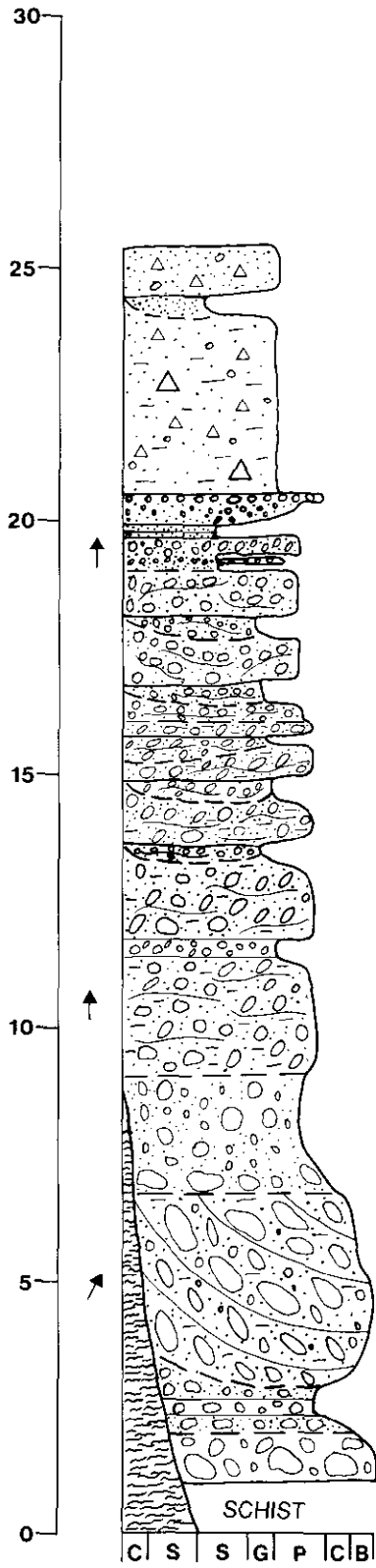


Figure 4-6-6. High-level buried-valley gravels overlain by till at the Streicek mine (Site 23).

BALLARAT MINE

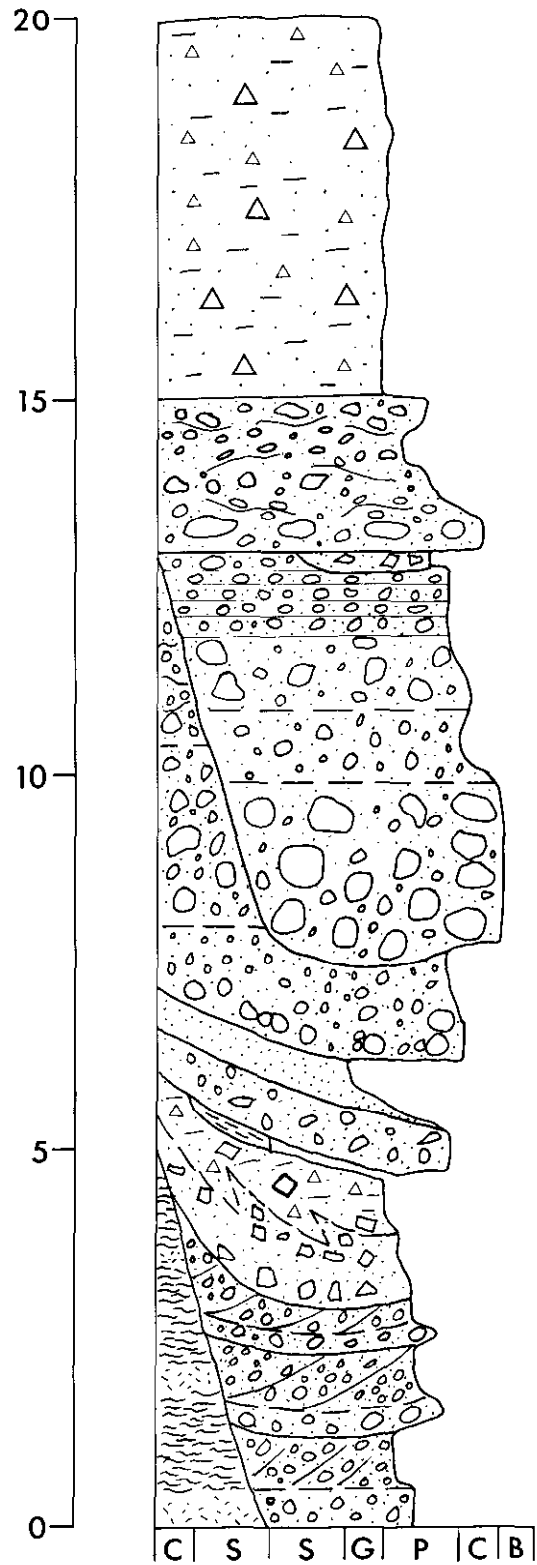


Figure 4-6-7. Paleochannel gravels overlain by till at the Ballarat mine (Site 29).

STEVENS GULCH

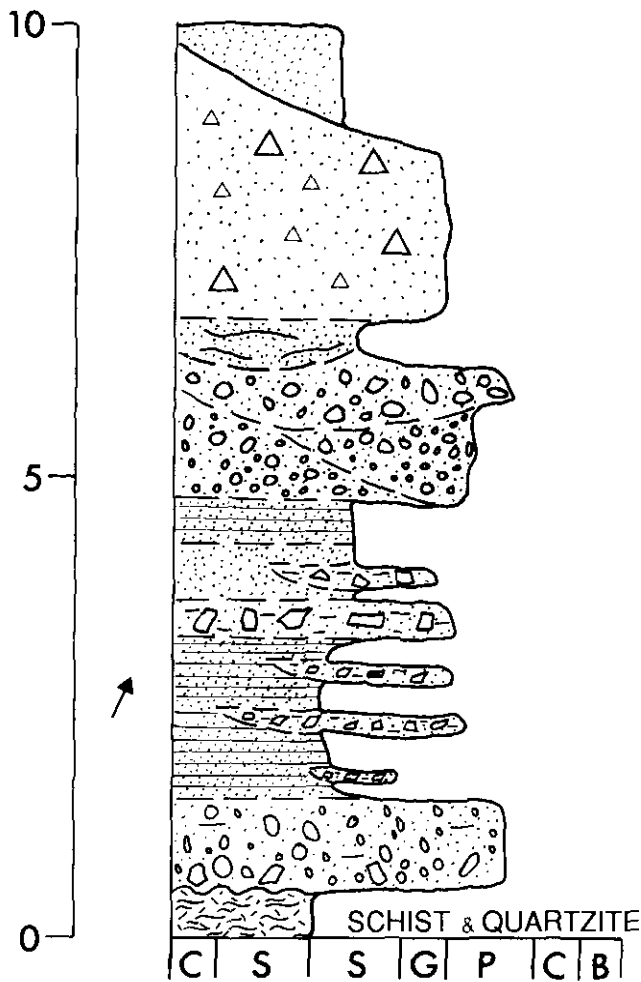


Figure 4-6-8. Gold-bearing, poorly sorted gravels overlain by colluvial diamicton, silt, sand and gravel at Stevens Gulch (Site 10).

matrix-supported diamicton interpreted as till. The lower gravels are poorly sorted, clast-supported and massive to crudely bedded. They were probably deposited by a flow with high discharge and sediment load, possibly in a gulch setting predating the last glaciation.

Mining activities in 1989 and 1990 at Beggs Gulch (Figure 4-6-3, Location 9) targeted a buried system that may parallel, and lie to the northwest of, the modern stream channel. Underground adits in both bedrock and unconsolidated materials have been excavated in the past in attempts to locate the buried channel. Modern mining has proceeded from near the valley bottom at about the 1190-metre level and has exposed well-sorted sand beds that dip up to 50° to the northwest (300°) and grade vertically into a sandy, boulder gravel. Sharp lateral and vertical variations in the grain size and sorting of the mined deposits are suggestive of highly variable flow conditions typical of gulch settings.

In addition to large buried-gulch placers, small abandoned channels adjacent to modern gulches are potential

SPANISH MOUNTAIN

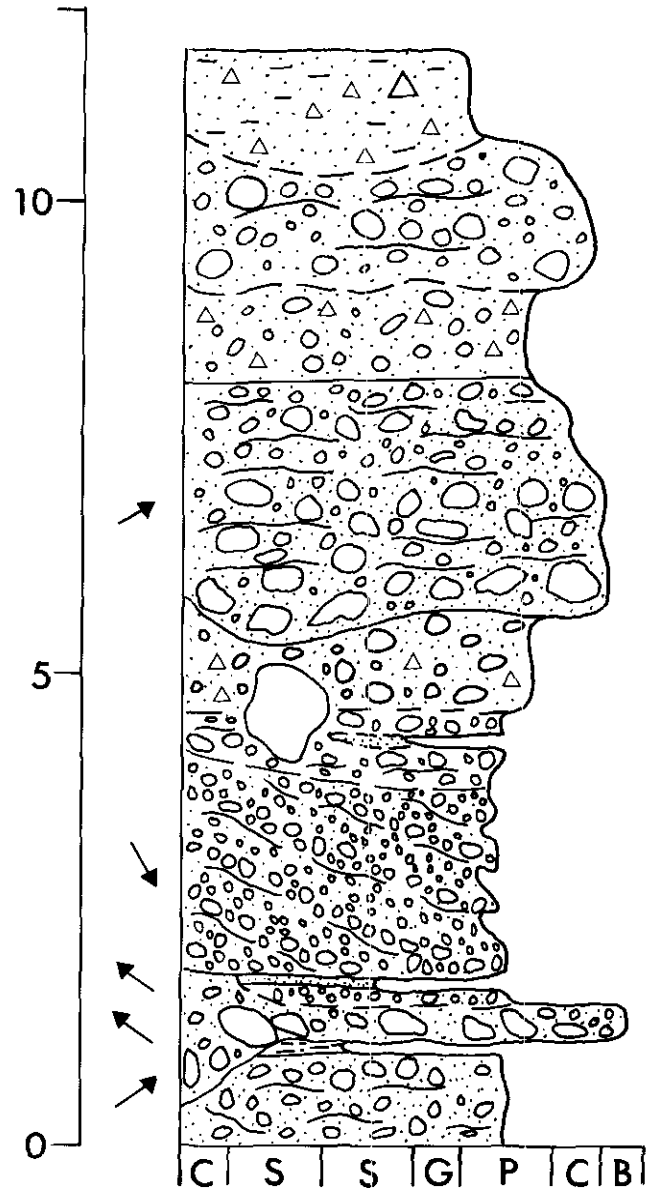


Figure 4-6-9. Gold-bearing gravels buried below till at the Spanish Mountain mine (Site 21).

placer targets. A small paleochannel along the southeastern margin of Beggs Gulch, at an elevation of about 1220 metres, has been mined for coarse gold with one small plunge pool being particularly lucrative. Bedrock exposed at the base of the channel has been smoothed by water action and the channel was filled with coarse gravels, some clasts being up to a few metres in diameter.

PALEOALLUVIAL FAN SETTINGS

At the Spanish Mountain mine (Figure 4-6-1, Location 21), gold is found in poorly sorted and crudely stratified coarse gravels interpreted as debris-flow deposits (Figure 4-6-9). Interbedded lenses of better sorted gravel,

sand and silt are interpreted as fluvial channel deposits. The gold-bearing gravels are capped by poorly exposed diamicton interpreted as till, suggesting that the placer deposits predate the last glaciation in the area. The sediments are mainly locally derived alluvium and may include some subglacial deposits. Gold content is generally consistent throughout the mined sequence, averaging about 1 gram per cubic metre, not including gold finer than 100 mesh (0.149 mm), and the gold appears to originate locally (V. McKeown, personal communication, 1989).

At the Ballarat mine, a complex unit of sands and gravels with gold concentrations up to approximately 2 grams per cubic metre, stratigraphically overlies older pay gravels (see Figure 6-3-6 in Levson *et al.*, 1990). Lithologic and paleoflow analyses of the lower gravels indicate that they were derived almost entirely from a small tributary stream. The characteristically steep (up to 25°) and consistent dip of massive gravel beds and the lateral continuity of strata suggest deposition in a fan-delta environment. Sedimentary structures representative of this unit, such as massive and normally graded sands, horizontally laminated silts and fine sands, climbing ripples and syndepositional deformation structures, are common in subaqueous environments. Interpretations of the overlying sediments indicate a progressive shift from a fan-delta to a dominantly subaerial alluvial fan environment.

In the fan centre, fining-upward channel-fill gravel sequences with erosional lower contacts probably represent deposition in main channels (Figure 4-6-7). Near the fan margins, poorly sorted gravel and diamicton beds are interpreted as gravelly debris-flow deposits (*c.f.* Larsen and Steel, 1978; Burgisser, 1984). Disorganized to weakly imbricated, large-clast clusters, such as those that occur in these beds, form during the waning stage of high-discharge events (Brayshaw, 1984). The uppermost deposits in the sequence are clast-supported, poorly sorted diamictons interpreted as debris-flow deposits. The diamictons exhibit crude horizontal bedding, minor openwork pebbly interbeds, weak imbrication and normal grading, sometimes with a thin, inversely graded basal zone. These characteristics are typical of debris-flow deposits (Burgisser, 1984; Kochel and Johnson, 1984). Lithologic and fabric data (Levson *et al.*, 1990) also support an alluvial-fan origin for these deposits.

GLACIAL PLACERS (TILL AND GLACIOFLUVIAL SEDIMENTS)

Glacial placers occur in sediments deposited directly by glacial ice or by meltwaters flowing near glaciers. Glacial processes that result in the deposition of tills do not allow for the removal of light minerals and the concentration of gold and other heavy minerals. Dilution of gold concentrations also occurs due to mixing of distally and locally derived sediments. In rare cases, subglacial meltwaters can concentrate gold from previously deposited sediments but these placers are usually small. Tills deposited by glaciers over-riding older stream placers can be locally productive where the gold concentration in the original placer was exceptionally high. At Cunningham Creek (Figure 4-6-3,

TREGILLUS LAKE

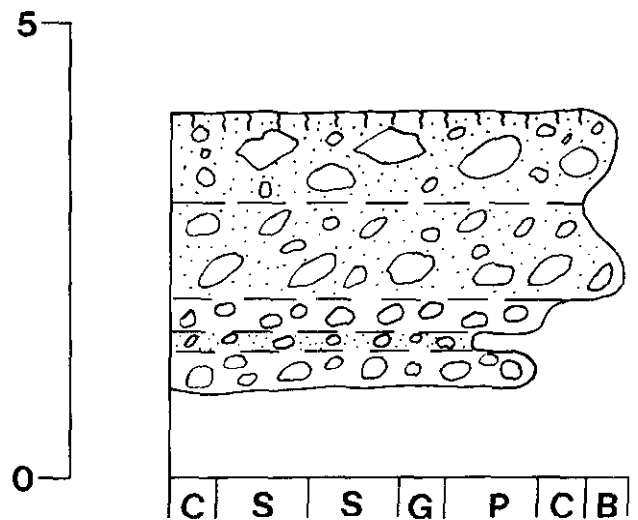


Figure 4-6-10. Stratigraphic column of mined glaciofluvial sediments at Tregillus Lake (Site 37).

Location 34), till and debris-flow deposits carry mineable quantities of gold. Glaciers flowing down the Cunningham Creek valley probably incorporated the gold from rich paleochannel placers upvalley.

Economic gold concentrations are also rare in glacial outwash deposits, usually being restricted to areas where meltwaters have reworked older placers. Outwash gravels along the northeast side of Tregillus Lake (Figure 4-6-3, Location 37) contain gold concentrations of approximately 0.15 to 0.35 gram per cubic metre. Gold within the gravels was probably derived from older placer deposits upstream. Placers underlying lodgement till at the south end of Tregillus Lake (Eyles and Kocsis, 1988) are a possible source. The glaciofluvial deposits at the north end of the lake are poorly to moderately sorted cobble gravels with clasts up to 2 metres in diameter overlying small to large-pebble gravels (Figure 4-6-10). Gold is most concentrated in the coarse gravels in the uppermost 1 to 2 metres, reflecting the typical association between coarse lag gravels and placer gold concentrations.

POSTGLACIAL PLACERS

Postglacial placer deposits occur in a variety of depositional environments. Postglacial gulch gravels were the most productive, accessible and easily mined of all the Cariboo placers and few remained beyond the turn of the century. Floodplain and low-terrace deposits were also largely mined out in the 1800s. However, fine gold carried many kilometres downstream from the original source area is still mined in some areas. In addition, higher terrace gravels can be locally productive. Postglacial colluvial and alluvial fan placers are also mined locally.

BURNS CREEK

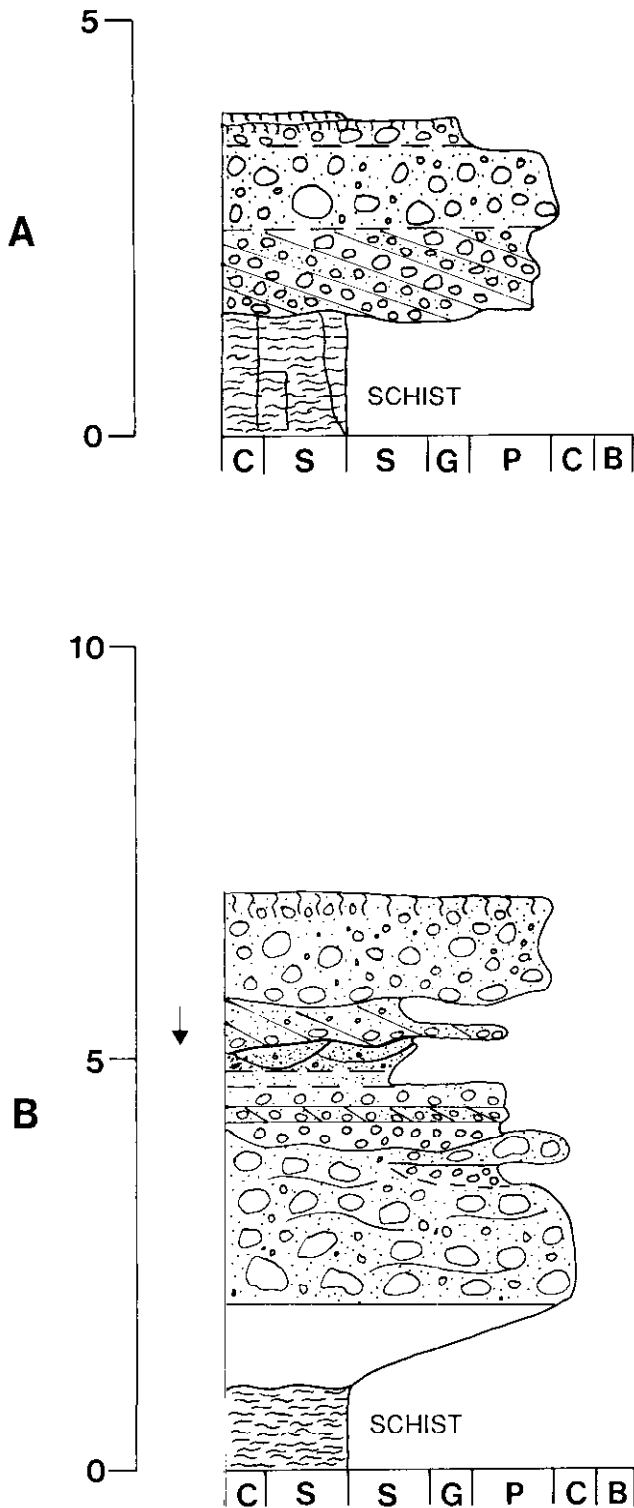


Figure 4-6-11. (A) Gold-bearing high-terrace gravels on Burns Mountain (Site 41), (B) Barren gravels upvalley of site A).

HIGH TERRACES

Terrace gravels occurring well above modern river levels were commonly formed in early postglacial times. It is often difficult to differentiate glaciofluvial gravels deposited in terraces near the ice margin from proximal, proglacial stream sediments deposited shortly after local deglaciation. Sedimentation in proximal braided streams is largely aggradational and characterized by multiple shifting channels. Consequently, the resultant gravels form large-volume deposits with low gold concentrations. Gold content is highest at the base of channel-fill sequences. Typical high-terrace gravels, are exposed at a mine on Burns Mountain (Figure 4-6-3, Location 41). Where the terrace gravels overlie older gulch-placer deposits they contain mineable quantities of gold (Figure 4-6-11a). Elsewhere, the gravels are almost devoid of gold (Figure 4-6-11b). Glaciofluvial streams reworked and, to a certain extent, diluted the older placers. Paleocurrent data indicate that flow was perpendicular to the older streams and consequently gold occurs only downstream of the intersection with the paleochannel.

LOW TERRACES

Low-terrace gravels are presently being mined at several locations on lower Lightning Creek and the Quesnel and Cottonwood rivers (Figures 4-6-1 and 2, Locations 48-57). The distribution of mines along the lower reaches of these rivers is only in part a reflection of geology. To a large extent, historical mining activity has depleted low-terrace placers in the upper reaches of these streams. Relatively coarse gold was recovered from these easily mined Holocene terrace placers. Progressively finer gold is carried farther downstream where mining activities are limited by the efficiency of fine gold recovery. The ability of the miner to locate sedimentary environments and specific facies where fine gold is concentrated is also a critical factor in these downstream placers.

Low-terrace gravels typically are well-sorted, horizontally stratified, imbricated, well-rounded pebble to cobble gravels (Figure 4-6-12). Planar and trough-crossbedded gravel beds occur locally. Sandy interbeds and lenses are common and the gravel sequences are typically capped by up to about 1 metre of overbank fines. The latter commonly exhibit weak horizontal laminations and contain abundant organic material. Scoured lower contacts in gravel beds are often overlain by concentrations of coarse clasts. Channel lags formed during periods of relative channel stability and are primary placer targets. Overlying bedded gravel sequences contain less gold and reflect bar sedimentation during aggradational phases.

Productive postglacial colluvial and alluvial placers are relatively rare in the Cariboo. A small operation along Williams Creek (Figure 4-6-3, Location 59) is recovering gold from a thin colluvial deposit overlying a bedrock surface that slopes 15° to 20° toward the valley centre (205°). A clast-supported, sandy pebble-gravel directly over bedrock is the most productive unit (Figure 4-6-13). Some gold is also recovered from overlying dredge tailings left from a previous operation that mined a small paleochannel

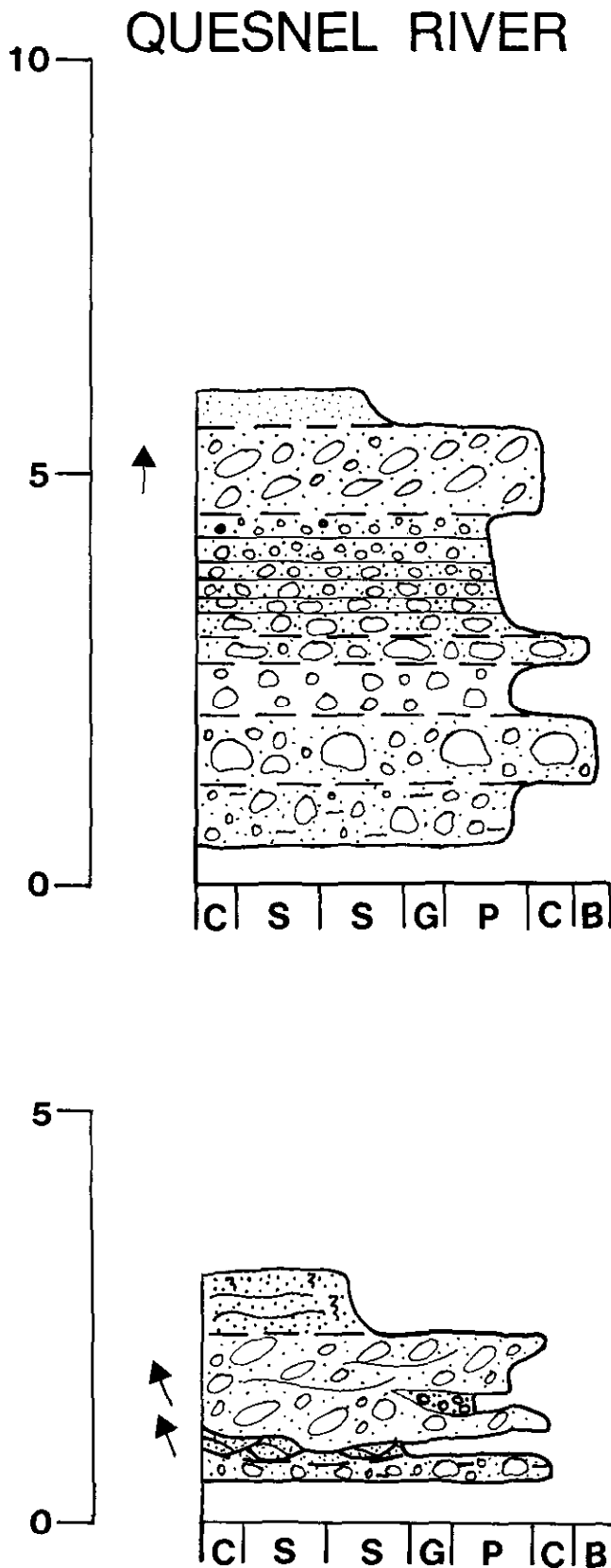


Figure 4-6-12. Low-terrace gravels on the lower Quesnel River (Site 49).

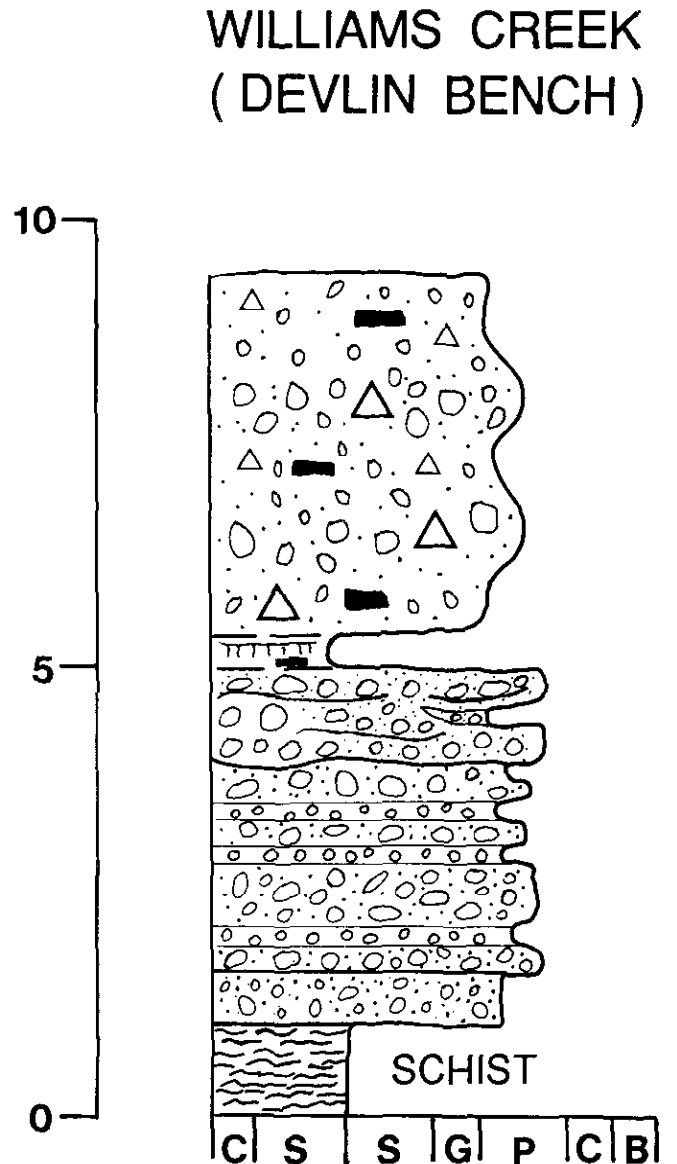


Figure 4-6-13. Colluvial sediments along Williams Creek (Site 59).

on the valley bottom. In the Nelson Creek area (Figure 4-6-3, Location 61) postglacial alluvial deposits consisting of interbedded diamicton and poorly sorted gravels (Figure 4-6-14) are gold bearing and currently being mined. Resedimentation of older deposits along the valley slope occurred by gravity-dominated processes with minor fluvial reworking. The reworked deposits include paleogulch gravels that were historically mined in the area and tills that incorporated older gold-bearing gravels during glaciation. Deposition occurred mainly in the period immediately following deglaciation, when lack of vegetation and climatic conditions enhanced slope instability.

CONCLUSIONS

Information gathered from geologic studies at active placer mines in the Cariboo region has identified several

ble gold-bearing deposits. Further development of these placers will require seismic and drilling exploration programs.

ACKNOWLEDGMENTS

The authors would like to thank all of the miners whose properties are described in this report for providing information and access to their properties. We acknowledge the support of the of Cariboo Mining Association. The manuscript was reviewed by Jonn Newell, Dan Kerr, Pete Bobrowsky and Paul Matysek. Diagrams were capably drafted by Chris Smith.

REFERENCES

- Anonymous (1963): Notes on Placer Mining in British Columbia; *B.C. Ministry of Energy, Mines and Petroleum Resources*, Bulletin 21, 42 pages.
- Boyle, R.W. (1979): The Geochemistry of Gold and its Deposits; *Geological Survey of Canada*, Bulletin 280, 584 pages.
- Brayshaw, A.C. (1984): Characteristics and Origins of Cluster Bedforms in Coarse-grained Alluvial Channels; in *Sedimentology of Gravels and Conglomerates*, E.H. Koster and R.J. Steel, Editors, *Canadian Society of Petroleum Geologists*, Memoir 10, pages 77-85.
- Bull, W.B. (1972): Recognition of Alluvial Fan Deposits in the Stratigraphic Record; in *Recognition of Ancient Sedimentary Environments*, J.K. Rigby and W.K. Hamblin, Editors, *Society of Economic Paleontologists and Mineralogists*, Special Publication 16, pages 63-83.
- Burgisser, H.M. (1984): A Unique Mass Flow Marker Bed in a Miocene Stream Flow Molasse Sequence, Switzerland; in *Sedimentology of Gravels and Conglomerates*, E.H. Koster and R.J. Steel, Editors, *Canadian Society of Petroleum Geologists*, Memoir 10, pages 147-163.
- Clague, J.J. (1987a): Quaternary History and Stratigraphy, Williams Lake, British Columbia; *Canadian Journal of Earth Sciences*, Volume 24, pages 147-158.
- Clague, J.J. (1987b): A Placer Exploration Target in the Cariboo District, British Columbia; *Geological Survey of Canada*, Paper 87-1A, pages 177-180.
- Clague, J.J. (1989): Gold in the Cariboo District, British Columbia; *Mining Review*, September/October, pages 26-32.
- Clague, J.J., Hebda, R.J. and Mathewes, R.W. (1990): Stratigraphy and Paleoecology of Pleistocene Interstadial Sediments, Central British Columbia; *Quaternary Research*, Volume 34, pages 208-228.
- Eyles, N. and Kocsis, S.P. (1988): Gold Placers in Pleistocene Glacial Deposits, Barkerville, British Columbia; *Canadian Institute of Mining and Metallurgy*, Bulletin, Volume 81, pages 71-79.
- Eyles, N. and Kocsis, S.P. (1989a): Sedimentological Controls on Gold Distribution in Pleistocene Placer Deposits of the Cariboo Mining District, British Columbia; *B.C. Ministry of Energy, Mines and Petroleum Resources*, Geological Fieldwork 1988, Paper 1989-1, pages 377-385.
- Eyles, N. and Kocsis, S.P. (1989b): Sedimentological Controls on Gold in a Late Pleistocene Glacial Placer Deposit, Cariboo Mining District, British Columbia, Canada; *Sedimentary Geology*, Volume 65, pages 45-68.
- Johnson, W.A. and Uglow, W.L. (1926): Placer and Vein Gold Deposits of Barkerville, Cariboo District, British Columbia; *Geological Survey of Canada*, Memoir 149, 246 pages.
- Kochel, R.C. and Johnson, R.A. (1984): Geomorphology and Sedimentology of Humid-temperate Alluvial Fans, Central Virginia; in *Sedimentology of Gravels and Conglomerates*, E.H. Koster and R.J. Steel, Editors, *Canadian Society of Petroleum Geologists*, Memoir 10, pages 109-122.
- Larsen, V. and Steel, R.J. (1978): The Sedimentary History of a Debris Flow Dominated Alluvial Fan: a Study of Textural Inversion; *Sedimentology*, Volume 25, pages 37-59.
- Levson, V.M., Giles, T.R., Bobrowsky, P.T. and Matysek, P.F. (1990): Geology of Placer Deposits in the Cariboo Mining District, British Columbia; Implications for Exploration; *B.C. Ministry of Energy, Mines and Petroleum Resources*, Geological Fieldwork 1989, Paper 1990-1, pages 519-530.
- Morison, S.R. and Hein, F.J. (1987): Sedimentology of the White Channel Gravels, Klondike Area, Yukon Territory: Fluvial Deposits of a Confined Valley; *Society of Economic Paleontologists and Mineralogists*, Special Publication 39, pages 205-216.
- Rouse, G.E. and Mathews, W.H. (1979): Tertiary Geology and Palynology of the Quesnel Area, British Columbia; *Canadian Petroleum Geology*, Bulletin, Volume 27, pages 418-445.
- Rouse, G.E., Lesack, K.A. and Hughes, B.L. (1990): Palynological Dating of Sediments Associated with Placer Gold Deposits in the Barkerville-Quesnel-Prince George Region, South-central British Columbia; *B.C. Ministry of Energy, Mines and Petroleum Resources*, Geological Fieldwork 1989, Paper 1990-1, pages 531-532.
- Sharpe, R.F. (1939): The Bullion Hydraulic Mine; *The Miner*, pages 37-40.
- Struick, L.C. (1982): Bedrock Geology of the Cariboo Lake (93A/14), Spectacle Lake (93H/3), Swift River (93A/13) and Wells (93H/4) Map Areas, Central British Columbia; *Geological Survey of Canada*, Open File 858.
- Tipper, H.W. (1971): Glacial Geomorphology and Pleistocene History of Central British Columbia; *Geological Survey of Canada*, Bulletin 196, 89 pages.



**RECONNAISSANCE QUATERNARY GEOLOGICAL INVESTIGATIONS IN
PEACE RIVER DISTRICT, BRITISH COLUMBIA
(93P, 94A)**

By **P.T. Bobrowsky,**
N. Catto, Memorial University of Newfoundland and V. Levson

KEYWORDS: Surficial geology, Quaternary, Pleistocene, Peace River, sedimentology, stratigraphy, Wisconsinan glaciation, diamicton, rhythmite, till, glaciolacustrine.

Study was restricted to the region extending from the town of Hudson Hope to directly east of the city of Fort St. John, and from Highway 97 to the north end of Charlie Lake (Figure 4-7-1). This area includes the northern half of NTS Sheet 93P (Dawson Creek) and the southern half of NTS Sheet 94A (Charlie Lake). Existing surficial mapping coverage for the region is available at a scale of 1:1 000 000

INTRODUCTION

Geologic investigations were undertaken in the area bordering the Peace River in northeastern British Columbia.

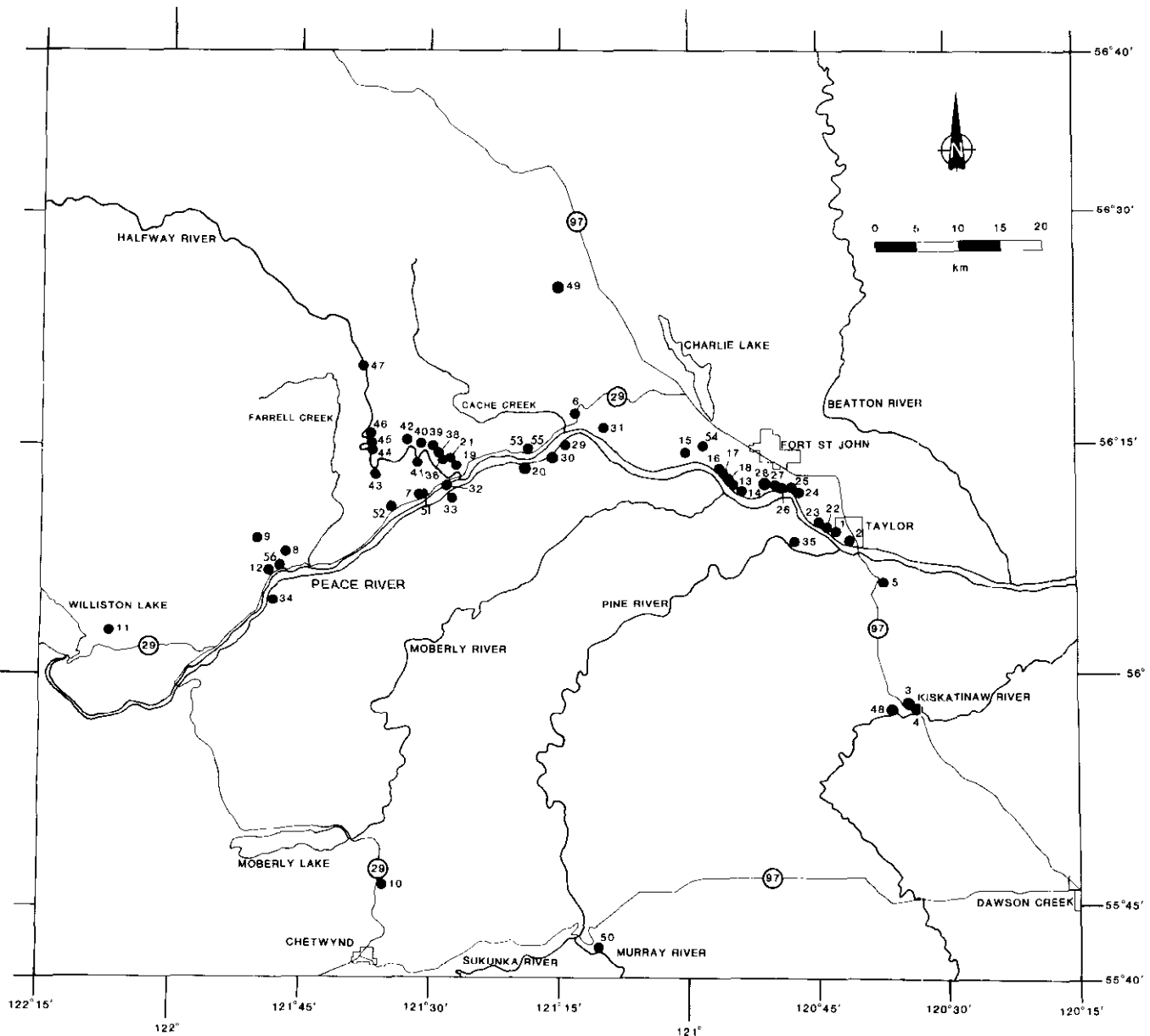


Figure 4-7-1. Location map of Quaternary sections in the Peace River study area. Coordinates for the sites given in Table 4-7-1.



Plate 4-7-1. Section PTB90-43 (Halfway River landslide). View to south of recent Attachie-like slope failure, which originally extended across the Halfway River and temporarily blocked drainage until breached several hours later. Note small channelling and leveeing along the surface formed during and after the failure. (GSB photo PTB90-13-15).

94 A/5 GROUND BIRCH	94 A/6 BEAR FLAT	94 A/7 NORTH PINE	94 A/8 ALCES RIVER
94 A/4 HUDSON HOPE	94 A/3 MOBERLY RIVER	94 A/2 FORT ST JOHN	94 A/1 SHEARER DALE
93 P/13 MOBERLY LAKE	93 P/14 FAVELS CREEK	93 P/15 SUNSET PRAIRIE	93 P/16 DAWSON CREEK
93 P/12 COMMOTION CREEK	93 P/11 EAST PINE	93 P/10 ARRAS	93 P/9 POUCE COUPE

Figure 4-7-2. Index map of 1:50 000-scale NTS map sheets comprising study area. Shaded sheets indicate regions mapped in 1990, and accompanying report by Catto (1991).

for NTS Sheet 94 (Beaton River; Mathews *et al.*, 1975) and at a scale of 1:250 000 for NTS Sheet 94A (Mathews, 1978a) and NTS Sheet 93P (Reimchen, 1980). Aggregate data for the area are poor, as are the data on peat deposits, both issues recommended as requiring attention (Hora, 1988; Maynard, 1988).

The objectives of this project are to provide detailed surficial geological maps (1:50 000 scale) of practical use to

industry, as well as municipal, regional and provincial governments; determine the occurrence of, and assess the exploration potential for, aggregate and peat deposits in the same area; study mass-movement deposits along the Peace River Canyon, and if possible determine the timing of occurrence of these past events (Plate 4-7-1); to contribute to the provincial geoscience database by refining the Quaternary geologic history of the Peace District through stratigraphic investigation. Field activities during the 1990 season included surficial mapping of four map sheets (Figure 4-7-2), as well as extensive reconnaissance to locate exposures and sections suitable for further detailed study. This paper presents the results of the reconnaissance efforts and therefore addresses the latter two project objectives, whereas the surficial maps and their accompanying interpretation which are published separately will cover the first two project objectives (Catto, 1991).

The earliest published description of the Peace River Canyon appears in the journal of Sir Alexander Mackenzie during his trip through the region in 1793. Almost 100 years later, in 1872, Captain W.F. Butler provided a detailed and picturesque description of the Peace River valley, and in 1875, A.R.C. Selwyn provided the first geologic description of the area, concentrating on the bedrock geology; only passing reference was made to the unconsolidated sediments by Selwyn (Beach and Spivak, 1943). The most significant contributions to the Quaternary geology of the Peace Region occurred in the period 1950-1980 by W.H. Mathews, and 1967-1977 by N.W. Rutter (Mathews, 1954, 1962, 1972, 1973, 1978a, b, 1980; Rutter, 1968, 1969a, b, 1974, 1976, 1977, 1980, 1981, 1984). However, recent geologic interpretations in the adjacent Rocky Mountain Trench (Bobrowsky, 1984, 1987, 1988, 1989a, b; Bobrowsky and Rutter, 1989, 1990) and the Peace District of Alberta (Liverman, 1987, 1989a, b; Liverman *et al.*, 1989) may have significant effects on interpretations presently applied to the study area. These recent investigations, coupled with the need for an assessment of aggregate and peat exploitation potential, and the continued threat of frequent mass movements, provide a necessary stimulus for renewed geologic work along the Peace River.

SETTING

The study area lies along the western edge of the Alberta Plateau within the Interior Plains (Mathews, 1986). Low-relief topography characterizes the region and consists of broad rolling plateaus and cuestas at elevations near 900 metres. These upland areas are dissected by the Peace River and its major tributaries including the Halfway, Moberly, Pine, Beaton and Kiskatinaw rivers, as well as Lynx, Farrell and Cache creeks (Holland, 1976). The elevation of the Peace River is 520 metres at Hudson Hope and less than 450 metres at the mouth of the Kiskatinaw. The disorganized drainage in the uplands is imprinted upon unconsolidated glacial deposits which cover flat-lying or gently east-dipping sedimentary bedrock of Cretaceous age. Most of the sedimentary rocks in the area belong to the Fort St. John Group. The oldest rocks, which belong to the Gates Formation, are composed of marine shale, siltstone and sandstone

MODEL 1

MODEL 2

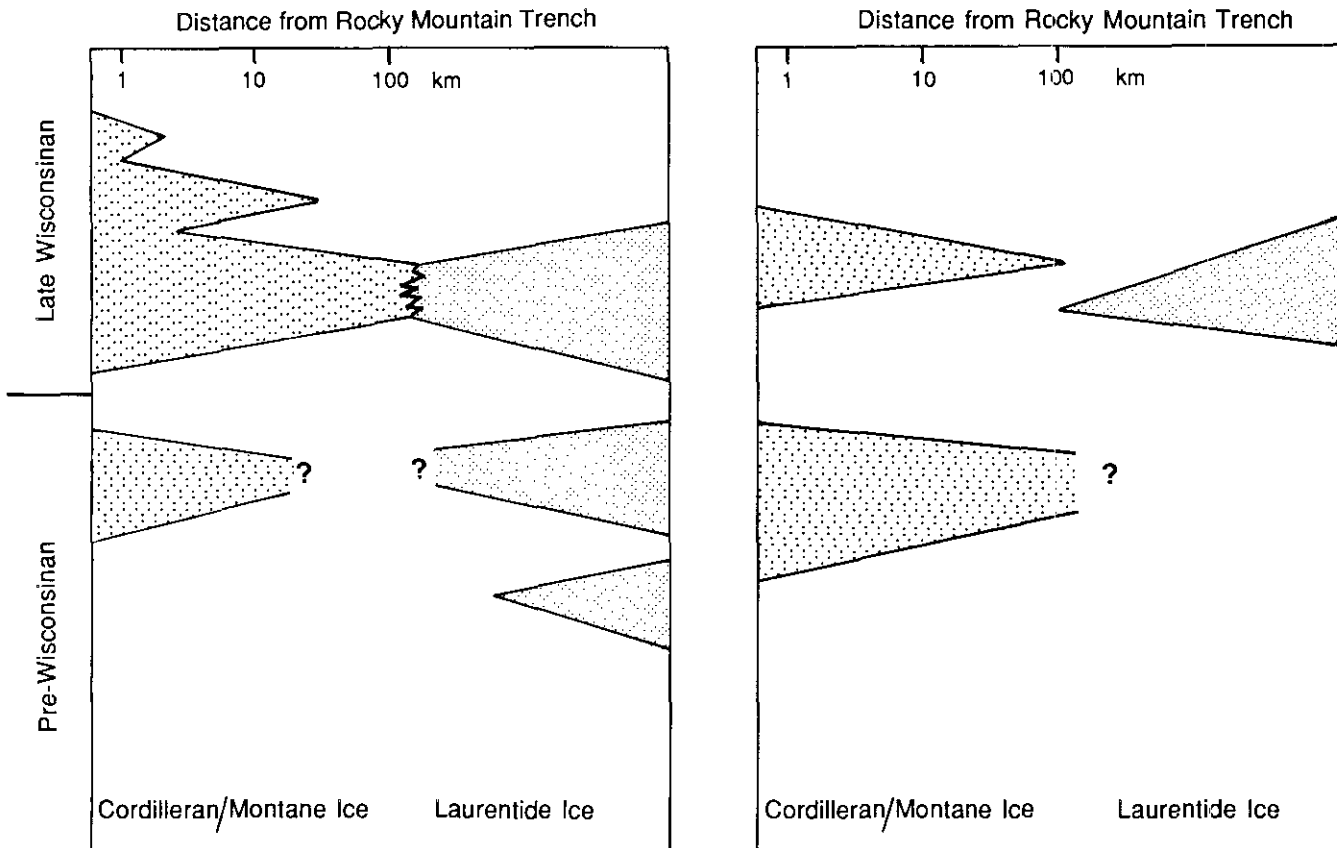


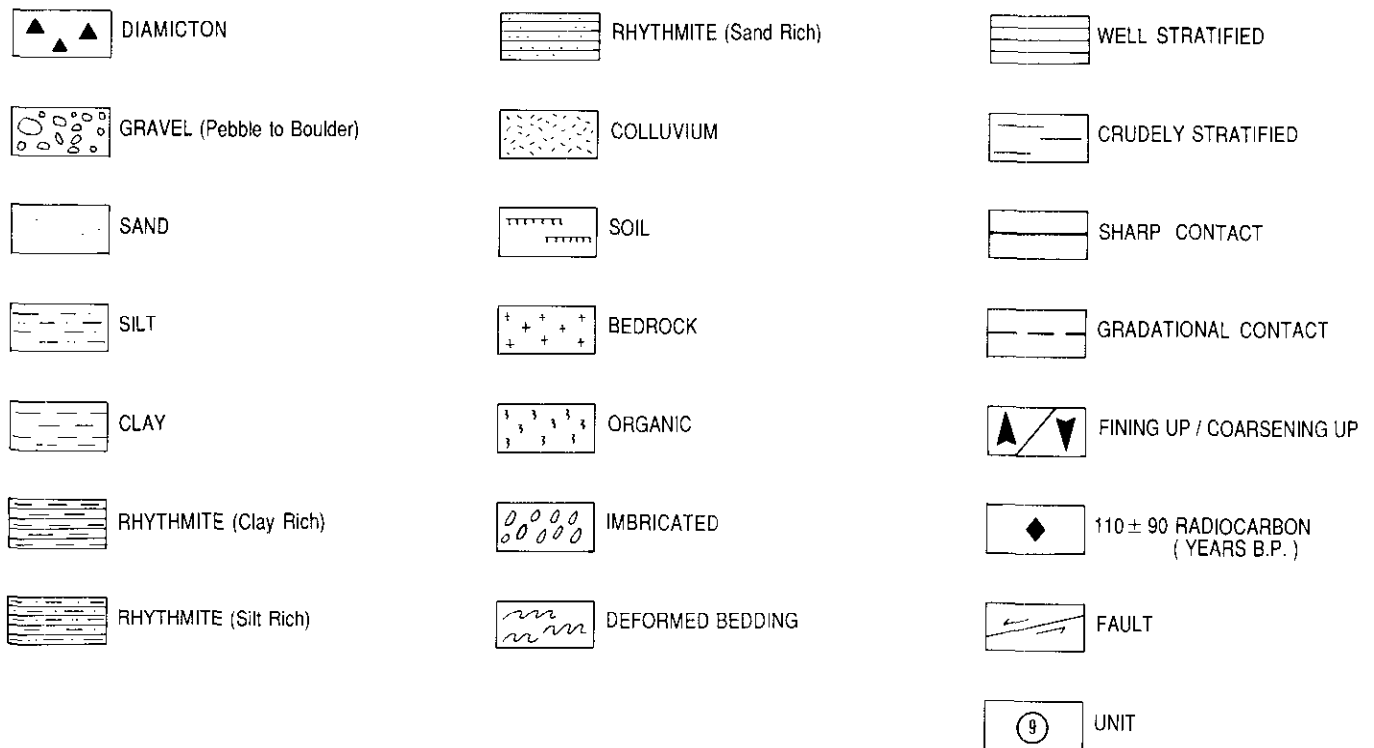
Figure 4-7-3. Time-distance diagram for Quaternary geologic history in the Peace River area. Model 1 based in part on Mathews (1978a, 1980) and Rutter (1976, 1977). Model 2 after Bobrowsky (1989a).

and outcrop in the west, near Hudson Hope. Marine siltstone, silty shale and shale belonging to the Shaftesbury Formation overlie the Gates Formation and outcrop in several places throughout the study area. These rocks, in turn, grade upward into more resistant siltstone and sandstone of the Dunvegan Formation (Mathews, 1978a).

The Peace River, which rises farther west at the Rocky Mountain Trench, is part of the Mackenzie River system, and is a preglacial feature which cuts across the Rocky Mountains perpendicular to the regional bedrock trend. It is likely that the course of the Peace River was established in the early Tertiary, and it is thus antecedent to the Rocky Mountain uplift which formed, in this area, during the late Tertiary (Holland, 1976). The preglacial Peace River occupied a much broader channel than the present river. Notable changes in its course include: a preglacial channel between Bull and Portage mountains (now occupied by the Portage Mountain moraine); paleoriver-flow 1 to 2 kilometres south of the present channel between Hudson Hope and Halfway River; and, paleoriver-flow 4 to 5 kilometres south of the present channel between Bear Flat and Fort St.

John (Beach and Spivak, 1963; Mathews, 1978a, 1980; Rutter, 1977; Seyers and Buchanan, 1990).

Historically the northwest part of British Columbia has long been favored as a primary centre for Pleistocene ice build-up (*cf.* Bobrowsky, 1989a for a detailed review). Modifications to this theme are minor and include recognition of other glacial ice accumulation centres such as the Cassiar, Cariboo and northern Rocky Mountains. The style, extent, intensity and timing of glaciations, however, attract a greater diversity of opinions and interpretations. The most contentious issue of the Pleistocene history in the study area centres on two aspects: the influence of Laurentide glacial ice in the province of British Columbia; and the number of glacial events. In the Peace District, two primary models and their variants have been put forward to describe the Pleistocene glacial history of the region (Figure 4-7-3). Model I recognizes two to three Laurentide and three to four Cordilleran glacial events, whereas Model II recognizes one Laurentide and two Cordilleran events. More importantly, Model I recognizes a coalescence of Cordilleran and Laurentide ice sheets, not recognized in Model II.



LEGEND FOR FIGURES 4-7-4 through 4-7-12.

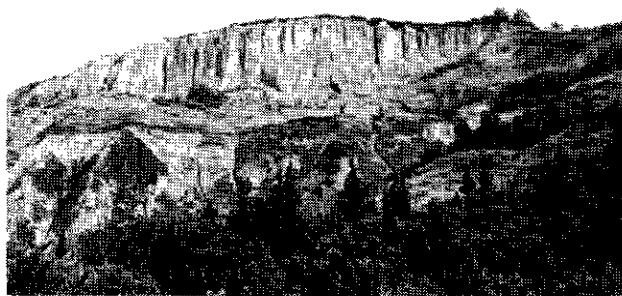


Plate 4-7-2. Section PTB90-26. View to north illustrates bluff exposure consisting of late Quaternary glacial sediments. Majority of exposed sediment at this site is late Wisconsinan diamicton deposited by Laurentide ice sheet. (GSB photo PTB90-11-34).

RESULTS AND INTERPRETATIONS

Field reconnaissance in the study area during 1990 resulted in the identification of 56 sites (Figure 4-7-1), providing some form of subsurface exposure of the unconsolidated sediments (Plate 4-7-2). Table 4-7-1 lists the coordinates and elevations of these sites. Preliminary sedimentologic and stratigraphic work at a few of these locations supports the contention of a complex glacial history for the area, involving ice interaction from three independent

sources (Laurentide, Cordilleran and Montane). Descriptions and genetic interpretations for several localities are discussed below.

DIAMICTON DEPOSITS

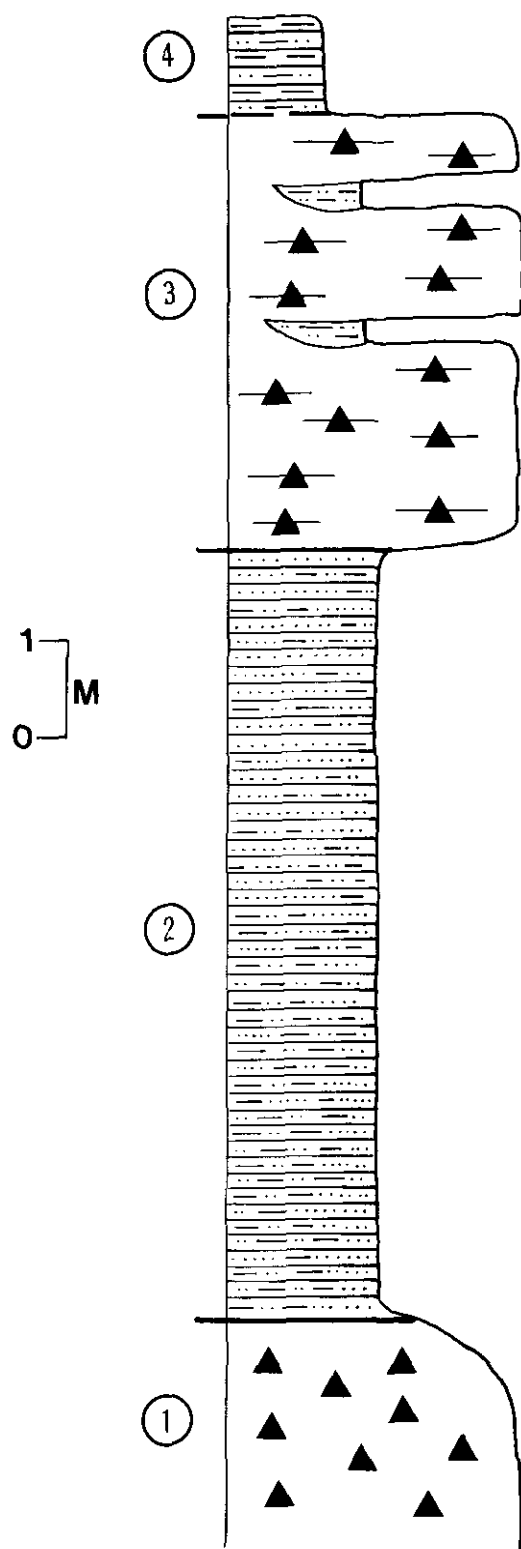
SECTION PTB90-06

Section PTB90-06 is located 17.1 kilometres west of Fort St. John, along Highway 29 (Figure 4-7-1). The 15.7 metres of sediment exposed at this locality comprises four units (Figure 4-7-4). Overlying the shaly bedrock along a brecciated regolith-like contact is a coarse, matrix-supported diamicton, 2.3 metres thick, containing planar silt lenses which are approximately 2 centimetres thick and 20 to 30 centimetres in length (Unit 1). Clasts in the unit are all angular and of local lithology. Unit 2 which is 8 metres thick, consists of 672, stone-free, normally graded silty sand and sandy silt rhythmite couplets, which are 1 to 5 centimetres thick. Both upper and lower contacts are sharp and erosional. The rhythmites are overlain by a stratified, matrix-supported diamicton, 4.3 metres thick, containing many planar and biconvex, fine silt lenses, which are 1 to 2 centimetres thick and up to 20 centimetres in length (Unit 3; Plate 4-7-3). The diamicton grades upward into approximately 1 metre of silt and clayey silt rhythmites which show postdepositional disturbance and pedogenesis (Unit 4). Large clasts, up to boulder size, are present in the upper rhythmites.

The lower diamicton, overlying bedrock, is interpreted to be local colluvium or debris-flow deposits. The remaining

PTB90-06

TABLE 4-7-1
LOCATION OF STUDY SITES IN PEACE RIVER AREA



LOCALITY	LATITUDE	LONGITUDE	UTM	ELEVATION	NTS NO.
90-01	56°09.2'	120°43.0'	FT 419252	472	94 A/2
90-02	56°08.7'	120°41.5'	FT 435243	472	94 A/2
90-03	55°57.9'	120°34.1'	FT 518048	540	93 P/15
90-04	55°57.6'	120°33.9'	FT 521041	579	93 P/15
90-05	56°06.3'	120°38.2'	FT 475201	579	94 A/2
90-06	56°17.2'	121°13.4'	FT 100391	594	94 A/6
90-07	56°11.6'	121°30.8'	ET 923285	488	94 A/4
90-08	56°07.5'	121°46.5'	ET 762205	610	94 A/4
90-09	56°07.8'	121°49.2'	ET 735209	655	94 A/4
90-10	55°47.7'	121°35.4'	ES 882839	792	93 P/13
90-11	56°02.7'	122°07.8'	ET 542113	1097	94 B/1
90-12	56°06.8'	121°47.9'	ET 747192	472	94 A/4
90-13	56°12.4'	120°55.0'	FT 292309	564	94 A/2
90-14	56°11.9'	120°49.5'	FT 296300	457	94 A/2
90-15	56°14.7'	121°00.5'	FT 234348	701	94 A/3
90-16	56°13.5'	120°56.5'	FT 275329	579	94 A/3
90-17	56°12.8'	120°55.5'	FT 287317	594	94 A/3
90-18	56°12.6'	120°55.2'	FT 289312	594	94 A/3
90-19	56°13.5'	121°27.3'	ET 958322	472	94 A/3
90-20	56°13.6'	121°18.9'	FT 045325	610	94 A/3
90-21	56°13.7'	121°27.9'	ET 952324	625	94 A/3
90-22	56°09.5'	120°43.6'	FT 412256	488	94 A/2
90-23	56°09.8'	120°44.1'	FT 407263	503	94 A/2
90-24	56°11.5'	120°47.1'	FT 375295	533	94 A/2
90-25	56°11.9'	120°47.4'	FT 371301	594	94 A/2
90-26	56°12.2'	120°47.9'	FT 365307	625	94 A/2
90-27	56°12.3'	120°48.7'	FT 357309	625	94 A/2
90-28	56°12.5'	120°50.2'	FT 341312	610	94 A/2
90-29	56°15.6'	121°13.2'	FT 102362	625	94 A/6
90-30	56°14.4'	121°15.8'	FT 077339	472	94 A/3
90-31	56°15.8'	120°09.8'	FT 138368	579	94 A/6
90-32	56°12.5'	121°27.5'	ET 956302	434	94 A/3
90-33	56°12.0'	121°27.2'	ET 961292	610	94 A/3
90-34	56°04.8'	121°49.8'	ET 738155	472	94 A/4
90-35	56°08.8'	120°48.1'	FT 366244	549	94 A/2
90-36	56°13.8'	121°29.2'	ET 939326	533	94 A/3
90-37	56°14.0'	121°29.0'	ET 941328	594	94 A/3
90-38	56°14.6'	121°29.5'	ET 945340	610	94 A/3
90-39	56°14.8'	121°29.8'	ET 932344	579	94 A/3
90-40	56°15.0'	121°30.5'	ET 924347	610	94 A/4
90-41	56°14.2'	121°31.2'	ET 916332	472	94 A/4
90-42	56°15.2'	121°31.6'	ET 913349	610	94 A/5
90-43	56°13.4'	121°36.1'	ET 867319	488	94 A/4
90-44	56°14.9'	121°36.6'	ET 862344	625	94 A/4
90-45	56°15.1'	121°37.0'	ET 857347	610	94 A/5
90-46	56°15.7'	121°36.8'	ET 858358	625	94 A/5
90-47	56°19.4'	121°37.8'	ET 847427	518	94 A/5
90-48	55°57.5'	120°36.5'	FT 494038	625	93 P/15
90-49	56°26.7'	121°15.6'	FT 073568	686	94 A/6
90-50	55°42.3'	121°10.7'	FS 146755	610	93 P/11
90-51	56°12.4'	121°29.6'	ET 936298	518	94 A/3
90-52	56°11.0'	121°33.6'	ET 894273	503	94 A/4
90-53	56°14.5'	121°18.4'	FT 049001	457	94 A/3
90-54	56°14.7'	120°57.8'	FT 262352	732	94 A/2
90-55	56°15.5'	121°16.7'	FT 067358	475	94 A/6
90-56	56°06.9'	121°47.5'	ET 753194	533	94 A/4

Figure 4-7-4. Composite stratigraphic column for Section PTB90-06.

units all represent facies formed in a glacial-lake environment. Unit 2 rhythmites probably represent sediment deposited during the early stages of glacial-lake formation as drainage to the east was blocked by Laurentide ice. The diamicton overlying these rhythmites is either a subaqueous sediment gravity-flow accumulation deposited in the impounded lake, or a deformation till of unknown provenance. The topmost rhythmites with drop-stones reflect the



Plate 4-7-3. Section PTB90-06 (Bear Flat section). Stratified glacial diamicton near top of section, approximately 5 metres thick, is interpreted to be either a subaqueous debris-flow deposit or deformation till related to the late Wisconsinan glaciation. (GSB photo PTB90-08-20).

retreating stages of the glacial event and thus the later stages of the lake history.

SECTION PTB90-09

This section is located 13 kilometres northeast of Hudson Hope, 2.5 kilometres north of Highway 29 in a small unnamed ravine (Figure 4-7-1). Nine units are represented in the 27.2 metres of sediment exposed in the section (Figure 4-7-5). At the base, 11 metres of horizontally stratified pebble-gravel, with some boulders (Unit 1), is gradually overlain by 3.4 metres of massive matrix-supported diamicton containing silty sand lenses (Unit 2). The Unit 2 diamicton grades upward into 2 metres of pebble-rich, slightly stratified, clast-supported diamicton (Unit 3), which in turn, grades up into 0.7 metre of poorly stratified, open-work pebble-gravel (Unit 4). Unit 5 comprises 1.1 metres of massive to slightly stratified matrix-supported diamicton which rests upon a sharp lower contact marked by a well-cemented, pebble lag bed. The upper contact shows sheared horizontal bedding with slickenside structures. Unit 6 consists of 1.8 metres of massive, matrix-supported diamicton

PTB90-09

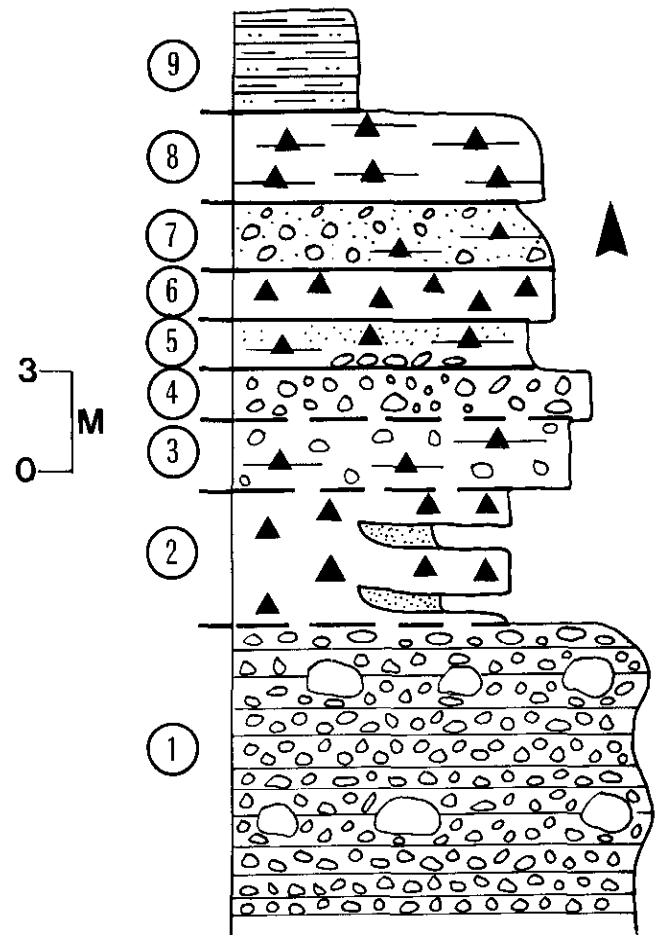


Figure 4-7-5. Composite stratigraphic column for Section PTB90-09.

with vertical jointing. Sharply overlying the diamicton is a 1.9-metre fining-upward sequence of horizontally stratified sand and imbricated gravel beds (Unit 7). Discontinuous and thin silty diamicton lenses are intercalated within the sand and gravel. A 2.3-metre matrix-supported diamicton, with some crude stratification and sharp upper and lower contacts overlies the sand and gravel (Unit 8). The top of the section consists of approximately 3 metres of sandy silt and clayey silt rhythmite couplets.

The complex sequence exposed at this section may reflect one or two glacial/nonglacial events. The interpretation that follows is tentative. The basal gravel represents fluvial deposition in a braided stream system, probably advance outwash (Unit 1). Over-riding ice may then have deposited the massive diamicton which is interpreted to be a till (Unit 2). As ice retreated, local deposition of resedimented diamicton within gravel occurred, as interpreted from the sediments in Unit 3. A second depositional cycle in a braided stream system is then inferred for the Unit 4 deposit. A period of erosion (= boulder lag) clearly pre-

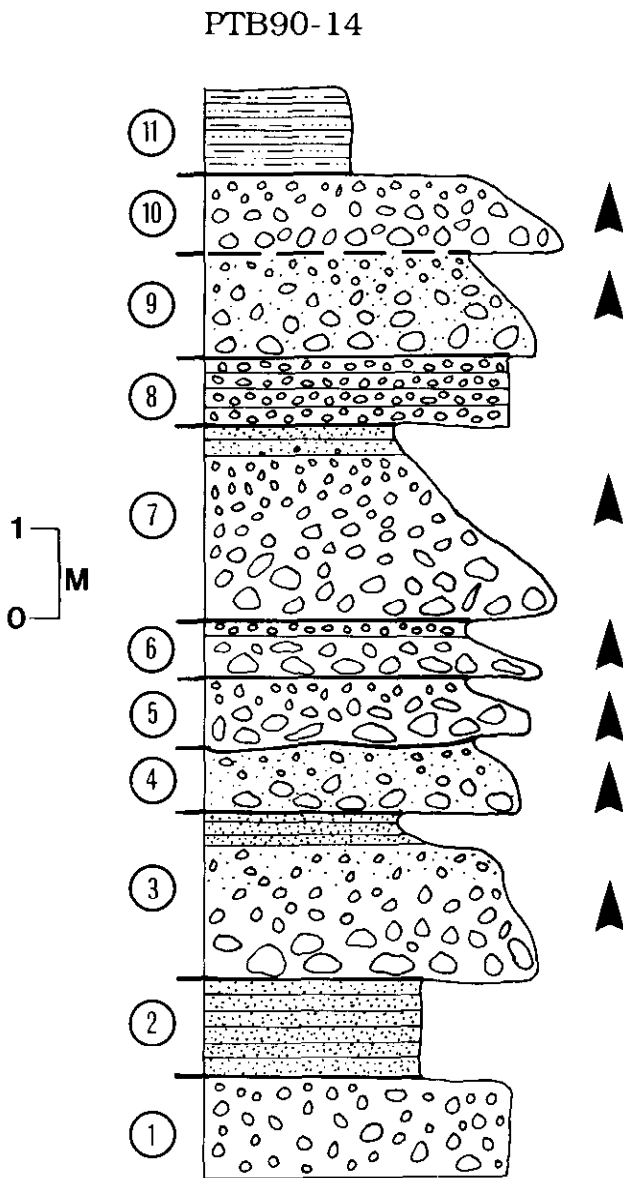


Figure 4-7-6. Composite stratigraphic column for Section PTB90-14.

ceded accumulation of the resedimented diamicton beds in gravel (Unit 5) and till (Unit 6) as ice once again advanced over the area. This was followed by additional resedimentation in ice-contact gravel deposits during ice retreat (Unit 7). Continued ice retreat blocked the regional drainage, resulting in a proglacial lake environment into which a subaqueous sediment gravity-flow would have deposited the stratified diamicton (Unit 8) and subsequently glaciolacustrine rhythmites (Unit 9).

COARSE-GRAINED DEPOSITS

SECTION PTB90-14

Section PTB90-14 is located 41.5 kilometres southwest of Fort St. John, along the north bank of Peace River (Figure

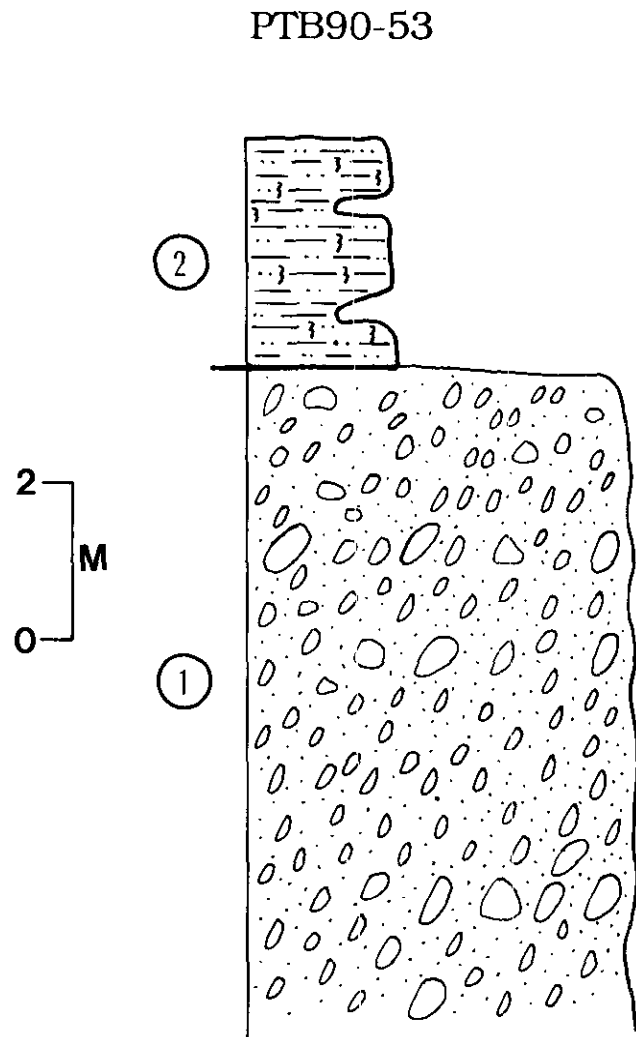


Figure 4-7-7. Composite stratigraphic column for Section PTB90-53.

4-7-1). With the exception of the upper 1 metre of sandy and clayey silt rhythmites, the remaining 14 metres of sediment exposed at this location is predominantly composed of sand and gravel interbeds (Units 1 to 10) (Figure 4-7-6). Several fining-upward cycles are evident in the deposit. Much of the sediment ranges from massive, open-work cobble-gravel to stratified and imbricated pebble-gravel with a sandy matrix. Horizontally laminated, well-sorted, medium sand is found near the base of the section (Unit 2).

This sequence is interpreted to represent fluvial deposition in a relatively high-energy channel of a braided or wandering stream system. The multiple fining-upward cycles of gravel, and sporadic interbeds of sand, reflect the shifting of channels and fluctuating energy levels which are characteristic of the braided stream environment.

SECTION PTB90-53

This section, located 27.2 kilometres west of Fort St. John, along the north side of Highway 29, is a currently

PTB90-55

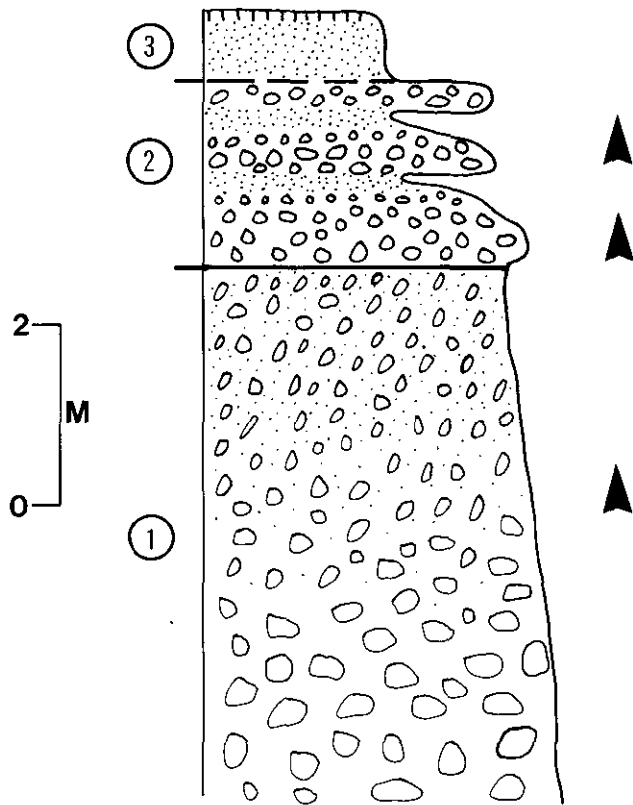


Figure 4-7-8. Composite stratigraphic column for Section PTB90-55.

inactive borrow pit (Figure 4-7-1). Exposed sediment totals 10.8 metres in thickness (Figure 4-7-7). At the base, Unit 1, is dominated by coarse, imbricated pebble-gravel, and shadow structures indicating consistent flow toward 105°. This unit is at least 8 metres thick. An abrupt, erosional upper contact separates the gravel from an interbedded sequence of clayey silt, silty clay and fibrous organic detrital beds totalling 2.8 metres in thickness (Unit 2). All beds within Unit 2 are internally structureless.

The sequence exposed in this section is interpreted to be a fluvial succession. The basal gravel unit is interpreted to represent thalweg deposition in a moderate to high-velocity stream, similar to the modern Peace River. The overlying unit represents overbank deposition in a similar environment. The sharp contact between the two units is either erosional and produced under conditions of a continuous single fluvial system, or represents a discontinuity in time.

SECTION PTB90-55

Section PTB90-55, located 2.8 kilometres northwest of Highway 29, along Road 167, is in a borrow pit exposing 8.7 metres of sediment (Figure 4-7-1). Three units are present at this site (Figure 4-7-8). Unit 1 is more than 6 metres thick and fines upward from open-worked cobble-

PTB90-52

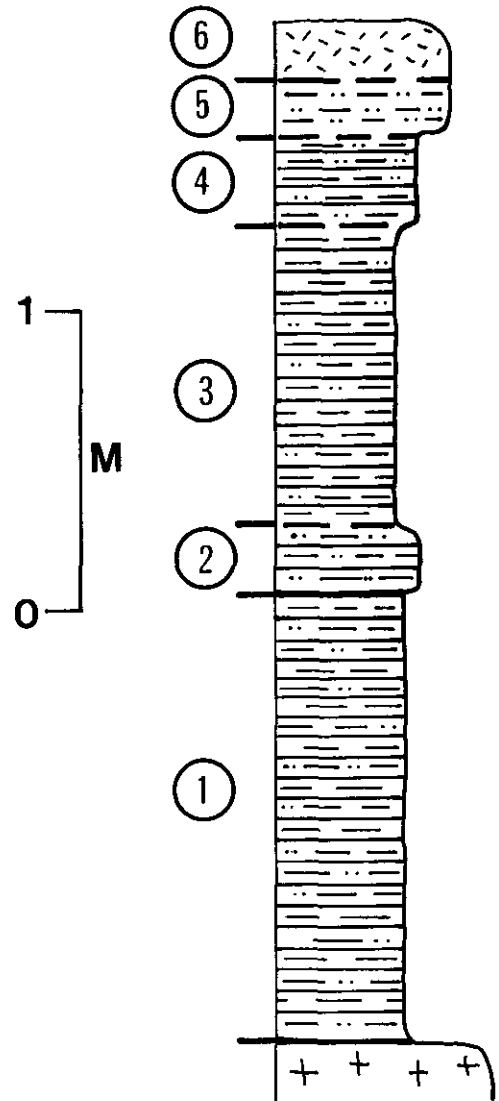


Figure 4-7-9. Composite stratigraphic column for Section PTB90-52.

gravel to matrix-filled coarse pebble-gravel. Imbricated bedding indicates depositional flow to the east and east-southeast. The mineralogy indicates derivation from western sources. The upper contact is erosional. Unit 1 is overlain by a pebble-gravel, 2 metres thick, with coarse and medium sand, consisting of several graded cycles (Unit 2). The uppermost Unit 3 gradually overlies the pebble-gravel and consists of structureless fine to medium sand which has been pedogenically altered in the upper part.

This sequence is interpreted to represent fluvial deposition in a relatively high-energy channel of a braided or wandering stream system. The absence of clasts from the Canadian Shield indicates that the exposure may lie beyond the limits of influence of Laurentide ice or the deposit predates Laurentide glaciation.

PTB90-56

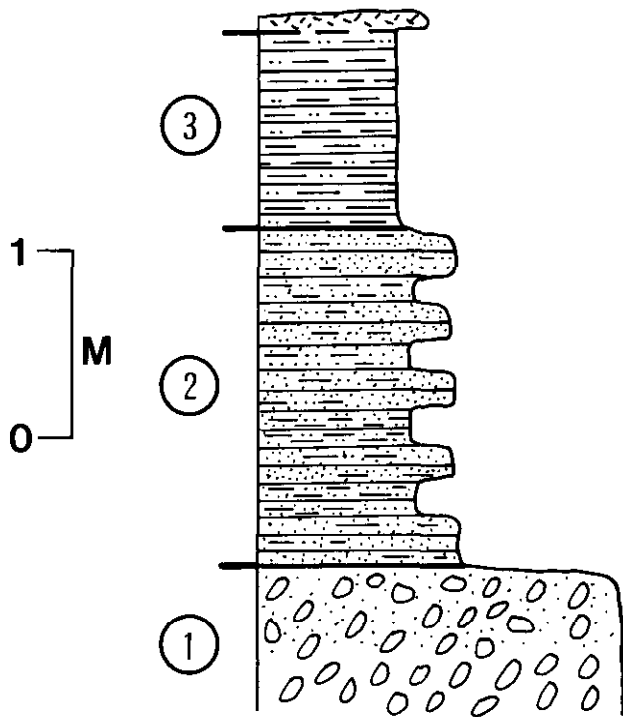


Figure 4-7-10. Composite stratigraphic column for Section PTB90-56.

PTB90-04

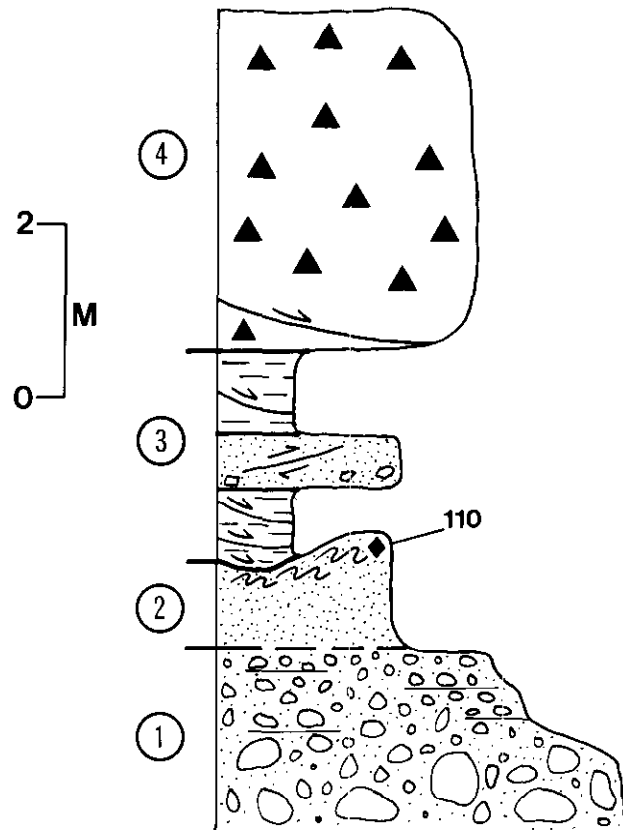


Figure 4-7-11. Composite stratigraphic column for Section PTB90-04.

FINE-GRAINED DEPOSITS

SECTION PTB90-51

This section is located 40.8 kilometres east of Hudson Hope, along the north side of Highway 29 (Figure 4-7-1). It consists of 18.6 metres of laminated silt and silty clay couplets, varying in thickness from 1 to 5 centimetres. Generally, the couplets at the base of the sequence are thicker than those in the upper 10 metres. Minor, structureless sand beds, 2 to 8 centimetres thick, are present in the basal 2 metres of the sequence. A total of 576 couplets were identified.

This sequence is interpreted as the product of low-density turbidity currents in a deep glaciolacustrine environment. In the basal part of the exposure, draped silt lenses, erosional structures and lateral textural gradation in some silt members suggest that flow during deposition was toward the northeast or east. Glaciolacustrine depositional environments were common during the Pleistocene in the Peace District and most often resulted from drainage impoundment to the east by the Laurentide ice sheet (Mathews, 1980). The gradual upward decrease in couplet thickness reflects either deepening of the lake waters or expansion of the lake to the west. The absence of a regressive sequence is probably due to subsequent erosion.

SECTION PTB90-52

Section PTB90-52 is located 35.4 kilometres east of Hudson Hope, along the north side of Highway 29 (Figure 4-7-1). This exposure consists of 3.36 metres of silty clay and clayey silt units overlying bedrock at road level, with a gradational upper contact to colluvium near the surface (Figure 4-7-9). A total of 193 couplets were counted. The basal 1.85 metres consists of silt and silty clay couplets, with a modal thickness of 2 centimetres (Unit 1). Contacts between the couplets are all sharp, but not necessarily erosional. These couplets are overlain, along a planar upper contact, by 15 centimetres of laminated clayey silt (Unit 2), which grades upward into couplets of silty clay and clay totalling 96 centimetres (Unit 3). Couplets in this sequence are generally thinner and finer in texture than those of Unit 2. The Unit 3 couplets are overlain by the 29-centimetre-thick Unit 4, along a gradational contact, by couplets similar to those of Unit 1. A gradational upper contact separates Unit 4 from 11 centimetres of structureless silt (Unit 5), which completes the exposed section.

The units exposed at this locality are interpreted as the products of low-density glaciolacustrine turbidity currents,

originating from the west. The fluctuations in couplet thickness and texture probably indicate changes in the energy regimes of the turbidity currents, induced either by fluctuations in shoreline position or by changes in the axis of deposition of the current.

SECTION PTB90-56

Section PTB90-56 is located 16.4 km east of Hudson Hope, along the north side of Highway 29 (Figure 4-7-1). The exposure consists of three units and is 3.73 metres thick (Figure 4-7-10). Unit 1 is more than 67 centimetres thick, and is composed of an imbricated pebble-gravel indicating flow to the east. Clasts indicate a western provenance. Overlying Unit 1 along an erosional contact are 187 centimetres of complexly interbedded, mottled sandy silt, silt and silty sand beds (Unit 2). The upper part of this unit is truncated along an erosional contact. The uppermost 119 centimetres (Unit 3) consists of silt to clay couplets, with gradational contacts between silt and clayey silt members, and erosional contacts between clay and silt members. A total of 44 couplets were counted in the unit, with a modal average of 3 centimetres in thickness.

Unit 1 is interpreted to be the product of a moderate-energy fluvial system. The overlying sediments may represent low-energy fluvial deposition, either as overbank deposits or in minor channels of a wandering stream. The high modal thickness of the uppermost rhythmites suggests that they represent periodic overbank sedimentation or paludal deposition in a fluvial system, rather than deposition in a lacustrine environment.

SLUMP DEPOSITS

SECTION PTB90-04

Section PTB90-04 is located 41.5 kilometres southeast of Fort St. John, along the north bank of the Kiskatinaw River



Plate 4-7-4. Section PTB90-15 (Target section). View of Unit 1, stratified glacial diamicton, containing prominent sand interbeds, numerous flat-lying boulders, and gradationally overlying Unit 2 rhythmites. Pebble fabric in diamicton approximately east-west. Pick for scale. Diamicton interpreted to be basal meltout-till. (GSB photo PTB90-11-08).

TABLE 4-7-2
SUMMARY STATISTICS FOR THREE-DIMENSIONAL PEBBLE-FABRIC ANALYSES

FABRIC	TREND	PLUNGE	S1	S2	S3	N
90-10A	029.0°	12.0°	0.8275	0.1618	0.0106	26
90-10B	163.3°	23.2°	0.7024	0.2374	0.0601	22
90-10C	143.4°	13.9°	0.8073	0.1390	0.0538	25
90-10D	154.4°	59.7°	0.5523	0.2592	0.1885	25
90-12	074.7°	06.9°	0.9783	0.0191	0.0026	26
90-06	265.9°	12.7°	0.8798	0.1082	0.0119	25
90-54	187.9°	13.1°	0.6596	0.2761	0.0643	25
90-15A	302.9°	04.1°	0.8143	0.1606	0.0252	25
90-15B	148.4°	30.0°	0.6765	0.2214	0.1021	25
90-08	210.9°	04.8°	0.6878	0.2802	0.0320	14

Note: Fabric number corresponds to section numbers listed elsewhere, S1 to S3 are normalized eigenvalues, and N is sample size.

TABLE 4-7-3
SUMMARY STATISTICS FOR TWO-DIMENSIONAL PEBBLE-FABRIC ANALYSES

FABRIC	VECTOR	R	S.E.	N	RAYLEIGH
90-03A	071.65°	0.9916	3.3140	6	0.0027
90-03B	136.55°	0.9715	2.8262	25	0.0000
90-03C	080.76°	0.9410	5.397	14	0.0000
90-12	107.22°	0.9940	2.7026	9	0.0001
90-10E	028.33°	0.9890	2.3463	12	0.0000

Note: Fabric number corresponds to section numbers listed in Table 4-7-1.

near the Highway 97 bridge (Figure 4-7-1). River erosion has resulted in a transverse section through the distal part of a slump. Approximately 9.5 metres of sediment is exposed (Figure 4-7-11). Horizontally bedded and well-imbricated boulder-gravel grading up into pebble-gravel (Unit 1) is conformably overlain by 1.5 metres of ripple-laminated sand (Unit 2). Climbing ripple sets, 2 to 15 centimetres thick, show convolution in the upper 0.5 metre of the unit. Wood and other organic debris, which is abundant in the upper 1 metre of Unit 2, has been dated to 110 ± 90 years B.P. (AECV-1213C). A sharp, subhorizontal erosional contact separates Unit 2 from the overlying 2 metres of sand and clay interbeds of Unit 3. Approximately 4 metres of clay-rich, matrix-supported diamicton occurs at the top of the section. Numerous subhorizontal slickensided surfaces, brecciated beds and faults are evident in Unit 3 and the lower part of Unit 4.

Units 1 and 2 in this section are interpreted to represent a fining-upward channel-gravel sequence and fine overbank sedimentation, respectively, of a moderate to high-energy wandering braided-stream system. Unit 3 represents the lower cohesive sediment or contact zone of the slump which shears during sediment remobilization. In this unit, sorted beds are still preserved but overprinted with numerous shear planes formed during slumping. The overlying diamicton is interpreted to be the product of an upper zone of viscous resedimentation which also resulted from the same event.

DISCUSSION

SEDIMENT TYPE

Based on a preliminary examination of several sections, Quaternary deposits in the study area can be grouped into

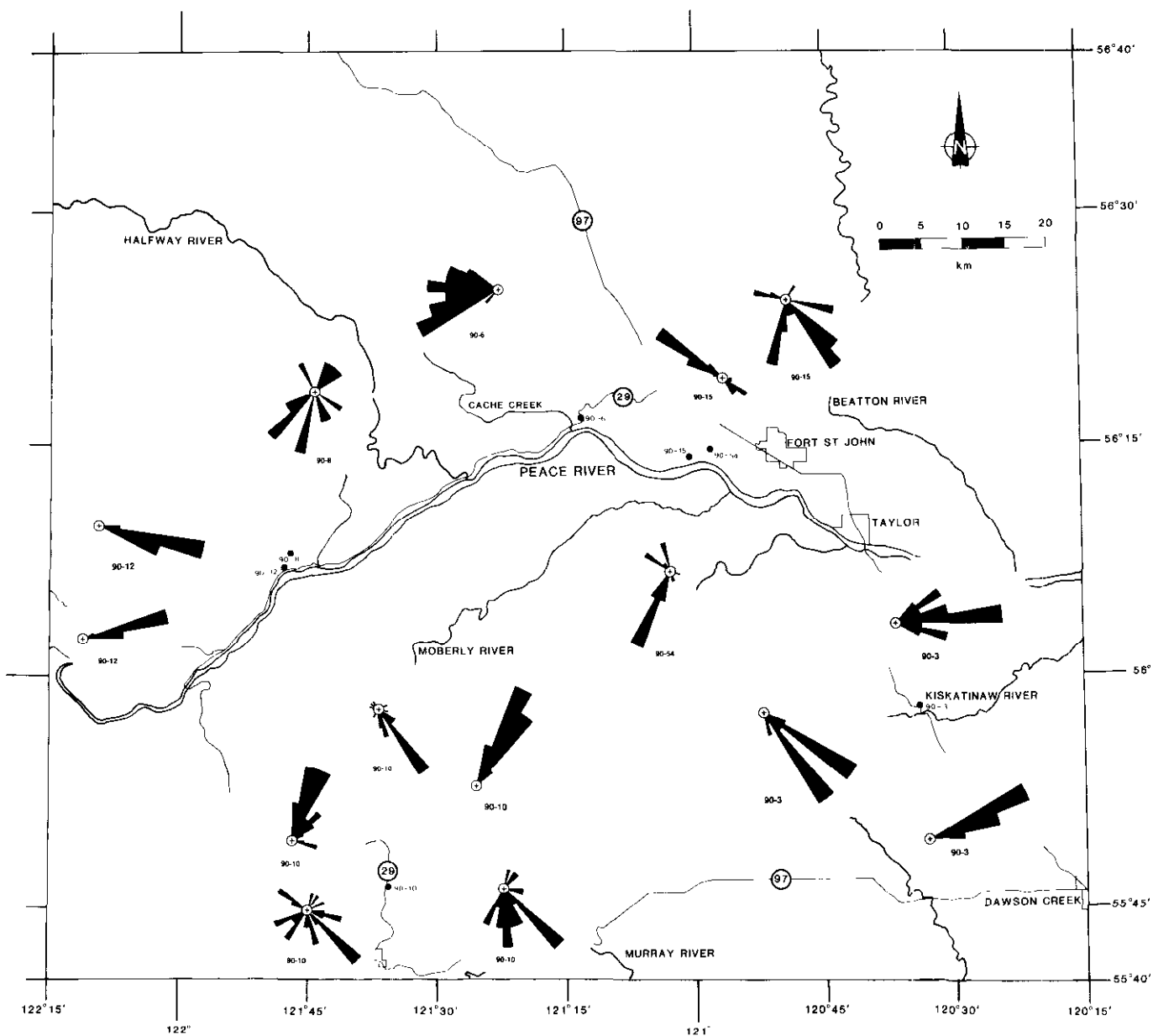


Figure 4-7-12. Pebble-fabric histograms for diamictons from seven locations. See Tables 4-7-2 and 4-7-3 for details of pebble-fabric data.

four broad textural groups including diamicton, gravel, sand and fines (silt and clay). Although additional work is required to identify and discuss all of the facies variations which may be present in these groups, a cursory review of some of the observations can be presented in this report.

Diamictons observed thus far include those that are structureless, stratified or massive with some interbeds (Plate 4-7-4). Their genesis is variable. For instance, the two diamictons (Units 2 and 6) observed at Section PTB90-09 are both interpreted to be basal till deposits, whereas the diamicton at the top of Section PTB90-04 is a debris-flow accumulation formed during slumping. The Unit 3 diamicton at Section PTB90-06 is interpreted to have been deposited by a subaqueous sediment gravity-flow. Detailed work

is still pending to fully quantify the sediment characteristics of the diamictons. As a start, pebble-fabric was measured in diamicton beds at seven locations. The results illustrate variation in fabric orientation and strength (eigenvalues) which can be expected in sediments of differing genesis, or sediments deposited under different flow directions (Figure 4-7-12; Tables 4-7-2 and 4-7-3).

Gravel and sand deposits are ubiquitous but deep below surface, thus precluding easy extraction for aggregate use. All gravel accumulations are either massive or stratified, and quite often normally graded; both open-work and matrix-filled deposits were observed (Plate 4-7-5). All size fractions of sand are present, as are sediments which are either massive and stratified (horizontal, planar and trough-



Plate 4-7-5. Section PTB90-14 (Rib section). View of Unit 7 illustrating the massive to crudely stratified, oxidized gravel with sand interbeds. Minor manganese staining. (GSB photo PTB90-10-28).

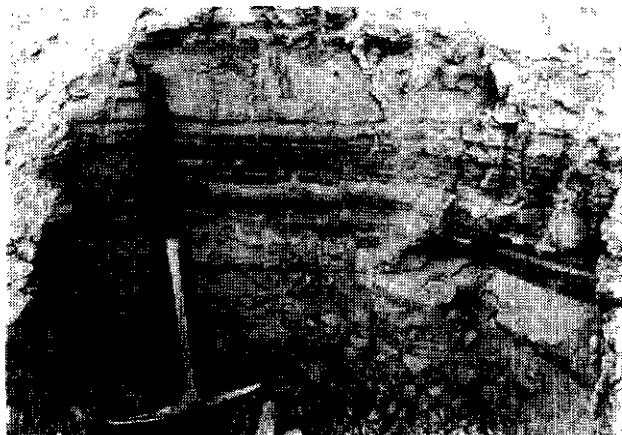


Plate 4-7-6. Section PTB90-12 (Red Paleosol section). View near base of section showing rhythmite variation in couplet thickness, and random interbeds of sand and granular diamiction. Couplets range from silty clay and clayey silt to sandy silt and silt textures. Charcoal wood fragments taken at top of paleosol (Sample PTB90-12-02) and below upper diamiction, radiocarbon dated to 3400 ± 90 years B.P. (AECV-1204C). (GSB photo PTB90-10-04).



Plate 4-7-7. Section PTB90-02. (Ostero Gravel Pit). View of *Bison* tibia (Sample PTB90-02-01) recovered 5.5 metres above base of gravel pit and 12.8 metres below upper ground surface. Proximal end of tibia broken during recovery; trowel for scale. Sample radiocarbon dated to $10\,240 \pm 160$ years B.P. (AECV-1206C). (GSB photo PTB90-07-36).

cross-stratified). Sand deposits occur either independently of the gravel or quite often interbedded with gravel as discrete beds or lenses. Most gravel deposits examined reflect deposition by moderate to high-energy braided-stream systems including cyclic fining-upward sequences characteristic of shifting channels (*e.g.* Section PTB90-14). Most sand deposits represent waning-flow conditions in braided channels (*e.g.* Section PTB90-14) or overbank sedimentation in general fluvial environments (*e.g.* Unit 2 at Section PTB90-53).

A significant portion of the unconsolidated sediment blanketing the study area consists of texturally fine rhythmites. Rhythmites observed in section exposures display considerable variability in bed thickness and integrity, with couplets ranging in texture from coarse sand to clay (Plate 4-7-6). Most of the couplet beds are normally graded and support scattered out-sized clasts. Load structures, rip-up clasts, graded beds and directional flow structures, as well as stratigraphic association with other sediment types indicate that the rhythmites represent episodic deposits resulting from sedimentation of turbid density-driven underflows into proglacial lake environments with intervening quiet-water sedimentation.

STRATIGRAPHY

The preliminary nature of the 1990 fieldwork restricts stratigraphic interpretations which would support either of the stratigraphic models presented earlier. Sections with multiple diamictions examined to date contain no more than two till units, but other sections with multiple diamictions (till?) have been recorded and have yet to be examined. Only a few radiocarbon dates were obtained during this season. Two mass movements were dated, indicating both recent [110 ± 90 years B.P. (AECV-1213C) at Section

PTB90-04] and Mid-Holocene [3400±90 years B.P. (AECV-1204C) at Section PTB90-12] slope-failure events.

One *Bison sp.* bone was recovered from stratified pebble-gravel at Section PTB90-02 and resulted in a radiocarbon date of 10 240±160 years B.P. (AECV-1206C; Plate 4-7-7). *Bison sp.* and other large mammals were common in the area as early as 10 000 years ago (Driver, 1988), so the bone discovery is not unusual. In fact, large game occupied the Rocky Mountain Trench before 9000 years ago (Rutter *et al.*, 1972). However, a previous date of 27 400±580 years B.P. (GSC-2034) on mammoth bone from this section led Mathews (1978a) to correlate the gravel with other gravel of mid-Wisconsinan age. In light of the new date, a reworked faunal assemblage in postglacial gravel seems warranted as a more plausible interpretation for the deposit. Spurious dates from elsewhere in the Peace District have resulted in considerable misinformation regarding late Pleistocene glaciation (*e.g.* White *et al.*, 1979, 1985).

SUMMARY AND IMPLICATIONS

Quaternary geologic investigations in the Peace River region of northeastern British Columbia provide an opportunity to address concerns of importance and interest to the general populace in the area and to Quaternary geoscientists. During the summer of 1990, 56 sites were located for further study to address the following issues:

- Given the high frequency of slope failures in the Peace area, dating of historic and prehistoric failures can shed light on the mitigation of future slope-instability issues;
- Detailed sedimentologic and stratigraphic study of these sites will improve understanding of the glacial and nonglacial history for the region.

Surficial mapping, not discussed here, but presented elsewhere, addresses the following two questions:

- What is the location and integrity of aggregate deposits in the Peace District?
- Do economically viable and potentially commercial peat deposits occur in the region?

Field activities are planned for the summers of 1991 and 1992 to meet the above objectives.

ACKNOWLEDGMENTS

The authors thank G. Bailey for assistance in the field and W. Speyers for providing unpublished B.C. Hydro reports. T. Giles drafted Figure 4-7-1. C. Smith drafted the remaining figures.

REFERENCES

- Beach, H.H. and Spivak, J. (1943): *The Origin of Peace River Canyon*, British Columbia; *American Journal of Science*, Volume 241, pages 366-376.
- Bobrowsky, P.T. (1984): Quaternary Geologic History of the North Central Rocky Mountain Trench, British Columbia; in *Proceedings of the 1st Northern Workshop*, A. S. Mohsen and W.C. MacKay, Editors; *Institute for Northern Studies, University of Alberta*, Edmonton, pages 59-60.
- Bobrowsky, P.T. (1987): Quaternary Stratigraphy of the Northern Canadian Cordillera Based on New Evidence from the Finlay River of Northeastern British Columbia; *International Quaternary Association, XIIth International Congress, Program with Abstracts*, Ottawa, page 132.
- Bobrowsky, P.T. (1988): Ice Free Conditions in the Northern Canadian Cordillera at 18 ka and the Timing of the Late Wisconsinan; *American Quaternary Association, Tenth Biennial Meeting, Abstracts and Program*, Amherst, page 108.
- Bobrowsky, P.T. (1989a): Late Cenozoic Geology of the Northern Rocky Mountain Trench, British Columbia; unpublished Ph.D. thesis, *University of Alberta*, Edmonton, 463 pages.
- Bobrowsky, P.T. (1989b): Quaternary Diamictos in the Inter-montane Environment of B.C.; *Geological Association of Canada, Program with Abstracts*, Montreal, Volume 14, page 89.
- Bobrowsky, P.T. and Rutter, N.W. (1989): Quaternary Stratigraphy of the Northern Cordillera in British Columbia; *Canadian Quaternary Association, 1989 Meeting, Program and Abstracts*, Edmonton, page 27.
- Bobrowsky, P.T. and Rutter, N.W. (1990): Geologic Evidence for an Ice-free Corridor in Northeastern British Columbia, Canada; *Current Research in the Pleistocene*, Volume 7, (in press).
- Catto, N. (1991): Surficial Geology of Peace River, British Columbia (NTS 94A/1, 2, 7, 8); *B.C. Ministry of Energy, Mines and Petroleum Resources*, in preparation.
- Driver, J.C. (1988): Late Pleistocene and Holocene Vertebrates and Palaeoenvironments from Charlie Lake Cave, Northeast British Columbia; *Canadian Journal of Earth Sciences*, Volume 25, pages 1545-1553.
- Holland, S.S. (1976): Landforms of British Columbia, a Physiographic Outline; *B.C. Ministry of Energy, Mines and Petroleum Resources*, Bulletin 48, 138 pages.
- Hora, Z.D. (1988): Sand and Gravel Study 1985; *B.C. Ministry of Energy, Mines and Petroleum Resources*, Open-File 1988-27, 41 pages.
- Liverman, D. (1987): Glaciolacustrine Sedimentation in the Grande Prairie Region, Alberta, Canada; *International Quaternary Association, XIIth International Congress, Program with Abstracts*, Ottawa, page 214.
- Liverman, D. (1989a): The Laurentide Ice Sheet in West-central Alberta – Implications for the Ice Free Corridor; *Canadian Quaternary Association 1989, Program and Abstracts*, Edmonton, page 36.

- Liverman, D. (1989b): The Quaternary Geology of the Grande Prairie Area, Alberta; unpublished Ph.D. thesis, *University of Alberta*, Edmonton.
- Liverman, D.G.E., Catto, N.R. and Rutter, N.W. (1989): Laurentide Glaciation in West-central Alberta: a Single (Late Wisconsinan) Event; *Canadian Journal of Earth Sciences*, Volume 26, pages 266-274.
- Mathews, W.H. (1954): Quaternary Stratigraphy and Geomorphology of the Fort St. John Area, Northeastern British Columbia; *Geological Society of America*, Bulletin 65, page 1345.
- Mathews, W.H. (1962): Quaternary Geology, Peace River District, British Columbia; in Peace River, *Edmonton Geological Society*, 4th Annual Field Trip, Guide Book, pages 1-4.
- Mathews, W.H. (1972): Quaternary Geology, Charlie Lake, British Columbia (94 A); in Report of Activities, Part A. *Geological Survey of Canada*, Paper 72-1A, pages 169-170.
- Mathews, W.H. (1973): Quaternary Geology, Charlie Lake, British Columbia; in Report of Activities, Part A. *Geological Survey of Canada*, Paper 73-1A, pages 210-211.
- Mathews, W.H. (1978a): Quaternary Stratigraphy and Geomorphology of Charlie Lake (94A) Map-area, British Columbia; *Geological Survey of Canada*, Paper 76-20, 25 pages. Includes Map 1460A.
- Mathews, W.H. (1978b): The Geology of the Ice-free Corridor – Discussion – Northeastern British Columbia and Adjacent Alberta; *American Quaternary Association*, Fifth Biennial Meeting, Program and Abstracts, Edmonton, pages 16-18.
- Mathews, W.H. (1980): Retreat of the Last Ice Sheets in Northeastern British Columbia and Adjacent Alberta; *Geological Survey of Canada*, Bulletin 331, 22 pages.
- Mathews, W.H. (1986): Physiographic Map of the Canadian Cordillera; *Geological Survey of Canada*, Map 1701A.
- Mathews, W.H., Gabrielse, H. and Rutter, N.W. (1975): Glacial Map, Beaton River Map Area, British Columbia (NTS 94); *Geological Survey of Canada*, Open File 274.
- Maynard, D.E. (1988): Peatland Inventory of British Columbia; *B.C. Ministry of Energy, Mines and Petroleum Resources*, Open File 1988-33, 73 pages.
- Reimchen, T.H.F. (1980): Surficial Geology, Dawson Creek; *Geological Survey of Canada*, Map 1467A.
- Rutter, N.W. (1968): Surficial Geology of the Peace River Dam and Reservoir Area, British Columbia; in Current Research, Part A, Report of Activities, *Geological Survey of Canada*, Paper 68-1A, pages 182-183.
- Rutter, N.W. (1969a): Summary of Preliminary Work on the Quaternary Geology of the Lake Williston Area, B.C.; in Field Conference Guidebook, P.A. Ziegler, Editor, *Edmonton Geological Society*, Field Conference 1969, pages 1-3.
- Rutter, N.W. (1969b): Surficial Geology of the Peace River Dam and Reservoir Area, British Columbia (Parts of 93N, O, 94B, C, E); in Report of Activities, Part A, *Geological Survey of Canada*, Paper 69-1A, pages 216-217.
- Rutter, N.W. (1974): Surficial Geology and Landforms, Williston Lake Area, British Columbia; *Geological Survey of Canada*, Maps 1381A, 1382A and 1383A.
- Rutter, N.W. (1976): Multiple Glaciation in the Canadian Rocky Mountains with Special Reference on Northeastern British Columbia; in Quaternary Stratigraphy of North America, W.C. Mahaney, Editor, *Dowden, Hutchinson & Ross*, Stroudsburg, Pennsylvania, pages 409-440.
- Rutter, N.W. (1977): Multiple Glaciation in the Area of Williston Lake, British Columbia; *Geological Survey of Canada*, Bulletin 273, 31 pages.
- Rutter, N.W. (1980): Late Pleistocene History of the Western Canadian Ice-free Corridor; *Canadian Journal of Anthropology*, Volume 1, pages 1-8.
- Rutter, N.W. (1981): Relationship between Late Pleistocene Laurentide and Cordilleran Glaciations, Canada; in Quaternary Glaciations in the Northern Hemisphere, V. Sibrava and F.W. Shotton, Editors, *Czechoslovakia Geological Survey*, Prague, IGCP Project 73/1/24, Report No. 6, pages 205-218.
- Rutter, N.W. (1984): Pleistocene History of the Western Canadian Ice-free Corridor; in Quaternary Stratigraphy of Canada – a Canadian Contribution to IGCP Project 24, R.J. Fulton, Editor, *Geological Survey of Canada*, Paper 84-10, pages 49-56.
- Rutter, N.W., Geist, V. and Schackleton, D.M. (1972): A Bighorn Sheep Skull 9280 Years Old from British Columbia; *Journal of Mammalogy*, Volume 53, pages 641-644.
- Seyers, W. and Buchanan, P. (1990): Assessment of Upper Left Bank Overburden Deposits – Task C9B-B03D, Peace River Site C; *Klohn-Crippen Consultants, Ltd.*, Report No. KC53.
- White, J.M., Mathewes, R.W. and Mathews, W.H. (1979): Radiocarbon Dates from Boone Lake and their Relation to the “Ice-free Corridor” in the Peace River District of Alberta, Canada; *Canadian Journal of Earth Sciences*, Volume 16, pages 1870-1874.
- White, J.M., Mathewes, R.W. and Mathews, W.H. (1985): Late Pleistocene Chronology and Environment of the “Ice-free Corridor” of Northwestern Alberta; *Quaternary Research*, Volume 24, pages 173-186.



TRACE ELEMENTS, MINERAL MATTER AND PHOSPHORUS IN BRITISH COLUMBIA COALS

By D.A. Grieve and M.E. Holuszko

KEYWORDS: Coal geology, coal quality, low-temperature ash, mineral matter, chlorine, fluorine, mercury, phosphorus.

INTRODUCTION

The objectives of the British Columbia Geological Survey Branch's Coal Quality Project are to collect, compile and interpret data concerning the intrinsic characteristics of the province's coal resources. Current studies fall into five categories, all of which are inter-related:

- Washability of coals — This study is concerned with the washability characteristics of coals from different seams, sites, geological formations, coalfields and regions.
- Trace elements and mineral matter in coals — This study addresses the nature of the inorganic constituents of coals, with emphasis on the trace element concentrations and mineralogy.
- Phosphorus content in coking coals — This study stems from the second, and focuses on the quantities and forms of association of this element in British Columbia coals.
- Coal petrography — Petrographic analyses to determine reflectance (rank) and maceral composition (type) of coal samples form a component of all other studies listed here. Separate petrographic studies are also underway or planned.
- Utilization potential of coals — The combination of various coal quality parameters determines the suitability of a coal for various end uses. This new study, in effect, combines and extends the data from the other studies. We are endeavouring to determine potential uses for coals from different parts of the province. The implications of the new "Alpern Classification System" (Alpern *et al.*, 1989) to our coals will also be addressed.

One planned study will be concerned with sulphur content and forms in British Columbia coals.

The current status and early results of the trace elements and phosphorus studies are outlined below. Preliminary results of the washability study are described in Holuszko and Grieve (1991, this volume).

Coals referred to in this paper are from two regions of British Columbia: the northeast or Peace River area, and the southeast or East Kootenay area (Figures 5-1-1 and 5-1-2). Peace River coals described here belong to the Gates Formation of the Lower Cretaceous Fort St. John Group. Kootenay coals belong to the Mist Mountain Formation of the Jurassic-Cretaceous Kootenay Group.

TRACE ELEMENTS AND MINERAL MATTER IN BRITISH COLUMBIA COALS

OBJECTIVES

Knowledge of the mineral matter and trace elements in coals is important for both technological and environmental reasons. For example, problems during combustion, such as slagging and fouling, are affected by the mineralogy and chemistry of the inorganic material. Determining the forms of association of minerals and elements in coal is also important. Washability of coal, for example, is affected by the forms of mineral matter association (*see* Holuszko and Grieve, 1991, this volume). Potential for improving a coal's quality with respect to concentrations of undesirable minerals or elements is also dependent on their affinity in the coal.

The aims of this study are to delineate both the amounts and forms of association of mineral matter and trace elements in British Columbia coals. These components are related, in the sense that it is impossible to discuss a trace element's associations in coals without knowing the minerals, particularly accessory minerals, present. This is because the accessory minerals usually contain a disproportionately large fraction of the trace elements in coal (Finkelman, 1980). Micron and submicron-sized inclusions of certain minerals also contain significant amounts of trace elements (Lyons *et al.*, 1990; Swaine, 1990).

To date, we have results of X-ray diffraction analysis of low-temperature ash (LTA) and analyses for the trace elements chlorine, fluorine and mercury in coal samples collected at operating coal mines in 1989 (*see* Van Den Busche and Grieve, 1990). These data have so far been evaluated with respect to the stratigraphic positions of samples. Determining the forms of association of the minerals and trace elements will be carried out at a later date.

The results of analysis of a large suite of trace elements determined by neutron activation on the same samples have yet to be received. This latter work is being carried out in conjunction with F. Goodarzi of the Geological Survey of Canada. The concentrations of phosphorus in the same samples are described in a subsequent section of this paper.

METHODS

SAMPLING

Channel samples were collected in July, 1989 at newly exposed coal faces at the following mines: Westar Mining Limited's Balmer and Greenhills operations, Esso Resources Canada Limited's Byron Creek Collieries, Crows Nest Resources Limited's Line Creek mine and Fording Coal Limited's Fording River operations in southeast Brit-

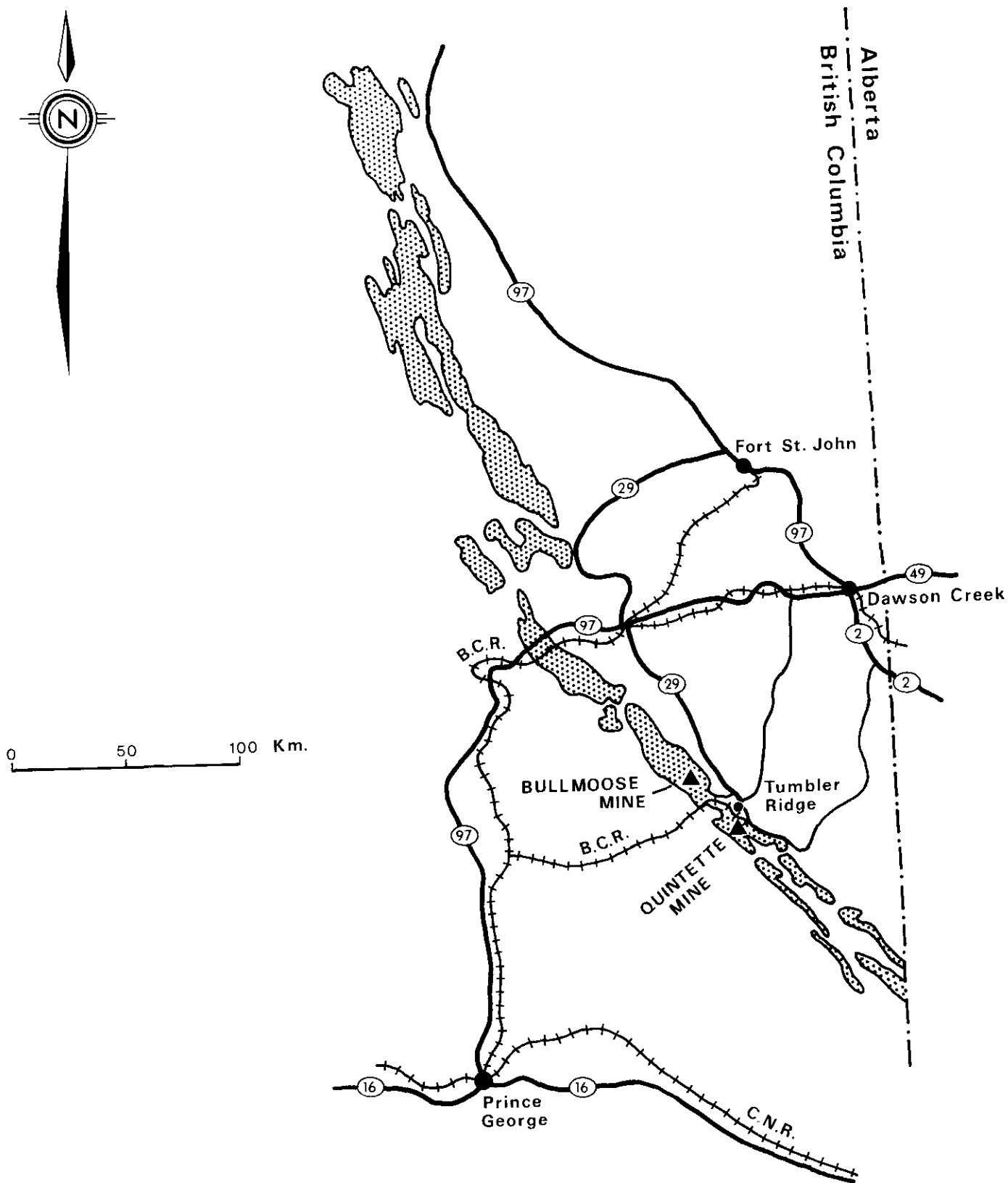


Figure 5-1-1. Distribution of coal deposits and locations of mines in the Peace River coalfield of northeastern British Columbia.

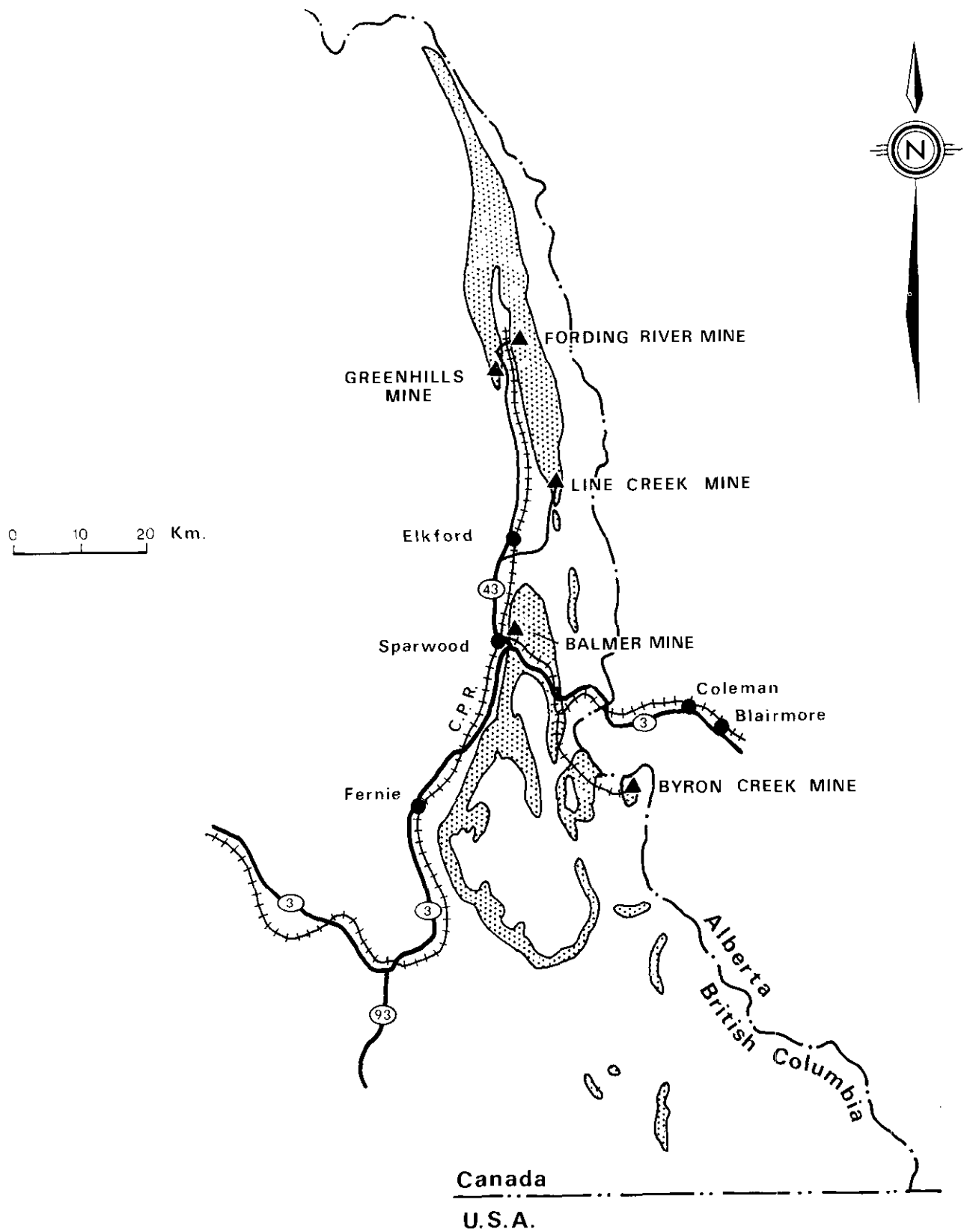


Figure 5-1-2. Distribution of coal deposits and locations of mines in the East Kootenay coalfields of southeastern British Columbia.

**TABLE 5-1-1
ASH, TRACE ELEMENTS AND PHOSPHORUS
BRITISH COLUMBIA COALS**

Sample Number	Property	Pit	Seam Name	Ash %	Cl %	F ppm (A.D. BASIS)	Hg ppb	P ₂ O ₅ %	Mineralogy of Low-Temperature Ash (LTA)
Q8901	FORDING	EAGLE	15	8.43	0.004	260	50	0.06	Quartz, kaolinite, illite/muscovite, calcite, fluorapatite, trace: - siderite?
Q8902	FORDING	EAGLE	14-9	21.18	0.009	650	130	0.27	Quartz, kaolinite, siderite, illite, pyrite
Q8903	FORDING	EAGLE	14-0	6.25	0.004	600	70	0.37	Quartz, kaolinite, goethite?, fluorapatite, siderite, trace: - pyrite, amphibole?
Q8904	FORDING	EAGLE	14-2	14.71	0.009	450	130	0.18	Quartz, kaolinite, dolomite/ankerite, illite, trace: - siderite, apatite, pyrite
Q8905	FORDING	TAYLOR	7	25.42	0.009	950	130	0.45	Quartz, kaolinite, siderite, illite, trace: - fluorapatite, pyrite?
Q8906	FORDING	TAYLOR	5	17.64	0.009	360	110	0.09	Quartz, kaolinite, illite, trace: - siderite, pyrite?
Q8907	FORDING	TAYLOR	9	19.61	0.009	750	100	0.37	Quartz, kaolinite, siderite, trace: - illite, pyrite, apatite?
Q8908	FORDING	POND	TAILINGS	21.35	0.004	470	60	0.16	Quartz, kaolinite, illite, magnetite, trace: - siderite, dolomite/ankerite, pyrite
Q8909	BYRON CREEK	12	MAMMOTH	21.71	0.004	380	80	0.07	Quartz, kaolinite, illite, calcite, dolomite/ankerite, trace: - siderite
Q8910	BYRON CREEK	51	MAMMOTH	21.32	0.007	340	50	0.08	Quartz, kaolinite, calcite, dolomite/ankerite, illite, trace: - siderite, rhodochrosite?
Q8911	BYRON CREEK	14	MAMMOTH	21.50	0.004	260	40	0.03	Quartz, kaolinite, dolomite, calcite, illite, trace: - siderite
Q8912	LINE CREEK	MAIN	10A (TOP)	55.97	0.004	680	130	0.17	Quartz, kaolinite, illite, trace: - pyrite
Q8913	LINE CREEK	MAIN	10A	26.50	0.009	320	40	0.08	Quartz, kaolinite, illite/mica, trace: - anatase
Q8914	LINE CREEK	MAIN	10A	17.32	0.009	160	30	0.03	Kaolinite, quartz, trace: - ilmenite?
Q8915	LINE CREEK	MAIN	10A	17.62	0.009	210	40	0.04	Quartz, kaolinite, trace: - illite, siderite
Q8916	LINE CREEK	MAIN	10A (BASE)	12.36	0.004	220	30	0.07	Quartz, kaolinite, trace: - siderite
Q8917	LINE CREEK	MAIN	10B (TOP)	15.49	0.013	180	30	0.02	Quartz, kaolinite, trace: - illite, siderite, calcite
Q8918	LINE CREEK	MAIN	10B	13.99	0.004	320	40	0.11	Quartz, kaolinite, calcite, trace: - siderite, pyrite, apatite
Q8919	LINE CREEK	MAIN	10B	24.86	0.007	260	30	0.05	Quartz, kaolinite, illite, trace: - siderite, anatase
Q8920	LINE CREEK	MAIN	10B	10.94	0.007	150	30	0.02	Quartz, kaolinite, trace: - calcite
Q8921	LINE CREEK	MAIN	10B (BASE)	15.80	0.011	260	40	0.03	Quartz, kaolinite, illite
Q8922	LINE CREEK	MAIN	9 (TOP)	12.62	0.009	230	50	0.06	Quartz, kaolinite, trace: - siderite, pyrite
Q8923	LINE CREEK	MAIN	9	18.34	0.009	420	30	0.09	Quartz, kaolinite, illite, fluorapatite, trace: - pyrite
Q8924	LINE CREEK	MAIN	9	12.88	0.009	500	40	0.14	Quartz, kaolinite, fluorapatite, trace: - pyrite
Q8925	LINE CREEK	MAIN	9	5.66	0.009	530	20	0.18	Quartz, kaolinite, fluorapatite, trace: - pyrite?
Q8926	LINE CREEK	MAIN	9	12.41	0.009	320	40	0.03	Quartz, kaolinite, illite, trace: - siderite
Q8927	LINE CREEK	MAIN	9	25.78	0.004	450	30	0.09	Quartz, siderite, kaolinite, trace: - illite
Q8928	LINE CREEK	MAIN	9	7.28	0.004	630	30	0.28	Quartz, kaolinite, fluorapatite, trace: - siderite, pyrite
Q8929	LINE CREEK	MAIN	9 (BASE)	22.20	0.004	470	70	0.10	Quartz, kaolinite, illite, trace: - anatase?
Q8930	LINE CREEK	MAIN	8 (TOP)	49.02	0.004	950	110	0.10	Quartz, kaolinite, illite, trace: - anatase?
Q8931	LINE CREEK	MAIN	8	13.07	0.009	800	50	0.30	Quartz, kaolinite, fluorapatite, trace: - illite, siderite
Q8932	LINE CREEK	MAIN	8	24.64	0.004	300	90	0.02	Kaolinite, quartz, trace: - illite
Q8933	LINE CREEK	MAIN	8	22.42	0.011	340	140	0.03	Kaolinite, quartz, trace: - illite
Q8934	LINE CREEK	MAIN	8	27.24	0.007	420	140	0.05	Kaolinite, quartz, trace: - siderite
Q8935	LINE CREEK	MAIN	8	8.41	0.013	400	100	0.12	Quartz, kaolinite, trace: - siderite
Q8936	LINE CREEK	MAIN	8	15.37	0.004	270	50	0.06	Kaolinite, quartz, trace: - siderite, illite
Q8937	LINE CREEK	MAIN	8	11.63	0.009	240	100	0.04	Quartz, kaolinite, siderite
Q8938	LINE CREEK	MAIN	8	24.81	0.009	370	40	0.02	Quartz, kaolinite, illite, siderite, trace: - anatase?
Q8939	LINE CREEK	MAIN	8	11.15	0.007	200	180	0.03	Quartz, kaolinite, siderite, trace: - fluorapatite, anatase?
Q8940	LINE CREEK	MAIN	8	17.34	0.009	600	40	0.26	Quartz, kaolinite, illite, fluorapatite, trace: - siderite?
Q8941	LINE CREEK	MAIN	8	13.40	0.007	360	70	0.15	Quartz, kaolinite, trace: - siderite, apatite, pyrite?
Q8942	LINE CREEK	MAIN	8	13.37	0.009	200	60	0.05	Kaolinite, quartz, trace: - dolomite/ankerite, siderite, anatase?
Q8943	LINE CREEK	MAIN	8	10.88	0.011	1350	70	0.78	Quartz, kaolinite, fluorapatite, trace: - siderite?
Q8944	LINE CREEK	MAIN	8	12.44	0.004	470	30	0.21	Quartz, kaolinite, fluorapatite, trace: - illite
Q8945	LINE CREEK	MAIN	8	19.77	0.009	240	50	0.04	Kaolinite, quartz, trace: - illite
Q8946	LINE CREEK	MAIN	8	17.21	0.004	350	80	0.07	Kaolinite, quartz, trace: - illite, siderite
Q8947	LINE CREEK	MAIN	8	13.07	0.011	430	50	0.16	Siderite, kaolinite, quartz, trace: - apatite?
Q8948	LINE CREEK	MAIN	8 (BASE)	56.54	0.011	950	140	0.06	Quartz, kaolinite, illite, trace: - pyrite, anatase?
Q8949	GREENHILLS	BLACKTAIL	25 EAST	7.63	0.007	340	10	0.08	Quartz, kaolinite, illite, trace: - Siderite, pyrite?, apatite?
Q8950	GREENHILLS	BLACKTAIL	16	16.84	0.009	410	90	0.09	Quartz, kaolinite, illite, trace: - pyrite, apatite
Q8951	GREENHILLS	N COUGAR	22 UPPER	6.12	0.011	310	40	0.08	Quartz, kaolinite, anatase?, trace: - siderite, apatite?
Q8952	GREENHILLS	BLACKTAIL	20 UPPER	32.72	0.009	750	50	0.13	Quartz, kaolinite, illite, siderite, trace: - pyrite, apatite, anatase?
Q8953	GREENHILLS	FALCON	1	9.25	0.004	430	40	0.19	Quartz, kaolinite, siderite, trace: - apatite, pyrite?
Q8954	GREENHILLS	FALCON	3	19.25	0.013	730	70	0.31	Quartz, kaolinite, siderite, trace: - pyrite, apatite?, illite
Q8955	BALMER	CAMP 8 EX	7R1	23.94	0.013	810	80	0.39	Quartz, kaolinite, illite, siderite, trace: - apatite, pyrite?
Q8956	BALMER	CAMP 8 EX	7RX	32.06	0.013	700	150	0.26	Quartz, kaolinite, illite, trace: - siderite, pyrite

TABLE 5-1-1
ASH, TRACE ELEMENTS AND PHOSPHORUS
BRITISH COLUMBIA COALS — Continued

Sample Number	Property	Pit	Seam Name	Ash	Cl	F	Hg	P ₂ O ₅	Mineralogy of Low-Temperature Ash (LTA)
				%	%	ppm (A.D. BASIS)	ppb	%	
Q8957	BALMER	CAMP 8 EX	7S	25.96	0.015	600	70	0.26	Quartz, kaolinite, illite, siderite, trace: - apatite, pyrite
Q8958	BALMER	CAMP 8 EX	8UX	34.74	0.015	1090	90	0.52	Quartz, kaolinite, illite, siderite, trace: - fluorapatite, pyrite, anatase?
Q8959	BALMER	BALDY 3, 4	4	24.83	0.022	680	110	0.27	Quartz, kaolinite, illite, trace: - fluorapatite, pyrite, siderite?
Q8960	BALMER	ADIT29E	8UC	28.03	0.013	610	80	0.27	Quartz, kaolinite, illite, siderite, trace: - dolomite?
Q8961	BALMER	POND	TAILINGS	38.28	0.018	660	100	0.15	Quartz, kaolinite, illite, trace: - dolomite/ankerite, siderite, pyrite?
Q8962	QUINTETTE	WOLVERINE	J3	13.77	0.015	230	40	0.03	Quartz, kaolinite, siderite, illite, trace: - apatite?
Q8963	QUINTETTE	WOLVERINE	G2	16.31	0.018	260	40	0.12	Quartz, kaolinite, dolomite/ankerite, trace: - siderite
Q8964	BULLMOOSE		A2	12.51	0.040	200	60	0.04	Quartz, kaolinite, siderite (manganous), dolomite/ankerite
Q8965	BULLMOOSE		B	11.05	0.031	190	180	0.07	Dolomite, quartz, calcite, kaolinite, trace: - pyrite, plagioclase?
Q8966	BULLMOOSE		A1	21.34	0.035	460	80	0.02	Quartz, kaolinite, illite, dolomite, pyrite
Q8967	BULLMOOSE		C	28.13	0.022	690	150	0.26	Quartz, illite/muscovite, kaolinite, dolomite/ankerite, trace: - pyrite, magnetite?
Q8968	BULLMOOSE		D	22.14	0.018	470	60	0.12	Quartz, kaolinite, dolomite, illite, trace: - pyrite, magnetite?
Q8969	BULLMOOSE		E	21.68	0.018	580	50	0.13	Quartz, kaolinite, illite, trace: - dolomite, pyrite, siderite, apatite?

Note: All results are based on raw coal samples and are not representative of clean, product coals.

ish Columbia; and Denison Mines Limited's Quintette mine and Teck Corporation's Bullmoose mine in northeast British Columbia (Figures 5-1-1 and 5-1-2; Table 5-1-1; see also Van Den Bussche and Grieve, 1990). The actual sample sites were chosen on the basis of availability on the day of sampling; consequently we were not able to acquire equal representation of the entire coal-bearing formation at all locations.

An attempt was made to make each sample as representative as possible, although at some locations, most notably at Byron Creek with its thick Mammoth seam, this was difficult. Of the total of 69 samples, 30 represent entire seams and were collected at all locations except Line Creek. At this last location, each of four seams was sampled on a ply-by-ply basis, in average intervals 0.50 metre thick, for a total of 37 samples (Table 5-1-1). In addition, one grab sample of tailings material (fine plant rejects) was taken at each of the Balmer and Fording mine sites.

SAMPLE PROCESSING

Sample drying, crushing, riffing and screening were carried out at a commercial laboratory in accordance with ASTM procedures (see Van Den Bussche and Grieve, 1990). A representative split of minus-60 mesh material was supplied to the authors for low-temperature ashing.

TRACE ELEMENT (Cl, F, Hg) DETERMINATIONS

Concentrations of chlorine, fluorine and mercury in whole coal were carried out by a commercial laboratory in accordance with the following standard procedures:

- Chlorine determinations were done by burning with Eschka mixture (ASTM D2361). The detection limit is 0.001 per cent by weight.

- Fluorine determinations were carried out using the oxygen-bomb digest method (ASTM D3761). The detection limit is 20 ppm.

- Mercury determinations were also carried out using the oxygen-bomb digest method (ASTM D3761). The detection limit is 1.0 ppb.

LOW-TEMPERATURE ASHING

Low-temperature ashing of coal using radio-frequency-generated (RF) oxygen plasma is a routine method of producing an ash with the original minerals essentially preserved (see for example, Miller *et al.*, 1979). The Branch's plasma asher is an LFE Corporation model LTA-504, which uses an RF power supply that operates at 13.56 megahertz. Five to ten grams of minus 60 mesh coal is placed in a silica sample boat. One boat is placed in each of the four 10-centimetre-diameter reaction chambers, which are then evacuated using a vacuum pump. Ashing is done using 200 watts total RF power (50 watts per chamber), and a total oxygen bleed-rate of about 30 cubic centimetres per minute. Samples are left exposed to the oxygen plasma round-the-clock, for a total of about 72 hours. They are stirred twice a day using a glass rod, in order to bring unreacted coal to the surface. At the end of the reaction process a small amount, less than 1 per cent (estimated) per volume, of unreacted organic material is left in the residue. This is assumed to be made up of inertinite. Low-temperature ashes are ground using an agate mortar and pestle, prior to X-ray diffraction analysis.

RESULTS

All results are reported on raw coals, and are not considered representative of product coals.

MINERAL MATTER

Lists of minerals in the low-temperature ashes (in relative order of abundance detected) are given in Table 5-1-1. Quartz and kaolinite are ubiquitous and are the most abundant minerals in almost all cases. Lesser and trace amounts of illite, illite/mica, calcite, apatite (mainly fluorapatite), siderite, pyrite and dolomite/ankerite were also detected. Tentatively or rarely identified minerals, which appear mainly in trace amounts, include anatase, ilmenite, magnetite, amphibole (species not identified), rhodochrosite and goeite.

There are no obvious differences between the mineral suites from the two regions of the province, with one possible exception. It appears that apatite is more commonly recognized in samples from southeast British Columbia. Within each region there are no obvious differences between the mineral suites from the various mine sites. The various seams at each site also do not appear, at first inspection, to be markedly different, and trends in variation within the seams at Line Creek are not apparent. Closer analysis may reveal systematic variations on some scale. The suites of minerals from the two tailings samples (Samples 8 and 61) are indistinguishable from those in the raw coals.

CHLORINE

Chlorine contents, on an air-dried basis, in the coal samples from southeast British Columbia (excluding the two tailings samples) range from 0.004 to 0.022 per cent, with a mean of 0.0084 (Table 5-1-1). There are no consistent trends in chlorine variation throughout either the Mist Mountain Formation (Figure 5-1-3A), or within individual coal seams at Line Creek (Figure 5-1-3B).

Chlorine values in samples from northeast British Columbia, with a range of 0.015 to 0.035 and a mean of 0.025 per cent, are somewhat higher than those from the southeast. There does not appear to be a trend in chlorine values throughout the coal-bearing section of the Gates Formation (Figure 5-1-3C).

FLUORINE

Values of fluorine concentrations, on an air-dried basis, in samples of coal from southeast British Columbia (excluding the two tailings samples) range from 150 to 1350 ppm and have a mean value of 475 ppm (Table 5-1-1). Lowest fluorine values appear to be associated with the base and top of the Mist Mountain Formation (Figure 5-1-4A). There are no consistent trends in fluorine values within individual coal seams at Line Creek (Figure 5-1-4B).

Values in samples from northeast British Columbia are very similar to those in samples from the southeast region. The range of concentrations is from 190 to 690 ppm, and the mean is 385 ppm. No systematic variation in fluorine contents with stratigraphic position is apparent within the Gates Formation coals (Figure 5-1-4C).

A cursory inspection of Table 5-1-1 suggests that some of the samples containing the highest fluorine values also contain relatively high amounts of phosphorus, and are likely to contain fluorapatite in their low-temperature ashes.

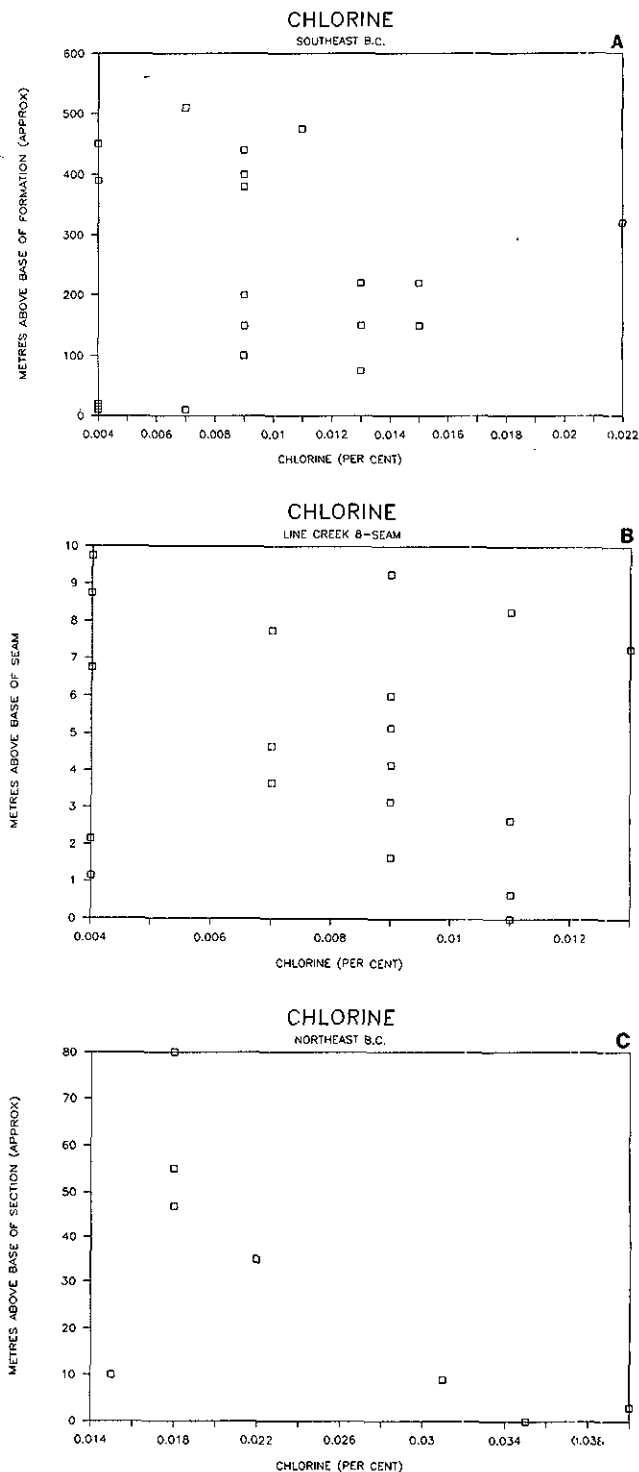


Figure 5-1-3. Variations in concentrations of chlorine in coal with stratigraphic position in southeast and northeast British Columbia. All results are based on raw coal samples and are not representative of clean, product coals.

Samples 43 and 58 from the southeast are good examples. This may be significant, but we cannot be sure until correlation analysis is carried out.

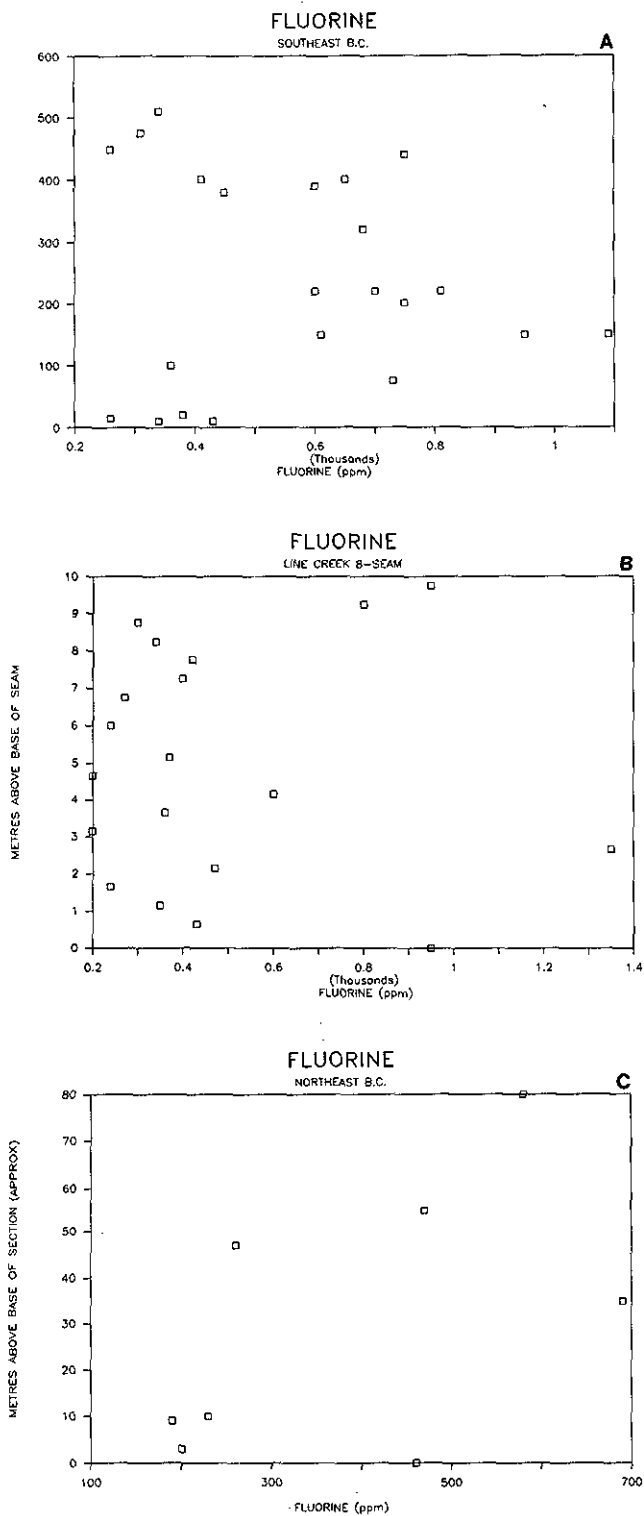


Figure 5-1-4. Variations in concentrations of fluorine in coal with stratigraphic position in southeast and northeast British Columbia. All results are based on raw coal samples are not representative of clean, product coals.

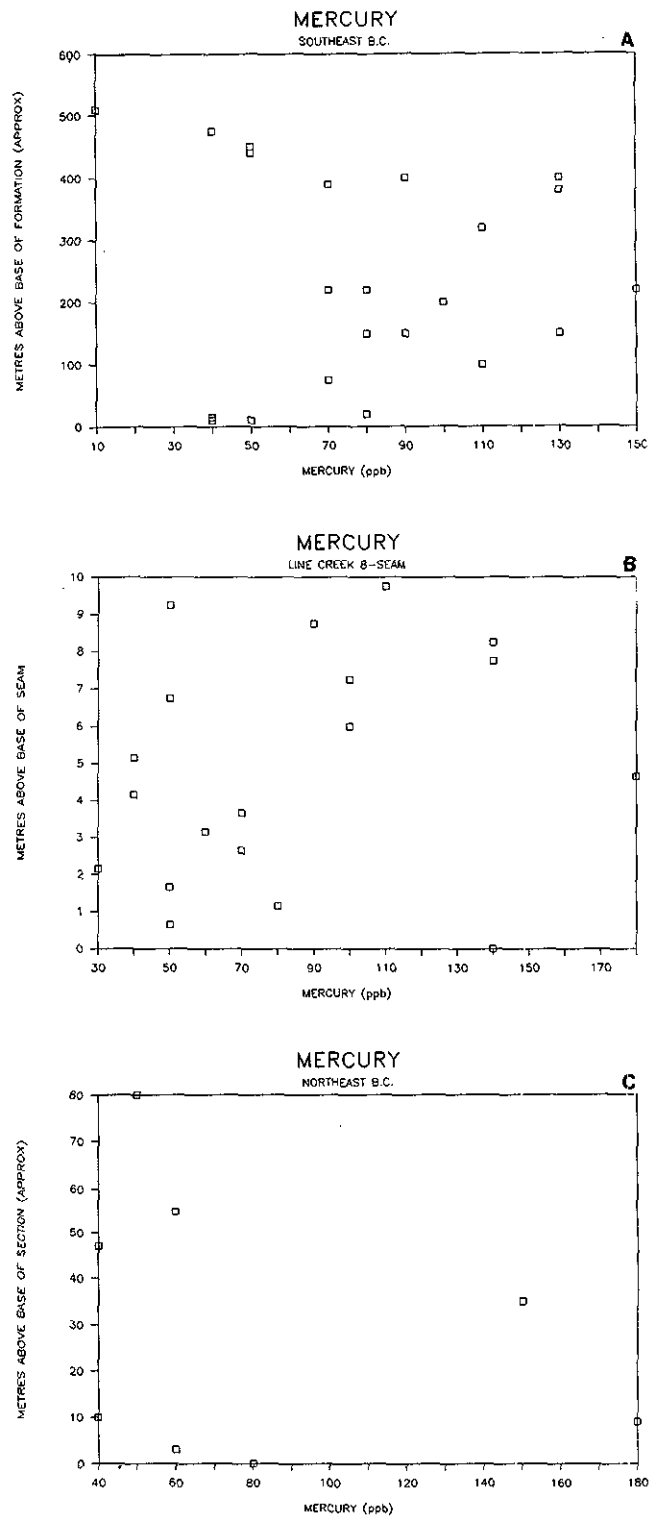


Figure 5-1-5. Variations in concentrations of mercury in coal with stratigraphic position in southeast and northeast British Columbia. All results are based on raw coal samples are not representative of clean, product coals.

MERCURY

Mercury concentrations, on an air-dried basis, in the samples from southeast British Columbia (excluding the two tailings samples) range from 10 to 180 ppb, with an average of 70 (Table 5-1-1). As was the case with fluorine, mercury values in the Mist Mountain Formation appear to be lowest at the base and top of the formation (Figure 5-1-5A). No trends within coal seams at Line Creek are observed (Figure 5-1-5B).

Values of mercury in samples from northeast British Columbia are very similar, with a range of 40 to 180 ppb, and a mean of 83 ppb. Again, no stratigraphic trends are observed in Gates Formation coals (Figure 5-1-5C).

DISCUSSION

The predominance of quartz and kaolinite in the low-temperature ashes of samples from southeast and northeast British Columbia in this study is consistent with nonmarine depositional conditions (see Pearson, 1980). This is also consistent with the generally low sulphur content of coals of the Gates and Mist Mountain formations (see British Columbia Geological Survey Branch Information Circulars 1989-22, *British Columbia Coal Quality Catalog*, and 1990-5, *British Columbia Coal Specifications*).

The origins of the various mineral species identified in these coals will not be delineated until forms of association are determined. Minerals in coal are both syngenetic and epigenetic.

Overall, chlorine values in the samples from both regions are relatively low. Finkelman, for example, cites 0.0629 per cent as the average of over 600 coal samples from the Appalachian region of the United States. Swaine (1990, page 101) suggests the probable range in chlorine values in most world coals is 0.005 to 0.2 per cent.

The causes of the difference between chlorine contents in samples from the two regions is not known at this time. Chlorine in coal can be an indicator of marine influence (Finkelman, 1980). A subtle marine influence (*i.e.* a slight brackishness) may be indicated for the Gates Formation coals of northeast British Columbia. Lamberson *et al.* (1990) state that although predominantly nonmarine conditions prevailed during deposition of the Gates Formation coal sequence, the paleoshoreline was situated just north of the Bullmoose mine site. Goodarzi (unpublished data) has inferred a slightly brackish depositional environment for coals of the Gates Formation in northeastern British Columbia, on the basis of geochemical data.

On the other hand, chlorine in coal has also been found to be sensitive to current groundwater chemistry (Gluskoter and Ruch, 1971), in which case the data do not reflect solely the depositional conditions.

No chloride minerals were found in the low-temperature ashes of samples used in this study. Minerals in coal which may contain chlorine include some clays and apatites (Finkelman, 1980). Finkelman (page 144) concluded, however, that it is possible that much of the chlorine in coals is associated with organic matter. Further study of these samples will be needed to discern its mode of occurrence.

Average values of fluorine in these British Columbia coals fall within the probable range of most world coals (20 to 500 ppm, Swaine, 1990, page 113). Some of the fluorine in these samples must reside in fluorapatite, which was detected in many of the low-temperature ashes, including some of those with the highest phosphorus contents, as noted above. This association, together with corresponding high phosphorus values, has been noted in other parts of the world (Gluskoter *et al.*, 1977; Finkelman, 1980). Finkelman notes that fluorine may have a very complex association in coals, although a strong organic affinity is not likely. Future work will delineate the forms of association of fluorine in these samples.

These coals appear to contain relatively low average mercury values when compared with the probable range of most world coals (20 to 1000 ppb, Swaine, 1990, page 133), and the mean of American coals (180 ppb, Swanson *et al.*, 1976, in Finkelman, 1980). It is not possible, at this stage, to speculate on the modes of occurrence of mercury in these samples. Finkelman (1980, page 177) notes that there is good evidence that a "significant proportion" of the mercury in coal is associated with pyrite. The scarcity of pyrite in these samples may then account for the relatively low mercury levels.

FUTURE PLANS

Coal petrographic analysis will be applied to these samples to determine both maceral compositions and forms of association of the minerals visible at standard magnification.

Results yet to be received include further trace element analyses carried out by neutron activation. This work is being done in conjunction with F. Goodarzi of the Geological Survey of Canada. When these data are available they will be treated in the same way as described here for chlorine, fluorine and mercury.

Further interpretation of all trace element data will focus on the forms of association of each element within the coals. This will involve, at the first stage, looking for correlations between each element and other fundamental parameters, especially the amount of ash, low-temperature ash mineralogy and maceral composition, and also between the various elements. At a later stage, samples will be subjected to scanning electron microscopy to refine the understanding of the modes of occurrence of both elements and minerals.

PHOSPHORUS IN BRITISH COLUMBIA COKING COALS

OBJECTIVES

Phosphorus can be an undesirable element in coking coals because of its potential to impart a brittle quality to steel. Other variables in this phenomenon include the phosphorus content of the iron ore, and the actual steel-making process used. Generally, eastern North American steel producers are more concerned about the amount of phosphorus in coals than are Asian producers, our traditional coking coal purchasers. Thermal coal users may also be concerned about phosphorus content in feedstocks.

The aims of this study are essentially identical to those of the previous study concerned with trace elements. We intend to determine the amount of phosphorus in British Columbia coals, and the nature of its association. To date we have the results of P_2O_5 analyses on the same coal samples referred to in the previous section. These have been evaluated with respect to variations in stratigraphic position.

In addition, the Branch's coal exploration assessment report files contain phosphorus concentration data determined by exploration companies. These data will be used, where not confidential, to complement phosphorus data described here.

METHODS

This study utilizes the same samples as the previous study on trace elements. Sampling and processing procedures were identical. Phosphorus contents were determined as P_2O_5 in coal in per cent by ASTM method D2795. The detection limit is 0.01 per cent.

RESULTS

All results are reported on raw coals, and are not considered representative of product coals.

Phosphorus contents, on an air-dried basis, in the coal samples from southeast British Columbia (excluding the two tailings samples) range from 0.02 to 0.78 per cent P_2O_5 , with a mean of 0.156 (Table 5-1-1). Phosphorus values are lowest at the base and top of the Mist Mountain Formation (Figure 5-1-6A). There are no clear trends within any of the four seams sampled at Line Creek (Figure 5-1-6B).

Phosphorus values from northeast British Columbia samples are in general lower than those from the southeast. The range is from 0.02 to 0.26 per cent P_2O_5 , and the mean is 0.099. There is a general increase in P_2O_5 concentrations up-section in the Gates Formation coal-bearing section, although the highest value occurs in a sample from the middle part of the section (Figure 5-1-6C).

As noted earlier, data in Table 5-1-1 suggest that some of the samples containing the highest P_2O_5 values also contain relatively high amounts of fluorine, and are likely to contain fluoroapatite in their low-temperature ashes.

DISCUSSION

Average phosphorus contents in raw British Columbia coking coals from both the Northeast and Southeast fall well within the probable range for most world coals (0.0023 to 0.69 per cent P_2O_5 , Swaine, 1990, page 140). The reason for the contrast between phosphorus contents from the two regions of the province is not known, although it is probably related to the more common occurrence of apatite in the southeast coals.

There is considerable disagreement in the literature concerning the modes of association of phosphorus in coal. Finkelman (1980, page 191) concludes that "substantial amounts of the phosphorus in many coals occur in rare-earth phosphates and/or apatite. The proportion of organically bound P is still to be determined." Certainly the common

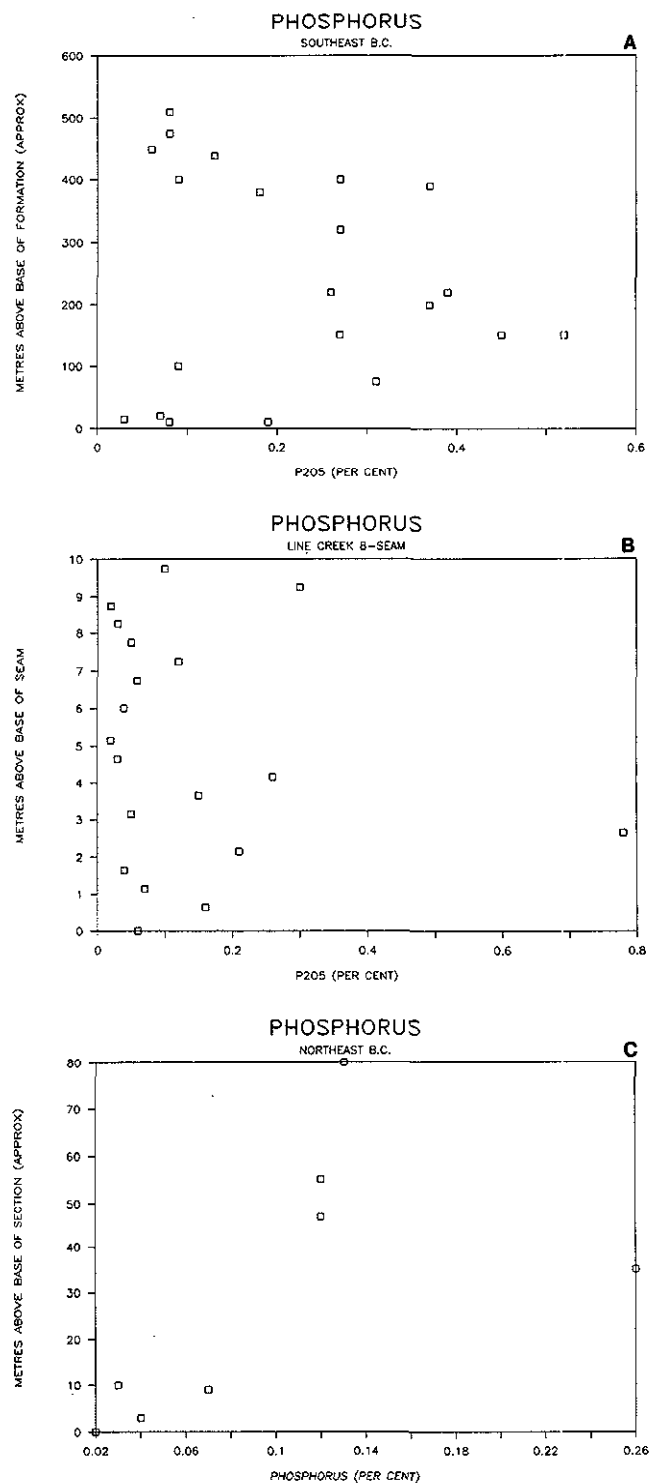


Figure 5-1-6. Variations in concentration of P_2O_5 in coal with stratigraphic position in southeast and northeast British Columbia. All results are based on raw coal samples and are not representative of clean, product coals.

occurrence of apatite and fluoroapatite in these coals, together with the observed correlation of phosphorus and fluorine in certain samples, argues for an inorganic association for a significant portion of the phosphorus. The tenta-

tive identification of gorceixite $(\text{Ba,Ca})\text{Al}_3(\text{PO}_4)_2(\text{OH})_5 \cdot \text{H}_2\text{O}$ in the low-temperature ash of one sample is further proof.

Studies of tonsteins in the southeast British Columbia coalfields (Grieve, 1984 and in preparation; Goodarzi *et al.*, 1990) have indicated that high phosphorus contents of many tonsteins are related to the presence of gorceixite and apatite. It is conceivable that some of the phosphorus observed in coal samples has a similar source to that contained in tonsteins. One of the likely sources of the tonsteins (Grieve, in preparation) is volcanic ash or reworked volcanic ash.

FUTURE PLANS

As in the case of the trace element study, future work will focus on the forms of association of phosphorus in coals. Correlations between phosphorus and ash content, maceral composition, and other elements of known affinity (for example, sulphur) will be determined, on both the data derived from these samples, and those compiled from the coal assessment reports. At a later stage, scanning electron microscopy will be used.

ACKNOWLEDGMENTS

We wish to express our gratitude to the geology staff at all of the province's coal mines, for their help and cooperation. Colleagues Barry Ryan and Ward Kilby read an earlier version of this paper.

REFERENCES

- Alpern, B., Lemos de Sousa, M.J. and Flores, D. (1989): A Progress Report on the Alpern Coal Classification; *International Journal of Coal Geology*, Volume 13, pages 1-19.
- Finkelman, R.B. (1980): Modes of Occurrence of Trace Elements in Coal; unpublished Ph.D. thesis, *University of Maryland*, 301 pages.
- Gluskoter, H.J. and Ruch, R.R. (1971): Chlorine and Sodium in Illinois Coals as Determined by Neutron Activation Analyses; *Fuel*, Volume 50, pages 65-76.
- Gluskoter, H.J., Ruch, R.R., Miller, W.G., Cahill, R.A., Dreher, G.B. and Kuhn, J.K. (1977): Trace Elements in Coal: Occurrence and Distribution; *Illinois State Geological Survey*, Circular 499.
- Goodarzi, F., Grieve, D.A. and Labonté, M. (1990): Petrological, Mineralogical and Elemental Composition of Tonsteins in Relation to the Origin and Degree of Physical and Chemical Alteration in the East Kootenay Coalfields, Southeastern British Columbia; *Energy Sources*, Volume 12, pages 265-295.
- Grieve, D.A. (1984): Tonsteins: Possible Stratigraphic Correlation Aids in East Kootenay Coalfields; *B.C. Ministry of Energy, Mines and Petroleum Resources*, Geological Fieldwork 1983, Paper 1984-1, pages 36-41.
- Grieve, D.A. (in prep.): Geology and Rank Distribution of the Elk Valley Coalfield, Southeastern British Columbia; *B.C. Ministry of Energy, Mines and Petroleum Resources*, Bulletin.
- Holuszko, M.E. and Grieve, D.A. (1991): Washability Characteristics of British Columbia Coals; *B.C. Ministry of Energy, Mines and Petroleum Resources*, Geological Fieldwork 1990, Paper 1991-1 (this volume).
- Lamberson, M.N., Bustin, R.M., Kalkreuth, W. and Pratt, K.C. (1990): Lithotype Characteristics and Variation in Selected Coal Seams of the Gates Formation, Northeastern British Columbia; *B.C. Ministry of Energy, Mines and Petroleum Resources*, Geological Fieldwork 1990, Paper 1990-1, pages 461-468.
- Lyons, P.C., Morelli, J.J., Hercules, D.M., Lineman, D., Thompson-Rizer, C.L. and Dulong, F.T. (1990): The Laser Microprobe Mass Analyser for Determining Partitioning of Minor and Trace Elements Among Intimately Associated Macerals: An Example from the Swallow Wood Coal Bed, Yorkshire, U.K.; *Fuel*, Volume 69, pages 771-775.
- Miller, R.N., Yarzab, R.F. and Given, P.H. (1979): Determination of the Mineral-matter Contents of Coals by Low-temperature Ashing; *Fuel*, Volume 58, pages 4-10.
- Pearson, D.E. (1980): The Quality of Western Canadian Coking Coal; *Canadian Institute of Mining and Metallurgy*, Bulletin, Volume 73, pages 70-84.
- Swaine, D.J. (1990): Trace Elements in Coal; *Butterworths*, London, 278 pages.
- Van Den Bussche, B.G. and Grieve, D.A. (1990): Phosphorus in British Columbia Coking Coals; *B.C. Ministry of Energy, Mines and Petroleum Resources*, Geological Fieldwork 1989, Paper 1990-1, pages 427-430.

WASHABILITY CHARACTERISTICS OF BRITISH COLUMBIA COALS

By M.E. Holuszko and D.A. Grieve

KEYWORDS: Coal geology, coal quality, washability, sink-and-float tests, degree of washing, washability number, mineral matter, lithotypes.

INTRODUCTION

As part of the British Columbia Geological Survey Branch's Coal Quality Project, washability characteristics of coals from all parts of the province are being compiled (see manuscript 5-1, this volume, for descriptions of other ongoing coal quality studies). The interpretation of these data will provide insight into the geological basis of washability, and hopefully provide practical information which will aid in the assessment and exploitation of our coal resources.

Coals described in this paper are from the Peace River coalfield of northeastern British Columbia. They occur in the Gates Formation of the Lower Cretaceous Fort St. John Group.

BACKGROUND

Washability is an essential factor in any coal seam or property evaluation. Washability provides practical information on those characteristics of coal that affect recovery, beneficiation and final use. It often determines the economic feasibility of a coal deposit.

In an assessment of any coal it is necessary to categorize it according to its rank, type and grade. Rank and type are related to the organic matter composing the coal, whereas grade refers to the quality of coal in terms of size and ash content. Washability analyses are carried out to determine how much coal, of what quality (in terms of grade), can be produced at a given specific gravity, or what the separation gravity should be to achieve desired coal quality.

Washability characteristics of a coal provide information to the design of the coal preparation processes. Most of the coal upgrading processes rely on gravity separation methods. This is because there is a significant difference in specific gravity between coal organic material (at any given rank of coal) and its associated mineral matter (specific gravity for macerals is 1.1 to 1.45, and for mineral matter is 2.0 to 5.0). Depending on the association between the coal macerals and mineral matter, the process of separating high-ash particles from low-ash particles may be easy or difficult. In general, the density of unliberated coal particles is proportional to the content of mineral matter.

Washability curves are constructed from sink-and-float analysis of a representative coal sample, carried out under ideal conditions, and are characterized by ash content and yield at a given density of separation. They are the best possible prediction of theoretical results for the gravity-based coal preparation processes.

MINERAL MATTER

The type and mode of occurrence of mineral matter in coal is particularly important to washability. The amount of inorganic matter associated with macerals has direct influence on the density of composite coal particles, while the type of minerals, and their association with the coal macerals, will have direct impact on the ease of gravity separation.

The mineral matter in coal occurs as inorganic matter from the original plant material, detrital particles and authigenic deposits associated with the first stage of coalification, or as deposits associated with the second stage of coalification after consolidation of the coal (Stach *et al.*, 1982, pages 153-171). The minerals which have formed together with the coal, or authigenically, are referred to as syngenetic, whereas the minerals formed later are commonly called epigenetic. The syngenetic minerals tend to be fine grained and are intimately intergrown with the coal, whereas epigenetic minerals occur in the cracks and fissures of macerals.

Minerals deposited in cleats and fissures are easier to remove by means of crushing and washing operations. Liberation of this type of mineral matter is relatively easy and results in good density separation between clean coal and shale particles, with very small amounts of middlings.

Syngenetic minerals occur either as finely disseminated mineral particles or in the form of larger species intimately intergrown with coal macerals. In western Canadian coals, pyrite occurs predominately in the latter form, whereas

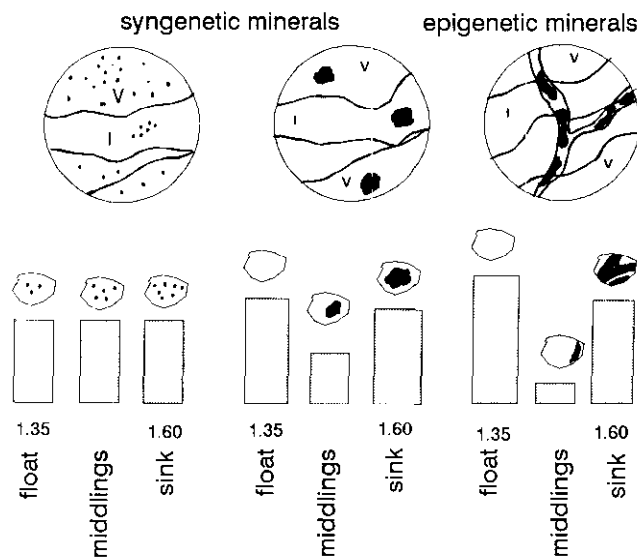


Figure 5-2-1. Types of mineral matter association and its effect on the washability. Adapted from Falcon and Falcon (1983).

**TABLE 5-2-1
COAL INORGANIC IMPURITIES**

Type	Origin	Examples	Physical Separation
Strongly chemically bonded elements	From coal-forming organic tissue material	Organic sulphur, nitrogen	No
Adsorbed and weakly bonded groups	Ash-forming components in pure water, adsorbed on the coal surface	Various salts	Very limited
Mineral matter			
a. Epiclastic	Minerals washed or blown into the sea during its formation	Clays, quartz	Partly separable by physical methods
b. Syngenetic	Incorporated into coal from the very earliest peat-accumulation stage	Pyrite, siderite, some clay minerals	Intimately intergrown with coal macerals
c. Epigenetic	Stage subsequent to syngenetic; migration of the mineral-forming solutions through coal fractures	Carbonates, pyrite, kaolinite	Vein type mineralization; epigenetic minerals concentrated along cleats, preferentially exposed during breakage; separable by physical methods

clays are found in both forms. Coals with fine syngenetic minerals will produce relatively equal amounts of light-density clean coal, middlings and high-density rejects when subjected to gravity separation. In this case liberation of the mineral matter can only be achieved by fine grinding.

Coarser syngenetic minerals display much better washability characteristics. Better washing characteristics are mainly due to greater degree of liberation of coarse minerals from coal. Figure 5-2-1 shows the type of mineral association and its effect on the washability. Table 5-2-1 presents the types of mineral phases in coal and their relation to physical separation.

LITHOTYPES

Another factor which contributes to the washability is the lithotype composition of the seam. Lithotypes are defined as the macroscopic bands of different types of coal in a given seam (ICCP Handbook of Coal Petrology, 1963; Stach *et al.*, 1982, page 376). The formation of various lithotypes is mainly a result of diverse environmental conditions at the time of deposition and subsequently differing rates of subsidence of a swamp. The composition of lithotypes is strongly dependent on the maceral make-up as well as their association with different proportions of mineral matter (*e.g.* Diesel, 1965). It is also known that different lithotypes are characterized by different density and hardness (Falcon and Falcon, 1987; Hower, 1988; Hower and Lineberry 1988; Hower *et al.*, 1987; Hsieh, 1976 in Hower *et al.*, 1987), the latter measured as the Hardgrove Grindability Index (HGI). It is expected that lithotype composition for a given rank of coal will influence the process of liberation of minerals as well as the density separation and washability characteristics.

Among lithotypes from the same coal, durain is the toughest and the hardest and would concentrate in the largest size fractions, whereas vitrain tends to be brittle and reports to the fines. Fusain is the most friable and concentrates in the dust, unless it is mineralized, in which case it will report to the coarse coal. Clarain is more resistant than vitrain and its hardness will depend on the thickness of lipinite bands or inherent mineral matter (Hower, 1988) For

any sized run-of-mine or bulk composite sample, different lithotypes will be found in different size fractions (Stach *et al.*, 1982, page 415). Since the washability tests are performed on different sizes, it is important to realize that washability will be controlled to some extent by the lithology of the seam.

Lithotypes also vary in density. Vitrain has the lowest density, unless contaminated with mineral matter, fusain is the next lightest, while clarain and durain, depending on their maceral and mineral composition, are the heaviest (Falcon and Falcon, 1987). Size fractions containing an abundance of one or the other lithotype will tend to have different washing characteristics as the washability depends on density. Figure 5-2-2 illustrates the effect of the microlithotype composition on washing characteristics (Falcon and Falcon, 1983). Microlithotypes form bands of lithotypes on the macroscopic scale.

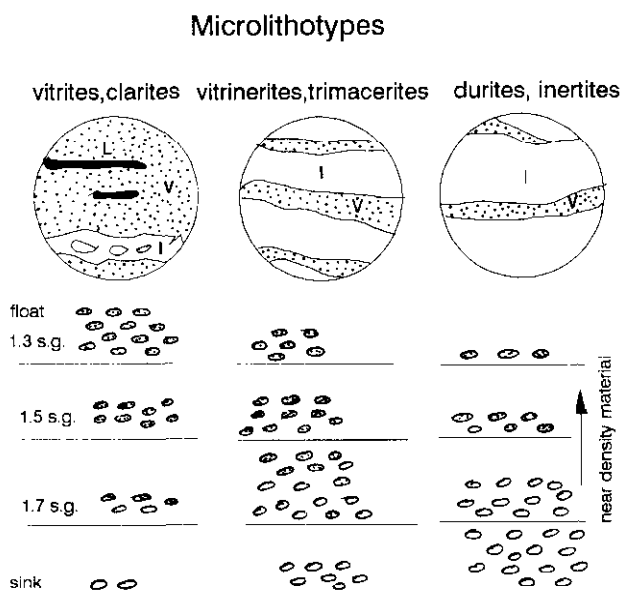


Figure 5-2-2. The effect of the microlithotype composition on the washability. Adapted from Falcon and Falcon (1983).

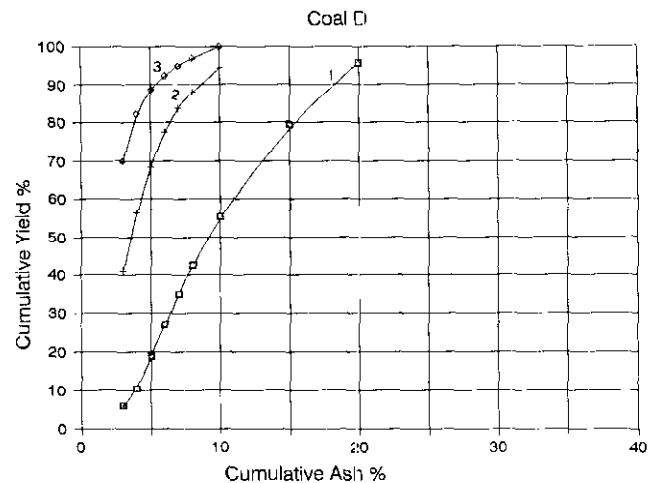
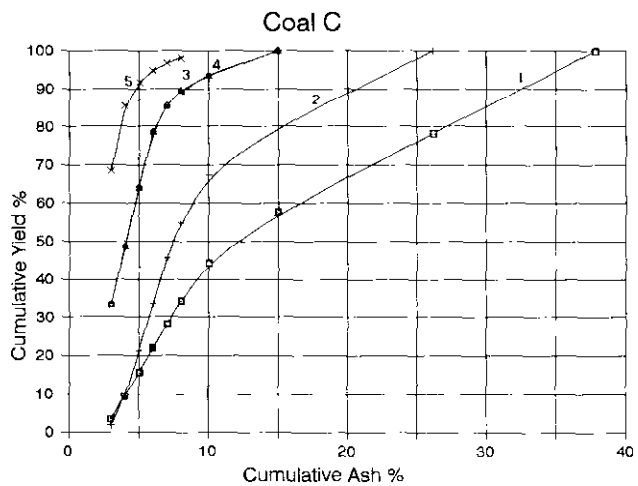
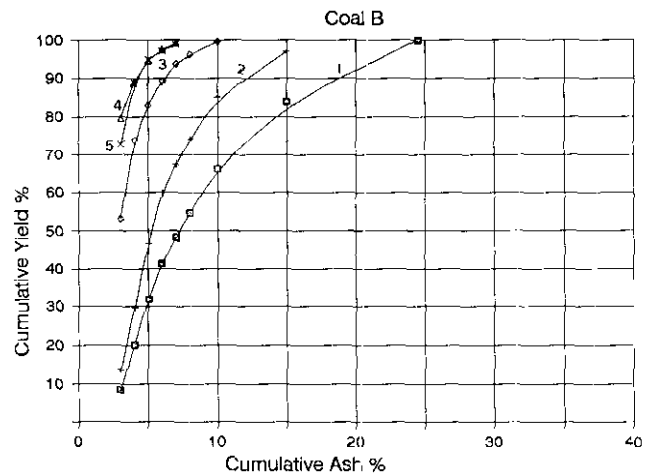
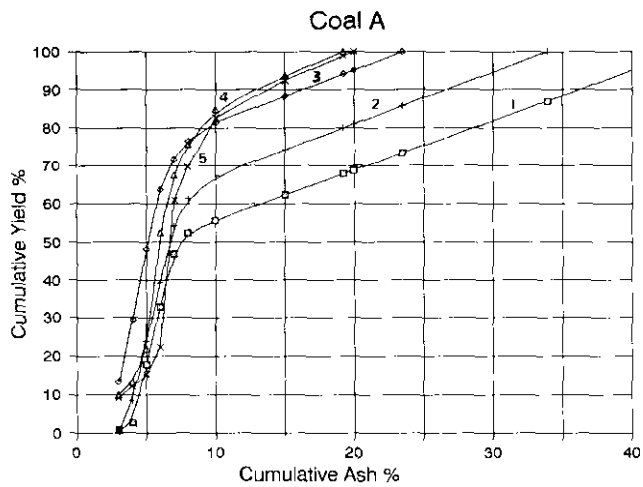


Figure 5-2-3. Plots of cumulative ash per cent versus cumulative yield per cent for different size fractions from four different British Columbia coals, referred to as A, B, C and D. For coals A, B and C size fraction 1 = 50-19 millimetres, 2 = 19-6.3 millimetres, 3 = 6.3-0.6 millimetres, 4 = 0.6 - 0.3, and 5 = 0.3-0.15 millimetre. For coal D size fraction 1 = 75-12.5 millimetre, 2 = 12.5-0.5 millimetres, and 3 = 0.5-0.15 millimetre.

Plots of ash in clean coal versus yield, for four different British Columbia coals, are presented in Figure 5-2-3. Washability improves as the particle size decreases. One reason for the better washing characteristics of fines is the fact that as the size is decreased, the liberation of mineral matter increases and gravity separation becomes more efficient. When the size becomes too fine, however, gravity separation itself becomes less ideal as the very fine coal or mineral (clay) particles remain suspended in the separating medium. Better washability of finer sizes can also be attributed to the increased presence of vitrain in the fines, vitrain being a natural concentration of light and low-ash vitrinite particles. It is important to be aware of the segregation of lithotypes and their liberation characteristics when comparing washability of different seams.

OBJECTIVES

The objectives of this coal quality study are to compile and study the washability characteristics of coals from different coalfields within the province.

Geological Fieldwork 1990, Paper 1991-1

Washability data from across the province are already available in the Ministry's collection of coal exploration assessment reports. Most of the washability results are in the form of sink-and-float analyses. These are usually carried out either on core or bulk samples representing individual seams. In accordance with ASTM D 437-84 methodology, sink-and-float tests are carried out on coarse and fine fractions separately. Frequently the analyses on the bulk samples are done on several size fractions, for more accurate predictions. All results reported in this paper are based on assessment report data.

Comparison of the washability of different coal seams and the coal regions of the province will be very useful in assessing coal quality. Coal washability data will be compiled in the form of an in-house catalogue, containing all possible washability parameters. Lithotype composition and the mineral matter studies will be merged with the washability evaluation. Publications arising out of washability data compilation and interpretation will honour the confidential nature of the data.

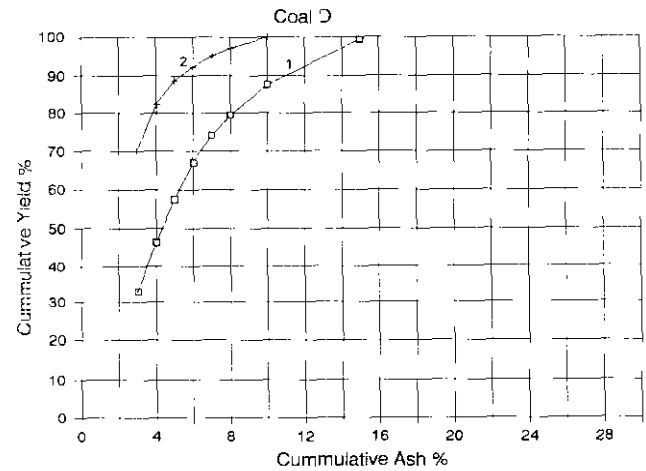
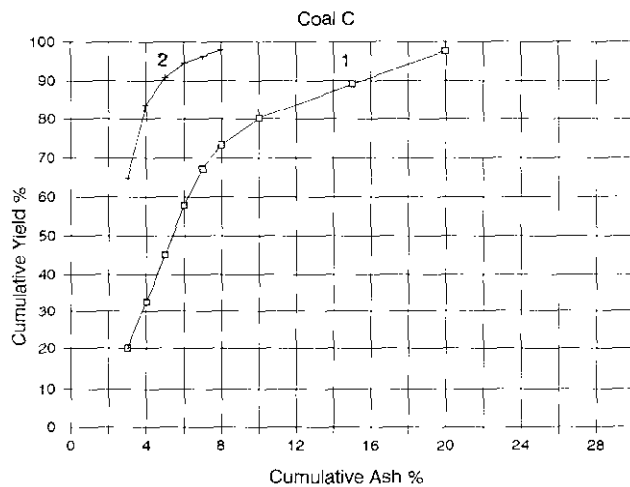
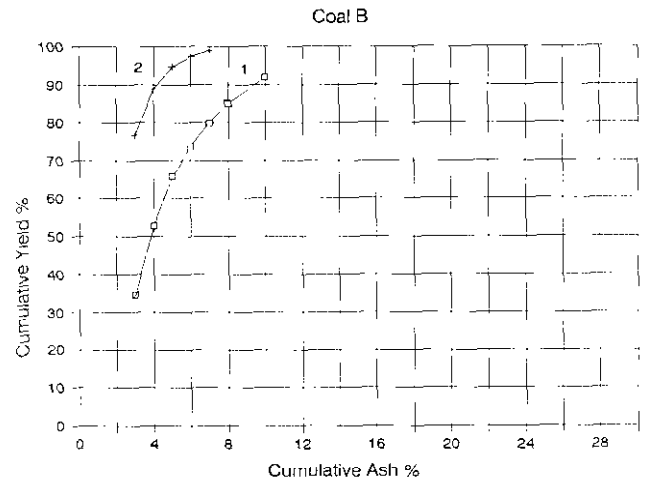
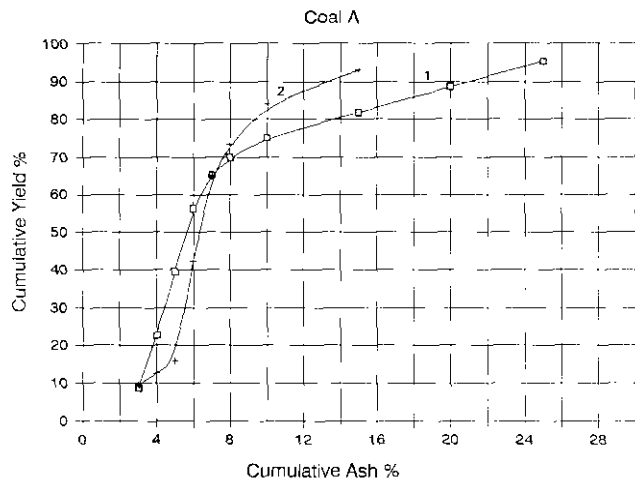


Figure 5-2-4. Cumulative clean coal curves for coarse and fine fractions from coals A, B, C and D: For coals A, B and C size fraction 1 = 50-0.6 millimetres (coarse) and 2 = 0.6-0.15 millimetre (fine). For coal D size fraction 1 = 75-0.5 millimetres (coarse) and 2 = 0.5-0.15 millimetre (fine).

At this time a number of washability curves have been constructed for four different properties from the Peace River coalfield. Each of the properties has washability data on four or five different seams. The form of the data is not uniform, as different size ranges have been used for sink-and-float analysis for different properties. For the purpose of comparison, data have to be converted into a more uniform format.

A computer program in BASIC was used to obtain washability calculations from sink-and-float tests. The set of washability curves for compiled data was plotted using in-house software.

To discuss and compare washing characteristics of different coal seams, sets of washability data for each of the samples are used. For carrying out the comparison between seams the following criteria have been applied:

- The washability data on separate size fractions have been combined into two size ranges, coarse and fine (upper limit for coarse is 150 millimetres and the lower limit is 0.5 to 0.6 millimetre, whereas the range for fines is 0.5 to 0.15 millimetre);

- Only bulk samples are studied, being the most representative of a seam.

For the comparison of different coalfields or regions the same criteria as above apply. As well, samples must be statistically representative of the region or coalfield.

METHODS

To compare washing characteristics of British Columbia coals, a number of parameters are used; yield and quality of clean coal and rejects at density of separation, near-gravity material, and densimetric distributions, together with the new washability measures such as degree of washing and washability number.

WASHABILITY CURVES

The most frequently used way of expressing concentration results is either by recovery of a valuable component, or by yield of concentrate, accompanied by the grade of the concentrate. However, a concentration process, as in the case of sink-and-float separation, is not carried out to com-

pletion, but stopped when an optimum concentration has been reached. Points given by yield and grade (ash content) at each step of density separation are used to construct washability curves.

The **primary curve** is obtained by plotting incremental ash content at each separation density versus incremental yield on the cumulative yield scale. The **clean coal curve** is obtained by plotting cumulative ash content at any given density versus cumulative yield. The **cumulative sink curve** predicts ash content of the sinks at any yield of clean coal. The fourth curve is the **cumulative density distribution**, which is plotted as density versus yield. The last curve is the curve of **near-gravity material**. It indicates the amount of material within ± 0.1 specific gravity of separation. For a full discussion of washability curves refer to Leonard (1979), Laskowski and Walters (1987).

Washability data are usually obtained for several different size fractions within a coal sample, and then combined to plot the total curves for coarse and fine fractions separately.

YIELD OF CLEAN COAL AND QUALITY OF REJECTS

The clean-coal curve, as derived from sink-and-float analysis, predicts the theoretical yield of clean coal product at any given ash content. For example, if the clean coal product has to meet market requirements of 10 per cent ash, then the yield of this product can be obtained from the curve. The higher the yield at the lowest ash content, the better the quality of the cleaned coal.

Figure 5-2-4 represents four different seams with different washability characteristics. Cumulative ash per cent of the floats, versus cumulative yield per cent, are plotted

TABLE 5-2-2
THE QUALITY OF CLEAN COAL AND REJECTS
Coarse

Clean Coal Ash %	CC yield %	Ash % reject	CC ash %	CC yield %	Ash % reject
Coal A				Coal B	
5	39.5	30.06	5	65.78	23.66
10	75.1	81.94	10	92.04	64.32
15	81.87	82.44			
Coal C				Coal D	
5	45.23	23.82	5	57.38	23.36
10	80.27	65.15	10	87.64	48.65
15	89.19	68.39	15	99.35	76.25

Fines

Clean Coal Ash %	CC yield %	Ash % reject	CC ash %	CC yield %	Ash % reject
Coal A				Coal B	
5	15.87	18.52	5	94.76	40.93
10	84.07	61.24			
15	93.22	76.06			
Coal C				Coal D	
5	90.88	46.06	5	88.64	44.12
			10	90.93	75.73

separately for coarse and fine fractions. If there were economic reasons for imposing strict limits on the yield of clean coal for these seams, as for instance 50 per cent yield at 5 per cent ash or 80 per cent yield at 10 per cent ash, it would be not feasible to process some of the seams.

From a theoretical point of view, reject is the coal which has higher ash content than feed sample as a result of the concentration process. The quality of the rejects is usually measured by ash content. The ash content of rejects can also be used as a measure of efficiency of the coal preparation. If, for example, the ash content of rejects is not sufficiently higher than ash of the feed sample, this is an indication of the loss of combustibles into the discard. Either the process of separation has not been efficient or liberation has not been adequate. Additional grinding would be required to liberate interlocked coal particles.

Table 5-2-2 shows the relationship between yield of clean coal at selected levels of ash and quality of rejects among four British Columbia coals. Industrial experience is that a reject ash content of about 65 per cent or more is expected for satisfactory recovery of combustibles from coal.

PREDICTING THE EASE OF WASHING

The "ease" of washing is a term to describe the way in which a given coal will respond to gravity separation. The difference in density between clean-coal particles and liberated mineral matter is sufficient to achieve complete separation. In this case, there will always be an intermediate density at which complete separation of two distinctly different components will occur. The difficulty in washing will be encountered with the particles of composite nature. Density distribution within the bulk sample may give some indication of the "ease" of washing. Density distributions of four coals are presented in Figure 5-2-5. All four samples contain high amounts of low-density material (1.3-1.4 relative density), very little of middlings (1.4-1.6 relative density) and varying amounts of high-density mineral matter particles. Therefore, coals A and C will be the easiest to wash, with samples B and D being somewhat more difficult. It is also interesting to notice that coal A has less of the 1.3 specific gravity material as compared to the others. This is in very good agreement with lithotype composition of this particular seam, which is known to be low in vitrain bands.

The shape of the primary curve and the yield of the clean-coal curve are other indications of whether a coal is easy or difficult to clean. The greater the change in shape of the primary or clean-coal curve in the range of low ash content, the more difficult it is to clean the coal (see Figure 5-2-4). When comparing a number of washability curves, it is difficult to assess the ease of washing by just comparing the shape of the different curves. A comparison of the yields of clean coal at selected ash levels and the quality of their sinks is more appropriate. The low ash content of the sinks at low separation densities indicates the presence of middlings, but this is not quantitative information on the ease of washing (see Table 5-2-2).

The quantitative measure of the ease of washing is the near-density material (0.1 relative density) curve. The greater the

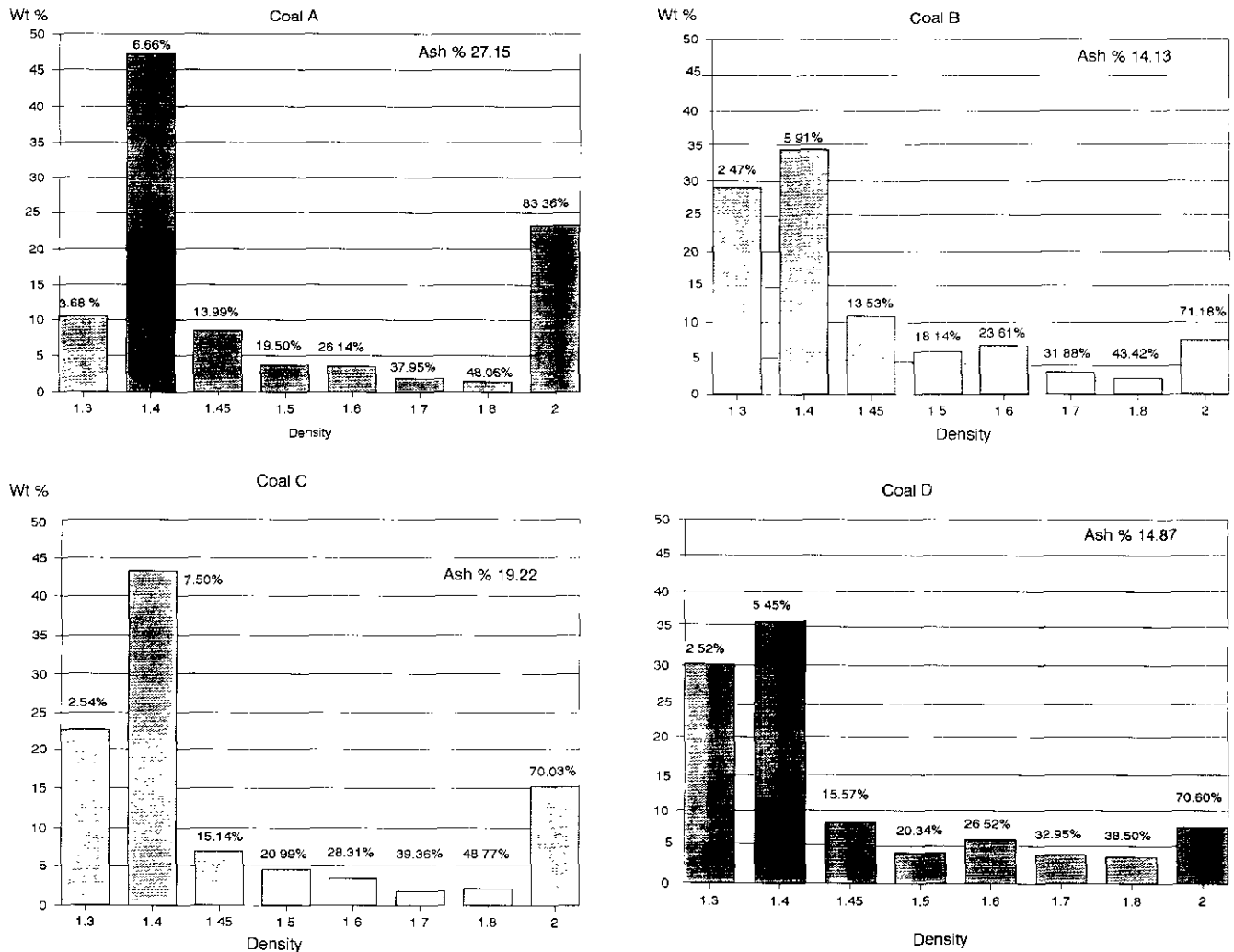


Figure 5-2-5. Density distribution for coals A, B, C and D. Total sample ash is given in the top right-hand corners, while ash contents for each density fraction are above the bars.

yield of the 0.1 fraction the more difficult it will be to carry out the separation at this relative density. The more the near-gravity material curve approximates the shape of a letter L, the easier it is to obtain good gravity separation. A sharp change in the shape of the curve indicates the presence of two different types of material: clean, low ash and heavy, mineral matter particles. This provides a basis for easy separation.

Figure 5-2-6 compares the near-gravity material curves for the four coals under discussion. For coals B, C and D, fine fractions have less near-density material than the coarse fractions, at any given density of separation. This confirms that fine size fractions are easier to wash because of the greater liberation of coal from mineral matter. Coal A is an exception; the fines have more near-density material, which may indicate the presence of clays. In this case separation becomes less efficient and this is reflected in a decrease of the ease of washing.

It is important to determine the amount of near-density material at the cut points required for good quality, clean coals.

DEGREE OF WASHING AS A NEW PARAMETER OF WASHABILITY

Washability takes into account a number of parameters such as ash, yield of floats and rejects, amount of near-gravity material and densimetric distribution.

As discussed by several authors (Sarkar and Das, 1974; Sanders and Brooks, 1986) it is useful to have a parameter which includes most of the variables. The degree of cleaning, or degree of washing, has been introduced to supplement the washability parameters. The degree of washing is expressed as:

$$N = \frac{w(a-b)}{a}$$

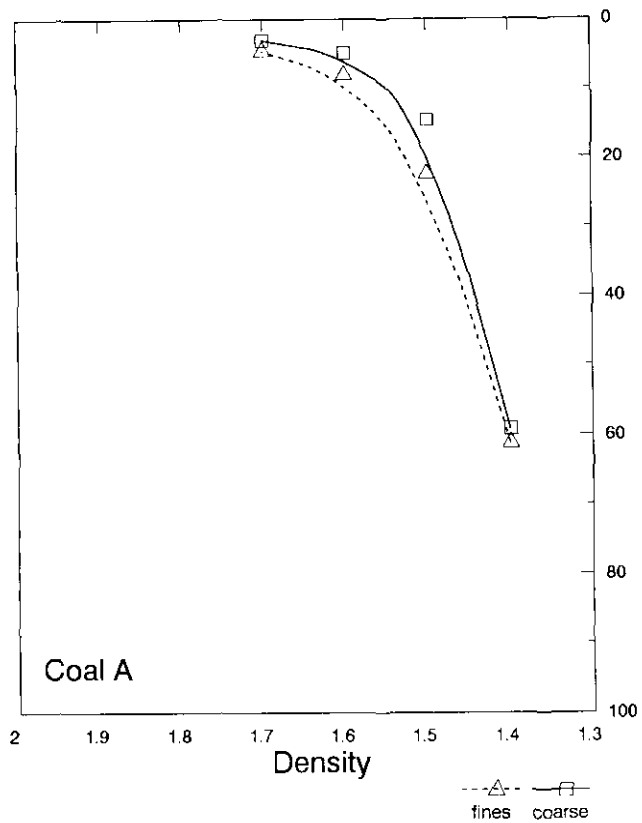
where: a = the ash content of the feed

b = the ash content of the clean coal at a given density of separation

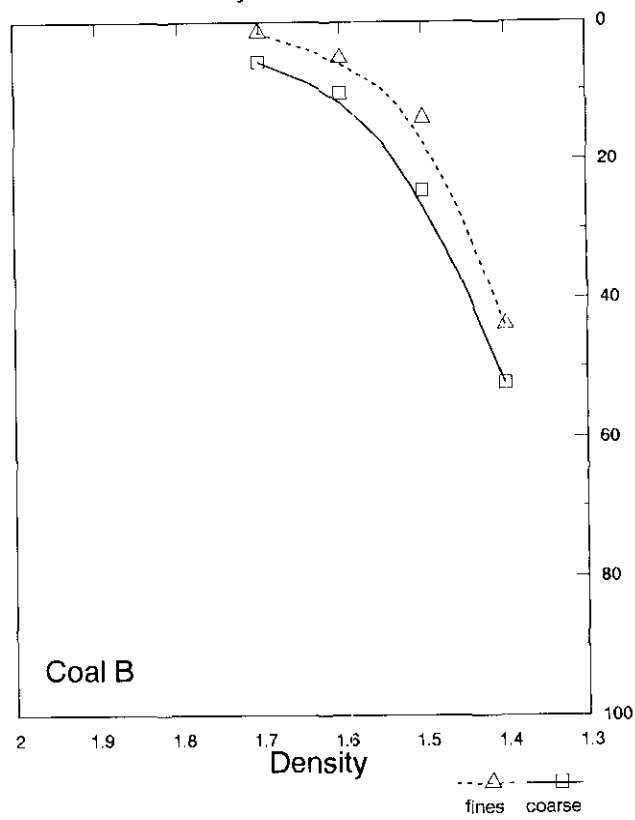
w = the yield of clean coal at a given density of separation.

The degree of washing N values, calculated as above and plotted as a function of density of coarse and fine fractions are presented in Figure 5-2-7. For each coal there is an

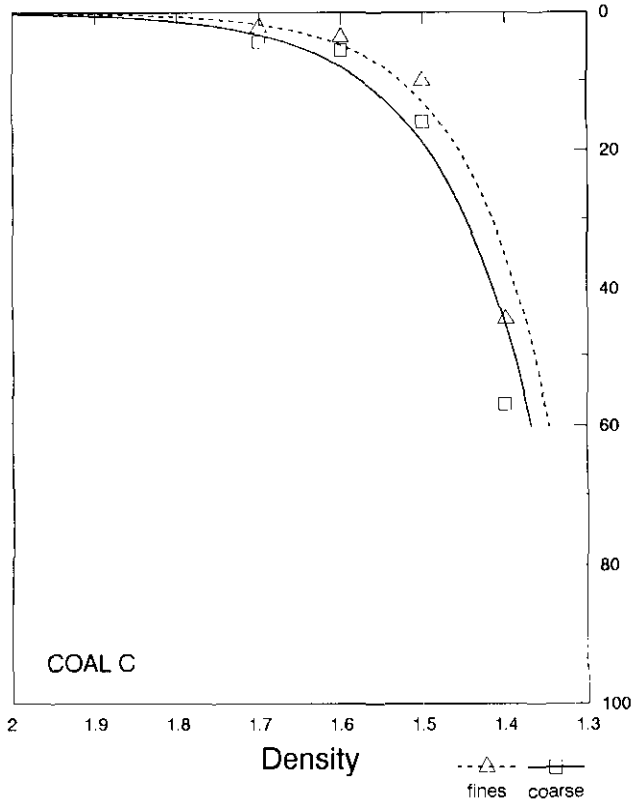
Wt % Near Gravity Material



Wt % Near Gravity Material



Wt % Near Gravity Material



Wt % Near Gravity Material

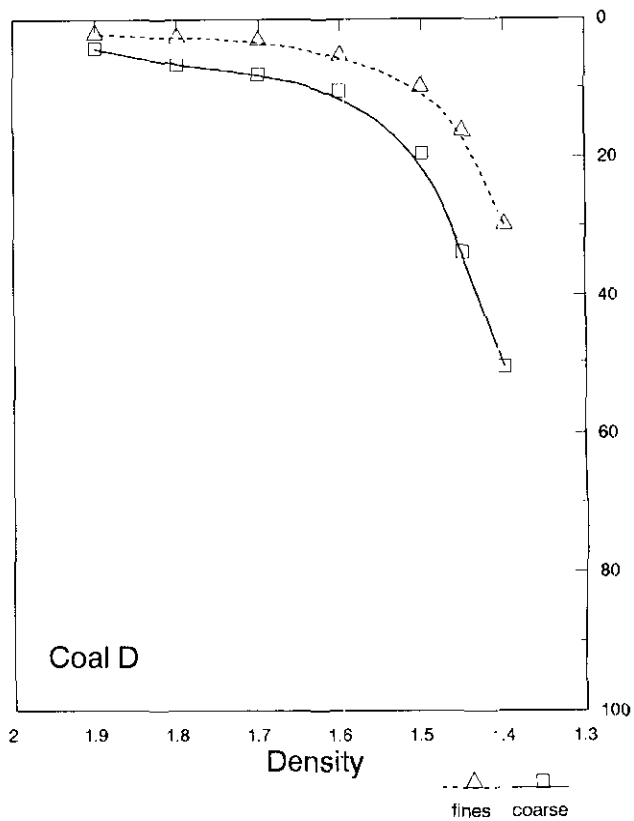


Figure 5-2-6. Near-gravity material (0.1 r.d.) curves for coals A, B, C and D.

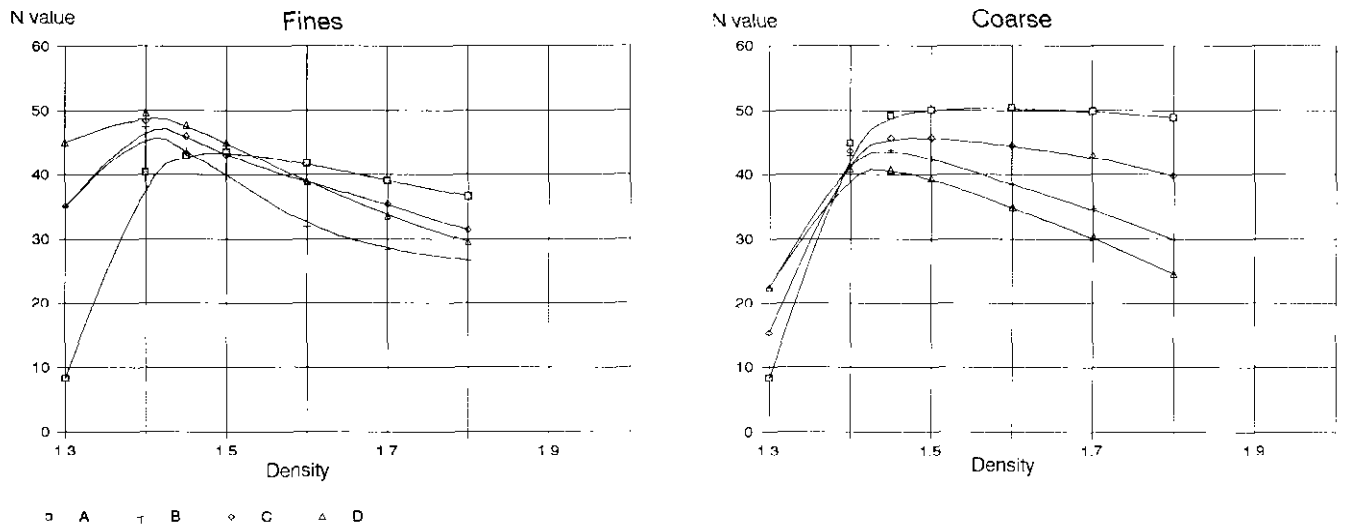


Figure 5-2-7. Degree of washing plots (N value versus separation density) for coals A, B, C and D.

optimum N value which is equivalent to the maximum of ash rejection at a given density. Ash rejection is proportional to the recovery of the combustibles from a given coal. The higher the rejection of ash the better the recovery of combustibles. For the coarse fractions the degree of washing (N), and therefore ease of washing increases in order D, B, C and A, whereas for the fines, the order is A, B, C and D.

The shape of the N-value curve indicates a change in ash rejection ability of a given coal for a different density of separation. For instance, the coarse fraction of coal A shows very little change in the N value over the range of densities increasing from 1.45 specific gravity. This means that ash rejection does not change in intermediate densities, because

there is very little middlings, and most of the material is either in the low-density fraction or in rejects.

For other samples, the N values change with increase in density. As the amount of middlings is increased, the ability to reject the ash is reduced. N values for fines are much higher in the low-density ranges than in the case of the coarse fractions. This is indicative of much better ash rejection in fines for light coal material, except for Sample A.

The ash rejection value is the parameter which can more precisely quantify the "ease" of washing.

For a better comparative measure, the N optimum value can be further developed (Sanders and Brooks, 1986). The "washability number" is calculated as:

$$W = (N_{opt}/b_{opt})10$$

where a_{opt} = ash content corresponding to the fraction at N_{opt} .

The washability number indicates differences in the ease of washing, taking into account conditions for the maximum ash reduction and the ash content of the product at the optimum. However, optimal conditions will not always satisfy the economic side of the processing, therefore the washability number should only be considered as an additional indicator of washing ease. It must also be used in conjunction with all the other parameters of the washability data, to confirm its validity. Table 5-2-3 presents the calculated washability numbers and other washability parameters which correspond to the optimum cut points.

TABLE 5-2-3
WASHING CHARACTERISTICS OF OPTIMUM
DEGREE OF WASHING

Coarse						
Coal	Cut Point Relative Density	Yield %	Ash %	Ash % in Rejects	Nopt Value	Wn Washability Number
A	1.60	68.63	7.64	68.92	50.45	66
B	1.40	73.14	5.92	31.63	43.07	73
C	1.50	69.49	7.29	46.11	45.86	63
D	1.40	73.42	6.89	33.16	40.82	59

Fines						
Coal	Cut Point Relative Density	Yield %	Ash %	Ash % in Rejects	Nopt Value	Wn Washability Number
A	1.50	77.98	8.59	48.56	43.69	51
B	1.40	87.77	3.83	26.83	47.50	124
C	1.40	87.89	4.46	36.01	48.42	109
D	1.40	81.90	3.96	29.51	29.8	75

SUMMARY AND CONCLUSIONS

The comparison between washability of coals or coal seams should always be considered on a much broader scale than just comparing the washability numbers derived from the sink-and-float analyses. The following factors should always be taken into account:

- mineral matter type and its mode of occurrence as the most important factor in the washability;
- lithology of a particular seam;
- the parameters such as optimum degree of washing and washability number, highlighting relative washing difficulties in relation to the optimal ash rejection, are recommended as a supplementary measure to the traditional washability parameters.

FUTURE PLANS

The compilation of the available washability data from coal seams across the province will continue. Washability curves will be obtained for a representative suite of coal seams in the province. The available computer programs will be used to obtain all possible combinations of washability parameters, and to find relationships between them. Values such as yield and quality of rejects at preselected ash levels will be calculated and compared. Degree of washing, together with the other measures of "ease" of cleaning, such as amount of near-gravity material, density distributions, and the "washability" number, will be used to compare different coals.

The washability data will be entered into in-house, catalogue-type files, where all washability parameters will be included. The computer software will be set up to maintain all possible washability information as active files. The system will be computerized for calculations and display of different washability parameters as needed.

As the new Alpern Classification System is being developed and approved (Alpern *et al.*, 1989) a further aim of this study is to compare British Columbia coals with coals from elsewhere.

The mineral matter content and its mode of occurrence significantly affects washability characteristics of any given coal, therefore it will be necessary to study mineral matter in conjunction with the washability. For the same reason, lithotype data will also be considered in conjunction with washability evaluations.

ACKNOWLEDGMENTS

We wish to express our gratitude to the geology staff at all of the province's coal mines, for their help and cooperation. Colleagues Barry Ryan and Ward Kilby read an earlier version of this paper. Ward Kilby also developed and provided computer washability programs.

REFERENCES

- Alpern, B., Lemos de Sousa, M.J. and Flores, D. (1989): A Progress Report on the Alpern Coal Classification; *International Journal of Coal Geology*, Volume 13, pages 1-19.
- Diessel, C.F.K. (1965): Correlation of Macro and Micro-petrography of Some New South Wales Coals; *Proceedings of 8th Commonwealth Mining and Metallurgical Congress*, Volume 6, pages 669-677.
- Falcon, L.M. and Falcon, R.M.S. (1983): The Application of Coal Petrography to Certain Beneficiation Techniques on South African Coal; *Geological Society of South Africa, Special Publication 7*, pages 137-148.
- Falcon, L.M. and Falcon R.M.S. (1987): The Petrographic Composition of Southern African Coals in Relation to Friability, Hardness and Abrasive Indices; *Journal of the South African Institute of Mining and Metallurgy*, Volume 87, No. 10, pages 323-336.
- Hower, J.C. (1988): Additivity of Hardgrove Grindability: a Case Study; *Journal of Coal Quality*, Volume 7, pages 68-70.
- Hower, J.C., Graese, A.M. and Klapheke, J.G. (1987): Influence of Microlithotype Composition on Hardgrove Grindability for Selected Eastern Kentucky Coals; *International Journal of Coal Geology*, Volume 7, pages 227-244.
- Hower, J.C. and Lineberry, G.T. (1988): The Interaction of Coal Lithology and Coal Cutting on the Breakage Characteristics of Selected Kentucky Coals; *Journal of Coal Quality*, Volume 7, pages 88-95.
- International Committee for Coal Petrology (1963): International Handbook of Coal Petrology, 2nd Edition; *Centre Nationale de la Recherche Scientifique*, Paris.
- Laskowski, J.S. and Walters, A.D. (1987): Coal Preparation; in *Encyclopedia of Physical Science and Technology*, Volume 3, *Academic Press*, pages 37-61.
- Leonard, J.W. (1979): Coal Preparation; 4th *American Institute of Mechanical Engineers*, New York.
- Sanders, G.J. and Brooks, G.F. (1986): Preparation of the "Gondwana" Coals. 1. Washability Characteristics; *Coal Preparation*, Volume 3, pages 105-132.
- Sarkar, G.G. and Das, H.P. (1974): A World Pattern of the Optimum Ash Levels on Cleans from the Washability Data of Typical Coal Seams; *Fuel*, Volume 53, page 74.
- Stach, E., Mackowsky, M.-Th., Teichmuller, M., Taylor, G.H., Chandra, D. and Teichmuller, R. (1982): Stach's Textbook of Coal Petrology, 3rd Edition; *Gebrüder Borntraeger*, Berlin, Stuttgart.

NOTES



GEOLOGY AND COAL RESOURCES OF THE NANAIMO GROUP IN THE ALBERNI, ASH RIVER, COWIE CREEK AND PARKSVILLE AREAS, VANCOUVER ISLAND (92F/2, 6, 7, 8)

C. Gwyneth Cathyl-Bickford and Georgia L. Hoffman
Consulting Geologists

KEYWORDS: Coal geology, stratigraphy, Vancouver Island, Comox sub-basin, Nanaimo Group, Comox Formation, Trent River Formation, coalbed mineability.

INTRODUCTION

This report is part of an ongoing study, begun in 1987, to establish the distribution and resource stratigraphy of the Vancouver Island coalfields. Knowledge of the extent of potentially underground-mineable coal resources will assist in the development of land-use guidelines for eastern Vancouver Island.

In this year's field program, we have investigated the extent and coal resource potential of the Comox Formation between Cowie Creek, Port Alberni and Parksville, in east-central Vancouver Island. We have also continued stratigraphic studies of the marine sediments of the middle Nanaimo Group, overlying the Comox Formation, in order to better ascertain the depth to the Comox in undrilled areas.

LOCATION AND ACCESS

The study area covers the central part of the eastern coastal plain of Vancouver Island and extends westward into the Alberni and Cameron River valleys (Figure 5-3-1). A dense network of public and private roads provides good access to most parts of the area, with the exception of the central peaks of the Beaufort Range, where rugged topography and low-grade timber resources have deterred road building. Elevations range from sea level to 1600 metres. Fairly gentle slopes on the coastal plain and in the large valleys are bounded by the steep slopes of the Beaufort Range, which forms a prominent mountain wall along the northeastern side of the Alberni Valley. Most of the region is covered by scrub forest, with small patches of merchantable timber along the higher slopes of the Beaufort Range.

Port Alberni is the major population centre in the study area; Qualicum and Parksville are the largest of several

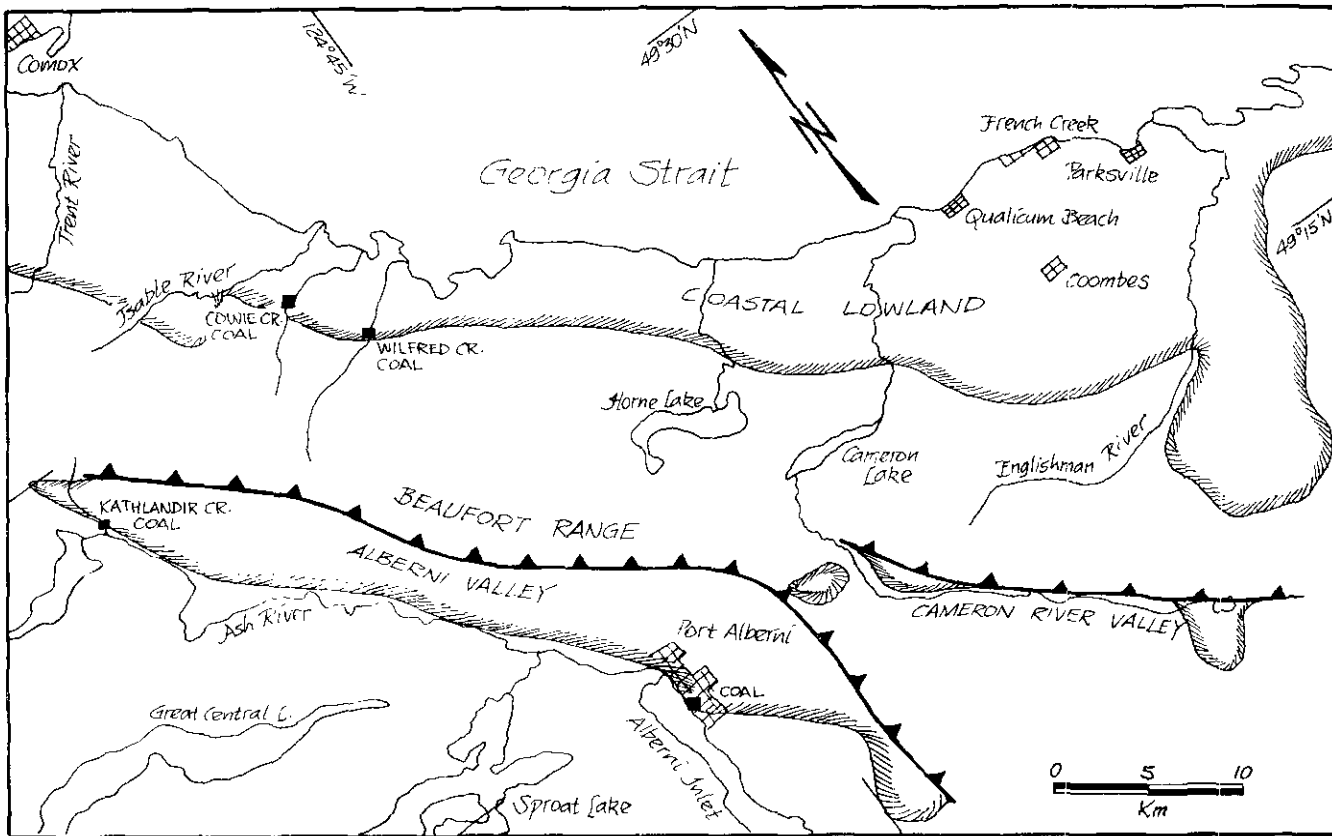


Figure 5-3-1. Location map.

resort communities along the eastern coast. Logging and pulp production are the major resource industries in the area, with tourism and real-estate development becoming increasingly important as the forest resources decline in volume and quality.

FIELDWORK

As in past years, geological mapping was done on aerial photographs and the observations transferred to base maps at 1:20 000 scale. Forest maps at the same scale, obtained from MacMillan Bloedel Ltd. and the Ministry of Forests, were used for orientation purposes in recently logged areas.

Samples of coal and carbonaceous mudstone were collected for petrographic study, and sandstones were collected for thin sectioning. Specimens were also collected, where appropriate, for paleontological and paleobotanical studies which should assist in refining the biostratigraphy of the lower Nanaimo Group.

GEOLOGICAL SETTING

The study area comprises the southerly half of the Comox sub-basin of the Late Cretaceous Georgia basin. The coal measures occur in the Cumberland and Dunsmuir members of the Comox Formation (Bickford and Kenyon, 1988). The Comox Formation outcrops on the eastern slopes of the Beaufort Range, and dips gently to moderately eastward beneath younger Cretaceous rocks and thick unconsolidated

Pleistocene sediments. Dikes and sills of probable Tertiary age frequently cut the Cretaceous rocks in the southeastern part of the area, at the headwaters of the Englishman River.

Large outliers of the Comox Formation and younger Cretaceous rocks occur in the Cameron River and Alberni valleys, west of the Beaufort Range. These rocks dip moderately to the east and northeast, and are locally warped into asymmetric, southwest-verging folds. Overthrusts form the eastern margins of both the Alberni and Cameron River outliers; pre-Cretaceous basement rocks have been thrust over the Cretaceous rocks and the resultant fault scarp forms the steep southwestern face of the Beaufort Range.

STRATIGRAPHY

Lithostratigraphic units of the lower Nanaimo Group are shown in Table 5-3-1 and illustrated in Figure 5-3-2. Formations and members have been traced into the study area, by mapping, from both the Cumberland (Bickford *et al.*, 1990) and Nanaimo (Bickford and Kenyon, 1988) coalfields

Contrary to the position presented by England (1989), the lower units of the Nanaimo Group may be readily traced from the Comox to the Nanaimo sub-basins of Georgia basin. The traceability of Cretaceous rock units between the two sub-basins suggests that the onshore portion of the Nanoose uplift (Muller and Jeletzky, 1970; Yorath and Sutherland Brown, 1984), at least during the Santonian and early Campanian stages, did not form a substantial barrier

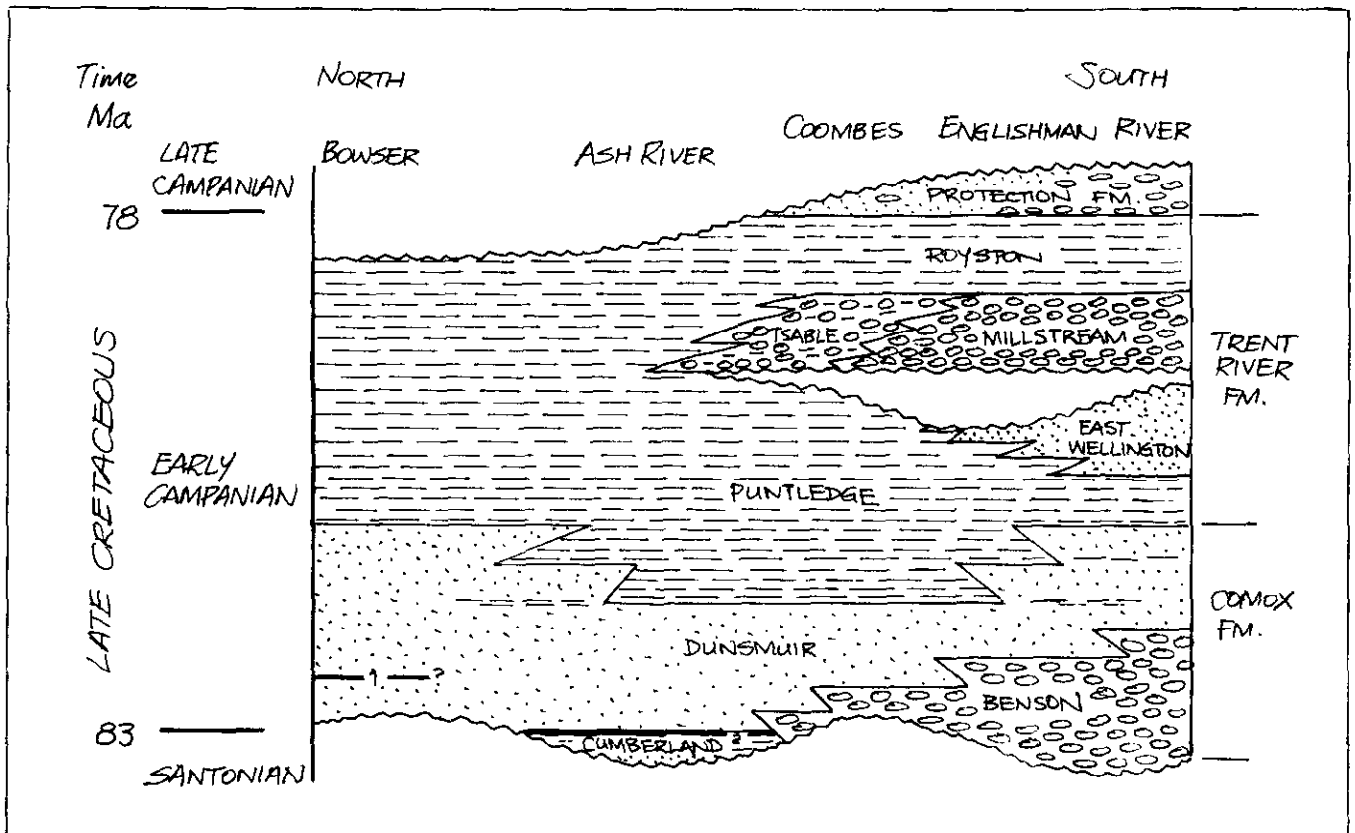


Figure 5-3-2. Chronostratigraphic diagram of lower Nanaimo Group, southern Comox sub-basin.

TABLE 5-3-1
LITHOSTRATIGRAPHIC UNITS OF THE
LOWER NANAIMO GROUP,
SOUTHERN HALF OF COMOX SUB-BASIN

Formation:	Member:	Lithology:
Protection		Conglomerate and sandstone
		-----Abrupt Contact-----
Trent River	Royston	Mudstone and siltstone
		-----Intertonguing Contact-----
	Tsable	Mud-matrix conglomerate and pebbly siltstone
		-----Intertonguing Contact-----
	Millstream	Conglomerate and gritstone
		-----Erosional Contact-----
	East Wellington	Sandstone
		-----Intertonguing Contact-----
	Puntledge	Mudstone; siltstone at top; minor glauconitic sandstone at base.
		-----Intertonguing Contact-----
Comox	Dunsmuir	Sandstone; minor siltstone and coal
		-----Abrupt Contact-----
	Cumberland	Siltstone; minor sandstone, shale and coal.
		-----Intertonguing Contact-----
	Benson	Conglomerate; minor red siltstone at top.
		-----Erosional Contact-----
Pre-Cretaceous volcanic, plutonic and metasedimentary basement.		

between the two sub-basins. There is no evidence to suggest that the Comox and Nanaimo sub-basins were ever separate depositional areas, and their existence as geographically separate entities can be wholly explained by post-Cretaceous erosion along the Nanoose uplift.

CONGLOMERATES NEAR PARKSVILLE

Ridge-forming conglomerates near Parksville were assigned to the Parksville member of the Trent River Formation by England (1989). In the course of this year's mapping, we have been able to distinguish three different types of conglomeratic units near Parksville. Two of these units we have assigned to the Millstream and Tsable members of the Trent River Formation, while the third we assign to the Protection Formation.

MILLSTREAM MEMBER

The Millstream member at Parksville consists of at least 90 metres of quartz, chert and basalt-pebble conglomerate and pebbly gritstone. It is well exposed along the Alberni Bypass Highway near Craig's Crossing and forms Little Mountain, a prominent hill south of the outskirts of Parksville. Distinguishing features of the Millstream conglomerates are absence of bioturbation, other than rare rooting at bed tops, excellent framework sorting and well-developed medium to very thick planar stratification and low-angle trough cross-stratification. We interpret the Millstream member near Parksville to be a delta-front deposit, sourced by streams carrying large amounts of gravel and grit as bed load.

The Millstream member was previously assigned to the Extension Formation of the Nanaimo coalfield (Bickford and Kenyon, 1988). Although we can confidently map this conglomeratic unit across the erosional gap of the Nanoose arch into the Parksville area, we cannot trace it across the remainder of the type Extension Formation and we therefore consider the Millstream member at Parksville to be a member of the Trent River Formation.

TSABLE MEMBER

The Tsable member at Parksville consists of mud-matrix, chert-pebble conglomerates with abundant interbeds of pebbly siltstone. It is well exposed in the canyon of French Creek above the Alberni Highway bridge at Coombes village where it is 20 to 30 metres thick. Distinguishing features of the Tsable conglomerates and pebbly siltstones are moderate bioturbation of bed tops (chiefly irregular grazing trails), good framework sorting with disorganized sedimentary fabric, and the sparse presence of broken pelecypod and ammonoid shells. We interpret the Tsable member at French Creek to be a submarine-canyon fill, sourced by the north-westward collapse of the Millstream delta-front.

PROTECTION FORMATION

The Protection Formation at Parksville consists of at least 30 metres of quartz-chert-basalt gritstone and sandy pebble conglomerate with abundant whole and broken pelecypod shells. It is well exposed along the coastline east of the mouth of French Creek and also forms low, north-dipping cuesta ridges at the east and west ends of the town of Parksville. Distinguishing features of the Protection conglomerates include their greenish or greenish grey coloration and their abundant content of shell debris. We interpret the Protection conglomerates at Parksville to be delta-front or barrier-bar deposits.

ECONOMIC GEOLOGY

Only four significant coal showings were identified during the 1990 field season. The lack of coal showings is partly due to poor exposure, but also to the general lack of suitable depositional conditions in the southern part of the Comox sub-basin. Three of the four showings are along the northern edge of the study area and represent extensions of prospective areas identified in previous studies. Details of

TABLE 5-3-2
SIGNIFICANT OCCURRENCES OF COAL AT OUTCROP IN THE
SOUTHERN PORTION OF THE COMOX SUB-BASIN

Locality	UTM Coordinates	Coal Bed	Thicknesses		Per Cent Coal by Thickness
			Gross	Net	
Cowie Creek	363510 E 5484425 N	No. 3	2.92 m	2.21 m	76
Wilfred Creek	366315 E 5481140 N	No. 2	1.99 m	1.27 m	64
Kathlandir Creek	348860 E 5480700 N	No. 2?	2.15 m	1.20 m	56
Port Alberni	368210 E 5454740 N	No. 3?	0.91 m	0.56 m	70

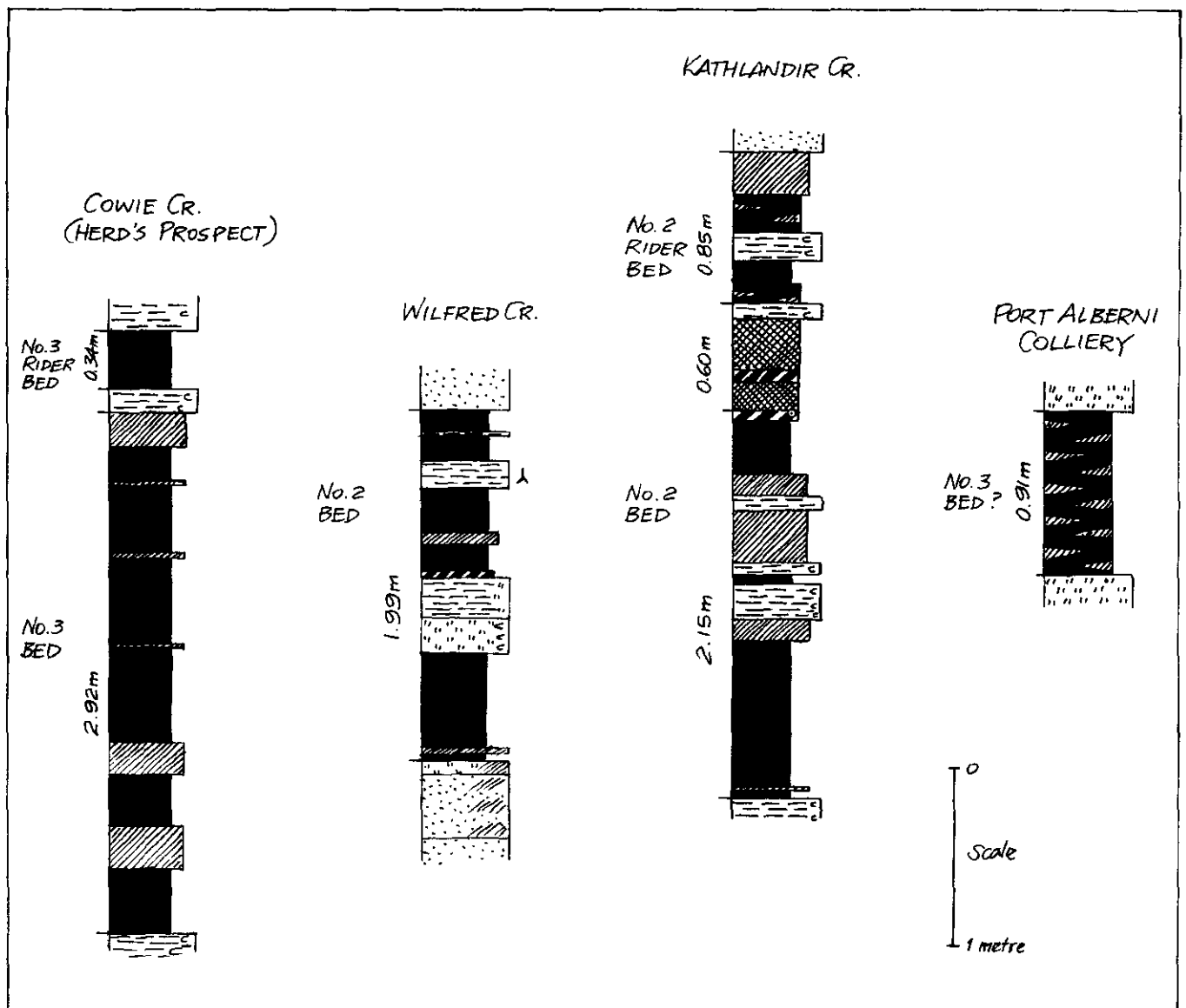


Figure 5-3-3. Measured sections of significant coal outcrops, southern Comox sub-basin.

the four coal showings are presented in Table 5-3-2, while graphic sections are shown as Figure 5-3-3.

The best showing is on Cowie Creek where an adit has been driven into the south bank of the creek, exposing a relatively clean bed of coking coal. This coal, which we correlate with the No. 3 bed of the type Comox section, is locally known as the Lower Seam and the adit is known as Herd's Prospect. Tests conducted on a bulk sample taken from the adit yielded a coke button which was described as "very hard, expanded, with metallic lustre (good coking)" (U.S. Steel Co., 1949). Although the U.S. Steel tests indicate that this coal is of good quality, its roof, which has caved near the portal of the adit, consists of a sheared carbonaceous mudstone with a thin rider coal band. Such a roof could be expected to cause problems in underground mining (Stan Lawrence, retired colliery manager, personal communication, 1990).

A short distance to the south, another old adit has been driven into the Comox No. 2 coal bed (locally known as the Upper Seam) on the south bank of Wilfred Creek. Despite an earlier report (Atchison, 1968) of thick and clean coal, this coal bed contains numerous partings of mudstone and on the whole is sheared and dirty. It has a strong sandstone roof which has stood, essentially unsupported, with only minor spalling, since the adit was driven in 1908. The net coal content of this bed, at 64 per cent, is marginal for underground mining, but should be an encouragement to further exploration in the area.

Approximately 18 kilometres to the east of the Wilfred Creek showing, a thick zone (>3.6 metres) of coal and shale is exposed on Kathlandir Creek, a south-flowing tributary to Ash River. This coal, discovered at the turn of the century, is locally known as the Ash River Seam; it is tentatively correlated with the Comox No. 2 and 2 Rider coal beds.

Only the lower, (No. 2) portion of this thick, dirty zone contains sufficient coal to have been considered as worthy of further investigation. Drilling in 1985 by Canadian Occidental Petroleum was aimed at establishing the continuity of the coal bed: results were not encouraging as the drilling showed the coal to be pockety and of local extent only.

On the eastern shore of Alberni Inlet, in Port Alberni city proper, a coal bed (possibly the Comox No. 3 bed) has been extensively prospected by trenching and underground development, and was unsuccessfully worked by the Port Alberni Colliery in 1911 and 1912 (Wilkinson, 1922; MacKenzie, 1923). Although the adit is now caved, the material dumped at the portal was sampled. The dump material consists of platy to blocky, bright coal with 30 per cent thin interbeds of black, coaly mudstone. Much of the coal shows woody surface markings, and it appears to be of allochthonous origin.

ACKNOWLEDGMENTS

We thank the forestry staff of Fletcher Challenge Canada Inc. and MacMillan Bloedel Ltd. for providing forest-cover maps of their land holdings, for the loan of surveying equipment, and for allowing access to closed forest areas. Stan Lawrence of Cumberland has continued to provide first-hand information on the existence and mineability of coal deposits in the Comox Formation. Esther Lobb and Marie Norsed provided assistance in geological mapping and paleobotanical sampling. We especially thank Kee Ming in Campbell River and Pat Armstrong in Cumberland for providing creature comforts to weary mappers.

REFERENCES

- Atchison, M. (1968): Stratigraphy and Depositional Environments of the Comox Formation (Upper Cretaceous), Vancouver Island, British Columbia; unpublished Ph.D. thesis, *Northwestern University*, Evanston, Illinois, 139 pages.
- Bickford, C.G.C. and Kenyon, C. (1988): Coalfield Geology of Eastern Vancouver Island (92F); *B.C. Ministry of Energy, Mines and Petroleum Resources*, Geological Fieldwork 1987, Paper 1998-1, pages 441-450.
- Bickford, C.G.C., Hoffman, G.L. and Kenyon, C. (1990): Geological Investigations in the Coal Measures of the Oyster River, Mount Washington and Cumberland Areas, Vancouver Island (92F/10, 11, 14); *B.C. Ministry of Energy, Mines and Petroleum Resources*, Geological Fieldwork 1989, Paper 1990-1, pages 431-437.
- England, T.D.J. (1989): Lithostratigraphy of the Nanaimo Group, Georgia Basin, Southwestern British Columbia; *Geological Survey of Canada*, in Current Research, Part E, Paper 1989-1E, pages 197-206.
- MacKenzie, J.D. (1923): Alberni Area, Vancouver Island, B.C.; *Geological Survey of Canada*, Summary Report for 1922, Part A, pages 51-67.
- Muller, J.E. and Jeletzky, J.A. (1970): Geology of the Upper Cretaceous Nanaimo Group, Vancouver Island and Gulf Islands, British Columbia; *Geological Survey of Canada*, Paper 69-25.
- U.S. Steel Co. (1949): Reports on Coking Tests of Vancouver Island Coal; *Provincial Archives of British Columbia*, Buckham Collection. Additional Manuscript 436.
- Wilkinson, G. (1922): Report of the Alberni and Port Alberni Townsite Area of the Alberni Coalfield; *B.C. Ministry of Energy, Mines and Petroleum Resources*, unpublished report in Alberni Community Archives.
- Yorath, C.J. and Sutherland Brown, A. (1984): Lithoprobe Geology; in Buttle Lake Mine and Lithoprobe Geology, *Geological Association of Canada, Pacific Section*, Guidebook for 2nd Annual Fall Field Trip, pages 20-26.

NOTES

**THE SUQUASH COALFIELD, VANCOUVER ISLAND
(92L/11)**

By Candace Kenyon

KEYWORDS: Coal geology, Vancouver Island, Suquash, sub-basin, vitrinite reflectance, coalbed methane.

INTRODUCTION

This report is part of an ongoing project, begun in 1987, to update knowledge of the coal basins of Vancouver Island. Limited information exists pertaining to coalmeasures of the Suquash coalfield or sub-basin (the terms coalfield and sub-basin are used interchangeably here). Geological descriptions by G.M. Dawson (1886) and Charles H. Clapp (1912) are contained in Geological Survey of Canada papers and a few unpublished reports are on file in Victoria with the B.C. Ministry of Energy, Mines and Petroleum Resources. The Buckham Collection, at the Provincial Archives of British Columbia, contains lithologic descriptions for some of the old boreholes. Due to recent industry interest in this area, this paper will summarize past activities and discuss recent coal-sampling results.

The coalfield is an isolated basin which covers 120 square kilometres near the northeast end of Vancouver Island (Figure 5-4-1). Access is possible by water, the Island Highway (No. 19), and secondary and logging roads. It is an area of predominantly low relief, with gently rolling

hills. It is heavily forested with cedar, fir and hemlock, and has many swampy areas, which hamper access. The Keogh and Cluxewe rivers flowing to the Queen Charlotte Strait drain the district. Most of the coalfield is covered by till which limits exposures to the shoreline, rivers and roadcuts. Climate is fairly mild and wet, and snowfall is common during the winter months.

GEOLOGICAL SETTING

The coal measures of eastern Vancouver Island are contained in Nanaimo Group rocks, which occupy the western erosional margin of the Late Cretaceous Georgia basin, which is largely concealed beneath the waters of Georgia Strait. The Suquash is a coal-bearing sub-basin within the Georgia basin. Crystalline basement rocks of Triassic and Jurassic age unconformably underlie the coal measures.

Sediments generally dip 5 to 10° to the northeast and consist mainly of sandstone, some shale, and minor amounts of conglomerate and coal. The total thickness of the sediments is unknown, but a borehole (BH 1), drilled in 1908, intersected weathered volcanics at a depth of 369 metres (Figure 5-4-1). Drilling has provided very little information concerning the paleotopography and how it affects sediment

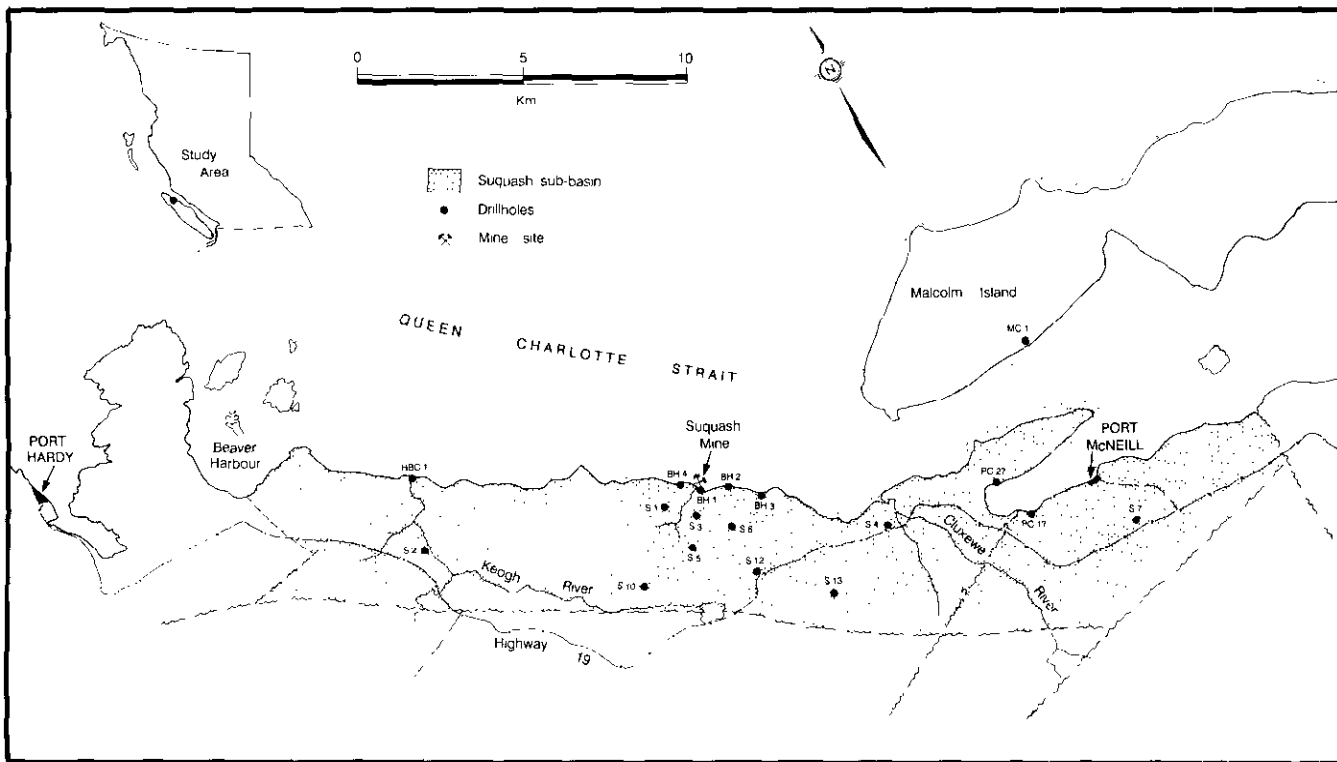


Figure 5-4-1. Location map, Suquash sub-basin.

distribution. There is also very little structural information available, but Clapp (1912) indicated that sediments in the coalfield are essentially flat-lying in what appears to be a broad, open syncline plunging at a low angle to the northeast. There are small intrusions of granitic and other igneous rocks along the coastline. Some localized folding has taken place, and there is probably localized faulting.

There are several coal zones in the Suquash coalfield, but individual seam thicknesses rarely exceed 1 metre. Eighteen drilling logs indicate coal or coaly material in all but two holes, S-2 and S-7. It cannot be described as clean coal because of multiple shale and mudstone partings in the zones. It appears that some zones may be laterally extensive. The coal in Hole MC 1, intersected at 166 metres, is thought to be the same zone as that worked at the Suquash mine.

HISTORY

The first samples of coal, from Beaver Harbour, were shown to the Hudson's Bay Company by native Indians in 1835. An exploration crew was sent to investigate the area and when fuel demands multiplied due to increased steamship fleets working on the west coast, it was decided to mine the deposit. In 1849, the company brought a party of workers from Scotland to operate the Suquash mine which was in production from 1849 to 1852. Three holes were drilled in 1852-1853, but only one location is known (HBC hole, Figure 5-4-1). When a richer deposit was discovered in the Nanaimo area, the company relocated its mining activities to the south.

There is evidence that a hole was drilled in 1890 and another in 1898, but unfortunately there are no logs or locations for these holes (Buckham, 1953).

Pacific Coast Coal Mines Ltd. drilled four exploratory holes in the old Suquash mine area in 1908 (BH holes). On the basis of the drilling results, it decided to work the property. At some time between 1908 and 1917, two holes were drilled on Malcolm Island. Only one is shown on Figure 5-4-1 (MC 1), the other is off the map. Two holes were drilled in the Port McNeill area (PC holes), but locations of these are vague. The outbreak of World War I and litigation regarding finances caused a shutdown of the mine in 1914 (Freeman, 1952). Following the war, small areas were mined until the closure in 1922. Total production from the coalfield, during the two mining stages was 23 600 tonnes.

Suquash Collieries Limited re-evaluated the underground mining potential in 1952 and dewatered an area of the old workings for a feasibility study of the deposit (Saunders, 1975). This was completed, but there were no mining operations to follow.

From October to November 1974, British Columbia Hydro and Power Authority drilled ten exploratory holes in the Suquash coalfield totalling 1910 metres (S holes). A total of 68 coal samples were taken from the drill core for proximate analysis. Geophysical logs were not run. Exploration activity ended as it appeared that the deposit was not economic for an underground coal mine at that time, due to relatively low calorific values.

RECENT WORK

In 1989, B.C. Hydro informed the Ministry of Energy, Mines and Petroleum Resources that it intended to dispose of the core from the 1974 drilling program (T. McCullough, personal communication). Hydro indicated that any core of interest to the ministry would be re-boxed and sent to Charlie Lake for storage. Only two of the holes (S-2 and S-5, Figure 5-4-1) were salvageable, as much of the core had deteriorated. Core from these two holes was sent for permanent storage. Coal in this core provided samples for the first vitrinite reflectance study of the Suquash coalfield.

Borehole S-2 did not contain any coal intervals, but ten coal samples were taken from S-5. The best possible samples were selected for vitrinite reflectance tests; in some intervals, much of the coal had already been removed for proximate analysis tests. Samples were crushed using a mortar and pestle. The -20 mesh fraction was combined with a mounting medium and pelletized. A Leitz MPV-3 reflecting microscope with an automated stage was used to determine the reflectance of the polished coal surfaces. On each sample, 50 randomly oriented vitrinite particles were measured for maximum and minimum apparent reflectance. A computer program developed by Kilby (1988) was used to produce on-screen crossplots for determining reflectance values.

RESULTS

Proximate analysis run on the B.C. Hydro samples (on an as-received basis), resulted in the following averaged values: moisture, 5.98 per cent; volatile matter, 23.31 per cent; fixed carbon, 25.38 per cent; ash, 45.34 per cent; sulphur, 2.21 per cent; and calorific value, 5969 Btu/lb. (Saunders, 1975).

A summary of the reflectance data from Borehole S-5 is presented in Table 5-4-1. Vitrinite reflectance values ranged from .63 to .81 per cent mean maximum and .60 to .80 per cent mean random. An examination of the coal pellets indicated that vitrinite was the predominant maceral, except for the uppermost sample in which the predominant maceral group was liptinite.

TABLE 5-4-1
VITRINITE REFLECTANCE DATA, BOREHOLE S-5

SAMPLE NUMBER	SAMPLE DEPTH (m)	MEAN MAXIMUM REFLECTANCE %	MEAN RANDOM REFLECTANCE %
1	19.8	.63	.60
2	48.6	.75	.73
3	66.8	.77	.76
4	74.7	.77	.73
5	84.4	.79	.78
6	106.4	.77	.76
7	190.2	.77	.76
8	214.9	.81	.80
9	216.1	.80	.79
10	234.7	.80	.79

DISCUSSION

There is limited distribution of exploration holes in this coalfield, and with the exception of one hole, none intersect basement rocks. There do not appear to be any useful horizons for correlating the coal zones from the available borehole information, with the exception of those close to

the old mine site. Consequently, there are not enough data available to provide a clear picture of the stratigraphy, structure, thickness and areal extent of the coal measures.

Vitrinite reflectance values and maceral content determined by this year's study indicate that the coal in the Suquash coalfield straddles the boundary between high volatile A and B bituminous rank (Figure 5-4-2). The moist ash-free calorific value places the coal in a high volatile C bituminous category based on B.C. Hydro's average values using A.S.T.M. standards (Saunders, 1975).

The area does not hold promise for development of an underground coal mine. When compared to other deposits, the dirty nature of the coal, due to multiple partings, and the relatively thin seams, do not make this an attractive venture.

An accurate estimate of reserves is difficult without sufficient data. B.C. Hydro calculated mineable reserves, from its

1974 drilling program, of 45 million tonnes of coal. The quality parameters used to determine this number were 6000 Btu/lb minimum and 50 per cent ash maximum (Saunders, 1975).

The recent vitrinite reflectance work places the coals of the Suquash sub-basin in the window of coalbed methane generation (Figure 5-4-2). Freeman (1952) stated, "I am certain when the mine has been cleared of gas, you will not be bothered with gas providing you have sufficient ventilation." This area deserves investigation of its coalbed methane potential. Certainly, more work is necessary.

ACKNOWLEDGMENTS

The author would like to thank Brad Van Den Bussche and Jim Hunter for sorting through the mounds of core

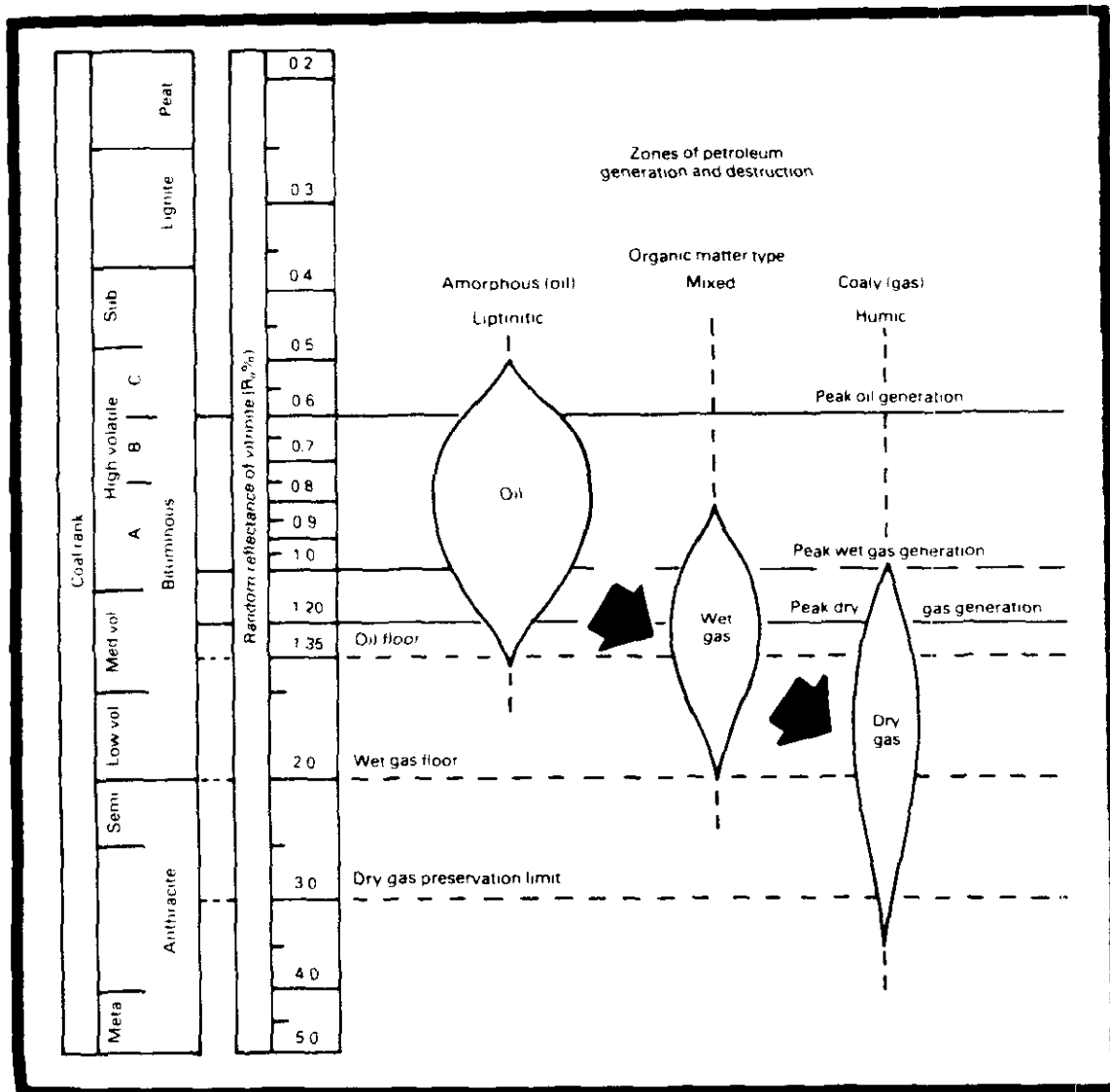


Figure 5-4-2. Correlation of coal rank scale with zones of petroleum generation (modified after Dow, 1977).

boxes, and to B.C. Hydro for re-boxing and shipping the core to Charlie Lake. Special thanks to Joanne Schwemler for her vitrinite reflectance work, and to Maria Holuszko for maceral identification.

REFERENCES

- Buckham, A.F. (1953): Suquash Borehole Records; *Provincial Archives of British Columbia*, Additional Manuscript 436, Box 76, File 5.
- Clapp, C.H. (1912): Geology of Nanaimo Sheet, Nanaimo Coalfield, Vancouver Island, British Columbia; *Geological Survey Branch of the Department of Mines*, Summary Report 1911, No. 26-1912, pages 106-107.
- Dawson, G.M. (1886): Coast from Port McNeill to Beaver Harbour; *Geological Survey of Canada*, Report of Progress, Volume 2, 1886, pages 61B-70B.
- Dow, W.G. (1977): Kerogen Studies and Geological Interpretations; *Journal of Geochemical Exploration*, No.7, pages 79-99.
- Freeman, H.N. (1952): Suquash Coalfield Report; unpublished report for *Suquash Collieries Ltd.* by Hope Engineering Ltd.
- Kilby, W.E. (1988): Tectonically Altered Coal Rank, Boulder Creek Formation, Northeastern British Columbia (93P/3); *B.C. Ministry of Energy, Mines and Petroleum Resources*, Geological Fieldwork 1987, Paper 1988-1, pages 565-570.
- Saunders, C.R. (1975): Suquash Drilling Project; unpublished report for *British Columbia Hydro and Power Authority* by Dolmage Campbell & Associates Ltd.



**SUBSURFACE COAL SAMPLING SURVEY, BOWRON RIVER
COAL DEPOSITS, CENTRAL BRITISH COLUMBIA
(93H/13)**

By Alex Matheson and Mansour Sadre

KEYWORDS: Coal geology, Bowron River, Tertiary deposits, coal measures, stratigraphy, drilling, sampling, analysis, coalbed methane, desorption tests.

INTRODUCTION

The 1990 coal subsurface sampling survey of the Bowron River coal deposits represents the third year of the program and the second year in which funding was provided jointly by the Institute of Sedimentary and Petroleum Geology and the B.C. Ministry of Energy, Mines and Petroleum Resources. A total of 300 metres of core (diameter 3.5 centimetres) was recovered from three diamond-drill holes. The drilling program was conducted, as in previous years, by Neill's Mining Company using a Prospector 89 drill manufactured by Hydrocore Drills Ltd.

Coal exposures on the west bank of the Bowron River, near the drill sites, were sampled, in addition to all the coal seams and bands recovered from the drill cores. Methane desorption tests were carried out on coal core from several horizons.

EXPLORATION HISTORY

The existence of coal on the Bowron River was first reported by G.M. Dawson in 1871. However, it was not until 1910-11 that development work started, with the construction of an adit and survey of the area. After a 35-year period of inactivity, diamond drilling and trenching was undertaken in 1946 and continued for a three year period. In

1967 work restarted with two exploration adits and several diamond-drill holes completed, and continued in a desultory manner until 1981. A total of about 140 holes, some as deep 1222 metres, were drilled over the entire exploration period from 1946 to 1981. The licenses were forfeited in 1982 and at present none are held in the area.

LOCATION OF THE STUDY AREA

The Bowron River coal deposit is within the Interior Plateau, in east-central British Columbia (Figure 5-5-1) 50 kilometres east-southeast of Prince George. Access is via a dirt road 55 kilometres east of Prince George on Highway 16 (Yellowhead Highway). The old adit site is reached by travelling 7 kilometres along this road to the south and a further 7 kilometres eastwards on a good forestry road. The adit is on the west bank of the Bowron River.

GEOLOGICAL SETTING

The Tertiary coal measures of the Bowron River graben overlie and are bounded by Mississippian volcanics and sediments of the Slide Mountain Group. Outcrop is sparse in the immediate vicinity of the graben due to the Quaternary overburden of alluvium and glacial deposits, which varies in thickness from a few metres to 300 metres.

The graben trends in a northwesterly direction. It is 2.5 kilometres wide and about 25 kilometres long. The coal measures occupy the lower 100 to 150 metres of the Tertiary sequence and consist of siltstone, sandstone, conglomerate and coal. The reported average thicknesses of the coal zones are: Upper, 2.4 metres; Middle, 3.4 metres; Lower, 4.0 metres (Borovic, 1980).

The regional strike varies from 325° to 330° and the dips along the western flank vary from 30° to 35° northeast, though dips appear to lessen with depth. The strike of the western boundary fault, as indicated by outcrop and drill-hole data, is roughly parallel to that of the Tertiary sediments. The position of the eastern boundary fault, which probably has a greater displacement, is inferred beneath the extensive overburden. Two minor, subparallel faults down-drop the strata toward the centre of the basin (Figure 5-5-2).

The 1981 drilling added little to this general picture, other than the fact that the basement surface below the area east of the Bowron River is very uneven. The lower coal zone has greater lateral continuity than the upper two, in which the coals are discontinuous and variable. Despite the close proximity of the three drill holes to one another along strike, correlation is difficult. A moderately active period of deposition is indicated by rapid facies changes, and flaser-

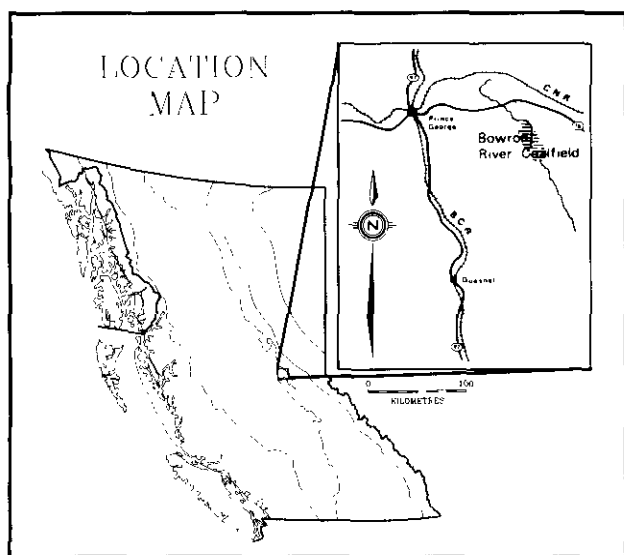


Figure 5-5-1. Location map.

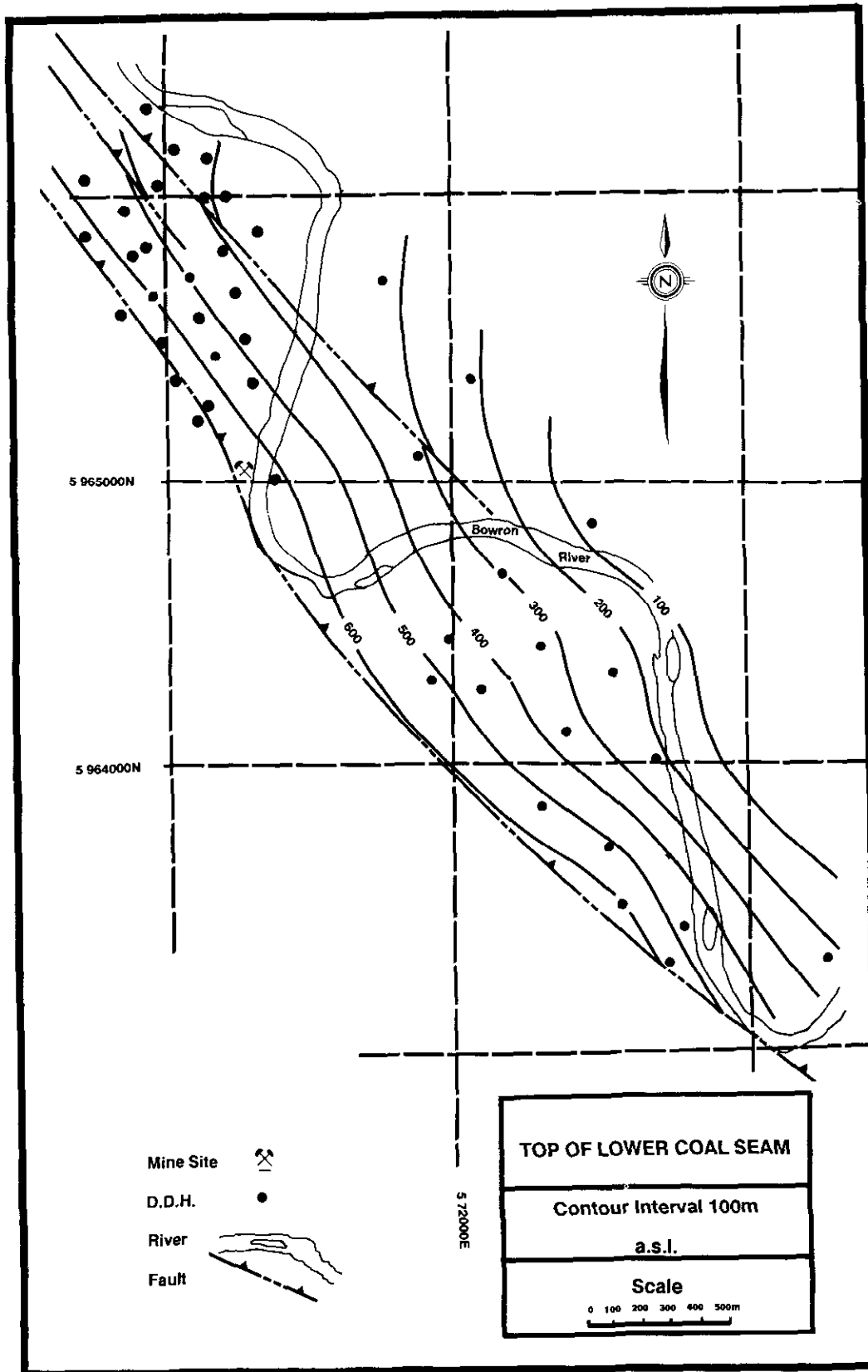


Figure 5-5-2. Contours of the top of lower coal seam.

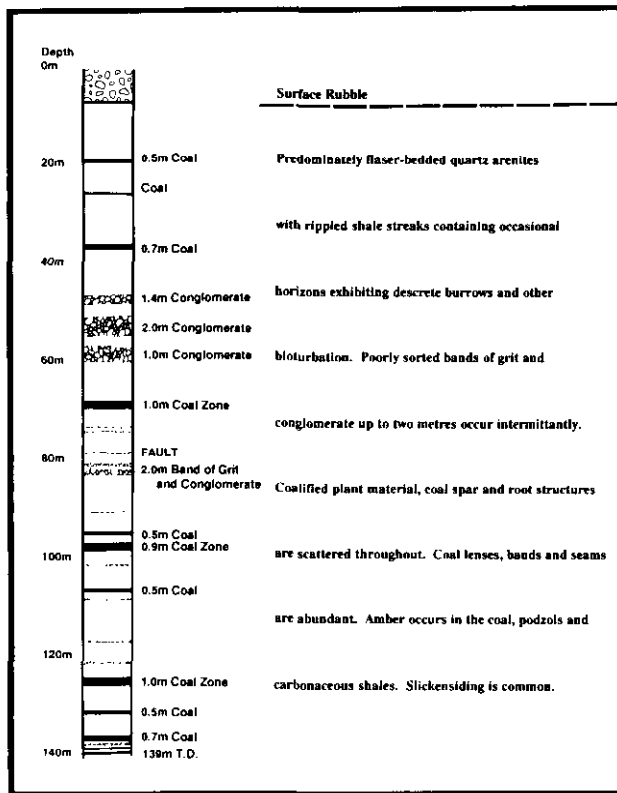


Figure 5-5-3. Simplified stratigraphic log of hole GSB-90-3.

bedded quartz arenites, accompanied by burrowing and other bioturbation. The presence of grits and conglomerates suggests various periods of high-energy sedimentation. Podzols containing distinct root structures and coalified plant remains occur throughout the section (Figure 5-5-3).

COAL QUALITY

The coal is described as a high-volatile B bituminous with an average R_o max of 0.65. A typical proximate analysis on an as-received basis is: moisture, 4.0 per cent; ash, 35.7 per cent; volatile matter, 26.4 per cent; fixed carbon, 33.9 per cent. The Hardgrove grindability index is 53 per cent and the average sulphur content is 1.6 per cent.

In outcrop, the cleat spacing is close (2 to 3 millimetres) suggesting a friable coal. This, however, is not consistent with the low Hardgrove Index. The total resin content is reported to be 8 per cent (Borovic, 1980), composed of 4 per cent Canadian resin-soluble and 4 per cent of insoluble resin. Sulphur bloom is abundant on coal outcrops.

DRILLING AND SAMPLING

The two major constraints regarding the siting of the drill holes were the highly variable thickness of overburden and the depth of the coal zones. Another consideration was the capability of the small drill which, in this instance, penetrated to depths of 140 metres. The coal zones are at their shallowest near the western fault. As a result, the holes were

sited along strike, close to the fault (Figure 5-5-4) and the southwest bank of the Bowron River. The spacing was about 100 metres to 120 metres. Depths of the holes are as follows: GSB-90-01, 130.3 metres; GSB-90-02, abandoned in overburden after two attempts; GSB-90-03, 139.0 metres; GSB-90-04, 24.5 metres.

The proximity of the coal zones to the fault decreased with depth in all holes. Coal bands greater than 5 centimetres thick were sampled, and the thicker seams were sampled in about 20-centimetre increments. Five grab samples of outcrop coal, exposed by the river, were taken near the site of GSB-90-04. Seventy samples were taken from GSB-90-01, thirty-five from GSB-90-03 (Figure 5-5-6) and thirty-three from GSB-90-04. All samples were forwarded to the Institute of Sedimentary and Petroleum Geology in Calgary for analysis. Eight samples were used for methane desorption tests.

SAMPLE ANALYSIS

All coal samples will be crushed to -20 mesh. Petrographic rank determinations will be carried out in-house by the vitrinite reflectance method. Analyses will also be made using X-ray defraction on low-temperature ash samples. The following analyses will be carried out by a private laboratory under the joint auspices of the Geological Survey Branch and the Institute of Sedimentary and Petroleum Geology: proximate; ultimate; sulphur forms; calorific value; ash analysis; chlorine, fluorine and mercury contents; and ash fusion. At the request of Dr. Fari Goodarzi the remainder of the core, after the coal had been removed, was sent to the Institute of Sedimentary and Petroleum Geology in Calgary, primarily for petrographic examination of the carbonaceous material in the mudstones, siltstones and shales, and trace element determination will be done on the coal using, among other techniques, neutron activation.

METHANE DESORPTION TESTS

1990 was the first year that the Geological Survey Branch attempted desorption tests, and we were more concerned with the methodology than the actual assessment of the methane potential of the coal deposit at this stage. Test canisters were made up from PVC plumbing pipe, with an internal diameter of 3.8 centimetres, and various plumbing accessories (Plate 5-5-1). The canisters were tested for an air-tight seal by sealing in baking soda and water, then holding them under water to detect any escaping gas. This check was made after the completion of each test. To ensure an effective seal the "O" ring was carefully examined. Teflon tape was wrapped around the thread of the sealing cap and all coal particles, which would prevent an efficient seal, were removed.

There are three components in the measurement of methane gas in coal (McCullough *et al.*, 1980):

- "Lost gas" is the methane which is given off from the time the coal sample is halfway out of the hole until the time it is sealed in the container (A in Figure 5-5-5), as

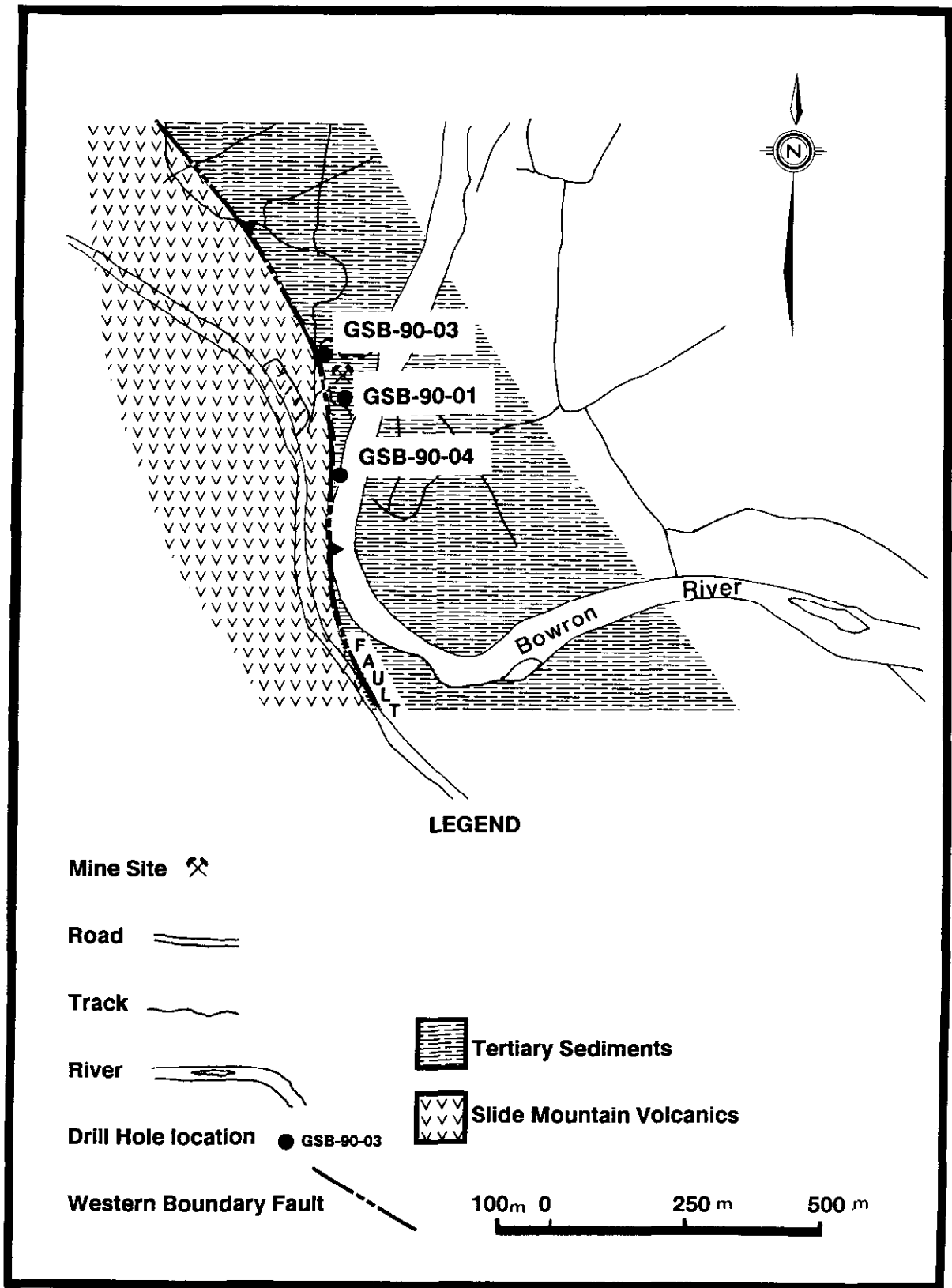


Figure 5-5-4. Location of GSB drill holes.

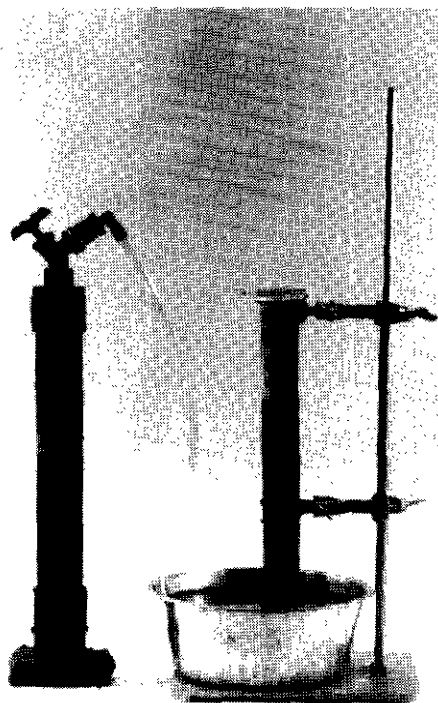


Plate 1. Desorption equipment.

in this case, where water is the drilling medium. If air or mist is used in drilling, it is assumed that the coal begins giving off gas immediately it is penetrated by the drill. This value is calculated by extrapolation back to zero time from the desorbed gas measurements. (e.g. Figure 5-5-5. McCullough *et al.*, 1980).

- “Desorbed gas” is the methane given off by the sample while in the cannister, and is the quantity measured as described below.
- “Residual gas” is retained by the coal and depends upon the fracture network that defines coal friability. The quantity is measured, in a sealed box filled with nitrogen, after desorption is completed by crushing in a mechanical grinder to about 200 mesh. This quantity is determined by gas chromatography and was not considered in this study.

Measurements were made of the desorbed methane at regular time intervals by releasing the gas through a valve into an inverted graduated cylinder filled with water (Plate 5-5-1). The volume of water displaced is then determined. Readings for the first two or three hours are taken at 15 minute intervals for an accurate determination of the lost gas (Figure 5-5-5, Line I) as the subsequent rate of desorption decreases (Figure 5-5-5, Line II). At Bowron River it was minimal, as the water table was just below surface and the hydrostatic pressure inhibited the release of gas during core recovery (Figure 5-5-5, Line I).

There should be a pressure gauge on the cannister to register the build up of pressure, as high pressure also inhibits the release of gas. The samples should be kept at a constant temperature of about 22°C, to allow free desorption. It was not possible to meet this condition in the field

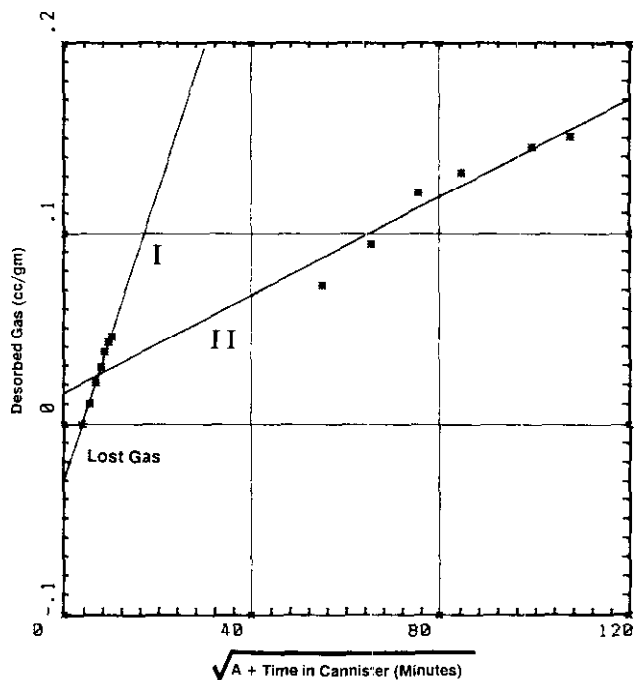


Figure 5-5-5. Desorbed gas and lost-gas calculation.

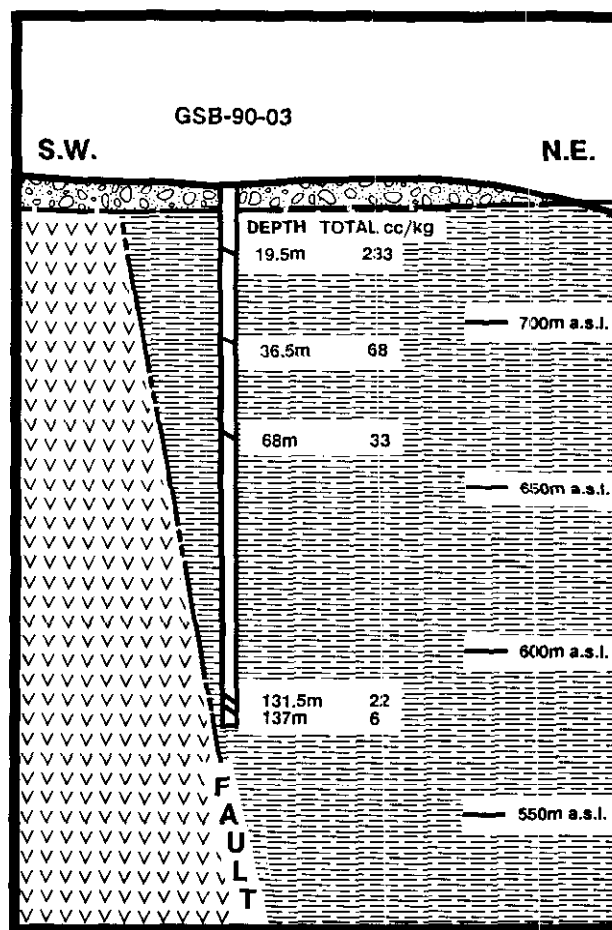


Figure 5-5-6. Section SW-NE through GSB-90-3 showing the coal horizons from which samples were taken for coalbed methane desorption tests and the results.

during the 1990 field season, with noticeable results (Table 5-5-1).

During this period, the night temperatures dropped to about 4°C. The time difference between the first and second reading is 22 hours and 10 minutes. Though the atmospheric temperature for the second reading was 22°C, the sample temperature lagged well below this level and there was no emission of methane. The third reading, taken only two hours later, by which time the temperature of the sample was probably appreciably higher, was 10 cubic centimetres. The same pattern was repeated the next day. Details of the procedures and calculations are given in various reports (McCullough *et al.*, 1980; Diamond and Levine, 1985).

**TABLE 5-5-1
METHANE GAS EMISSIONS INHIBITED BY
LOWER SAMPLE TEMPERATURES**

Sample #7 Date	Time	Weight of sample 0.37 kg		Temperature
		Gas Released	Total Gas	
21-IX	3:20 p.m.	8 cc	35 cc	22°C
22-IX	1:30 p.m.	0	35 cc	22°C
22-IX	3:30 p.m.	10 cc	45 cc	28°C
23-IX	10:45 a.m.	0	45 cc	23°C
23-IX	3:00 p.m.	4 cc	49 cc	28°C

**TABLE 5-5-2
COALBED METHANE DESORPTION TESTS**

Samples of coal taken from different coal horizons	
GSB-90-03	
Depth	Total cc/kg
19.5 metres	233
36.5 metres	68
68 metres	33
131.5 metres	22
137 metres	6

**TABLE 5-5-3
BOWRON RIVER COAL DEPOSITS
COAL RESOURCES AND POTENTIAL COALBED METHANE RESOURCE**

GENERALIZED SECTION								
DEPTH IN METRES								
FROM	0	200	400	600	800	1000	TOTALS	
TO	200	400	600	800	1000	1200	0 to 1200	
			COAL					
TOTAL (million tonnes)	33.75	60.0	64.5	64.5	78.75	91.5	393.0	
			METHANE					
TOTAL (million cubic feet)								
A	4219	9300	12255	13868	18900	23790	82332	
B	423	8100	12384	14835	20239	25620	81651	

A – Values calculated from Figure 5-5-8 (Ryan, this volume).

B – Values calculated from Equation 2, Table 5-5-1 (Ryan, this volume) R_0 max = 0.65.

RESULTS

Due to the attitude of the strata, it was necessary to place the holes close to the fault, with predictable results with respect to the methane emitted (Figure 5-5-5; Table 5-5-2). The deeper the coal samples, the closer they were to the fault, and the less the coalbed methane retention, contrary to normal conditions where coalbed methane content increases with depth (Eddy *et al.*, 1982).

RESOURCES

It has been postulated that the Tertiary sequence occurs as an asymmetrical syncline (Borovic, 1981). There is little evidence of this in the existing drill-hole data. Assuming, however, that it is not a syncline, the thickness of the Tertiary deposit would be 1200 metres, which is not unreasonable. The beds strike 325° to 330° and dip 30° to 35° northeast near the western fault boundary, but flatten towards the centre of the basin.

The resource calculations are based on the most simple monoclinical structure. The coal resource of the lower coal seam only, assumed to be a constant 4 metres thick, is estimated at 400 million tonnes (SG 1.5) down to a depth of 1200 metres [where drill hole 81-22 (Norco) penetrated the lower coal seam at a depth of 1172 metres]. If the beds are folded into an asymmetrical syncline, the figure for the coal resources is not appreciably different, though it would be less for coalbed methane. Table 5-5-3 gives a breakdown of the coal resources for each 200-metre depth increment and two methods of assessing the coalbed methane potential.

CONCLUSION AND RECOMMENDATIONS

Despite the badly broken core and abundant slickensiding, recovery at 95 per cent was good. Further drilling would resolve the structure and delineate the resources. More accurate desorption tests should be carried out on coal

at greater depths and distance from the boundary fault. Rigorous desorption tests would take several weeks, continuing until the rate is less than 0.05 cubic centimetres per gram for five consecutive days. Indications are that the Bowron River coal is blocky in nature, in which case it would only emit about 60 per cent of its total gas by desorption (McCullough *et al.*, 1980). On the other hand, friable coals emit nearly 96 per cent of the total gas. Hydrofracturing would release most of the residual gas within an area with a diameter of 50 metres to 100 metres, depending upon the severity of the fracturing, virtually converting a blocky coal to a friable coal (personal communication, D. Richardson, 1990).

It is unlikely that the Bowron River deposit is capable of supporting a viable mining operation. An interesting alternative for the exploitation of the existing energy resources may lie in coalbed methane extraction.

ACKNOWLEDGMENTS

The authors would like to extend their appreciation to Dr. Fari Goodarzi for his keen interest and participation in the program, their colleagues in the Coal Unit, Barry Ryan and Dave Grieve, to the personnel of the Ministry's Prince George District Office, and to Julie Hutchins for her stenographic support.

REFERENCES

- Borovic, I. (1980): Exploration Report; *Norco Resources Ltd.*
- Borovic, I. (1981): Explorations Report, *Norco Resources Ltd.*
- Diamond, W.P. and Levine, J.R. (1985): Direct Method Determination of the Gas Content of Coal: Procedures and Results; Report of Investigations 8515, *United States Department of the Interior, Bureau of Mines.*
- Eddy, G.E., Rightmire, C.T. and Byren, C.W. (1982): Content of Coal Rank and Depth: Relationship of Methane; Proceedings of the *Society of Petroleum Engineers/Department of Environment, Unconventional Gas Recovery Symposium*, Pittsburg, Pennsylvania, 10800, Pages 117-122.
- McCullough, C.M., Levine, J.R., Kissell, F.N. and Duell M. (1980): Measuring the Methane Content of Bituminous Coal Beds; Report of Investigations 8043, *United States Department of the Interior, Bureau of Mines.*
- Ryan, B.D. (1991): Geology and Potential Coal and Coalbed Methane Resource of the Tuya River Coal Basin; *B.C. Ministry of Energy, Mines and Petroleum Resources, Geological Fieldwork 1990, Paper 1991-1, this volume.*

NOTES



**DENSITY OF COALS FROM THE TELKWA COAL PROPERTY,
NORTHWESTERN BRITISH COLUMBIA
(93L/11)**

By Barry Ryan

KEYWORDS: Coal geology, coal density, *in situ* moisture, porosity, Telkwa.

INTRODUCTION

It is important, for mining feasibility studies, to be able to accurately convert *in situ* coal volumes to tonnages using coal densities. The density of coal of constant rank varies depending on the amount of included rock (mineral matter), water, and void porosity. Actual measurements of density often require adjustment because data are needed at different ash, water or porosity values. Data from the Telkwa Coal property are used to validate a density equation. The equation predicts density given per cent ash or, per cent ash given the density. It requires the following constants to be defined; density of dry zero-ash coal (DC), density of dry mineral matter (DMM), weight per cent water (TM), volume per cent void porosity (VP) and the ratio weight of mineral matter divided by weight of resultant ash (WTLOS). The equation (Equation 1, Table 5-6-1) has the form;

$$BD = 100 \times DC \times DMM / [DC \times DMM \times (TM + VP) + MM \times (DC - DMM) + DMM \times (100 - TM)];$$

MM is the weight of mineral matter, and is given by;

$$MM = WTLOS \times \text{per cent ash.}$$

**TABLE 5-6-1
DEVELOPMENT OF DENSITY EQUATIONS**

Specific gravity	= mass/volume × density of water.
Bulk density	= mass/volume (grams/cubic centimetre).
DC	= apparent specific gravity of dry, zero-ash coal.
DMM	= apparent specific gravity of dry, pure mineral matter.
TM	= mass of water in sample including inherent and surface water.
MD	= moisture difference.
ADM	= mass of air dried moisture.
VP	= volume of air or gas-filled voids.
BD	= <i>in situ</i> specific gravity or bulk density.
MM	= mass of mineral matter.
MC	= mass of zero-ash coal.
WTLOS	= mass mineral matter divided by mass of ash.
	$BD = (MC + MM + TM) / (MC/DC + MM/DMM + TM + VP)$
	$MC + MM + TM = 100 \text{ grams}$
	$DC \times DMM = K$
	$BD = 100 \times K / (K \times (TM + VP) + MM \times (DC - DMM) + DMM \times (100 - TM))$ (Equation 1)
	$BD = 1/(A + B \times \text{Ash})$ simplified form Equation 1
	$MM = 1.08 \times \text{Ash} + .55 \times PY$ (Rees, 1966)
	PY = per cent pyrite
	MM = WTLOS × Ash as described in text
	$VP = 100 \times (1 - BD/ASG)$ (Equation 2)
	$MD = 100 \times (ASG - BD) / (BD \times (ASG - 1))$ (Equation 3)
	$A = (VP + TM) + (1 - TM)/DC$ (Equation 4)
	$B = -(DMM - DC) / (DMM \times DC) \times WTLOS$ (Equation 5)
	$TM = (ADM \times (100 - ADM) + MD \times 100) / 100$ (Equation 6)

The Telkwa coal property is located in northwestern British Columbia, 15 kilometres south of Smithers. In the area, Cretaceous sediments of the Skeena Group contain a coal-bearing succession which includes ten seams over approximately 300 metres of section (Figure 5-6-1). Exploration on the property by Crows Nest Resources Limited (geological assessment reports submitted to B.C. Ministry of Energy, Mines and Petroleum Resources, 1981 to 1989) has culminated in a submission to the provincial government seeking approval to develop an open-pit coal mine on the property. The data discussed in this study were collected as part of the mining feasibility study for one of the proposed open pits which is located on the north side of the Telkwa River (Pit 7). One hundred and eighty seven samples of NQ diamond-drill core from Seams 2 to 8 (Figure 5-6-1), representing approximately 50 metres of section, were analyzed on an air-dried basis (ADB) for apparent specific gravity (ASG), per cent ash, per cent sulphur and per cent moisture. The apparent specific gravity was measured on 60-mesh sized particles, using ASTM procedure D167.

Previous discussions of coal density versus ash relationships have taken two general directions. Some fit mathematical curves to data sets of ash and density measurements (Ward, 1984). This approach lacks flexibility and requires a new set of sample analyses if rank or moisture content of coal change. Other papers take a more theoretical approach and develop equations which predict coal density using real variables such as per cent ash and per cent moisture (Smith, 1989). This paper takes the latter approach; Equation 1 was developed over a number of years while working in industry and is similar to, though less rigorous than that used by Smith.

COAL DENSITY

A number of concepts require clarification before embarking on a discussion of the subtleties of coal density versus ash relationships. Analytical laboratories measure per cent ash in coal; a coal seam actually contains mineral matter. When ash is extracted by burning off the coal there is a weight loss experienced by the mineral matter as it is in part volatilized and converted to ash. The ratio, weight of mineral matter divided by weight of resultant ash, is referred to in this study as the "weight loss value" (WTLOS). Coal in the ground or in a stockpile may contain air or gas-filled fractures or spaces which make up a volume referred to in this study as "void porosity". Void porosity (VP) is a volume which is in addition to, and does not include "water-filled porosity". The water content of the coal (TM) is expressed as a weight per cent; some of the water is in fractures, some in small-scale porosity and some is associated with the microporosity. In rough terms, total moisture

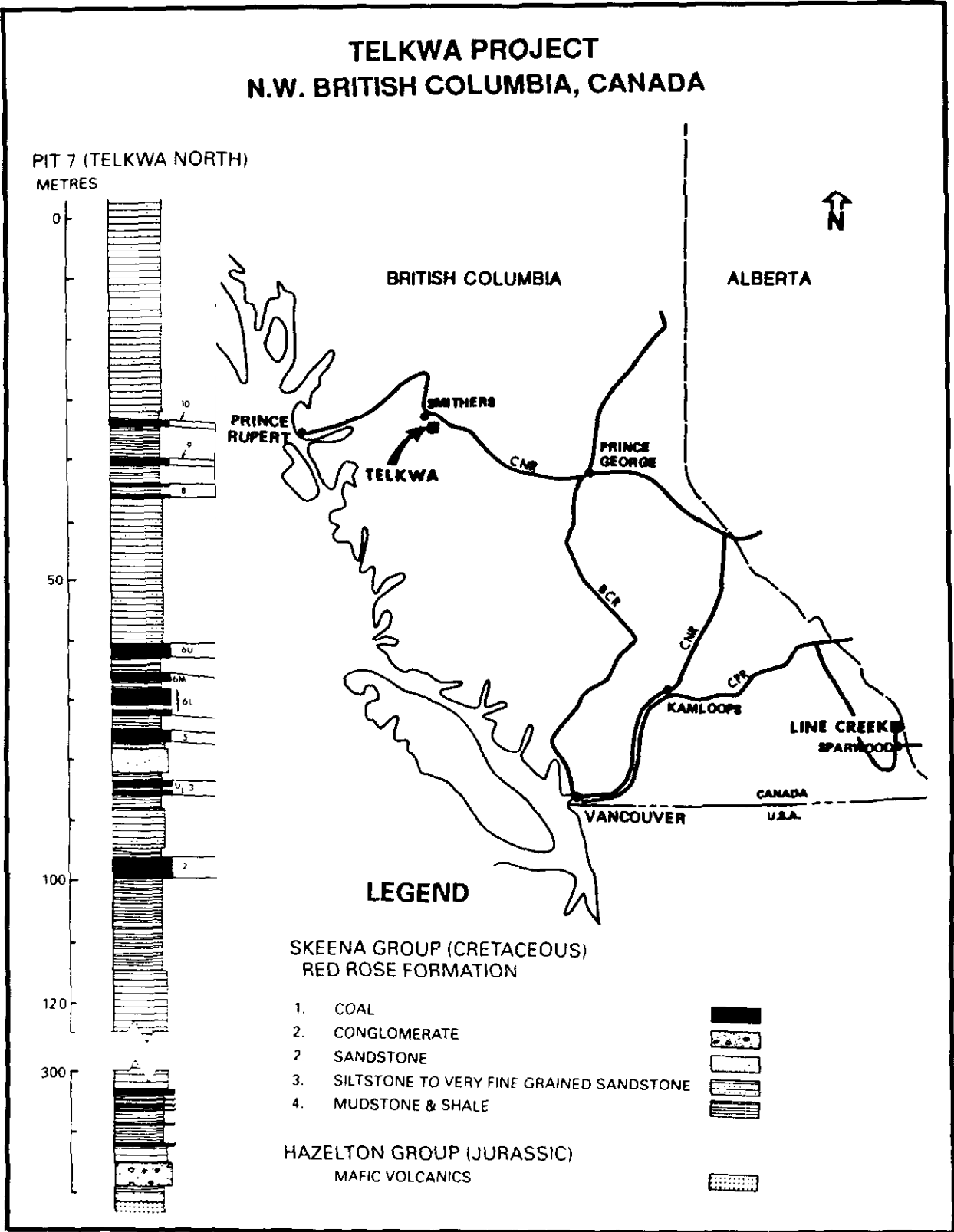


Figure 5-6-1. Telkwa project; location and stratigraphic section.

is equivalent to "in situ moisture", water in small-scale and microporosity is equivalent to as-received or equilibrium moisture and water in microporosity only is equivalent to air-dried or inherent moisture.

The true density of dry, zero-ash coal cannot, in reality, be measured. It is possible to remove all the water from coal but it is not possible to remove all the ash. It is also very difficult to measure true density corrected for microporosity (coal pores up to 200 Å units in size). The microporosity is filled with water, methane or other gases and density measurements which do not take microporosity into account will be lower than true density and should be referred to as "apparent density" or "apparent specific gravity" (ASG).

The terms density and specific gravity are often used interchangeably. Density is mass divided by volume often expressed as grams per cubic centimetre; the specific gravity of a substance is the ratio obtained by dividing its density by the density of water and is therefore dimensionless. In the rest of the text, general discussion may refer to densities, but all detailed discussion will refer to specific gravity, sometimes abbreviated to SG.

Measurements of apparent SG are usually made on samples with air-dried moisture and variable ash contents. Data are projected to give a values of apparent SG at zero per cent ash and moisture (DC) and specific gravity of the mineral matter at zero per cent void porosity and moisture (DMM).

It is important to differentiate between the concept of *in situ* SG or "bulk density" (BD) and particle apparent SG (ASG). Measurements of *in situ* SG incorporate open or water-filled fracture porosity. Measurements of apparent SG, utilizing 60-mesh sized grains, do not take into account fracture porosity and are normally higher than *in situ* SG measurements on the same coal. Romaniuk (1987) discusses the concepts of true, apparent and *in situ* SG. He also discusses the difficulties in making direct measurements of *in situ* SG and presents the limited amount of *in situ* SG data he could locate in the literature.

The *in situ* SG of a sample is usually less than the apparent specific gravity (ASG) on an air-dried basis (ADB). If this difference is because of the destruction of void porosity during preparation of the sample for ASG

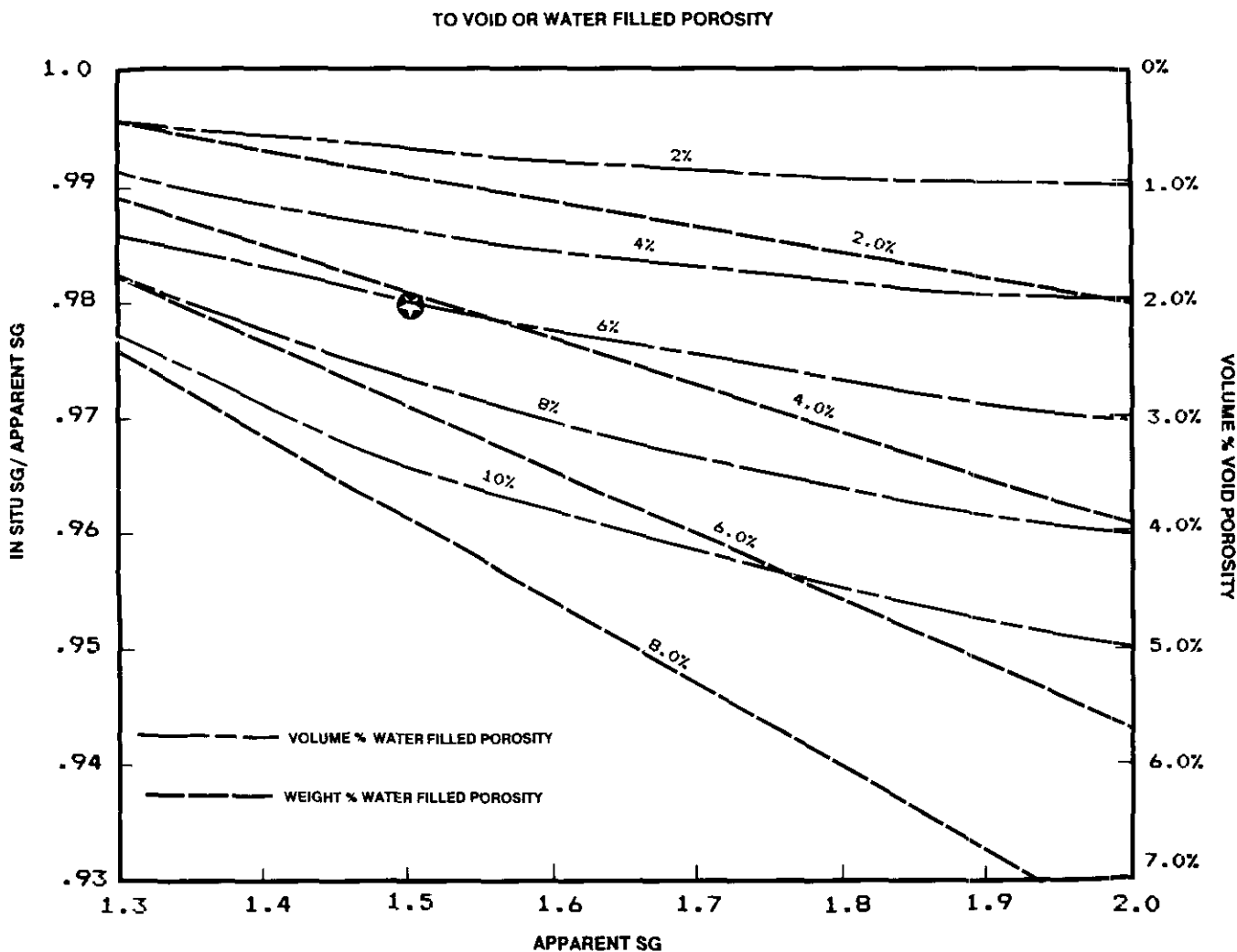


Figure 5-6-2. Relationship of *in situ* specific gravity and sample apparent specific gravity to air or water-filled porosity.

measurements then the per cent void porosity volume change is given by:

$$100 \times (1 - BD/ASG) \quad (\text{Equation 2, Table 5-6-1}).$$

On the other hand, if the decrease is because of destruction of water-filled fracture porosity then the per cent porosity volume change is still given by Equation 2 and the change in weight per cent water (or water-filled volume) is given by:

$$MD = 100 \times (ASG - BD) / [BD \times (ASG - 1)]. \quad (\text{Equation 3, Table 5-6-1}).$$

A plot of X axis = ASG, left Y axis = BD/ASG and right Y axis = void porosity (Figure 5-6-2) can be contoured using the two relationships above with iso-volume and iso-weight of water-filled porosity lines. An example point [X = 1.5 (ASG); left Y = .98 (BD/ASG = 1.47/1.5); Figure 5-6-2] predicts a void fracture porosity of 2 per cent (right Y axis) or a water-filled porosity volume of 6 per cent corresponding to 4 weight per cent water. The 6 per cent porosity volume and 4 per cent water content are in addition to the porosity or water values in the sample measured on an air-dried basis. Actual fracture porosity will probably be close to the 6 per cent by volume value, indicating close to 100 per cent saturation.

DEVELOPMENT AND JUSTIFICATION OF THE DENSITY EQUATION

Equation 1 incorporates values of apparent specific gravity of dry zero-ash coal (DC); apparent specific gravity of dry mineral matter (DMM); volume of void porosity (VP) weight per cent of total water (TM), and a method of converting per cent ash to per cent mineral matter. Per cent ash can be converted to per cent mineral matter using the Parr Equation (Rees, 1966) or by using the value WTLOS. Equation 1 has the general form;

$$BD = 1/[A + (B \times \text{ash})],$$

where BD is *in situ* SG or bulk density. The values A and B are constant if per cent ash and BD are the only variables; in which case;

$$A = (VP + TM) + (1 - TM)/DC \quad (\text{Equation 4, Table 5-6-1})$$

$$B = -(DMM - DC)/(DMM \times DC) \times WTLOS$$

$$(\text{Equation 5, Table 5-6-1}).$$

Constant A provides a unique value for DC and constant B provides a set of paired DMM and WTLOS values.

TABLE 5-6-2
APPARENT SPECIFIC GRAVITY ANALYSES,
TELKWA PROPERTY

Seam	Data Count	ASG	Moisture ARB %	Moisture ADB %	Ash ADB %	Sulphur ADB %
8	6	1.47	3.29	0.7	18.00	1.62
6	52	1.49	3.49	0.83	17.56	1.51
5	33	1.58	3.74	0.79	23.99	1.23
4	22	1.70	3.46	0.63	30.45	1.38
3	25	1.60	4.25	0.95	25.72	1.54
2	49	1.50	3.97	0.84	21.09	1.03
Total	187					
Averages		1.547	3.75	0.81	22.2	1.33

Note: ASG apparent specific gravity measured on an ADB
ADB air-dried basis
ARB as-received basis
Seam averages are weighted based on sample size

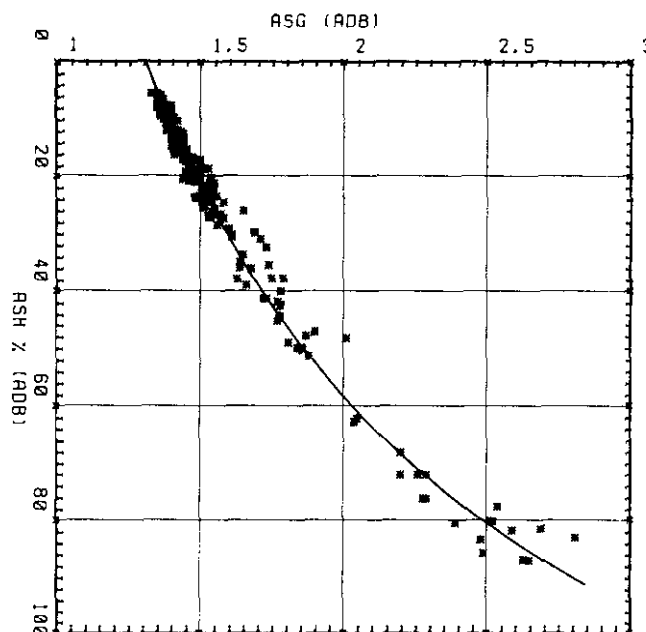


Figure 5-6-3. Telkwa data; apparent specific gravity versus per cent ash, both on an air-dried basis.

TABLE 5-6-3
RESULTS OF CURVE FITTING TO TELKWA DENSITY DATA

Equations fitted to all ash versus density data			
No.	Equation	r ²	
1	Y = 1/(A.(X + B) ² + C)	.983	
2	Y = A.e ^{-((X - B)/2)}	.983	
3	Y = 1/(A + B.X)	.982	
4	Y = A.X'(B.X)	.982	
5	Y = A.B'X.X'C	.982	
6	Y = A(X/B)'C.c'(X/B)	.982	
7	Y = A + B.X + C.X ²	.980	
8	Y = A.B'X	.980	
9	Y = A.e'((Ln(X) - B)'2/C)	.972	
10	Y = A + B.X + C/X	.971	
11	Y = A + B.X	.960	

Constants from equation No. 3 Y = 1/(A + B.X)				
Data	Constant A	Constant B	r ²	Clean-Coal Density DC
All Seams	.76230	-.00450	.982	1.315
Seams 6 + 8	.76376	-.00463	.975	1.313
Seams 2 + 3	.7597	-.00439	.981	1.320

Calculated paired values of DMM and WTLOS using Equations 4 and 5, Table 5-6-1 (VP=0% TM=0.8%)			
DMM	All Seams	Seams 6 + 8	Seams 2 + 3
2.6	1.198	1.23	1.18
2.62	1.98	1.22	1.17
2.64	1.179	1.21	1.16
2.66	1.171	1.20	1.15
2.68	1.162	1.19	1.14(b)
2.7	1.154	1.18	1.13
2.72	1.146(b)	1.17	1.13
2.74	1.138	1.17	1.12
2.76	1.131	1.16(b)	1.11
2.78	1.123	1.15	1.10
2.8	1.154	1.14	1.10

(b) = Best fit with plasma ashing data
Note: DMM density dry mineral matter
WTLOS (weight of mineral matter)/(weight of ash)

TABLE 5-6-4
PLASMA ASHING XRD AND REFLECTANCE DATA FOR FOUR TELKWA SAMPLES

Seam	Coal Samples				Plasma-ashed Samples		
	R _v Max %	Ash %	Mineral Matter%	WTLOS	Ash %	WTLOS high%-low%	Minerals
6	.963	26.2	30.26	1.155	85.92	1.164	KQCDSF
5	.957	10.5	12.03	1.146	86.45	1.157	QKDCPS
3	.901	27.0	30.08	1.114	86.44	1.157	QKDCPS
2	.976	19.8	22.24	1.123	86.9	1.151	KQPCDS
Average				1.135		1.157	

Mineral Data					
Mineral	Code	Density g/cc	WTLOS	Weight Loss % of Mineral	
Kaolinite	K	2.63	1.162	14	
Quartz	Q	2.65	1	0	
Calcite	C	2.72-2.94	1.785	44	
Dolomite	D	2.86-2.93	1.913	47.7	
Siderite	S	3.5-3.96	1.613	38	
Pyrite	P	4.95-5.03	1.5-1.67	33.4-40	

Note: R_v Max = reflectance of vitrinite in oil
WTLOS (weight mineral matter)/(weight ash)1

The Telkwa data are plotted on Figure 5-6-3 and averaged in Table 5-6-2. Data in the plot of apparent specific gravity (ADB) versus per cent ash (ADB) (Figure 5-6-3) scatter along a curve rather than a straight line. A freeware program, CURVEFIT based on equations in Kolb (1984), fits 25 different equations to X versus Y data. Using regression analysis and r² values it assigns the best constants to each equation and ranks the equations in terms of their ability to fit curves through the data. The results of applying the CURVEFIT computer program to the Telkwa data are presented in Table 5-6-3. Equations are ranked based on r² values from the best (r² = .983) to a straight line (r² = .960). An equation of the form $Y = 1/[A + (B \times X)]$ which has the structure of Equation 1 is ranked third. Obviously Equation 1 has a structure which enables it to fit the Telkwa data well, which, to some extent, validates the theory and assumptions used to develop it. The constants A and B from Equation 3 (Table 5-6-3) provide a unique value of 1.315 for DC and a set of possible paired values for DMM and WTLOS (Table 5-6-4).

Generally, Equation 1 is used to generate data sets of apparent specific gravity (ASG) versus per cent ash at different void porosity volumes and weight per cent moisture contents. Data sets can be tabulated or plotted as curves; usually it is assumed that values DC, DMM and WTLOS remain constant for a single data set. In fact the density of the inherent mineral matter in coal seams is probably different from the density of rock splits that contribute to the per cent ash at high ash concentrations. The value DMM probably varies with the ash content. It is also dangerous to assume total moisture is constant over a range of ash concentrations. The inherent moisture in coal is unlikely to be the same as the inherent moisture in rock, nor is the fracture porosity likely to remain constant as the ash content of a seam varies from 10 to 50 per cent. Thus, in reality, *in situ* moisture content probably varies with ash content.

Computer programs were written to calculate the various specific gravity versus ash relationships and to plot the

results. These programs and the CURVEFIT freeware program are available from the author on an informal basis.

TELKWA COAL

APPARENT SPECIFIC GRAVITY OF COAL AND MINERAL MATTER

The curve generated using Equation 1 (Figure 5-6-3) represents the ASG versus ash relationship for Telkwa coals at ADB moisture averaging about 0.8 weight per cent (Table 5-6-2) and zero volume void porosity. Once values of DC, DMM and WTLOS are established, it is possible to vary the weight per cent water and volume void porosity in Equation 1 and develop a curve of *in situ* specific gravity (BD) versus ash (ADB) which can be used for *in situ* tonnage calculations. It is therefore important to confirm the accuracy of the value DC and to choose the most appropriate paired values of DMM and WTLOS.

The predicted value of apparent specific gravity for dry zero-ash coal (DC) for Telkwa coal is 1.315 (Table 5-6-4) which is reasonable, based on the rank of the coal (high volatile bituminous A) and agrees with density ranges suggested by Smith (1989). Clean coal density is rank dependent, higher rank seams lower in the stratigraphic section will have higher densities. To test if variations in the value DC are contributing to data scatter in Figure 5-6-3, data were divided into upper-seam data (Seams 6+8) and lower-seam data (Seams 2+3). The upper and lower seam data sets represent an average stratigraphic separation of 40 metres. The upper-seam data predict a DC value of 1.31 and the lower-seam data a value of 1.32 (Table 5-6-3). It is unlikely that this is a statistically significant difference, certainly it contributes very little to the data scattering on Figure 5-6-2.

The mean maximum reflectance of vitrinite in oil was measured on the four composite samples of Seams 6, 5, 3 and 2. Values range from .98 per cent to .9 per cent and average .95 per cent (Table 5-6-4) indicating a rank of high volatile bituminous A. Values do not correlate with stratigraphic position.

The values of DMM and WTLOS are higher for the upper seams than for the lower seams (Table 5-6-3). This implies that mineral matter associated with the upper seams is composed of heavier minerals which undergo a greater weight loss when ashed than minerals associated with the lower seams. Such minerals could be carbonates and pyrite. Data collected for an acid rock-drainage study (Norecol, 1990) indicated a net neutralizing potential of 35 and pyritic sulphur content 2.49 per cent for a composite Seam Six sample compared to 25 and 0.25 per cent for a composite Seam Two sample. The net neutralizing potential is usually proportional to the amount of carbonate in a sample.

PLASMA ASHING AND X-RAY DEFFRACTION RESULTS AND THE WTLOS VALUE

The four composite samples of raw coal from Seams 2, 3, 5 and 6 were ashed in a plasma furnace. Sample weights ranged from 9 to 12 grams. Samples were oxidized in an oxygen atmosphere at a pressure of less than 1 millimetre of mercury and a temperature of 50°C for four days. The resulting mineral matter consisted of fine, white to grey powder with no visible coal. One split of the mineral matter was used for X-ray defraction analysis and another split was ashed in the conventional manner at 850°C in air.

Data are presented in Table 5-6-4. The average WTLOS value calculated from the mineral matter after plasma ashing is 1.135. This value may be low because of the difficulty of recovering all the sample from the quartz boat used in the plasma furnace. The average WTLOS value obtained after conventional ashing of the mineral matter is 1.157, which may be high because of incomplete oxidation of carbon in the plasma furnace. The average WTLOS value obtained from both procedures is 1.145 which implies a DMM value of 2.72 for all the data (Table 5-6-3). The average WTLOS for the two upper-seam samples is 1.156 and 1.136 for the two lower-seam samples. These values are flagged in Table 5-6-3 and imply DMM values of 2.76 (upper seams) and 2.68 (lower seams).

The X-ray defraction analyses of the four samples identified a simple suite of minerals which are listed in order of abundance in Table 5-6-4. Also listed in Table 5-6-4 is the theoretical maximum weight loss experienced by each mineral if totally oxidized. Obviously mineral matter composed of quartz experiences no weight loss whereas mineral matter composed of carbonates may experience a weight loss of up to 50 per cent. All samples contain some carbonates, consequently DMM values greater than 2.67 are to be expected.

IN SITU SPECIFIC GRAVITY AND MOISTURE OF TELKWA COALS

Down-hole sidewall geophysical logging, using a calibrated long-spaced density sond, can provide reasonably accurate values of *in situ* specific gravity of coal or rock. Generally it is difficult to establish a range of ash versus *in situ* specific gravity readings because of the resolution of the sond. *In situ* specific gravity values were read off Telkwa geophysical logs for thicker, cleaner seams where the interval could be matched to a sample interval and the

thickness was greater than the limit of resolution of the sond. This provided a set of values for ash (ADB), ASG (ADB) and matching *in situ* specific gravity measurements. The data provide average values for the upper seams of 9.01 per cent ash, 1.382 (ASG) and 1.351 (BD) and for the lower seams of 11.25 per cent ash, 1.397 (ASG) and 1.369 (BD). In all, thirteen values from the upper seams were averaged and nine values from the lower seams.

The difference in weight of water between *in situ* samples and samples at ADB can be read from Figure 5-6-2 and is a measure of the water-filled fracture porosity. The difference can also be calculated using;

$$MD = 100 \times (ASG - BD) / [BD \times (ASG - 1)]$$

(Equation 3, Table 5-6-1).

Total *in situ* moisture is given by;

$$TM = (ADM \times (100 - ADM) + MD \times 100) / 100$$

(Equation 6, Table 5-6-1);

where ADM = air-dried moisture, which in this case is 0.8 per cent. Using the average upper and lower seam data from above, the average *in situ* moisture for the upper and lower seams is 7 per cent and 6 per cent, respectively. Average equilibrium moisture for the seams is 3.4 per cent and average as-received moisture (Table 5-6-2) is 3.7 per cent. The moisture difference from an ARB of 3.7 per cent to an ADB moisture of 0.8 per cent is a measure of the small-scale water-filled porosity of coal fragments. The moisture difference from an *in situ* moisture of about 7 per cent to an ARB moisture of 3.7 per cent is a measure of the water-filled fracture porosity. A water-filled fracture porosity of about 3.5 per cent (upper seams) and 2.5 per cent (lower seams) is implied. Three per cent water by weight at 10 per cent ash corresponds to about 4 per cent volume for water-filled fractures; at higher ash contents, 3 per cent water by

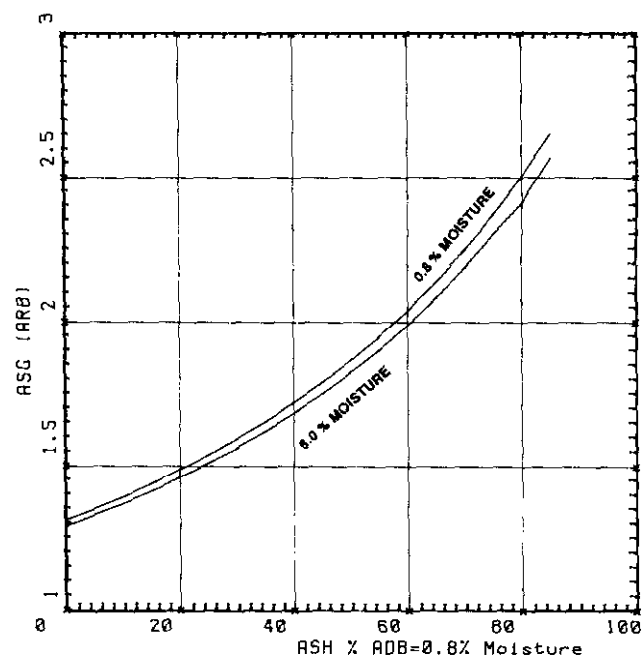


Figure 5-6-4. Apparent specific gravity at 6% and 0.8% moisture versus per cent ash at 0.8% moisture.

TABLE 5-6-5
APPARENT SPECIFIC GRAVITY AND IN SITU DENSITY
FOR TELKWA COALS

Ash %(ADB)	ASG (ADB)	BD (Case 1) 6% moisture	BD (Case 2) 6% moisture	BD (Case 3) 6% moisture
5	1.35	1.32	1.32	1.33
10	1.38	1.36	1.36	1.36
15	1.42	1.40	1.39	1.40
20	1.47	1.44	1.43	1.44
25	1.51	1.48	1.47	1.49
30	1.56	1.53	1.52	1.53
35	1.61	1.58	1.56	1.58
40	1.66	1.63	1.61	1.64
45	1.72	1.68	1.66	1.70
50	1.78	1.74	1.71	1.76

ASG = apparent specific gravity

BD = In situ density

Case 1 WTLOS = 1.146 DMM = 2.72

Case 2 WTLOS = 1.20 DMM = 2.6

Case 3 WTLOS = 1.12 DMM = 2.8

Note: All calculations at clean coal specific gravity(DC) = 1.315

weight will correspond to a greater volume of water-filled fractures (Figure 5-6-2).

The average interburden rock *in situ* specific gravity read from the geophysical logs is 2.45; if a dry specific gravity of 2.67 for interburden rock is assumed, then this predicts an *in situ* moisture content for the rock of 5 per cent.

The estimate of *in situ* moisture of 6 to 7 per cent for the coal does not contradict equilibrium moisture data and rock density data. An apparent specific gravity (at 6 weight per cent moisture) versus per cent ash (ADB) curve is plotted on Figure 5-6-4 and for comparison the curve for ASG (at 0.8 weight per cent moisture) versus ash per cent (ADB) is also plotted. The same data are tabulated in Table 5-6-5.

In situ specific gravity versus per cent ash (ADB) relationships are essential for converting *in situ* volumes to tonnages. *In situ* coal tonnages represent the starting database for all mine feasibility studies; if *in situ* tonnages are not well defined then all subsequent analysis is suspect.

Once values of DC, DMM and WTLOS are established it is possible, using Equation 1, to construct *in situ* specific gravity versus ash ADB at a number of possible *in situ* moisture weight per cents for comparison purposes. It is also possible to construct curves which incorporate volume of void porosity for stockpile bulk densities.

It is important to know *in situ* weight of water in order to estimate "run-of-mine moisture". An *in situ* moisture content of 6 to 7 per cent for Telkwa coals probably translates into a "run-of-mine moisture" of about 8 per cent. If product coal were to be shipped at 10 per cent moisture then the company would in effect be selling 2 per cent water as coal.

DISCUSSION

The proceeding discussion outlines a way of combining laboratory analyses, a density equation and geophysical log data to derive *in situ* specific gravity versus ash relationships. A number of potentially complicating factors have been ignored.

Equation 1 assumes that mineral matter density, and the value WTLOS, remain constant as per cent ash varies,

which is not necessarily the case. Coal contains a background concentration of inherent ash which varies from 0 to 5 per cent. Inherent ash is derived from material that may be bound elementally with the organic material or exist as oxides dispersed within it. Ashing inherent ash will not result in a weight loss and may in fact result in a weight gain. The WTLOS value for low-ash samples may therefore approach 1 or be less than 1 (Gray, 1982). At intermediate ash concentrations the ash is probably derived from authogenic minerals such as carbonates and pyrite which will ensure high values for DMM and WTLOS. At high ash concentrations, the ash is dominated by interburden rock which is likely to have intermediate values of DMM and WTLOS.

Much of the data scatter at higher ash concentrations in Figure 5-6-3 is probably caused by variation in individual WTLOS values. Mineral matter composition varies from sample to sample, independently of variation in per cent mineral matter. It may be possible to reduce the scatter by using the simplest form of the Parr Equation (Table 5-6-1) to convert ash to mineral matter. This requires a pyritic sulphur analysis for each ash analysis. It should be realized that if a constant sulphur value is used then this forces the Parr Equation to predict higher WTLOS values at low ash contents, which is unrealistic. If the sulphur is in the mineral matter then the sulphur content of the coal sample will decrease as the per cent ash decreases. Data from a separate acid rock-drainage study at Telkwa (Norecol, 1990) established the relationship, per cent pyritic sulphur = 0.9935 × per cent total sulphur - 0.206, for Telkwa coals. Using this relationship, the Parr Equation and data from Table 5-6-3, average WTLOS values were calculated for each seam (Table 5-6-6); values average 1.11 which is distinctly lower than the measured values in Table 5-6-4. It appears that the simple version of the Parr Equation provides unreliable estimates of the WTLOS value for Telkwa coal.

The WTLOS value can be derived without resorting to the use of a plasma furnace. The relationship between volatile matter, dry mineral matter free basis (VM dmmf), and ash, and volatile matter (VM), as-received basis (ARB) and moisture content (TM) can be written as:

$$VM \text{ dmmf} = VM/[1 - TM - (WTLOS \times ash)] - (WTLOS - 1) \times ash.$$

On a plot of volatile matter versus ash the Y intercept is VM dmmf (1 - TM) and the slope is WTLOS × (1 - VM dmmf) - 1. These equations can be solved for VM dmmf

TABLE 5-6-6
CALCULATION OF WTLOS USING PARR EQUATION

Seam	Average Ash %	Average Total Sulphur %	Average Pyritic Sulphur %	WTLOS
8	18	1.62	1.23	1.118
6	17.56	1.51	1.29	1.120
5	23.99	1.23	1.02	1.103
4	30.45	1.38	1.17	1.101
3	25.72	1.54	1.32	1.108
2	21.09	1.03	0.82	1.101

WTLOS = 1.08 ash + 0.55 Pyrite/Ash (Parr Equation)

Pyritic sulphur calculated using

Pyrite = .9935 × total sulphur - .206

and WTLOS. In practice, a good data set with a range in ash values is required. Normally volatile matter is measured on washed samples which have a limited range of ash contents, making it difficult to fit a line through the data. This approach assumes that the weight loss incurred by mineral matter during a volatile matter analysis is the same as the weight loss incurred during an ash analysis. The two analyses are performed under different conditions and the assumption is not always correct.

In most cases reasonable estimates of the DMM and WTLOS values will suffice for *in situ* specific gravity calculations because most studies are of coal with less than 40 per cent ash. Table 5-6-3 outlines a range of possible DMM, WTLOS pairs from 2.6, 1.198 to 2.8, 1.116. Table 5-6-6 illustrates the effect on *in situ* specific gravity calculations of choosing either of the two extremes. At 50 per cent ash results are 1.7 per cent low to 1.2 per cent high. Obviously, for ash concentrations less than 50 per cent DMM and WTLOS values can generally be estimated using previous experience without incurring large errors in the calculation of *in situ* specific gravity.

The apparent specific gravity of dry zero-ash coal (DC) at constant rank varies with changes in petrographic composition. Different macerals have different densities and micro- porosities. Coal with higher contents of fusinite and semi-fusinite have higher densities than vitrinite-rich coals. It is difficult to quantify the variation in DC caused by changes in petrographic composition but it is probably not significant.

CONCLUSIONS

Equation 1 fits specific gravity measurements from the Telkwa property well. The combination of Equation 1, a set of apparent specific analyses on an air-dried basis and data from geophysical logs is sufficient to fully describe the *in situ* specific gravity or bulk density versus ash relationships required for mine planning. Equation 1 can generate *in situ* specific gravity versus ash curves at different *in situ* moistures for comparison purposes, and can also be used to predict stockpile bulk densities which incorporate a void porosity.

Coals in the Telkwa deposit have a clean coal apparent specific gravity of 1.31 to 1.32 on an ADB of about 0.8 per cent moisture. *In situ* moisture is approximately 6 per cent.

The WTLOS value for Telkwa coals is higher than is predicted by the Parr Equation and is influenced by the presence of carbonates in the mineral matter. In most cases it is not necessary to independently measure the values of WTLOS and DMM; reasonable estimates do not introduce large errors.

Reserve calculations and mining feasibility studies represent a sequence of calculation steps, like links in a chain, each of which has its own associated errors and possible bias. These errors and biases accumulate to effect the uncertainty and possible bias in the final conclusions. It seems that in many studies the unappreciated weak link in the chain is the conversion of volumes to tonnages. This note may help to ensure that the weak link is elsewhere in the chain, at a point less easy to quantify and more deserving of the notoriety.

ACKNOWLEDGMENTS

The author wishes to thank Brian McKinstry of Crows Nest Resources Limited for providing the density data from the Telkwa property. Studies of this type are not possible without access to data which often sits under-utilized in company files. Thanks are also extended to JoAnne Schwemler who carried out the petrographic analyses and to Dave Grieve and Ward Kilby who provided comments on the manuscript.

REFERENCES

- Gray, V. R. (1982): A Formula for the Mineral Matter to Ash Ratio for Low Rank Coals; *Fuel*, Volume 62, pages 94-97.
- Kolb, W. M. (1984): Curve Fitting for Programmable Calculators; *IMTEC*, PO Box 1402, Bowie, MD 20716, USA.
- Norecol (1990): Evaluation of Potential for Acid Generation, North Side of the Telkwa River Coal Project, British Columbia; *Norecol Environmental Consultants Ltd.*
- Rees, O.W. (1966): Chemistry, Uses and Limitations of Coal Analyses; *Illinois State Geological Survey*, Report INV 220, page 55.
- Romaniuk, A. (1987): Assessment of Field Techniques Used to Determine *In Situ* Bulk Density of Coal; *Northwest Resources Consultants Ltd.*, unpublished report for CANMET, contract 23440-6-9057/01-SQ.
- Smith, G.G. (1989): The Required Use of Coal Density Values for Calculating Average Composition of *In Situ* Coals; Contributions to Canadian Coal Science, *Geological Survey of Canada*; Paper 89-8, pages 131-136.
- Ward, C. R. (1984): Coal Geology and Coal Technology; *Blackwell Scientific Publications*, page 51.



**BURNT RIVER MAPPING AND COMPILATION PROJECT
(93 P/5, 6)**

By D.J. Hunter and J.M. Cunningham

KEYWORDS: Coal geology, Peace River, Burnt River, Gwillim Lake, Boulder Creek, Gates, Gething, structure, coal rank, coalbed methane.

INTRODUCTION

This study continues the 1:50 000-scale geologic mapping program in the Peace River coalfield. The study area is adjacent to the recently completed mapping of the Bullmoose and Kinuseo map sheets to the south (Kilby and Wrightson, 1987a, b, c; Kilby and Johnston, 1988a, b, c; Kilby and Hunter, 1990). The objective is to produce Open File maps of 93P/5 and the southwest half of 93P/6 to be released in early 1991 (Figure 5-7-1). These maps will display data collected in the field in June, July and August 1990, as well as substantial outcrop and borehole data from coal and gas exploration reports.

LOCATION

The study area encompasses approximately 1300 square kilometres in the Rocky Mountain Foothills of northeastern British Columbia. Located midway between Chetwynd and Tumbler Ridge, the area is predominantly tree covered with topography ranging in elevation from 600 to 1700 metres. Vegetation varies from alpine tundra (in the extreme southwest) to mature stands of pine and spruce.

The Burnt River map area is trisected at the confluence of Burnt and Sukunka rivers which provide the main drainage. The rivers follow U-shaped valleys carved during the Pleistocene glaciation. Geologically, the area is bounded by the Rocky Mountains just west of the southwest corner of 93P/5 and the outer foothills structure of the Gwillim Lake area to the east. Access to most of the area is provided by a network of cut lines, logging, drilling and well-site roads, all accessible from the major highways.

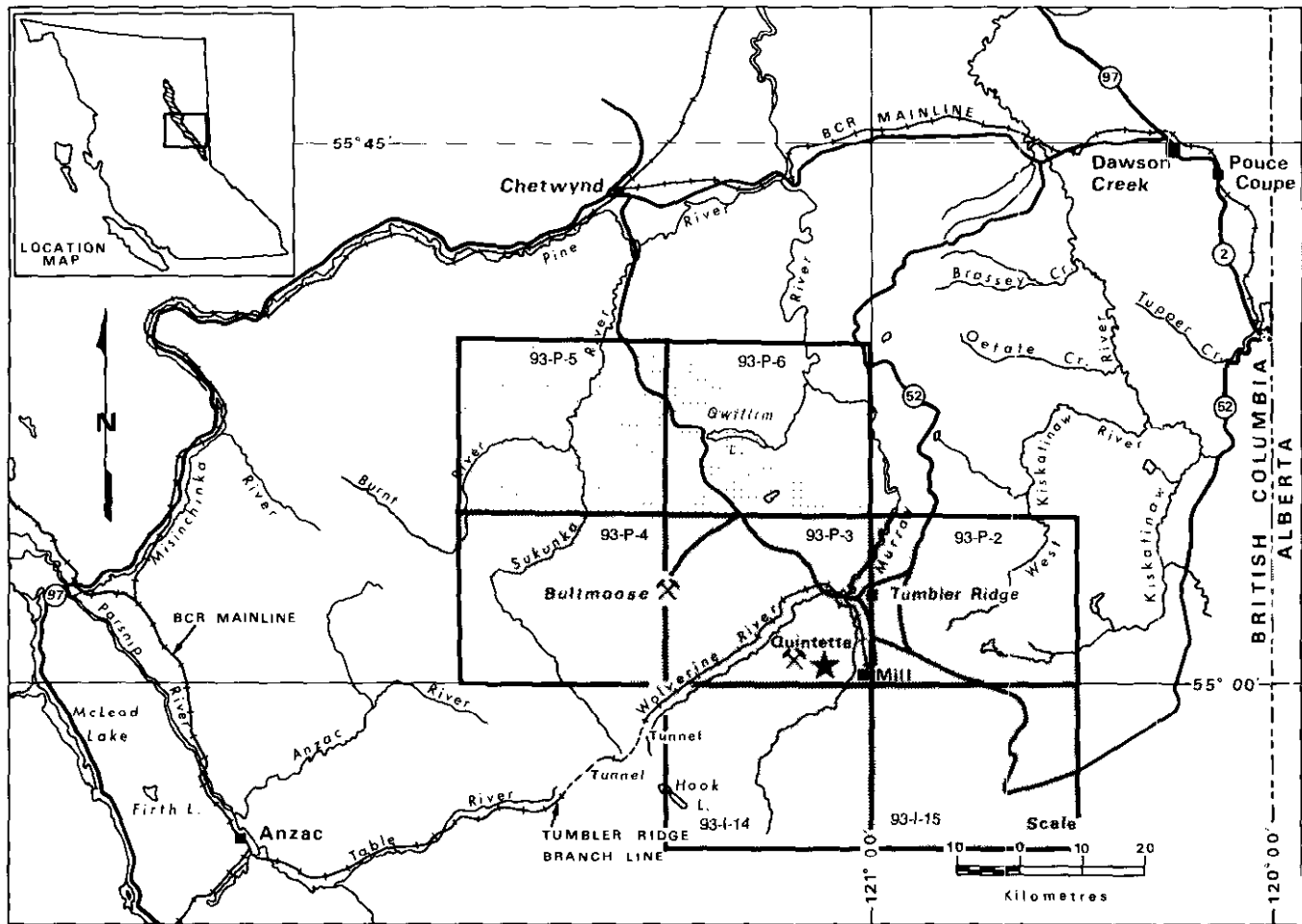


Figure 5-7-1. Location map. Dark stipple shows previous mapping, light stipple shows area of 1990 mapping.

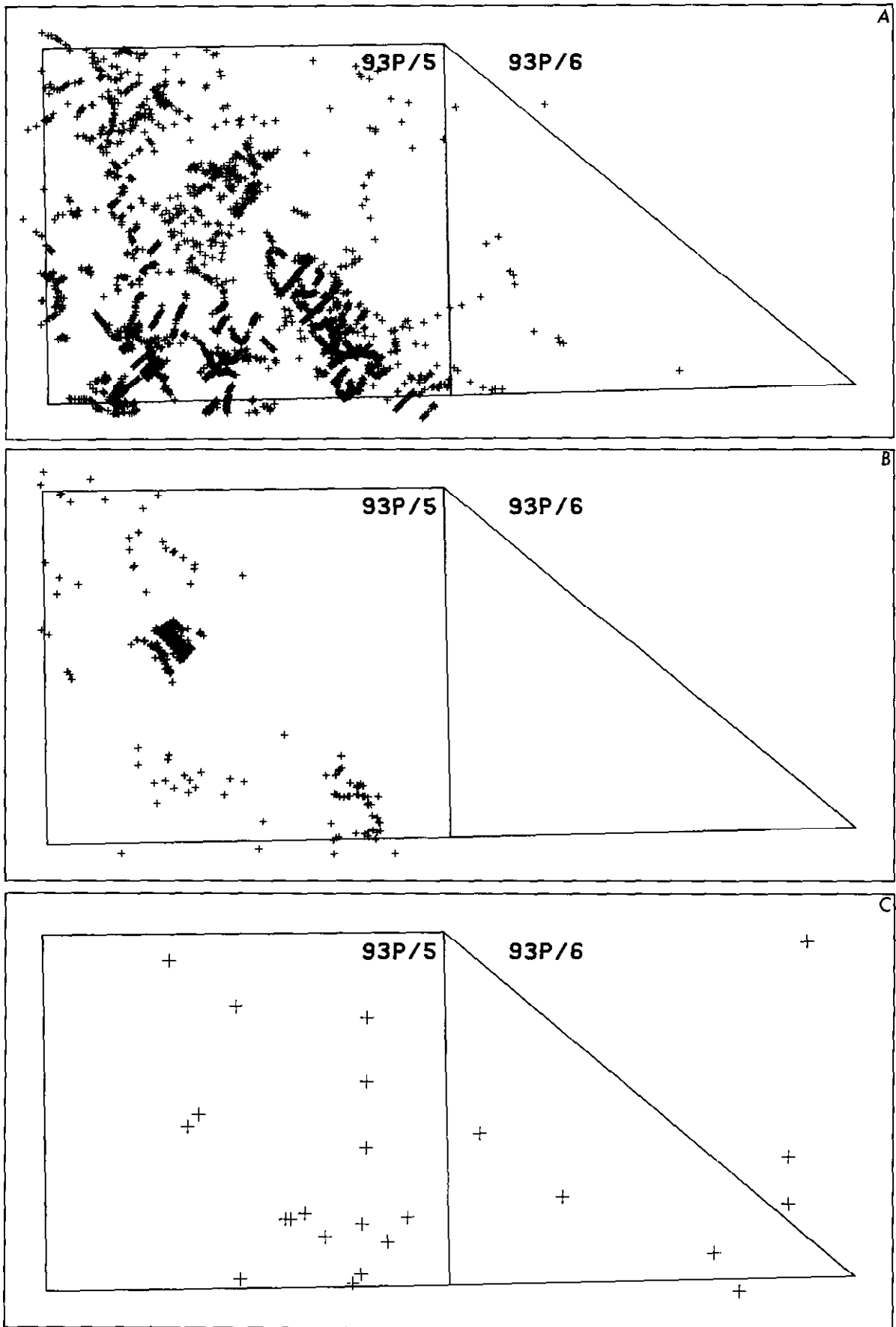


Figure 5-7-2. Locations of a) outcrops b) coal boreholes and c) petroleum exploration wells in Burnt River database.

SERIES	GROUP	MAP SYMBOL	FORMATION	THICKNESS IN METRES	LITHOLOGY	
QUATERNARY		Q AL	QUATERNARY	?	Alluvial deposits; sands and gravels	
UPPER CRETACEOUS	SMOKY	UKW	WAPITI	1000	Nonmarine interbedded conglomerate, sandstone, mudstone and coal	
		UKP	PUSKWASKAU	210	Concretionary grey marine shale; coarsens upward to marine sandstone (Chungo)	
		UKB	BAD HEART	10	Marine and nonmarine quartz sandstone	
		UKM	MUSKIKI	65	Grey marine shale; rust weathering; concretionary	
		UKC	CARDIUM	40	Marine and nonmarine sandstone; conglomerate in upper part	
		UKK	KASKAPAU	750	Dark grey marine shales; interbedded sandstone and shale in lower part	
		UKD	DUNVEGAN	475	Marine and nonmarine sandstone, shale and coal	
	LOWER CRETACEOUS	FORT ST. JOHN	UKCR	CRUISER	150	Dark grey marine shale with sideritic concretions; some sandstone.
			KGO	GOODRICH	150	Fine-grained, crossbedded sandstone; shale and mudstone
			KHA	HASLER	300	Silty dark grey marine shale with sideritic concretions; siltstone in lower part
			KBC	BOULDER CREEK	120	Fine-grained, well-sorted sandstone; massive conglomerate; nonmarine sandstone and mudstone and coal
			KH	HULCROSS	100	Dark grey marine shale with sideritic concretions
			Ke	GATES	130	Fine-grained, marine and nonmarine sandstones; conglomerate; coal; shale and mudstone
KM			MOOSEBAR	130	Dark grey marine shale with sideritic concretions; glauconitic sandstone and pebbles at base	
BULLHEAD		KGE	GETHING	375	Fine- to coarse-grained, brown, calcareous, carbonaceous sandstone; coal, carbonaceous shale, and conglomerate	
		KCD	CADOMIN	40	Massive conglomerate containing chert and quartzite pebbles and sandstone	
JURASSIC		MINNES	JKM	UNDIFFERENTIATED	1700	Thinly to thickly interbedded, shale, sandstone, siltstone and coals.

Figure 5-7-3. Stratigraphic table (modified after Stott, 1982).

DATA

Mapping was aided by surface and subsurface data from several sources. The complete database includes 3084 outcrop locations with orientation data, 325 coal company boreholes and associated maps, and 23 petroleum company exploration wells (Figure 5-7-2). Outcrop and coal-borehole data were obtained from assessment reports on file with the Geological Survey Branch. Gas-well data was created by analysis of geophysical logs available through the Petroleum Resources Division of the Ministry of Energy, Mines and Petroleum Resources. Microcomputers are being used for the storage and manipulation of these data. A standardized format has been established for all the surface and subsurface information so that it may be released in conjunction with the Open File maps. The geological maps are also stored digitally in the form of CAD files.

In several areas with limited access or outcrop, mapping has been based on air-photo interpretation and the information contained within this database.

STRATIGRAPHY

The Foothills of the map area are underlain by Upper and Lower Cretaceous strata with progressively older formations exposed southwestward. This succession is predomi-

nantly an alternating series of marine and nonmarine clastic sediments with dark grey marine shales (Figure 5-7-3). This represents several transgressive-regressive cycles depositing a complete succession of over 4500 metres thickness. Triassic carbonates of the Rocky Mountain Front Ranges are exposed southwest of the Burnt River map area. Fieldwork during 1990 covered all formations from the Puskawaskau Formation to the Minnes Group. Coal occurrences were noted in the Boulder Creek, Gates and Gething formations as well as the Minnes Group. Regionally, coal is also present in the Dunvegan, Cardium and Wapiti formations. The major coal-bearing sequence of the map area is the lower Gething. Regional stratigraphy of the Cretaceous sequence has been extensively described by Stott (1967, 1968, 1973, 1982), by Kilby and Wrightson (1987a, b, c) and Kilby and Johnston (1988a, b, c).

There are some significant stratigraphic variations found within several formations between the Burnt River area and previous geological investigations to the southeast. These are best illustrated by a comparison of the geophysical log traces for these formations (Figure 5-7-4). The figure shows three types of geophysical log. The gamma ray log (GR) measures the natural radioactivity of rock. Clay-rich rocks such as shales have a high gamma reading while clean sandstones, conglomerates and coal will move the curve to the left, reflecting their low radioactivity. The sonic tool

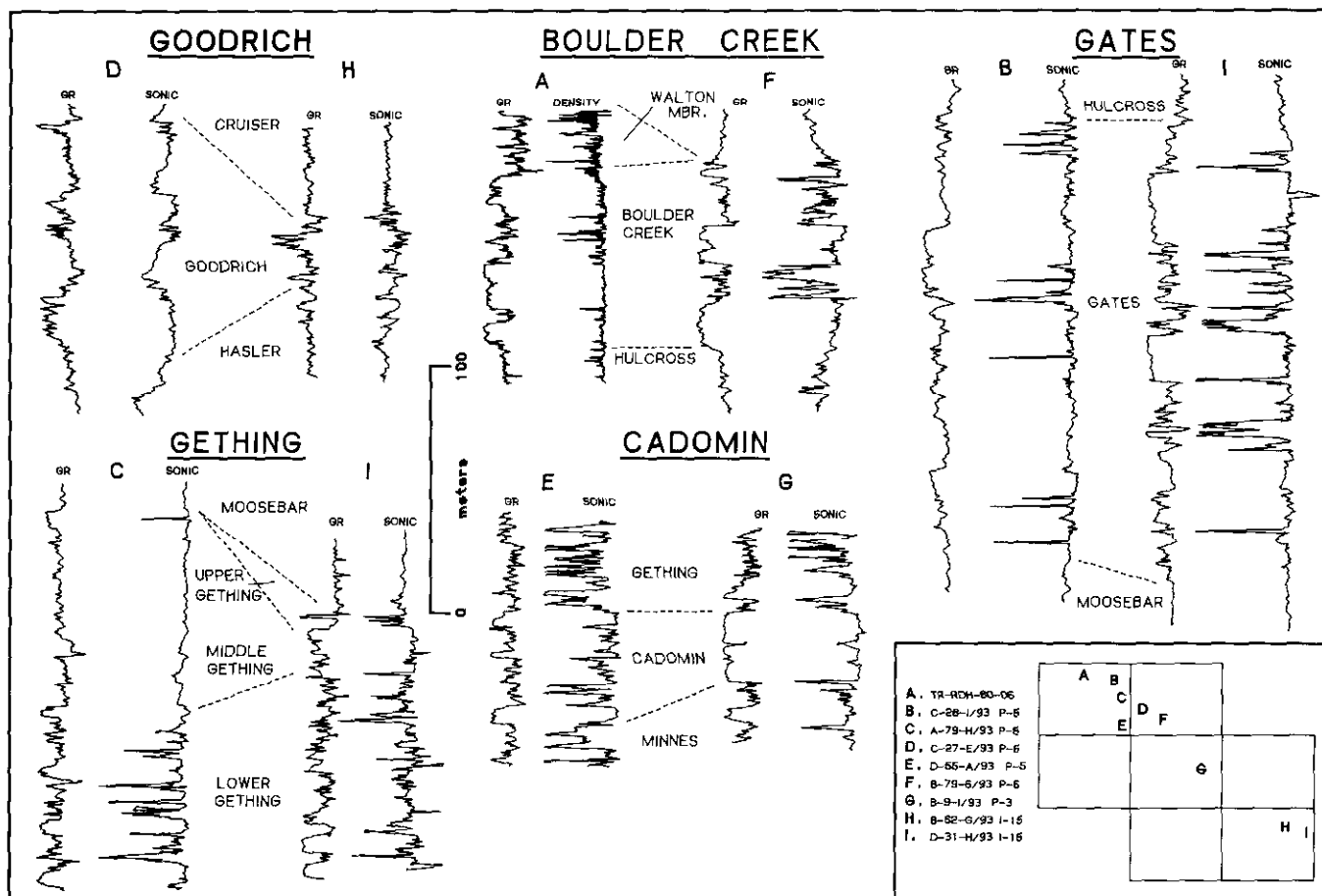


Figure 5-7-4. Geophysical log comparisons for Goodrich, Boulder Creek, Gates, Gething and Cadomin formations.

records the "interval transit time" for a sound wave to pass through a formation and return to the tool. The travel time is partly dependant on the density of the rocks. The low density of a coal seam will give a long travel time which appears as a strong kick to the left on the sonic log. The density tool emits gamma rays and counts the number which are scattered back to the tool. This is dependant on the number of electrons in the rock which, in turn, is related to the bulk density. Higher densities are reflected by a log reading to the right. Coal, consisting mainly of carbon and hydrogen with low atomic numbers, gives a low bulk-density reading showing up as a sharp kick to the left on the density log.

STRATIGRAPHIC VARIATIONS

GOODRICH

The Goodrich Formation becomes increasingly important as a prominent ridge-capping formation to the northeast. Regionally, the formation shales out to both the south and east (Stott, 1982). South of the Murray River (93I/15), the Goodrich consists of only of a few thin sands. Mapping in 93P/5 indicates the fine-grained Goodrich sandstones and interbedded shales increase to over 150 metres in thickness (Figure 5-7-4) and they are best developed on the western limb of a broad syncline west of Gwillim Lake. Subsurface geophysical logs show three distinct coarsening-upward cycles which can be correlated laterally to the eastern edge of 1990 mapping.

BOULDER CREEK

The Boulder Creek Formation is a prominent ridge-forming unit of conglomerates, sandstones and carbonaceous sediments. It is easily recognized in the subsurface by the presence of the two thick conglomerates that generally define the upper and lower boundaries of the formation. These units are known as the Paddy and Cadotte formations in the subsurface (Figure 5-7-4). Most coal in the Boulder Creek Formation is found between the upper and lower conglomerates as shown in the figure close to Borehole F. North of the Sukunka River, however, carbonaceous sediments and coal seams up to 1.5 metres thick have been deposited above the upper conglomerates, and this package has been named the Walton member. Coal seams from both stratigraphic intervals were sampled.

GATES

The most dramatic stratigraphic variation is the loss of thick, laterally extensive coal seams in the Gates Formation. Mapping this season identified only a few thin coals seams (<1 metre thick) at the southern edge of the map area. Northward from that point, the Gates Formation is composed dominantly of more marine-influenced shelf-facies sediments (Stott, 1982). The geophysical log comparison shows only a few thin carbonaceous horizons in Well B, compared to the thick coal seams of Well I in the Kinuseo Creek area.

GETHING

The major target for coal exploration in the Burnt River area is the Gething Formation. As with the Gates Formation, the southern limit of the map area also marks a major change in deposition for the Gething. Previous work in the southern area has divided it into three distinct units. The upper and lower Gething are mainly coal-bearing non-marine sediments which are separated by the coarsening-upward middle Gething marine package (Figure 5-7-4). Gas-well logs clearly show the pinching out of the upper coal measures and thickening of the middle Gething in the Gwillim Lake region (Legun, 1985).

The lower Gething coals have been extensively explored for in the Burnt River map area. The thickest seams (>5 metres) are found in the Burnt River deposit just north of the Sukunka River. This prospect has been closely drilled and sampled as a high-rank thermal coal deposit.

CADOMIN

The Cadomin Formation within the 1990 map area is in a transitional location as far as stratigraphic nomenclature is concerned. While the authors have kept the formation definitions used previously (Kilby *et al.*) and as set out by Stott (1982) it became apparent that the Cadomin becomes a less distinct marker horizon north of the Sukunka River. The conglomerates are not as thick or as laterally continuous and may be absent in some areas. Mapping farther to the north may have to use the stratigraphic divisions set up by Hughes (1964) which redefine the lower Bullhead Group and subdivide the Minnes Group into three separate formations.

Figure 5-7-4 shows the typical log signature of a thick Cadomin conglomerate from the southern region at Well G. Well E, however, has only two thinner conglomerates defining the top and bottom of the formation, with sands and siltstones in between. This well was previously interpreted as a thrust-faulted Cadomin section, however, log signatures for the formation do not indicate any repetition of units.

STRUCTURE

The map area covers the complete range of structures in the inner and outer Rocky Mountain Foothills. Structural traces of faults and fold axes generally follow the north-westerly regional trends (Figures 5-7-5 and 6).

In the Gwillim Lake area the Upper Cretaceous Smoky Group is exposed by the broad gentle folds of the outer foothills. Westward, folding of the Dunvegan Formation and Fort St. John Group becomes increasingly narrow and more complex. The Boulder Creek, Hulcross and Gates formations, being relatively competent units, are exposed as tight chevron folds that are clearly visible on air photographs. Farther west is a broad area of the more subdued topography underlain by the Gething Formation. The lack of outcrop and traceable resistant horizons in the Gething make determination of structure extremely difficult. Folding is believed to be fairly complex and is complicated by more faulting than is seen farther east. Structural interpretations of the Gething Formation are based mainly upon drilling results, especially for the Burnt River deposit north of the Sukunka River.



Figure 5-7-6. Geologic map – Gwillim Lake map sheet (93P/6). For legend see Figure 5-7-3.

been received for all samples. Rm Readings range from 1.03 to 1.76, placing all samples in the high to low-volatile bituminous rank using the ASTM (American Standard Testing Methods) classification scheme (Stach, 1982).

Reflectance values for samples from the Boulder Creek Formation ranged from 1.06 Rm for Walton member coal, to 1.19 for thin seams in the lower stratigraphic horizons. This places the coal at or near the high-medium volatile boundary.

Most lower Gething Formation coals ranged from 1.38 to 1.76 Rm, placing them in the low-volatile or upper-medium volatile bituminous categories. The one sample falling outside this range has an Rm value of 1.03 with over 80 per cent of the macerals being thought to be coarse micrinite. Samples with similar characteristics have previously been associated with devolatilization of the coal macerals, trans-

forming the vitrinite into the anisotropic mosaic of micrinite particles (Kilby, 1989).

Samples taken from the Minnes coal measures have Rm values ranging from 1.10 to 1.69. The low-rank samples were taken from the most western coal outcrops in the southwest corner of 93P/5 on Mount Jilg. This decrease in rank is attributed to thrust faulting early in the coalification process as has been noted previously for Gething coals in the subsurface (Karst and White, 1980).

ECONOMIC GEOLOGY

Exploration in the region has mainly been limited to conventional structural gas-traps and surficial coal prospecting in the lower Gething Formation. Vitrinite reflectance values (all in the bituminous range), and the number of coal-bearing formations, also make the area of potential interest

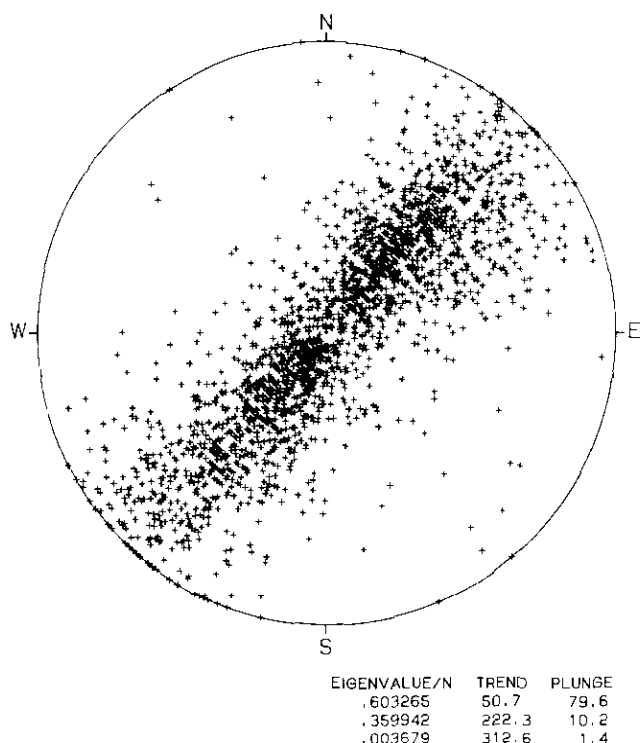


Figure 5-7-7. Pi diagram of poles to bedding for all outcrops in Burnt River Project database.

for the development of coalbed methane production. The most obvious targets would be the thicker seams of the lower Gething and the thinner but more numerous seams of the Minnes Group. The Burnt River thermal coal deposit is apparently not economically viable at this time, but future development of the Sukunka deposit just south of 93P/5 may improve that situation.

ACKNOWLEDGMENTS

The authors would like to thank Ward Kilby for his valuable input into this project. Also special thanks to Joanne Schwemler for her expeditious sample preparation and vitrinite reflectance observations, and to Julie Hutchins for typing the manuscript. Our excellent accommodations in Chetwynd were provided by Robert and Jean Pohl who's kindness was greatly appreciated.

REFERENCES

- Hughes, J.E. (1964): Jurassic and Cretaceous Strata of the Bullhead Succession in the Peace River Foothills; *B.C. Ministry of Energy, Mines and Petroleum Resources*, Bulletin 51, 73 pages.
- Karst, R.H. and White, G.V. (1980): Coal Rank Distribution within the Bluesky-Gething Stratigraphic Horizon of Northeastern British Columbia (93 I, O, P); *B.C. Ministry of Energy, Mines and Petroleum Resources*, Geological Fieldwork 1979, Paper 1980-1, pages 103-107.
- Kilby, W.E. and Hunter, D.J. (1990): Tumbler Ridge, Northeastern British Columbia (93P/2, 3, 4.; 93I/14, 15); *B.C. Ministry of Energy, Mines and Petroleum Resources*, Geological Fieldwork 1989, Paper 1990-1, pages 455-459.

- Kilby, W.E. and Johnston, S.T. (1988a): Kinuseo Mapping and Compilation Project (93I/14, 15; 93P/3); *B.C. Ministry of Energy, Mines and Petroleum Resources*, Geological Fieldwork 1987, Paper 1988-1, pages 463-470.
- Kilby, W.E. and Johnston, S.T. (1988b): Bedrock Geology of the Kinuseo Falls Area, Northeast British Columbia, NTS 93I/14; *B.C. Ministry of Energy, Mines and Petroleum Resources*, Open File 1988-22.
- Kilby, W.E. and Johnston, S.T. (1988c): Bedrock Geology of the Kinuseo Creek Area, Northeast British Columbia, NTS 93I/15; *B.C. Ministry of Energy, Mines and Petroleum Resources*, Open File 1988-21.
- Kilby, W.E. and Wrightson, C.B. (1987a): Bullmoose Mapping and Compilation Project (93P/3, 4); *B.C. Ministry of Energy, Mines and Petroleum Resources*, Geological Fieldwork 1986, Paper 1987-1, pages 373-378.
- Kilby, W.E. and Wrightson, C.B. (1987b): Bedrock Geology of the Bullmoose Creek Area, Northeast British Columbia, NTS 93P/3; *B.C. Ministry of Energy, Mines and Petroleum Resources*, Open File 1987-6.
- Kilby, W.E. and Wrightson, C.B. (1987c): Bedrock Geology of the Sukunka River Area, Northeast British Columbia, NTS 93P/4; *B.C. Ministry of Energy, Mines and Petroleum Resources*, Open File 1987-7.
- Kilby, W.E. (1989): Tectonically Altered Coal Rank, Boulder Creek Formation, Northeastern British Columbia (93P/3); *B.C. Ministry of Energy, Mines and Petroleum Resources*, Geological Fieldwork 1988, Paper 1989-1, pages 565-570.
- Legun, A. (1985): Eastern Limit of Upper Coal Measures of the Gething Formation (Chamberlain Member) Peace River Coalfield; *B.C. Ministry of Energy, Mines and Petroleum Resources*, Geological Fieldwork 1984, Paper 1985-1, pages 250-255.
- McMechan, M.E. (1985): Low-taper Triangle-zone Geometry: An Interpretation for the Rocky Mountain Foothills, Pine Pass – Peace River Area, British Columbia; *Bulletin of Canadian Petroleum Geology*, Volume 33, No. 1 (March 1985), pages 31-38.
- Stach, E. (1982): Coal Petrology; *Gebrüder Borntraeger Publishing*, 535 pages.
- Stott, D.F. (1967): The Cretaceous Smoky Group, Rocky Mountain Foothills, Alberta and British Columbia; *Geological Survey of Canada*, Bulletin 132, 133 pages.
- Stott, D.F. (1968): Lower Cretaceous Bullhead and Fort St. John Groups between Smoky and Peace Rivers, Rocky Mountain Foothills, Northeastern British Columbia; *Geological Survey of Canada*, Bulletin 152, 279 pages.
- Stott, D.F. (1973): Lower Cretaceous Bullhead Group between Bullmoose Mountain and Tetsa River, Rocky Mountain Foothills, Northeastern British Columbia; *Geological Survey of Canada*, Bulletin 219, 228 pages.
- Stott, D.F. (1982): Lower Cretaceous Fort St. John Group and Upper Cretaceous Dunvegan Formation of the Foothills and Plains of Alberta, British Columbia, District of Mackenzie and Yukon Territory; *Geological Survey of Canada*, Bulletin 328, 124 pages.



COAL-BEARING FACIES IN THE NORTHERN BOWSER BASIN (104A, H)

By H. O. Cookenboo and R. M. Bustin
The University of British Columbia

KEYWORDS: Coal geology, Groundhog coalfield, Ashman Formation, Currier Formation, McEvoy Formation, Devils Claw Formation, facies variations, coal-bearing facies, deltaic deposition, delta-plain deposits.

INTRODUCTION

Strata exposed in the drainage of the Klappan and Nass rivers were examined during the 1990 field season as part of an ongoing sedimentological study of the Groundhog coalfield and the surrounding area in the northern Bowser basin (Figure 5-8-1). The field program consisted of measurement, sampling and detailed description of outcrops chosen from airphotos and airborne reconnaissance based on their continuity and location relative to sections measured during prior field seasons. Sections examined are now being integrated with earlier sections to delineate the geographic limits of coal-bearing stratigraphic units across a

wide area of the northern Bowser basin and to better understand the depositional history of the rocks. Coal-bearing strata studied during the 1990 field season belong to the Currier and McEvoy formations as originally described and defined in the Groundhog coalfield (Bustin and Moffat, 1983; Cookenboo and Bustin, 1989). Based on their gross lithology and facies characteristics, rocks examined south of Maitland Creek, near the headwaters of Konigus Creek, and south of Currier Creek are assigned to the Jurassic Currier Formation and strata at the southern end of Konigus Creek and west of the Nass River are assigned to the Cretaceous McEvoy Formation.

STRATIGRAPHY

Four lithostratigraphic units outcrop in the vicinity of the Groundhog coalfield (from oldest to youngest): Ashman, Currier, McEvoy and Devils Claw formations.

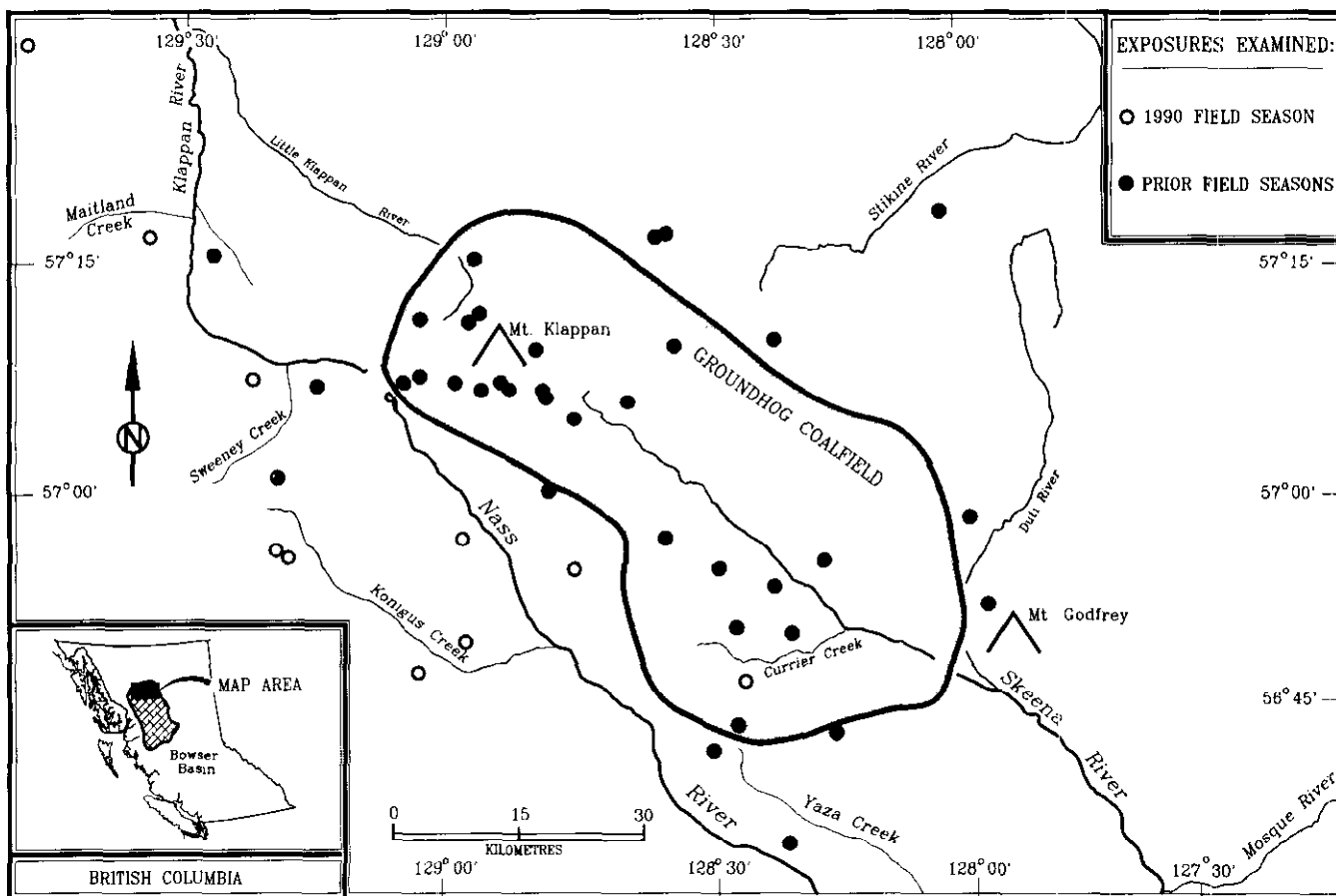


Figure 5-8-1. Map of the study area showing outcrops examined as part of this study and the Groundhog coalfield.

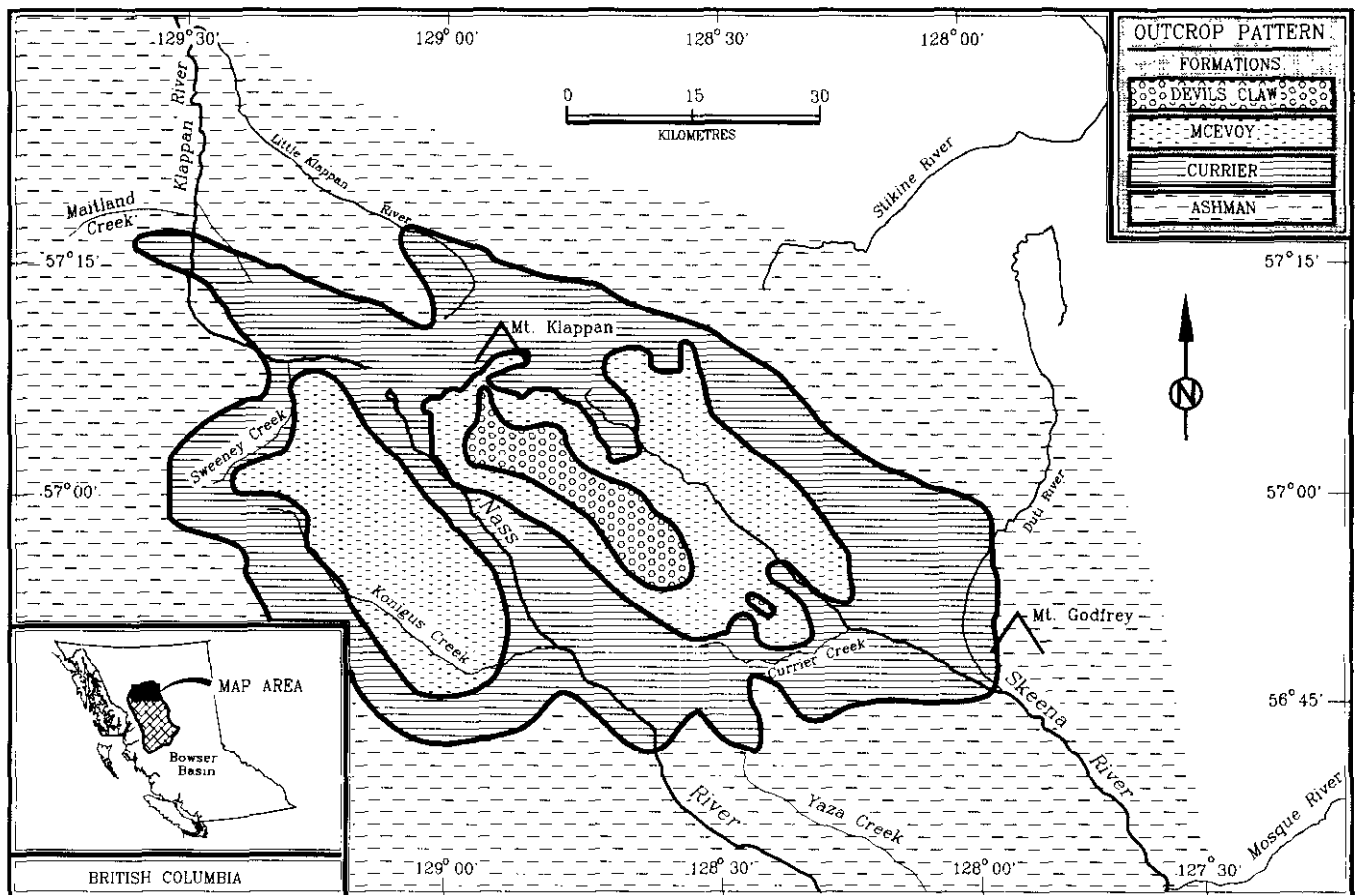


Figure 5-8-2. Outcrop patterns based on sections measured in this study.

The lowermost unit is correlated with the Jurassic Ashman Formation as described in the southern Bowser basin (Tipper and Richards, 1976). The Ashman Formation is exposed around the margins of the coalfield. It is a fully marine, clastic unit composed mostly of dark bluish grey to black shale that coarsens upwards repetitively to shallow-marine sandy mudstone and sandstone. The name Ashman Formation, as it is used here, may include coarser grained strata in its upper portions than are included elsewhere in the formation.

The Currier and McEvoy formations are coal-bearing deltaic and fluviodeltaic units. The thickest coals are restricted to the lower part of the Currier Formation. The Cretaceous Devils Claw Formation is a dominantly conglomeratic unit more than 600 metres thick that caps the succession exposed in the Groundhog coalfield.

OUTCROP EXTENTS

Exposures examined during the 1990 field season were chosen, in part, to establish the southwestern and western limits of coal-bearing strata in the Groundhog coalfield as well as to document variations in the depositional facies. The transition from coal-bearing rocks of the Currier Formation to underlying fully marine strata of the Ashman

Formation was established in the western part of the coalfield, but the southwestern limit of the Currier Formation was not determined. The most southwestern sections examined are assigned to the McEvoy Formation, suggesting that either more coal-bearing rocks of the Currier Formation, or its marine equivalents, may outcrop farther to the southwest. The geographic limits of the Currier, McEvoy and Devils Claw formations, based on sections measured last season and prior fieldwork, are shown in Figure 5-8-2.

COAL-BEARING STRATA

CURRIER FORMATION

The Currier Formation was originally defined for coal-bearing strata exposed between the Skeena and Nass rivers, from Mount Klappan in the north to Currier Creek in the south (Cookenboo and Bustin, 1989). Study during the 1989 and 1990 field seasons has extended the range of known Currier Formation occurrence north to the Klappan River watershed, southeast to Mount Godfrey (east of the Duti River), and west to the headwaters of Konigus Creek (Figure 5-8-2).

The formation consists of up to 1000 metres of alternating beds of shale and sandstone, with lesser amounts of siltstone, conglomerate and coal. Strata are arranged in generally coarsening-upward units ranging from 30 to 60 metres thick in the lower part of the formation. The coarsening-upward units thin to 6 to 10 metres toward the top of the section. Thick (1 to 4 m) seams of anthracite coal are notable in the lower part of the formation, although coal is only a minor component (comprising less than 3%) of the total stratigraphic thickness. Marine trace fossils (including *Teichicnus*, *Zoophycus* and *Helminthopsis*), a diverse suite of dinoflagellate cysts and marine macrofauna are common in the lower Currier Formation. Higher in the formation, plant fossils are common, trace fossils are rare and marine macrofauna are absent. The diversity of dinocysts and an oyster bed identified at the headwaters of Konigus Creek suggest that marine and brackish water conditions persisted during Currier deposition. Criteria used to recognize the formation are dominance of shale in the fine-grained deposits, local occurrence of thick coals, and increasing plant fossils and decreasing marine shells and trace fossils up stratigraphy.

The contact of the Currier Formation with the underlying marine rocks of the Ashman Formation is gradational and placed at the first occurrence of coals or abundant fossil leaves. The contact with the overlying McEvoy Formation is recognized by a change from Currier Formation facies to a dominance of siltstone in the fine-grained deposits, lack of thick coals, and an increase in conglomerates.

The Currier Formation is interpreted to be deltaic in origin, recording a change to alternating marine and non-marine deposition from fully marine deposition in the underlying Ashman Formation. The coarsening-upward units that comprise the Currier indicate repeated aggradation and progradation of deposition, and are interpreted as delta or subdelta (crevasse splay) lobes. In the lower Currier, the thickness of coarsening-upward units and widespread marine influence suggests that each individual unit represents a prograding delta lobe. Higher in the formation, marine influence is less clear, although saline to brackish conditions are suggested by the dinoflagellate assemblages, and the thinner coarsening-upward units probably represent splay or subdelta lobes. Pervasive marine influence suggests most of the deposits accumulated in the subaqueous delta and lower delta plain.

COAL-BEARING FACIES OF THE CURRIER FORMATION

Coals of the Currier Formation occur within a black shale facies and commonly directly overlie sandstones that form the top of the underlying delta lobes. The black shales are in part carbonaceous and homogeneous, and in part laminated with lighter brown silty layers. The black shale facies is commonly rich in plant fossils and some beds are intensely burrowed by *Helminthopsis*. Although the shales commonly overlie delta sandstones, the peats that were the direct precursors of Currier Formation coals may have accumulated at considerable distance from active deltaic deposition, as suggested by depositional models proposed by McCabe (1986).

McEVoy FORMATION

The McEvoy Formation was originally defined for rocks exposed in the Groundhog coalfield. Fieldwork during the last two seasons has expanded its extent westward to include rocks in the Konigus Creek watershed (Figure 5-8-2). The formation consists of between 600 and 1000 metres of siltstone, shale, sandstone, conglomerate and minor thin coal of subanthracite to anthracite rank. Coarsening-upward silty mudstones are the dominant facies. The mudstones occur in stacked units, typically 3 to 5 metres thick, which grade upward from black or dark grey and often carbonaceous claystone at the base, to dark grey to brown siltstone with increasing sand content. The units may or may not be topped by trough-crossbedded, very fine grained sandstone. The top and bottom contacts are sharp, with the top surface commonly rooted. Thick black shale beds (up to 20 m thick) occur interspersed within the coarsening-upward siltstone. These shales are variously silty to carbonaceous and are rich in plant remains.

Coarse-grained deposits form resistant layers in the McEvoy Formation and include fine-grained sandstones and chert-pebble conglomerates which become thicker and more common higher in the formation. Erosive based and lens-shaped sandstone and conglomerate beds, and consistent southwesterly directed current indicators (measured from cross laminae) are common, indicating McEvoy deposition is dominantly fluvial.

The lower contact of the formation is recognized by a marked upward increase in the occurrence of silt in the mudstones relative to the Currier Formation, a dearth of thick coals, and an increase in the proportion of conglomerate above the contact. The upper contact with the overlying Devils Claw Formation is gradational, and recognized by a further increase in conglomerate to the extent that the Devils Claw Formation is dominantly conglomerate.

Plant remains including plant debris, wood, and well-preserved leaves are common in the McEvoy Formation; no marine macrofossils are known. A broad suite of dinoflagellate cysts recovered from throughout the fine-grained deposits suggests a brackish to marine depositional environment.

McEvoy strata are interpreted as paralic marine or brackish water deposits of a fluvially dominated delta system. The repeated vertical stacking of coarsening-upward mudstones are analogous to overbank or crevasse splay deposits of the Mississippi River and other fluvially dominated delta systems (Coleman, 1982). Lack of marine fauna suggests a fluvially dominated upper delta plain, above the reach of open-marine conditions. A similar depositional environment was recently suggested by Macleod and Hills (1990).

COAL-BEARING FACIES OF THE McEVoy FORMATION

Coals occur within two facies of the McEvoy Formation. The thickest coals are in the thick shale facies interbedded with carbonaceous shales, and are associated with a wide

variety of well-preserved fossil leaves and wood. The best developed coals in this facies are exposed southeast of Sweeney Creek, where six seams in excess of 1 metre thick crop out. The thick shale facies is interpreted as fine-grained bay or lacustrine-fill deposits in an upper delta plain environment.

The second coal-bearing facies is a sequence of coarsening-upward siltstones. Coals in this facies are generally less than 20 centimetres thick and argillaceous. These thin coals may have accumulated following emergence of overbank splay deposits more closely associated with the active depositional system than the somewhat thicker coals of the thick shale facies.

ACKNOWLEDGMENTS

This research was supported in part by the British Columbia Geoscience Research Grant Program (reference number RG90-7) and received additional logistical support from the Institute of Sedimentary and Petroleum Geology, for which the authors are sincerely grateful. The authors benefited from lengthy discussions with geologists Barry Ryan of the British Columbia Geological Survey Branch and Mike Dawson of the Institute of Sedimentary and Petroleum Geology which have added to our understanding of Bowser basin geology. Arne Toma is thanked for able assistance in the field.

REFERENCES

- Bustin, R.M. and Moffat, I. (1983): Groundhog Coalfield, Central British Columbia: Reconnaissance Stratigraphy and Structure; *Bulletin of Canadian Petroleum Geology*, Volume 31, pages 231-245.
- Coleman, J.M. (1982): Deltas; *International Human Resources Development Corporation*, 124 pages.
- Cookenboo, H.O. and Bustin, R.M. (1989): Jura-Cretaceous (Oxfordian to Cenomanian) Stratigraphy of the North-central Bowser Basin, Northern British Columbia; *Canadian Journal of Earth Sciences*, Volume 26, pages 1001-1012.
- Macleod, S.E. and Hills, L.V. (1990): Conformable Late Jurassic (Oxfordian) to Early Cretaceous Strata, Northern Bowser Basin, British Columbia: A Sedimentological and Paleontological Model; *Canadian Journal of Earth Sciences*, Volume 27, pages 988-998.
- McCabe, P.J. (1986); Facies Studies of Coal and Coal-bearing Strata, in Coal and Coal-bearing Strata: Recent Advances; A.C. Scott, Editor, *Geological Society*, Special Publication 32, pages 51-67.
- Tipper, H.W. and Richards, T.A. (1976). Jurassic Stratigraphy and History of North-central British Columbia; *Geological Survey of Canada*, Bulletin 270. 73 pages.

GEOLOGY AND POTENTIAL COAL AND COALBED METHANE RESOURCE OF THE TUYA RIVER COAL BASIN (104J/2, 7)

By Barry Ryan

KEYWORDS: Coal geology, Tuya River, coal basin, coalbed methane.

INTRODUCTION

This article forms part of an ongoing study of the coal and coalbed methane resource potential of northwestern British Columbia. Other areas under study include the Bowser basin coalfield, Telkwa coalfield and Tertiary coalfields of the Bulkley Valley.

Tertiary sediments survive in many major watersheds in British Columbia. The sediments are generally not well consolidated, poorly exposed and their subcrop extent is arbitrarily delineated by adjacent high ground underlain by pre-Tertiary rocks. Many of these Tertiary basins contain

coal, varying in rank from lignite to medium-volatile bituminous and seam thickness varies from a few centimetres to many metres.

The Tuya River Tertiary coal basin is located between the communities of Dease Lake and Telegraph Creek in northwestern British Columbia (Figure 5-9-1). The basin straddles the drainage of Tuya River and its tributaries Little Tuya River and Mansfield Creek. Tuya River flows south, joining the Stikine River 60 kilometres southwest of Dease Lake. Access is via the Dease Lake to Telegraph Creek gravel road, which at 52 kilometres is 5 kilometres south of the coal basin, or by a 15-minute helicopter flight from Dease Lake.

The Tuya River basin is potentially quite large, yet it has escaped detailed study. Limits of the basin are poorly defined and in places it is overlain by Recent volcanic rocks. However, it is estimated that the basin covers approximately 150 square kilometres and contains over 600 million tonnes of high-volatile B bituminous coal; a sizeable coalbed methane resource up to 0.04 Tcf (trillion cubic feet) may also exist.

Five field days were spent in the area. All known coal outcrops were sampled and the major drainages mapped.

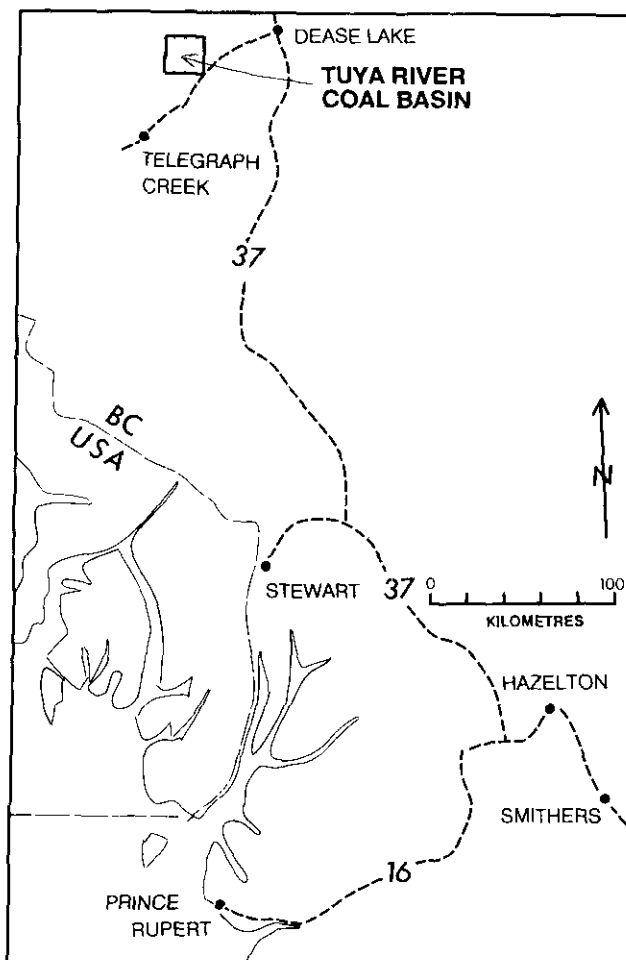


Figure 5-9-1. Tuya River coal basin location map; northwestern British Columbia.

PREVIOUS WORK

The earliest recorded description of coal in the Tuya River area is by R.D. Featherstonhaugh in 1904 (Dowling, 1915). He describes large seams in Tuya River (11.6 metres and 7.9 metres) and a 12.2-metre seam probably in and near the mouth of Little Tuya River. Dowling notes the existence of 13 coal leases and provides a single coal analysis which, based on analyses of ash and heating value, indicates a high-volatile bituminous C rank. Smitheringale (1953) mapped Tuya River and had only partial success in locating the coal outcrops described by Dowling. He also mapped the Tahltan River canyon where he located Tertiary lignite coal zones ranging up to 4 metres in thickness. The Tahltan River coal occurrences are about 20 kilometres southwest of the Tuya River coal basin and may be part of an outlier to it.

The Tuya River coal basin was drilled and mapped in detail in the period 1979 to 1980 when interest in coal was high. PetroCanada mapped and drilled the western half of the basin (Reid, 1980; De Nys, 1980) and Esso Minerals Canada (Vincent, 1979) mapped the eastern half. Ten cored holes were drilled and a number of hand trenches dug. Analytical results indicate a coal rank of sub-bituminous B to high-volatile bituminous C. A potential of 200 million tonnes of surface-mineable coal was outlined in the western half of the basin to a depth of 500 metres. Data were

insufficient to define measured reserves. The low rank of the coal, geographic isolation and general down-turn in coal utilization made the property unattractive to coal companies, and all coal licences in the area were allowed to lapse.

REGIONAL GEOLOGY

The Tuya River coal basin is within the Intermontane Belt of the Cordillera. Basement is composed of deformed Paleozoic and Mesozoic strata. Palynology (Vincent, 1979; De Nys, 1980) dates the coal-bearing rocks as not younger than early Eocene and not older than Paleocene. They may be equivalent to the Tango Formation of the Sustut Group (Eisbacher, 1974).

The basin is bounded on the north by basic rocks, possibly part of the Recent Level Mountain Complex. The eastern and western boundaries are probably fault-controlled, with pre-Tertiary rocks to the east and younger volcanic rock to the west. The southern boundary is arbitrarily

defined by thick postglacial drift and absence of outcrop. The basin is covered by the regional map of Gabrielse and Souther (1962) and is mentioned briefly in a number of coal compilation articles, the most recent of which is by Smith (1989).

The basin lies within the Stikine Plateau physiographic division. The topography in the Tuya River area is subdued with an average elevation of 800 metres. The area is lightly treed with patches of swamp. The Tuya and Little Tuya rivers and Mansfield Creek have incised meandering canyons up to 200 metres deep. Outcrop is restricted to the canyon floors.

LOCAL GEOLOGY

Sediments within the basin are generally coarse grained and poorly consolidated. In order of decreasing abundance, rock types are: sandstone, conglomerate and mudstone. The sandstones are medium to coarse grained, orange weathering and greyish when fresh. They contain numerous pebble

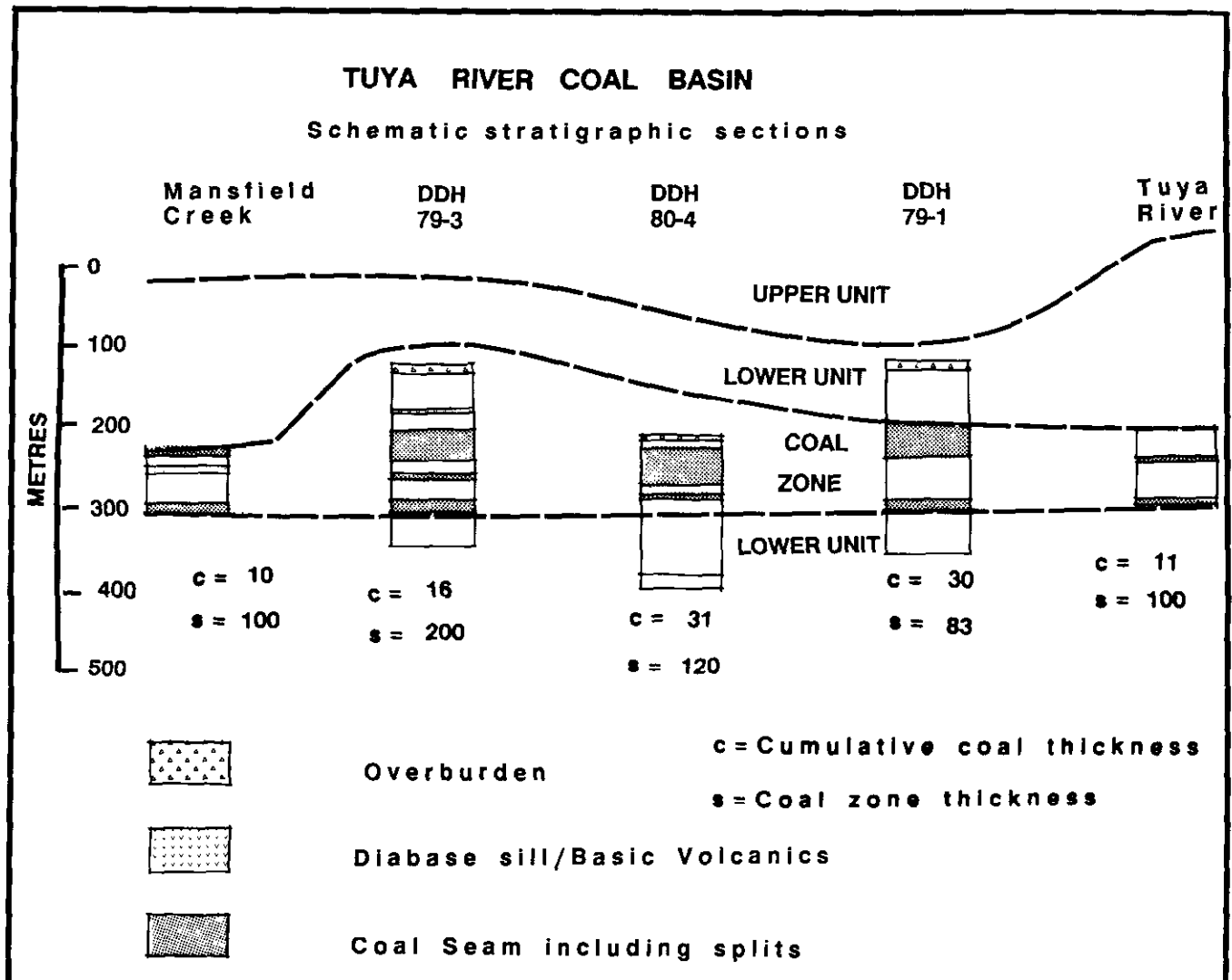


Figure 5-9-2. Stratigraphic sections of coal-bearing zone.

and grit bands and coal fragments; clasts are usually quartz or chert in a grey clay matrix; some lithic fragments have weathered to limonite. Conglomerates contain rounded volcanic and chert clasts ranging in size from granules to boulders, with pebbles predominating. They are yellow to orange weathering and form cliffs along the banks of the Little Tuya River. The mudstones are brown, sideritic and soft, and generally contain fine silty laminations. Vesicular basalts and diabases crop out in the basin.

It is difficult to establish a detailed stratigraphy in the area because of the lack of outcrop. Rocks structurally low in the succession in Mansfield Creek are mudstones, sandstones and a diabase sill, whereas rocks low in the succession in Tuya River are sandstones. Generally rocks high in the succession are conglomerates with volcanic clasts or basalt flows. Coal seams appear restricted to a zone fairly low in the succession.

A tentative stratigraphic succession is outlined in Figure 5-9-2. A lower unit, 200 to 300 metres thick, is composed of mudstones and sandstones in the west and sandstones and chert-pebble conglomerates in the east; it contains a single coal zone. The coal zone, described in detail later, is about 100 metres thick and contains from 5 to 30 metres of coal. The lower unit is overlain by an upper unit at least 300 metres thick which is composed of volcanic-pebble conglomerate, sandstones and volcanics.

STRUCTURAL GEOLOGY

There are insufficient data to adequately describe regional faults or folds. The simplest interpretation, presented here, represents the basin as an open, northerly plunging syncline, complicated by smaller scale faults and folds. Beds in Little Tuya River and Mansfield Creek dip to the east; beds in Tuya River dip to the north or west (Figure 5-9-3).

All available bedding orientation data are plotted on Figure 5-9-4; the eigen values/eigen vector technique was then used to calculate a best-fit cylindrical fold axis of $019^{\circ}/13^{\circ}$ (trend/plunge) for the data. Local, open, low-amplitude folds are outlined by bedding in Mansfield Creek, and isolated outcrops with steep bedding in Tuya River are probably evidence of faulting. Generally, interpretation of structures is complicated by extensive block-slumping off the valley walls and toward the rivers, causing detachment and rotation of some outcrops.

COAL GEOLOGY AND QUALITY

No detailed depositional model is postulated for coal in the Tuya River coal basin; certainly it would not be the same as that for Cretaceous coals. Depositional models for Cretaceous coals in British Columbia postulate large coastal swamps and cyclic deposition leading to fining-upwards sequences topped with coal. At Tuya River the surrounding rocks are sandier and contain evidence of rapid deposition in high-energy environments. Long (1981) suggests that the boundaries of Tertiary intermontane coal basins in the Cordillera and the type of sedimentation found in them were

controlled by penecontemporaneous faulting. The abundant coarse detritus and apparent lateral and/or temporal variability of depositional environment lend support to this suggestion.

In outcrop the coal is blocky, well banded and usually clean. It is often harder than the enclosing poorly consolidated sandstones. A burn zone was noted above one coal seam in Mansfield Creek, but in general the coal does not appear susceptible to rapid oxidation or spontaneous combustion. Seams vary in thickness up to 20 metres. Mudstone bands are common in the coal seams; bentonite layers are also conspicuous but are not radioactive on geophysical logs. The coal seams do not form part of fining-upwards sequences, and hanging and footwall contacts are sharp, with no particular enclosing rock type predominating. The coal is vitrain rich and contains an unusually high percentage of resin; some bands contain up to 5 per cent resin blebs ranging up to 5 millimetres in diameter. In places, the vitrain bands have a waxy lustre and conchoidal fracture which forms a distinctive eyed pattern on the fracture surfaces (Plate 5-9-1).

Coal seams were trenched and were intersected by three drill holes (Figures 5-9-2 and 3) in the Little Tuya and Tuya rivers and Mansfield Creek areas. Correlation of coal seams is made difficult by the sparsity of drill and surface data and by the lateral variability of the coal stratigraphy. A conservative approach is adopted in this report and most of the coal is assigned to a single coal-bearing zone. Stratigraphic sections (see Figure 5-9-2) measured in outcrop, represent approximate thickness, except for coal-seams. All coal-seam thicknesses include minor rock bands; where possible rock bands thicker than 50 centimetres are noted separately.

Coal seams forming part of the coal-bearing zone are exposed in Mansfield Creek. A thick seam outcropping below a 5-metre-thick diabase sill was trenched in three locations, providing: 3.89 metres of coal (hanging and footwalls not exposed); 6.6 metres of coal in a 7.7-metre zone; and a 2.7-metre zone of coal and mudstone below a burn zone. Above the diabase sill a 4.22-metre coal seam was trenched without exposing the hangingwall. The total coal-bearing section is about 100 metres thick and contains about 9.5 metres of coal.

The lower part of the coal-bearing zone is intersected by holes 79-3 and 80-4 (Figure 5-9-2). It is assumed that both holes are collared below the 4.22-metre seam, which is above the diabase sill in Mansfield Creek. In this case, the total coal-bearing zone at location 79-3 should be 200 metres thick with 16 metres of coal and, at location 80-4, 120 metres with 31 metres of coal. Hole 79-1 (Figure 5-9-3) is collared near an outcrop in Little Tuya River which has 6.1 metres of coal over 7.1 metres. The hole intersects this seam, and others lower in the section, for a cumulative coal thickness of 31 metres over an 83-metre section, which is assumed to be the full width of the coal-bearing zone.

The coal-bearing zone extends across the syncline to Tuya River where a zone 100 to 150 metres thick contains three coal seams with a cumulative coal thickness of 11 metres (Figures 5-9-2 and 3). A second coal zone, down

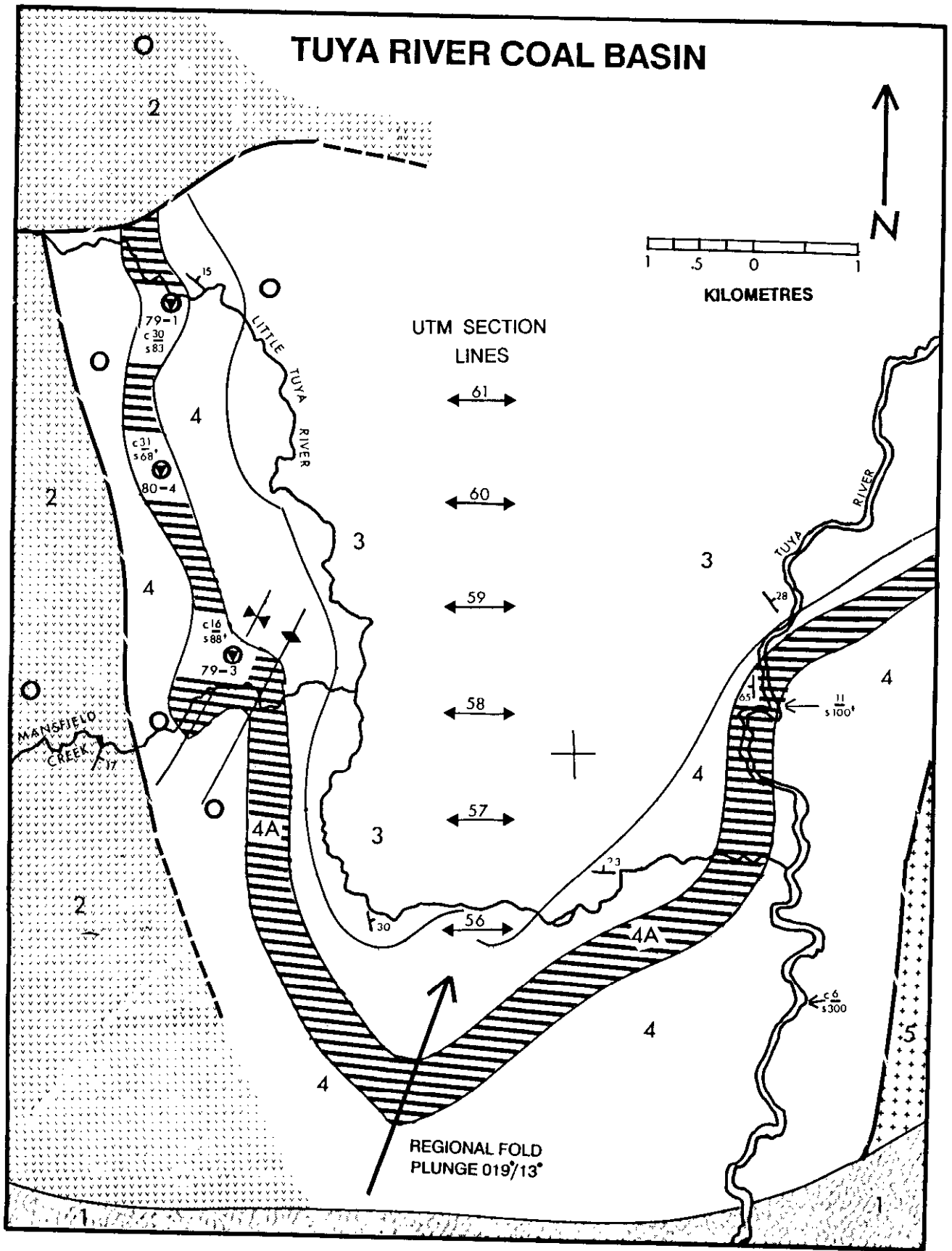


Figure 5-9-3. Regional map of Tuya River coal basin.

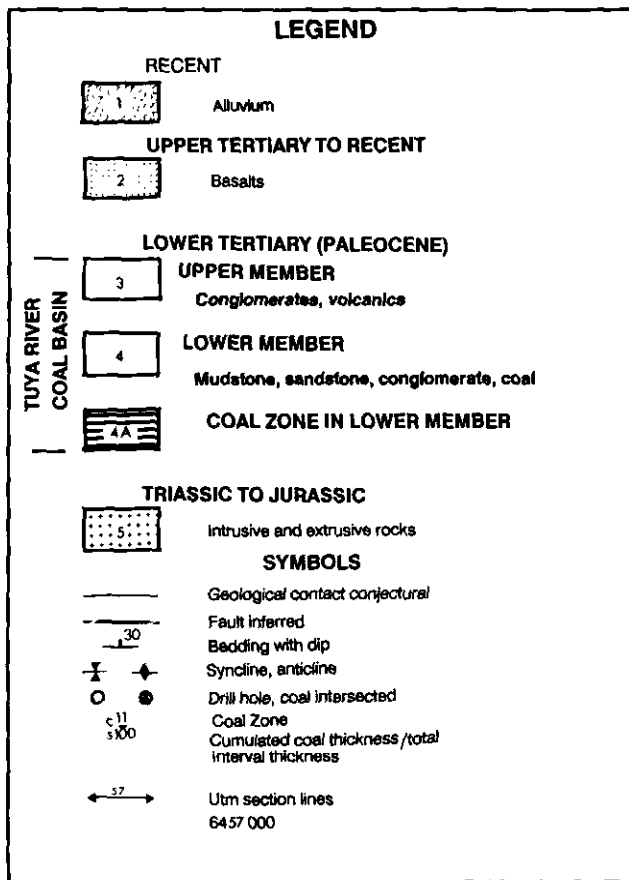


Figure 5-9-3A. Legend for Tuya River map.

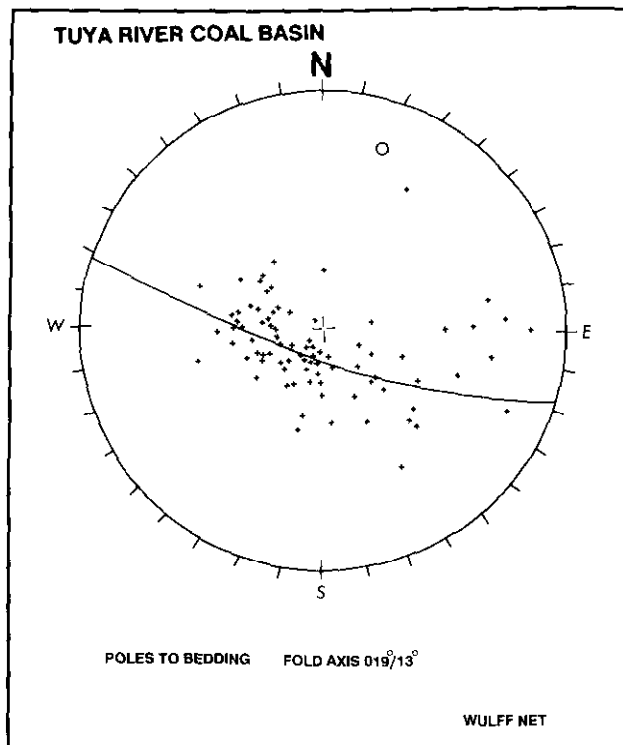


Figure 5-9-4. Stereonet of poles to Tuya River bedding data and best-fit great circle.

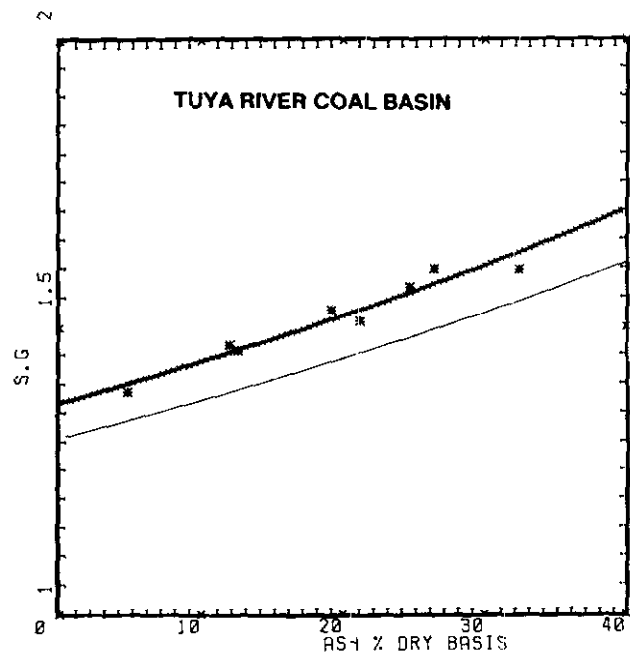


Figure 5-9-5. Plot of specific gravity versus ash data from drill holes; Tuya River.

TABLE 5-9-1
EQUATIONS USED IN TEXT

EQUATION 1 Derived by author for estimating specific gravity (S.G.)

$$S.G. = 100 \times K / (K + (TM + VP) + MM \times (DC - DMM) + DMM) \times (100 - TM)$$

DC = Specific gravity dry zero-ash coal

DMM = Specific gravity dry rock

VP = Void porosity

TM = total moisture

MM = weight dry mineral matter

K = DC × DMM

MM = WTLOS × Ash

Ash = per cent dry ash

WTLOS = ratio mineral matter/ash; 1.17 used in Figure 3-9-5.

S.G. = Specific gravity of coal ash-mixture at TM moisture

EQUATION 2 Empirical fit to Figure 3-9-7 (derived by author)

$$CBM = (\log(H \times (R^{2.5} - .2)) - 1.095) / .003913$$

CBM = coalbed methane in cubic feet per short ton

H = depth in metres

R = Ro Max

Note equation limits Ro Max > .6

EQUATION 3 From Kim (1977)

For estimating adsorption capacity of coal

$$MA = (1 - M - A) \times Vw/Vd \times (K \times (.096 \times H)^N - B \times (1.8 \times H / 100 + 11))$$

MA = methane: cubic centimetres/gram

M = moisture per cent/100

A = Ash per cent/100

K = .8 × FC/VM + .56

N = .315 - .01 × FC/VM

B = .14 cubic centimetres/gram/°C

H = depth in metres

FC = fixed carbon per cent

VM = volatile matter per cent

Vw/Vd = ratio of adsorption capacity wet coal: adsorption capacity dry coal

Vw/Vd = 1/(1.067 + .24337 × M ARB)

M ARB = Moisture on an as-received basis or equilibrium moisture

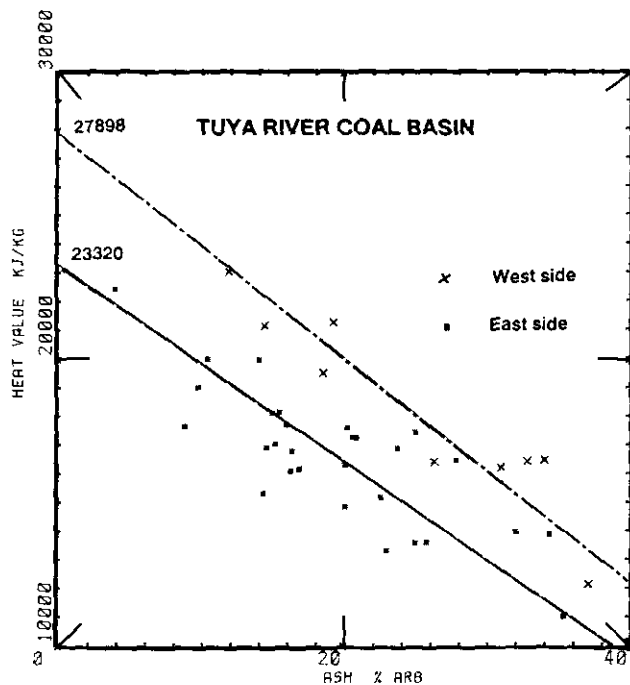


Figure 5-9-6. Plot of heat value versus ash; surface and drill-hole data.

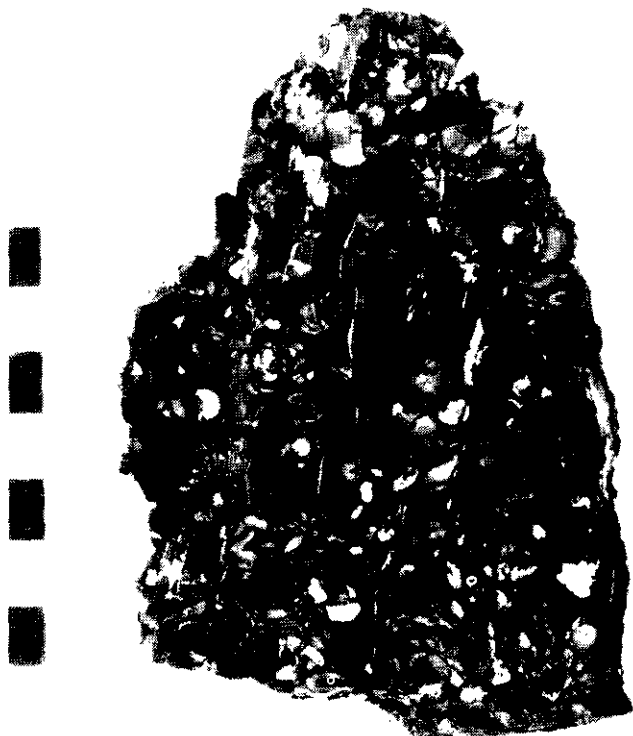


Plate 5-9-1. Eyed coal from Tuya River.

river, contains approximately 6 metres of coal and carbonaceous shale over 300 metres of section; it is not correlated with any other outcrop.

Existing coal-quality data are available from Dowling (1915), Vincent (1979) and De Nys (1980). Data from the western side of the basin were obtained from NQ diamond-drill core and on the eastern side from hand trenches. Samples were analyzed for per cent moisture (as received basis, ARB and air dried basis, ADB), ash, volatile matter, fixed carbon, sulphur and heat value. Data from the drill holes provide average, as received values of 12.4 per cent moisture, 19.1 per cent ash, 30.7 per cent volatile matter, 37.8 per cent fixed carbon and 0.5 per cent sulphur. Some specific gravity (S.G.) and Hardgrove index (HGI) data are also available from some drill-core samples. Eight petrographic analyses will be carried out during the present study and will be described in detail in a later report.

Eight S.G. determinations on air-dried core samples are reported by De Nys (1980); data are plotted in Figure 5-9-5 and a curve derived from a theoretical density equation (Equation 1, Table 5-9-1) is fitted to the data. A dry, clean coal specific gravity of 1.37 is calculated from the curve, based on the eight data points. This dry ash-free specific gravity is high for low-rank coals which usually have values in the range 1.2 to 1.3. The S.G. data were measured on air-dried core with a moisture content averaging 8 per cent; the thin line (Figure 5-9-5) illustrates the ash (DB) versus S.G. relationship at an *in situ* moisture of 12.5 per cent and provides an S.G. of 1.48, for an ash of 22.5 per cent ADB and 8 per cent moisture. This value is used as an average for deriving tonnages from *in situ* volumes in the resource calculation (next section).

Hardgrove index values are a measure of the friability of coal; small numbers indicate hard or non-friable coal, large numbers indicate soft or friable coal. Two HGI values from drill core (De Nys, 1980) average 52.5, indicating a moderately hard coal in agreement with outcrop observations.

Rank can be estimated from the projected moist, ash-free heat value of the coal. The western and eastern surface data sets were treated separately and lines fitted to each using the method of York (1969) (Figure 5-9-6). The western data predict a moist, ash-free heat value of 27 898 kilojoules per kilogram and the eastern data 23 322 kilojoules per kilogram. These values are compatible with ranks of high-volatile bituminous C on the west and sub-bituminous B on the east. Oxidation of surface samples may have lowered the heat content of coal for the eastern side of the basin.

Seven samples from the coal basin were analyzed for per cent mean maximum reflectance of vitrinite in oil (referred to in the text as reflectance). Reflectances of the samples from Tuya River and Mansfield Creek range from 0.60 to 0.79 and average 0.68 per cent, indicating a rank of high-volatile bituminous B. The reflectance value of a single sample of float from the mouth of the Tahltan River, 20 kilometres southwest of Tuya River, is 0.71; previous references to coal in the area postulate a rank of lignite to sub-bituminous. If the sample is representative of coal from the Tahltan River then there is a possibility that the high-volatile coal of the Tuya River coal basin extends to the

southwest. The preliminary petrographic data indicate a rank of high-volatile B extending to high-volatile A based on rank versus reflectance relationships provided by Ward (1984). This rank is higher than previously expected and increases the potential for a coalbed methane resource. The preliminary data indicate reflectances of 0.61 from Tuya River above Little Tuya River, 0.72 from the Tuya River south of Little Tuya River and 0.79 from Mansfield Creek.

POTENTIAL COAL AND COALBED METHANE RESOURCE

COALBED METHANE IN COAL

It is unlikely that the Tuya River coal basin will be of interest as a source for surface-minable coal for a long time; however, the deposit could be a source of coalbed methane. Natural gas is 74 per cent methane, while the gas desorbed from coal is 98 per cent methane and is invariably low in SO_2 (despite varying sulphur contents in the coal) and has a heat value similar to natural gas. Coalbed methane is a safety hazard in underground mining. Its presence has long been monitored and steps taken to vent it safely. More recently, especially in the U.S.A., coalbed methane is collected as a viable replacement for natural gas. Wells drilled into deeply buried coal seams decrease the overburden pressure on the coal and allow methane to desorb from the coal and rise to the surface. The process has similarities to natural gas exploration; the technology, depth of holes and gas composition, are all similar; differences exist in the process of recovering the methane.

Coalbed methane is released slowly after water is pumped out of the seam and the overburden pressure reduced. The amount of methane trapped by coal is in part proportional to the surface area of the coal structure. To use an analogy, coal is like a book in which the amount of methane retained is proportional to the cumulative surface area of all the pages, while a sandstone reservoir is like a block of styrofoam in which the amount of natural gas retained is proportional to the cumulative volume of voids in the styrofoam. It is easy to imagine how, on a volume to volume comparison, coal can retain up to five times more gas than a sandstone reservoir.

Coalbed methane occupies three general sites in the coal seam: (1) fractures and large pores in the coal; (2) adsorbed onto the coal structure; and (3) absorbed into the coal structure. When coalbed-methane measurements are made on core, Type 1 methane is lost prior to the desorption measurement and is referred to as "lost gas"; Type 2 methane, which usually accounts for most of the reservoir potential, is referred to as the desorbed component, and Type 3 methane is the residual component which is generally not measured. Theoretical estimates of coalbed methane attempt to estimate the content of Type 2 and some of the Type 3 methane and refer to this as the "adsorbed component".

Coal rank and depth of burial are important controls on the amount of gas coal can retain. Figure 5-9-7, adapted from Hunt (1979), tracks cumulative and incremental meth-

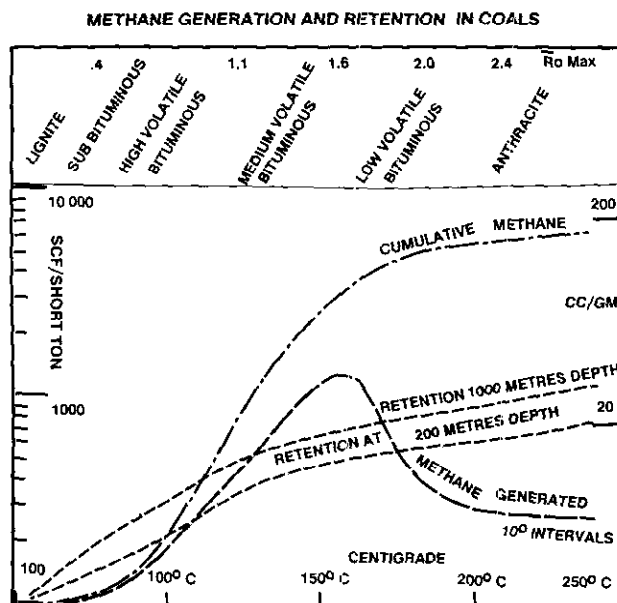


Figure 5-9-7. Methane generation and retention by temperature. modified from Hunt (1979).

ane generated by coals from lignite to anthracite rank. It illustrates the limited proportion of methane that is retained; the rest being available to charge sandstone reservoirs. A cubic metre of coal can charge up to 60 cubic metres of sandstone reservoir with expelled coalbed methane. The figure shows that for low-rank coals, methane generated is close to or less than retention capability. This means that the coal will not have charged the surrounding rocks by expelling methane. The coalbed gas expelled at greater depths from coals of higher rank can migrate upwards and actually be adsorbed by lower rank coals with a retention capacity exceeding their cumulative methane generation value. Figure 5-9-8, derived from Eddy *et al.* (1982) with minor extrapolation of some lines by the author, plots lost and desorbed gas contents of fresh drill-core coal samples of different ranks against depth. The lost gas component is lost before the desorption test but its value can be determined by extrapolation. The methane retention curves in Figure 5-9-3 can be approximated by a single equation developed by the author, which has reflectance and depth as variables (Equation 2, Table 5-9-1). The equation provides approximate values of coalbed methane for any combination of reflectance and depth (reflectance >0.6) and therefore offers more flexibility than the six curves in Figure 5-9-8. Kim (1977) developed a theoretical equation (Equation 3 in Table 5-9-1) which predicts methane adsorption capacity by rank and depth.

The experimental approach of Eddy *et al.* (1982) and the theoretical approach of Kim (1977) measure different combinations of the types of methane in coal. Figure 5-9-8 provides information on the amount of lost and desorbed gas; residual gas is assumed to remain in the core. Eddy *et al.* indicate that residual gas can vary from 5 to 32 per cent of the total with low-rank coals having more than higher rank coals. McCulloch *et al.* (1975) estimate residual

METHANE RETENTION AS A FUNCTION OF RANK AND DEPTH

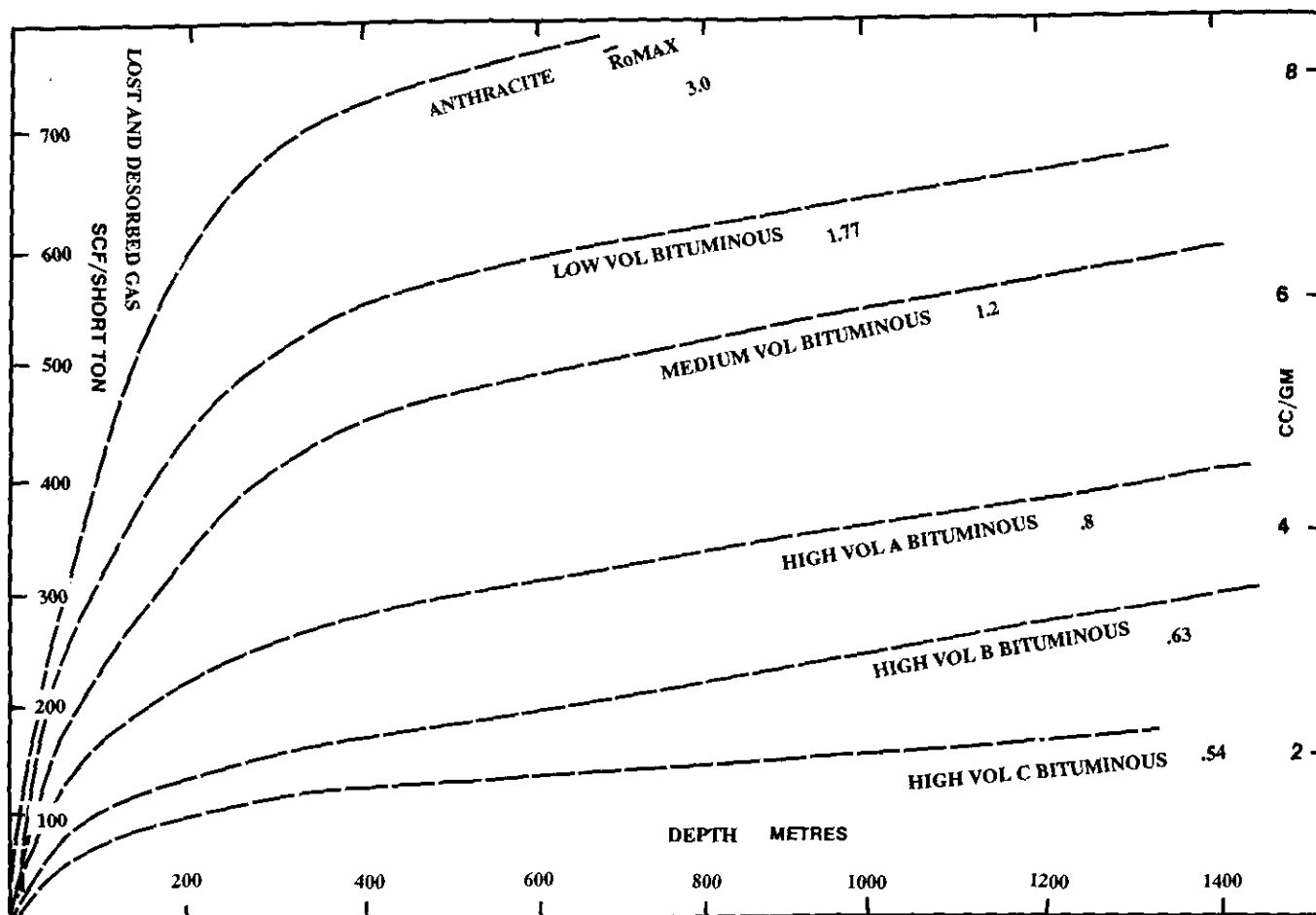


Figure 5-9-8. Methane retention by rank and depth, modified from Eddy *et al.* (1982).

gas using HGI values. A value of 52.5 defines the coal as blocky, which represents a potential residual gas content of 39 per cent. Diamond *et al.* (1981) found a less reliable relationship between HGI and residual gas. McCulloch *et al.* note that the lost gas component for blocky coals is smaller than for friable coals. Eddy *et al.* indicate that lost gas ranges from 5 to 17 per cent of the total gas. Equation 3 (Table 5-9-1) from Kim (1977) does not predict lost gas components. It is a theoretical estimate of the adsorptive capacity of coal and corresponds with the desorption component measured by Eddy *et al.*, and some of the residual gas component which is not incorporated in Figure 5-9-8. If residual gas is greater than lost gas for Tuya River coals then Equation 3 may tend to overestimate recoverable methane.

CALCULATION OF COAL AND COALBED METHANE RESOURCE

The amount of methane retained by Tuya River coals is limited by the low rank (though the rank is higher than previously reported). However, the large tonnage of coal and permeable interburden lithologies, all point to the pos-

sibility of a sizeable coalbed methane resource. Volcanic flows and sills in the succession may have raised the rank and helped contain the methane.

An estimate of the potential resource requires first a coal tonnage calculation and then information on how gas retention varies with depth. The coal resource at Tuya River was estimated using six 1:10 000-scale sections (Figure 5-9-3). The coal-bearing zone was drawn on the sections using the sparse surface and drill data and assuming fold plunge orientation 019°/13°(trend/plunge). The numerical average, vertical coal-thickness in the coal-bearing zone is 19.6 metres; this was converted to an estimated true thickness of 17 metres assuming an average dip of 30°. The true thickness was reduced by 20 per cent to account for rock splits. Coal volumes were calculated for each 1000-metre section-strip using 200-metre vertical slices; volumes were converted to tonnages using an S.G. of 1.48. Table 5-9-2 tabulates the results: there is a total potential coal resource of over 600 million tonnes, of which 416 million tonnes are within 1600 metres of surface (Table 5-9-2).

Variation of methane retention with depth has been investigated in a number of ways. Coals of sub-bituminous to

**TABLE 5-9-2
TUYA RIVER COAL BASIN
POTENTIAL COAL AND COALBED METHANE RESOURCE**

Section 6400 x1000	FROM TO	Depth in Metres										TOTAL
		0 200	200 400	400 600	600 800	800 1000	1000 1200	1200 1400	1400 1600	0 1600	+ 1600	
Million Tonnes												
61		9.5	6.8	10.8	19	12.2	13.6	13.6	13.6			
60		9.5	12.2	17.6	10.8	13.6	13.6					
59		16.3	10.8	12.2	13.6	17.6						
58		27.1	8.1	10.8	16.3							
57		21.7	8.1	12.2								
56		65										
TOTAL TONNES		149.1	46	63.6	59.7	43.4	27.2	13.6	13.6	416	232	648
(A) Methane cft/ton		25	25	25	25	25	25	25	25	25	0	.01Tcf
(B) Methane cft/ton		72	108	117	125	133	150	150	150	0	0	.039Tcf
(C) Methane cft/ton		89	98	114	126	132	141	146	151	0	0	.038Tcf

- (A) uses constant 25 cubic feet per short ton
- (B) values derived from Figure 3-9-8
- (C) values derived from Equation 3, Table 3-9-1

Note 1 sections located in Figure 3-9-3

Note 2 half of 491.1 million tonnes used to calculate CBM

high-volatile bituminous rank do not generate or retain much methane. Meissner (1984) states that catagenic methane generation starts when the volatile matter (dry, ash-free basis) is less than 37.8 per cent, equivalent to a rank of high-volatile A. The dry, ash-free volatile matter of Tuya River coals is about 45 per cent though the rank may be as high as high-volatile bituminous A. Figure 5-9-8 indicates that high-volatile bituminous C coals can retain up to 150 cubic feet of methane per short ton (4 cubic centimetres per gram) at depths of 1500 metres. Equation 2 provides ranges of 0 to 250 cubic feet per short ton (reflectance=0.6) and 0 to 350 cubic feet per short ton (reflectance=0.7) for depths 0 to 1500 metres. These values assume that the rank of coal at 1500 metres is not higher than that at surface. In the case of Tuya River, if folding predates coalification, then the rank in the core of the syncline could be as high as medium-volatile bituminous and the coal at depth capable of retaining two to three times more methane. A high-volatile bituminous C rank is assumed for the purpose of estimating the coalbed methane resource at Tuya River.

The resource has been estimated for other low-rank coal basins. Choate *et al.* (1989) estimate an average gas content of 25 cubic feet per short ton for coals in the Powder River basin where rank is sub-bituminous to high volatile C. Recently, desorption tests from the Powder River basin have provided values of 56 and 74 cubic feet per short ton (McBane, 1990) McCord (1989) uses a range of 0 to 100 cubic feet per short ton for sub-bituminous coal when estimating the methane resource of the Greater Green River coal region. Equation 3 (Table 5-9-1) from Kim (1977) is described later, but it predicts a range of gas contents of 69 to 151 cubic feet per short ton from 100 metres to 1500 metres depth. Obviously there is a wide range of uncertainty in trying to predict the methane contents for low-rank coals.

The coalbed methane resource was calculated in this study in three ways. A minimum estimate was obtained by

multiplying the total tonnage to a depth of 1600 metres by 25 cubic feet per short ton derived from Choate *et al.* (1989), to give a resource value of 0.01 trillion cubic feet. The second and third approaches involved multiplying the coal tonnages, distributed by depth of burial, by methane-retention values derived from the data of Eddy *et al.* (1982; Figure 5-9-8 high volatile bituminous C line) and from Equation 3 (Table 5-9-1) from Kim (1977).

Application of Equation 3 to Tuya River coals predicts a methane resource of 0.038 trillion cubic feet, with retention values ranging from 67 to 151 cubic feet per short ton. Equation 3 requires coal-quality data and estimates of the pressure and temperature acting on the coal as well as an estimate of the ratio of gas-adsorption capacity for wet coal divided by gas-adsorption capacity for dry coal (V_w/V_d , Table 5-9-1). The coal-quality data were averaged from coal

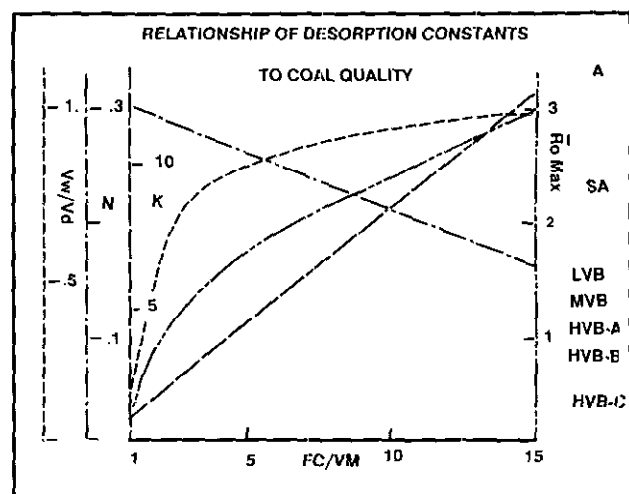


Figure 5-9-9. Plot of fixed carbon/volatile matter ratio versus reflectance and desorption constants from Kim (1977).

intersections in the drill holes which provided values of 12.4 per cent moisture, 19.1 per cent ash, 30.7 per cent volatile matter, 37.8 per cent fixed carbon (all AR). These data are incorporated into Equation 3 (Table 5-9-1) using constants K and N which are derived from the ratio of fixed carbon divided by volatile matter. This ratio is related to rank and reflectance measurements in Figure 5-9-9 (data from Stach, 1982) which also illustrates the relationship of K and N to reflectance.

The pressure acting on the coal seam is an important constraint on methane retention. Usually pressure will equal hydrostatic pressure, but drill results indicate cases where pressures are less than hydrostatic or more than hydrostatic and approach lithostatic pressure (over-pressure situations). For this study hydrostatic pressure is assumed.

Methane retention decreases as the moisture content of the coal increases. High moisture contents are an important limiting factor on methane retention by low-rank coals. The effect of moisture content on methane retention is accounted for in Equation 3 by the ratio V_w/V_d which was derived for Tuya River coals by curve fitting and extrapolation using data in Table B-1 of Kim (1977); a value of 0.25 was determined. Methane retention decreases with temperature, which increases with depth. The factor B (Table 5-9-1) takes into account temperature and the term following B in the equation assumes a geothermal gradient of 18° C per 1000 metres.

Coalbed methane retention values from Figure 5-9-8 (high-volatile bituminous C line) range from 72 cubic feet per short ton at 100 metres depth to 150 cubic feet per short ton at 1500 metres; the upper value was fixed at 150 cubic feet per short ton because the original diagram by Eddy *et al.* (1982) does not extrapolate beyond this point. Using these values a coalbed methane resource of 0.039 trillion cubic feet is calculated (Table 5-9-2). The resource calculated using Equation 2 would be even larger because reflectance values, on average, indicate a rank up to high-volatile A. A resource of 0.062 trillion cubic feet is predicted using Equation 2 and an average reflectance of 0.68.

DISCUSSION

The three methods of estimating coalbed methane resources to a depth of 1600 metres produce values of 0.01, 0.038 and 0.039 trillion cubic feet. These values are based on minimal data and are at the low end of the scale for methane retention. This approach was taken because at the moment no desorption data are available for Tuya River coals. The same approach is being applied more usefully to the Telkwa deposit where coal rank for the lowest seam is favorable for methane retention.

It is useful to make some order of magnitude comparisons between coal and coalbed methane as fuels. A tonne of coal mined and burned will provide about sixty times more energy than the methane extracted from one tonne of coal. This means that extracting methane decreases the energy content of the coal by about 2 per cent and represents about 1 per cent of the volatile matter in the coal. Therefore its extraction has little if any effect on the quality of the coal

because the gas would probably also be lost during conventional mining.

A single house using electricity derived from coal for all its energy needs requires from 1 to 5 tonnes of coal per year; in contrast, if the house were using coalbed methane, the coal requirement would be from 40 to 200 tonnes. The increased requirement of coal may be offset as the end-use efficiency for natural gas or coalbed methane can be much higher than for coal. A resource of 400 million tonnes or 0.04 trillion cubic feet is sufficient to service up to 5000 houses for 100 years.

The environmental impact of burning coal is greater than the impact of burning the same energy-equivalent of coalbed methane. Burning methane provides two times more energy than coal per unit CO₂ generated (Fulkerson, 1990). Although using coal only as a source of gas requires a larger coal resource, and may be considered an inefficient use of the resource, it is environmentally much cleaner. Recovering the methane does not detract from the value of the coal for future use when coal-burning technologies have improved. Also, on a molecule for molecule basis, methane is twenty times more potent as a greenhouse gas than CO₂ (although its residence time in the atmosphere is one-tenth that of CO₂). Collecting and burning methane that might otherwise escape into the atmosphere should help to reduce the overall impact of greenhouse gases.

SUMMARY

A review of existing data, with the addition of some 1990 fieldwork, indicates that the Tuya River coal basin is large with a potential resource of 650 million tonnes of high-volatile B bituminous coal and a possible coalbed-methane resource of up to 0.04 trillion cubic feet. A resource of this magnitude could make a significant contribution to the energy requirements of the region, as it develops, while minimizing impact on the environment.

In the long term, the isolation of the basin might be a positive factor in its development; it might be more economic and environmentally sound to sustain development in northwestern British Columbia using a local energy source than to continue to use high-priced petroleum products and build expensive transmission systems. The methane could be distributed by truck as pressurized gas and used for local industry as well as to run motor vehicles and heat houses.

Petrographic and coal-quality analyses of the 1990 samples are ongoing and will be discussed in depth in a later report. The next stage in clarifying the potential for a coalbed-methane resource should be a drilling program to provide fresh samples for methane desorption tests, petrography and coal quality analyses. Some existing drill sites could be used and new ones cleared in Tuya River. The program would have to be helicopter supported from Dease Lake which is 15 minutes flying time away.

There are numerous poorly explored Tertiary coal-bearing sedimentary basins in British Columbia. It is intriguing to speculate that some may, in the future, provide local, environmentally sound sources of energy to help in the development of the province.

ACKNOWLEDGMENTS

The author wishes to thank J. Whittles for providing cheerful and reliable field support and for helping with map and illustration preparation; and David Grieve for spending precious time reviewing the manuscript and providing many helpful comments. Thanks are extended to Joanne Schwemler who performed the petrographic analyses in time for inclusion in the report.

REFERENCES

- Choate R. Johnson C.A. and McCord J.P. (1989): Geological Overview, Coal Deposits, and Potential for Methane Recovery from Coalbeds – Powder River Basin; in Coalbed Methane Resources of the United States, *American Association of Petroleum Geologists studies in Geology*, Series 17, pages 335-351.
- De Nys, F.J.G. (1980): Thundercloud Coal Project Technical Report; PetroCanada Exploration, *B.C. Ministry of Energy, Mines and Petroleum Resources*, Coal Assessment Report 00243.
- Diamond, W.P. and Levine, J.R. (1981): Direct Method Determination of the Gas Content of Coal, *Procedures and Results*; *U.S. Bureau of Mines*, Report of Investigations 8515.
- Dowling, D.B. (1915): Coal Fields of British Columbia; *Geological Survey of Canada*, Memoir 309, pages 324-326.
- Eddy, G.E., Rightmire, C.T. and Byren, C.W. (1982): Content of Coal Rank and Depth: Relationship of Methane; *Proceedings of the SPE/Department of the Interior, Unconventional Gas Recovery Symposium*, Pittsburg, Pennsylvania SPE/DOE 10800, pages 117-122.
- Eisbacher, G.H. (1974): Sedimentary History and Tectonic Evolution of the Suskut and Sifton Basins, North-central British Columbia, *Geological Survey of Canada*, Paper 73-31.
- Fulkerson, W., Judkins, R.R. and Sanghvi, M.K. (1990): Energy From Fossil Fuels; *Scientific American*, September 1990, Pages 129-135.
- Gabrielse, H., and Souther, J.G. (1962): Dease Lake, British Columbia; *Geological Survey of Canada*, Map 21-1992.
- Hunt, J.M. (1979): Petroleum Geochemistry and Geology; *W.H. Freedman and Company*.
- Kim, A.G. (1977): Estimating Methane Content of Bituminous Coalbeds from Adsorption Data; *U.S. Bureau of Mines*, Report of Investigations 8245.
- Long, D.G.F. (1981): Dextral Strike Slip Faults in the Canadian Cordillera and Depositional Environment of Related Fresh-water Intermontane Coal Basins; *Geological Association of Canada*, Special Paper No. 23 pages 153-186.
- McBane R.A. (1990): Basin Activities, Powder River Basin, Wyoming and Montana; *Quarterly Review of Methane from Coal Seams Technology*, Volume 7, Number 4, page 3.
- McCord J.P. (1989): Geologic Overview, Coal and Coalbed Methane Resources of the Greater Green River Coal Region – Wyoming and Colorado; in Coalbed Methane Resources of the United States, *American Association of Petroleum Geologists Studies in Geology*, Series 17, pages 271-332.
- McCulloch, C.M., Levine, J.R., Kissell, F.N. and Deul, M. (1975): Measuring the Methane Content of Bituminous Coalbeds; *U.S. Bureau of Mines*, Report of Investigations 8043.
- Meissner F.F. (1984): Cretaceous and Lower Tertiary Coals as Sources for Gas Accumulations in the Rocky Mountain Area; in *Hydrocarbon Source Rocks of the Greater Rocky Mountain Region*, J. Woodward, F.F. Meissener and J.L. Clayton, Editors, *Rocky Mountain Association of Geologists 1984 Symposium*, pages 401-431.
- Reid, J.L. (1980): Thundercloud Coal Project Technical Report, PetroCanada Exploration Inc; *B.C. Ministry of Energy, Mines and Petroleum Resources*, Coal Assessment Report 00242.
- Smith, G.G. (1989): Coal Resources of Canada; *Geological Survey of Canada*; Paper 89-4, page 41.
- Smitheringale, W.Y. (1953): Report on Coal Occurrences Tuya and Tahltan Rivers, Telegraph Creek Area. B.C.. *B.C. Ministry of Energy, Mines and Petroleum Resources*, Coal Assessment Report 00245.
- Stach, E. (1982): Coal Petrology; *Gebruder Borntraeger*, Berlin, page 45.
- Vincent, B.D. (1979): Geological Mapping, Tuya River Property, British Columbia; *Esso Minerals Canada*; *B.C. Ministry of Energy, Mines and Petroleum Resources*, Coal Assessment Report 00246.
- Ward C. R. (1984): Coal Geology and Coal Technology; *Blackwell Scientific Publications*, page 96.
- York, D. (1969): Least Squares Fitting of a Straight Line with Correlated Errors; *Earth and Planetary Science Letters* Volume 5, pages 320-324.

NOTES

UNIVERSITY RESEARCH IN BRITISH COLUMBIA

THE UNIVERSITY OF BRITISH COLUMBIA, 1989

- Armstrong, C.R.: Preliminary Evaluation of the Pit Valley Region for Aggregate Deposits. (B.A.Sc.)
- Beyers, J.M.: Upper Permian and Triassic Conodont Biostratigraphy of the Cache Creek Group, Marble Range, South-central British Columbia. (M.Sc.)
- Bryan, C.: Site Selection and Monitoring Network Design Based on Contaminant Transport Models. (B.A.Sc.)
- Chapman, A.E.: Simulated Annealing: Its Application to Fluid Distribution in the Void Space of a Rock. (B.Sc.)
- Cookenboo, H.O.: Lithostratigraphy, Palynostratigraphy, and Sedimentology of the Northern Skeena Mountains and their Implications to the Tectonic History of the Canadian Cordillera. (M.Sc.)
- Coasdale, D.A.: A Small Scale Translational Rock Failure Affecting the Basal Failure Surface of the 1965 Hope Slide. (B.A.Sc.)
- Feeney, T.: The Petrology, Morphology and Tectonics of Explorer Seamount. (B.Sc.)
- Fogarassy, J.A.S.: Stratigraphy, Diagenesis and Petroleum Reservoir Potential of the Cretaceous Haida, Skidegate and Honna Formations, Queen Charlotte Islands, British Columbia. (M.Sc.)
- Greig, C.J.: Geology and Geochronology of the Eagle Plutonic Complex, Coquihalla Area, Southwestern British Columbia. (M.Sc.)
- Hammack, J.L.: The Effect of Deformational Mechanisms on the Permeability of Upper Paleozoic Limestone, Dolostone and Sandstone Near Overfold Mountain, 55 Kilometres Southeast of Fernie, British Columbia. (M.Sc.)
- Hood, C.: Geology of the Iron Hill Calcic Iron Skarn, Central-east Vancouver Island, British Columbia. (B.Sc.)
- Keep, M.: The Geology and Petrology of the Averill Alkaline Plutonic Complex Near Grand Forks, British Columbia. (M.Sc.)
- Laesecke, R.F.: Factors Causing Instability of Rock Slopes Along the Vancouver-Squamish Highway in Southwestern British Columbia. (B.A.Sc.)
- Leitch, C.H.B.: Geology, Wallrock Alteration and Characteristics of the Ore Fluid At the Bralorne Mesothermal Gold Vein Deposit, Southwestern British Columbia. (Ph.D.)
- Leslie, D.R.: Petrography and Sedimentology of an Unnamed Upper Cretaceous to Lower Paleocene Sedimentary Unit, Queen Charlotte Basin, British Columbia. (B.A.Sc.)
- McCleachern, D.: Salinity Effect on the Hydraulic Conductivity of Samples of a Typical Coastal Aquifer. (B.A.Sc.)

- Neilson, B.: Diagenesis of Tricyclic Diterpenoids Used as Biomarkers in an Anoxic Lake. (M.Sc.)
- Presch, G.: Geology of the 2800-Level Access Adit of Northair Mine, Southwestern British Columbia. (B.A.Sc.)
- Pritchard, M.A.: Numerical Modelling of Large Scale Toppling. (M.A.Sc.)
- Radloff, J.K.: Origin and Obduction of the Ophiolitic Redfern Complex on the Omineca-Intermontane Belts Boundary, Western Cariboo Mountains, British Columbia. (M.Sc.)
- Reddy, D.G.: Geology of the Indian River Area, Southwestern British Columbia. (M.Sc.)
- Rose, N.D.: A Petrographic and Chemical Analysis of Altered Mafic Metavolcanic Rocks from Sinmax Valley, Adams Lake, South-central British Columbia. (B.A.Sc.)
- Stevens, L.A.: The Application of a Correction Procedure for Metasomatism to a Suite of Rocks From the Fennell Formation in South-central British Columbia. (B.A.Sc.)
- VanDer Heyden, P.: U-Pb and K-Ar Geochronometry of the Coast Plutonic Complex, 53°N to 54°N, British Columbia and Implications for the Insular-Intermontane Superterrane Boundary. (Ph.D.)
- Wise, M.P.: Calculations of Seismic Velocities to Monitor Steamfront Advance In Tar Sands: Velocities after Kuster and Toksoz, 1974. (B.A.Sc.)

THE UNIVERSITY OF BRITISH COLUMBIA, 1990

- Boychuk, K.: Extensometer Analysis of Rock Deformation in ALRT Tunnels and Pillars Produced by Excavation at the Burrard and Granville Street Stations. (B.A.Sc.)
- Carmichael, D.A.: A Geological Engineering Evaluation of Whistler Village, Southwestern British Columbia. (B.A.Sc.)
- Gant, M.: Preliminary Design Guidelines for an Openpit Highwall at Quintette Coal Limited, Northeastern British Columbia. (B.A.Sc.)
- Gillstrom, G.O.: Geology, Mining History and Ore Petrology of the Exposed Skarns of the Copper Duke Deposit, Lynn Creek, North Vancouver, British Columbia. (B.A.Sc.)
- Hedberg, S.A.: The NMR Response of Sandstones and its Application to the Detection of the Hydrocarbon Contamination. (B.A.Sc.)
- Higman, S.L.: Chemical Discrimination of the Cheakamus Valley Basalt Lava Flows, Southwestern British Columbia: Statistical Constraints. (B.A.Sc.)

Irwin, S.E.B.: Late Devonian Conodont Biostratigraphy of the Earm Group with Age Constraints for Stratiform Mineral Deposits, Selwyn and Kechika Basins, Northern British Columbia. (M.Sc.)

Jurbin, T.: Lightweight Materials for Construction Fills. (B.A.Sc.)

Kokan, M.J.: Evaluation of Resistivity Cone Penetrometer in Studying Groundwater Quality. (B.A.Sc.)

Leir, M.C.: Preliminary Wall Design of the East Pit, Ajax Project. (B.A.Sc.)

Nader, U.K.: Carbon Dioxide and Carbon Dioxide — Water Mixtures: P-V-T. Properties and Fugacities to High Pressure and Temperature Constrained by Thermodynamic Analysis and Phase Equilibrium Experiments. (Ph.D.)

Mahood, R.: Design Considerations for a Tailings Dike. (B.A.Sc.)

McMullin, D.W.A.: Thermobarometry of Pelitic Rocks Using Equilibria Between Quartz-Garnet-Aluminosilicate-Muscovite-Biotite, with Application to Rocks of Quesnel Lake Area, British Columbia. (Ph.D.)

Naumann, C.M.: The Cheam Slide: A Study of Interrelationship of Rock Avalanches and Seismicity. (M.A.Sc.)

Palsgrove, R.J.: Stratigraphy, Sedimentology and Coal Quality of the Lower Skeena Group, Telkwa Coalfield, Central British Columbia. (M.Sc.)

Risk, Z.V.: Structural Interpretation of the T-Bone Coal, Mesa Pit, Quintette Coal Limited. (B.A.Sc.)

Thomas, D.G.: Methods of Estimating the Strength and Index Properties for the Basal Failure Plane of the Cheam Slide and Implications on Slide Development. (B.A.Sc.)

Wallis, C.C.: A Proposed Guideline for Investigations for Siting and Designing Tailings Dams. (B.A.Sc.)

UNIVERSITY OF ALBERTA, 1989

Bobrowsky, P.T.: Late Cenozoic Sedimentology and Stratigraphy of the Northern Rocky Mountain Trench, British Columbia. (Ph.D.)

Maheux, P.J.: A Fluid Inclusion and Light Stable Isotope Study of Antimony-associated Gold Mineralization in the Bridge River District, British Columbia. (M.Sc.)

Oppelt, H.P.: Stratigraphy, Sedimentology and Ichnology of the Bluesky Formation in Northeastern British Columbia. (M.Sc.)

UNIVERSITY OF ALBERTA, 1990

Marsh, I.K.: A Description of Glass Phases in the Columbia River Basalt Group. (M.Sc.)

Shaw, R.P.: Geology and Geochemistry of Gold Mineralization at Athabasca Pass, Central Rocky Mountains, British Columbia. (M.Sc.)

MCGILL UNIVERSITY, 1990

Minehan, K.: Paleotectonic Setting of Takla Group Volcano-sedimentary Rocks of Quesnellia, North Central British Columbia. (M.Sc.)

UNIVERSITY OF WESTERN ONTARIO, 1990

Diakow, L.J.: Volcanism and Evolution of the Early and Middle Jurassic Toadogone Formation, Toadogone Mining District British Columbia. (Ph.D.)

McDonald, D.W.A.: The Silbak Premier Silver-Gold Deposit: A Structurally-controlled, Base Metal Rich Cordilleran Epithermal Deposit, Stewart, British Columbia. (Ph.D.)

UNIVERSITY OF CALGARY, 1989

Bloch, J.D.: Diagenesis and Rock-Fluid Interaction of Cretaceous Harmon Member (Fort St. John Group) Mudstones, Alberta and British Columbia. (Ph.D.)

Gal, L.P.: Metamorphic and Structural Geology of the Northern Solitude Range, Western Rocky Mountains, British Columbia. (M.Sc.)

McDonough, M.R.: The Structural Geology and Strain History of the Northern Selwyn Range, Rocky Mountains, near Valemount, British Columbia. (Ph.D.)

Schiarizza, A.P.: Structural and Stratigraphic Relationships Between the Fennell Formation and Eagle Bay Assemblage, Western Omineca Belt, South-central British Columbia: Implications for Paleozoic Tectonics along the Paleocontinental Margin of Western North America. (M.Sc.)

Walker, R.T.: Geology of the Mt. Lulu Area, Southern Cariboo Mountains, British Columbia. (M.Sc.)

UNIVERSITY OF CALGARY, 1990

Green, K.C.: Structure, Stratigraphy and Alteration of Cretaceous and Tertiary Strata in the Gang Ranch Area, British Columbia. (M.Sc.)

Kubli, T.E.: Geology of the Dogtooth Range, Northern Purcell Mountains, British Columbia. (Ph.D.)

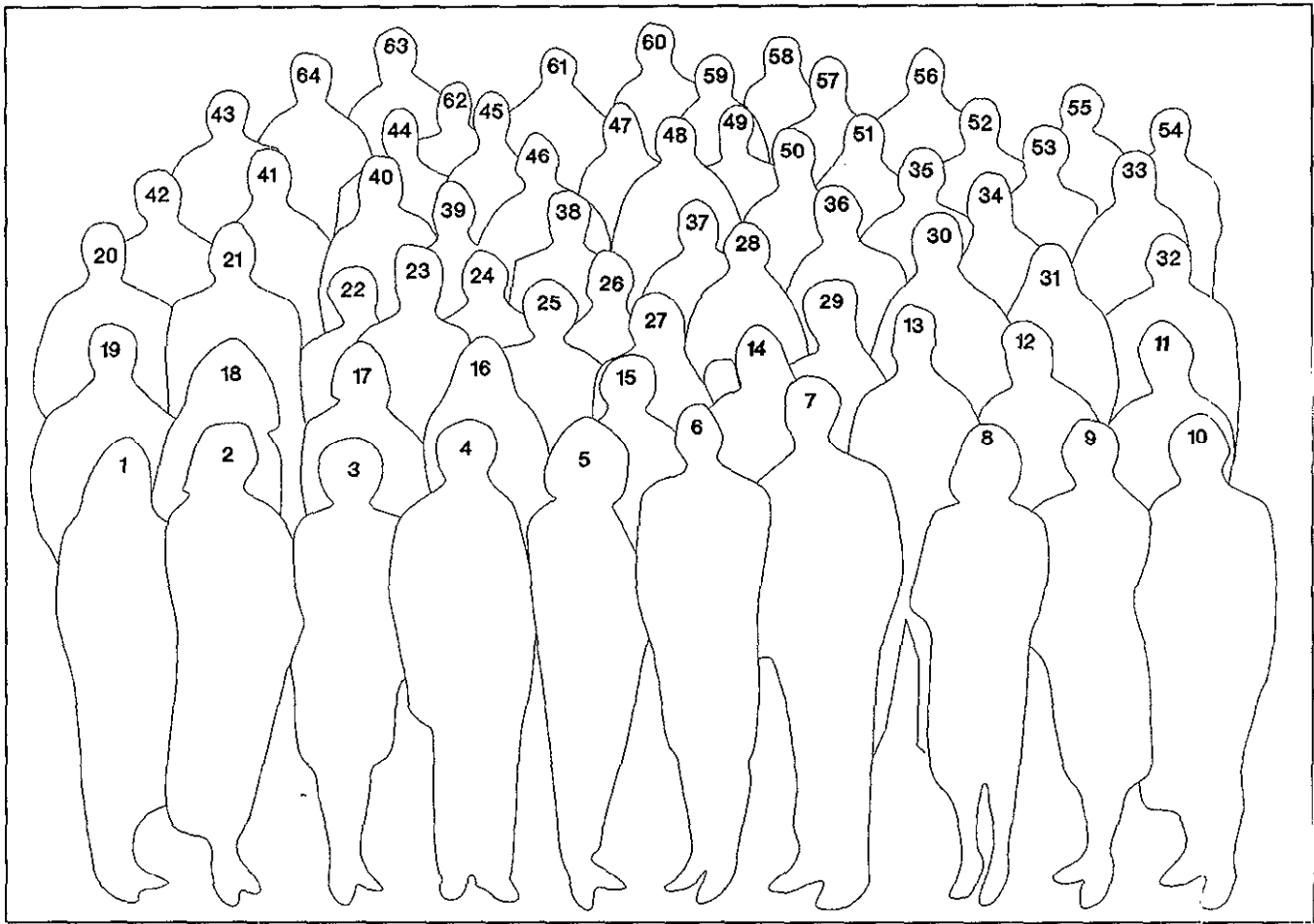
WESTERN WASHINGTON UNIVERSITY

Bennett, J.D.: Timing and Conditions of Deformation and Metamorphism of the Structural Packages East of Harrison Lake, British Columbia. (M.Sc.)

Hettinga, M.P.: Metamorphic Petrology, Geothermobarometry and Structural Analysis of a Portion of the Area East of Harrison Lake, British Columbia. (M.Sc.)

Lindsay, C.S.: The Effects of Urbanization on the Water Balance of the Fishtrap Creek Basin, Northwest Washington and South-central British Columbia, 1988. (M.Sc.)





GEOLOGICAL SURVEY BRANCH PERSONNEL, 1990

- | | | |
|----------------------------|-----------------------|----------------------|
| 1. Laura de Groot | 23. Keith Mountjoy | 44. Dave Melville |
| 2. Cindy McPeck | 24. Heather Blyth | 45. Bob Lane |
| 3. Gerri Magee | 25. Dorthe Jakobsen | 46. Talis Kalnins |
| 4. Bill McMillan | 26. Victor Koyanagi | 47. Kathy Colbourne |
| 5. Candace Kenyon | 27. Kim Bellefontaine | 48. Alex Matheson |
| 6. Claudia Logan | 28. Mike Fournier | 49. Ray Lett |
| 7. Ron Smyth | 29. Kathryn Andrew | 50. Dave Grieve |
| 8. Dawna Biffert | 30. Chris Ash | 51. Wayne Jackaman |
| 9. Shielagh Pfuetzenreuter | 31. Sabine Feulgen | 52. Bob Paul |
| 10. Mary Lou Malott | 32. Ted Faulkner | 53. George Simandi |
| 11. Brian Grant | 33. Gib McArthur | 54. John Gravel |
| 12. Bev Wendt | 34. Steve Sibbick | 55. Don MacIntyre |
| 13. Jim Hunter | 35. Ward Kilby | 56. Derek Brown |
| 14. Jan Hammack | 36. Jim Logan | 57. Rick Meyers |
| 15. Marilyn Demarchi | 37. Barry Ryan | 58. Pat Desjardins |
| 16. Pauline Loos | 38. Paul Wilton | 59. Bish Bhagwanani |
| 17. Beverly Brown | 39. Peter Bobrowsky | 60. Andre Panteleyev |
| 18. Julie Hutchins | 40. Gary Payie | 61. Dick Player |
| 19. Vic Levson | 41. George Owsiacki | 62. Joanne Schwerler |
| 20. Dan Kerr | 42. Mitch Mihalynuk | 63. Bob Gaba |
| 21. Paul Matysek | 43. Dave Lefebure | 64. Vic Preto |